NASA Contractor Report 198413

Measurements in Transitional Boundary Layers Under High Free-Stream Turbulence and Strong Acceleration Conditions

Ralph J. Volino and Terrence W. Simon
University of Minnesota
Minneapolis, Minnesota

October, 1995

Prepared for
Lewis Research Center
Under Grant NAG3–1249

National Aeronautics and
Space Administration

ACKNOWLEDGMENTS

This work was sponsored by the NASA Lewis Research Center under grant NASA/NAG3-1249. The authors thank the grant monitor, Fred Simon, for his guidance. Development of the three-wire probe and associated signal processing was done previously by Professor Jungho Kim, and the initial development of the intermittency measurement techniques was by Professor Jungho Kim and Professor Michael Kestoras. Development of near-wall measurement techniques was with the assistance of Professor Michael Kestoras and Mr. Songgang Qiu.

ABSTRACT

Measurements from transitional, heated boundary layers along a concave-curved test wall are presented and discussed. A boundary layer subject to low free-stream turbulence intensity (FSTI), which contains stationary streamwise (Görtler) vortices, is documented. The low FSTI measurements are followed by measurements in boundary layers subject to high (initially 8%) free-stream turbulence intensity and moderate to strong ($K = \frac{\nu}{U_\infty^2}\frac{dU_\infty}{dx}$ as high as 9×10^{-6}) acceleration. The high FSTI experiments are the main focus of the work. Conditions were chosen to simulate those present on the downstream half of the pressure side of a gas turbine airfoil. The high FSTI boundary layers undergo transition from a strongly disturbed non-turbulent state to a fully-turbulent state. Due to the stabilizing effect of strong acceleration, the transition zones are of extended length in spite of the high FSTI. Transitional values of skin friction coefficients and Stanton numbers drop below flat-plate, low FSTI, turbulent flow correlations, but remain well above laminar flow values. Mean velocity and temperature profiles exhibit clear changes in shape as the flow passes through transition. Turbulence statistics, including the turbulent shear stress, turbulent heat flux, and turbulent Prandtl number, are documented. Turbulent transport is strongly suppressed below values in unaccelerated turbulent boundary layers. A technique called "octant analysis" is introduced and applied to several cases from the literature as well as to data from the present study. Octant analysis shows a fundamental difference between transitional and fully-turbulent boundary layers. Transitional boundary layers are characterized by incomplete mixing compared to fully-turbulent boundary layers. Similar octant analysis results are observed in both low and high FSTI cases. Spectral analysis suggests that the non-turbulent zone of the high FSTI flow is dominated by large scale fluctuations induced by the free-stream unsteadiness. The large scale fluctuations cause some turbulent mixing, but are not as

effective at promoting turbulent transport as are smaller scale fluctuations resulting from near wall production in the turbulent boundary layer. To the authors' knowledge, this is the first detailed documentation of boundary layer transition under such high free-stream turbulence conditions.

TABLE OF CONTENTS

	Page
Acknowledgments	i
Abstract	ii
Table of Contents	iv
List of Figures	xi
List of Tables	xix
Nomenclature	xx
Chapter 1: Introduction	1
History of Transition Research	1
Bypass Transition	4
Bypass Transition Experiments	5
Bypass Transition Computations	10
Transition Modeling	11
Immediate Needs	12
Outline of Present Work	12
Chapter 2: Experimental Facility and Measurement Techniques	14
Wind Tunnel	14
Flow Preparation	14
Turbulence Generating Grid	16
Test Section	16
Instrumentation and Measurements	18
Mean Temperature	18
Profile measurement, probe traversing	20

Wall temperature 21

Wall heat flux 22

Mean and Fluctuating Velocity 23

Hot wire calibration 23

Single-wire profiles 24

Near wall correction 25

Digitizers 26

Cross-wire profiles 27

Simultaneous Velocity and Temperature - Turbulent Heat Flux 28

Cold wire frequency compensation 29

Intermittency 31

Data Processing 34

Skin Friction and Stanton Number 34

Turbulent Prandtl Number 34

Free-Stream Velocity 35

Boundary Layer Thickness 36

Octant Analysis 37

Spectral Analysis and Transfer Functions 37

Integral length scales 39

Transfer functions 39

Two Point Correlations 40

Chapter 3: Low FSTI, Concave Wall Transition 52

Background 52

Free-Stream Turbulence 53

Boundary Layer Spectra and Transfer Functions 54

Streamwise Velocity Profiles 57

Mean Velocity 57

Skin Friction 58

Fluctuating Velocities 59

Intermittency 60

Transition location 61

Intermittency distribution 62

Turbulent spot propagation rate 63

Conclusions 65

Chapter 4: An Application of Octant Analysis to Turbulent and Transitional Flow Data 100

Summary 100

Introduction 101

Quadrant and Octant Analysis 102

Results and Discussion 105

Base Case: The Fully-Turbulent, Flat-Wall Boundary Layer with Low-to-Moderate Free-Stream Turbulence Intensity Levels 105

The Effects of Curvature on the Fully-Turbulent Boundary Layer 107

Effects of High Free-Stream Turbulence Intensity 107

Transitional Flow 108

Modeling Implications 110

Conclusions and Recommendations 111

Chapter 5: High FSTI, $K=0.75\times10^{-6}$ Results 130

Experimental Conditions 130

Free-Stream Conditions 131

Free-stream spectra 132
Two point correlations 132
Boundary Layer Growth 133
Energy and Momentum Balances 133
Strength of Curvature 134
Mean Velocity Profiles 135
Skin Friction Coefficients 135
Mean Temperature Profiles 136
Stanton Numbers 137
Fluctuating Velocity Measurements 138
$\overline{u'}$ Profiles 138
$\overline{v'}$ Profiles 138
Turbulent Shear Stress Profiles 139
Eddy Viscosity 140
Mixing Length of Momentum 140
Turbulent Heat Flux Measurements 140
Conclusions 141

Chapter 6: High FSTI, $dU_{cw}/dx=29\ s^{-1}$ Results 171
Experimental Conditions 172
Free-Stream Conditions 172
Free-stream spectra 172
Boundary Layer Growth 174
Energy Balance 174
Strength of Curvature 175
Mean Velocity Profiles 175
Skin Friction Coefficients 176

Mean Temperature Profiles 176

Stanton Numbers 177

Intermittency Profiles 177

Fluctuating Velocity Measurements 178

$\overline{u'}$ Profiles 178

$\overline{v'}$ Profiles 179

Turbulent Shear Stress Profiles 179

Eddy Viscosity 180

Mixing Length of Momentum 180

Fluctuating Temperature and Velocity Measurements 180

$\overline{t'}$ Profiles 180

$\overline{v't'}$ Profiles 181

$-\overline{u't'}$ Profiles 181

Eddy Diffusivity of Heat 182

Mixing Length of Heat 182

Turbulent Prandtl Number 182

Cross Transport of Turbulent Shear Stress and Turbulent Heat Flux 183

Octant Analysis 183

Boundary Layer Spectra and Transfer Functions 185

Transfer Functions 186

Conclusions 187

Chapter 7: High FSTI, $dU_{cw}/dx=14\ s^{-1}$ Results 253

Experimental Conditions 253

Free-Stream Conditions 254

Free-stream spectra 254

Boundary Layer Growth 256
Energy Balance 257
Strength of Curvature 257
Mean Velocity Profiles 257
Skin Friction Coefficients 258
Mean Temperature Profiles 259
Stanton Numbers 261
Intermittency Profiles 262
Fluctuating Velocity Measurements 263
$\overline{u'}$ Profiles 263
$\overline{v'}$ Profiles 264
Turbulent Shear Stress Profiles 264
Eddy Viscosity 265
Mixing Length of Momentum 265
Fluctuating Temperature and Velocity Measurements 266
$\overline{t'}$ Profiles 266
$\overline{v't'}$ Profiles 266
$-\overline{u't'}$ Profiles 267
Eddy Diffusivity of Heat 267
Mixing Length of Heat 267
Turbulent Prandtl Number 268
Cross Transport of Turbulent Shear Stress and Turbulent Heat Flux 268
Octant Analysis 268
Boundary Layer Spectra and Transfer Functions 270
Transfer Functions 271
Turbulent shear stress 273

Conclusions 274

Chapter 8: Discussion and Recommendations 353

Nature of High FSTI Transition 353

Acceleration Effect 354

Curvature Effect 354

Görtler vortices 354

Transition Modeling 356

Chapter 9: Conclusions 358

References 360

Appendix A: Velocity and Temperature Profiles in Turbulent Boundary Layers Experiencing Streamwise Pressure Gradients 368

Summary 368

Introduction 368

Analysis 373

Velocity Profile 373

Temperature Profile 379

Calculation of Pr_t 382

Results and Discussion 383

Temperature Profile 386

Calculation of Pr_t 387

Conclusions 388

Appendix B: Program Listings 400

Appendix C: Tabulated Data 400

LIST OF FIGURES

Figure

2.1 Schematic of Test Facility

2.2 Turbulence Generator

2.3 Cross Section of Test Wall

2.4 Schematic of Triple-Wire Probe used to measure Turbulent Heat Fluxes

2.5 Cold Wire Compensation Calibration

2.6 Velocity Time Trace from Intermittent Flow

2.7 Typical Spectrum Before and After Smoothing

2.8 Configuration for Two-Point Correlation Measurements

3.1 Schematic of Görtler Vortices

3.2 Free-Stream u′ Spectra, Low FSTI Case

3.3 Free-Stream v′ Spectra, Low FSTI Case

3.4 Boundary Layer u′ Spectra at y^+=6, Low FSTI Case

3.5 Boundary Layer u′ Spectra at y^+=35, Low FSTI Case

3.6 Transfer Function of u′ Between y^+=6 and Free-Stream, Low FSTI Case

3.7 Depiction of u′ Caused by Large-Scale Free-Stream Eddies Buffeting the Boundary Layer

3.8 Transfer Function of u′ Between y^+=35 and Free-Stream, Low FSTI Case

3.9 Mean Streamwise Velocity Profiles at a) Lowest Re_x ($=3.7\times10^5$) and b) Highest Re_x ($=4.4\times10^5$), Low FSTI Case

3.10 Upwash and Downwash Profiles Cutting Through "Tilted" Vortices

3.11 Mean Streamwise Velocity Profiles at a) Lowest Re_x ($=3.7\times10^5$) and b) Highest Re_x ($=4.4\times10^5$), Low FSTI Case, wall coordinates

3.12 Mean Streamwise Velocity Profiles at a) Downwash Locations and b) Upwash Locations, Low FSTI Case

3.13 Mean Streamwise Velocity Profiles at a) Downwash Locations and b) Upwash Locations, Low FSTI Case, wall coordinates

3.14 Skin Friction Coefficient vs a) Re_x and b) Re_θ, Low FSTI Case

3.15 Fluctuating Streamwise Velocity Profiles at a) Downwash Locations and b) Upwash Locations, Low FSTI Case

3.16 Fluctuating Streamwise Velocity Profiles at a) Downwash Locations and b) Upwash Locations, Low FSTI Case, wall coordinates

3.17 Intermittency Profiles at a) Downwash Locations and b) Upwash Locations, Low FSTI Case

3.18 Intermittency Distributions Through Transition

3.19 Turbulent Spot Production Rate Based on γ

4.1 Octant Names

4.2 Conceptual Drawing of Eddies in Each Octant

4.3 Turbulent Shear Stress Profiles, 1.5% FSTI Flat-Wall Case, Fully Turbulent-Flow

4.4 Normal Component of Turbulent Heat Flux Profiles, 1.5% FSTI Flat-Wall Case, Fully-Turbulent Flow

4.5 Turbulent Shear Stress versus hole size at $y/\delta_{99.5}$=0.39, 1.5% FSTI Flat-Wall Case, Fully-Turbulent Flow

4.6 Fraction of Points in Octant versus Hole Size at $y/\delta_{99.5}$=0.39, 1.5% FSTI Flat-Wall Case, Fully-Turbulent Flow

4.7 Turbulent Shear Stress Profiles, 0.6% FSTI Concave-Wall Case, Fully Turbulent-Flow

4.8 Turbulent Shear Stress Profiles, 0.68% FSTI Convex-Wall Case, Fully Turbulent-Flow

4.9 Turbulent Shear Stress Profiles, 8.3% FSTI Flat-Wall Case, Fully-Turbulent Flow

4.10 Normal Component of Turbulent Heat Flux Profiles, 8.3% FSTI Flat-Wall Case, Fully-Turbulent Flow

4.11 Turbulent Shear Stress Profiles, 1.5% FSTI Flat-Wall Case, Transitional Flow

4.12 Normal Component of Turbulent Heat Flux Profiles, 1.5% FSTI Flat-Wall Case, Transitional Flow

4.13 Turbulent Shear Stress versus Hole Size at $y/\delta_{99.5}$=0.43, 1.5% FSTI Flat-Wall Case, Transitional Flow

4.14 Fraction of Points in Octant versus Hole Size at $y/\delta_{99.5}$=0.43, 1.5% FSTI Flat-Wall Case, Transitional Flow

4.15 Normal Component of Turbulent Heat Flux Profiles, 0.6% FSTI Concave-Wall Case, Transitional Flow, H′=0

4.16 Normal Component of Turbulent Heat Flux Profiles, 0.6% FSTI Concave-Wall Case, Transitional Flow, H′=10

4.17 Proposed Differences Between Fully-Turbulent and Transitional Flow Structures

5.1 Typical Pressure Side Acceleration Profiles

5.2 Pressure Side KRe_c Profiles for Two Airfoils

5.3 Free-Stream Turbulence Levels, $K=0.75\times10^{-6}$ Case

5.4 Station 1 Free-Stream Spectra, $K=0.75\times10^{-6}$ Case

5.5 Two Point Correlation of Streamwise Velocity Fluctuations, Station 1, $K=0.75\times10^{-6}$ Case

5.6 Momentum and Thermal Boundary Layer Growth

5.7 Shape Factor vs Re_x

5.8 Energy Balance, $K=0.75\times10^{-6}$ Case

5.9 Strength of Curvature for Experiment and Pressure Side of Two Typical Airfoils

5.10 Mean Velocity Profiles, $K=0.75\times10^{-6}$ Case

5.11 Mean Velocity Profiles, Wall Coordinates, $K=0.75\times10^{-6}$ Case

5.12 Skin Friction Coefficients vs Re_θ, $K=0.75\times10^{-6}$ Case

5.13 Mean Temperature Profiles, $K=0.75\times10^{-6}$ Case

5.14 Mean Temperature Profiles, Wall Coordinates, $K=0.75\times10^{-6}$ Case

5.15 Comparison of Calculated Profile to Data, $K=0.75\times10^{-6}$ Case

5.16 Mean Temperature Profiles, Unaccelerated, Concave-Wall Case

5.17 Stanton Number vs Re_{Δ_2}

5.18 Fluctuating Streamwise Velocity Profiles, $K=0.75\times10^{-6}$ Case

5.19 Fluctuating Streamwise Velocity Profiles, Wall Coordinates, $K=0.75\times10^{-6}$ Case

5.20 Fluctuating Normal Velocity Profiles, $K=0.75\times10^{-6}$ Case

5.21 Fluctuating Normal Velocity Profiles, Wall Coordinates, $K=0.75\times10^{-6}$ Case

5.22 Turbulent Shear Stress Profiles, $K=0.75\times10^{-6}$ Case

5.23 Turbulent Shear Stress Profiles, Wall Coordinates, $K=0.75\times10^{-6}$ Case

5.24 Eddy Viscosity Profiles, $K=0.75\times10^{-6}$ Case

5.25 Mixing Length of Momentum Profiles, $K=0.75\times10^{-6}$ Case

6.1 K Profiles for $dU_{cw}/dx=29\ s^{-1}$ Experiment and the Pressure Side of Typical Turbine Airfoils

6.2 Free-Stream Turbulence Levels, $dU_{cw}/dx=29\ s^{-1}$ Case

6.3 Free-Stream Spectra of Streamwise Velocity Fluctuations, $dU_{cw}/dx=29\ s^{-1}$ Case

6.4 Free-Stream Spectra of Cross-stream Velocity Fluctuations, $dU_{cw}/dx=29\ s^{-1}$ Case

6.5 Momentum and Thermal Boundary Layer Growth, $dU_{cw}/dx=29\ s^{-1}$ Case

6.6 Shape Factor vs Re_x, $dU_{cw}/dx=29\ s^{-1}$ Case

6.7 Energy Balance, $dU_{cw}/dx=29\ s^{-1}$ Case

6.8 Strength of Curvature for $dU_{cw}/dx=29\ s^{-1}$ Case and Pressure Side of Two Typical Airfoils

6.9 Mean Velocity Profiles, $dU_{cw}/dx=29\ s^{-1}$ Case

6.10 Mean Velocity Profiles, Wall Coordinates, $dU_{cw}/dx=29\ s^{-1}$ Case

6.11 Skin Friction Coefficients vs Re_θ, $dU_{cw}/dx=29\ s^{-1}$ Case

6.12 Mean Temperature Profiles, $dU_{cw}/dx=29\ s^{-1}$ Case

6.13 Mean Temperature Profiles, Wall Coordinates, b) Comparison of Calculated Profile to Data, $dU_{cw}/dx=29\ s^{-1}$ Case

6.14 Stanton Number vs $Re_{\Delta 2}$, $dU_{cw}/dx=29\ s^{-1}$ Case

6.15 Intermittency Profiles Based on u′ Fluctuations, $dU_{cw}/dx=29\ s^{-1}$ Case

6.16 Intermittency Profiles Based on t′ Fluctuations, $dU_{cw}/dx=29\ s^{-1}$ Case

6.17 Fluctuating Streamwise Velocity Profiles, $dU_{cw}/dx=29\ s^{-1}$ Case

6.18 Fluctuating Streamwise Velocity Profiles, Wall Coordinates, $dU_{cw}/dx=29\ s^{-1}$ Case

6.19 Fluctuating Cross-stream Velocity Profiles, $dU_{cw}/dx=29\ s^{-1}$ Case

6.20 Fluctuating Cross-stream Velocity Profiles, Wall Coordinates, $dU_{cw}/dx=29\ s^{-1}$ Case

6.21 Turbulent Shear Stress Profiles, $dU_{cw}/dx=29\ s^{-1}$ Case

6.22 Turbulent Shear Stress Profiles, Wall Coordinates, $dU_{cw}/dx=29\ s^{-1}$ Case

6.23 Eddy Viscosity Profiles, $dU_{cw}/dx=29\ s^{-1}$ Case

6.24 Mixing Length of Momentum Profiles, $dU_{cw}/dx=29\ s^{-1}$ Case

6.25 Fluctuating Temperature Profiles, $dU_{cw}/dx=29\ s^{-1}$ Case

6.26 Fluctuating Temperature Profiles, Wall Coordinates, $dU_{cw}/dx=29\ s^{-1}$ Case

6.27 Normal Component of Turbulent Heat Flux Profiles, $dU_{cw}/dx=29\ s^{-1}$ Case

6.28 Normal Component of Turbulent Heat Flux Profiles, Wall Coordinates $dU_{cw}/dx=29\ s^{-1}$ Case

6.29 Streamwise Component of Turbulent Heat Flux Profiles, Wall Coordinates $dU_{cw}/dx=29\ s^{-1}$ Case

6.30 Eddy Diffusivity of Heat Profiles, $dU_{cw}/dx=29\ s^{-1}$ Case

6.31 Mixing Length of Heat Profiles, $dU_{cw}/dx=29\ s^{-1}$ Case

6.32 Turbulent Prandtl Number Profiles, $dU_{cw}/dx=29\ s^{-1}$ Case

6.33 Cross Transport of Turbulent Shear Stress Profiles, $dU_{cw}/dx=29\ s^{-1}$ Case

6.34 Cross Transport of Turbulent Heat Flux Profiles, $dU_{cw}/dx=29\ s^{-1}$ Case

6.35 Octant Decomposition of Turbulent Shear Stress, $dU_{cw}/dx=29\ s^{-1}$ Case

6.36 Octant Decomposition of Turbulent Heat Flux, $dU_{cw}/dx=29\ s^{-1}$ Case

6.37 Boundary Layer u' Spectra at $y^+=5$, $dU_{cw}/dx=29\ s^{-1}$ Case

6.38 Boundary Layer u' Spectra at $y^+=17$ $dU_{cw}/dx=29\ s^{-1}$ Case

6.39 Boundary Layer u' Spectra at $y^+=100$, $dU_{cw}/dx=29\ s^{-1}$ Case

6.40 Boundary Layer v' Spectra at $y^+=100$, $dU_{cw}/dx=29\ s^{-1}$ Case

6.41 Turbulent Shear Stress Spectra at $y^+=100$, $dU_{cw}/dx=29\ s^{-1}$ Case

6.42 Transfer Function of u′ Between Boundary Layer and Free-Stream, $dU_{cw}/dx=29\ s^{-1}$ Case

6.43 Transfer Function of v′ Between Boundary Layer at $y^+=100$ and Free-Stream, $dU_{cw}/dx=29\ s^{-1}$ Case

6.44 Transfer Function Between u′v′ and u′ at $y^+=100$, $dU_{cw}/dx=29\ s^{-1}$ Case

6.45 Transfer Function Between u′v′ and v′ at $y^+=100$, $dU_{cw}/dx=29\ s^{-1}$ Case

7.1 K Profiles for $dU_{cw}/dx=14\ s^{-1}$ Experiment and the Pressure Side of Typical Turbine Airfoils

7.2 Free-Stream Turbulence Levels, $dU_{cw}/dx=14\ s^{-1}$ Case

7.3 Free-Stream Spectra of Streamwise Velocity Fluctuations, $dU_{cw}/dx=14\ s^{-1}$ Case

7.4 Free-Stream Spectra of Cross-stream Velocity Fluctuations, $dU_{cw}/dx=14\ s^{-1}$ Case

7.5 Momentum and Thermal Boundary Layer Growth, $dU_{cw}/dx=14\ s^{-1}$ Case

7.6 Shape Factor vs Re_x, $dU_{cw}/dx=14\ s^{-1}$ Case

7.7 Energy Balance, $dU_{cw}/dx=14\ s^{-1}$ Case

7.8 Mean Velocity Profiles, $dU_{cw}/dx=14\ s^{-1}$ Case

7.9 Mean Velocity Profiles, Wall Coordinates, $dU_{cw}/dx=14\ s^{-1}$ Case

7.10 Comparison of Calculated Profiles to Data, $dU_{cw}/dx=14\ s^{-1}$ Case

7.11 Skin Friction Coefficients vs Re_θ, $dU_{cw}/dx=14\ s^{-1}$ Case

7.12 Skin Friction Coefficients vs Re_θ and Re_x, Comparison of High-FSTI Cases

7.13 Mean Temperature Profiles, $dU_{cw}/dx=14\ s^{-1}$ Case

7.14 Mean Temperature Profiles, Wall Coordinates, $dU_{cw}/dx=14\ s^{-1}$ Case

7.15 Comparison of Calculated Profiles to Data, $dU_{cw}/dx=14\ s^{-1}$ Case

7.16 Stanton Number vs $Re_{\Delta 2}$, $dU_{cw}/dx=14\ s^{-1}$ Case

7.17 Stanton Number vs $Re_{\Delta 2}$ and Re_x, Comparison of High-FSTI Cases

7.18 Intermittency Profiles Based on u′ Fluctuations, $dU_{cw}/dx=14\ s^{-1}$ Case

7.19 Intermittency Profiles Based on t′ Fluctuations, $dU_{cw}/dx=14\ s^{-1}$ Case

7.20 Fluctuating Streamwise Velocity Profiles, $dU_{cw}/dx=14\ s^{-1}$ Case

7.21 Fluctuating Streamwise Velocity Profiles, Wall Coordinates, $dU_{cw}/dx=14\ s^{-1}$ Case

7.22 Fluctuating Cross-stream Velocity Profiles, $dU_{cw}/dx=14\ s^{-1}$ Case

7.23 Fluctuating Cross-stream Velocity Profiles, Wall Coordinates, $dU_{cw}/dx=14\ s^{-1}$ Case

7.24 Turbulent Shear Stress Profiles, $dU_{cw}/dx=14\ s^{-1}$ Case

7.25 Turbulent Shear Stress Profiles, Wall Coordinates, $dU_{cw}/dx=14\ s^{-1}$ Case

7.26 Eddy Viscosity Profiles, $dU_{cw}/dx=14\ s^{-1}$ Case

7.27 Mixing Length of Momentum Profiles, $dU_{cw}/dx=14\ s^{-1}$ Case

7.28 Fluctuating Temperature Profiles, $dU_{cw}/dx=14\ s^{-1}$ Case

7.29 Fluctuating Temperature Profiles, Wall Coordinates, $dU_{cw}/dx=14\ s^{-1}$ Case

7.30 Normal Component of Turbulent Heat Flux Profiles, $dU_{cw}/dx=14\ s^{-1}$ Case

7.31 Normal Component of Turbulent Heat Flux Profiles, Wall Coordinates $dU_{cw}/dx=14\ s^{-1}$ Case

7.32 Streamwise Component of Turbulent Heat Flux Profiles, Wall Coordinates $dU_{cw}/dx=14\ s^{-1}$ Case

7.33 Eddy Diffusivity of Heat Profiles, $dU_{cw}/dx=14\ s^{-1}$ Case

7.34 Mixing Length of Heat Profiles, $dU_{cw}/dx=14\ s^{-1}$ Case

7.35 Turbulent Prandtl Number Profiles, $dU_{cw}/dx=14\ s^{-1}$ Case

7.36 Cross Transport of Turbulent Shear Stress Profiles, $dU_{cw}/dx=14\ s^{-1}$ Case

7.37 Cross Transport of Turbulent Heat Flux Profiles, $dU_{cw}/dx=14\ s^{-1}$ Case

7.38 Octant Decomposition of Turbulent Shear Stress, $dU_{cw}/dx=14\ s^{-1}$ Case

7.39 Octant Decomposition of Turbulent Heat Flux, $dU_{cw}/dx=14\ s^{-1}$ Case

7.40 Boundary Layer u′ Spectra at $y^+=5$, $dU_{cw}/dx=14\ s^{-1}$ Case

7.41 Boundary Layer u′ Spectra at $y^+=17$ $dU_{cw}/dx=14\ s^{-1}$ Case

7.42 Boundary Layer u′ Spectra at y^+=50, dU_{cw}/dx=14 s^{-1} Case

7.43 Boundary Layer v′ Spectra at y^+=50, dU_{cw}/dx=14 s^{-1} Case

7.44 Turbulent Shear Stress Spectra at y^+=50, dU_{cw}/dx=14 s^{-1} Case

7.45 Transfer Function of u′ Between Boundary Layer at y^+=5 and Free-Stream, dU_{cw}/dx=14 s^{-1} Case

7.46 Transfer Function of u′ Between Boundary Layer at y^+=17 and Free-Stream, dU_{cw}/dx=14 s^{-1} Case

7.47 Transfer Function of u′ Between Boundary Layer at y^+=50 and Free-Stream, dU_{cw}/dx=14 s^{-1} Case

7.48 Transfer Function of v′ Between Boundary Layer at y^+=50 and Free-Stream, dU_{cw}/dx=14 s^{-1} Case

7.49 Transfer Function Between u′v′ and u′ at y^+=50, dU_{cw}/dx=14 s^{-1} Case

7.50 Transfer Function Between u′v′ and v′ at y^+=50, dU_{cw}/dx=14 s^{-1} Case

A.1 Velocity Profile in Laminar Unaccelerated Flow

A.2 Velocity and Temperature Profiles Including Various Correction Terms

A.3 Comparison of Experimental and Calculated Velocity Profiles

A.4 Force Fit of Experimental Velocity Date to Standard Law of the Wall

A.5 Comparison of Experimental and Calculated Temperature Profiles

A.6 Comparison of Calculated and Measured Pr_t, Unaccelerated, High FSTI, Concave-Wall Case

LIST OF TABLES

Table

3.1 Conditions for Kim and Simon's (1991) Low FSTI Concave-Wall Case

3.2 Conditions for Streamwise Velocity Profiles, Low FSTI Concave-Wall Case

3.3 Transition Start and End, and Turbulent Spot Propagation Rates Based on Intermittency Measurements, Low FSTI Concave-Wall Case

4.1 Cases Considered (for Octant Analysis)

5.1: Parameters for the $K=0.75\times10^{-6}$ Case

6.1: Parameters for the $dU_{cw}/dx=29\ s^{-1}$ Case

7.1: Parameters for the $dU_{cw}/dx=14\ s^{-1}$ Case

A.1 Experimental Data

NOMENCLATURE

A^+	constant in van Driest damping model
A^+_{eq}	equilibrium value of A^+ (eq. A.17a)
a	hot wire radius
b	y/a, dimensionless distance from the wall
C	constant in standard law of the wall
C_f	$\frac{\tau_w}{\rho U_\infty^2 / 2}$, skin friction coefficient
C_μ	empirical constant
C_t	constant in standard thermal law of the wall
c	chord length
c_p, c	specific heat at constant pressure
cfv	correction to v' for tangential cooling of hot wires (eq. 2.8)
cfuv	correction to $u'v'$ for tangential cooling of hot wires (eq. 2.8)
d	hot wire diameter
E	hot wire voltage
FSTI	free-stream turbulence intensity
f	frequency
f_1	$\frac{\nu}{U_\infty \frac{C_f}{2}} \frac{d\sqrt{\frac{C_f}{2}}}{dx}$
f_2	$\frac{\nu t_\infty^{+2}}{U_\infty \frac{C_f}{2}} \frac{dSt}{dx}$
$f(\gamma)$	function of intermittency (eq. 3.1)
f_μ	empirical function
G	$Re_\theta \sqrt{\frac{\theta}{R}}$, Görtler number

G_t $\frac{U_{cw}\theta}{\varepsilon_M}\sqrt{\frac{\theta}{R}}$, turbulent Görtler number

H shape factor, δ^*/θ

H' hole size parameter (eq. 4.2)

I indicator function

K $\frac{\nu}{U_\infty^2}\frac{dU_\infty}{dx}$, acceleration parameter

k turbulence intensity

k_{cc} cold wire compensation constant (eq. 2.10)

k_w near wall correction term for hot-wire-measured velocities (eq. 2.5)

k_t term in Champagne correction for tangential cooling of hot wires (eq. 2.9)

ℓ, ℓ_M mixing length of momentum

ℓ_H mixing length of heat

N number of points in sample

n turbulent spot production rate

$\hat{n}$ $\frac{n\sigma}{U_s^3}$, dimensionless turbulent spot production rate

P pressure

p^+ $\frac{\nu}{\rho u_\tau^3}\frac{dP}{dx}$, pressure in wall units $= -K\left(\frac{C_f}{2}\right)^{-3/2}$

PSD power spectral density, $\frac{\overline{u'^2(f,df)}}{df}$, $\frac{\overline{v'^2(f,df)}}{df}$, or $\frac{\overline{-u'v'(f,df)}}{df}$

Pr Prandtl number

Pr_t $\varepsilon_M/\varepsilon_H$, turbulent Prandtl number

q heat flux

q_o wall heat flux (in Appendix A)

R radius of curvature of test wall

Re_c Reynolds number based on chord length of airfoil

Re_x Reynolds number based on distance from leading edge

Re_{Δ_2} enthalpy thickness Reynolds number

Re_θ momentum thickness Reynolds number

r recovery factor

St $\frac{q}{\rho c U_\infty (T_w - T_\infty)}$, Stanton number

T instantaneous local temperature

T_{rec} recovery temperature

T_{static} static temperature, T

T_s stagnation temperature

T_{s_∞} stagnation temperature in free-stream

T_w wall temperature

T_∞ free-stream temperature

t time

t' fluctuating component of temperature

$\overline{t'}$ $\sqrt{\overline{t'^2}}$, rms fluctuating temperature

$\overline{t'^2}$ mean square of fluctuating temperature

t^+ $\frac{(T - T_w)\rho c u_\tau}{q}$, local temperature in wall coordinates

U instantaneous local streamwise velocity

U_c core velocity

U_{cw} core velocity extrapolated to the wall

U_{cw_o} core velocity at entrance to the test section

U_∞ free-stream velocity

U_s free-stream velocity at transition start

u mean velocity component in streamwise direction (used in Appendix A)

u^+ $\frac{U}{u_\tau}$, local velocity in wall coordinates

u' fluctuating component of streamwise velocity

$\overline{u'}$ $\sqrt{\overline{u'^2}}$, rms streamwise fluctuating velocity component

$\overline{u'^2}$ mean square of fluctuating streamwise velocity, based on full spectrum

$\overline{u'^2(f,df)}$ contribution to $\overline{u'^2}$ from a frequency band of width df, centered at f, $\lim_{\Delta f \to df} \int_f^{f+\Delta f} \overline{u'^2(f)} df$

u_τ $\sqrt{\tau_w/\rho}$, friction velocity

$-\overline{u't'}$ streamwise component of turbulent heat flux

$-\overline{u'v'}$ turbulent shear stress

$-\overline{u'v'(f,df)}$ contribution to $-\overline{u'v'}$ from a frequency band of width df, centered at f, $\lim_{\Delta f \to df} \int_f^{f+\Delta f} -\overline{u'v'(f)} df$

$\overline{u'v'^2}$ cross-transport of turbulent shear stress

V instantaneous local cross-stream velocity

v mean velocity component in cross-stream direction (used in Appendix A)

v′ fluctuating component of cross-stream velocity

$\overline{v'}$ $\sqrt{\overline{v'^2}}$, rms cross-stream fluctuating velocity component

$\overline{v'^2}$ mean square of fluctuating normal velocity, based on full spectrum

$\overline{v'^2(f,df)}$ contribution to $\overline{v'^2}$ from a frequency band of width df, centered at f, $\lim_{\Delta f \to df} \int_f^{f+\Delta f} \overline{v'^2(f)} df$

V_c compensated voltage from the cold wire (eq. 2.10)

V_1 measured voltage across the cold wire (eq. 2.10)

V_2 voltage across one of the hot wires (eq. 2.10)

V_{21} (cold wire current) × (hot wire resistance) (eq. 2.10)

$\overline{v't'}$ normal component of turbulent heat flux

$\overline{v'^2t'}$ cross-transport of normal component of turbulent heat flux

W instantaneous local spanwise velocity

w′ fluctuating component of spanwise velocity

$\overline{w'}$ $\sqrt{\overline{w'^2}}$, rms cross-stream fluctuating velocity component

$\overline{w'^2}$ mean square of fluctuating normal velocity, based on full spectrum

x streamwise coordinate

x_o x at start of heating on test wall

x_e x at end of transition

x_s x at start of transition

x^+ $\frac{xu_\tau}{\nu}$, distance in streamwise direction in wall coordinates

y coordinate normal to the wall

y^+ $\frac{yu_\tau}{\nu}$, distance from wall in wall coordinates

α thermal diffusivity

γ intermittency (fraction of time flow is turbulent)

Δ_2 enthalpy thickness

δ boundary layer thickness

δ^* displacement thickness

$\delta_{99.5}$ 99.5% boundary layer thickness

$\delta_{t99.5}$ 99.5% thermal boundary layer thickness

ε turbulence dissipation, also resistance ratio (eq. 2.10)

ε_H $\overline{v't'} / \frac{d\overline{T}}{dy}$, eddy diffusivity of heat

ε_M $-\overline{u'v'} / \frac{d\overline{U}}{dy}$, eddy viscosity

ζ' $\frac{u}{U_\infty}$, dimensionless velocity

η $\frac{y}{\sqrt{\frac{\nu x}{U_\infty}}}$, Blasius similarity coordinate

θ momentum thickness

κ von Kármán constant

$\Lambda_{u'}$ integral length scale, $\frac{U}{4\overline{u'^2}}\frac{\overline{u'^2(f=0,df)}}{df}$

$\Lambda_{v'}$ integral length scale, $\frac{U}{4\overline{v'^2}}\frac{\overline{v'^2(f=0,df)}}{df}$

$\Lambda_{w'}$ integral length scale, $\frac{U}{4\overline{w'^2}}\frac{\overline{w'^2(f=0,df)}}{df}$

ν kinematic viscosity

ν_T eddy viscosity

ξ dimensionless position within transition zone (eq. 1.1)

ρ density

σ turbulent spot propagation parameter

τ shear stress

τ_w wall shear stress

Subscripts

e end of transition

i index for octant number

j index for data point number

s start of transition or stagnation temperature

w quantity evaluated at the wall

∞ quantity evaluated in the free-stream

overbar time-averaged

CHAPTER 1: INTRODUCTION

Transition to turbulence is a complex phenomenon which has been studied extensively but is still not well understood. A better understanding of transition is needed since the transition process is an important factor in determining the distribution of heat transfer and drag on a surface. Transition is generally accepted to be an important phenomenon experienced by many flows of engineering significance, including the flow through the core of gas turbine engines. Better prediction of gas turbine flows is the motivation for the present work. Mayle (1991) stated that a substantial fraction of the boundary layer on each side of a gas turbine airfoil may be transitional. The ability to understand and predict transition in turbine environments is potentially very important since airfoil heat transfer and drag coefficients may increase severalfold when a boundary layer undergoes transition. Boundary layer separation, which is seen in adverse pressure gradient regions of turbine airfoils, may also depend on transition, since laminar boundary layers are more susceptible to separation than are turbulent boundary layers. For these reasons, it is important to know the location and length of the transition region as well as the behavior of the flow and heat transfer within the transition zone.

HISTORY OF TRANSITION RESEARCH

Laminar-turbulent transition has been recognized and studied for over 100 years. Osborne Reynolds (1883) observed transition in pipe flows, noting the intermittent nature of the laminar and turbulent regions of the flow. Prandtl (1935) studied boundary layer transition, noting a transition zone of "appreciable length", and that the position at which "turbulence commences oscillates with time." Dryden (1939) studied velocity traces obtained with hot wires in transitional boundary layers and stated that transition occurs suddenly but that the transition point moves back and forth in the streamwise direction.

Much of the early transition research focused on transition in low disturbance environments, where analytical study was possible. Tollmien (1931, 1936) and Schlichting (1933) applied linear stability theory to laminar boundary layers to predict when the boundary layer would become unstable to small disturbances. Stability plots were produced to show the frequencies at which disturbances would be amplified by the boundary layer at different Reynolds numbers. The amplification of disturbances at unstable frequencies is the first step in the transition process under low-disturbance conditions. Perturbations at unstable frequencies grow as two dimensional disturbances, now known as Tollmien-Schlichting, or, TS waves. These disturbances or "wave packets" become three-dimensional due to secondary instabilities as they move downstream and eventually culminate as turbulent spots in the boundary layer. This type of transition is known as Tollmien-Schlichting or TS transition, and has been described by several authors, including Schlichting (1979).

In the 1940's, Görtler (1940) predicted streamwise vortices in boundary layers along concave-curved walls. These vortices, now known as Görtler vortices, can lead to a breakdown to turbulence if they become unstable. Liepmann (1943) also studied transition along curved walls. Schubauer and Skramstad (1943) experimented in boundary layers grown in very low free-stream turbulence environments (free-stream turbulence intensity, FSTI, below 0.03%). They introduced disturbances into the boundary layer at various frequencies with a vibrating ribbon, and confirmed Schlichting's (1933) stability plots. With hot wires, they observed TS waves.

Emmons (1951) observed the intermittent nature of transitional flow using flow visualization in a water channel. He reported turbulent spots moving along in otherwise laminar flow. The spots grew as they moved downstream, eventually merging and forming a fully turbulent boundary layer. At any fixed point in the transitional flow, one would observe the passage of regions of laminar and turbulent flow. The nature of the

turbulent spots (e.g. their shape and rate of growth) were later documented by researchers such as Schubauer and Klebanoff (1955).

Narasimha (1957) proposed a theory which quantified the intermittent nature of the flow described by Emmons. He suggested a "concentrated breakdown" in which all turbulent spots in a flow are produced at a single streamwise position. This is obviously an approximation to the actual production of the spots. In a zero pressure gradient flow, spots are produced in a zone which is narrow compared to the overall length of the transition zone, and the concentrated breakdown model works well. Dhawan and Narasimha (1958) proposed the following equation for the intermittency within the transition zone.

$$\gamma = 1 - e^{-0.412\xi^2} \tag{1.1}$$

The intermittency, γ, is the fraction of the time the flow is turbulent (i.e. within a turbulent spot), and ξ is a dimensionless streamwise coordinate within the transition zone, given as $\xi = (x - x_s) / (x_{\gamma=75\%} - x_{\gamma=25\%})$. The concentrated breakdown (transition start) location is at x_s. Dhawan and Narasimha showed that Eqn. (1.1) agrees well with their own experimental data and data from Schubauer and Klebanoff (1955). Later, measurements by other researchers confirmed this agreement. Some of these comparisons are presented by Volino and Simon (1991). In accelerated flows, Narasimha (1984) noted an exception to the concentrated breakdown model. Acceleration tends to stabilize the boundary layer, resulting in a longer region in which turbulent spots are produced. Narasimha referred to this as a subtransition.

The studies described above focused on low disturbance flows. There were several reasons for this. Some important applications, such as transition on aircraft bodies and wings, are associated with low disturbance conditions. Low disturbance flows are amenable to linear stability analysis, making comparison between experiment and

theory possible. Under low disturbance conditions, there is also better control over discrete perturbations introduced into the flow with devices such as vibrating ribbons. In highly disturbed environments, the perturbations introduced with a vibrating ribbon would be present only along with many other uncontrolled disturbances. The study of low-disturbance flows is continuing. A review of this work was given by Narasimha (1985).

BYPASS TRANSITION

The work done in low-disturbance flows is good background material for better understanding of transition in general, but, unfortunately, is not directly applicable to highly-disturbed flows, such as those in gas turbine engines. Under high-disturbance conditions, the linear growth stages of TS transition appear to be bypassed. Morkovin (1978) defined "bypass transition" as "those roads to transition which cannot be identified as starting from a known linear instability." Bypass transition is characterized by the sudden appearance of turbulent spots.

Bypass can be caused by any disturbance of the boundary layer. Some examples of disturbances are: high free-stream turbulence (considered in the present work), surface roughness, and acoustic disturbances. The precise conditions under which bypass transition occurs are not well defined. Narasimha (1985) identified three modes of transition at different ranges of free-stream turbulence. These are "disturbance limited" transition at FSTI<1%, "turbulence driven" transition at 0.1%<FSTI<4%, and "stability limited" transition at FSTI>4%. The mechanism for the first mode is TS transition and the third is clearly bypass transition. The intermediate cases exhibit some elements of both TS and bypass transition. Sohn and Reshotko (1991) presented spectral measurements from boundary layers at six different FSTI levels. At the three lowest turbulence levels (nominal 0.45%, 0.83% and 1.1%) evidence of TS waves appeared as broadband humps in the spectra at the unstable frequencies predicted by linear stability

theory. In the 0.45% FSTI case the perturbations in the unstable range were amplified at downstream stations, while the disturbances outside this frequency range were damped. This behavior is in agreement with linear stability theory and provides evidence of TS transition. At 0.83% and 1.1%, however, perturbations at frequencies both within the band predicted to be unstable by linear theory and at higher frequencies were amplified. These two cases could be considered bypass cases since they show deviations from linear theory, despite evidence of TS-type disturbances at upstream stations. Cases which show no evidence of TS transition, particularly those which occur when linear stability theory predicts stable flow at all frequencies, are known as strong bypass cases. Cases with evidence of TS transition are weak bypass cases.

In gas turbine engines, where FSTI of 3% to over 20% are possible, transition is clearly in the bypass range. Mayle (1991) states that recent measurements in turbine and compressor rigs show FSTI values of 5 to 10%, except in the wakes of upstream blades and vanes, where values as high as 15 to 20% are found.

BYPASS TRANSITION EXPERIMENTS

Some information concerning bypass transition has come from experiments in actual gas turbine engines or turbine cascades which simulate the geometry of turbine engine passages. Such experiments are valuable, for they include all or most of those effects present in the engine which can affect the transition process. Measurements of heat transfer coefficients from these experiments provide evidence that transition is important in gas turbines. This is particularly clear on the suction side of airfoils, where heat transfer coefficients can show a sudden rise, indicating transition. The evidence is less clear on the pressure side of the airfoils, but transition may be important there as well. Some examples of turbine experiments are available in Dring et al. (1986), Hylton et al. (1983), and Bridgeman et al. (1983). Many more examples exist; Mayle (1991) provides a review of relevant experiments.

While valuable, the information available from turbine experiments is limited. The geometry of turbines is complicated, making access for detailed measurements difficult. In an actual fired engine, the difficulty of taking measurements is even more severe. When measurements are made, they can be very difficult to explain. Because the flow is complicated, with many effects present simultaneously, it is not always possible to sort out which effects are dominant, or which effects cause specific events observed in the transition process. So, while turbine experiments are valuable and can have some direct usefulness for design purposes, they cannot be used to fully explain bypass transition and are of limited use for the development of improved transition models.

To gain more insight into the mechanisms governing bypass transition, experiments are conducted in simpler flows. Geometries are chosen to allow better access of probes and more detailed measurements than in gas turbines. The complicating effects present in the experiments are also limited to allow better explanation of the results. From these results, transition models can be developed. Later, after the separate effects are better understood, experiments with several effects combined can be conducted.

While most of the early transition research focused on low disturbance cases, some bypass transition experiments have been done. Some of the older work was reviewed by Abu-Ghannam and Shaw (1980), who developed a transition correlation relating transition location to free-stream turbulence level. The last 15 years has seen considerable experimental work. Much of this work was reviewed in detail by Volino and Simon (1991), who recast data from several studies into local (Re_θ) coordinates for comparison purposes. New information, such as turbulent spot propagation rates, was also extracted from the existing data. A summary of the results of this review are presented below. A summary is also available in Volino and Simon (1995a).

Wang, Simon and Buddhavarapu (1985) studied transition on a flat plate in unaccelerated flows with FSTI of 0.6 and 2.0%. Transition occurred earlier at the higher

turbulence level, as expected. Wang and Simon (1987) considered flow along a convex curved wall at the same two turbulence levels. Strengths of curvature, $\delta_{99.5}/R$, of as high as 4% were considered. They found that convex curvature stabilized the flow and delayed transition at 0.6% FSTI. At the higher turbulence level, the free-stream turbulence effect dominated over the curvature effect, so that curvature had little effect on the transition location.

Blair (1983) studied unaccelerated boundary layers on a flat plate with FSTI ranging from 0.2% to 7.6%. Although his focus was on fully-turbulent boundary layers, Stanton numbers were documented through transition for the cases with FSTI up to 2.6%. Stanton number was increased and transition occurred earlier at the higher turbulence levels. Blair (1992) considered accelerated boundary layers with FSTI ranging from 1% to 5%. The acceleration parameter, $K = \frac{\nu}{U_\infty^2}\frac{dU_\infty}{dx}$, was held fixed at values of 0.2×10^{-6} and 0.75×10^{-6}. Acceleration, which tends to stabilize the boundary layer, delayed the onset of transition and extended the length of the transition zone at all turbulence levels.

Kuan and Wang (1990) documented an unaccelerated, 1% FSTI case on a flat plate.

Suder, O'Brien and Reshotko (1988) considered unaccelerated flow along a flat plate with FSTI ranging from 0.3% to 6.6%. Sohn and Reshotko (1991) repeated these cases and extended the results using new experimental techniques. At the lower FSTI they were able to documented the full transition zone. For FSTI over 2.6%, however, transition started before their first measurement station and they were able to see only the end of transition.

Rued and Wittig (1985) considered unaccelerated, flat plate cases with FSTI ranging from 1.3% to 8.7%. They documented surface heat transfer coefficients, but did not make detailed flow measurements. For the lower-FSTI cases, the full transition zone was documented. Above 2.1%, transition occurred quickly and only the end of transition

was documented. Rued and Wittig (1986) also considered several accelerated flow cases with K as high as 6×10^{-6} and FSTI up to 11%. Their measurements suggest that for FSTI>5%, acceleration at $K=2\times10^{-6}$ is not strong enough to influence transition, but that acceleration with $K>5\times10^{-6}$ can extend the transition zone, even at 11% FSTI. Acceleration rates in gas turbines can exceed 20×10^{-6}; thus, high-FSTI transition is expected to be important to gas turbine design. More details of Rued and Wittig's work are available in Rued (1987).

Kim, Simon and Russ (1992) and Kim, Simon and Kestoras (1994) considered unaccelerated flow on flat walls with FSTI of 0.3%, 1.5% and 8%. At the two lower turbulence levels, complete transition was documented. At 8% FSTI, transition occurred near the leading edge of the test wall and only one transitional station was captured. Downstream, the flow was fully turbulent. Kim et al. (1992) also considered unaccelerated flow along a concave wall at 0.6% and 8% FSTI. The strength of curvature reached 5% at the downstream stations. At 0.6% FSTI, curvature caused the formation of stable Görtler vortices and led to earlier transition than on the flat wall at the same FSTI. Further documentation of this case is given in Chapter 3. At 8% FSTI, as on the flat wall, Kim et al. (1992) reported transition near the leading edge and were only able to document only one station, near the end of transition. More details of Kim et al.'s (1992, 1994) work are available in Kim and Simon (1991). Kestoras (1993) repeated the measurements of Kim and Simon's 8% FSTI concave curved wall case, providing information on boundary layer thicknesses which were not given in the original study.

In addition to the above works, which are reviewed in more detail in Volino and Simon (1991), Keller and Wang (1993) investigated transition in accelerated flow along a flat plate under low (<1%) FSTI conditions. Zhou and Wang (1993) considered various acceleration rates and FSTI values up to about 6%. In adverse pressure gradient flows, which are not considered in this study, Gostelow and Walker (1991) conducted a series of transition studies. Walker (1993) provides a review of this work.

From the existing literature, some conclusions can be drawn concerning bypass transition. The general trends of high FSTI, concave curvature, and adverse pressure gradients causing early transition are confirmed. Convex curvature and favorable pressure gradients delay transition. In many of the cases considered, correlations such as the Abu-Ghannam and Shaw (1980) correlation and a more recent correlation by Mayle (1991) do reasonably well in predicting transition location (start and end) in terms of the momentum thickness Reynolds number, Re_θ, as a function of FSTI. Turbulent spot growth rates for most cases agreed with a correlation given by Mayle (1991). The distribution of intermittency closely followed Eqn. (1.1) from Dhawan and Narasimha (1958), in most cases. An exception to the above statements was Kim and Simon's (1991) 0.6% FSTI concave wall case. This case showed earlier transition and higher spot propagation rates than the correlations predict. It also deviated substantially from the expected intermittency behavior. Transition in this case was driven by a Görtler instability. More evidence of this is provided in Chapter 3.

A few shortcomings have been identified in the existing bypass transition literature. One is inadequate documentation of the free-stream disturbance in many of the experiments. Volino and Simon (1991) noted some discrepancies in the order in which cases went through transition. That is, some cases with low FSTI levels went through transition upstream of cases with higher FSTI levels. In most cases, a single FSTI value is given to describe the free-stream disturbance. Apparently, more is needed. Mayle (1991) and Volino and Simon (1991) both reached this conclusion independently. Hancock and Bradshaw (1989) considered the effects of both free-stream turbulence intensity and length scale on fully turbulent boundary layers. Free-stream spectral measurements and length scale documentation in transitional boundary layers could be very useful. More of such measurements have been included in the present study.

A second shortcoming in the literature is the lack of transition documentation at FSTI levels above 3%. In unaccelerated flow at high FSTI, transition occurs very near

the leading edge of the test wall, so no appreciable transition zone can be documented. In these cases, transition is of little practical significance, and the flow can be treated as fully turbulent from the leading edge. In accelerated flow, however, transition may be important even at very high FSTI. Blair (1992) provided some evidence of this, but only to 5% FSTI. Rued and Wittig (1986) provided interesting results showing the possible importance of transition at 11% FSTI, but these results were limited to surface heat transfer measurements. The nature of high-FSTI transition processes is unknown.

BYPASS TRANSITION COMPUTATIONS

The governing equations for bypass transition are the Navier-Stokes equations. These equations are known and can, in principle, be solved for any flow. Saying we don't understand transition really means that we cannot solve the equations in our heads, as Bradshaw (1994a) pointed out. Some work in direct numerical simulation (DNS) of bypass transition cases has already been done. Most notable is the work of Rai and Moin (1991), who performed a DNS of a 3%-FSTI case on a flat wall. DNS can provide valuable information not available from conventional experiments. The entire time-resolved flow field is available at the end of the calculation, and no intrusive probes are needed to acquire the data. Quantities such as the vorticity field can be easily calculated.

DNS does, however, have its limitations. DNS requires no turbulence modeling, but accurate specification of initial and boundary conditions is required. An accurate DNS result cannot be expected if the free-stream conditions are not well known. A sufficiently fine computational grid must also be used. Rai and Moin (1991) saw differences between results obtained for the same flow conditions with different grids. DNS computations are currently very expensive. Rai and Moin's case, requiring 400 hours of CPU time on a Cray YMP computer, is the only bypass transition case documented in the literature. Computers are becoming faster, but, for the immediate future, DNS of bypass transition will not be practical for general application. Large eddy

simulations (LES), in which the smallest scales in the flow are modeled, may become practical sooner. Large eddy simulations are less computationally intensive than direct numerical simulations, but they require subgrid scale models which require development. LES has not yet been successfully applied to bypass transition calculations.

TRANSITION MODELING

The most common calculations are those which use some type of turbulence model for closure of the time-averaged Navier-Stokes and energy equations. Since DNS and LES are not ready for general use, gas turbine designers are dependent on turbulence models and will remain dependent on them in the near future. Mayle (1991) refers to such models as the mainstay of the industry. Models range from relatively simple mixing length models to full Reynolds stress models in which differential equations are solved for each of the terms in the Reynolds stress tensor. A review of various models is provided by Reynolds (1975).

The simplest transition models use an empirical correlation such as Abu-Ghannam and Shaw's (1980) to force the calculation to change from laminar to turbulent when the laminar boundary layer reaches a given state of maturity (usually based on Re_θ). These models are only as good as is the transition correlation, in the particular flow of interest. They assume that the pre-transitional flow is steady, laminar flow, which may not be a good assumption at high FSTI levels. With high FSTI, the non-turbulent boundary layer may be highly disturbed by buffeting from free-stream eddies.

Most current efforts are focused on two-equation, k-ε models, which can capture the effects of changing FSTI. Such models can be used to calculate through transition without a transition model. Standard turbulence models tend to predict transition too far upstream and transition zones which are too short, however. Stephens and Crawford (1990) concluded that current transition and turbulence models are generally poor predictors of transition. Mayle (1991) reached the same conclusion. Schmidt and

Patankar (1991) developed a two-equation transition model using "production term modification." They started with the Lam-Bremhorst (1981), low-Reynolds-number turbulence model and set the production term for turbulence kinetic energy to zero in the upstream part of the flow. When the Abu-Ghannam and Shaw (1980) correlation indicated that transition should begin, the production term was turned on. This model was fairly successful in calculating transition for a number of cases, but it is still empirical in nature. Models can be tuned to predict transition under limited sets of conditions, but they are generally not robust. Given the dependence of designers on transition modeling, a better understanding of transition and better transition models are needed for improved turbine design. This will entail more experimental work to expand the existing data base and advance our understanding of transition.

IMMEDIATE NEEDS

From the above discussion, it is clear that transition experiments should be conducted under high (>5%) FSTI conditions. These must be done under strong acceleration conditions, because extended transition zones at high FSTI are possible only in the presence of some stabilizing effect, such as acceleration. There is also a need to provide better documentation of experimental conditions, particularly free-stream conditions. Turbulence quantities which are useful to modelers, such as the turbulent shear stress and turbulent heat flux should be provided with the experimental results. Volino and Simon (1991) provide a discussion of important modeling terms which can be measured.

OUTLINE OF PRESENT WORK

To address the needs given above, experiments were conducted and are presented as outlined below.

Chapter 2: A discussion of the experimental apparatus and the measurements is presented.

Chapter 3: Further documentation of Kim and Simon's (1991) 0.6% FSTI concave-wall transition case is given. Included are more spectral data and extensive velocity profile data taken within the transition zone.

Chapter 4: Octant analysis of new data and data from the literature is presented to better explain the structure of transitional and turbulent flows. Octant analysis is an extension of quadrant analysis, as presented by Willmarth and Lu (1972).

Chapters 5-7: Results of three accelerating-flow cases done under high FSTI conditions on a concave test wall are discussed. Material in these chapters shows the main focus of the work and represents a logical extension of the studies mentioned above. An extended transition zone was documented in two of the three cases.

Chapter 8: The experimental results are discussed and recommendations are made. Included is a recommendation for a new transition model.

Chapter 9: Conclusions from these data are given.

CHAPTER 2: EXPERIMENTAL FACILITY AND MEASUREMENT TECHNIQUES

WIND TUNNEL

All experiments were performed in the blown-type wind tunnel sketched in Fig. 2.1. The air delivery section, built and described by Wang (1984), consists of a fan, header, heat exchanger, settling chamber and nozzle.

Flow Preparation

The fan used in the early cases considered in this study was a New York Blower model 224, centrifugal blower with a rated capacity of 5500 cfm. It was driven by a 3 phase, 230 V, 10 hp electric motor (Westinghouse model 680B103G37). The motor and fan speed were controlled with a Louis-Allis Lancer Jr., Type VT, 10 hp variable frequency motor controller (model 92245), which was added to the facility by Kim (1990). In the latter cases of this study, a high pressure drop was introduced when strong acceleration and high free-stream turbulence were added to the flow. This moved the fan's operating point onto the unstable region of its operating curve, causing a coherent 20 Hz oscillation which could be heard, felt, and seen in hot-wire anemometer traces. The frequency of oscillation was identified with spectral analysis. The oscillation was intermittent, coming and going in a random fashion, shaking the tunnel for periods of tens of seconds separated by periods of comparable length. The effect of the oscillation on the flow, though unknown, was of concern. Thus, the unstable fan was replaced with two 5 hp, Dayton Blowers (model 3N669) running in parallel. The new fans were designed for higher pressure drops and lower flow rates than was the original fan. The variable-frequency motor controller was used to control the speed of both of the new fans. Replacing the fans eliminated the oscillation. A very low-amplitude, 20 Hz oscillation could occasionally be detected in the flow, but it was apparently not affected by the fans.

Data taken with both the old and new fans under the same operating conditions showed no significant differences (other than the presence of the 20 Hz oscillation), indicating that the 20 Hz oscillation did not have a significant effect on the flow.

Downstream of the fans is a header (see Fig. 2.1) used to redirect the flow and improve its uniformity. Following the header is a heat exchanger used to improve the thermal uniformity of the flow. Water is circulated through the heat exchanger from a 40 gallon storage tank with a 3/4 hp centrifugal pump (Dayton model 98K588). Tap water is added to the storage tank and excess water is discharged to a drain at a low flow rate, to maintain a constant tank temperature. Once steady state is reached at the room temperature, the heat exchanger can maintain the flow temperature uniformity to within 0.1°C, both spatially and temporally. The flow through the tunnel is maintained near room temperature. The tunnel flow can be cooled to approximately 10 degrees below room temperature by increasing the tap water flow rate into the storage tank, but high tap water flow rates result in spatial nonuniformities in the air flow temperature of as high as 0.5°C.

Experiments were run under low and high free-stream turbulence conditions. In the low free-stream turbulence configuration (Fig. 2.1a) two settling chambers and a screen pack are placed downstream of the heat exchanger. These are used to reduce the free-stream turbulence level. Following the settling chambers and screen pack is a 10.7:1 contraction ratio nozzle. The inlet area is 0.914 m $\times$ 0.914 m, and the exit area is 0.685 m $\times$ 0.114 m. The nozzle increases the flow velocity and lowers the free-stream turbulence level. The 6:1 aspect ratio at the nozzle exit insures that secondary flows are minimized and that the end walls do not influence the flow on the centerline of the test wall. In the low-FSTI configuration, the nozzle is followed by the test section. The flow enters the test section with a nominal 0.6% FSTI. In the high free-stream turbulence configuration (Fig. 2.1b), the settling chambers are removed, The screen pack is left in place (mainly as

a spacer and to improve flow uniformity, since it is not needed to reduce the FSTI level), the nozzle is followed by a turbulence generating grid.

Turbulence Generating Grid

The grid used to generate high FSTI was designed and built by Russ (1989). It is described by Kim, Simon and Russ (1992) and is based on the design of O'Brien and vanFossen (1985). A sketch of the grid is shown in Fig. 2.2. It is constructed of 4.2 cm OD PVC pipes and has 60% blockage. The grid was designed for use as a blown jet grid, but, for the present study, it was used only as a passive grid. The grid is follow by a 96.5 cm long rectangular settling section of the nozzle exit dimensions. The flow exiting the settling section enters the test section with a nominal 8% FSTI. The turbulence intensity is approximately independent of the mean flow velocity over the range used in this study. The mean streamwise velocity is uniform to within 3% and the fluctuating component of the streamwise velocity is uniform to within 6% at the exit of the settling section. Russ (1989) indicates that the turbulence leaving the settling section is nearly isotropic.

Test Section

The test section was built by Kim (1990) and is described by Kim and Simon (1991). The test wall is concave, with a constant radius of curvature, R, of 0.97 m. It is 0.686 m high by 1.3 m long. The wall is constructed of several layers, as shown in Fig. 2.3. A 4.76 mm thick Lexan® sheet is covered with a 1.59 mm thick electrical resistance heater. The heater is a foil-type heater covered on both sides with a rubber sheet. Wang (1984) measured the uniformity of the heat flux from an identical heater to be within 1%, although the uniformity of heat flux of the present test wall surface is not so good, as is discussed below. Over the heater is a layer of 0.25 mm-thick, double-sided tape, in which thermocouples are embedded. Over the tape is a 0.8 mm-thick Lexan sheet. Over the Lexan is a liquid crystal sheet used for visualization of wall temperature. The top

surface of the liquid crystal sheet, a smooth mylar sheet, forms the test wall surface. Kim (1990) measured the emmisivity of the liquid crystal to be 0.85. Radiation losses from the test wall are significant and can exceed 20% of the input power from the heater. The radiative heat flux can be calculated and subtracted from the total heat flux to give the convective heat flux at the surface. The back of the test wall is supported with Lexan ribs, and is covered with 10 cm of fiberglass insulation. This limits the back heat loss to 1.5% of the power input to the heater under steady state conditions.

At the leading edge of the test wall is a suction slot, used to bleed off the boundary layer which grows in the settling section. For the low-FSTI, unaccelerated flow, suction was applied with a 2 hp centrifugal Dayton Blower (model 3N085). For the accelerated flow cases, the pressure in the test section was sufficiently high relative to atmospheric pressure that the flow exited the suction slot without the use of the blower. The flow direction around and through the suction slot was checked with a tuft wand (a tuft secured to the end of a thin rod) to insure that flow was properly going into the slot. The core flow in the test section was also checked with the tuft wand, and did not appear to be significantly affected by the suction slot.

The outer wall of the test channel is a flexible, 0.476 cm-thick, Lexan sheet which can be positioned to produce any desired streamwise velocity distribution. For unaccelerated cases, the channel width was held approximately constant at 0.114 m. For the accelerated flow cases, the channel was narrowed in the streamwise direction. Eleven, 2.54 cm-diameter access holes distributed in the streamwise direction along the centerline of the outer wall were used for insertion of probes for velocity and temperature profile measurements. The holes were plugged when not in use. A hole in use was covered with masking tape and the probe was inserted through a small hole in the tape at the center of the access hole. This prevented the escape of air from the pressurized test section. The test wall and outer wall are vertical. They sit on a table, which serves as the bottom end-wall of the test channel. The top end-wall is a 1.27 cm thick Plexiglas®

sheet. For the unaccelerated flow cases, pressure taps in the top wall were used to check the pressure distribution in the channel during positioning of the outer wall. The outer wall was adjusted until the static pressure variation within the channel was within 4% of the dynamic head. For the accelerated-flow cases, a significant total (or stagnation) pressure drop though the test section prevented the use of the pressure taps in setting the velocity distribution in the channel. Instead, the core velocity distribution in the channel was measured with a hot wire as the outer wall was adjusted.

The position in the test section is described with a standard coordinate system. The streamwise coordinate is x, measured from the leading edge of the test wall along the concave surface. The coordinate normal to the test wall is y, measured from y=0 at the test wall surface. The spanwise coordinate is z. The velocity components in the x, y, and z directions are U, V, and W, respectively.

INSTRUMENTATION AND MEASUREMENTS

Mean Temperature

Mean temperatures were measured with Type-E (chromel-constantan) thermocouples. One thermocouple was inserted into the flow through the top end-wall near the entrance of the test section to measure the free-stream temperature, T_∞. A traversing thermocouple probe, constructed by You (1986), following the design of Blackwell and Moffat (1975), was used for temperature profile measurements in the boundary layer. The thermocouple wire in this probe was 0.076 mm in diameter, and the butt-welded junction could be brought into contact with the test wall.

All thermocouples were referenced to an isothermal box, as described by Kim and Simon (1991). The box consisted of two 20.3 cm × 30 cm × 2.54 cm aluminum blocks which were used to sandwich the thermocouple wires. Foam was used to seal the edges of the blocks, and the package was wrapped in fiberglass insulation. The isothermal box was referenced to an ice bath. Two thermocouples led from the isothermal box to the ice

bath. The ice bath thermocouples were placed at different depths in the ice bath. When the ice bath was fresh, the voltages across these thermocouples were equal. As the ice began to melt, and some temperature stratification occurred, and the voltages from the two thermocouples began to differ. This voltage difference was checked periodically during experiments, and when it exceeded 0.003 mV (0.05°C) the ice bath was replaced.

The thermocouples were originally calibrated by You (1986), and the calibration was confirmed by Kim (1990). The free-stream and traversing thermocouple were recalibrated against each other and a mercury-in-glass thermometer at temperatures ranging from 15°C to 30°C. No measurable deviation from You's calibration was found, and the original calibration has been used in this study. This calibration is also in good agreement with reference tables for Type-E thermocouples, provided by Powell et al. (1974). The uncertainty in mean temperature measurements was 3 to 5% of the total wall-to-free-stream temperature difference.

Thermocouple voltages were read with a multimeter (Fluke model 8842). A scanner (Fluke model 2205A) allowed switching, for consecutive readings of the ice bath, traversing, and free-stream thermocouples. The scanner and multimeter were controlled and read with a computer though an IEEE interface bus. For the earliest experiments in this study, a Hewlett Packard model 216 desktop computer was used for experiment control, data acquisition and data processing. Software was written in HP Basic. Some of this software was based on programs provided by Kim (1990). For the latter experiments, including those described in chapters 6 and 7, the HP computer was replaced with a 386 based computer with a Unix (System V) operating system. Software was rewritten for this computer in C language. The 386 computer was connected through a network to a Sun workstation, which was used for most data processing and plotting. Listings of C and FORTRAN programs used for data acquisition and processing are provided in Appendix B.

Profile measurements, probe traversing. The traversing thermocouple probe was positioned with a two-dimensional, automated, motorized traverse. The probe was clamped to a stand mounted on a manual slide (Daedal model CR4419 with 10 μm resolution), which was used for moving the probe in the spanwise direction. The manual slide was mounted on a second slide (Velmex model B2509Q1J) equipped with a stepper motor (Slo-Syn model MO63-LF-401). The motorized slide was used for traversing normal to the test wall with a minimum step size of 0.005 mm. The stepper motor was controlled with a driver (Superior Electric model PDM155) and controller (Superior Electric chassis SCA311, controller card IOD010, and indexer card IDD008). The controller could be operated manually for initial positioning of the probe, or with a computer for profile measurements. Remote control from the computer was accomplished through the IEEE interface bus.

Temperature was measured at approximately 50 y-positions in each temperature profile. Points were concentrated near the wall, where temperature gradients are highest. Logic written into the data acquisition program controlled the traverse to maintain approximately constant-ΔT steps between points in the profile. This was accomplished using the y-distance and temperature difference between two adjacent measurement points to extrapolate to the position of the next point in the profile. At each point in the profile, 5 thermocouple readings were taken over a 5 second period and then averaged. The probe measures the recovery temperature. Recovery temperatures were converted to static temperatures using data from the velocity profile measurements, described below, and the equation:

$$T_{static} = T_{rec} - \frac{r\overline{U}^2}{2c_p} \tag{2.1}$$

where c_p is the specific heat of air, and r is the recovery factor, taken to be 0.88 (Kays and Crawford, 1993).

Wall temperature. The wall temperature, T_w, was found by extrapolation of the near-wall temperature profile data, taken with the traversing probe, to the wall surface at y=0. This technique requires accurate knowledge of the probe position relative to the wall. The position is found by springing the thermocouple wire against the test wall, then backing the probe away from the wall in 5 μm increments. While the wire remains on the wall, its temperature remains nearly constant, but when it leaves the wall, its temperature drops noticeably. The y-position where the wire leaves the wall is taken to be one thermocouple-wire radius (0.038 mm) from the wall surface. The uncertainty of the y-position is 0.02 mm. For a typical wall heat flux of 200 W/m^2, this uncertainty in y results in 0.15°C uncertainty in T_w. This is approximately 3% of the total wall to free-stream temperature difference. Further documentation of the technique used to find local wall temperatures and local wall heat flux values is available in Qiu et al. (1995).

In previous studies in this facility, wall temperature was measured using thermocouples embedded in the test wall. The temperature at the thermocouple was measured and extrapolated to the wall surface using the wall heat flux and the thermal resistance of the material between the thermocouple and the surface. The thermal resistance of the test wall was determined in independent tests using small samples of wall composed of the same materials as those of the test wall. Kim (1990) and Kestoras (1993) describe these tests. The temperature correction from the thermocouple to the wall surface was sizable, since the wall was constructed of relatively low-conductivity materials, a compromise made so that the wall could be bent. The measured thermal resistance varied from 8.5×10^{-3} °Cm^2/W as found by Kim, to 6.5×10^{-3} °Cm^2/W as found by Kestoras, to 9.0×10^{-3} °Cm^2/W as found by the present authors. Also, the present authors found a spatial variability over the range $7.5\text{-}10\times10^{-3}$ °Cm^2/W. Because of this variability in wall resistance, which appears to have an uncertainty of about 25% (leading to a contribution to uncertainty in Stanton number of about 7%), the embedded thermocouples were not used. Stanton numbers were evaluated with the temperature

probe measurements. A complete discussion of the expected shapes of mean temperature profiles is given in Appendix A.

Wall heat flux. The local convective wall heat flux, q, was determined from the slope of the near-wall temperature profiles. The uncertainty in q is 5%. Convective heat fluxes obtained using the power to the test wall heater with corrections for radiation losses from the surface agreed with values computed from the temperature profiles, to within 12%. Some of this variability is considered to be due to slight spatial variability in the thermal resistance of the test wall. Variations in the color of the liquid crystal on the test wall support the suggestion of slight nonuniformity of the wall heat flux. The present technique of determining the heat flux from the profile measurements accounts for these variations. In earlier studies done in this facility (Kim and Simon, 1991 and Kestoras, 1993) the uniformity of the test wall was believed to be better, based on the uniformity of the liquid crystal color and the better match between the average heat flux and the local heat fluxes determined from near wall temperature profiles. Some deterioration of the surface had apparently occurred over time. The present technique is not influenced significantly by this apparent deterioration.

Mean and Fluctuating Velocity

Mean and fluctuating velocities were measured using a four-channel, hot-wire anemometer (TSI model IFA-100). Each channel was equipped with a signal conditioner (TSI model 157), which was used for amplification and filtering of the anemometer output. A 5000 Hz cutoff frequency, low-pass filter was used on most signals. This eliminated most high frequency noise, but the cutoff frequency was above the expected frequencies of most turbulent fluctuations of interest in the flow. This is demonstrated below with spectral measurements, for which the filter was set to a higher frequency. The offset and gain of the signal conditioner were set to improve the resolution with which voltage fluctuations could be digitized.

Hot wire calibration. Hot wires are best calibrated in-situ; but, because of the complex nature of the flows under study (curvature, acceleration, and high-turbulence effects, all simultaneously present), this was not possible. Instead, hot wires were calibrated in a laminar jet device described by Wilson (1970). Air was supplied to the device from the building air supply. Air exited as a laminar jet though a contoured nozzle. The jet velocity was set using a pressure regulator at the inlet. The pressure drop through the nozzle was measured using a variable-reluctance type pressure transducer (Validyne model DP45) with a carrier demodulator (Validyne model CD15). The transducer has a pressure range of 0 to 8.9 cm H_2O. Its accuracy is given by the manufacturer as 0.5% of full scale over the full range. The pressure transducer was calibrated against a micro-manometer. The calibration was linear and very stable, unchanging to three significant digits over a three year period. The jet velocity was calculated using the Bernoulli equation, the measured pressure drop, and the dimensions of the nozzle.

The probe was placed in the center of the jet and aligned by eye. Since the probe would later be aligned by eye for use in the wind tunnel, efforts to improve the accuracy of the alignment in the jet would not have improved the overall accuracy of subsequent measurements. The "eyeball alignment" was accurate to within ±1°. This introduces almost no uncertainty into the single-wire velocity measurements described below, but does contribute to the uncertainty in velocities measured with a cross-wire probe, also described below. The error introduced in $\overline{U}$ by a 1° misalignment is negligible, and the errors introduced into the turbulence quantities $\overline{u'}$, $\overline{v'}$, and $\overline{u'v'}$ are less than 0.5%. The error introduced in $\overline{V}$ is approximately 2% of the local $\overline{U}$. All of these contributions to the uncertainty are small compared to the total uncertainty in the various quantities. Probe alignment, therefore, is not a matter of concern.

Calibrations were conducted over the velocity range of interest, typically from about 2 m/s to 20 or 30 m/s. Anemometer voltage and pressure data were collected over

a 40 second period at each velocity in the calibration and then time averaged. The calibration is dependent on the jet temperature. To eliminate this dependence, all calibrations were normalized to 25°C by multiplying all anemometer voltages by the correction factor $\left(\frac{225}{250-T}\right)^{1/2}$. The wire temperature is 250°C, and T is the jet temperature in °C as measured with a thermometer. The same correction was used during measurements, with T in the measurements corresponding to the local flow temperature. The time averaged velocities and temperature-normalized anemometer voltages were least-squares curve fit to determine the constants A and B in a King's law (1914a, 1914b, 1915) type calibration:

$$\overline{U} = \left(A + B\overline{E}^2\right)^{1/0.435} \tag{2.2}$$

E is the hot wire voltage.

Single-wire profiles. For streamwise velocity measurements, a single-wire, boundary layer type probe (TSI model 1218-T1.5) was used. This probe has a 3.81 μm diameter tungsten wire with a active length to diameter ratio, l/d, of 320. The active length of the wire is approximately 2/3 of the total length. The ends are platinum plated. The wire is run in the constant-temperature mode at 250°C. All velocity measurements made with this probe and the cross-wire probe, described below, were done in isothermal flow. Kim et al. (1994) showed that at FSTI>1.5%, wall heating at the levels considered in this study does not affect transition. The single-wire probe was used for measurements very near the wall. The probe could be brought in contact with the test wall without breaking the hot wire. Profile measurements were made with a procedure similar to that described above for the mean temperature profiles. The probe was manually brought in contact with and sprung against the test wall. The stepper motor was then used to back the probe away from the wall in 0.005 mm increments. The voltage from the anemometer changed slowly while the hot wire was against the wall, but rose

significantly at the point where the wire lifted off of the wall. The magnitude of this rise depended on the flow velocity. The point where the probe lifted off of the wall was taken as y=0. Data were taken at approximately 50 y-positions for each velocity profile. In most cases, the raw voltage data from the digitizers were stored and processed at a later time. As with the mean temperature profiles, data points were concentrated near the wall, and the probe was traversed to maintain an approximately constant $\Delta\overline{U}$ between points. For time-average profile measurements, data were acquired at a 100 Hz sampling rate for 40 s at each measurement point. The uncertainty in the mean streamwise velocity, $\overline{U}$, is 3 to 5%. The uncertainty in the rms fluctuating component, $\overline{u'}$, is 5%.

Near wall correction. Velocities at points very near the wall (y less than approximately 0.1 mm) were affected by conduction between the hot wire and the wall. This effect causes falsely high velocity readings. An empirical scheme proposed by Wills (1962) was used to correct the near-wall velocities. Wills developed his correction in laminar flow and proposed that half of the correction be used in turbulent boundary layers. It was found in this study that 84% of the laminar correction worked best in correcting near-wall data obtained by Kim (1990) in a simple, unaccelerated, fully-turbulent boundary layer on a flat plate. The data from this flow, when plotted in wall coordinates, should follow the standard law of the wall. This makes it possible to calibrate the correction in the near-wall region. Eighty-four percent of Wills' correction has been used throughout this study. The scheme used in the correction is outlined below:

$$U_{corrected} = 0.84U_{Wills} + 0.16U_{uncorrected} \tag{2.3}$$

where

$$U_{Wills} = \left(U^{0.45}_{uncorrected} - \left(\frac{\nu}{2a}\right)^{0.45} k_w \right)^{1/0.45} \tag{2.4}$$

$$k_w = \begin{cases} 4.53b^{-1.0278} & \text{when } b < 40 \\ 76.524b^{-1.7893} & \text{when } b \geq 40 \end{cases} \tag{2.5}$$

and

$$b = \frac{y}{a}. \tag{2.6}$$

The correction goes to zero for large y. The kinematic viscosity, ν, is evaluated at the film temperature between the hot-wire and the free-stream. The constant, a, is the hot-wire radius. For the present study, $a=1.905\times10^{-4}$ cm, and $\left(\frac{\nu}{2a}\right)^{0.45}=2.423$.

Digitizers. Data were acquired using two, 12-bit-resolution digital oscilloscopes (Norland Prowler) with variable voltage ranges from ±100 mV to ±20 V. The voltage range was minimized for each experiment to improve the resolution of the measurements. Sampling rate could be adjusted from 1 Hz to 100 kHz. Each oscilloscope has two channels, and each channel has a 4096 point data buffer. By linking the two oscilloscopes in a master-slave configuration, four channels of simultaneous data could be acquired. Data were transferred from the digitizers to the controlling computer through the IEEE bus in binary form, and converted to decimal form in post processing. The routine used for this processing was originally written by Kim (1990), modified by Kestoras (1993), and further modified in the present study when the routine was translated from HP Basic to C. The routine is included in several of the programs in Appendix B.

Cross-wire profiles. Mean and fluctuating velocities in the streamwise and normal directions were measured using a boundary layer type cross-wire probe (TSI model 1243-T1.5). The same 3.81 μm diameter tungsten wires are used with this probe as with the single-wire probe described above. The wires are perpendicular to each other and are inclined at 45° to the main flow. The wires are spaced 1 mm apart in the spanwise direction. The wires of the cross-wire probe were calibrated in the calibration device described above, with the wires inclined at 45° to the jet (the same position as is used in

measurements). The effective wire cooling velocity, $U_{eff} = U\cos(45°)$, is used in the calibration in place of the jet velocity, U. For measurements of normal velocity fluctuations, v', and turbulent shear stress, $u'v'$, a correction proposed by Champagne et al. (1967a, 1967b) was used to account for the effects of cooling by the velocity component tangential to the hot wires. The corrections are as follows:

$$v'_{corrected} = cfv \times v'_{measured} \qquad \text{and} \qquad u'v'_{corrected} = cfuv \times u'v'_{measured} \tag{2.7}$$

where

$$cfv = \frac{1+k_t^2}{1-3k_t^2+4k_t^4} \qquad \text{and} \qquad cfuv = \frac{1+k_t^2}{1-k_t^2} \tag{2.8}$$

and

$$k_t = -5\times10^{-4}\frac{l}{d} + 0.3 \tag{2.9}$$

where l/d is the length-to-diameter ratio of the hot wires.

The center of the cross-wires can be placed within 0.6 mm of the test wall, but, due to spatial resolution problems, reasonable data can be taken only for y greater than approximately 1 mm. The closest y position at which the data could be trusted was determined by comparing $\overline{u'}$ measured with the single-wire probe and with the cross-wire probe. At y greater than approximately 1 mm, the two measurements agreed. Closer to the wall, $\overline{u'}$ measured with the cross-wire was significantly lower than the value measured with the single-wire. Care must be exercised when the cross-wire probe is brought near the wall. Unlike the single-wire described above, the cross-wires will break if the probe touches the test wall. For profile measurements, the probe was traversed through the same positions as in the corresponding single-wire profile for y>0.6 mm. Also like the single-wire profile, data were acquired at a 100 Hz sampling rate for 40 s at each measurement point.

The uncertainty in the mean normal velocity, $\overline{V}$, is 3 to 5% of $\overline{U}$. The uncertainty in the normal rms fluctuating component, $\overline{v'}$, is 10%. The uncertainty in the

turbulent shear stress, $\overline{u'v'}$, is also 10%. The uncertainty in the triple correlation, $\overline{u'v'^2}$, which represents the transport of shear stress normal to the wall, is 15%.

Simultaneous Velocity and Temperature - Turbulent Heat Flux

A three wire, boundary layer type probe (TSI model 1295AM-T1.0) was used to simultaneously measure the instantaneous U and V components of velocity and the instantaneous temperature, T. The probe is described in detail by Kim and Simon (1991) and is sketched in Fig. 2.4. Two of the wires of the probe are arranged in a standard cross-wire arrangement and are used for measuring velocity. These wires are 2.54 μm diameter tungsten wires with l/d=200. They are run in constant-temperature mode at 250°C. The third wire is an uncoated, 1.27 μm-diameter platinum wire, run as a cold wire. This wire is parallel and adjacent to one of the hot-wires. The spacing between adjacent wires is 0.35 mm. The overall distance between the outside hot wire and the cold wire, then, is 0.7 mm. The cold wire is run in constant-current mode as a resistance thermometer with a 1 mA current. The heating of the cold wire by the 1 mA current is insignificant, which implies that apparent t' temperature fluctuations caused by u' velocity fluctuations are also insignificant. This was checked by running the cold wire with a 0.25 mA current and comparing results to those obtained with the 1 mA current. Changes in mean T and t' were negligible.

Cold wire frequency compensation. The circuit used to drive the cold wire was designed and built by the Analog Circuit company of Minneapolis. The circuit outputs the voltage across the cold wire, amplified by a factor of 25. The circuit also supplies the instantaneous time derivative of the amplified cold wire signal. The derivative was used for frequency compensation. Kim and Simon (1991) determined that frequency compensation was needed to improve the response of the cold wire. They introduced a scheme similar to one used by Hishida and Nagano (1978), which they found improved

the frequency response to 4 kHz. The voltage from the cold wire is compensated as follows:

$$V_c = \frac{\frac{k_{cc}}{V_2^2} V_{21} \frac{dV_1}{dt} + V_1}{1 + \varepsilon \frac{k_{cc}}{V_2^2} \frac{dV_1}{dt}} \tag{2.10}$$

where V_c = compensated voltage from the cold wire

V_1 = measured voltage across the cold wire

V_2 = voltage across one of the hot wires

V_{21} = (cold wire current) × (hot wire resistance)

ε = ratio of the hot and cold wire resistances at 0°C

k_{cc} = empirical constant determined from a frequency response test

The constant k_{cc} is determined empirically. The probe is placed in the isothermal calibration jet, and a 6 mA current is supplied to the cold wire. This current causes a slight heating of the wire. A switch is then thrown, dropping the supply current to 1 mA. The wire then cools. The voltage across the cold wire and one hot wire, V_1 and V_2 respectively, are digitized at a 100 kHz sampling rate during this process. The cold wire voltage drops sharply when the switch is thrown to drop the current, then continues to drop more slowly as the wire cools, approaching a steady state value asymptotically. This is depicted in Fig. 2.5. If the cold wire had infinite frequency response, its voltage would drop immediately to the final, 1 mA current, steady state value. The constant k_{cc} is set so that the compensated voltage, V_c, approaches this infinite-frequency-response step change. During actual measurements of temperature fluctuations, the time derivative of the cold wire voltage, $\frac{dV_1}{dt}$, is provided by the analog circuit supplying the constant current to the wire. When the switch is thrown in the calibration test, however, $\frac{dV_1}{dt}$

becomes momentarily very large, and the circuit used to find the derivative saturates. This makes direct measurement of this derivative impossible during calibration. For calibrations, the derivative was calculated numerically from the V_1 trace. Some researchers, such as Sohn and Reshotko (1991), calculate the derivative numerically at all times when the actual data are taken. This requires a high sampling rate, which was not practical in the present study (except during calibration) because of the limited size (4096 points) of the digitizer buffers.

Data for profile measurements were digitized at a 100 Hz sampling rate for 40 s at each measurement point. Measurements could be taken as close to the test wall as 0.5 mm, but as with the cross-wire described above, data taken at $y<1$ mm were discarded due to spatial resolution problems. The probe was traversed to the same y positions at which data were acquired with the thermocouple probe described above. The two hot wire signals, cold wire signal, and cold wire derivative signal were digitized with the four available oscilloscope channels. Using the procedure of Kim (1990), the hot and cold wire signals were low-pass filtered at 5 kHz, and the cold wire derivative was filtered at 3 kHz. The filters on the TSI 157 signal conditioners mentioned above were used. Filtering of the cold wire signal was found to have no noticeable effect on the signal, since the uncompensated response of the cold wire is well below 5 kHz and electronic noise was apparently small. In some of the latter tests, this filter was not used. Signal conditioners were used to offset and amplify the hot and cold wire signals, improving the accuracy with which the signals could be digitized. The TSI signal conditioners and a signal conditioner built by Analog Circuit were used.

In addition to the quantities mentioned above with reference to the cross-wire, the fluctuating temperature, $\overline{t'}$, the normal component of the turbulent heat flux, $\overline{v't'}$, the streamwise component of the turbulent heat flux, $\overline{u't'}$, and the turbulent transport of the normal component of the turbulent heat flux, $\overline{v'^2t'}$, were measured. The Champagne et al. (1967a, 1967b) correction mentioned above with reference to $\overline{u'v'}$ (Eqn. 2.8) was also

applied to the turbulent heat flux, $\overline{v't'}$. The uncertainties in the measurements are 5% in $\overline{t'}$, 15% in $\overline{v't'}$, 10% in $\overline{u't'}$, and 20% in $\overline{v'^2t'}$. Because the raw data from the digitizers were stored, other quantities in addition to those listed above could also be determined.

Intermittency

In transitional flow, the flow can be divided into turbulent and non-turbulent zones. Figure 2.6 shows typical time traces of streamwise velocity from low and high FSTI flows. In the low FSTI flow (Fig. 2.6a), the non-turbulent part of the flow appears very laminar-like. In the high FSTI flow (Fig. 2.6b), the non-turbulent zone is characterized by large amplitude fluctuations. This zone is not laminar-like, but the fluctuations are of relatively low frequency and the non-turbulent fluctuations are distinctly different than the high frequency fluctuations in the turbulent zone. In both the low and high FSTI cases, the intermittency, γ, can be defined at any position as the fraction of time that the flow is turbulent. The intermittency was determined with an analog circuit described by Kim et al. (1994) and Kim and Simon (1991). This circuit was based on the design of Kim, Kline and Johnston (1978). The circuit takes the voltage across a hot or cold wire as an input, and determines the first and second time derivative of the input signal. The derivatives are then rectified. If either or both of the derivatives exceed an adjustable threshold level, the circuit declares the flow turbulent and outputs a +3.9 V signal. If both derivatives fall below their thresholds, the circuit declares the flow non-turbulent and outputs a 0.1 V signal. Both the first and second derivatives are used to determine the intermittency in order to eliminate drop outs when one or the other of the derivatives crosses zero. For example, if the first derivative is fluctuating between large positive and negative values in a turbulent flow, it must pass through zero. If the intermittency function were based only on the first derivative, the flow would be declared non-turbulent during these zero crossings. The second derivative will be large if the first derivative is rapidly changing signs, and will not be zero during the first derivative zero

crossings. Using both first and second derivatives for the intermittency function helps to minimize drop-outs in turbulent flow. When the intermittency circuit is used in conjunction with the single hot-wire or one of the wires of the cross-wire probe, the intermittency signal is digitized with a separate channel on one of the digital oscilloscopes. When the circuit is used in conjunction with the triple-wire probe, the voltage across the cold wire is used as the input to the intermittency circuit, and the intermittency function is added to the time derivative of the cold wire signal with a second analog circuit. This combined signal is then digitized with one of the oscilloscopes. Adding the signals in this way was necessary, since only four digitizer channels were available. The cold wire derivative signal is small compared to the 3.9 V intermittency signal, allowing digital separation of these two signals in post processing. The response of the intermittency circuit is generally fast, but some of the op-amps in the circuit can not keep up with the most rapid change between turbulent and non-turbulent flow. This results in an occasional output from the circuit between the 0.1 V non-turbulent and 3.9 V turbulent values. Up to 2% of the points in a digitized signal may fall into this category. These points are discarded before γ is calculated.

The threshold values for the derivatives used in determining the intermittency must be set for each flow. This is done by observing the input and output of the intermittency circuit on the screen of an oscilloscope and adjusting the threshold levels until the circuit appears to be giving the "correct" intermittency. This "tuning" of the circuit is fairly straightforward in low-FSTI flows, where the distinction between laminar and turbulent flow is clear. The tuning is more difficult in high FSTI flows where the distinction between turbulent and non-turbulent flows is less clear. This can be seen in Fig. 2.6b. The derivatives in the non-turbulent portion of the flow are occasionally high. If the circuit is adjusted to declare these high derivative zones as non-turbulent, then parts of the turbulent zone will also be falsely declared non-turbulent. Alternatively, if the circuit is adjusted so that all of the turbulent zone is declared turbulent, then parts of the

non-turbulent zone will be declared turbulent. Some compromise must be made and this makes the tuning of the circuit somewhat subjective. This is to be expected, and is to some extent unavoidable since the distinction between the two zones of the flow is somewhat blurred. The uncertainty in the intermittency is high in the high-FSTI flows. This prevented conditional sampling based on intermittency in this study. Uncertainty in the intermittency values approached 50% in the early part of transition and decreased to 20% by the end of transition. Despite the high uncertainty, the intermittency function is still useful. Once the circuit is tuned, all intermittencies are determined with respect to a common reference. While the absolute values have a high uncertainty, the trends in γ with position are more reliable. The intermittency determined from hot and cold wire signals are different. The hot-wire based intermittency tends to be a good indicator of whether the flow is turbulent or non-turbulent within the boundary layer, while the cold wire based intermittency is better for separating boundary layer flow from free-stream flow in the wake region of the boundary layer. Keller and Wang (1995) discuss the use of various criteria for determining the intermittency.

DATA PROCESSING

Skin Friction and Stanton Number

In addition to the quantities listed above, several more quantities were calculated based on the data described above. Uncertainties for these processed quantities were determined using a standard propagation of errors as presented by Kline and McClintock (1953). Skin friction coefficients, C_f, were determined from the mean streamwise velocity profiles by a profile fitting technique. In unaccelerated turbulent flow, the profile data are fit to the standard turbulent law of the wall using the "Clauser" (1956) fitting technique. In accelerated flow, the law of the wall is not applicable, and the technique developed and presented in Appendix A is used. This technique is also documented in condensed form in Volino and Simon (1994a). The uncertainty in C_f is 7

to 8%. Local Stanton numbers (dimensionless heat transfer coefficients), St, were determined directly from the wall heat flux and the wall and free-stream temperatures. The uncertainty in St is 7 to 8%.

Turbulent Prandtl Number

The turbulent Prandtl number, Pr_t, is calculated from the measured turbulent shear stress and turbulent heat flux. The turbulent Prandtl number is defined as:

$$Pr_t = \frac{\overline{u'v'} \Big/ \frac{\partial \overline{U}}{\partial y}}{\overline{v't'} \Big/ \frac{\partial \overline{T}}{\partial y}} = \frac{\varepsilon_M}{\varepsilon_H} \tag{2.11}$$

ε_M is the eddy viscosity, and ε_H is the eddy diffusivity of heat. The mean velocity and temperature gradients, $\frac{\partial \overline{U}}{\partial y}$ and $\frac{\partial \overline{T}}{\partial y}$, were found at each point in a profile by curve fitting 5 points (the point in question and two points to either side) with a cubic polynomial and calculating the derivative of this polynomial. Kim and Simon (1991) estimated that the uncertainties in the derivatives $\frac{\partial \overline{U}}{\partial y}$ and $\frac{\partial \overline{T}}{\partial y}$ range from 12% near the wall where the derivatives are large to 53% in the outer part of the boundary layer where the derivatives are small. These estimates are accepted here. The uncertainties in ε_M range from 16% near the wall to 54% in the outer part of the boundary layer. The uncertainties in ε_H range from 19% to 55%. The uncertainties in Pr_t ranges from 25% to 77%. Obviously, Pr_t measurements are only valuable fairly close to the wall. The data presented in the following chapters support this. The uncertainties, even near the wall, are large, but they are typical of direct turbulent Prandtl number measurements. The mixing lengths of momentum and heat are defined as:

$$\ell_M = \left(-\overline{u'v'}\right)^{1/2} \Big/ \frac{\partial \overline{U}}{\partial y} \qquad \text{and} \qquad \ell_H = \left(\overline{v't'}\right)^{1/2} \Big/ \frac{\partial \overline{T}}{\partial y} \tag{2.12}$$

The uncertainties in ℓ_M range from 13% to 53%, and in ℓ_H range from 16% to 54% (the former values relate to the near-wall and log regions of the profiles).

Free-Stream Velocity

The free-stream velocity is not uniform in curved channels, nor does it follow a potential flow solution when FSTI levels are high. The curvature and high FSTI cause cross transport of momentum, as described by Eckert (1987). Although this prevents the core velocity distribution from following a potential flow or free-vortex solution, the velocity profile in the core of the channel is, to a close approximation, linear. Using the technique of Kestoras and Simon (1993), a line, $U_C(y)$, fit to the core velocity measurements, is extrapolated to the test wall to give the reference velocity U_{CW}. The boundary layer thickness, $\delta_{99.5}$, is taken as the point where the data, U(y), and the line $0.995U_C(y)$ cross. The reference velocity, U_{CW}, is used for normalization in the same way as the free-stream velocity, U_∞, is used on flat-plate boundary layers. The value of U_{CW} is fairly insensitive to the fitting of the core velocities and has an uncertainty of 3-5%. The boundary layer thickness, $\delta_{99.5}$, in contrast, is quite sensitive to the choice of which points are fit and has an uncertainty of 20%.

Boundary Layer Thickness

Integral quantities such as the displacement thickness, δ^*, the momentum thickness, θ, and the enthalpy thickness, Δ_2, were calculated as follows from the mean velocity and temperature profiles:

$$\delta^* = \frac{-U_{cw} + \left(U_{cw}^2 + 2\frac{\partial U_c}{\partial y}\int_0^{\delta_{99.5}} \left(U_c - \overline{U}(y)\right)dy \right)^{1/2}}{\frac{\partial U_c}{\partial y}} \qquad (2.13)$$

$$\theta = R\left(1 - \frac{1}{1 + \frac{1}{RU_{cw}^2}\int_0^{\delta_{99.5}}\left[\overline{U}(y)\left(U_c - \overline{U}(y)\right)\right]dy}\right) \tag{2.14}$$

$$\Delta_2 = \frac{-U_{cw} + \left(U_{cw}^2 + \frac{2}{(T_w - T_\infty)}\frac{\partial U_c}{\partial y}\int_0^{\delta_{99.5}}\left[\overline{U}(y)\left(\overline{T}(y) - T_\infty\right)\right]dy\right)^{1/2}}{\frac{\partial U_c}{\partial y}} \tag{2.15}$$

These definitions were taken from Kestoras (1993). Constant fluid properties have been assumed, a good assumption since the wall to free-stream temperature difference was only about 5°C in the experiments. Stagnation temperatures, as opposed to static temperatures, are used in the enthalpy thickness calculation. The definitions take curvature effects into account, but when the strength of curvature is weak, as it was in the present study, these definitions are essentially equivalent to the standard definitions for boundary layers on flat plates. The uncertainties in these boundary layer thicknesses are about 10%. The momentum and enthalpy thicknesses are used in place of $\delta_{99.5}$ for data reduction because of their lower uncertainty. The uncertainty in the shape factor, $H = \frac{\delta^*}{\theta}$, would be 14% by a standard propagation of errors, but it is likely that errors in δ^* and θ will be related, making the uncertainty in H smaller. The uncertainty in H is taken to be 10%.

Octant Analysis

Octant analysis, described in detail in Chapter 4, was done on the data obtained with the triple-wire probe. Octant analysis is an extension of quadrant analysis, which was introduced by researchers such as Willmarth and Lu (1972).

Spectral Analysis and Transfer Functions

Spectral analysis was done on the fluctuating velocities in the free-stream and boundary layer. Data were acquired using the single-wire and cross-wire probes described above. Single-wire data for $\overline{u'^2}$ spectra were acquired in the viscous sublayer at $y^+ \approx 5$, near the position of maximum turbulence intensity ($y^+ \approx 17$), and in the free-stream. Because the cross-wire probe could not be positioned close to the wall, data for $\overline{u'^2}$, $\overline{v'^2}$, and $-\overline{u'v'}$ spectra were acquired at y^+ between 50 and 100 and in the free-stream. Free-stream $\overline{w'^2}$ spectra were acquired in a few cases by inserting the cross-wire probe through the top wall of the wind tunnel. In this configuration, the probe measured the U and W components of velocity.

For each spectrum, data were acquired in four sections at sampling rates of 100 Hz, 1 kHz, 10 kHz and 100 kHz. The data were low-pass filtered at 1/10th the sampling rate (10 Hz, 100 Hz, 1 kHz and 10 kHz for the four sections, respectively). Twenty sets of 4096 data points were acquired for each of the four sections. A Fast Fourier Transform (FFT) was performed on each set of 4096 points to compute the power spectral density (PSD). Routines for performing the FFT and calculating the PSD were taken from Press et al. (1988). After the 20 PSD from each section of the spectrum were averaged for smoothing, the sections were pieced together to form the full spectrum. The data obtained with the 100 Hz sampling rate were used to provide the section of the spectrum from 0 to 5 Hz, the 1 kHz sampled data provided the section from 5 to 50 Hz, the 10 kHz sampled data provided the section from 50 to 500 Hz, and the 100 kHz sampled data provided the final section of the spectrum from 500 to 5000 Hz. Acquiring the spectra in sections allowed better resolution of the lower frequencies. For most of the high-FSTI work, the 100 Hz sampled data were not acquired, after it was recognized that very little energy resided in the 0 to 5 Hz band. For these spectra, the 1-kHz-sampled data provided the 0 to 50 Hz section of the spectrum. The choices of sampling rates, filters, sample size, etc. were primarily functions of the equipment used in the

measurements (e.g. a digitizer with 4096-point buffer) and the flow in question. Under different conditions, other choices might be more appropriate. Once the full spectrum had been pieced together, further smoothing was done through curve fitting. At each frequency in the spectrum, 60 points (30 to each side of the point in question) were curve fit with a power law. The value at each frequency was presented as the value of the curve fit at that frequency. The spectra were always checked for spikes before smoothing to insure that no important information was lost in the smoothing process. Figure 2.7 shows a typical power spectrum before and after the curve-fit smoothing. In Fig. 2.7a the PSD is plotted versus frequency in log coordinates. In Fig. 2.7b the PSD is multiplied by the frequency and plotted on a linear axis versus frequency on a log axis. In the coordinates of Fig. 2.7b, the area under the curve in any frequency band is proportional to the energy in that frequency band. The spectra are plotted in dimensional coordinates for lack of a clear choice of nondimensionalizing parameter. A discussion of possible choices for nondimensionalization of the spectra is presented in Chapter 7.

The uncertainty in the time-averaged quantities $\overline{u'^2}$, $\overline{v'^2}$, and $-\overline{u'v'}$ are 5%, 10%, and 10%, respectively, as noted above. Local (frequency) uncertainty values in the smoothed spectra are the same as the respective time-averaged values.

Integral length scales. Integral length scales were determined from spectral measurements using the following formulas, which are based on formulas presented by Hinze (1975):

$$\Lambda_{u'} = \frac{\overline{U}\,\overline{\frac{u'^2(f=0,df)}{df}}}{4\overline{u'^2}}, \quad \Lambda_{v'} = \frac{\overline{U}\,\overline{\frac{v'^2(f=0,df)}{df}}}{4\overline{v'^2}}, \quad \Lambda_{w'} = \frac{\overline{U}\,\overline{\frac{w'^2(f=0,df)}{df}}}{4\overline{w'^2}} \qquad (2.16)$$

where $\overline{\frac{u'^2(f=0,df)}{df}}$, $\overline{\frac{v'^2(f=0,df)}{df}}$ and $\overline{\frac{w'^2(f=0,df)}{df}}$ are the values of the PSD of $\overline{u'^2}$, $\overline{v'^2}$ and $\overline{w'^2}$ at zero frequency. These values are found graphically by extrapolating a

spectrum, plotted in log-log coordinates (such as the spectrum plotted in Fig. 2.7a), to f=0. The uncertainties in the integral length scales are 30%. Integral length scales can also be computed from autocorrelations of fluctuating velocities. Kim and Simon (1991) used autocorrelations to find integral length scales. In the present study, autocorrelations were computed for a few cases and integral scales were determined from both the autocorrelations and the spectra. The scales computed by the two techniques matched.

Transfer functions. Some spectral results are presented in terms of "transfer functions". The transfer function is used to examine the relationship between fluctuations in the boundary layer and in the free-stream. The transfer function, commonly used in controls or vibration analyses, is a ratio of an output function PSD to an input function PSD. The ratio is taken at each represented frequency over the full range of frequencies in the signals. In this study, a transfer function is calculated by dividing the PSD from the boundary layer (considered to be the output or dependent function) by the PSD of the free-stream (considered to be the input or independent function) at each frequency over the full range of frequencies represented. The boundary layer can be considered to be the system. When a system has a single input and a single output, the transfer function gives a clear indication of which frequencies in the input are amplified by the system and, thus, are present in the output signal. The relationship between the free-stream and boundary layer turbulence spectra is not so simple. Certainly, the free-stream turbulent kinetic energy has an influence on the boundary layer, but boundary layer turbulence is also generated by other mechanisms, such as near-wall bursting during which mean-flow kinetic energy in the external flow is converted to turbulence energy in the boundary layer. The transfer function can show evidence of free-stream influences on the boundary layer. Also, energy in the boundary layer spectra which is not visible in the free-stream indicates a direct origin from sources other than the free-stream. The transfer function between the spectra of the turbulent shear stress, $-\overline{u'v'}$, and the turbulent kinetic energy, $\overline{u'^2}$, tells how turbulent transport is related to the overall fluctuation level in the

boundary layer. The uncertainties in the transfer functions, taken as the combined error in the two spectra used to compute them, range from ~10% for transfer functions involving only $\overline{u'^2}$ spectra, to 15% for transfer functions involving $\overline{v'^2}$ and $-\overline{u'v'}$ spectra. More on the transfer function is available in Volino and Simon (1994b).

Two Point Correlations

Two point correlation measurements of streamwise velocity were made in the free-stream using two single-wire probes. The boundary layer type single-wire probe describe above and a straight single-wire probe (TSI model 1210-T1.5) were placed in the flow with the two wires nearly touching, as shown in Fig. 2.8. The probes were then separated, and data were simultaneously taken from both probes for various separation distances. The correlation, $\overline{u_1'u_2'}$ was then determined as a function of the separation distance (u_1' and u_2' are the fluctuating components recorded by the two probes). Separations in the y and z directions were considered. For z separation, the probes were inserted through the top wall of the wind tunnel.

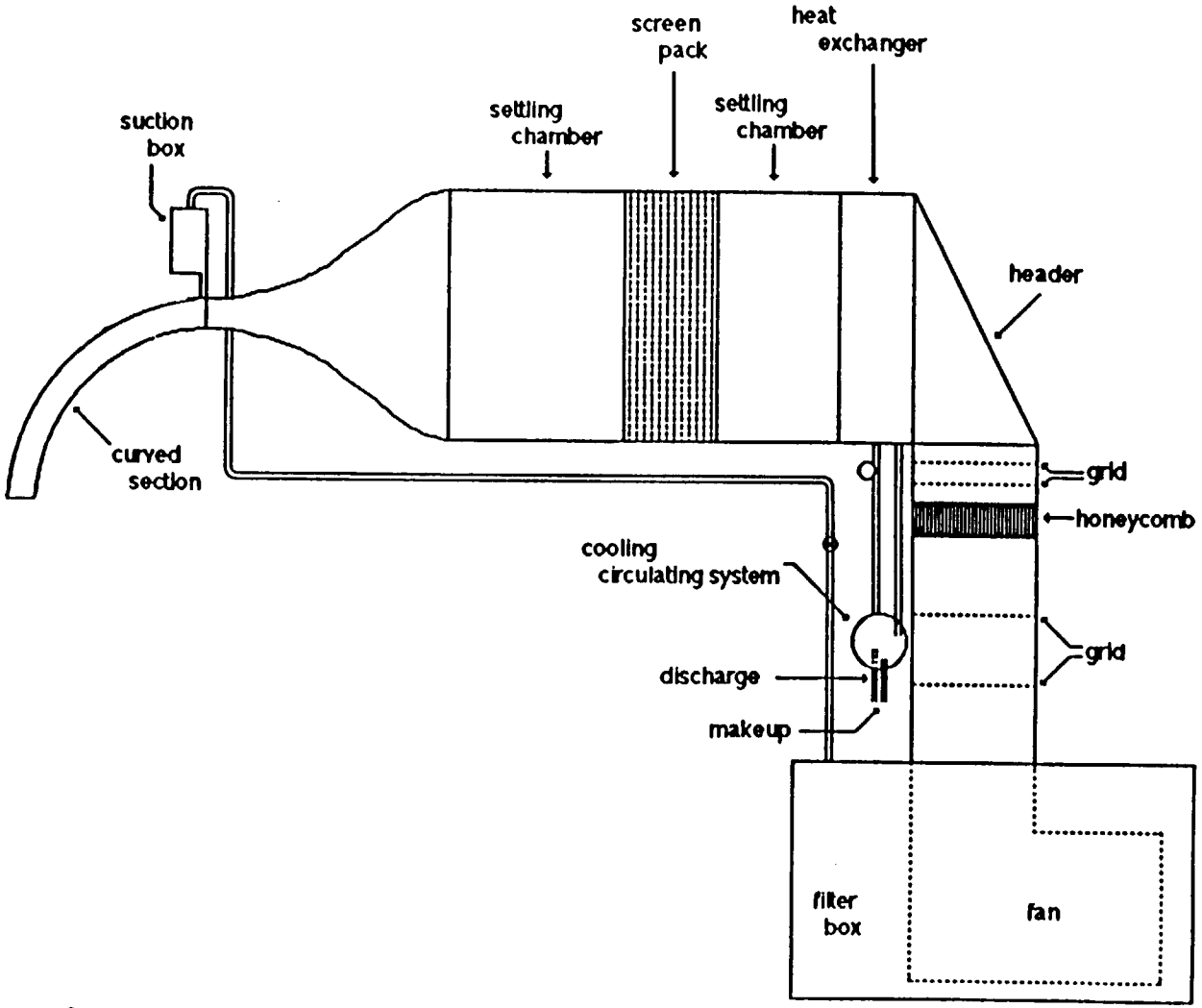

Fig. 2.1a: Schematic of Test Facility, Low FSTI configuration (from Kim, 1990)

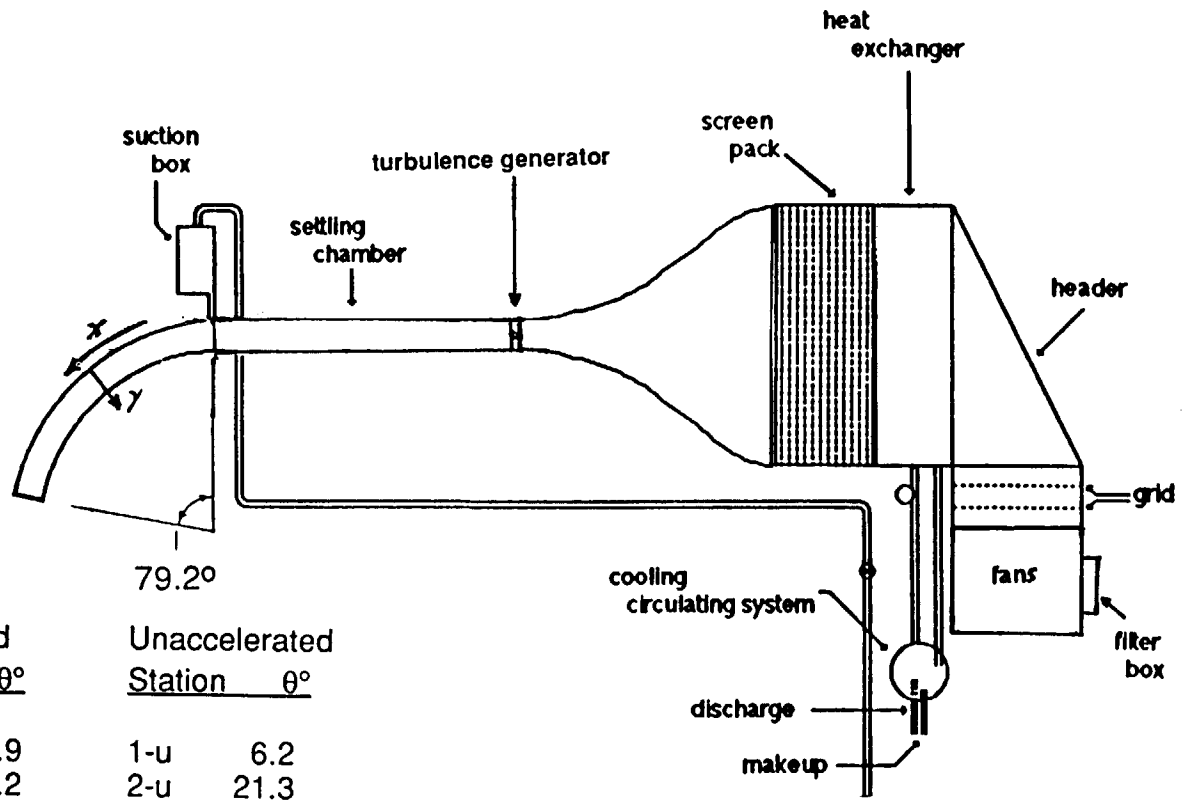

Accelerated		Unaccelerated	
Station	θ°	Station	θ°
1	5.9	1-u	6.2
2	11.2	2-u	21.3
3	15.4	3-u	36.4
4	20.4	4-u	51.7
5	25.0	5-u	66.9
6	29.7		
7	34.3		
8	38.9		
9	43.4		
10	48.2		

Fig. 2.1b: Schematic of Test Facility, High FSTI configuration

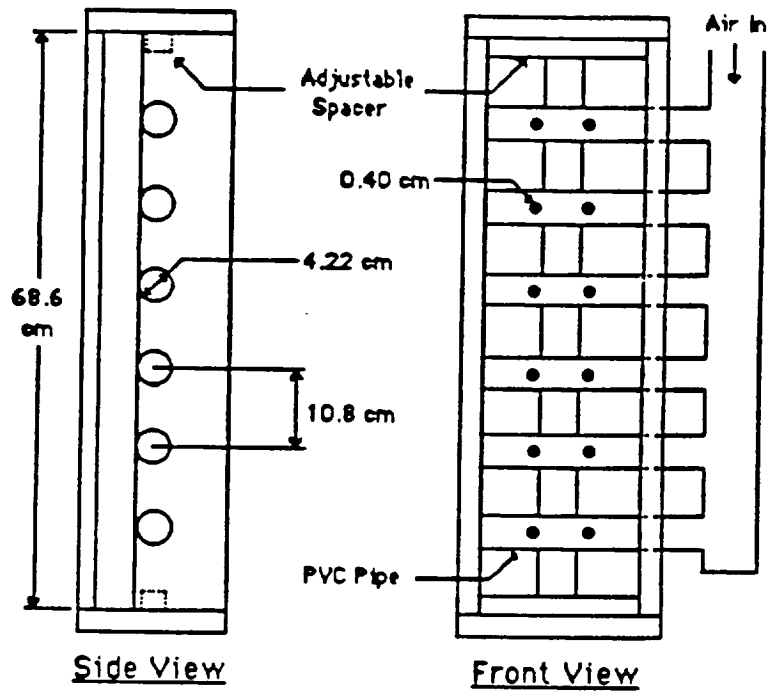

Fig. 2.2: Turbulence Generator (from Russ, 1989)

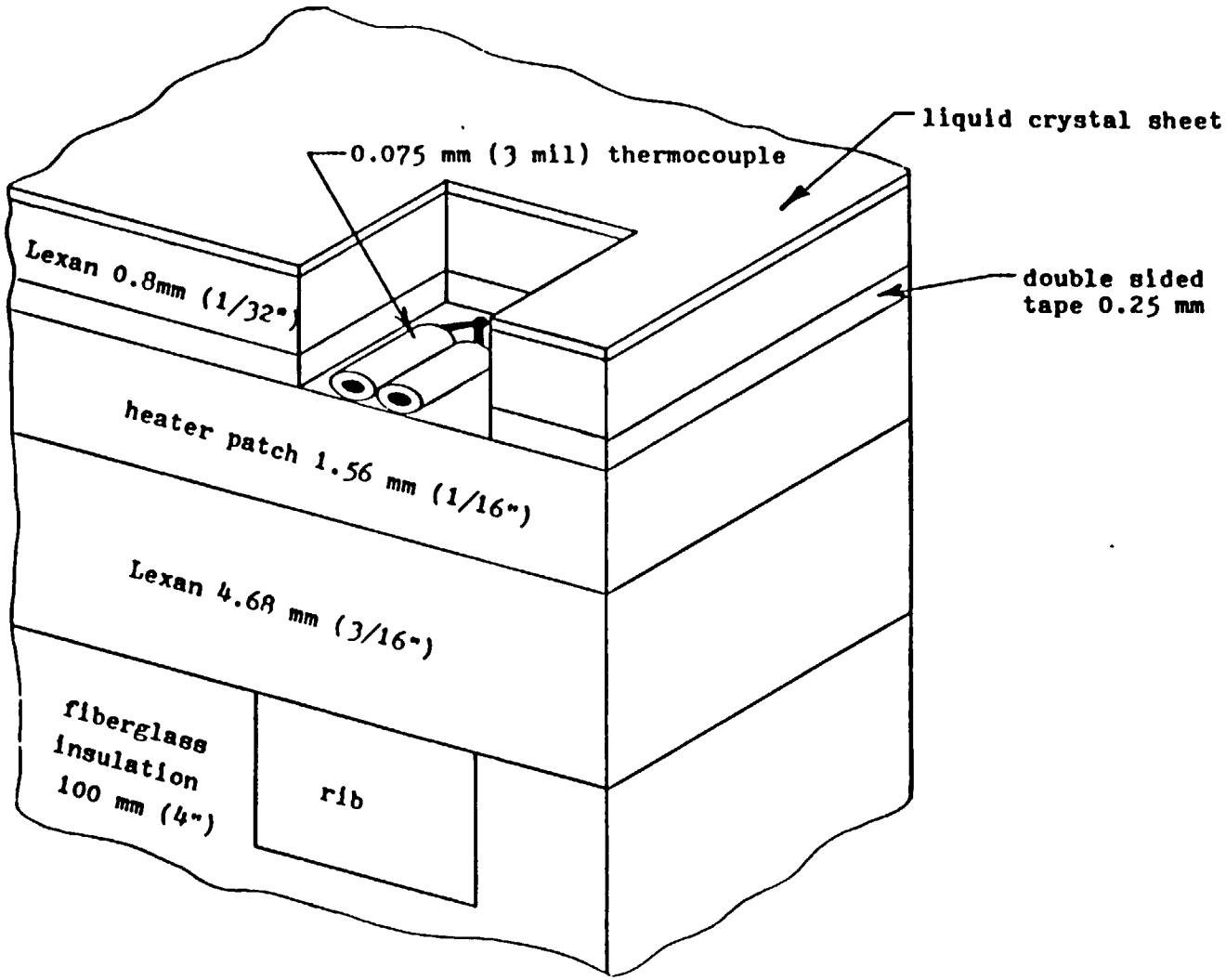

Fig. 2.3: Cross Section of Test Wall (not to scale) (from Kim, 1990)

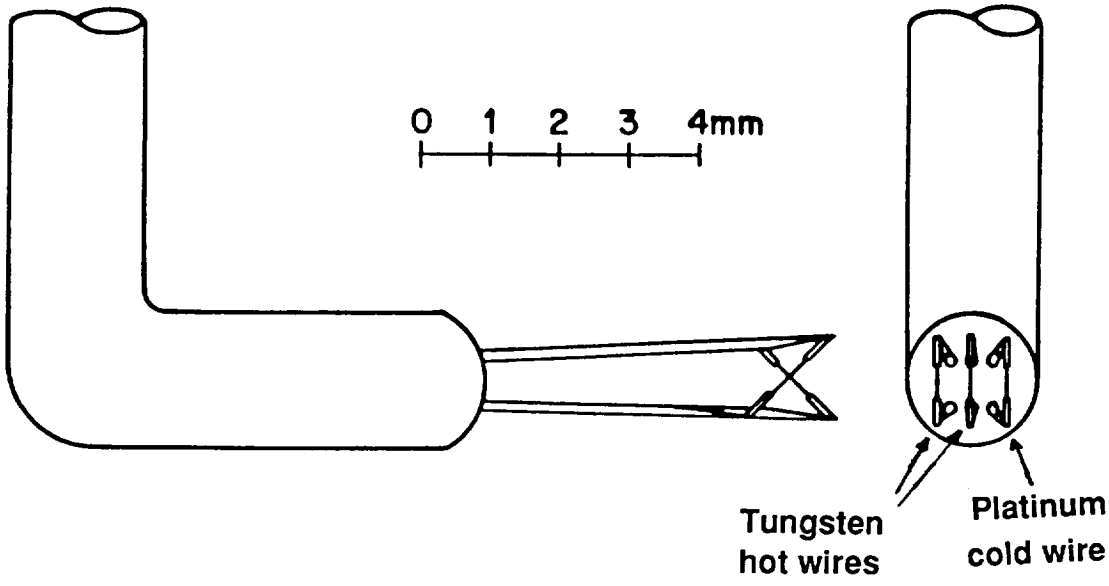

- 1, 1.27 μm dia. unplated platinum wire
- 2, 2.54 μm dia. platinum plated tungsten wire
  l/d=200, l=0.5 mm
- Separation between wires: 0.35 mm

Fig. 2.4: Schematic of Triple-Wire Probe used to measure Turbulent Heat Fluxes (from Kim, 1990)

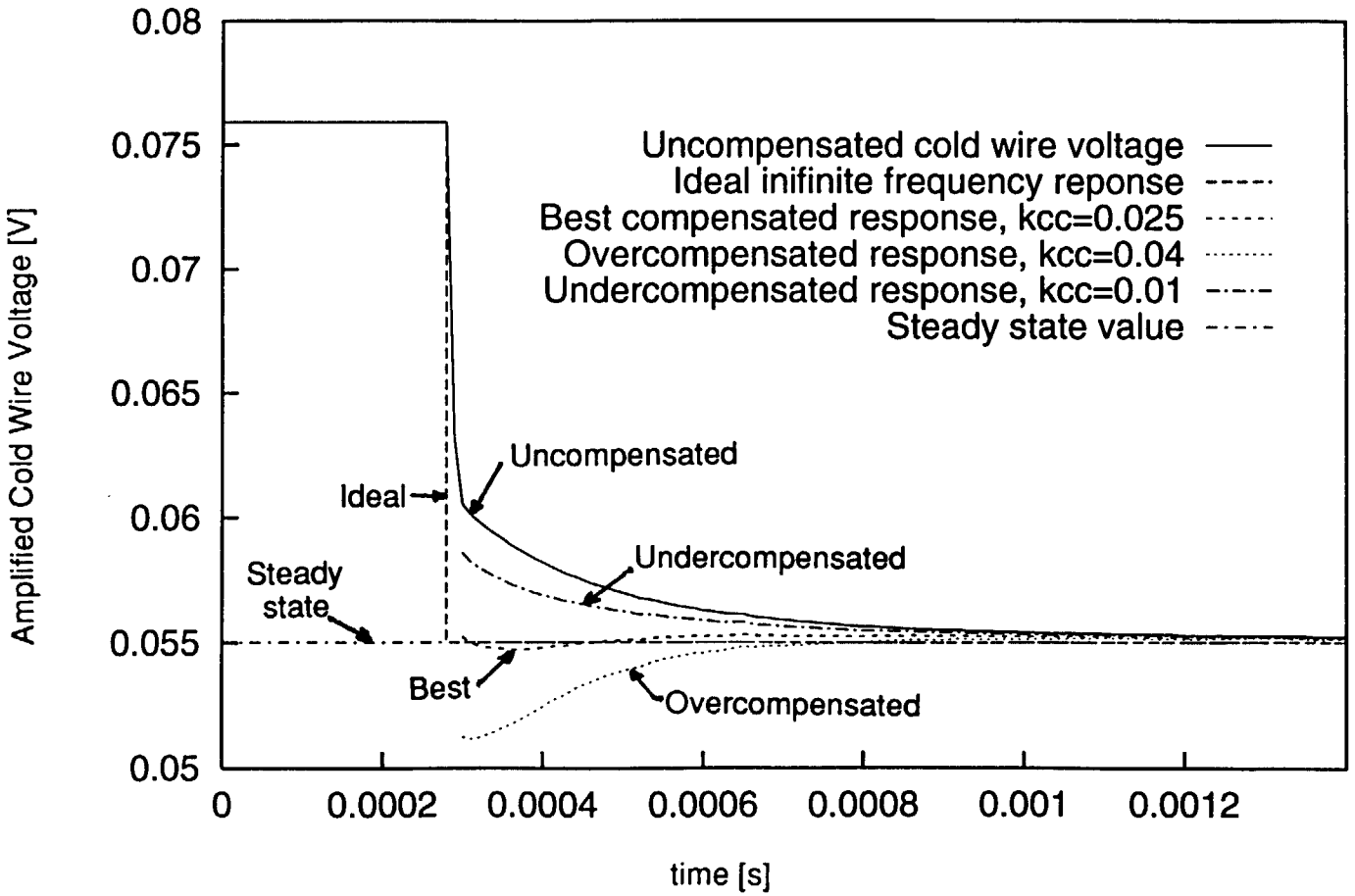

Fig. 2.5: Cold Wire Compensation Calibration

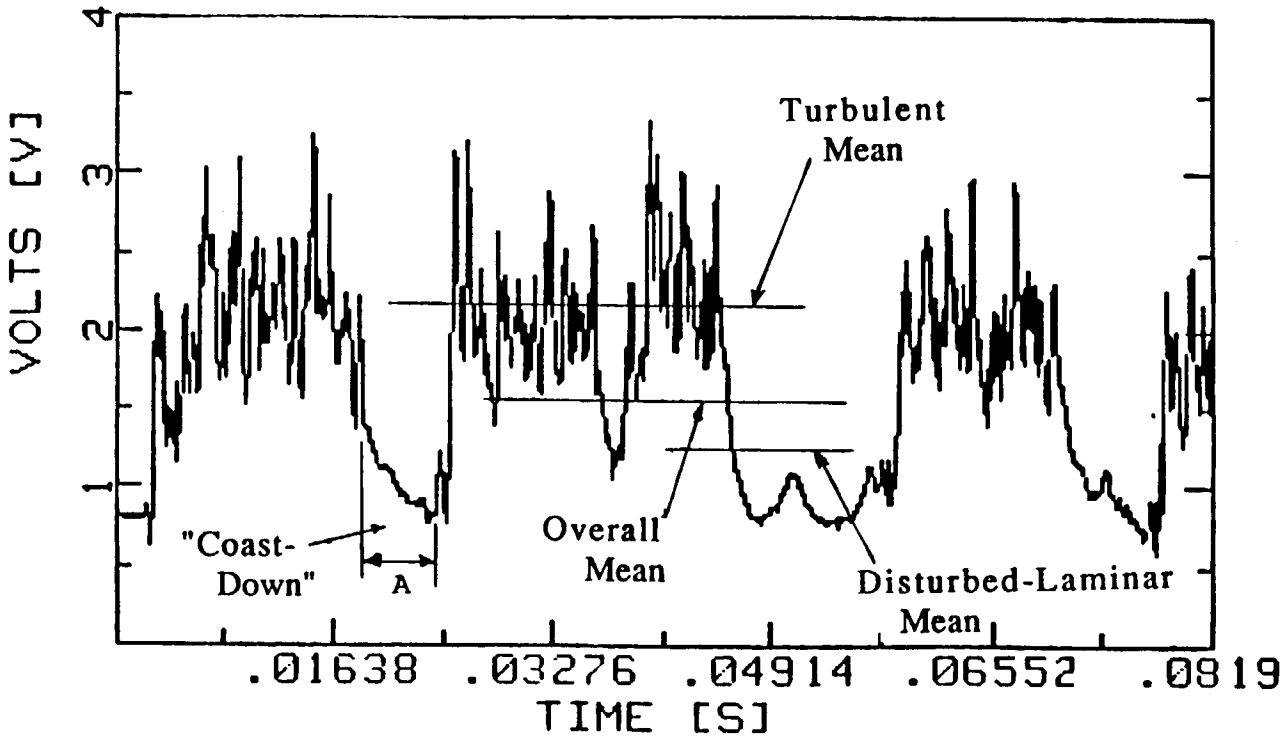

Fig. 2.6a: Velocity Time Trace from Intermittent Flow, Low FSTI (from Kim, 1990)

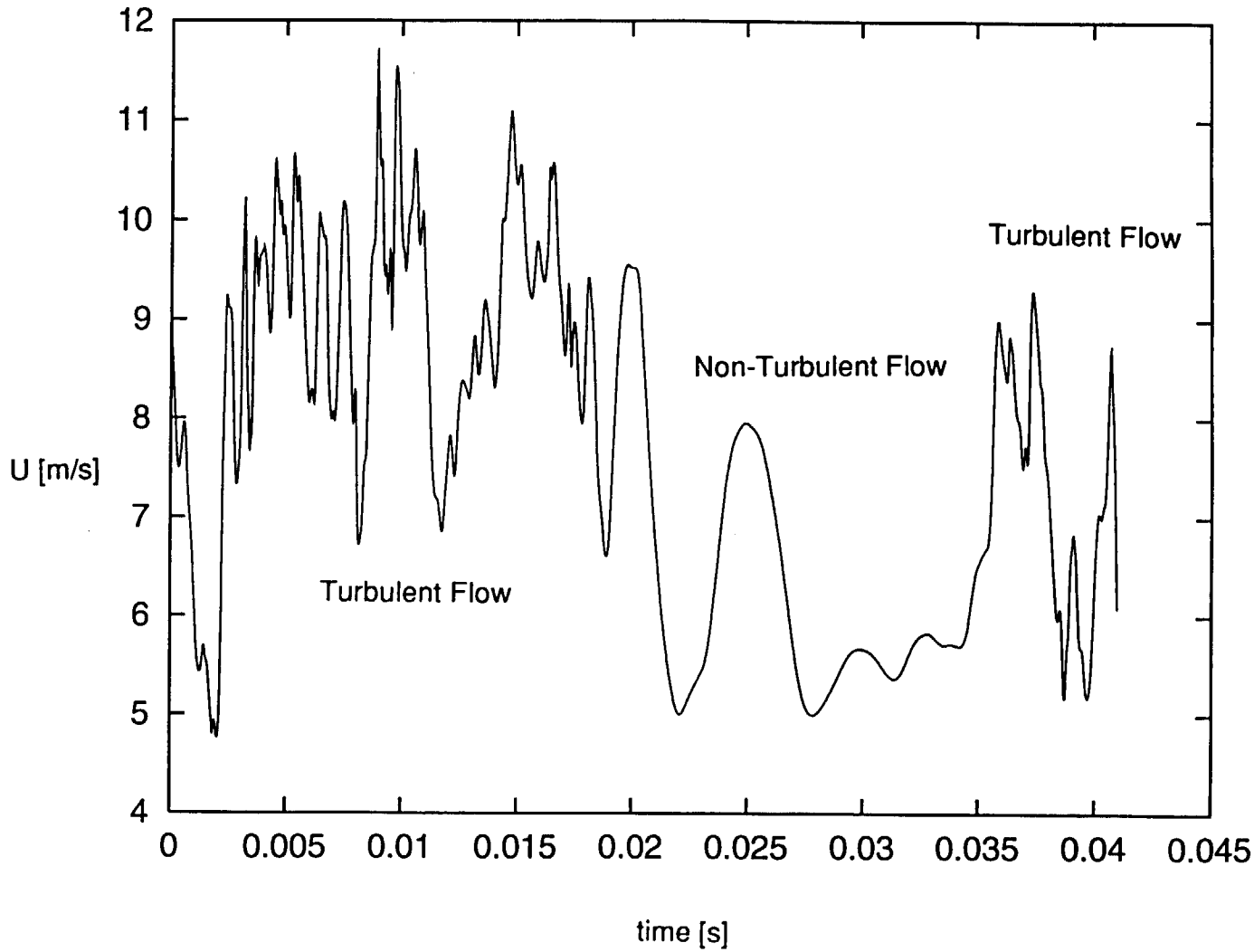

Fig. 2.6b: Velocity Time Trace from Intermittent Flow, High FSTI

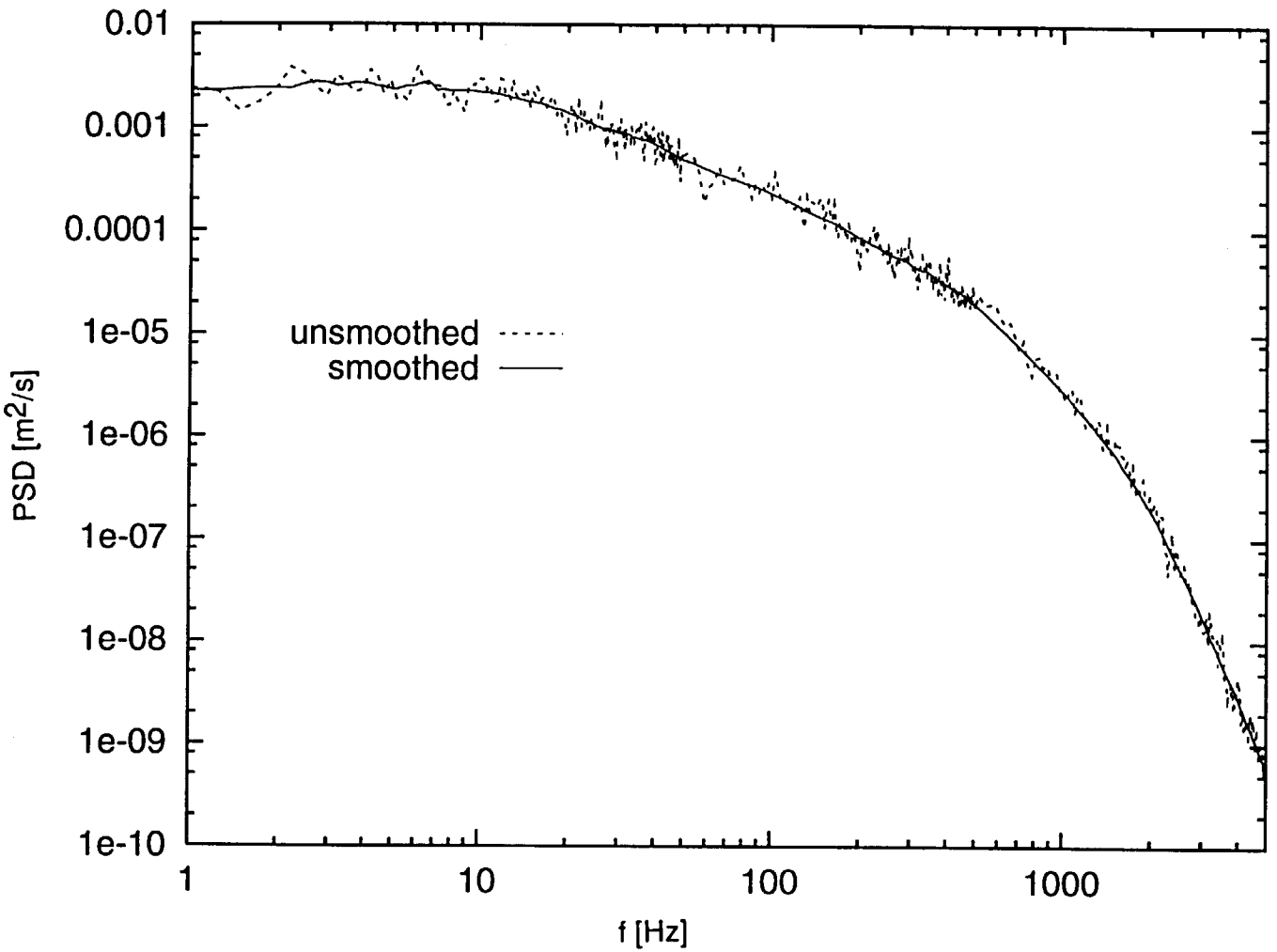

Fig. 2.7a: Typical Spectrum Before and After Smoothing, standard coordinates

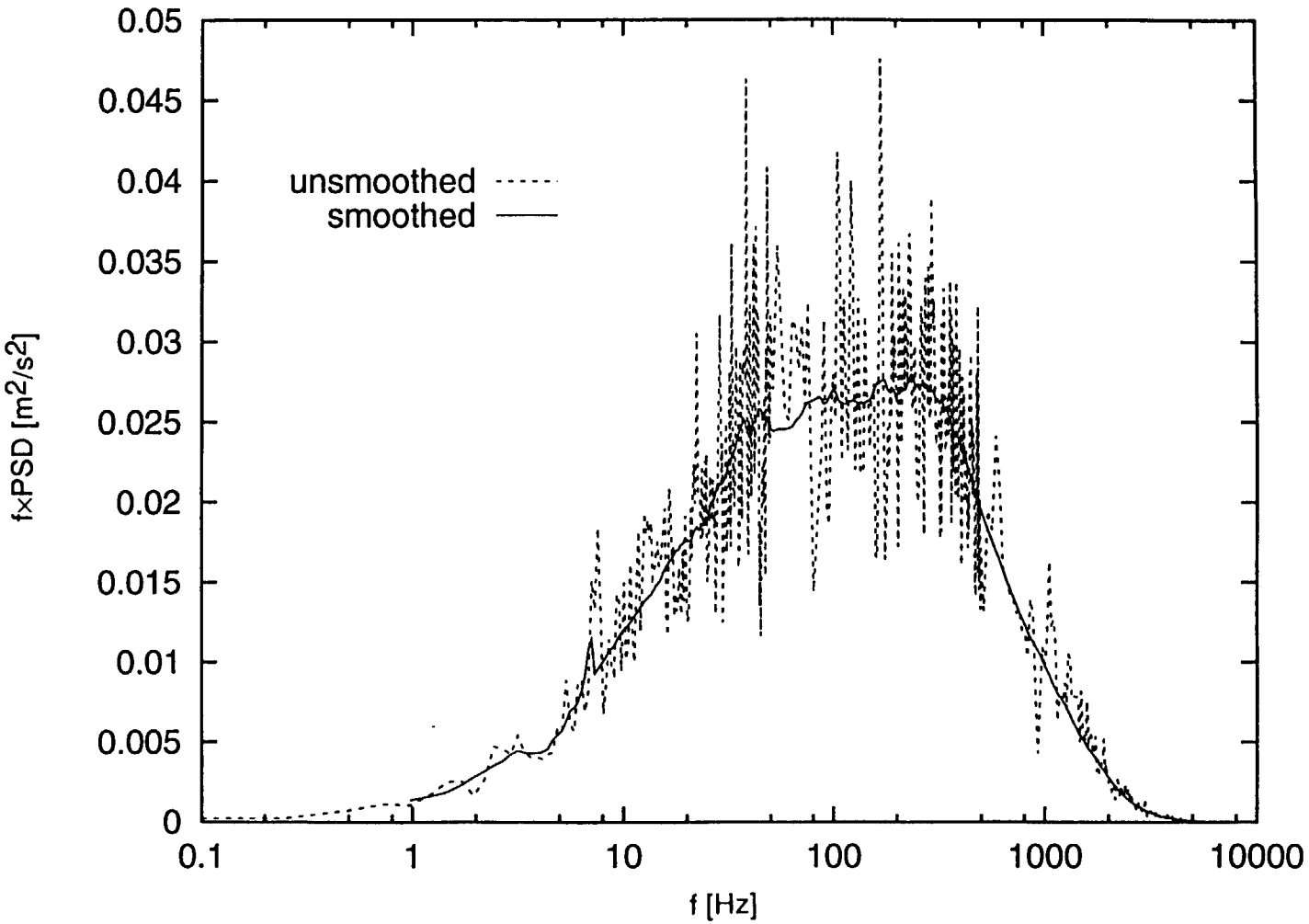

Fig. 2.7b: Typical Spectrum Before and After Smoothing, energy coordinates (frequency×PSD vs log frequency)

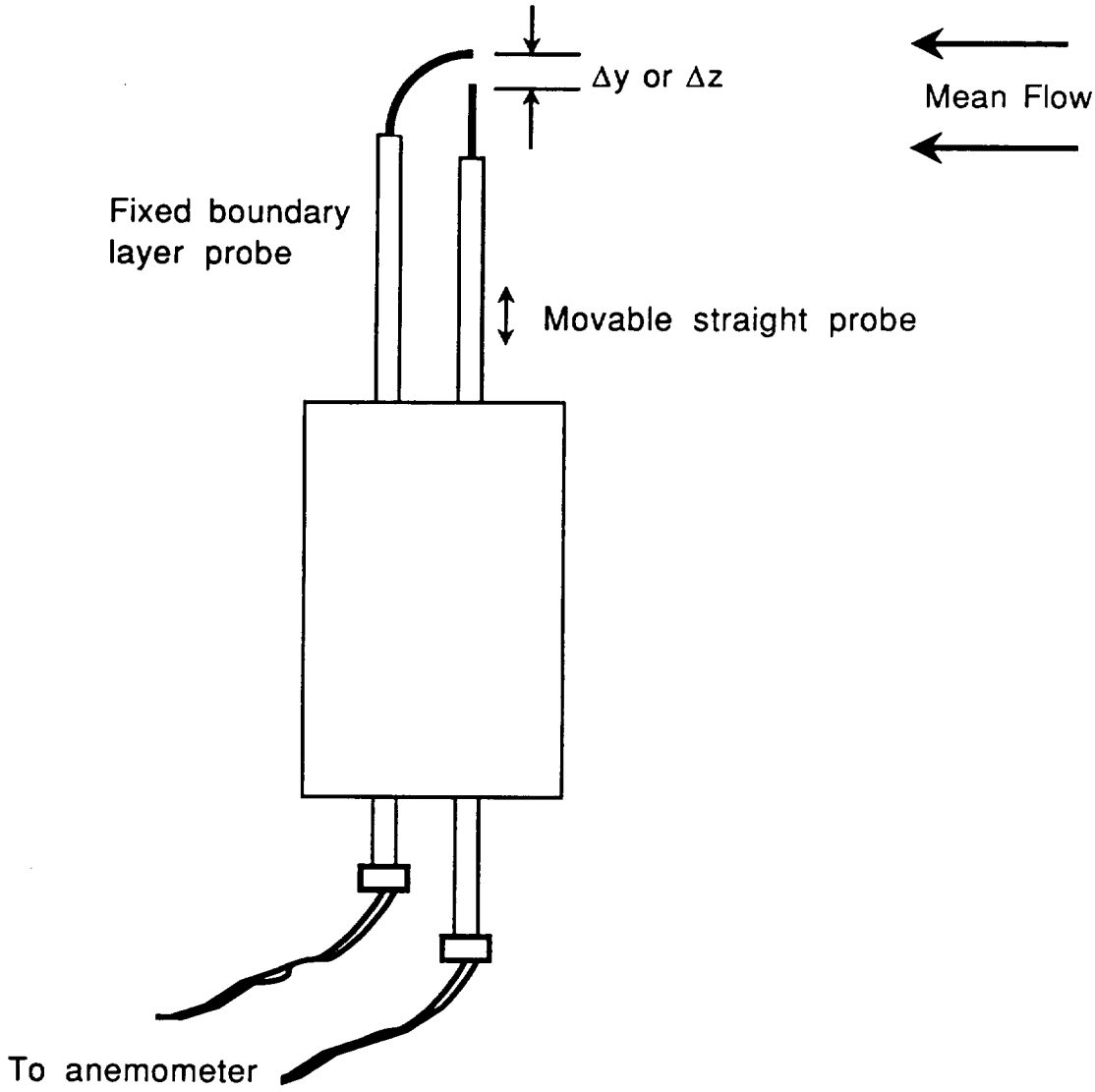

Fig. 2.8: Configuration for Two-Point Correlation Measurements

CHAPTER 3: LOW FSTI, CONCAVE WALL TRANSITION

BACKGROUND

Kim and Simon (1991) considered cases on the same concave wall as used in the present study. One case which they documented was taken under low (0.6%) FSTI conditions. The flow entered the test section at 17.2 m/s and was unaccelerated. The concave curvature led to the formation of stable streamwise (Görtler) vortices, which were observed downstream of the first measurement station. A sketch of Görtler vortices is presented in Fig. 3.1. Floryan (1991) provides a review of the Görtler instability in boundary layers. The vortices in Kim and Simon's (1991) flow originated in the laminar flow region and persisted through transition into the fully-turbulent boundary layer downstream. The vortices increased in size as the boundary layer grew and remained visible to the end of the test section. The vortices were observed with the liquid crystal on the test wall surface as warm and cold streaks. Kim and Simon (1991) took measurements at five streamwise stations in this flow. Conditions for these stations are listed in Table 3.1. Also included in the table are the results of some length scale measurements from the present study. The flow was laminar at the first station, transitional at the second, and fully-turbulent by the third. Transition occurred farther upstream in this flow than in a similar low FSTI case done on a flat wall. Velocity and temperature profiles at station 3 followed the turbulent velocity and temperature laws of the wall in the inner part of the boundary layer, but the wake was strongly affected by the curvature and vortices. Data were acquired at the upwash and downwash locations of the vortices at each station. These locations appear to be stable in that they always appeared at the same spanwise positions.

Kim and Simon did not observe stable Görtler vortices under high (8%) free-stream turbulence conditions on the concave test wall. This was believed to be due in

part to the absence of an extended laminar region for vortex development in the high-FSTI case. It was considered possible that vortices might re-emerge in a high FSTI case if a strong favorable pressure gradient were imposed to extend the non-turbulent region of the flow. To provide comparison data for such a case, better documentation of transition in the presence of Görtler vortices was sought under low FSTI conditions. In the end, no vortices were observed in high FSTI cases, even with strong acceleration. The results from the low FSTI case are still interesting, however, and are presented below.

In this study, more detailed documentation of Kim and Simon's (1991) case is provided. Spectral measurements in the boundary layer and free-stream were made by the present author to better document the boundary conditions and to provide another perspective to the transition process. The spectral documentation presented for this case is not as complete as for some of the high-FSTI cases presented in later chapters. The use of spectral information was introduced to the measurement program during the course of this study and more data were acquired in later cases. In addition to the spectral data, streamwise velocity profiles were acquired in the transition region at several spanwise positions to better document the effect of the Görtler vortices on transition. Octant analysis of data from this case is discussed in Chapter 4.

FREE-STREAM TURBULENCE

Free-stream u' spectra were acquired at Kim and Simon's stations 1, 2 and 5. Free-stream v' spectra were acquired at stations 1 and 2. The u' spectra are presented in Fig. 3.2 in both of the coordinate systems described in Chapter 2 The spectra do not change greatly in the streamwise direction. The integral length scale based on u' in the free-stream is $\Lambda_{u'}$=6.7 m. This is a very large dimension, and obviously cannot be associated with turbulent eddies in the free-stream. The frequency associated with this length scale, $U_\infty/\Lambda_{u'}$, is 2.6 Hz. The energy in the fluctuations, as shown in Fig. 3.2b, is centered around 0.8 Hz. Fluctuations at these low frequencies are associated with

streamwise unsteadiness, and, as stated above, are not due to eddy motion. Nearly all of the energy in $\overline{u'^2}$ lies below 20 Hz. A two-point correlation with separation in the y direction showed almost perfect correlation between u′ fluctuations measured with two probes, independent of the probe separation distance. This supports the conclusion that most of the u′ fluctuations are due to streamwise unsteadiness, not turbulent eddies. There is a very small peak in the u′ spectra centered around 100 Hz. This peak shows a slight growth in the streamwise direction, and may be associated with turbulent eddies in the free-stream.

Figure 3.3 shows the free-stream v′ spectra at the first and second measurement stations. Note the change in scale between Figs. 3.2b and 3.3b. Below 10 Hz, there is much less energy in $\overline{v'^2}$ than in $\overline{u'^2}$. Above 90 Hz, u′ and v′ are similar, indicating that the flow is fairly isotropic. The integral length scale associated with v′, $\Lambda_{v'}$, is 11 cm. This length scale is still large, but it could be associated with the largest eddies in the flow. The frequency associated with this length scale, $U_\infty/\Lambda_{v'}$, is 150 Hz. As shown in Fig. 3.3b, the energy in $\overline{v'^2}$ is centered around 20 Hz, in contrast to the $\overline{u'^2}$ PSD, where the energy was centered around 0.8 Hz. The component $\overline{v'^2}$ appears to be a better descriptor of eddy motion in this case. It will also be shown below, for both this case and the high-FSTI cases considered, that free-stream v′ fluctuations have a more important influence on the boundary layer than u′ fluctuations.

BOUNDARY LAYER SPECTRA AND TRANSFER FUNCTIONS

Figure 3.4 shows u′ spectra taken in the boundary layer very near the wall at y^+=6. Data were acquired at stations 1, 2 and 5. The energy in the fluctuations is so low at station 1, that it cannot be seen in the coordinates of Fig. 3.4b. This is to be expected since the flow is laminar at station 1. There is a sharp rise in u′ at all frequencies between stations 1 and 2, as transition begins. Data were acquired at both the upwash and downwash locations of the Görtler vortices at station 2. The upwash and downwash

spectra were similar, with the energy in the upwash spectrum only slightly higher than at the downwash. Only the downwash spectra are shown in Fig. 3.4. Between stations 2 and 5, there is little change in the spectra below 35 Hz, but a significant rise in energy is visible at higher frequencies. The peak in energy shifts from 35 Hz at station 2 to about 200 Hz at station 5. As expected, the lower frequencies associated with larger scales, become important early in the transition process, but the smaller scales do not become developed until later in transition. The cascade of energy from large scales to small scales takes some time to develop. The integral length scales associated with the spectra in Fig. 3.4 are approximately 0.5 m at stations 1 and 2, decreasing to 8 cm at station 5. At the upstream stations, the fluctuations even very near the wall appear to be dominated by low-frequency unsteadiness. Downstream, the contribution from turbulent eddies becomes more important.

Figure 3.5 shows boundary layer spectra from stations 1 and 5 taken at $y^+=35$. The results are similar to those seen at $y^+=6$ in Fig. 3.4. There is little energy in u' at station 1, although the level is higher than at $y^+=6$, and the spectrum is barely visible in Fig. 3.5b. At station 5, the peaks in the spectra in Figs. 3.4b and 3.5b agree. The fluctuation level at station 5 is somewhat higher at $y^+=35$ than at $y^+=6$. The integral scales associated with the spectra in Fig. 3.5 are 3.3 m at station 1 and 5 cm at station 5. As stated above, the fluctuations at the upstream stations are dominated by streamwise unsteadiness, while the downstream station show the influence of turbulent eddies.

Figure 3.6 shows the transfer function of $\overline{u'^2}$ between the boundary layer at $y^+=6$ and the free-stream at stations 1, 2, and 5. Essentially, the spectra of Fig. 3.4 were divided by the spectra of Fig. 3.2 at each station. At the first measurement station, the boundary layer contains more energy than does the free-stream in the frequency range 13 to 150 Hz. The low-frequency, $f<13$ Hz, streamwise unsteadiness is "damped" by the boundary layer, as are the higher frequencies, $f>150$ Hz. The boundary layer is apparently amplifying the free-stream turbulence for $13<f<150$ Hz. This is the range

containing most of the energy associated with eddy motion in the free-stream (Fig. 3.3b). A possible explanation for the amplification follows: Large-scale, free-stream eddies buffet the boundary layer, causing a displacement of fluid in the y direction (normal to the wall). This displacement causes v' fluctuations in the boundary layer at the frequency associated with the free-stream eddies. It also causes u' fluctuations within the boundary layer at the same frequency due to the normal gradient of streamwise velocity, $\partial U/\partial y$, as depicted by Fig. 3.7. Amplification occurs because $\partial U/\partial y$ is much larger in the boundary layer than in the free-stream. Bradshaw (1994a) used the terms "inactive motion" and "splat mechanism" to describe this effect. The low-frequency unsteadiness discussed with the u' spectra, which is a streamwise unsteadiness, would not produce this effect because it would not cause a displacement of fluid in the y direction.

At the downstream measurement stations (Fig. 3.6) where the boundary layer has become turbulent, the broad-band peak of station 1 has grown, and a new broad-band peak, centered almost two decades higher, has emerged. The higher frequencies are probably associated with boundary layer turbulence, originating from near-wall production of turbulence rather than amplification of anything present in the free-stream. The transfer functions at the two downstream stations are very similar to each other, although there is growth at the higher frequencies between the two stations.

Figure 3.8 shows the transfer function of $\overline{u'^2}$ between the boundary layer at $y^+ \approx 35$ and the free-stream at stations 1 and 5. The spectra of Fig. 3.5 are divided by the spectra of Fig. 3.2 at each station. At the upstream station, the boundary layer and free-stream have approximately equal energies (transfer function = 1) below 2 Hz and above 800 Hz. At the intermediate frequencies, centered around 20 Hz, the boundary layer has more energy than the free-stream. The transfer function is qualitatively similar to that at $y^+=6$ (Fig. 3.6), but with less "damping" of the high and low frequencies and higher

values at the intermediate frequencies. If the low transfer function values are due to near-wall viscous effects, the lower values at $y^+=6$ compared to those at $y^+=35$ should be expected.

STREAMWISE VELOCITY PROFILES

Mean Velocity

To better document the transition zone, velocity profiles were measured within the transition region. Instead of moving the probe to different streamwise positions within the transition zone, all measurements were taken at x=0.36 m (station 2) and the free-stream velocity was varied from 16.5 m/s to 20 m/s. The Reynolds number, Re_X, ranged from 3.7×10^5 to 4.4×10^5 as the velocity was increased. The free-stream turbulence level remained nearly constant at 0.6% as the velocity was varied. As stated above, the free-stream turbulence in this case is dominated by streamwise unsteadiness. Twenty five profiles were acquired at 5 free-stream velocities and 5 spanwise positions. Some of the results from these profiles are listed in Table 3.2. The profiles are numbered 1 through 5 depending on their free-stream velocity, with 1 corresponding to 16.5 m/s and 5 corresponding to 20 m/s. The profiles are also given a letter designation from a to e corresponding to their spanwise position. The downwash of a Görtler vortex pair is designated "a" and is located at z=-1.59 mm relative to the channel centerline. The upwash is designated "e" and is located at z=-3.79 mm relative to the channel centerline. Positions b, c, and d were evenly spaced between the upwash and downwash. The location and size of the vortices remained approximately constant over the free-stream velocity range considered. The vortices were approximately 2.2 mm wide. This compares to a boundary layer thickness, $\delta_{99.5}$, of approximately 3 mm.

Figure 3.9a shows mean velocity profiles at $Re_X=3.7\times10^5$. Streamwise velocity is normalized with U_{CW} and the distance from the wall is normalized on the momentum

thickness. The variation with spanwise position is obvious. The profiles are most full at the downwash positions. Since the boundary layer tends to be thinner at the downwash, the velocity gradients tend to be higher there. Some of the profiles, particularly the downwash profile, have strange shapes with inflection points. These are believed to be caused by spanwise "tilting" of the Görtler vortices, as depicted in Fig. 3.10. Similar behavior was noted by Wortmann (1969). A profile taken normal to the test wall will cut through a tilted vortex. As the probe is moved away from the wall, its position relative to the upwash and downwash will change. The upwash and downwash positions listed in Table 3.2 and in Fig. 3.9a, therefore, are only accurate at the test wall. This makes the definition of the various boundary layer thicknesses somewhat ambiguous.

Figure 3.9b shows the mean velocity profiles at $Re_X=4.4\times10^5$. The near wall gradients are higher than in the lower Reynolds number profiles. This is expected, since the skin friction should increase as the boundary layer proceeds through transition. The profiles also appear more inflectional than at the lower Reynolds numbers.

Figure 3.11 shows the mean velocity profiles from Fig. 3.9 plotted in wall coordinates. The low-Re_X profiles in Fig. 3.11a appear somewhat laminar-like. The high-Re_X profiles in Fig. 3.11b appear more turbulent-like, and are closer to the turbulent law of the wall. This is particularly true near the upwash. Because the boundary layer is thickest at the upwash, the boundary layer there should tend to be more mature, and should therefore tend to be farther along in the transition process. As stated above, the effective thickness of the boundary layer is not necessarily represented correctly in Table 3.2, due to the tilting of the vortices.

For another perspective, Figs. 3.12 and 3.13 show mean velocity profiles at the upwash and downwash positions. Figure 3.12a shows the downwash profiles plotted in outer coordinates. The profiles collapse fairly well, particularly in the outer part of the boundary layer. The profiles become somewhat fuller in the inner region, with increasing

Re_x. Figure 3.12b shows the upwash profiles. As in the downwash profiles, the collapse in the outer part of the boundary layer is good, but in the inner part of the boundary layer the progression through transition is more distinct. Figure 3.13 shows the profiles from Fig. 3.12 plotted in wall coordinates.

Skin Friction

Skin friction coefficients were determined from the velocity profiles by fitting the very near-wall data to the line $u^+=y^+$. Skin friction coefficient values are plotted versus Re_x and Re_θ in Fig. 3.14. In general, C_f is highest at the downwash locations, where the boundary layer is thinnest. Skin friction coefficients increase at each spanwise position as the Reynolds numbers increase and the boundary layer proceeds through transition. The exceptions to the general trends may be explainable in terms of the tilting vortices, described above. In Fig. 3.14b, standard correlations for laminar and fully-turbulent boundary layers on flat plates are shown for reference. The laminar correlation follows from the Blasius solution and the turbulent correlation is from Schlichting (1979). The data lie between the laminar and turbulent correlations, as expected for a transitional boundary layer.

Fluctuating Velocities

Profiles of fluctuating streamwise velocity, $\overline{u'}$, are plotted in outer coordinates in Fig. 3.15. The fluctuations are normalized on U_{cw}. The downwash profiles are shown in Fig. 3.15a. The fluctuation level rises as Re_x is increased. There is a near-wall peak in all of the profiles at $y/\theta \approx 1$ and a second, larger peak at $y/\theta \approx 5$. The near-wall peak is typical of all boundary layers. The second peak is caused by the Görtler vortices. A peak in the outer part of a boundary layer with Görtler vortices was also reported by Swearingen and Blackwelder (1987). The peak at $y/\theta \approx 5$ occurs at the location of the local minimum in the mean velocity profiles (Fig. 3.12a). Figure 3.15b shows the

upwash profiles. The fluctuation levels at the upwash are higher than those in the corresponding downwash profiles of Fig. 3.15a. The near-wall peak is broader at the upwash than at the downwash. At the higher Re_x, the near-wall peak shows some signs of dividing into two peaks, one at $y/\theta \approx 1$ and the second at $y/\theta \approx 2.5$. This second peak corresponds to the emergence of an inflection point in the mean velocity profiles at the upwash (Fig. 3.12b).

The fluctuating velocity profiles of Fig. 3.15 are plotted in wall coordinates in Fig. 3.16. At the downwash (Fig. 3.16a), the near-wall peak is at $y^+=22$. Its magnitude is between 1.7 and 2.6, rising with increasing Re_x. The magnitude of the peak is typical of most turbulent boundary layers. The second peak is at $y^+ \approx 100$. At the upwash (Fig. 3.16b), the fluctuation levels are much higher than at the downwash. At some Re_x, the fluctuation levels observed in profiles taken between the upwash and downwash (not plotted) were even higher than the values at the upwash. High fluctuation levels are generally expected in transitional flows and have been observed in studies such as Sohn and Reshotko (1991). The reasons for such high levels at the upwash locations in the present flow, however, have not been determined. The high levels must result from the presence of the Görtler vortices. Such high levels were not observed in cases without stable vortices, such as the high-FSTI cases discussed below in Chapters 5-7.

Intermittency

Profiles of the intermittency, γ, were measured along with the velocity profiles. These are shown for the downwash and upwash locations in Fig. 3.17. In the downwash profiles (Fig. 3.17a) the near-wall intermittency rises from near zero at the lowest Re_x to about 85% at the highest Re_x. There is a peak in γ near $y/\theta=5$. This peak corresponds to the local minimum in the mean velocity seen in Fig. 3.12a, and the second peak in $\overline{u'}$ seen in Fig. 3.15a. The inflection point in the mean velocity profile, caused by a tilting of

the vortices, appears be a source of turbulence production. This causes a local rise in the intermittency above the near-wall values. This suggests that the instability which causes the tilting of the Görtler vortices may be driving the transition process in this flow. Figure 3.17b shows the intermittency profiles at the upwash locations. As at the downwash locations, there is a regular progression through transition. A comparison of Figs. 3.17a and 3.17b shows that the intermittency tends to be slightly higher at the upwash locations than at the corresponding downwashes. As stated above, the boundary layer is thicker at the upwash locations, so it is reasonable to expect that transition would occur there first, resulting in higher intermittencies. The intermittency drops very near the wall in the upwash profiles. The intermittency should go to zero at the wall, where the velocity goes to zero and viscous effects dominate. This near-wall drop was not resolved in the downwash profiles, possibly because the boundary layer is thinner at the downwash locations. In agreement with the above results, Leoutsakos and Crane (1990) studied a boundary layer with Görtler vortices and noted that transition began at upwash locations, near a region of high shear, and proceeded rapidly through lateral spreading.

Transition location. The transition start and end locations can be determined, based on the intermittency, using Narasimha's (1984) theory, which, in turn, was derived from Emmons' (1951) theory of turbulent spots. The highest γ value in the γ vs y profile at each streamwise measuring station in a test are selected and used to calculate the function

$$f(\gamma) = \left(-\ln(1-\gamma)\right)^{-1/2}, \tag{3.1}$$

which is then plotted versus x or Re_x (plotting versus x is equivalent to plotting versus Re_x in cases with unaccelerated flow and constant fluid properties, such as the present case). In most flows along flat-walls, the data lie along a straight line in these coordinates, although some exceptions are seen at low γ (particularly in accelerated flow)

in a region which Narasimha (1984) referred to as the "subtransition" region. To determine the start and end of transition, attention is focused on the data points downstream of any subtransition. A least-squares fit to these data points is extrapolated to $f(\gamma)=0$ and $f(\gamma)=2.146$, which correspond to $\gamma=0$ and $\gamma=0.99$, respectively. The corresponding Re_x values at the two extrapolated points are taken as the locations of the start and end of transition, Re_{x_s} and Re_{x_e}, respectively. Volino and Simon (1991) applied this technique to find the transition start and end locations in several flows along flat plates. The extrapolation technique could not be applied in a straightforward manner in the present case along the concave wall. The present data, when plotted as $f(\gamma)$ vs Re_x, do not lie along a straight line. The trajectory of $f(\gamma)$ vs Re_x changes slope in the middle of the transition region. Thus, Re_{x_s} and Re_{x_e} were determined in this case using two extrapolations. The data near the start of transition were extrapolated to $f(\gamma)=0$ to determine Re_{x_s}, and the high-γ data were extrapolated to $f(\gamma)=2.146$ to find Re_{x_e}. This was done at three of the spanwise locations for this case, corresponding to the downwash (a), upwash (e) and mid-vortex (c) locations of the Görtler vortices. Transition start and end are given in terms of Re_x and Re_θ in Table 3.3. At the three spanwise positions, Re_θ was between 361 and 403 at the start of transition, and between 500 and 686 at the end of transition. At the 0.6% FSTI of the present case, correlations such as those given by Abu-Ghannam and Shaw (1980) or Mayle (1991) predict transition start at $Re_\theta \approx 600$ and transition end at $Re_\theta \approx 1600$. Concave curvature is causing early transition in the present case.

Intermittency distribution. The intermittency within the transition zone is plotted as a function of the dimensionless streamwise coordinate $\frac{Re_x - Re_{x_s}}{Re_{x_e} - Re_{x_s}}$ in Fig. 3.18. The abscissa is a modified version of Dhawan and Narasimha's (1958) coordinate, mentioned above in Chapter 1. Dhawan and Narasimha used $\frac{x - x_s}{x_e - x_s}$, with x_s taken at $\gamma=0.25$ and x_e taken at $\gamma=0.75$. Here, Re_{x_s} is taken at the extrapolated $\gamma=0$ location and

Re_{x_e} at the extrapolated γ=0.99 location. The modification was done to give Re_x estimates which are closer to the actual start and end of transition. The change was purely algebraic; the theory remains exactly as Dhawan and Narasimha presented it. Dhawan and Narasimha present a formula (given above as Eqn. 1.1) which, when modified to take the changed abscissa into account is

$$\gamma = 1 - \exp\left(-4.6\left(\frac{Re_x - Re_{x_s}}{Re_{x_e} - Re_{x_s}}\right)^2\right) \tag{3.2}$$

This curve is plotted along with the experimental data in Fig. 3.18. Volino and Simon (1991) found good agreement between the theoretical curve and data from several studies done in unaccelerated and accelerated flow along flat plates. Gostelow and Walker (1991) showed that the agreement is also good for adverse pressure gradient cases on flat plates. The present data indicate that the theory does not always hold when curvature effects are introduced. Although it is possible to force any two data points from an experimental case to fit the theoretical curve (through appropriate choice of Re_{x_S} and Re_{x_e}), it is impossible to fit all of the concave-wall data to the theoretical curve. This behavior is believed to be due to a change in the transition mechanism associated with the Görtler vortices in the low-FSTI concave-wall flow. Transition tends to progress more slowly, in a relative sense, during early transition and more quickly during later stages of transition, compared to flat-wall behavior.

Turbulent spot propagation rate. The production and growth of turbulent spots in the transition region can be calculated using the information provided above and Dhawan and Narasimha's (1958) theory. As given by Mayle (1991),

$$\gamma = 1 - \exp\left(-\frac{n\sigma}{U_\infty}(x - x_s)^2\right) \tag{3.3}$$

where n is the turbulent spot production rate and σ is the turbulent spot propagation parameter. A dimensionless spot production rate, $\hat{n}$, is defined as $\frac{n\nu^2}{U_s^3}$. The velocity, U_S, is the free-stream velocity at the start of transition. The product $\hat{n}\sigma$ is directly related to the length of the transition zone. Given the location of the transition start and $\hat{n}\sigma$, it should be possible to calculate the location of the end of transition and the intermittency within the transition region. From the discussion above, one can show

$$\hat{n}\sigma = \frac{4.6}{\left(Re_{x_e} - Re_{x_s}\right)^2} \tag{3.4}$$

in unaccelerated flow, where Re_{x_S} and Re_{x_e} are taken at γ=0 and γ=0.99. A single value of $\hat{n}\sigma$ is applied through transition.

Spot propagation rates were calculated for the present case and are plotted in Fig. 3.19. Also shown is a correlation given by Mayle (1991). Mayle (1991) and Volino and Simon (1991) showed that data from several flat-wall studies agreed well with this correlation. In flat-wall cases, where the intermittency data agree with Narasimha's (1984) theory, the choice of a single $\hat{n}\sigma$ for the entire transition region is appropriate. For the concave-wall case, however, the local effective $\hat{n}\sigma$ values increase as one moves downstream through transition. The first three γ values in each of the three concave-wall curves in Figure 3.18 were used to determine an effective local $\hat{n}\sigma$ at the start of transition. Similarly, the last two γ values in each curve were used to determine an effective local $\hat{n}\sigma$ for the end of transition. These are presented in Table 3.3 for the upwash, downwash and mid-vortex locations of this case. In Fig. 3.19, all the concave wall $\hat{n}\sigma$ lie significantly above Mayle's correlation. The effective $\hat{n}\sigma$ increases by an order of magnitude between the beginning and end of transition. An effective overall $\hat{n}\sigma$ is also presented based on the extrapolated Re_{x_S} and Re_{x_e} given in Table 3.3.

CONCLUSIONS

The flow in this case is interesting and complex due to the presence of the stable Görtler vortices. These vortices appear to dominate the transition process. Transition occurs farther upstream than in comparable FSTI flows along flat walls. The transition zone is shortened and the path through transition, in terms of the intermittency, is altered by the presence of the vortices.

Station	x [m]	U_{cw} [m/s]	δ^* [mm]	θ [mm]	H	Re_x	$Re\theta$	C_f $\times 10^3$	$\overline{v'_\infty}$ [m/s]	$\Lambda_{v'}$ [cm]	$U_{cw}/\Lambda_{v'}$ [Hz]
1	0.089	16.53	0.541	0.213	2.54	91700	219.	2.23	0.022	10.3	167.
2 dw	0.356	17.24	0.317	0.164	1.93	376000	173.	4.60	0.024	11.5	149.
2 uw	0.356	17.23	1.160	0.531	2.18	375700	561.	2.10	0.024	11.5	149.
3 dw	0.610	17.08	1.407	0.996	1.41	638900	1044.	4.80			
3 uw	0.610	17.11	1.623	1.124	1.44	640300	1181.	4.15			
4 dw	0.876	17.14	1.532	1.167	1.31	924400	1231.	5.20			
4 uw	0.876	17.13	2.487	1.820	1.37	923400	1917.	4.20			
5 dw	1.130	16.76	2.436	1.898	1.28	1164000	1954.	4.70			
5 uw	1.130	16.76	3.679	2.718	1.35	1650000	2801.	3.70			

Table 3.1: Conditions for Kim and Simon's (1991) Low FSTI Concave-Wall Case Upwash and Downwash denoted by uw and dw respectively

Station	z [mm]	U_{cw} [m/s]	$\delta_{99.5}$ [mm]	δ^* [mm]	θ [mm]	H	Re_x	Re_θ	$C_f \times 10^3$
1a (dw)	-1.59	16.51	3.33	0.675	0.409	1.65	372541.	422.	3.60
1b	-2.19	16.44	2.81	0.515	0.282	1.83	371070.	289.	3.70
1c	-2.69	16.48	3.08	0.602	0.306	1.96	372139.	316.	3.20
1d	-3.24	16.46	2.80	0.771	0.349	2.21	371417.	359.	2.45
1e (uw)	-3.79	16.47	2.90	0.881	0.376	2.34	371893.	389.	2.10
2a (dw)	-1.59	17.60	3.32	0.668	0.419	1.59	397613.	462.	3.70
2b	-2.19	17.62	3.31	0.504	0.298	1.69	399538.	329.	4.00
2c	-2.69	17.57	3.16	0.560	0.304	1.84	398231.	336.	3.80
2d	-3.24	17.54	2.69	0.726	0.358	2.03	396826.	393.	3.25
2e (uw)	-3.79	17.60	2.71	0.912	0.396	2.30	397769.	436.	2.20
3a(dw)	-1.59	18.06	3.42	0.636	0.408	1.56	403395.	456.	4.10
3b	-2.19	18.03	3.16	0.498	0.288	1.73	402930.	322.	3.80
3c	-2.69	18.02	3.00	0.595	0.319	1.86	402800.	356.	3.25
3d	-3.24	17.98	2.84	0.815	0.381	2.14	402222.	424.	2.40
3e (uw)	-3.79	18.00	2.84	0.935	0.412	2.27	402787.	460.	2.25
4a (dw)	-1.59	19.11	3.55	0.639	0.425	1.50	424556.	499.	4.45
4b	-2.19	19.14	3.61	0.510	0.307	1.66	425738.	362.	3.85
4c	-2.69	19.12	3.13	0.593	0.329	1.80	426042.	389.	3.40
4d	-3.24	19.23	3.67	0.780	0.404	1.93	429139.	479.	2.90
4e(uw)	-3.79	19.23	3.35	0.920	0.440	2.09	429367.	523.	2.45
5a (dw)	-1.59	20.03	5.12	0.645	0.439	1.47	443653.	540.	4.47
5b	-2.19	20.02	4.62	0.518	0.330	1.57	443368.	406.	4.13
5c	-2.69	19.98	4.14	0.579	0.348	1.66	442133.	427.	4.27
5d	-3.24	19.99	3.86	0.768	0.418	1.84	441987.	512.	3.15
5e (uw)	-3.79	20.03	3.83	0.890	0.460	1.94	442726.	564.	2.85

Table 3.2: Conditions for Streamwise Velocity Profiles, Low FSTI Concave-Wall Case, (dw) and (uw) denote downwash and upwash respectively

Position	$Re_{x_S} \times 10^{-6}$	$Re_{x_e} \times 10^{-6}$	Re_{θ_S}	Re_{θ_e}	effective $\hat{n}\sigma \times 10^{11}$ at transition start	effective $\hat{n}\sigma \times 10^{11}$ at transition end	effective overall $\hat{n}\sigma \times 10^{11}$
Upwash	0.350	0.468	361	586	5.9	91.7	33.0
Mid-Vortex	0.353	0.467	363	500	11.7	105.2	35.4
Downwash	0.356	0.472	403	686	14.2	93.4	34.2

Table 3.3: Transition Start and End, and Turbulent Spot Propagation Rates Based on Intermittency Measurements

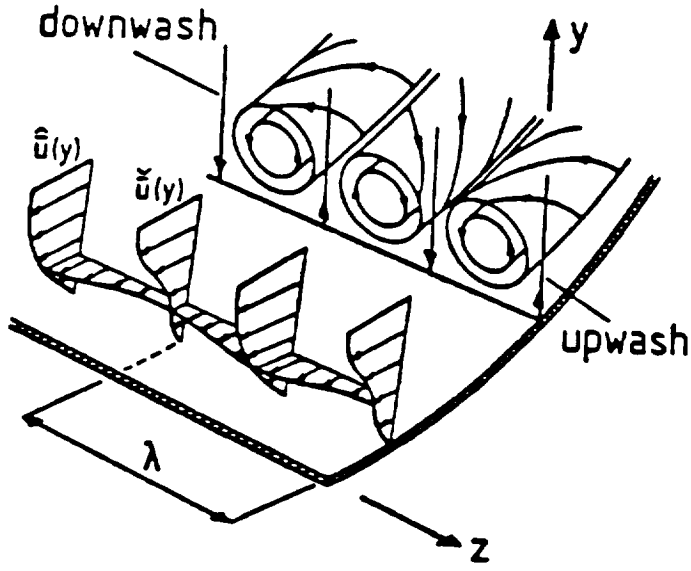

Fig. 3.1: Schematic of Görtler Vortices (from Crane and Sabzvari, 1984)

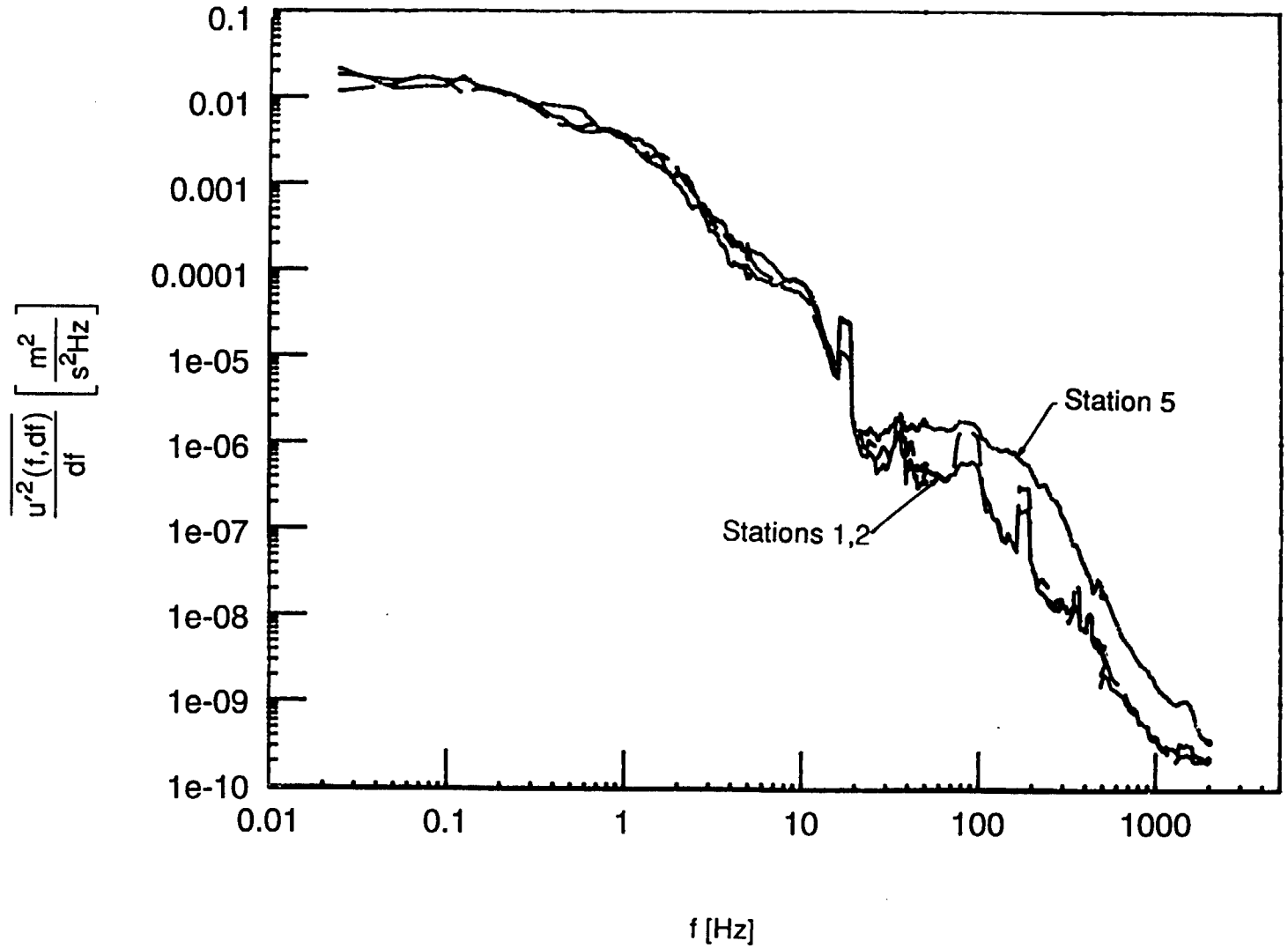

Fig. 3.2a: Free-Stream u′ Spectra, Low FSTI Case

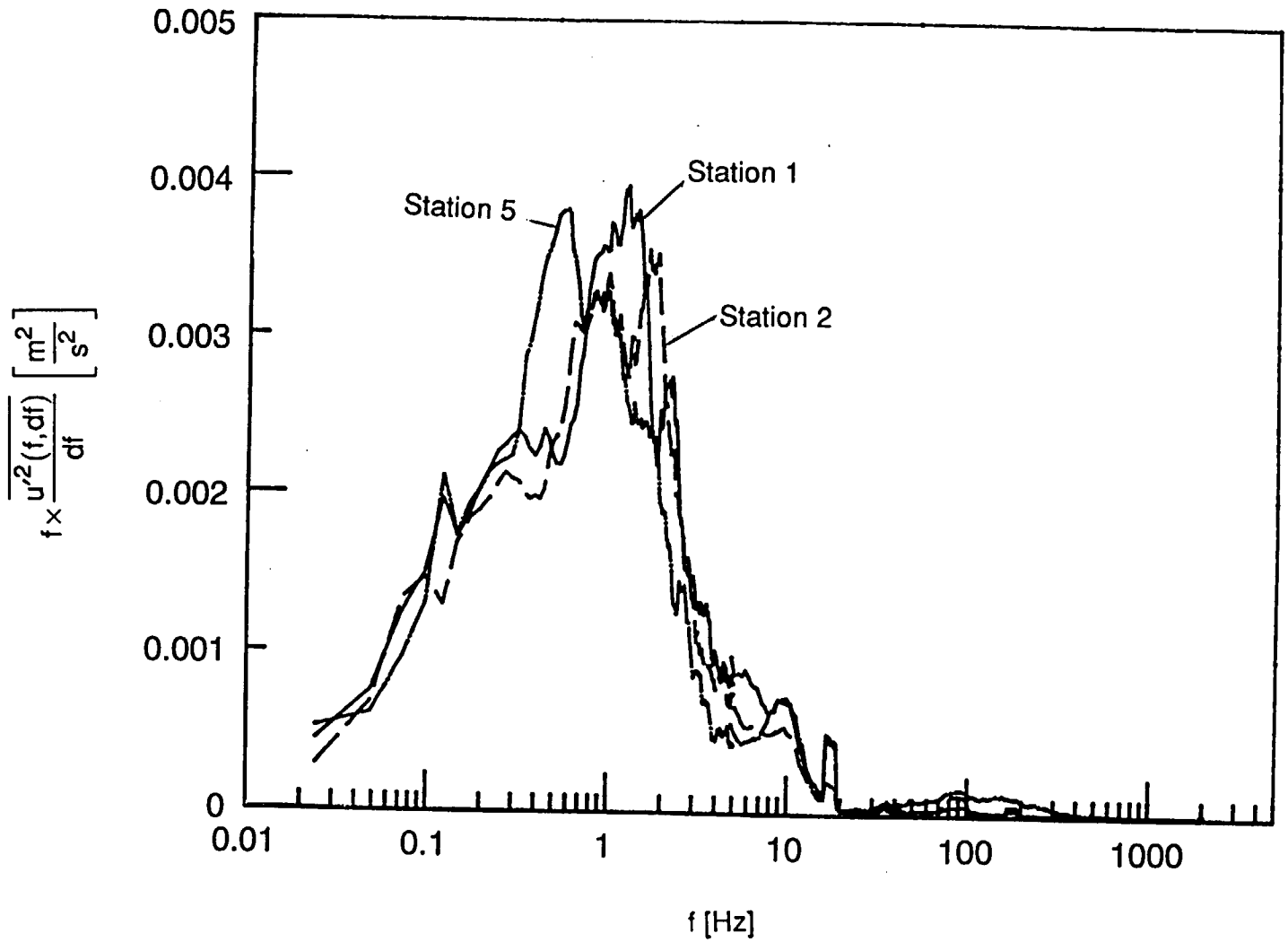

Fig. 3.2b: Free-Stream u′ Spectra, Low FSTI Case, Energy Coordinates

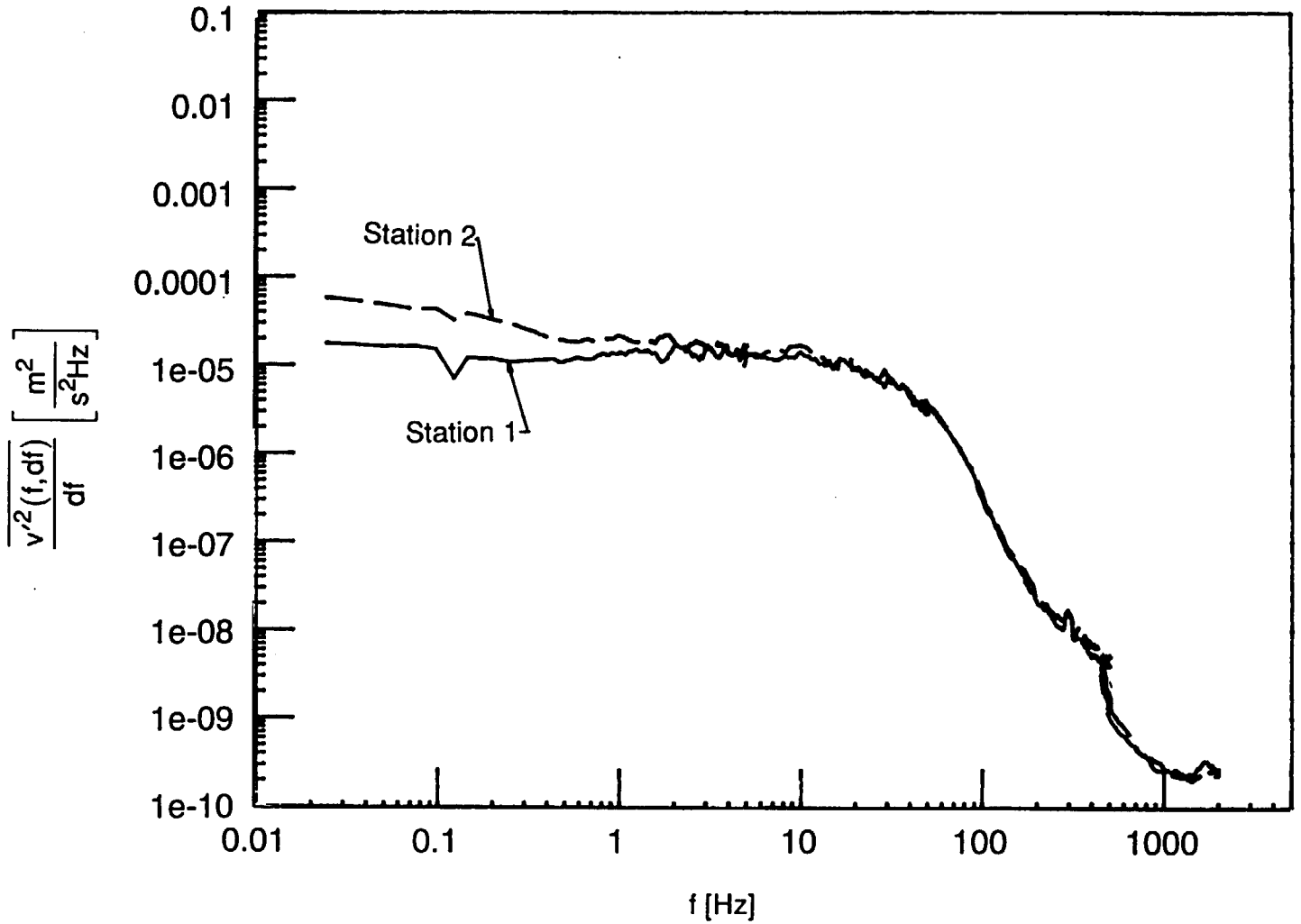

Fig. 3.3a: Free-Stream v′ Spectra, Low FSTI Case

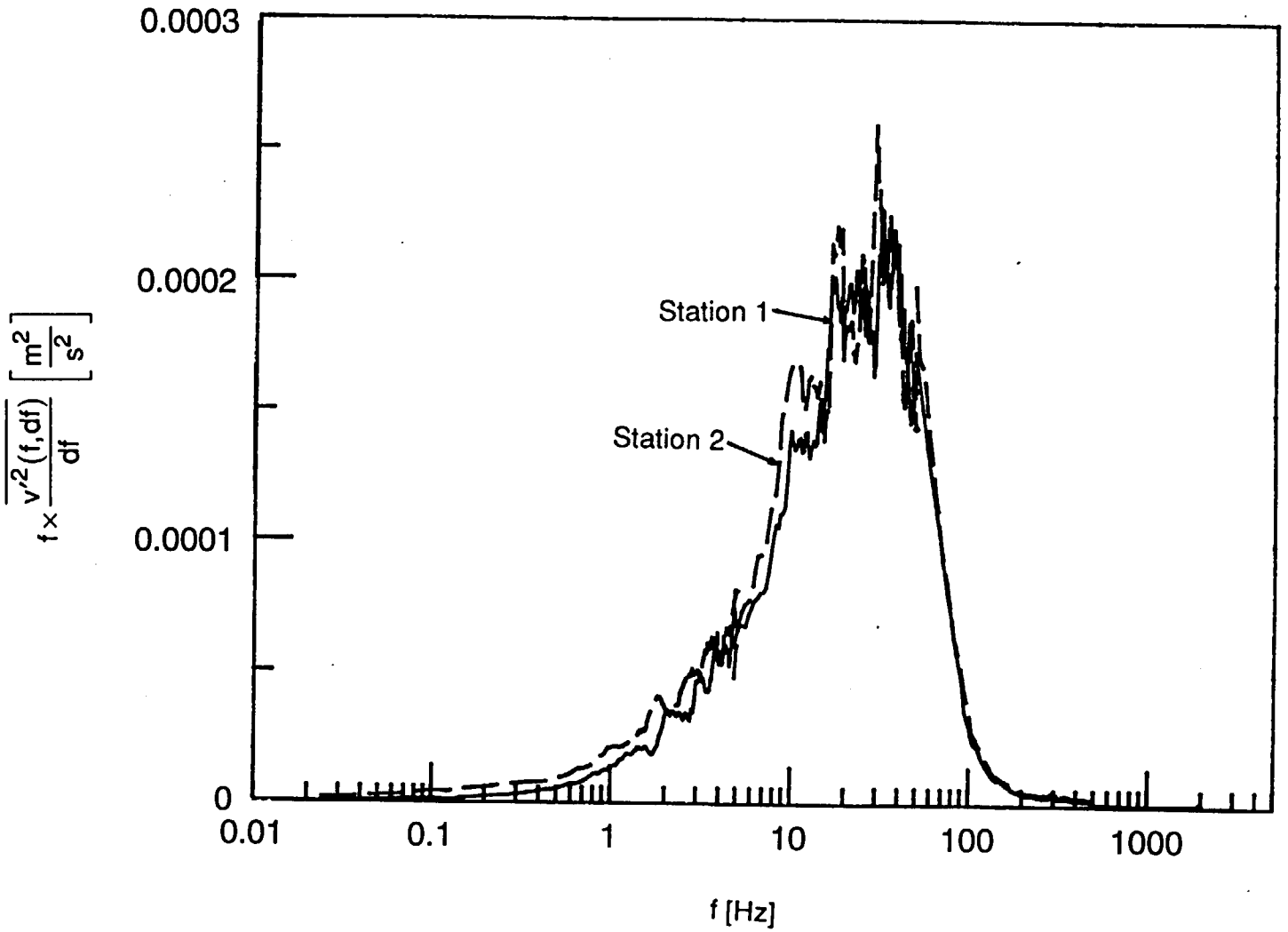

Fig. 3.3b: Free-Stream v′ Spectra, Low FSTI Case, Energy Coordinates

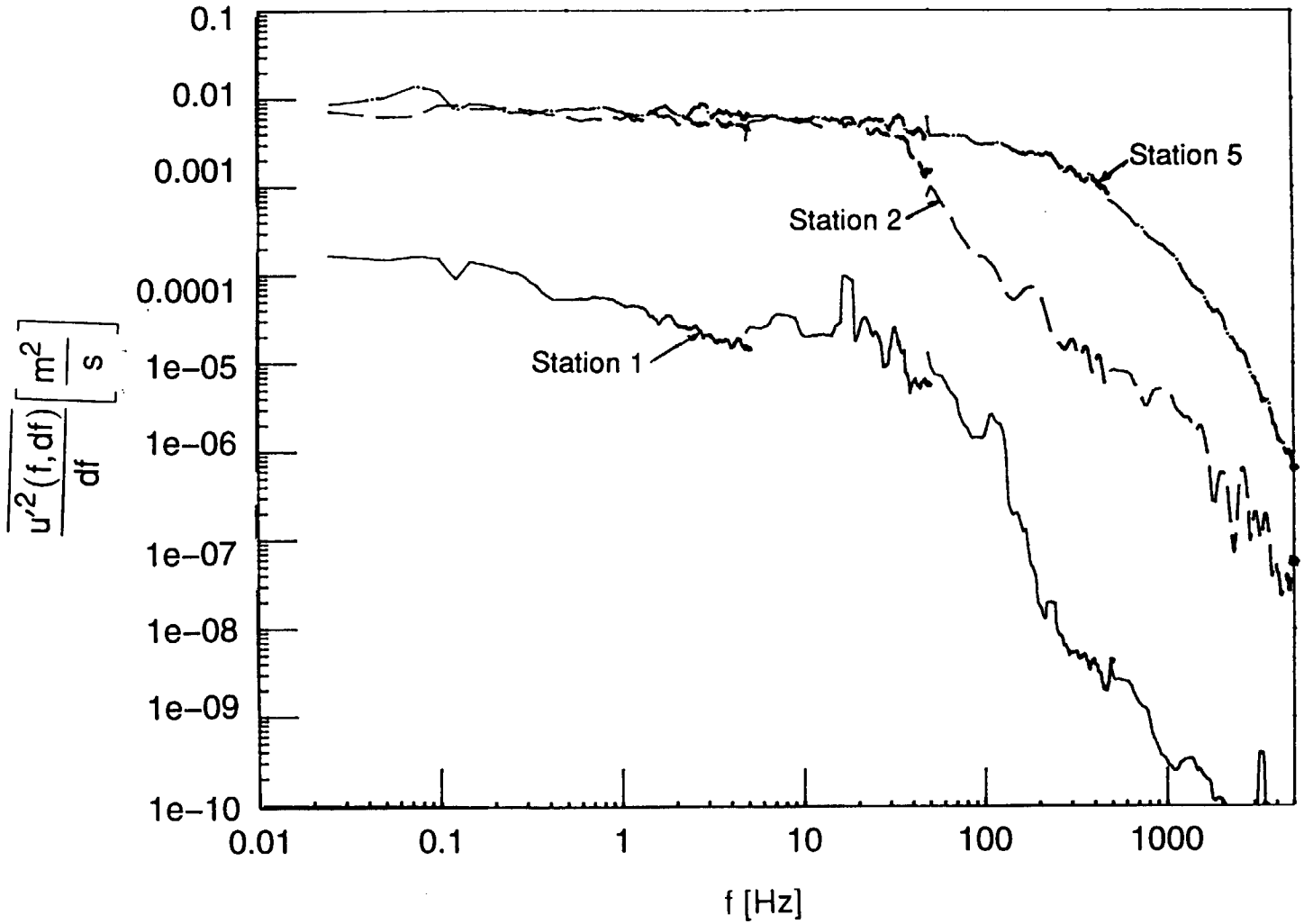

Fig. 3.4a: Boundary Layer u′ Spectra at y+=6, Low FSTI Case

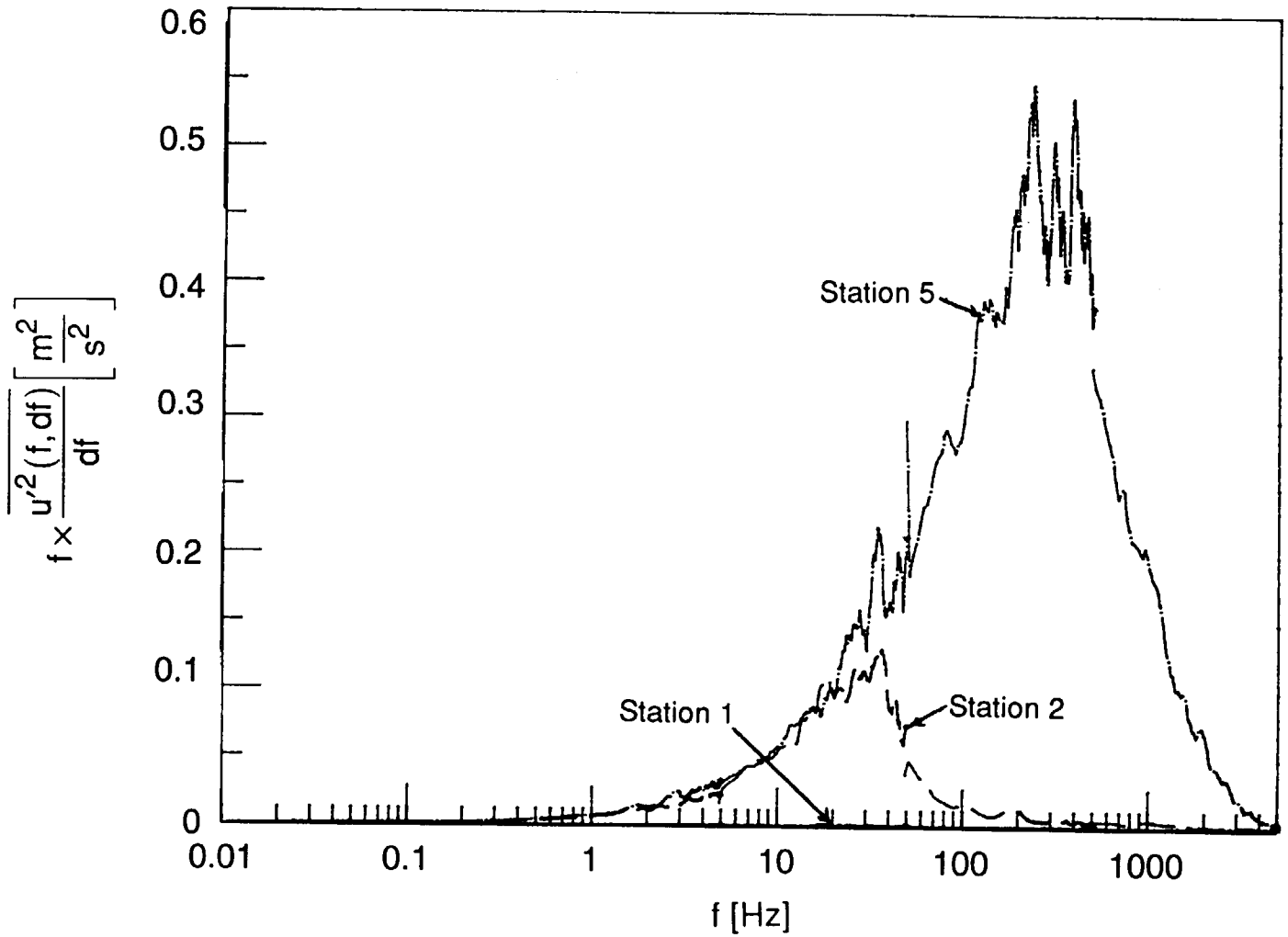

Fig. 3.4b: Boundary Layer u′ Spectra at y^+=6, Low FSTI Case, Energy Coordinates

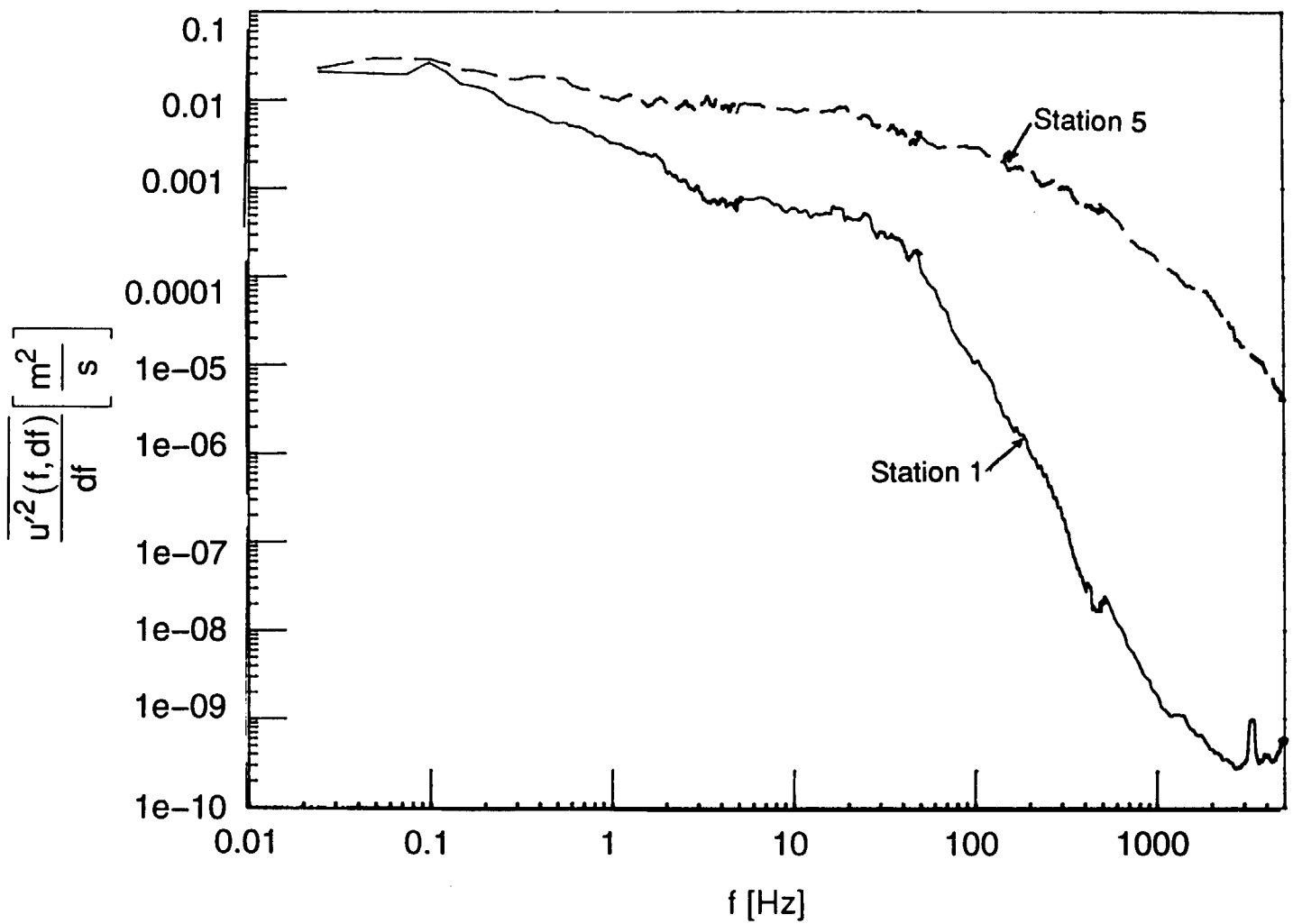

Fig. 3.5a: Boundary Layer u′ Spectra at y+=35, Low FSTI Case

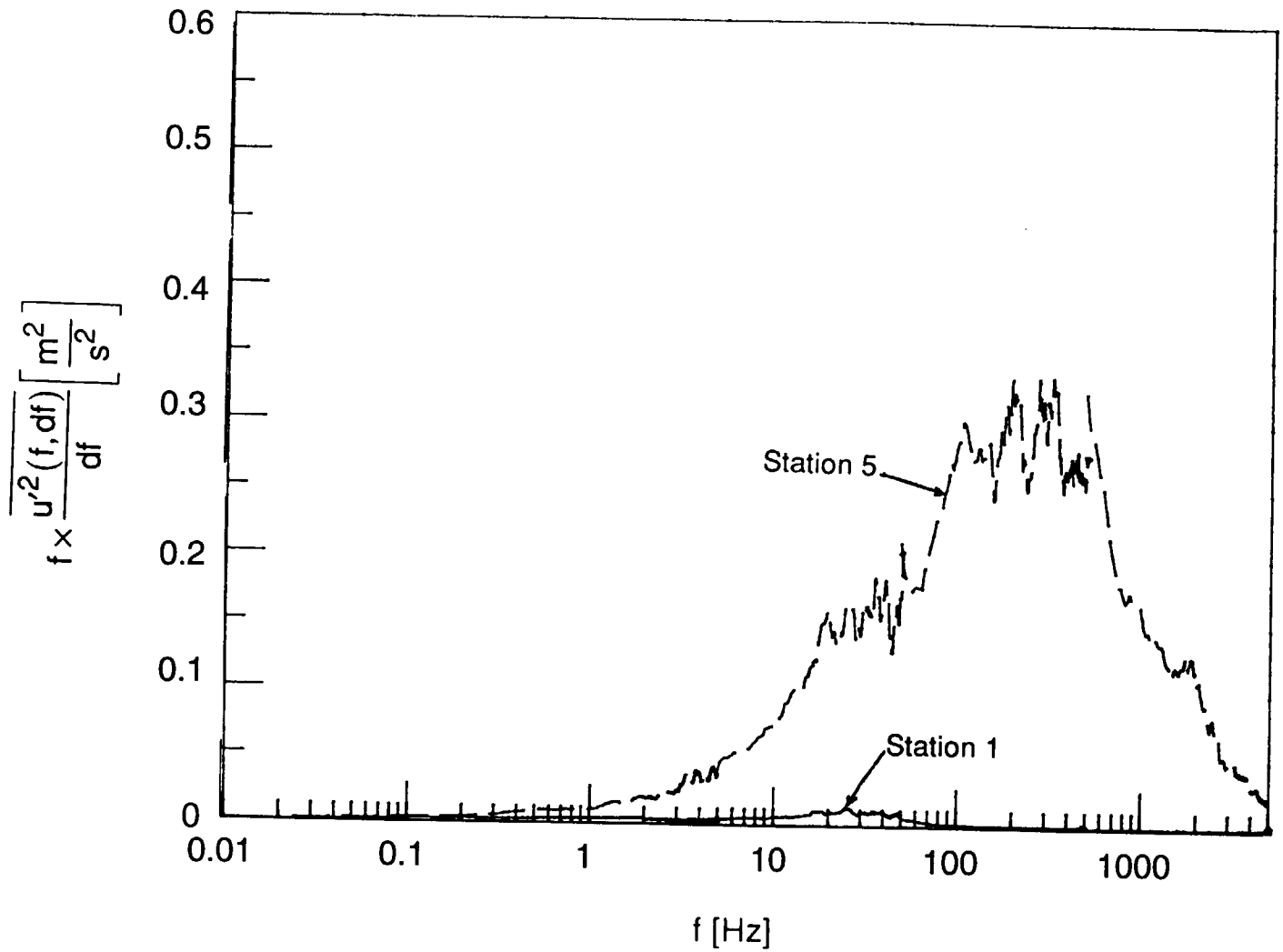

Fig. 3.5b: Boundary Layer u′ Spectra at y^+=35, Low FSTI Case, Energy Coordinates

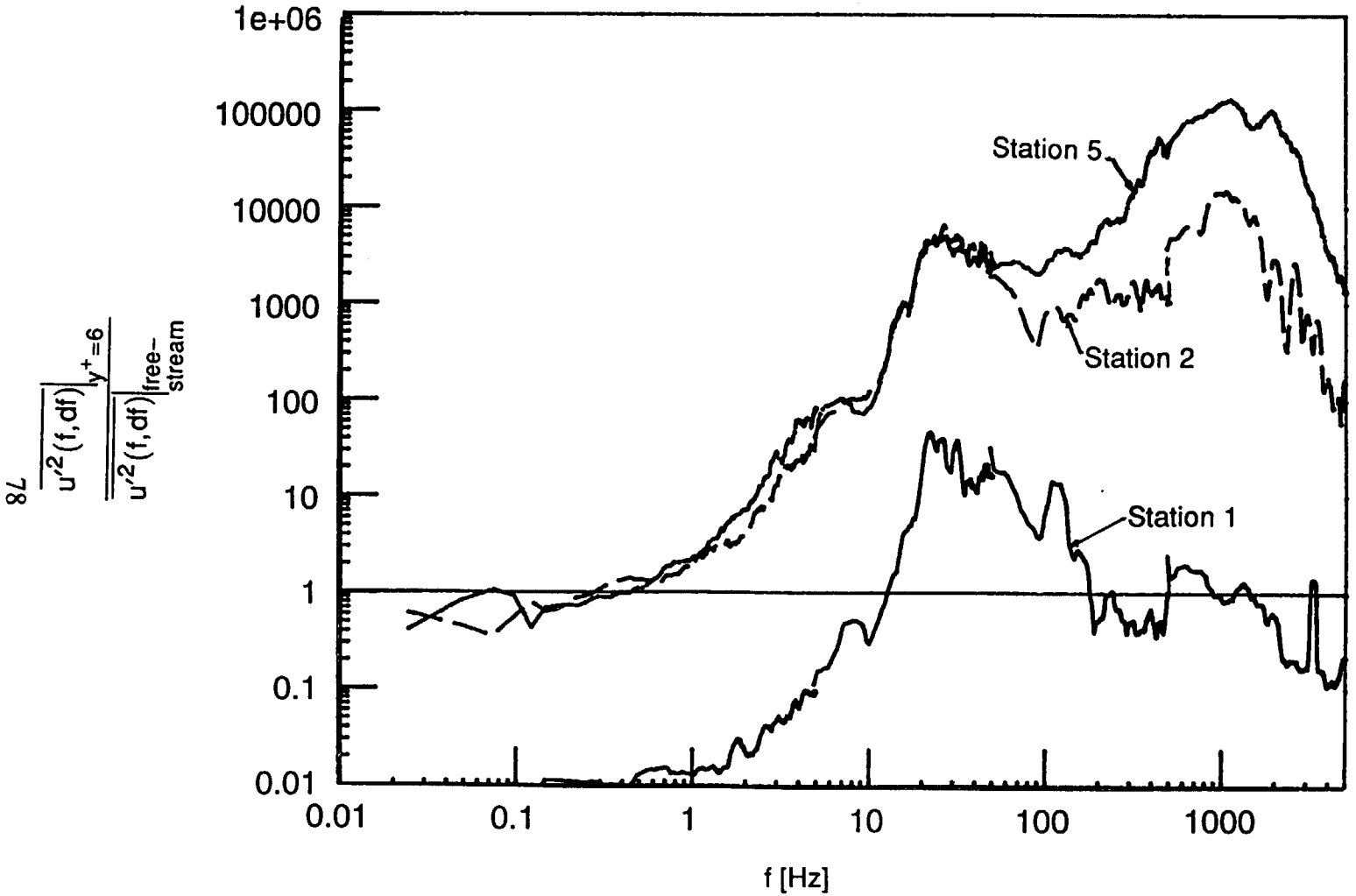

Fig. 3.6: Transfer Function of u′ Between $y^+=6$ and Free-Stream, Low FSTI Case

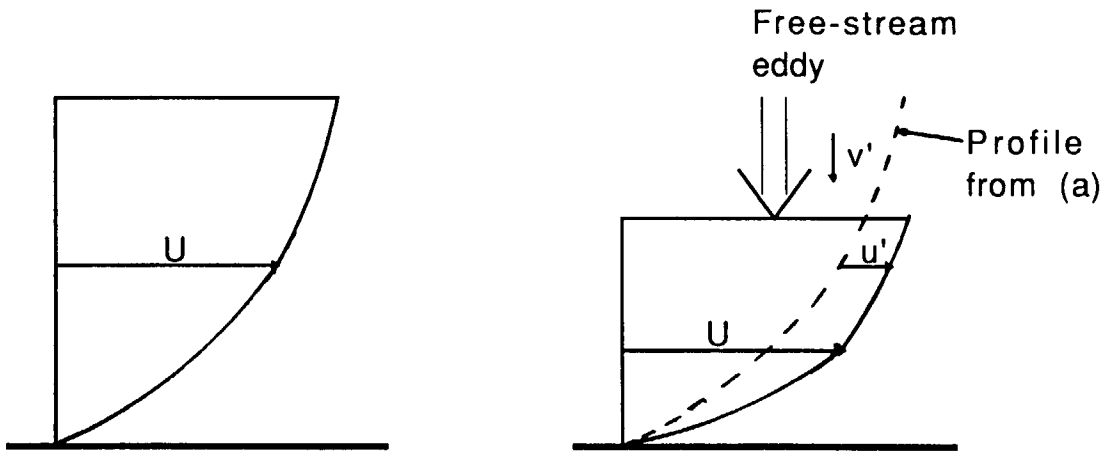

(a) undisturbed profile

(b) profile disturbed by free-stream eddy

Fig. 3.7: Depiction of u′ Caused by Large-Scale Free-Stream Eddies Buffeting the Boundary Layer

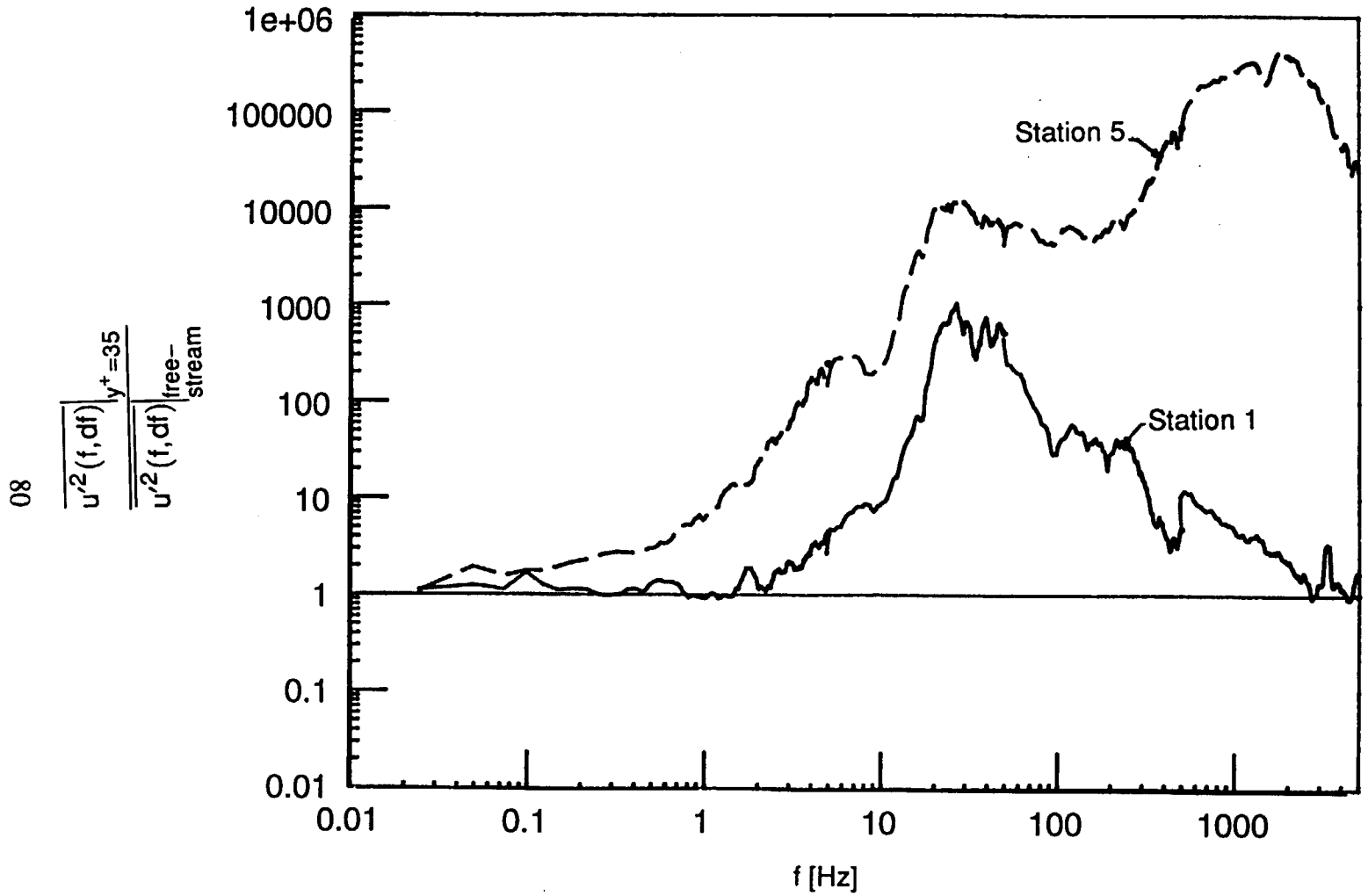

Fig. 3.8: Transfer Function of u′ Between y^+=35 and Free-Stream, Low FSTI Case

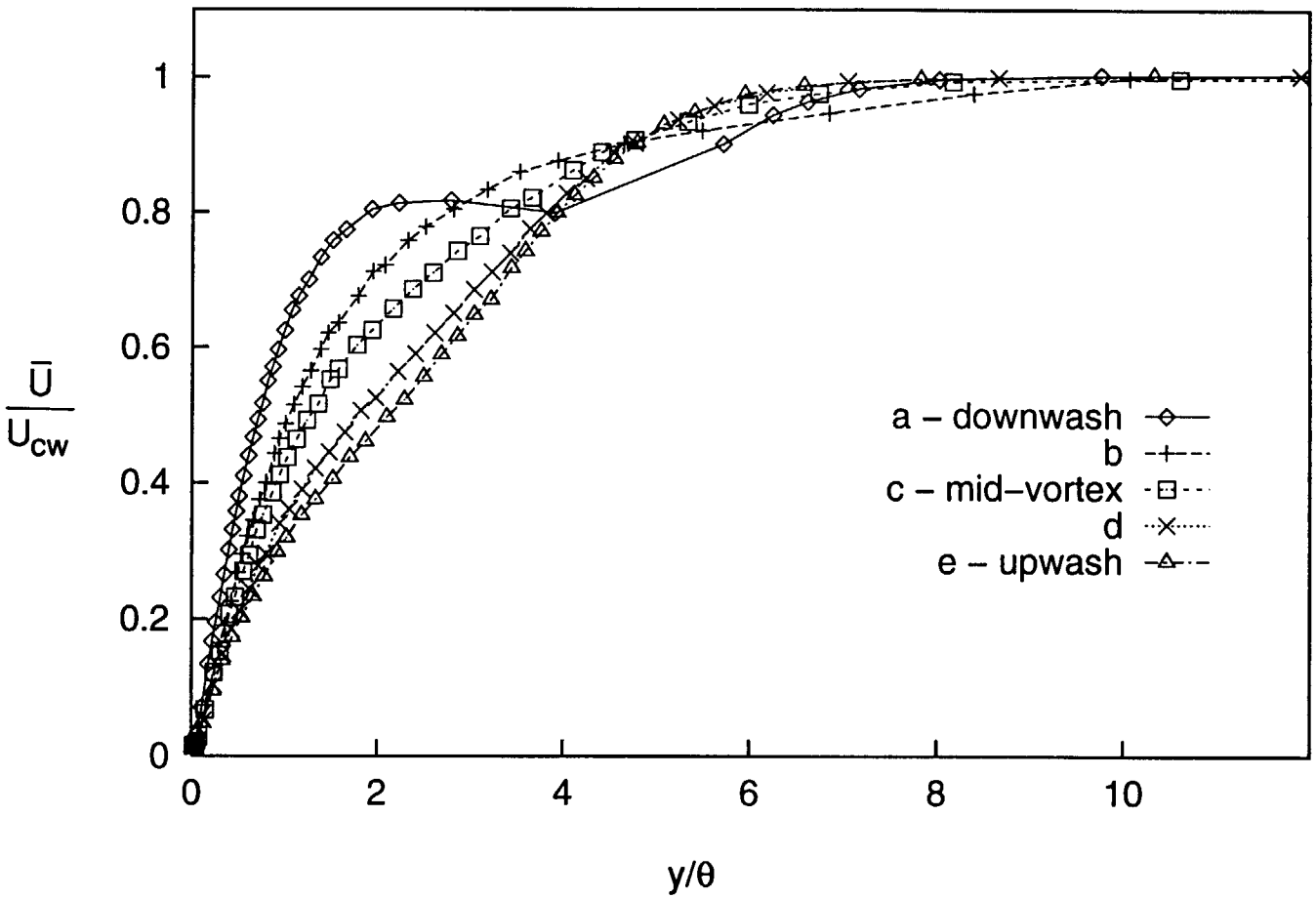

Fig. 3.9a: Mean Streamwise Velocity Profiles at Lowest Re_x (=3.7×10^5), Low FSTI Case

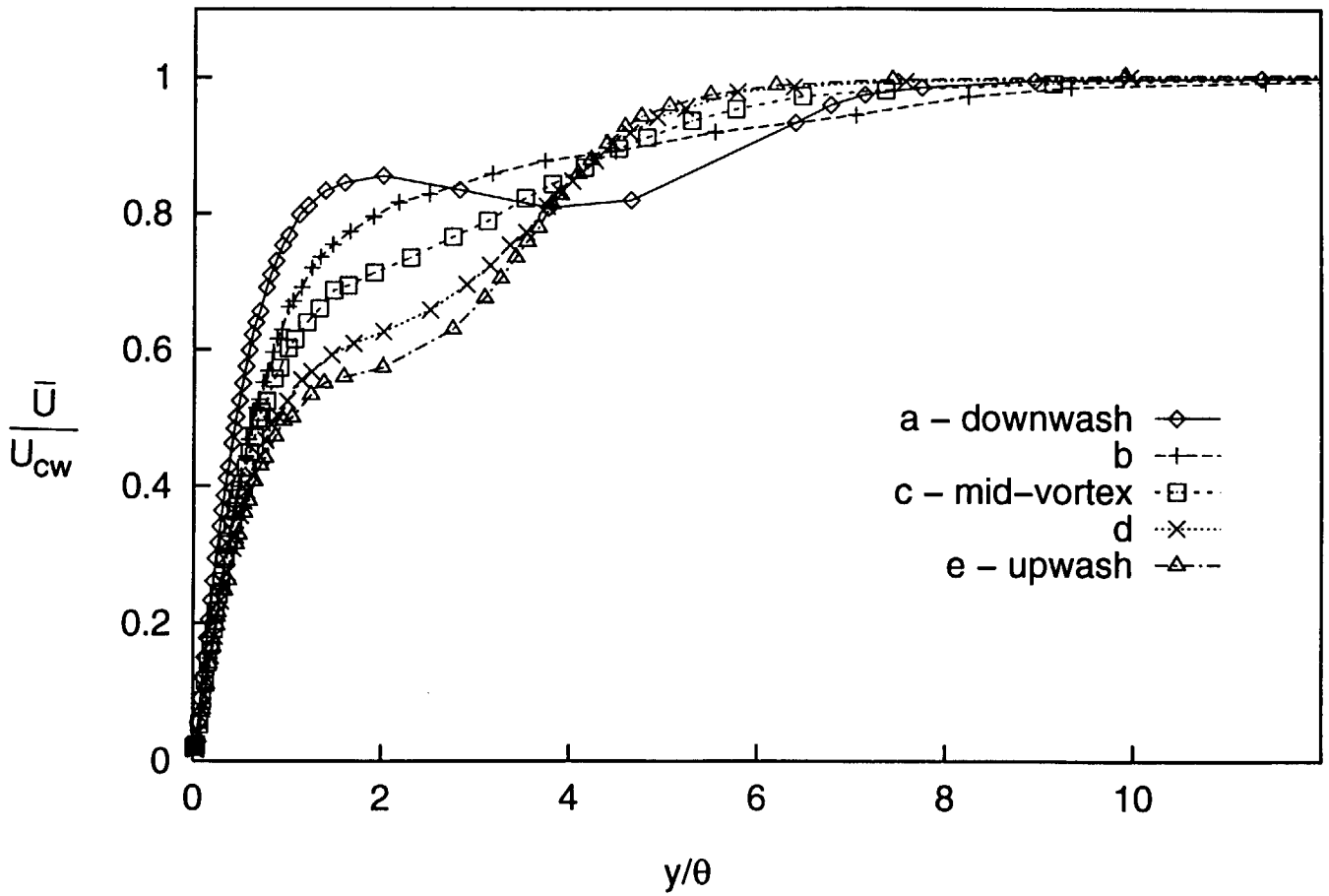

Fig. 3.9b: Mean Streamwise Velocity Profiles at Highest Re_x (=4.4×10^5), Low FSTI Case

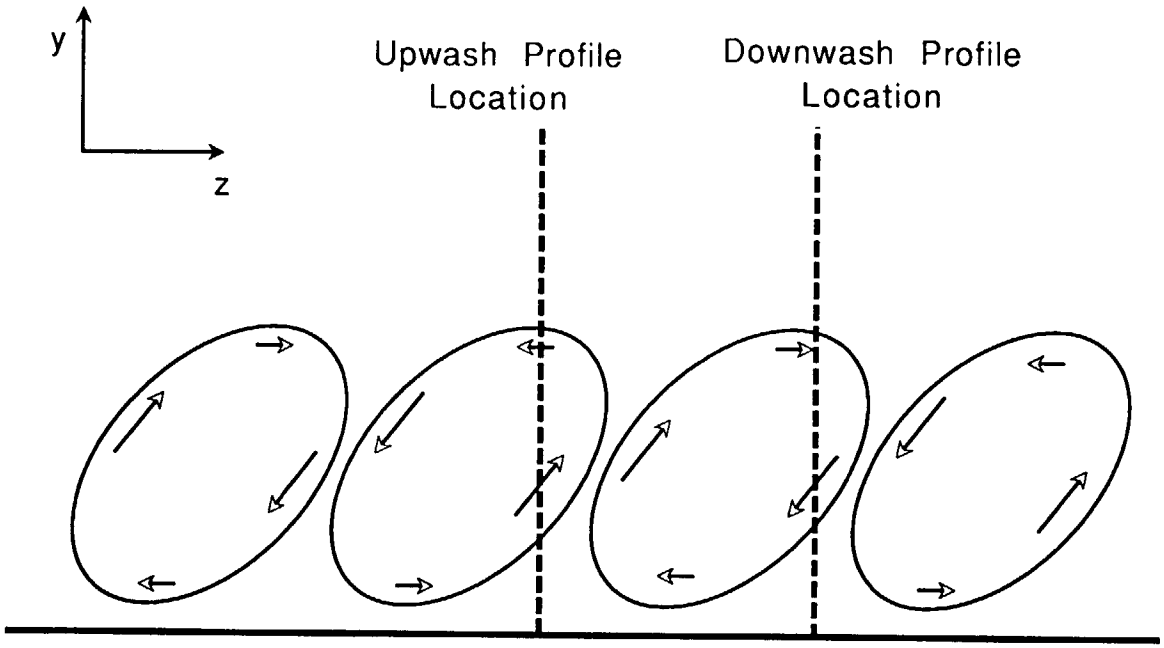

Fig. 3.10: Upwash and Downwash Profiles Cutting Through "Tilted" Vortices

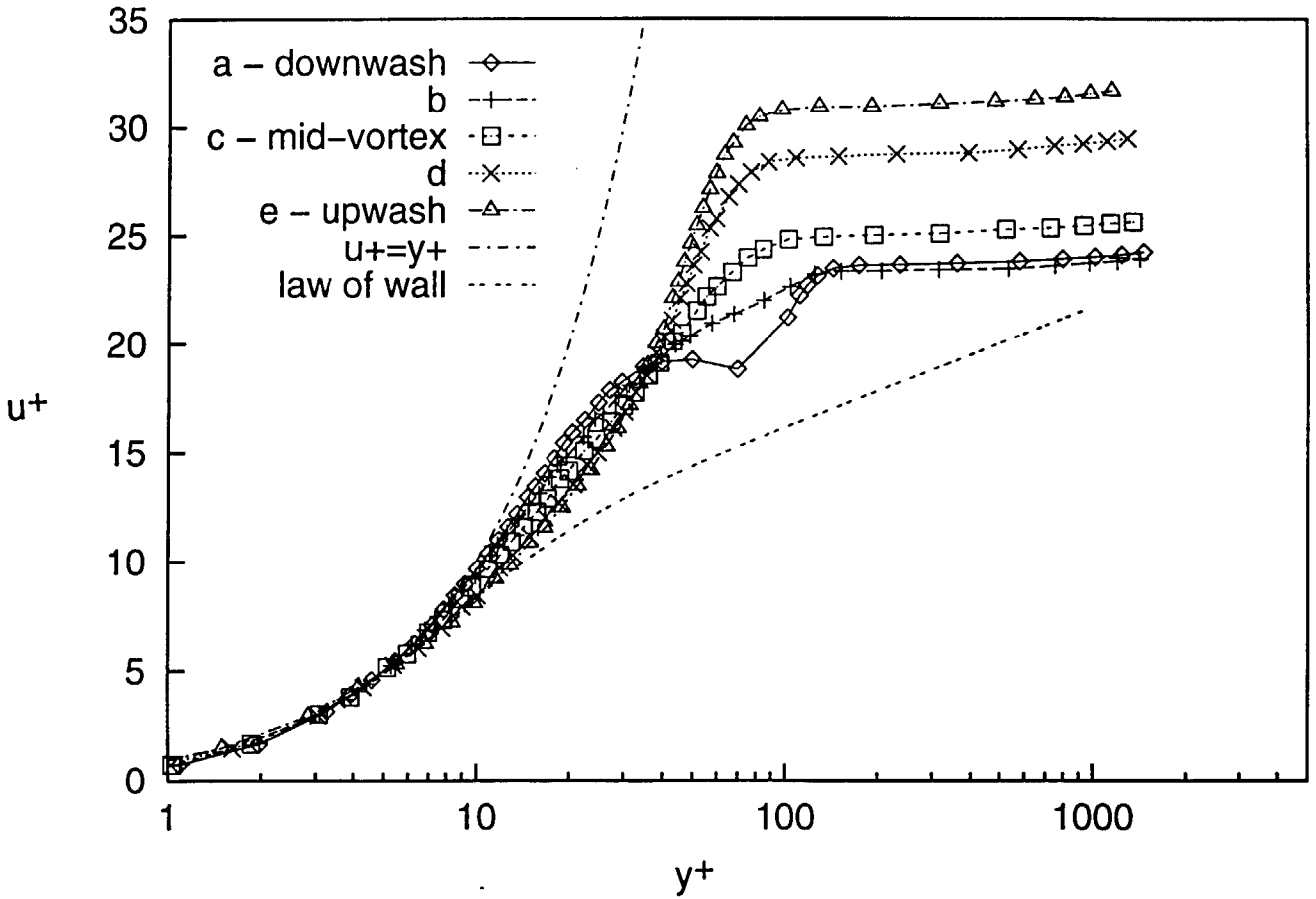

Fig. 3.11a: Mean Streamwise Velocity Profiles at Lowest Re_x (=3.7×10^5), Low FSTI Case, wall coordinates

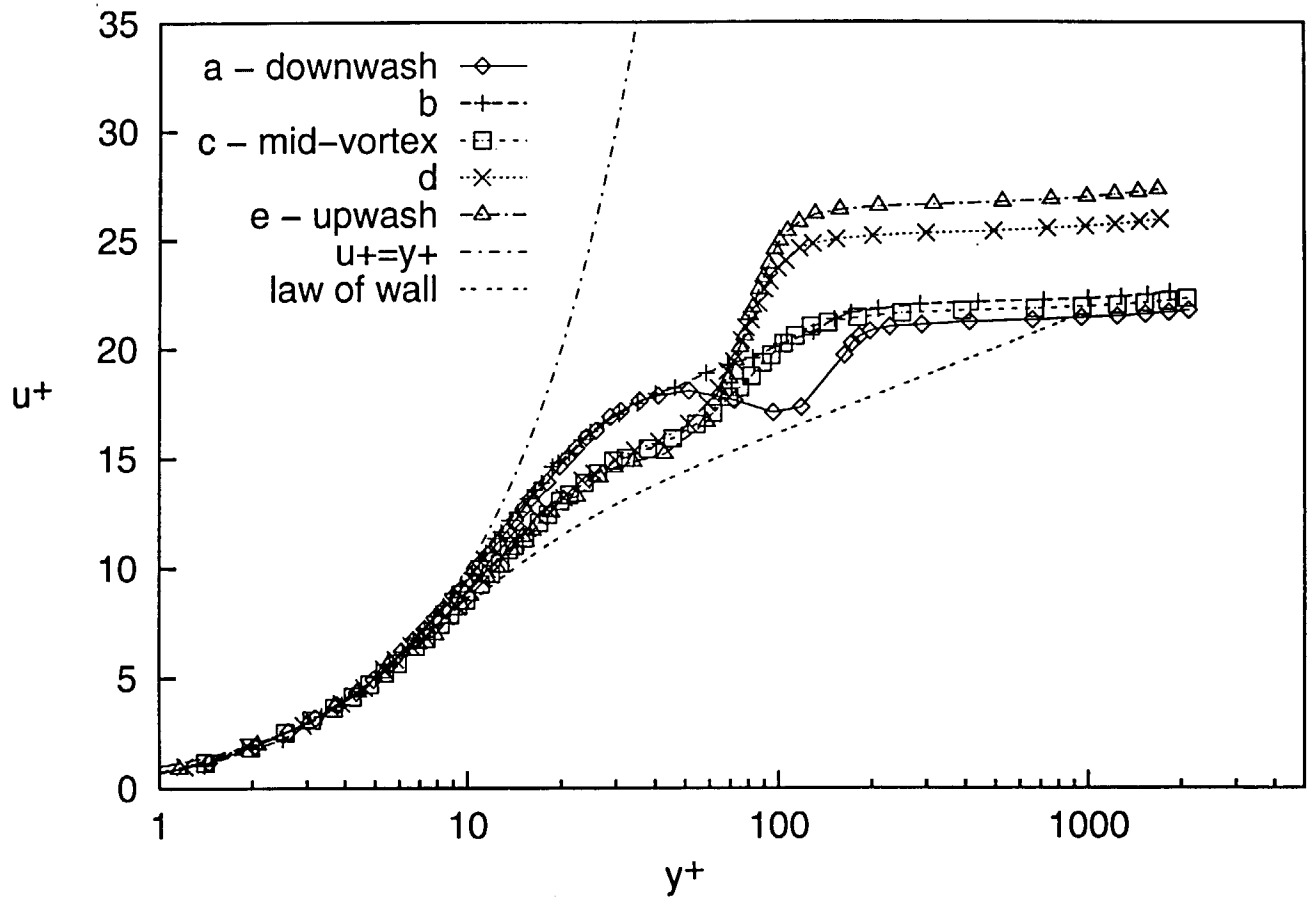

Fig. 3.11b: Mean Streamwise Velocity Profiles at Highest Re_x (=4.4×10^5), Low FSTI Case, wall coordinates

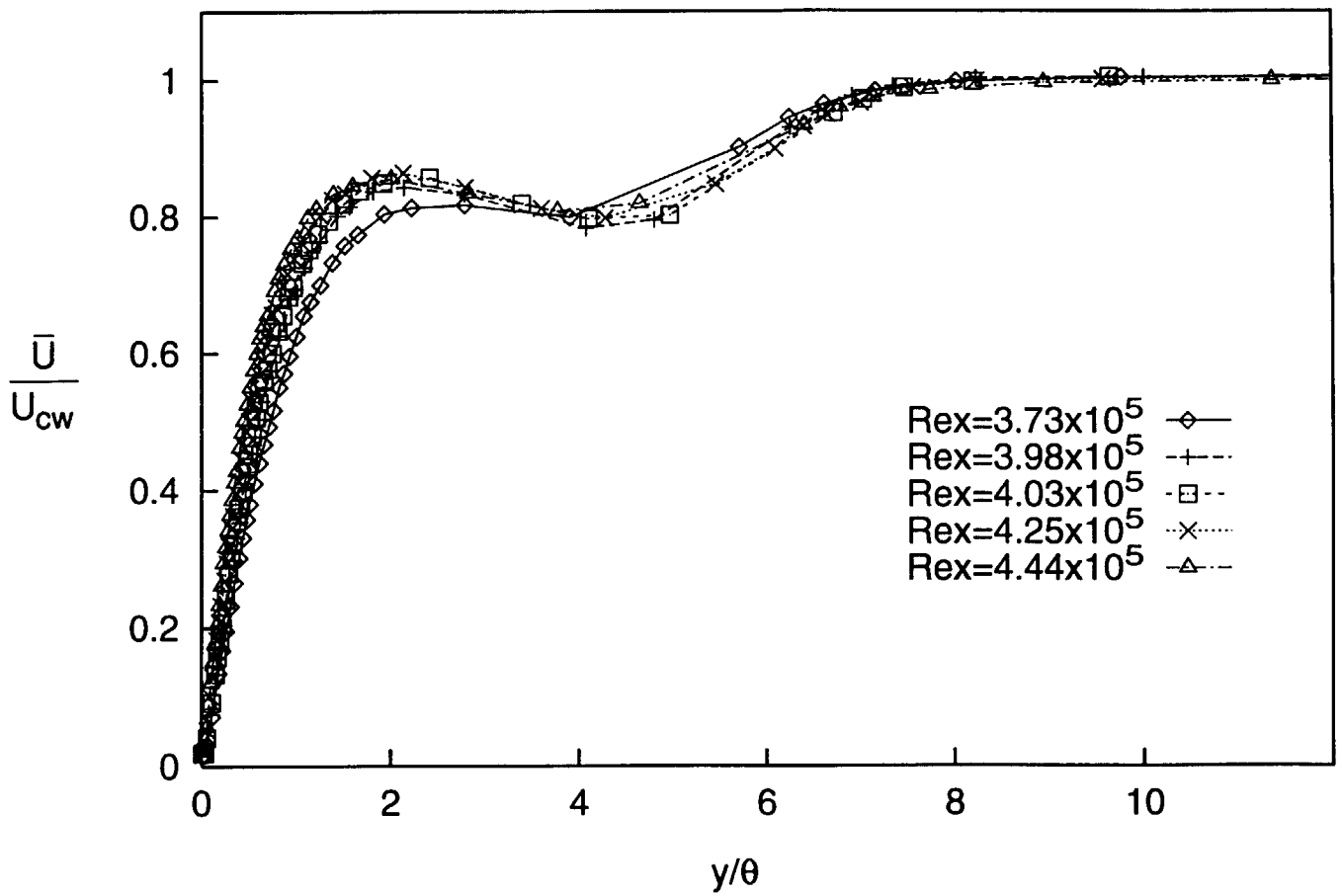

Fig. 3.12a: Mean Streamwise Velocity Profiles at Downwash Locations, Low FSTI Case

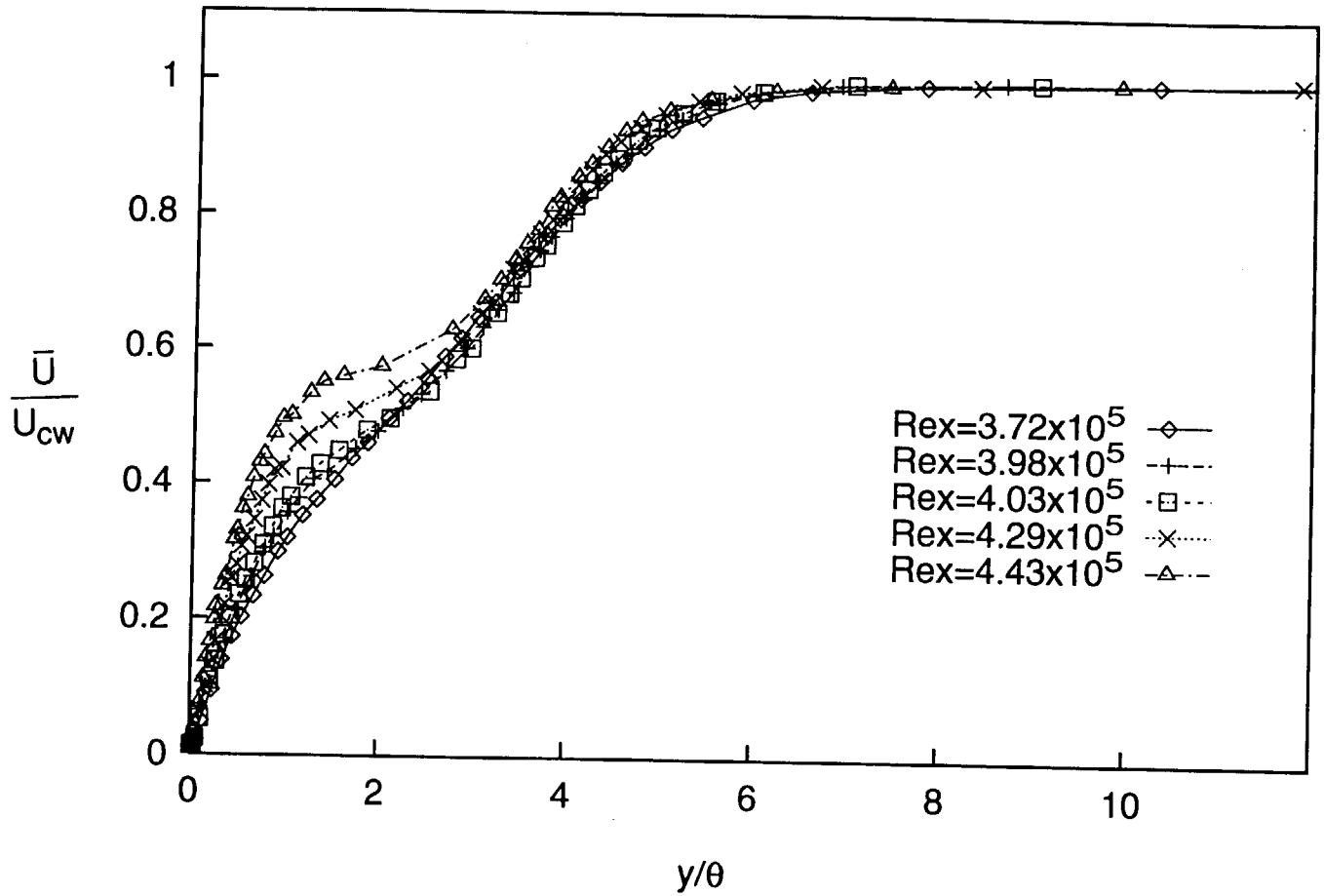

Fig. 3.12b: Mean Streamwise Velocity Profiles at Upwash Locations, Low FSTI Case

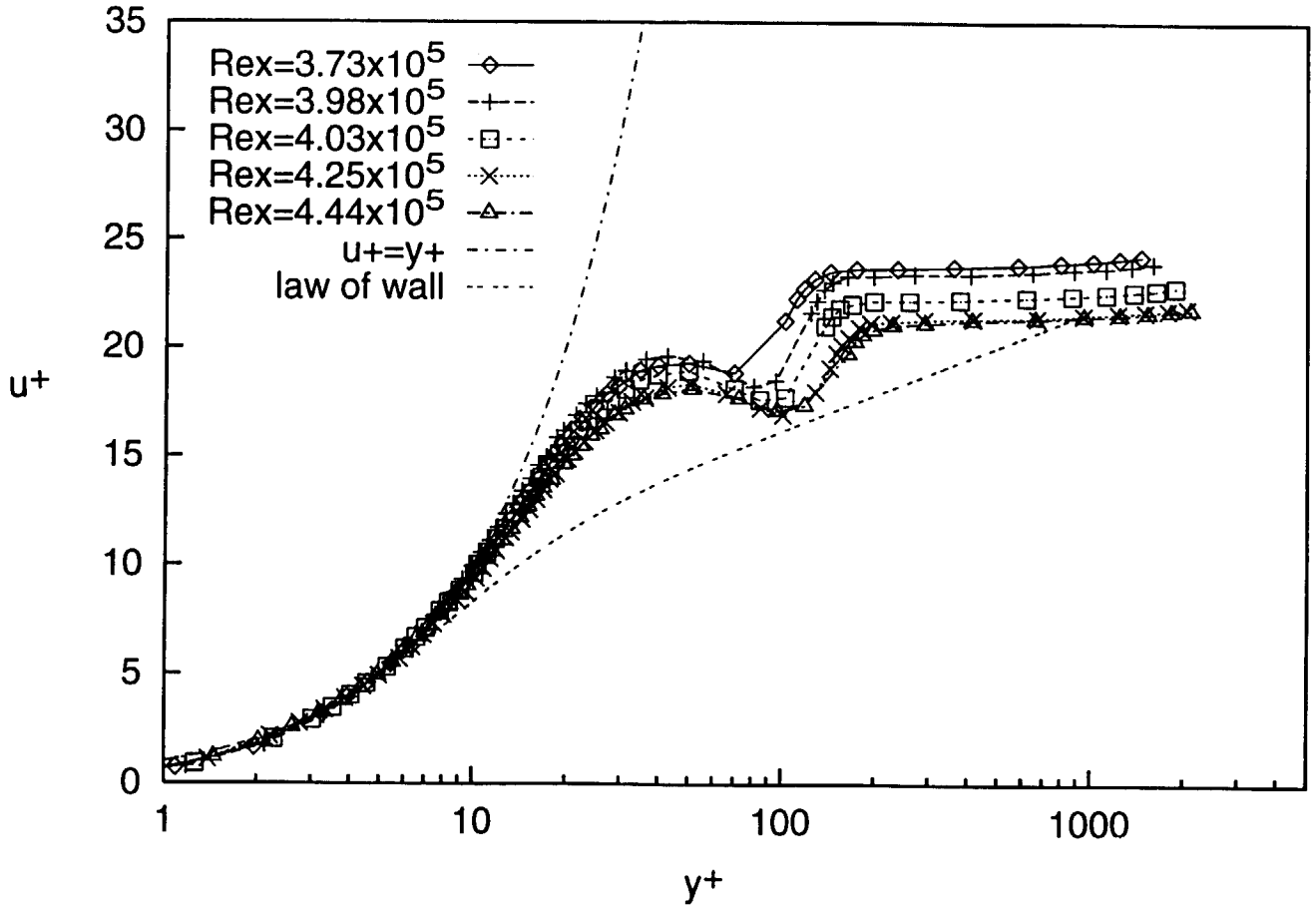

Fig. 3.13a: Mean Streamwise Velocity Profiles at Downwash Locations, Low FSTI Case, wall coordinates

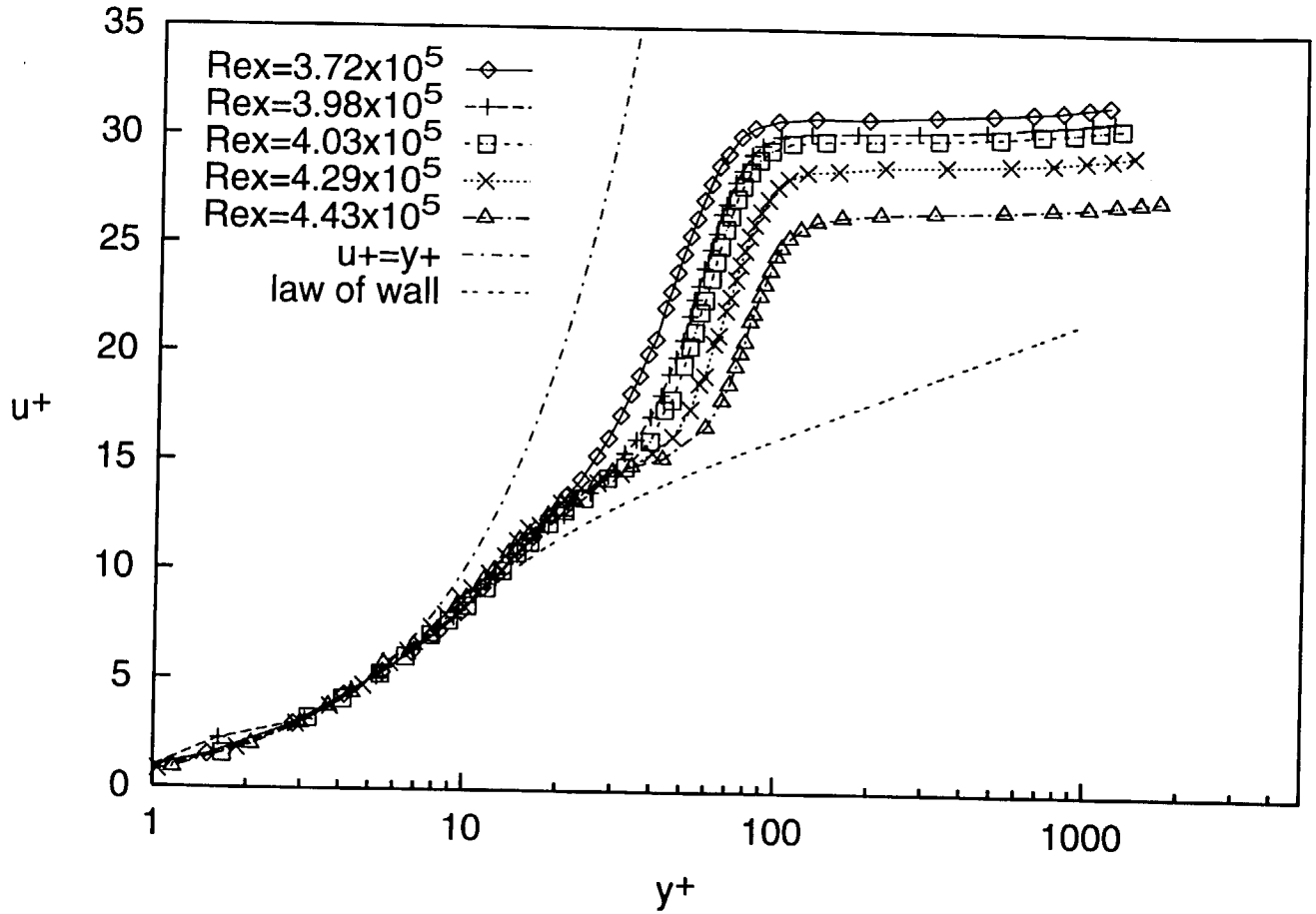

Fig. 3.13b: Mean Streamwise Velocity Profiles at Upwash Locations, Low FSTI Case, wall coordinates

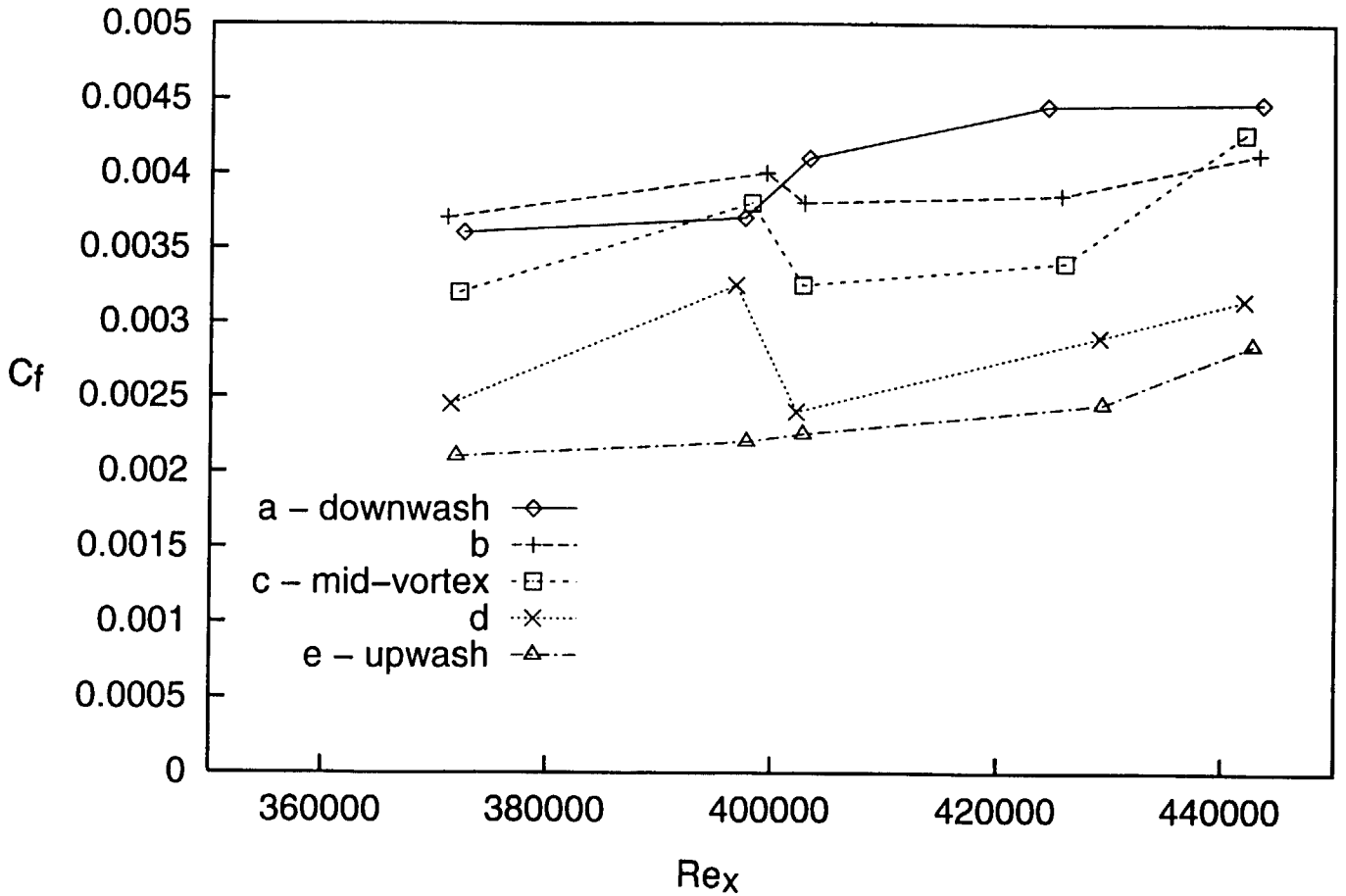

Fig. 3.14a: Skin Friction Coefficient vs Re_x, Low FSTI Case

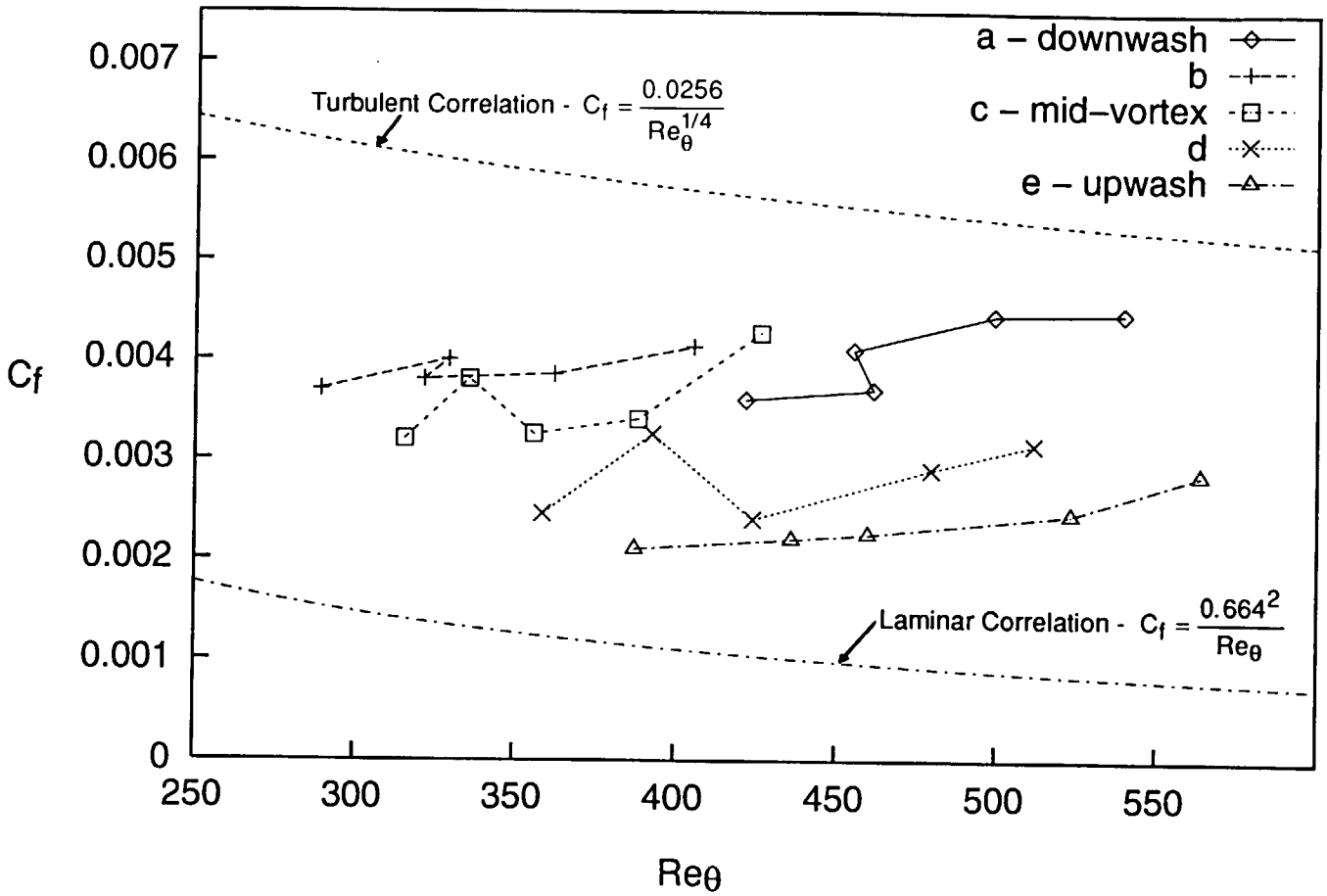

Fig. 3.14b: Skin Friction Coefficient vs Re_θ, Low FSTI Case

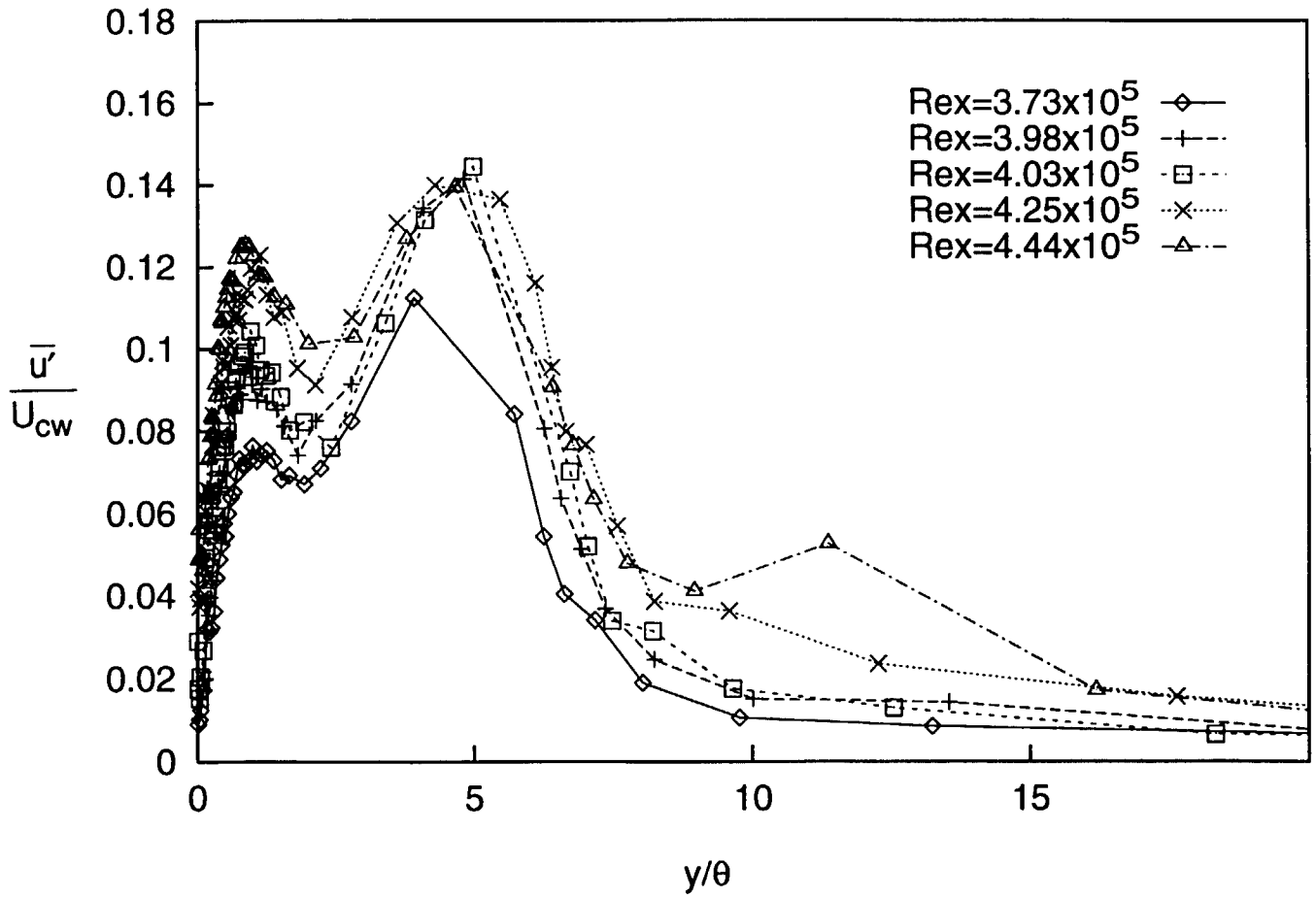

Fig. 3.15a: Fluctuating Streamwise Velocity Profiles at Downwash Locations, Low FSTI Case

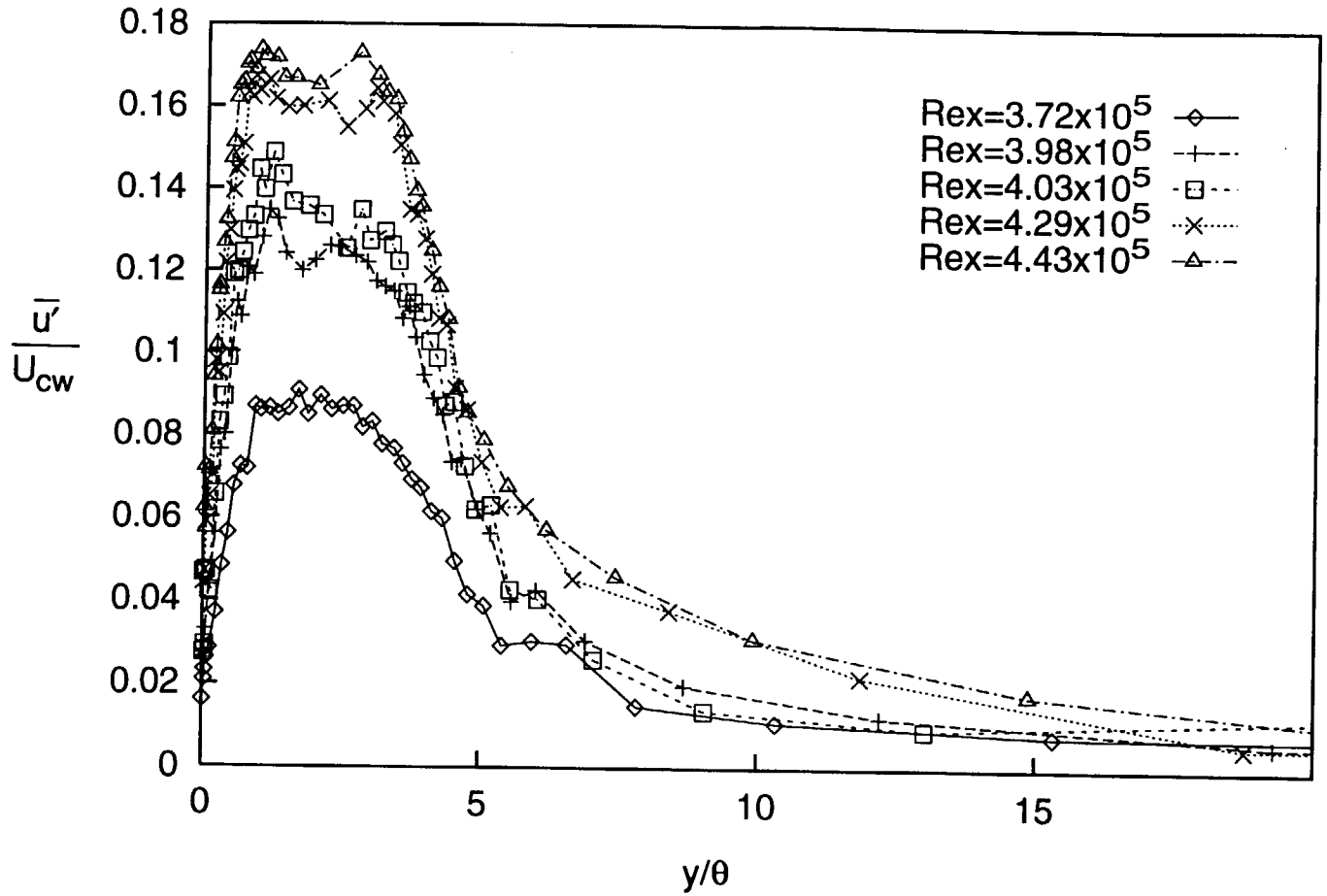

Fig. 3.15b: Fluctuating Streamwise Velocity Profiles at Upwash Locations, Low FSTI Case

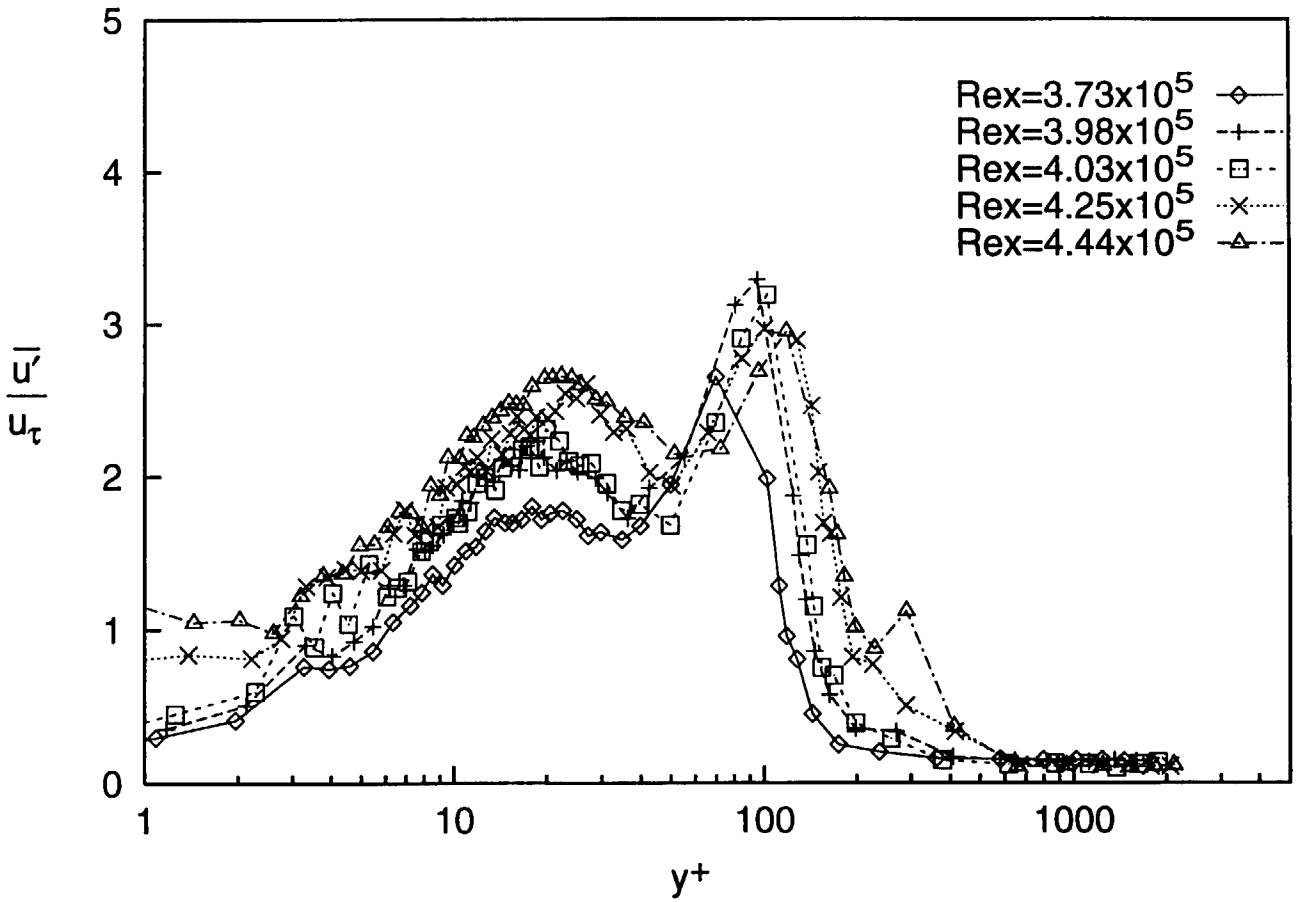

Fig. 3.16a: Fluctuating Streamwise Velocity Profiles at Downwash Locations, Low FSTI Case, wall coordinates

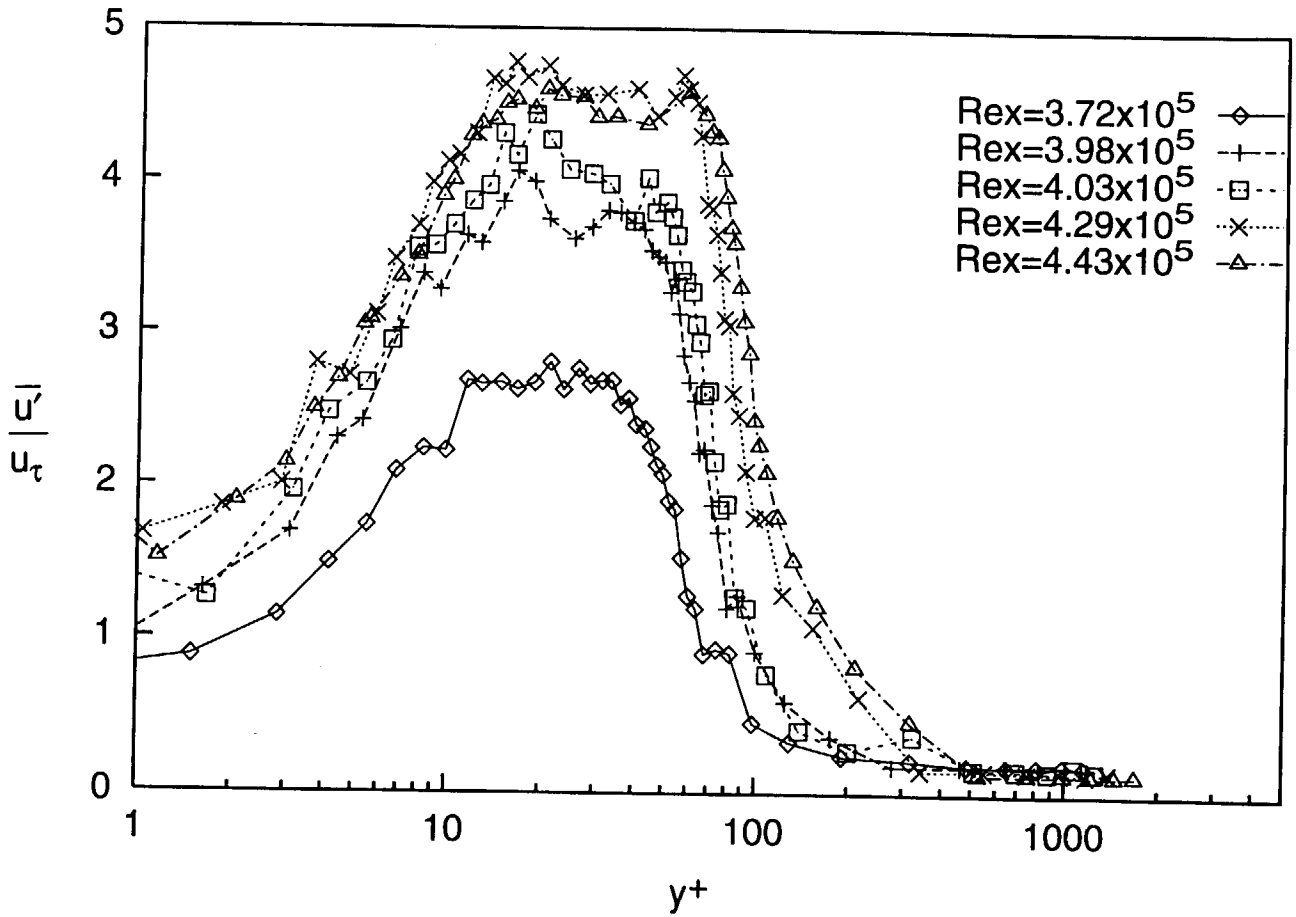

Fig. 3.16b: Fluctuating Streamwise Velocity Profiles at Upwash Locations, Low FSTI Case, wall coordinates

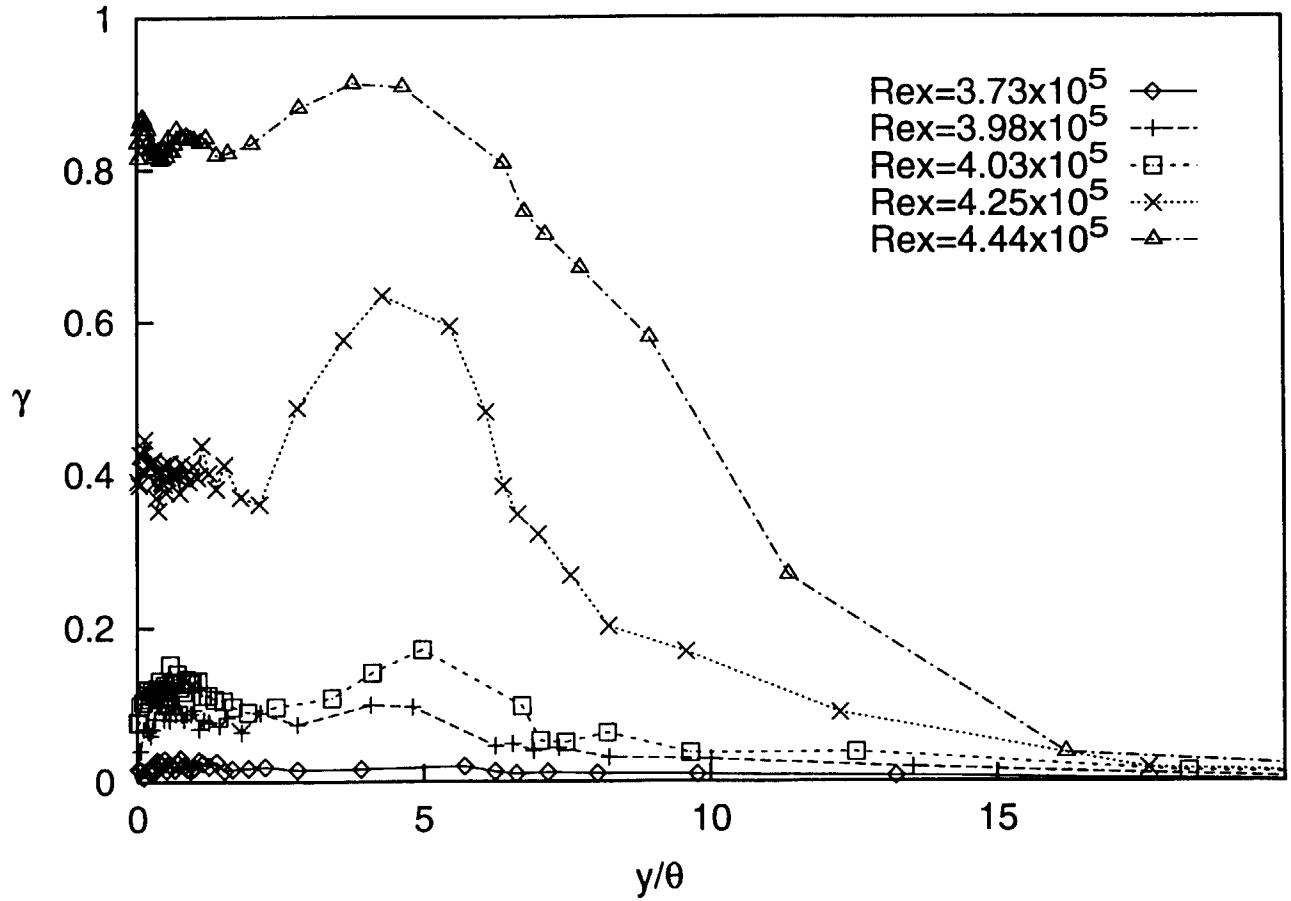

Fig. 3.17a: Intermittency Profiles at Downwash Locations, Low FSTI Case

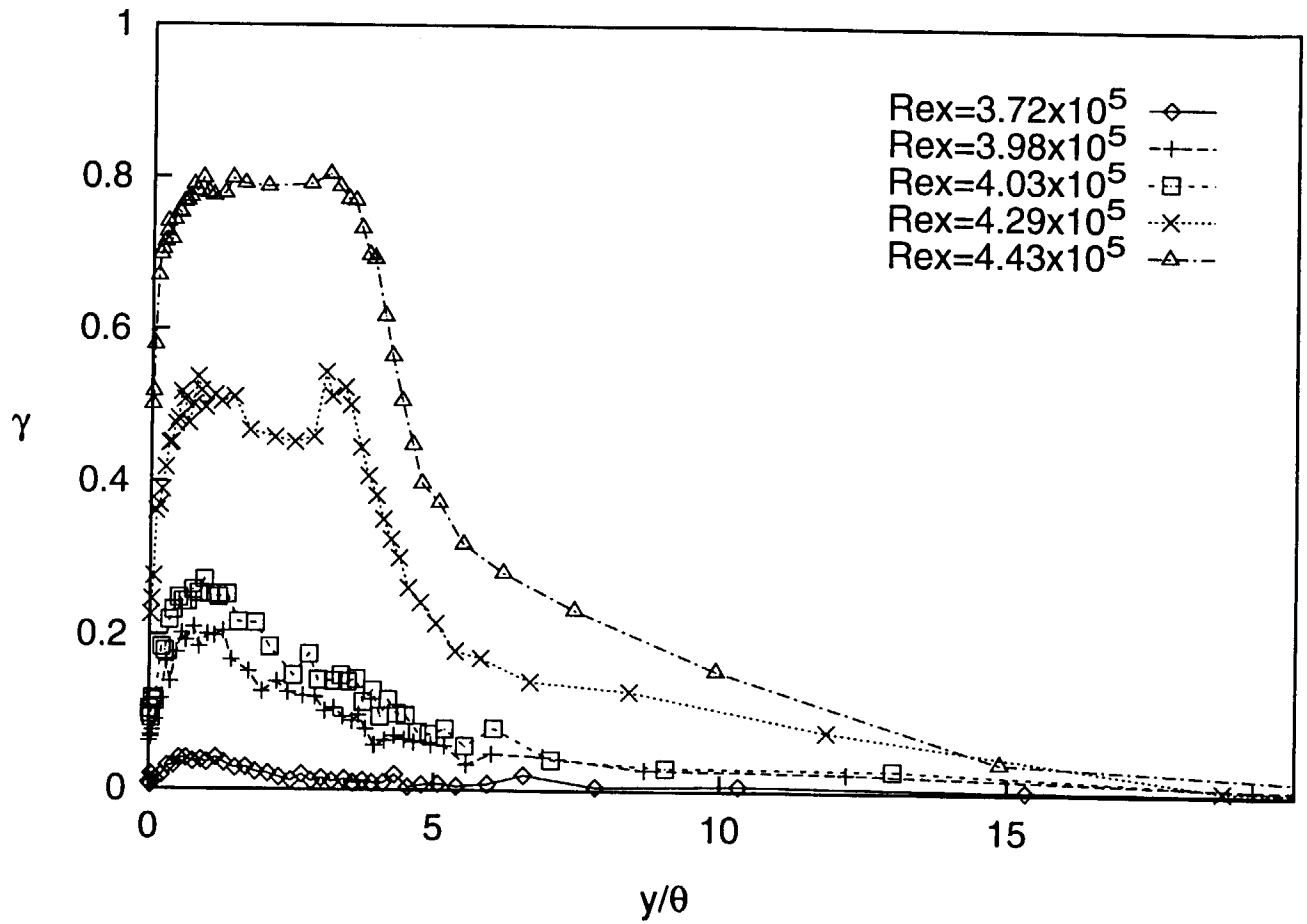

Fig. 3.17b: Intermittency Profiles at Upwash Locations, Low FSTI Case

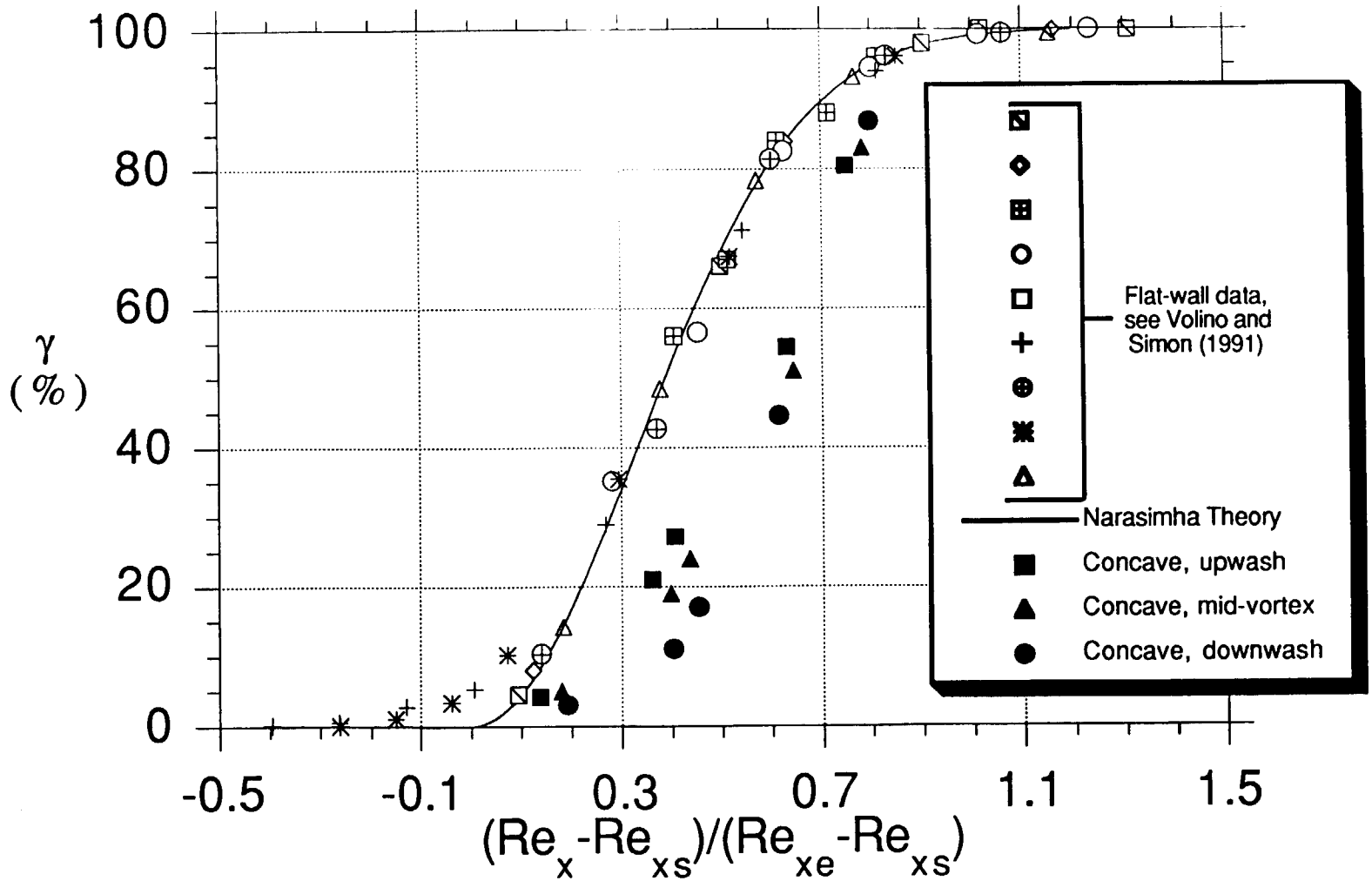

Fig. 3.18: Intermittency Distributions Through Transition

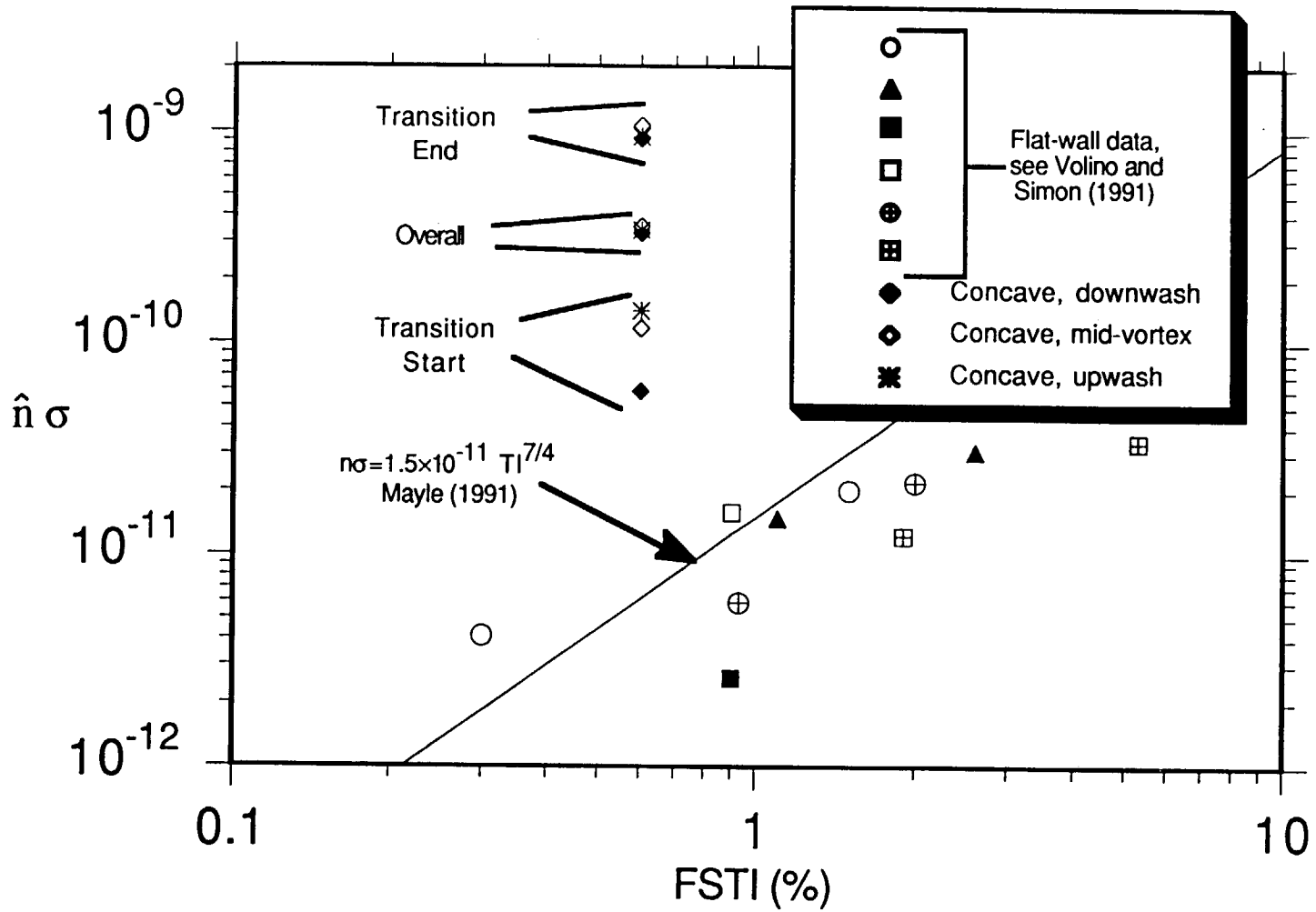

Fig. 3.19: Turbulent Spot Production Rate Based on γ

CHAPTER 4: AN APPLICATION OF OCTANT ANALYSIS TO TURBULENT AND TRANSITIONAL FLOW DATA

SUMMARY

A technique called "octant analysis" was used to examine the eddy structure of turbulent and transitional heated boundary layers on flat and curved surfaces. The intent was to identify important physical processes that play a role in boundary layer transition on flat and concave surfaces. Octant processing involves the partitioning of flow signals into octants based on the instantaneous signs of the fluctuating temperature, t'; streamwise velocity, u'; and cross-stream velocity, v'. Each octant is associated with a particular eddy motion. For example, $u'<0$, $v'>0$, $t'>0$ is associated with an ejection or "burst" of warm fluid away from a heated wall. Within each octant, the contribution to various quantities of interest (such as the turbulent shear stress, $-\overline{u'v'}$, or the turbulent heat flux, $\overline{v't'}$) can be computed. By comparing and contrasting the relative contributions from each octant, the importance of particular types of motion can be determined. If the data within each octant are further segregated, based on the magnitudes of the fluctuating components, so that minor events are eliminated, the relative importance of particular types of motion to the events that are important can also be discussed. In fully-developed, turbulent boundary layers along flat plates, trends previously reported in the literature were confirmed. A fundamental difference was observed in the octant distribution between the transitional and fully-turbulent boundary layers, however, showing incomplete mixing and a lesser importance of small scales in the transitional boundary layer. Such observations were true on both flat and concave walls. The differences are attributed to incomplete development of the turbulent kinetic energy cascade in transitional flows. The findings have potential application to modeling, suggesting the utility of incorporating multiple length scales in transition models. The data presented below are from unaccelerated flow cases. Most of

the information can also be found in Volino and Simon (1994c). Additional octant analysis results from accelerated flows are presented below in Chapters 6 and 7.

INTRODUCTION

Turbulent flow has long been known to contain considerable structure. Flow visualization shows the presence of turbulent eddies, near-wall "streaks" and "bursts", turbulent spots in transitional flow, and other structures. More recently, full Navier-Stokes solutions have reproduced these structures computationally. These structures play important roles in the overall flow behavior. Turbulent eddies, for example, are responsible for the high level of mixing (eddy transport) in turbulence, which would not be present if the turbulent fluctuations were completely uncorrelated.

Most efforts to document turbulent structure have concentrated on mean transport quantities, such as the turbulent shear stress, $-\overline{u'v'}$, and the turbulent heat flux, $\overline{v't'}$. These quantities provide important information about effective mixing within particular flows, but they offer only limited information about the actual eddy structure which produces the effective mixing. Turbulence models derived from mean transport measurements in one flow should be applicable only to flows with similar eddy structure. If a model derived from one flow were applied to a flow with a fundamentally different structure, there is good reason to expect a poorer prediction of the mean transport quantities and, thus, poorer prediction of the overall flow behavior. Fortunately, there appears to be considerable similarity in the structure of many turbulent flows. This has allowed development of rather robust turbulence models. There are, however, some important situations such as transitional flows where conventional models seem to be lacking of important physics, as documented by Schmidt and Patankar (1991) and Rodi and Scheuerer (1985). In at least some of these cases, the reason for the poor performance may be a difference in the flow structure. There is, therefore, a need for a more detailed study of flow structure in transitional flow. A better understanding of the flow will help provide

explanations for some of the unexpected behavior seen in experiments and point the way toward development of better computational models.

QUADRANT AND OCTANT ANALYSES

One means of investigating flow structure is the quadrant analysis. It was first used approximately twenty years ago by researchers such as Wallace et al. (1972) and Willmarth and Lu (1972). The technique involves partitioning of the flow signal into four quadrants, based on the instantaneous signs of the fluctuating velocity components u' and v'. Each quadrant is associated with a particular eddy motion. In quadrant 2, for example, low streamwise momentum (relative to the mean) fluid is moving with high cross-stream momentum (relative to the mean). In a turbulent boundary layer, this motion is attributed to turbulent "bursts" originating near the wall. The contribution to a quantity of interest (e.g. $-\overline{u'v'}$) is then calculated for each quadrant based on the data points which lie within it.

$$\left(\overline{u'v'}\right)_1 = \frac{1}{N}\left[\sum_1^N Iu'v'\right]_1 \tag{4.1}$$

where I=1 if the point is within quadrant 1 (zero otherwise) and N is the total number of points (all quadrants). A data point refers to an instantaneous u-v pair. The relative contributions from the four quadrants can then be compared to show which eddy motions are more important. The turbulent shear stress is the sum of the contributions from the four quadrants.

The quadrant analysis data can be further partitioned, based on the "strength" of the entries. One method of doing this uses the following filter function given by Willmarth and Lu (1972):

$$\overline{u'v'}_i = \frac{\sum_{j=1}^{N} I u'v'_i}{N} \quad \text{where} \quad I = \begin{cases} 1 \text{ if } u'v' \text{ lies in quadrant i} \\ \text{and } |u'v'| > |H'\overline{u'v'}| \\ \\ 0 \text{ otherwise} \end{cases} \tag{4.2}$$

H' is termed the hole size parameter, and $\overline{u'v'}_i$ is the contribution to $\overline{u'v'}$ from that portion of quadrant i which is outside the hole described by the parameter H'. When $H'=0$, Eqn. (4.2) becomes (4.1). For large H', only the strongest eddies are considered, as shown in the I function definition of Eqn. (4.2).

Quadrant analyses can be extended in heated flows by inclusion of the temperature fluctuations, t'. If both positive and negative values of u', v' and t' are considered, eight possible combinations arise. The eight-way partitioning will be referred to as octant separation and the technique is called the octant analysis. The octants are identified using names assigned by Kawaguchi et al. (1984) as shown in Fig. 4.1. Figure 4.2 is a conceptual drawing of the eddies responsible for the motion in each octant.

In a fully-developed turbulent boundary layer on a heated flat plate, octants 4 and 6 should be the most significant. A turbulent "parcel" of fluid moving away from the wall ($v'>0$)† would most likely be of relatively low velocity ($u'<0$) and high temperature ($t'>0$), when the wall is heated. Such a motion would be characteristic of a turbulent burst and would be classified as a hot ejection (octant 6). Similarly, a fluid packet moving toward the wall ($v'<0$) would most likely have originated in the faster ($u'>0$), cooler ($t'<0$) fluid away from the wall. Such a motion, a cold sweep (octant 4), would be expected after a hot ejection as fluid moves in to replace that which had left. Motions in all eight octants would be present but on the average the hot ejections and cold sweeps should be the largest contributors to quantities of interest. This is confirmed by the measurements of Suzuki et al. (1988) and those of the present study.

---

† $\overline{V} \approx 0$ is assumed when stating that $v'>0$ indicates motion away from the wall. This is satisfactory for discussing boundary layers. It must be remembered, however, that u', v' and t' are given relative to the mean quantities at the probe location.

The above simple representation of turbulent flows, depicting them as a series of predominantly ejections and sweeps, agrees with the assumptions used in most turbulence models. The arguments are basically those of the Prandtl mixing length model. In many cases they provide an adequate description of the eddy structure. In cases where they do not, differences become apparent in the octant analysis. Suzuki et al. (1988), for example, placed a heated horizontal cylinder normal to the flow direction above a heated flat wall. The thermal boundary conditions at the cylinder surface and on the wall were the same. Given the similarity in the heat and momentum boundary conditions, one might expect the presence of the cylinder to have similar effects on the wall heat transfer and skin friction. Surprisingly, the wall heat transfer was augmented, but the skin friction was not. An octant analysis showed a jump in the significance of octant 5, the hot outward interaction, when the cylinder was added. The increased significance of this octant agrees with the wall heat transfer and skin friction behavior and explains the dissimilarity between the near-wall heat and momentum transport rates.

In the present study the flow structures of two-dimensional heated boundary layers with zero streamwise pressure gradients are considered. The data used for this study include both new data and data taken in earlier studies: Kim (1986), Kim and Simon (1988), Kim et al. (1992, 1994) and Kim and Simon (1991) using triple wire probes. The three wires of the probes were used to measure instantaneous U, V and T. Details of the wind tunnel, probes, measurement techniques and flow conditions, as well as presentations of the processed data, including profiles of mean velocities, temperatures, and transport quantities, are available in those references. New measurements taken for this study are described above in Chapter 2. Data were acquired using the same probe and essentially the same techniques as used by Kim and Simon (1991).

In this study, data were processed in terms of the octant analysis. The correlations $u'v'$, $v't'$, $u't'$, $u'v'^2$ and v'^2t' were calculated. The hole size, H', as used in Eqn. (4.2), was varied from 0 to 10. In total, seven separate cases of differing curvature,

boundary layer maturity and free-stream turbulence intensity (FSTI) were considered. On a flat wall, Kim and Simon (1991) studied boundary layers subject to FSTI values of 0.3%, 1.5% and 8.3%. The flow underwent natural transition in each case, and, at the upstream stations of the 0.3% and 1.5% FSTI cases, transitional profiles were obtained. The boundary layers at the other stations were fully turbulent. On a convex wall, with a radius of curvature of 90 cm, Kim (1986) acquired fully-turbulent boundary layer data at 0.68% and 2.0% FSTI. On a concave wall, with a radius of curvature of -97 cm, Kim and Simon (1991) acquired fully-turbulent boundary layer data at FSTI levels of 0.6% and 8.3%. Additional transitional boundary layer data, not previously reported, was acquired for the present study at an upstream location in the 0.6% FSTI concave-wall case. The FSTI values for the flat wall cases are based on the full spectra of the u', v' and w' fluctuations. For the curved wall cases, the FSTI are based on the full spectra of the u' and v' fluctuations. Because the data are extensive, only a sample is presented herein to demonstrate the utility of the octant technique and to show the most important effects of streamwise wall curvature, free-stream turbulence level and transition, as revealed by octant decomposition. Emphasis is placed on the turbulent shear stress, $-u'v'$, and the normal component of the turbulent heat flux, $v't'$. Table 4.1 gives pertinent information regarding the six profiles presented.

RESULTS AND DISCUSSION

Base Case: The Fully-Turbulent, Flat-Wall Boundary Layer with Low-to-Moderate Free-Stream Turbulence Intensity Levels

Figure 4.3 shows profiles of the octants of the turbulent shear stress from the 1.5% FSTI, fully-turbulent, flat-wall case, normalized on the friction velocity, u_τ. All data are shown with $H'=0$, unless otherwise specified. As expected, octants 4 and 6 are the major contributors, with the other octants remaining near zero over the entire profile. Octant 6 is

larger than octant 4 and its effects persist farther toward the edge of the boundary layer. Near the wall, the total $\frac{-\overline{u'v'}}{u_\tau^2}$, found by summing the contributions from all the octants, approaches 1, as expected. The peak in all octants is near the wall, dropping toward zero at the free-stream. Figure 4.4 shows similar results for the normal component of the turbulent heat flux, normalized as $\frac{\overline{v't'}}{q/(\rho c_p)}$.

Figures 4.5 and 4.6 show the effect of the hole size parameter at $y/\delta_{99.5}$=0.387. The data at this position are typical of the distributions at other y locations. In Fig. 4.5, the normalized shear stress contributions of the octants are plotted vs H′. Figure 4.6 shows the number of points in each octant normalized on the total number of points in the sample and plotted versus H′. Well over half the events are in octants 4 and 6. Octant 4 contains the most points, but the eddies in octant 6 are stronger. Octant 7 is a distant third in importance. For H'>4, only octant 6 makes a significant contribution.

Clearly, the hot ejection, which is associated with turbulent bursting, is the dominant structure in the turbulent boundary layer. Over one quarter of the data fall in this octant, and within this data lie the strongest eddies. The effects of the bursts extend farther toward the edge of the boundary layer than do the effects of the other octants. The cold sweeps also make an important contribution, occupying as much of the total time as do the hot ejections, but consisting mainly of somewhat weaker eddies. Octants 1 and 7, the cold outward interaction and hot wallward interactions, are next in importance, but appear to be of little significance. These octants are believed to result from the remnants of hot ejections and cold sweeps which reverse direction normal to the wall. More discussion on this subject will be given below in conjunction with the transitional flow data, where these octants, particularly 7, play a more important role.

The Effects of Curvature on the Fully-Turbulent Boundary Layer

Figures 4.7 and 4.8 show octant decomposition of shear stress for the 0.6% FSTI concave-wall and the 0.68% FSTI convex-wall, fully-turbulent cases, respectively. Concave curvature leads to increased instability and, hence, enhanced mixing in the boundary layer. Additionally, stationary, streamwise (Görtler) vortices were observed in this flow, as described above in Chapter 3. The profile shown here was taken at the upwash location of a pair of these vortices. The increased scale of mixing is evidenced by the fuller profiles in Fig. 4.7 compared to those of Figs. 4.3 and 4.8. Convex curvature tends to increase stability, thereby reducing mixing and leading to less full profiles, as a comparison of Figs. 4.8 and 4.3 shows. The influence of curvature was evident in the mean $-\overline{u'v'}$ profiles and is supported by the octant decomposition. There appears to be little reordering of the importance of the octants when curvature is introduced to the low-FSTI, fully-turbulent boundary layer, however. Octants 4 and 6 continue to play essentially the same relative roles in the curved-wall as they do in the flat-wall cases.

Effects of High Free-Stream Turbulence Intensity

Figure 4.9 shows shear stress profiles from the 8.3% FSTI, flat-wall case. The stated FSTI is the nominal value. At the location of this profile, the FSTI has decayed to 5.4%. The results appear similar to those of the low FSTI cases (Fig. 4.3) in that octants 4 and 6 dominate. The main differences are observed near the edge of the boundary layer. The free-stream velocity fluctuations do not approach zero in the high-turbulence case, so $u'v'$ remains significant in octants 4 and 6 to well beyond $\delta_{99.5}$. The other octants also show an increase in activity in the free-stream, indicating a higher level of uncorrelated fluctuations than in the low FSTI case. The sum of the octants goes to zero at $y/\delta \approx 1.2$; the free-stream $\overline{u'v'}=0$. The octants of the $v't'$ decomposition, shown in Fig. 4.10, each go to zero at the edge of the boundary layer since the free-stream temperature is uniform and, thus, t' goes to zero. A high FSTI concave-wall profile, not shown here, displayed the

expected combination of larger uncorrelated fluctuations near the edge of the boundary layer along with the generally fuller profiles seen in the low-FSTI, concave-wall case.

Transitional Flow

Figure 4.11 shows the shear stress distribution in a transitional flow from the 1.5% FSTI, flat-wall case. At this location, transition is 9.8% complete. Figure 4.12 shows $v't'$ for this case. The transitional profiles are quite different from the fully-turbulent cases shown above. Octants 4 and 6 are still significant in transition, but they are joined in importance by other octants, particularly octant 7, the hot wallward interaction. Octant 6 gives the largest contribution, and the difference between 4 and 6 is larger than in the fully-turbulent cases. At some locations, octant 7 has a larger magnitude than octant 4. Octants 1 and 7 also make contributions in the fully-turbulent cases, as mentioned above, but they are much less important in those cases. Octants 1 and 7 are of opposite sign to octants 4 and 6, for both $u'v'$ and $v't'$. They therefore act to decrease the total turbulent shear stress and normal component of turbulent heat flux. Figures 4.13 and 4.14 show the shear stress data at $y/\delta_{99.5}$=0.425 plotted verses H'. Octants 6 and 7 dominate. There are many data points in octant 4, but they are associated with weaker eddies and only make a minor contribution to $-u'v'$. The contributions to octants 6 and 7 persist even at H'=10, indicating that large eddies constitute the major contributions to $-\overline{u'v'}$. This contrasts with the fully-turbulent flow shown in Fig. 4.6, where $-u'v'$ drops more steeply with H'. This indicates that a wider range of scales is contributing to the shear stress in the fully-turbulent flow.

The transitional flow on the concave wall is similar to that on the flat wall. In Fig. 4.15, the octant decomposition of $v't'$ is shown with H'=0. The data were acquired at the downwash location of a Görtler vortex pair at a point where transition was 56% complete. The hot ejection (octant 6) dominates, with the hot wallward interaction (octant 7) making a secondary contribution. In Fig. 4.16 the same profiles of $v't'$ are shown again with

$H'=10$. Comparing Figs. 4.15 and 4.16 shows that there is little change in octants 6 or 7 with a change of H', indicating the importance of large scale eddies for these two octants.

The octant analysis shows a fundamental difference between transitional and fully-turbulent flow structures. The differences are believed to be caused by incomplete development of the turbulence in the transitional region. In particular, the transitional flow is dominated by large-scale eddies since the cascade of energy from large scales to small is not yet established and the small scales have not had a chance to develop. The consequence is an incomplete mixing. An illustration of the proposed difference in mechanisms is given in Fig. 4.17. In fully-turbulent flow, a parcel of low-speed, warm fluid is ejected from the wall in a relatively large scale motion. Upon reaching the outer part of the boundary layer, the parcel is immediately acted upon by small-scale eddies which disperse it by way of eddy straining and "turbulent diffusion." Mixing is fairly complete. A parcel of fluid moving with a cold sweep would be similarly dispersed. In transitional flow, the behavior is different. A burst still transports a parcel of warm, low-speed fluid to the outer part of the boundary layer, but there are few small-scale eddies present to act upon it. The parcel tends to remain intact for some time as a warm, low-speed entity. If it is next carried toward the wall, the parcel would be involved in a hot wallward interaction (octant 7). Similarly a parcel from a previous cold sweep might be thrown away from the wall as a cold outward interaction (octant 1). If the small-scale mixing were sufficiently poor, one could conceive of octants 1 and 7 approaching the levels of octants 4 and 6 with a net of zero turbulent mixing. In general, 1 and 7 do follow 4 and 6, but are of lesser importance.

Another feature in transitional flows is the larger difference between octants 4 and 6. Transition starts with near-wall bursting, so octant 6 should become dominant early in transition. Figure 4.14 supports this by showing that, although the total number of events in octants 4 is nearly twice that in octant 6, the events in octant 4 are much "weaker." The number of events in octant 4 with $H'>2$ is near zero, while there are a significant number of events in octant 6 with $H'=10$.

Modeling Implications

The above results suggest a potential benefit of incorporating an additional length scale or scales into existing transition models. A standard k-ε model bases the effective eddy viscosity on the turbulence intensity using a relation of the form $\nu_T = C_\mu f_\mu \frac{k^2}{\varepsilon}$. The coefficient C_μ is an empirical constant and f_μ is an empirical function. If this relationship were employed for prediction of the transport by turbulent eddies in a transitional flow, it would predict excessive eddy viscosity even if k and ε were accurate, since C_μ and f_μ are based on fully-turbulent flow where only octants 4 and 6 are important. Also, because of a falsely large contribution by turbulent eddies, a prediction of the streamwise distance within which the boundary layer is transitional would be too short. This is typical of existing models. The octant analysis results suggest that the standard k-ε modeling cannot fully capture the physics of the transitional flow structure. It suggests that an improvement to the situation would be a model that properly accommodates the larger-scale eddies in the transitional flow. Such a model may be an expansion of the standard k-ε model to two k equations with one k for the large scales and the other for the small scales. Turbulent energy would be mainly produced in the large scales by the standard production terms and would be transferred from the large scales to the small scales through a cascade model. Energy would be dissipated at the small scales. Contributions to $-\overline{u'v'}$ or eddy viscosity would come from both the large- and small-scale k, but the large scale contribution would be dominant. Since the small-scale energy would depend on transfer from the large scales, the turbulent kinetic energy in the small scales would lag that in the large scales as the boundary layer passes through transition. These measurements indicate that this lag would represent an improvement in predicting transition.

CONCLUSIONS AND RECOMMENDATIONS

Octant analysis was applied to transitional and fully-turbulent boundary layer data from both flat and curved walls. The following conclusions can be drawn:

1. In fully-turbulent flow, hot ejections and cold sweeps are the dominant flow structures. Eddies over a range of sizes contribute to quantities of interest, as evidenced by the sensitivity of these quantities to the hole size parameter, H′.

2. Curvature has an effect on the boundary layer, but does not appear to have a significant effect on the relative importance of the octants.

3. Octant decomposition in cases subject to high free-stream disturbance shows the difference between the uncorrelated fluctuations associated with free-stream "turbulence" and the highly correlated turbulence of the boundary layer. At, and beyond, the edge of the boundary layer, for the high free-stream turbulence case, the octant contributions do not approach zero, though their sum does.

4. Transitional flow is dominated by large scales, particularly hot ejections, and is characterized by incomplete mixing due to the incomplete development of small scale eddies. The octant analysis shows a decreased importance of the cold sweep and an increased importance of the hot wallward interaction in transitional flow. The hot wallward interaction is believed to follow directly from the hot ejection and acts to counteract the effects of ejections on the transport terms $-\overline{u'v'}$ and $\overline{v't'}$

5. The differences between transitional and fully-turbulent flows suggest the utility of multiple length scales in turbulence models that may be used to compute through transition.

No.	Ref.	Geometry	FSTI	x [m]	U_∞ [m/s]	q [W/m^2]	T_w-T_∞ [°C]	θ [cm]	H	$\delta_{99.5}$ [cm]	$\delta_{t99.5}$ [cm]	C_f $\times 10^3$	St $\times 10^3$	γ
1	†	flat	1.5%	1.029	16.86	154.8	3.56	0.154	1.361	1.749	2.025	4.05	2.201	100%
2	†	concave	0.6%	0.876	17.13	147.6	3.78	0.182	1.367	1.603	1.868	4.20	1.946	100%
3	‡	convex	0.68%	0.528	15.10	160.7	6.87	0.493	1.54	3.572	3.590	2.61	1.330	100%
4	†	flat	8.3%	0.800	9.19	181.9	6.07	0.191	1.364	2.451	3.012	4.70	2.528	100%
5	†	flat	1.5%	0.343	16.86	137.3	6.56	0.038	2.256	0.318	0.355	1.70	1.086	9.8%
6	*	concave	0.6%	0.610	9.58	170.9	4.12	-	-	0.788	0.813	3.00	3.686	56%

† Kim and Simon (1991); ‡Kim (1986); *present study

Table 4.1: Cases Considered

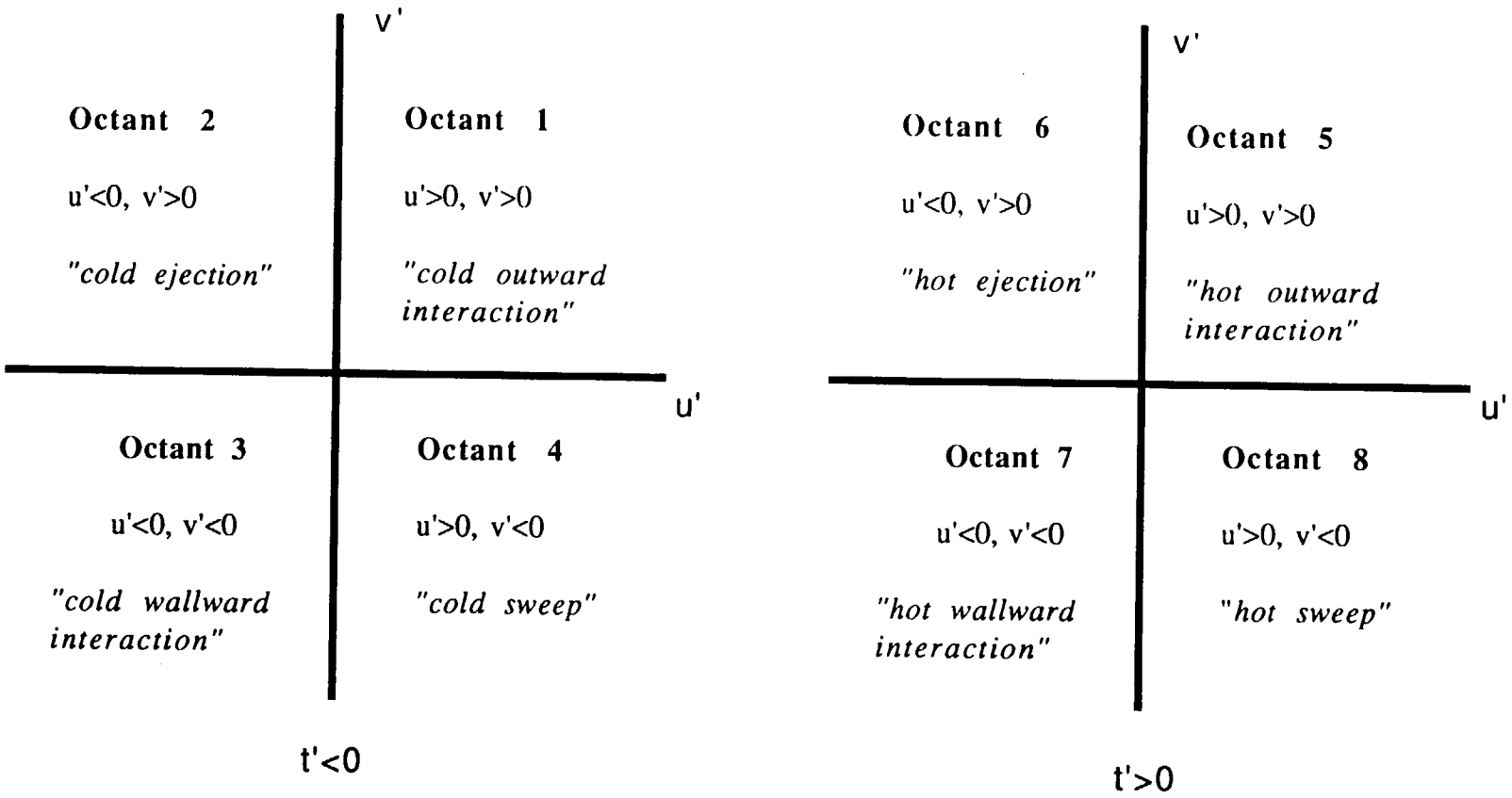

Fig. 4.1: Octant names

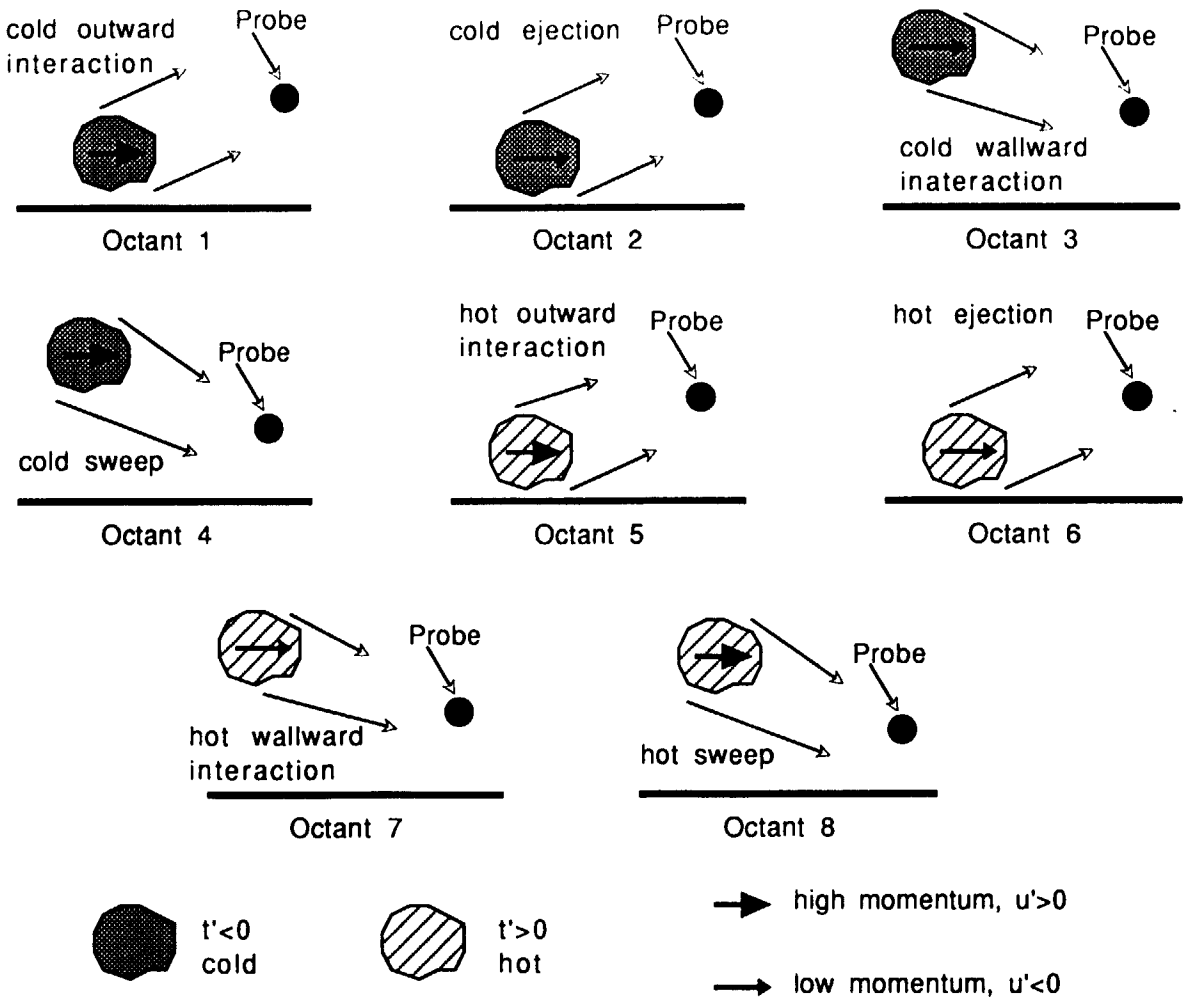

Fig. 4.2: Conceptual drawing of eddies in each octant

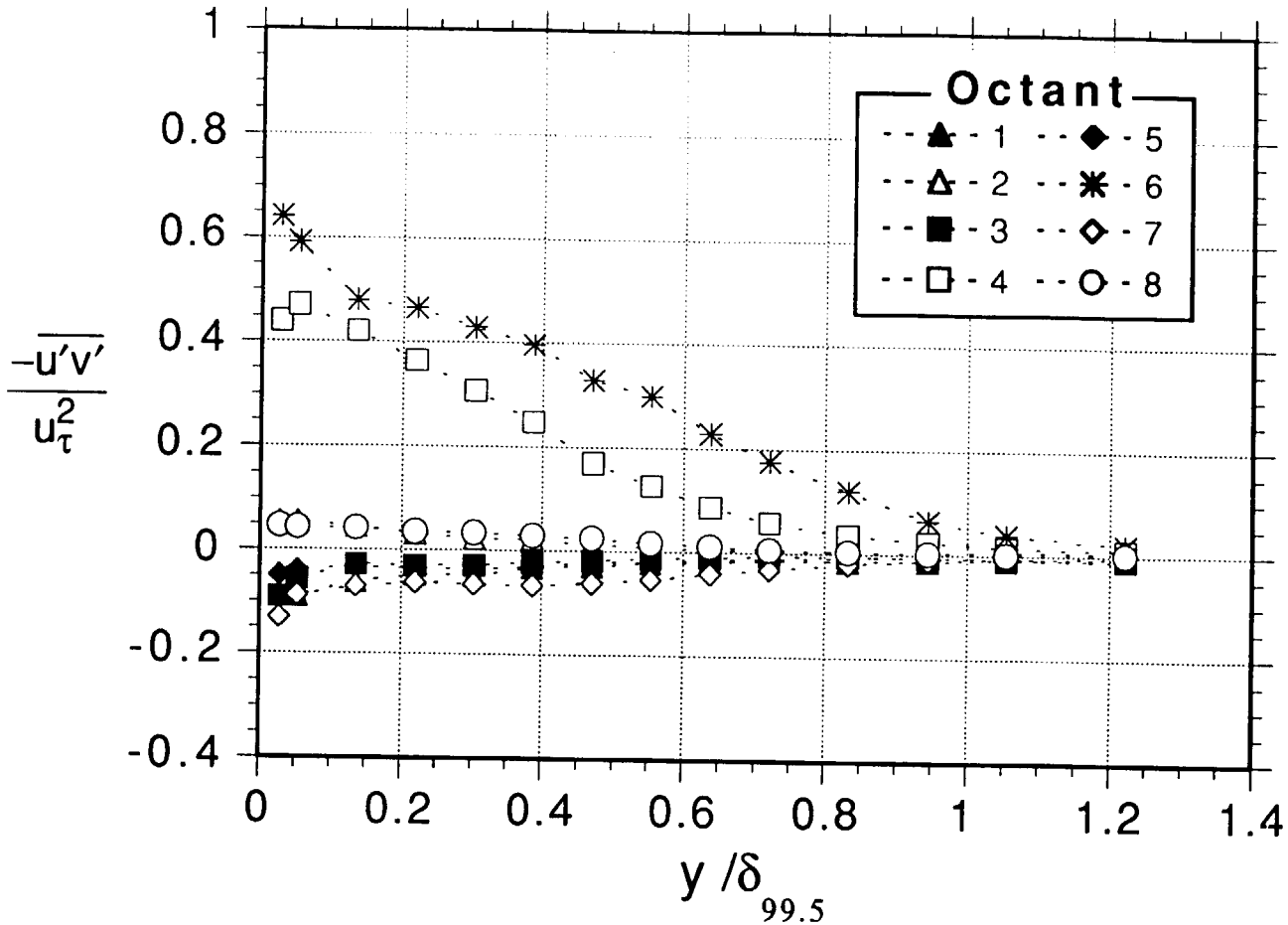

Fig. 4.3: Turbulent shear stress profiles, 1.5% FSTI flat-wall case, fully-turbulent flow

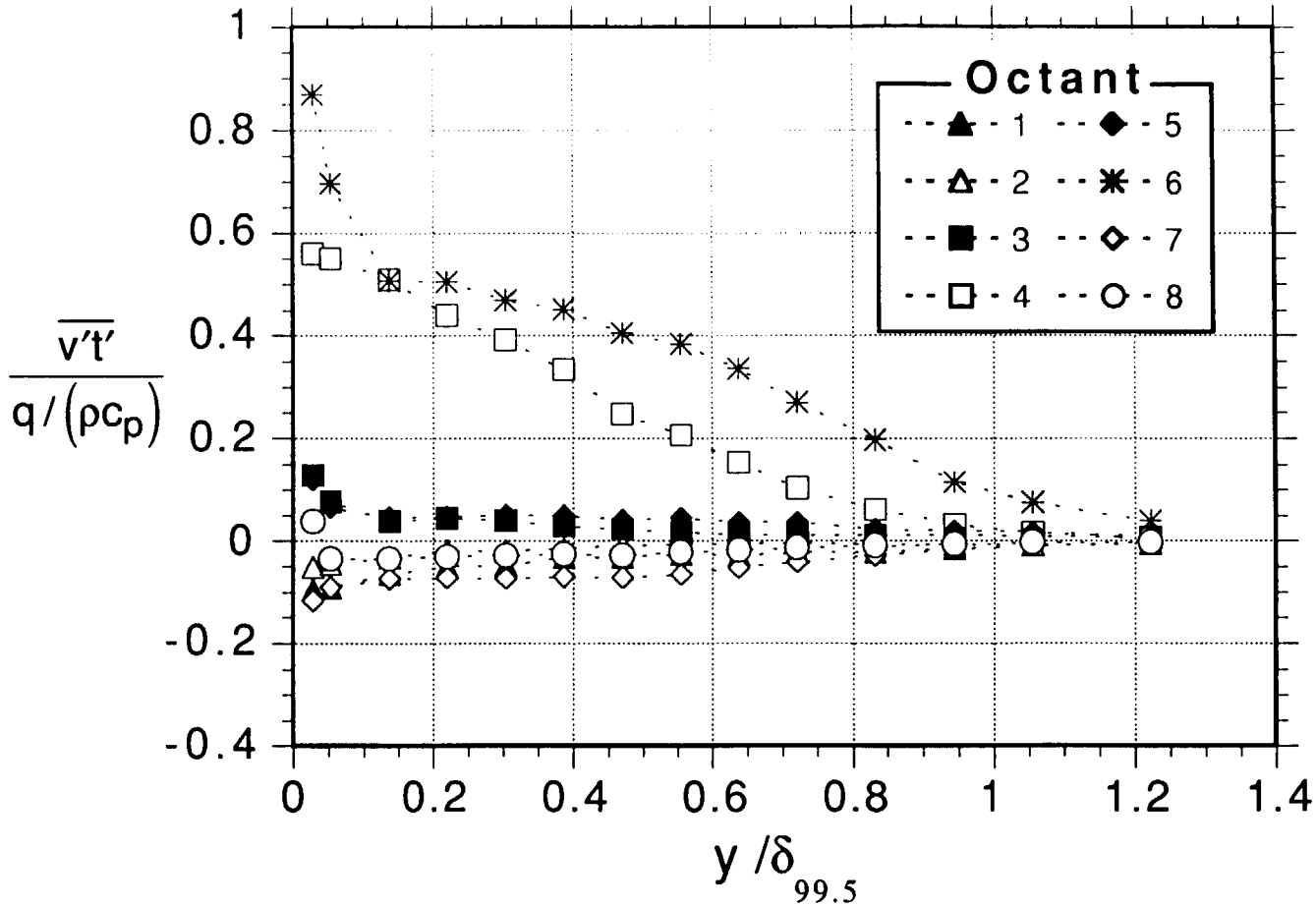

Fig. 4.4: Normal component of turbulent heat flux profiles, 1.5% FSTI flat-wall case, fully-turbulent flow

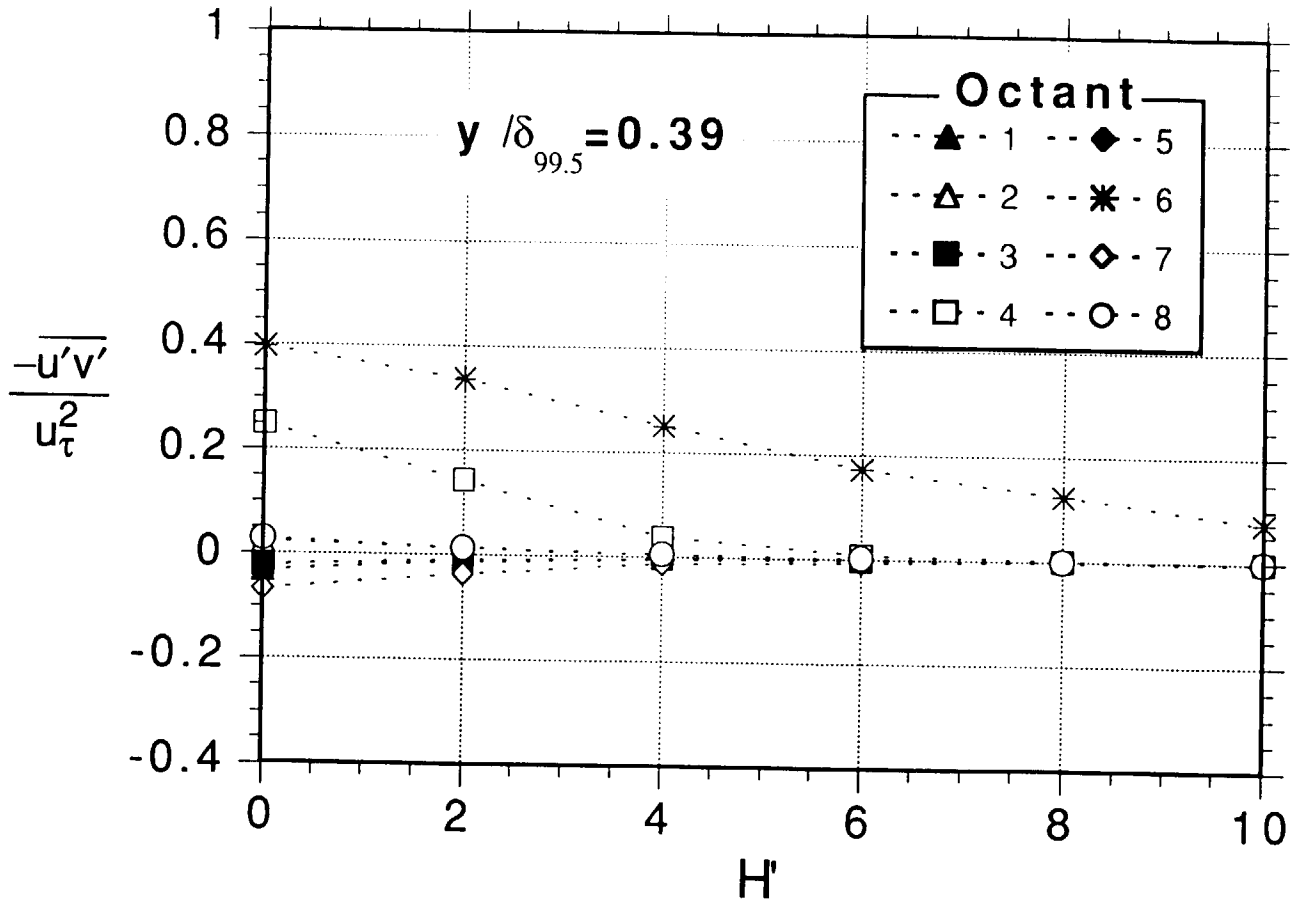

Fig. 4.5: Turbulent shear stress vs hole size at $y/\delta_{99.5}$=0.39, 1.5% FSTI flat-wall case, fully-turbulent flow

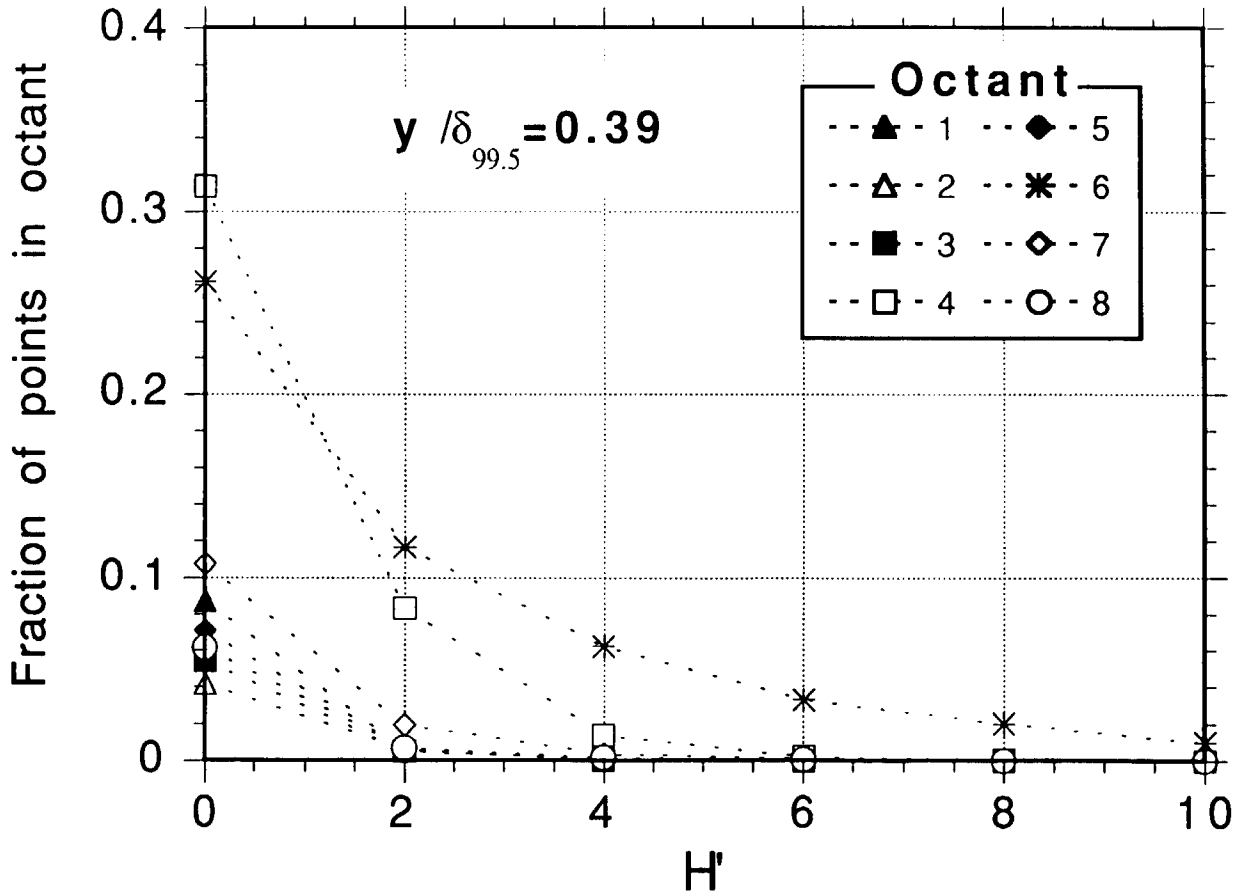

Fig. 4.6: Fraction of points in octant vs hole size at $y/\delta_{99.5}$=0.39, 1.5% FSTI flat-wall case, fully-turbulent flow

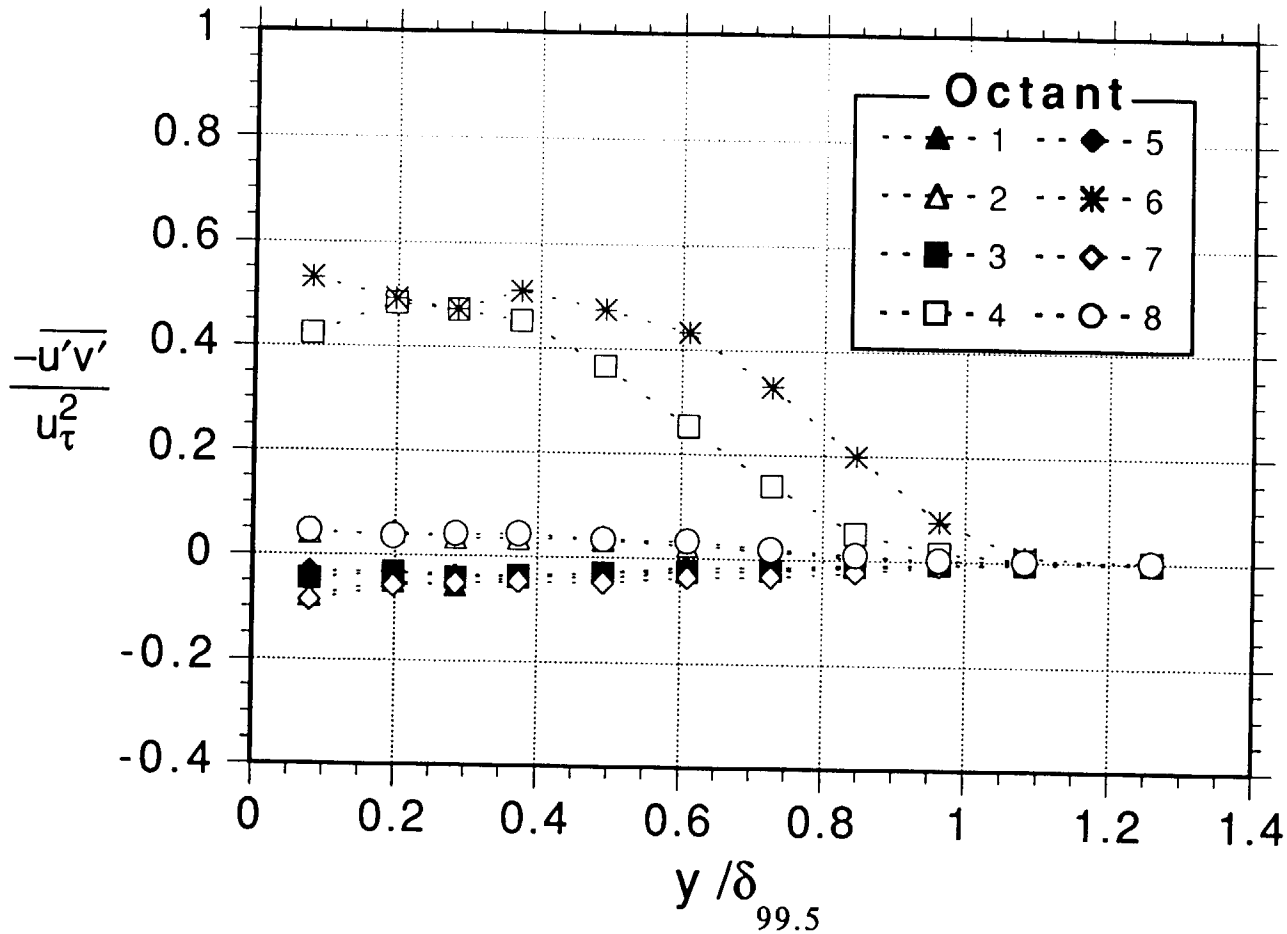

Fig. 4.7: Turbulent shear stress profiles, 0.6% FSTI concave-wall case, fully-turbulent flow

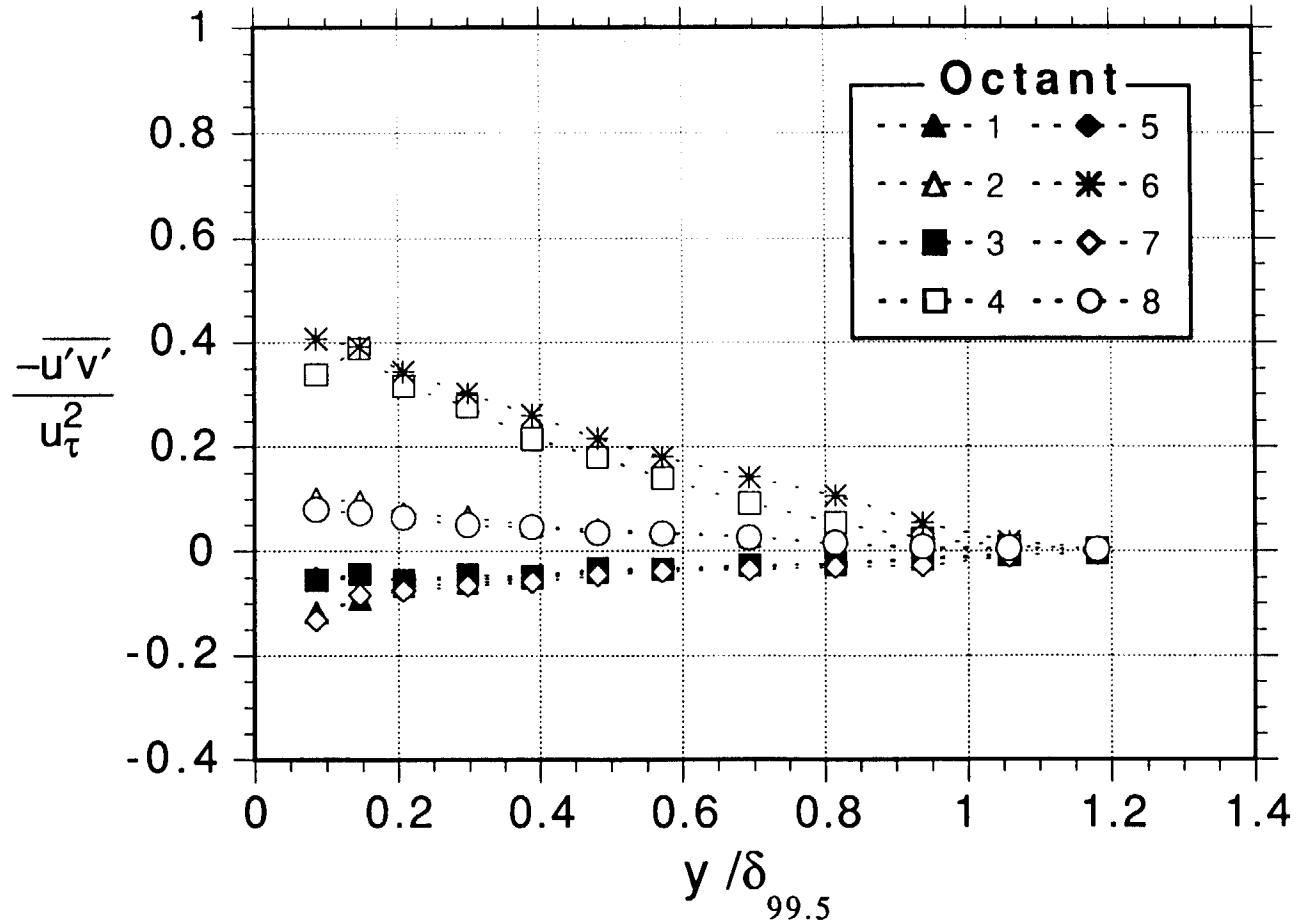

Fig. 4.8: Turbulent shear stress profiles, 0.68% FSTI convex-wall case, fully-turbulent flow

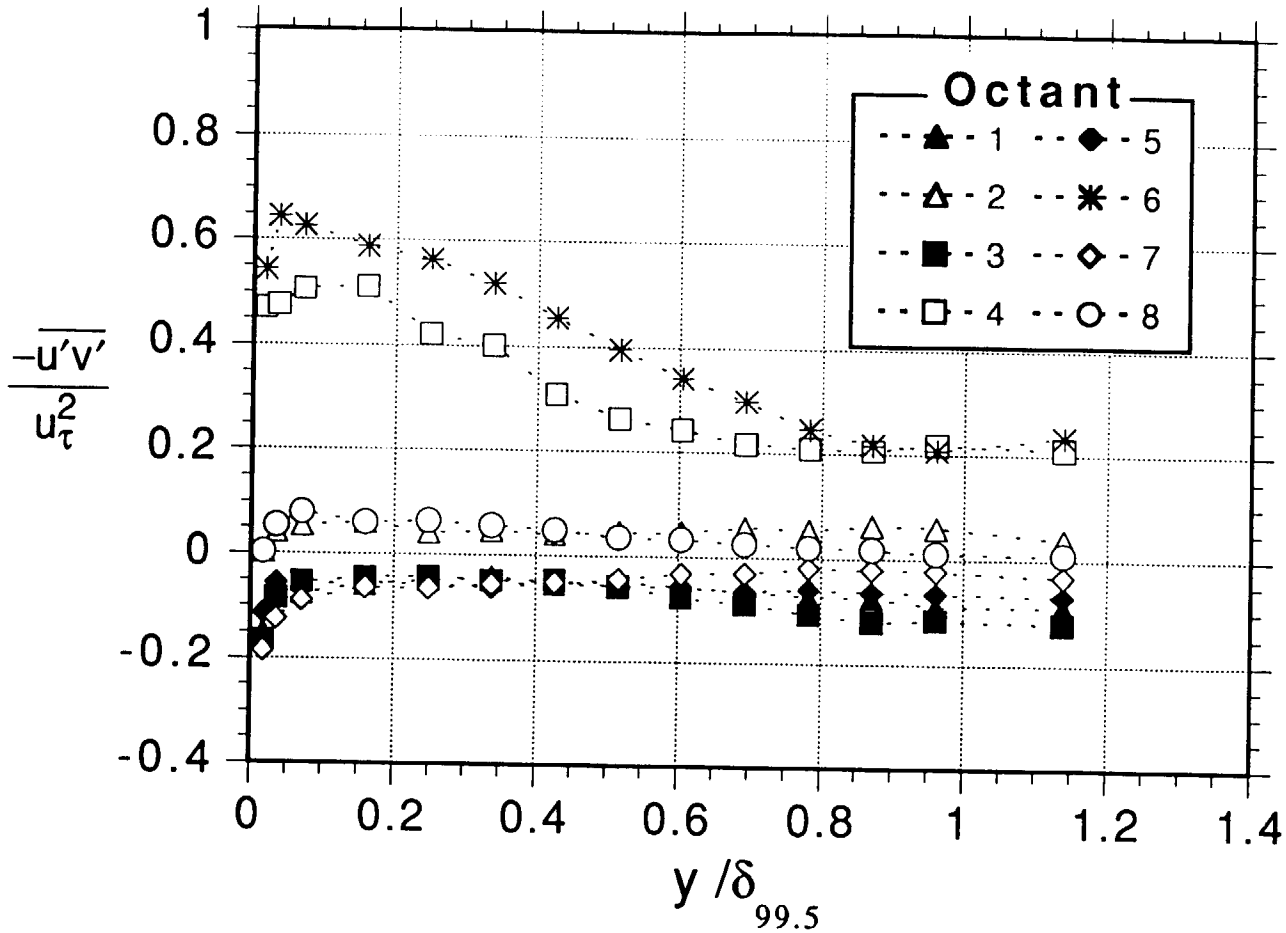

Fig. 4.9: Turbulent shear stress profiles, 8.3% FSTI flat-wall case, fully-turbulent flow

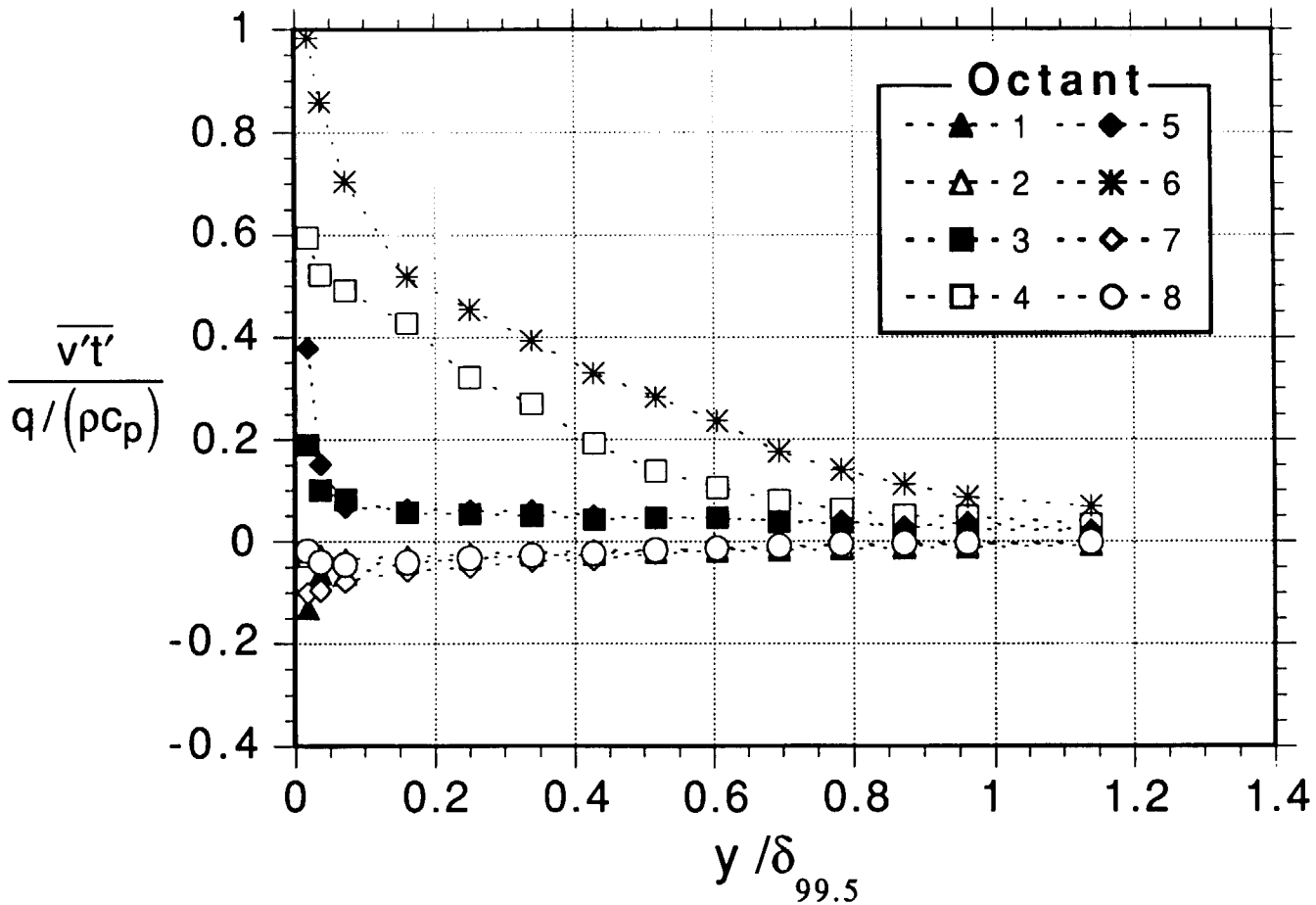

Fig. 4.10: Normal component of turbulent heat flux profiles, 8.3% FSTI flat-wall case, fully-turbulent flow

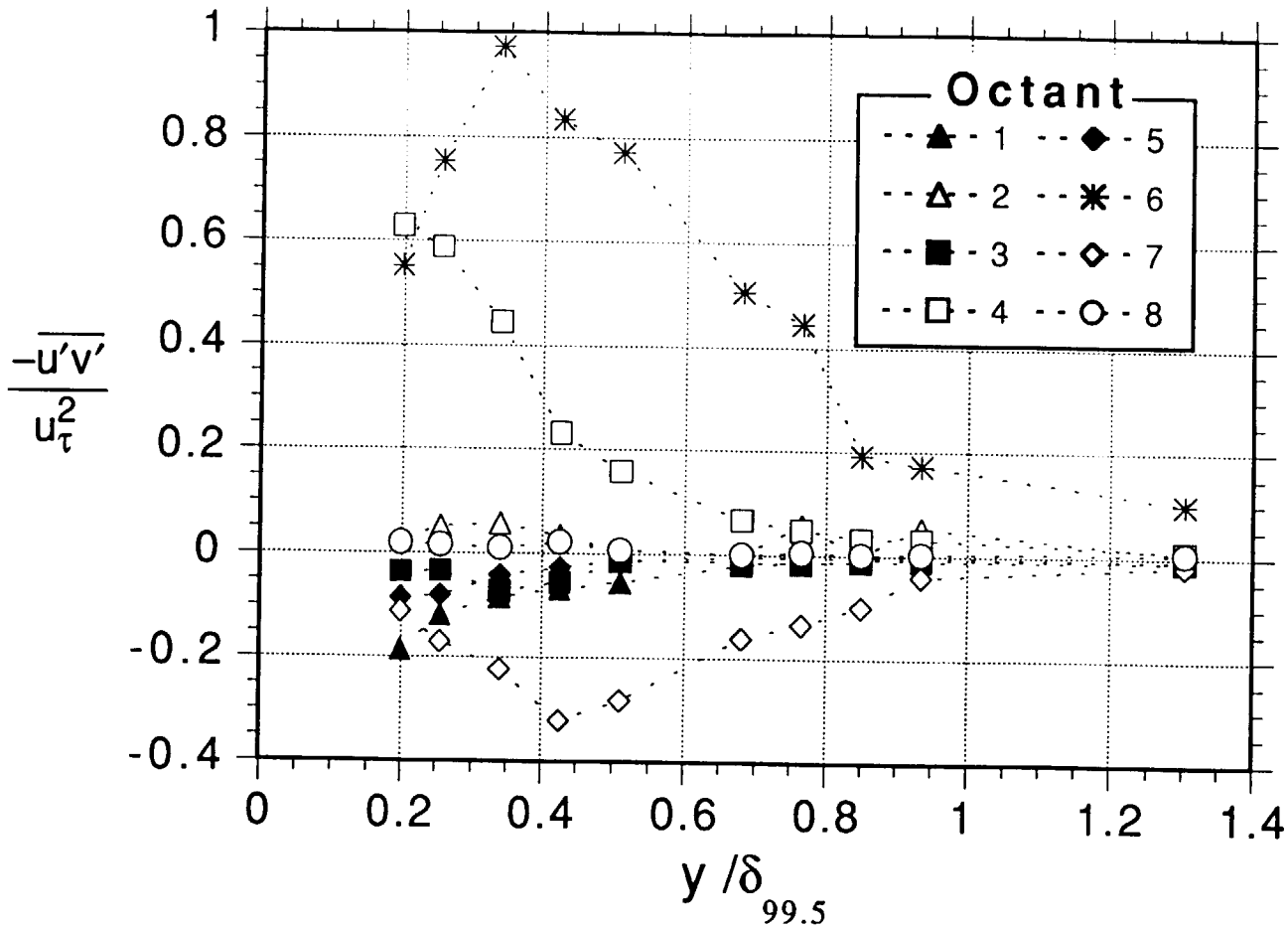

Fig. 4.11: Turbulent shear stress profiles, 1.5% FSTI flat-wall case, transitional flow

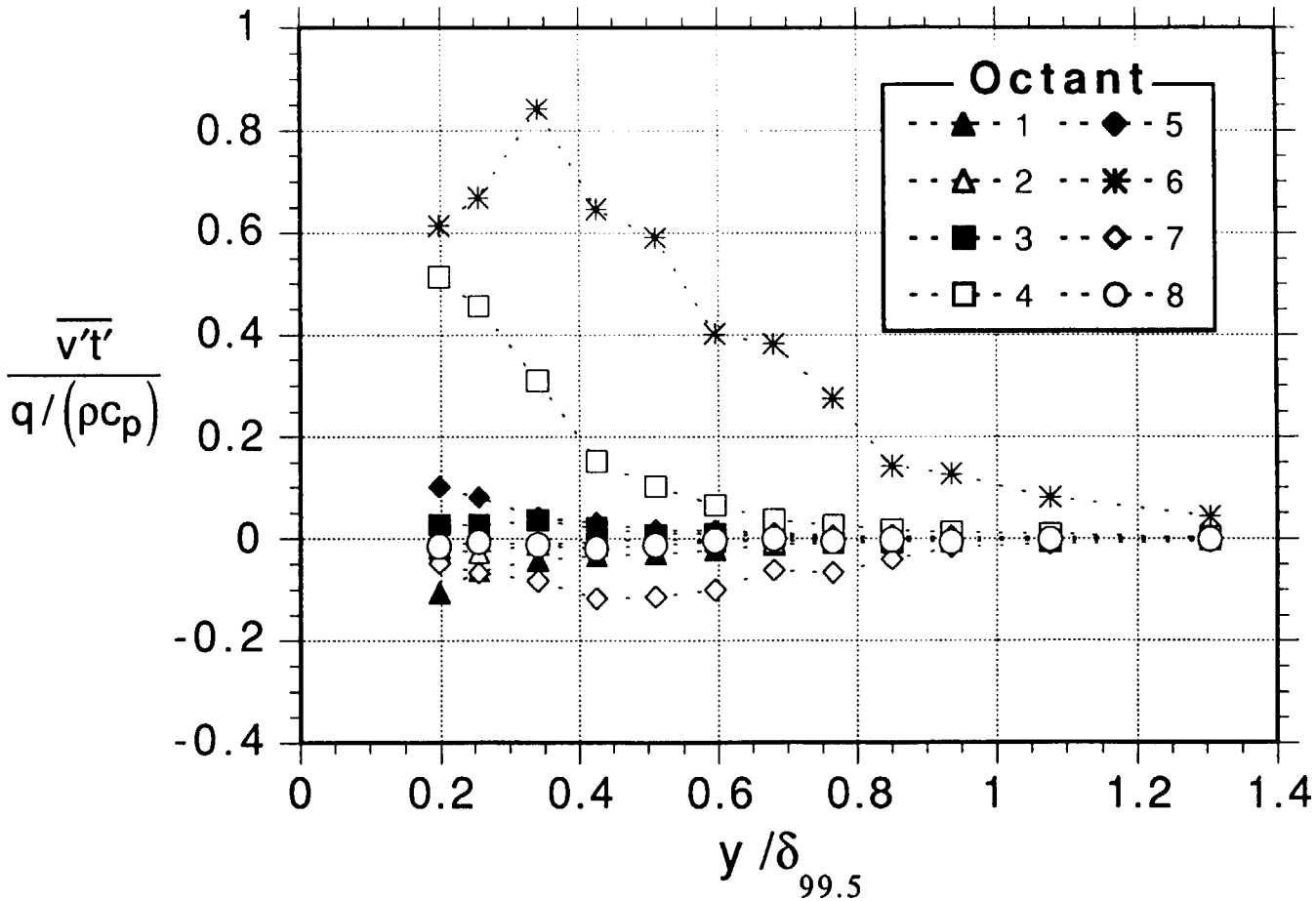

Fig. 4.12: Normal component of turbulent heat flux profiles, 1.5% FSTI flat-wall case, transitional flow

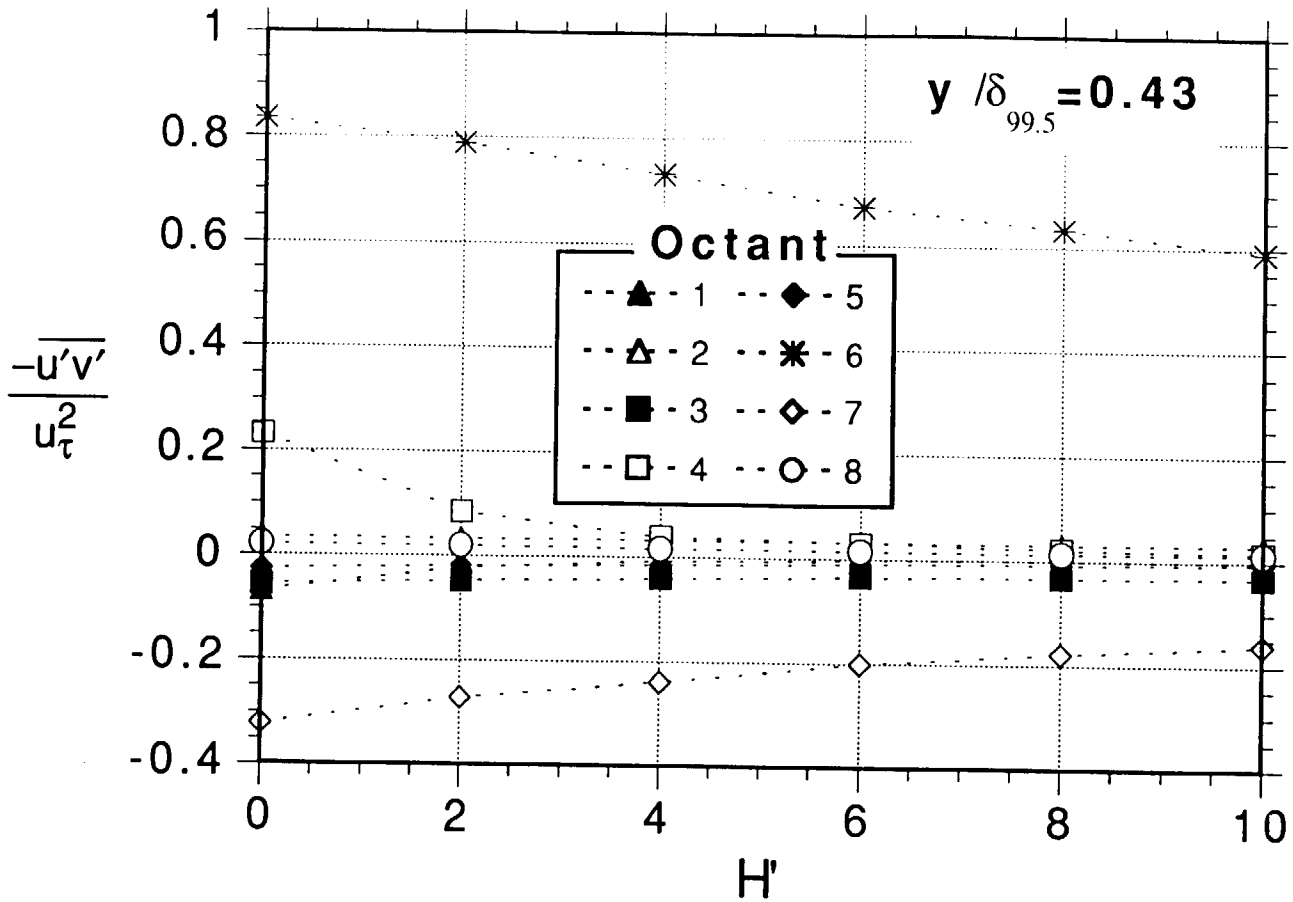

Fig. 4.13: Turbulent shear stress vs hole size at $y/\delta_{99.5}=0.43$, 1.5% FSTI flat-wall case, transitional flow

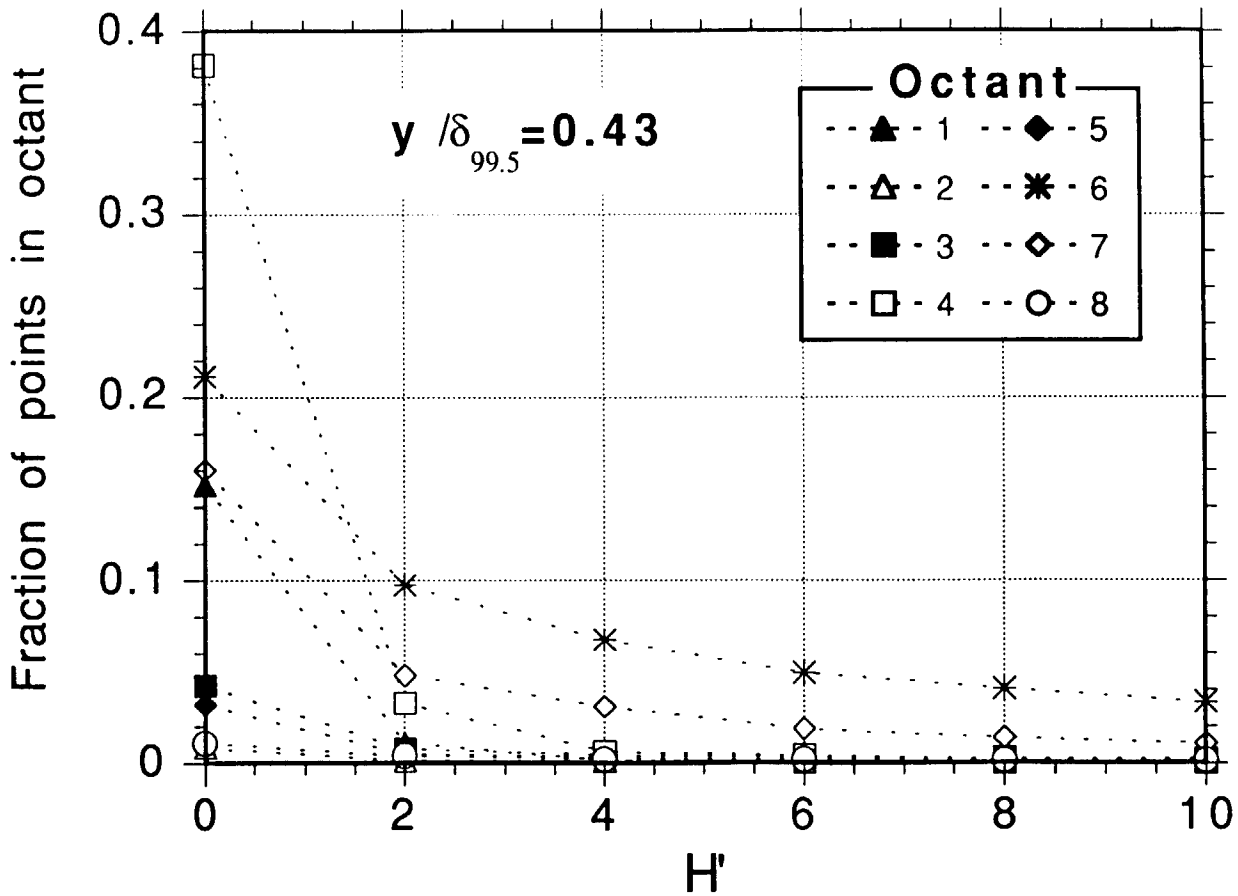

Fig. 4.14: Fraction of points in octant vs hole size at $y/\delta_{99.5}$=0.43, 1.5% FSTI flat-wall case, transitional flow

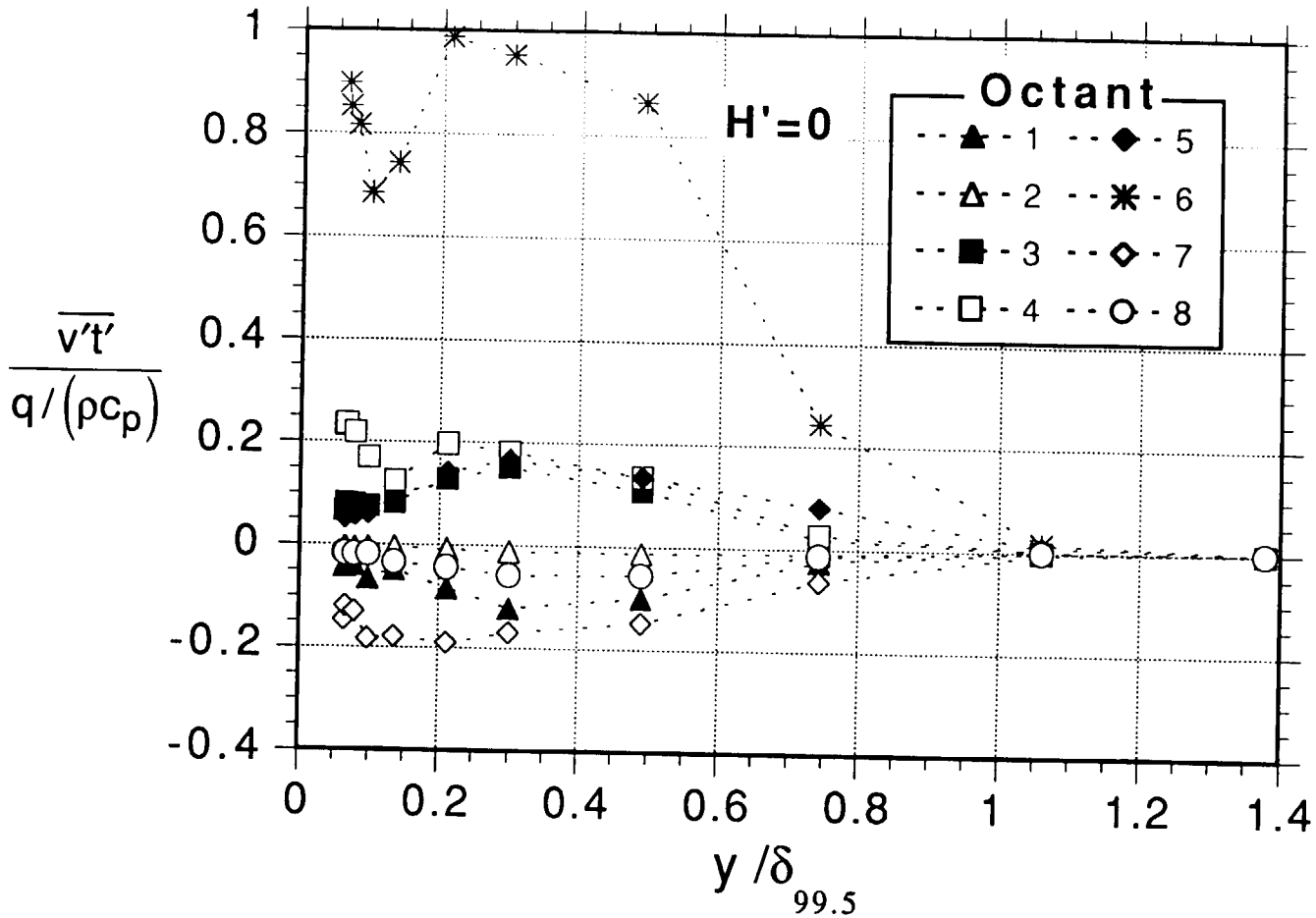

Fig. 4.15: Normal component of turbulent heat flux profiles, 0.6% FSTI concave-wall case, transitional flow, H'=0

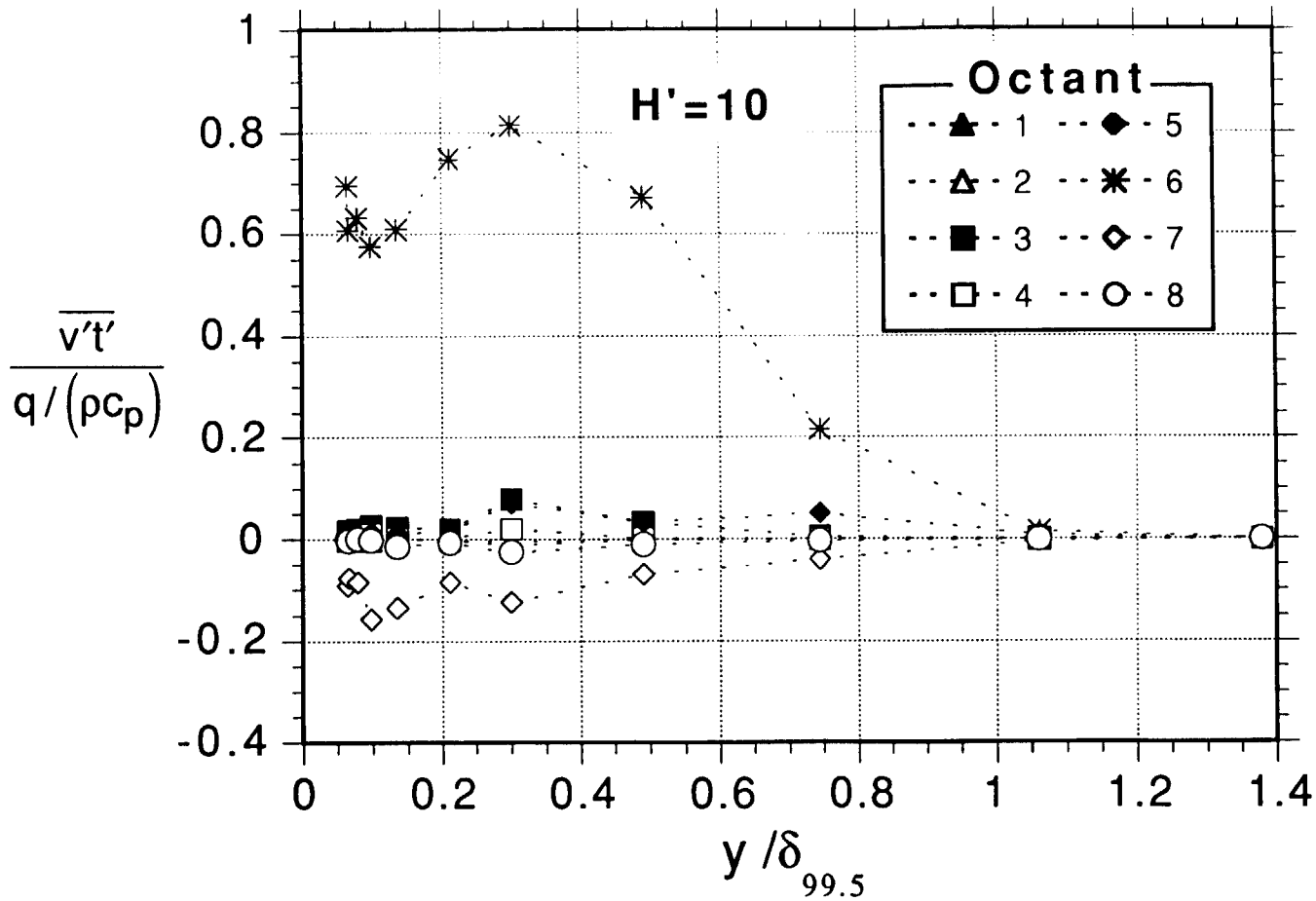

Fig. 4.16: Normal component of turbulent heat flux profiles, 0.6% FSTI concave-wall case, transitional flow, H'=10

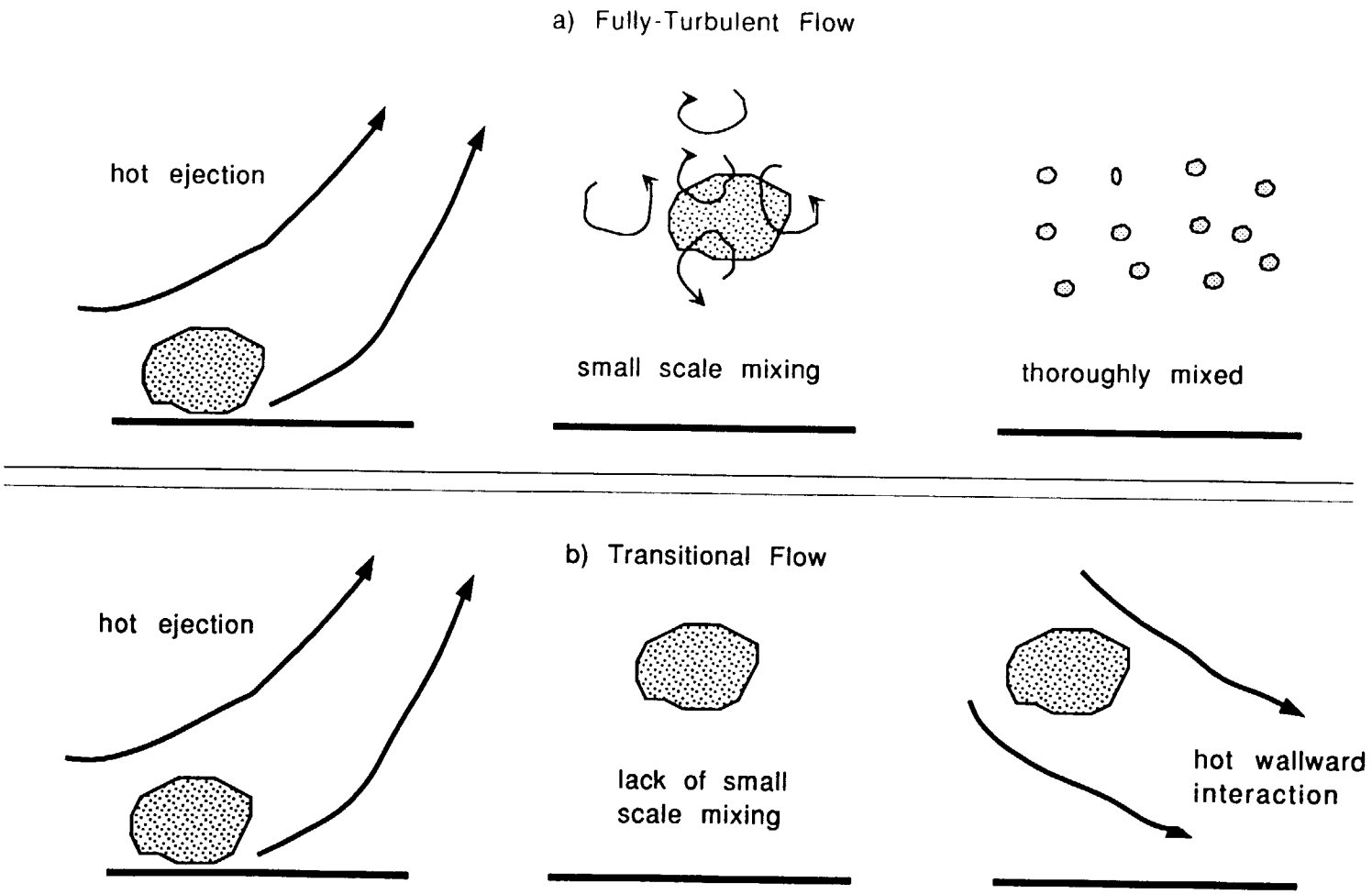

Fig. 4.17: Proposed differences between fully-turbulent and transitional flow structures

CHAPTER 5: HIGH FSTI, $K=0.75\times10^{-6}$ RESULTS

The following documents the first case of a study of the effects of acceleration at high FSTI. In this case, the acceleration parameter was held constant at $K=0.75\times10^{-6}$. This acceleration was found to be too weak to significantly affect the transition process, but the acceleration did influence the fully turbulent boundary layer, as documented below. The boundary layer was two-dimensional in a time-averaged sense; no stationary streamwise vortices were observed.

EXPERIMENTAL CONDITIONS

The flow entered the test section with a velocity of 8 m/s and a nominal FSTI of 8%. The Reynolds number, Re_x, reached 9.23×10^5 by the end of the test section. This value is comparable to the chord Reynolds numbers seen in high pressure gas turbines. The chord Reynolds number, Re_c, is based on the airfoil chord length, c, and the free-stream velocity downstream of the airfoil. The constant-K boundary condition was chosen for the experiment to provide a relatively simple condition. The value, $K=0.75\times10^{-6}$, was chosen to match the higher of two accelerations used by Blair (1992). This acceleration rate is high compared to the acceleration rates used in most of the experimental transition studies documented in the literature, but is low compared to the acceleration rates seen on the pressure side of modern gas turbine airfoils. Figure 5.1 shows the acceleration profiles from the pressure sides of two airfoils operating under cruise conditions at altitude. The acceleration parameter, K, is plotted verses Re_x. Data for the curve labeled "CF6" in Fig. 5.1 were taken from Chung (1992), who used a cascade with an airfoil shape based on the high pressure turbine blades in the General Electric CF6 engine. Data for the curve labeled "Modern Airfoil" were taken from a study by Smith (1993), who used a more modern airfoil shape. The peak accelerations on

the airfoils are 10 to 20 times higher than in the present experiment. For reference, relaminarization is expected under low FSTI conditions for sustained-K values of greater than 3×10^{-6} (Jones and Launder, 1972). For another perspective, Fig. 5.2 shows the product KRe_C plotted verses x/c for the same two airfoils. The product KRe_C depends only on the geometry of the airfoil passage, and remains constant when operating conditions are changed (i.e. for a given airfoil, the KRe_C profile is the same for takeoff and cruise conditions).

Blair (1992) investigated transition on a flat wall at FSTI up to 5%. At FSTI=5%, he observed that acceleration with $K=0.75\times10^{-6}$ extended the transition zone. The inlet free-stream velocity in Blair's case was 10 m/s, and his maximum Re_X was approximately 3.5×10^6. Since the free-stream velocities and Re_X were higher in Blair's case than in the present case, it was expected that an extended transition zone might be observed in the present experiment. This was not the case, however. The concave curvature and higher FSTI in the present case (8% here, compared to 5% in Blair's experiment) led to a more rapid transition than in Blair's experiment. Based on surface heat transfer and velocity profile measurements (see Volino and Simon, 1995a), the start of transition in Blair's experiment was observed at $Re_X=0.8\times10^5$ and $Re_\theta=130$. Transition end was at $Re_X=2.4\times10^5$ and $Re_\theta=490$. In the present case, the boundary layer was transitional at the first measurement station, where $Re_X=0.5\times10^5$ and $Re_\theta=190$, but fully-turbulent by the second station, where $Re_X=2.0\times10^5$ and $Re_\theta=590$.

Free-Stream Conditions

Data were acquired in the present case at five streamwise stations. The locations of these stations, along with corresponding Reynolds numbers and other important parameters are listed in Table 5.1. The free-stream turbulence levels at these stations are shown in Fig. 5.3. In Fig. 5.3a, $\overline{u'_\infty}$ and $\overline{v'_\infty}$ are plotted in dimensional coordinates. Both quantities decay somewhat in the streamwise direction. The free-stream turbulence

intensities are shown in dimensionless coordinates in Fig. 5.3b. Also shown is the FSTI, taken here as $\sqrt{\frac{\overline{u'^2}+2\overline{v'^2}}{3U_{cw}^2}}$. The FSTI drops from 7.6% at the first station to 3.2% at the last station. Most of the drop is due to the increase in U_{cw} in the streamwise direction.

Free-stream spectra. The free-stream spectra of u′, v′, and w′, acquired at station 1, are presented in Fig. 5.4. Below 20 Hz, u′ contains more energy than v′ or w′. This low-frequency streamwise unsteadiness was also seen in the low-FSTI flow of Chapter 3, shown in Fig. 3.2. In the low-FSTI case, nearly all of the fluctuation energy was found in u′, and the energy in the u′ spectra was concentrated around a peak at 0.8 Hz (Fig. 3.2b). These low frequencies were associated with streamwise unsteadiness, as opposed to turbulent eddies. In the present case, the fluctuation energy is more evenly distributed between the three velocity components, and the peak shown in Fig. 5.4b is near 50 Hz. The integral length scales associated with the fluctuating velocity components are $\Lambda_{u'}$=5 cm, $\Lambda_{v'}$=1.3 cm, and $\Lambda_{w'}$=0.8 cm. The integral length scales were obtained from the free-stream spectra using Eqn. 2.16. The frequencies associated with the integral scales are $U_\infty/\Lambda_{u'}$=170 Hz, $U_\infty/\Lambda_{v'}$=650 Hz, and $U_\infty/\Lambda_{w'}$=1050 Hz. All three components of the high FSTI fluctuations can be associated with turbulent eddies.

Two-point correlations. Two-point spatial correlations of the free-stream u′ fluctuations are shown in Fig. 5.5. The correlations for y and z separations are nearly identical. The integral length scales associated with these correlations are equal to the areas under the curves in Fig. 5.5. The integral scales for the y and z separations are both equal 1.7 cm. This is smaller than $\Lambda_{u'}$=5 cm taken from the spectra (associated with separation in the x direction), suggesting that the free-stream eddies are somewhat elongated in the streamwise direction.

Boundary Layer Growth

The growth of the momentum and thermal boundary layers are shown in Fig. 5.6, where Re_θ and $Re_{\Delta 2}$ are plotted verses Re_x. Also shown for comparison are curves from an unaccelerated, 8%-FSTI experiment done on the same concave test wall by Kim and Simon (1991) (and repeated by Kestoras (1993) who provided additional boundary layer thickness data). Acceleration should not have a direct effect on the thermal boundary layer, and, as expected, the thermal boundary layer growth is not strongly affected by the acceleration. The growth of the momentum boundary layer, however, is suppressed. By $Re_x=1\times10^6$, Re_θ has been reduced from 1800 in the unaccelerated boundary layer to 950 in the accelerated flow. Although the acceleration is not strong enough to significantly delay transition, it does have a significant impact on the fully-turbulent boundary layer.

The shape factor, $H=\delta^*/\theta$, is shown in Fig. 5.7. The shape factor drops from a transitional value of 1.8 at the first station, to a fully-turbulent value of 1.3 by the second station. The fully-turbulent value in the unaccelerated flow case is only slightly lower at 1.25. For reference, the laminar unaccelerated (Blasius solution) value is 2.6.

Energy and Momentum Balances

The energy convected away from the heated test wall must be present in the boundary layer. This requires that

$$\int_0^\infty \left[\rho c_p \overline{U}\left(\overline{T}_s - T_{s\infty}\right)\right]dy = \int_0^x q\,d\varsigma \qquad (5.1)$$

where q is the convective heat flux from the test wall, and T_s and $T_{s\infty}$ are stagnation temperatures. The test wall has an unheated starting length of 2.54 cm. Downstream of this, the heat flux is approximately uniform. Using the definition of the enthalpy thickness (Eqn. 2.15), Eqn. 5.1 reduces to

$$\rho c_p U_{cw}\left(T_w - T_{s_\infty}\right)\Delta_2 = q(x - x_0) \qquad (5.2)$$

where x_0 is the unheated starting length. Curvature effects, which were omitted in Eqn. 5.1, are included in Eqn. 5.2 through the definition of Δ_2. The two sides of Eqn. 5.2 are plotted verses the streamwise position, x, in Fig. 5.8. The energy balance is within 12% at all stations. This balance is good, particularly when the actual spatial variability in the wall heat flux (described above in Chapter 2) is taken into consideration.

In simple boundary layer flows, a momentum balance can be computed between the drag force at the wall and the momentum deficit in the fluid. This is not possible in the present study, however. The combination of high FSTI and streamwise curvature leads to cross transport of momentum across the channel, as described by Eckert (1987). To properly determine the momentum balance, the momentum deficit across the whole channel must be computed, and the shear stresses on both the concave and convex walls must be measured. Since measurements were not taken in the convex wall boundary layer, the momentum balance cannot be assessed. Attempts to compute the momentum balance with only the concave wall data proved unsatisfactory.

Strength of Curvature

The strength of curvature, θ/R, is shown in Fig. 5.9 along with data from the Kim and Simon (1991) 8%-FSTI, unaccelerated flow case and estimates of the curvature profiles for the CF6 and modern airfoils mentioned above in the discussion of Fig. 5.1. The airfoil values are based on rough estimates of momentum thickness computed using the TEXSTAN program (Kays and Crawford, 1993; Crawford and Kays, 1976), k-ε closure, high FSTI, and design pressure profiles, without consideration of curvature effects. In the unaccelerated flow experiment, θ/R rose steadily to a maximum value of 1.8×10^{-3}. In the accelerated flow, the strength of curvature is suppressed, with θ/R

reaching a maximum of 1.3×10^{-3} by the third station and decreasing at the downstream stations. In terms of the boundary layer thickness, $\delta_{99.5}$, the accelerated flow case has a strength of curvature between 2 and 3%. This curvature is weak, but still potentially significant. The strength of curvature is slightly below that of the CF6 airfoil, and significantly lower than that of the more modern airfoil.

MEAN VELOCITY PROFILES

Figure 5.10 shows mean streamwise velocity profiles from the present case, plotted as $\overline{U}/U_{CW}$ verses y/θ. The edge of the momentum boundary layer, $\delta_{99.5}$, corresponds to $y/\theta\approx20$. Stations 2 through 5 collapse on one another. The station 1 profile is less full, supporting the conclusion that the flow there is transitional. Figure 5.11 shows the profiles plotted in wall coordinates. The station 1 profile again appears transitional, while the rest appear fully turbulent and collapse onto the standard law of the wall. The acceleration is too weak to cause significant deviation from the law of the wall. This behavior agrees with what is predicted by the method given in Appendix A. The profiles in Fig. 5.11 exhibit no wake. Similar behavior was observed in the Kim and Simon (1991) 8%-FSTI, concave-wall, unaccelerated flow case. The high FSTI and concave curvature promote mixing in the outer part of the boundary layer, thereby reducing the gradients in the outer region and suppressing the wake. One consequence of this enhanced mixing is higher gradients near the wall, resulting in high skin friction coefficients, as is shown below.

SKIN FRICTION COEFFICIENTS

Skin friction coefficients are plotted versus Re_θ in Fig. 5.12. Shown, for reference, are correlations for laminar and fully-turbulent flows on flat walls under low-FSTI, unaccelerated flow conditions. The station 1 data point falls slightly below the

turbulent correlation. In the fully-turbulent boundary layer at stations 2 through 5, the data fall above the turbulent correlation. As stated above, the increased mixing caused by the high FSTI and concave curvature leads to high near-wall velocity gradients and skin friction coefficients. The same behavior was observed in the Kim and Simon (1991) unaccelerated flow, 8%-FSTI, concave wall case.

MEAN TEMPERATURE PROFILES

Mean temperature profiles from the five streamwise measurement stations are shown in Fig. 5.13. The edge of the thermal boundary layer, $\delta_{t99.5}$, corresponds to $y/\Delta_2 \approx 15$. As with the mean velocity profiles of Fig. 5.10, the stations 2 through 5 profiles collapse on one another and are much fuller than is the station 1 profile. As stated above, this supports the conclusion that the boundary layer is transitional at station 1 and fully-turbulent by station 2.

The temperature profiles are shown in wall coordinates in Fig. 5.14. Also shown for reference are the line $t^+=Pry^+$ and the thermal law of the wall. The station 1 profile falls below the others, but the others fall above the law of the wall. The profiles exhibit no wake, agreeing with the velocity profiles of Fig. 5.11. As stated above, this is caused by the high FSTI and concave curvature, which lead to high levels of mixing in the outer part of the boundary layer. The temperature profiles are more sensitive to acceleration than are the velocity profiles. This difference between the velocity and temperature profiles is caused by the different effects of the pressure gradient, dP/dx, on the momentum and thermal boundary layers. These effects are explained in Appendix A. Temperature profiles can be calculated for accelerated flows using the method given in Appendix A. Figure 5.15 shows the station 3 profile data along with the calculated profile corresponding to the conditions at this station. The agreement in good.

In unaccelerated flow along the concave wall at 8% FSTI, the temperature profiles agree with the standard thermal law of the wall. Figure 5.16 shows unaccelerated flow results. The raw thermocouple voltage data for these profiles were acquired during the study of Kestoras (1993), and were processed here using the method explained above in Chapter 2. The stations 2, 3 and 5 profiles lie just below the law of the wall. The station 4 profile shows more deviation, which is probably caused by a higher uncertainty in T_w at this station. This uncertainty resulted from a sparsity of very near-wall data points at this station. As in the accelerating flow (Fig. 5.14), no wakes appear in the unaccelerated flow profiles of Fig. 5.16.

STANTON NUMBERS

Stanton numbers are plotted verses $Re_{\Delta 2}$ in Fig. 5.17. Data are shown for the present case; the 8%-FSTI, unaccelerated, concave-wall case corresponding to the profiles of Fig. 5.16; and the 8%-FSTI, flat-wall case of Kim and Simon (1991). Shown for reference are correlations from Kays and Crawford (1993) for low FSTI, unaccelerated laminar and turbulent boundary layers on flat walls. The flat-wall data agree with the turbulent correlation. The concave wall cases agree with each other, and the data lie well above the turbulent correlation. By the last measurement station, the Stanton numbers in the accelerated concave wall cases lie 20% above the correlation. In the unaccelerated case, this difference reaches 40%.

The Reynolds analogy factor, $\frac{2St}{C_f}$, drops from about 1.13 in the unaccelerated flow cases to 1.0 in the accelerated flow. This drop is attributed to the mismatch between the momentum and thermal boundary layer thicknesses in the accelerated flow. Because the thermal boundary layer is thicker than the momentum boundary layer in the accelerated flow (see Fig. 5.6), one should expect low heat transfer coefficients relative to skin friction coefficients at a given streamwise position.

FLUCTUATING VELOCITY MEASUREMENTS

$\overline{u'}$ Profiles

Profiles of $\overline{u'} / U_{cw}$ are plotted verses y/θ in Fig. 5.18. Figure 5.18a shows the full boundary layer, and Fig. 5.18b is an expanded view of the near wall region. Also shown for comparison are profiles from unaccelerated, 8% FSTI flows on flat and concave walls from Kim and Simon (1991). The peaks in the profiles shift from 1.8 at station 1 to 0.4 at station 2. The levels of the peaks drop from 0.16 to 0.14 between these two stations. As the flow proceeds downstream, the peaks continue to drop in magnitude and move toward the wall, although much more slowly than between stations 1 and 2. The high peak at station 1 is typical of transitional flows, as documented by others, such as Sohn and Reshotko (1991) and Kim and Simon (1991). The drop in the free-stream turbulence level with streamwise distance can be seen in Fig. 5.18a.

Fig 5.19 shows the $\overline{u'}$ profiles in wall coordinates. The peaks at all stations are at $y^+=17$, which is typical for turbulent boundary layers. The levels of the peaks drop from a high value of 3 at station 1 to 2.4 at the downstream stations. Peaks between 2 and 2.5 are typical of most turbulent boundary layers. The profiles at stations 2 through 5 collapse everywhere except near the free-stream. The unaccelerated flow profiles are much fuller in the outer part of the boundary layer than are the accelerated flow profiles. This is particularly true for the unaccelerated concave-wall case. The acceleration suppresses the turbulence in the outer part of the boundary layer below flat-wall levels. A small bump can be seen in the accelerated flow profiles near $y^+=100$. This is a remnant of the plateau observed in the unaccelerated flow.

$\overline{v'}$ Profiles

Figure 5.20 shows profiles of $\overline{v'} / U_{cw}$ plotted versus y/θ. The profiles drop from a peak near the wall to a minimum near $y/\theta=9$ ($\delta_{99.5}\approx 0.5$). The profiles then rise to the

free-stream value. Similar behavior is seen in unaccelerated, high-FSTI flows, such as those presented by Kestoras (1993). The near-wall fluctuations are caused by turbulence production in the boundary layer. The free-stream fluctuations appear to be damped near the wall, resulting in the minimum. The $\overline{v'}$ profiles may be useful for determining the extent to which parts of the boundary layer are influenced by the free-stream turbulence.

Figure 5.21 shows the $\overline{v'}$ profiles in wall coordinates. With the exception of the station 1 profile, the profiles collapse in the near wall region. The minimum noted above falls near y^+=200. The minimum becomes less clear at the downstream stations as the free-stream values drop.

Turbulent Shear Stress Profiles

Profiles of the turbulent shear stress are plotted as $-\overline{u'v'} / U_{cw}^2$ versus y/θ in Fig. 5.22. Also shown are unaccelerated, 8% concave- and flat-wall profiles from Kim and Simon (1991). There is considerable shear stress activity beyond $\delta_{99.5}$ ($y/\theta \approx 20$). This is caused by the combined destabilizing effects of high FSTI and concave curvature, and indicates considerable mixing in the outer part of the boundary layer. This activity decreases at the downstream stations, as the acceleration suppresses the turbulence. At all stations, the accelerated flow profiles fall below Kim and Simon's concave wall profile, and by the downstream stations, there is agreement with the flat wall profile. The acceleration is counteracting the curvature effect.

The profiles are plotted in wall coordinates in Fig. 5.23. The accelerated flow profiles collapse on a straight line in these coordinates, and appear to extrapolate to 1 at the wall. Unity is the expected near-wall value for a fully-turbulent boundary layer. The profiles are much less full than those of the unaccelerated-flow comparison cases.

Eddy Viscosity

Profiles of the eddy viscosity, ε_M, are shown in Fig. 5.24. The magnitudes are comparable to those seen by Kestoras (1993) in 8% FSTI, unaccelerated flow along the same concave wall. Kestoras (1993) found the eddy viscosity was an order of magnitude higher in his high FSTI flow than in low (0.6%) FSTI flows along flat and concave walls. In the low-FSTI cases, the ε_M profiles reached a maximum at $y/\delta_{99.5}$=0.5, and decreased toward zero in the outer part of the boundary layer. In the high-FSTI cases, the eddy viscosity rises monotonically from the wall. The combined effects of high FSTI and concave curvature cause a rise in ε_M, particularly in the outer part of the boundary layer.

Mixing Length of Momentum

Profiles of the mixing length, ℓ_M, are shown in Fig. 5.25. Near the wall, the profiles are expected to follow the line $\ell_M = \kappa y$, where κ=0.41 is the von Kármán constant. The profiles follow the line from the wall to y/θ=8 ($y/\delta_{99.5}$≈0.4). Farther from the wall, the mixing length rises above the line. Kays and Crawford (1993) present data from low disturbance flows which show the mixing length following the line $\ell_M = \kappa y$ to $y/\delta_{99.5}$≈0.2, then leveling off at ℓ_M=0.085$\delta_{99.5}$. In the present case, ℓ_M rises well above these expectations in the outer part of the boundary layer. As stated above, this indicates increased mixing in the high-FSTI, concave wall flow. Kestoras (1993) observed the same behavior in unaccelerated flow.

TURBULENT HEAT FLUX MEASUREMENTS

Attempts to measure fluctuating temperatures and the turbulent heat flux failed in the present case. Time traces of instantaneous temperature consistently contained data points with temperature well above the wall temperature (by as much as 7°C). Given that the wall to free-stream temperature difference was about 5°C, and that the temperature at the wall should have been higher than anywhere in the flow, these measurements were

obviously unreasonable. The erroneous readings were traced to cross-talk between the wires of the three-wire probe. The errors may have been caused by electrical induction effects between the wires, or by convection of hot fluid from the region adjacent to one of the hot wires (which are held at 250°C) to the temperature sensor (cold wire). These errors were peculiar to the present case. No such errors were observed in earlier studies in which this probe was used (e.g. Kim and Simon (1991) and Kestoras (1993)), and no errors were observed in the latter cases of the present study. Since, at this time, a higher-acceleration case was of pressing concern, it was decided to proceed with a higher-K case while diagnosing and correcting the $\overline{v't'}$ measurement technique in preparation for that case. Turbulent heat flux results for these latter cases are presented below in Chapters 6 and 7.

CONCLUSIONS

Acceleration with $K=0.75\times10^{-6}$ did not significantly affect the transition process, but did have a significant effect on the fully-turbulent boundary layer. This acceleration caused a reduction in various turbulence quantities, particularly in the outer part of the boundary layer. Concave curvature has been shown to be destabilizing and to promote turbulent mixing, particularly in high-FSTI flows (Kim and Simon, 1991). Acceleration has been shown here to counteract this effect.

More information about the transition region in this flow might have been obtained if the measurement stations had been spaced more closely in the upstream region of the flow. It was decided, however, that more interesting results might be obtained in a more strongly accelerated boundary layer. Further measurements in the $K=0.75\times10^{-6}$ case were not taken, and attention was shifted to the two cases presented below in Chapters 6 and 7.

Station	1	2	3	4	5
x [m] †	0.106	0.353	0.610	0.861	1.108
U_{cw} [m/s]	8.20	9.15	10.34	11.59	13.30
FSTI [%]	7.6	6.2	5.4	4.4	3.2
$Re_x \times 10^{-5}$	0.5488	2.0342	3.9647	6.2605	9.2345
$\delta_{99.5}$ [cm]	0.450	2.196	2.766	2.333	2.534
δ^* [mm]	0.691	1.371	1.645	1.556	1.476
θ [mm]	0.374	1.025	1.261	1.201	1.143
H	1.845	1.337	1.305	1.296	1.291
Re_{δ^*}	357	790	1069	1131	1230
Re_θ	194	591	819	873	953
$\theta/R \times 10^3$	0.386	1.057	1.300	1.238	1.178
$\delta_{99.5}/R$ [%]	0.46	2.26	2.85	2.41	2.61
$C_f \times 10^3$	6.00	6.40	6.00	5.80	5.60
T_w [°C]	29.72	30.25	30.42	30.31	30.10
T_∞ [°C]	28.03	28.03	28.01	27.98	27.94
$\delta_{t99.5}$ [cm]	0.280	1.521	2.371	3.643	3.153
Δ_2 [mm]	0.237	1.111	1.534	2.296	2.336
$Re_{\Delta 2}$	120	626	973	1639	1896
$St \times 10^3$	4.474	3.212	2.931	2.910	2.650
$2St/C_f$	1.49	1.00	0.98	1.00	0.95

† Mean temperature profiles were acquired 2 cm upstream of these locations. Velocity profile data were extrapolated 2 cm upstream for calculation of Δ_2.

Table 5.1: Parameters for the $K=0.75\times10^{-6}$ Case

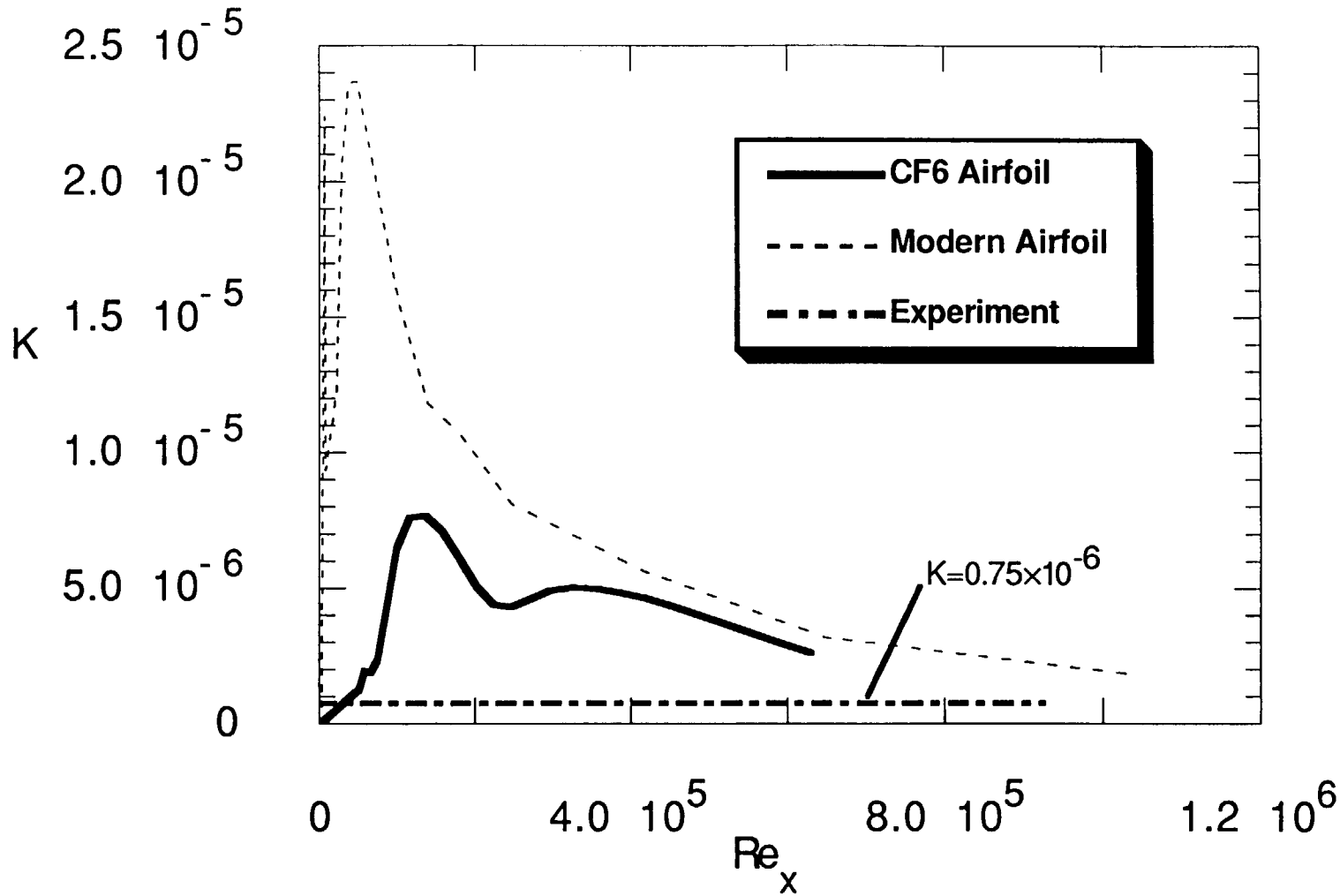

Fig. 5.1: Typical Pressure Side Acceleration Profiles

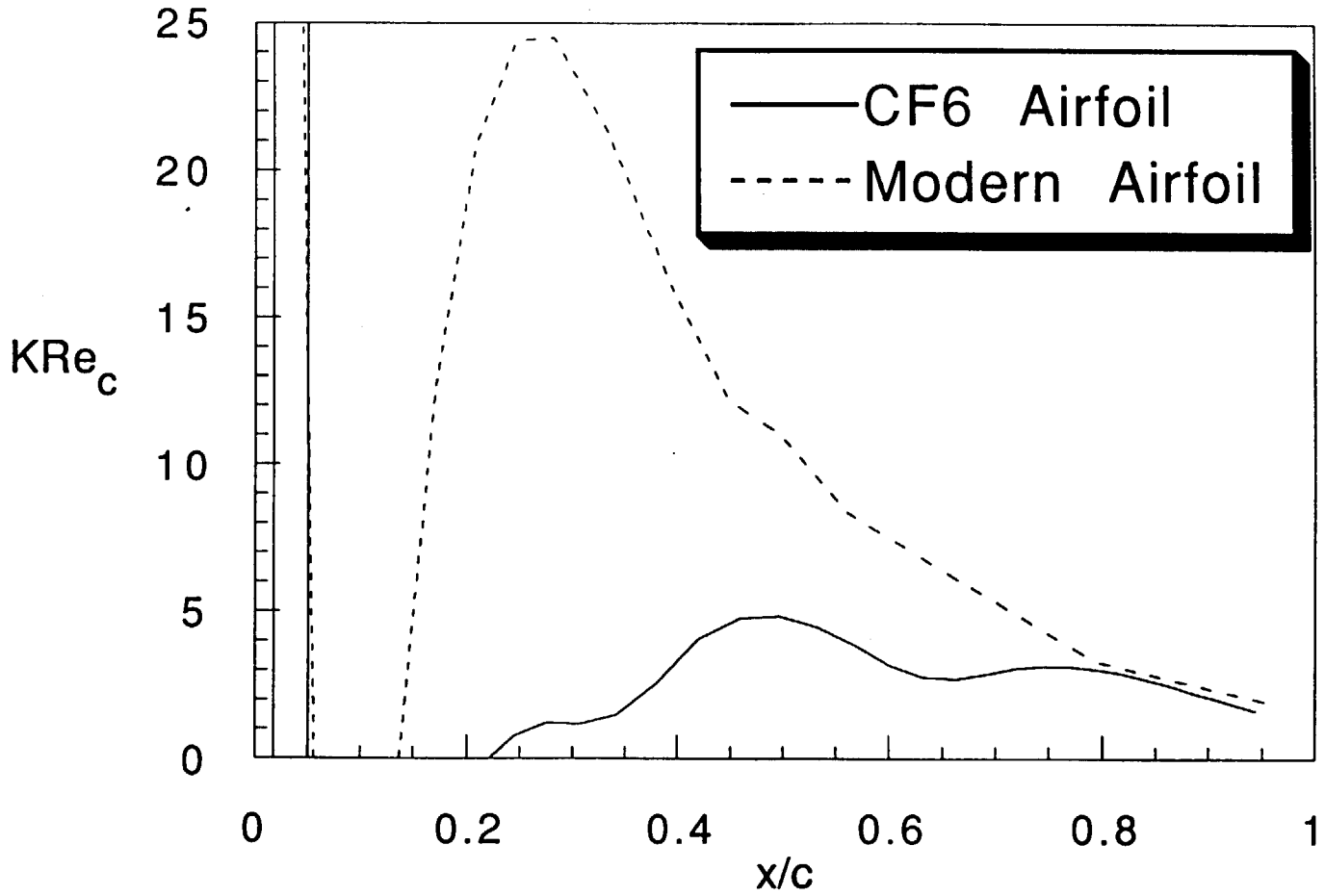

Fig. 5.2: Pressure Side KRe$_c$ Profiles for Two Airfoils

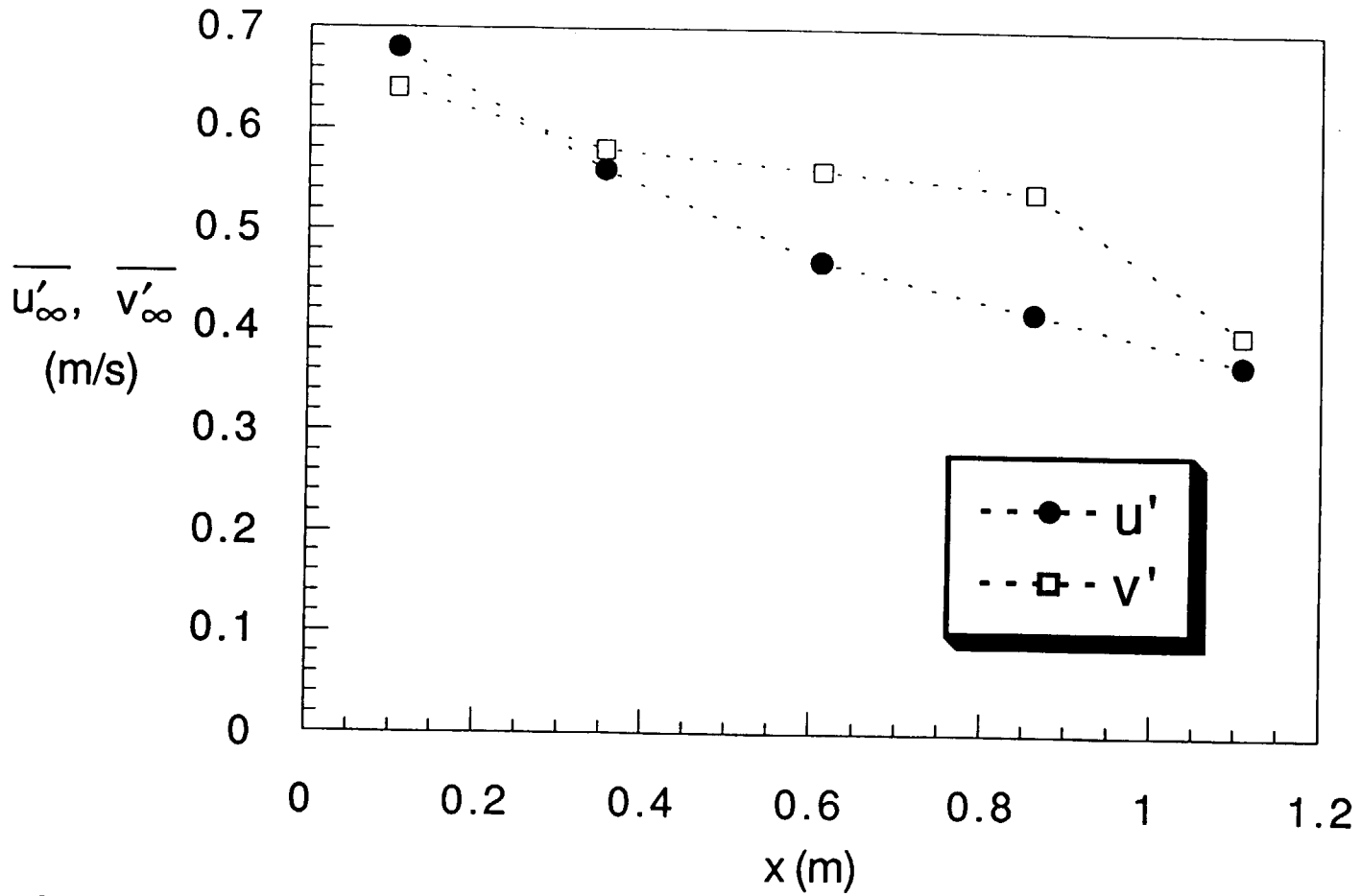

Fig. 5.3a: Free-Stream Turbulence Levels, Dimensional Coordinates, $K=0.75\times10^{-6}$ Case

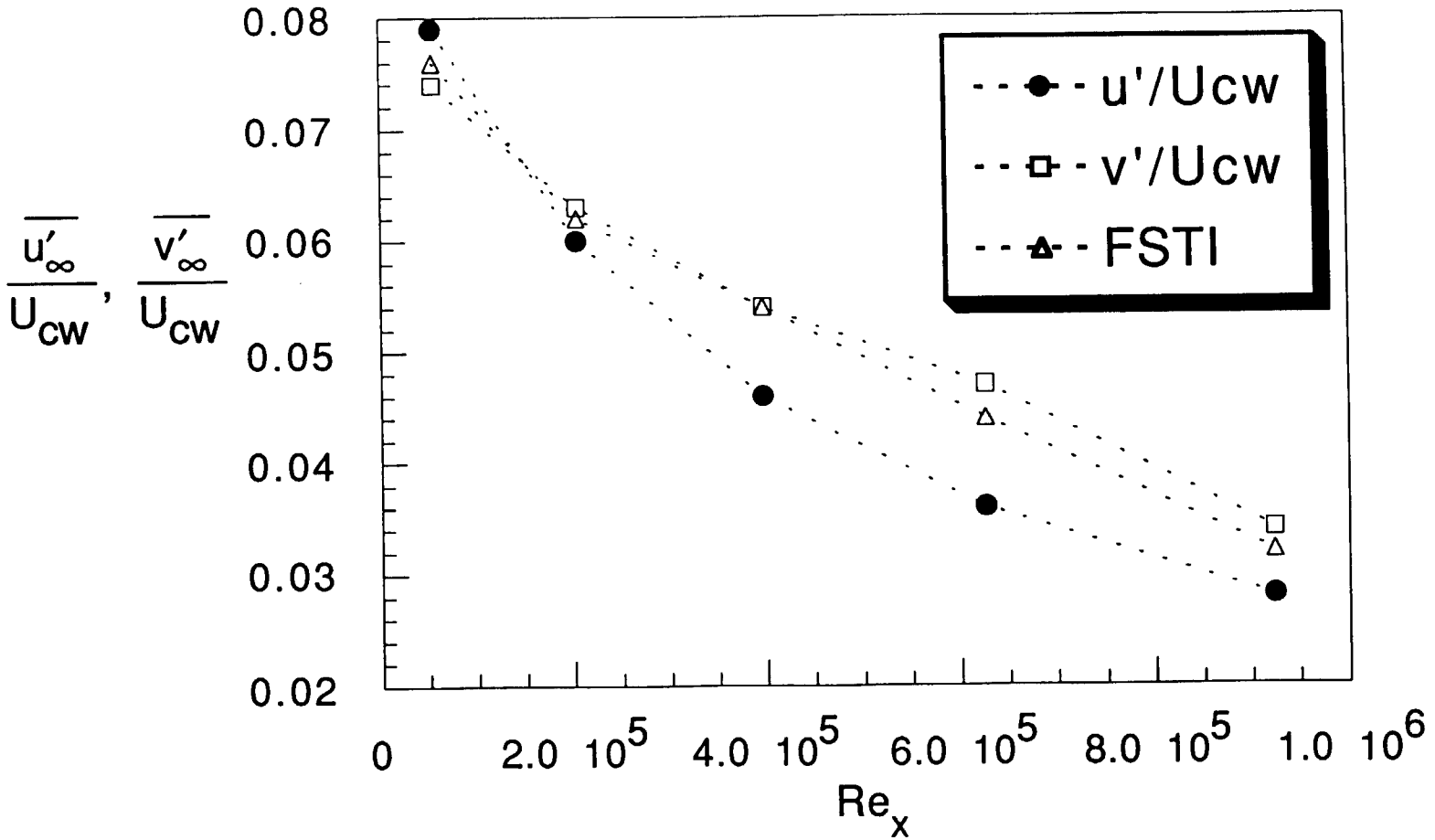

Fig. 5.3b: Free-Stream Turbulence Levels, Nondimensional Coordinates, K=0.75×1 0^{-6} Case

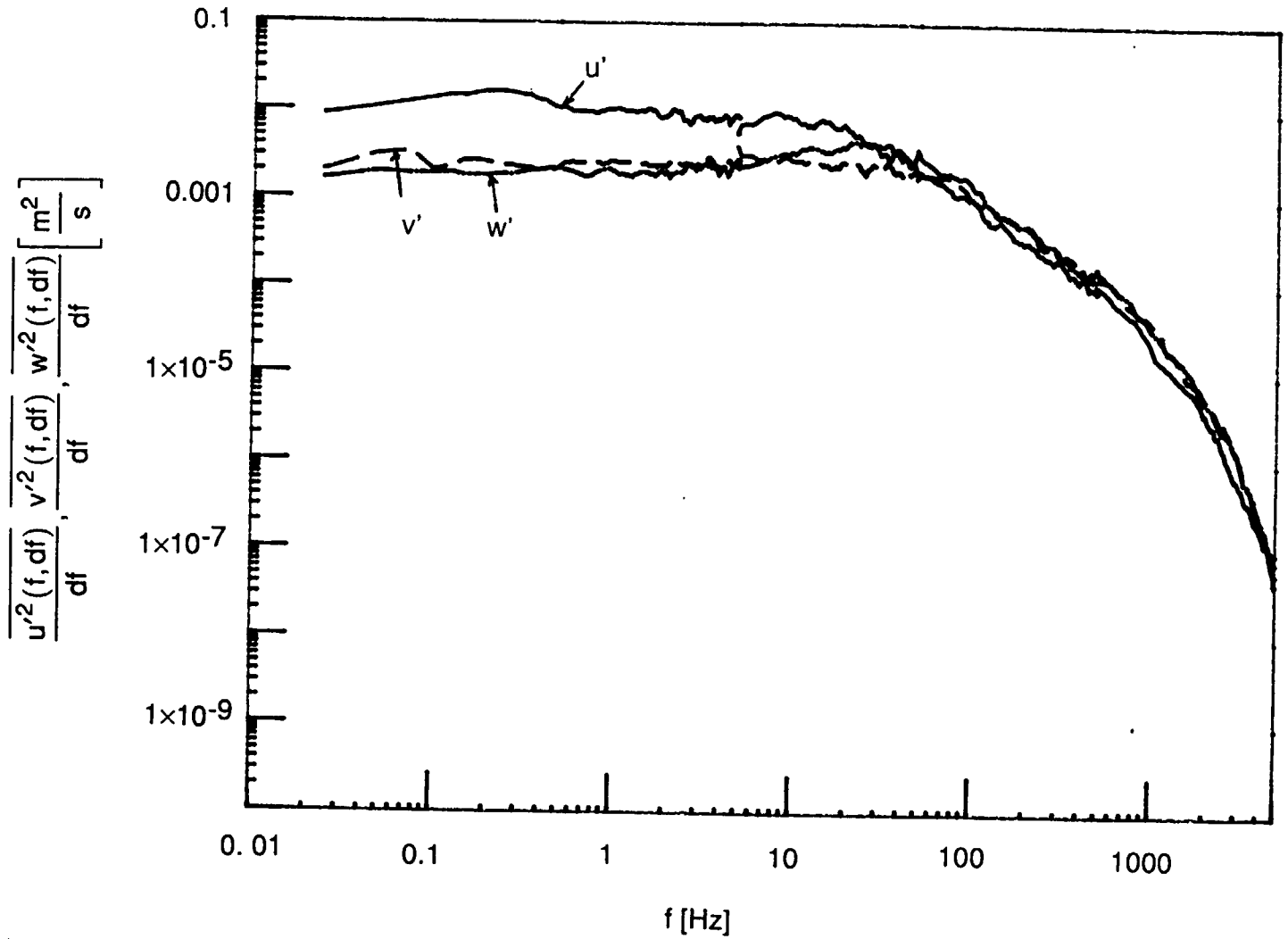

Fig. 5.4a: Station 1 Free-Stream Spectra, K=0.75×10-6 Case

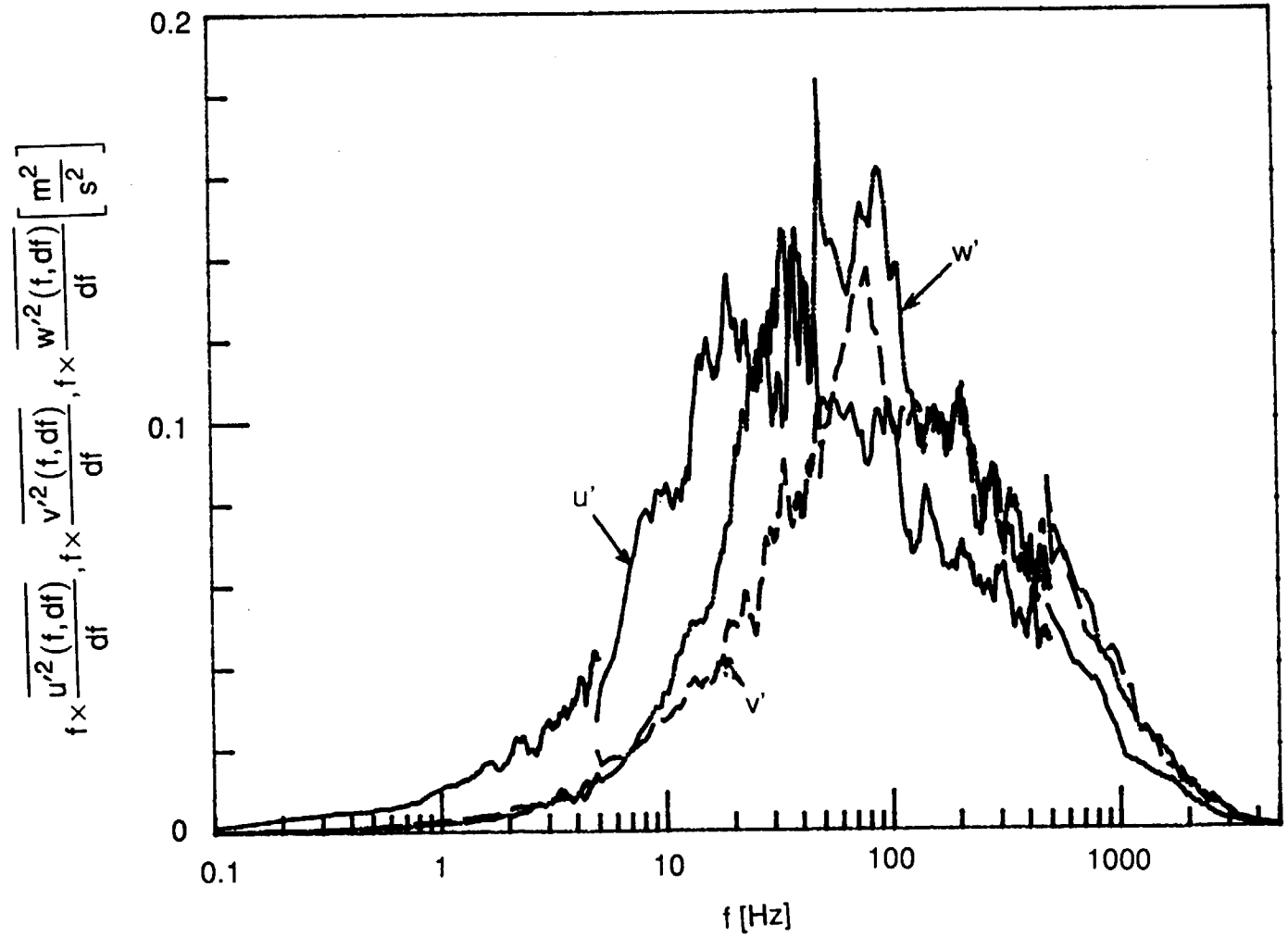

Fig. 5.4b: Station 1 Free-Stream Spectra, K=0.75×10^{-6} Case, Energy Coordinates

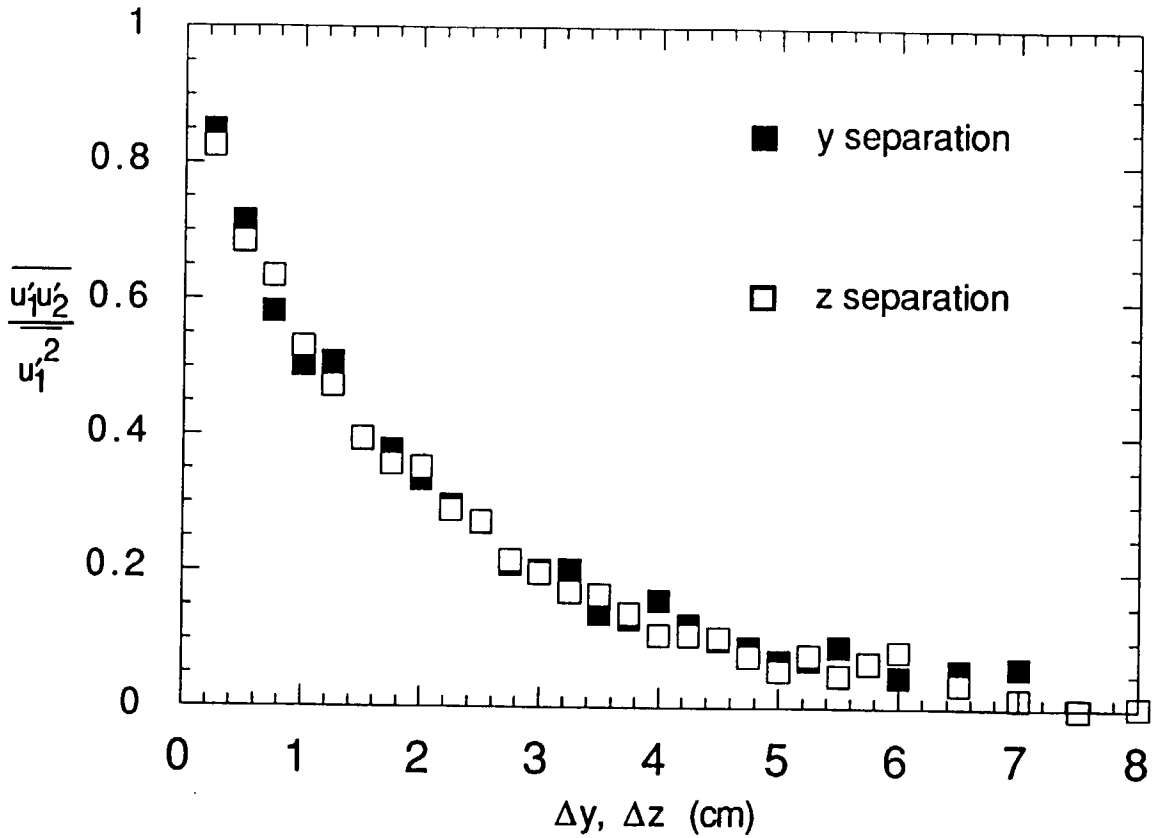

Fig. 5.5: Two Point Correlation of Streamwise Velocity Fluctuations, Station 1, K=0.75×1 0^{-6} Case

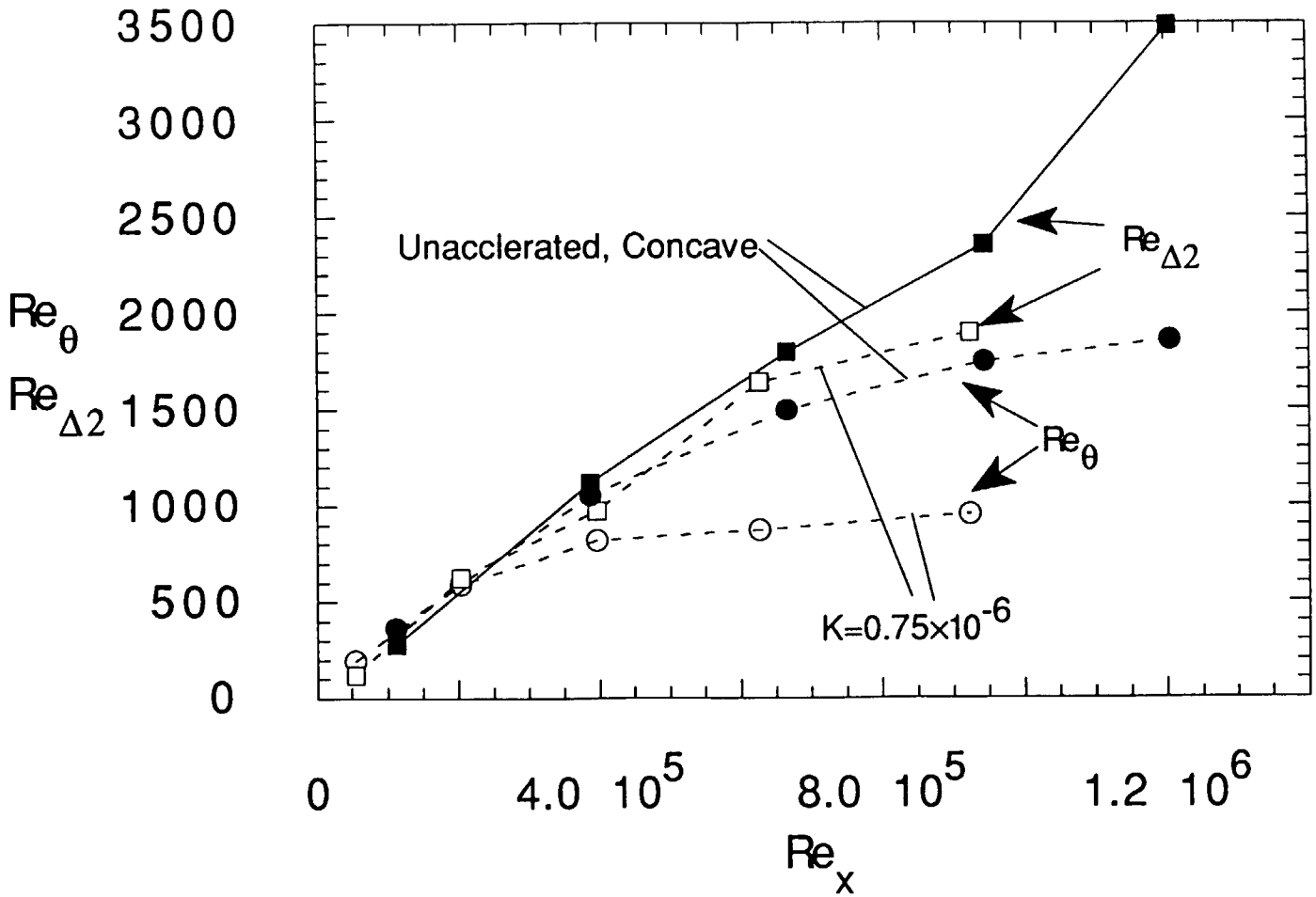

Fig. 5.6: Momentum and Thermal Boundary Layer Growth

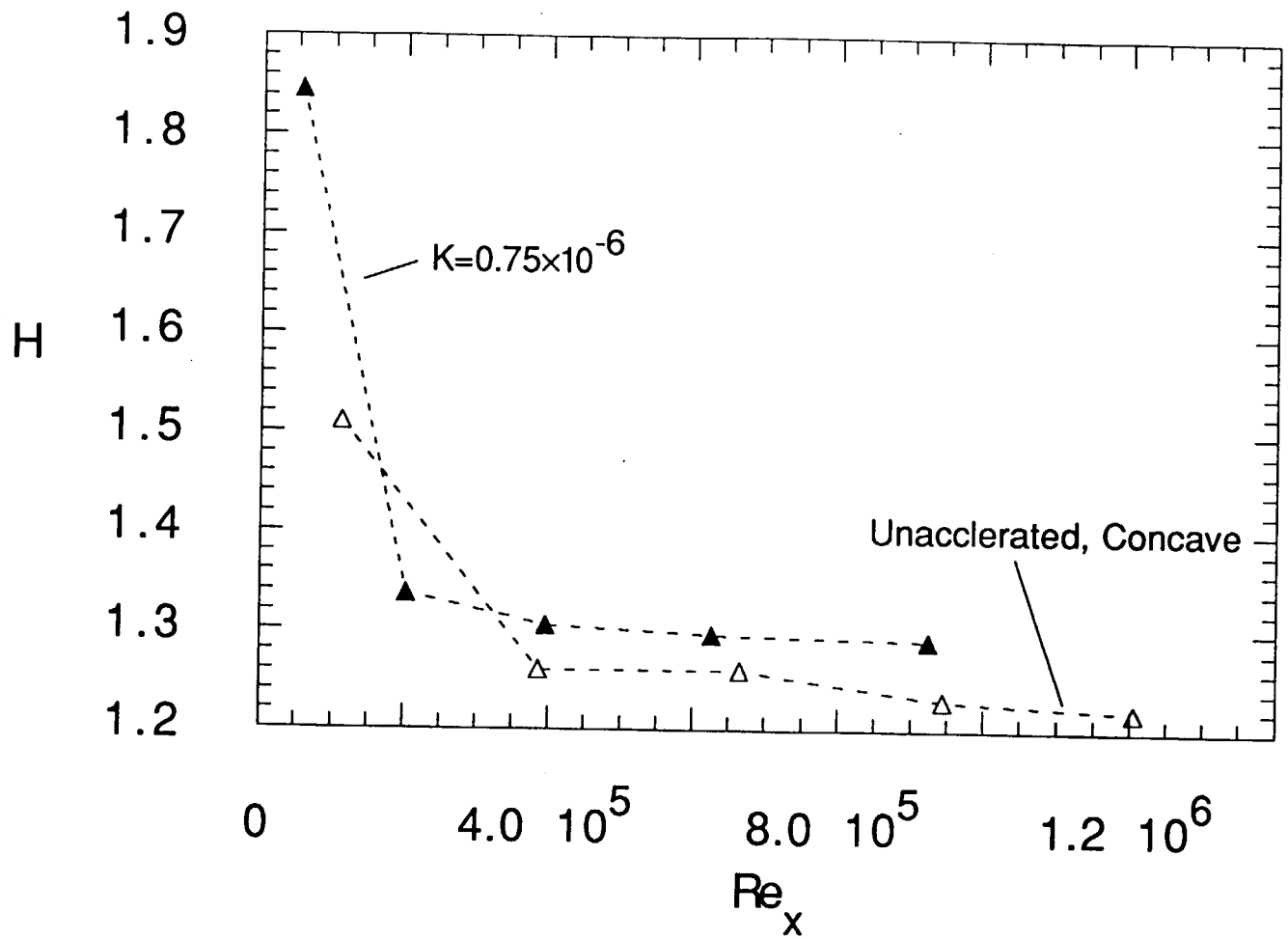

Fig. 5.7: Shape Factor vs Re_x

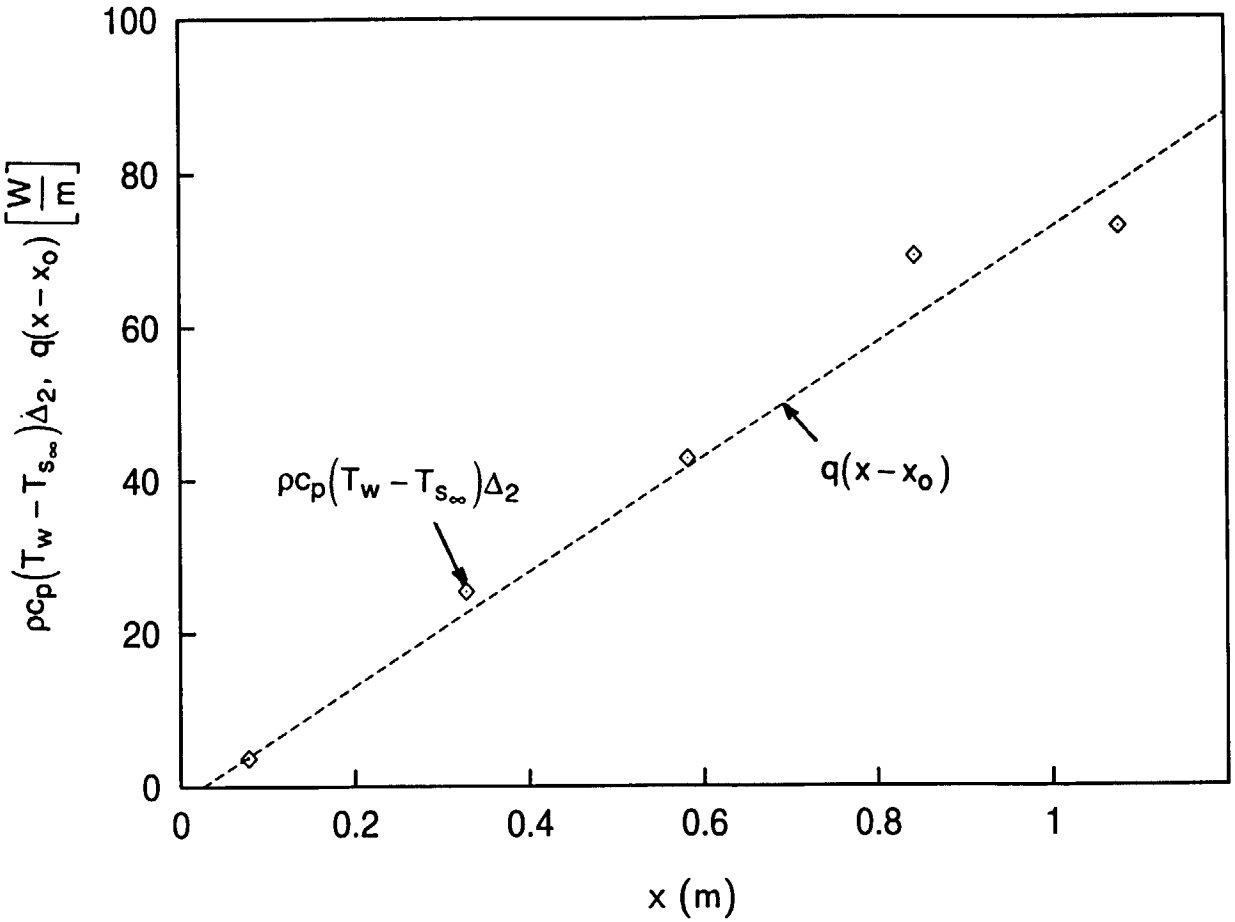

Fig. 5.8: Energy Balance
K=0.75x10^{-6} Case

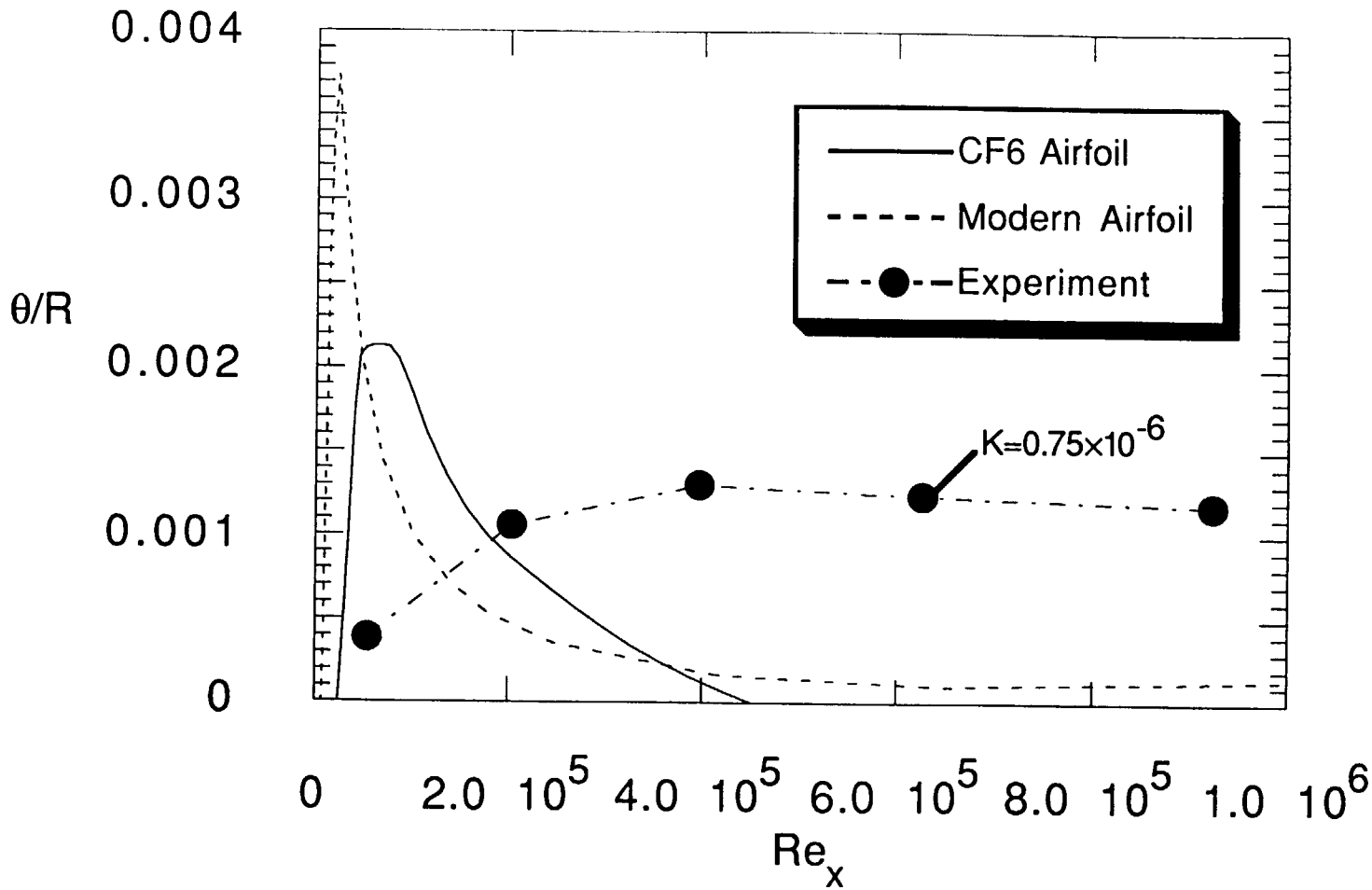

Fig. 5.9: Strength of Curvature for Experiment and Pressure Side of Two Typical Airfoils

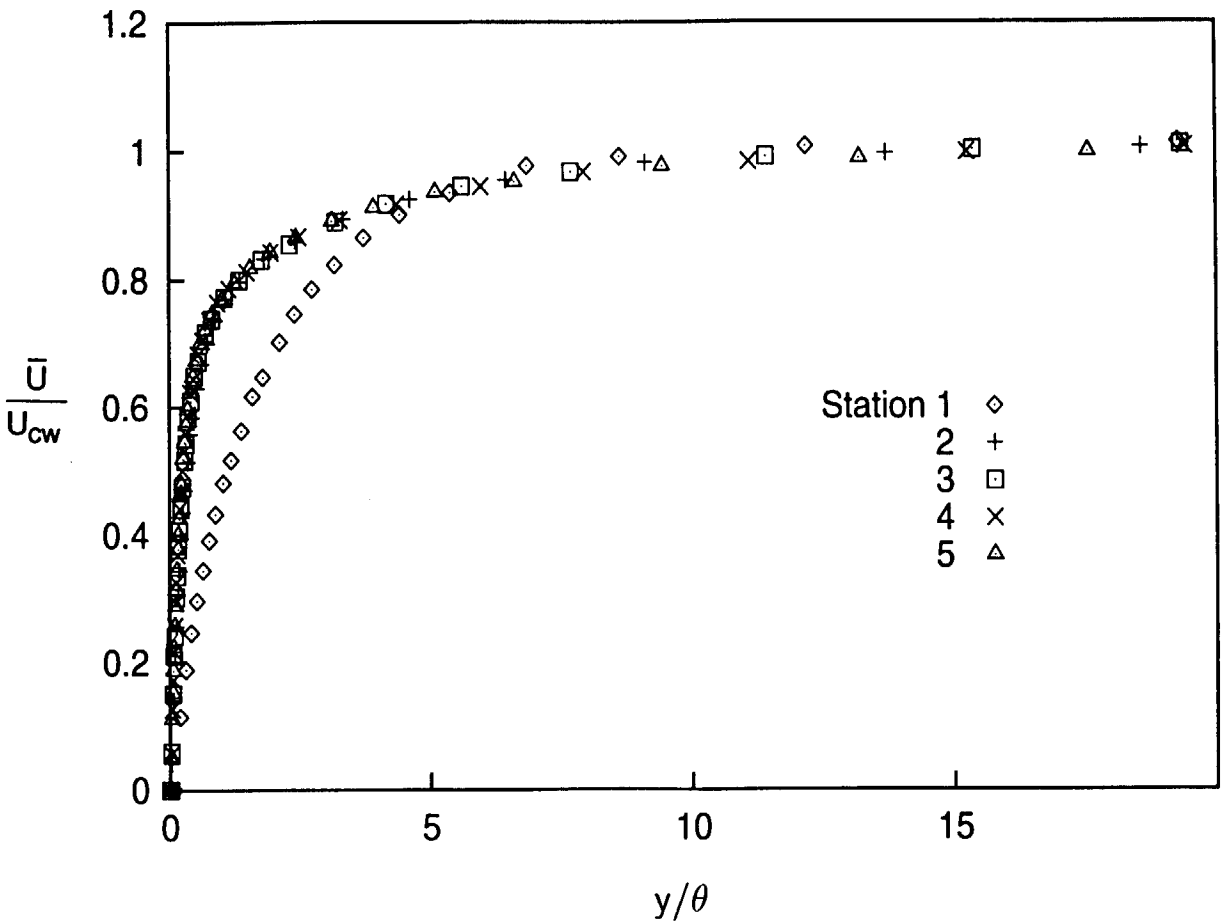

Fig. 5.10: Mean Velocity Profiles
K=0.75x10^{-6} Case

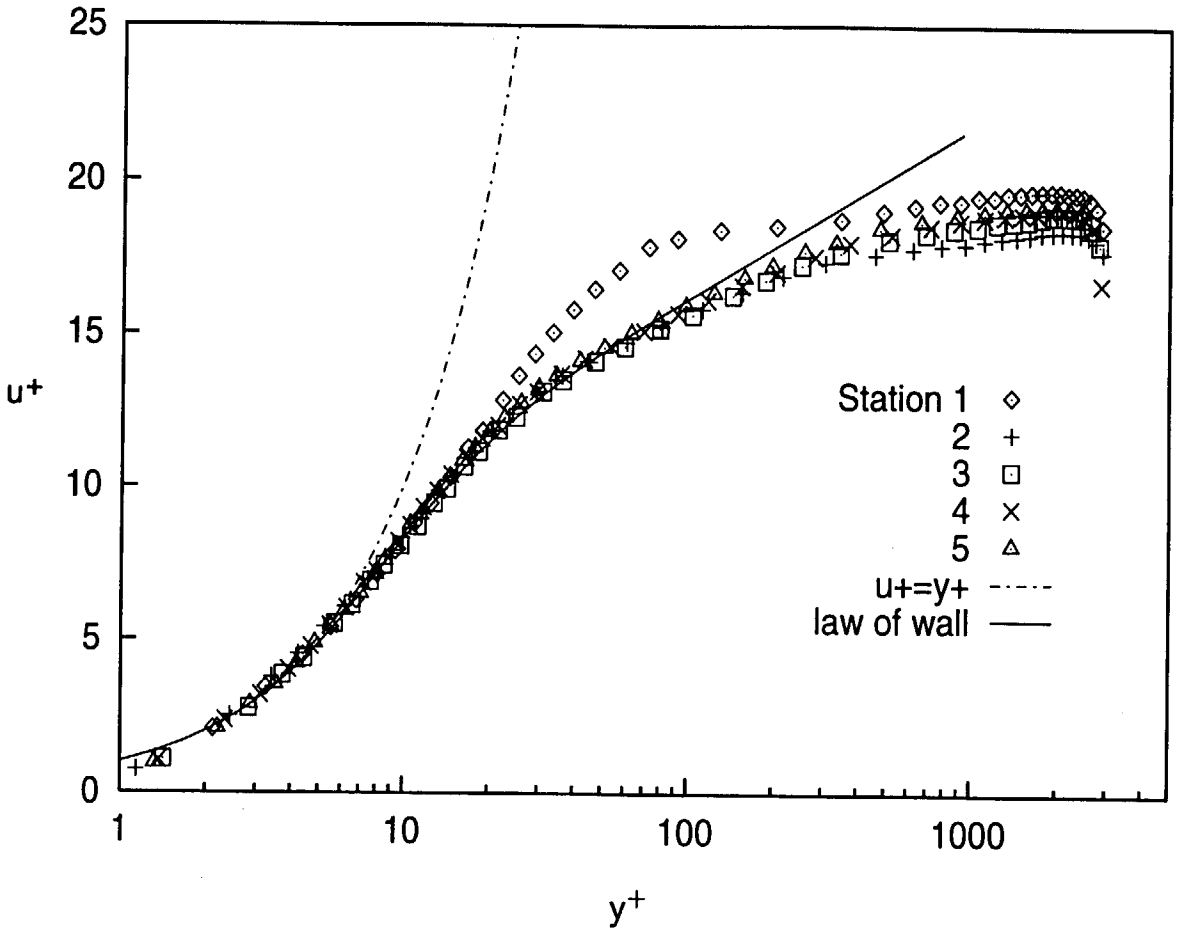

Fig. 5.11: Mean Velocity Profiles,Wall Coordinates
K=0.75x10^{-6} Case

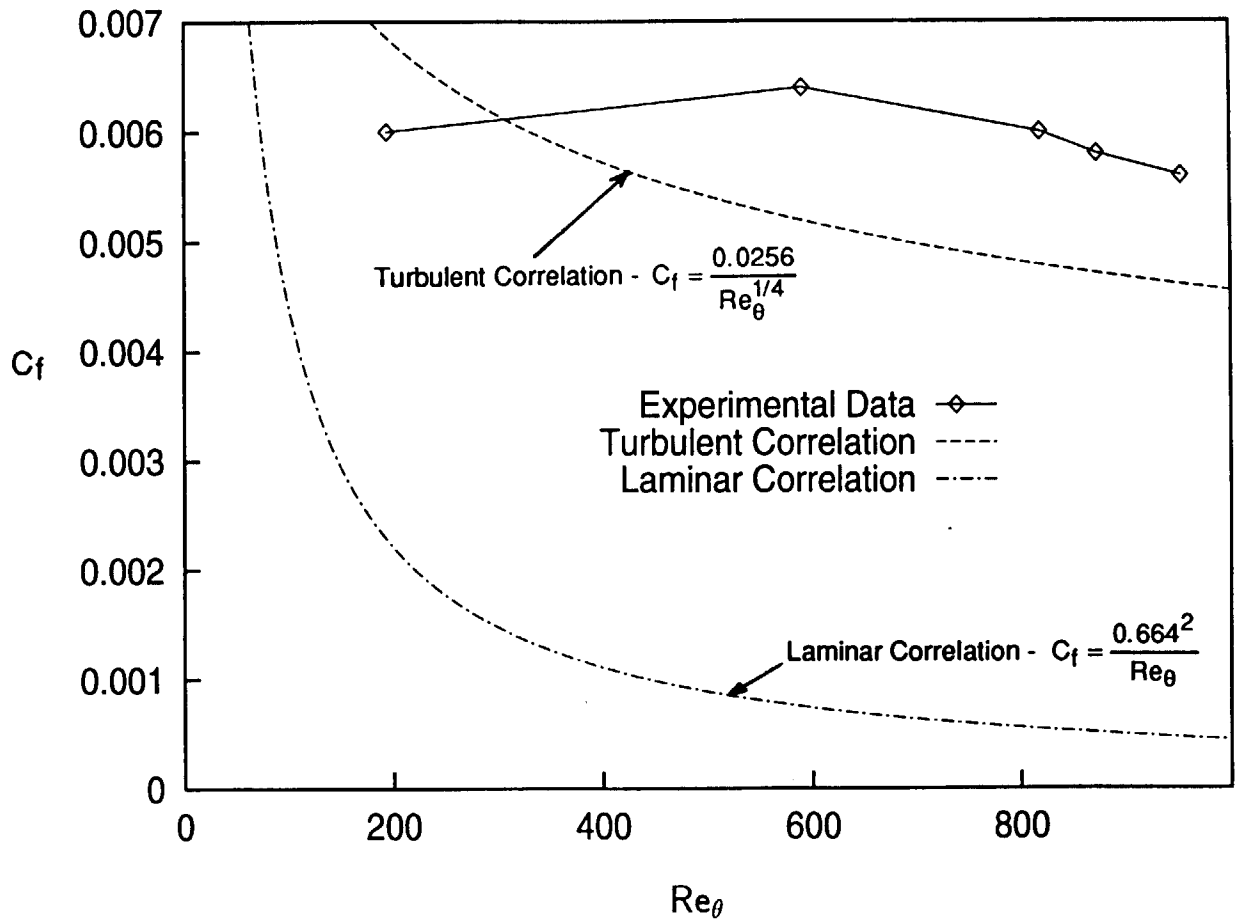

Fig. 5.12: Skin Friction Coefficients vs Re_θ
K=0.75x10^{-6} Case

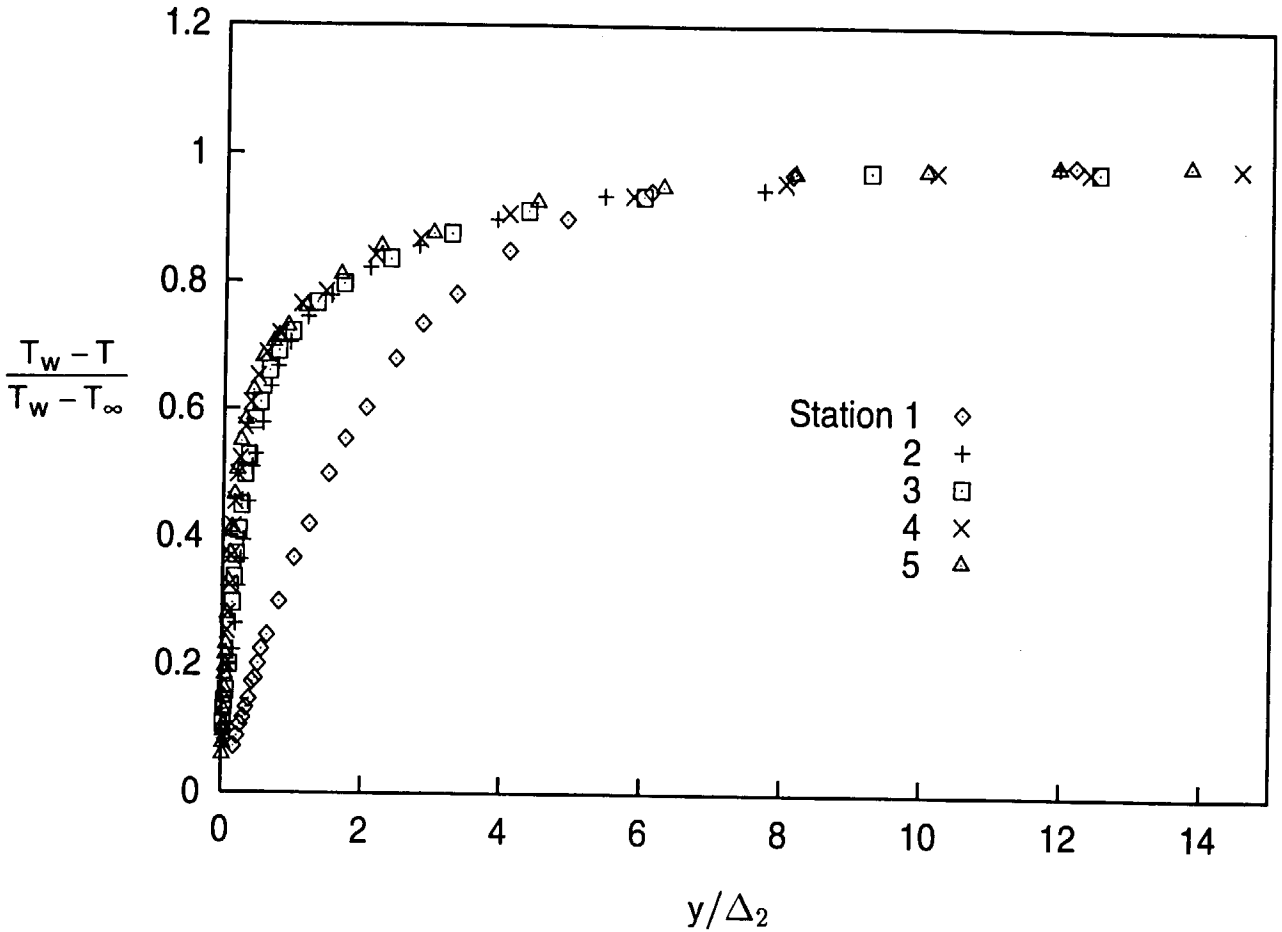

Fig. 5.13: Mean Temperature Profiles
K=0.75x10^{-6} Case

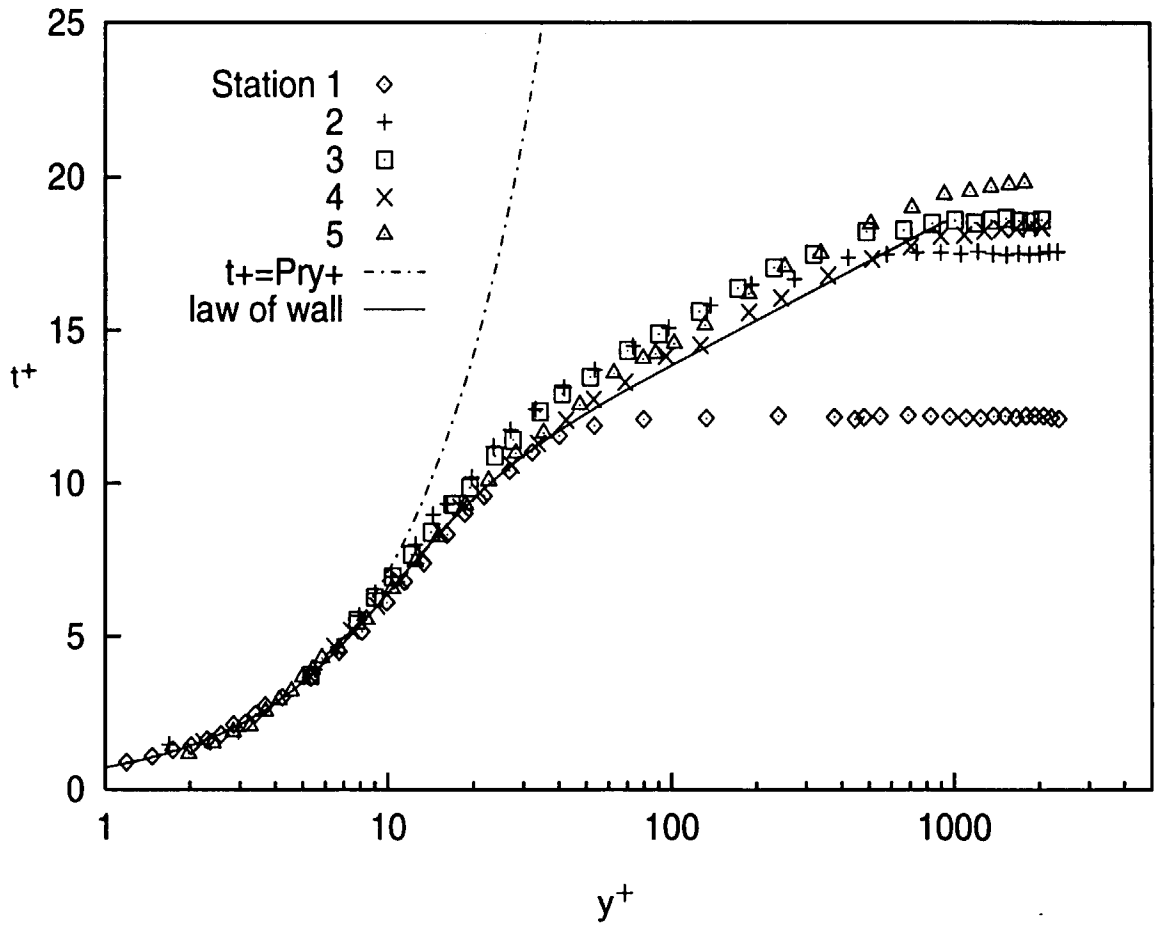

Fig. 5.14: Mean Temperature Profiles,Wall Coordinates
K=0.75x10^{-6} Case

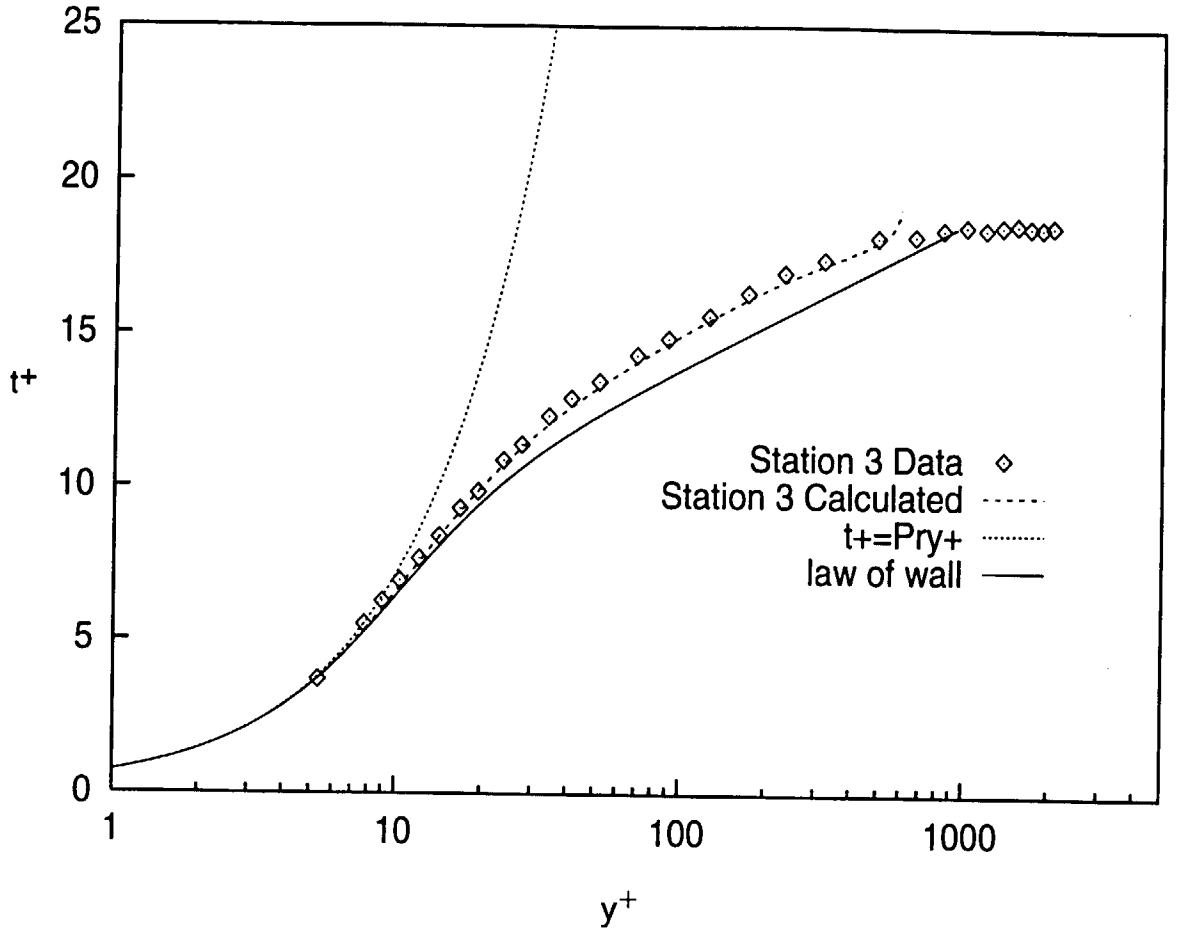

Fig. 5.15: Comparison of Calculated Profile to Data
K=0.75x10^{-6} Case

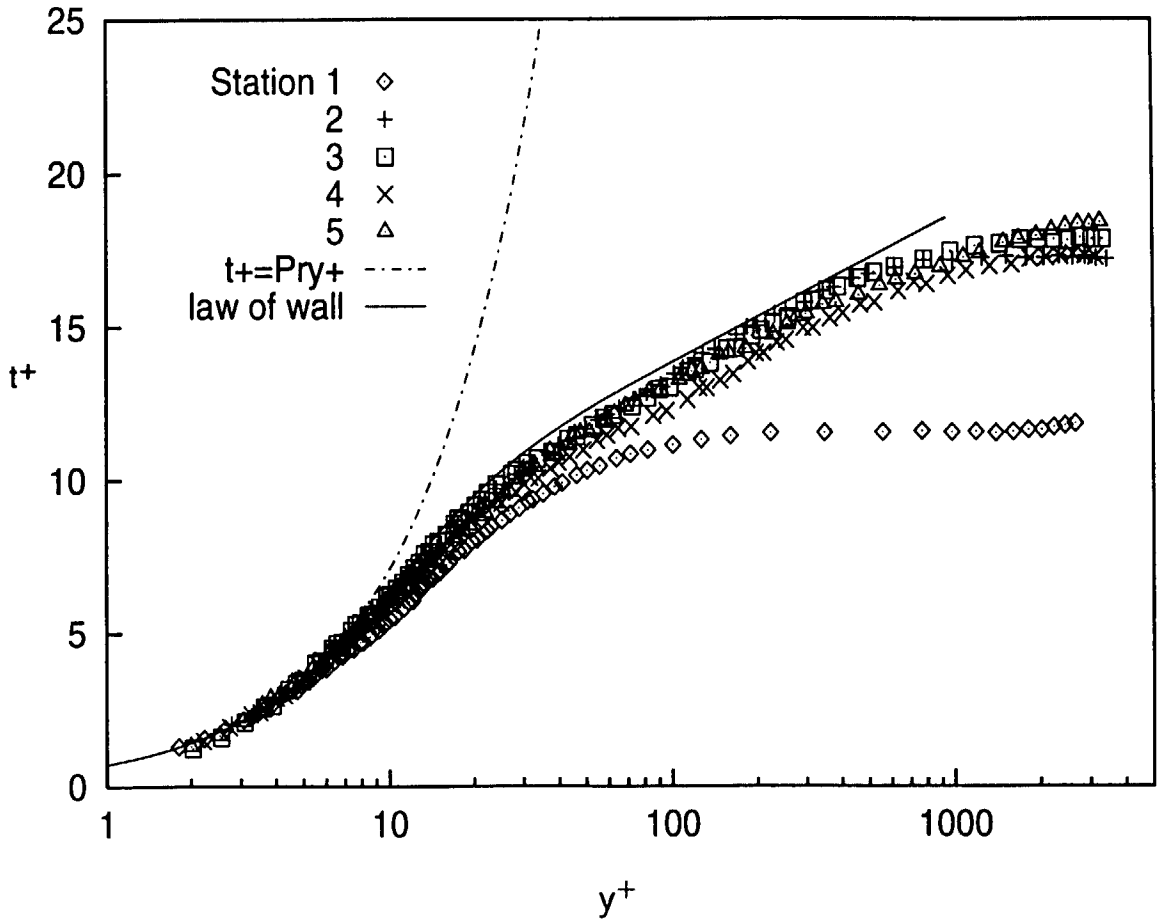

Fig. 5.16: Mean Temperature Profiles Unaccelerated, Concave-Wall Case

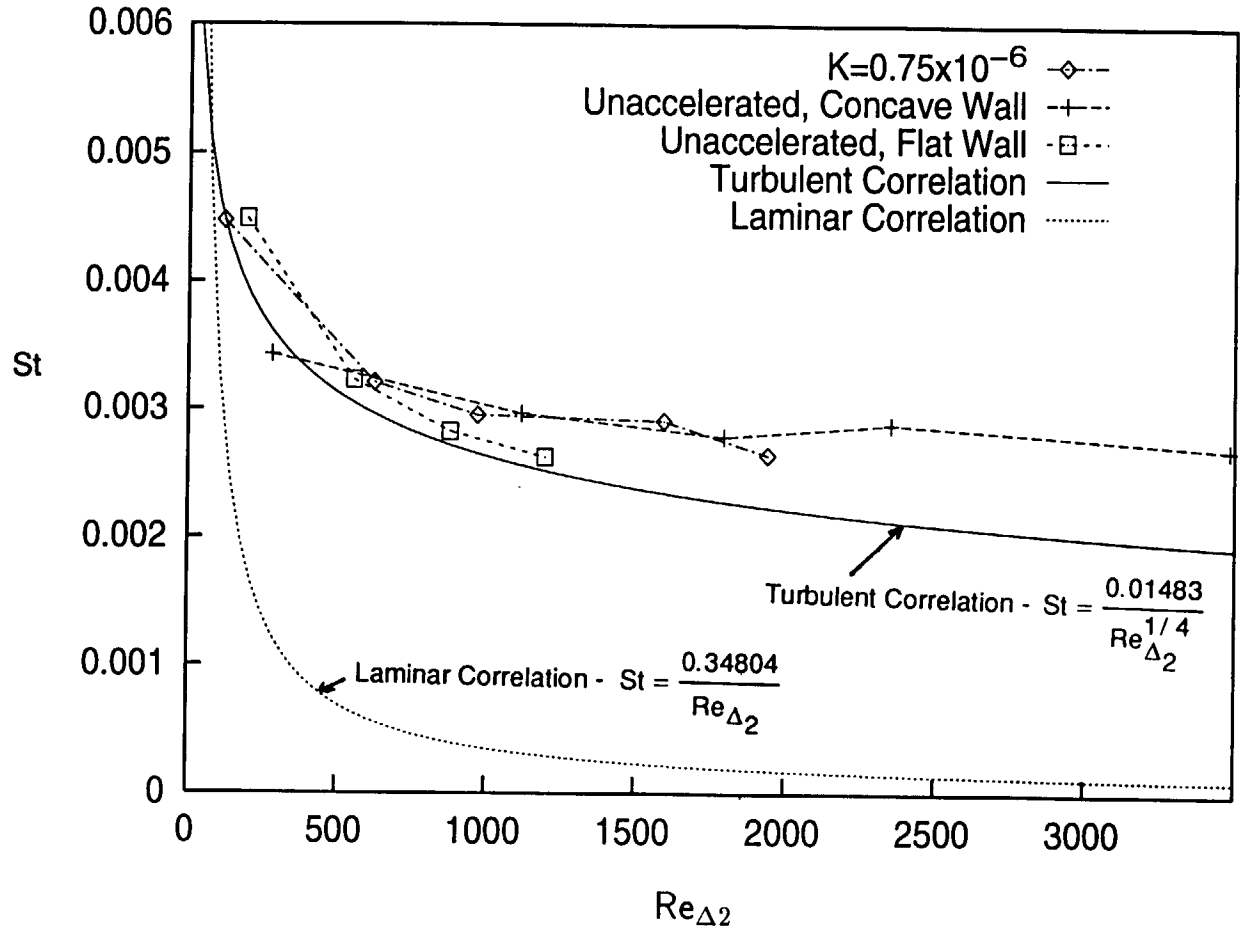

Fig. 5.17: Stanton Number vs $Re_{\Delta 2}$

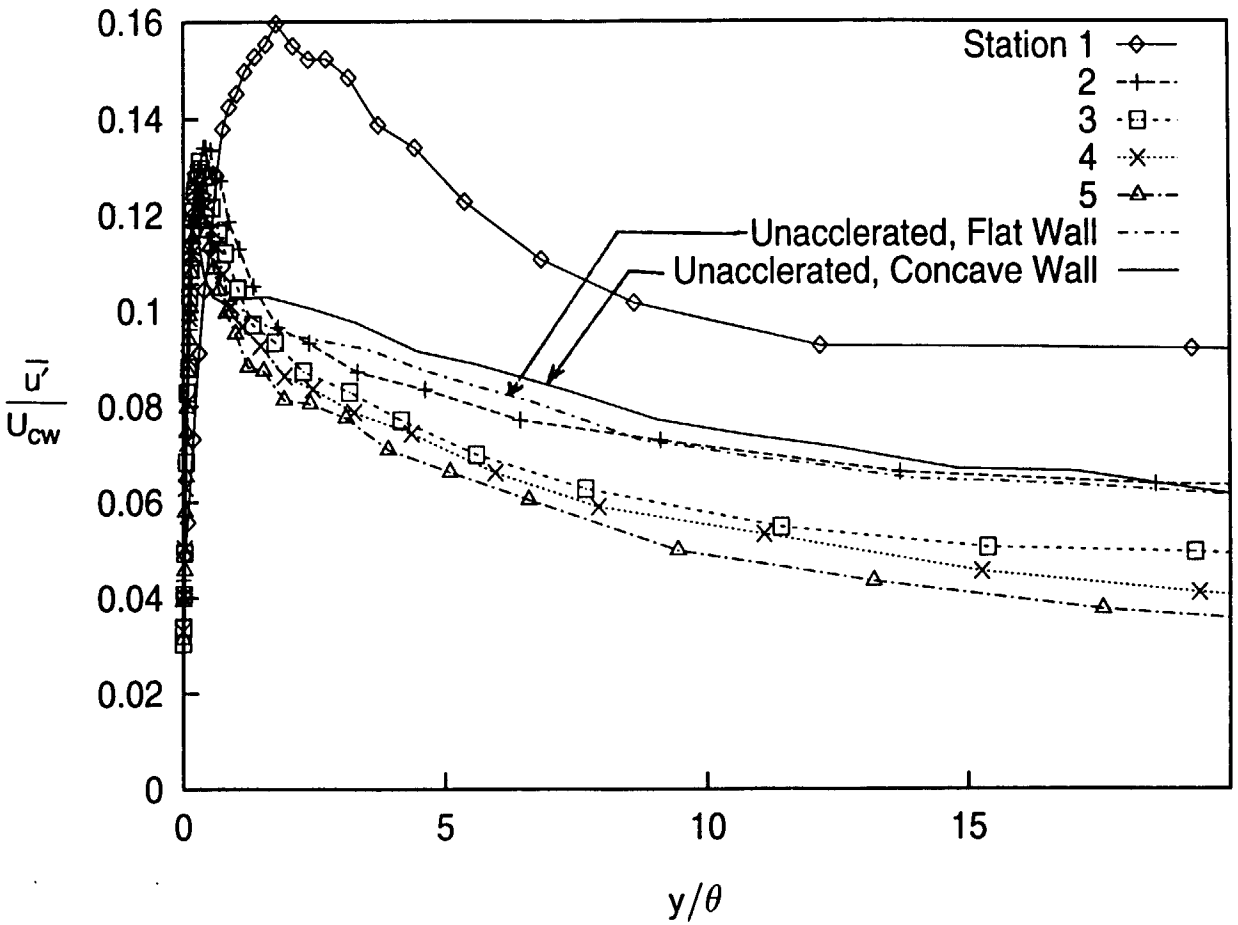

Fig. 5.18a: Fluctuating Streamwise Velocity Profiles
K=0.75x10^{-6} Case

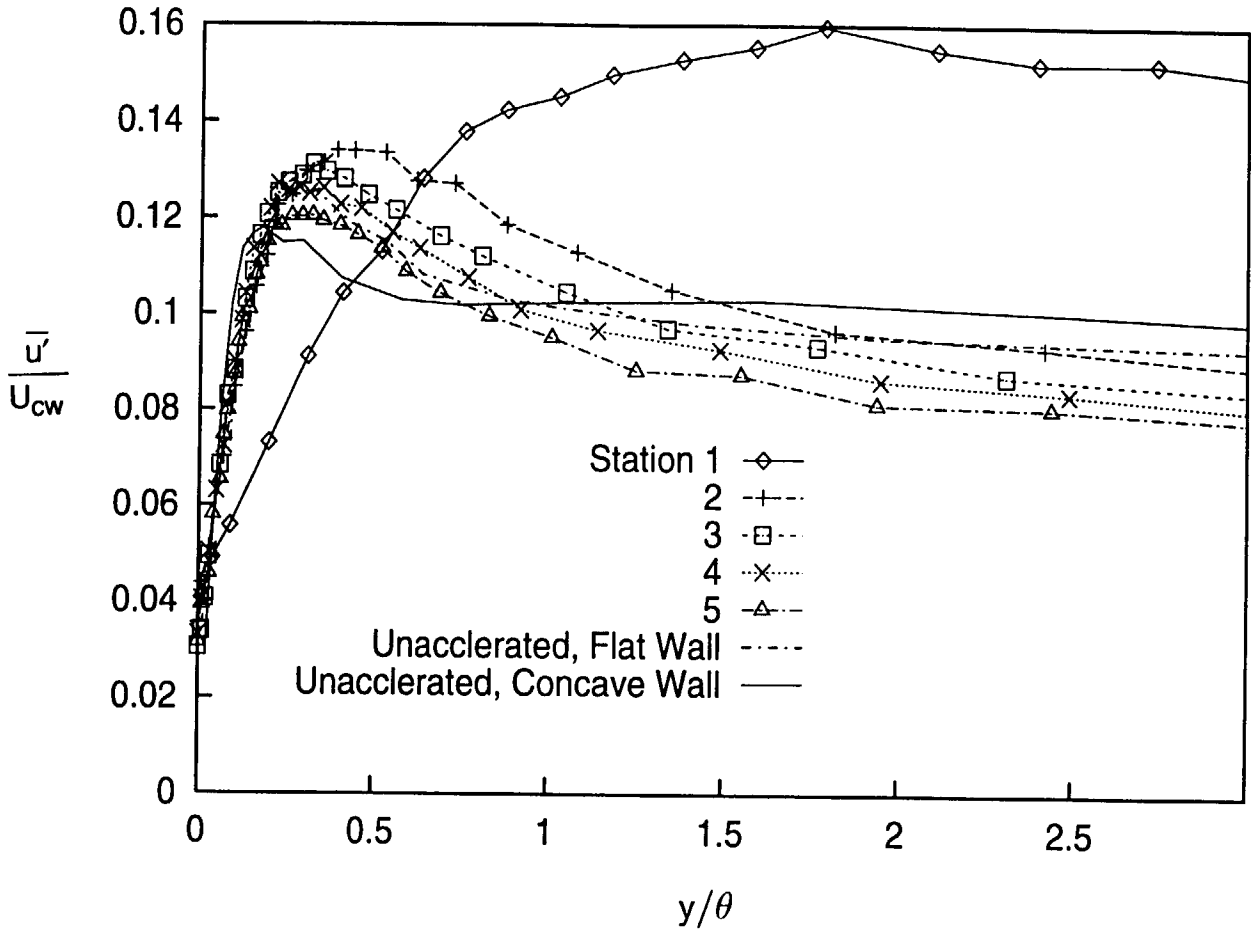

Fig. 5.18b: Fluctuating Streamwise Velocity Profiles
K=0.75x10^{-6} Case

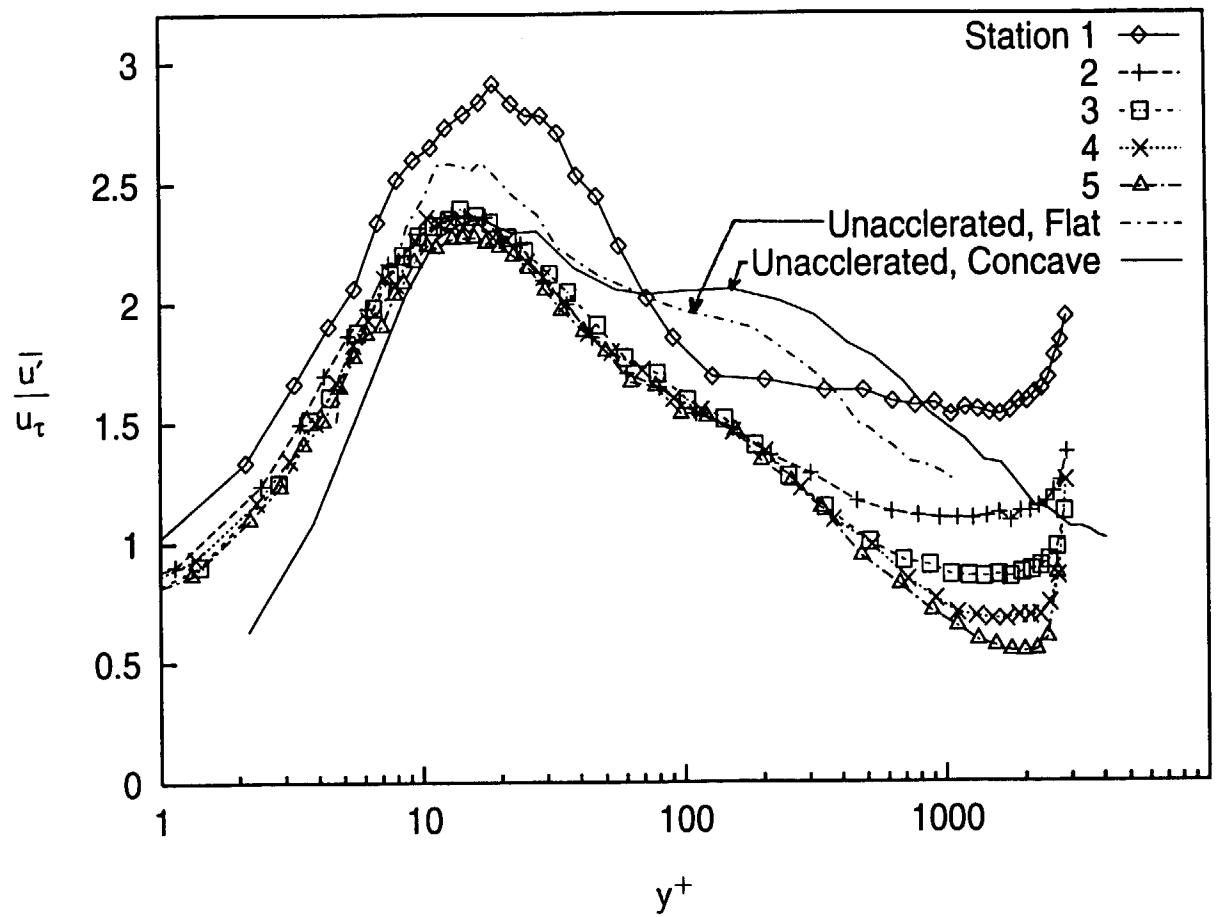

Fig. 5.19: Fluctuating Streamwise Velocity Profiles, Wall Coordinates
K=0.75x10^{-6} Case

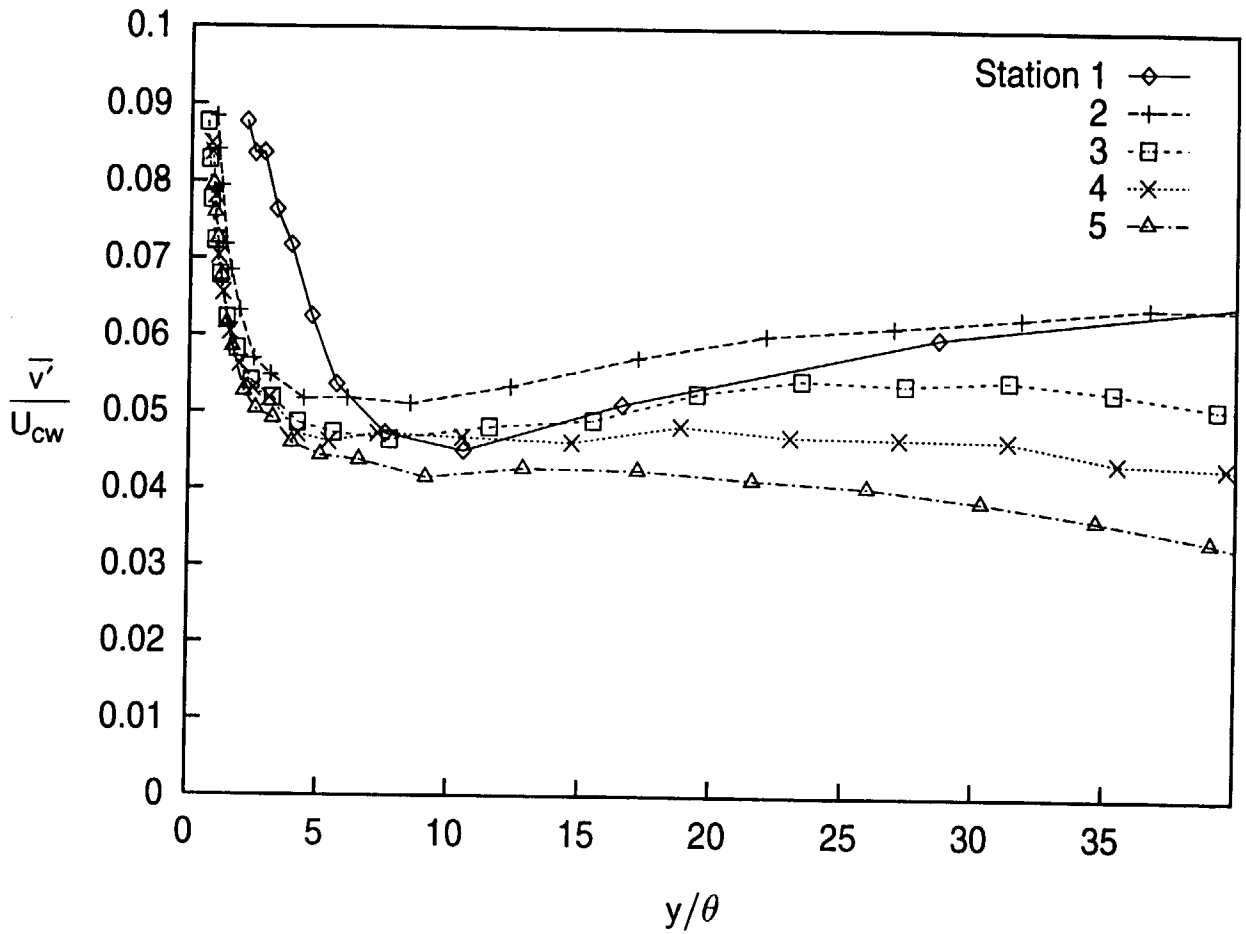

Fig. 5.20: Fluctuating Normal Velocity Profiles
K=0.75x10^{-6} Case

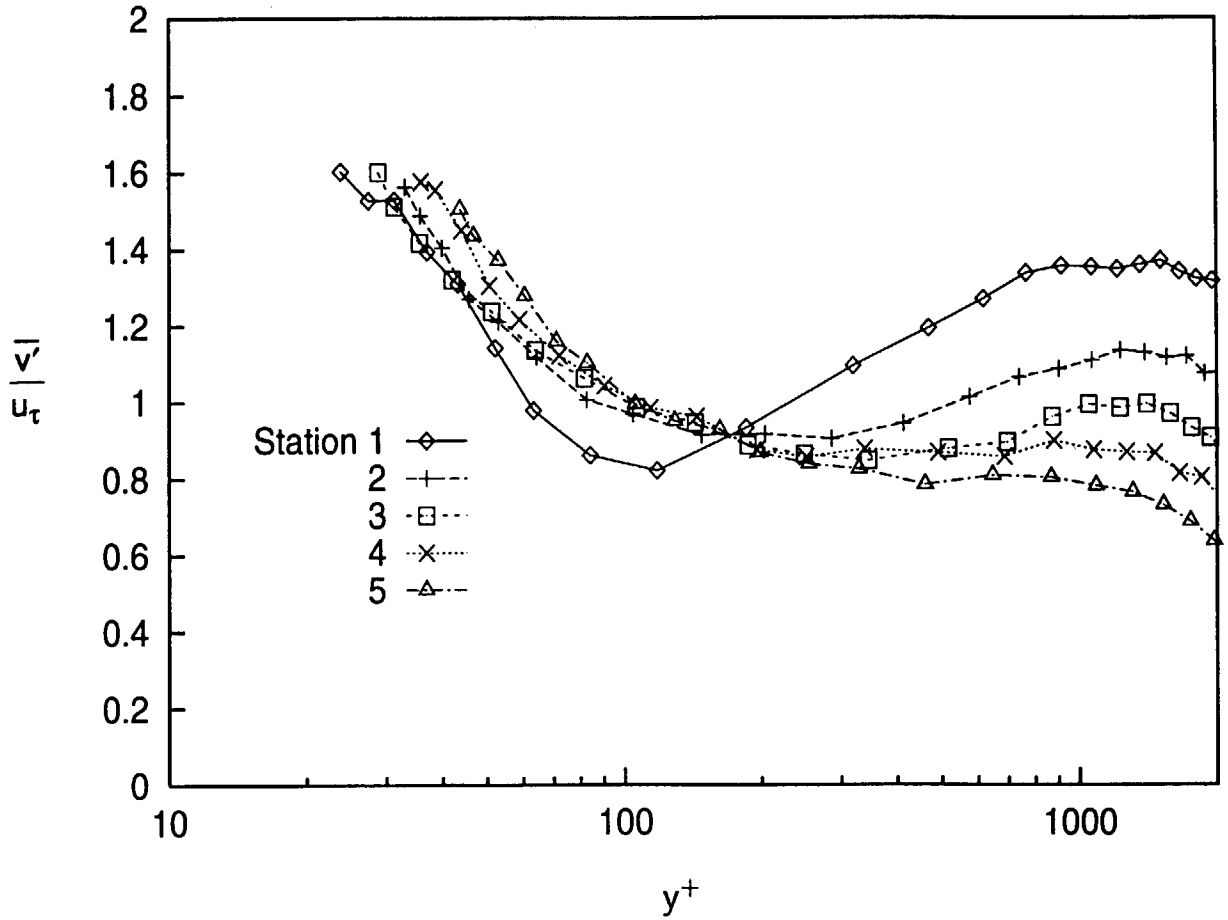

Fig. 5.21: Fluctuating Normal Velocity Profiles, Wall Coordinates
K=0.75x10^{-6} Case

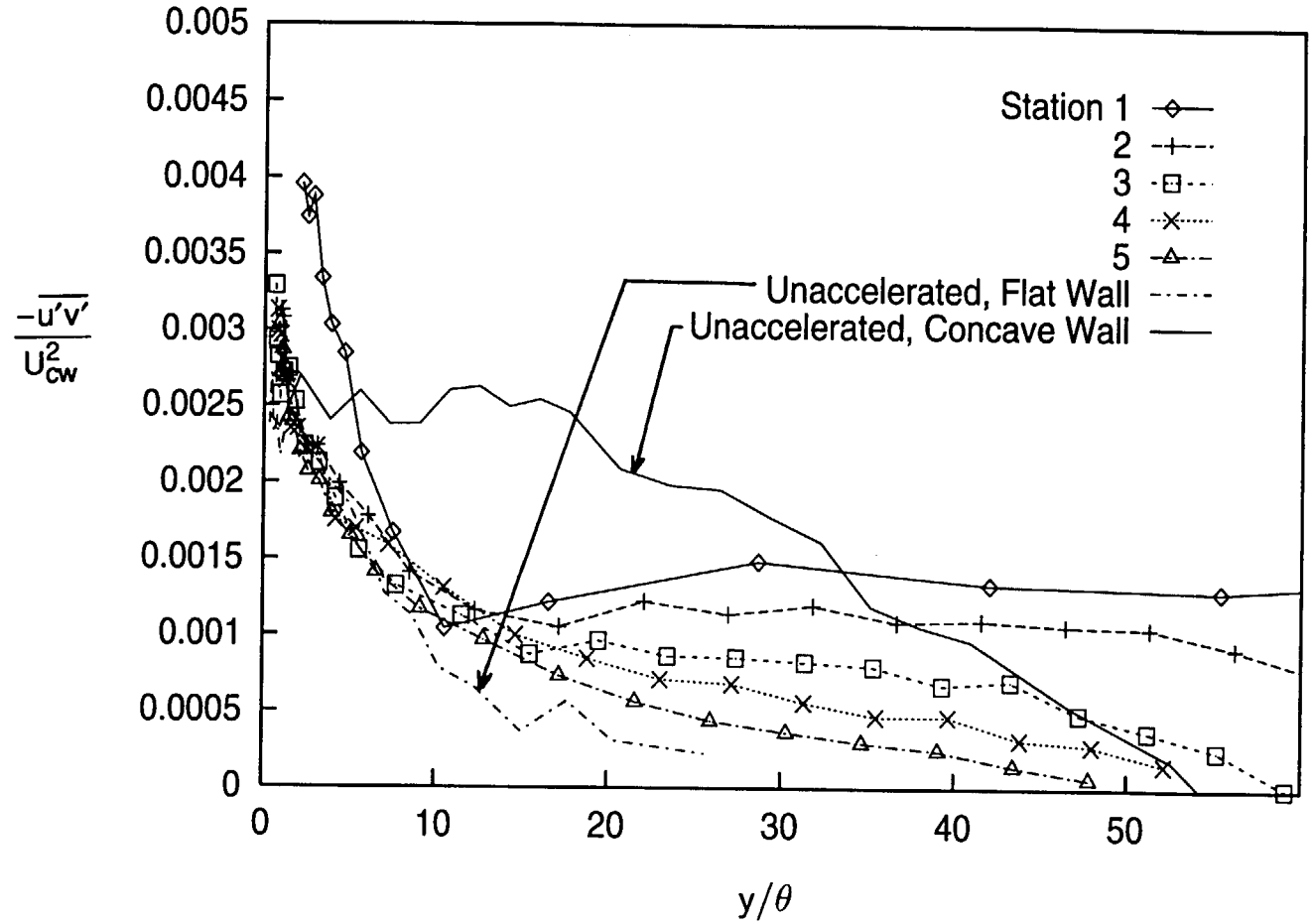

Fig. 5.22: Turbulent Shear Stress Profiles
K=0.75x10^{-6} Case

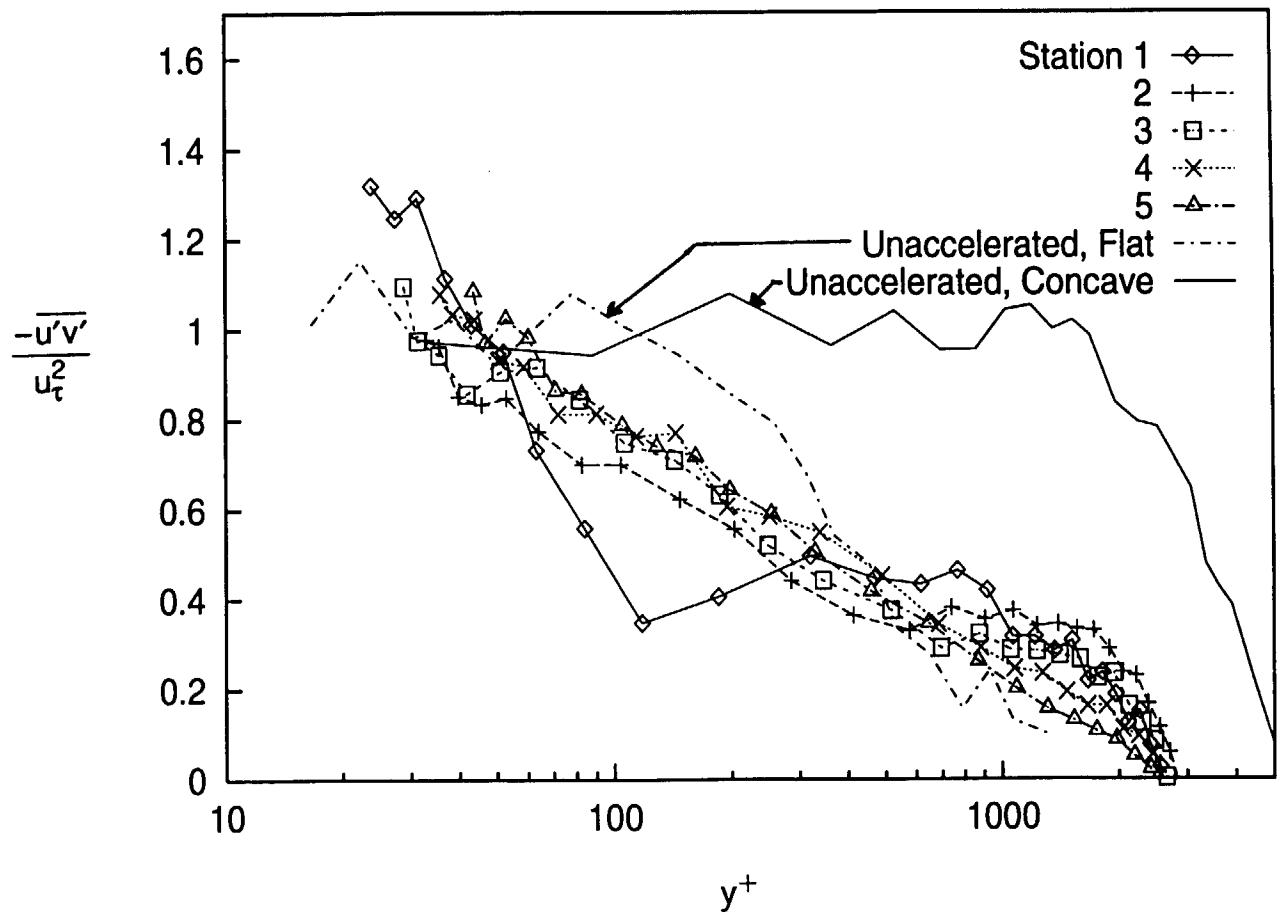

Fig. 5.23: Turbulent Shear Stress Profiles, Wall Coordinates
K=0.75x10^{-6} Case

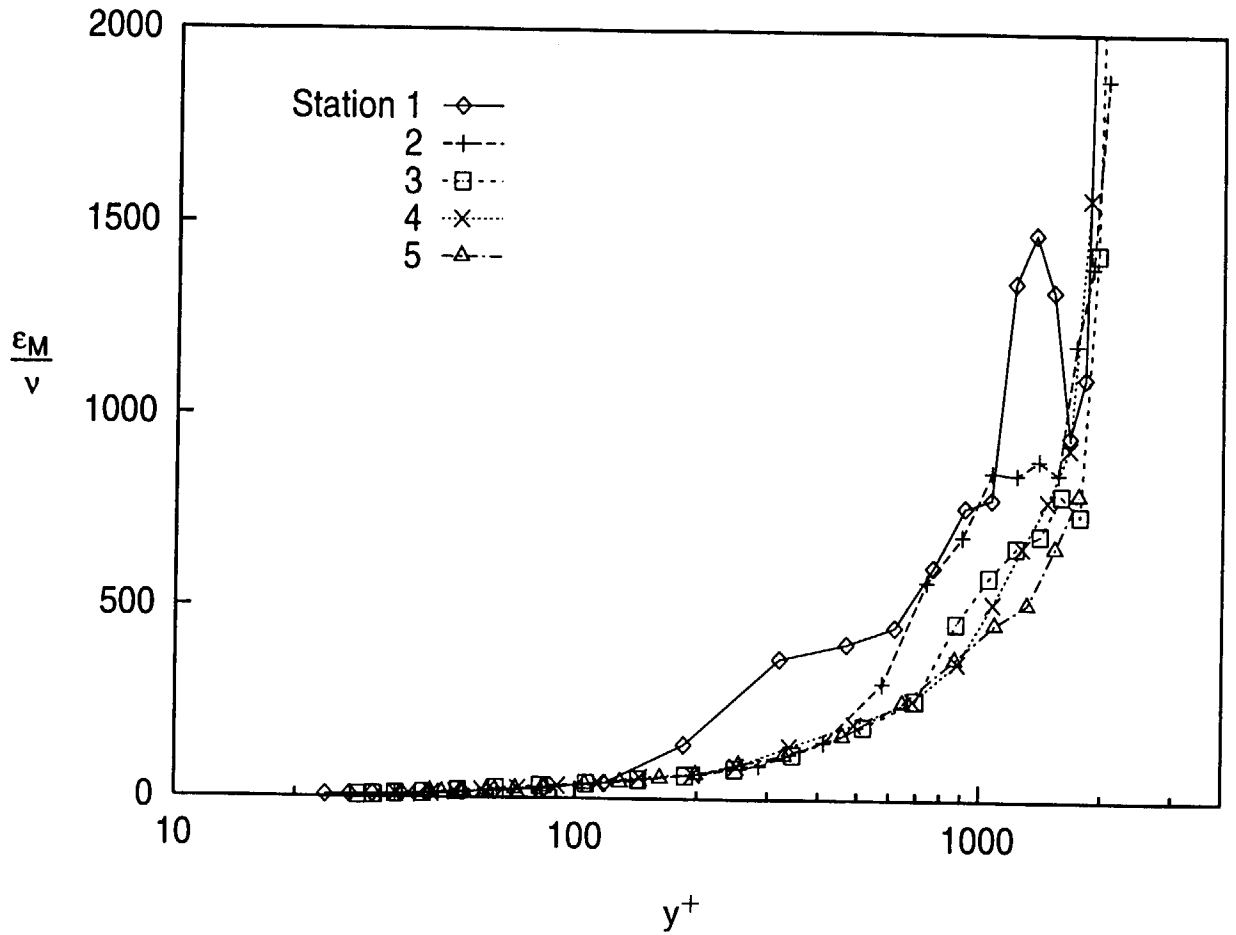

Fig. 5.24: Eddy Viscosity Profiles
K=0.75x10^{-6} Case

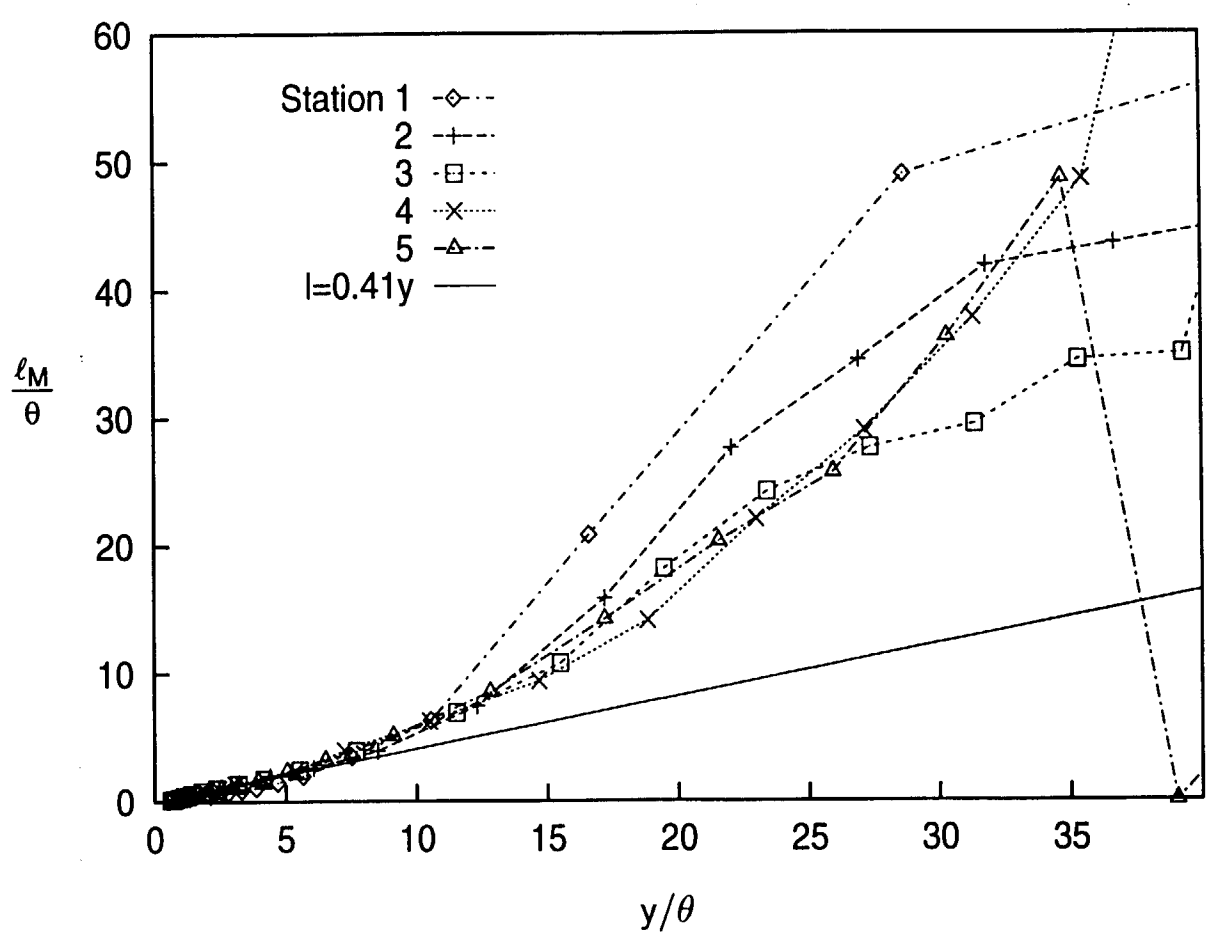

Fig. 5.25: Mixing Length of Momentum Profiles K=0.75x10^{-6} Case

CHAPTER 6: HIGH FSTI, $dU_{cw}/dx=29\ s^{-1}$ RESULTS

The results described above in Chapter 5 showed that acceleration with $K=0.75\times10^{-6}$ is not strong enough to significantly affect the transition process on the concave test wall under high (8% at the inlet) FSTI conditions. The acceleration rates on the pressure side of modern turbine airfoils are much higher than $K=0.75\times10^{-6}$, as shown in Fig. 5.1. It was therefore decided to investigate a case with stronger acceleration. When K is held constant, the free-stream velocity varies as

$$U_{cw} = \frac{1}{\frac{1}{U_{cw_o}} - \frac{Kx}{\nu}}, \tag{6.1}$$

where U_{cw_o} is the free-stream velocity at the inlet to the test section. The inlet velocity, the acceleration rate and the length of the test section are related, so Re_x and K cannot be set independently. If K could be held constant indefinitely, U_{cw} would become infinite at $x=\nu/KU_{cw_o}$. Since this is not possible, the length of the test section or the inlet velocity must be decreased to achieve higher K. To maintain a representative Reynolds number range for the experiment while increasing the acceleration rate, a variable-K boundary condition was substituted with an acceleration boundary condition of a uniform free-stream velocity gradient, dU_{cw}/dx. This gave a K distribution which decreased from a maximum at the leading edge. The decreasing K distribution is similar to that on the downstream section of the pressure side of turbine airfoils, as shown in Fig. 5.1.

As in the case described in Chapter 5, the boundary layer in the present case was two-dimensional in a time averaged sense. An extended transition zone, described below, was observed. Many of the phenomena observed in the present case can be seen more clearly in a case with even stronger acceleration, documented in Chapter 7.

EXPERIMENTAL CONDITIONS

The flow entered the test section with a velocity of 10.3 m/s and a nominal FSTI of 8%. The free-stream velocity gradient was held at 29.4 s^{-1}. Profile data were acquired at ten streamwise stations. The locations of these stations, along with other important parameters, are listed in Table 6.1. The stations were more closely spaced than those of the previous cases, to provide better documentation of the transition zone. At the last measurement station, $Re_x=17.7\times10^5$. The acceleration parameter dropped from $K=4.4\times10^{-6}$ at the leading edge to 0.39×10^{-6} at the last measurement station. The K profile from the experiment, along with the profiles from the airfoils of Fig. 5.1, is shown in Fig. 6.1. The acceleration in the experiment is still weaker than on the airfoils, but is at least of the same order of magnitude.

Free-Stream Conditions

The free-stream turbulence level is shown in Fig. 6.2. In Fig. 6.2a, $\overline{u'_\infty}$ and $\overline{v'_\infty}$ are plotted in dimensional coordinates. The streamwise component, $\overline{u'_\infty}$, decays to about half of its inlet value by the last measurement station. The normal component, $\overline{v'_\infty}$, decays more slowly. The free-stream turbulence intensities are shown in dimensionless coordinates in Fig. 6.2b. Also shown is the FSTI, taken as stated above, as $\sqrt{\frac{\overline{u'^2}+2\overline{v'^2}}{3U_{cw}^2}}$. The FSTI drops from its inlet value (~8%) to 5.7% at the first station and 1.6% at the last station. Most of the drop is due to the increase in U_{cw} in the streamwise direction.

Free-stream spectra. Free-stream spectra of u′ and v′ were acquired at stations 1, 3, 5, 7 and 9. The u′ spectra are shown in Fig. 6.3. Below 1000 Hz, u′ decays in the streamwise direction. There is some growth at higher frequencies, which may be associated with the cascade of energy from large scales to small scales. It is also possible that this high-frequency energy is transported by turbulent diffusion from the boundary

layer into the core of the channel. A third possibility is the production of high-frequency turbulence in the free-stream. Production in the free-stream is possible because of the non-zero mean velocity gradient in the free-stream, which results from the curvature of the channel. The fluctuation energy at the upstream stations is centered around 50 Hz, as is shown in Fig. 6.3b. The station 1 spectrum is similar to the u' spectrum in Fig. 5.4, which should be expected since the inlet conditions for the present case and the case described in Chapter 5 are similar. Hence, the station 1 free-stream data presented in Chapter 5 (including the two-point spatial correlations) are expected to be applicable to the present case. As the low frequencies decay, the peak in Fig. 6.3b shifts to about 1000 Hz. The length scale associated with 1000 Hz at station 9, U_{cw}/f, is 3 cm. This scale could be associated with large scale turbulent eddies. The integral length scale associated with the u' fluctuations, $\Lambda_{u'}$, remains constant at about 4 cm at all stations (see Table 6.1). This scale can also be associated with large scale eddies. The frequency associated with the integral scale, $U_\infty/\Lambda_{u'}$, increases from 300 Hz at station 1 to 800 Hz at station 9.

The v' spectra are shown in Fig. 6.4. The peak in the v' energy, as shown in Fig. 6.4b, is centered around 150 Hz at station 1. The v' fluctuations decay for frequencies below 600 Hz. By station 9 the energy is centered at 300 Hz, in a broad peak, or plateau, between 100 Hz and 1000 Hz. A comparison of Figs. 6.3b and 6.4b shows much less decay in v' than in u'. The decay in u' may be due to straining of the eddies in the streamwise direction, caused by the acceleration. The integral length scale associated with the v' fluctuations, $\Lambda_{v'}$ (obtained using Fig. 6.4a and Eqn. 2.16), rises from 2 cm at station 1 to 3.6 cm at station 9 (see Table 6.1). The frequency associated with the integral scale, $U_\infty/\Lambda_{v'}$, rises from 700 Hz at station 1 to 900 Hz at station 9.

The u' fluctuations show significant change in the streamwise direction, both in magnitude and spectral distribution. This is probably due to streamwise straining caused

by the acceleration. The v′ fluctuations show less change, behaving more like "frozen turbulence."

Boundary Layer Growth

The growths of the momentum and thermal boundary layers are shown in Fig. 6.5, where Re_θ and Re_{Δ_2} are plotted verses Re_x. The momentum thickness Reynolds number drops from 440 to 400 between stations 1 and 2, and then begins to rise slowly. The beginning of the rise in Re_θ corresponds to a drop in the acceleration parameter, K, below 2×10^{-6}. A comparison to the unaccelerated and $K=0.75\times10^{-6}$ cases of Fig. 5.6 shows the strong suppression of the momentum boundary layer growth in the present case. A comparison of Figs. 6.5 and 5.6 shows that thermal boundary layer growth, in terms of Re_{Δ_2}, is not strongly affected by the acceleration. This leads to an even larger mismatch between Re_θ and Re_{Δ_2} in the present case than in the $K=0.75\times10^{-6}$ case.

The shape factor, $H=\delta^*/\theta$, is shown in Fig. 6.6. The shape factor has a value of 1.46 at the first two stations, and drops slowly to 1.31 at the last station. The unaccelerated, fully-turbulent, high-FSTI, concave-wall value shown in Fig. 5.7 is 1.25. The laminar flow value for a boundary layer with the acceleration rates of the present case (calculated for flow on a flat plate with the TEXSTAN program (Kays and Crawford, 1993; Crawford and Kays, 1976)) is between 2.2 and 2.3. These values suggest that the flow in the present case is transitional at the upstream stations, and reaches fully-turbulent behavior by the end of the test section.

Energy Balance

The energy balance for the present case is shown in Fig. 6.7. The energy balance is within 12% at station 1, and within 7% at the rest of the stations. Given the variability in the wall heat flux and the uncertainty in the data (described above in Chapter 2), the energy balance is acceptable.

Strength of Curvature

The strength of curvature, θ/R, is shown in Fig. 6.8. Also plotted are the data from Fig. 5.9. The strength of curvature in the present case is only half of that in the $K=0.75\times10^{-6}$ case. Levels are between 15 and 25% of the peak values of typical airfoils. In terms of the boundary layer thickness, $\delta_{99.5}$, the strength of curvature has been reduced to about 0.8%. The curvature may still influence the flow, but it is weak.

MEAN VELOCITY PROFILES

Figure 6.9 shows mean streamwise velocity profiles from the present case plotted as $\overline{U}/U_{CW}$ verses y/θ. The edge of the momentum boundary layer, $\delta_{99.5}$, corresponds to $y/\theta\approx15$ to 20. The profiles appear to collapse in Fig. 6.9a. In Fig. 6.9b, a closer look at the near wall region shows that the profiles become fuller, or more turbulent like, in the streamwise direction. Figure 6.10 shows the profiles in wall coordinates. The profiles fall somewhat above the law of the wall at the first four stations. This behavior is expected with the local acceleration, and the data is well predicted by profiles calculated using the method of Appendix A. At the downstream stations, as the flow becomes fully-turbulent and the acceleration weakens, the profiles collapse onto the law of the wall. As in the high-FSTI case shown in Fig. 5.11 and the high FSTI cases presented by Kim and Simon (1991), the profiles exhibit no wake.

Very near the wall, in the region $y^+<5$, the agreement between the data and the line $u^+=y^+$ is not as good as that observed in the other cases of this study (compare Figs. 3.11, 3.13, 5.11, 6.10 and 7.9). The data in Figs. 3.11, 3.13, 5.11 and 7.9 lie on the line $u^+=y^+$, while the data in Fig. 6.10 lie somewhat above the line, particularly at the downstream stations. The near wall data are corrected for conduction effects as described in Chapter 2. The applied correction was developed by Wills (1962) in laminar flows. It appears to work well in turbulent boundary layers when the free-stream velocity is below

about 20 m/s. At the downstream stations in the present case, where the free-stream velocity is above 20 m/s, it appears that Wills' correction has been extrapolated somewhat beyond its useful range.

SKIN FRICTION COEFFICIENTS

Skin friction coefficients are plotted verses Re_θ in Fig. 6.11. Shown for reference are correlations for laminar and fully-turbulent flows on flat walls under low FSTI, unaccelerated flow conditions. For the first 3 stations, C_f lies just above the turbulent correlation, and Re_θ and C_f are nearly constant, as the acceleration slows development of the boundary layer. Downstream, Re_θ begins to grow and C_f rises above the turbulent correlation by about 12%.

MEAN TEMPERATURE PROFILES

Mean temperature profiles are shown in Fig. 6.12. The edge of the thermal boundary layer, $\delta_{t99.5}$, corresponds to $y/\Delta_2 \approx 11$. The full profiles are shown in Fig. 6.12a. The profile becomes fuller between stations 1 and 2. At the downstream stations, the profiles appear to collapse. Figure 6.12b shows an expanded view of the near wall region. In this view, the profiles become fuller between stations 1 and 4, and the profiles collapse downstream. These profiles provide evidence that the first four stations are transitional, and that the boundary layer is fully-turbulent by station 5.

The temperature profiles are shown in wall coordinates in Fig. 6.13. Also shown for reference are the line $t^+=Pry^+$ and the thermal law of the wall. The profiles rise through the first 5 stations. At the downstream stations, the profiles collapse onto a turbulent-like shape as the boundary layer becomes fully-turbulent and the acceleration weakens. The temperature profiles do not agree with the thermal law of the wall. The deviation is even greater in this case than in the $K=0.75\times10^{-6}$ case (Fig. 5.14). This is expected since the acceleration is stronger in the present case. Figure 6.13b shows the

station 9 profile data along with a profile calculated for the conditions at this station by the method of Appendix A. The agreement is good to $y^+ \approx 500$. The calculated profile makes no attempt to capture the wake, so no agreement at higher y^+ should be expected.

STANTON NUMBERS

Stanton numbers are plotted verses $Re_{\Delta 2}$ in Fig. 6.14. Shown for reference are correlations from Kays and Crawford (1993) for low FSTI, unaccelerated laminar and turbulent boundary layers on flat walls. Also shown for the comparison are data from unaccelerated, 8% FSTI flows along flat and concave walls from Kim and Simon (1991). In the accelerated flow, Stanton numbers drop in the streamwise direction and agree with the turbulent correlation. The data never approach the laminar correlation, although the flow is transitional at the upstream stations. The data do not rise above the turbulent correlation, unlike the unaccelerated-flow, high-FSTI, concave-wall data of Fig. 5.17, in which Stanton numbers as high as 40% above the correlation are observed. The stabilizing effect of strong acceleration in the present case counteracts the destabilizing effects of high FSTI and concave curvature, and lowers the Stanton numbers back to flat wall values.

The Reynolds analogy factor, $\frac{2St}{C_f}$, drops to 0.8 in the present case. This compares to 1.13 in unaccelerated flow, and 1.0 in the $K=0.75\times10^{-6}$ case. The drop is attributed to the difference between the momentum and thermal boundary layer thicknesses, shown in Fig. 6.5.

INTERMITTENCY PROFILES

Profiles of the intermittency, γ, are shown in Fig. 6.15. These profiles are based on u' fluctuations. The intermittency is low at the wall, rises to a peak at $y/\theta \approx 1$, and drops to a free-stream value of about 20%. The non-zero free-stream value results from

the high FSTI and the tuning of the intermittency circuit, as described in Chapter 2. The intermittency has a peak of 73% at station 1. The peak rises steadily, reaching a maximum near 100% by station 5. The measurements suggest that the flow is well into transition at station 1, and fully-turbulent by station 5. Intermittency profiles based on the fluctuating temperature, t', are shown in Fig. 6.16. The profiles all have a high peak near the wall and go to zero at the free-stream, where the flow is isothermal. The progression though transition, seen in Fig. 6.15, is not apparent in Fig. 6.16. The t' based intermittency appears to provide a good means of separating the boundary layer flow from the free-stream, but is not as useful for determining the state of the boundary layer with respect to transition.

FLUCTUATING VELOCITY MEASUREMENTS

$\overline{u'}$ Profiles

Profiles of $\overline{u'} / U_{cw}$ are plotted verses y/θ in Fig. 6.17. Figure 6.17a shows the full boundary layer, and Fig. 6.17b is an expanded view of the near wall region. The peaks in the profiles drop in magnitude and shift toward the wall as the flow proceeds downstream. This behavior, as noted above in the discussion of Fig. 5.18, is expected in transitional flows.

Figure 6.18 shows the $\overline{u'}$ profiles in wall coordinates. There are peaks at all stations at $y^+=17$, which is typical of turbulent boundary layers. The levels of the peaks drop from a high value of 2.4 at station 1, to 1.6 at the station 10. Peaks between 2 and 2.5 were observed in the other cases in this study. The reason for the lower peaks in the present case is not clear. The profile rises between stations 5 and 6 at $y^+\approx150$. This rise develops into a plateau between $y^+=100$ and $y^+=200$ at the downstream stations. The

plateau is typical of unaccelerated and weakly accelerated flows, as shown in Fig. 5.19. It appears in the present case, when K drops below 0.8×10^{-6}.

$\overline{v'}$ Profiles

Figure 6.19 shows profiles of $\overline{v'} / U_{cw}$ plotted verses y/θ. As in the $K=0.75\times10^{-6}$ case (Fig. 5.20), the profiles drop from peaks near the wall to minimum values between $y/\theta=5$ and 10 ($\delta_{99.5}\approx0.25$ to 0.5) and then rise to the free-stream values. Figure 6.20 shows the $\overline{v'}$ profiles in wall coordinates. The profiles appear to reach an asymptotic shape by station 7, where the flow is fully-turbulent and the acceleration has dropped to $K=0.64\times10^{-6}$.

Turbulent Shear Stress Profiles

Profiles of the turbulent shear stress are plotted as $-\overline{u'v'} / U_{cw}^2$ verses y/θ in Fig. 6.21. Also shown are unaccelerated, 8% FSTI, concave- and flat-wall profiles from Kim and Simon (1991). The profiles appear to collapse at all stations. The shear stress is lower than in the $K=0.75\times10^{-6}$ case (Fig. 5.22), and even falls below the unaccelerated flat-wall curve.

The profiles are plotted in wall coordinates in Fig. 6.22. The profiles rise as the flow moves downstream, appearing to reach an asymptote by station 8 or 9. At the downstream stations the dimensionless shear stress appears to extrapolate to 1 at the wall, as expected for a turbulent boundary layer. Upstream, the lower shear stress indicates that the flow is still transitional. As in the coordinates of Fig. 6.21, the profiles all fall well below those of the unaccelerated flow cases.

Eddy Viscosity

Profiles of the eddy viscosity, ε_M, are shown in Fig. 6.23. The eddy viscosity is an order of magnitude lower than in the $K=0.75\times10^{-6}$ case of Fig. 5.24.

Mixing Length of Momentum

Profiles of the mixing length, ℓ_M, are shown in Fig. 6.24. Near the wall, the profiles drop with streamwise distance, reaching an asymptote by station 6. The slope of the downstream profiles, ℓ_M/y, is about 0.3, which is below the expected value of 0.41 (the von Kármán constant). The slope very near the wall ($y^+<100$) could not be measured due to probe size limitations, and it is possible that the profiles have the standard, 0.41, slope very near the wall. The profiles follow the line $\ell_M=0.3y$ to the edge of the boundary layer. There is a rise above the line at higher y, but it is not as pronounced as in the $K=0.75\times10^{-6}$ case (Fig. 5.25). The turbulent shear stress, eddy viscosity, and mixing length profiles all show that strong acceleration greatly reduces the turbulent transport in the boundary layer.

FLUCTUATING TEMPERATURE AND VELOCITY MEASUREMENTS

$\overline{t'}$ Profiles

Profiles of the fluctuating temperature are shown in Fig. 6.25. The profiles appear similar at all stations in these coordinates. Unlike the velocity fluctuations, the temperature fluctuations go to zero in the free-stream, where the flow is isothermal. Figure 6.26 shows the temperature profiles in wall coordinates. The profiles become fuller at the downstream stations in these coordinates. At the downstream stations, there is a near wall plateau in dimensionless $\overline{t'}$ with a level of about 2.5. Kim and Simon (1991) saw levels of about 1.7 in this region in unaccelerated flow.

$\overline{v't'}$ Profiles

Profiles of the component of the turbulent heat flux normal to the wall, $\overline{v't'}$, are shown in Fig. 6.27. Near the wall, at $y/\Delta_2<3$, normalized values of $\overline{v't'}$ as high as 1.8 were measured, particularly at the first four stations. The normal component of the turbulent heat flux is not expected to exceed the wall heat flux, so the values above 1 were not believed, and are not presented. These high values appeared only at the upstream stations, where the boundary layer is thinnest, so it is possible that they are due to measurement error caused by spatial resolution problems.

The profiles in Fig. 6.27 all appear similar. They reach a maximum value of about 0.7 near the wall. As stated above, a value of 1 is expected at the wall, but accurate measurements could not be taken close enough to the wall to resolve this. The profiles are plotted in wall coordinates in Fig. 6.28. The profiles rise in these coordinates, becoming fuller at the downstream stations. A similar rise was seen in the shear stress profiles in Fig. 6.22. Unlike the shear stress, $\overline{v't'}$ has a near wall plateau at the downstream stations with a value of 0.7. Also shown in Fig. 6.28 are profiles from Kim and Simon's (1991) 8% FSTI unaccelerated flat- and concave-wall cases. The effect of acceleration on the turbulent heat flux is not as strong as its effect on the turbulent shear stress, shown in Fig. 6.22. The accelerated $\overline{v't'}$ profiles at the downstream stations have higher values than the unaccelerated flat-wall profile. The accelerated shear stress profiles, in contrast, were well below the unaccelerated flat-wall values.

$-\overline{u't'}$ Profiles

Profiles of the streamwise component of the turbulent heat flux, $-\overline{u't'}$, are shown in Fig. 6.29. The $-\overline{u't'}$ values are 2 to 3 times larger than the $\overline{v't'}$ values shown in Figs. 6.27 and 6.28. Qualitatively, however, $-\overline{u't'}$ and $\overline{v't'}$ are similar. A comparison of Figs. 6.17, 6.19, 6.27 and 6.29 shows that the correlation coefficient for the normal component

of the turbulent heat flux, $\frac{\overline{v't'}}{(\overline{v'})(\overline{t'})}$, is about 0.3, while the streamwise component correlation, $\frac{-\overline{u't'}}{(\overline{u'})(\overline{t'})}$, is about 0.6.

Eddy Diffusivity of Heat

Profiles of the eddy diffusivity, ε_H, are shown in Fig. 6.30. The results are similar to the eddy viscosity results of Fig. 6.23.

Mixing Length of Heat

Profiles of the thermal mixing length, ℓ_H, are shown in Fig. 6.31. In low-FSTI, unaccelerated flow on flat walls, ℓ_H is expected to follow the line $\ell_H = \frac{\kappa}{Pr_t} y$ near the wall. The expected value of Pr_t is about 0.9, and κ=0.41. Like the mixing length of momentum, shown in Fig. 6.24, ℓ_H values rise above the expected line to high values at the edge of the boundary layer. Near the wall, the ℓ_H data lie fairly close to the line, unlike the mixing length of momentum, which had a lower slope than expected near the wall.

Turbulent Prandtl Number

Profiles of the turbulent Prandtl number, Pr_t, are shown in Fig. 6.32. Very near the wall ($y^+<100$) the measurements cannot be trusted due to spatial resolution problems. Far from the wall ($y^+>800$) the mean velocity and temperature gradients become too small for accurate calculation of Pr_t (the uncertainty rises to several hundred percent). In the range $100<y^+<800$, Pr_t lies between 1 and 1.2. This range is slightly above the standard value of 0.9, but given the uncertainty in the measured data, this difference is not significant. It appears that Reynold's analogy between eddy transport of heat and momentum is obeyed in this flow.

Cross Transport of Turbulent Shear Stress and Turbulent Heat Flux

Profiles of the triple correlations $\overline{u'v'^2}$ and $\overline{v'^2t'}$ are shown in Figs. 6.33 and 6.34. These terms are related to the rate at which the turbulent shear stress and turbulent heat flux are transported away from the wall by turbulent diffusion. Shown for comparison are profiles from 8% FSTI, unaccelerated, flat-wall and concave-wall cases from Kim and Simon (1991). The accelerated flow profiles rise as the flow proceeds downstream, through transition. Values of normalized $\overline{u'v'^2}$ are approximately equal to values from the unaccelerated flat-wall case. The values are roughly half those from the unaccelerated concave-wall case. Values of normalized $\overline{v'^2t'}$ are 1.5 times those of the unaccelerated concave-wall case, and three times those of the flat-wall case. The acceleration has a much stronger effect on the momentum boundary layer than on the thermal boundary layer in counteracting the effects of curvature.

OCTANT ANALYSIS

The octant analysis, described above in Chapter 4, has been applied to the present, accelerated flow. Profiles of the octant decomposition of the turbulent shear stress are shown in Fig. 6.35. The flow is transitional at station 2, as shown in Fig. 6.35a. The octant decomposition is similar to that of the unaccelerated transitional flows discussed in Chapter 4. Octant 6, the hot ejection, makes the largest contribution to $-\overline{u'v'}$, about double the contribution of octant 4, the cold sweep. Near the wall, some of the other octants become significant. Included among these is octant 7, the hot wallward interaction. Similar behavior was seen in the unaccelerated transitional flows, and was attributed to incomplete turbulent mixing. Also significant in the present case is octant 3, which has the same sign and magnitude as octant 7. Octant 3 is the cold wallward interaction. Cold, slow fluid moves toward the wall causing a reduction in the overall turbulent shear stress. The mechanism responsible for the octant 3 motion is not known,

but it may be related to the difference between the momentum and thermal boundary layer thicknesses. A direct numerical simulation might be useful for determining the source of the octant 3 data.

The octant distributions are approximately the same at stations 1 through 4. The distribution begins to change at station 5, as shown in Fig. 6.35b. The results presented above suggest that the flow at the downstream stations is fully-turbulent. In agreement with this, the octant distributions at stations 6 through 10 are characteristic of a fully-turbulent boundary layer. The station 10 distribution is shown in Fig. 6.35c. Near the wall at station 10, octants 4 and 6 are of comparable magnitude. The octant 4 contribution is approximately 80% of the octant 6 contribution. Octants 4 and 6, the cold sweep and hot ejection, account for nearly all of the turbulent shear stress.

The octant decomposition of the normal component of the turbulent heat flux, $\overline{v't'}$, is shown for stations 2, 5 and 10 in Fig. 6.36. The results are similar to those for the turbulent shear stress, but some differences appear. At station 2 (Fig. 6.36a), octant 3 makes a significant contribution, as it did with the shear stress, but while octant 3 causes a reduction in the turbulent shear stress, it makes a positive contribution to $\overline{v't'}$. Octant 5 also makes a contribution to $\overline{v't'}$. It has the same sign and magnitude as octant 3. Octant 5 is the hot outward interaction. High speed, warm fluid moves away from the wall. Octant 5 corresponds to u', v' and t' all positive. It is the counter-motion to octant 3, which corresponds to u', v' and t' all negative. One might expect that octant 3 and 5 motions would lead to high $\overline{v't'}$ relative to $-\overline{u'v'}$, resulting in lower turbulent Prandtl numbers. This was not observed, however, indicating that differences between the mean velocity and temperature gradients (which also factor into Pr_t) are important.

At the downstream stations (Figs. 6.36b and 6.36c) nearly all of $\overline{v't'}$ results from octant 4 and 6 contributions, as expected for a fully-turbulent boundary layer, and in agreement with the results for the turbulent shear stress.

BOUNDARY LAYER SPECTRA AND TRANSFER FUNCTIONS

Boundary layer spectra were measured at stations 1, 3, 5, 7 and 9. The u′ spectra acquired near the wall at y^+=5 are shown in Fig. 6.37. The peak in u′ energy is at 200 Hz at station 1 (Fig. 6.37b). The peaks rise continuously and shift to higher frequencies at the downstream stations, reaching 700 Hz by station 9. The u′ spectra acquired at y^+=17 are shown in Fig. 6.38. The spectra at y^+=5 and y^+=17 are similar. The fluctuation levels are higher at y^+=17, since this is the location of maximum $\overline{u'}$ in the boundary layer (Fig. 6.18). Near wall damping results in lower values at y^+=5. The u′ spectra acquired at y^+=100 are shown in Fig. 6.39. The peak energy is at 30 Hz at station 1. The peaks rise in magnitude to a broad peak centered at 700 Hz at station 9. At the high frequencies centered around 700 Hz, there is less fluctuation energy at y^+=100 than at y^+=17 or y^+=5. These frequencies are associated with near-wall turbulence production, so it is expected that fluctuation levels should decrease with increasing distance from the wall. At frequencies below 100 Hz, the spectra at y^+=100 and y^+=17 are more comparable. The lower frequencies are associated with free-stream unsteadiness.

The v′ spectra acquired at y^+=100 are shown in Fig. 6.40. The peak in v′ energy is at 1000 Hz at stations 1 through 5, shifting to 2000 Hz at stations 7 and 9. The levels of the peaks rise somewhat between stations 1 and 3, but rise more rapidly between stations 3 and 5 as the boundary layer becomes fully-turbulent. A comparison of Figs. 6.39 and 6.40 shows that there is more low-frequency energy in u′ than in v′ at y^+=100. This supports the conclusion that the low-frequency fluctuations are associated with streamwise unsteadiness.

The turbulent shear stress spectra acquired at y^+=100 are shown in Fig. 6.41. The energy level is low at station 1 and has no clear peak frequency (Fig. 6.41b). Between stations 1 and 3 there is some increase in the shear stress, and a peak emerges at, approximately, 1000 Hz. As the flow becomes fully-turbulent at the downstream

stations, and turbulence production becomes significant in the boundary layer, the peaks rise rapidly and shift to between 2000 and 3000 Hz.

Transfer Functions

Figure 6.42 shows transfer functions of u' between the boundary layer and the free-stream. Transfer functions between $y^+=5$ and the free-stream are shown in Fig. 6.42a. At the upstream stations, there is a peak at 300 Hz. This is believed to result from amplification of the free-stream disturbance. The v' energy in the free-stream (Fig. 6.4b) is also centered around 300 Hz. Downstream, there is significant activity at frequencies above 1000 Hz. These higher frequencies are associated with turbulence production in the near-wall region. The trends seen at $y^+=5$ are also seen at $y^+=17$ (Fig. 6.42b). The transfer functions between $y^+=100$ and the free-stream (Fig. 6.42c) are similar, but the 300 Hz peak, although still present, is less distinct. As explained for the low FSTI case in Chapter 3, the low-frequency peak is believed to be caused by "inactive" disturbances in the free-stream. As depicted in Fig. 3.7, free-stream v' fluctuations displace fluid across the mean streamwise velocity gradient, $\frac{\partial \overline{U}}{\partial y}$, causing large u' fluctuations in the boundary layer. Since $\frac{\partial \overline{U}}{\partial y}$ is lower at $y^+=100$ than at $y^+=17$ or $y^+=5$, the 300 Hz peak is less distinct at $y^+=100$.

The transfer functions of v' between $y^+=100$ and free-stream are shown in Fig. 6.43. Unlike the u' transfer functions, there are no peaks at 300 Hz. At the higher frequencies, u' and v' are similar. As explained above, the low-frequency u' fluctuations in the boundary layer result from amplification of free-stream v' fluctuations. There is no similar mechanism for amplification of v' in the boundary layer, and there is no low frequency peak in the v' transfer function.

Figure 6.44 shows the transfer function between $-\overline{u'v'}$ at $y^+=100$ and u' at the same position. This transfer function can be considered to be a correlation coefficient on

a frequency basis. The transfer function is about 0.1 for frequencies below 50 Hz, and rises to between 0.4 and 0.7 at 5000 Hz. The high-frequency values tend to rise with streamwise distance, reaching an asymptotic position in downstream station profiles. The low-frequency u′ fluctuations, which result from "inactive" motions caused by the free-stream unsteadiness, are relatively inefficient at promoting turbulent mixing. The low-frequency fluctuations can still make a significant contribution to the turbulent shear stress in the high-FSTI flow, but they are not so effective as are high frequency fluctuations resulting from turbulent eddies produced in the boundary layer. Figure 6.45 shows the transfer function between $-\overline{u'v'}$ and v′ at $y^+=100$.

CONCLUSIONS

The flow is transitional in the present case, in spite of the high free-stream disturbance level. The boundary layer appears to be well into the transition process at the first measurement station, and transition proceeds steadily through station 5, where the momentum thickness Reynolds number is 570. Downstream of station 5, the boundary layer appears to be fully-turbulent. The momentum thickness Reynolds number is only 1120 at the last measurement station, indicating that, although the boundary layer is fully-turbulent, it probably is not a mature, turbulent boundary layer. Evidence of the change from transitional to fully-turbulent behavior was provided through the intermittency profiles, the shapes of the mean temperature profiles, octant decompositions, spectral analysis, and other data.

The nature of the transition under high-FSTI conditions is different from that observed in low-FSTI flows. The flow never appears laminar. Fluctuating velocity and temperature are always high, and skin friction coefficients are always above a correlation for fully-turbulent boundary layers on flat walls. Stanton numbers are always well above laminar values, and agree with a flat-wall turbulent flow correlation, even in the transition

region. The acceleration causes high skin friction coefficients relative to Stanton numbers. This does not result from differences in the eddy transport of heat and momentum. The turbulent Prandtl number remains near 1 in the accelerated flow. The differences between St and C_f are caused by a mismatch in the thicknesses of the momentum and thermal boundary layers. This acceleration level suppresses the growth of the momentum boundary layer (which results in the extended transition zone), but the thermal boundary layer growth is largely unaffected.

Station	1	2	3	4	5	6	7	8	9	10
x [m] †	0.1003	0.1885	0.2597	0.3519	0.4213	0.5043	0.5825	0.6611	0.7393	0.8175
U_{cw} [m/s]	13.13	15.59	17.81	21.01	23.58	25.41	27.19	29.17	31.86	34.72
FSTI [%]	5.47	4.44	3.71	3.08	2.75	2.46	2.23	2.08	1.74	1.61
$\Lambda_{u'_\infty}$ [cm]	3.90	--	3.99	--	3.83	--	4.66	--	4.41	--
$\Lambda_{v'_\infty}$ [cm]	1.96	--	2.80	--	3.07	--	3.40	--	3.59	--
$K \times 10^6$	2.73	1.94	1.44	1.07	0.85	0.73	0.64	0.55	0.46	0.39
$Re_x \times 10^{-5}$	0.8236	1.8358	2.8883	4.6171	6.2301	8.0073	9.8930	12.039	14.703	17.702
$\delta_{99.5}$ [cm]	1.006	0.783	0.793	0.720	0.662	0.742	0.770	0.656	0.865	0.847
δ^* [mm]	0.784	0.595	0.585	0.540	0.543	0.642	0.703	0.625	0.727	0.676
θ [mm]	0.539	0.408	0.409	0.385	0.386	0.465	0.519	0.460	0.548	0.517
H	1.45	1.46	1.43	1.40	1.41	1.38	1.35	1.36	1.33	1.31
Re_{δ^*}	644	580	651	709	800	1020	1194	1138	1446	1463
Re_θ	443	397	454	505	569	738	882	838	1090	1119
$\theta/R \times 10^3$	0.556	0.421	0.422	0.399	0.398	0.479	0.535	0.474	0.565	0.533
$\delta_{99.5}/R$ [%]	1.04	0.81	0.82	0.74	0.68	0.76	0.79	0.68	0.89	0.87
$C_f \times 10^3$	5.70	5.90	5.80	5.90	5.65	5.30	5.10	5.30	5.00	5.10
T_w [°C]	35.34	36.4	36.4	35.72	35.79	35.20	35.07	35.03	35.35	34.87
T_∞ [°C]	30.37	29.84	29.78	29.76	29.75	29.68	29.65	29.63	29.72	29.38
$\delta_{t99.5}$ [cm]	0.328	0.582	0.852	0.965	1.146	1.307	1.304	1.416	1.454	1.917
Δ_2 [mm]	0.237	0.450	0.631	0.880	0.970	1.106	1.269	1.383	1.543	1.579
$Re_{\Delta 2}$	177	399	654	1067	1336	1657	2034	2394	2910	3246
$St \times 10^3$	5.24	3.54	3.20	2.69	2.42	2.36	2.10	2.24	2.01	2.01
$2St/C_f$	1.84	1.20	1.10	0.912	0.857	0.892	0.822	0.845	0.804	0.787

† Mean temperature profiles were acquired 2 cm upstream of these locations. Velocity profile data were extrapolated 2 cm upstream for calculation of Δ_2.

Table 6.1: Parameters for the dU_{cw}/dx=29 s^{-1} Case

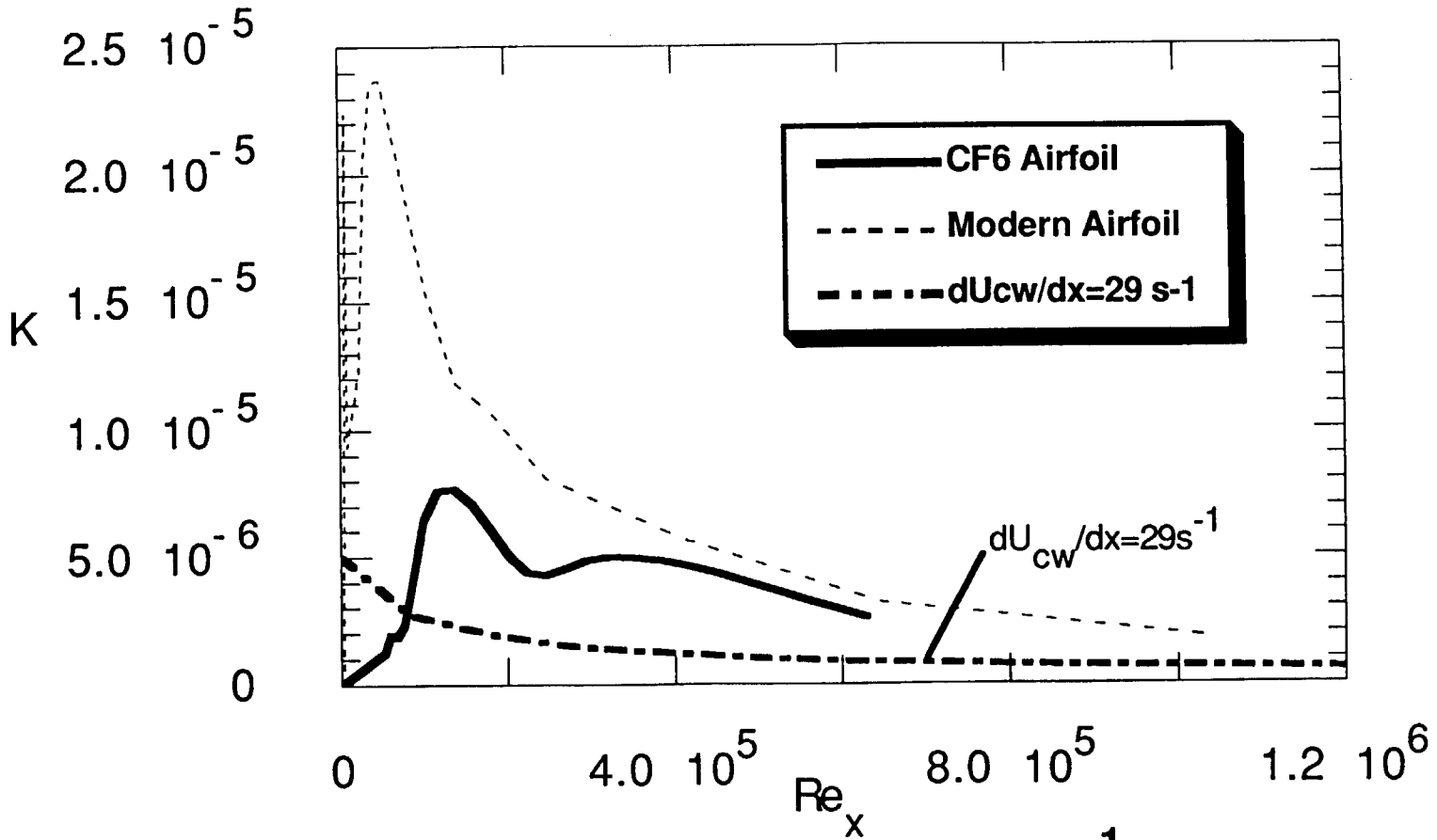

Fig. 6.1: K Profiles for $dU_{cw}/dx = 29 s^{-1}$ Experiment and the Pressure Side of Typical Turbine Airfoils

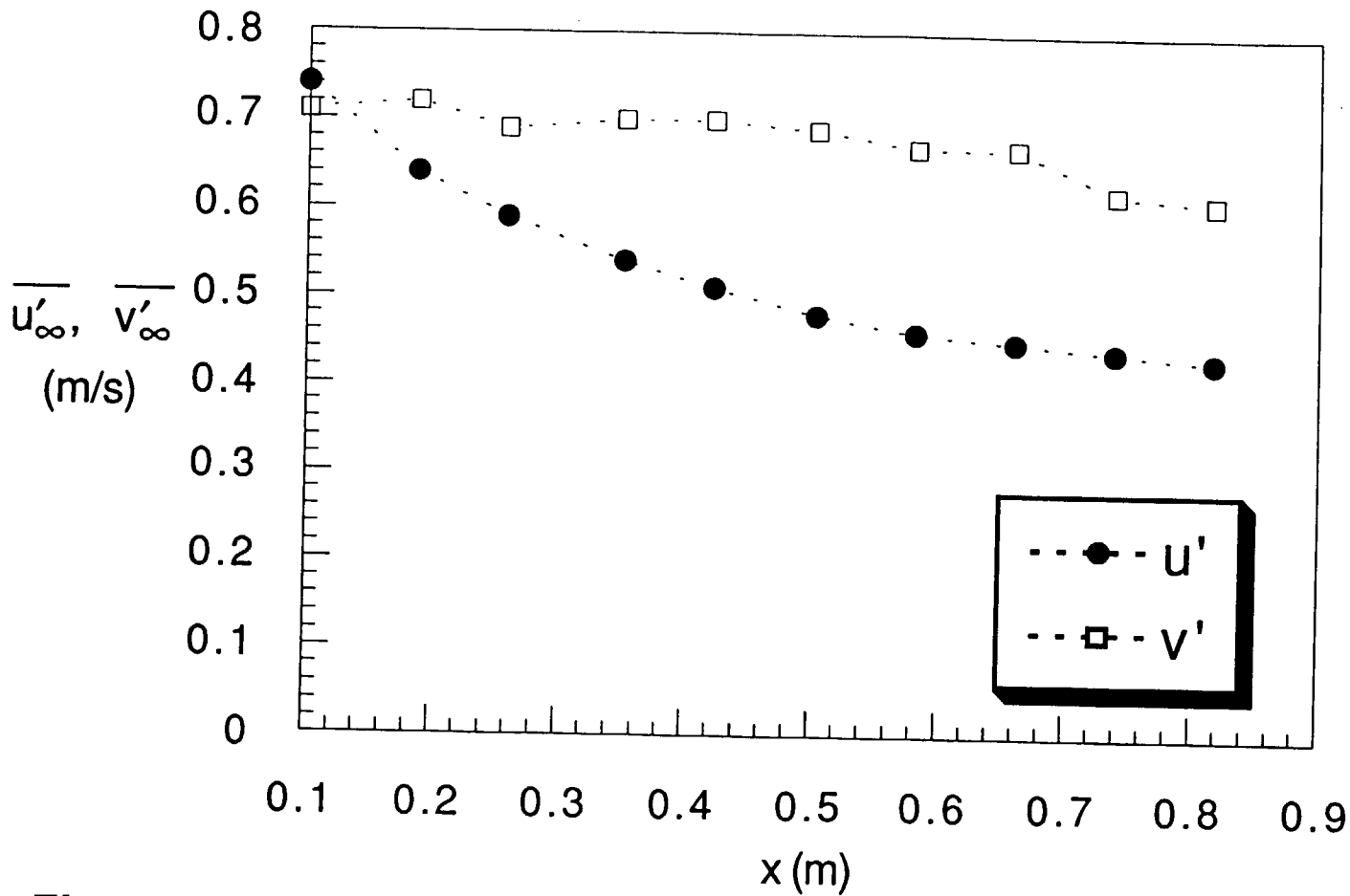

Fig. 6.2a: Free-Stream Turbulence Levels, Dimensional Coordinates, $dU_{cw}/dx=29s^{-1}$ Case

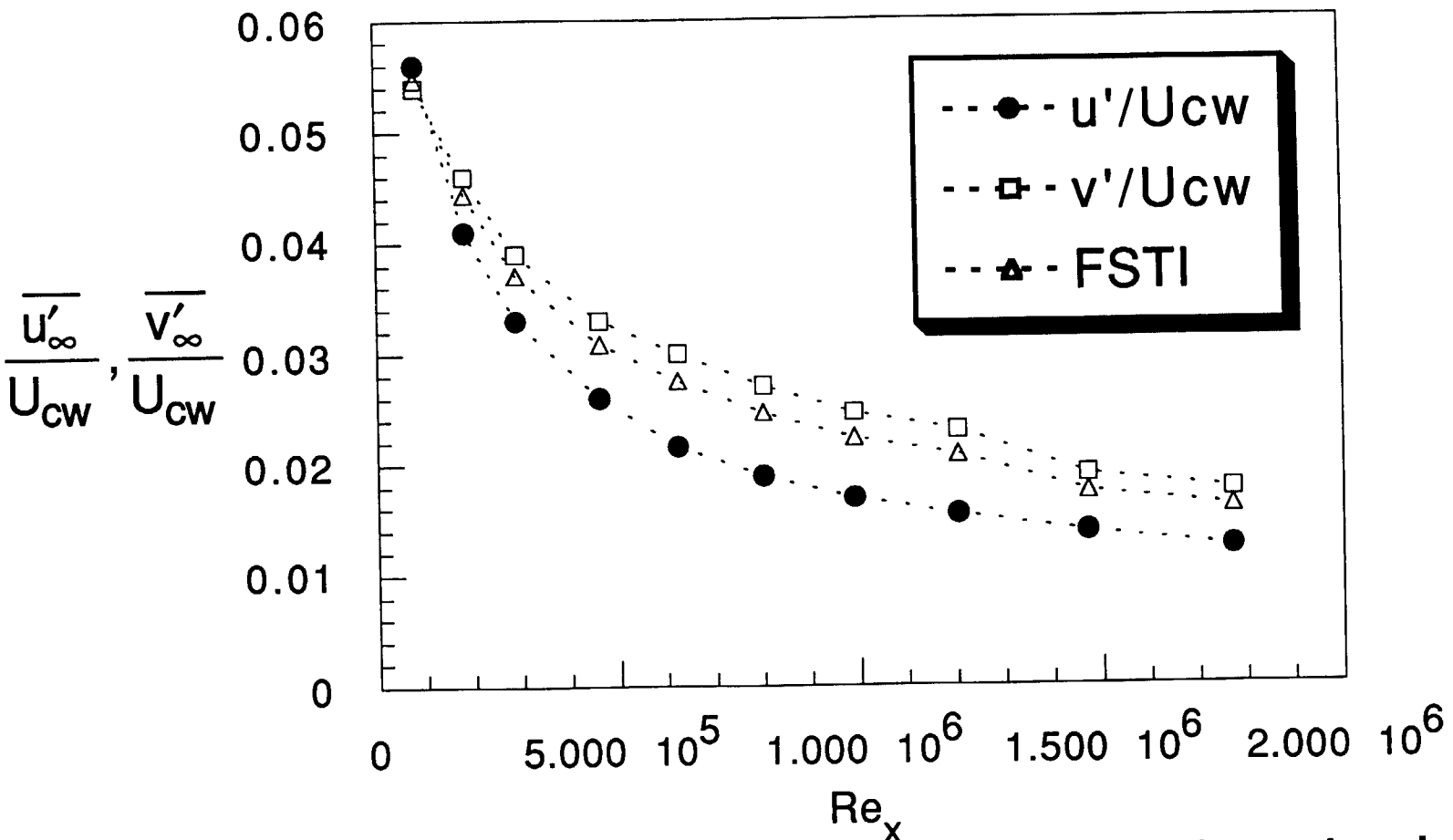

Fig. 6.2b: Free-Stream Turbulence Levels, Nondimensional Coordinates, $dU_{cw}/dx=29s^{-1}$ Case

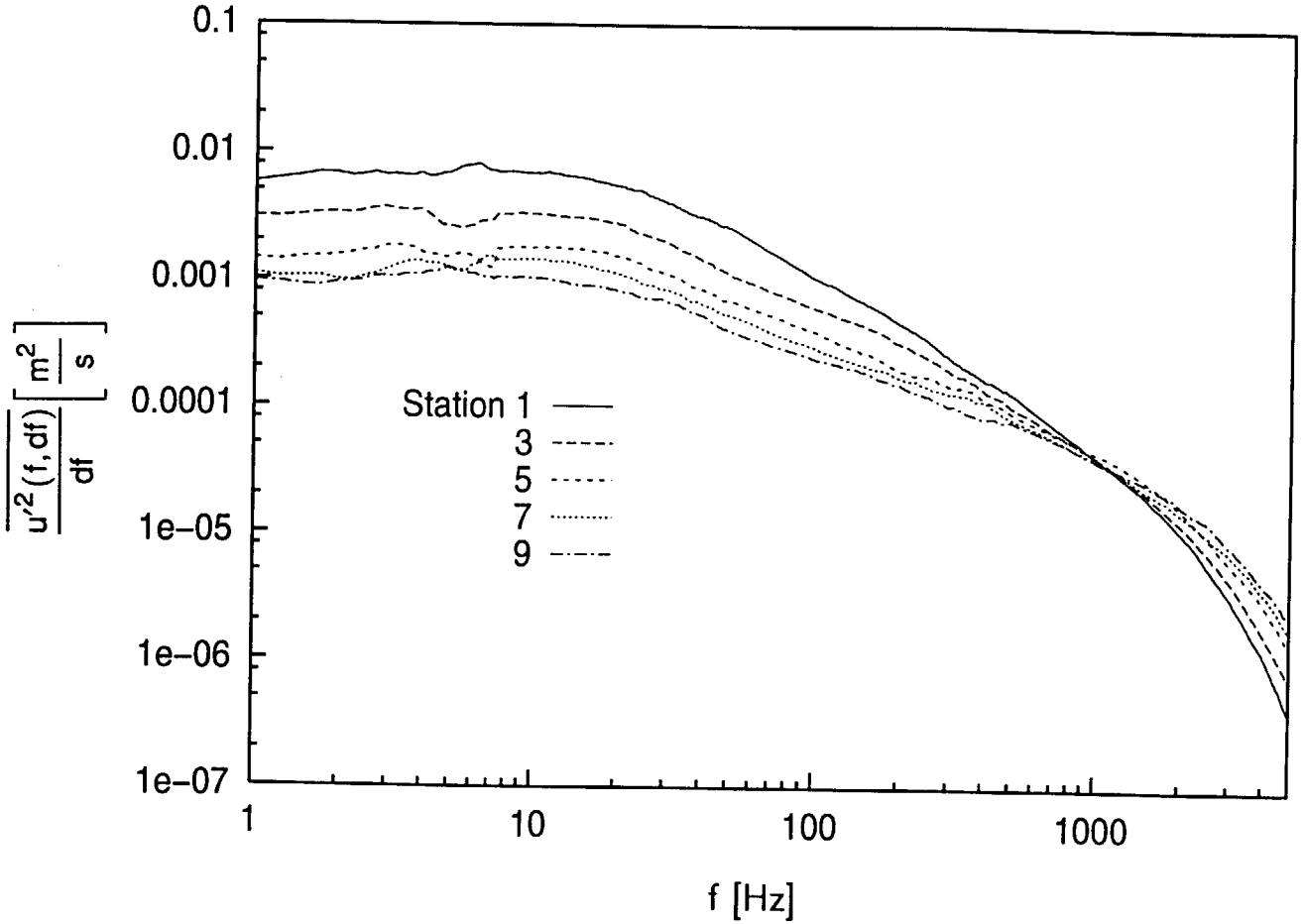

Fig. 6.3a: Free-Stream Spectra of Streamwise Velocity Fluctuations, dU_{cw}/dx=29 s^{-1} Case

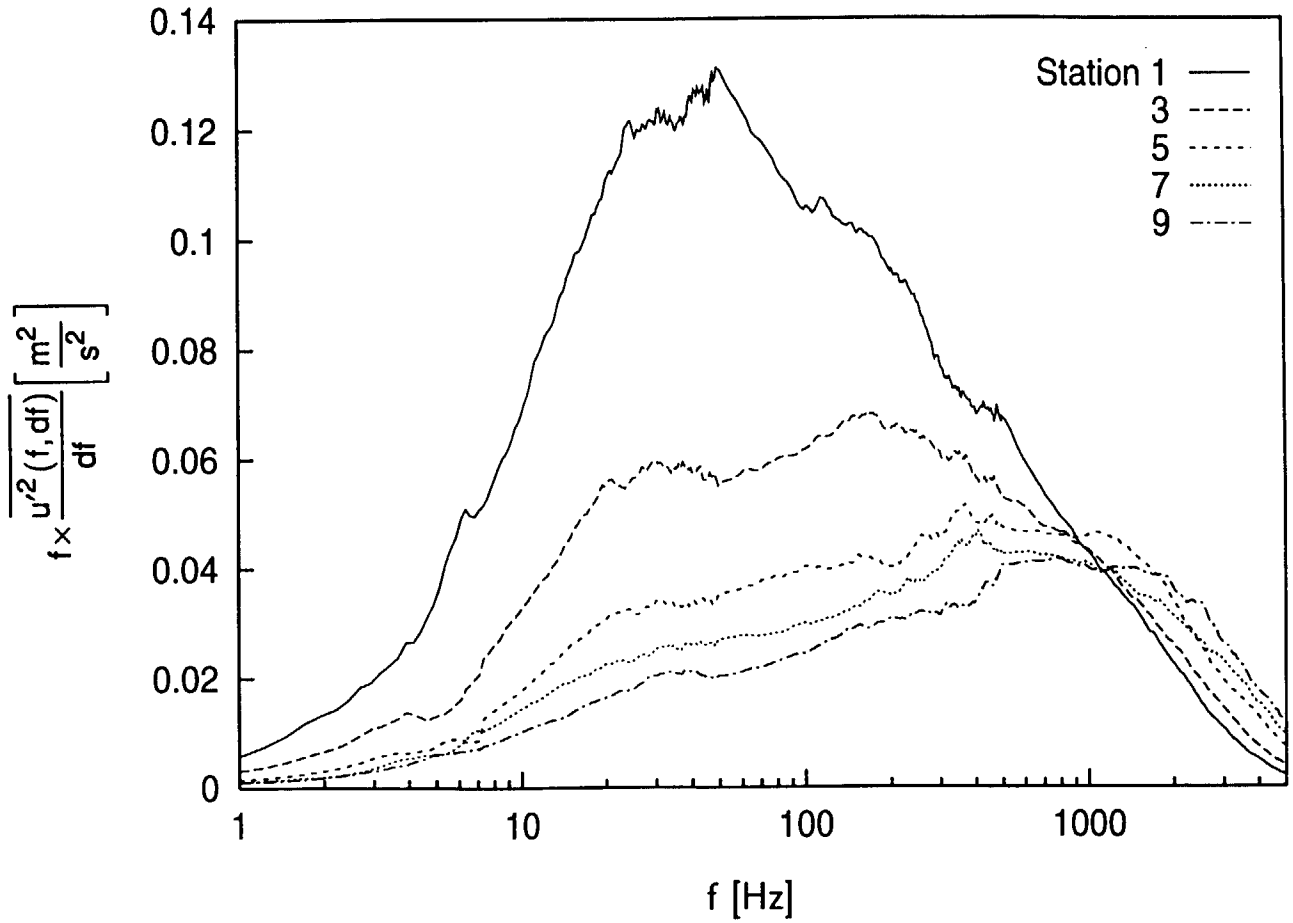

Fig. 6.3b: Free-Stream Spectra of Streamwise Velocity Fluctuations, Energy Coordinates, dU_{cw}/dx=29 s^{-1} Case

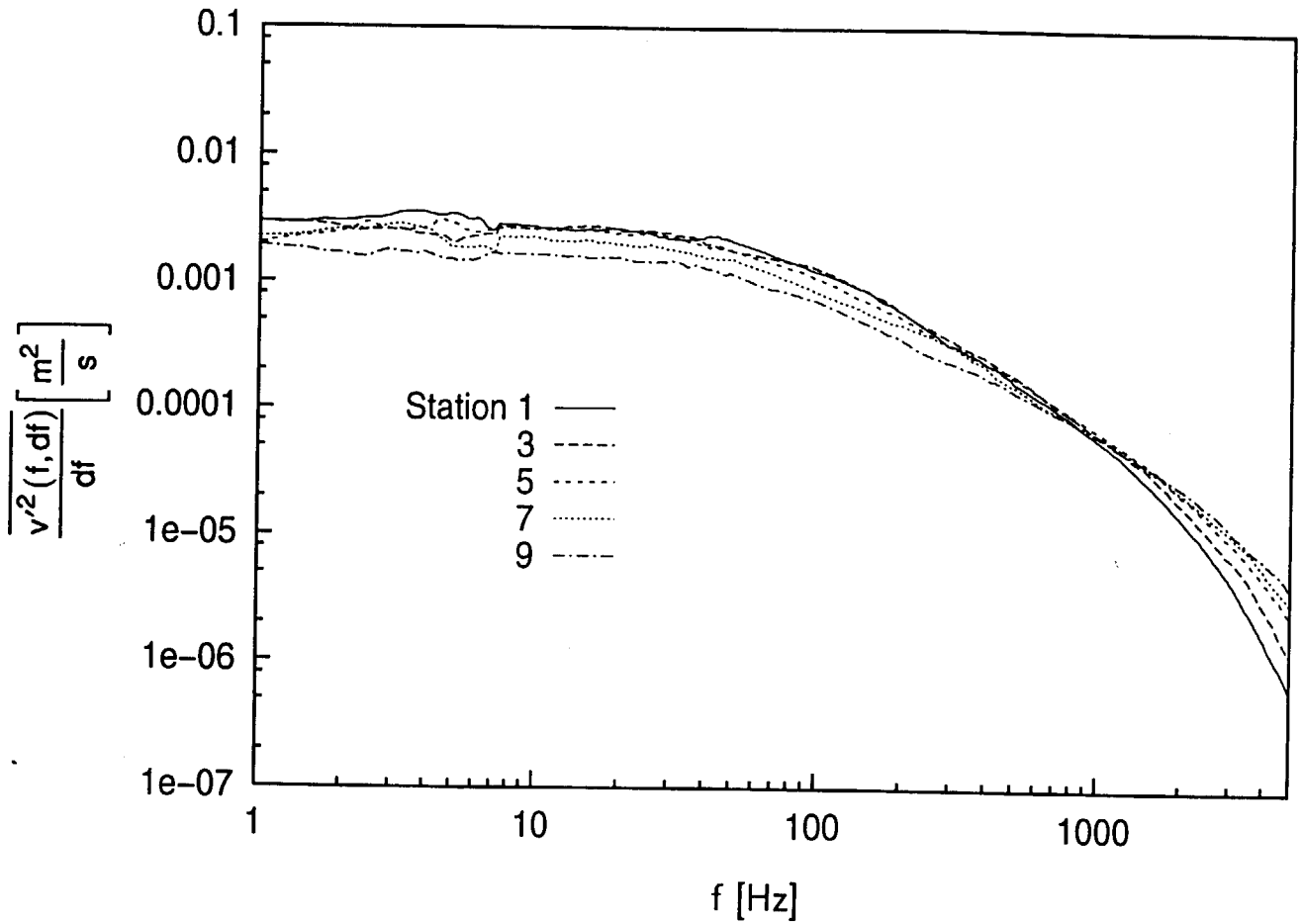

Fig. 6.4a: Free-Stream Spectra of Cross-stream Velocity Fluctuations, dU_{cw}/dx=29 s^{-1} Case

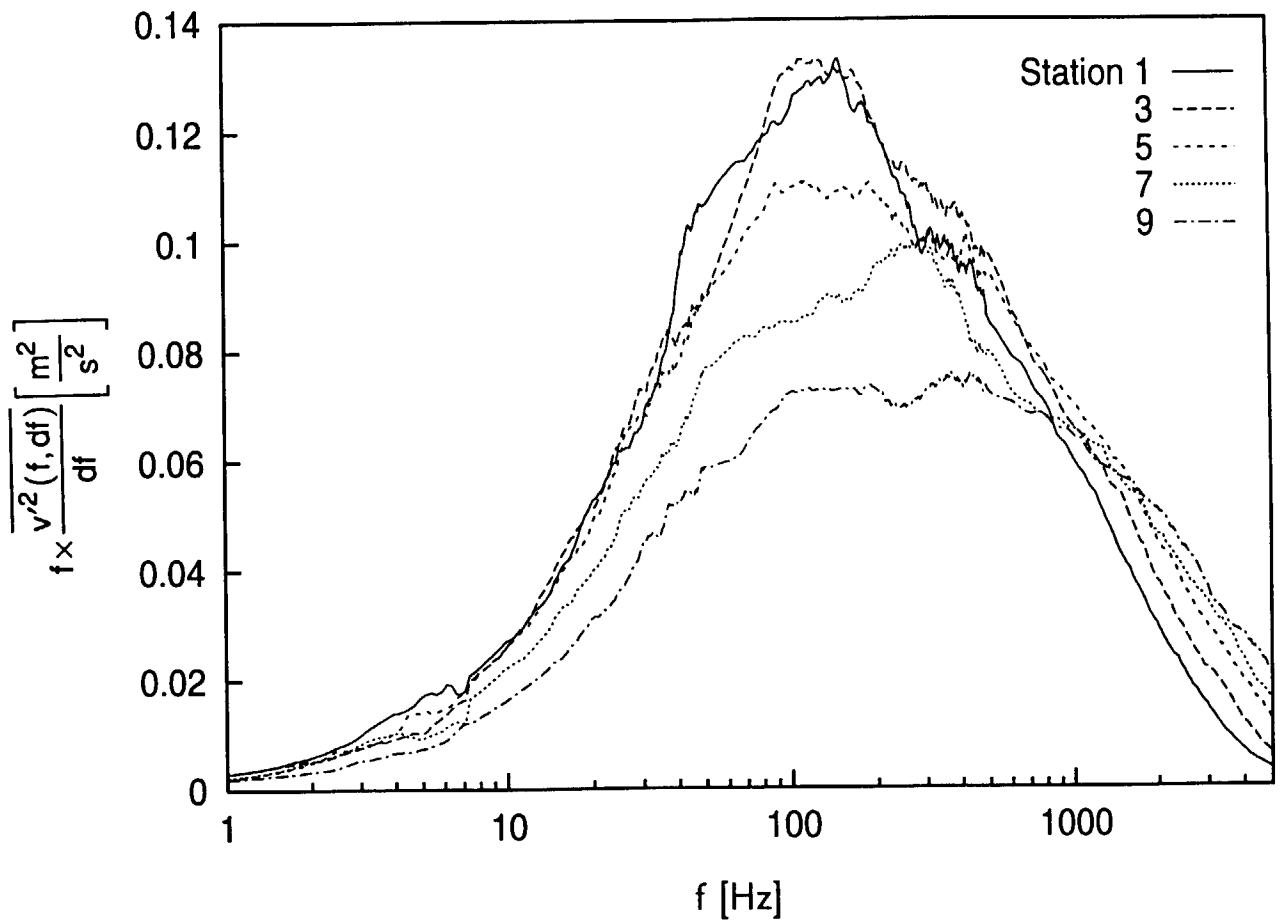

Fig. 6.4b: Free-Stream Spectra of Cross-stream Velocity Fluctuations, Energy Coordinates, dU_{cw}/dx=29 s^{-1} Case

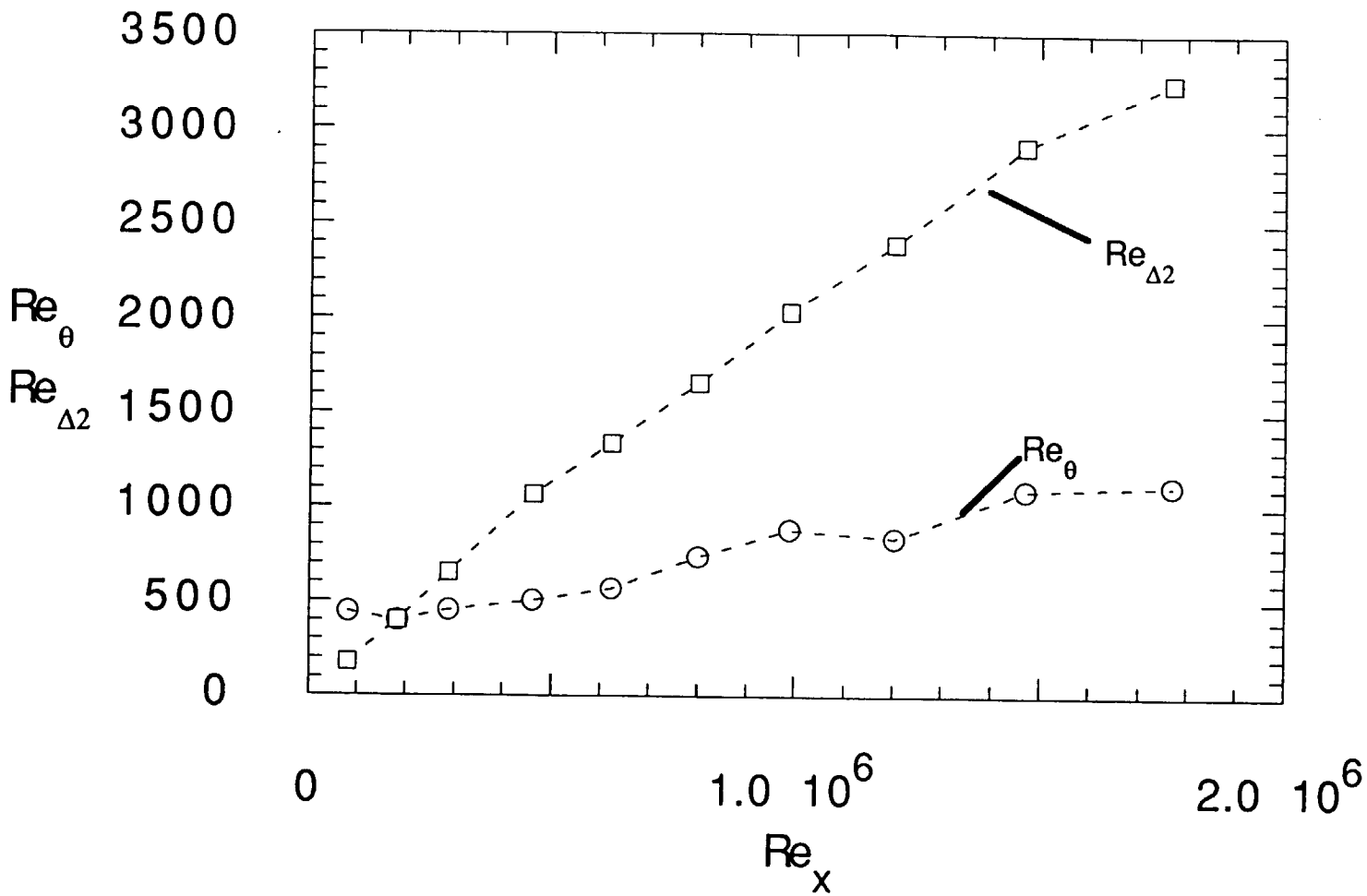

Fig. 6.5: Momentum and Thermal Boundary Layer Growth $dU_{cw}/dx=29s^{-1}$ Case

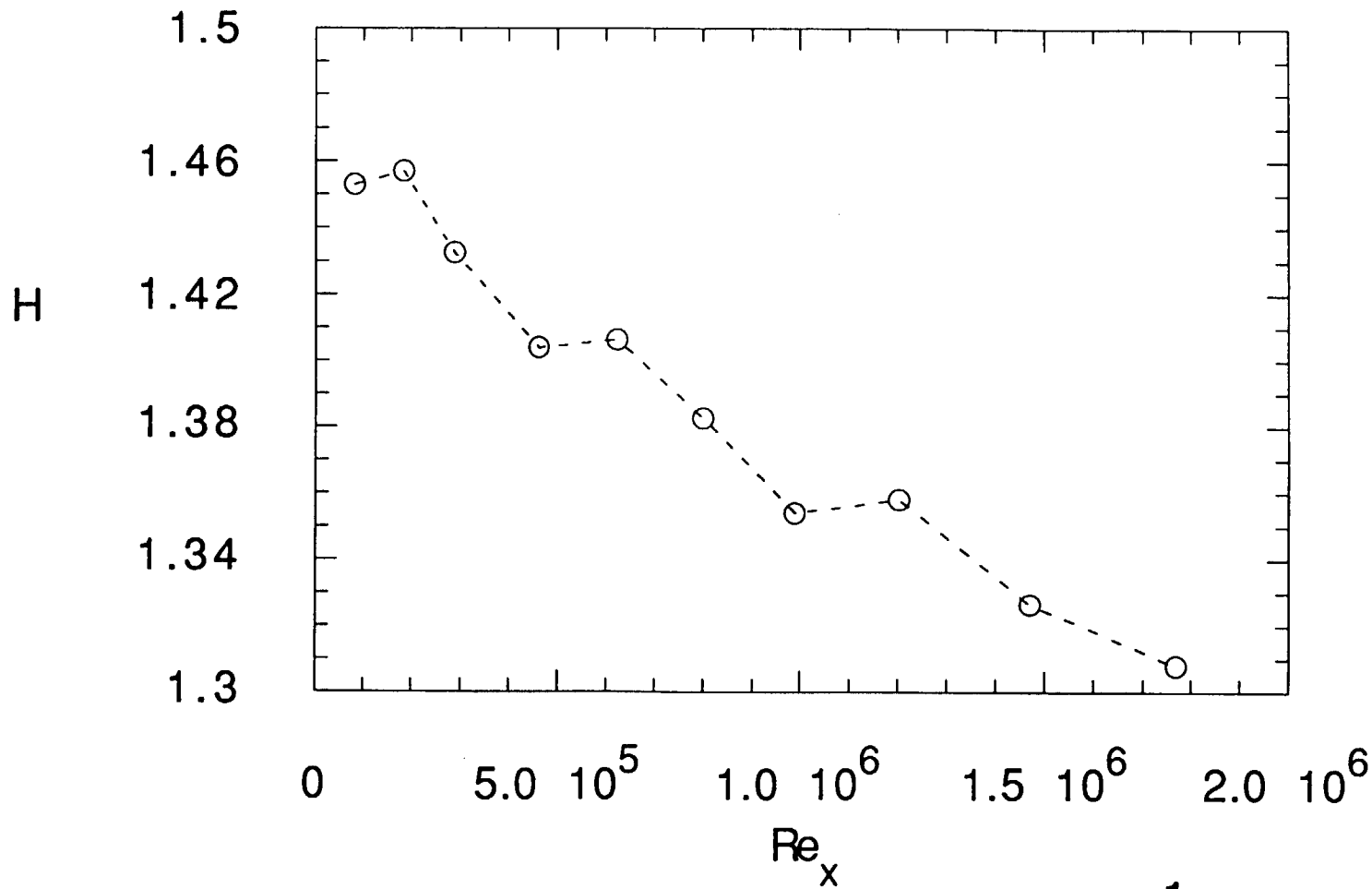

Fig. 6.6: Shape Factor vs Re_x, $dU_{cw}/dx=29s^{-1}$ Case

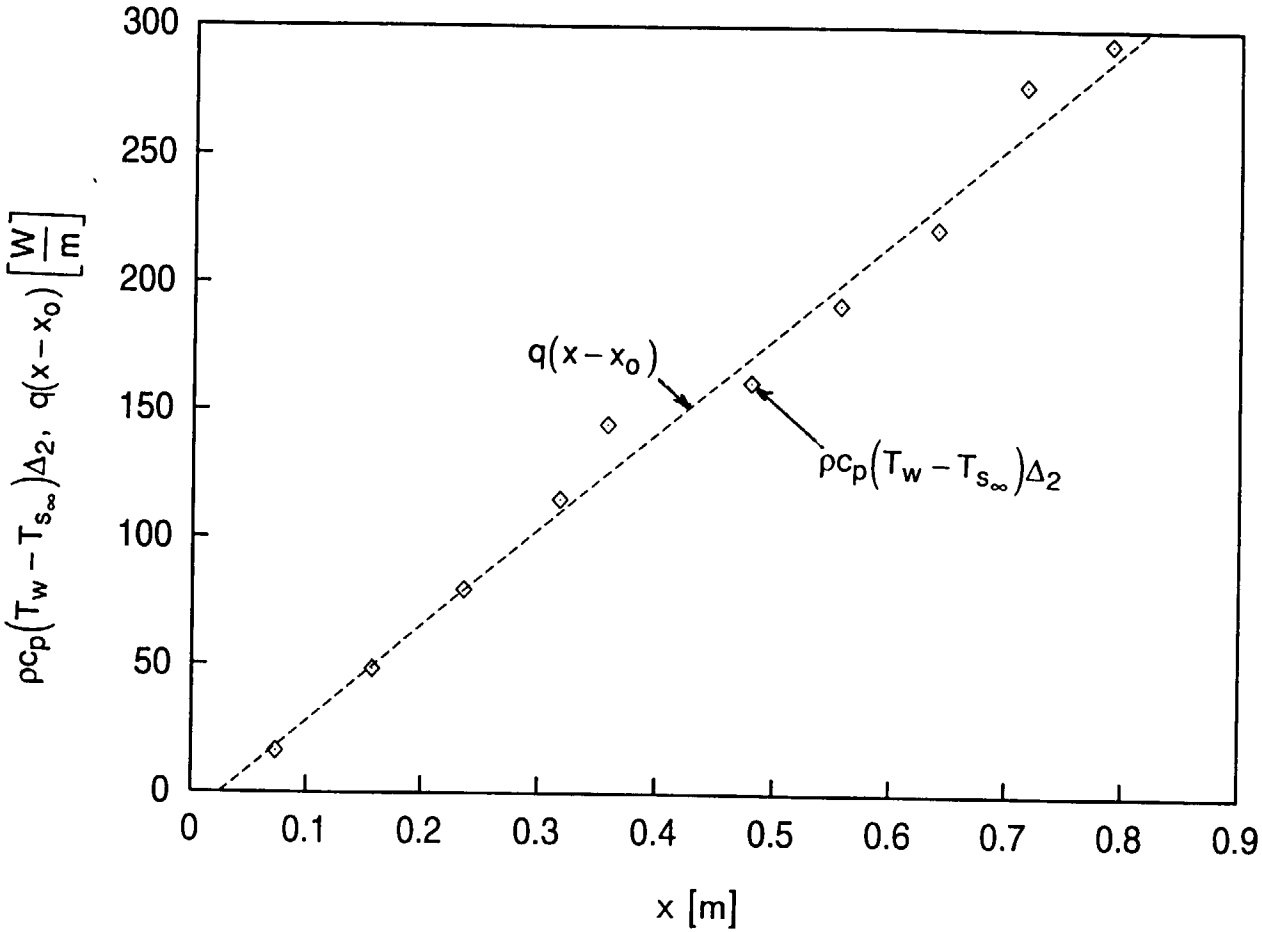

Fig. 6.7: Energy Balance
dU_{cw}/dx=29 s^{-1} Case

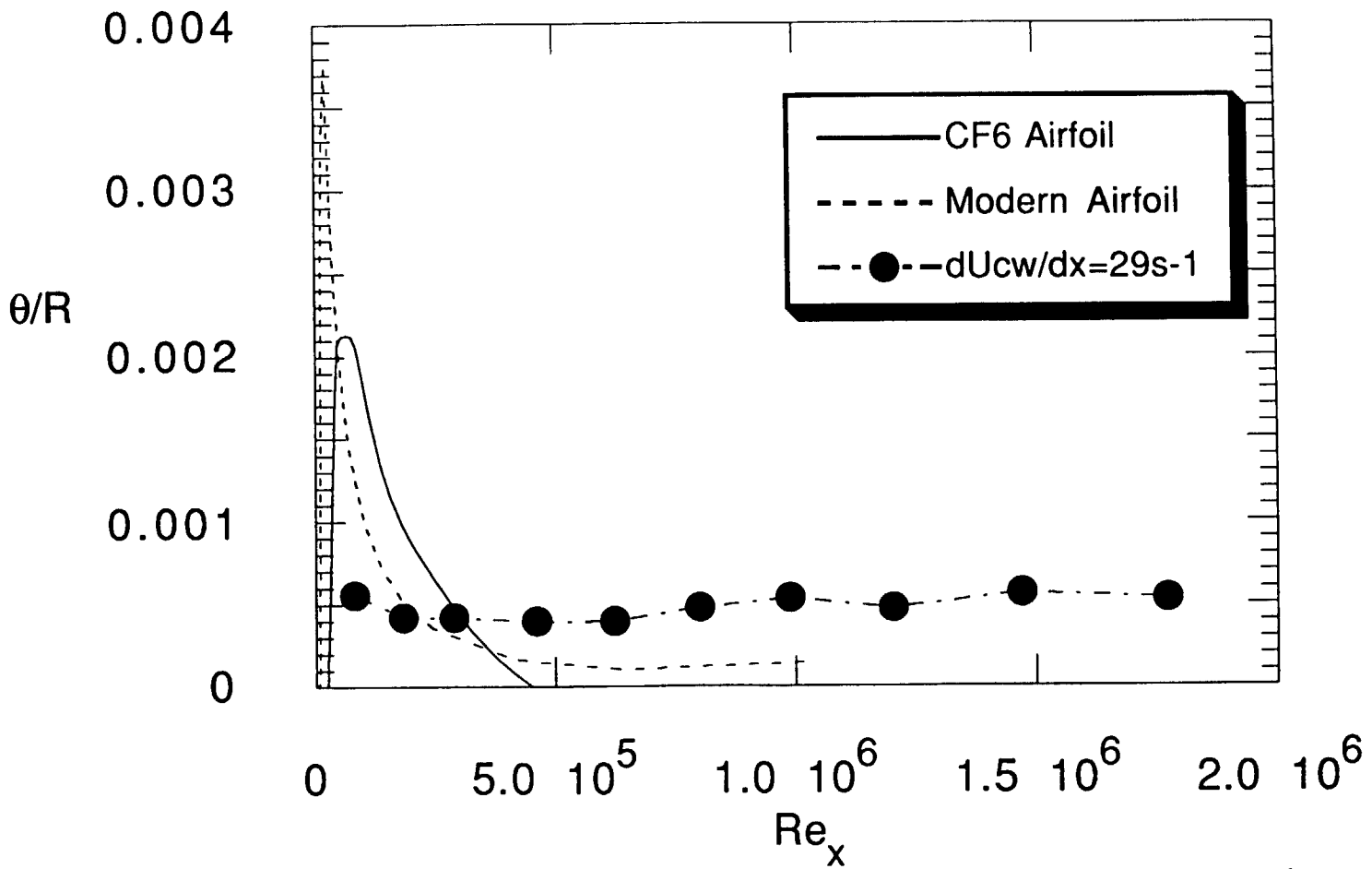

Fig. 6.8: Strength of Curvature for $dU_{cw}/dx=29s^{-1}$ Case and Pressure Side of Two Typical Airfoils

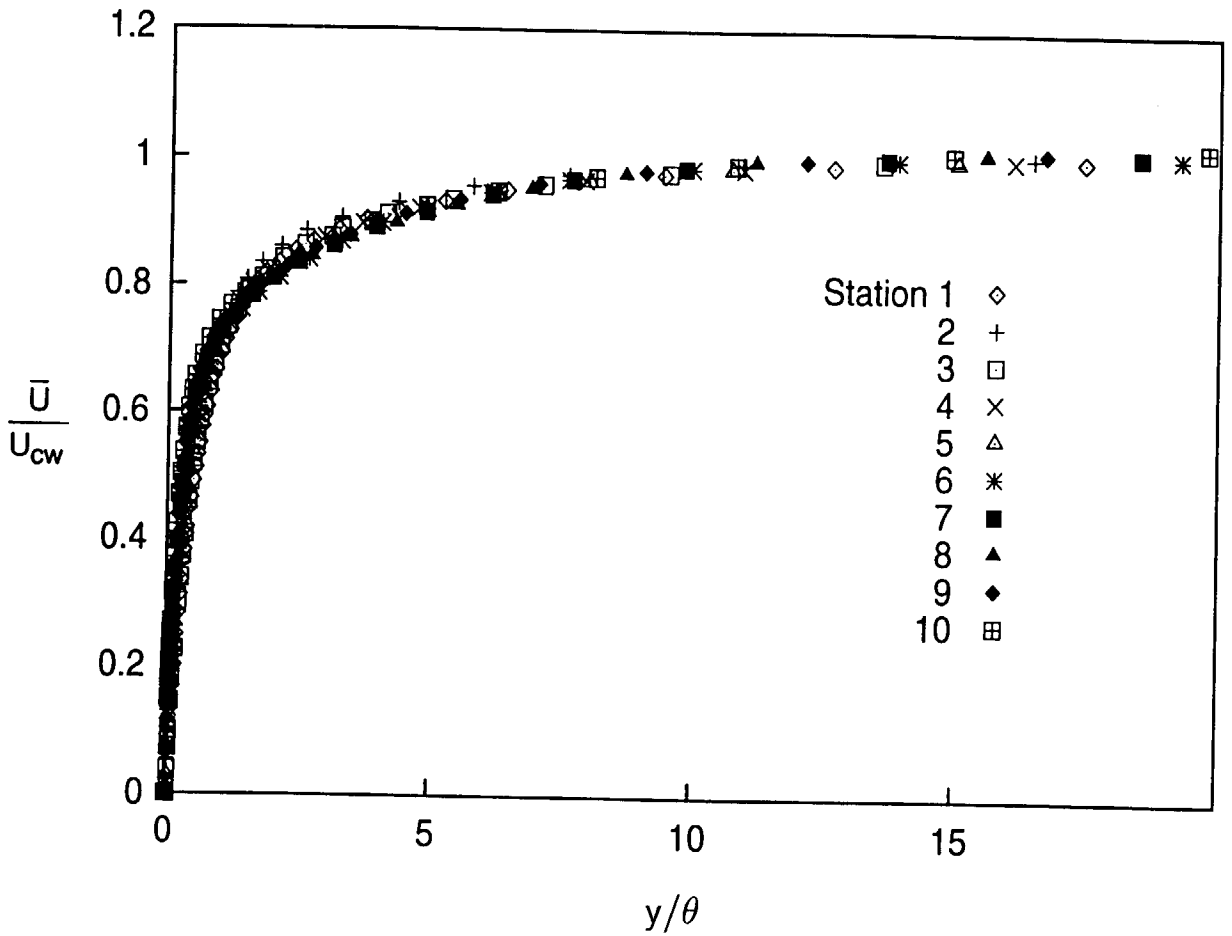

Fig. 6.9a: Mean Velocity Profiles
$dU_{cw}/dx=29\ s^{-1}$ Case

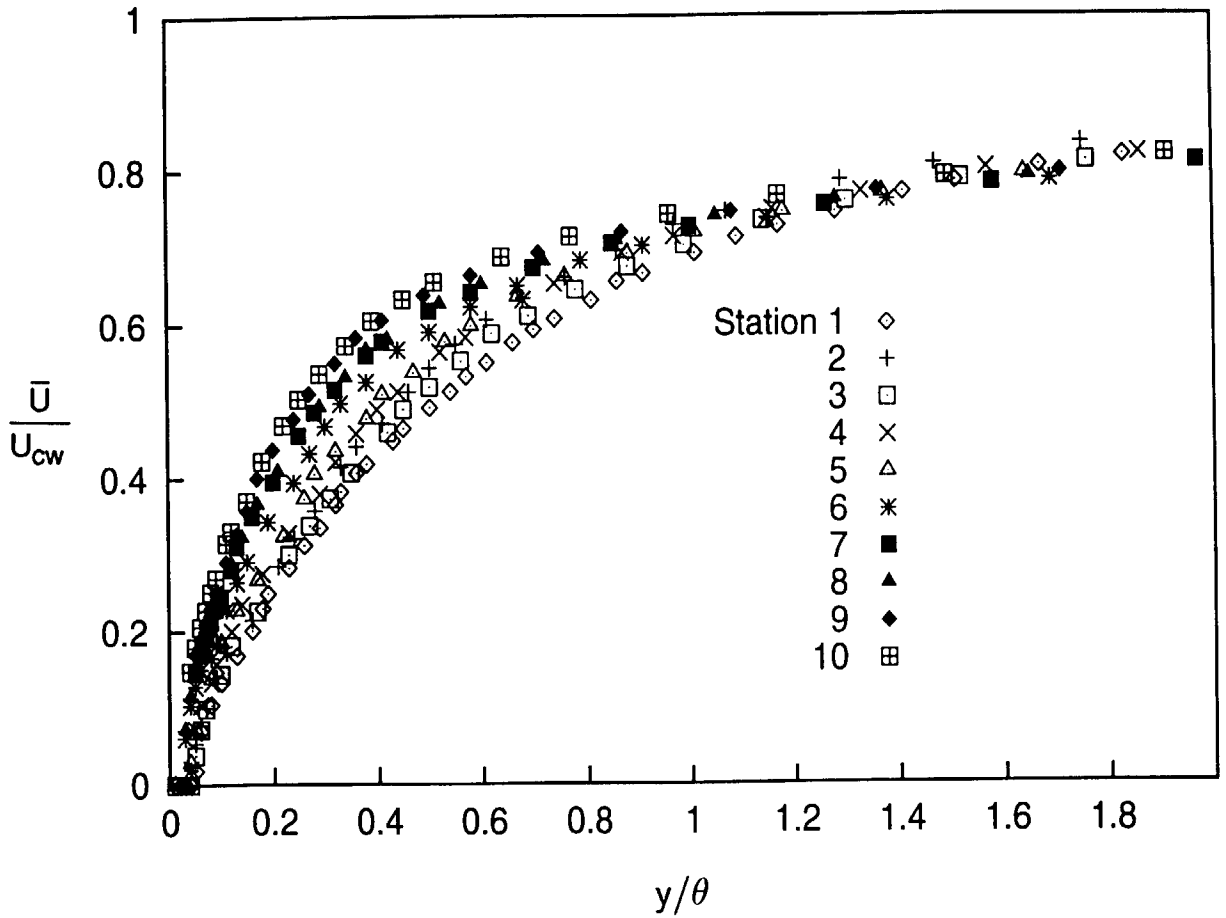

Fig. 6.9b: Mean Velocity Profiles
$dU_{cw}/dx=29\ s^{-1}$ Case

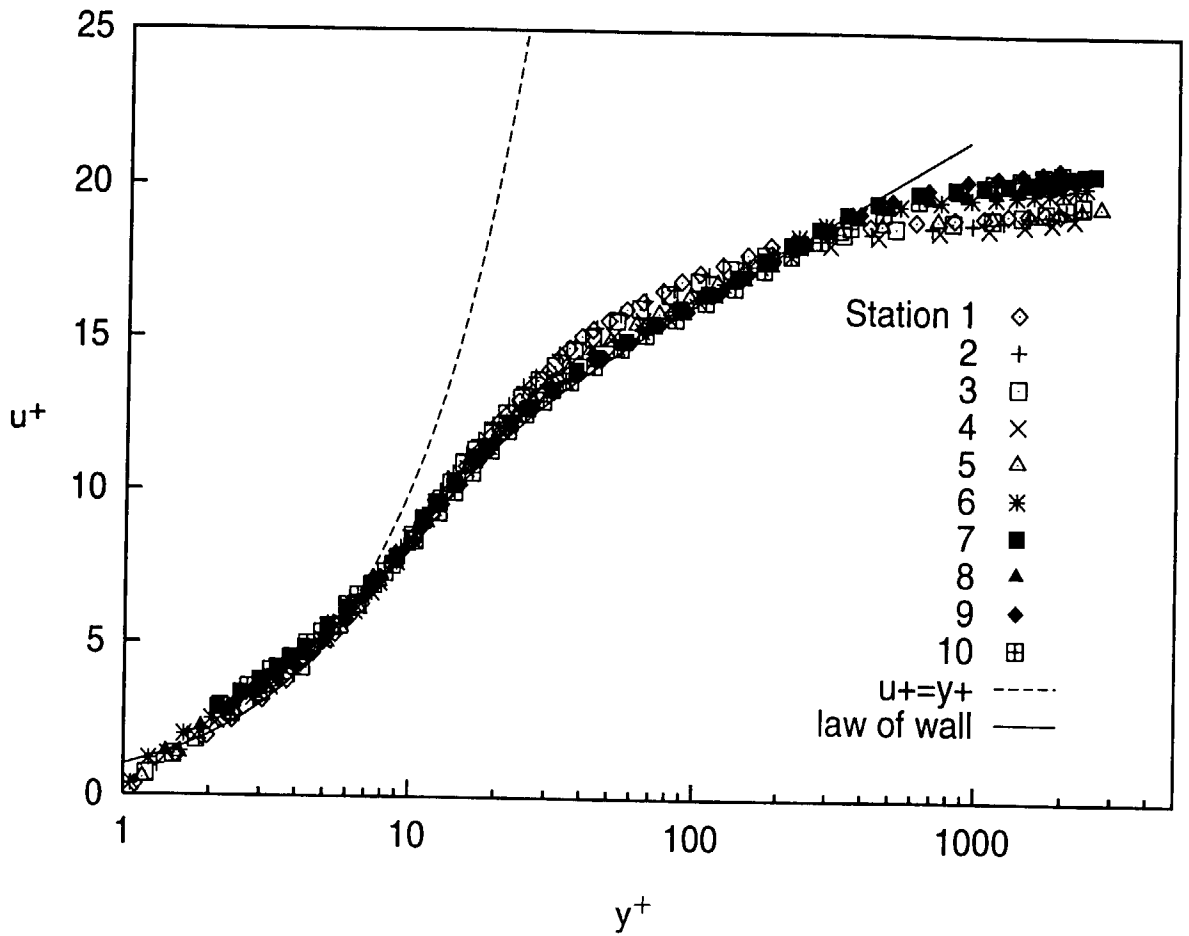

Fig. 6.10: Mean Velocity Profiles, Wall Coordinates
dU_{cw}/dx=29 s^{-1} Case

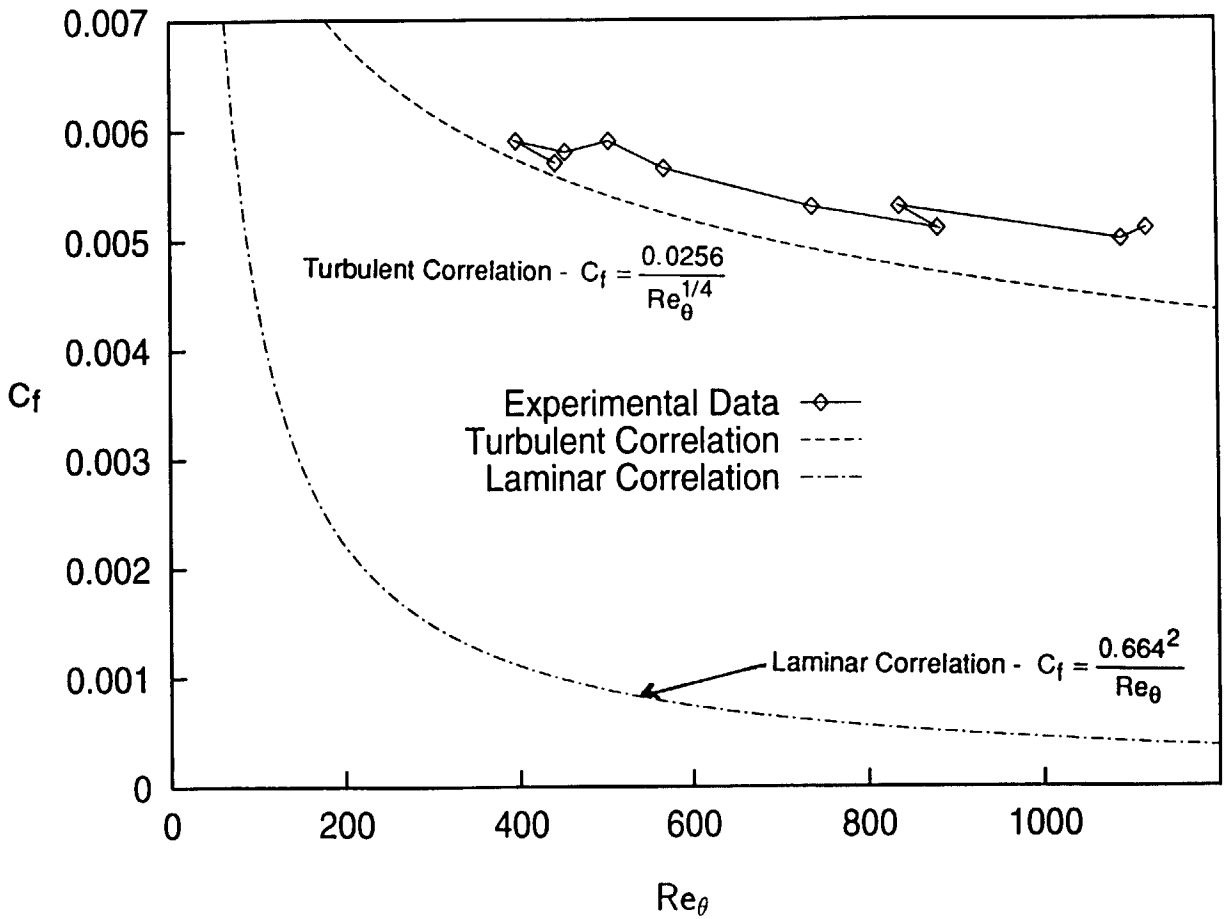

Fig. 6.11: Skin Friction Coefficients vs Re_θ dU_{cw}/dx=29 s^{-1} Case

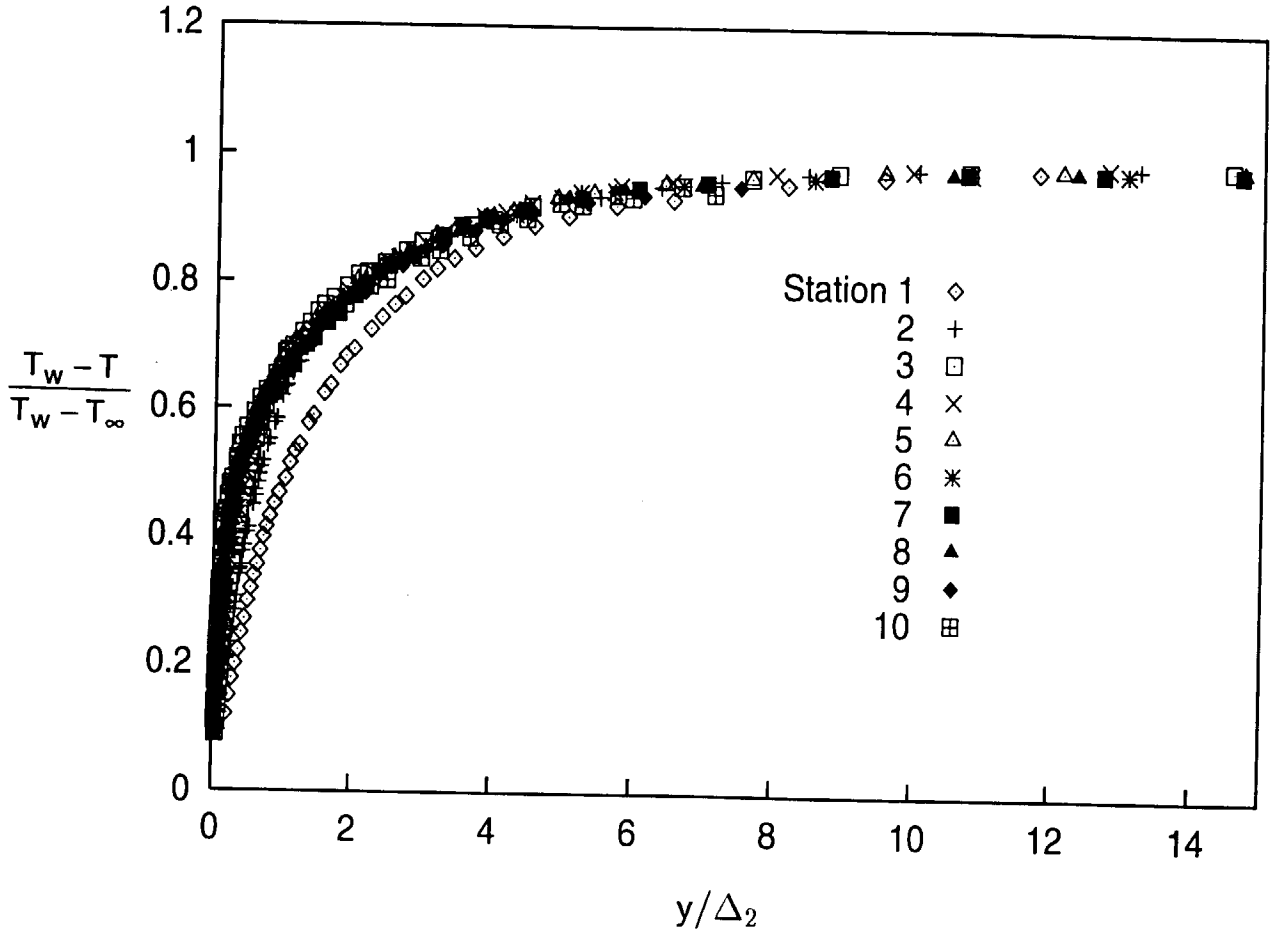

Fig. 6.12a: Mean Temperature Profiles
dU_{cw}/dx=29 s^{-1} Case

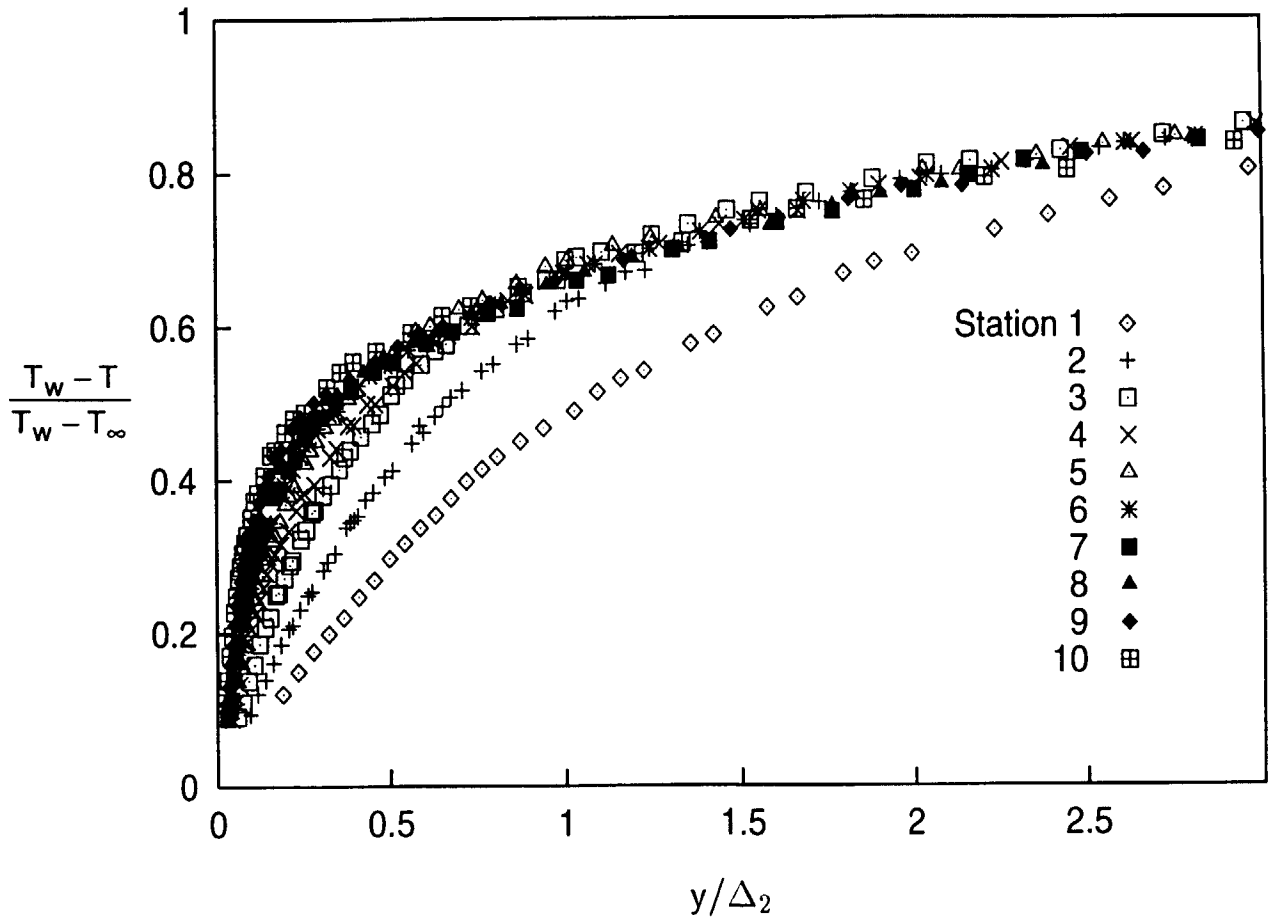

Fig. 6.12b: Mean Temperature Profiles
dU_{cw}/dx=29 s^{-1} Case

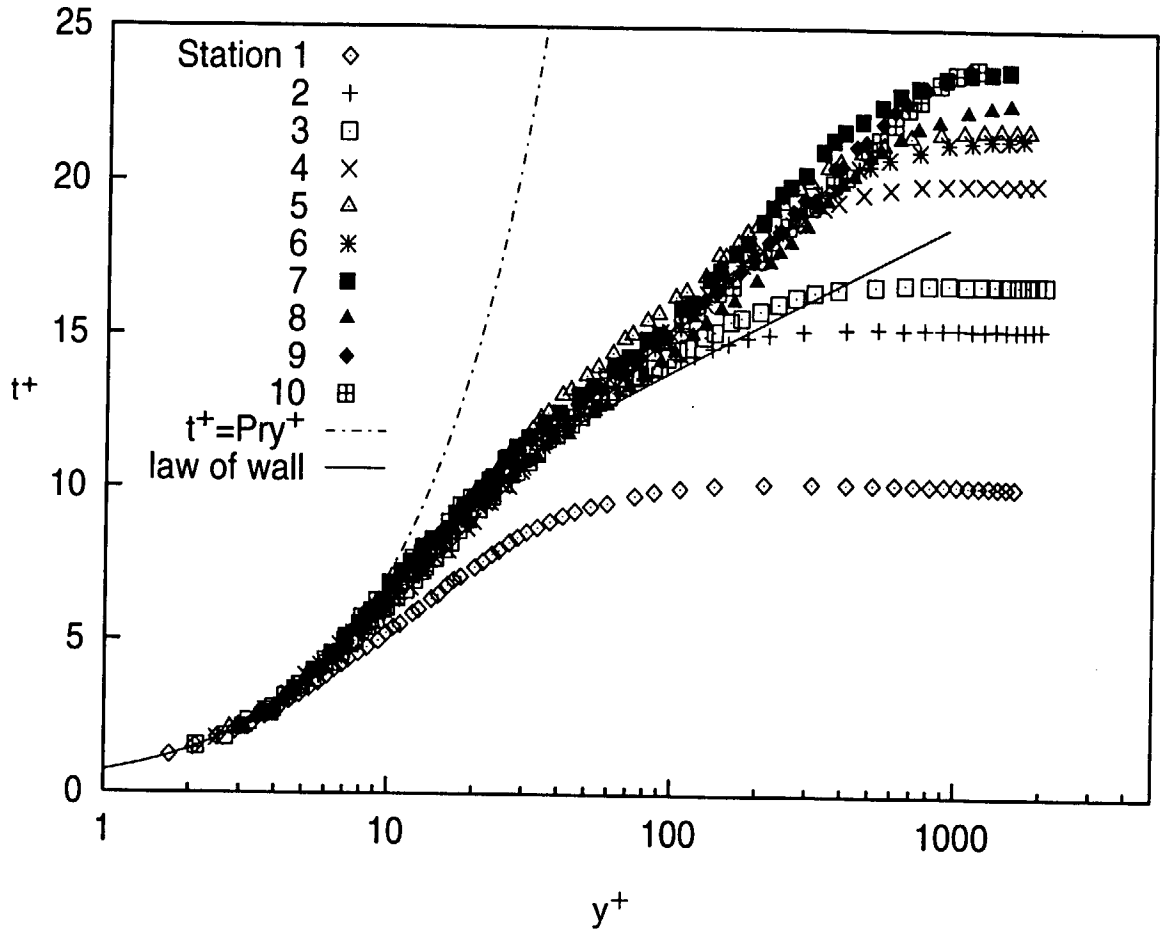

Fig. 6.13a: Mean Temperature Profiles, Wall Coordinates $dU_{cw}/dx=29\ s^{-1}$ Case

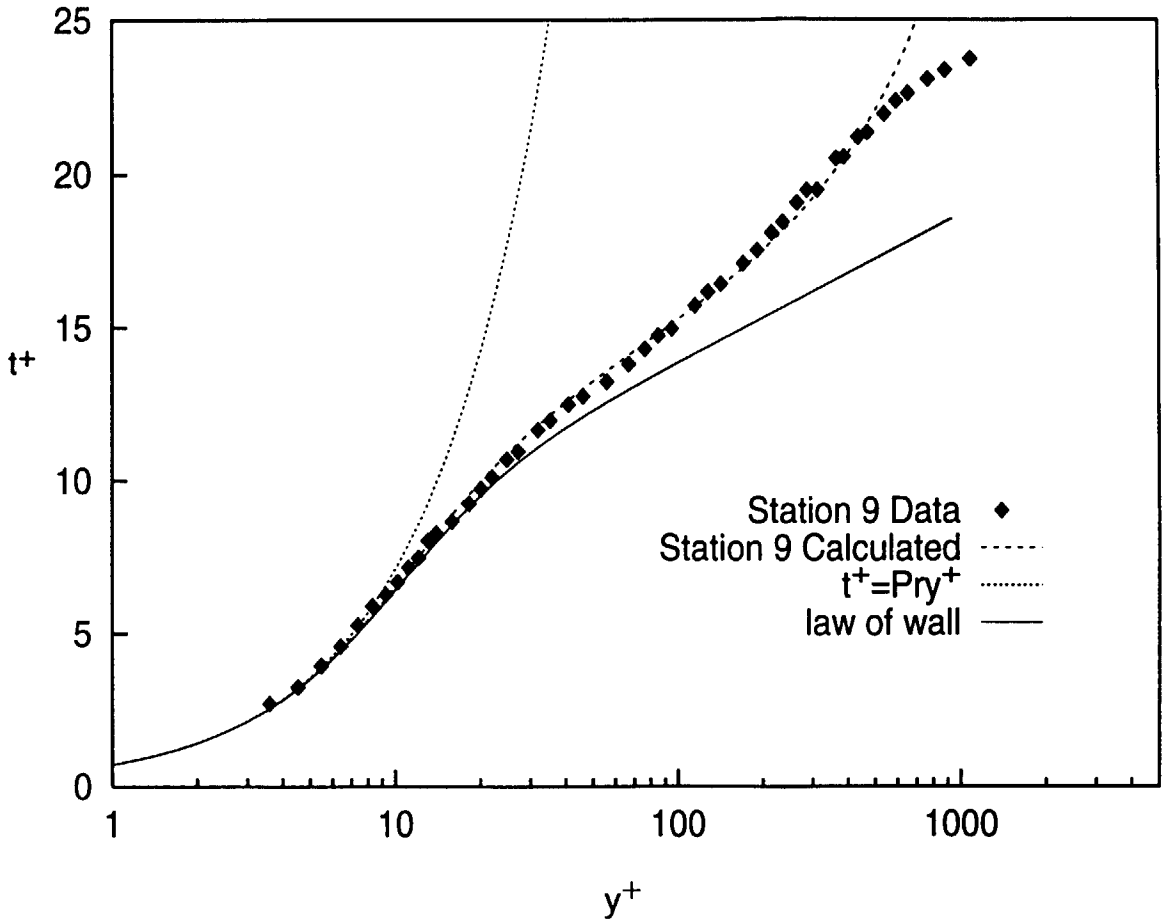

Fig. 6.13b: Comparison of Calculated Profile to Data
dU_{cw}/dx=29 s^{-1} Case

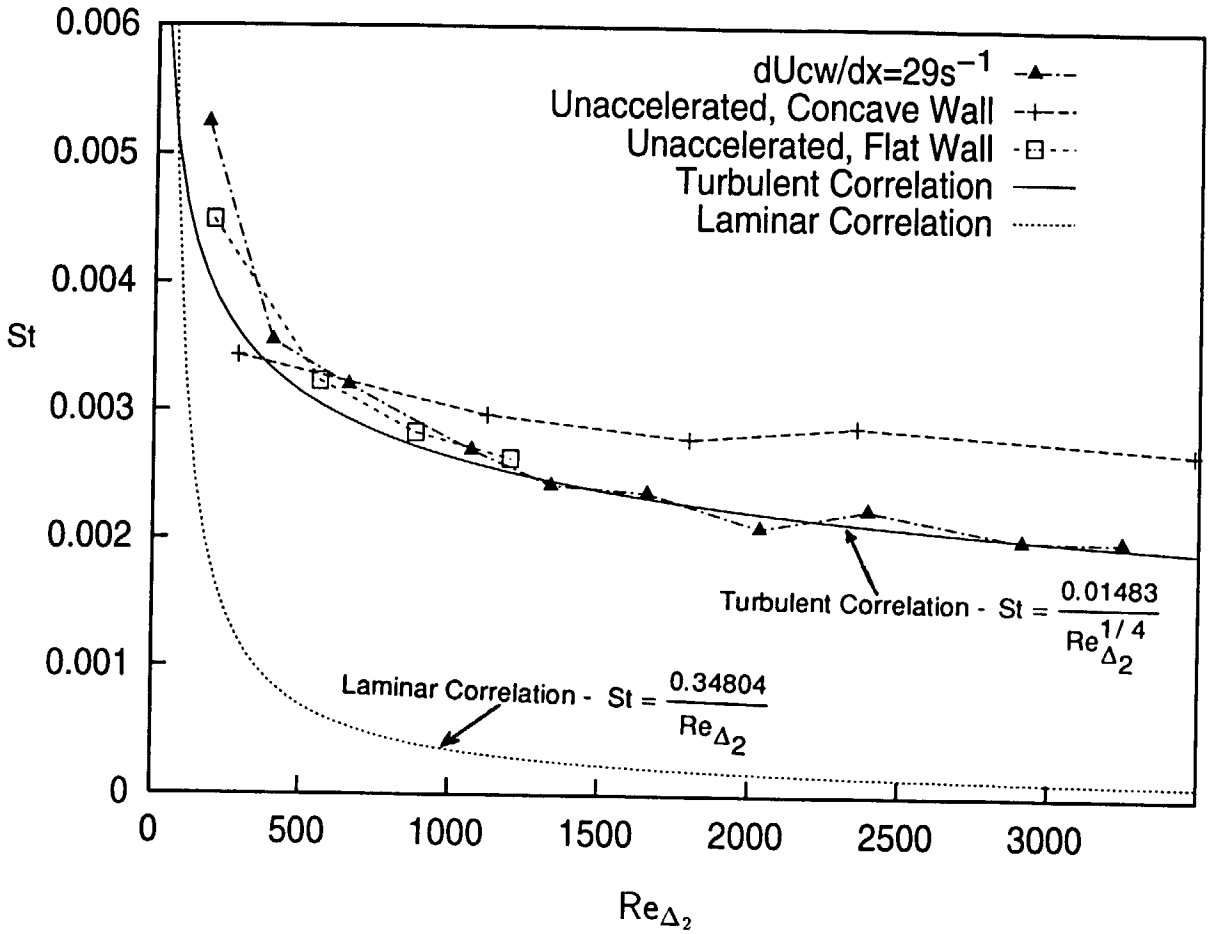

Fig. 6.14: Stanton Number vs Re_{Δ_2}
$dU_{cw}/dx=29\ s^{-1}$ Case

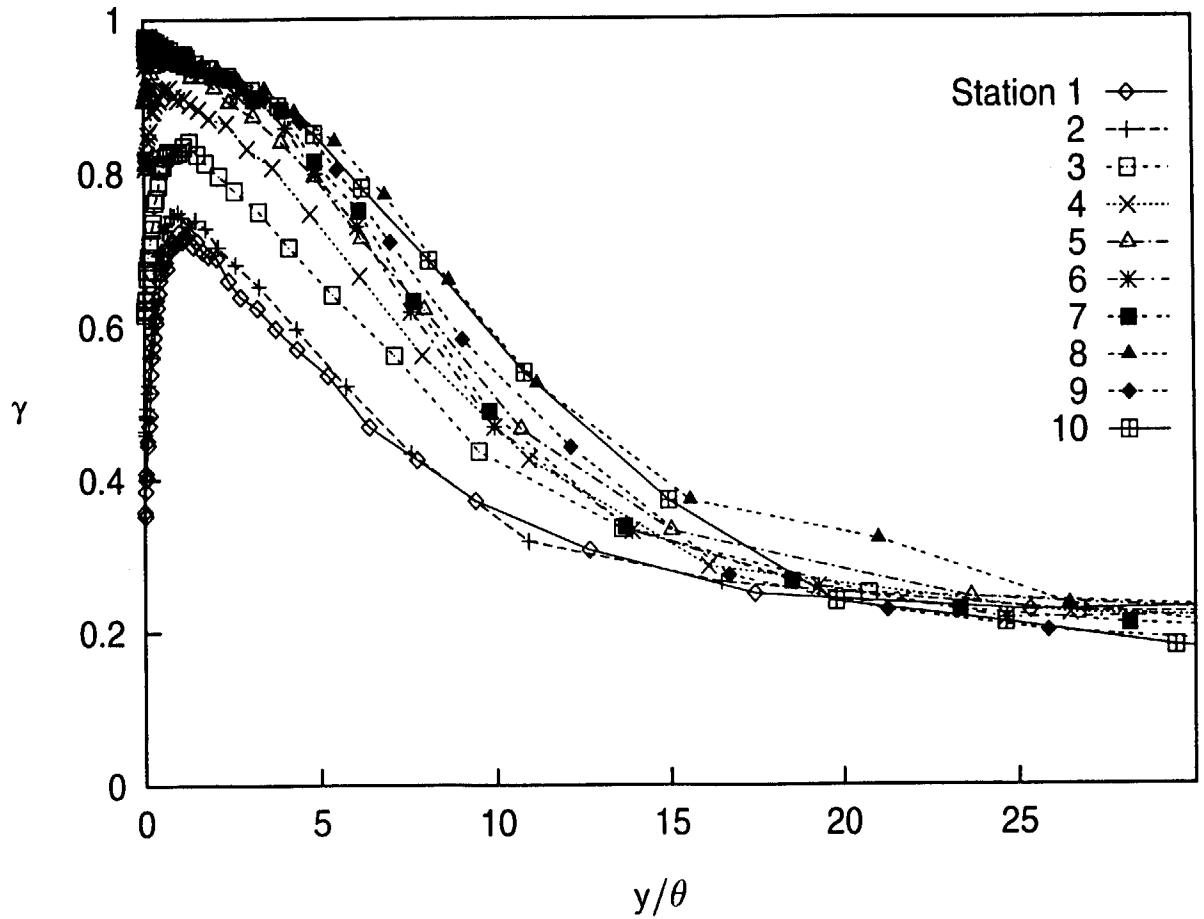

Fig. 6.15: Intermittency Profiles Based on u' Fluctuations
dU_{cw}/dx=29 s^{-1} Case

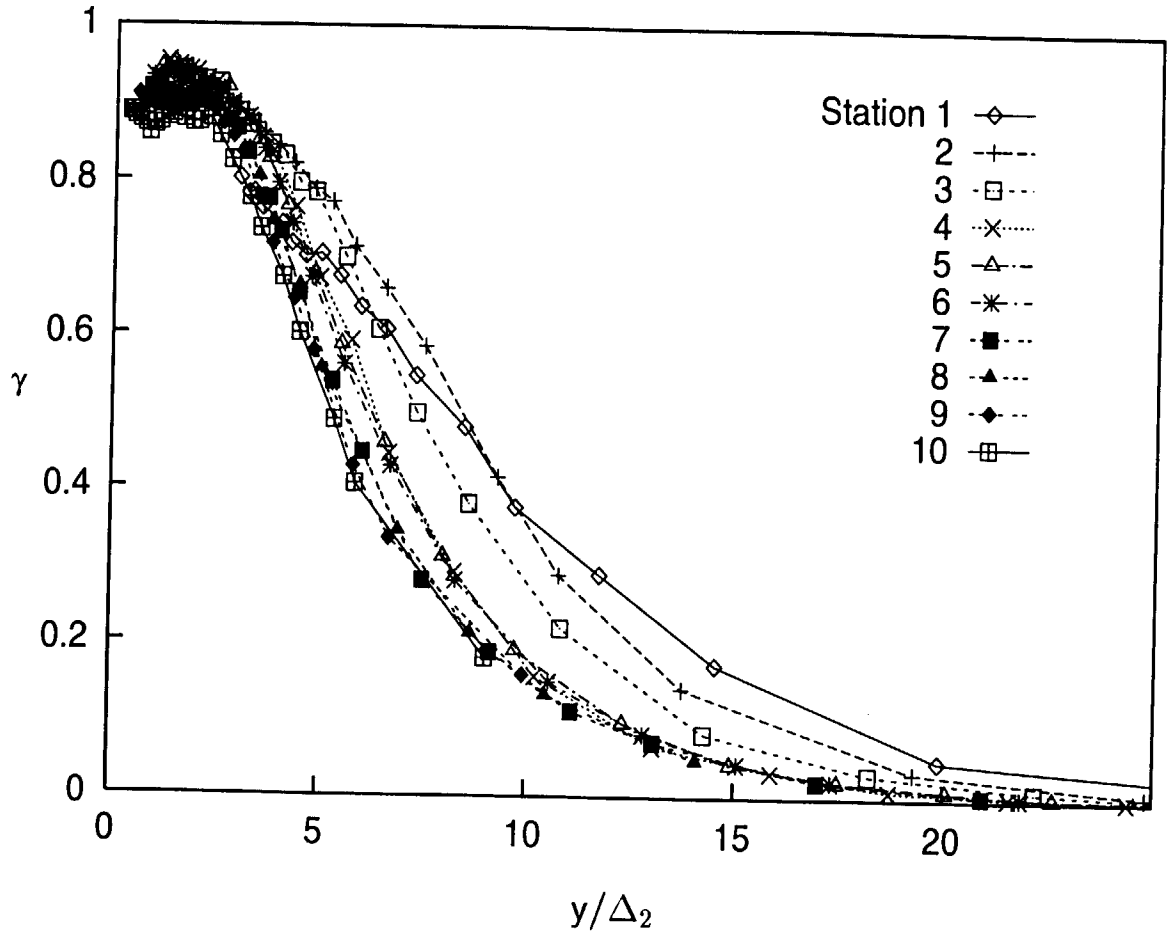

Fig. 6.16: Intermittency Profiles Based on t' Fluctuations dU_{cw}/dx=29 s^{-1} Case

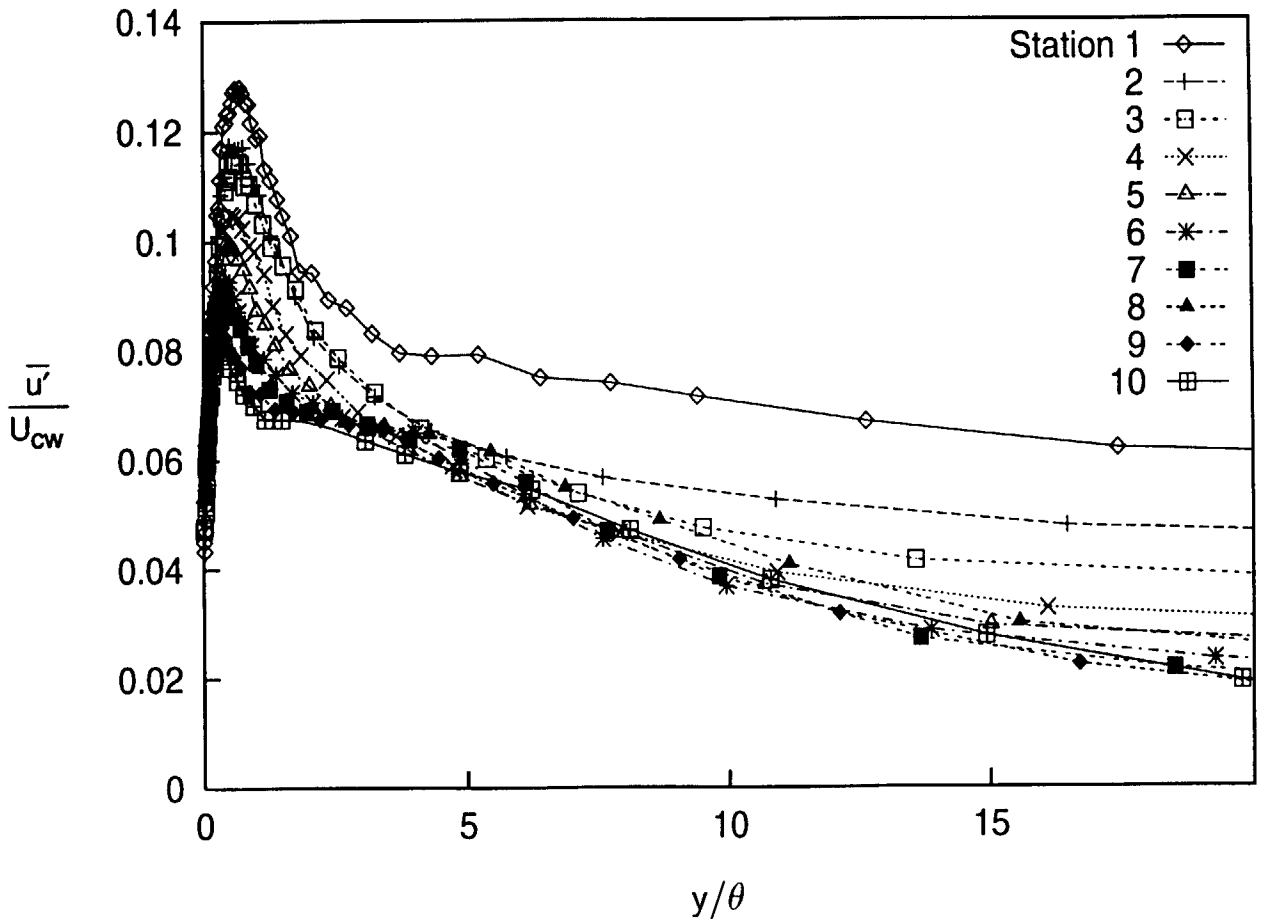

Fig. 6.17a: Fluctuating Streamwise Velocity Profiles $dU_{cw}/dx=29\ s^{-1}$ Case

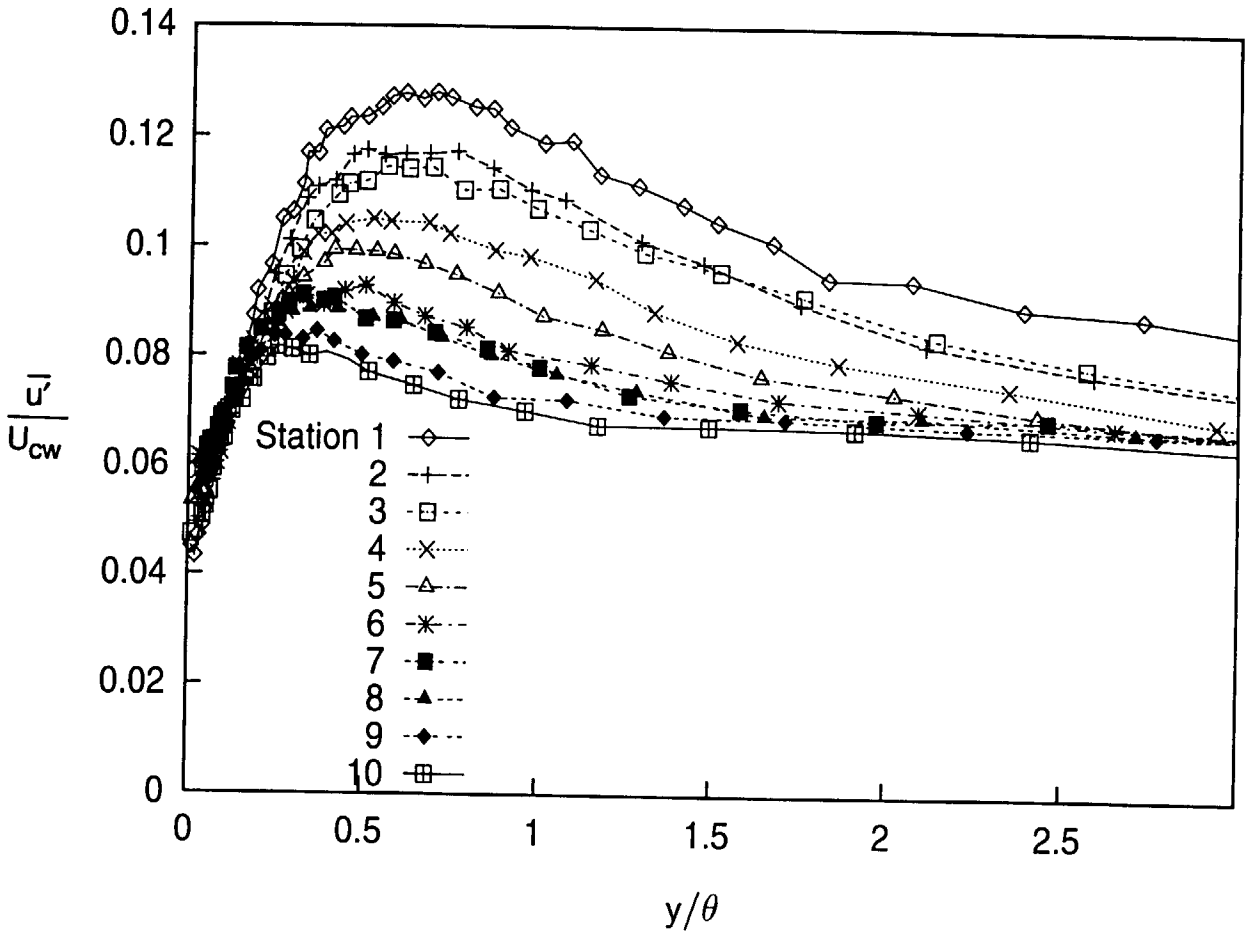

Fig. 6.17b: Fluctuating Streamwise Velocity Profiles $dU_{cw}/dx=29\ s^{-1}$ Case

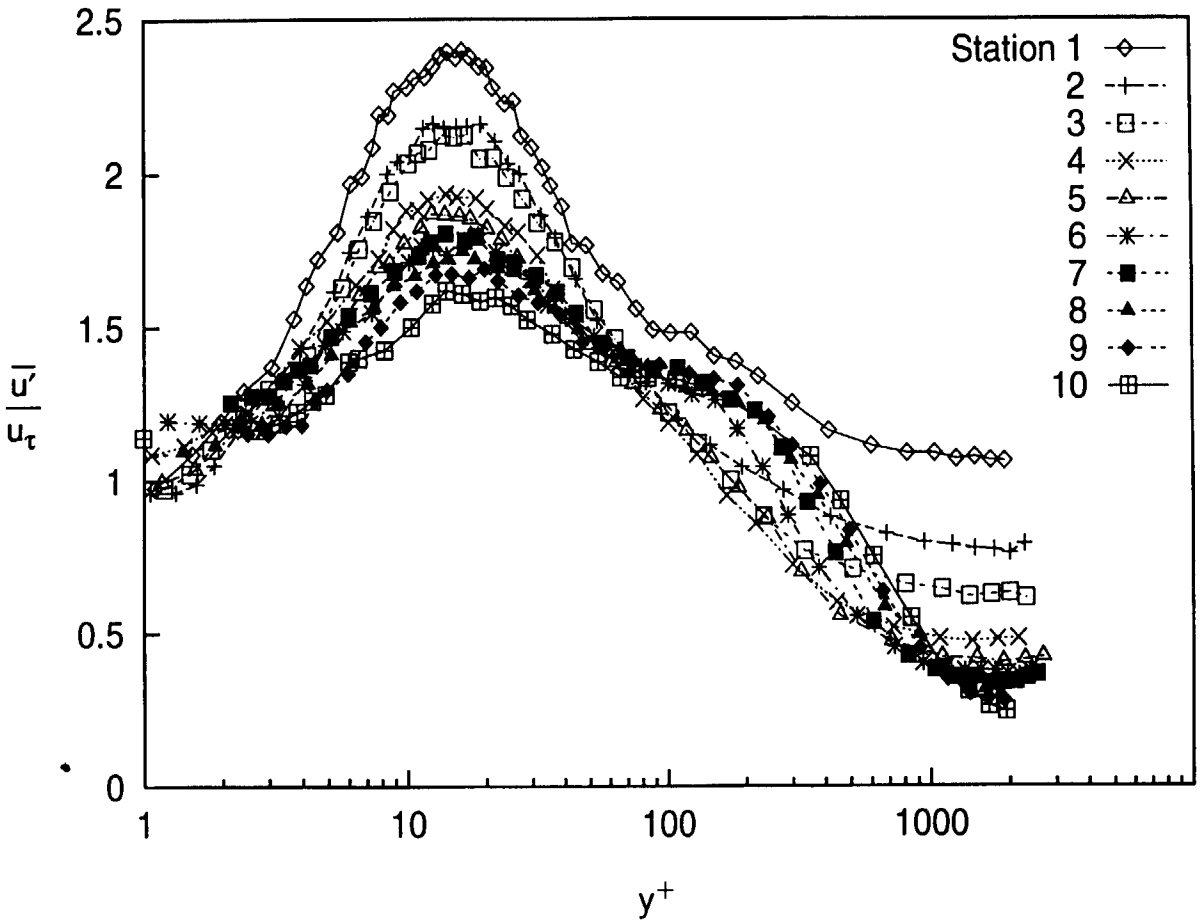

Fig. 6.18: Fluctuating Streamwise Velocity Profiles, Wall Coordinates $dU_{cw}/dx=29\ s^{-1}$ Case

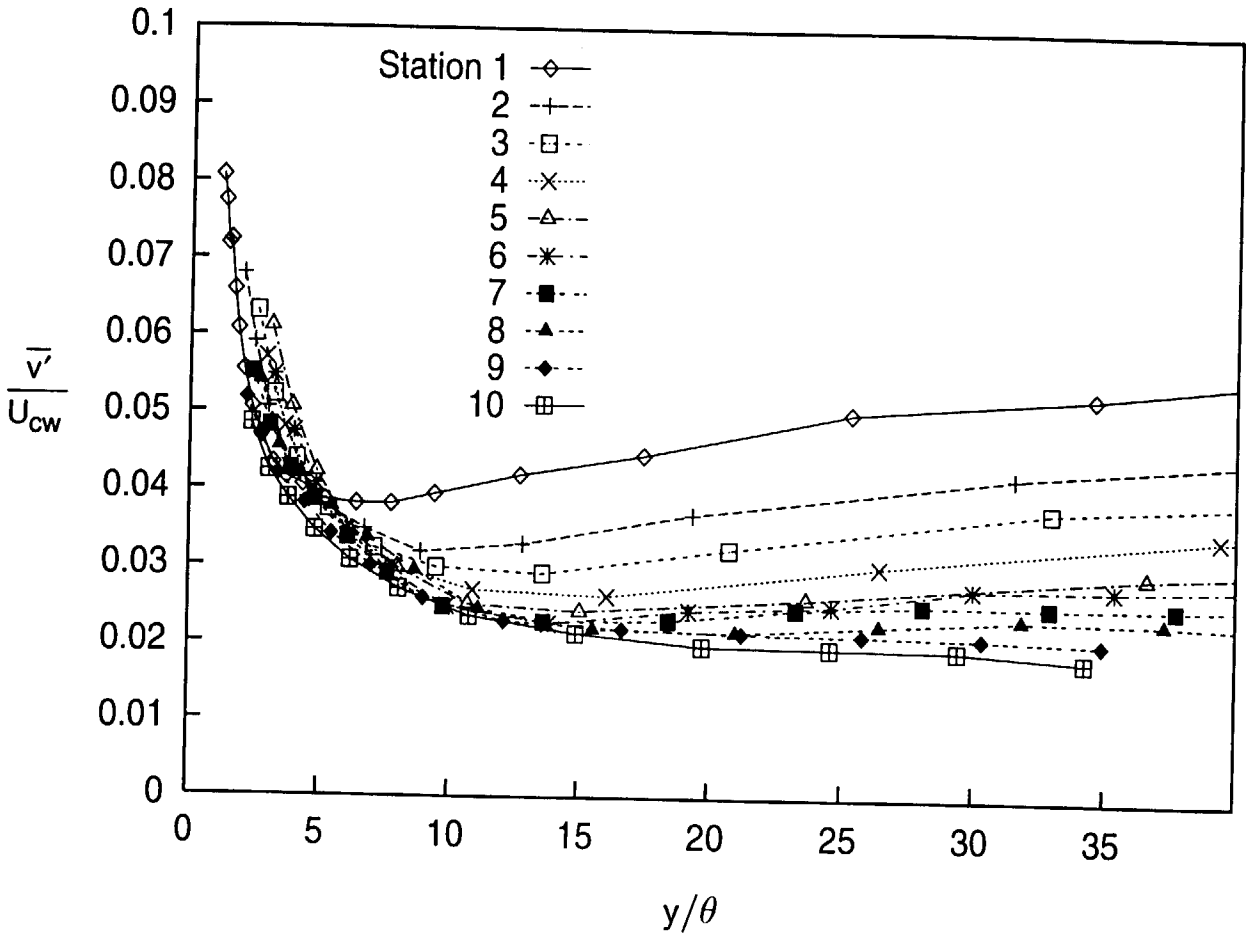

Fig. 6.19: Fluctuating Cross-stream Velocity Profiles dU_{cw}/dx=29 s^{-1} Case

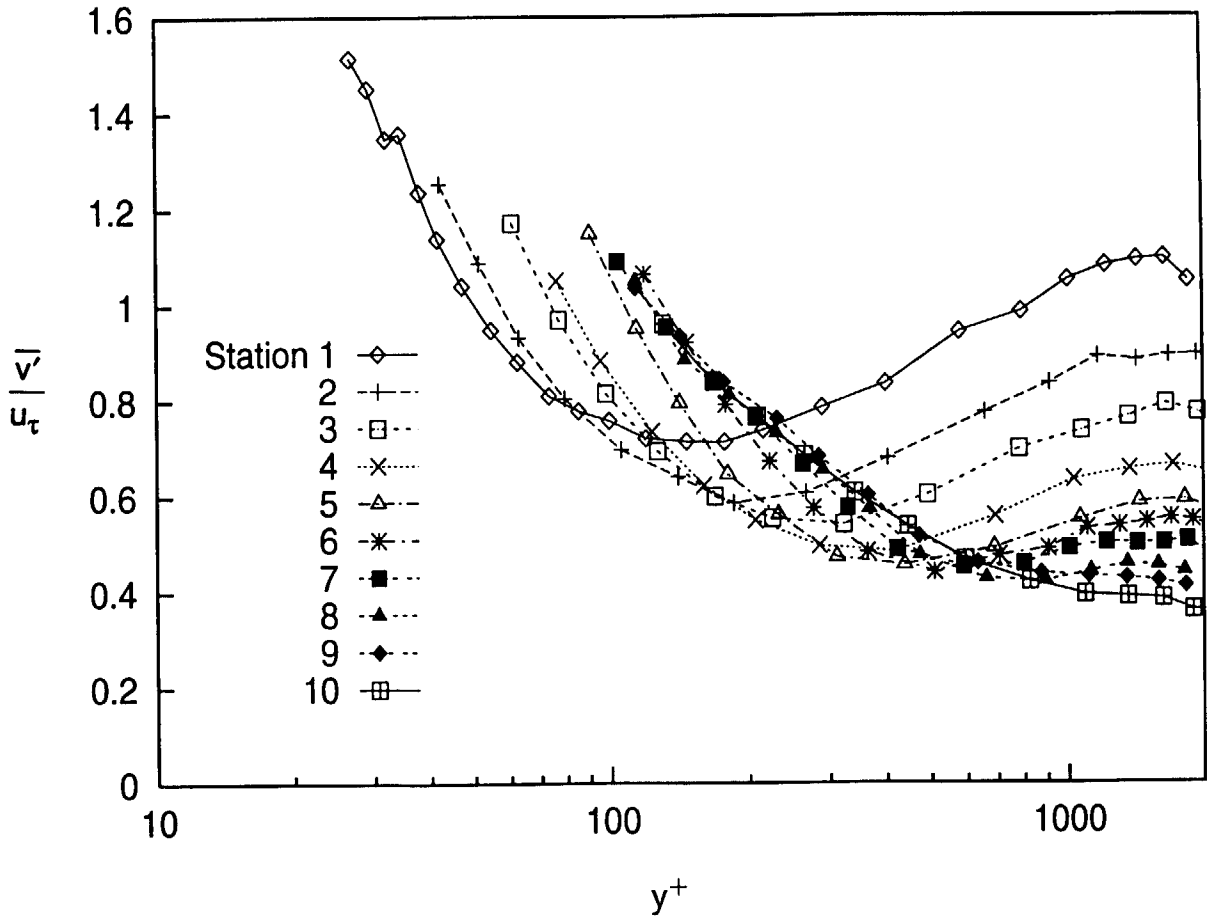

Fig. 6.20: Fluctuating Cross-stream Velocity Profiles, Wall Coordinates $dU_{cw}/dx=29\ s^{-1}$ Case

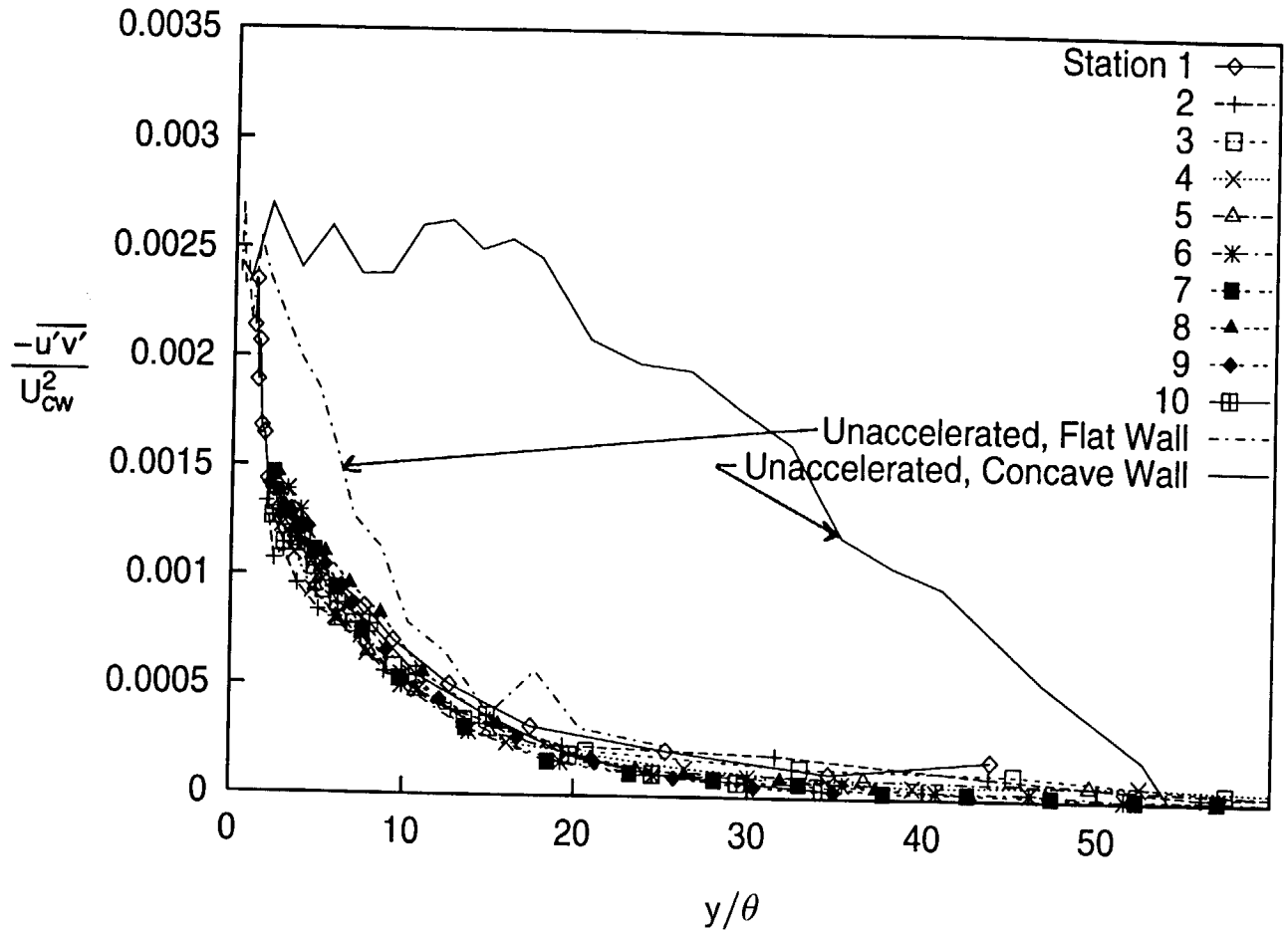

Fig. 6.21: Turbulent Shear Stress Profiles
dU_{cw}/dx=29 s^{-1} Case

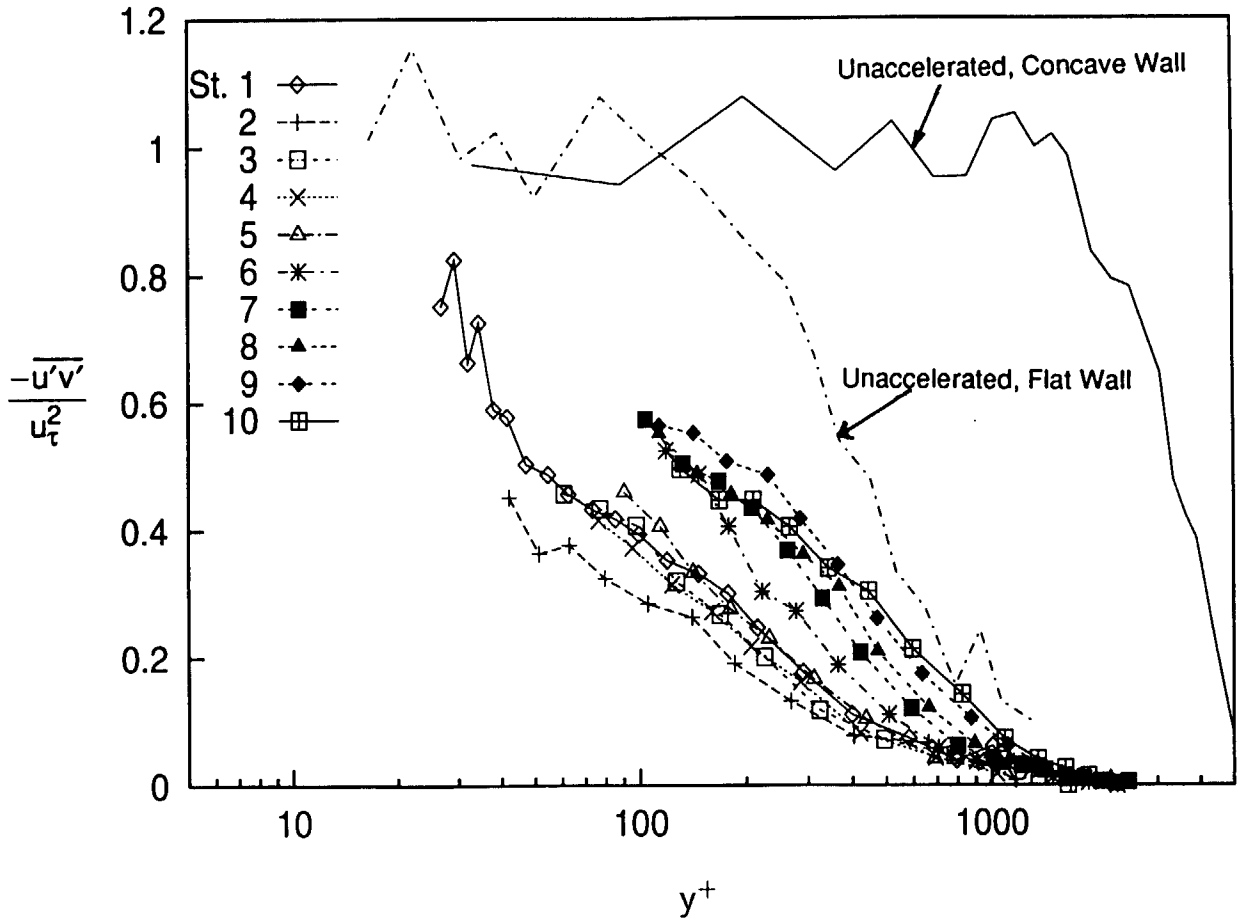

Fig. 6.22: Turbulent Shear Stress Profiles, Wall Coordinates $dU_{cw}/dx=29\ s^{-1}$ Case

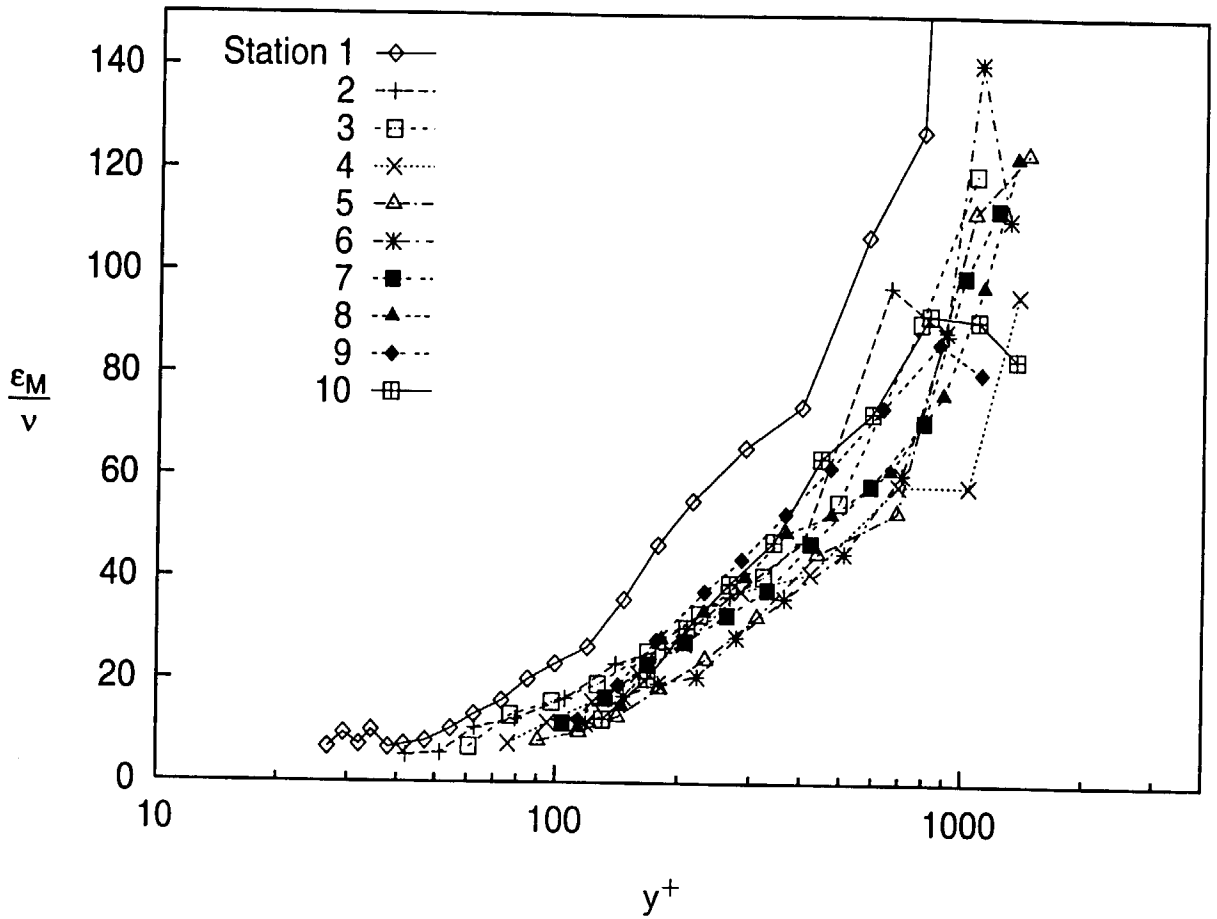

Fig. 6.23: Eddy Viscosity Profiles
dU_{cw}/dx=29 s^{-1} Case

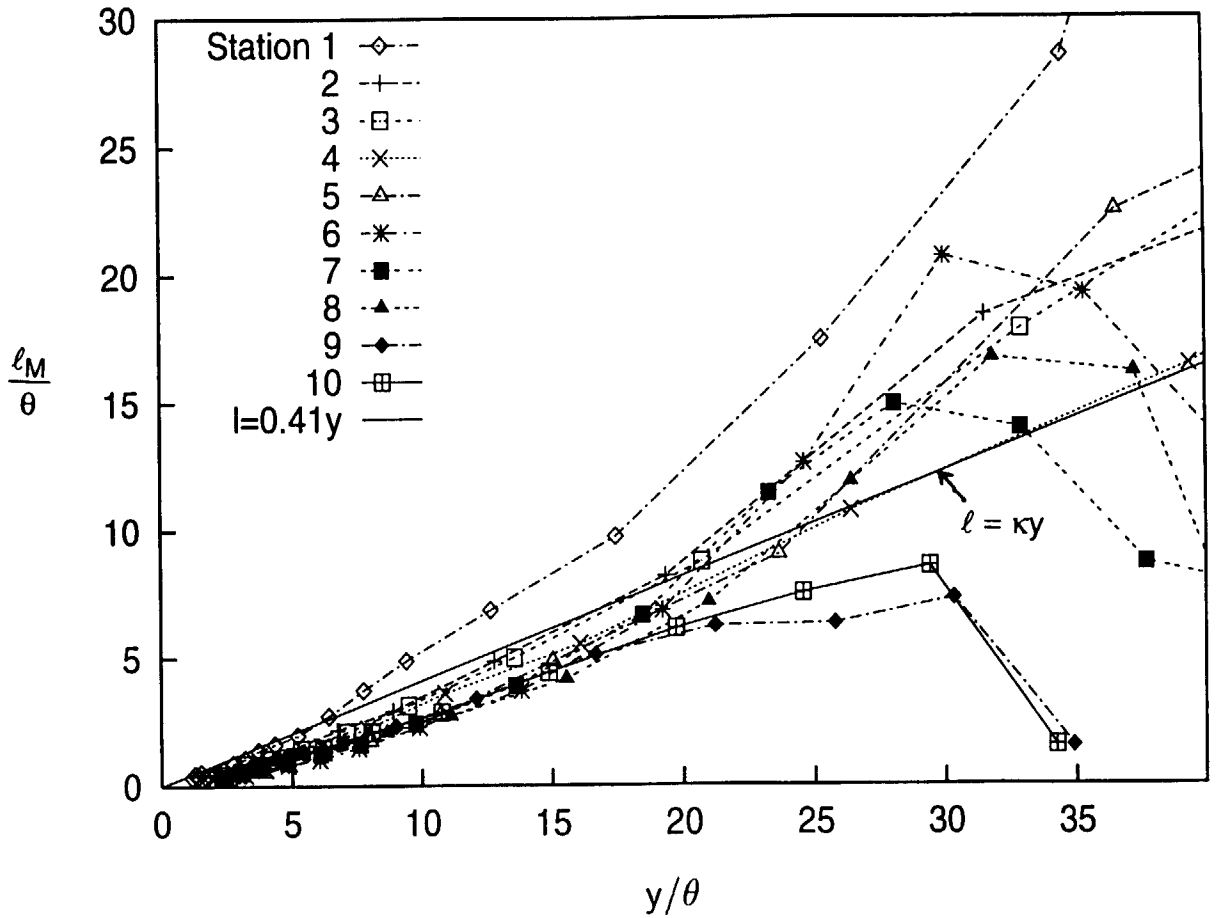

Fig. 6.24: Mixing Length of Momentum Profiles dU_{cw}/dx=29 s^{-1} Case

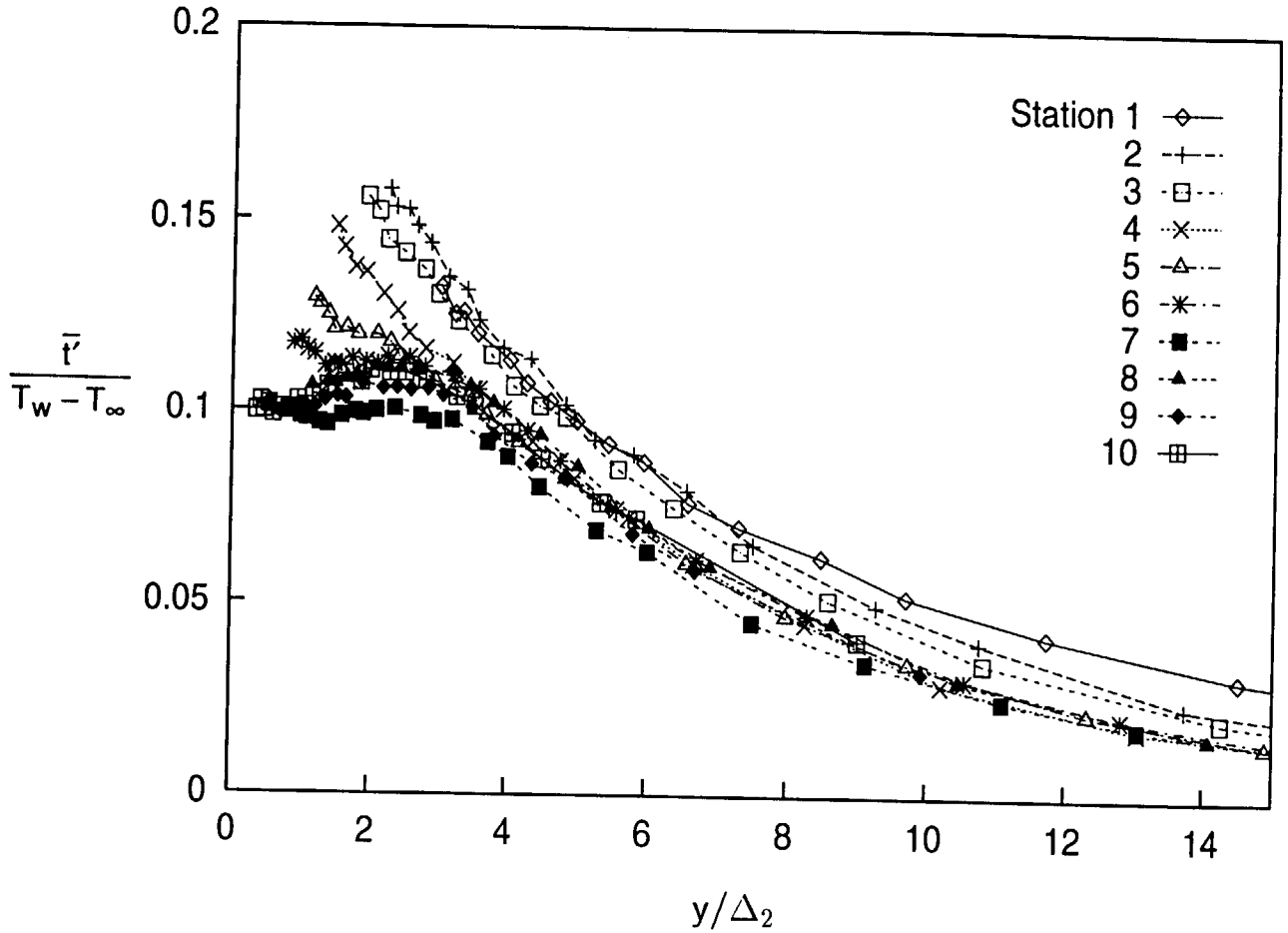

Fig. 6.25: Fluctuating Temperature Profiles dU_{cw}/dx=29 s^{-1} Case

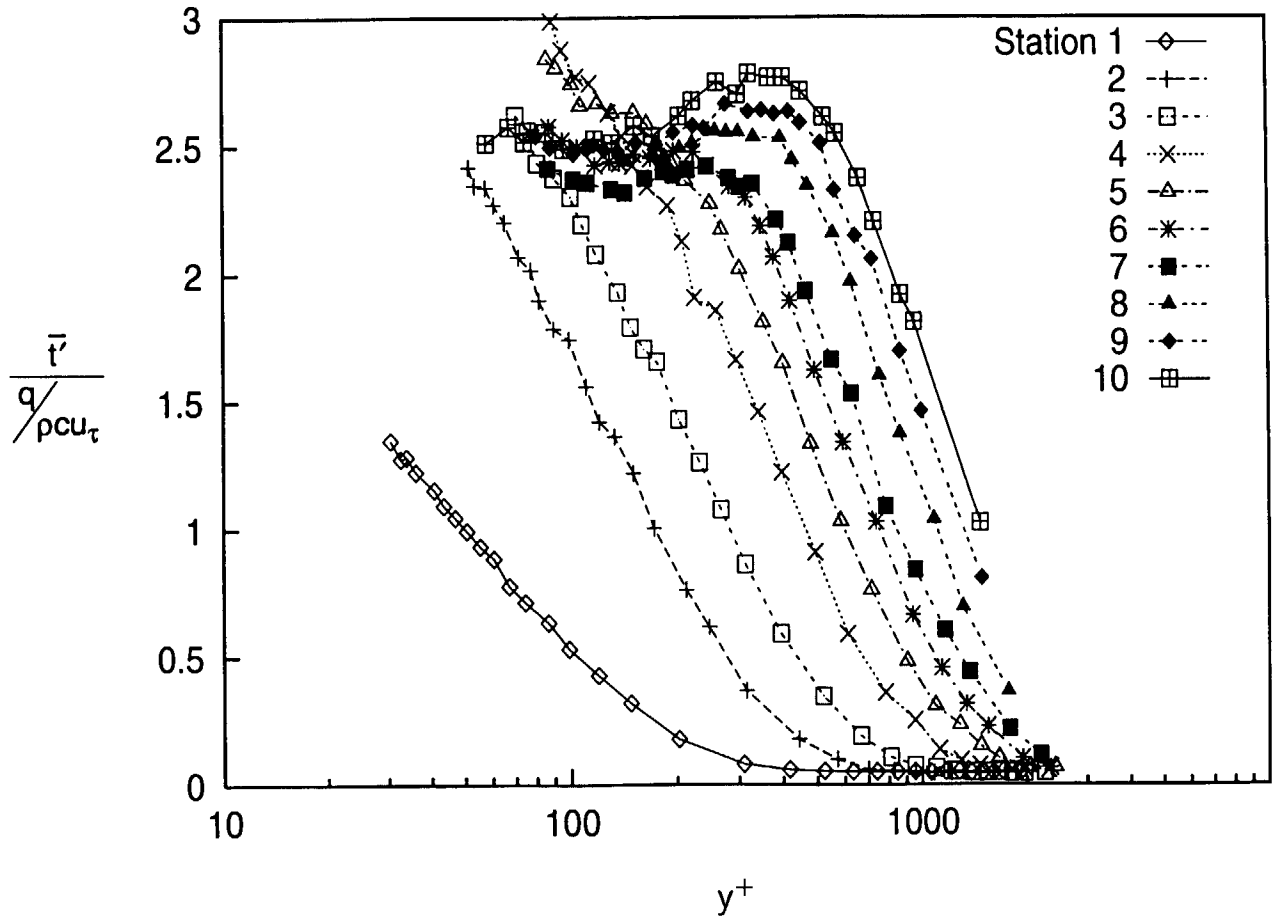

Fig. 6.26: Fluctuating Temperature Profiles, Wall Coordinates dU_{cw}/dx=29 s^{-1} Case

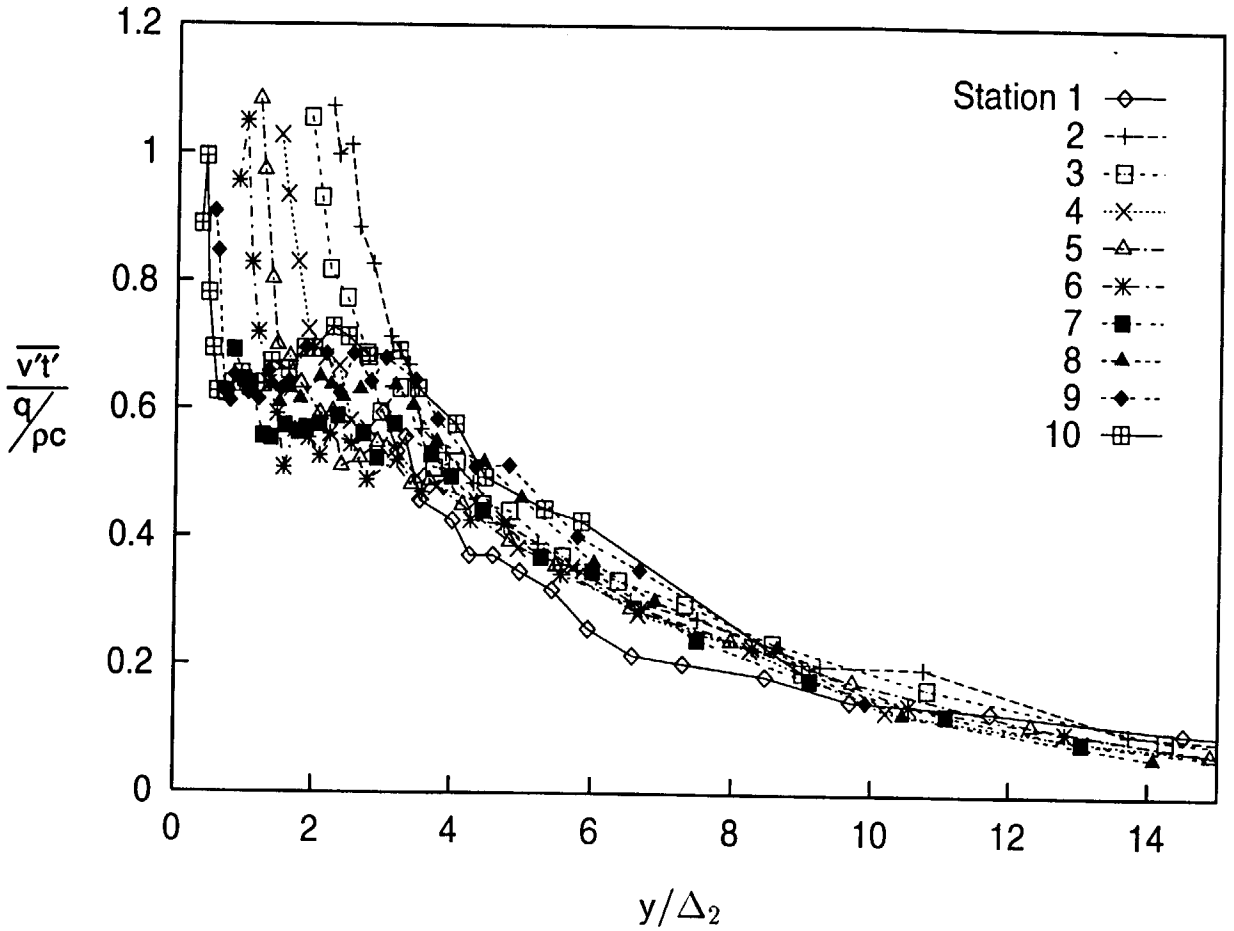

Fig. 6.27: Normal Component of Turbulent Heat Flux Profiles $dU_{cw}/dx=29\ s^{-1}$ Case

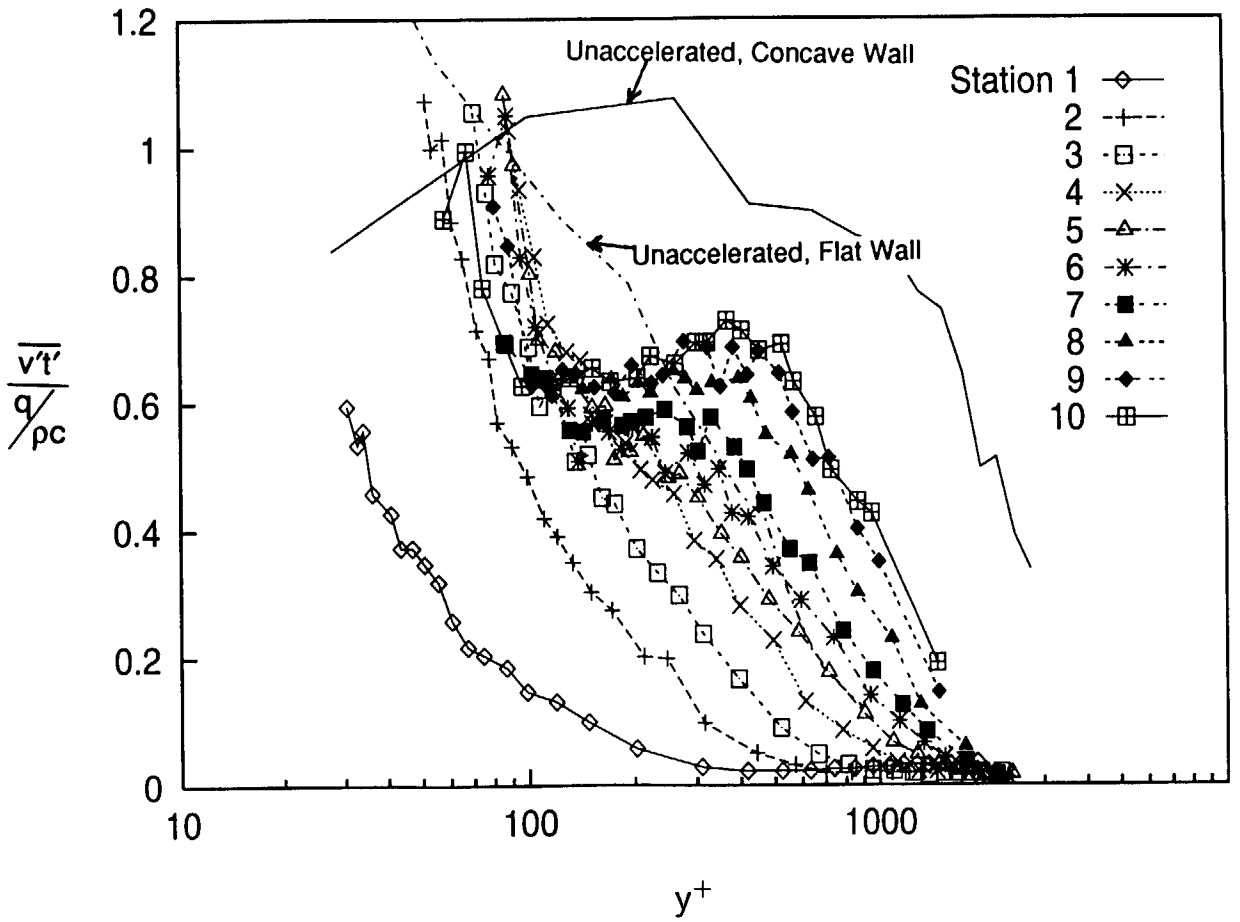

Fig. 6.28: Normal Component of Turbulent Heat Flux Profiles, Wall Coordinates, dU_{cw}/dx=29 s^{-1} Case

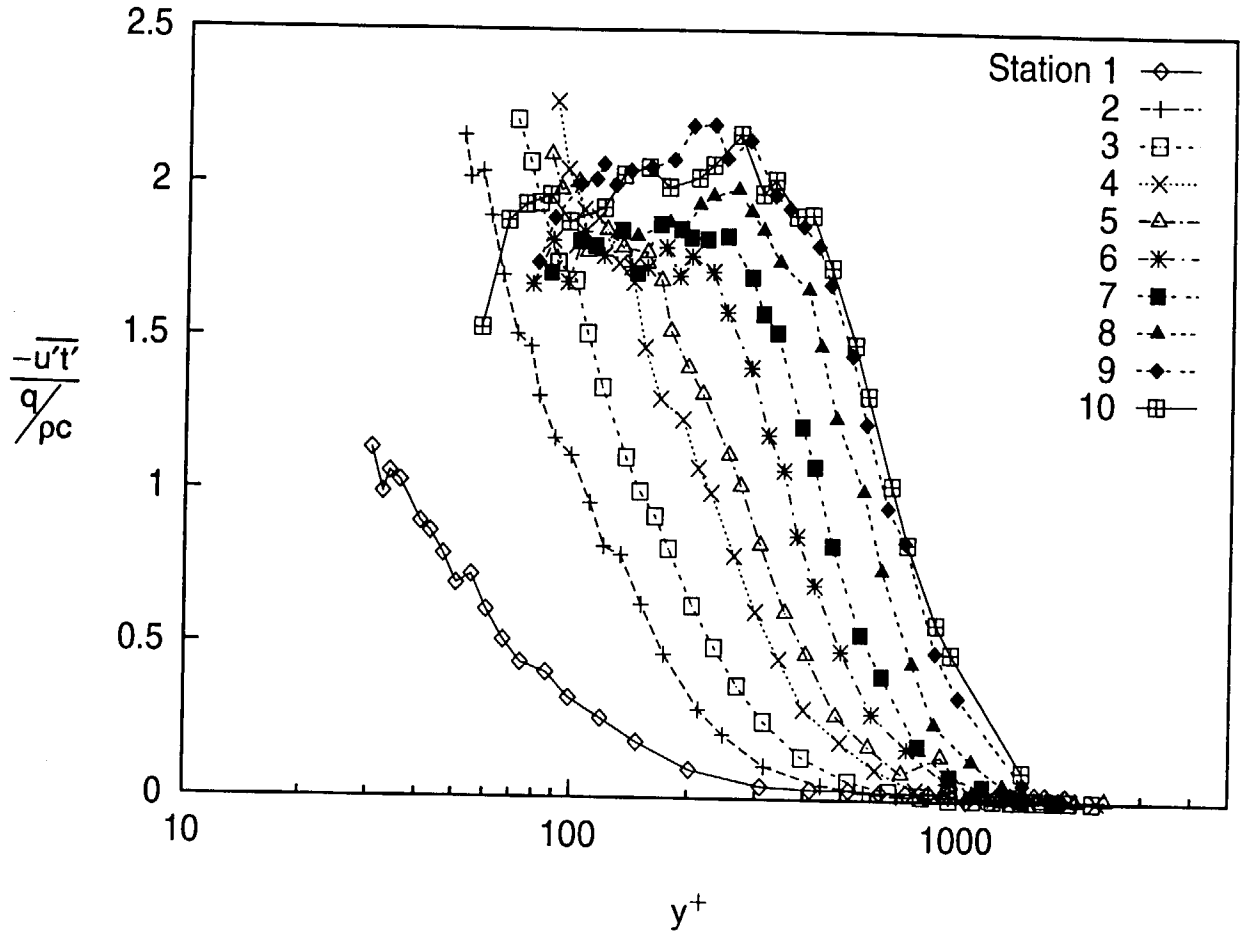

Fig. 6.29: Streamwise Component of Turbulent Heat Flux Profiles, Wall Coordinates, dU_{cw}/dx=29 s^{-1} Case

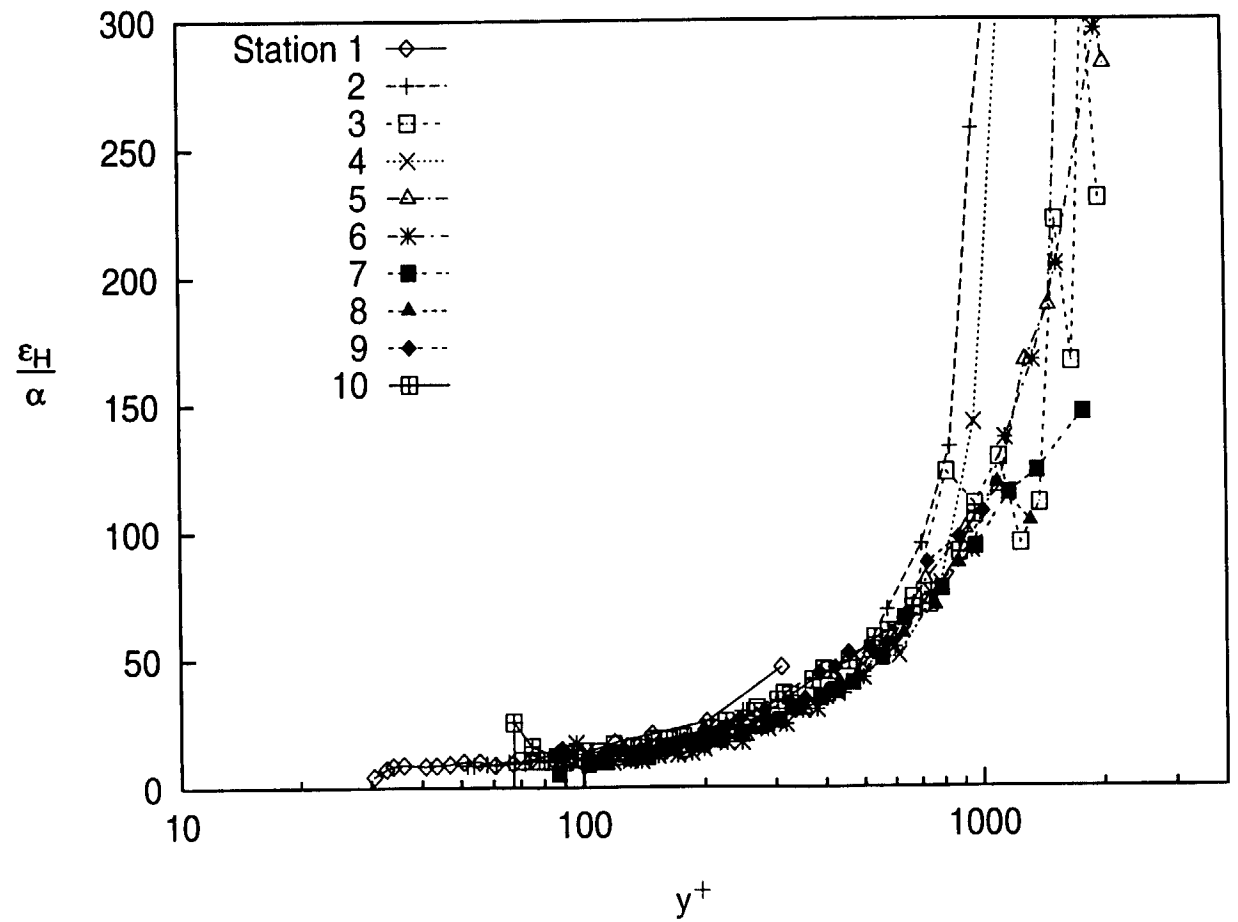

Fig. 6.30: Eddy Diffusivity of Heat Profiles dU_{cw}/dx=29 s^{-1} Case

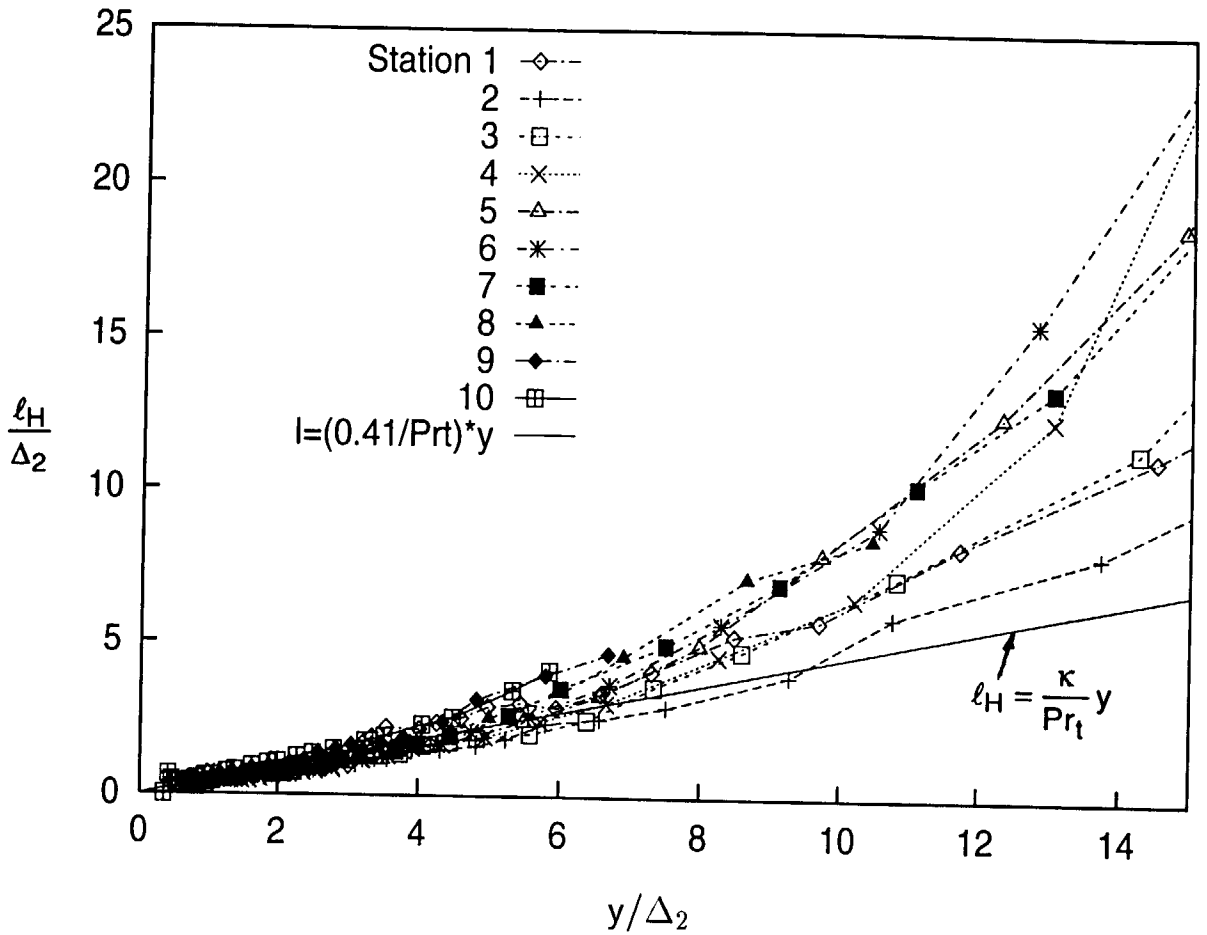

Fig. 6.31: Mixing Length of Heat Profiles $dU_{cw}/dx=29\ s^{-1}$ Case

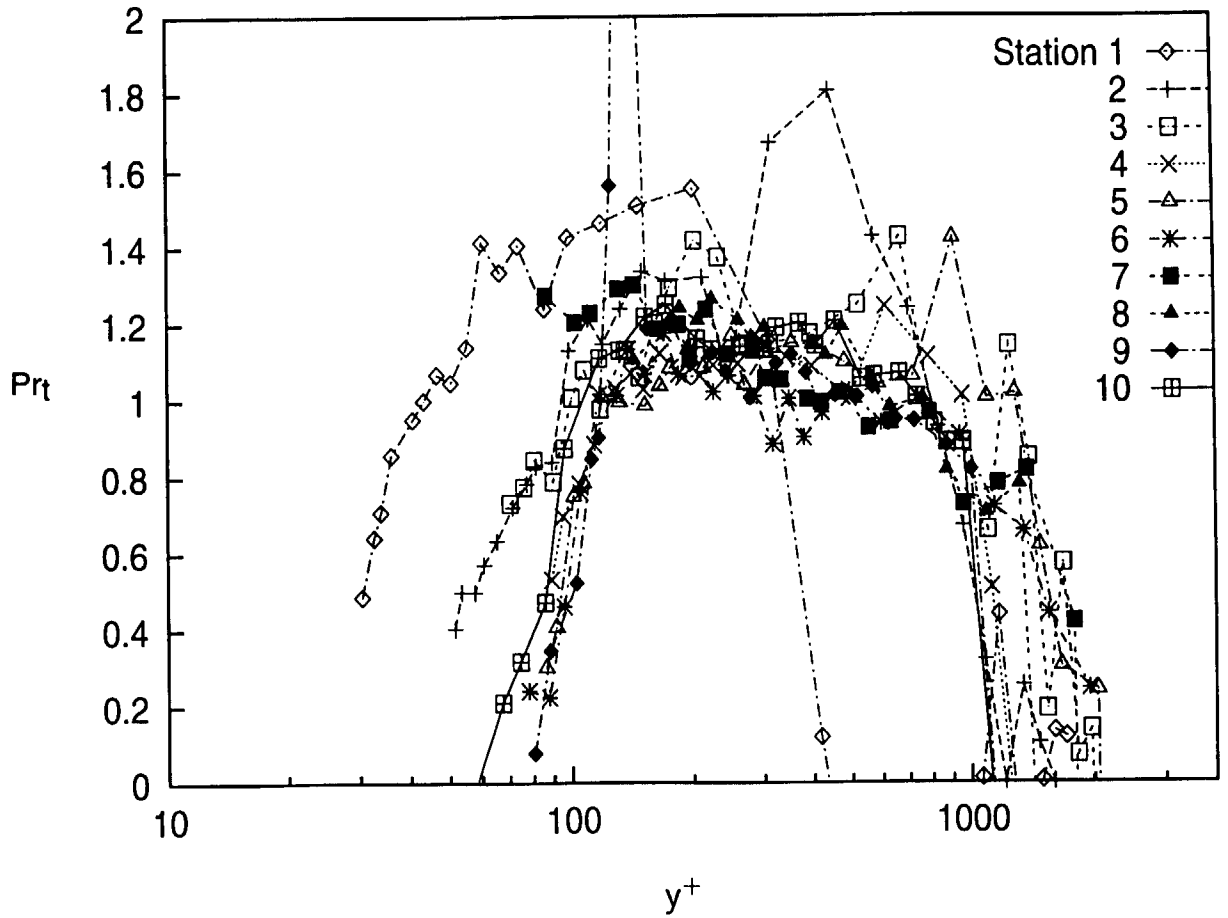

Fig. 6.32: Turbulent Prandtl Number Profiles
dU_{cw}/dx=29 s^{-1} Case

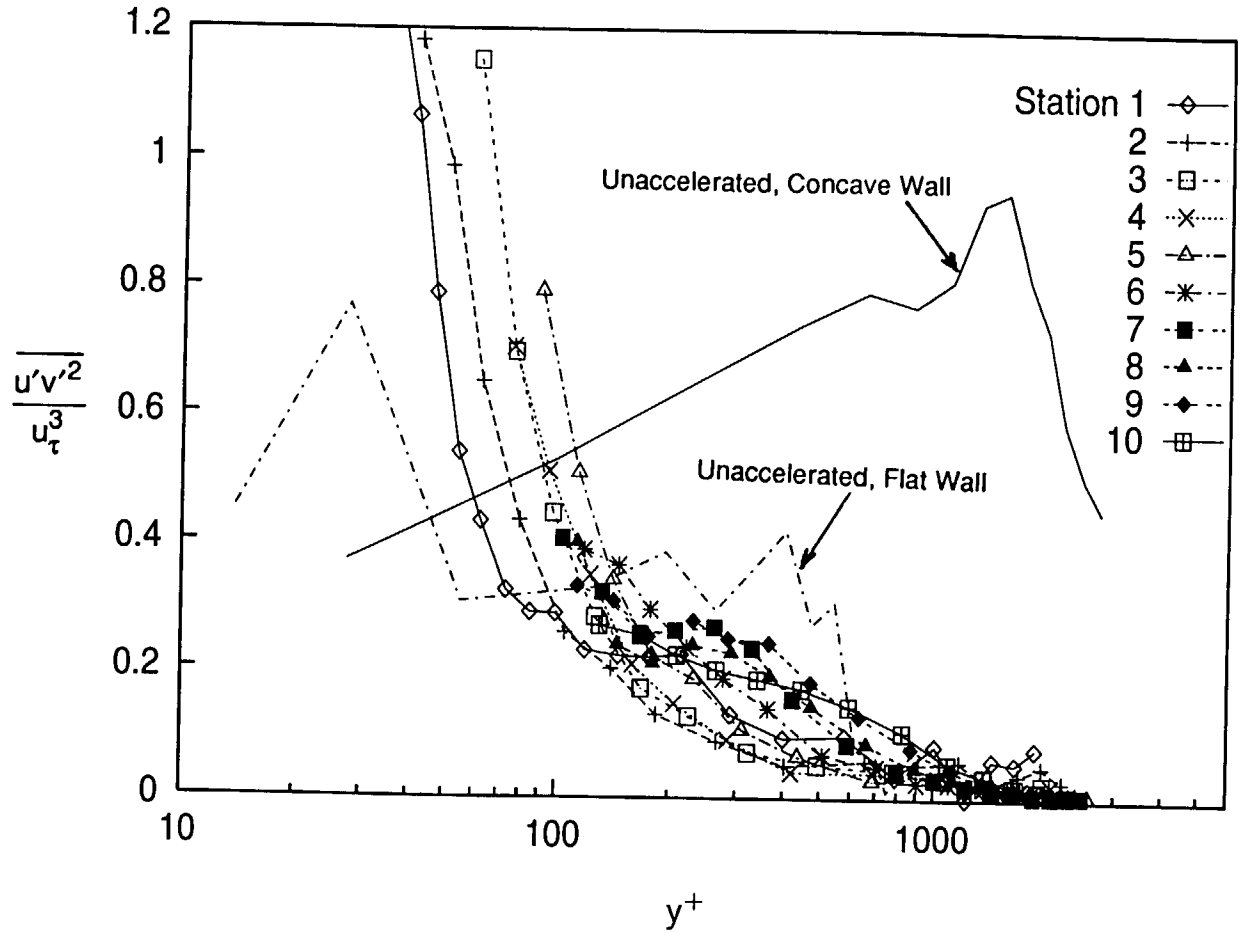

Fig. 6.33: Cross Transport of Turbulent Shear Stress Profiles dU_{cw}/dx=29 s^{-1} Case

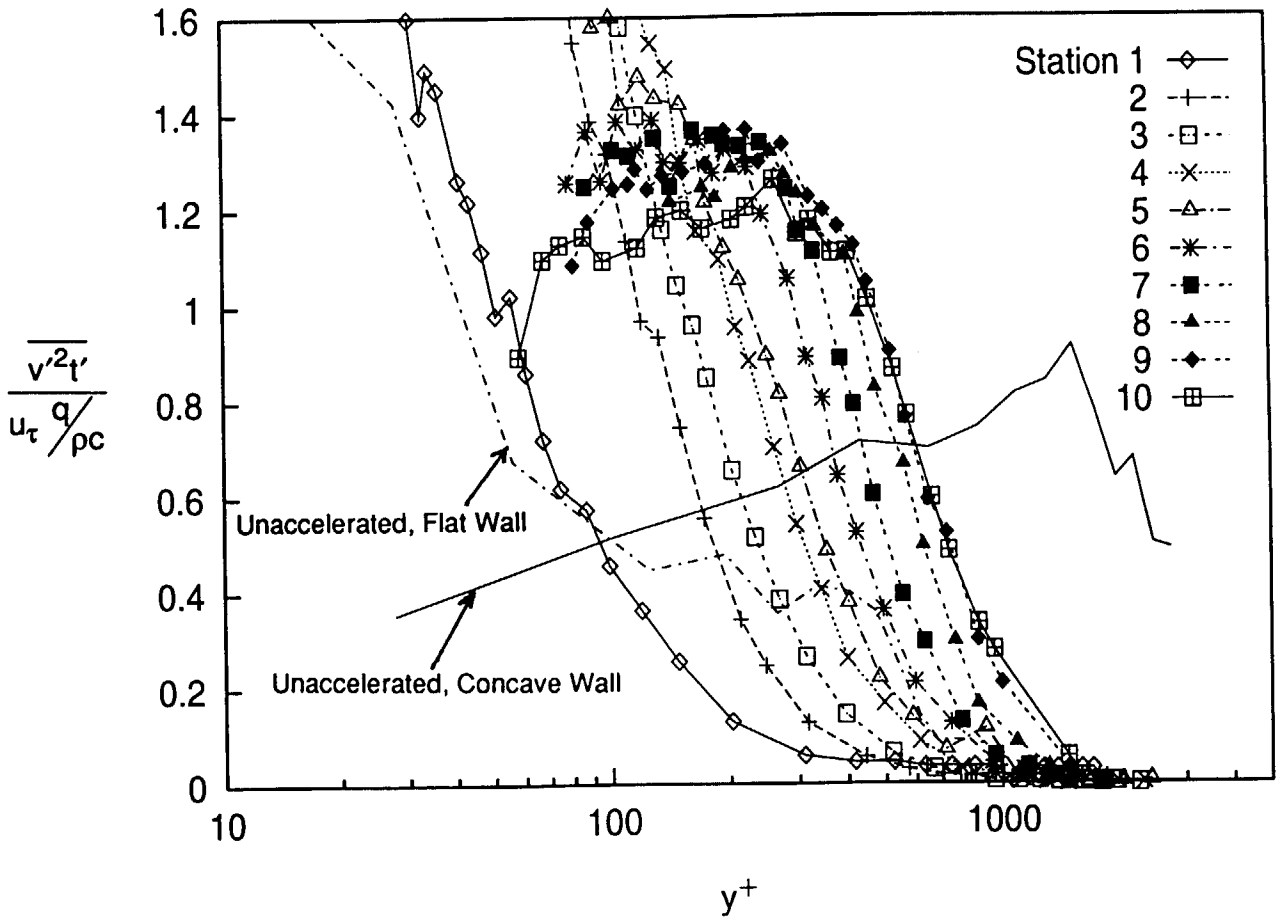

Fig. 6.34: Cross Transport of Turbulent Heat Flux Profiles dU_{cw}/dx=29 s^{-1} Case

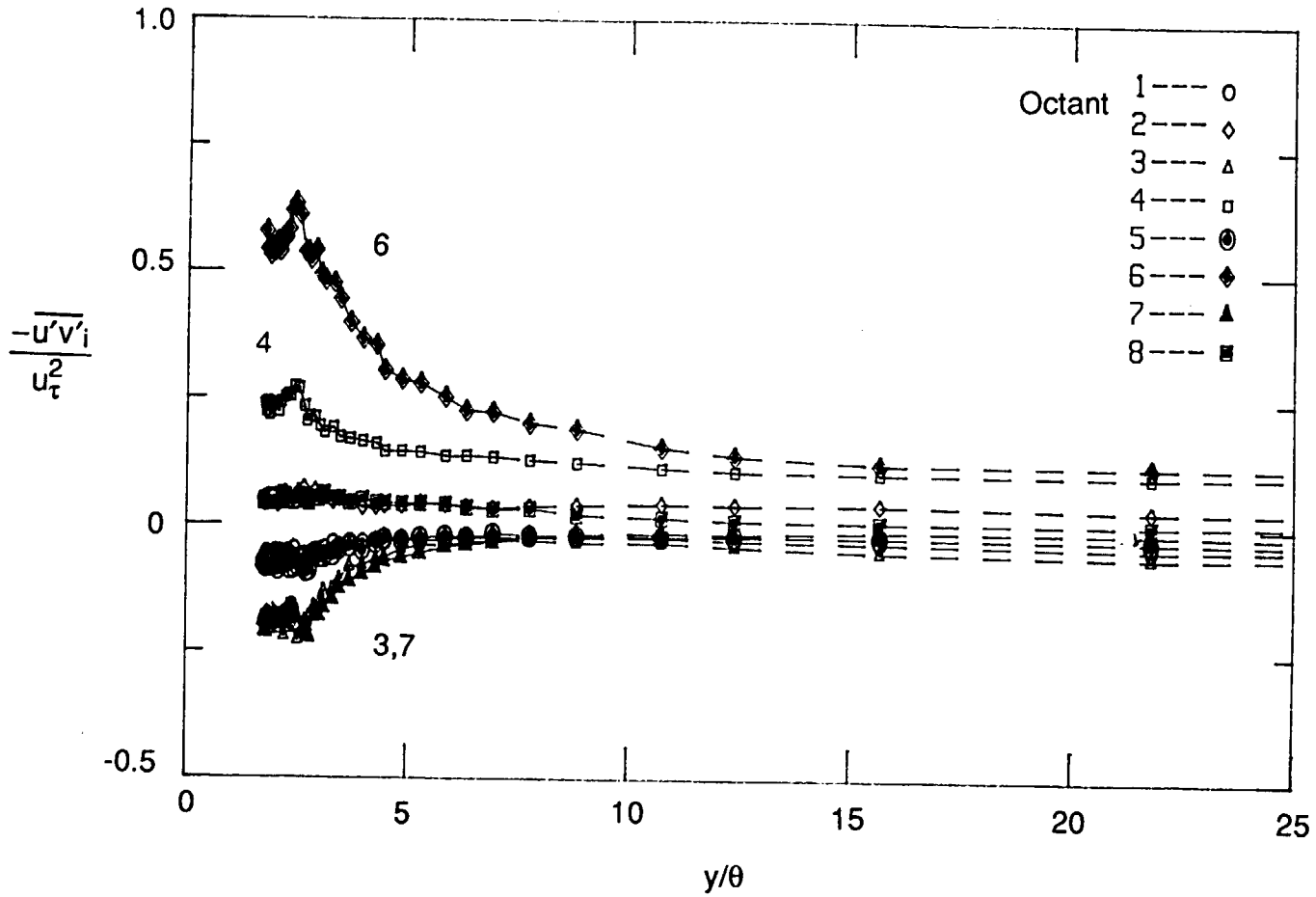

Fig. 6.35a: Octant Decomposition of Turbulent Shear Stress Station 2, $dU_{cw}/dx=29\ s^{-1}$ Case

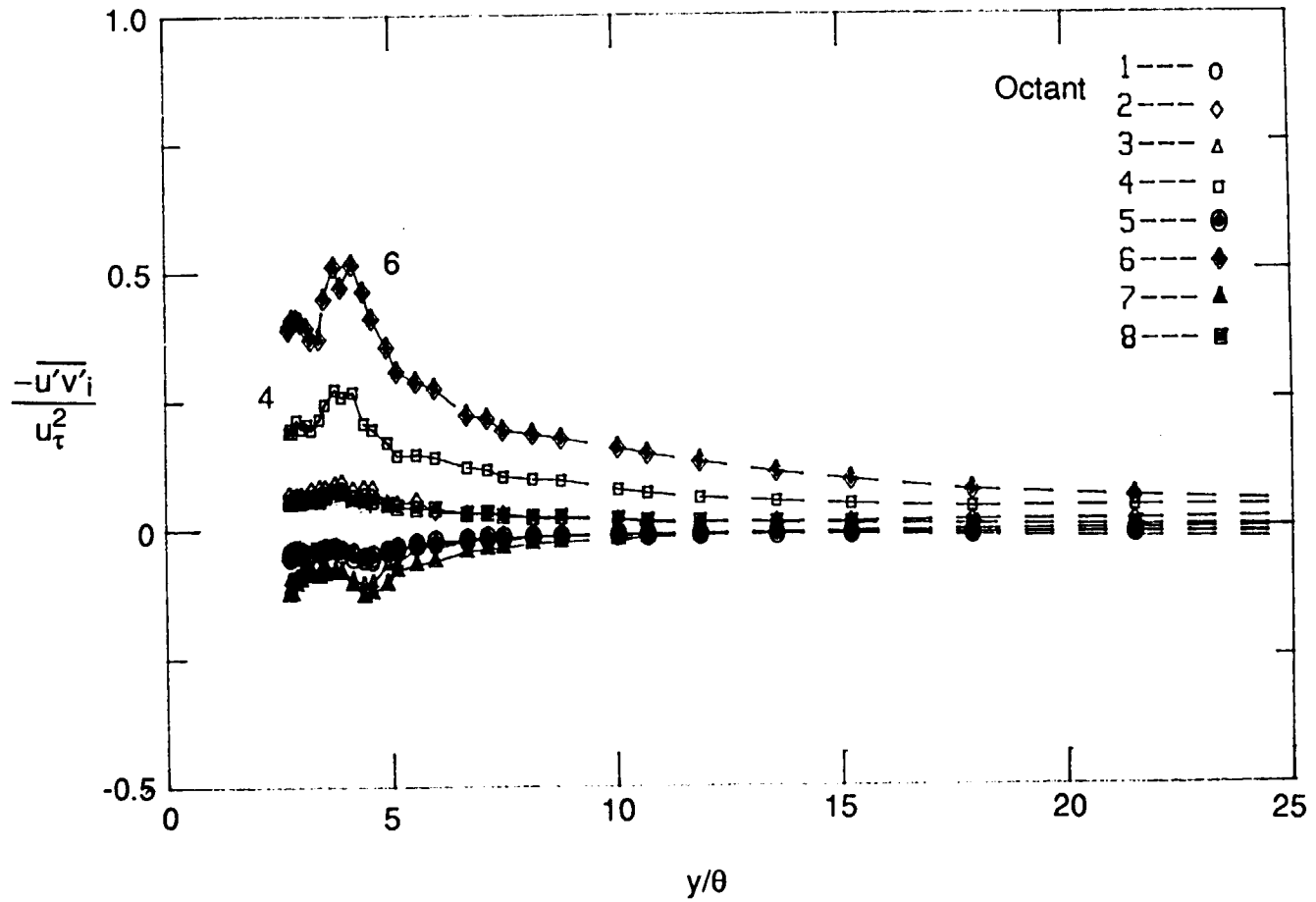

Fig. 6.35b: Octant Decomposition of Turbulent Shear Stress Station 5, $dU_{CW}/dx=29\ s^{-1}$ Case

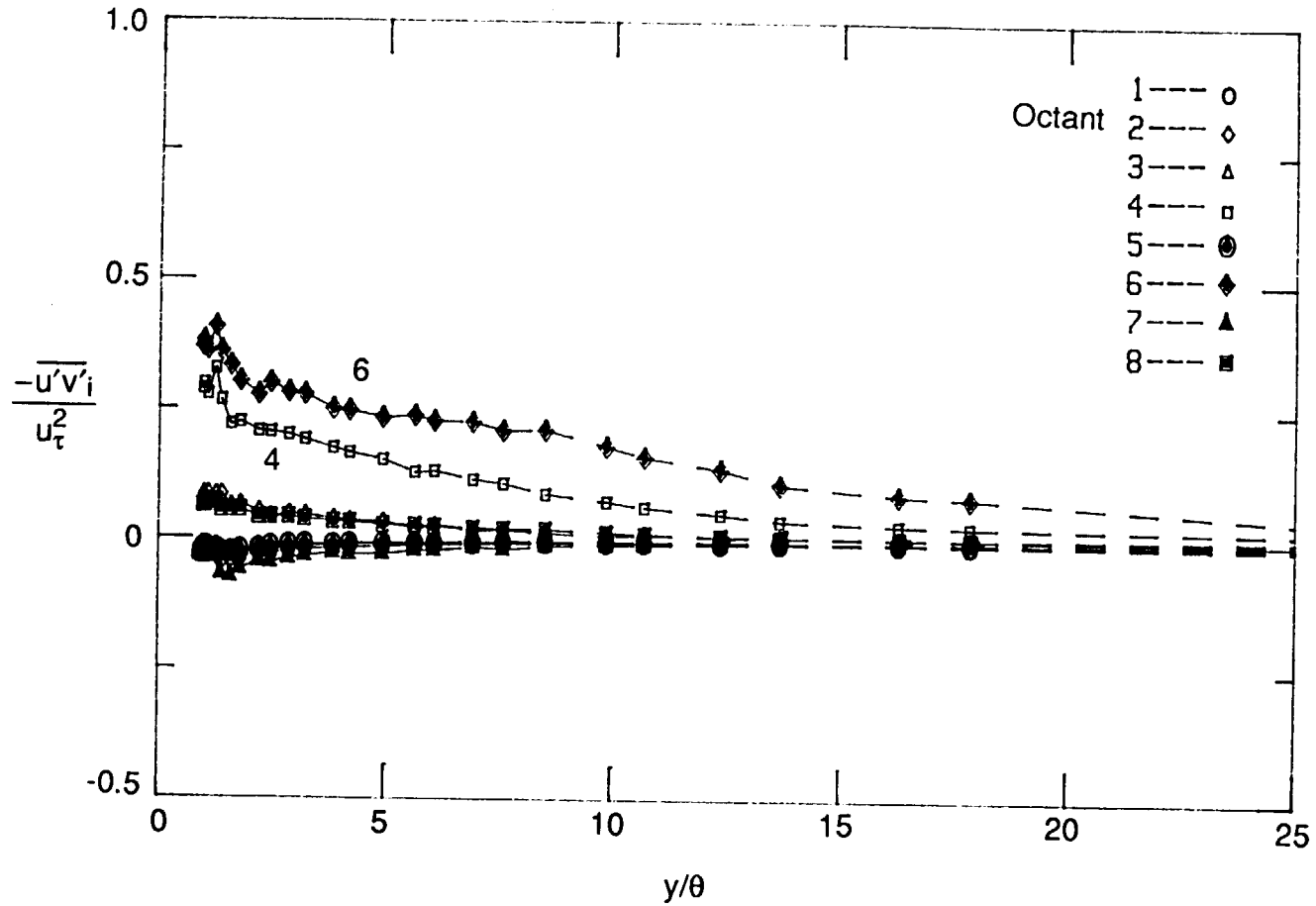

Fig. 6.35c: Octant Decomposition of Turbulent Shear Stress Station 10, $dU_{CW}/dx=29\ s^{-1}$ Case

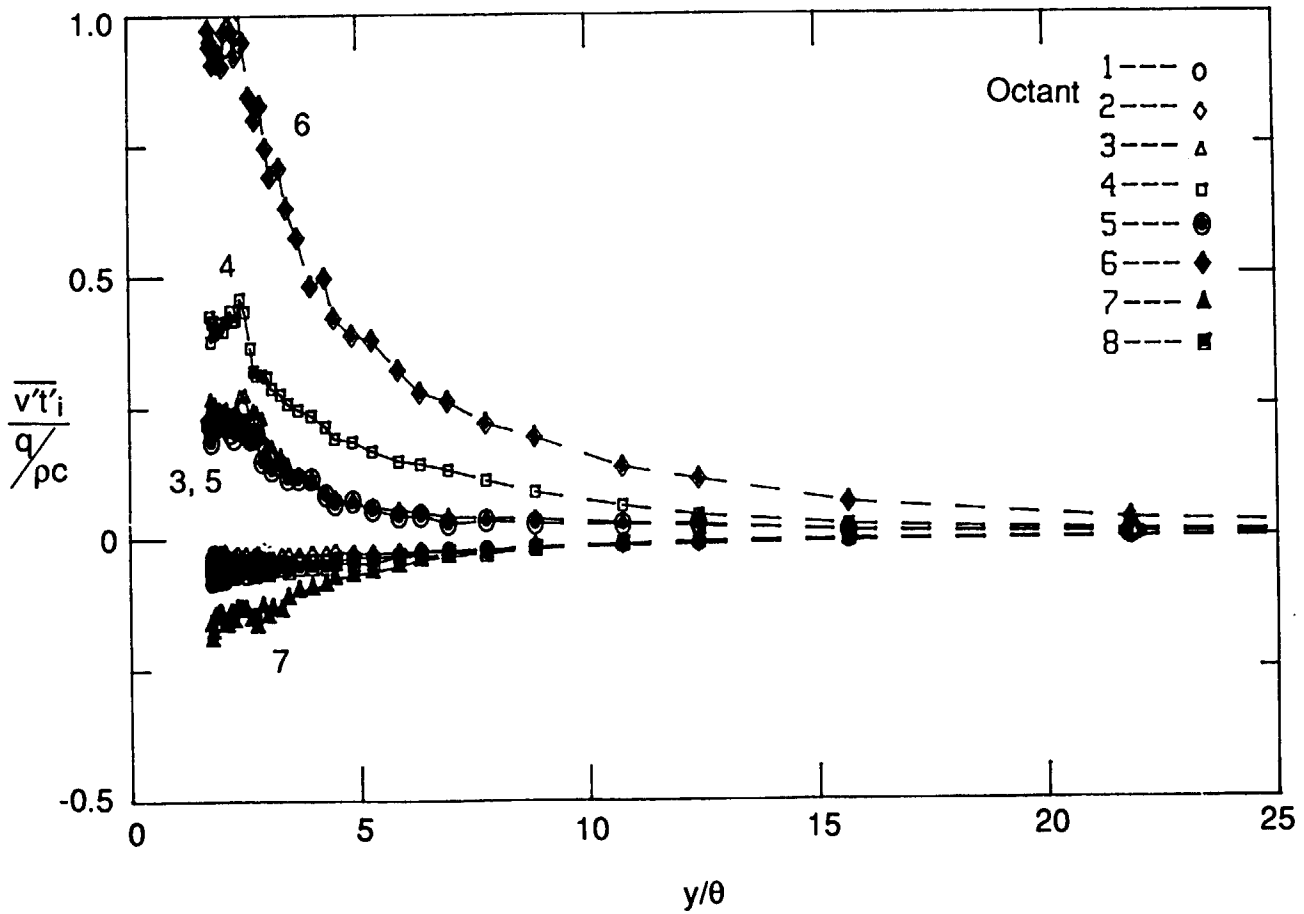

Fig. 6.36a: Octant Decomposition of Turbulent Heat Flux Station 2, $dU_{cw}/dx=29\ s^{-1}$ Case

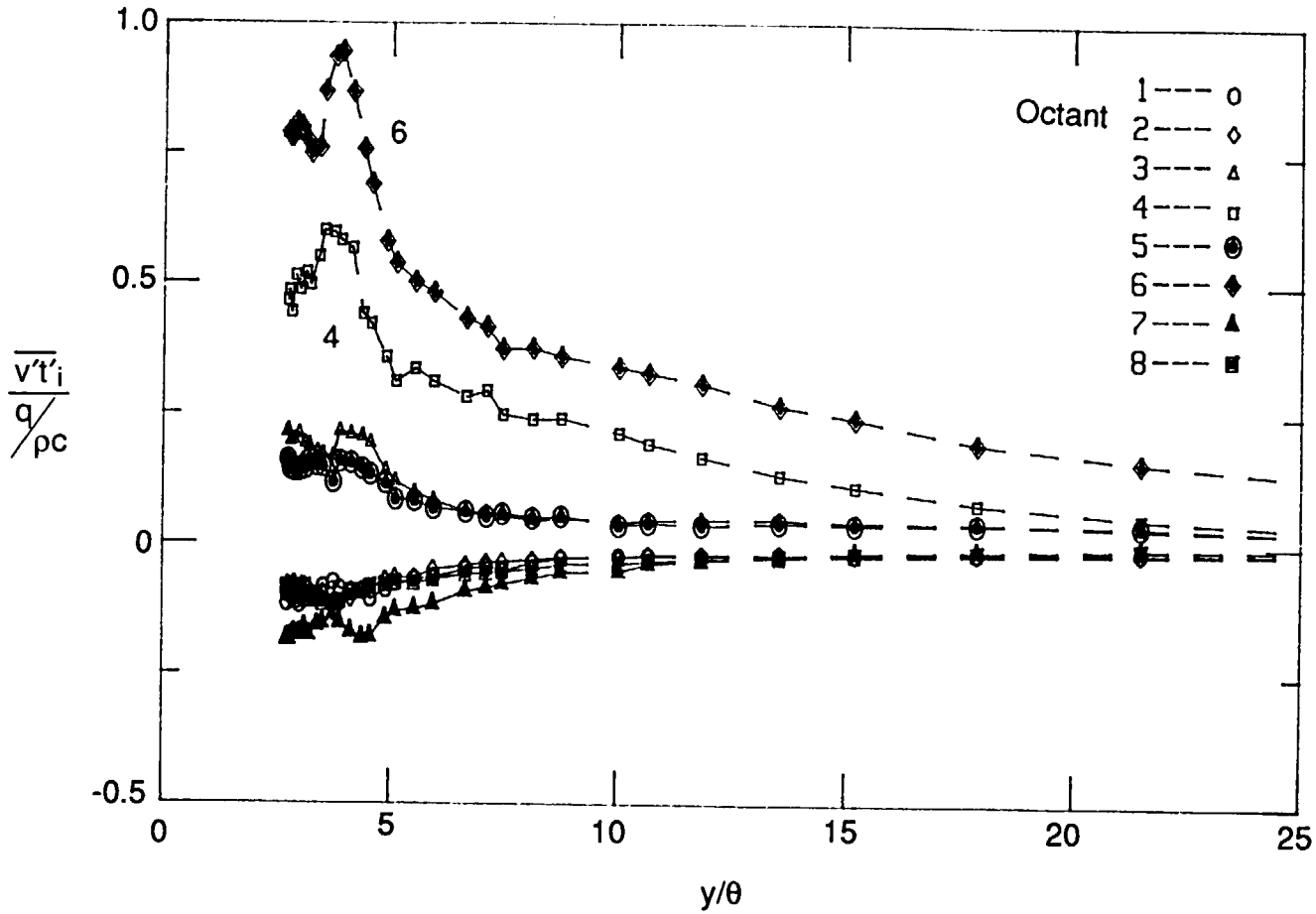

Fig. 6.36b: Octant Decomposition of Turbulent Heat Flux Station 5, $dU_{cw}/dx=29\ s^{-1}$ Case

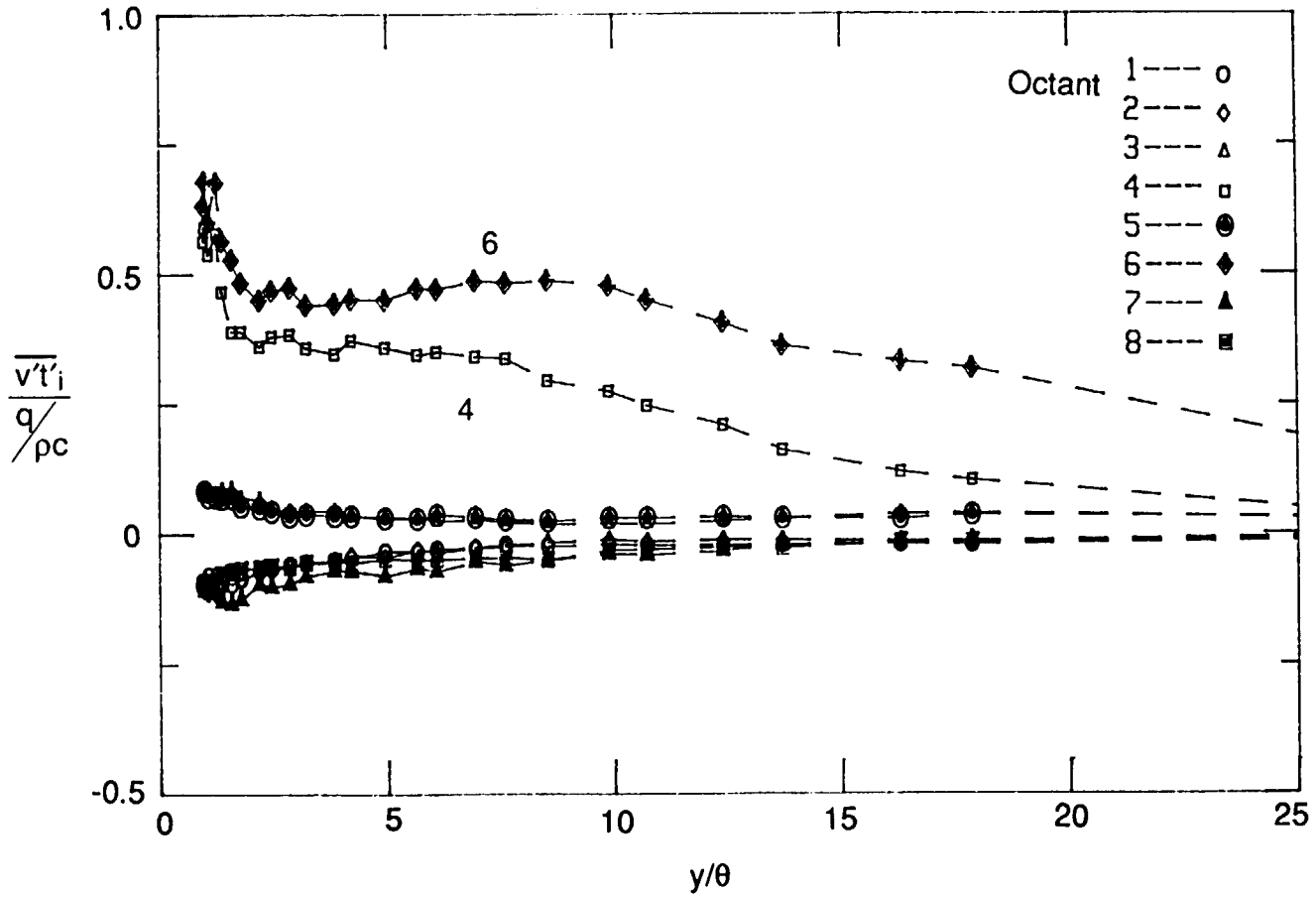

Fig. 6.36c: Octant Decomposition of Turbulent Heat Flux Station 10, $dU_{CW}/dx=29\ s^{-1}$ Case

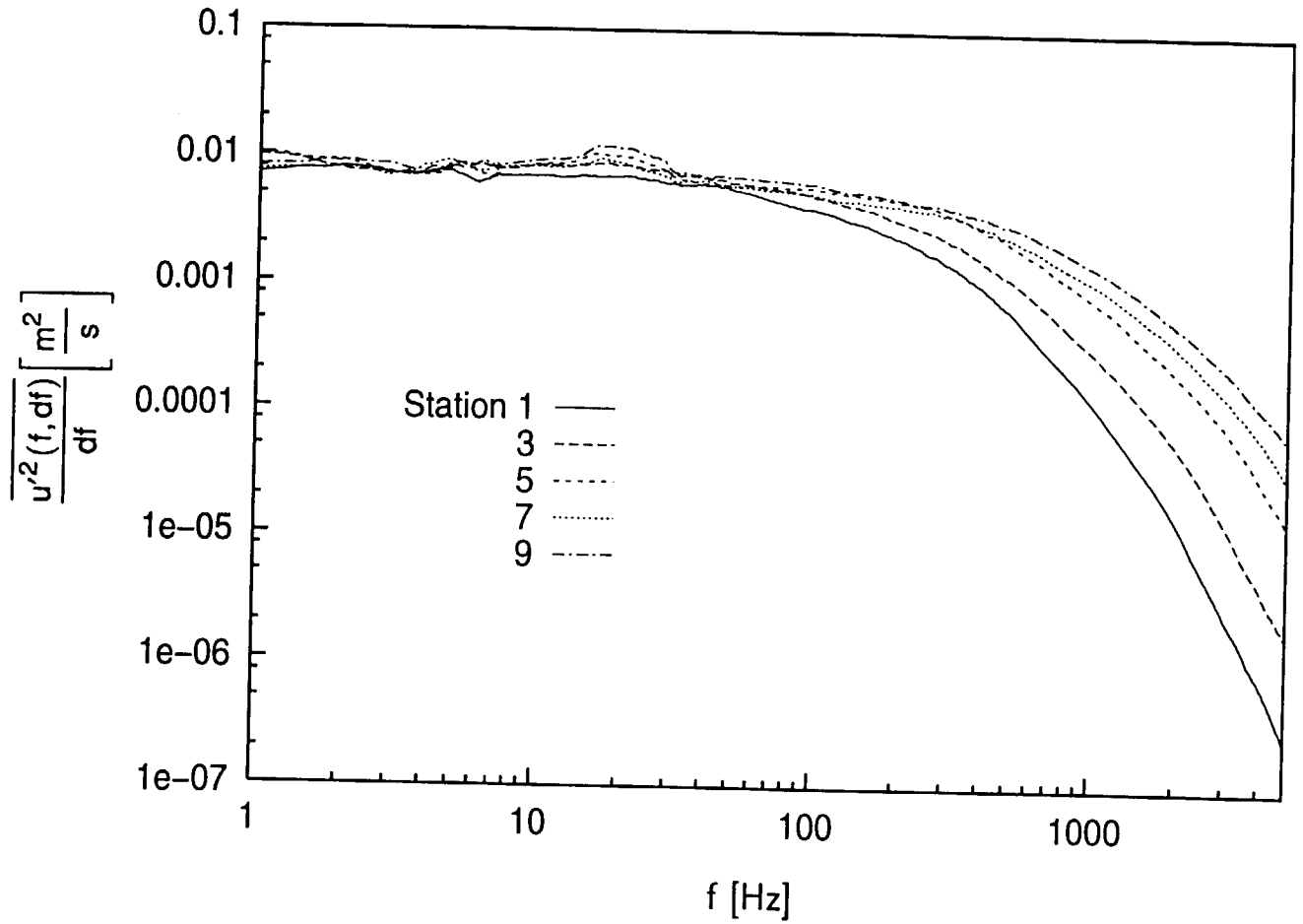

Fig. 6.37a: Boundary Layer u' Spectra at y^+=5 dU_{cw}/dx=29 s^{-1} Case

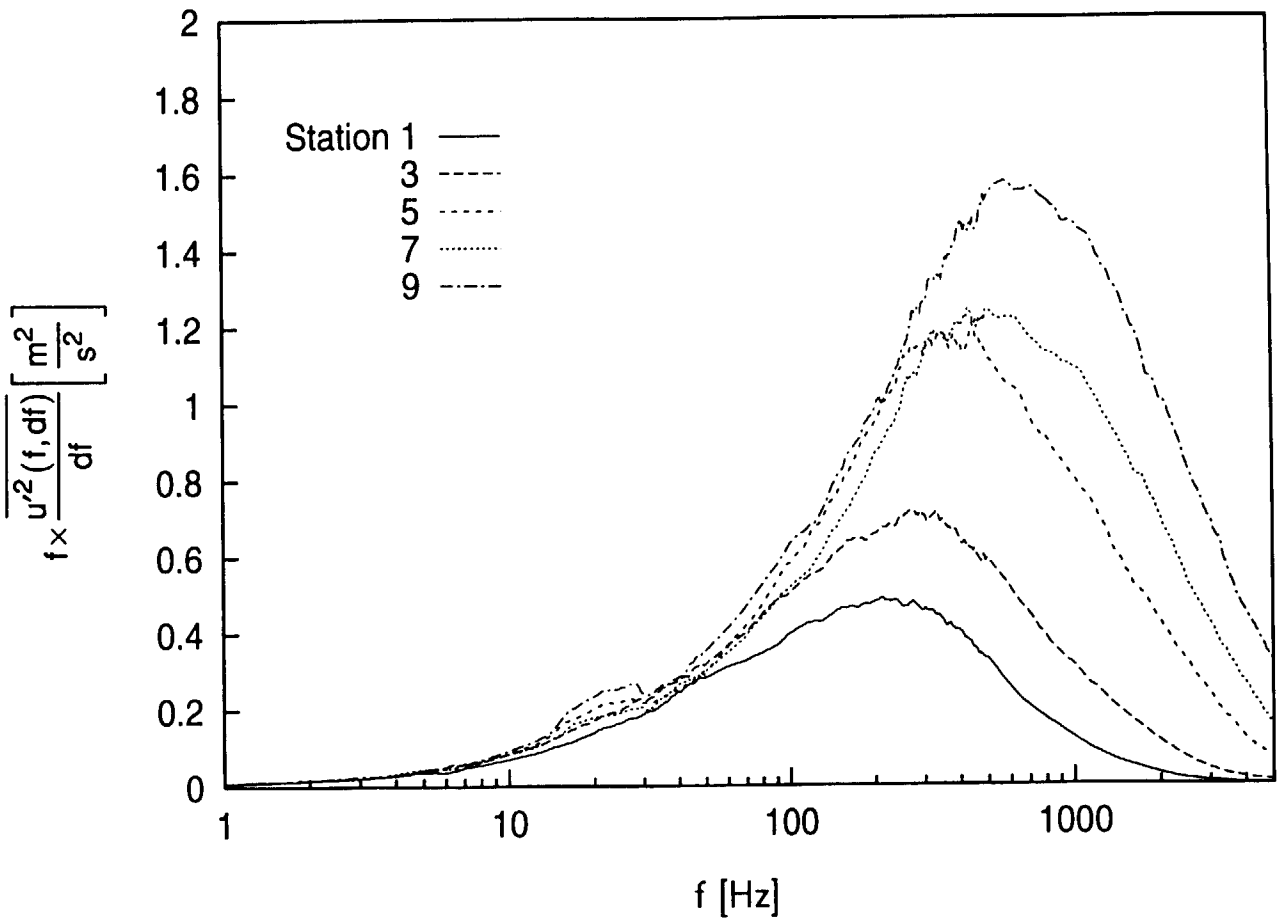

Fig. 6.37b: Boundary Layer u' Spectra at y^+=5, Energy Coordinates, dU_{cw}/dx=29 s^{-1} Case

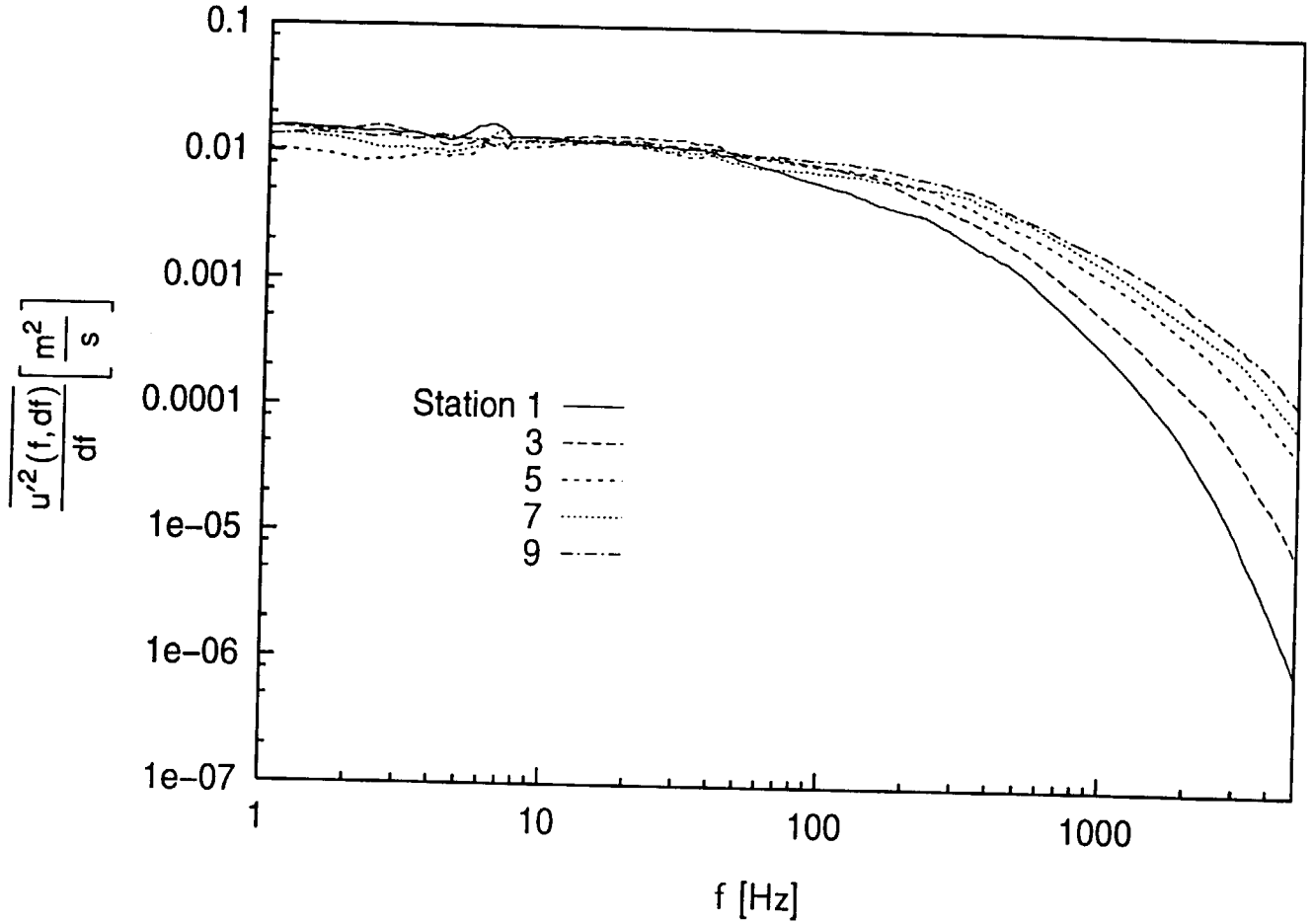

Fig. 6.38a: Boundary Layer u' Spectra at y^+=17 dU_{cw}/dx=29 s^{-1} Case

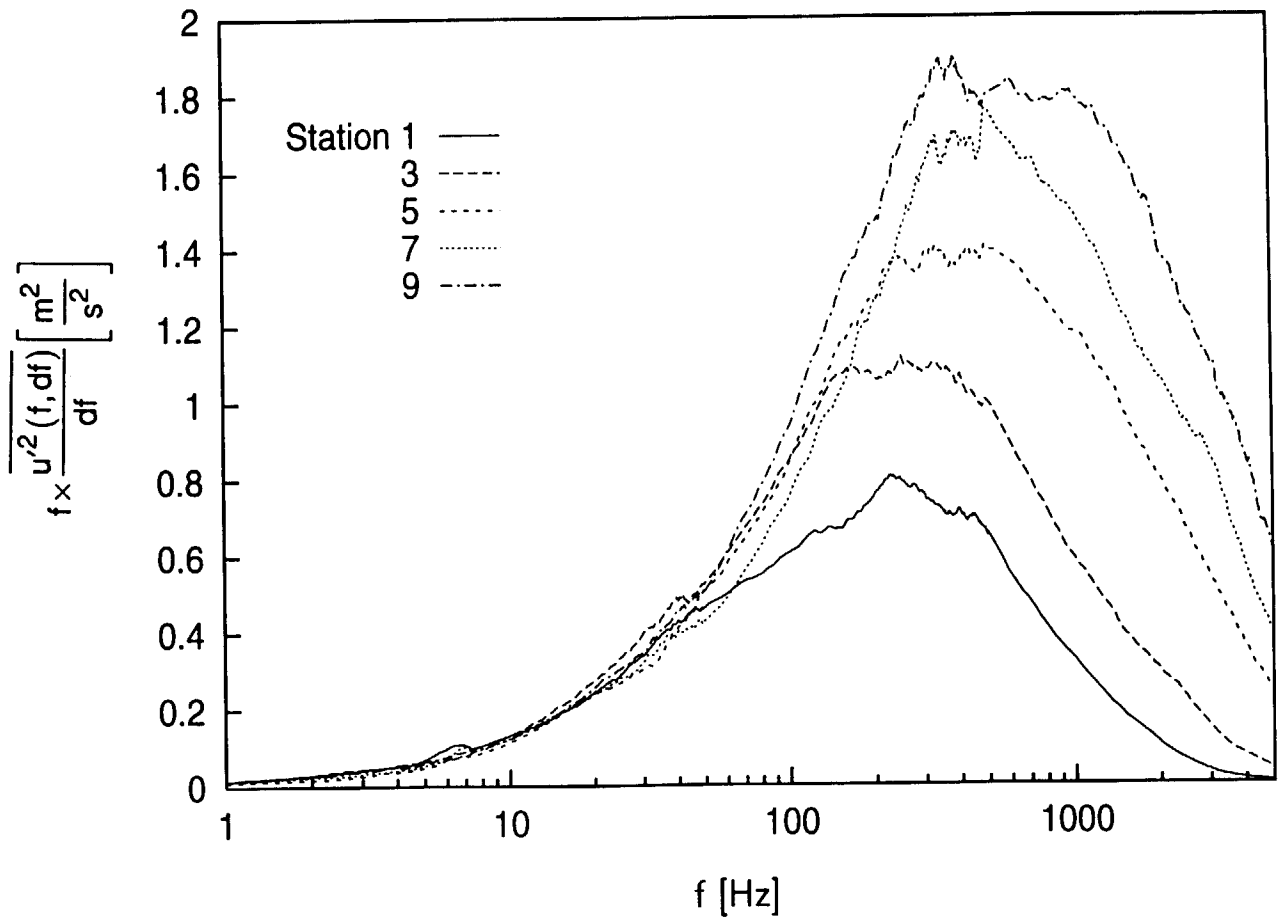

Fig. 6.38b: Boundary Layer u' Spectra at y^+=17, Energy Coordinates, dU_{cw}/dx=29 s^{-1} Case

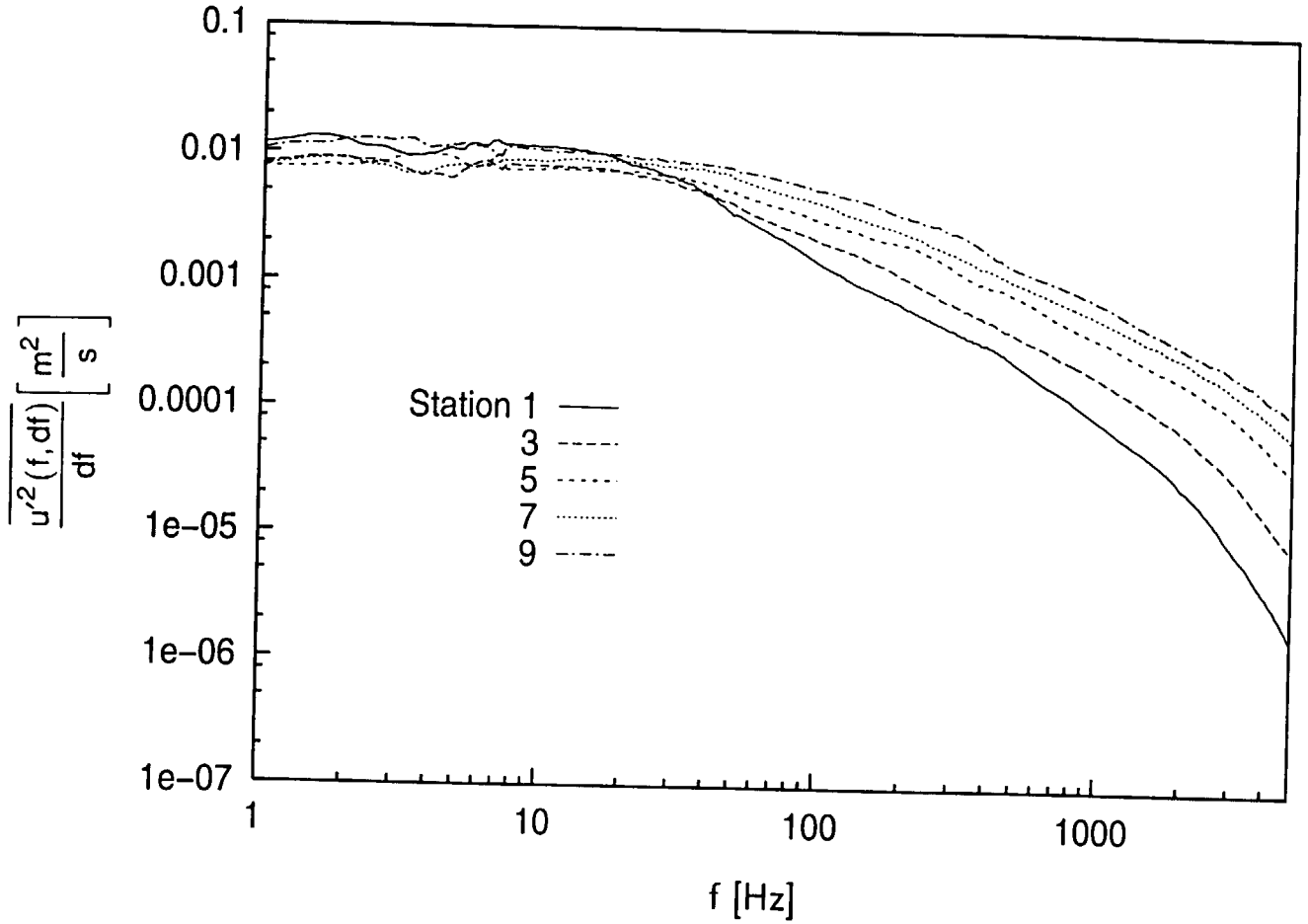

Fig. 6.39a: Boundary Layer u' Spectra at y^+=100 dU_{cw}/dx=29 s^{-1} Case

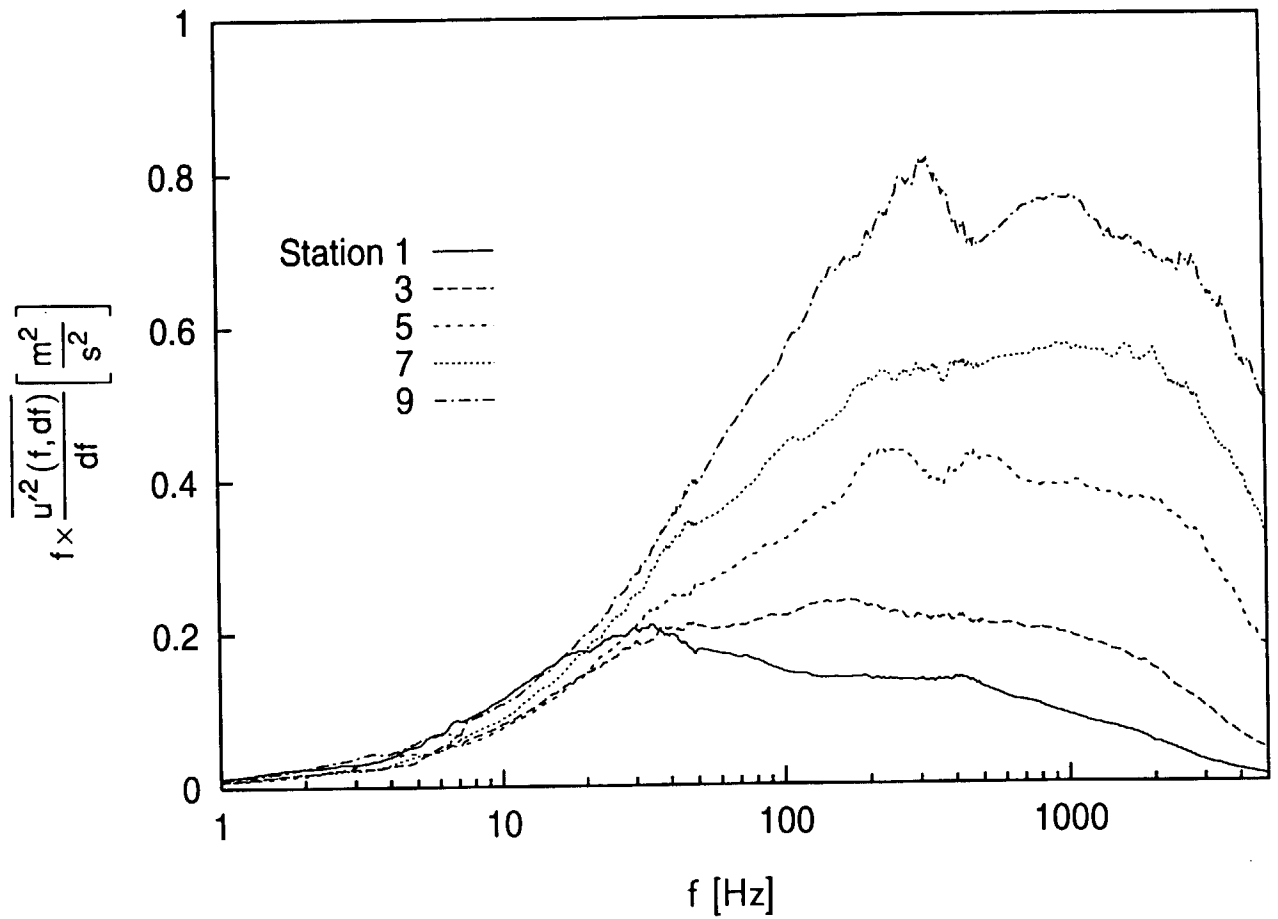

Fig. 6.39b: Boundary Layer u' Spectra at y^+=100, Energy Coordinates, dU_{cw}/dx=29 s^{-1} Case

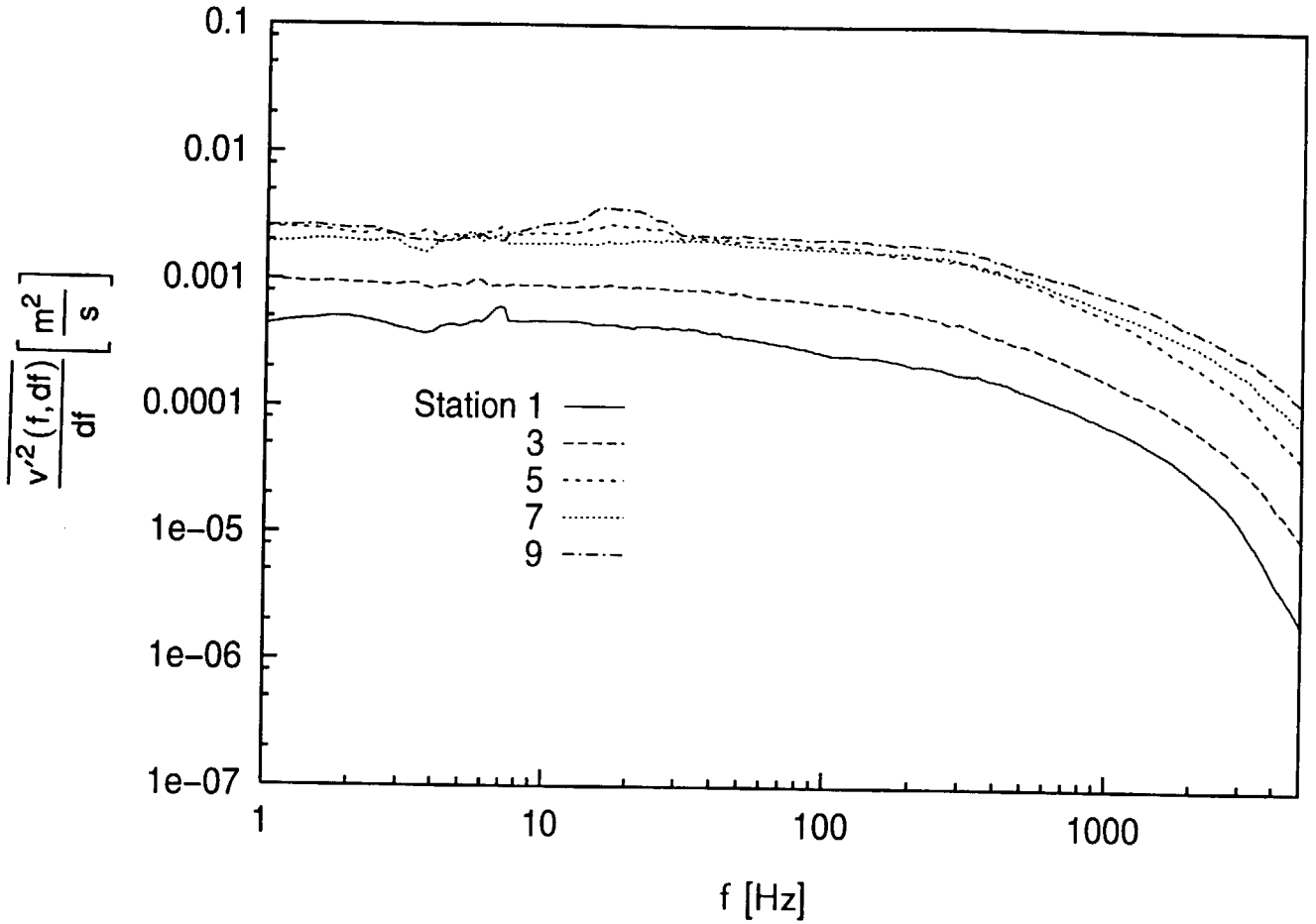

Fig. 6.40a: Boundary Layer v' Spectra at y^+=100 dU_{cw}/dx=29 s^{-1} Case

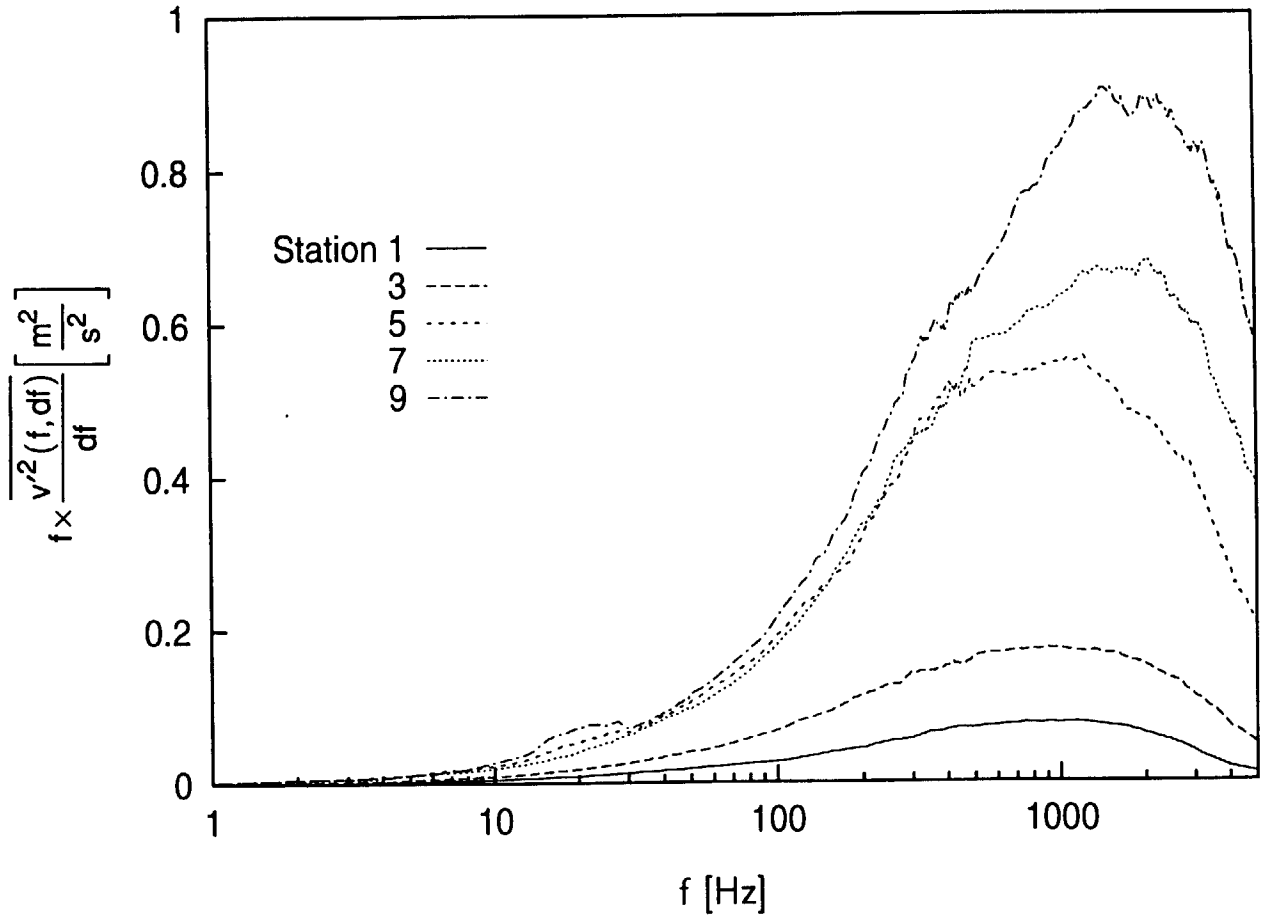

Fig. 6.40b: Boundary Layer v' Spectra at y^+=100, Energy Coordinates, dU_{cw}/dx=29 s^{-1} Case

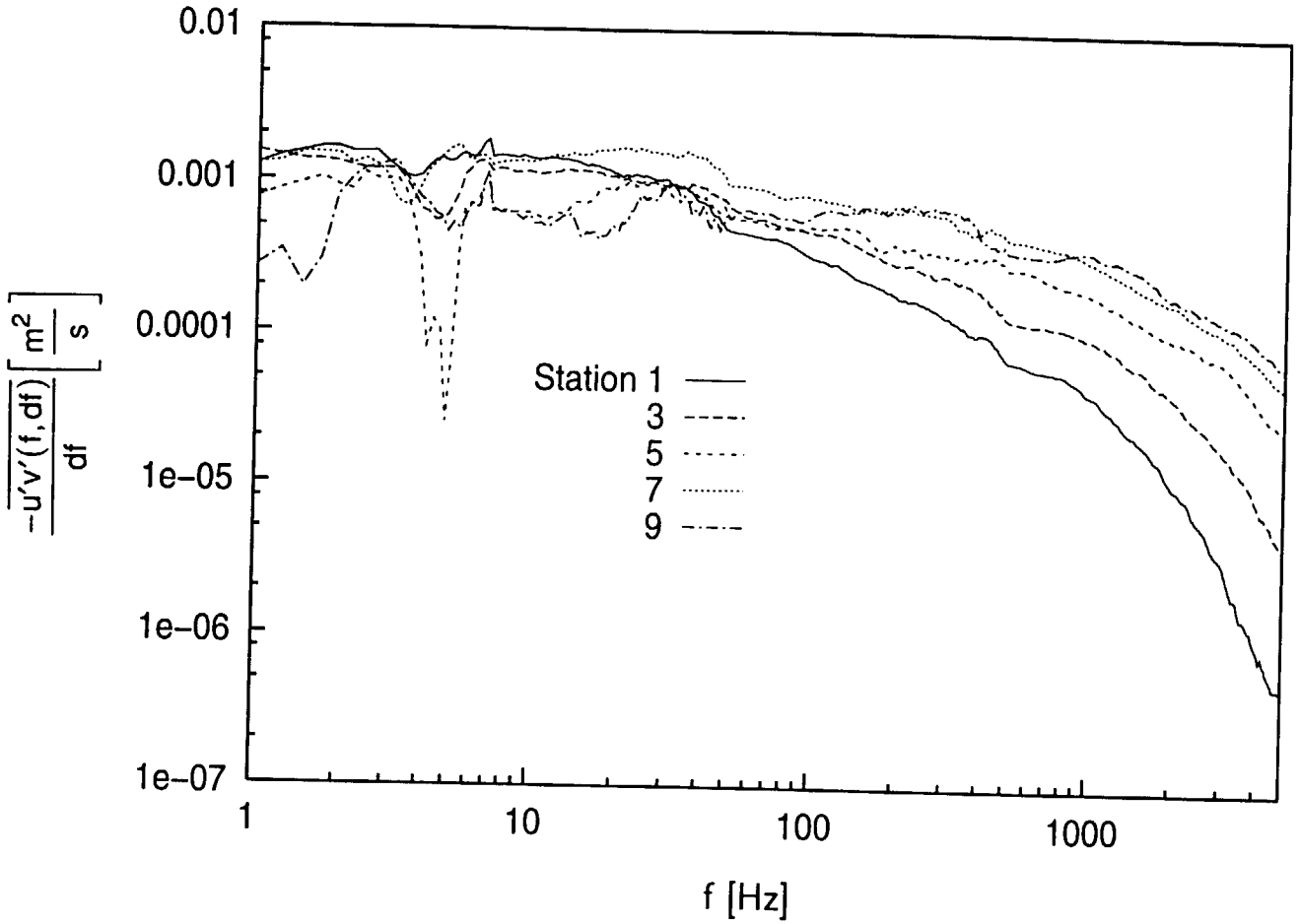

Fig. 6.41a: Turbulent Shear Stress Spectra at y^+=100 dU_{cw}/dx=29 s^{-1} Case

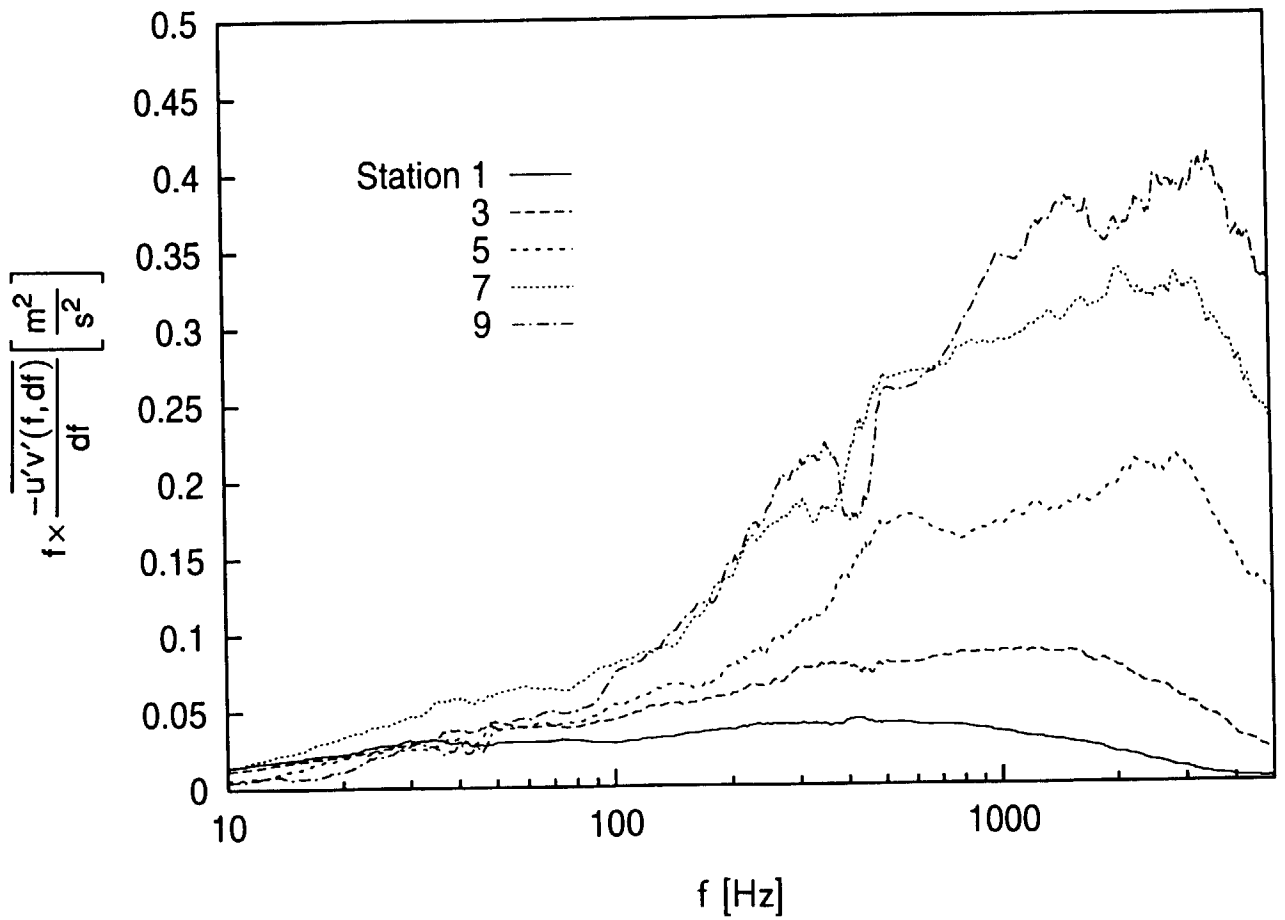

Fig. 6.41b: Turbulent Shear Stress Spectra at y^+=100, Energy Coordinates, dU_{cw}/dx=29 s^{-1} Case

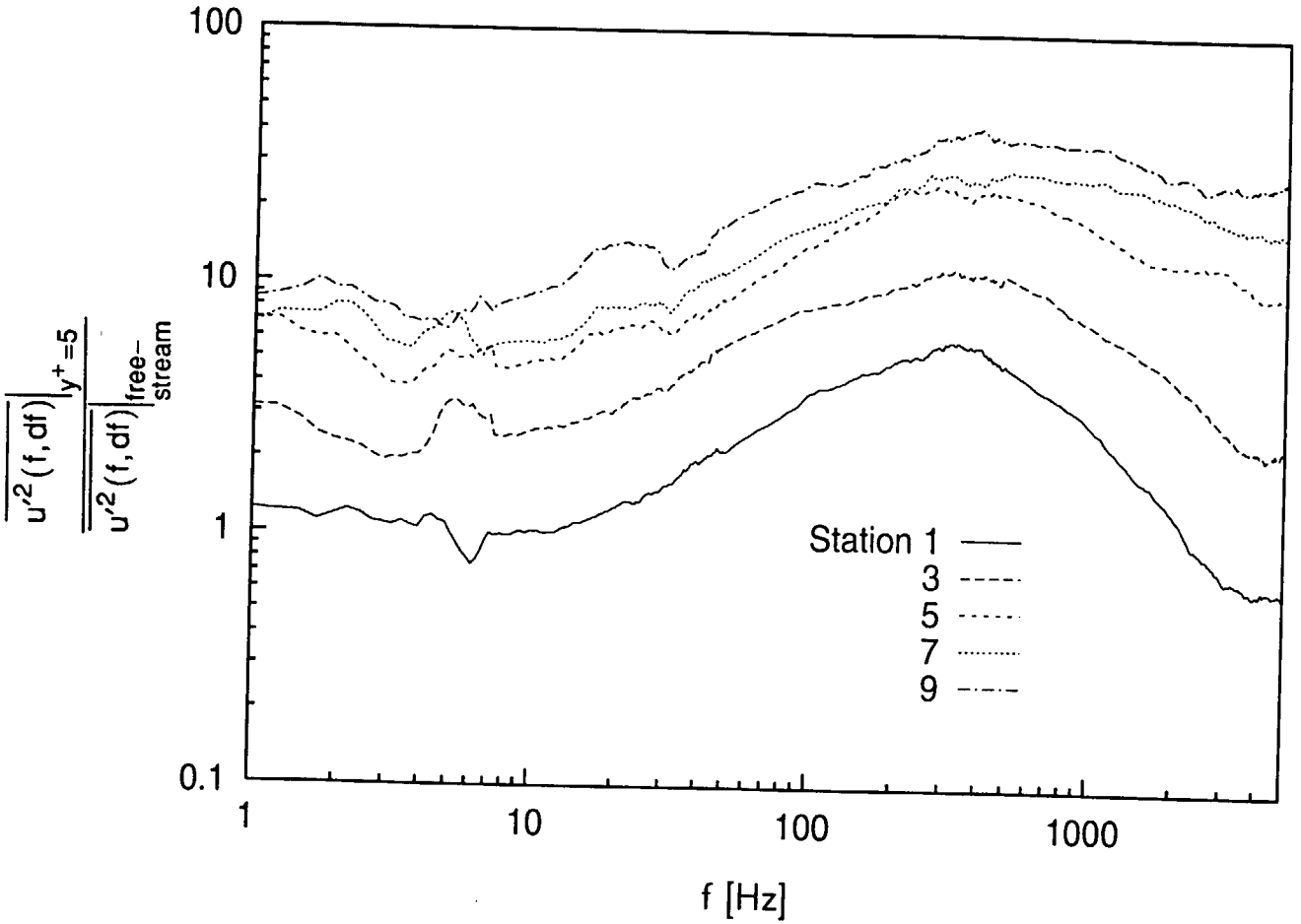

Fig. 6.42a: Transfer Function of u' Between Boundary Layer at y^+=5 and Free-Stream, dU_{cw}/dx=29 s^{-1} Case

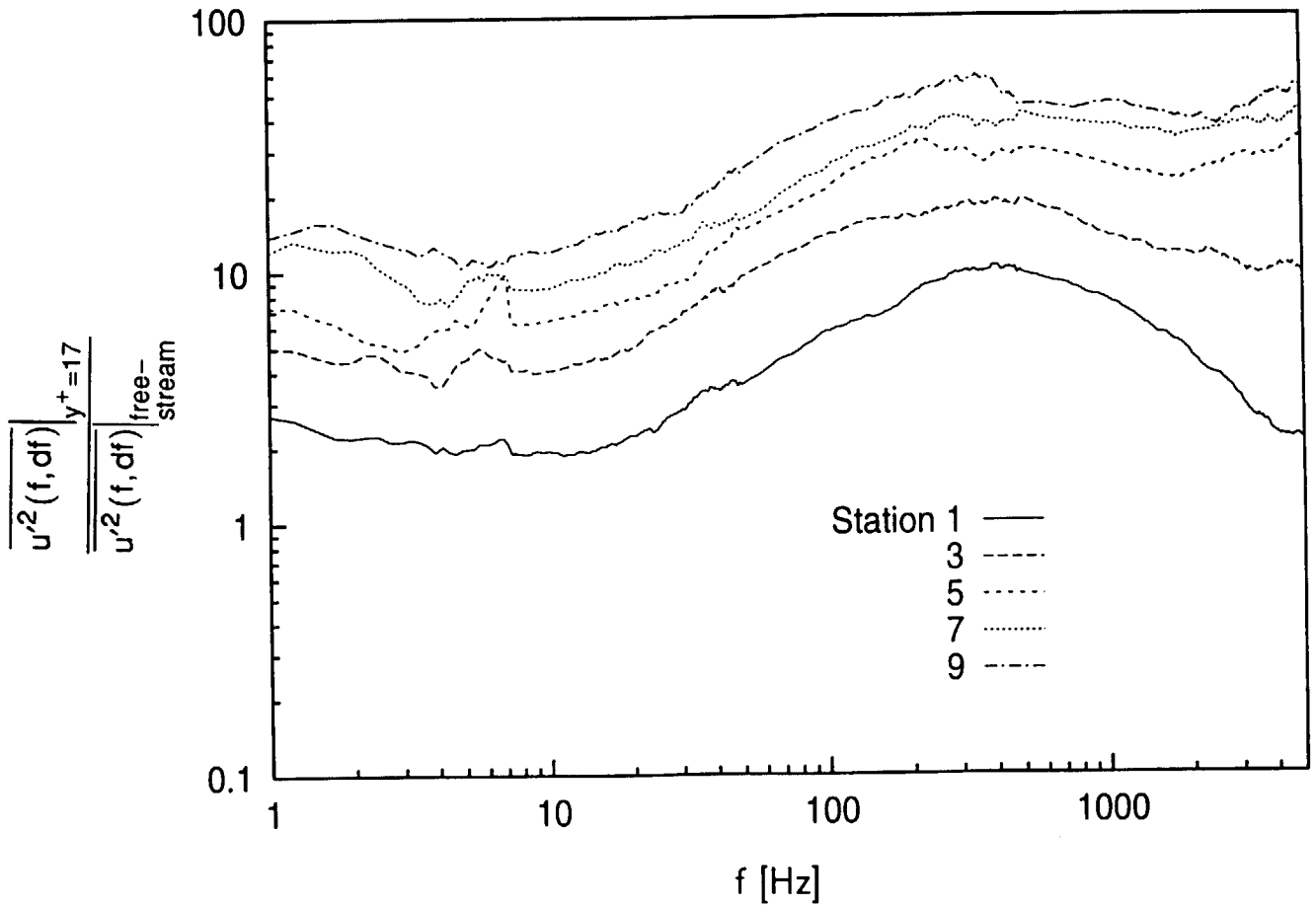

Fig. 6.42b: Transfer Function of u' Between Boundary Layer at y^+=17 and Free-Stream, dU_{cw}/dx=29 s^{-1} Case

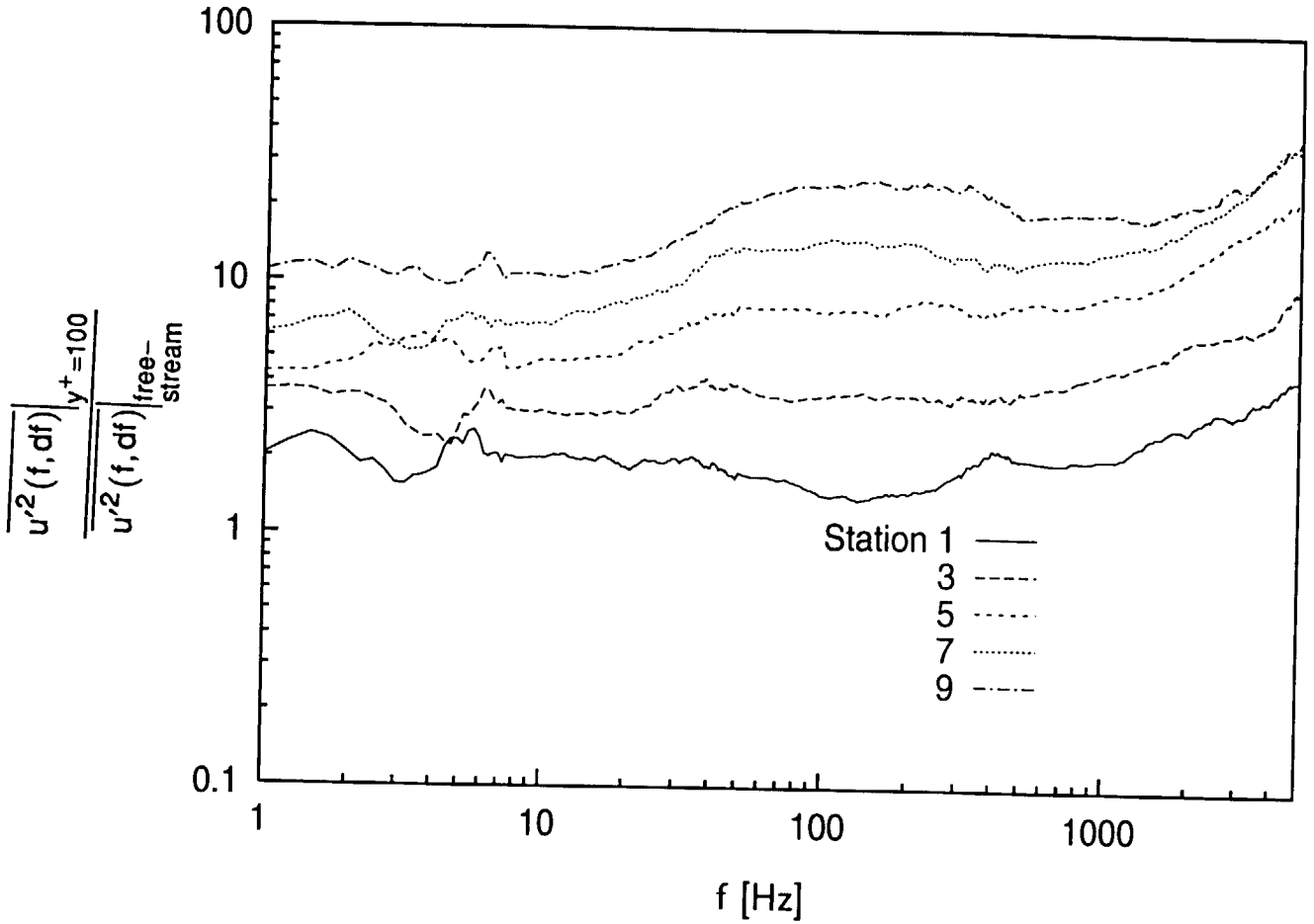

Fig. 6.42c: Transfer Function of u' Between Boundary Layer at y^+=100 and Free-Stream, dU_{cw}/dx=29 s^{-1} Case

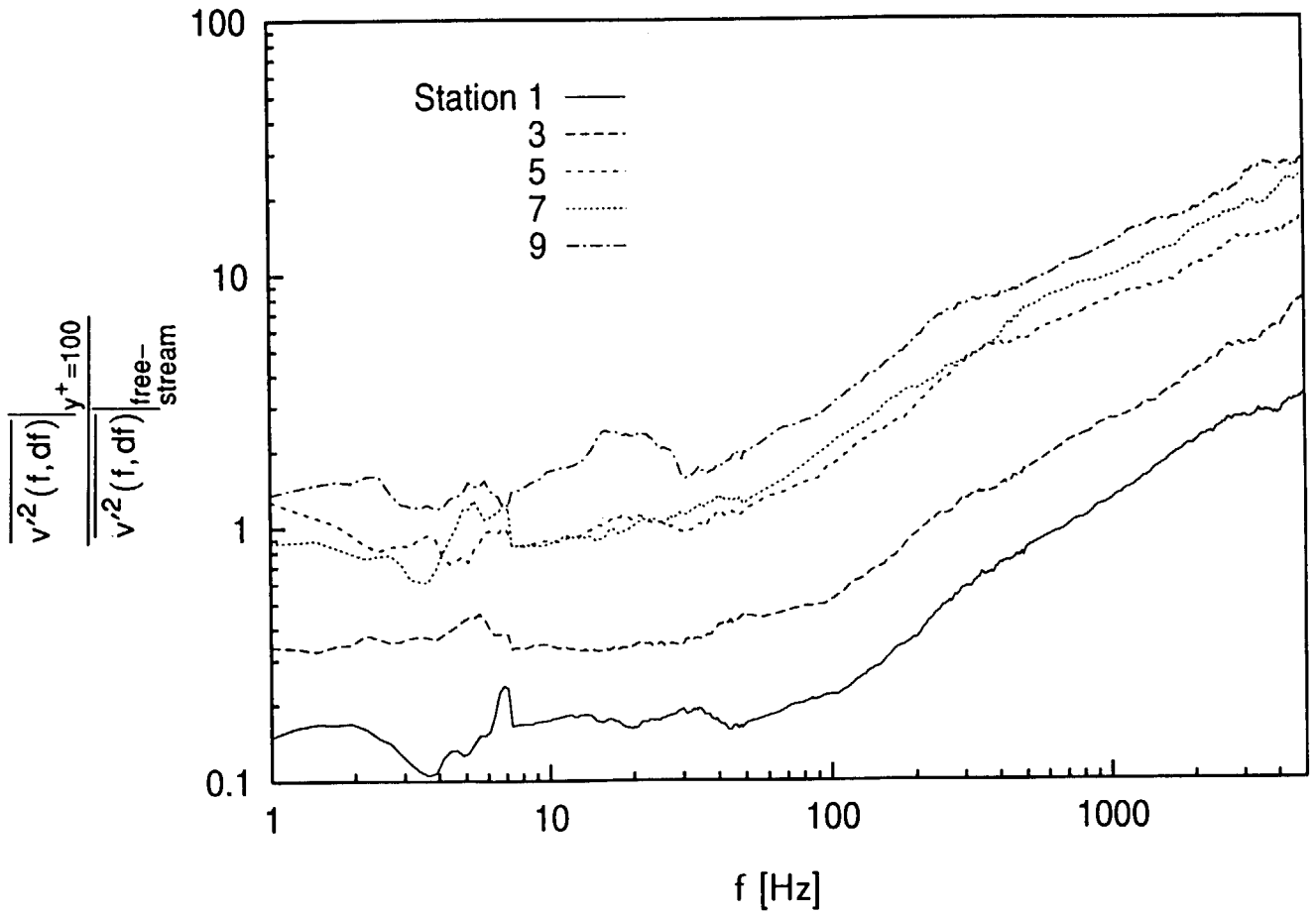

Fig. 6.43: Transfer Function of v' Between Boundary Layer at y^+=100 and Free-Stream, dU_{cw}/dx=29 s^{-1} Case

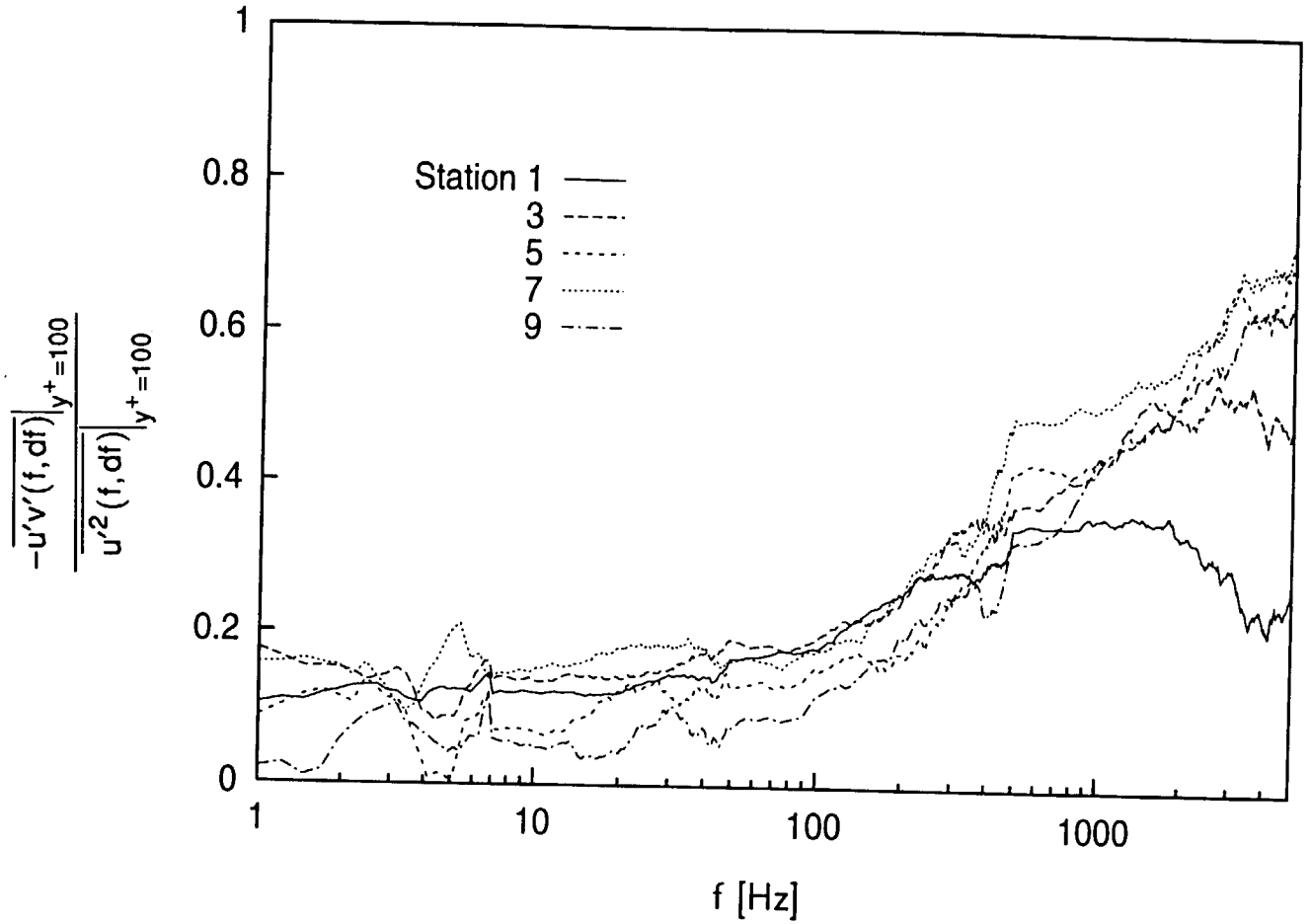

Fig. 6.44: Transfer Function Between u'v' and u' at y^+=100 dU_{cw}/dx=29 s^{-1} Case

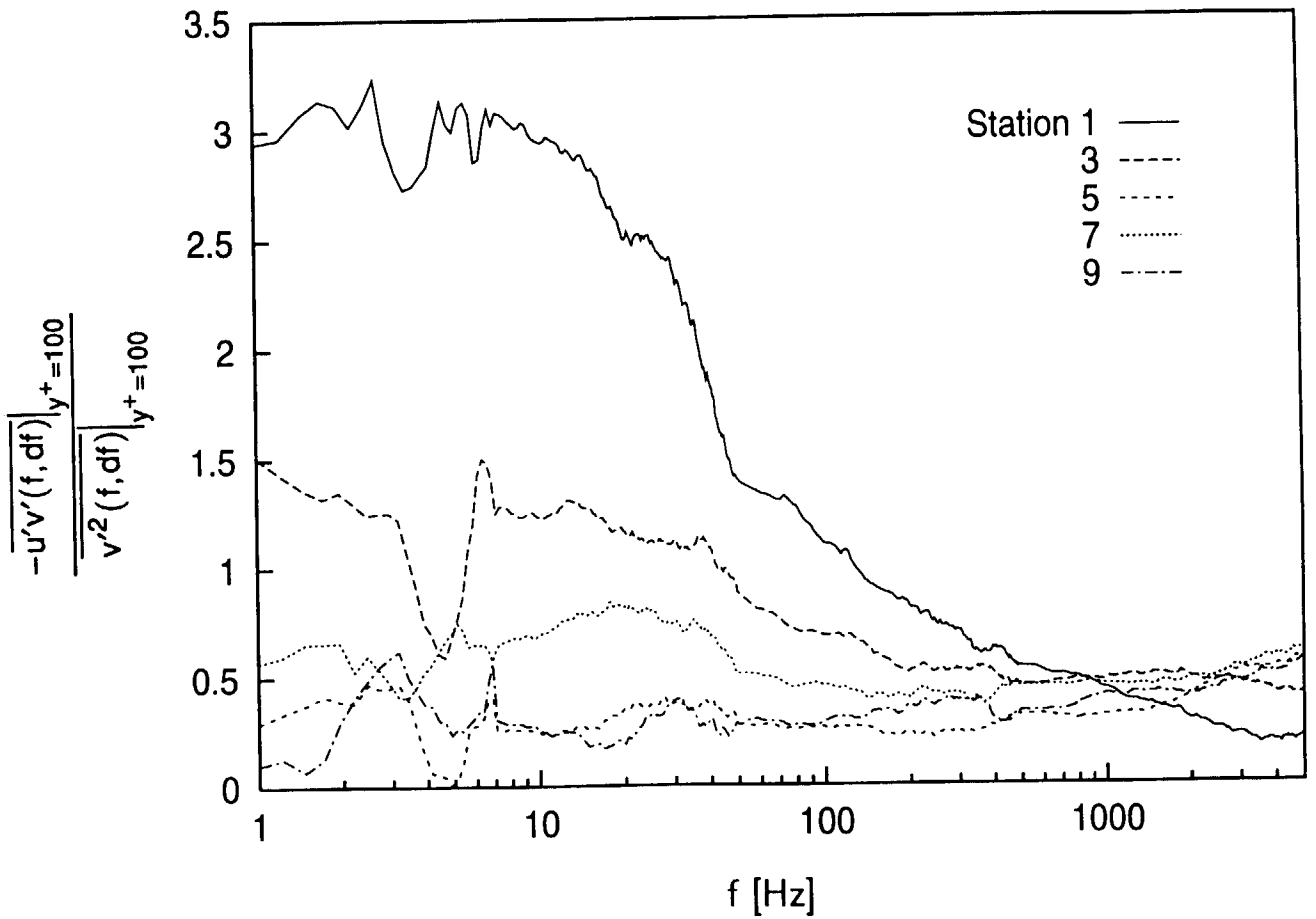

Fig. 6.45: Transfer Function Between u'v' and v' at y^+=100 dU_{cw}/dx=29 s^{-1} Case

CHAPTER 7: HIGH FSTI, $dU_{cw}/dx=14\ s^{-1}$ RESULTS

To expand on the results presented in Chapter 6 and better document the early stages of transition, a case with a longer transition zone was investigated. The test section was left in the geometry of the $dU_{cw}/dx=29\ s^{-1}$ case described in Chapter 6, and the inlet velocity was reduced to half the value used in that case. This reduced the local free-stream velocities and Re_x throughout the test section to half the values of the $dU_{cw}/dx=29\ s^{-1}$ case. For a given geometry, the KRe_x product remains constant as the velocity is changed. Local K parameters were, therefore, doubled. The lower Reynolds numbers and higher acceleration parameters both acted to extend the transition zone in the present case. As in the two high-FSTI cases described above, the boundary layer in the present case was two-dimensional in a time-averaged sense. Some of the results presented below are also available in Volino and Simon (1994b, 1995b, 1995c).

EXPERIMENTAL CONDITIONS

The flow entered the test section with a velocity of 5.2 m/s and a nominal FSTI of 8%. The free-stream velocity gradient was held at $14.35\ s^{-1}$. Profile data were acquired at ten streamwise measurement stations. The locations of these stations, along with other important parameters, are listed in Table 7.1. At the last measurement station, $Re_x=8.7\times10^5$. The acceleration parameter dropped from $K=8.6\times10^{-6}$ at the leading edge of the test wall to 0.80×10^{-6} at the last measurement station. The K profile from the experiment and the profiles from the airfoils of Fig. 5.1 are shown in Fig. 7.1. The maximum acceleration is roughly the same as that of the CF6 airfoil, and about half that of a more modern airfoil. The chord Reynolds numbers for the experiment and the airfoils are roughly the same.

Free-Stream Conditions

The free-stream turbulence level is shown in Fig. 7.2. In Fig. 7.2a, $\overline{u'_\infty}$ and $\overline{v'_\infty}$ are plotted in dimensional coordinates. The streamwise component, $\overline{u'_\infty}$, decays to about 70% of its inlet value by the last measurement station. The normal component, $\overline{v'_\infty}$, decays only slightly. The free-stream turbulence intensities are shown in dimensionless coordinates in Fig. 7.2b. Also shown is the FSTI, taken as stated above, as $\sqrt{\frac{\overline{u'^2}+2\overline{v'^2}}{3U_{cw}^2}}$. The FSTI drops from its inlet value (~8%) to 5.3% at the first station and 1.7% at the last station. Most of the drop is due to the increase in U_{cw} in the streamwise direction. In terms of the streamwise position, x, the FSTI are nearly equal to those of the $dU_{cw}/dx=29\ s^{-1}$ case, presented in Fig. 6.2b. Since the same turbulence generating grid and the same geometry were used in the $dU_{cw}/dx=29\ s^{-1}$ case and the present case, it is not surprising that the free-stream turbulence level scales with the free-stream velocity. In terms of Re_x, the FSTI drops twice as fast in the present case as in the $dU_{cw}/dx = 29\ s^{-1}$ case.

Free-stream spectra. Free-stream spectra of u′ and v′ were acquired at stations 1, 2, 3, 4, 5, 7 and 9. The u′ spectra are shown in Fig. 7.3. Below 400 Hz, u′ decays in the streamwise direction. There is some slight growth at higher frequencies. The overall energy in the free-stream drops at first before settling out to a more constant value at the downstream stations. The fluctuation energy at the upstream stations is centered around 20 Hz, as shown in Fig. 7.3b. As the low frequencies decay, the peaks in Fig. 7.3b shift to about 500 Hz. The length scale associated with 500 Hz at station 9, U_{cw}/f, is 3 cm. This scale could be associated with large scale turbulent eddies. The integral length scale associated with the u′ fluctuations, $\Lambda_{u'}$ (obtained using Fig. 7.3a and Eqn. 2.16), is 4.4 cm at the first measurement station, and remains in the 3.4 cm to 4.4 cm range as the flow moves downstream (see Table 7.1). This scale can also be associated with large scale eddies. The frequency associated with the integral scale, $U_\infty/\Lambda_{u'}$, increases from 150

Hz at station 1 to 420 Hz at station 9. A comparison of Figs. 6.3 and 7.3 shows that the length scales in the flow do not change as the free-stream velocity is changed, but the frequencies associated with the spectra vary directly with the free-stream velocity. The free-stream velocity and frequencies of the $dU_{cw}/dx=29\ s^{-1}$ case (Fig. 6.3) are both twice those of the present case. The levels of the peaks in Fig. 6.3b are four times the levels of the peaks in Fig. 7.3b. This implies variation with the free-stream velocity squared. Such variation was noted above with the FSTI levels presented in Fig. 7.2.

The v' spectra are shown in Fig. 7.4. The peak in the v' energy, as shown in Fig. 7.4b, is centered around 70 Hz at station 1. There is less evolution of v' in the streamwise direction than was observed in u'. By station 9 the energy is centered at 150 Hz, in a broad peak, or plateau, between 40 Hz and 300 Hz. The integral length scale associated with the v' fluctuations, $\Lambda_{v'}$, rises from 1.6 cm at station 1 to 3.7 cm at station 9. The frequency associated with the integral scale, $U_\infty/\Lambda_{v'}$, remains between 350 Hz and 440 Hz at all stations. As with the u' spectra, a comparison of Figs. 6.4 and 7.4 shows that the frequencies and magnitudes of the v' spectra for the $dU_{cw}/dx=29\ s^{-1}$ case and the present case scale with the free-stream velocity. The integral length scales are approximately the same for the two cases.

The variation of the frequencies and length scales noted above suggests that the frequencies of the free-stream spectra could be nondimensionalized using the quantity $U_\infty/\Lambda_{v'}$. The integral scale based on v' is suggested for the nondimensionalization since the free-stream v' fluctuations are believed to have more of an influence on the boundary layer than the u' fluctuations. The magnitude of the spectra could be nondimensionalized using the local free-stream velocity. This choice would allow comparison of the spectra of dimensionless FSTI between various flows, but could give a false impression of turbulence decay in an accelerating flow. Another possibility is to normalize with $\overline{v_\infty'^2}$. This choice eliminates distortion of the results due to acceleration, but would mask differences between spectra in comparisons of high- and low-FSTI

flows. There does not appear to be a general purpose way of nondimensionalizing the spectra. Different choices are appropriate for different comparisons. For this reason, the spectra are left in dimensional form in this study.

Boundary Layer Growth

The growth of the momentum and thermal boundary layers is shown in Fig. 7.5, where Re_θ and Re_{Δ_2} are plotted verses Re_x. The momentum thickness Reynolds number remains nearly constant for the first five measurement stations, rising thereafter. There is some evidence of a reverse transition between the first and second stations, as Re_θ drops from 274 to 207. The beginning of the rise in Re_θ corresponds to a drop in the acceleration parameter, K, below 2×10^{-6}. The same behavior was observed in the lower acceleration case discussed in Chapter 6. In that case, Re_θ began to rise after the second station, also when K dropped below 2×10^{-6}. A comparison of Figs. 5.6, 6.5 and 7.5 shows that the momentum boundary layer growth is more strongly suppressed in the present case than in any of the cases with weaker acceleration. The comparison also confirms that thermal boundary layer growth, in terms of Re_{Δ_2}, is not strongly affected by the acceleration.

The shape factor, $H=\delta^*/\theta$, is shown in Fig. 7.6. The shape factor increases from 1.5 to 1.7 between stations 1 and 2, providing further evidence of a reverse transition between these stations. The shape factor remains between 1.6 and 1.7 between stations 2 and 6. Downstream, H drops to about 1.4 at the last measurement station. At no point is H near the laminar, low-disturbance value, which for the acceleration rates present would be about 2.3 (calculated for flow on a flat plate with the TEXSTAN program (Kays and Crawford, 1993; Crawford and Kays, 1976)). In a low FSTI flow, boundary layers relaminarize at $K>3\times10^{-6}$ (Jones and Launder, 1972) and at the acceleration rates of this case, they would be laminar. The H values of the present case are all above the fully-turbulent values of 1.2 to 1.3 observed in the flows of Chapters 5 and 6. These results

suggest that the boundary layer in the present case is in the early stages of transition at the upstream stations, and is nearing the end of transition by the end of the test section.

Energy Balance

The energy balance for the present case is shown in Fig. 7.7. The energy balance is within 12% at station 7, and within 6% at the rest of the stations. Given the variability in the wall heat flux and the uncertainty in the data (described above in Chapter 2), the energy balance is acceptable.

Strength of Curvature

The strength of curvature of the present case is nearly the same as that of the $dU_{cw}/dx=29\ s^{-1}$ case of Chapter 6 (see Fig. 6.8). Local values are tabulated in table 7.1. As stated in Chapter 6, the curvature may influence the flow, but it is weak. No stable streamwise vortices were observed in the extended transition zone. The Görtler number, $G = Re_\theta \sqrt{\frac{\theta}{R}}$, remained between 4 and 5 in the transition region. Floryan (1991) states that boundary layers become unstable to Görtler vortices when G=0.3, but that the vortices do not become detectable until G>5.5. Thus, the absence of vortices was expected.

MEAN VELOCITY PROFILES

Figure 7.8 shows mean streamwise velocity profiles from the present case plotted as $\overline{U}/U_{cw}$ verses y/θ. The edge of the momentum boundary layer, $\delta_{99.5}$, corresponds to $y/\theta \approx 14$ to 21. The full boundary layer is shown in Fig. 7.8a. The profiles become fuller at the downstream stations. Figure 7.8b shows the near wall region more closely. The profile is less full at station 2 than at station 1, indicating possible reverse transition. The

profiles become fuller, or more turbulent like, from station 2 through 10. The most significant change occurs between stations 6 and 7.

Figure 7.9 shows mean velocity profiles plotted in wall coordinates. Over the first five stations, the profiles rise to higher u^+ values while keeping approximately the same shape. The profiles appear somewhat laminar-like. Below are comparisons to expected accelerating-flow profiles. At station 6, the profile shape begins to change to one that is more turbulent-like. This trend is more obvious at station 7, and by stations 9 and 10 the profiles are almost in agreement with the unaccelerated flow law of the wall. The change in profile shape at station 6 is consistent with the beginning of the rise in Re_θ (Fig. 7.5) and the drop in the shape factor, H (Fig. 7.6). The profiles exhibit no wake region. The absence of a wake is consistent with previous observations in accelerated and unaccelerated high-FSTI turbulent boundary layers, as noted in Chapter 6. It indicates considerable turbulent mixing in the outer part of the boundary layer.

The mean velocity data agree well with profiles calculated by the method of Appendix A, as demonstrated in Fig. 7.10. Data from stations 3 and 8 are shown. The data agree with the line $u^+=y^+$ in the viscous sublayer, and deviations from the unaccelerated flow law of the wall are well predicted.

SKIN FRICTION COEFFICIENTS

Figure 7.11 shows skin friction coefficients, C_f, plotted verses Re_θ. Also shown are flat-plate, low-FSTI, unaccelerated flow correlations for laminar and fully-turbulent boundary layers. At the upstream stations, C_f drops while Re_θ remains nearly constant. The flow appears to be relaminarizing in some sense, although C_f values always remain much closer to the turbulent correlation than to the laminar correlation. Once the flow proceeds toward fully-turbulent behavior (between stations 6 and 7, as indicated by the velocity profiles of Figs. 7.8 and 7.9), C_f rises above the turbulent correlation. By station 10, the data are 11% above the correlation. Acceleration, high FSTI, and concave

curvature all tend to produce a rise in C_f at a given Re_θ. The trend observed here is, therefore, expected. The extent to which each effect is separately responsible for the rise in C_f cannot be determined. The effects interact with one another; for example, acceleration was shown above to reduce FSTI and the strength of curvature.

Figure 7.12 shows C_f plotted verses Re_θ and Re_x for the 8% FSTI cases of this study, and unaccelerated cases from Kim and Simon (1991). As a function of Re_θ (Fig. 7.12a), curvature causes a significant increase in C_f, and acceleration has the opposite effect. Acceleration alone tends to cause a slight rise in C_f (Volino and Simon, 1995a), but when acting in combination with concave curvature, the acceleration acts to keep the boundary layer thin, reduce the strength of curvature, and thereby reduce C_f below unaccelerated concave-wall values. It would be useful to compare the data from the present study to data from accelerated, high FSTI, boundary layers on flat plates or surfaces with stronger curvature, but such data do not exist. As a function of Re_x (Fig. 7.12b) both curvature and acceleration cause C_f to rise. The unaccelerated flat-wall data lie close to a turbulent correlation from Kays and Crawford (1993). The unaccelerated concave-wall data fall above the correlation due to the destabilizing effects of concave curvature. The accelerated flow data have the highest C_f values in these coordinates, because the acceleration keeps the boundary layer thin, thereby increasing near wall velocity gradients and increasing wall shear stress. Comparisons and correlations in terms of Re_x are of limited use because they do not take the maturity of the boundary layer (i.e. the boundary layer thickness) into account.

MEAN TEMPERATURE PROFILES

Mean temperature profiles are shown in Fig. 7.13. The edge of the thermal boundary layer, $\delta_{t99.5}$, corresponds to $y/\Delta_2 \approx 10$ to 14. The full profiles are shown in Fig. 7.13a. The profiles become fuller between stations 1 and 3. At the downstream stations,

the profiles appear to collapse. Figure 7.13b shows an expanded view of the near-wall region. In this view, the profiles are seen to become fuller between stations 1 and 9, only appearing to collapse at stations 9 and 10. There is a significant change between stations 6 and 7, agreeing with the velocity profiles of Fig. 7.8b.

Figure 7.14 shows temperature profiles plotted in wall coordinates. The trends are similar to those observed in the velocity profiles in Fig. 7.9. The profiles rise in t^+ through the first five stations, with a laminar-like shape. At station 6 the trend is reversed, and the profiles begin to collapse onto a turbulent-like shape. At the downstream stations, a wake emerges, which is contrary to velocity profile development. The wakes in the temperature profiles may be due to the thickness of the thermal boundary layer relative to the momentum boundary layer, a product of acceleration's suppression of the momentum boundary layer growth. High FSTI, combined with concave curvature, results in high levels of turbulent mixing in the outer part of the momentum boundary layer, suppressing the wake. The thermal boundary layer extends beyond the edge of the momentum boundary layer into a region of lower mixing. The presence of the thermal wake suggests that surface heat transfer should be relatively low compared to skin friction, as shown below. Although not so obvious, the emergence of a wake can be seen in the thermal boundary layer of the lower acceleration case of Chapter 6 (Fig. 6.13).

At the downstream stations (Fig. 7.14) the temperature profiles do not agree with the unaccelerated flow law of the wall, although there is reasonable agreement between the velocity profiles and the momentum law of the wall (Fig. 7.9). As explained in Appendix A, acceleration tends to stabilize the boundary layer and reduce turbulence, causing a rise in both the velocity and temperature profiles when plotted in wall coordinates. The favorable pressure gradient also has a direct effect on the velocity profile, causing it to drop, somewhat negating the rise caused by the reduction in

turbulence. The pressure gradient has no similar effect on the temperature profiles, so the temperature profiles remain high, relative to those in unaccelerated flow.

The temperature profiles agree with profiles calculated according to Appendix A. Figure 7.15 shows the temperature profile data from stations 6 and 8 along with the calculated profiles for the conditions present at these stations. The matches between the data and the calculated profiles are good. Some difference should be expected since the calculated profiles account for the effect of acceleration, but do not include curvature or free-stream turbulence effects. The calculated profiles do not attempt to capture the wake, so no agreement at high y^+ should be expected. In this flow, however, the wake is suppressed, so the calculated and measured profiles agree almost to the free-stream.

STANTON NUMBERS

Figure 7.16 shows Stanton number plotted verses enthalpy thickness Reynolds number, Re_{Δ_2}, for the present case. Also shown are flat plate, low-FSTI, unaccelerated flow correlations for laminar and fully-turbulent flow. The data drop below the turbulent correlation in the transition region and rise to meet the correlation at the downstream stations. The rise in St occurs between stations 6 and 7, agreeing with the rise in C_f seen in Fig. 7.11. The Stanton numbers in the transition region are much closer to the turbulent correlation than to the laminar correlation, as with the skin friction coefficients. At the downstream stations, the integrated effect of acceleration has kept the curvature effect small and has also led to a reduction in FSTI. At the end of the test section, the three effects are apparently weak, with a remaining acceleration effect compensating the remaining enhancement due to FSTI (1.6% at this point) and curvature ($\delta_{99.5}/R \approx 1\%$ at this point). The data agree with the unaccelerated, flat-wall, turbulent correlation. Since the drop in FSTI and strength of curvature did not cause a reduction in C_f to flat wall levels, it is assumed that the mismatch between the thickness of the thermal and momentum boundary layers is an important effect in reducing the Stanton numbers. The

Reynolds analogy factor, $\frac{2St}{C_f}$, drops from a value of 1.1 in unaccelerated flow to a value of 0.8 in the present case, as it did in the case described in Chapter 6.

Figure 7.17 shows St plotted verses Re_{Δ_2} and Re_x for the 8% FSTI cases of this study and the 8% FSTI unaccelerated cases from Kim and Simon (1991). The data look similar in both coordinate systems since acceleration does not have a strong effect on the thermal boundary layer growth. The unaccelerated concave-wall data show no sign of transition and are significantly higher than the flat-wall correlation. The combined effects of FSTI and concave curvature raise the Stanton numbers by as much as 40% above the flat wall correlation. The rise in Stanton number is large, but not unexpected. Simonich and Moffat (1982) reported a significant (~20%) rise in Stanton numbers above flat plate values in a low-FSTI, concave wall boundary layer with a strength of curvature which is comparable to the unaccelerated case presented here. Simonich and Bradshaw (1978) reported a 5% increase in Stanton number for every 1% increase in FSTI in boundary layers on flat plates. This is roughly consistent with the data of Blair (1983). They considered FSTI up to 7%. Acceleration counteracts the FSTI and curvature effects, as stated above.

INTERMITTENCY PROFILES

Profiles of the intermittency, γ, are shown in Fig. 7.18. These profiles are based on u' fluctuations. At the first three stations, the intermittency is near zero at the wall, rises to a peak of 30 to 35% at $y/\theta \approx 4$ ($y^+ \approx 60$), and drops to a free-stream value of between 10 and 20%. As noted in Chapter 6, the non-zero free-stream value results from the high FSTI and the tuning of the intermittency circuit (described in Chapter 2). The intermittency drops slightly between stations 1 and 2, supporting the suggestion of reverse transition between these stations mentioned above. Between station 3 and 8, the intermittency rises. By stations 9 and 10, the peak intermittency is nearly 100%,

indicating fully-turbulent flow at these last two stations. The measurements suggest that the flow is in the early stages of transition at station 1 and that the strong acceleration at the first three stations prevents further progress of the transition process. The intermittency starts to increase between stations 3 and 4, when K drops below 3×10^{-6}. Given the uncertainty associated with the tuning of the intermittency circuit, it could also be argued that the flow is pre-transitional at the first three stations, and transition begins after station 3.

Intermittency profiles based on the fluctuating temperature, t', are shown in Fig. 7.19. The intermittency values in Fig. 7.19 are different from those based on u', which are presented in Fig. 7.18. As stated in Chapter 6, intermittency based on t' is believed to useful for separating boundary layer flow from free-stream flow, but it is not as useful for distinguishing between turbulent and non-turbulent flow in the boundary layer.

FLUCTUATING VELOCITY MEASUREMENTS

$\overline{u'}$ Profiles

Profiles of $\overline{u'} / U_{cw}$ are plotted verses y/θ in Fig. 7.20. Figure 7.20a shows the full boundary layer, and Fig. 7.20b is an expanded view of the near-wall region. The peak in the profiles shifts out between stations 1 and 2, providing further evidence of reverse transition between these stations. The profiles appear similar at stations 2 through 5, with peaks of magnitude 0.13 at $y/\theta=1.2$. At station 6 the peak begins to move toward the wall and increases in magnitude. Between stations 6 and 10, the peaks continue to shift toward the wall, and the peak magnitudes drop to about 0.11 at station 10. The rise, then fall, of the peak values, and the shift of the peaks toward the wall are both characteristic of transitional flow. Others, such as Sohn and Reshotko (1991), have noted such behavior in low-FSTI, transitional flows. It appears that most of the transition

process has been captured in the present case. In the $dU_{cw}/dx=29\ s^{-1}$ case, discussed in Chapter 6, only the latter stages of transition were seen. As shown in Fig. 6.17b, the peak $\overline{u'}/U_{cw}$ in the previous case moved continuously toward the wall, and the peak magnitude decreased from a maximum of 0.13 at station 1 to 0.08 at stations 9 and 10. This behavior corresponds to what is observed between stations 6 and 10 in the present case.

Fig 7.21 shows the $\overline{u'}$ profiles in wall coordinates. There is a peak at each station at $y^+=17$, which is typical of turbulent boundary layers. The levels of the peaks remain between 2 and 2.5 at all stations, as they did in the $K=0.75\times10^{-6}$ case of Chapter 5 (Fig. 5.19). As the acceleration parameter drops downstream of station 5, the profiles begin to rise in the outer part of the boundary layer ($70<y^+<500$). Similar behavior was observed in the cases described in Chapters 5 and 6. The $\overline{u'}$ levels in the outer part of the boundary layer are well below the levels of the 8% FSTI, unaccelerated comparison cases taken from Kim and Simon (1991).

$\overline{v'}$ Profiles

Figure 7.22 shows profiles of $\overline{v'}/U_{cw}$ plotted verses y/θ. As in the lower acceleration cases (Figs. 5.20 and 6.19), the profiles drop from peaks near the wall to minimum values between $y/\theta=5$ and 10 ($\delta_{99.5}\approx0.25$ to 0.5) followed by rises to the free-stream values. Figure 7.23 shows the $\overline{v'}$ profiles in wall coordinates. The profiles appear to reach an asymptotic shape by station 7, where the flow is near the end of transition and the acceleration has dropped to $K=1.3\times10^{-6}$.

Turbulent Shear Stress Profiles

Profiles of the turbulent shear stress are plotted as $-\overline{u'v'}/U_{cw}^2$ verses y/θ in Fig. 7.24. Also shown are unaccelerated, 8% FSTI concave- and flat-wall profiles from Kim

and Simon (1991). In these coordinates, the shear stress in the outer part of the boundary layer drops in the streamwise direction through the first four stations. By station 5, the profiles reach an asymptotic shape, which is the same as that seen in the $dU_{cw}/dx=29\ s^{-1}$ case of Fig. 6.21.

The profiles are plotted in wall coordinates in Fig. 7.25. The behavior is similar to that seen in the $dU_{cw}/dx=29\ s^{-1}$ case of Fig. 6.22. The profiles rise as the flow moves downstream, appearing to reach an asymptote between stations 7 and 10. At the downstream stations, the dimensionless shear stress profiles appear to extrapolate to 1 at the wall, as expected for a turbulent boundary layer. Upstream, the lower shear stress values indicate that the flow is still transitional. As is the coordinates of Fig. 7.24, the profiles all fall well below those of the unaccelerated flow cases.

Eddy Viscosity

Profiles of the eddy viscosity, ε_M, are shown in Fig. 7.26. With the exception of station 1, where high values are seen at the edge of the boundary layer, the profiles appear similar at all stations. The eddy viscosity in this case is equal that in the $dU_{cw}/dx=29\ s^{-1}$ case of Fig. 6.23. It is an order of magnitude lower than in the $K=0.75\times10^{-6}$ case of Fig. 5.24.

Mixing Length of Momentum

Profiles of the mixing length, ℓ_M, are shown in Fig. 7.27. Near the wall, the profiles drop with streamwise distance, reaching an asymptote by station 4. The slopes of the downstream profiles, ℓ_M/y, are about 0.3, which agrees with the profiles of the $dU_{cw}/dx=29\ s^{-1}$ case shown in Fig. 6.24, and which is below the von Kármán constant ($\kappa=0.41$). The slopes very near the wall ($y^+<50$) could not be measured due to probe size limitations, and it is possible that the profiles have the standard, 0.41, slope very near the

wall. As in the lower-acceleration cases, the turbulent shear stress, eddy viscosity, and mixing length profiles all show that strong acceleration greatly reduces the turbulent transport in the boundary layer.

FLUCTUATING TEMPERATURE AND VELOCITY MEASUREMENTS

$\overline{t'}$ Profiles

Profiles of the fluctuating temperature are shown in Fig. 7.28. Fluctuating temperature and turbulent heat flux data were acquired at stations 1 though 8. The profiles appear similar at all stations in these coordinates. Unlike the velocity fluctuations, the temperature fluctuations go to zero in the free-stream, where the flow is isothermal. Figure 7.29 shows the fluctuating temperature profiles in wall coordinates. The profiles become fuller at the downstream stations in these coordinates. At the downstream stations, there are near-wall plateaus in dimensionless $\overline{t'}$ with levels of about 3.6. This compares to plateaus at 2.5 in the $dU_{cw}/dx=29\ s^{-1}$ case (Fig. 6.26) and plateaus of 1.7 in the Kim and Simon (1991) concave-wall, unaccelerated flow.

$\overline{v't'}$ Profiles

Profiles of the component of the turbulent heat flux normal to the wall, $\overline{v't'}$, are shown in Fig. 7.30. Results appear very similar to those of the $dU_{cw}/dx=29\ s^{-1}$ case in Fig. 6.27. The profiles are plotted in wall coordinates in Fig. 7.31. Also shown in Fig. 7.31 are profiles from the Kim and Simon (1991), 8%-FSTI, unaccelerated flat- and concave-wall cases. The accelerated flow profiles rise in these coordinates, becoming fuller at the downstream stations. A similar rise was seen in the shear stress profiles in Fig. 7.25. There is some sign that a plateau is forming in $\overline{v't'}$ in the outer part of the boundary layer at station 8, but this plateau is not so pronounced as in the $dU_{cw}/dx = 29$

s^{-1} case of Fig. 6.28. The boundary layer in the present case does not reach the level of maturity seen in the $dU_{cw}/dx=29\ s^{-1}$ case. This is expected, since the acceleration rates are higher and the Reynolds numbers are lower in the present case.

$-\overline{u't'}$ Profiles

Profiles of the streamwise component of the turbulent heat flux, $-\overline{u't'}$, are shown in Fig. 7.32. The $-\overline{u't'}$ values are 2 to 3 times larger than the $\overline{v't'}$ values shown in Fig. 7.31. As in the $dU_{cw}/dx=29\ s^{-1}$ case, the correlation coefficient for the normal component of the turbulent heat flux, $\frac{\overline{v't'}}{(\overline{v'})(\overline{t'})}$, is about 0.3, while the streamwise component correlation, $\frac{-\overline{u't'}}{(\overline{u'})(\overline{t'})}$, is about 0.6.

Eddy Diffusivity of Heat

Profiles of the eddy diffusivity, ε_H, are shown in Fig. 7.33. The profiles collapse in these coordinates and are similar to the eddy viscosity results of Fig. 7.26.

Mixing Length of Heat

Profiles of the thermal mixing length, ℓ_H, are shown in Fig. 7.34. In low FSTI, unaccelerated flow on flat walls, ℓ_H is expected to follow the line $\ell_H = \frac{\kappa}{Pr_t} y$ near the wall. The expected value of Pr_t is about 0.9, and κ=0.41. The ℓ_H values rise above the expected line to high values at the edge of the boundary layer. Near the wall, the ℓ_H data lie fairly close to the line, unlike the mixing length of momentum (Fig. 7.27), which had a lower slope than expected near the wall. The data is this case agree with the data of the $dU_{cw}/dx=29\ s^{-1}$ case shown in Fig. 6.31.

Turbulent Prandtl Number

Profiles of the turbulent Prandtl number, Pr_t, are shown in Fig. 7.35. Very near the wall ($y^+<50$) the measurements cannot be trusted due to spatial resolution problems. Far from the wall ($y^+>400$) the mean velocity and temperature gradients become too small for accurate calculation of Pr_t (the uncertainty rises to several hundred percent). In the range $50<y^+<400$, Pr_t lies between 0.9 and 1.3. This range is slightly above the standard value of 0.9, but, given the uncertainty in the measured data, this difference may not be significant. It appears that Reynold's analogy between eddy transport of heat and momentum is obeyed in this flow, as it was in the $dU_{cw}/dx=29\ s^{-1}$ case.

Cross Transport of Turbulent Shear Stress and Turbulent Heat Flux

Profiles of the triple correlations $\overline{u'v'^2}$ and $\overline{v'^2t'}$ are shown in Figs. 7.36 and 7.37. These terms are related to the rate at which the turbulent shear stress and turbulent heat flux are transported away from the wall by turbulent diffusion. Shown for comparison are profiles from 8% FSTI, unaccelerated, flat-wall and concave-wall cases from Kim and Simon (1991). The accelerated flow profiles rise as the flow proceeds downstream, through transition. Values of normalized $\overline{u'v'^2}$ are lower than those of the $dU_{cw}/dx=29\ s^{-1}$ case (Fig. 6.33) and lower than the values from the unaccelerated flat-wall case. The stronger acceleration of the present case suppresses the $\overline{u'v'^2}$ values. Values of normalized $\overline{v'^2t'}$ are over double those of the $dU_{cw}/dx=29\ s^{-1}$ case (Fig. 6.34), and as much as 12 times the values in the unaccelerated flow cases. Possibly, a different choice of non-dimensionalization would help in analyzing the data.

OCTANT ANALYSIS

The octant analysis, described above in Chapter 4, has been applied to the present, accelerated flow. In general, the results agree with those discussed in the preceding chapters. Profiles of the octant decomposition of the turbulent shear stress are shown in

Fig. 7.38. Data were acquired at stations 1 through 8. The flow appears transitional at all stations. The octant decomposition is similar to that of the unaccelerated transitional flows discussed in Chapter 4. Octant 6, the hot ejection, makes the largest contribution to $-\overline{u'v'}$. At the upstream stations, the octant 6 contribution is about three times the octant 4 (cold sweep) contribution. At the downstream stations, the octant 6 contribution is about twice the octant 4 contribution. Near the wall, octants 7 and 3 are significant. Octant 7 is the hot wallward interaction. It was seen in the unaccelerated transitional flows and was attributed to incomplete turbulent mixing. Also significant in the present case is octant 3, which has the same sign and magnitude as octant 7. Octant 3 is the cold wallward interaction. Cold, slow fluid moves toward the wall causing a reduction in the overall turbulent shear stress. The mechanism responsible for the octant 3 motion is not known, but it may be related to the difference between the momentum and thermal boundary layer thicknesses. A direct numerical simulation might be useful for determining the source of the octant 3 data.

The octant distributions never reach the fully-turbulent distribution described in Chapter 4 and seen at the downstream stations in the $dU_{cw}/dx=29\ s^{-1}$ case (Fig. 6.35c). Even at the most downstream station in the present case (station 8, Fig. 7.38h), a transitional distribution is observed. The strong acceleration prevents the present flow from achieving a mature turbulent state.

The octant decomposition of the normal component of the turbulent heat flux, $\overline{v't'}$, is shown for stations 1 through 8 in Fig. 7.39. The results are similar to those for the turbulent shear stress, but some differences appear. Octant 3 makes a significant contribution, as it did with the shear stress, but while octant 3 causes a reduction in the turbulent shear stress, it makes a positive contribution to $\overline{v't'}$. Octant 5 also makes a contribution to $\overline{v't'}$. It has the same sign and magnitude as octant 3. Octant 5 is the hot outward interaction. High speed, warm fluid moves away from the wall. Octant 5 corresponds to u', v' and t' all positive. It is the counter-motion to octant 3, which

corresponds to u′, v′ and t′ all negative. Octants 3 and 5 cause high $\overline{v't'}$ relative to $-\overline{u'v'}$. This was noted above (Figs. 7.25 and 7.31), and indicates that the acceleration has a stronger influence on the momentum boundary layer than the thermal boundary layer. As noted in Chapter 6, the turbulent Prandtl number is not changed by the octant 3 and 5 contributions. Although $\overline{v't'}$ and $-\overline{u'v'}$ are affected differently by acceleration, the differences between the mean velocity and temperature gradients (which also factor into Pr_t) keep Pr_t approximately equal to 1.

BOUNDARY LAYER SPECTRA AND TRANSFER FUNCTIONS

Boundary layer spectra were measured at stations 1, 2, 3, 4, 5, 7 and 9. The u′ spectra acquired near the wall at y^+=5 are shown in Fig. 7.40. The peak in u′ energy is at 70 Hz at station 1 (Fig. 6.37b). The peak rises steadily and remains at 70 Hz through station 5. Between stations 5 and 7 the growth in u′ is accelerated and the peaks shift to 200 Hz. Between stations 7 and 9 the peaks continue to shift to 300 Hz, as higher frequency fluctuations become more significant. The u′ spectra acquired at y^+=17 are shown in Fig. 7.41. The spectra at y^+=5 and y^+=17 are similar. Fluctuations are concentrated at the same frequencies at both y positions. The spectra have larger magnitudes at y^+=17, since this is the location of maximum $\overline{u'}$ in the boundary layer (Fig. 7.21). Near-wall damping results in lower values at y^+=5. The u′ spectra acquired at y^+=50 are shown in Fig. 7.42. The peak energy is at 60 Hz at station 1. The peaks rise in magnitude and remain at 60 Hz through station 5. Between stations 5 and 9, there is little change below 100 Hz, but significant growth at higher frequencies. At station 9, the fluctuation energy is centered around 300 Hz, agreeing with the results at y^+=5 and y^+=17.

The v′ spectra acquired at y^+=50 are shown in Fig. 7.43. The peaks in v′ energy are at 200 Hz at stations 1 through 5, shifting to 400 Hz at stations 7 and 9. The levels of

the peaks rise steadily between stations 1 and 5, but rise more rapidly between stations 5 and 7, as the boundary layer undergoes the end stages of transition. A comparison of Figs. 7.42 and 7.43 shows that there is more low-frequency energy in u' than in v' at $y^+=50$. The same trends were observed in the $dU_{cw}/dx=29\ s^{-1}$ case in Chapter 6 (Figs. 6.39 and 6.40). The low-frequency behavior supports the conclusion that the low-frequency fluctuations are associated with streamwise unsteadiness.

The turbulent shear stress, $-\overline{u'v'}$, is the important turbulence quantity for transport of momentum. Figure 7.44 shows the spectra of $-\overline{u'v'}$ measured at $y^+=50$. At the station 1, there is relatively little energy in $-\overline{u'v'}$ and the peak is around 100 Hz. Between stations 1 and 2 there is little change, suggesting a lack of near-wall turbulence production. Moving to the third, fourth and fifth stations, there is some growth in $-\overline{u'v'}$, particularly at the higher frequencies, but the overall levels remain relatively low compared to downstream levels. The correlation $-\overline{u'v'}$ rises sharply as the flow moves to stations 7 and 9, and the peak in $-\overline{u'v'}$ shifts to 600 Hz. These stations correspond to the end of transition where near-wall turbulence production at higher frequencies is believed to be important. At station 9, the flow is fully turbulent, although not mature. The behavior of the turbulent shear stress is similar to that observed in v' in Fig. 7.43, but the change between station 5 and 7 is more pronounced in $-\overline{u'v'}$ than in v'. The growth in v' and $-\overline{u'v'}$ observed at the downstream stations in the present case were observed from the first station in the $dU_{cw}/dx=29\ s^{-1}$ case of Chapter 6 (Figs. 6.40 and 6.41). In the present case, the upstream stations are either pre-transitional or "frozen" in the early stages of transition by the strong acceleration.

Transfer Functions

Figure 7.45 shows the transfer function of u' between the boundary layer at $y^+=5$ and the free-stream. At the first streamwise position, the boundary layer and free-stream have about the same energy between 0 and 10 Hz. Between 10 and 400 Hz there is more

energy in the boundary layer. This peak in the transfer function is centered around 100 Hz, which corresponds to the peak in the free-stream v′ spectra in Fig. 7.4. This correlation between the u′ transfer function and the free-stream v′ spectrum was also seen in the low-FSTI case in Figs. 3.3, 3.6 and 3.8. The same correlation was seen in the $dU_{cw}/dx=29\ s^{-1}$ case, as shown in Figs. 6.4 and 6.42. In the present case, there is much less energy above 400 Hz in the boundary layer than in the free-stream. The boundary layer appears to damp out the high-frequency fluctuations, acting as a low-pass filter. This behavior also agrees with that of the low-FSTI case. At the downstream stations, the transfer functions remain above 1.0 for all frequencies. The peaks at 100 Hz remain, but the most significant growth occurs above 400 Hz. This again agrees with the low-FSTI case, although the actual values of the transfer functions are lower in the high-FSTI case, due to the higher levels of free-stream u′ in this case.

Figure 7.46 shows the u′ transfer function between the boundary layer at the position of maximum u′ ($y^+=17$) and the free-stream. The level of the transfer function is higher at this location than at $y^+=5$ (Fig. 7.45), but the trends are the same in both figures. The same general trends can be seen in the u′ transfer function between the boundary layer at $y^+=50$ and the free-stream, as shown in Fig. 7.47. Note that there is less high frequency damping at $y^+=50$ than at $y^+=5$.

Figure 7.48 shows the v′ transfer function between $y^+=50$ and the free-stream. The transfer function increases with frequency at all streamwise positions and increases across the entire spectrum with streamwise position. Above 400 Hz, the u′ and v′ transfer functions of Figs. 7.47 and 7.48 are similar. Below 400 Hz they are quite different. The v′ transfer function is lower and does not exhibit the 100 Hz peak seen in the u′ transfer function.

The results presented in Figs. 7.47 and 7.48 are consistent with the explanations proposed in Chapter 3 for the low-FSTI case. Free-stream eddies buffet the boundary layer causing a displacement of fluid in the y direction. As depicted in Fig. 3.7, this

displacement, combined with the normal gradient of streamwise velocity, $\frac{\partial \overline{U}}{\partial y}$, leads to an amplification of u' fluctuations at a frequency which is associated with the free-stream eddies. This explains the 100 Hz peak in Fig. 7.47. One would not expect a similar amplification of v', since the gradient $\frac{\partial \overline{V}}{\partial y}$ is small. As expected, there is no 100 Hz peak in Fig. 7.48. The highest frequencies in the boundary layer are associated with turbulence produced in the near-wall region. At these frequencies, u' and v' are similar, suggesting isotropy of the smaller eddies.

Turbulent shear stress. The transfer function can be used to relate the turbulent shear stress to the fluctuation levels of u' or v'. Figure 7.49 shows the transfer function between $-\overline{u'v'}$ at $y^+=50$ and u' at the same position. The transfer function is about 0.1 for frequencies below 50 Hz and rises to between 0.4 and 0.7 at 5000 Hz. The high-frequency values tend to rise with increasing streamwise distance, reaching an asymptotic position at downstream stations. The $dU_{cw}/dx=29\ s^{-1}$ case, as shown in Fig. 6.44, exhibited the same asymptotic values. Figure 7.50 shows the transfer function between $-\overline{u'v'}$ and v'. At the first station, $-\overline{u'v'}$ is much higher than v' in the low-frequency range. At the other stations, the transfer function is fairly flat with frequency. There does not appear to be any consistent trend with streamwise position after station 2.

The 100 Hz peaks in $-\overline{u'v'}$ at the upstream stations, shown in Fig. 7.44, suggest that the free-stream does have an effect in enhancing the momentum transport in the boundary layer. Free-stream eddies buffeting the boundary layer could enhance mixing in the boundary layer to levels which are significantly above the level in a truly laminar flow, but the free-stream eddies would not be so effective in promoting mixing as are the turbulent eddies produced and residing within the boundary layer. This speculation is supported by the lower correlation between $-\overline{u'v'}$ and u' at the lower frequencies than at the high frequencies, as shown in Fig. 7.49. In agreement with this, Hancock and

Bradshaw (1989) reported a stronger effect of the free-stream turbulence on $\overline{u'^2}$ than on $-\overline{u'v'}$.

The above results are complemented and supported by the octant analysis results presented above. Based on the octant distribution, it was concluded that the lower $-\overline{u'v'}$ levels in the transitional flow are due to a lack of small-scale eddies.

CONCLUSIONS

An extended transition zone has been documented in the present case. Included is documentation of pre-transitional or early transitional flow at the upstream stations. The upstream flow is badly disturbed, with high levels of turbulent transport compared to laminar flows, but with lower transport levels than the fully-turbulent flow at the downstream stations. Fluctuations at the upstream stations appear to be induced mainly by the free-stream at relatively low frequencies. Downstream, near wall turbulence production results in higher frequency fluctuations. Skin friction coefficients and Stanton numbers drop below flat-wall turbulent correlations in the transitional flow. As the flow becomes fully-turbulent, C_f rises above a low-FSTI flat-wall correlation, and Stanton number rises to match a flat-wall correlation.

Station	1	2	3	4	5	6	7	8	9	10
x [m] †	0.0993	0.1895	0.2607	0.3449	0.4231	0.5033	0.5805	0.6587	0.7353	0.8165
U_{cw} [m/s]	6.56	7.71	8.74	10.26	11.58	12.53	13.60	14.56	15.40	16.93
FSTI [%]	5.30	4.31	3.78	3.06	2.76	2.46	2.19	2.08	1.90	1.73
$\Lambda_{u'_\infty}$ [cm]	4.37	3.34	4.18	3.91	4.72	–	3.42	–	3.79	–
$\Lambda_{v'_\infty}$ [cm]	1.60	2.01	2.26	2.81	3.39	–	3.76	–	3.67	–
$K \times 10^6$	5.29	3.83	2.98	2.18	1.71	1.46	1.24	1.08	0.96	0.80
$Re_x \times 10^{-5}$	0.4102	0.9199	1.4354	2.2111	3.0635	3.9470	4.9460	6.0113	7.1046	8.6686
$\delta_{99.5}$ [cm]	1.610	0.809	0.903	0.628	0.653	0629	0.753	0.741	0.763	0.867
δ^* [mm]	1.00	0.722	0.703	0.573	0.595	0.656	0.712	0.698	0.766	0.771
θ [mm]	0.665	0.427	0.433	0.344	0.358	0.410	0.481	0.484	0.540	0.555
H	1.51	1.69	1.62	1.67	1.66	1.60	1.48	1.44	1.42	1.39
Re_{δ^*}	414	351	387	367	431	514	606	637	740	819
Re_θ	274	207	239	220	259	321	410	442	522	589
$\theta/R \times 10^3$	0.686	0.440	0.446	0.355	0.370	0.423	0.496	0.499	0.557	0.572
$\delta_{99.5}/R$ [%]	1.66	0.83	0.93	0.65	0.67	0.65	0.78	0.76	0.79	0.89
$C_f \times 10^3$	7.20	6.40	6.10	6.20	5.50	5.30	5.85	6.00	5.90	5.80
T_w [°C]	31.30	32.63	33.06	33.32	33.15	32.99	32.60	31.96	31.56	31.24
T_∞ [°C]	27.36	27.32	27.38	27.34	27.33	27.40	27.35	27.39	27.30	27.26
$\delta_{t99.5}$ [cm]	0.410	0.634	0.868	0.909	1.155	1.188	1.791	1.467	1.434	2.420
Δ_2 [mm]	0.306	0.518	0.656	0.740	0.855	0.941	1.321	1.408	1.683	1.867
$Re_{\Delta 2}$	117	232	337	447	589	679	1076	1237	1574	1915
$St \times 10^3$	5.77	3.94	3.22	2.86	2.51	2.57	2.57	2.58	2.44	2.25
$2St/C_f$	1.60	1.23	1.05	0.923	0.914	0.971	0.879	0.859	0.828	0.775

† Mean temperature profiles were acquired 2 cm upstream of these locations. Velocity profile data were extrapolated 2 cm upstream for calculation of Δ_2.

Table 7.1: Parameters for the $dU_{cw}/dx=14\ s^{-1}$ Case

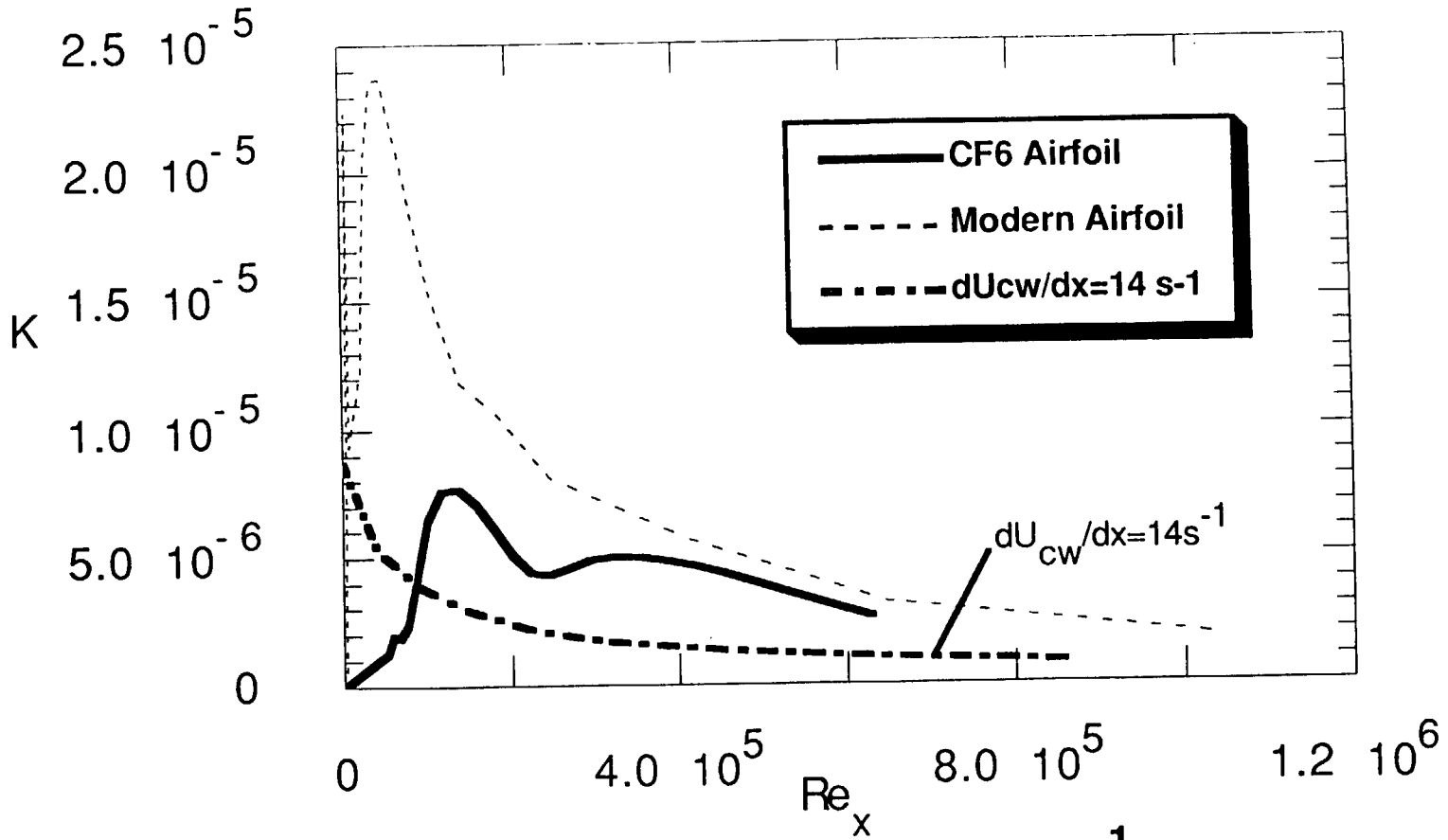

Fig. 7.1: K Profiles for $dU_{cw}/dx = 14\,s^{-1}$ Experiment and the Pressure Side of Typical Turbine Airfoils

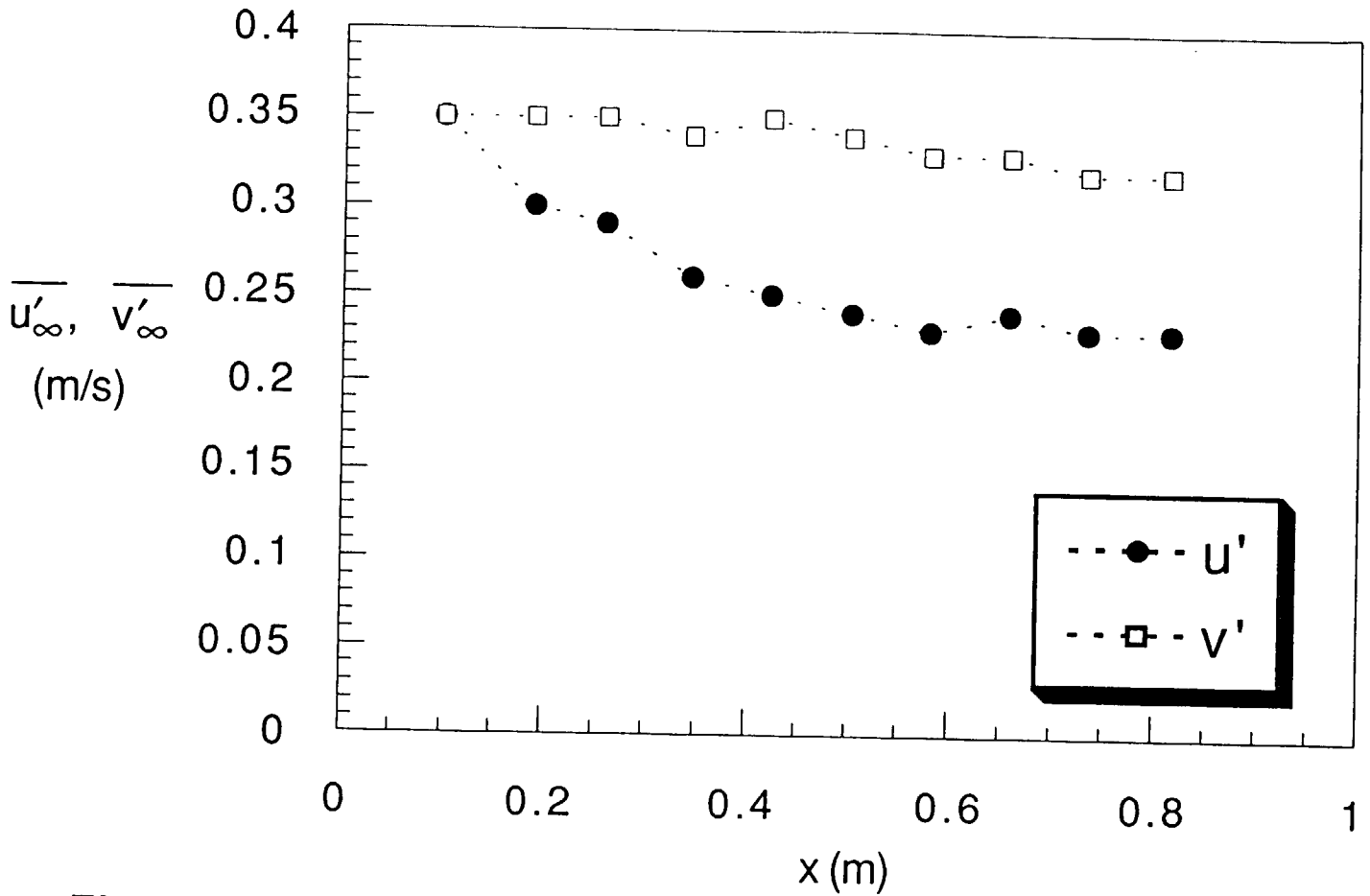

Fig. 7.2a: Free-Stream Turbulence Levels, Dimensional Coordinates, $dU_{cw}/dx=14s^{-1}$ Case

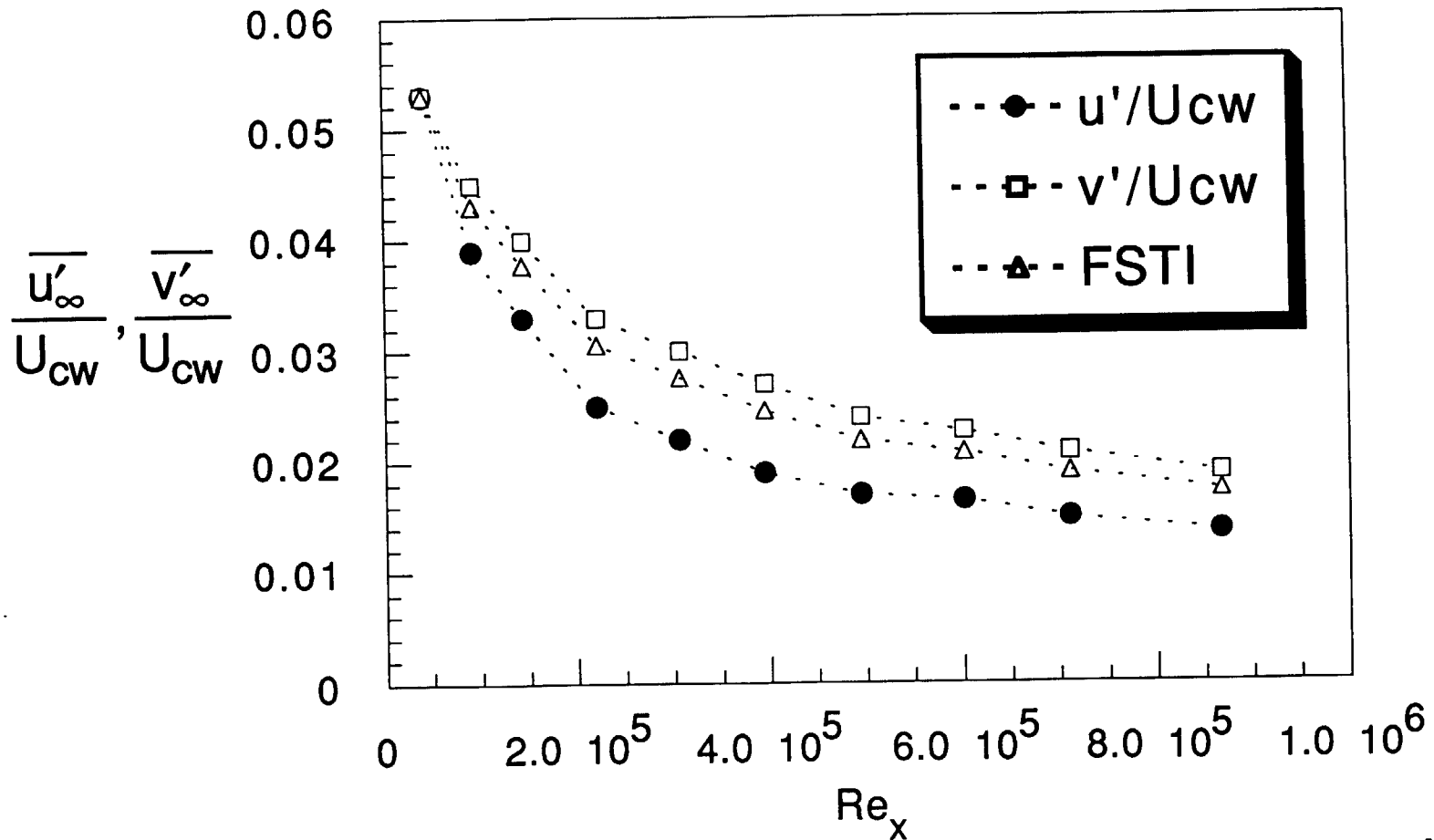

Fig. 7.2b: Free-Stream Turbulence Levels, Nondimensional Coordinates, $dU_{cw}/dx=14s^{-1}$ Case

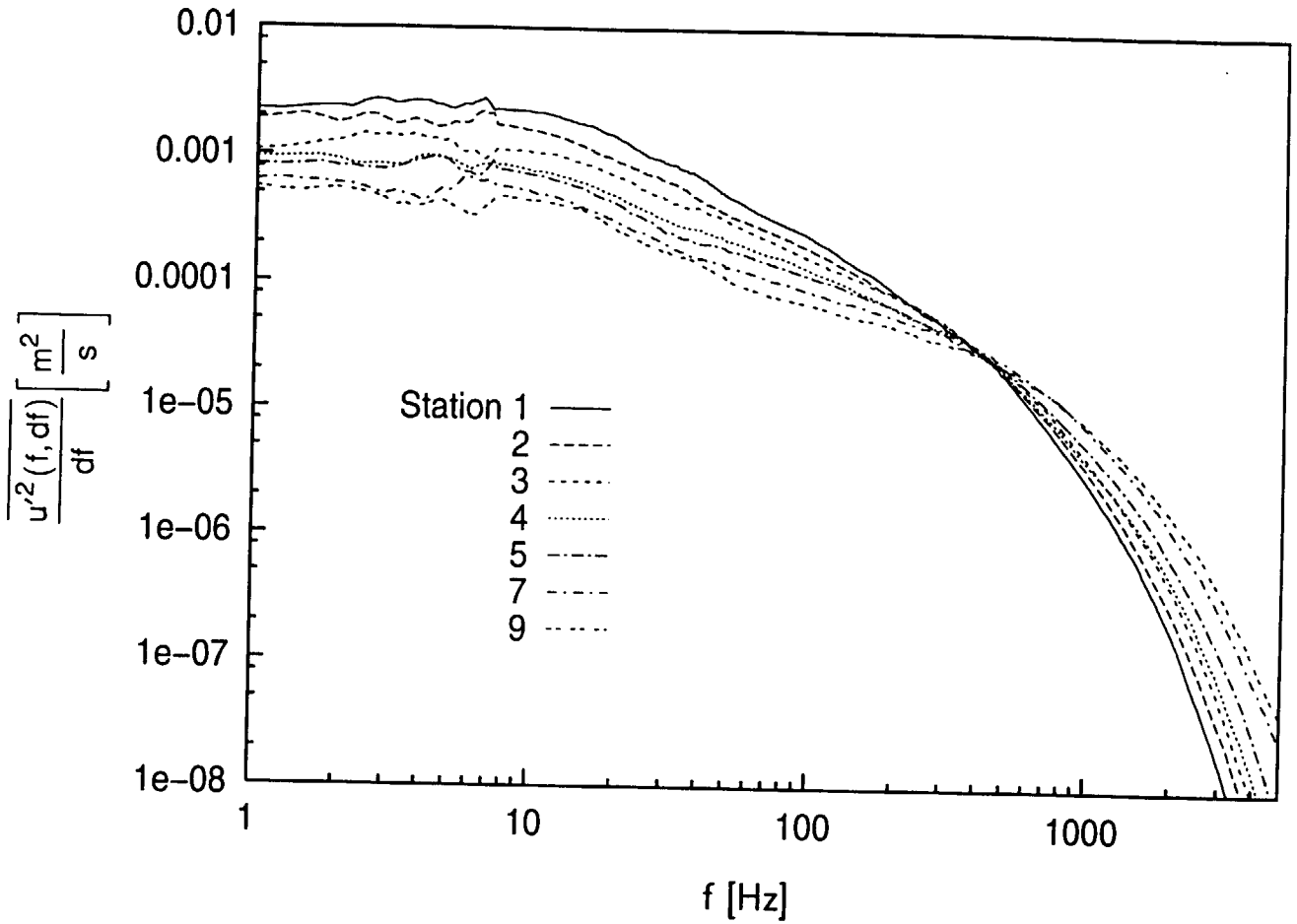

Fig. 7.3a: Free-Stream Spectra of Streamwise Velocity Fluctuations, dU_{cw}/dx=14 s^{-1} Case

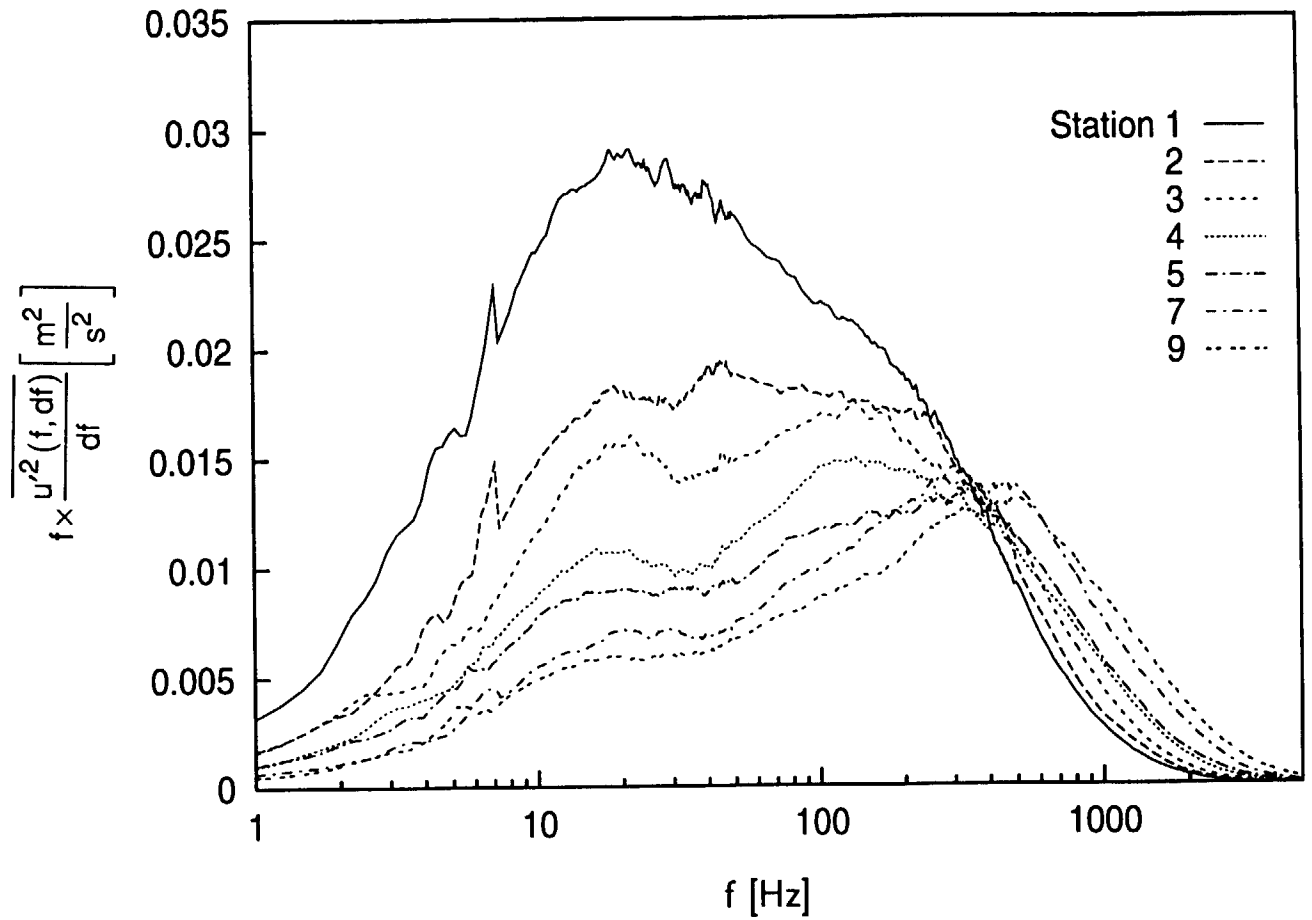

Fig. 7.3b: Free-Stream Spectra of Streamwise Velocity Fluctuations, Energy Coordinates, dU_{cw}/dx=14 s^{-1} Case

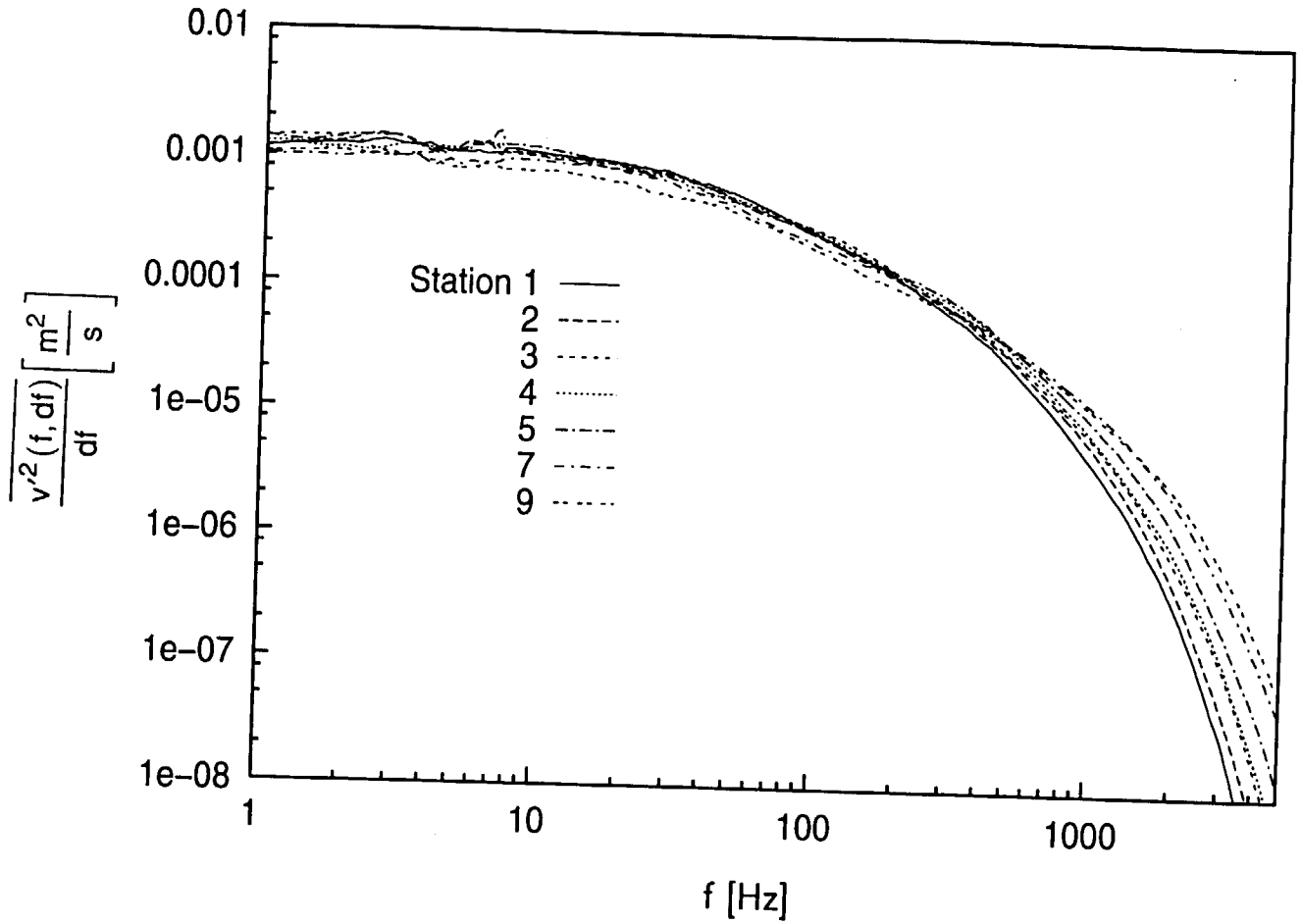

Fig. 7.4a: Free-Stream Spectra of Cross-stream Velocity Fluctuations, $dU_{cw}/dx=14\ s^{-1}$ Case

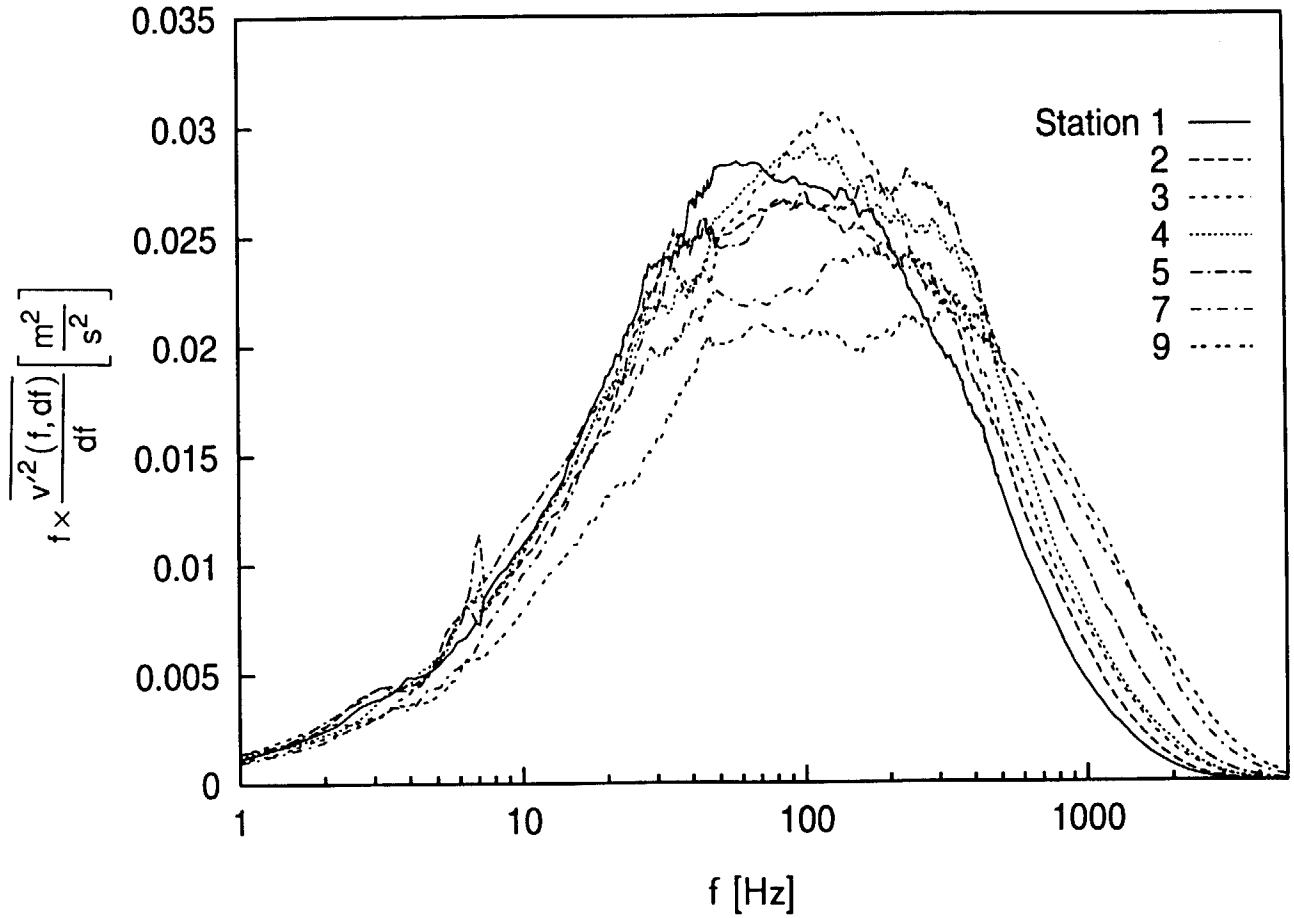

Fig. 7.4b: Free-Stream Spectra of Cross-stream Velocity Fluctuations, Energy Coordinates, dU_{cw}/dx=14 s^{-1} Case

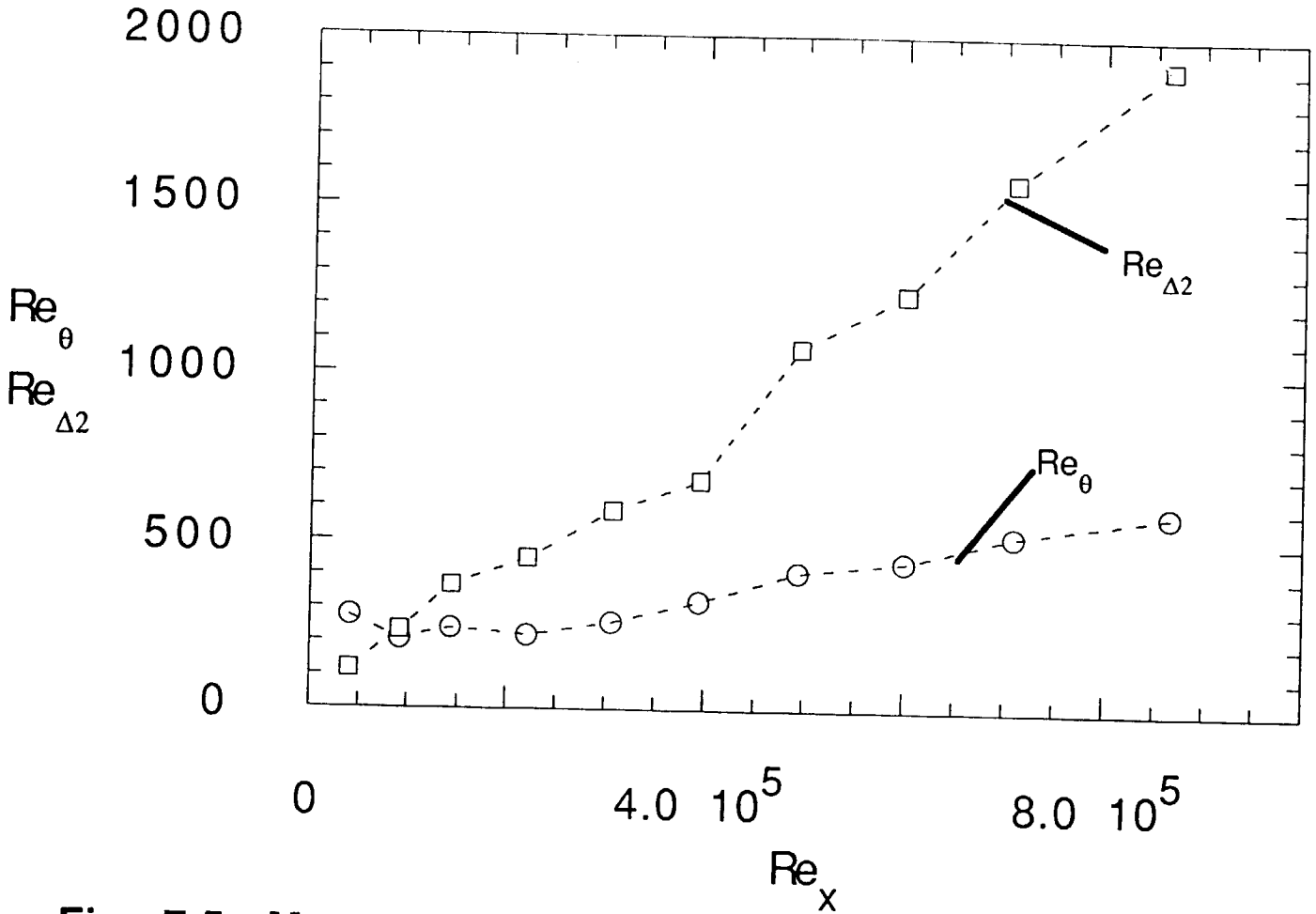

Fig. 7.5: Momentum and Thermal Boundary Layer Growth $dU_{cw}/dx=14s^{-1}$ Case

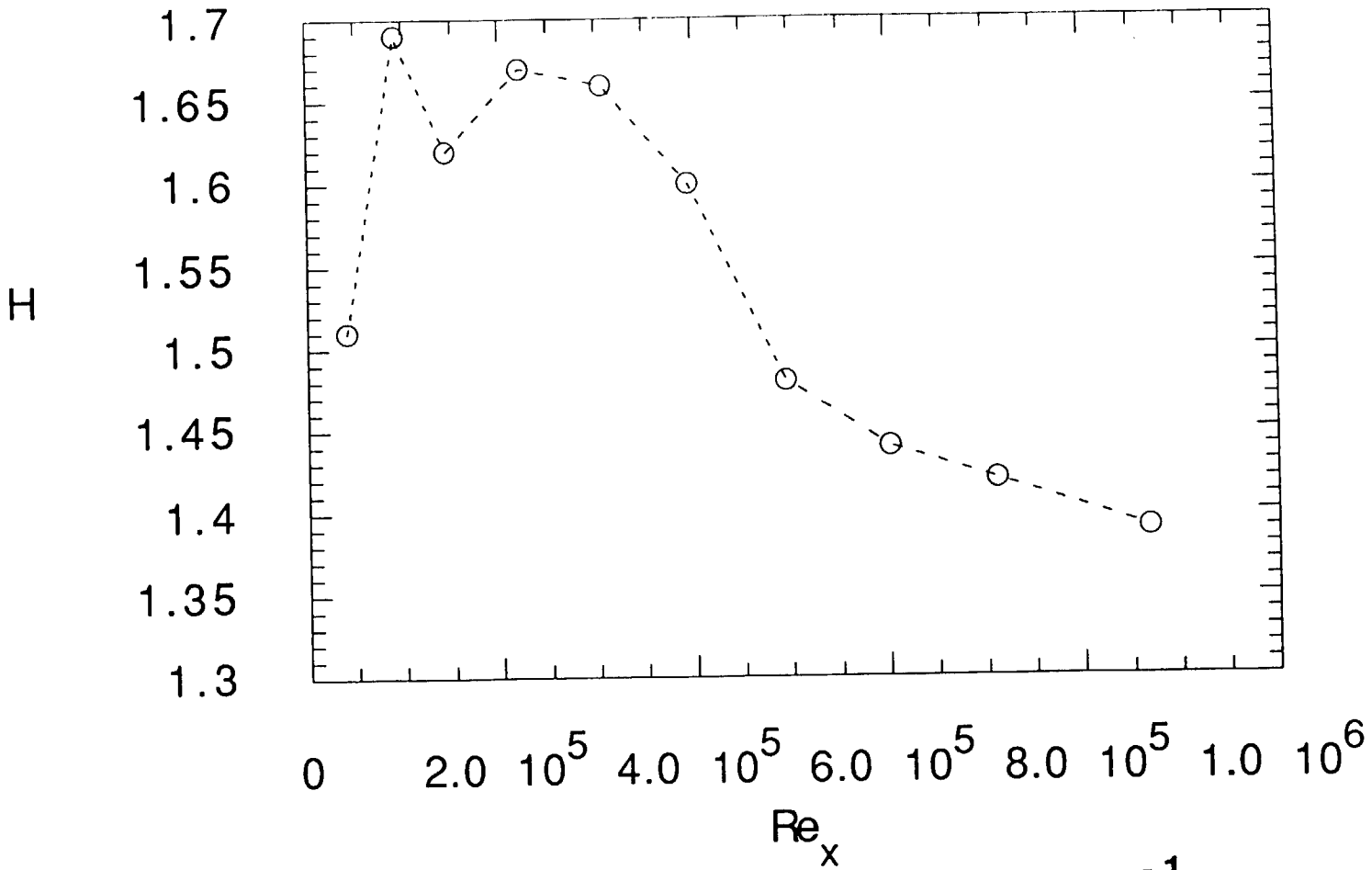

Fig. 7.6: Shape Factor vs Re_x, $dU_{cw}/dx=14s^{-1}$ Case

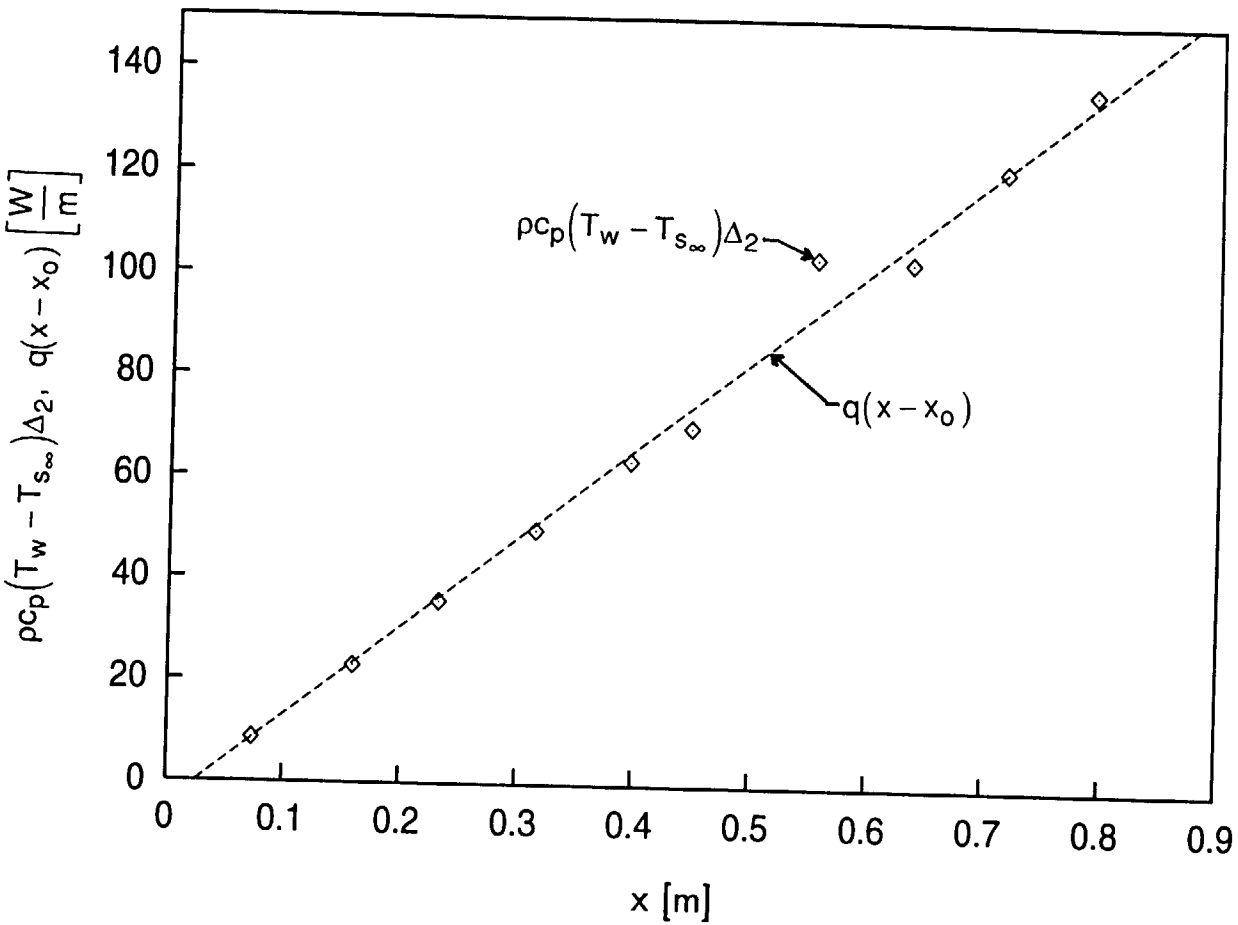

Fig. 7.7: Energy Balance
dU_{cw}/dx=14 s^{-1} Case

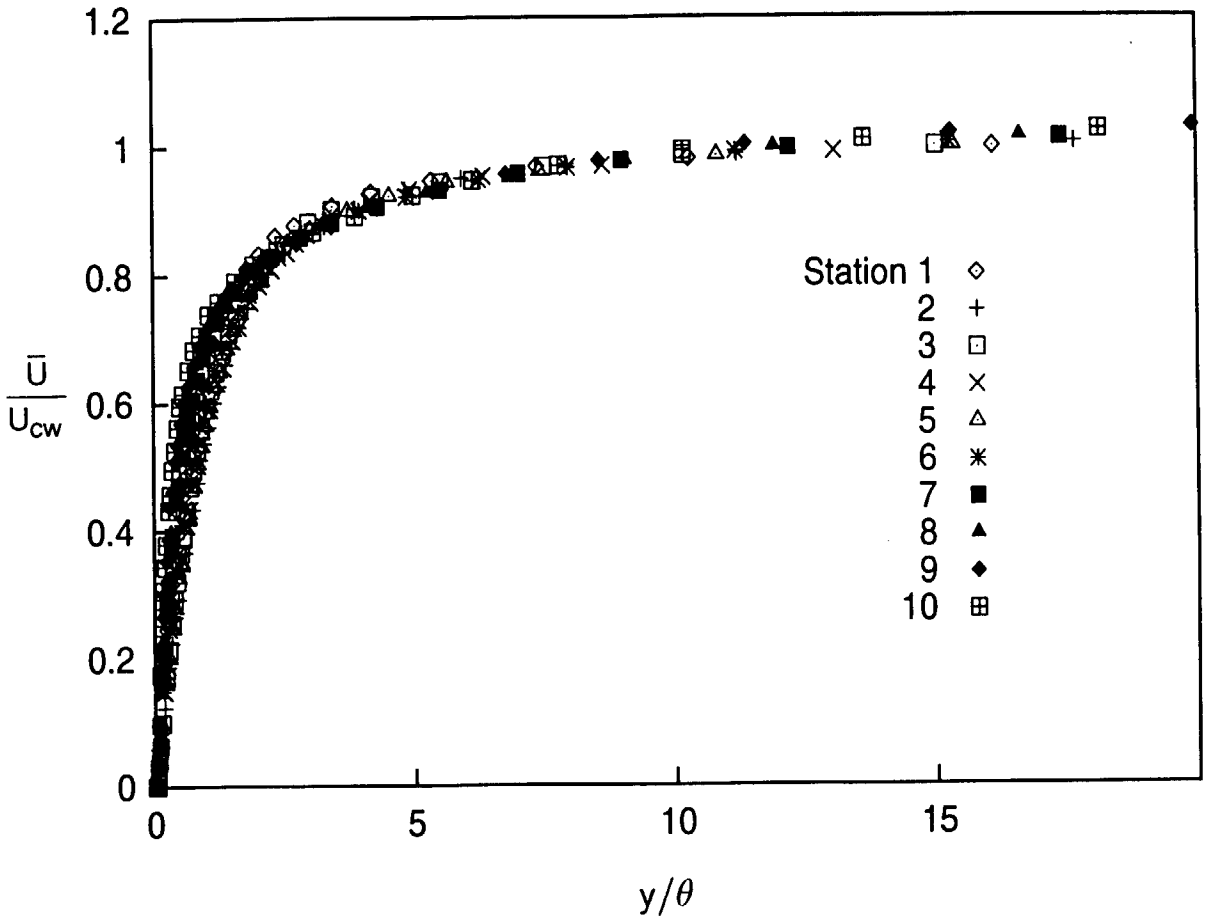

Fig. 7.8a: Mean Velocity Profiles
$dU_{cw}/dx=14\ s^{-1}$ Case

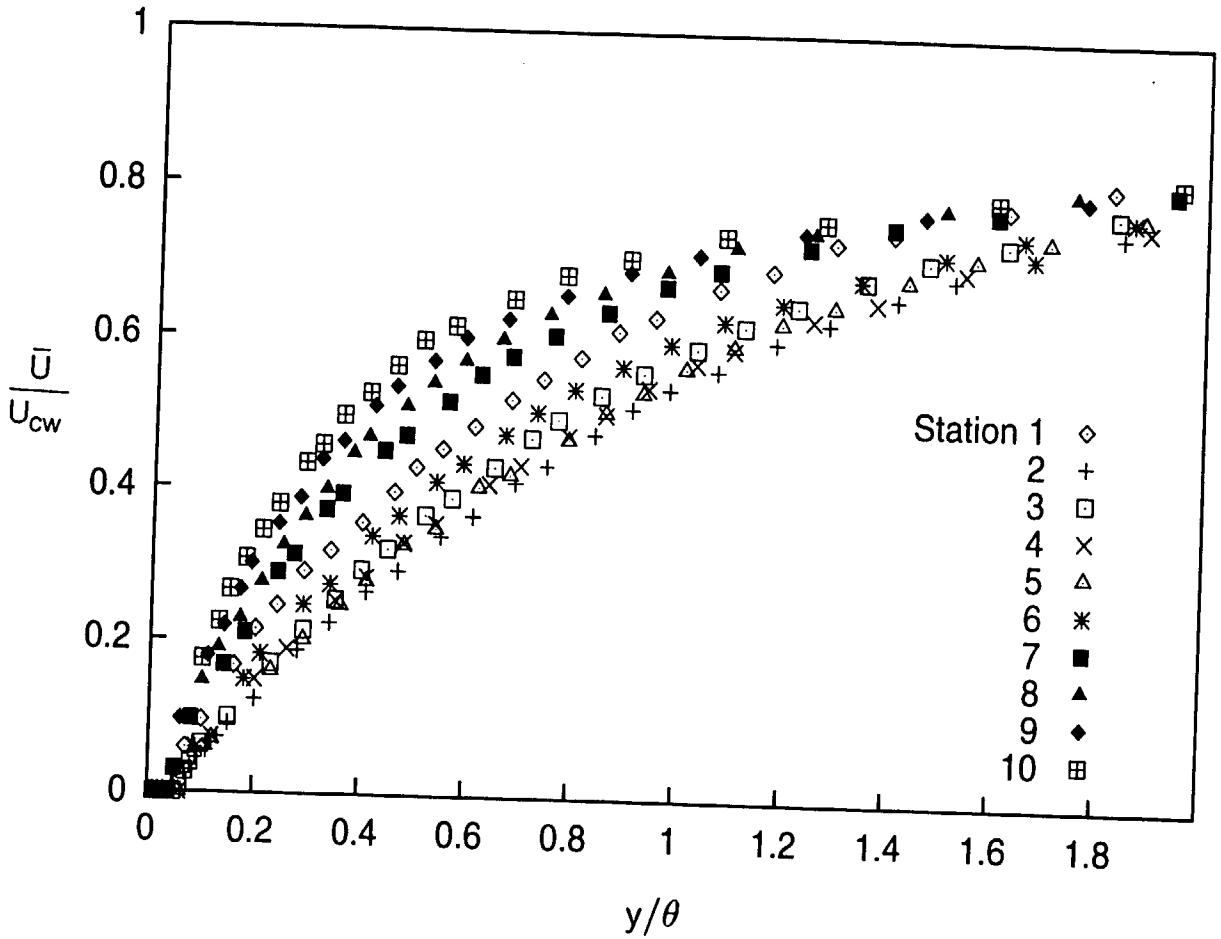

Fig. 7.8b: Mean Velocity Profiles
$dU_{cw}/dx=14\ s^{-1}$ Case

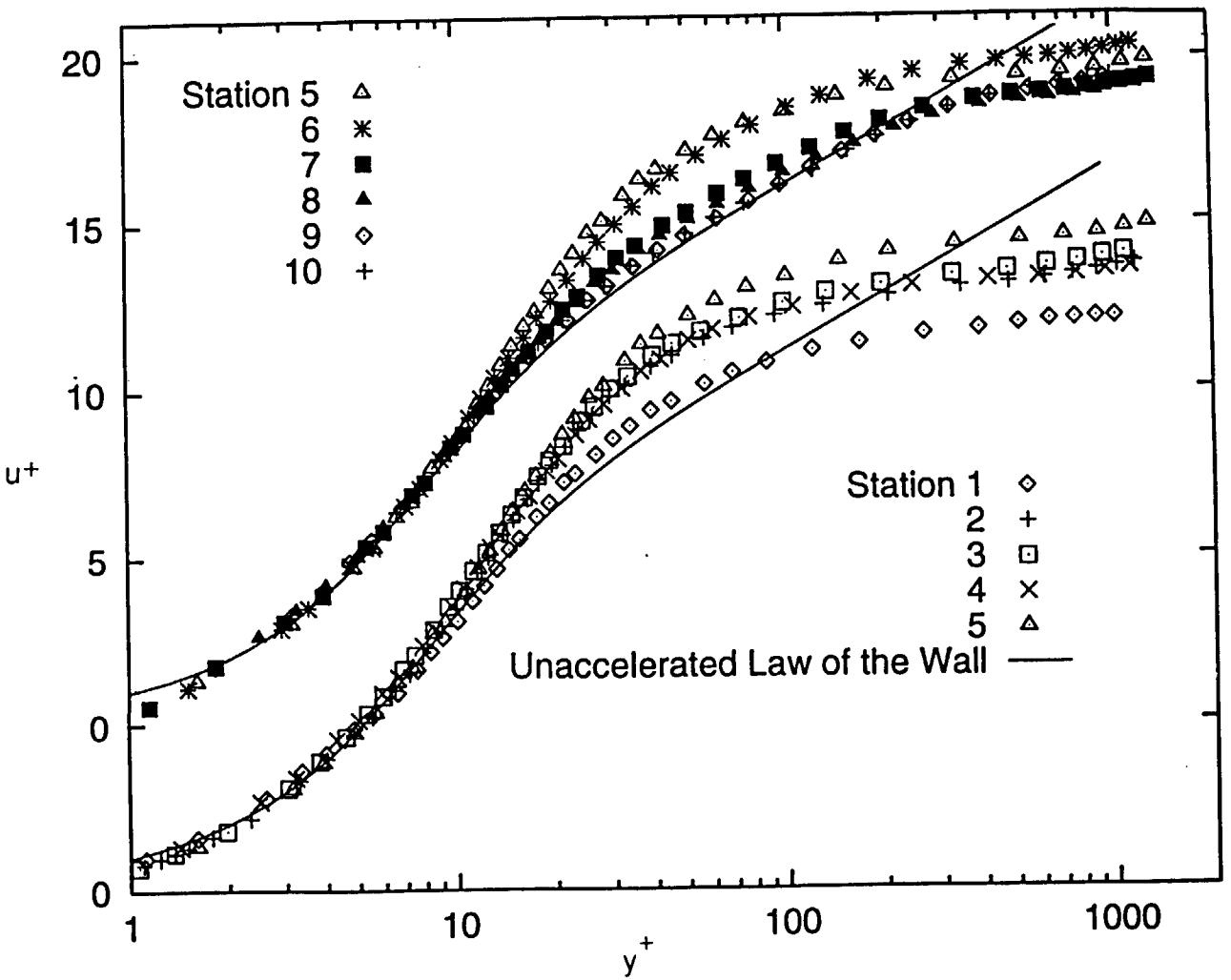

Fig. 7.9: Mean Velocity Profiles, Wall Coordinates
dU_{cw}/dx=14 s^{-1} Case

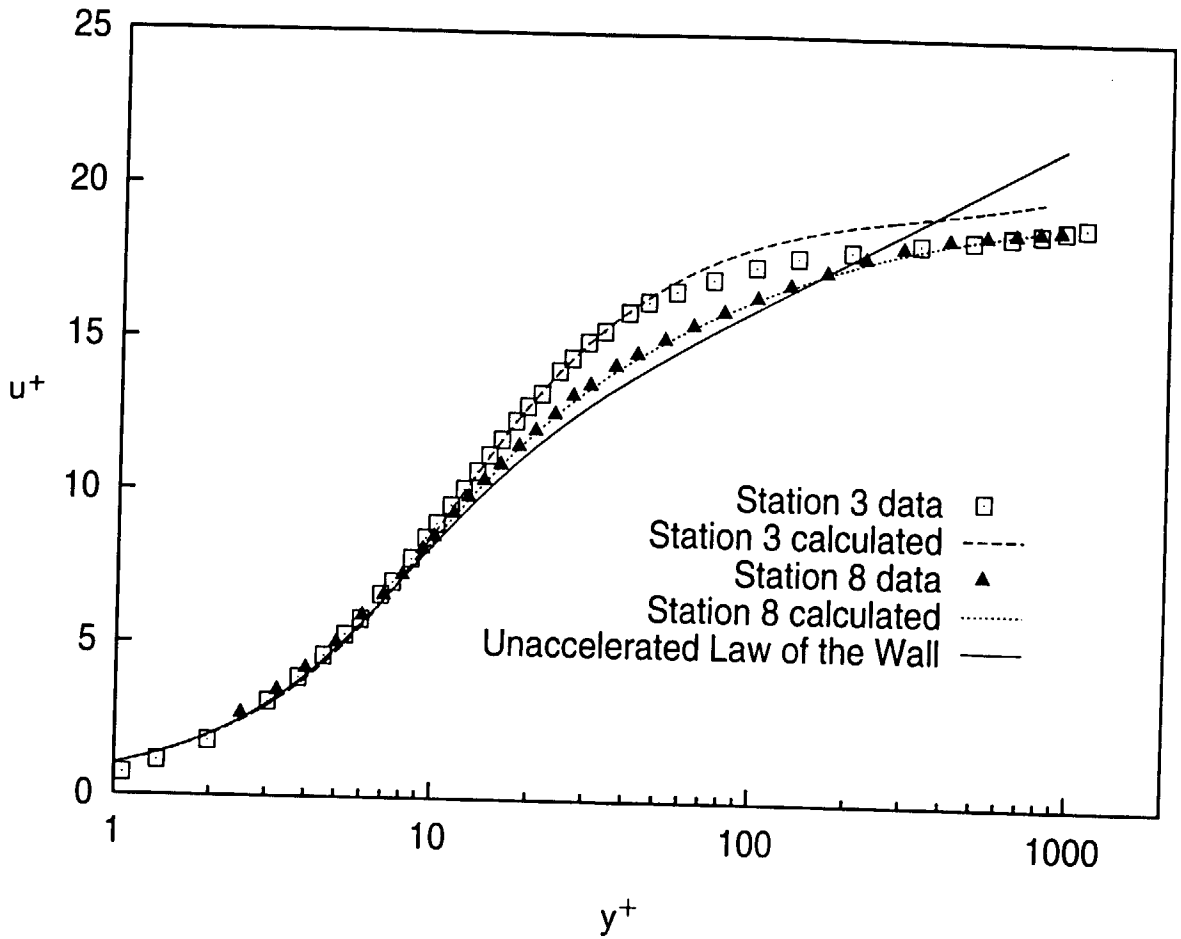

Fig. 7.10: Comparison of Calculated Profiles to Data dU_{cw}/dx=14 s^{-1} Case

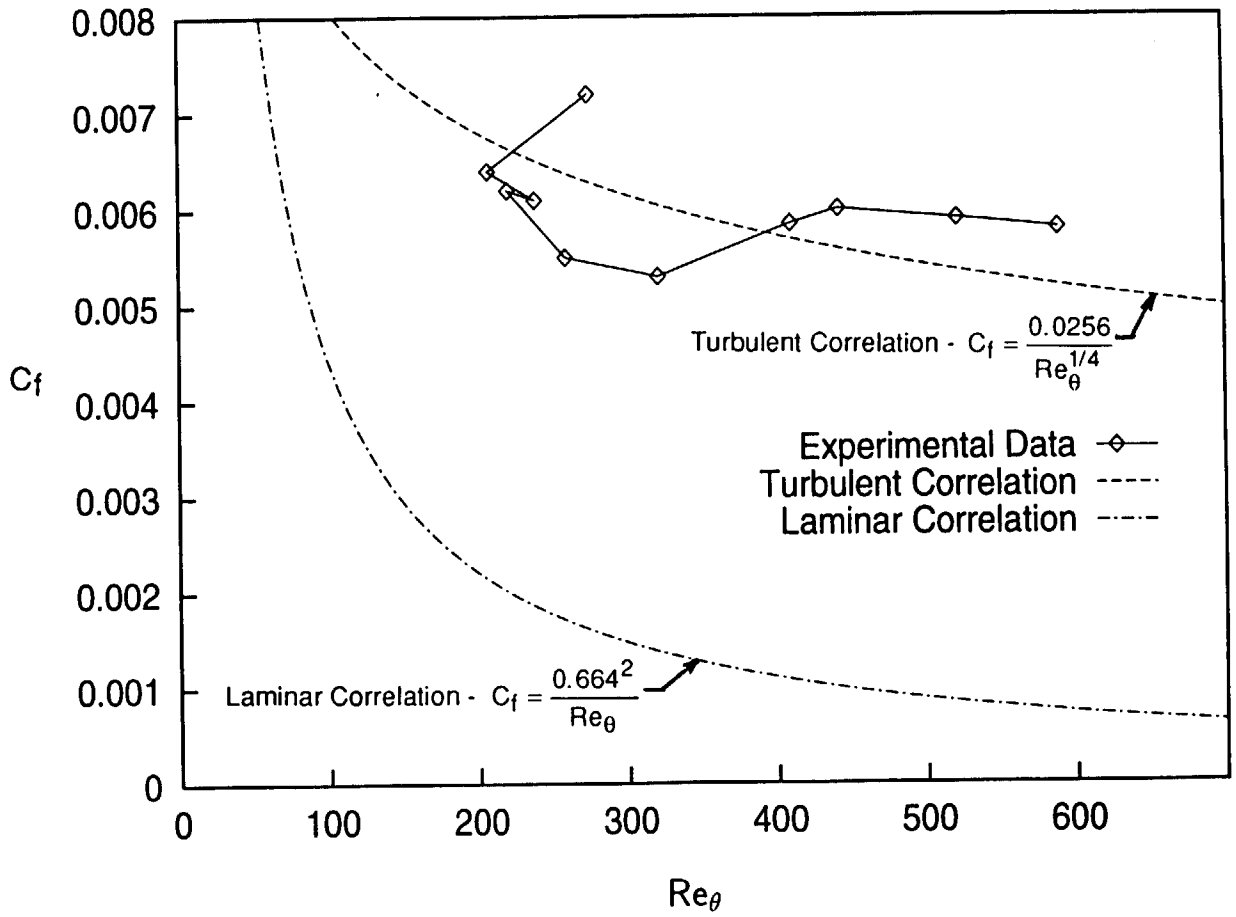

Fig. 7.11: Skin Friction Coefficients vs Re_θ dU_{cw}/dx=14 s^{-1} Case

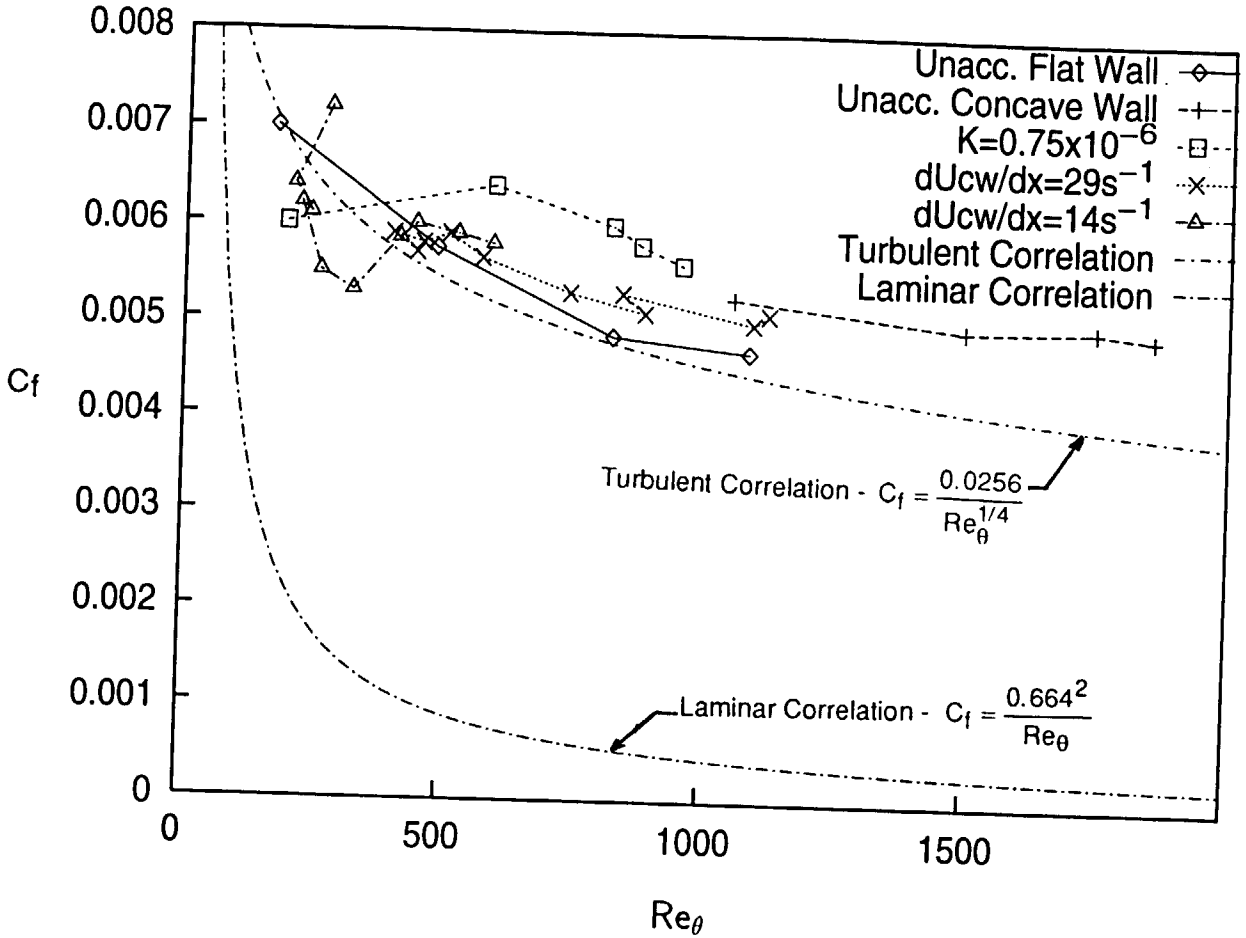

Fig. 7.12a: Skin Friction Coefficients vs Re_θ Comparison of High-FSTI Cases

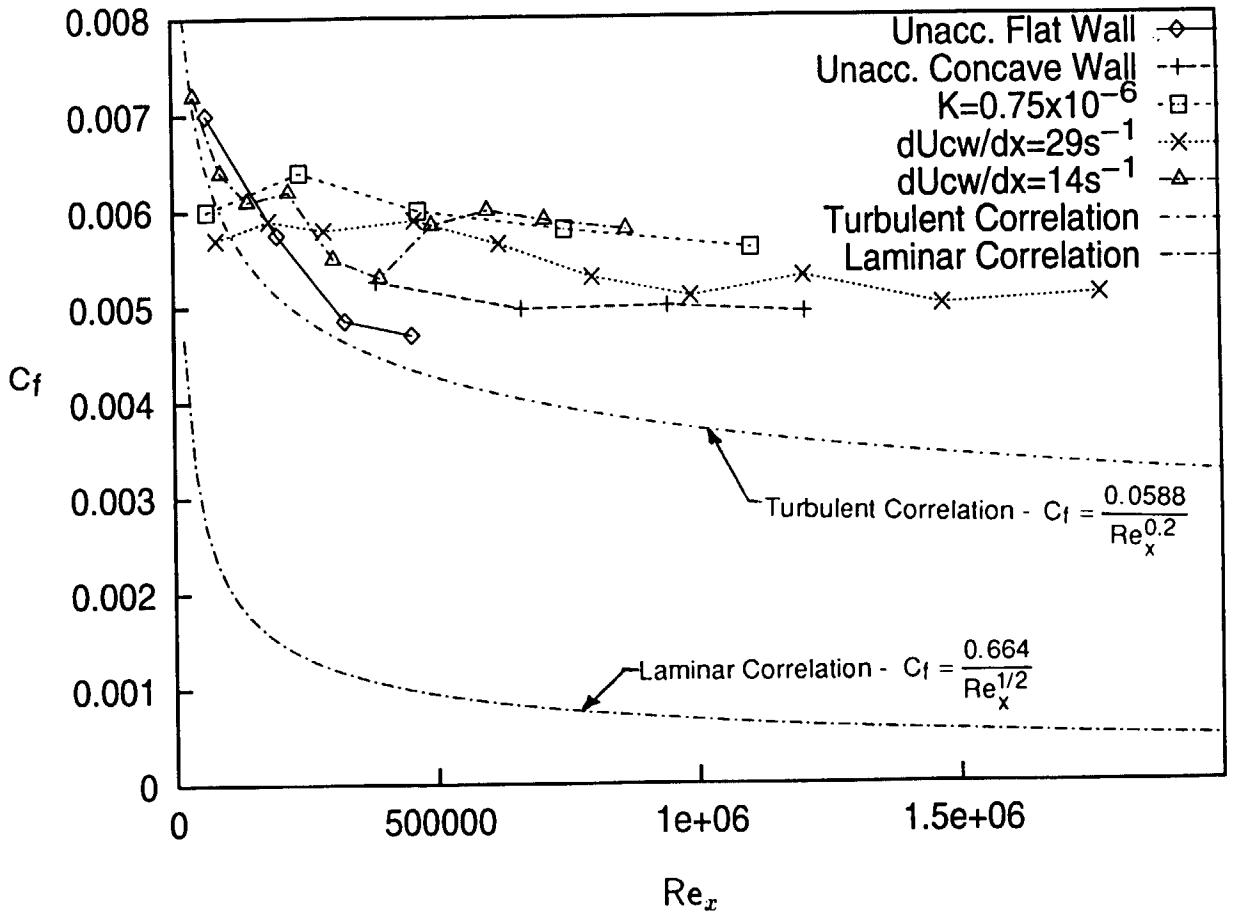

Fig. 7.12b: Skin Friction Coefficients vs Re_x
Comparison of High-FSTI Cases

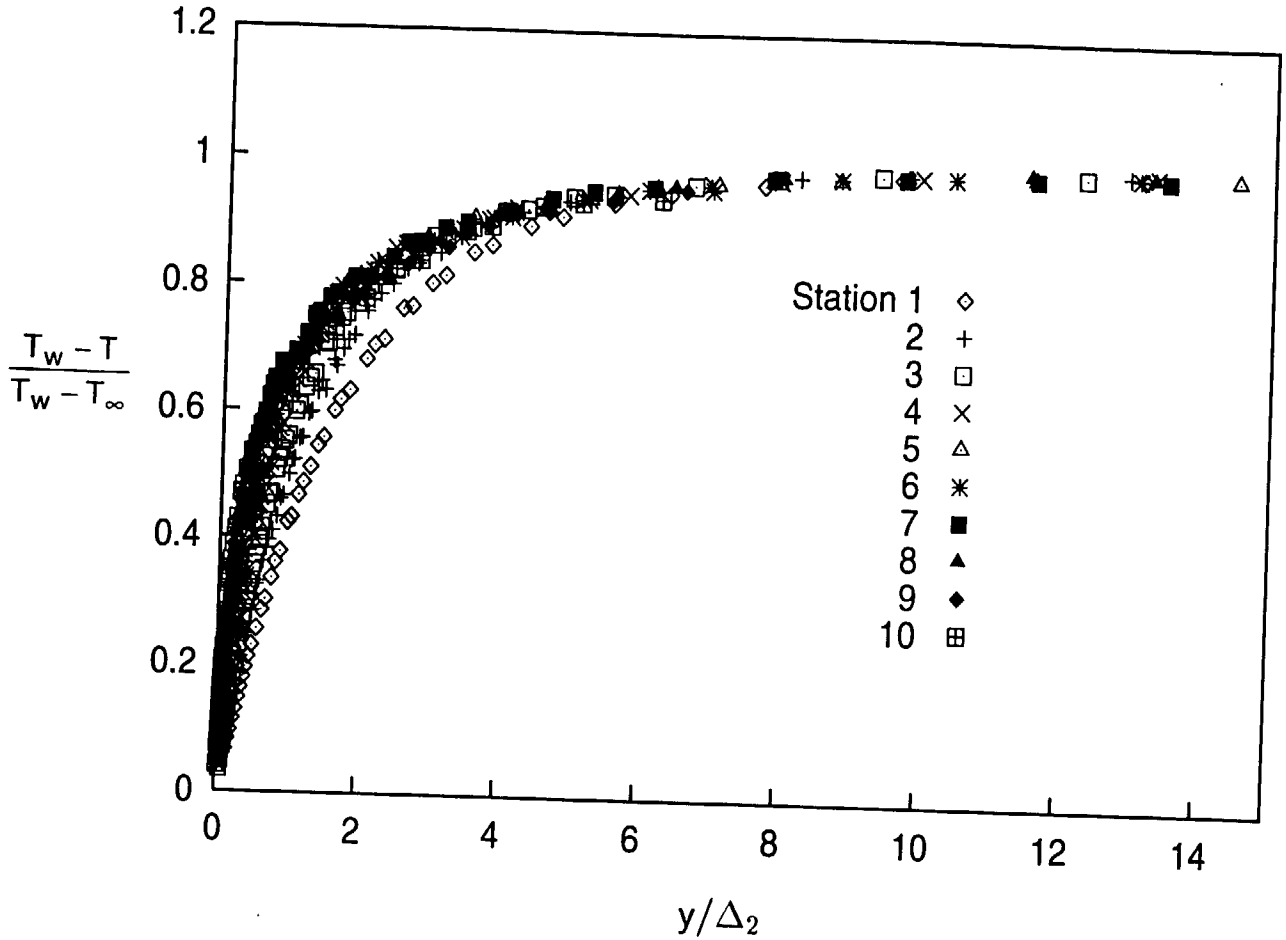

Fig. 7.13a: Mean Temperature Profiles
dU_{cw}/dx=14 s^{-1} Case

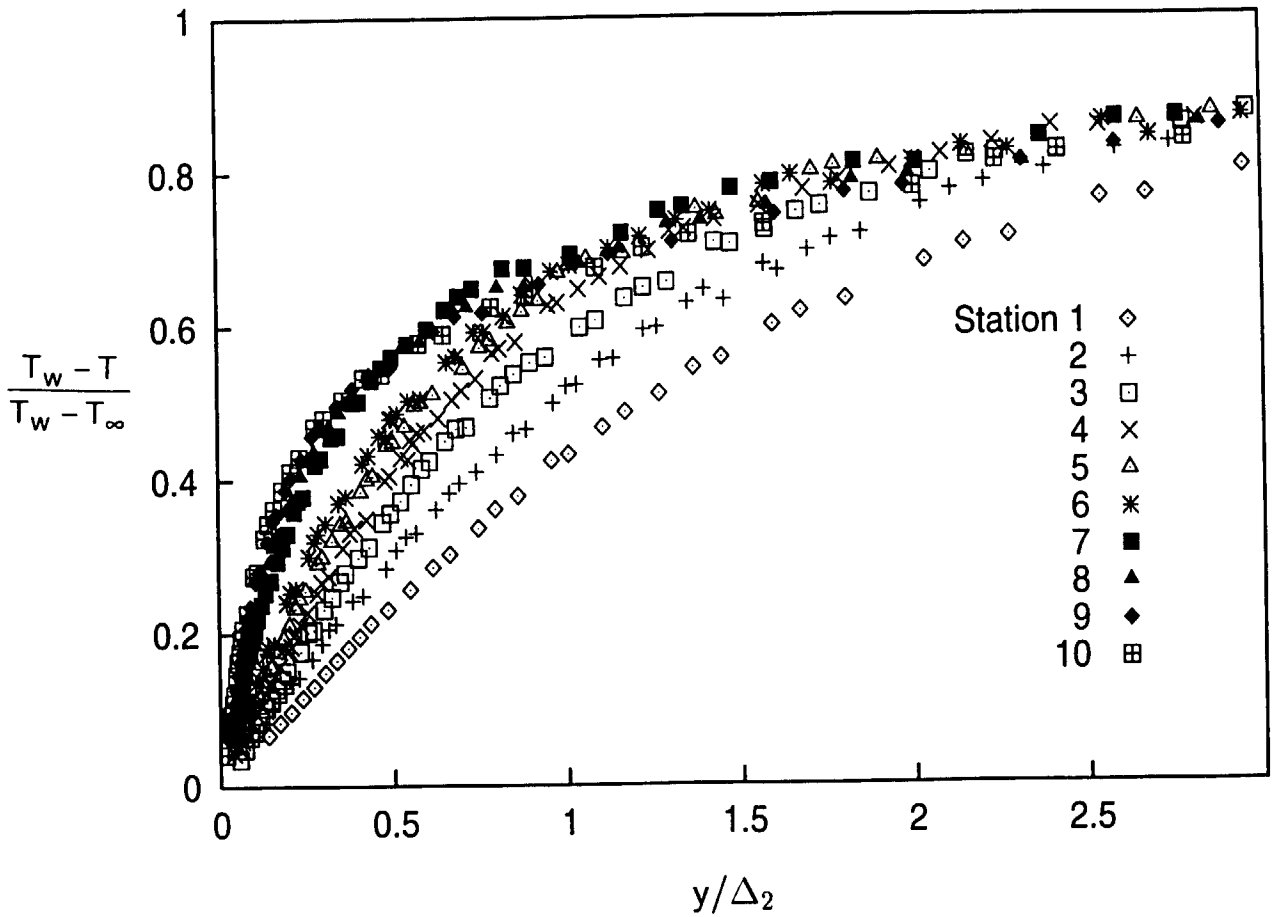

Fig. 7.13b: Mean Temperature Profiles
dU_{cw}/dx=14 s^{-1} Case

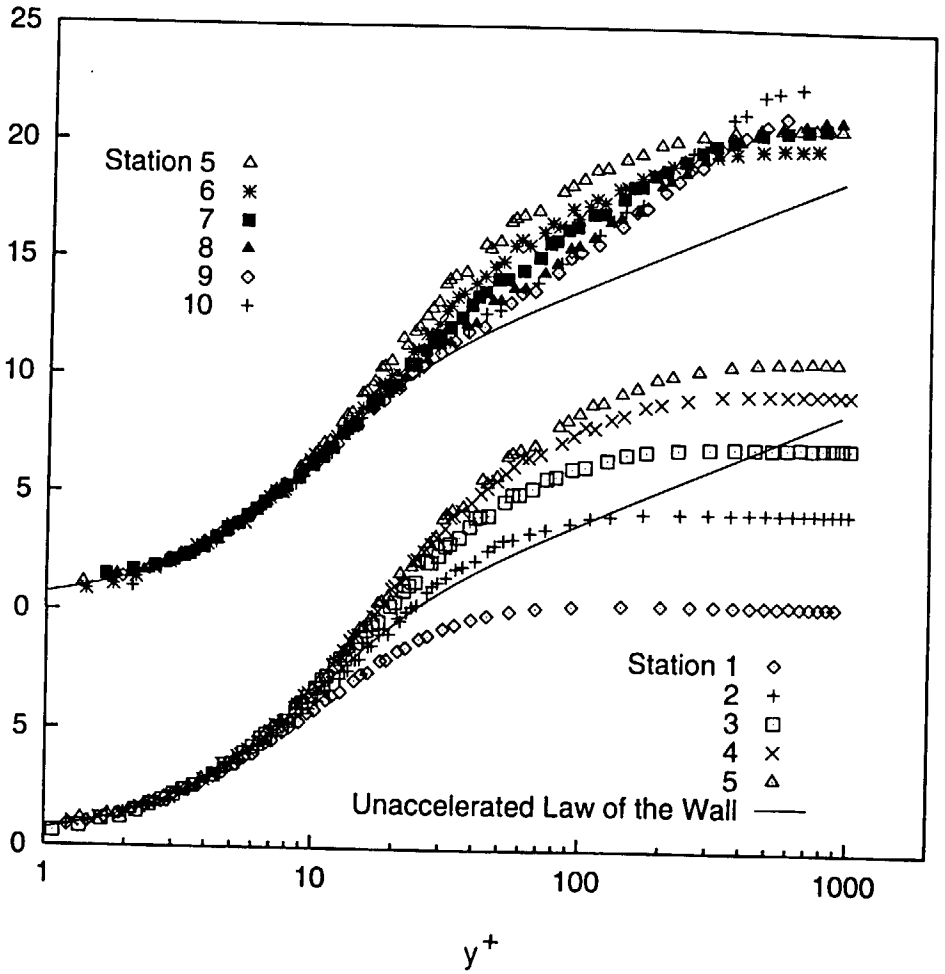

Fig. 7.14: Mean Temperature Profiles, Wall Coordinates, $dU_{cw}/dx=14\ s^{-1}$ Case

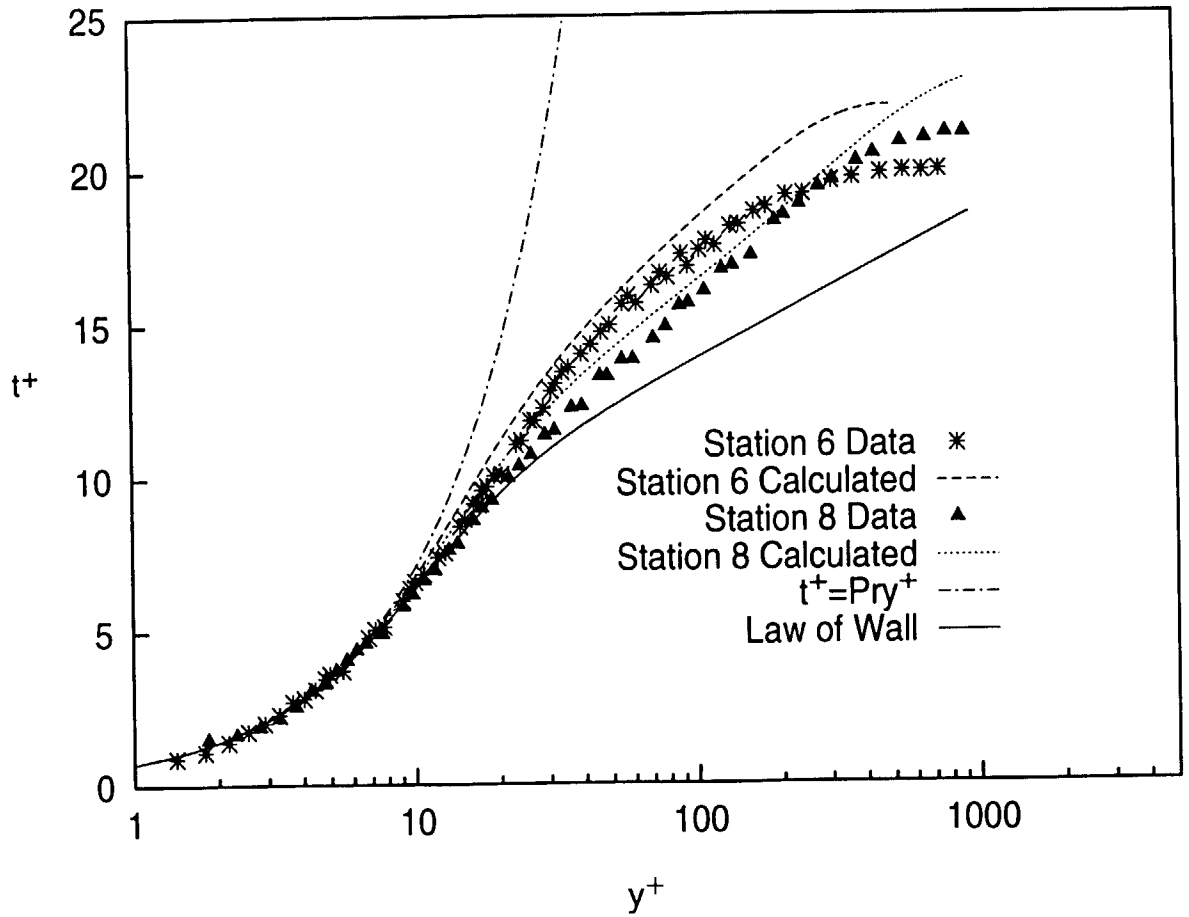

Fig. 7.15: Comparison of Calculated Profiles to Data dU_{cw}/dx=14 s^{-1} Case

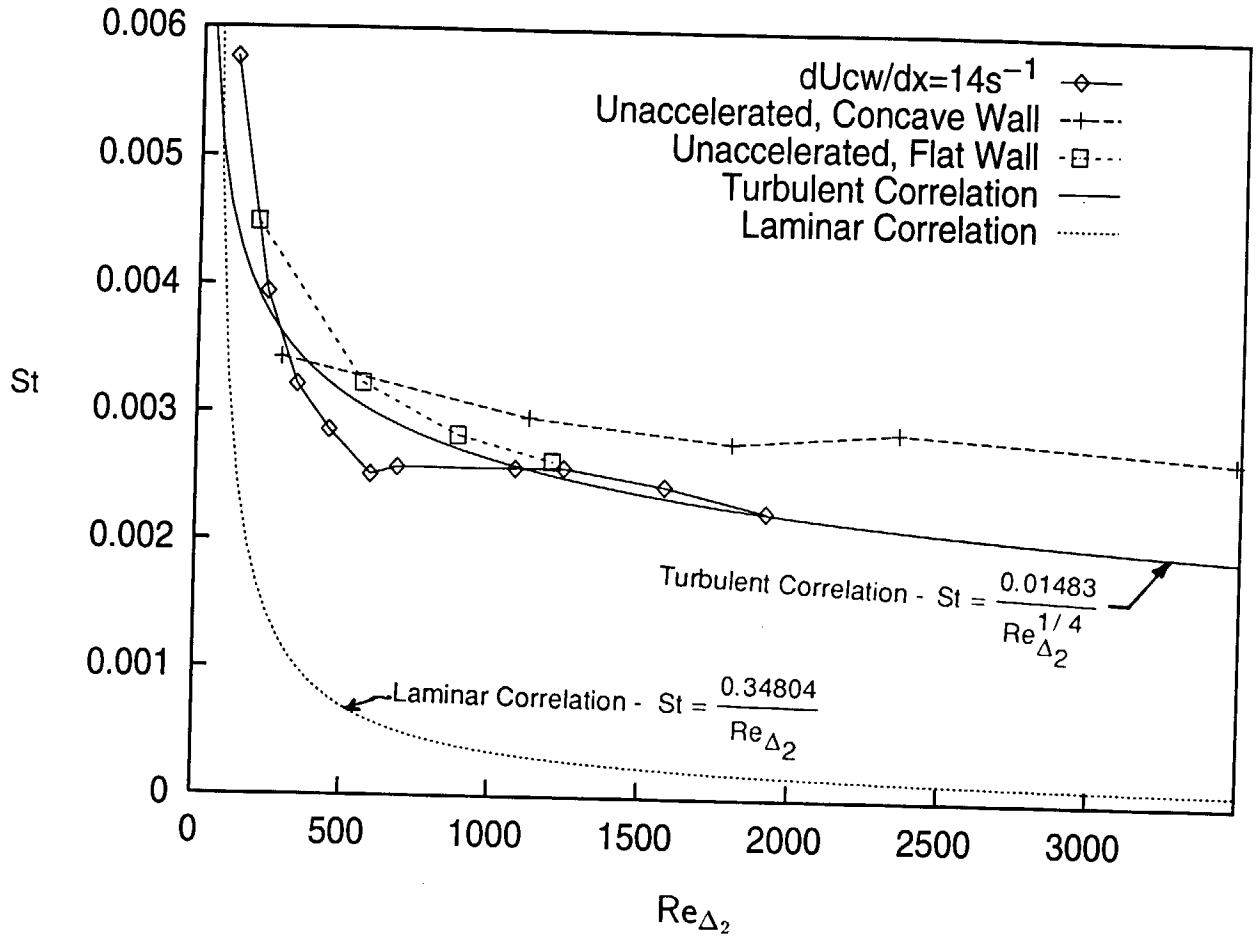

Fig. 7.16: Stanton Number vs Re_{Δ_2}
dU_{cw}/dx=14 s^{-1} Case

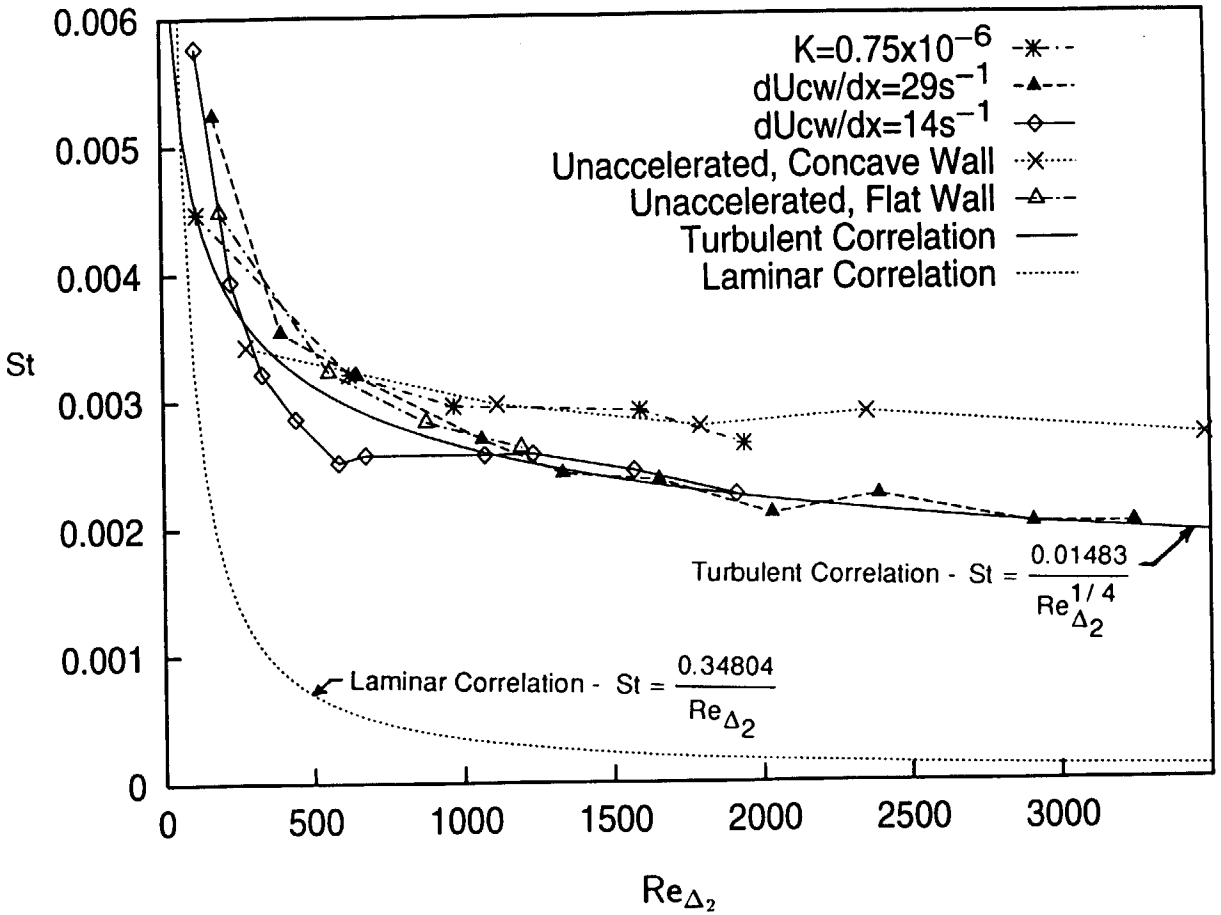

Fig. 7.17a: Stanton Number vs Re_{Δ_2} Comparison of High-FSTI Cases

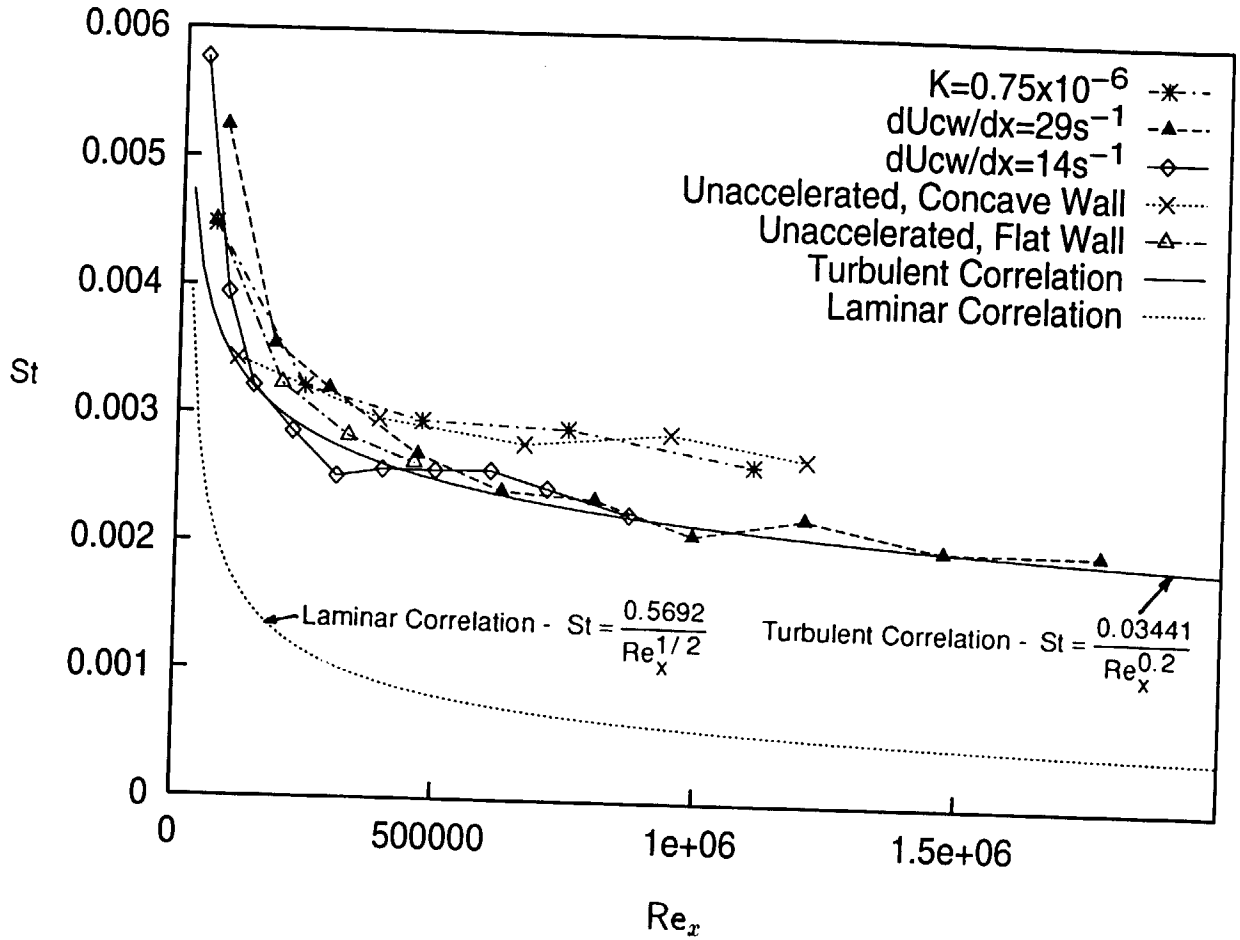

Fig. 7.17b: Stanton Number vs Re_x
Comparison of High-FSTI Cases

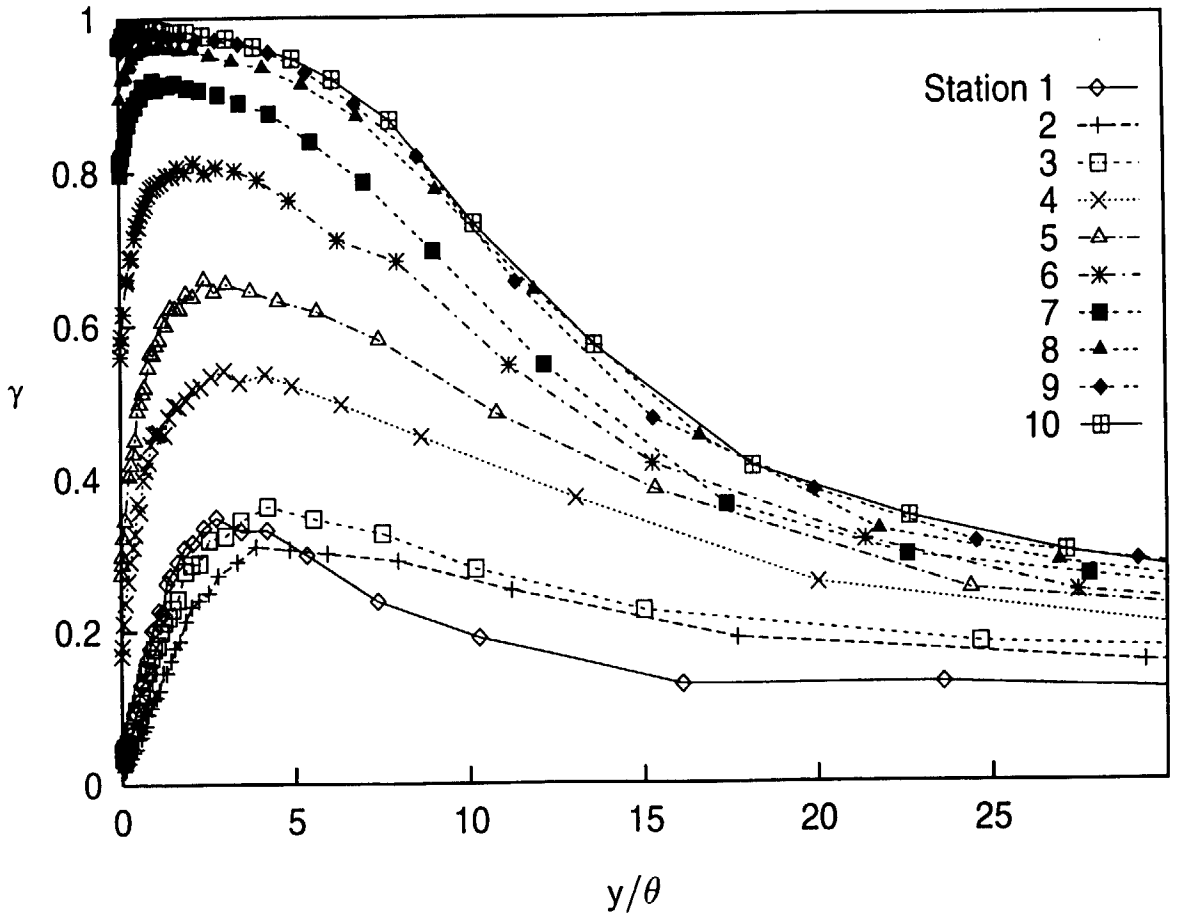

Fig. 7.18: Intermittency Profiles Based on u' Fluctuations
dU_{cw}/dx=14 s^{-1} Case

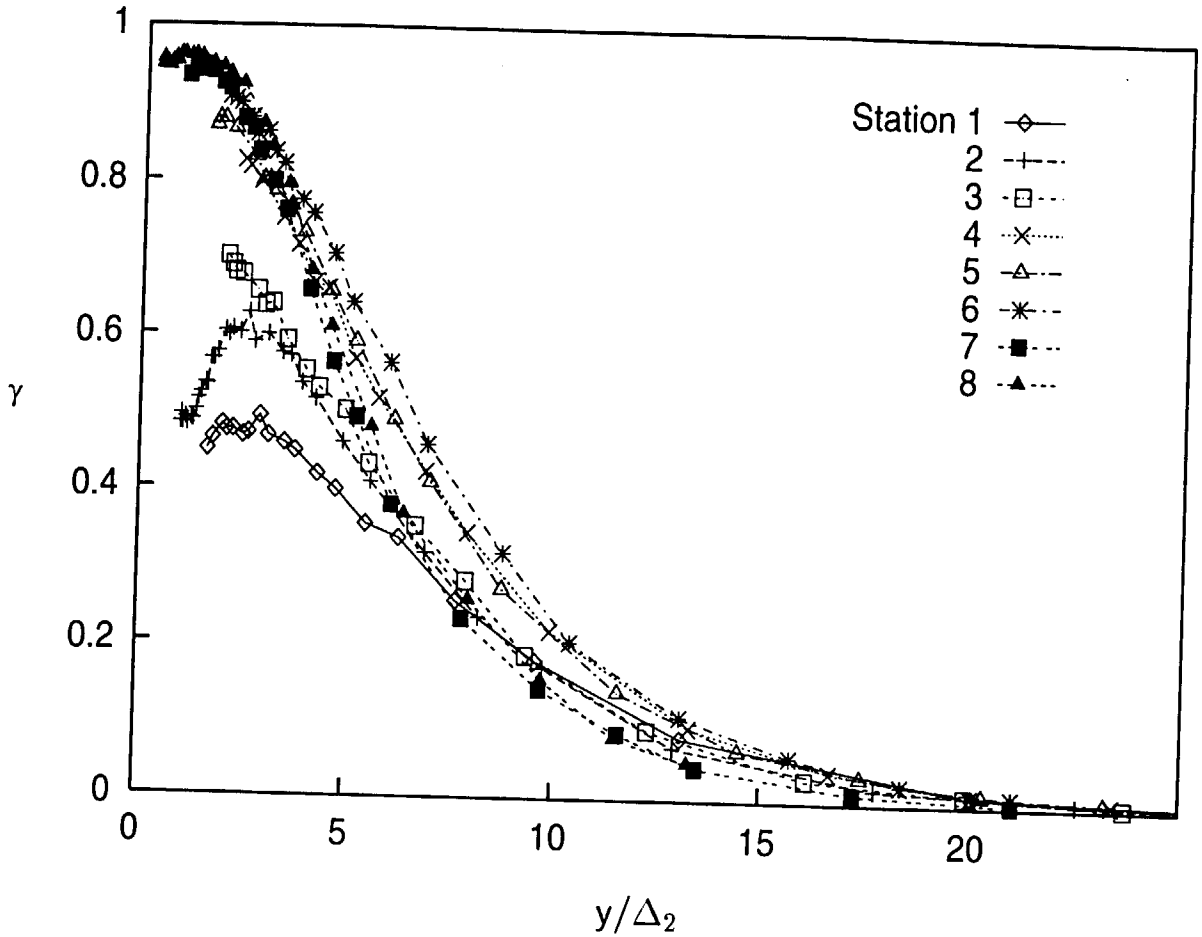

Fig. 7.19: Intermittency Profiles Based on t' Fluctuations dU_{cw}/dx=14 s^{-1} Case

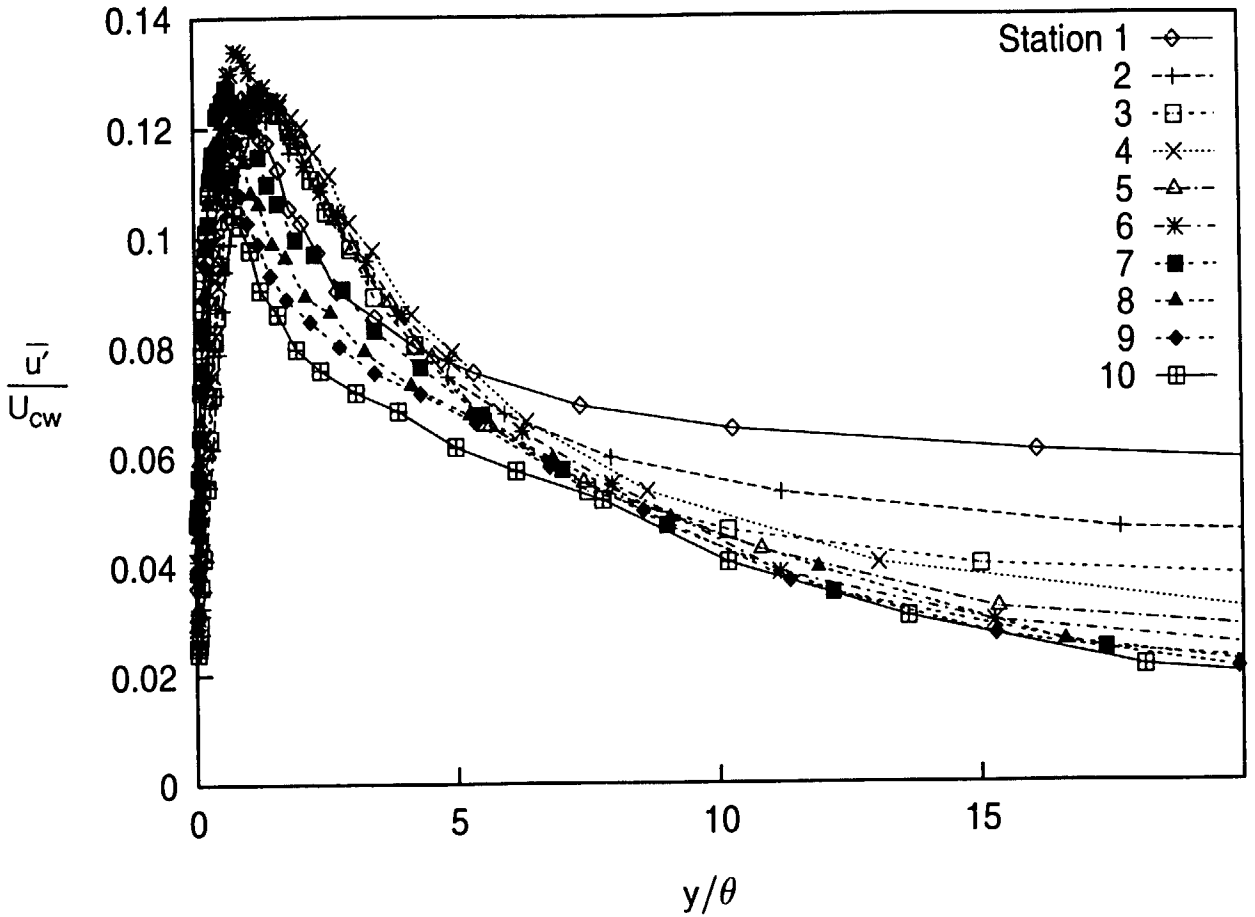

Fig. 7.20a: Fluctuating Streamwise Velocity Profiles dU_{cw}/dx=14 s^{-1} Case

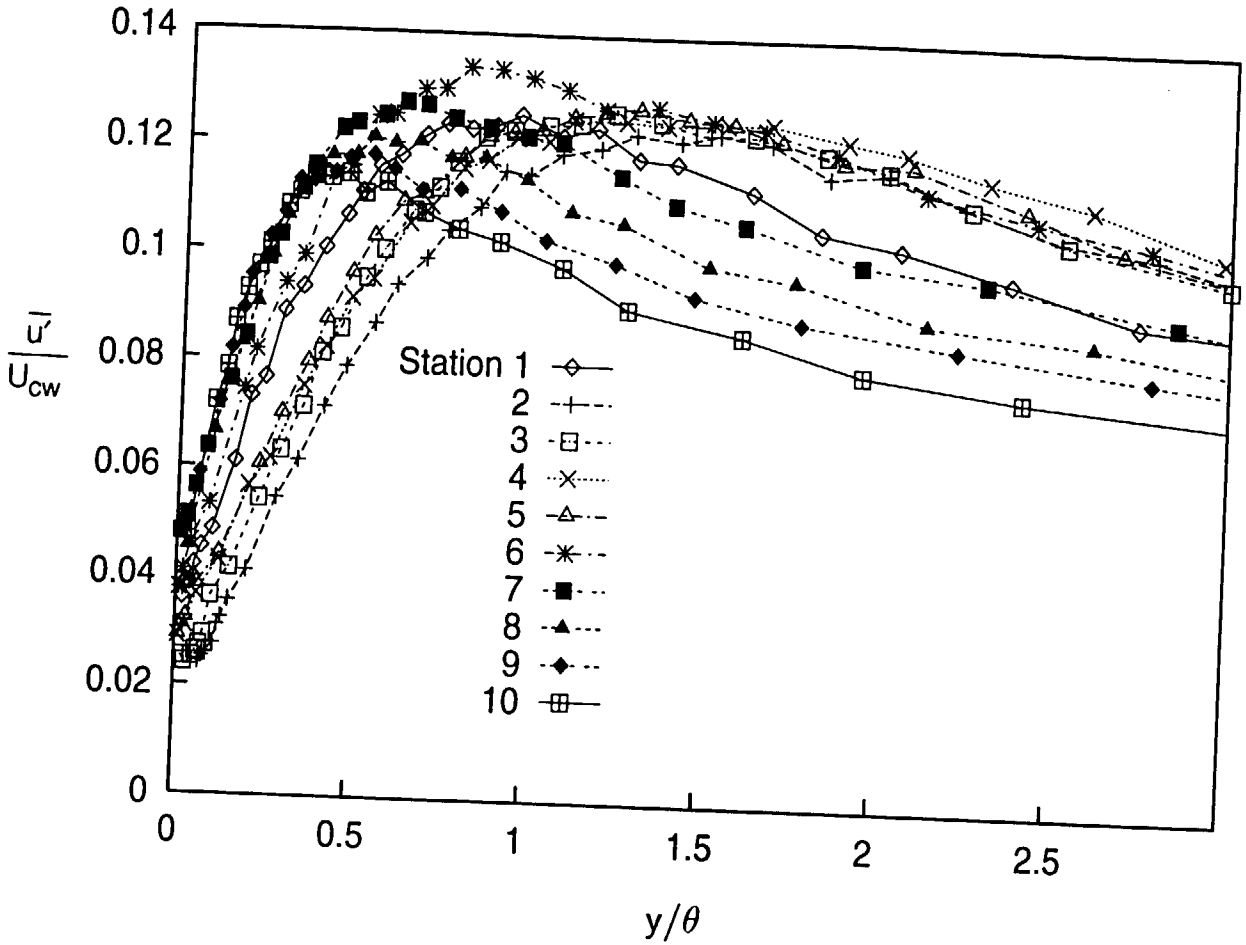

Fig. 7.20b: Fluctuating Streamwise Velocity Profiles dU_{cw}/dx=14 s^{-1} Case

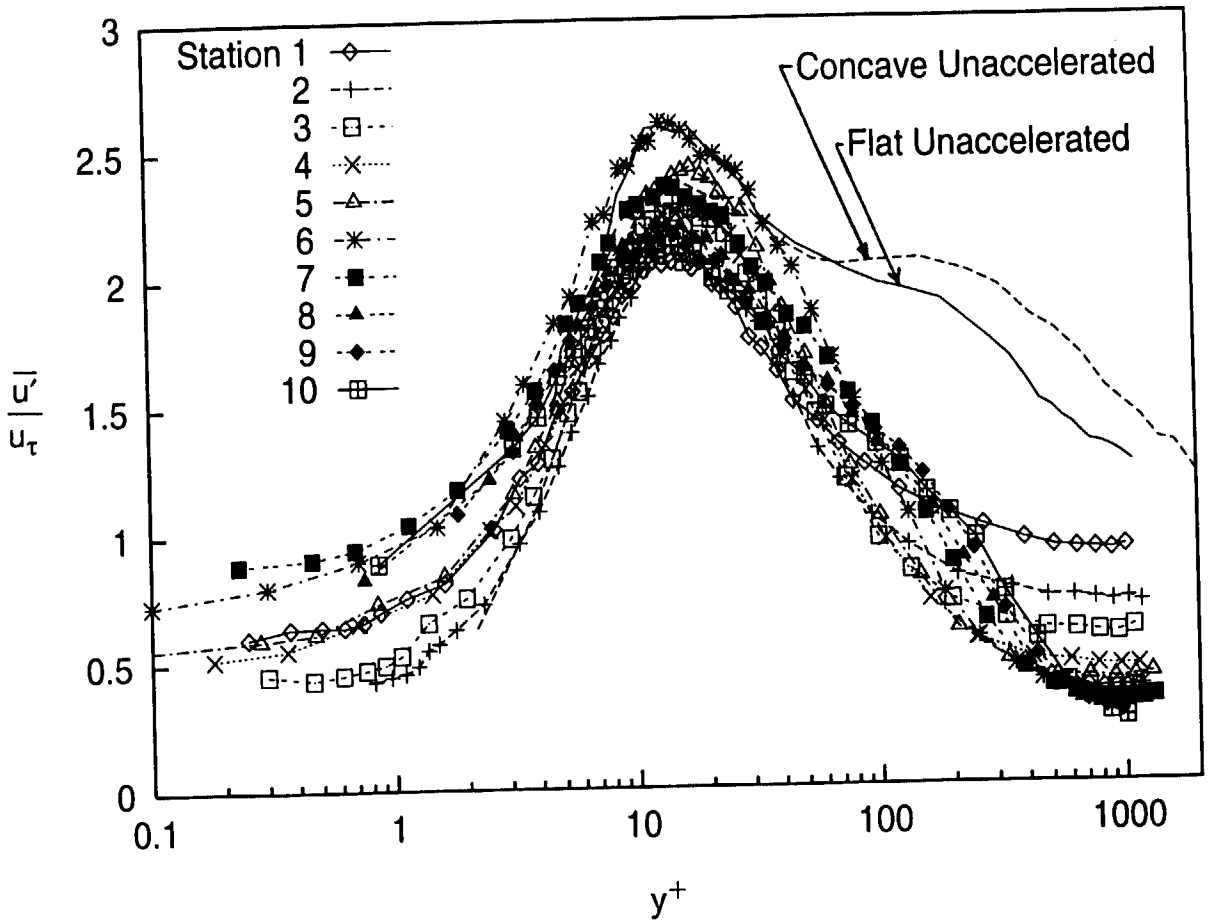

Fig. 7.21: Fluctuating Streamwise Velocity Profiles, Wall Coordinates dU_{cw}/dx=14 s^{-1} Case

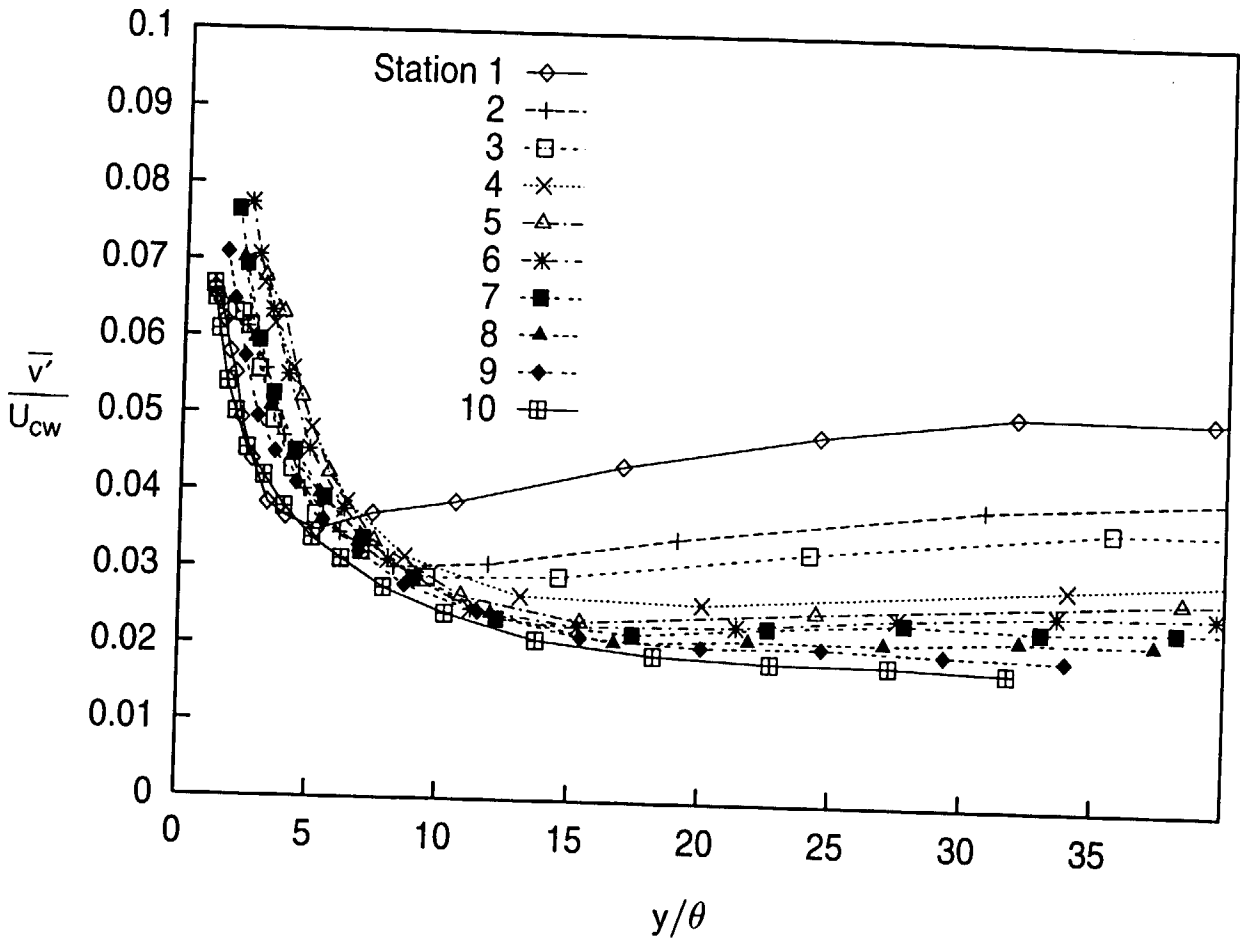

Fig. 7.22: Fluctuating Cross-stream Velocity Profiles $dU_{cw}/dx=14\ s^{-1}$ Case

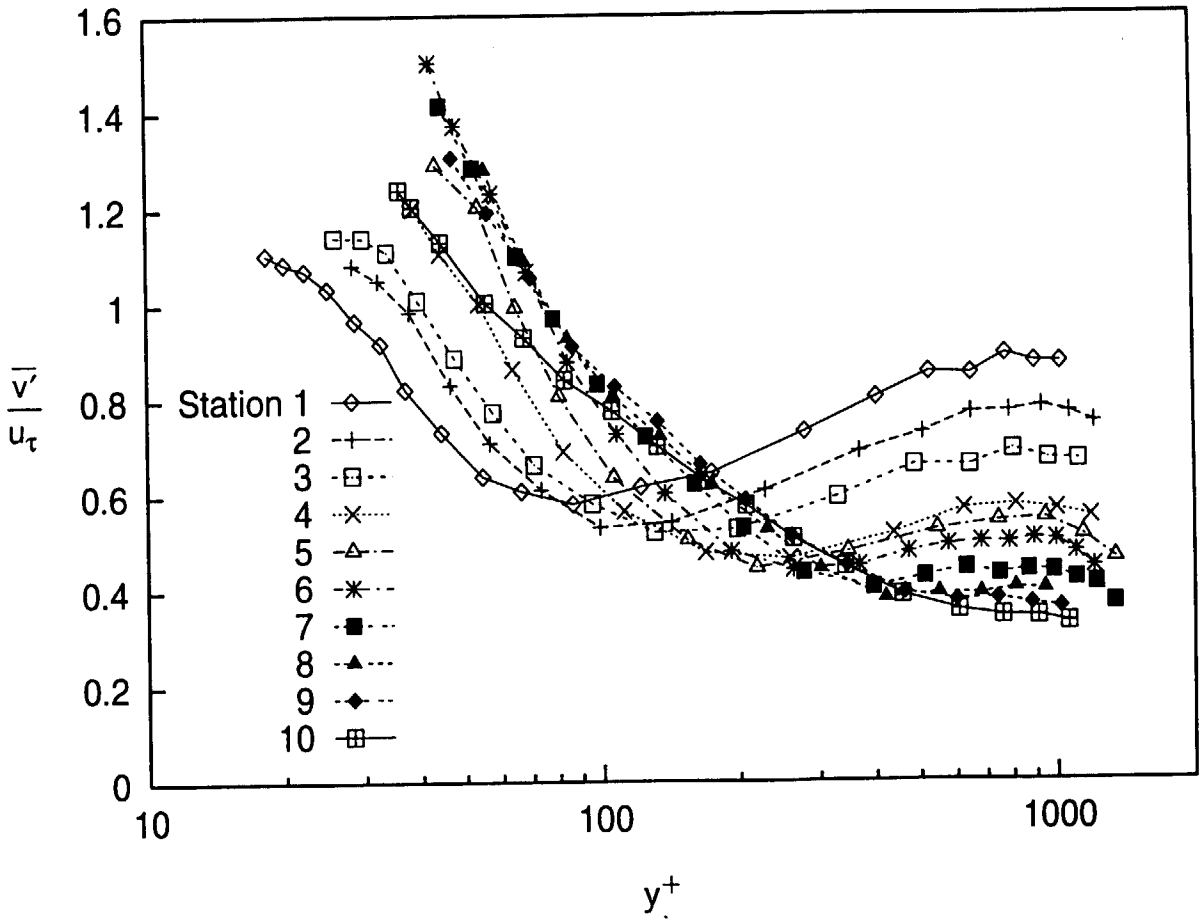

Fig. 7.23: Fluctuating Cross-stream Velocity Profiles, Wall Coordinates dU_{cw}/dx=14 s^{-1} Case

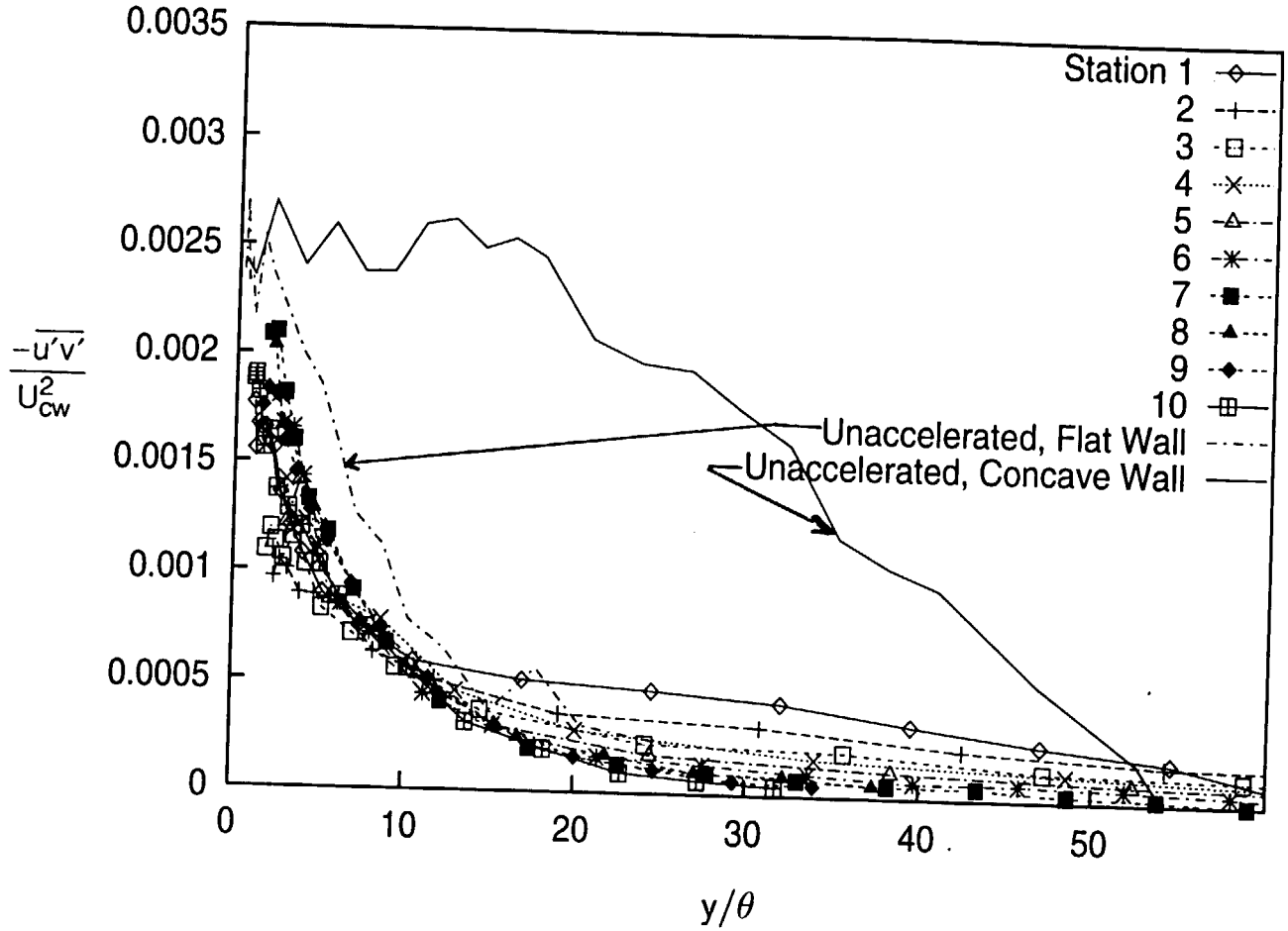

Fig. 7.24: Turbulent Shear Stress Profiles
dU_{cw}/dx=14 s^{-1} Case

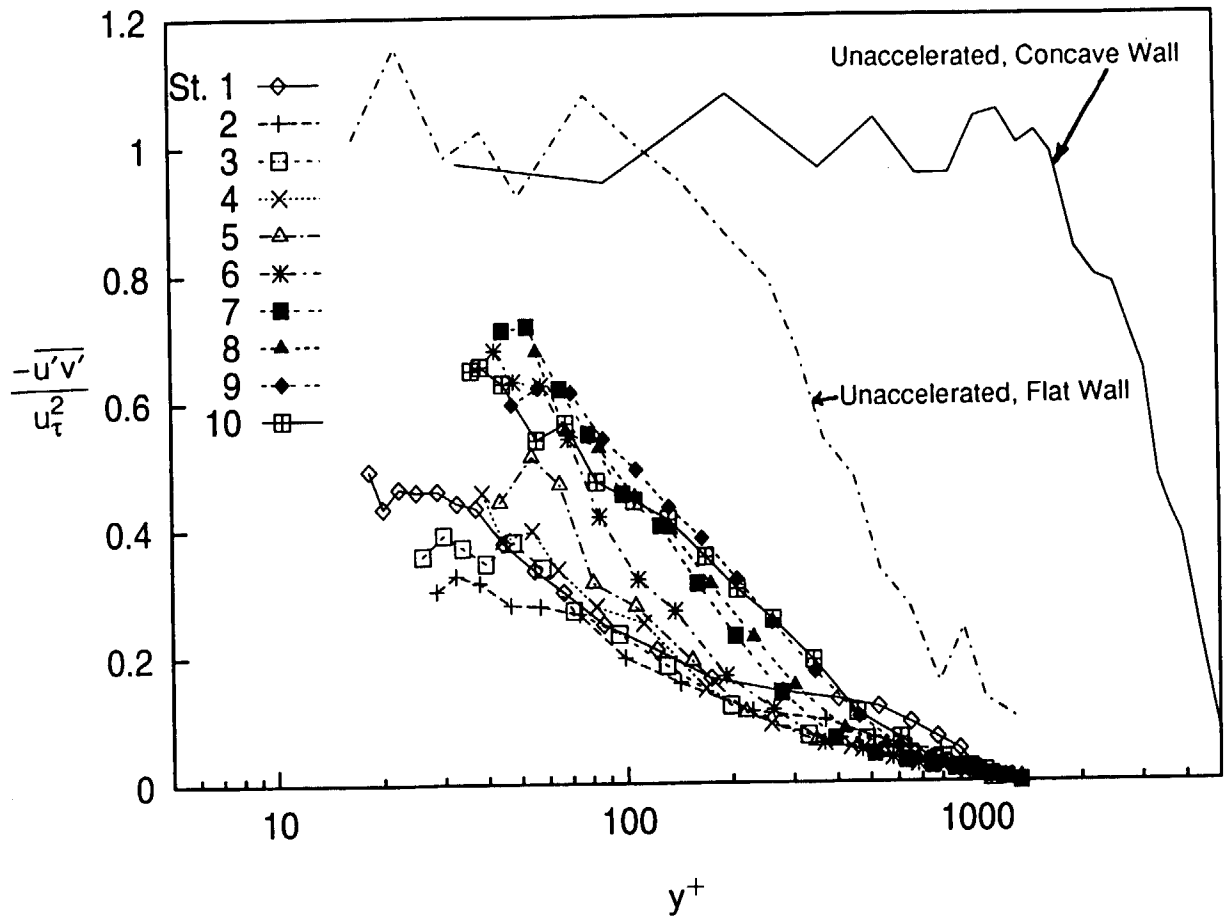

Fig. 7.25: Turbulent Shear Stress Profiles, Wall Coordinates dU_{cw}/dx=14 s^{-1} Case

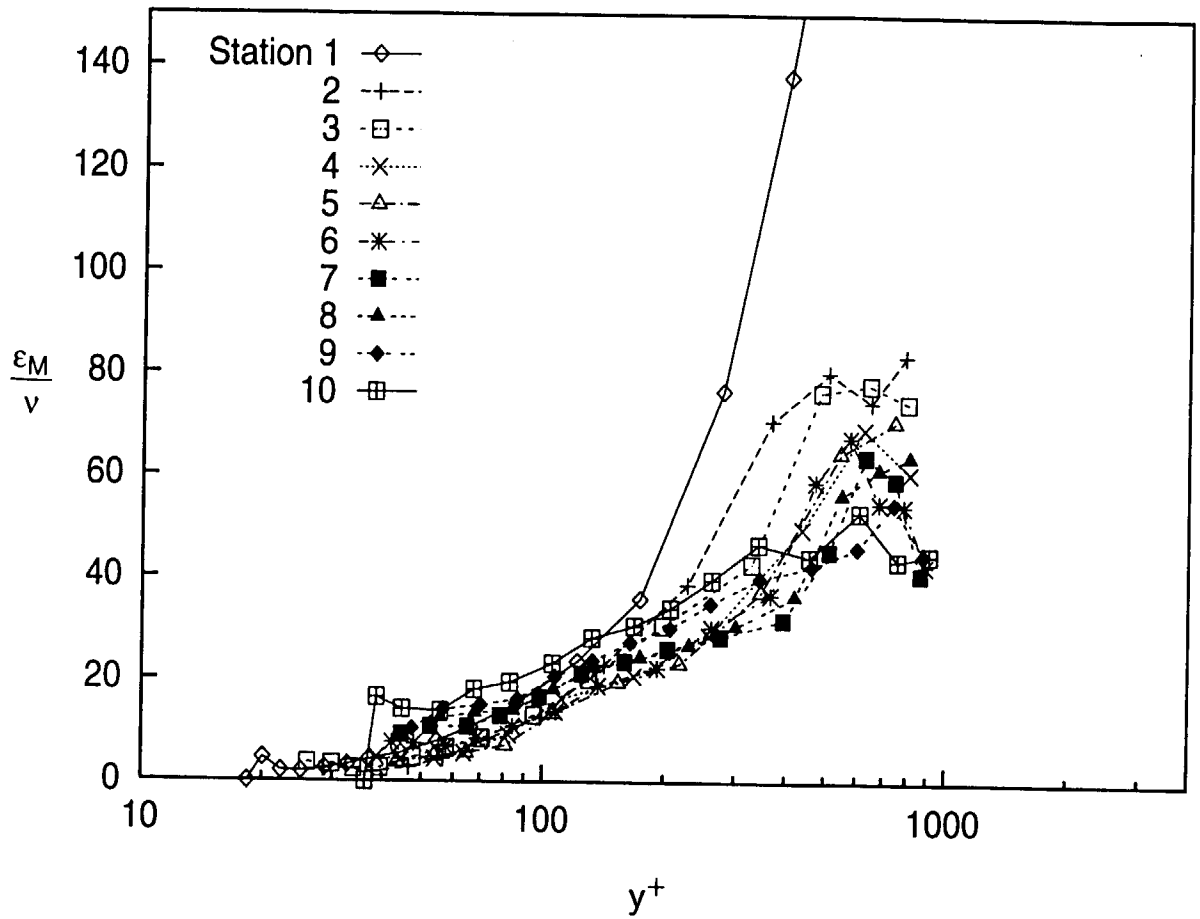

Fig. 7.26: Eddy Viscosity Profiles
dU_{cw}/dx=14 s^{-1} Case

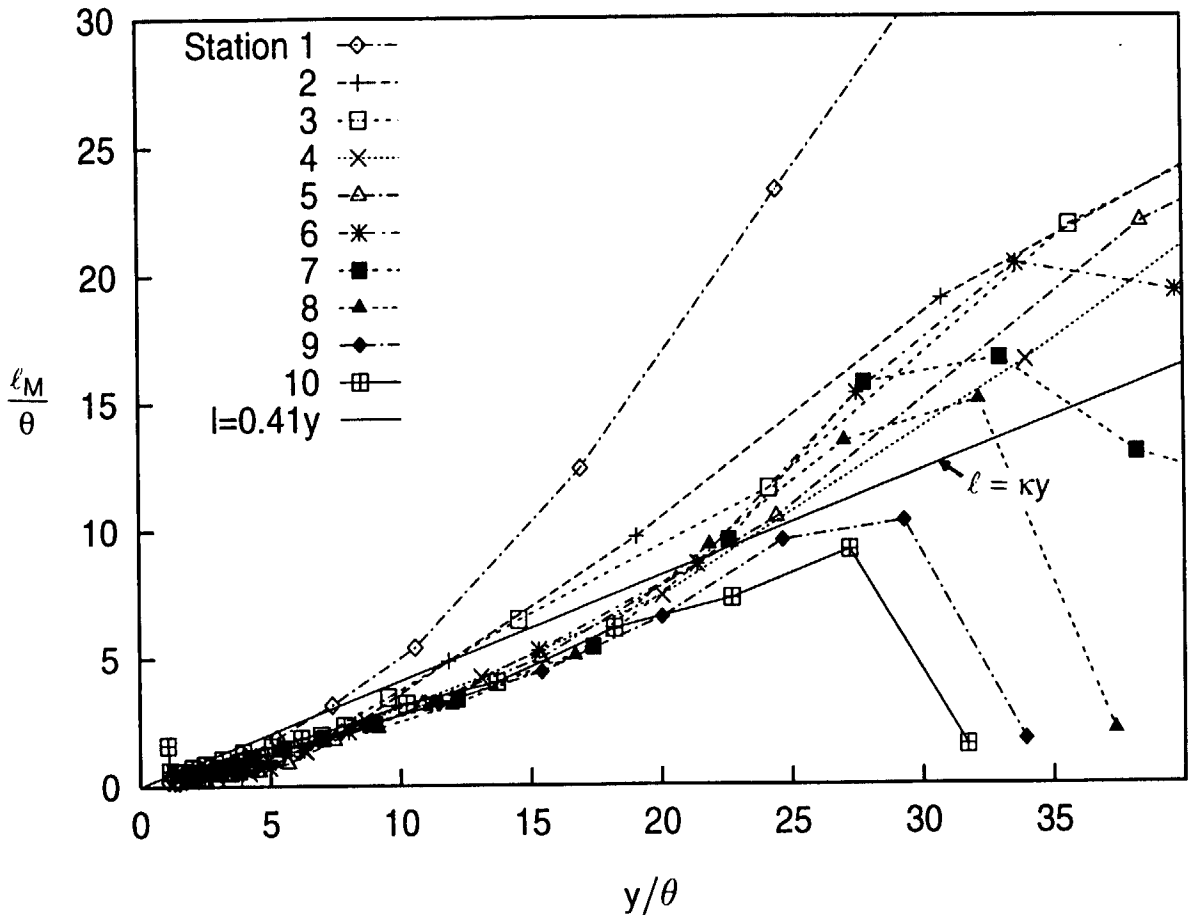

Fig. 7.27: Mixing Length of Momentum Profiles dU_{cw}/dx=14 s^{-1} Case

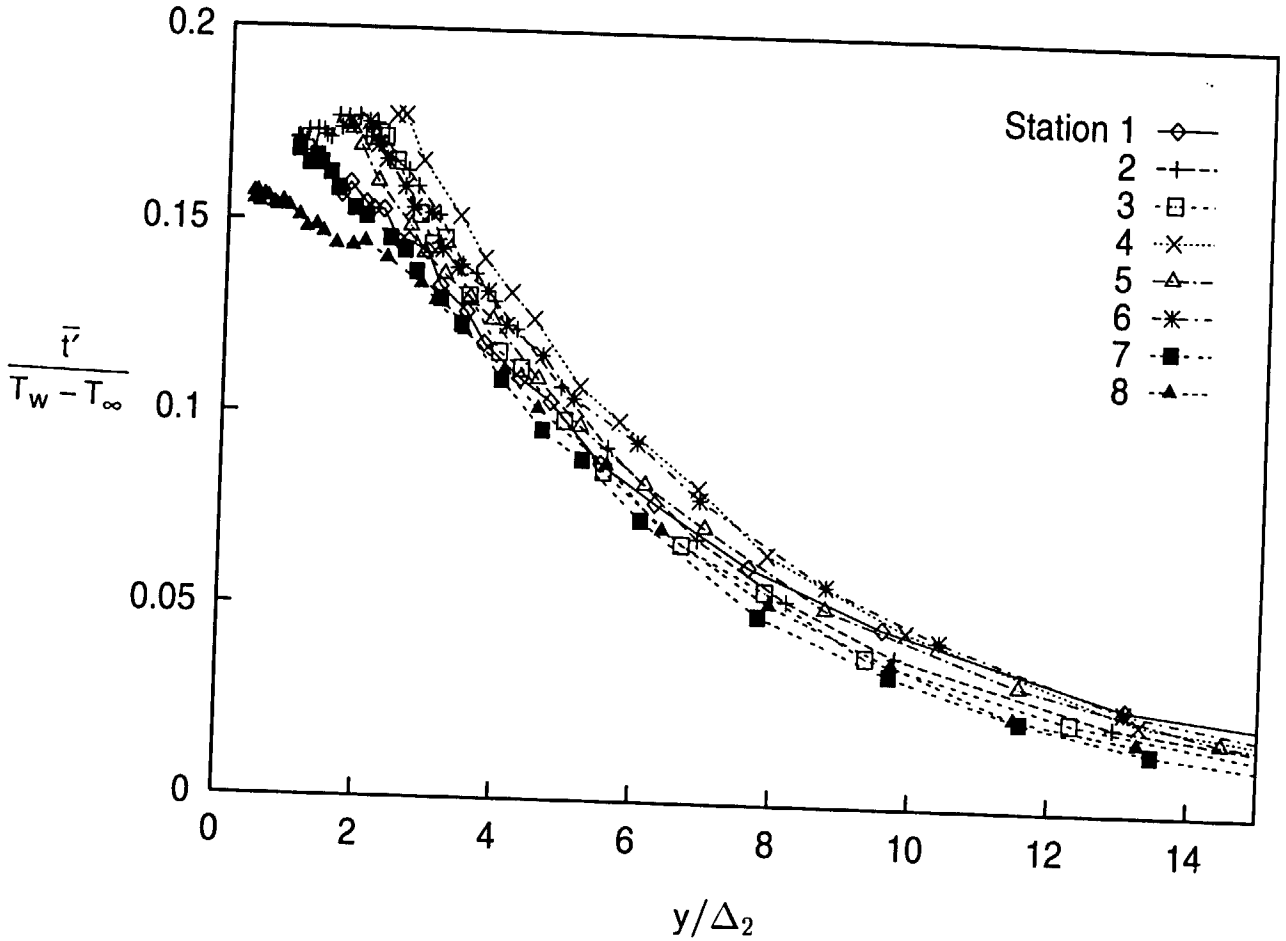

Fig. 7.28: Fluctuating Temperature Profiles dU_{cw}/dx=14 s^{-1} Case

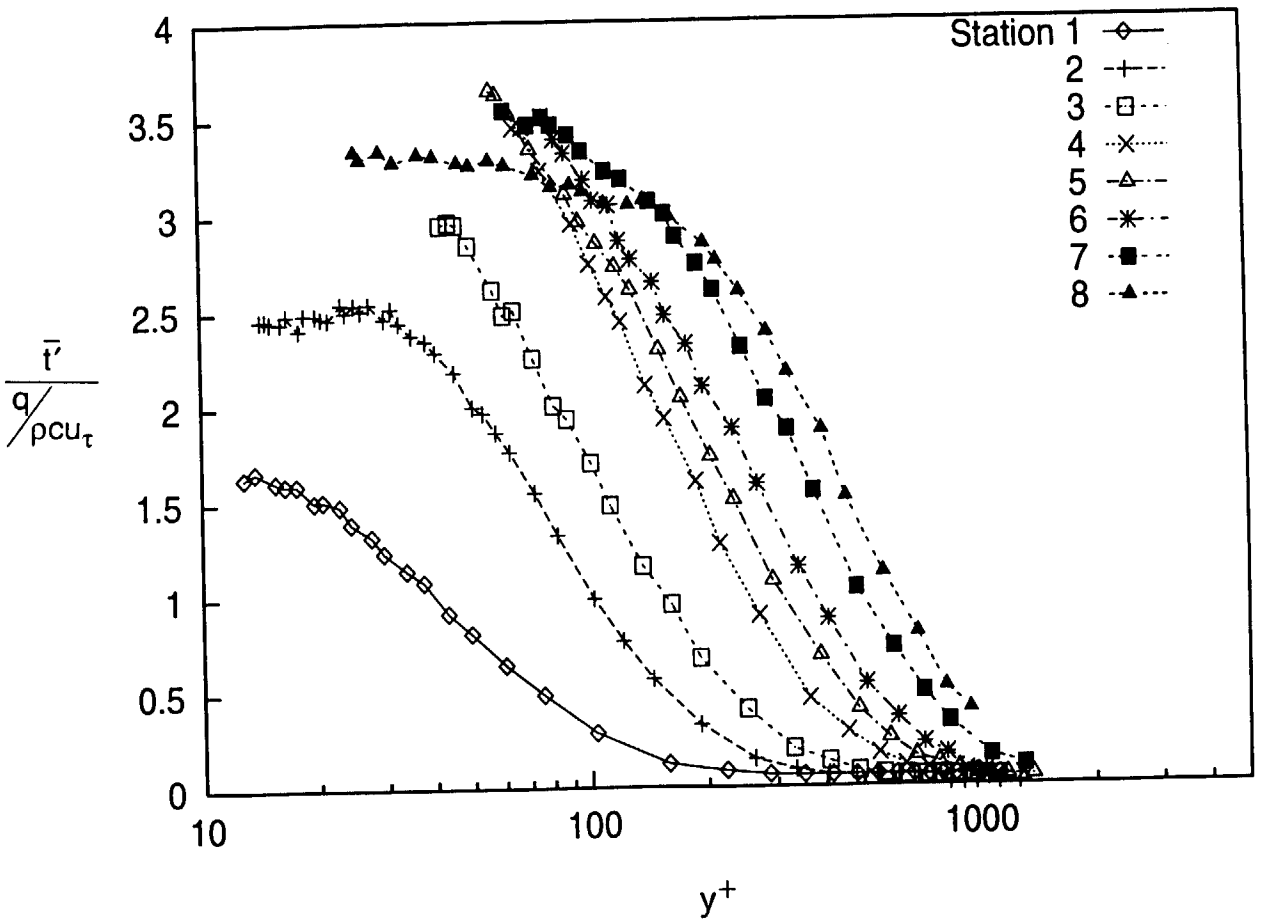

Fig. 7.29: Fluctuating Temperature Profiles, Wall Coordinates dU_{cw}/dx=14 s^{-1} Case

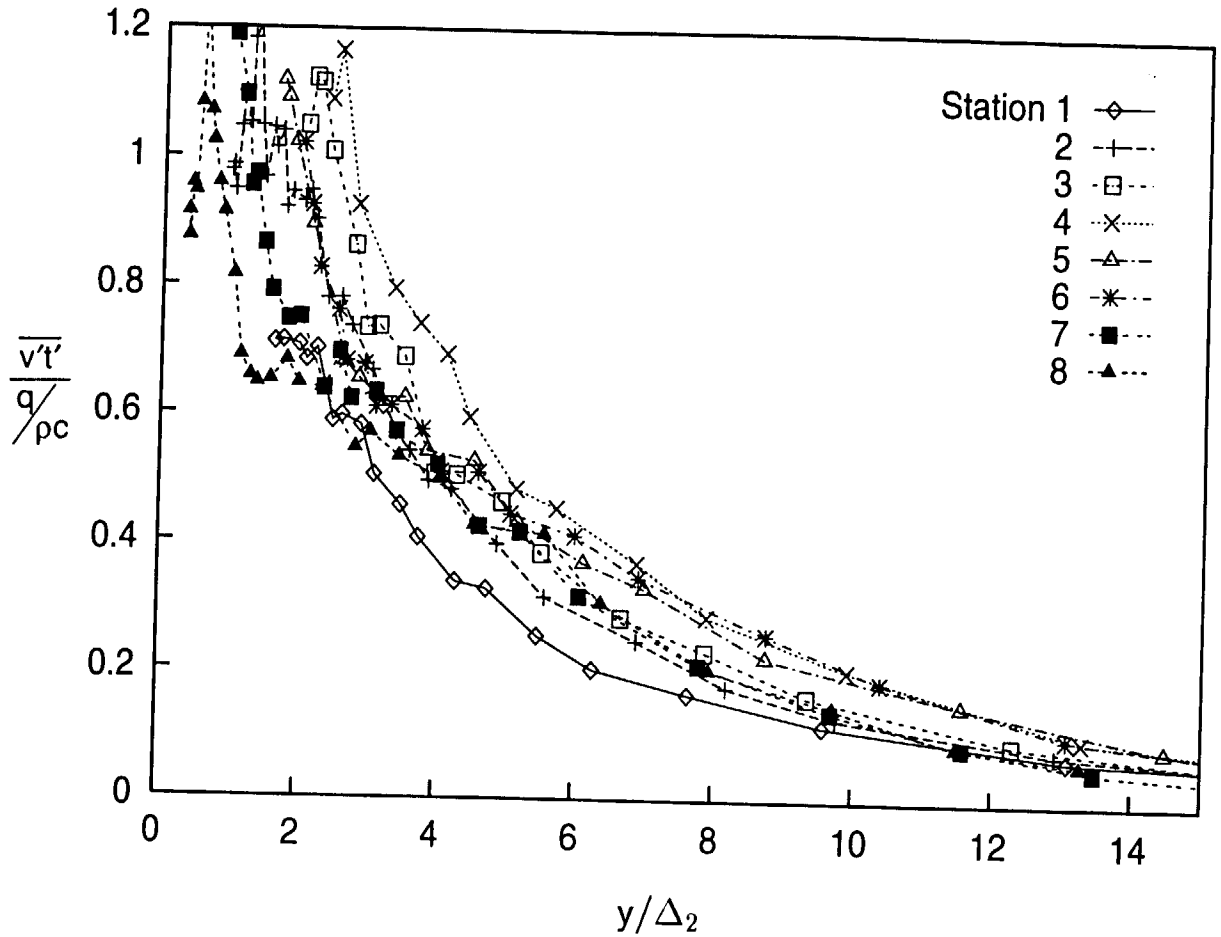

Fig. 7.30: Normal Component of Turbulent Heat Flux Profiles dU_{cw}/dx=14 s^{-1} Case

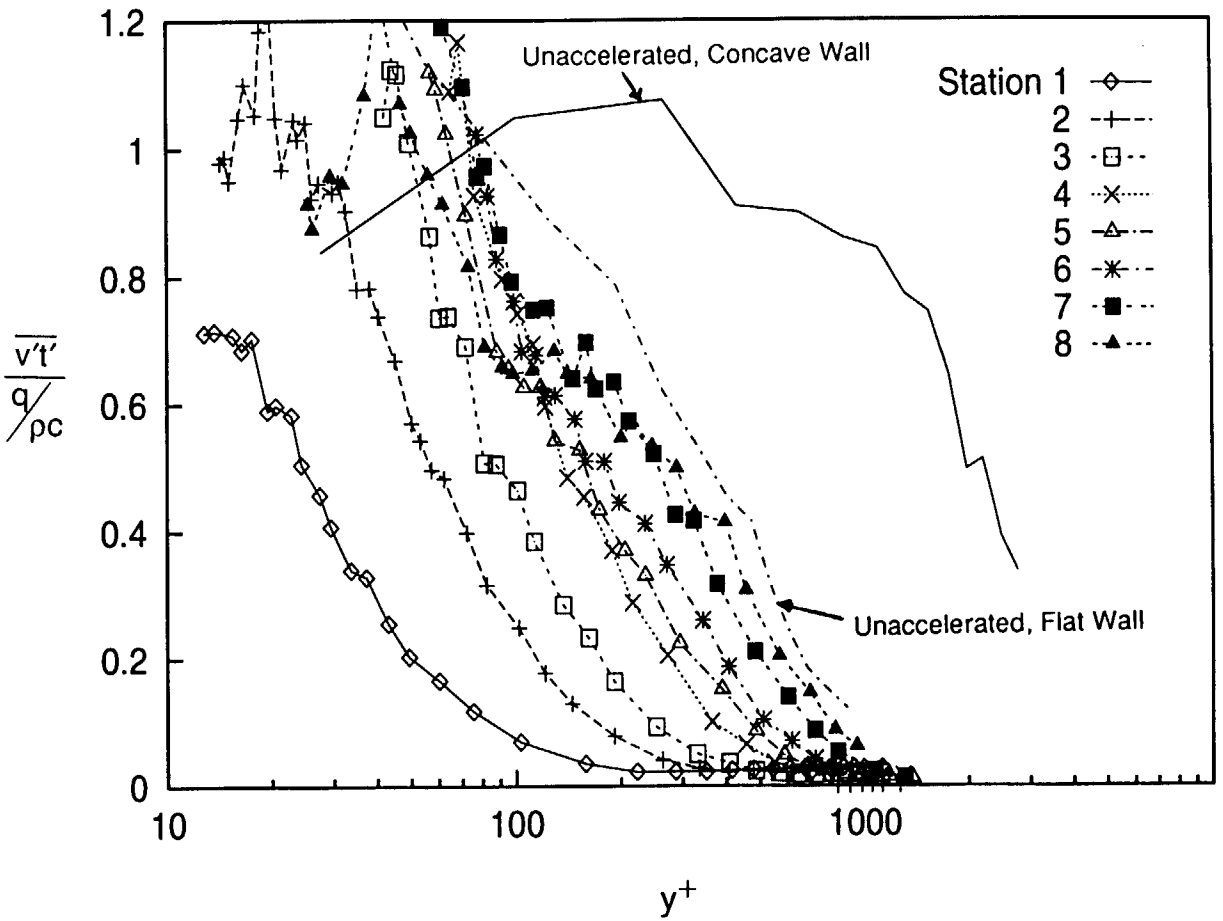

Fig. 7.31: Normal Component of Turbulent Heat Flux Profiles, Wall Coordinates, dU_{cw}/dx=14 s^{-1} Case

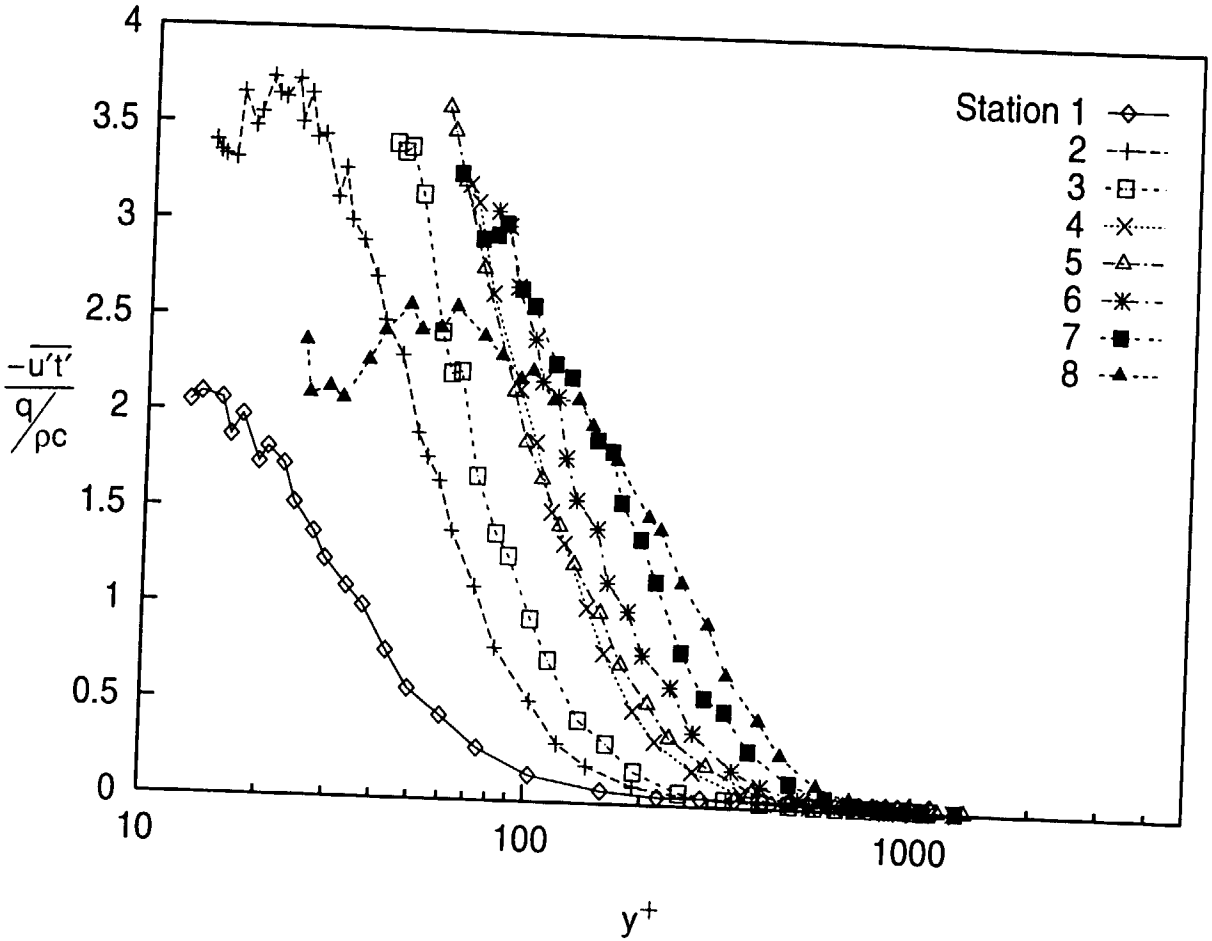

Fig. 7.32: Streamwise Component of Turbulent Heat Flux Profiles, Wall Coordinates, dU_{cw}/dx=14 s^{-1} Case

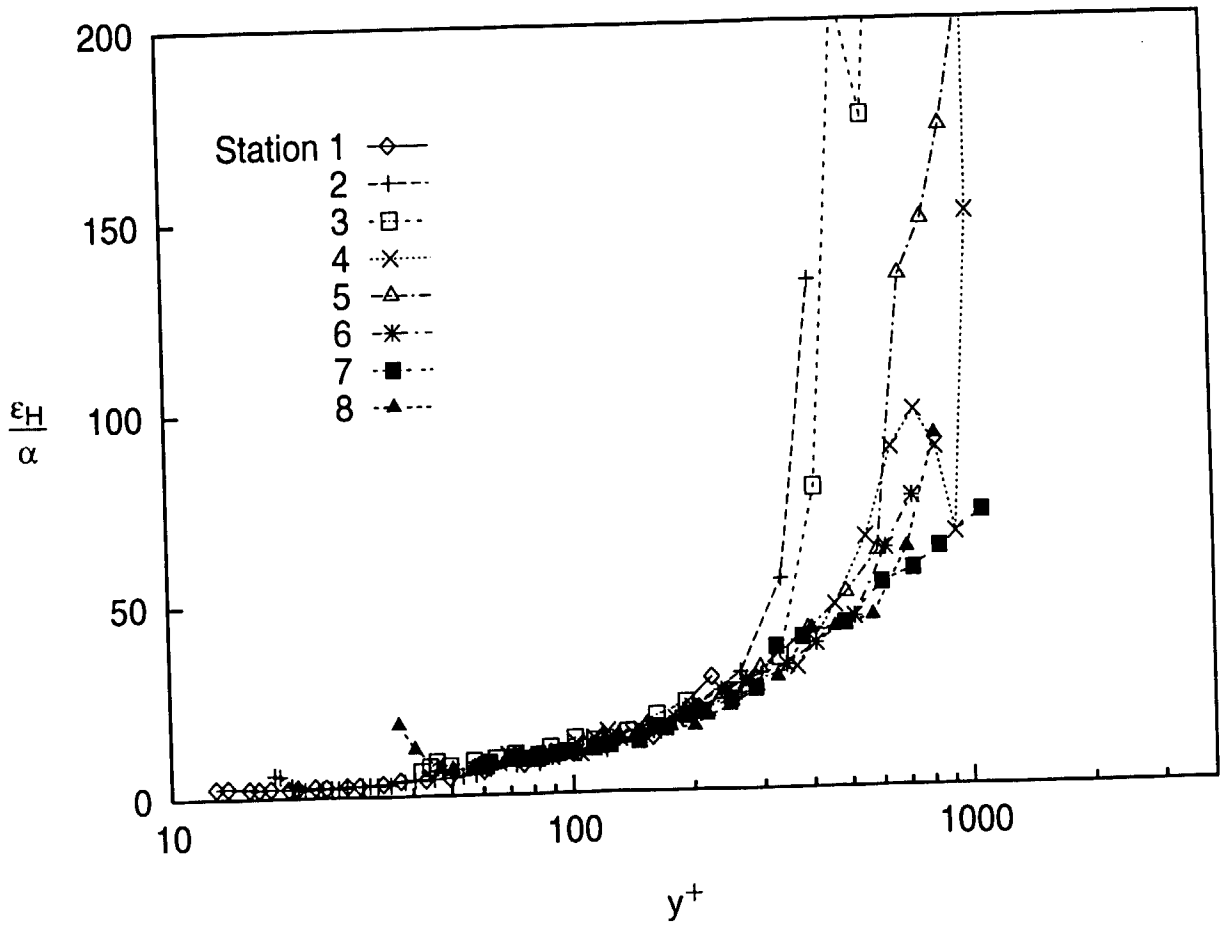

Fig. 7.33: Eddy Diffusivity of Heat Profiles dU_{cw}/dx=14 s^{-1} Case

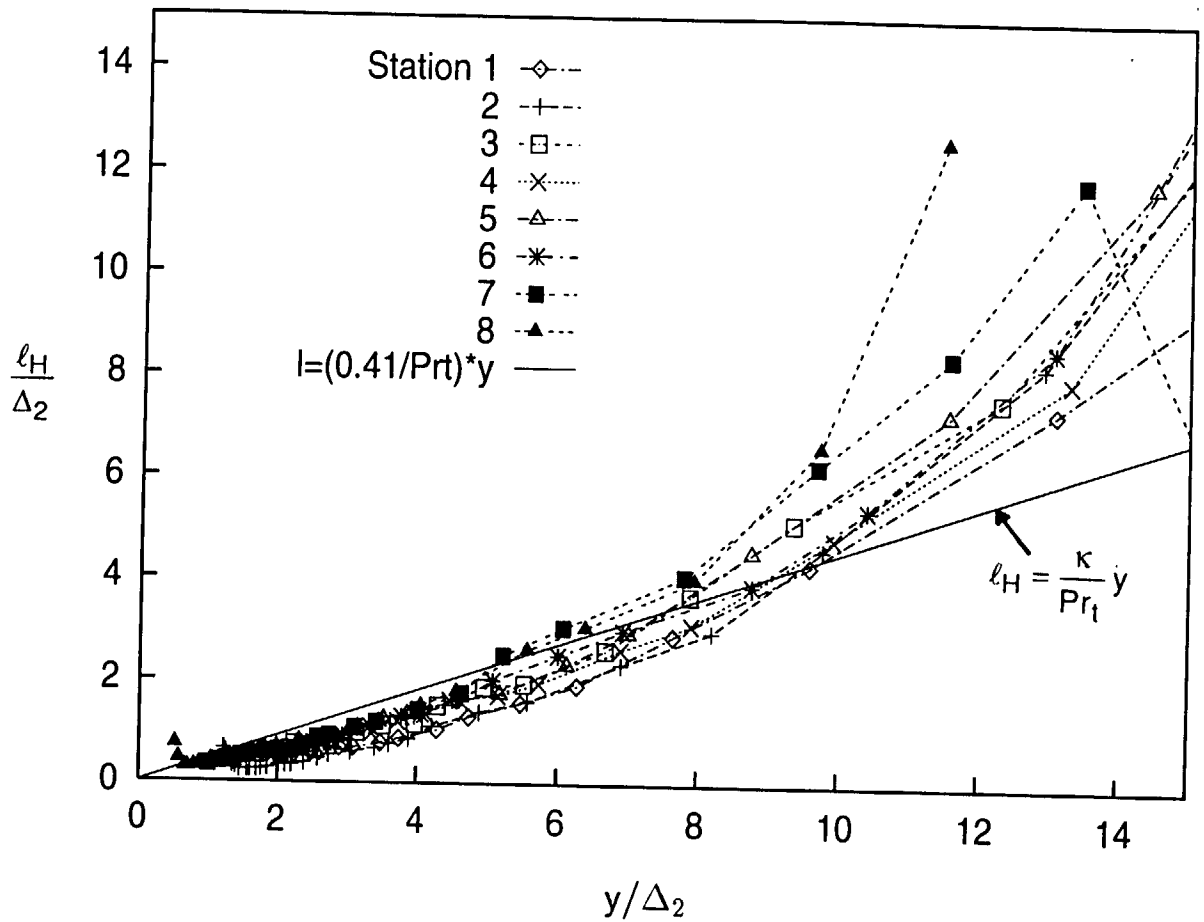

Fig. 7.34: Mixing Length of Heat Profiles $dU_{cw}/dx=14\ s^{-1}$ Case

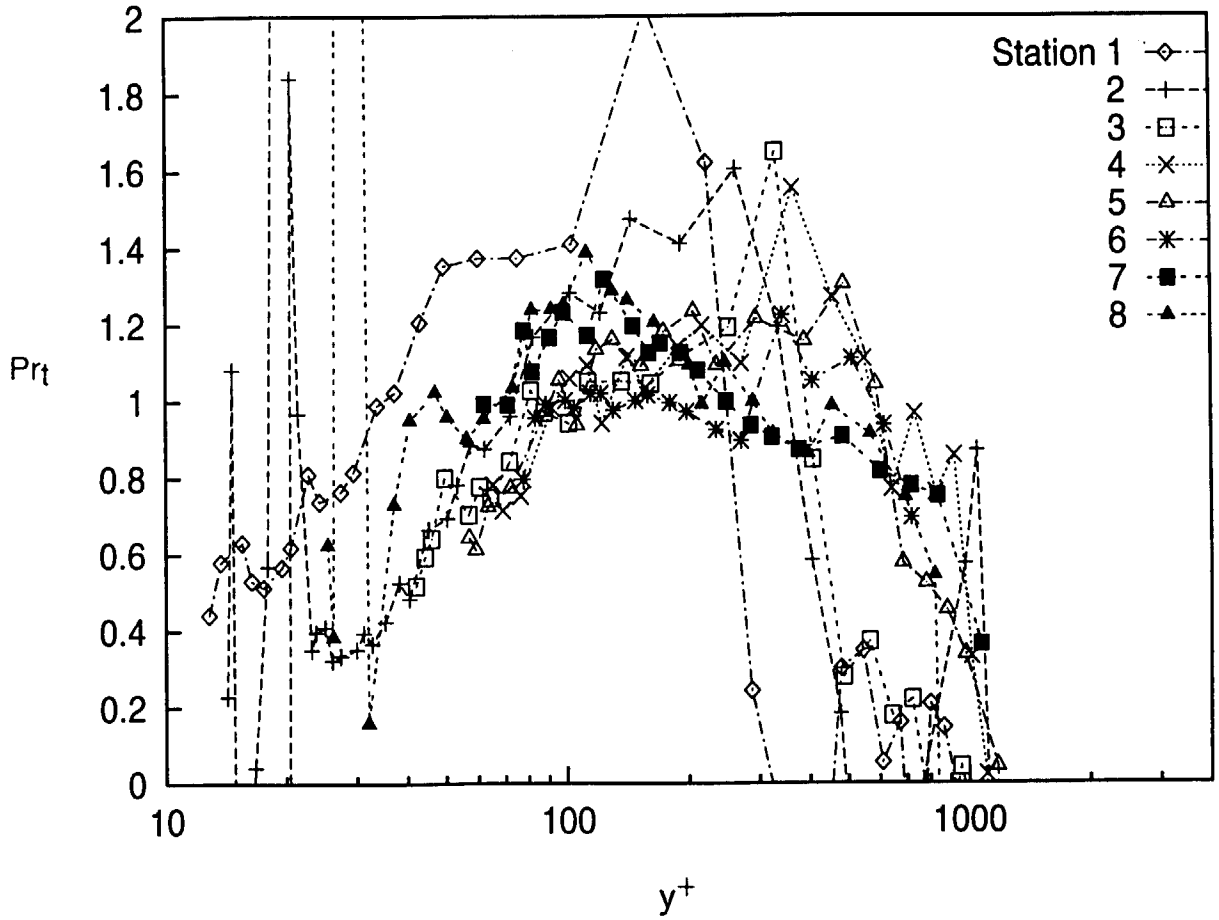

Fig. 7.35: Turbulent Prandtl Number Profiles
dU_{cw}/dx=14 s^{-1} Case

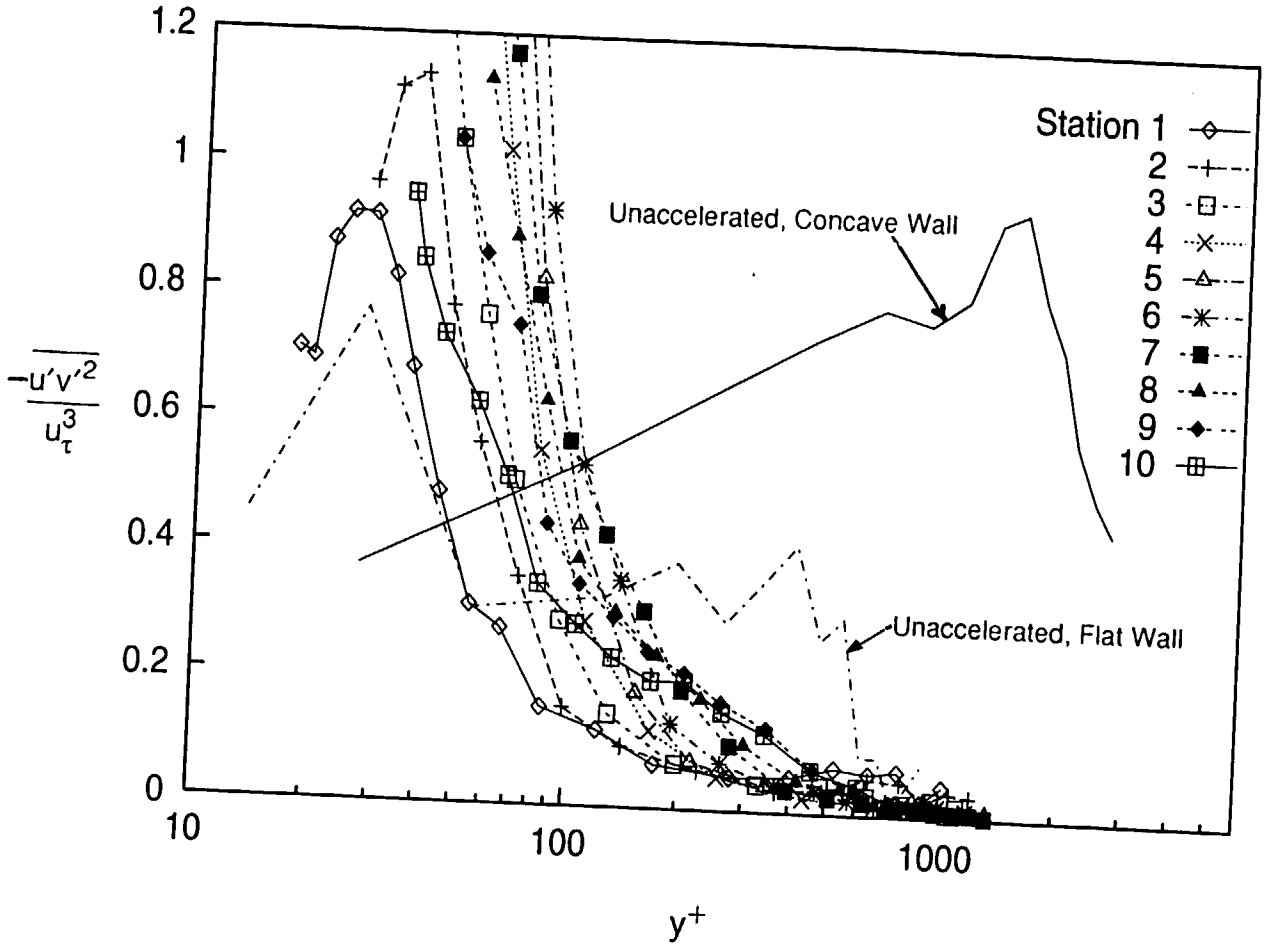

Fig. 7.36: Cross Transport of Turbulent Shear Stress Profiles dU_{cw}/dx=14 s^{-1} Case

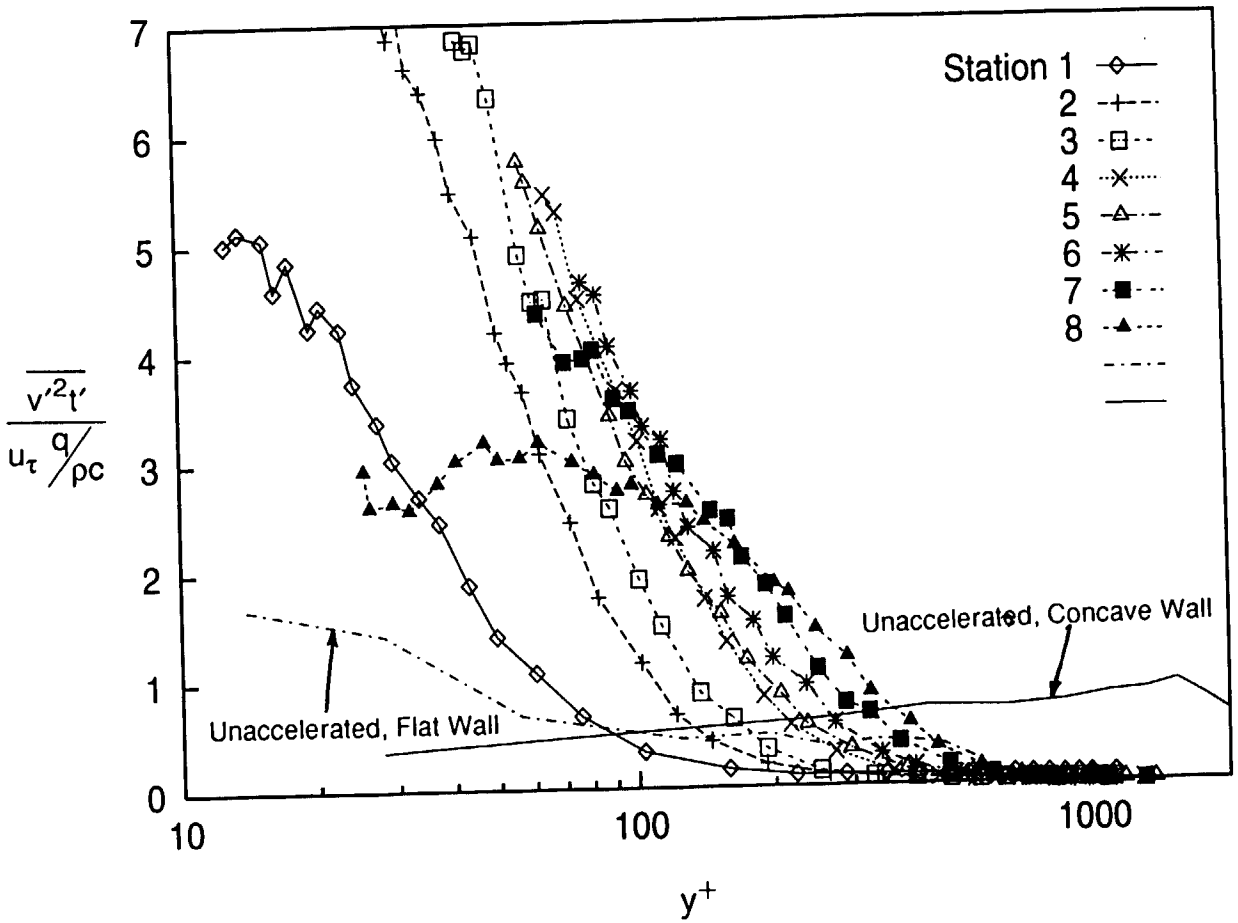

Fig. 7.37: Cross Transport of Turbulent Heat Flux Profiles dU_{cw}/dx=14 s^{-1} Case

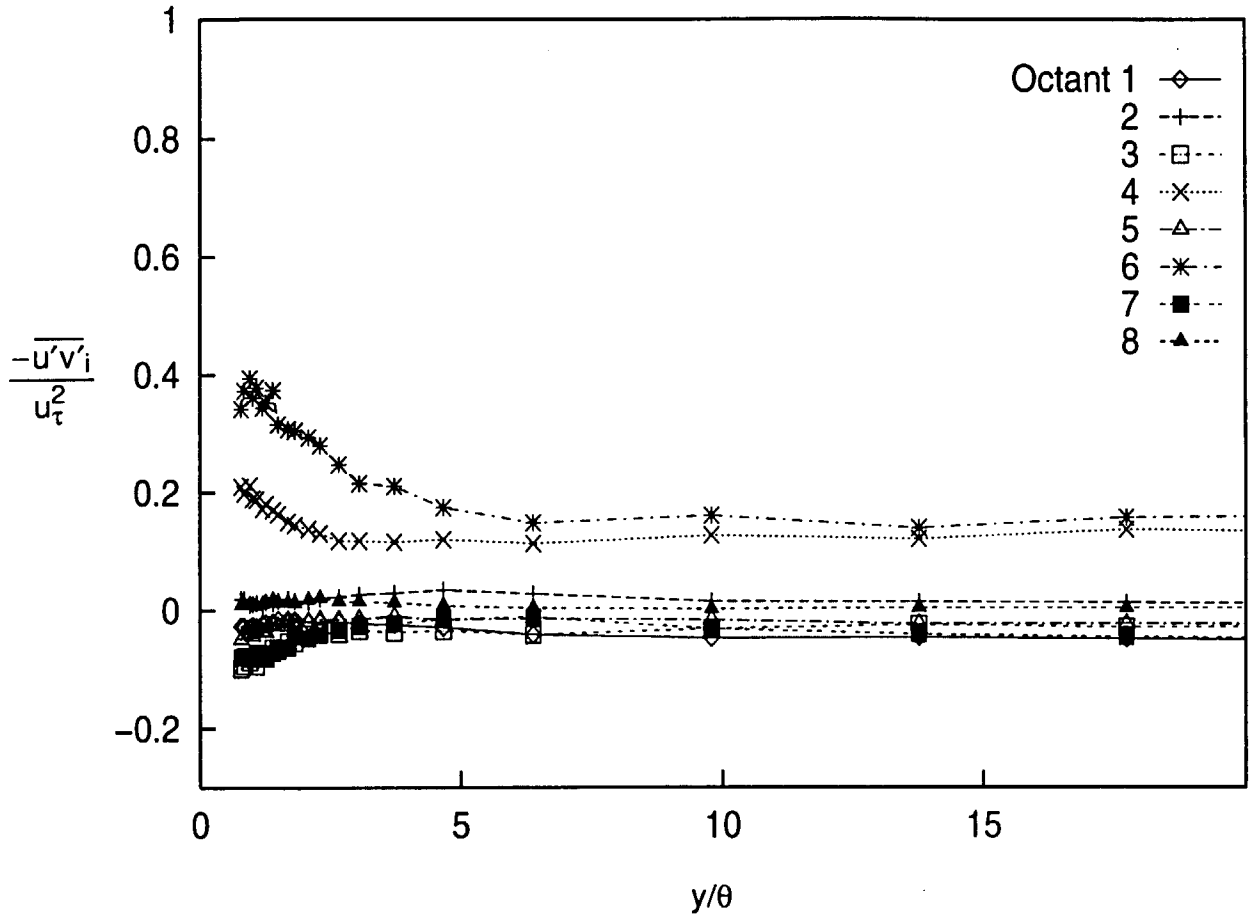

Fig. 7.38a: Octant Decomposition of Turbulent Shear Stress Station 1, dU_{cw}/dx=14 s^{-1} Case

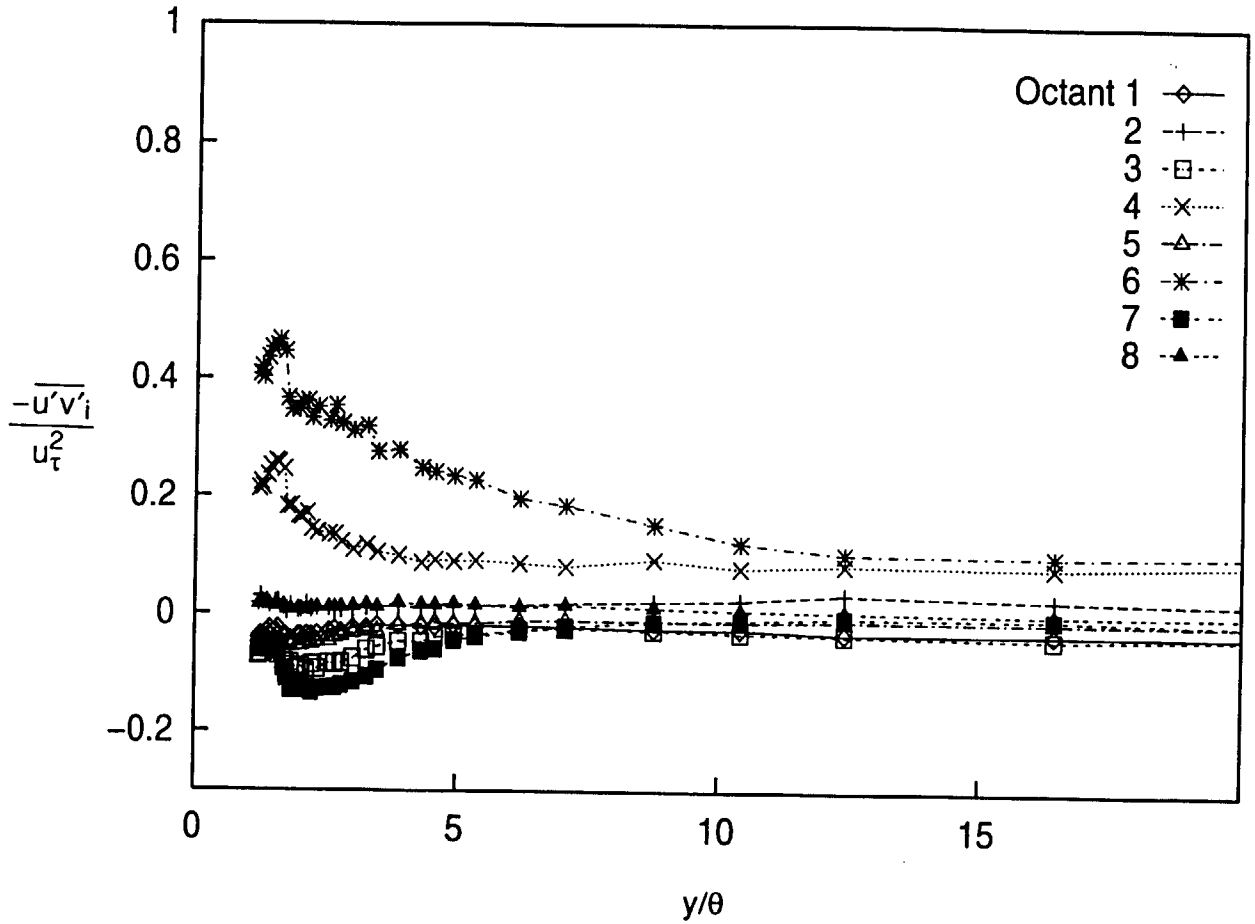

Fig. 7.38b: Octant Decomposition of Turbulent Shear Stress Station 2, dU_{cw}/dx=14 s^{-1} Case

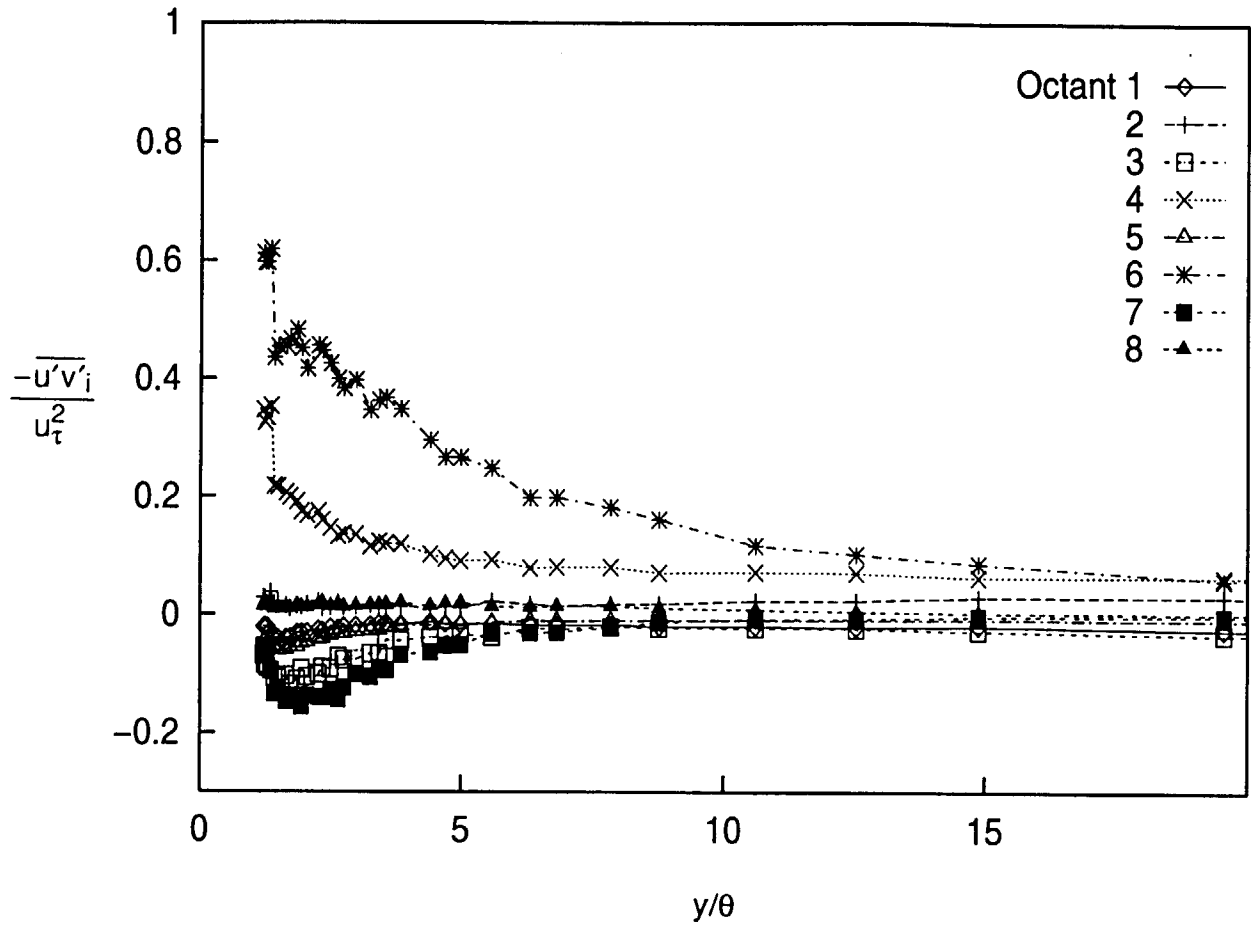

Fig. 7.38c: Octant Decomposition of Turbulent Shear Stress Station 3, dU_{cw}/dx=14 s^{-1} Case

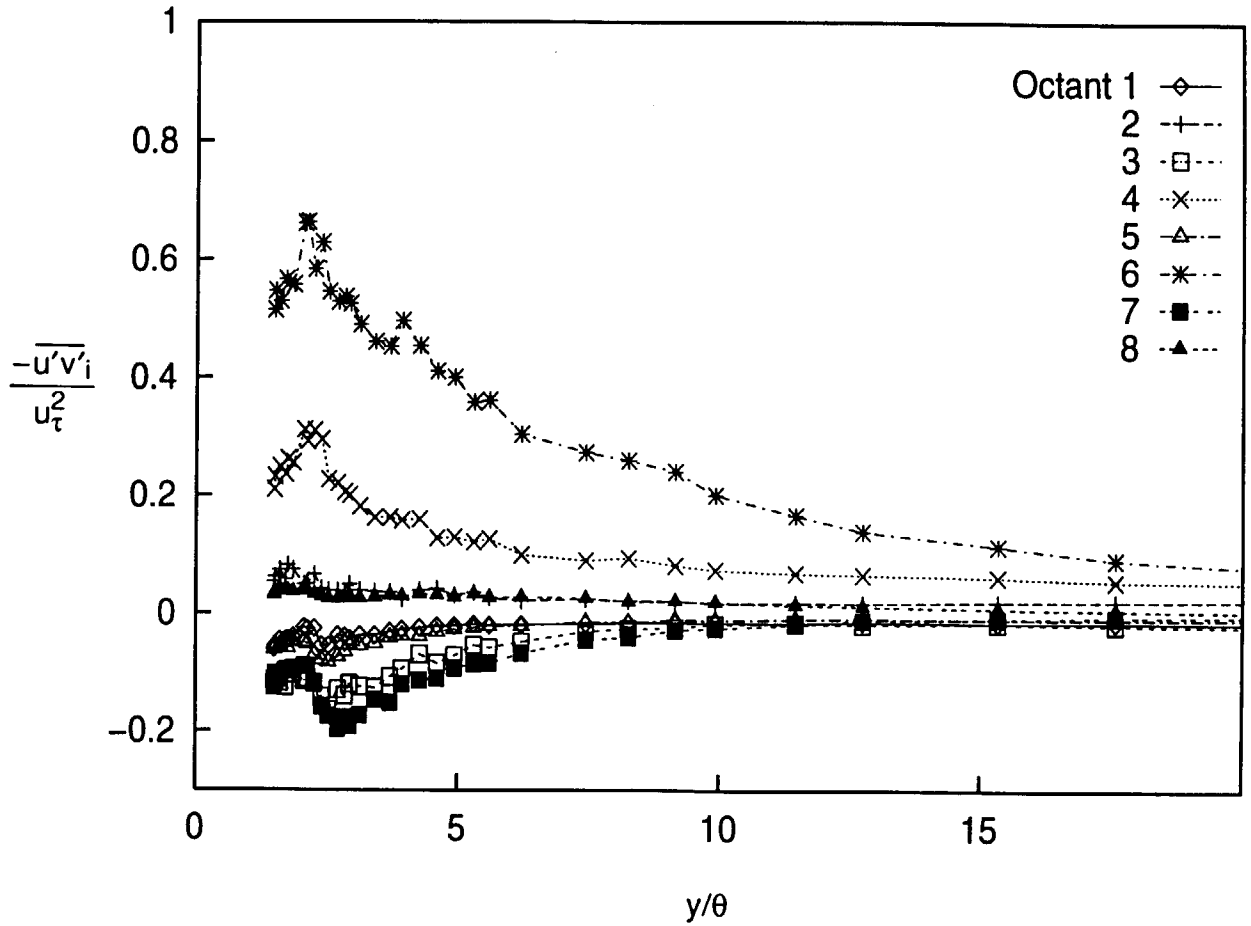

Fig. 7.38d: Octant Decomposition of Turbulent Shear Stress Station 4, dU_{cw}/dx=14 s^{-1} Case

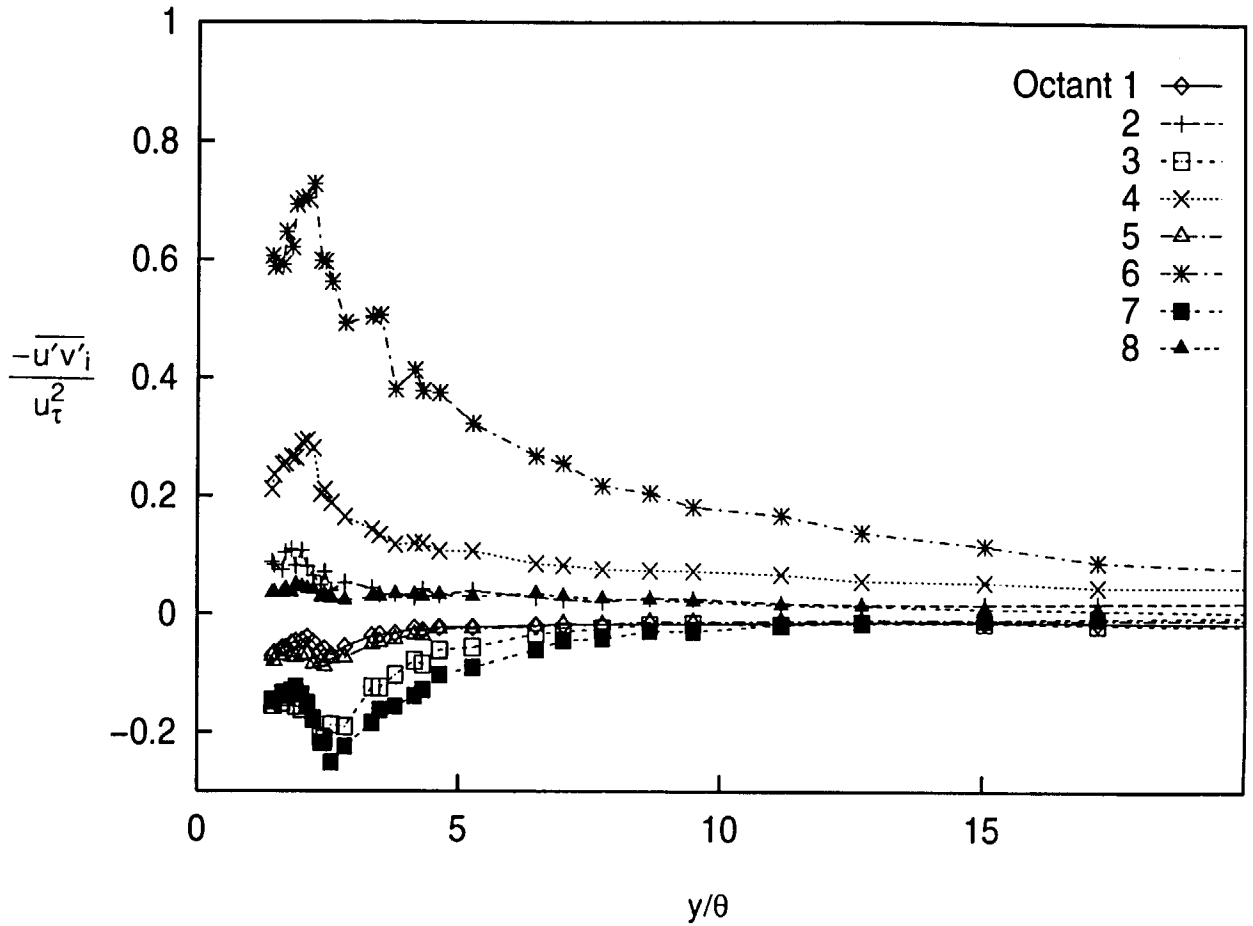

Fig. 7.38e: Octant Decomposition of Turbulent Shear Stress Station 5, dU_{cw}/dx=14 s^{-1} Case

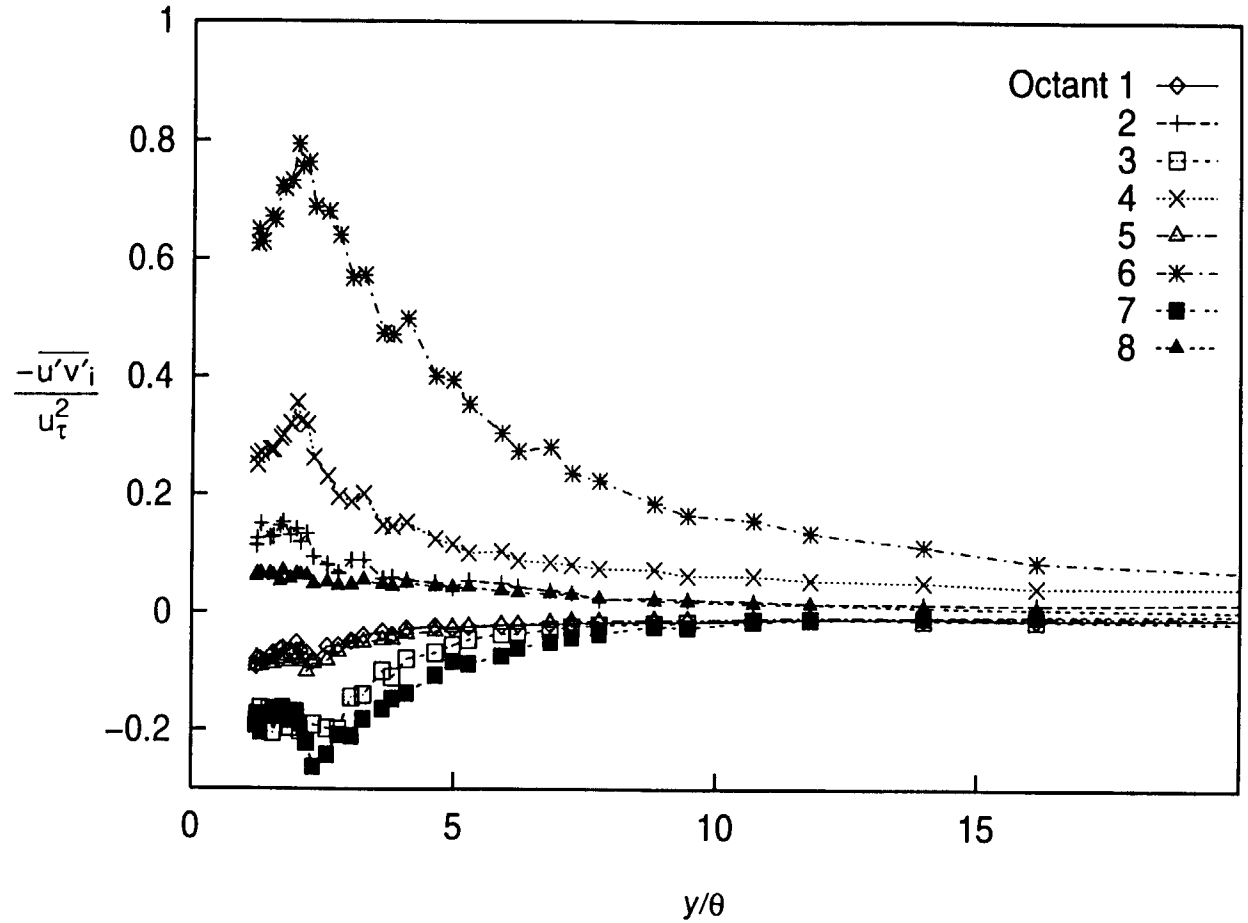

Fig. 7.38f: Octant Decomposition of Turbulent Shear Stress Station 6, dU_{cw}/dx=14 s^{-1} Case

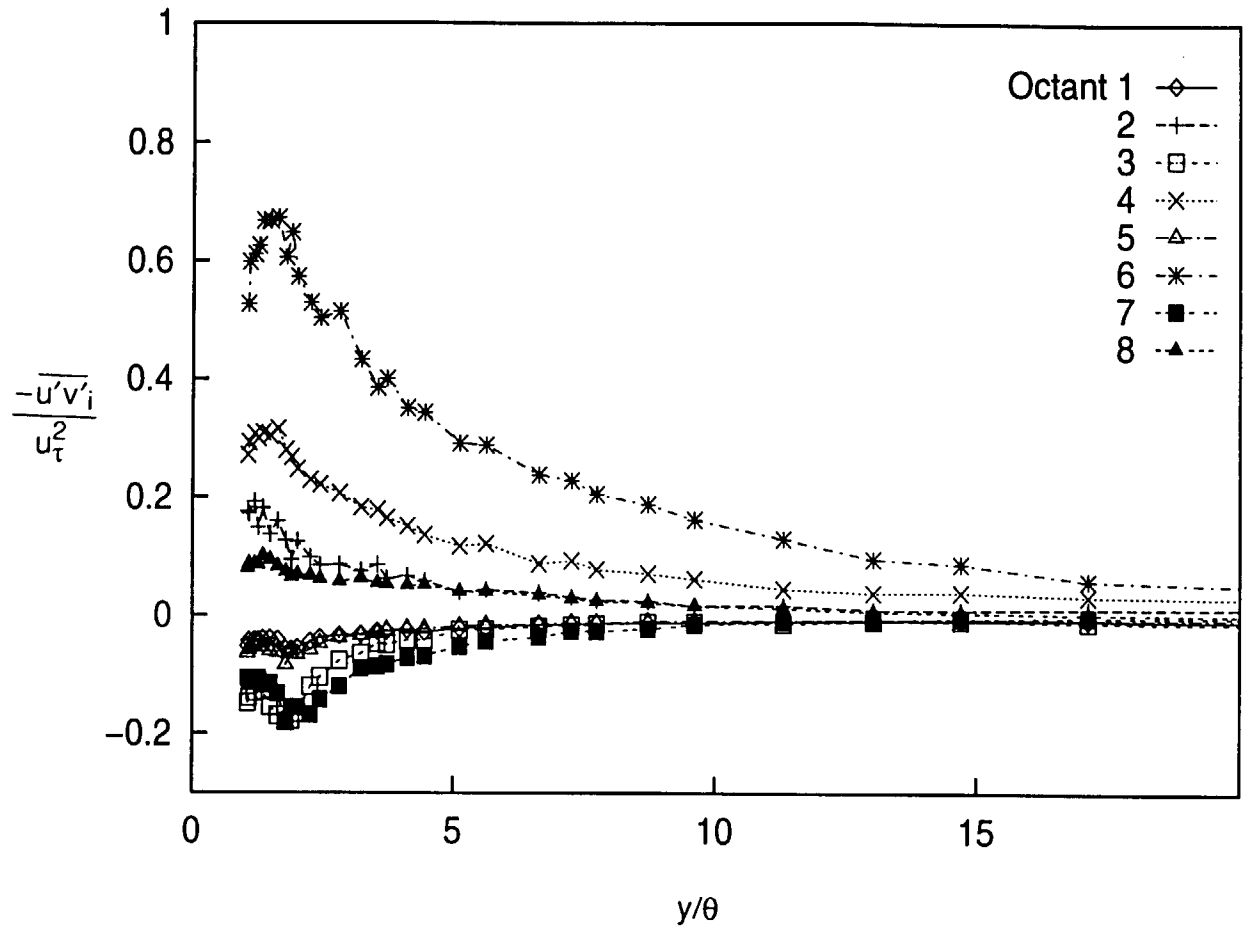

Fig. 7.38g: Octant Decomposition of Turbulent Shear Stress Station 7, dU_{cw}/dx=14 s^{-1} Case

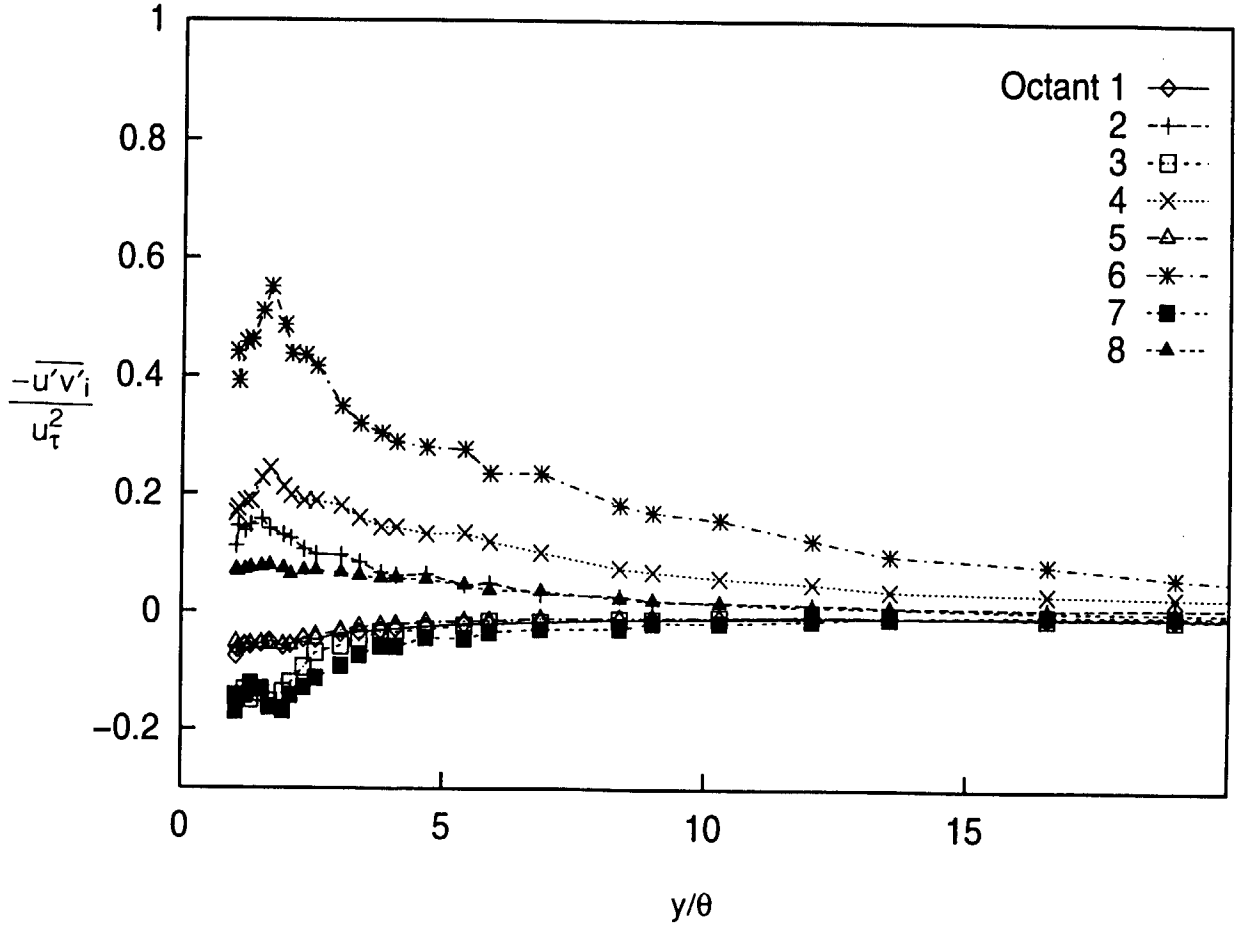

Fig. 7.38h: Octant Decomposition of Turbulent Shear Stress Station 8, dU_{cw}/dx=14 s^{-1} Case

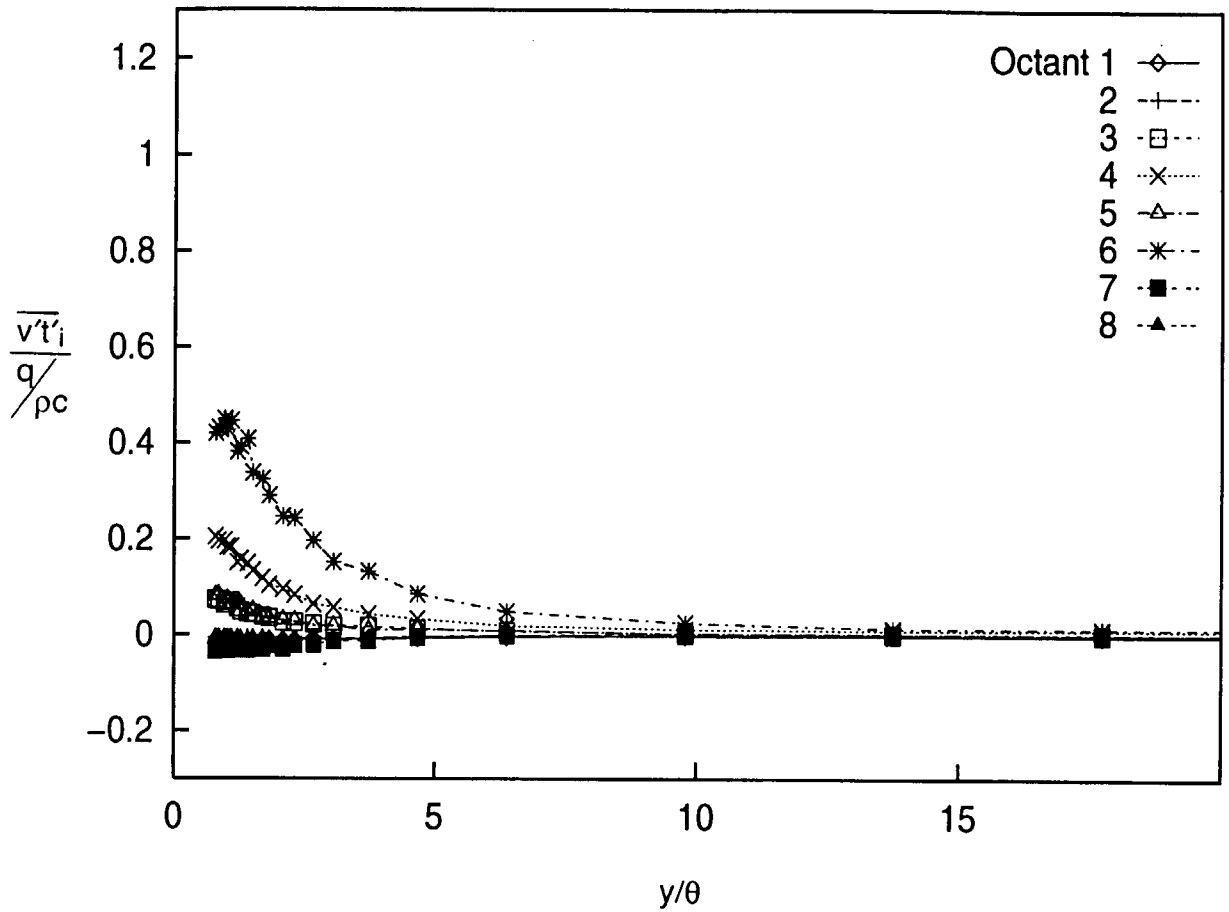

Fig. 7.39a: Octant Decomposition of Turbulent Heat Flux Station 1, dU_{cw}/dx=14 s^{-1} Case

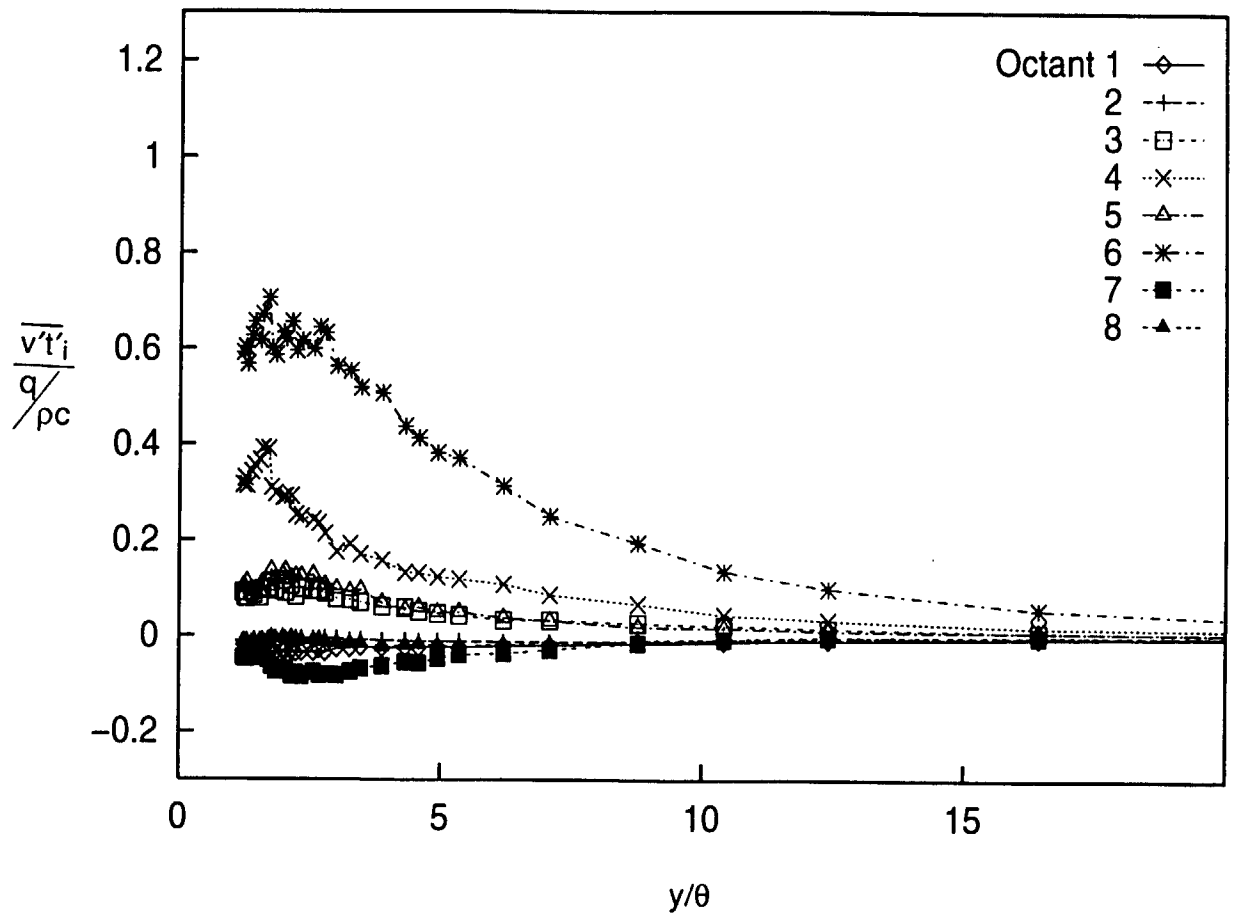

Fig. 7.39b: Octant Decomposition of Turbulent Heat Flux Station 2, dU_{cw}/dx=14 s^{-1} Case

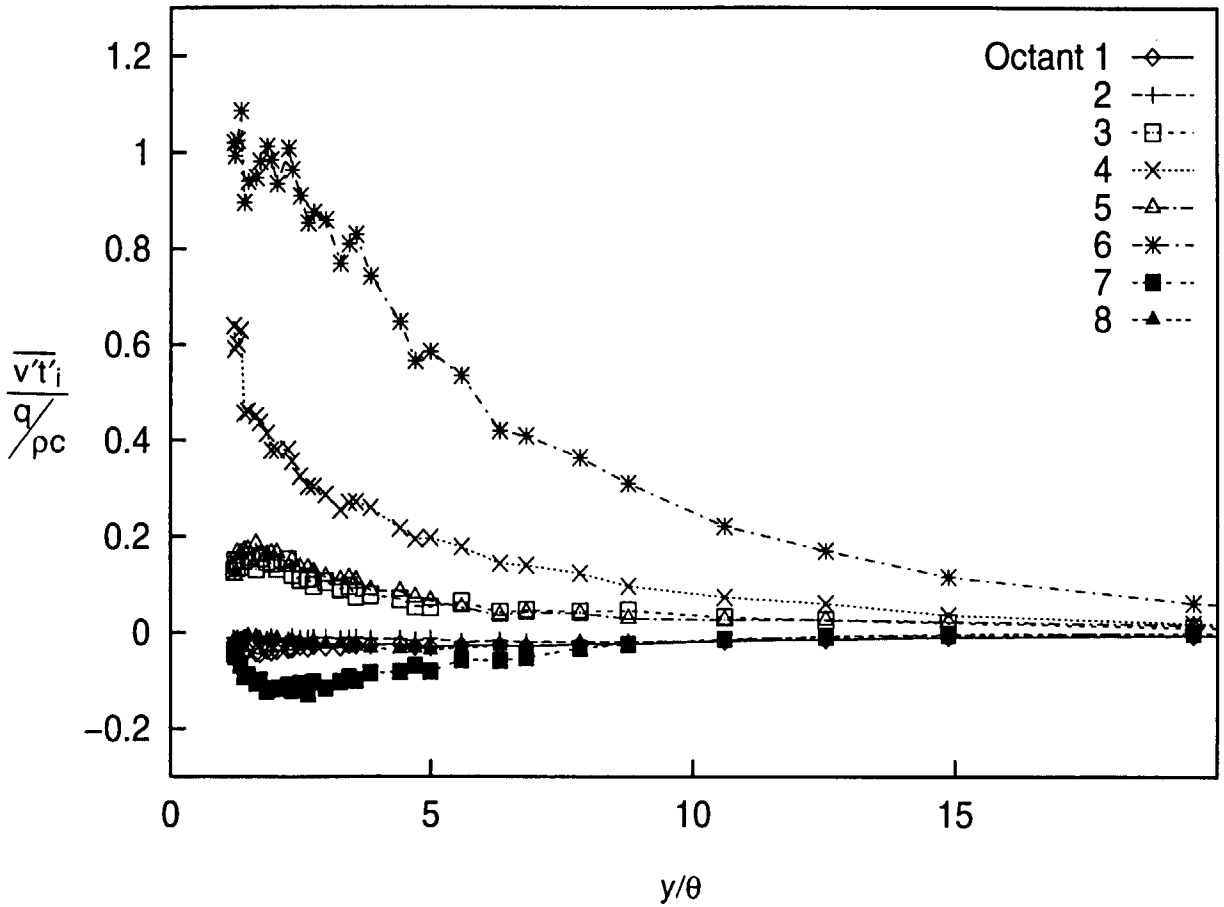

Fig. 7.39c: Octant Decomposition of Turbulent Heat Flux Station 3, dU_{cw}/dx=14 s^{-1} Case

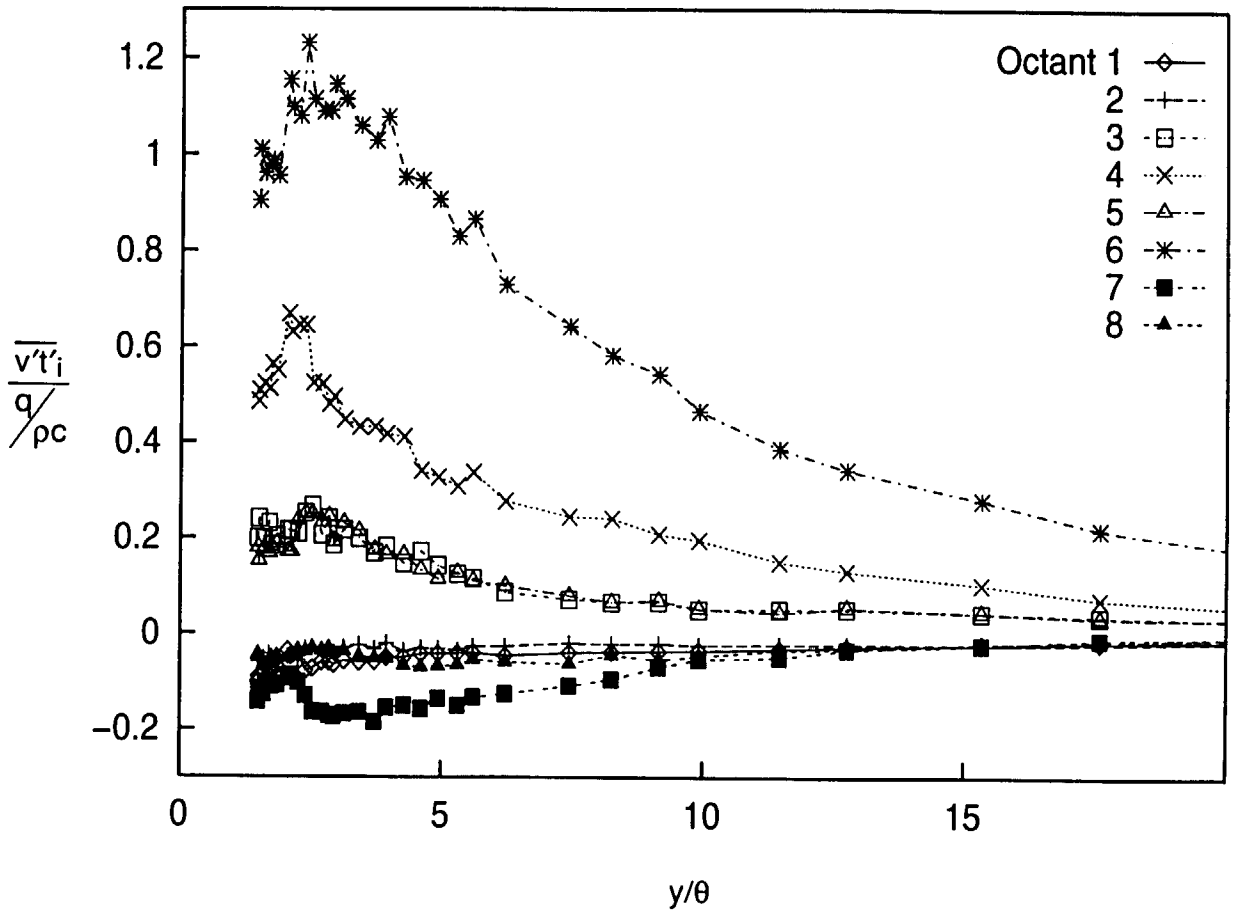

Fig. 7.39d: Octant Decomposition of Turbulent Heat Flux Station 4, dU_{cw}/dx=14 s^{-1} Case

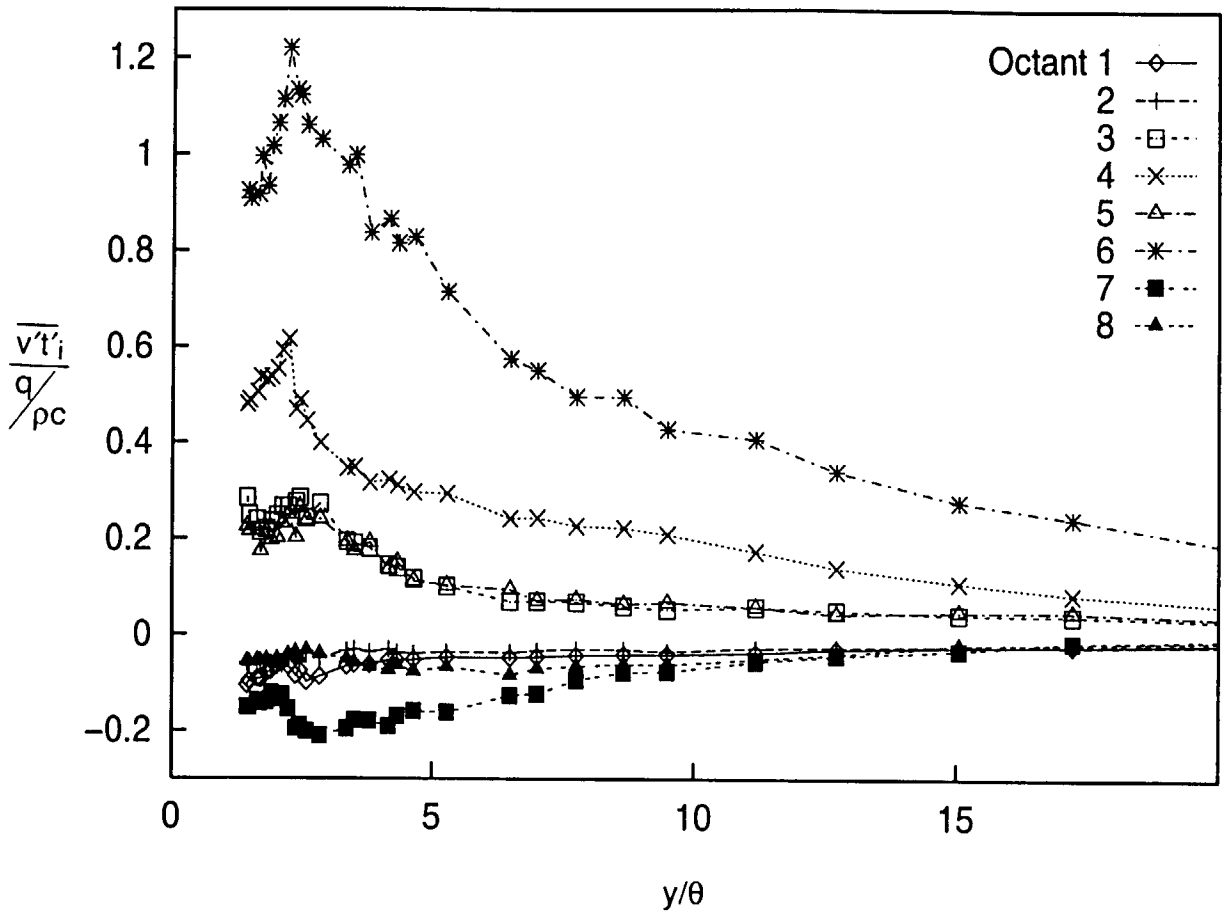

Fig. 7.39e: Octant Decomposition of Turbulent Heat Flux Station 5, dU_{cw}/dx=14 s^{-1} Case

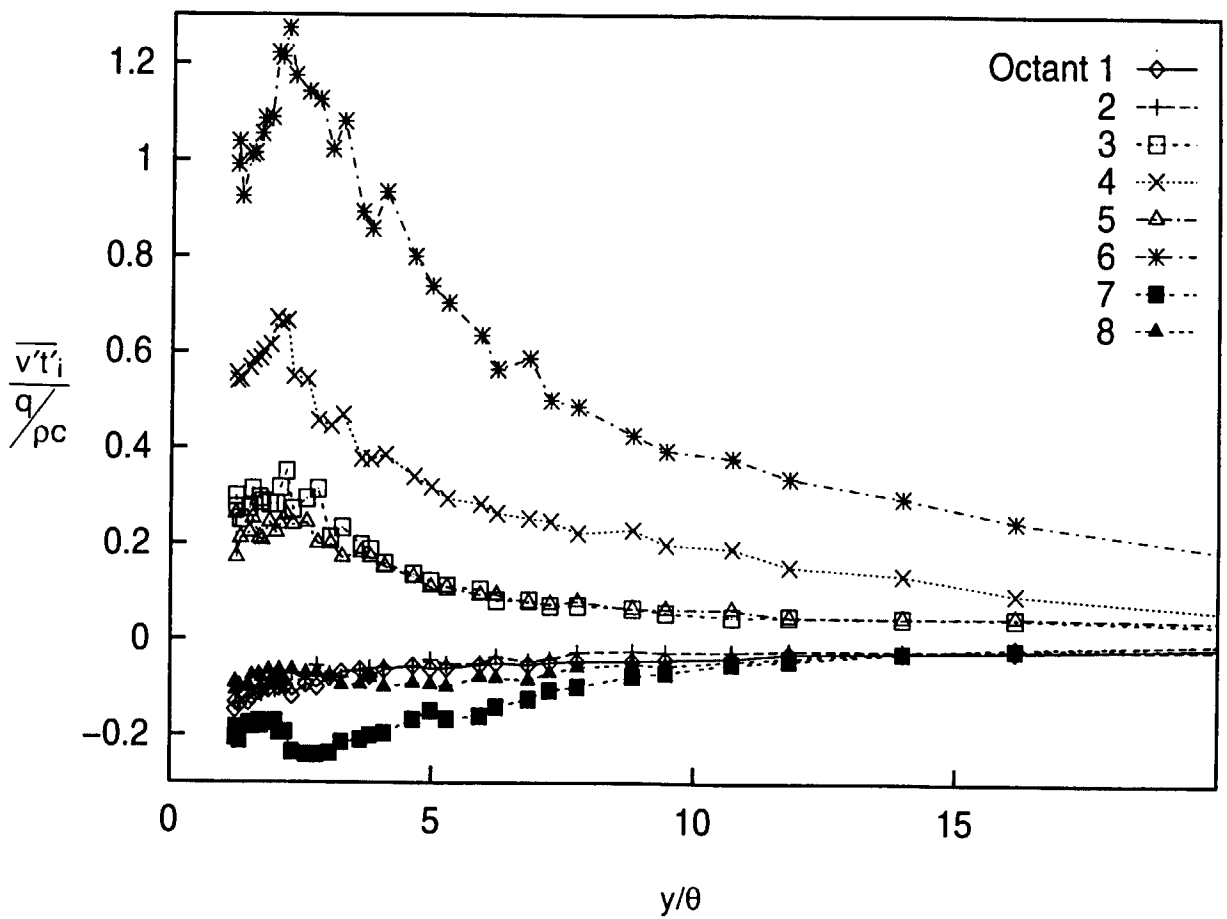

Fig. 7.39f: Octant Decomposition of Turbulent Heat Flux Station 6, dU_{cw}/dx=14 s^{-1} Case

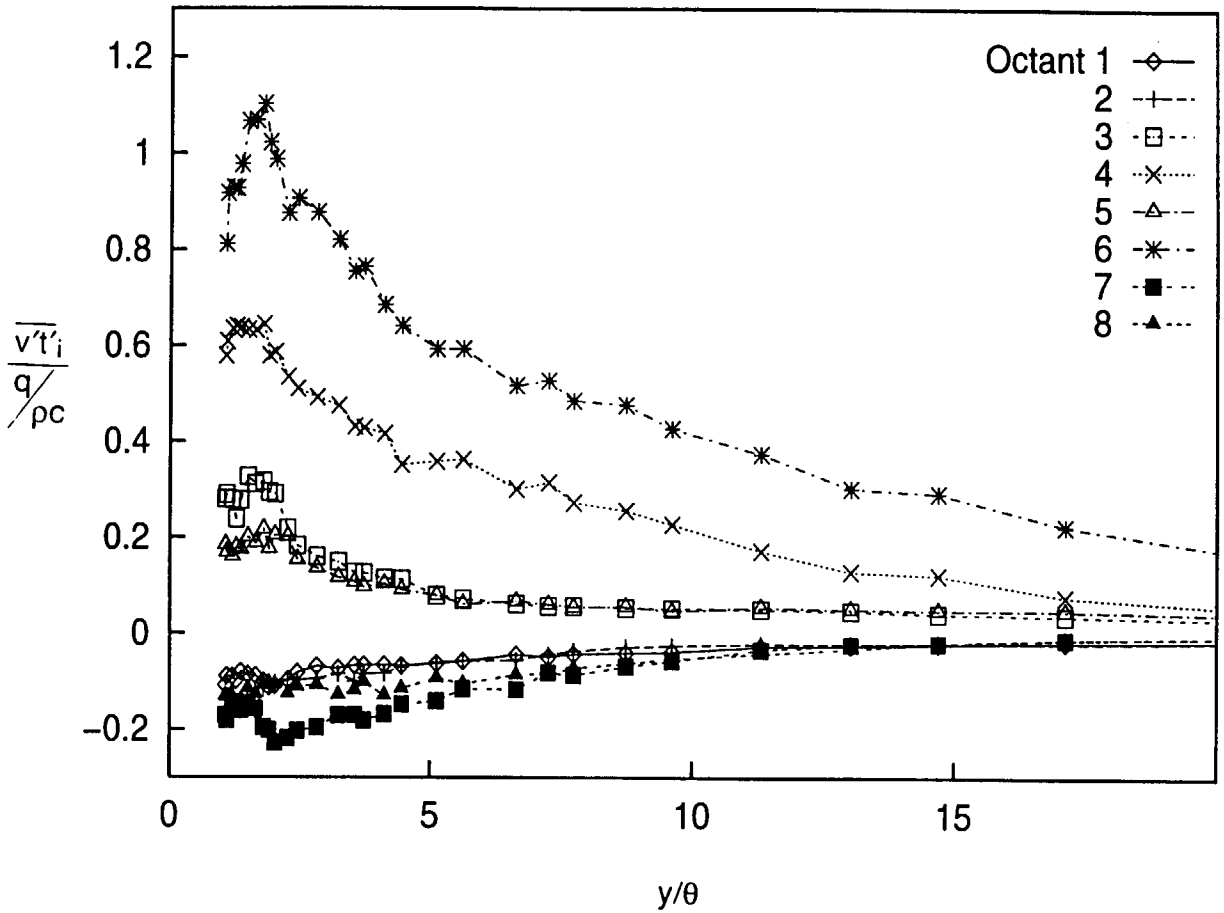

Fig. 7.39g: Octant Decomposition of Turbulent Heat Flux Station 7, dU_{cw}/dx=14 s^{-1} Case

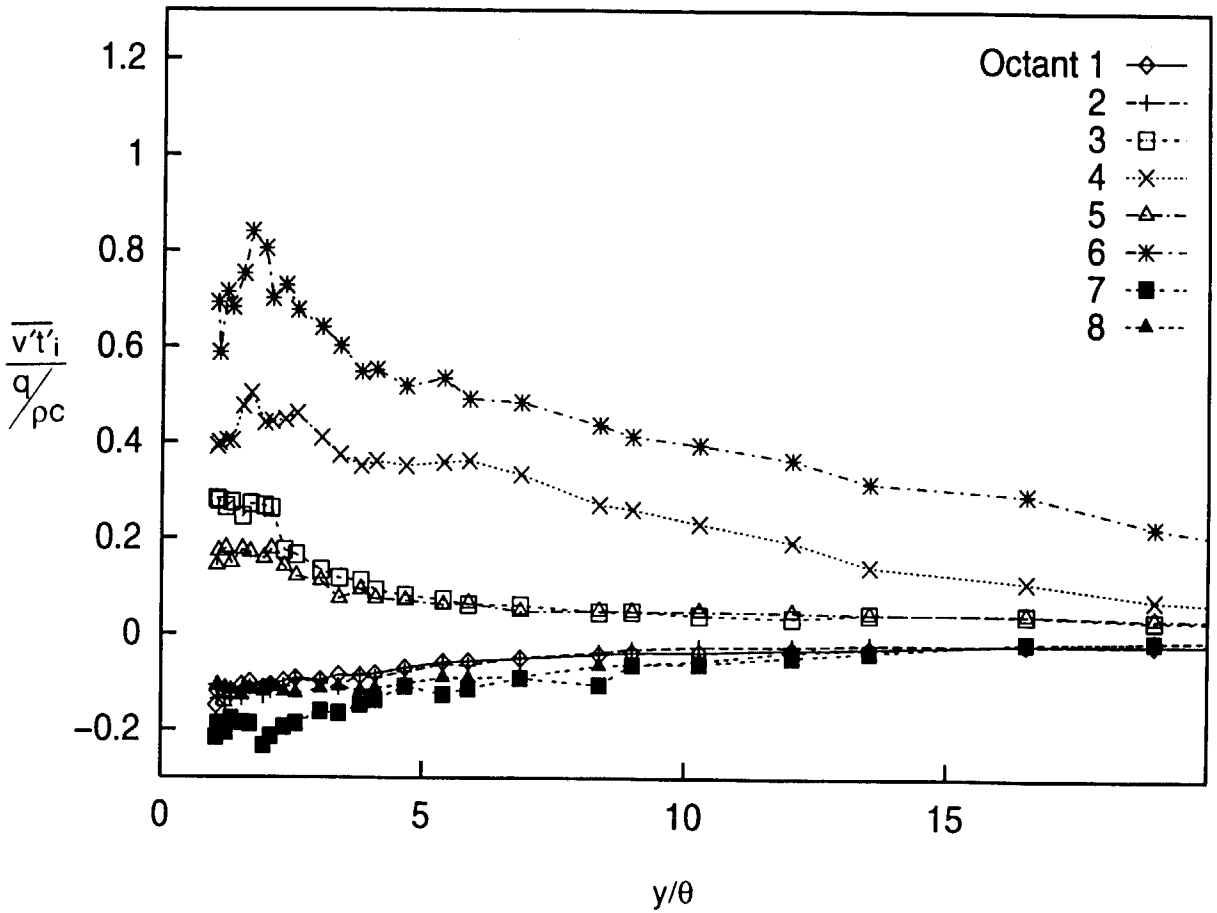

Fig. 7.39h: Octant Decomposition of Turbulent Heat Flux Station 8, dU_{cw}/dx=14 s^{-1} Case

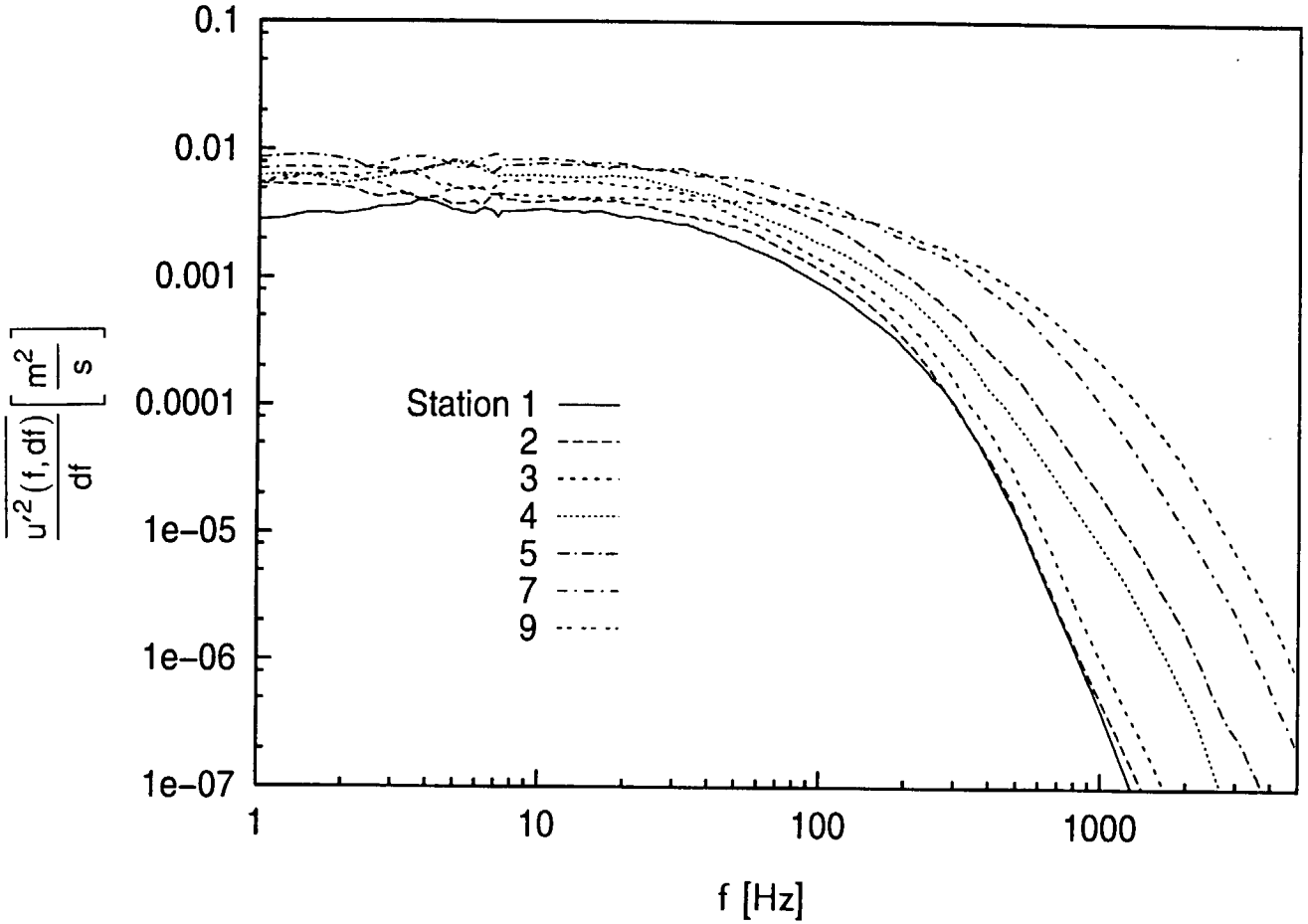

Fig. 7.40a: Boundary Layer u' Spectra at y^+=5 dU_{cw}/dx=14 s^{-1} Case

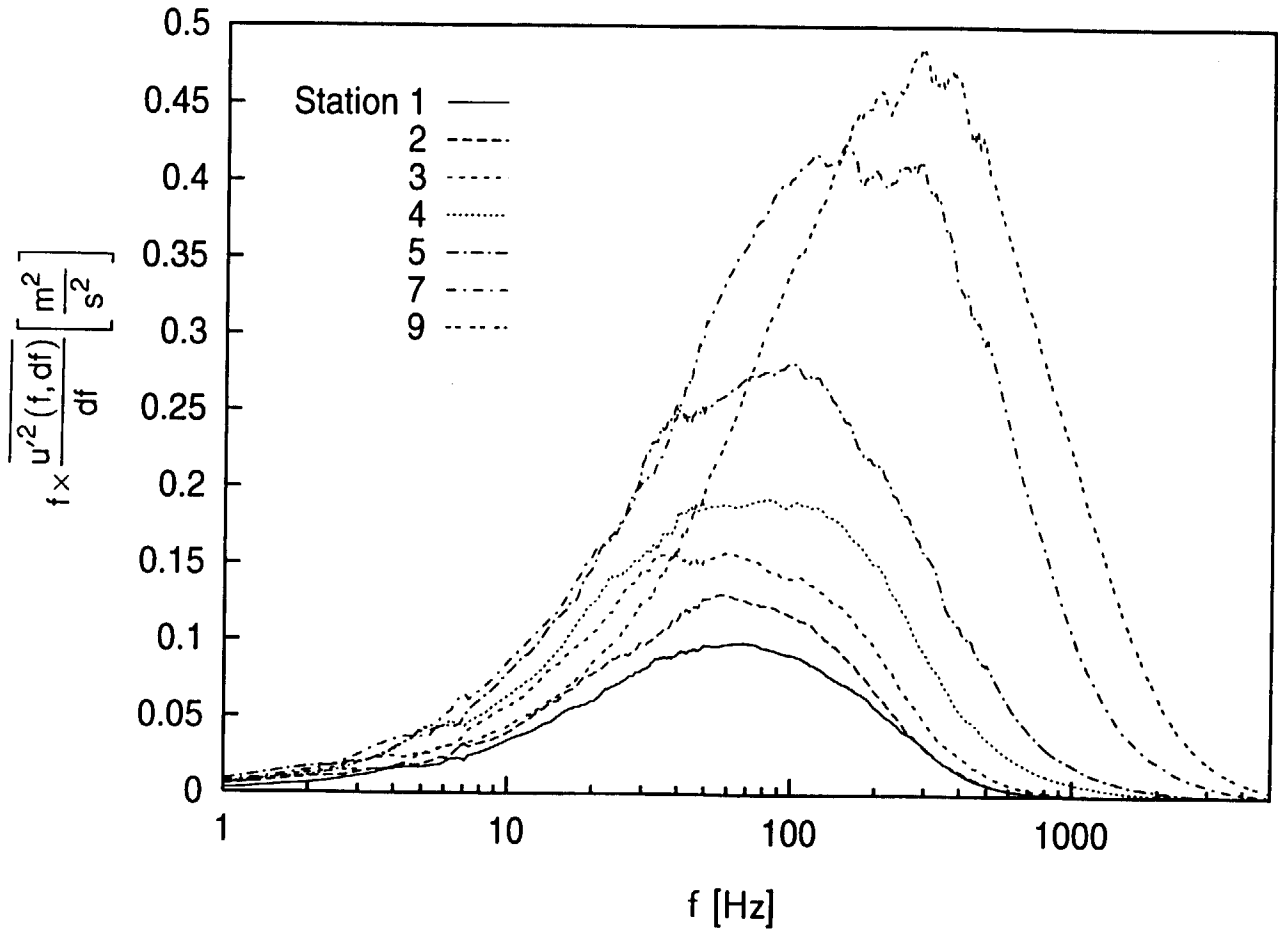

Fig. 7.40b: Boundary Layer u' Spectra at y^+=5, Energy Coordinates, dU_{cw}/dx=14 s^{-1} Case

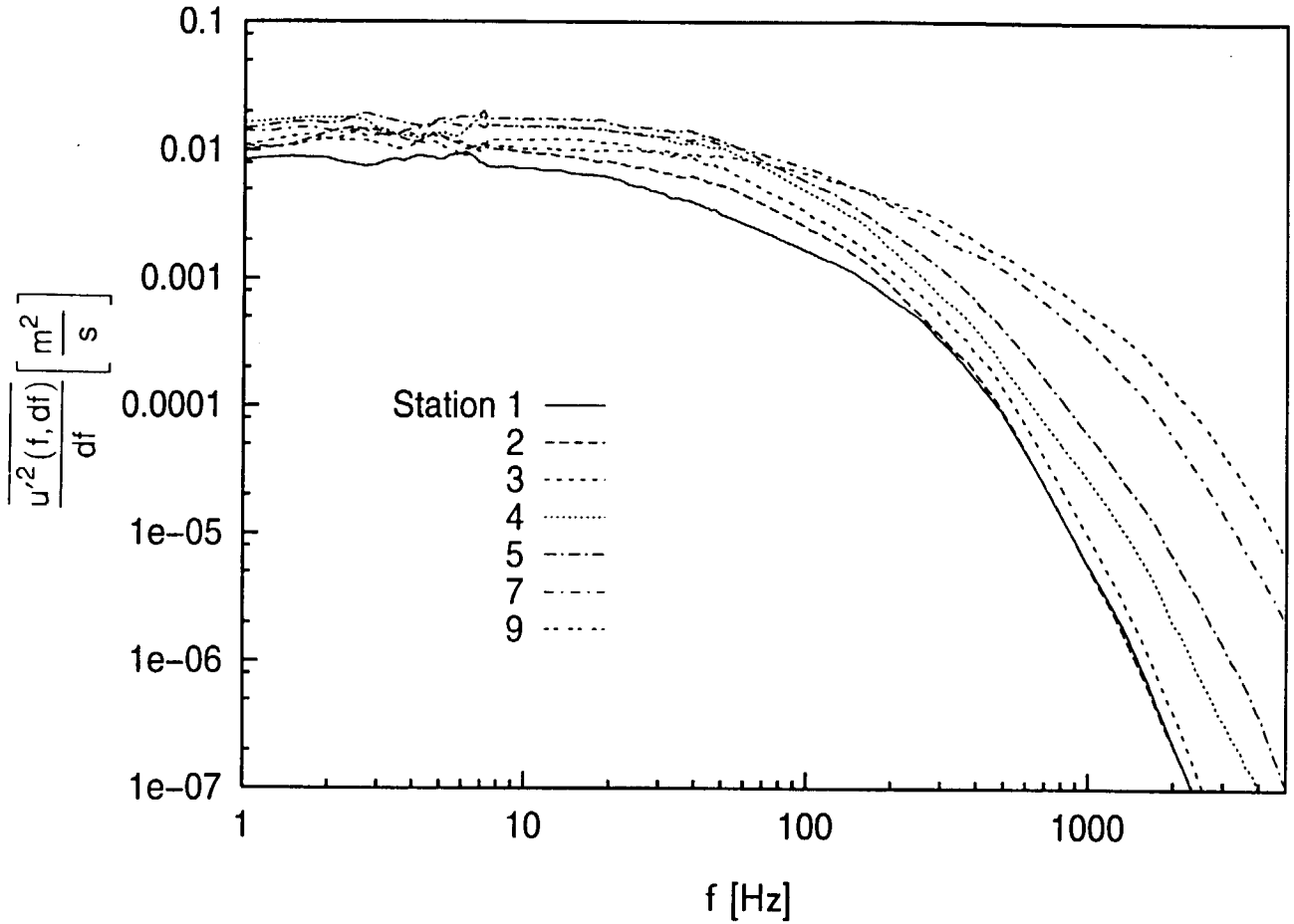

Fig. 7.41a: Boundary Layer u' Spectra at y^+=17 dU_{cw}/dx=14 s^{-1} Case

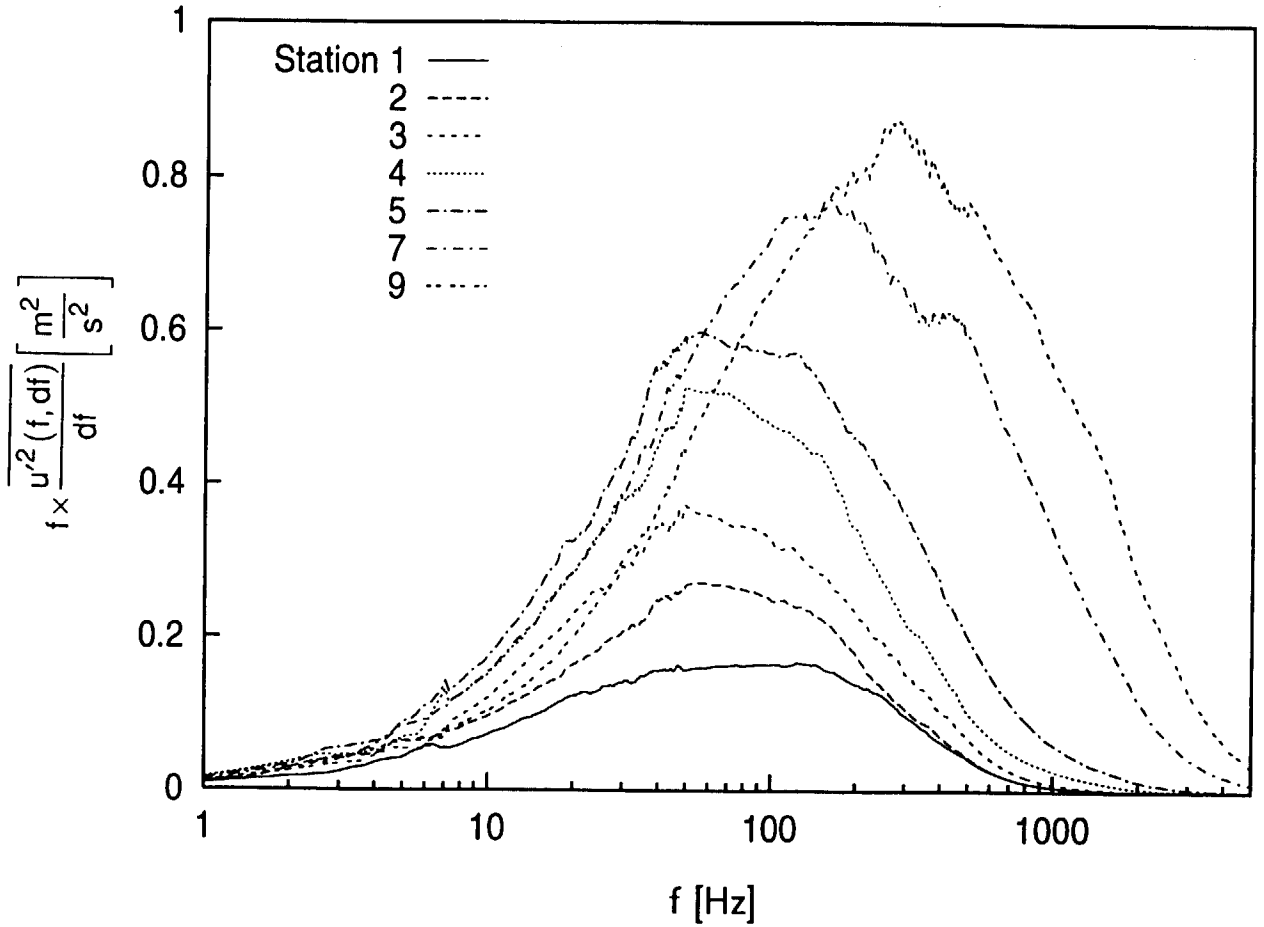

Fig. 7.41b: Boundary Layer u' Spectra at y^+=17, Energy Coordinates, dU_{cw}/dx=14 s^{-1} Case

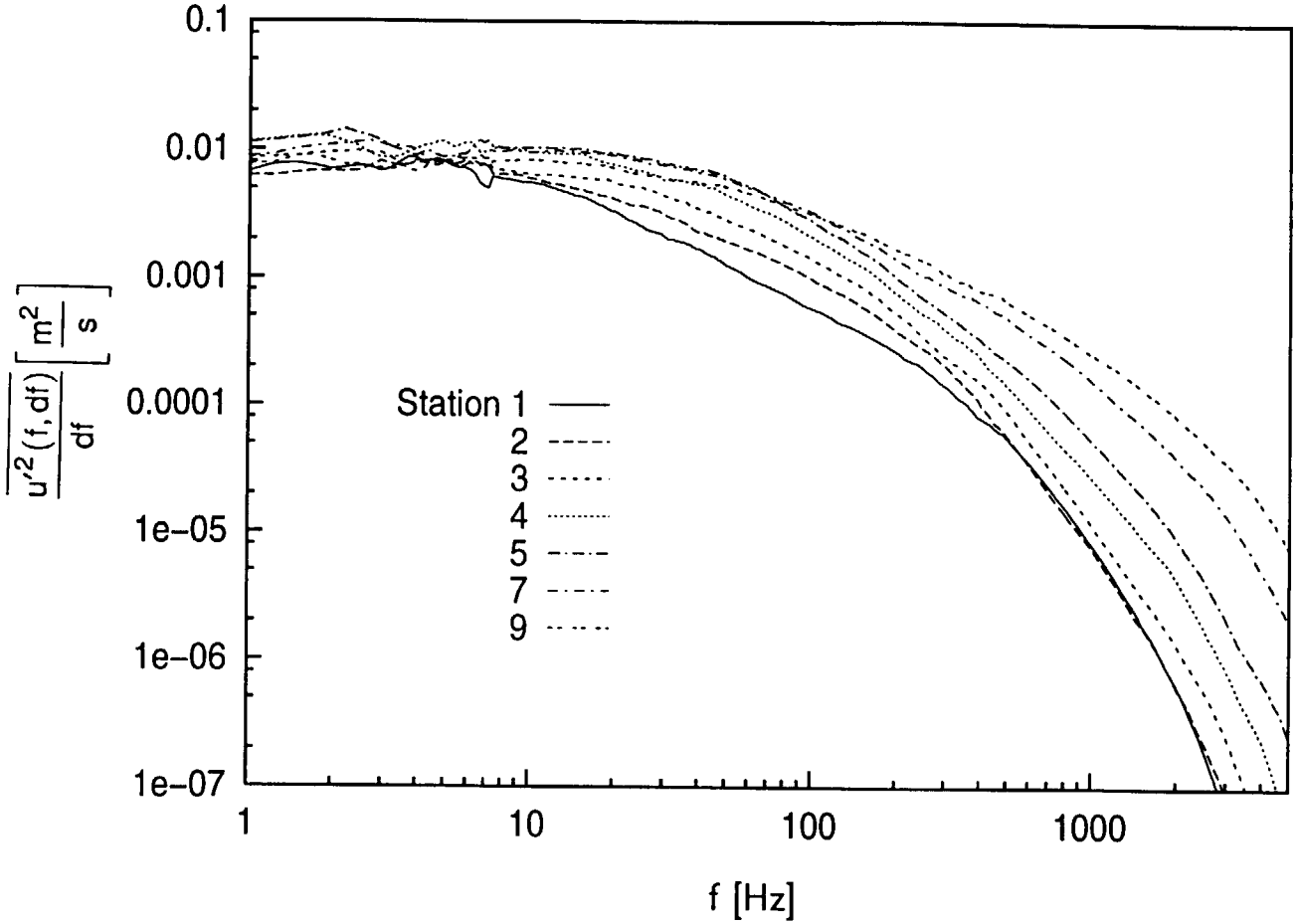

Fig. 7.42a: Boundary Layer u' Spectra at y^+=50 dU_{cw}/dx=14 s^{-1} Case

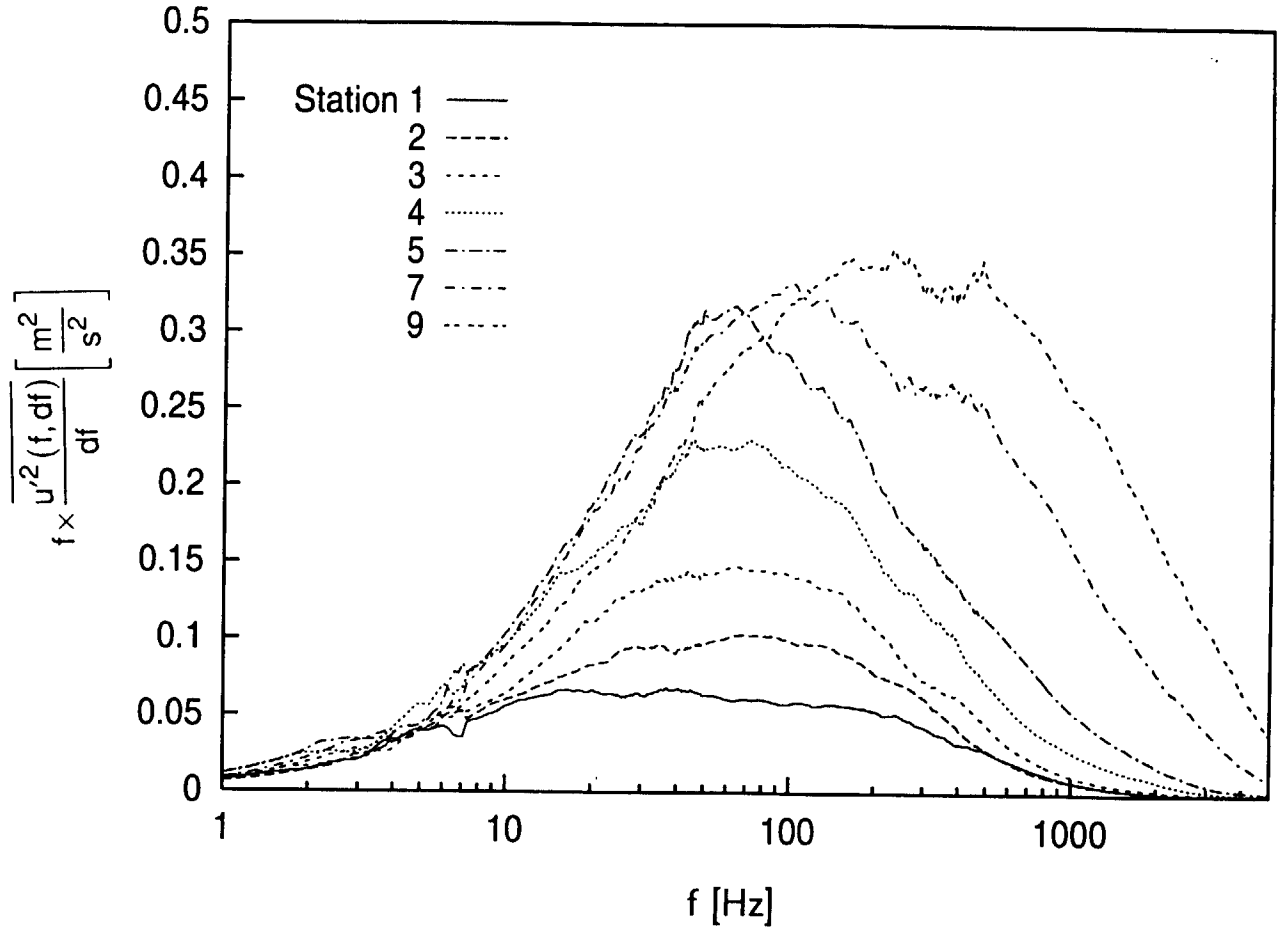

Fig. 7.42b: Boundary Layer u' Spectra at y^+=50, Energy Coordinates, dU_{cw}/dx=14 s^{-1} Case

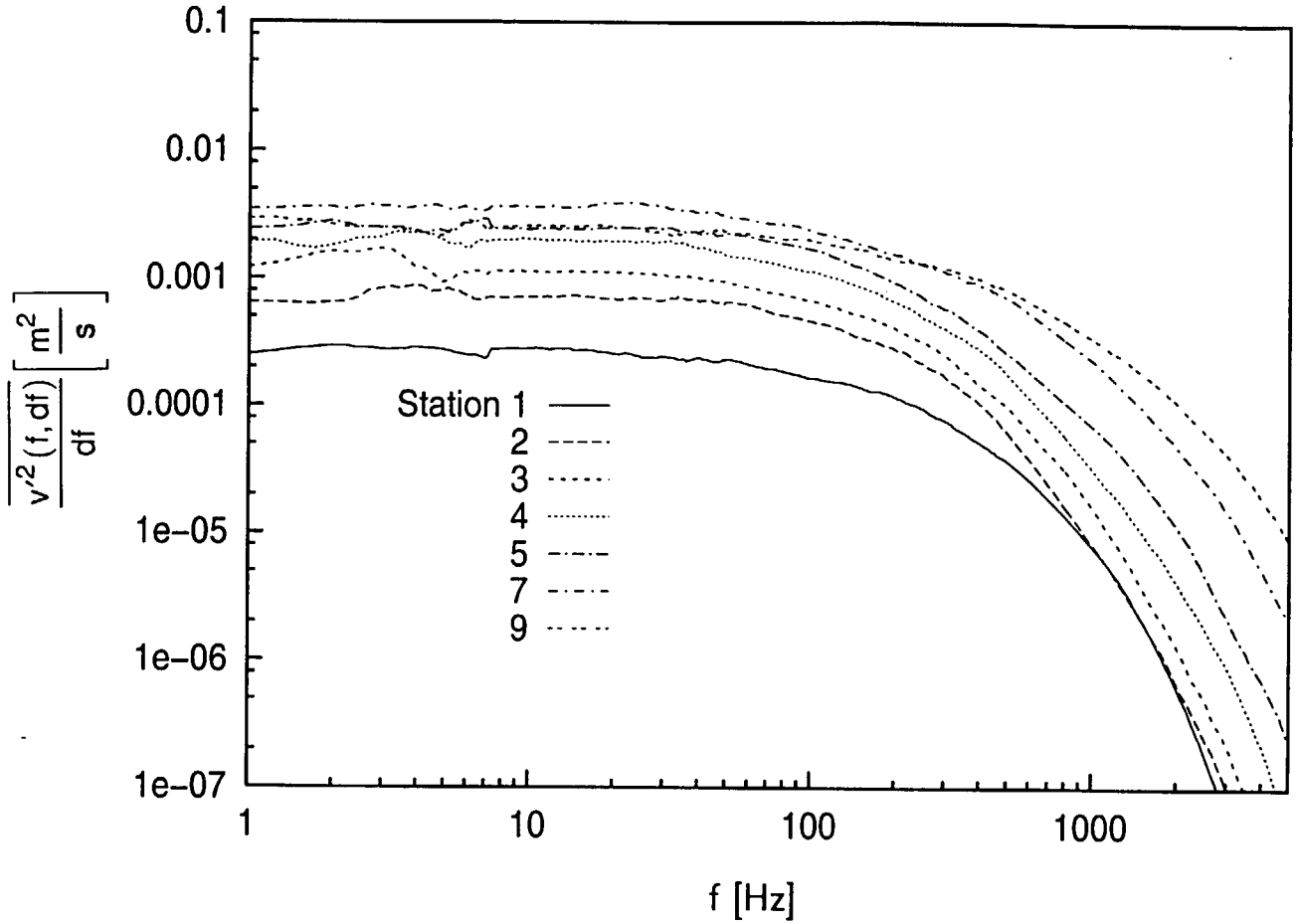

Fig. 7.43a: Boundary Layer v' Spectra at y^+=50 dU_{cw}/dx=14 s^{-1} Case

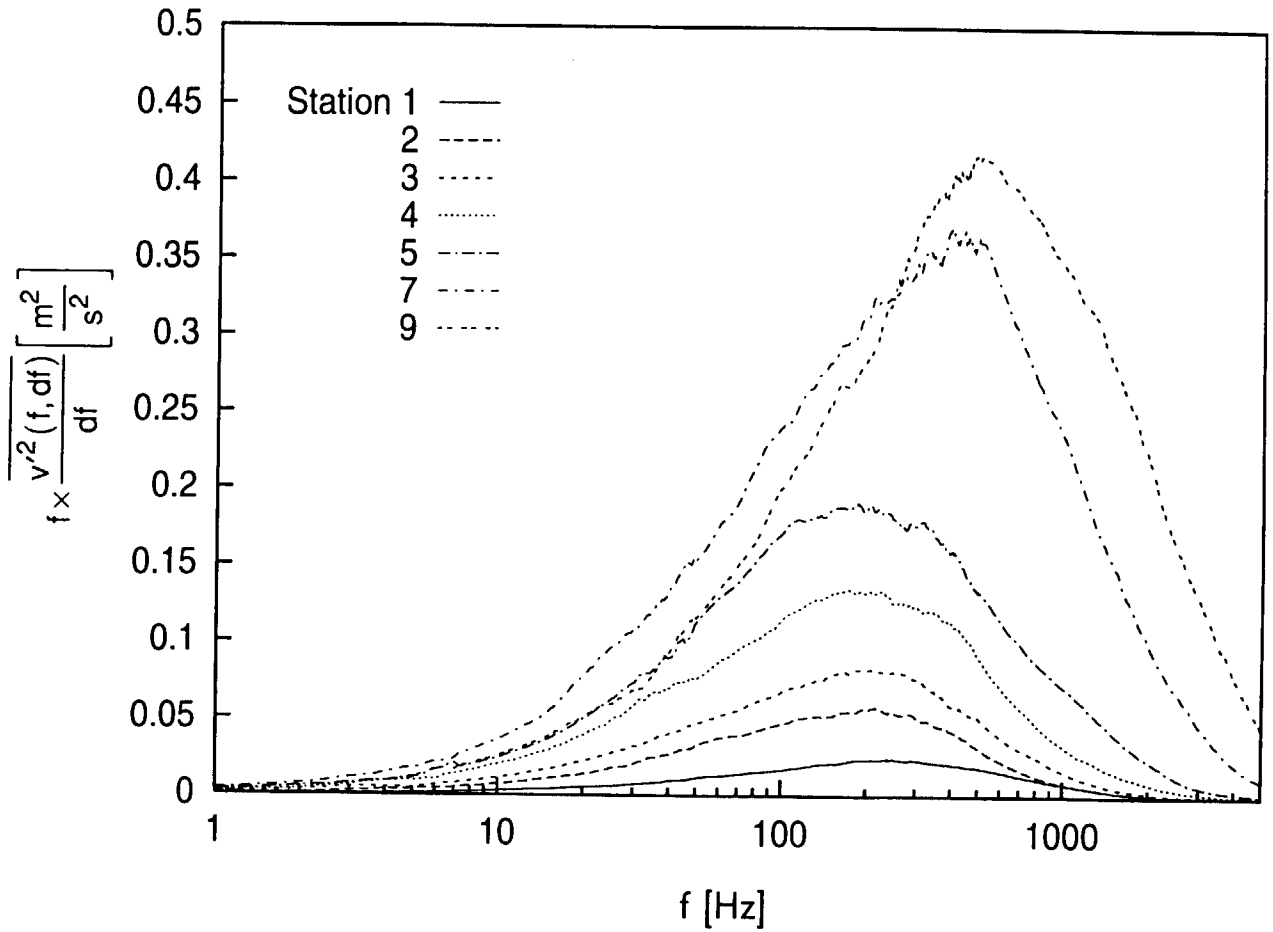

Fig. 7.43b: Boundary Layer v' Spectra at y^+=50, Energy Coordinates, dU_{cw}/dx=14 s^{-1} Case

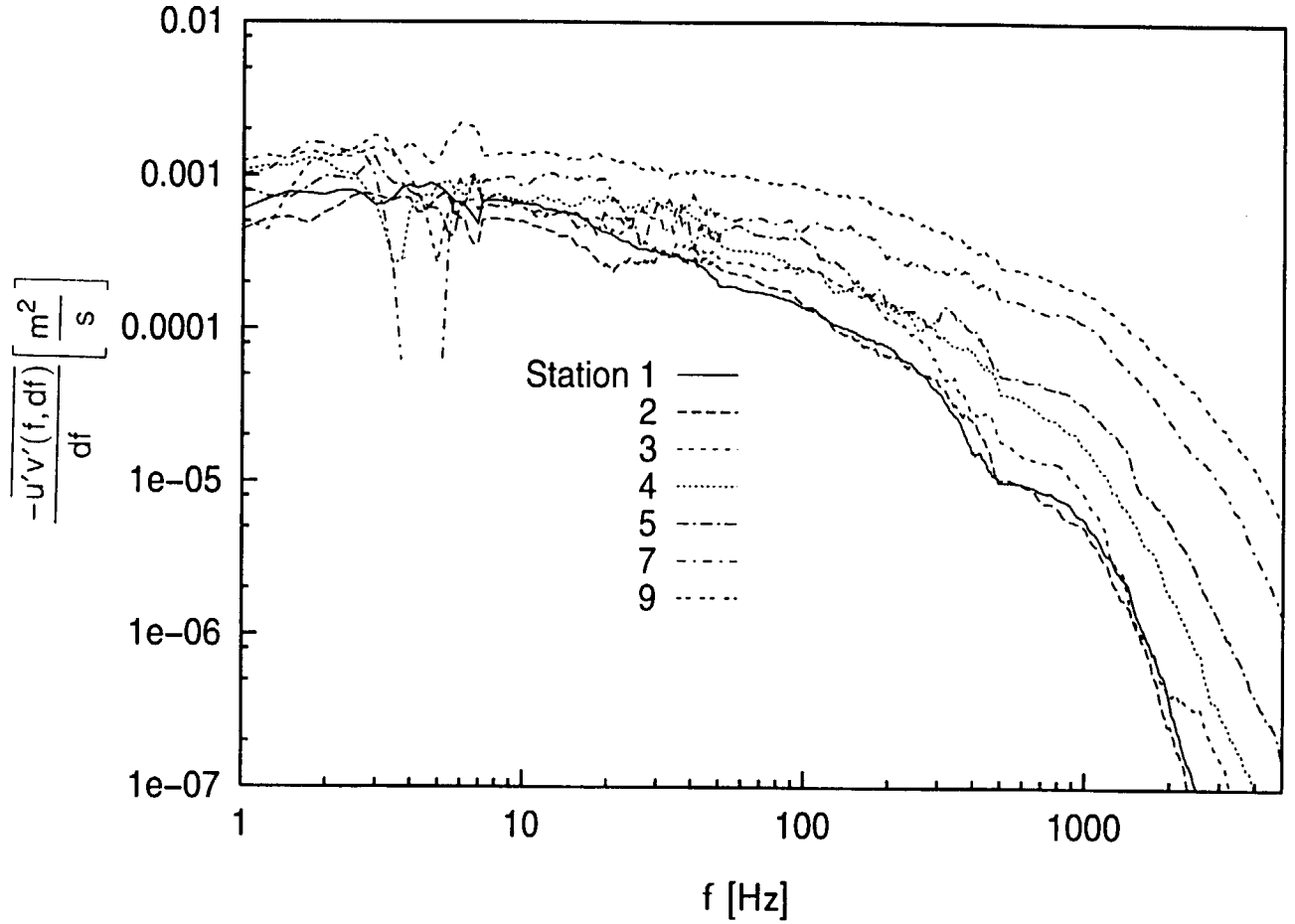

Fig. 7.44a: Turbulent Shear Stress Spectra at y^+=50 dU_{cw}/dx=14 s^{-1} Case

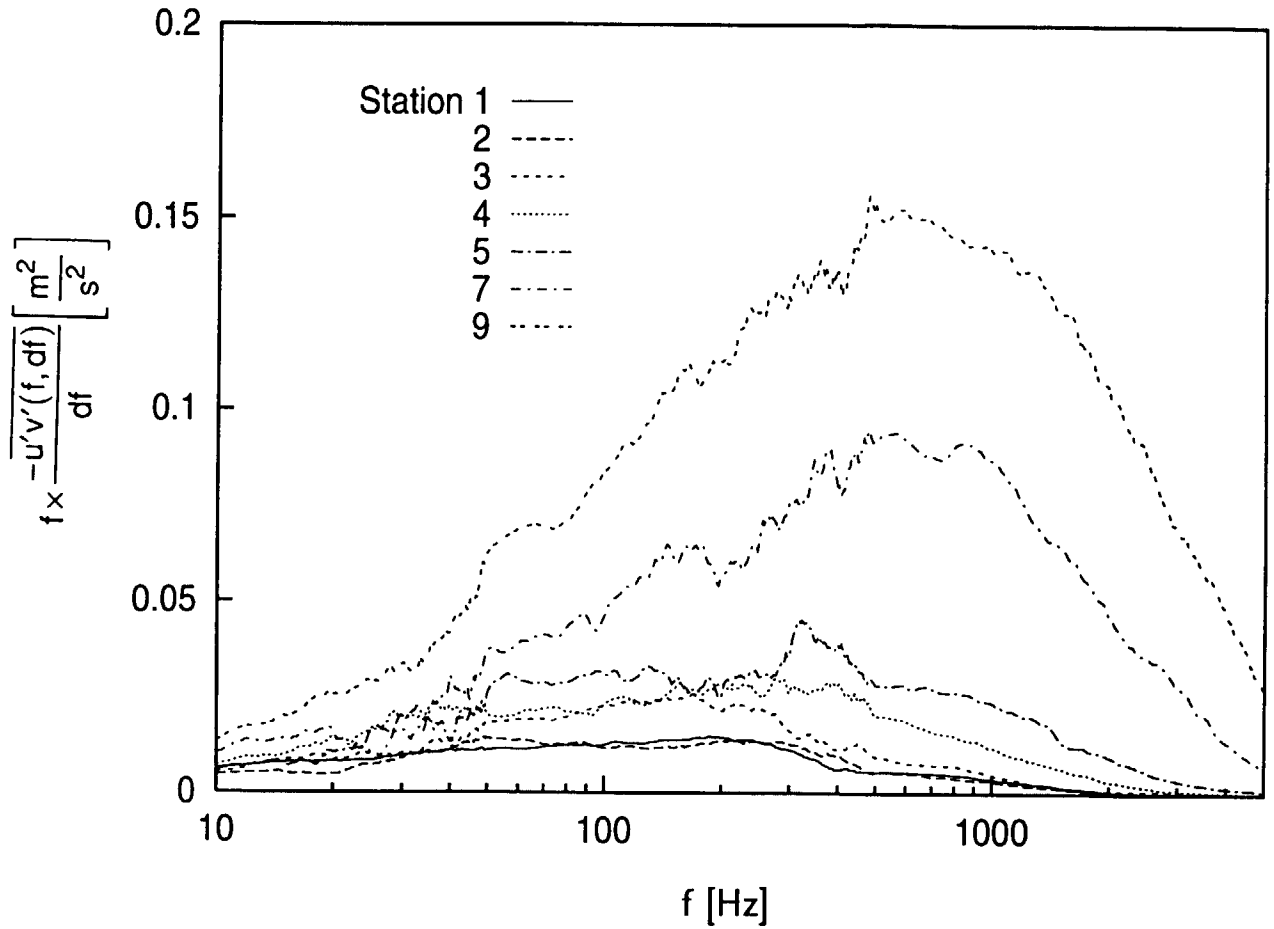

Fig. 7.44b: Turbulent Shear Stress Spectra at y^+=50, Energy Coordinates, dU_{cw}/dx=14 s^{-1} Case

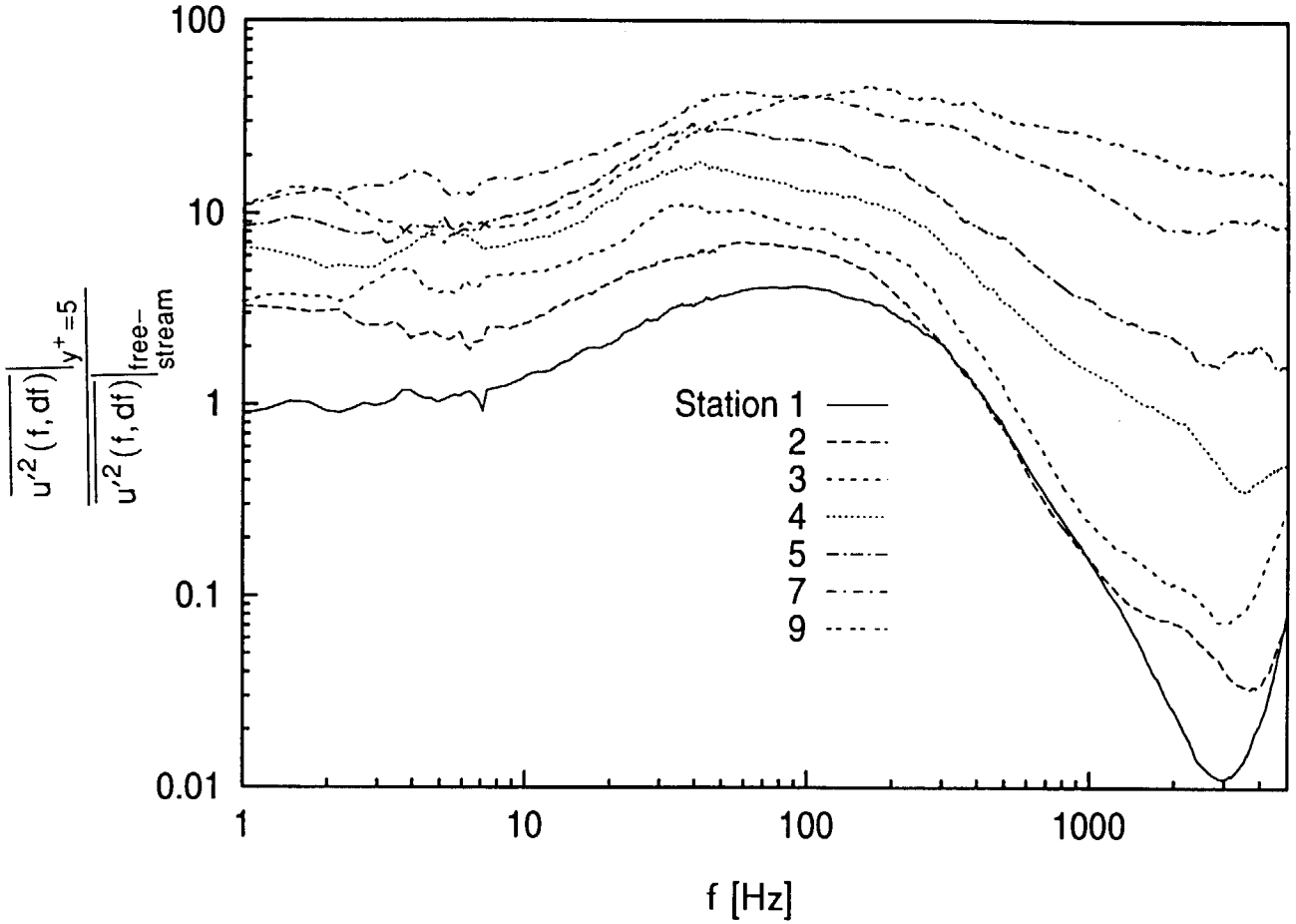

Fig. 7.45: Transfer Function of u' Between Boundary Layer at y^+=5 and Free-Stream, dU_{cw}/dx=14 s^{-1} Case

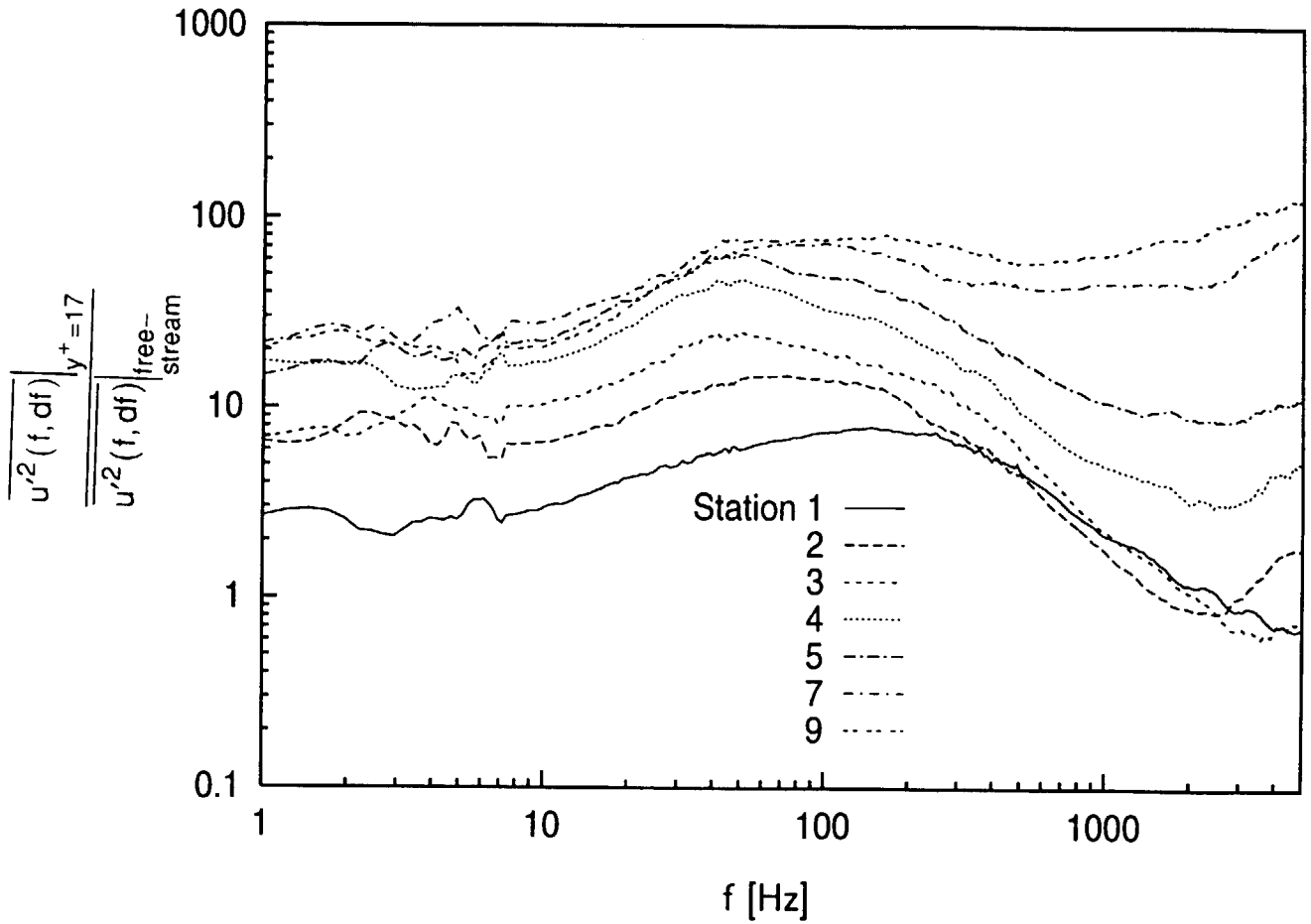

Fig. 7.46: Transfer Function of u' Between Boundary Layer at y^+=17 and Free-Stream, dU_{cw}/dx=14 s^{-1} Case

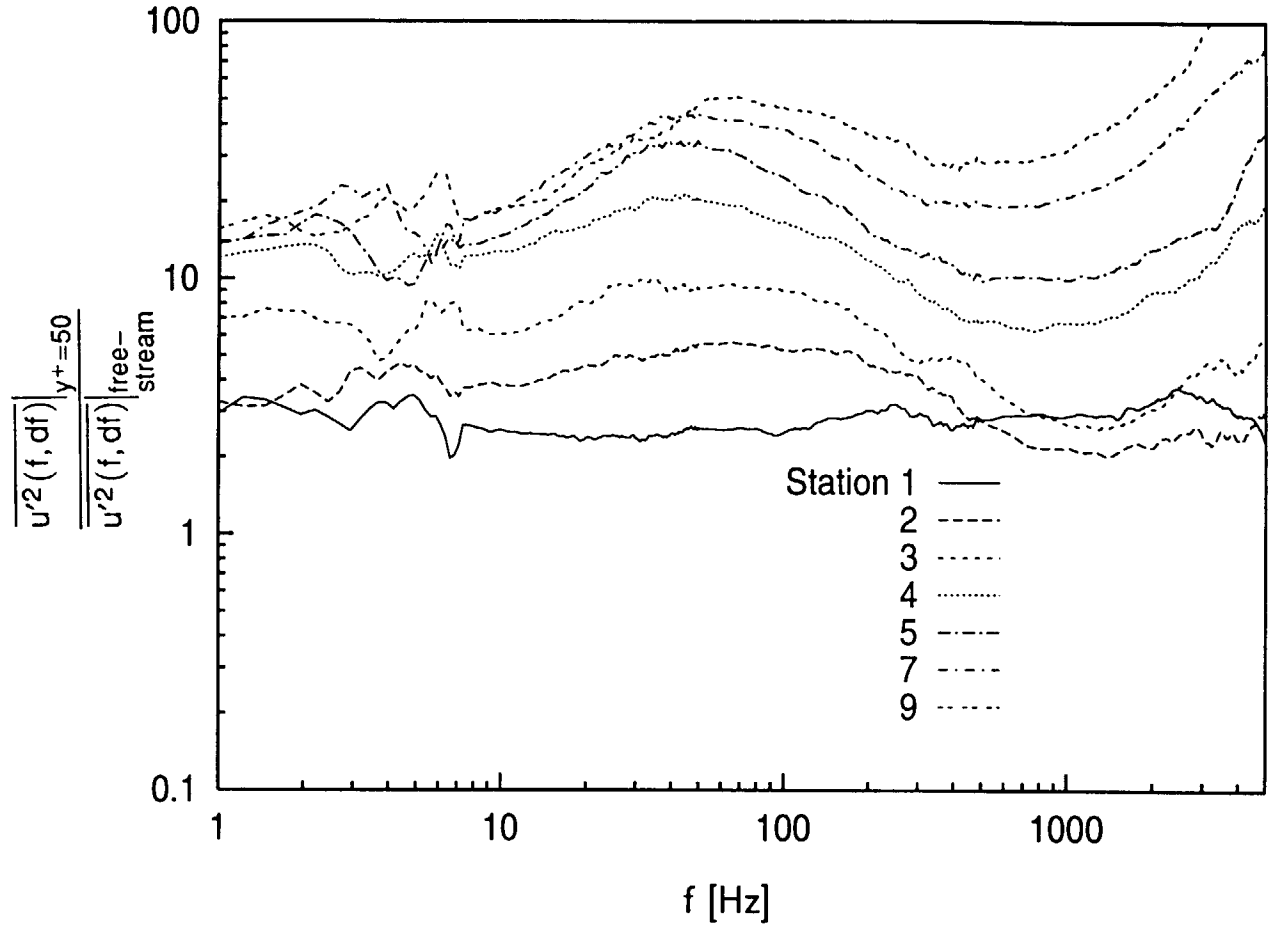

Fig. 7.47: Transfer Function of u' Between Boundary Layer at y^+=50 and Free-Stream, dU_{cw}/dx=14 s^{-1} Case

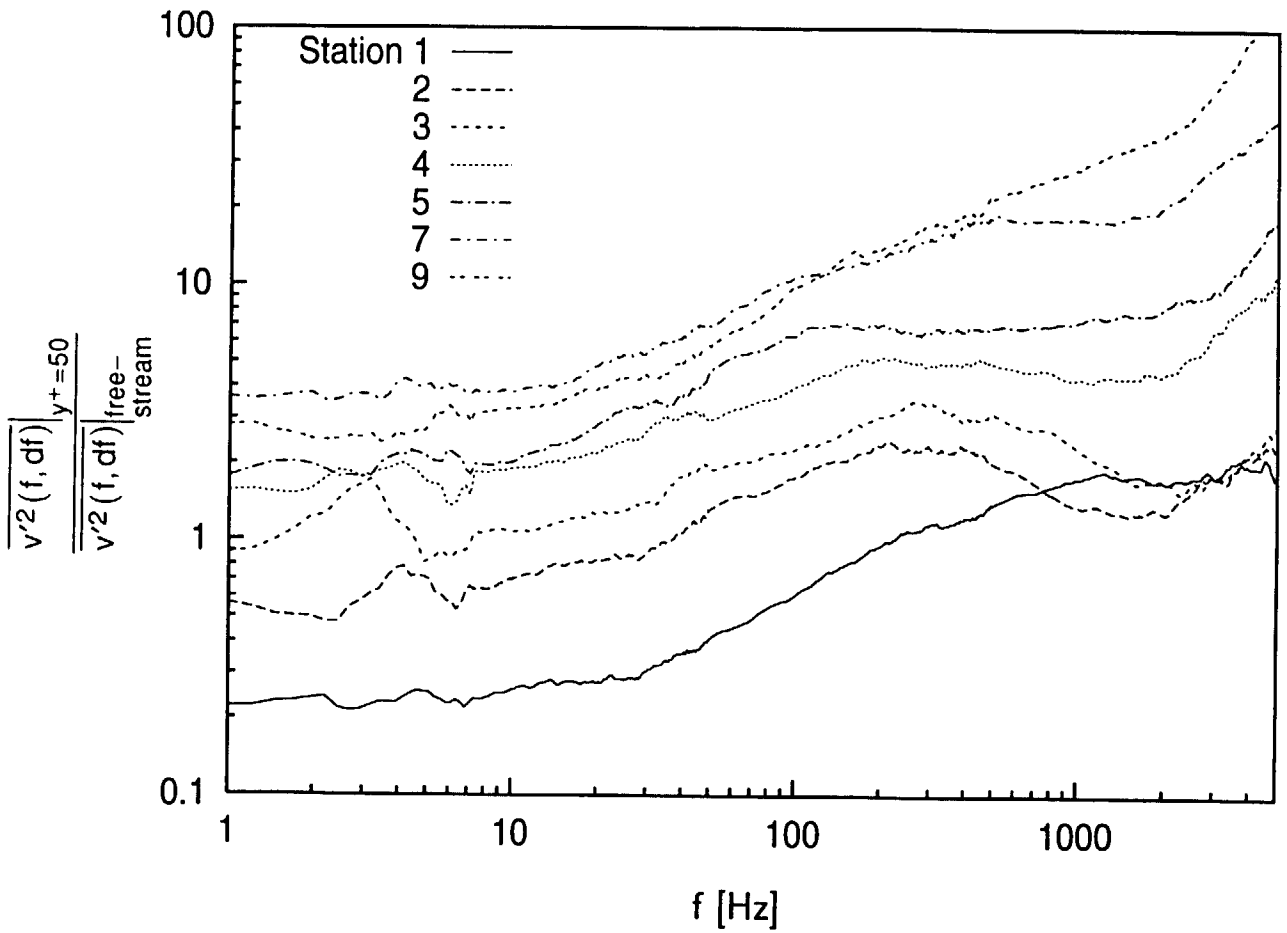

Fig. 7.48: Transfer Function of v' Between Boundary Layer at y^+=50 and Free-Stream, dU_{cw}/dx=14 s^{-1} Case

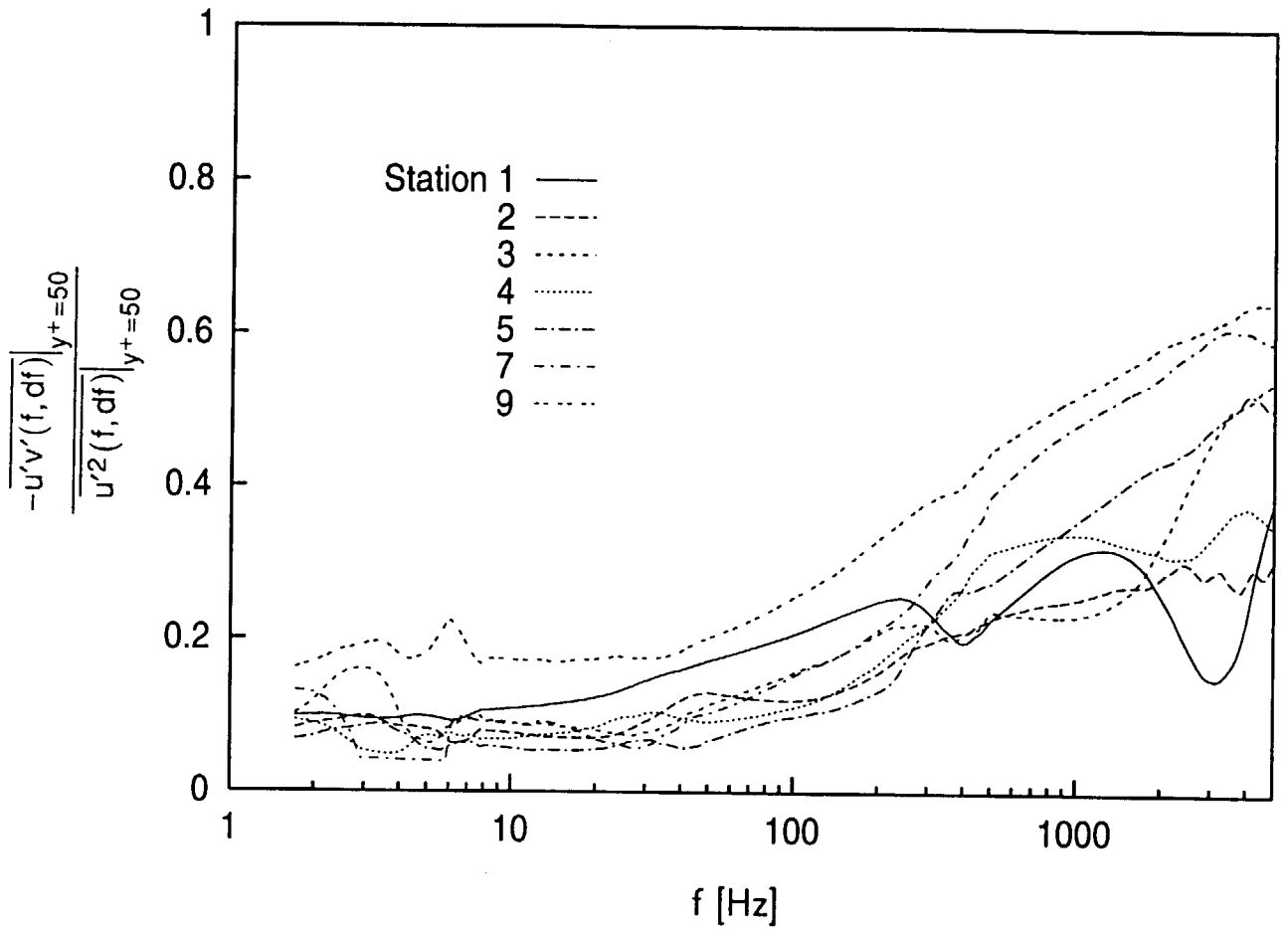

Fig. 7.49: Transfer Function Between u'v' and u' at y^+=50 dU_{cw}/dx=14 s^{-1} Case

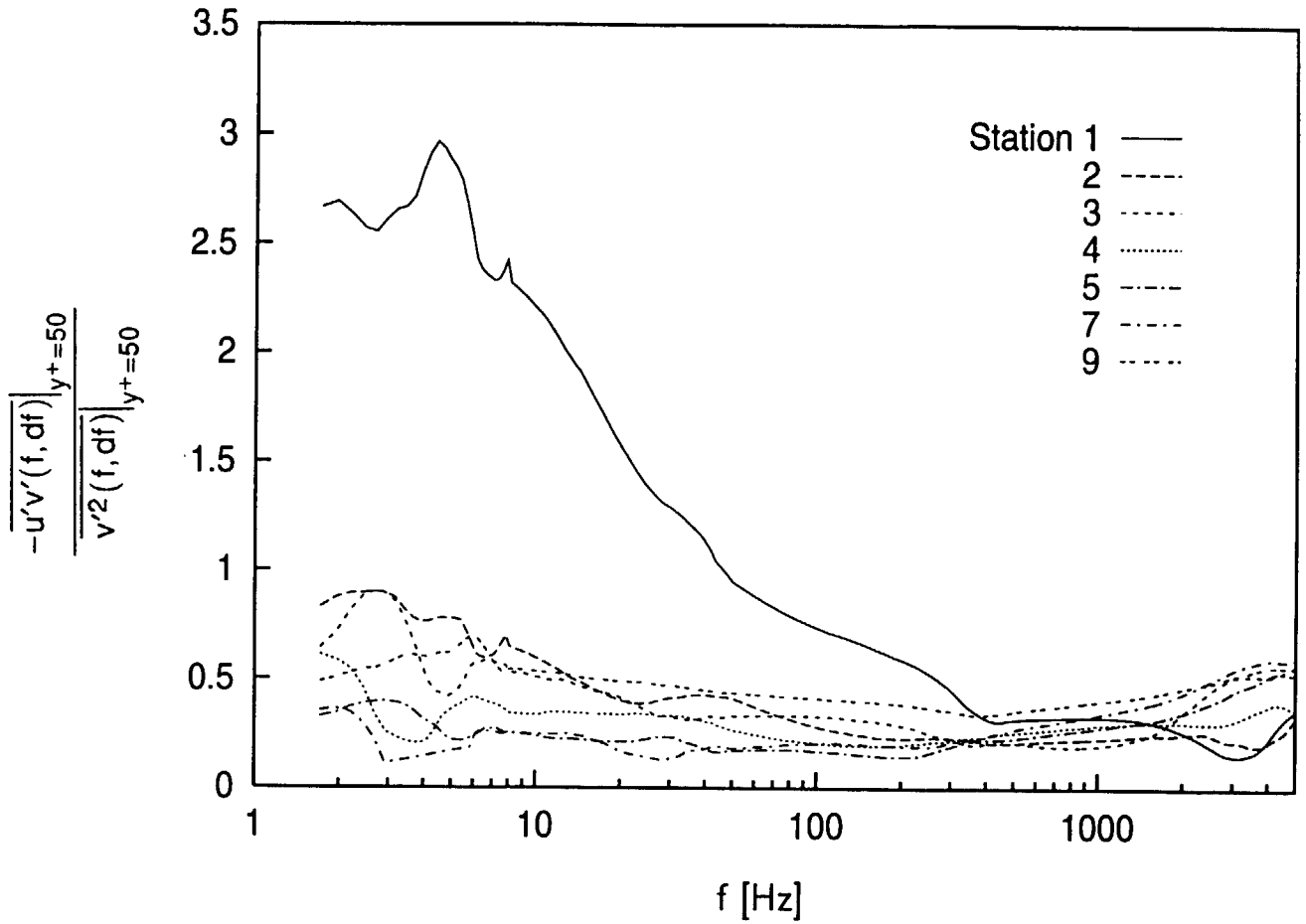

Fig. 7.50: Transfer Function Between u'v' and v' at y^+=50 dU_{cw}/dx=14 s^{-1} Case

CHAPTER 8: DISCUSSION AND RECOMMENDATIONS

NATURE OF HIGH FSTI TRANSITION

The transition process has been documented in boundary layers subject to high free-stream turbulence levels. This transition is considerably different than Tollmien-Schlichting transition, which is observed under low-FSTI conditions. The flow in the transition region is intermittent, alternating between a badly disturbed, non-turbulent state and a turbulent-like state. The non-turbulent zone is characterized by high-amplitude, low-frequency fluctuations. These fluctuations are believed to be induced directly by the free-stream unsteadiness. The non-turbulent zone lacks high-frequency, small-scale fluctuations. This suggests a lack of near-wall turbulence production in the non-turbulent flow. The fluctuations in the non-turbulent zone lead to enhanced transport relative to that in a laminar flow, but relatively low transport compared to that in a fully-turbulent boundary layer. The large-scale motions, which are induced by the free-stream, promote mixing in the boundary layer, but they are not so efficient as eddies produced and residing in the boundary layer. Skin friction and heat transfer coefficients in the transition region are well above laminar flow values, but below the values observed in fully-turbulent flow.

The octant analysis shows considerable similarity between high-FSTI transition and low-FSTI transition. The octant distributions in both the high- and low-FSTI transitional flows include octant 6 (hot ejection) as the major contributor to the turbulent heat flux and shear stress, with octants 4 (cold sweep) and 7 (hot wallward interaction) as important secondary contributors. The similarity in the octant distributions suggests similarity in the eddy structure of the flows. The octant 7 motion is associated with incomplete mixing due to a lack of small scale eddies, as depicted in Fig. 4.17. The octant 7 motions may be related to the "inactive" motions suggested though spectral

analysis and transfer functions, as depicted in Fig. 3.7. Large-scale, free-stream eddies buffeting the boundary layer would cause octant 4, 6 and 7 motions in the boundary layer.

ACCELERATION EFFECT

Strong acceleration prevents the transition process from proceeding. The intermittency remains nearly constant when the acceleration parameter, K, is above 3×10^{-6}. The acceleration prevents near-wall turbulence production. When K drops below about 2×10^{-6}, transition begins. When near-wall production begins, the intermittency increases, and a range of smaller-scale eddies are observed. Mayle (1991) suggested a transition model which does not allow transition to begin unless $K<3\times10^{-6}$. The present study tends to support this model.

CURVATURE EFFECT

Curvature may play a significant role in the transition process, but more work is needed. Kim and Simon (1991) showed the importance of curvature on transition in low FSTI flows, and showed the strong influence of curvature on fully-turbulent boundary layers subject to high FSTI. In the present study, the importance of Görtler vortices in the transition process was shown at low FSTI. In the high-FSTI cases of the present work, the strength of curvature was reduced to low levels by the strong acceleration, which kept the boundary layer thin. No strong effects of curvature were apparent in the present study.

Görtler vortices. No streamwise, Görtler vortices were observed in any of the high FSTI cases. In the cases with weaker acceleration, transition occurred far upstream, before vortices could form. In the case with the strongest acceleration, the Görtler number in the transition region was between 4 and 5, which is below the level at which vortices are expected to form. Floryan (1991) states that Görtler vortices are observed when G>5.5. Several investigators have observed that Görtler vortices cause transition to

turbulence when G> 6 to 9. Swearingen and Blackwelder (1987), for example, saw the beginning of transition at G between 6.7 and 9.

On a modern gas turbine airfoil, the acceleration rates and strength of curvature can be stronger than those in the present experiments. It is conceivable that stable vortices could form on the pressure side of an airfoil and influence the transition process. There are, however, reasons to doubt that vortices would form. Even on a strongly curved airfoil surface, Görtler numbers would tend to be low, due to the strong acceleration, which would keep the boundary layer thin. Finnis and Brown (1994) state that in the presence of favorable pressure gradients, the flow is stabilized and the Görtler instability mechanism is suppressed, meaning that higher Görtler numbers would be needed to cause transition than in an unaccelerated flow. High free-stream turbulence, by promoting mixing in the outer part of the boundary layer, would also tend to inhibit the formation of vortices. Kim and Simon (1991), following the suggestion of Tani (1962), proposed that the eddy viscosity be used in place of the molecular viscosity to define a "turbulent Görtler number," $G_t = \frac{U_{cw}\theta}{\varepsilon_M}\sqrt{\frac{\theta}{R}}$. Kim and Simon (1991) observed stable Görtler vortices in a low-FSTI flow with G_t between 1 and 2. In the present, high-FSTI cases, the eddy viscosity is 1 to 2 orders of magnitude greater than the kinematic viscosity, and G_t is reduced below 0.1. It therefore seems unlikely that Görtler vortices will form under high free-stream turbulence conditions.

It is still possible that curvature may influence the high-FSTI transitional boundary layer, even if stable vortices do not form. To better determine the effects of curvature on high-FSTI transition, experiments should be conducted on flat walls and walls with strong streamwise curvature, under the same FSTI and acceleration conditions as were considered in the present work.

TRANSITION MODELING

The results presented in this study suggest the potential utility of a two-scale transition model. The spectral analysis and octant analysis indicate that the flow is influenced by large scales originating in the free-stream and smaller scales produced in the near-wall region. The large scales promote some turbulent transport in the boundary layer and thereby influence the shape of the mean velocity and temperature profiles. As the mean profiles are changed, the rate of near-wall turbulence production will be affected. Beyond this influence of the large scales on the small, however, the two scales may be largely uncoupled. A model based on the presumption that the scales are uncoupled follows.

The effect of the large scales in the flow could be captured with an algebraic model. The level of the fluctuations in the free-stream would be specified, and the level of the fluctuations induced in the boundary layer would be calculated. The level of the induced fluctuations would decrease from a maximum at the edge of the boundary layer to zero at the wall. The $\overline{v'}$ profiles from Figs. 6.19 and 7.22, which show $\overline{v'}$ decreasing from a maximum value in the free-stream to a minimum near $y/\theta=5$, could be used to guide the modeling. An algebraic expression would then be used to calculate local contributions to the turbulent shear stress. Experimental data would be used to guide the choice of algebraic expressions and constants. The low-frequency data in Figs. 6.44 and 7.49 suggest that the large-scale contribution to $-\overline{u'v'}$ should be about 10% of the local $\overline{u'^2}$ induced by the free-stream.

The effect of the small scales in the boundary layer could be captured with an existing turbulence model, such as a low-Reynolds-number k-ε model. A k-ε model should capture the effects of acceleration. If necessary, however, an existing model could be modified to limit turbulence production whenever $K>2\times10^{-6}$. To limit production, a "production term modification" model, such as that suggested by Schmidt and Patankar

(1991) might be used. The turbulent shear stress calculated for the small scales would be added to the contribution from the large scales, to give the full turbulent shear stress.

CHAPTER 9: CONCLUSIONS

1. Transition to turbulence has been documented in a boundary layer subject to high (initially 8%) free-stream turbulence, strong acceleration and moderate to weak concave curvature. This is believed to be the first detailed fluid mechanics and heat transfer documentation of transition under such high free-stream turbulence conditions.

2. The non-turbulent zone of the transitional boundary layer is one of strong unsteadiness and moderate eddy transport, but without near-wall turbulence production. The boundary layer unsteadiness appears to be induced directly by the free-stream.

3. Skin friction and heat transfer coefficients in the transition zone drop below turbulent correlations but never approach laminar values. They remain above laminar flow values due to the influence of the high free-stream turbulence on the boundary layer. The rises in skin friction coefficients and Stanton numbers during transition are, therefore, less than in a low-FSTI flow. Transition models which predict skin friction and heat transfer by some combination of laminar and fully-turbulent values will not be accurate in high FSTI cases until the high-disturbance non-turbulent flow is properly modeled.

4. The levels of turbulent fluctuations, particularly transport quantities such as the turbulent shear stress, are strongly suppressed by favorable pressure gradients. When the acceleration parameter, K, is above 3×10^{-6}, turbulence production and further development of the transition process are stopped.

5. The transitional flow is characterized by two scales. Large scale, low frequency fluctuations are induced by the free-stream, and smaller scales are produced in the near wall region. This conclusion is supported by spectral analysis and octant analysis results. It suggests the utility of a two-scale transition model which would successfully compute the effects of free-stream turbulence and near-wall bursting on production of the large-scale turbulence, the cascading of energy to the small scales, and the dissipation of the small scales. The k-ε type model elements should adequately provide the near-wall bursting production term and the dissipation term.

6. Under low-FSTI conditions on a concave wall, transition is strongly influenced, if not governed, by the presence of stable streamwise (Görtler) vortices. Under high-FSTI conditions, no streamwise Görtler vortices were observed and the time averaged flow was two-dimensional.

7. Free-stream turbulence, acceleration and concave curvature interact to produce the results presented. The effect of curvature on accelerated flow transition is still unclear. There is an interaction of effects, for acceleration affects the streamwise variation of FSTI and curvature strength. To help separate effects, experiments should be conducted for the high-K, high-FSTI conditions described here but on a flat wall and, perhaps, on a wall with stronger curvature.

REFERENCES

Abu-Ghannam, B. J. and Shaw, R. (1980). "Natural Transition of Boundary Layers - The Effects of Turbulence, Pressure Gradient and Flow History," *J. Mechanical Engineering Science*, Vol. 22, No. 5, pp. 213-228.

Blackwell, B. F., Kays, W. M. and Moffat, R. J. (1972). "The Turbulent Boundary Layer on a Porous Plate: an Experimental Study of the Heat Transfer Behavior with Adverse Pressure Gradients," HMT-16, Thermosciences Division, Mechanical Engineering Department, Stanford University, Stanford, Calif.

Blackwell, B. F. and Moffat, R. J. (1975). "Design and Construction of a Low Velocity Boundary Temperature Probe," *J. Heat Transfer*, Vol. 97, No. 2, pp. 313-315.

Blair, M. F. (1981). "Final Data Report - Vol. II -Velocity and Temperature Profile Data for Accelerating, Transitional Boundary Layers," United Technologies Research Center report R81-914388-16.

Blair, M.F. (1983). "Influence of Free-Stream Turbulence on Turbulent Boundary Layer Heat Transfer and Mean Profile Development, Part-1, Experimental Data," *J. Heat Transfer*, Vol. 150, pp. 33-40.

Blair, M.F. (1992). "Boundary-Layer Transition in Accelerating Flows With Intense Freestream Turbulence: Part 1 - Disturbances Upstream of Transition Onset, Part 2 - The Zone of Intermittent Turbulence," *J. Fluids Engineering*, Vol. 114, pp. 313-332.

Bradshaw, P. (1967). "The Turbulent Structure of Equilibrium Turbulent Boundary Layers," *J. Fluid Mech.*, Vol. 29, pp. 625-645.

Bradshaw, P. (1994a). "Turbulence: the chief outstanding difficulty of our subject," *Experiments in Fluids*, Vol. 16, pp. 203-216.

Bradshaw, P. (1994b). "The Law of the Wall," lecture at the Osborne Reynolds Centenary Symposium, UMIST, Manchester, May 24, 1994.

Bridgeman, M. J., Cherry, D. G. and Pedersen, J. (1983) "NASA/GE Energy Efficient Engine Low Pressure Turbine Scaled Test Vehicle Performance Report," NASA CR 168290.

Champagne, F. H., Sleicher, C. A. and Wehrmann, O. H. (1967a). "Turbulence Measurements with Inclined Hot-Wires, Part 1. Heat Transfer Experiments with Inclined Hot-Wire," *J. Fluid Mech.*, Vol. 28, pp. 153-175.

Champagne, F. H. and Sleicher, C. A. (1967b). "Turbulence Measurements with Inclined Hot-Wires, Part 2. Hot-Wire Response Equations," *J. Fluid Mech.*, Vol. 28, pp. 177-182.

Chung, J. T. (1992). "Flow and Heat Transfer Experiments in the Turbine Airfoil/Endwall Region," Ph.D. Thesis, Department of Mechanical Engineering, University of Minnesota.

Clauser, F. H. (1956). "The Turbulent Boundary Layer," *Advances in Applied Mechanics*, Vol. 4, pp. 1-51, Academic Press, New York.

Crane, R. I. and Sabzvari, J. (1984). "Laser-Doppler Measurements of Görtler Vortices in Laminar and Low-Reynolds-Number Turbulent Boundary Layers," Laser Anemometry in Fluid Mechanics, pp. 19-35 (ed. R. J. Adrian et al.), LADOAN - Instituto Superior Téchnico, Lisbon.

Crawford, M. E. and Kays, W. M. (1976). "STAN5 - A Program for Numerical Computation of Two-Dimensional Internal and External Boundary Layer Flows," NASA CR 2742.

Dhawan, S. and Narasimha, R. (1958). "Some Properties of Boundary Layer Flow During the Transition from Laminar to Turbulent Motion," *J. Fluid Mech.*, Vol. 3, pp. 418-436.

Dring, R. P., Blair, M. F., Joslyn, H. D., Power, G. D. and Verdon, J. M. (1986). "The Effect of Inlet Turbulence and Rotor/Stator Interactions on the Aerodynamics and Heat Transfer of a Large-Scale Rotating Turbine Model," NASA CR 4079.

Dryden, H. L. (1939). "Turbulence and the Boundary Layer," *J. Aero. Sci.*, Vol. 6, pp. 85-100.

Eckert, E. R. G. (1987). "Cross Transport of Energy in Fluid Streams," *Wärme- und Stoffübertragung*, Vol. 21, pp. 73-81.

Emmons, H. W. (1951). "The Laminar-Turbulent Transition in a Boundary Layer - Part I," *J. Aeronautical Science*, Vol. 18, pp. 490-498.

Finnis, M. V. and Brown, A. (1994). "The Streamwise Development of Görtler Vortices in a Favorable Pressure Gradient," ASME paper 94-GT-166.

Floryan, J. M. (1991). "On the Görtler Instability of Boundary Layers," *Prog. Aerospace Sci.*, Vol. 28, pp. 235-271.

Galbraith, R. A. McD. and Head, M. R. (1975). "Eddy Viscosity and Mixing Length from Measured Boundary Layer Developments," Aeronautical Quarterly, Vol. 26, pp. 133-154.

Görtler, H. (1940). "Uber eine Dreidimensionale Instabilität Laminarer Grenschichten an Konkaven Wänden," Ges. d. Wiss. Göttingen, Nachr. a. d. Math.-Phys. Kl. 2:1 (also NACA TM 1375, 1954).

Gostelow, J. P. and Walker, G. J. (1991). "Similarity Behavior in Transitional Boundary Layers Over a Range of Adverse Pressure Gradients and Turbulence Levels," *J. Turbomachinery*, Vol. 113, pp. 617-625.

Hancock, P. and Bradshaw, P. (1989). "Turbulence Structure of a Boundary Layer beneath a Turbulent Free-Stream," *J. Fluid Mech.*, Vol. 205, pp. 45-76.

Hinze, J. (1975). Turbulence, Second Edition, McGraw Hill, New York.

Hirt, F. and Thomann, H. (1986). "Measurement of Wall Shear Stress in Turbulent Boundary Layers Subject to Strong Pressure Gradients," *J. Fluid Mech.*, Vol. 171, pp. 547-562.

Hishida, M. and Nagano, Y. (1978). "Simultaneous Measurements of Velocity and Temperature in Nonisothermal Flows," *J. Heat Transfer*, Vol. 100, pp. 340-345.

Huffman, G. D. and Bradshaw, P. (1972). "A Note on von Kármán's Constant in low Reynolds Number Turbulent Flows," *J. Fluid Mech.*, Vol. 53, pp. 45-60.

Hylton, L. D., Mihelc, M. S., Turner, E. R., Nealy, D. A., and York, R. E. (1983). "Analytical and Experimental Evaluation of the Heat Transfer Distribution Over the Surfaces of Turbine Vanes," NASA CR 168015.

Jones, W. P. and Launder, B. E. (1972). "Some properties of sink-flow turbulent boundary layers," *J. Fluid Mech.*, Vol. 56, pp. 337-351.

Julien, H. L., Kays, W. M. and Moffat, R. J. (1971). "Experimental Hydrodynamics of the Accelerated Turbulent Boundary Layer With and Without Mass Injection," *J. Heat Transfer*, Vol. 93, pp. 373-379.

Kawaguchi, Y., Matsumori, Y. and Suzuki, K. (1984). "Structural Study of Momentum and Heat Transport in the Near Wall Region of a Disturbed Boundary Layer," 9th Biennial Symposium on Turbulence.

Kays, W. M. (1994). "Turbulent Prandtl Number - Where Are We?" *J. Heat Transfer*, Vol. 116, pp. 284-295.

Kays, W. M. and Crawford, M. E. (1993). Convective Heat and Mass Transfer, McGraw-Hill Inc., New York.

Kearney D. W., Moffat, R. J. and Kays, W. M. (1970). "The Turbulent Boundary Layer: Experimental Heat Transfer with Strong Favorable Pressure Gradients and Blowing," HMT-12, Thermosciences Division, Mechanical Engineering Department, Stanford University, Stanford, Calif.

Keller, F. J. and Wang, T. (1993). "Flow and Thermal Structures in Heated Transitional Boundary Layers With and Without Streamwise Acceleration," Final Report, Department of Mechanical Engineering, Clemson University. Also Ph.D. Dissertation of F. J. Keller, Department of Mechanical Engineering, Clemson Univerisity, 1993.

Keller, and Wang, T. (1995). "Effects of Criterion Functions on Intermittency in Heated Transitional Boundary Layers with and without Streamwise Acceleration," *J. Turbomachinery*, Vol. 117, pp. 154-165.

Kestoras, M. D. (1993). "Heat Transfer and Fluid Mechanics Measurements in a Turbulent Boundary Layer: Introduction and Removal of Concave Curvature under High Free-Stream Turbulence Conditions," Ph.D. Thesis, Department of Mechanical Engineering, University of Minnesota.

Kestoras, M.D. and Simon, T.W. (1993). "Combined Effects of Concave Curvature and High Free-stream Turbulence Intensity on Boundary Layer Heat and Momentum Transport," ASME paper 93-WA/HT-56.

Kim, J., Kline, S. J. and Johnston, J. P. (1978). "Investigation of Separation and Reattachment of a Turbulent Shear Layer: Flow Over a Backward-Facing Step," Report MD-37, Thermosciences Division, Department of Mechanical Engineering, Stanford University, Stanford, CA.

Kim, J. (1986). "The Development of a Turbulent Heat Flux Probe and its use in a 2-D Boundary Layer over a Convex Surface," MSME Thesis, Department of Mechanical Engineering, University of Minnesota.

Kim, J. (1990). "Free-stream Turbulence and Concave Curvature Effects on Heated, Transitional Boundary Layers," Ph.D. Thesis, Department of Mechanical Engineering, University of Minnesota.

Kim, J. and Simon, T. W. (1988). "Measurements of the Turbulent Transport of Heat and Momentum in Convexly Curved Boundary Layers: Effects of Curvature, Recovery, and Free-Stream Turbulence," *J. Turbomachinery*, Vol. 110, pp. 80-87.

Kim, J. and Simon, T. W. (1991). "Free-Stream Turbulence and Concave Curvature on Heated, Transitional Boundary Layers, Volume I - Final Report," NASA CR 187150, "Volume II - Program Listings and Tabulated Data," NASA CR 187151.

Kim, J., Simon, T.W. and Kestoras, M. (1994). "Fluid Mechanics and Heat Transfer Measurements in Transitional Boundary Layers Conditionally Sampled on Intermittency," *J. Turbomachinery*, Vol. 116, pp. 405-416.

Kim, J., Simon, T. W. and Russ, S. G. (1992). "Free-Stream Turbulence and Concave Curvature Effects on Heated Transitional Boundary Layers," *J. Heat Transfer*, Vol. 114, No. 2, pp. 338-347.

King, L. V. (1914a). "On the Convection of Heat from Small Cylinders in a Stream of Fluid: Determination of the Convection Constants of Small Platinum Wires with Application to Hot-Wire Anemometry," *Proc. R. Soc. Lond.*, Vol. 90, pp. 563-570.

King, L. V. (1914b). "On the Convection of Heat from Small Cylinders in a Stream of Fluid," *Phil. Trans. R. Soc.*, Vol. A214, pp. 373-432.

King, L. V. (1915). "On the Precision Measurements of Air Velocity by Means of the Linear Hot-Wire Anemometer," *Phil. Mag. Vol.* 29, pp. 556-577.

Kline, S. J. and McClintock, F. A. (1953). "Describing Uncertainties in Single-Sample Experiments," *J. Mech. Engr. Sci.*, Vol. 75, pp. 3-8.

Kuan, C. L. and Wang, T. (1990). "Investigation of the Intermittent Behavior of Transitional Boundary Layer Using a Conditional Averaging Technique," *Experimental Thermal and Fluid Science*, Vol. 3, pp. 157-173.

Lam, C. K. G. and Bremhorst, K. (1981). "A Modified Form of the k-ε Model for Predicting Wall Turbulence," *J. Fluids Engineering*, Vol. 103, pp. 456-460.

Leoutsakos, G. and Crane, R. I. (1990). "Three-Dimensional Boundary Layer Transition on a Concave Surface," *Int. J. Heat and Fluid Flow*, Vol. 11, pp. 2-9.

Liepmann, H. W. (1943). "Investigation of Laminar Boundary-Layer Stability and Transition on Curved Boundaries," NACA Wartime Report W-107. Originally issued 1943 as NACA ACR 3H30.

Mayle, R. E. (1991). "The Role of Laminar-Turbulent Transition in Gas Turbine Engines," *J. Turbomachinery*, Vol. 113, pp. 509-537.

McDonald, H. (1969). "The Effect of Pressure Gradient on the Law of the Wall in Turbulent Flow," J. Fluid Mech., Vol. 35, pp. 311-336.

Morkovin, M. V. (1978). "Instability, Transition to Turbulence and Predictability," AGARD-AG-236.

Nagano, Y., Tagawa, M. and Tsuji, T. (1992). "Effects of Adverse Pressure Gradient on Mean Flows and Turbulence Statistics in a Boundary Layer," Turbulent Shear Flows 8 (ed. F. Durst et al.), Springer-Verlag, Berlin.

Narasimha, R. (1957). "On the Distribution of Intermittency in the Transition Region of a Boundary Layer," *J. Aero. Sci.*, Vol. 24, pp. 711-712.

Narasimha, R. (1984). "Subtransitions in the Transition Zone," Proc. 2nd IUTAM Symposium on Laminar-Turbulent Transition, Novosibirsk, pp. 141-151.

Narasimha, R. (1985). "The Laminar - Turbulent Transition Zone in the Boundary Layer," *Progress in Aerospace Science*, Vol. 22, No. 1, pp. 29-80.

O'Brien, J. E. and vanFossen, G. J. (1985). "The Influence of Jet Grid Turbulence on Heat Transfer from the Stagnation Region of a Cylinder in Cross Flow," ASME paper 85-HT-58.

Powell, R. L., Hall, W. J., Hyink, C. H. Jr., Sparks, L. L., Burns, G. W., Scroger, M. G. and Plumb, H. H. (1974). "Thermocouple Reference Tables Based on the IPTS-68," NBS Monograph 125.

Prandtl, L. (1935). *Aerodynamic Theory*, Vol. 3, p. 152 (Durand, L. F. ed.).

Press, W. H., Flannery, B. P., Teukolsky, S. and Vetterling, W. T. (1988). Numerical Recipes in C, The Art of Scientific Computing, Cambridge University Press, Cambridge.

Qiu, S., Simon, T. W. and Volino, R. J. (1995). "Evaluation of Local Wall Temperature, Heat Flux, and Convective Heat Transfer Coefficient from the Near-Wall Temperature Profile," to be presented at the 1995 ASME IMEC, San Francisco, CA, November 1995.

Rai, M. M. and Moin, P. (1991). "Direct Numerical Simulation of Transition and Turbulence in a Spatially Evolving Boundary Layer," AIAA paper 91-1607.

Reynolds, O. (1883). "An Experimental Investigation of the Circumstances Which Determine Whether the Motion of Water Shall be Direct or Sinuous and of the Law of Resistance in Parallel Channels," *Phil. Trans. Roy. Soc.*, Vol. 174, pp. 935-982.

Reynolds, W. C. (1976). "Computation of Turbulent Flows," *Annual Review of Fluid Mechanics*, Vol. 8, pp. 183-208.

Rodi, W. and Scheuerer, G. (1985). "Calculation of Laminar-Turbulent Boundary Layer Transition of Turbine Blades," Heat Transfer and Cooling in Gas Turbines, AGARD-CP-390, pp. 18-1 through 18-13.

Rued, K. (1987). "Transitional Boundary Layers under the Influence of High Free Stream Turbulence, Intensive Wall Cooling and High Pressure Gradients in Hot Gas Circulation," NASA TM 88254.

Rued, K. and Wittig, S. (1985). "Free-Stream Turbulence and Pressure Gradient Effects of Heat Transfer and Boundary Layer Development on Highly Cooled Surfaces," *J. of Engineering for Gas Turbines and Power*, Vol. 107, pp. 54-59.

Rued, K. and Wittig, S. (1986). "Laminar and Transitional Boundary Layer Structures in Accelerating Flow With Heat Transfer," *J. Turbomachinery*, Vol. 108, pp. 116-123.

Russ, S.G. (1989). "The Generation and Measurement of Turbulent Flow Fields," M.S. Thesis, Department of Mechanical Engineering, University of Minnesota.

Samuel, A. E. and Joubert, P. N. (1974). "A Boundary Layer Developing in an Increasingly Adverse Pressure Gradient," *J. Fluid Mech.*, Vol. 66, pp. 481-505.

Schlichting, H. (1933). "Zur Entstehung der Turbulenz bei der Plattenströmung," Nachr. Ges. Wiss. Göttingen, Math. Phys. Klasse, pp. 182-208. See also ZAMM, Vol. 13, pp. 171-174.

Schlichting, H. (1979). Boundary Layer Theory, 7th Edition, McGraw Hill, New York.

Schmidt, R. C. and Patankar, S. V. (1991). "Simulating Boundary Layer Transition with Low-Reynolds-Number k-epsilon Turbulence Models, Part 1 - An Evaluation of Prediction Characteristics, Part 2 - An Approach to Improving the Predictions," *J. Turbomachinery*, Vol. 113, No. 1 pp. 10-26.

Schubauer, G. B. and Klebanoff, P. S. (1955). "Contributions on the Mechanics of Boundary-Layer Transition," NACA Tech. Note 3489.

Schubauer, G. B. and Skramstad, H. K. (1948). "Laminar-Boundary-Layer Oscillations and Transition on a Flat Plate," NACA report 909. Originally issued 1943 as NACA ACR.

Simonich, J. C. and Bradshaw, P. (1978). "Effect of Free-Stream Turbulence on Heat Transfer through a Turbulent Boundary Layer," *J. Heat Transfer*, Vol. 100, pp. 671-677.

Simonich, J. C. and Moffat, R. J. (1982). "Local Measurements of Turbulent Boundary Layer Heat Transfer on a Concave Surface Using Liquid Crystals," HMT-35, Thermosciences Division, Department of Mechanical Engineering, Stanford University.

Smith, D. J. (1993). "Fluid Mechanics Measurements in a Cascade Simulator Which Models the Gas Turbine Environment," M.S.M.E. Thesis, Department of Mechanical Engineering, University of Minnesota.

Sohn, K. H. and Reshotko, E. (1991). "Experimental Study of Boundary Layer Transition with Elevated Freestream Turbulence on a Heated Flat Plate," NASA CR 187068.

Spalart, P. R. (1986). "Numerical Study of Sink-Flow Boundary Layers," *J. Fluid Mech.*, Vol. 172, pp. 307-328.

Spalart, P. R. and Watmuff, J. H. (1993). "Experimental and Numerical Study of a Turbulent Boundary Layer with Pressure Gradients," *J. Fluid Mech.*, Vol. 249, pp. 337-371.

Stephens, C.A. and Crawford, M.E. (1990). "An Investigation into the Numerical Prediction of Boundary Layer Transition Using the K.Y. Chien Turbulence Model," NASA CR 185252.

Suder, K. L., O'Brien, J. E. and Reshotko, E. (1988). "Experimental Study of Bypass Transition in a Boundary Layer," NASA TM 100913.

Suzuki, H., Suzuki, K. and Sato, T. (1988). "Dissimilarity Between Heat and Momentum Transfer in a Turbulent Boundary Layer Disturbed by a Cylinder," *Int. J. Heat Mass Transfer*, Vol. 31, No. 2, pp. 259-265.

Swearingen, J. D. and Blackwelder, R. F. (1987). "The Growth and Breakdown of Streamwise Vortices in the Presense of a Wall," *J. Fluid Mech.*, Vol. 182, pp. 255-290.

Tani, I. (1962). "Production of Longitudinal Vortices in the Boundary Layer along a Concave Wall," *J. Geophysical Research*, Vol. 67, pp. 3075-3080.

Thielbahr, W. H., Kays, W. M. and Moffat, R. J. (1969). "The Turbulent Boundary Layer: Experimental Heat Transfer with Blowing, Suction, and Favorable Pressure Gradient," HMT-5, Thermosciences Division, Mechanical Engineering Department, Stanford University, Stanford, CA.

Tollmien, W. (1931). "The Production of Turbulence," NASA TM 609.

Tollmien, W. (1936). "General Instability Criterion of Laminar Velocity Distributions," NACA TM No. 792.

van Driest, E. R. (1956). "On Turbulent Flow Near a Wall," *J. Aero. Sci.*, Vol. 23, pp. 1007-1011.

Volino, R.J. and Simon, T.W. (1991). "Bypass Transition in Boundary Layers Including Curvature and Favorable Pressure Gradient Effects," NASA CR 187187.

Volino, R.J. and Simon, T.W. (1994a) "Velocity and Temperature Profiles in Turbulent Boundary Layer Flows Experiencing Streamwise Pressure Gradients," Fundamentals of Heat Transfer in Forced Convection 1994, ASME HTD-Vol. 285, pp. 17-24. Presented at the 1994 ASME Winter Annual Meeting.

Volino, R.J. and Simon, T.W. (1994b) "Transfer Functions for Turbulence Spectra," Unsteady Flows in Aeropropulsion, ASME AD-Vol. 40, pp. 147-155. Presented at the 1994 ASME Winter Annual Meeting.

Volino, R. J. and Simon, T. W. (1994c). "An Application of Octant Analysis to Turbulent and Transitional Flow Data," *J. Turbomachinery*, Vol. 116, pp. 752-758.

Volino, R.J. and Simon, T.W. (1995a). "Bypass Transition in Boundary Layers Including Curvature and Favorable Pressure Gradient Effects," *J. Turbomachinery*, Vol. 117, pp. 166-174.

Volino, R. J. and Simon, T. W. (1995b). "Boundary Layer Transition under High Free-Stream Turbulence and Strong Acceleration Conditions: Mean Flow Results," proceedings of the 4th ASME/JSME Thermal Engineering Joint Conference, Vol. 1, pp. 335-342.

Volino, R. J. and Simon, T. W. (1995c). "Measurements of Turbulent Transport in Transitional Boundary Layers Under High Free-Stream Turbulence and Strong Acceleration Conditions," to be presented at the 10th Turbulent Shear Flows Conference, University Park, PA, August 1995.

Walker, G. J. (1993). "The Role of Laminar-Turbulent Transition in Gas Turbine Engines: A Discussion," *J. Turbomachinery*, Vol. 115, pp. 207-217.

Wallace, J. M., Eckelmann, H. and Brodkey, R. S. (1972). "The Wall Region in Turbulent Shear Flow," *J. Fluid Mech.*, Vol. 54, Part 1, pp. 39-48.

Wang, T. (1984). "An Experimental Investigation of Curvature and Freestream Turbulence Effects on Heat Transfer and Fluid Mechanics in Transitional Boundary Layer Flows," Ph.D. Thesis, Department of Mechanical Engineering, University of Minnesota.

Wang, T. and Simon, T.W. (1987). "Heat Transfer and Fluid Mechanics Measurements in a Boundary Layer Undergoing Transition on a Convex-Curved Wall," *J. Turbomachinery*, Vol. 109, No. 3, pp. 443-452.

Wang, T., Simon, T. W. and Buddhavarapu, J. (1985). "Heat Transfer and Fluid Mechanics Measurements in Transitional Boundary Layer Flows," *J. Engineering for Gas Turbines and Power*, Vol. 107, No. 4, pp. 1007-1015.

Wills, J. A. B. (1962). "The Correction of Hot-Wire Readings for Proximity to a Solid Boundary," *J. Fluid Mech.*, Vol. 12, pp. 388-396.

Willmarth, W. W. and Lu, S. S. (1972). "Structure of the Reynolds Stress Near the Wall," *J. Fluid Mech.*, Vol. 55, Part 1, pp. 65-92.

Wilson, D. J. (1970). "An Experimental Investigation of the Mean Velocity, Temperature and Turbulence Fields in Plane and Curved Two-Dimensional Wall Jets: Coanda Effect," Ph.D. Thesis, Department of Mechanical Engineering, University of Minnesota.

Wortmann, F. X. (1969). "Visualization of Transition," *J. Fluid Mech.*, Vol. 38, pp. 473-480.

You, S. M. (1986). "Turbulent Boundary Layer Heat Transfer and Fluid Mechanics Measurements on a Curved Convex Wall," M.S.M.E. Thesis, Department of Mechanical Engineering, University of Minnesota.

Zhou, D. and Wang, T. (1993). "Combined Effects of Elevated Free-Stream Turbulence and Streamwise Acceleration on Flow and Thermal Structures in Transitional Boundary Layers," ASME HTD-Vol. 242, Gas Turbine Heat Transfer 1993, ed. D. M. McEligot, pp. 41-52.

APPENDIX A:

VELOCITY AND TEMPERATURE PROFILES IN TURBULENT BOUNDARY LAYER FLOWS EXPERIENCING STREAMWISE PRESSURE GRADIENTS

SUMMARY

The standard turbulent law of the wall, devised for zero pressure gradient flows, has been previously shown to be inadequate for accelerating and decelerating turbulent boundary layers. Here, formulations for mean velocity profiles from the literature are applied and formulations for the temperature profiles are developed using a mixing length model. These formulations capture the effects of pressure gradients by including the convective and pressure gradient terms in the momentum and energy equations. The profiles which include these terms deviate considerably from the standard law of the wall; the temperature profiles more so than the velocity profiles. The new profiles agree well with experimental data. The modification to the velocity profile is useful for evaluation of more accurate skin friction coefficients from experimental data by the near-wall fitting technique. The temperature profile modification improves the accuracy with which one may extract turbulent Prandtl numbers from near-wall mean temperature data when they cannot be determined directly.

INTRODUCTION

When presented in wall coordinates (u^+ vs y^+), mean velocity profiles plotted using data from turbulent boundary layers seem to be self similar in the near-wall region over a wide range of conditions. In the viscous sublayer ($y^+<5$)

$$u^+=y^+. \tag{A.1a}$$

Outside the viscous sublayer ($30<y^+<150$), in the so called "log region", the standard law of the wall

$$u^+ = \frac{1}{\kappa} \ln y^+ + C \tag{A.1b}$$

holds. The von Kármán constant, κ, and the offset constant, C, are most commonly taken from data as 0.41 and 5.0, respectively. The extent of the log region varies with the flow conditions, extending to higher y^+ as Reynolds number is increased. In the outer, or wake, region of the boundary layer, the self similarity of profiles expressed in wall units breaks down, being influenced by Reynolds number, curvature, pressure gradient, and free-stream turbulence effects.

In the turbulent thermal boundary layer, the mean temperature profile can be expressed as

$$t^+ = Pr\, y^+ \tag{A.2a}$$

in the conduction layer which, for a $Pr \approx 1$ fluid corresponds to the viscous sublayer and

$$t^+ = \frac{Pr_t}{\kappa} \ln y^+ + C_t \tag{A.2b}$$

in the log region. The turbulent Prandtl number, Pr_t, is typically taken as 0.9, and C_t is assigned to be 13.2Pr-5.66, based upon experimental data. The choices of constants and functions in the velocity and temperature profiles have been supported by time-averages of Direct Numerical Simulations (DNS).

The self-similarity of the velocity profile lends considerable utility in the determination of skin friction coefficients, C_f. Preston tube and Stanton probe measurements of shear stress, for example, depend on the standard relationship so that, with calibration, they can be employed to measure wall shear stress in terms of measured pressure. Using measured velocity distributions to compute wall shear stress also

requires an assurance that the mean velocity profile can be cast in terms of a self similar form. For unaccelerated, high-Reynolds-number, turbulent boundary layers, this is the "law" given as Eqns. (A.1a) and (A.1b). If the actual velocity profile were to deviate from the standard profile but the technique were mistakenly applied, assuming that the standard profile holds, errors in C_f could be expected. Hirt and Thomann (1986) discussed such errors with Preston tube measurements in adverse pressure gradient flows.

The temperature law of the wall expressed by Eqns. (A.2a) and (A.2b) has utility in the calculation of local turbulent Prandtl number, Pr_t, from measured wall heat flux, wall temperature, boundary layer mean temperature profile data and wall shear stress. Numerous instances have been documented where Pr_t deviated from the commonly assumed value of 0.9 (e.g. Kays (1994) and Kim and Simon (1991)).

The standard law of the wall velocity and temperature distributions were derived for zero-pressure-gradient flows. For such flows they are generally accepted as correct. In the presence of adverse or favorable pressure gradients, however, there remains some controversy over the appropriate form which one should apply for an equivalent analysis. Rued (1987), for example, concluded that pressure gradients do have an effect on the wake regions of velocity profiles, and small effects on the viscous sublayer region, but no effect on the log region. He cites several references, including Samuel and Joubert (1974), which support the conclusion that the law of the wall is applicable to flows with streamwise pressure gradients. Galbraith and Head (1975) also concluded that the log-law of Eqn. (A.1b) is universal and more fundamental than is the standard near-wall mixing length distribution, $\ell=\kappa y$, upon which the standard law of the wall for velocity was originally derived. To explain discrepancies noted with pressure gradients, they concluded that κ is the variable. They assert that their assumption is correct and supported by Bradshaw's (1967) strong adverse pressure gradient measurements.

On the other side of the controversy are instances of deviation from the standard profile. Jones and Launder (1972) considered sink flows with constant-K $\left(=\frac{\nu}{U_\infty^2}\frac{dU_\infty}{dx}\right)$ values of 1.5×10^{-6}, 2.5×10^{-6}, and 3.0×10^{-6}. The velocity profile data fell above (higher u^+ at a given y^+) the standard log-law at all three accelerations, with the deviation increasing with K. Spalart (1986) performed a Direct Numerical Simulation (DNS) of Jones and Launder's (1972) experiments, finding agreement with their results. He also presented a plot of mixing length, ℓ, vs y, showing that the slope is not a constant. This would imply that κ is not constant. He went on to suggested that Galbraith and Head (1975) may be correct in stating that the log-law is a more universal relationship than the assumption of a constant κ. The assumption of a universal profile may not be entirely accurate, however, for Spalart's (1986) DNS results showed a displacement and change in slope of the log region as the acceleration strength-parameter, K, was changed. McDonald (1969) derived corrections to the mean velocity profile for pressure gradient flows. These corrections have the opposite trend, with acceleration, to that seen in the Jones and Launder (1972) data.

Huffman and Bradshaw (1972) examined the velocity profiles in boundary layers, channels, pipes, annuli, and wall jets to conclude that κ=0.41 is a constant, even when there is no log region in the data. Nagano, Tagawa, and Tsuji (1992) concluded that the standard log-law does not apply and that $\kappa\approx0.4$ is unchanging in adverse pressure gradient flows. They stated that "over-fitting" of data to the standard log-law (using the fitting technique in situations where doing so is not justified) is the reason for claims that the standard log-law is universal. Essentially, with an incorrect choice of C_f, one can always force at least some of the data in a profile to fall along the standard log-law. Nagano, Tagawa, and Tsuji proceed to warn against the use of wall functions in turbulence models due to these deviations from the standard law of the wall.

Spalart and Watmuff (1993) compared DNS and experimental results for a flow which is subject to an acceleration, followed by a deceleration. Skin friction coefficients were obtained from Preston tube measurements in the experiment. Velocity profiles from the DNS results deviated from the log-law in a manner which was consistent with that described by Jones and Launder (1972). The experimental results showed a better match to the standard log-law. In the laminar sublayer, however, the DNS results showed a good fit to the expected $u^+=y^+$ line, while the experiments showed deviations from the line for y^+ values as low as 2. Spalart and Watmuff (1993) point out that the Preston tube measurements may have been in error due to these deviations from the standard law of the wall. Differences in C_f between the experiment and DNS of as high as 12% were reported in this study. Spalart and Watmuff (1993) stated that the DNS results added to the evidence which indicates a moderate failure of the law of the wall in flows with pressure gradients. They also stated that the body of evidence in support of this statement is small and not conclusive.

Data from the Heat Transfer Laboratory of the University of Minnesota taken in a favorable pressure gradient flow, suggest that the conclusions of Nagano, Tagawa and Tsuji (1992) are correct -- that the standard log-law fails in pressure gradient flows. The present work was initiated after attempts to fit experimental data from a favorable pressure gradient flow to the standard law of the wall failed. The log-region tends to be short in such flows due to the immaturity of the boundary layer (indicated as low values of Re_θ) as a result of the acceleration. With an appropriate choice of C_f, one can make a "reasonable" fit of most, if not all, of the log-region to the standard profile. When this is done, however, the fit in the sublayer, while still within a possibly acceptable range, is clearly not as close as the fits routinely obtained in zero pressure gradient flows. Since the behavior in the sublayer is known with more certainty than that in the van Driest damped layer or the log layer, accurately fitting the very near-wall data is important. Given that the attempted fits of the accelerated flow data to the standard log law were

unacceptable, an alternative was sought which would allow more accurate determination of skin friction coefficients.

There has been much less work in the literature on documentation of pressure gradient effects on the temperature profile. Because no pressure gradient term appears explicitly in the boundary layer energy equation, it is not clear at first glance that a pressure gradient should directly affect the temperature profile. The data which do exist (some of which are presented below) show that the deviations from the standard temperature profile are even stronger than the deviations discussed above for the velocity profiles, however.

The following section presents derivations of mean velocity and temperature profiles which can be applied in pressure gradient flows. The velocity law profile is similar to that presented by Huffman and Bradshaw (1972) for accelerated flows. The derivation for the temperature profile is believed to be new. The derived forms are verified by comparisons to experimental data for accelerated and decelerated, turbulent boundary layer flows.

ANALYSIS

The following development of velocity and temperature profiles starts with the boundary layer momentum and energy equations and proceeds in a manner similar to that used in the derivation of the standard law of the wall, but without the deletion of terms which are considered to be relevant in accelerated boundary layer flow. The mixing length model is used for closure of the momentum equation with κ=0.41 which is assumed to be constant and with van Driest (1956) damping using the variable A^+ model documented in Kays and Crawford (1993).

Velocity Profile

We start with the boundary layer momentum equation:

$$\rho u\frac{\partial u}{\partial x}+\rho v\frac{\partial u}{\partial y}-\frac{\partial \tau}{\partial y}+\frac{dP}{dx}=0 \tag{A.3}$$

and do not make the Couette flow assumption to eliminate the convection terms. Also, the pressure gradient term is kept. In the standard law of the wall development, these terms are dropped. Next, we substitute for the normal velocity, v, using the continuity equation:

$$\rho u\frac{\partial u}{\partial x}-\rho\frac{\partial u}{\partial y}\int_0^y\frac{\partial u}{\partial x}dy-\frac{\partial \tau}{\partial y}+\frac{dP}{dx}=0 \tag{A.4}$$

This is then integrated with respect to y and rearranged to have:

$$\frac{\tau}{\tau_o}=1+\frac{y}{\tau_o}\frac{dP}{dx}+\frac{\rho}{\tau_o}\int_0^y\left[u\frac{\partial u}{\partial x}-\frac{\partial u}{\partial y}\int_0^y\frac{\partial u}{\partial x}dy\right]dy \tag{A.5}$$

For the standard law of the wall, $\frac{\tau}{\tau_o}=1$.

Next, we convert from x-y coordinates to x-y^+ coordinates, replacing u with u^+u_τ and replacing $\frac{y}{\tau_o}\frac{dP}{dx}$ with p^+y^+. For the transformation,

$$\left.\frac{\partial u}{\partial x}\right|_y=\left.\frac{\partial\left(u^+u_\tau\right)}{\partial x}\right|_y=y^+\frac{du_\tau}{dx}\left.\frac{\partial u^+}{\partial y^+}\right|_x+u^+\frac{du_\tau}{dx}+u_\tau\left.\frac{\partial u^+}{\partial x}\right|_{y^+} \tag{A.6}$$

$$\left.\frac{\partial u}{\partial y}\right|_x=\left.\frac{\partial\left(u^+u_\tau\right)}{\partial y}\right|_x=\frac{u_\tau^2}{\nu}\left.\frac{\partial u^+}{\partial y^+}\right|_x \tag{A.7}$$

$$dy=\frac{\nu}{u_\tau}dy^+-\frac{y^+\nu}{u_\tau^2}\frac{du_\tau}{dx}dx \tag{A.8}$$

Since the integration is at a fixed streamwise position, Eqn. (A.8) reduces to $dy = \frac{\nu}{u_\tau} dy^+$.

With the transformation, Eqn. (A.5) becomes

$$\frac{\tau}{\tau_o} = 1 + p^+ y^+ + \frac{1}{u_\tau^2}\int_0^{y^+}\left[u^+ u_\tau\left(y^+\frac{du_\tau}{dx}\frac{\partial u^+}{\partial y^+} + u^+\frac{du_\tau}{dx} + u_\tau\frac{\partial u^+}{\partial x}\right)\right. \tag{A.9}$$
$$\left. -\frac{u_\tau^2}{\nu}\frac{\partial u^+}{\partial y^+}\int_0^{y^+}\left(y^+\frac{du_\tau}{dx}\frac{\partial u^+}{\partial y^+} + u^+\frac{du_\tau}{dx} + u_\tau\frac{\partial u^+}{\partial x}\right)\frac{\nu}{u_\tau}dy^+\right]\frac{\nu}{u_\tau}dy^+$$

After integrating the inner integral by parts and rearranging:

$$\frac{\tau}{\tau_o} = 1 + p^+ y^+ + \frac{\nu}{u_\tau^2}\frac{du_\tau}{dx}\int_0^{y^+} u^{+2} dy^+ + \frac{2\nu}{u_\tau}\int_0^{y^+} u^+\frac{\partial u^+}{\partial x}dy^+ - \frac{\nu u^+}{u_\tau}\int_0^{y^+}\frac{\partial u^+}{\partial x}dy^+ \tag{A.10}$$

Introducing $u_\tau = \sqrt{\frac{C_f}{2}}U_\infty$ and $K = \frac{\nu}{U_\infty^2}\frac{dU_\infty}{dx}$, yields,

$$\frac{\tau}{\tau_o} = 1 + p^+ y^+ + \left(\frac{K}{\sqrt{\frac{C_f}{2}}} + \frac{\nu}{U_\infty\frac{C_f}{2}}\frac{d\sqrt{\frac{C_f}{2}}}{dx}\right)\int_0^{y^+} u^{+2} dy^+ \tag{A.11}$$
$$+\frac{2\nu}{U_\infty\sqrt{\frac{C_f}{2}}}\int_0^{y^+} u^+\frac{\partial u^+}{\partial x}dy^+ - \frac{\nu u^+}{U_\infty\sqrt{\frac{C_f}{2}}}\int_0^{y^+}\frac{\partial u^+}{\partial x}dy^+$$

As a check, Eqn. (A.11) was solved for unaccelerated laminar flow, where $\frac{\tau}{\tau_o} = \frac{\partial u^+}{\partial y^+}$, K=0 and $p^+ = \frac{-K}{\left(\frac{C_f}{2}\right)^{3/2}} = 0$. For this case, Eqn. (A.11) becomes

$$u^+ = \int_0^{y^+}\left[1+\frac{\nu}{U_\infty\frac{C_f}{2}}\frac{d\sqrt{\frac{C_f}{2}}}{dx}\int_0^{y^+}u^{+2}dy^+ + \frac{2\nu}{U_\infty\sqrt{\frac{C_f}{2}}}\int_0^{y^+}u^+\frac{\partial u^+}{\partial x}dy^+ - \frac{\nu u^+}{U_\infty\sqrt{\frac{C_f}{2}}}\int_0^{y^+}\frac{\partial u^+}{\partial x}dy^+\right]dy^+ \qquad (A.12)$$

Values for C_f, $\frac{d\sqrt{\frac{C_f}{2}}}{dx}$ and $\frac{\partial u^+}{\partial x}$ were taken from the Blasius solution at a given x and with assigned values of U_∞ and ν. Numerical integration of Eqn. (A.12) reproduced the Blasius solution for u^+ vs y^+. This is not a practical technique for arriving at a Blasius solution since the Blasius solution was required to supply the above streamwise gradients for the integration. To make Eqn. (A.11) useful, an approximation must be made. We will assume that $\left.\frac{\partial u^+}{\partial x}\right|_{y^+}$ is negligible. This reduces Eqn. (A.11) to

$$\frac{\tau}{\tau_o} = 1 + p^+y^+ + \left(\frac{K}{\sqrt{\frac{C_f}{2}}}+f_1\right)\int_0^{y^+}u^{+2}dy^+ \qquad (A.13)$$

where $f_1 \equiv \frac{\nu}{U_\infty\frac{C_f}{2}}\frac{d\sqrt{\frac{C_f}{2}}}{dx}$. For turbulent flow, the assumption of $\left.\frac{\partial u^+}{\partial x}\right|_{y^+} \approx 0$ is reasonable and is consistent with the use of wall coordinates for presentation of the data (i.e. $u^+=u^+(y^+)$ assumed for the near wall flow). Figure A.1 shows the solution to Eqn. (A.13) for laminar unaccelerated flow along with the Blasius solution and the line $u^+=y^+$ (which results if the Couette flow assumption is applied and the convection terms are dropped from Eqn. (A.3)). The results are converted to Blasius similarity coordinates for generality. Note the good agreement between Eqn. (A.13) and the Blasius solution in the

inner part of the boundary layer ($\eta<2$). This exercise has shown that the streamwise term $\left.\frac{\partial u^+}{\partial x}\right|_{y^+}$ is not an important term for evaluation of the near-wall profile.

For turbulent flow, the mixing length model is applied for $\frac{\tau}{\tau_o}$ as follows:

$$\frac{\tau}{\tau_o} = \frac{(\nu + \varepsilon_M)}{u_\tau^2}\frac{du}{dy} \tag{A.14}$$

$$\varepsilon_M = \ell^2 \frac{du}{dy} \tag{A.15}$$

$$\ell = \kappa y\left(1 - e^{-y^+/A^+}\right) \tag{A.16}$$

ε_M is the eddy viscosity, and ℓ is the mixing length. The term $\left(1 - e^{-y^+/A^+}\right)$ is the van Driest (1956) damping term which provides a continuous transition from the viscous sublayer, which is dominated by molecular diffusion, to the outer boundary layer flow, which is dominated by eddy transport.

To proceed, we will assume that κ is a constant (=0.41) in spite of the controversy discussed above.

The damping model parameter, A^+, is assumed to vary with the pressure gradient, as recommended by Kays and Crawford (1993):

$$A^+ = \frac{25}{1 + ap^+} \quad \text{where } a = \begin{cases} 20.59 \text{ for } p^+ > 0 \\ 30.18 \text{ for } p^+ < 0 \end{cases} \tag{A.17a}$$

In flows with rapidly changing acceleration rates, the lag model suggested by Kays and Crawford (1993),

$$\frac{dA^+}{dx^+} = \frac{A_{eq}^+ - A^+}{4000} \tag{A.17b}$$

is used to prevent sudden changes in the sublayer thickness. The equilibrium value, A^+_{eq}, is the local value given by Eqn. (A.17a).

Substituting the mixing length into Eqn. (A.14) and converting to wall coordinates,

$$\frac{\tau}{\tau_o} = \left(1 + \left[\kappa y^+ \left(1 - e^{-y^+/A^+}\right)\right]^2 \frac{du^+}{dy^+}\right)\frac{du^+}{dy^+} \tag{A.18}$$

Equating from Eqn. (A.18) and Eqn. (A.13), solving for $\frac{du^+}{dy^+}$, and integrating, yields:

$$u^+ = \int_0^{y^+} \left[\frac{-1 + \sqrt{1 + 4\left(1 + p^+ y^+ + \left(\frac{K}{\sqrt{\frac{C_f}{2}}} + f_1\right)\int_0^{y^+} u^{+2} dy^+\right)\left(\kappa y^+\left(1 - e^{-y^+/A^+}\right)\right)^2}}{2\left(\kappa y^+\left(1 - e^{-y^+/A^+}\right)\right)^2} \right] dy^+ \tag{A.19}$$

A profile can be generated with the assignment of K, C_f and f_1(ν, C_f, U_∞, $\frac{dC_f}{dx}$). When fitting experimental data, the local value of the acceleration constant, K, is known, and C_f is adjusted until the data in u^+-y^+ coordinates and calculated profile, also in u^+-y^+ coordinates, match. The process is iterative because C_f must be determined at two or more streamwise positions before an accurate calculation of f_1 is available. The value of f_1 is usually small and the calculated profile is fairly insensitive to its value, however, so the convergence is quick.

Temperature Profile

The temperature profile is generated in the same manner. Starting with the boundary layer energy equation,

$$u\frac{\partial T}{\partial x}+v\frac{\partial T}{\partial y}+\frac{1}{\rho c}\frac{\partial q}{\partial y}=0 \tag{A.20}$$

and applying continuity to substitute for v, then integrating with respect to y, one obtains:

$$\frac{q}{q_o}=1-\frac{\rho c}{q_o}\int_0^y\left[u\frac{\partial T}{\partial x}-\frac{\partial T}{\partial y}\int_0^y\frac{\partial u}{\partial x}dy\right]dy. \tag{A.21}$$

The next development is to transform Eqn. (A.21) to x-y^+ coordinates. First, using:

$$T=T_w-\frac{q_o}{\rho c u_\tau}t^+ \tag{A.22}$$

and

$$\frac{\partial T}{\partial y}=-\frac{q_o}{\rho c v}\frac{\partial t^+}{\partial y^+} \tag{A.23}$$

and, for the uniform heat flux case, q_o=constant, the streamwise gradient becomes:

$$\left.\frac{\partial T}{\partial x}\right|_y=-\frac{y^+}{u_\tau^2}\frac{du_\tau}{dx}\left.\frac{\partial t^+}{\partial y^+}\right|_x-\frac{1}{U_\infty St^2}\frac{dSt}{dx}-\frac{1}{U_\infty^2 St}\frac{dU_\infty}{dx}+\frac{t^+}{u_\tau^2}\frac{du_\tau}{dx}-\frac{1}{u_\tau}\left.\frac{\partial t^+}{\partial x}\right|_{y^+} \tag{A.24}$$

where $St=\dfrac{q_o}{\rho c U_\infty(T_w-T_\infty)}$.

With substitution, the transformed Eqn. (A.21) becomes

$$\begin{aligned}\frac{q}{q_o}=1-\int_0^{y^+}\Bigg[u^+u_\tau\Bigg(&-\frac{y^+}{u_\tau^2}\frac{du_\tau}{dx}\frac{\partial t^+}{\partial y^+}-\frac{1}{U_\infty St^2}\frac{dSt}{dx}-\frac{1}{U_\infty^2 St}\frac{dU_\infty}{dx}+\frac{t^+}{u_\tau^2}\frac{du_\tau}{dx}-\frac{1}{u_\tau}\frac{\partial t^+}{\partial x}\Bigg)\\&-\frac{1}{\nu}\frac{\partial t^+}{\partial y^+}\int_0^{y^+}\left(y^+\frac{du_\tau}{dx}\frac{\partial u^+}{\partial y^+}+u^+\frac{du_\tau}{dx}+u_\tau\frac{\partial u^+}{\partial x}\right)\frac{\nu}{u_\tau}dy^+\Bigg]\frac{\nu}{u_\tau}dy^+\end{aligned} \tag{A.25}$$

After simplifying the inner integral,

$$\frac{q}{q_o} = 1 + \left(\frac{1}{U_\infty^2 St} \frac{dU_\infty}{dx} + \frac{1}{U_\infty St^2} \frac{dSt}{dx} \right) \int_0^{y^+} u^+ dy^+ - \frac{\nu}{u_\tau^2} \frac{du_\tau}{dx} \int_0^{y^+} u^+ t^+ dy^+ \qquad (A.26)$$
$$+ \frac{\nu}{u_\tau} \int_0^{y^+} u^+ \frac{\partial t^+}{\partial x} dy^+ + \frac{\nu t^+}{u_\tau} \int_0^{y^+} \frac{\partial u^+}{\partial x} dy^+ - \frac{\nu}{u_\tau} \int_0^{y^+} t^+ \frac{\partial u^+}{\partial x} dy^+$$

As with the velocity profile, the terms $\left.\frac{\partial u^+}{\partial x}\right|_{y^+}$ and $\left.\frac{\partial t^+}{\partial x}\right|_{y^+}$ are assumed to be insignificant and are set to zero, leaving

$$\frac{q}{q_o} = 1 + \left(\frac{K t_\infty^+}{\sqrt{\frac{C_f}{2}}} + f_2 \right) \int_0^{y^+} u^+ dy^+ - \left(\frac{K}{\sqrt{\frac{C_f}{2}}} + f_1 \right) \int_0^{y^+} u^+ t^+ dy^+ \qquad (A.27)$$

where $f_2 \equiv \frac{\nu t_\infty^{+2}}{U_\infty \frac{C_f}{2}} \frac{dSt}{dx}$.

For computing $\frac{q}{q_o}$, the mixing length model is used:

$$\frac{q}{q_o} = \frac{\alpha + \varepsilon_H}{\nu} \frac{dt^+}{dy^+} = \left(\frac{1}{Pr} + \frac{\varepsilon_H}{\nu} \right) \frac{dt^+}{dy^+} \qquad (A.28)$$

To eliminate ε_H, we use the turbulent Prandtl number, Pr_t, as:

$$\frac{\varepsilon_M}{\varepsilon_H} = Pr_t \quad , \quad \frac{\varepsilon_H}{\nu} = \frac{\left(\kappa y^+ \left[1 - e^{-y^+/A^+} \right] \right)^2 \frac{du^+}{dy^+}}{Pr_t} \qquad (A.29)$$

Equating (A.27) and (A.28) and solving for $\frac{dt^+}{dy^+}$,

$$\frac{dt^+}{dy^+} = \frac{1 + \left(\frac{Kt_\infty^+}{\sqrt{\frac{C_f}{2}}} + f_2\right)\int_0^{y^+} u^+ dy^+ - \left(\frac{K}{\sqrt{\frac{C_f}{2}}} + f_1\right)\int_0^{y^+} u^+ t^+ dy^+}{\frac{1}{Pr} + \frac{\left(\kappa y^+\left[1 - e^{-y^+/A^+}\right]\right)^2 \frac{du^+}{dy^+}}{Pr_t}} \qquad \text{(A.30)}$$

Integrating,

$$t^+ = \int_0^{y^+} \left[\frac{1 + \left(\frac{Kt_\infty^+}{\sqrt{\frac{C_f}{2}}} + f_2\right)\int_0^{y^+} u^+ dy^+ - \left(\frac{K}{\sqrt{\frac{C_f}{2}}} + f_1\right)\int_0^{y^+} u^+ t^+ dy^+}{\frac{1}{Pr} + \frac{\left(\kappa y^+\left[1 - e^{-y^+/A^+}\right]\right)^2 \frac{du^+}{dy^+}}{Pr_t}} \right] dy^+ \qquad \text{(A.31)}$$

Equation (A.31) can be integrated numerically. The values of u^+ and $\frac{du^+}{dy^+}$ are from the velocity profile, Eqn. (A.19). The required inputs to Eqn. (A.31) are K, C_f, f_1, t_∞^+, f_2, and Pr_t. The turbulent Prandtl number, Pr_t, can be taken from a correlation such as the following proposed by Kays and Crawford (1993),

$$Pr_t = \frac{1}{\frac{1}{2Pr_{t_\infty}} + CPe_t\sqrt{\frac{1}{Pr_{t_\infty}}} - (CPe_t)^2\left[1 - \exp\left(-\frac{1}{CPe_t\sqrt{Pr_{t_\infty}}}\right)\right]} \qquad \text{(A.32)}$$

where C=0.2, $Pe_t = \frac{\varepsilon_M}{\nu} Pr$, and Pr_{t_∞}, the turbulent Prandtl number in the log region of the boundary layer, is either measured, assigned the flat plate value of 0.85, or found by fitting the t^+-y^+ profile to temperature profile data.

If q_o and T_w are both known along the test wall, no "fitting" of the data is required. Recall that such fitting was required with the velocity profile processing when C_f was to be evaluated. Equation (A.31) can be integrated without iteration, then compared to the experimental data.

The above development was for the case of a uniform heat flux. For the case of uniform wall temperature (T_w=constant), the derivation is similar, and the final result is

$$t^+ = \int_0^{y^+} \left[\frac{1 + \left(\frac{f_2}{t_\infty^+} - f_1 \right) \int_0^{y^+} u^+ t^+ dy^+}{\frac{1}{Pr} + \frac{\left[\kappa y^+ \left(1 - e^{-y^+/A^+} \right) \right]^2 \frac{du^+}{dy^+}}{Pr_t}} \right] dy^+ \qquad \text{(A.33)}$$

Calculation of Pr_t

Equation (A.30) can be solved for Pr_t, as:

$$Pr_t = \frac{\left[\kappa y^+ \left(1 - e^{-y^+/A^+} \right) \right]^2 \frac{du^+}{dy^+}}{1 - \left(\frac{K}{\sqrt{\frac{C_f}{2}}} + f_1 \right) \int_0^{y^+} u^+ t^+ dy^+ + \left(\frac{K t_\infty^+}{\sqrt{\frac{C_f}{2}}} + f_2 \right) \int_0^{y^+} u^+ dy^+}{\frac{dt^+}{dy^+}} - \frac{1}{Pr} \qquad \text{(A.34)}$$

If experimental data from the temperature profile are available, Eqn. (A.34) can be used to evaluate $Pr_t(y)$. All terms are calculated or are available, except for $\frac{dt^+}{dy^+}$, which is taken directly from the experimental data.

RESULTS AND DISCUSSION

The following demonstrates the importance of the corrections for pressure gradient and discusses the utility of the profiles developed above.

Figures A.2a and A.2b compare velocity and temperature profiles generated for one example set of conditions; $K=2.0\times10^{-6}$, $C_f=6.0\times10^{-3}$, $f_1=-5.0\times10^{-6}$, $t_\infty^+=20$, and $f_2=-1.0\times10^{-4}$, with various terms in Eqns. (A.19) and (A.31) set to zero to demonstrate the importance of each in the profile evaluation. Included are (a) the standard law of the wall (K, f_1, f_2 and p^+ set to zero), (b) correction for acceleration using just the A^+ term (K, f_1, f_2 and p^+ set to zero, but $A^+=40$, which is consistent with the actual p^+), (c) correction with just the p^+ term (K, f_1 and f_2 set to zero and $A^+=25$), (d) correction with A^+ and p^+ (K, f_1 and f_2 set to zero and $A^+=40$), and (e) the full correction as given by Eqns. (A.19) and (A.31). From the differences in the curves, one can see that each part of the correction makes a significant contribution to the total profile. An explanation for the effect of each term follows.

In a favorable pressure gradient, the p^+ term causes a drop in u^+ values below those of the standard law of the wall (compare curves a and c of Fig. A.2a), and a rise in t^+ values above those of the standard thermal law of the wall (compare curves a and c of Fig. A.2b). To explain this, consider a momentum balance on an element of fluid in the boundary layer. If the convection terms in the boundary layer momentum equation (Eqn. (A.3)) were set to zero, the resulting equation would be $\frac{dP}{dx}=\frac{\partial\tau}{\partial y}$; the normal gradient of shear stress balances the streamwise pressure gradient. For an accelerating flow, $\frac{dP}{dx}<0$, τ must therefore decrease with distance from the wall. Since $\tau\propto\frac{\partial u}{\partial y}$, $\frac{\partial u}{\partial y}$ must also decrease with distance from the wall. This results in a drop in u^+ values below those of the standard law of the wall. In turbulent flow, the p^+ term also has a secondary effect. Since the eddy viscosity is proportional to $\frac{\partial u}{\partial y}$, Eqn. (A.15), ε_M must drop in response to

the favorable pressure gradient effect described above. In a turbulent flow, the eddy viscosity enhances mixing outside of the viscous sublayer, thereby increasing wall shear and reducing $\frac{\partial u}{\partial y}$ and τ outside the sublayer, relative to their values at the wall. In dimensionless variables, $\frac{\partial u^+}{\partial y^+}$ drops. In favorable pressure gradients, the reduced eddy viscosity causes a rise in $\frac{\partial u^+}{\partial y^+}$ back toward laminar values, somewhat mitigating the drop in $\frac{\partial u^+}{\partial y^+}$ caused by the direct effect of the p^+ term.

The p^+ term has no direct effect on the temperature profile, since the pressure gradient does not appear explicitly in the boundary layer energy equation (Eqn. (A.20)). The secondary effect described above is present, however. As $\frac{\partial u^+}{\partial y^+}$ drops in a favorable pressure gradient, the eddy diffusivity, ε_H, must also fall (Eqn. (A.29)). The result is a rise in t^+ values above those predicted by the standard thermal law of the wall (compare curves a and c in Fig. A.2b).

The A^+ term is used to model the thickness of the viscous sublayer. Favorable pressure gradients (or acceleration) strain the flow in the streamwise direction, causing a reduction in eddy transport and an increase in sublayer thickness. This is a stabilizing effect. The reduction in eddy transport has the same effect described above with regard to the secondary effect of the p^+ term. When ε_M and ε_H drop, the velocity and temperature profiles both rise above the standard profiles.

When the A^+ and p^+ effects are combined, they tend to cancel each other in the velocity profile, but are additive for the temperature profile (due to the absence of a direct p^+ effect for temperature). The result is a larger deviation of the temperature profile from the standard profile as a result of acceleration than for the velocity profile. Herein lies the reason for the apparent robustness of the velocity profiles to different accelerations which

is not shared by the temperature profiles. Such behavior was noted by Bradshaw (1994b).

The remainder of the corrections in Eqns. (A.19) and (A.31) are due to the convection terms in Eqns. (A.3) and (A.20). The magnitudes and signs of these corrections will depend on local conditions, including, for example, the rate at which the free-stream is being accelerated and the rate at which the boundary layer is growing. In Eqns. (A.19) and (A.31), these effects are expressed in terms of K, f_1, and f_2.

To evaluate velocity profiles given by Eqn. (A.19), experimental velocity profile data from four studies are plotted in Fig. A.3a along with calculated profiles corresponding to each. Data were taken from Blair (1981), Blackwell, Kays and Moffat (1972), Thielbahr, Kays and Moffat (1969), and Kearney, Moffat and Kays (1970). All but the first were taken from Kays and Crawford (1993). Pertinent constants from these profiles are given in Table A.1. All four studies were done on flat plates, with K held constant. Blair's mild acceleration case deviates only slightly from the standard, zero pressure gradient law of the wall, and the data match the calculated profile well. The fits of the other three profiles are reasonable, but could stand improvement. Blackwell et al.'s adverse pressure gradient data, and Thielbahr et al.'s favorable pressure gradient data do not match the calculated profile particularly well in the viscous sublayer region (where acceleration effects on the calculated profile are small), indicating that better estimates of C_f than those given with the experimental data might be possible. As shown in Fig. A.3b, if C_f were increased by approximately 8%, to 0.0022 in Blackwell's case and to 0.0053 in Thielbahr's case, the experimental data and the calculated profiles could be brought into good agreement. For Blackwell et al.'s and Thielbahr et al.'s flows, the 8% change discussed above is within the expected experimental uncertainty in C_f. Julien, Kays and Moffat (1971), who provided the velocity profiles used in Thielbahr et al.'s study, estimate an uncertainty of $\pm 10\%$ in C_f in this case. Fitting to Eqn. (A.19) is believed to reduce this uncertainty and improve C_f estimation. Figure A.4 shows a force

fit of Thielbahr et al.'s velocity data to the standard law of the wall. The required Cf was 0.0061. This is a 15% increase above the value estimated above using a fit to Eqn. (A.19) and a 23% increase above their published value. The Kearney et al. data could not be brought into good agreement with the calculated profile. Given the relatively strong acceleration parameter in this case, relaminarization effects may have become strong enough to explain the discrepancy between the data and the turbulent flow calculation. Perhaps the flow was stabilized to the point (low momentum thickness Reynolds number) where the mixing length, A^+ and turbulent Prandtl number models were not so accurate.

Temperature Profiles

The measured and calculated temperature profiles corresponding to the flat wall velocity profiles in Fig. A.3a are shown in Fig. A.5a. The unadjusted C_f values given with the data sets and used in Fig. A.3a were used in the data reduction. Blair's (1981) case was subject to a uniform wall heat flux boundary condition. The other three cases had uniform wall temperature boundary conditions. The matches between calculation and data are reasonable for all four cases.

If the updated Cf values used with Fig. A.2b were applied to Blackwell et al.'s and Thielbahr et al.'s temperature profile data, the results would appear as shown in Fig. A.5b. The match between Blackwell et al.'s data and Thielbahr et al.'s data and the calculated profiles improves.

An examination of the near-wall region ($y^+<10$) shows some discrepancies between the measured data and the calculated profiles. In this region, acceleration effects are minimal, and all data should fall near the line $t^+=Pr\ y^+$. Thielbahr et al.'s and Kearney et al.'s data fall noticeably above this line in both Figs. A.5a and A.5b. If at each point in the profile the temperature difference (T_W-T) is decreased by 0.47°C below the reported value in Kearney et al.'s case and 0.84°C in Thielbahr et al.'s case, the near-wall data is brought into good agreement with $t^+=Pr\ y^+$, as shown in Fig. A.5c. The

required shift could be due to error in the measurement of T_w, the profile temperatures, or some combination of both. The shifts in T_w given above represents about 3.5% of the overall temperature difference (T_w-T_∞) in both cases. Kearney et al. note the discrepancy between their data and the $t^+=Pr\ y^+$ line, and suggest that their measured temperature in this region may be in error by as much as 1.3°C. They also checked their energy balance by calculating the enthalpy thickness, Δ_2, using mean temperature profile, wall temperature, and heat flux data, along with the energy integral equation. Differences in Δ_2 of as high as 8.4% were reported. This discrepancy is not large, given the nature of the measurements, but with the shift in T_w proposed above, the discrepancy in Δ_2 decreases from 8.4% to about 5%. The shifts in T_w given above, therefore, appear reasonable and within the experimental uncertainty.

Note that the deviations of the temperature profile data from the standard unaccelerated law of the wall values are much larger than those for the velocity profile in all cases. This is particularly apparent in Blair's mild, favorable pressure gradient flow and Blackwell et al.'s adverse pressure gradient flow. In these cases, the deviations of the velocity profile from the unaccelerated law of the wall are small, but the deviations of the temperature profiles are significant and Eqns. (A.31) and (A.33) represent major improvements.

Calculation of Pr_t

The temperature profiles presented above were calculated using the turbulent Prandtl number distribution given in Eqn. (A.32), with Pr_{t_∞}=0.85. The good match between the experimental data and the calculated profiles in Fig. A.5c indicate that this model is adequate, and suggests that pressure gradients, alone, do not significantly affect the turbulent Prandtl number distribution. In some flows, however, this distribution may change. Eqn. (A.34) could be applied in an attempt to calculate the Pr_t distributions. As an example of such an application, Kim and Simon (1991) and Kestoras (1993) measured

Pr_t directly (as explained above in Chapter 2) in an unaccelerated, nominal 8% FSTI flow, along the concave wall used in the present study. They were able to take direct measurements for $y^+>100$. Probe size limitations prevent measurements within $y^+<100$ of their flows. Mean temperature profile data, acquired by Kestoras (1993), was processed in the present study to determine local values of Pr_t, using Eqn. (A.34). The results for four streamwise stations are shown in Fig. A.6. Profiles of Pr_t determined from Eqn. (A.34) and from direct measurements are plotted versus y^+. Below $y^+=100$, the measured data can not be trusted due to spatial resolution problems. Above $y^+=400$, the calculated profiles lose accuracy as the mean velocity and temperature gradients become small. In the range $100<y^+<400$, the calculated and measured results agree, within the uncertainty of the data.

CONCLUSIONS

1. New formulations have been developed for mean velocity and temperature profiles in turbulent flows. The velocity profile is similar to one in the literature. No equivalent to the temperature formulation has been found in the literature. These profiles capture the effects of non-zero pressure gradients and match experimental data well.

2. The improvements to the velocity profiles allow an improved determination of skin friction coefficients from experimental data using a near-wall fitting technique. It was shown that "force fits" to the standard law of the wall can lead to errors of as large as 15%.

3. The profiles presented here are dependent on the mixing length model which assumes $\kappa=0.41$ and are based upon a documented variable-A^+ model. As shown, inclusion of this variable-A^+ model is quite important. While this model appears to be adequate, further work to clarify the behavior of κ and A^+ under various conditions would be desirable.

4. The model has been tested through comparison to some data from pressure gradient flows. Further testing in both favorable and adverse pressure gradient cases would be useful.

APPENDIX A REFERENCES

Blackwell, B. F., Kays, W. M. and Moffat, R. J. (1972). "The Turbulent Boundary Layer on a Porous Plate: an Experimental Study of the Heat Transfer Behavior with Adverse Pressure Gradients," HMT-16, Thermosciences Division, Mechanical Engineering Department, Stanford University, Stanford, Calif.

Blair, M. F. (1981). "Final Data Report - Vol. II -Velocity and Temperature Profile Data for Accelerating, Transitional Boundary Layers," United Technologies Research Center report R81-914388-16.

Bradshaw, P. (1967). "The Turbulent Structure of Equilibrium Turbulent Boundary Layers," *J. Fluid Mech.*, Vol. 29, pp. 625-645.

Bradshaw, P. (1994b). "The Law of the Wall," lecture at the Osborne Reynolds Centenary Symposium, UMIST, Manchester, May 24, 1994.

Galbraith, R. A. McD. and Head, M. R. (1975). "Eddy Viscosity and Mixing Length from Measured Boundary Layer Developments," Aeronautical Quarterly, Vol. 26, pp. 133-154.

Hirt, F. and Thomann, H. (1986). "Measurement of Wall Shear Stress in Turbulent Boundary Layers Subject to Strong Pressure Gradients," *J. Fluid Mech.*, Vol. 171, pp. 547-562.

Huffman, G. D. and Bradshaw, P. (1972). "A Note on von Kármán's Constant in low Reynolds Number Turbulent Flows," *J. Fluid Mech.*, Vol. 53, pp. 45-60.

Jones, W. P. and Launder, B. E. (1972). "Some properties of sink-flow turbulent boundary layers," *J. Fluid Mech.*, Vol. 56, pp. 337-351.

Julien, H. L., Kays, W. M. and Moffat, R. J. (1971). "Experimental Hydrodynamics of the Accelerated Turbulent Boundary Layer With and Without Mass Injection," *J. Heat Transfer*, Vol. 93, pp. 373-379.

Kays, W. M. (1994). "Turbulent Prandtl Number - Where Are We?" *J. Heat Transfer*, Vol. 116, pp. 284-295.

Kays, W. M. and Crawford, M. E. (1993). Convective Heat and Mass Transfer, McGraw-Hill Inc., New York.

Kearney D. W., Moffat, R. J. and Kays, W. M. (1970). "The Turbulent Boundary Layer: Experimental Heat Transfer with Strong Favorable Pressure Gradients and Blowing,"

HMT-12, Thermosciences Division, Mechanical Engineering Department, Stanford University, Stanford, Calif.

Kestoras, M. D. (1993). "Heat Transfer and Fluid Mechanics Measurements in a Turbulent Boundary Layer: Introduction and Removal of Concave Curvature under High Free-Stream Turbulence Conditions," Ph.D. Thesis, Department of Mechanical Engineering, University of Minnesota.

Kim, J. and Simon, T. W. (1991). "Free-Stream Turbulence and Concave Curvature on Heated, Transitional Boundary Layers, Volume I - Final Report," NASA CR 187150, "Volume II - Program Listings and Tabulated Data," NASA CR 187151.

McDonald, H. (1969). "The Effect of Pressure Gradient on the Law of the Wall in Turbulent Flow," J. Fluid Mech., Vol. 35, pp. 311-336.

Nagano, Y., Tagawa, M. and Tsuji, T. (1992). "Effects of Adverse Pressure Gradient on Mean Flows and Turbulence Statistics in a Boundary Layer," Turbulent Shear Flows 8 (ed. F. Durst et al.), Springer-Verlag, Berlin.

Rued, K. (1987). "Transitional Boundary Layers under the Influence of High Free Stream Turbulence, Intensive Wall Cooling and High Pressure Gradients in Hot Gas Circulation," NASA TM 88254.

Samuel, A. E. and Joubert, P. N. (1974). "A Boundary Layer Developing in an Increasingly Adverse Pressure Gradient," *J. Fluid Mech.*, Vol. 66, pp. 481-505.

Spalart, P. R. (1986). "Numerical Study of Sink-Flow Boundary Layers," *J. Fluid Mech.*, Vol. 172, pp. 307-328.

Spalart, P. R. and Watmuff, J. H. (1993). "Experimental and Numerical Study of a Turbulent Boundary Layer with Pressure Gradients," *J. Fluid Mech.*, Vol. 249, pp. 337-371.

Thielbahr, W. H., Kays, W. M. and Moffat, R. J. (1969). "The Turbulent Boundary Layer: Experimental Heat Transfer with Blowing, Suction, and Favorable Pressure Gradient," HMT-5, Thermosciences Division, Mechanical Engineering Department, Stanford University, Stanford, CA.

van Driest, E. R. (1956). "On Turbulent Flow Near a Wall," *J. Aero. Sci.*, Vol. 23, pp. 1007-1011.

Case	$K \times 10^6$	$C_f \times 10^3$	$f_1 \times 10^6$	$f_2 \times 10^4$	t_∞^+	A^+	Re_θ	$Re_{\Delta 2}$
Blair	0.75	4.98	-34.0	-0.065	31.6	30.6	838	2730
Blackwell	-0.31	2.02	-4.43	-1.25	15.2	20.8	4533	2459
Thielbahr	1.67	4.96	-0.88	-1.37	24.9	42.2	747	1880
Kearney	2.68	4.96	-3.88	-7.90	31.3	72.5	550	1345

Table A.1: Experimental Data

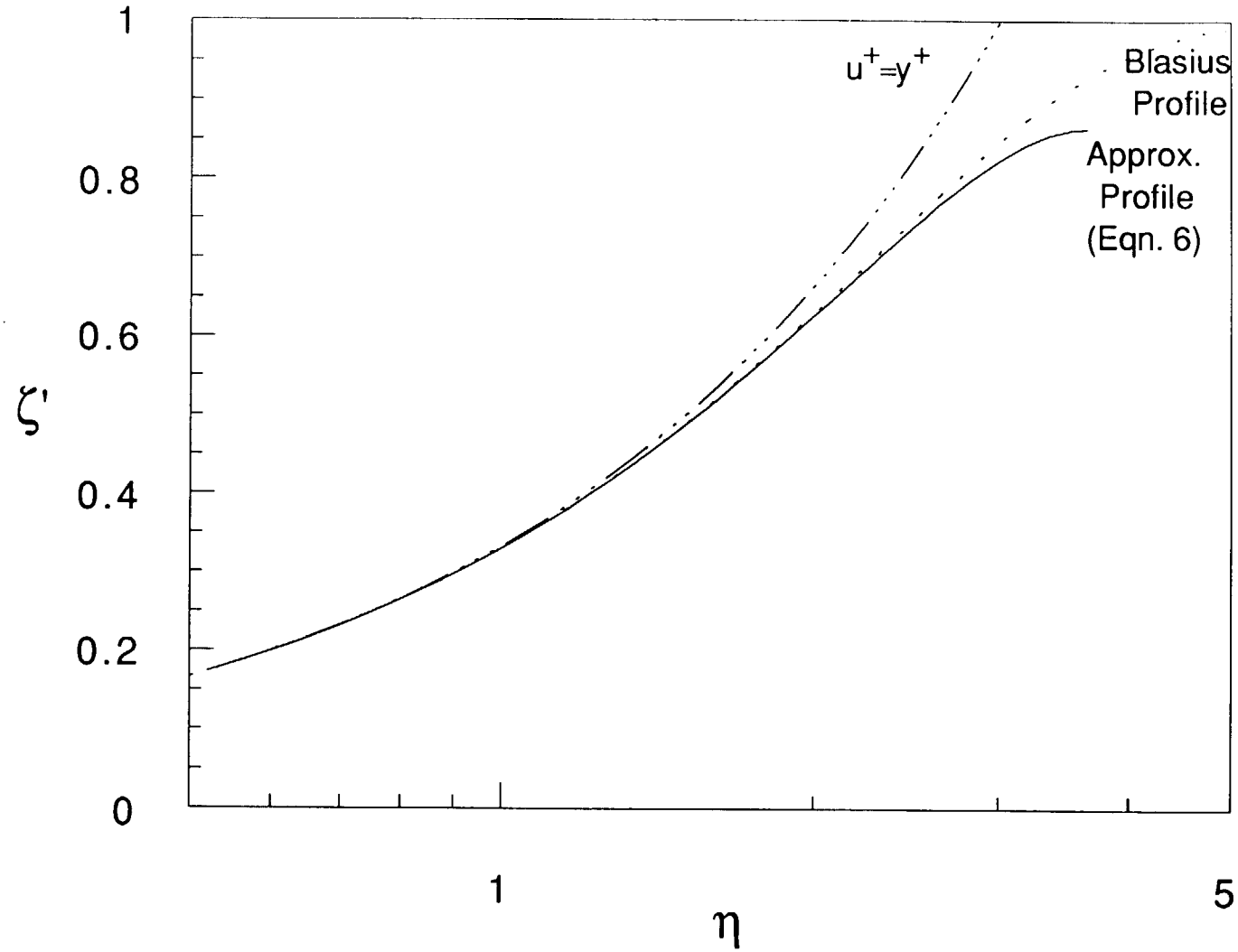

Fig. A.1: Velocity Profile in Laminar Unaccelerated Flow

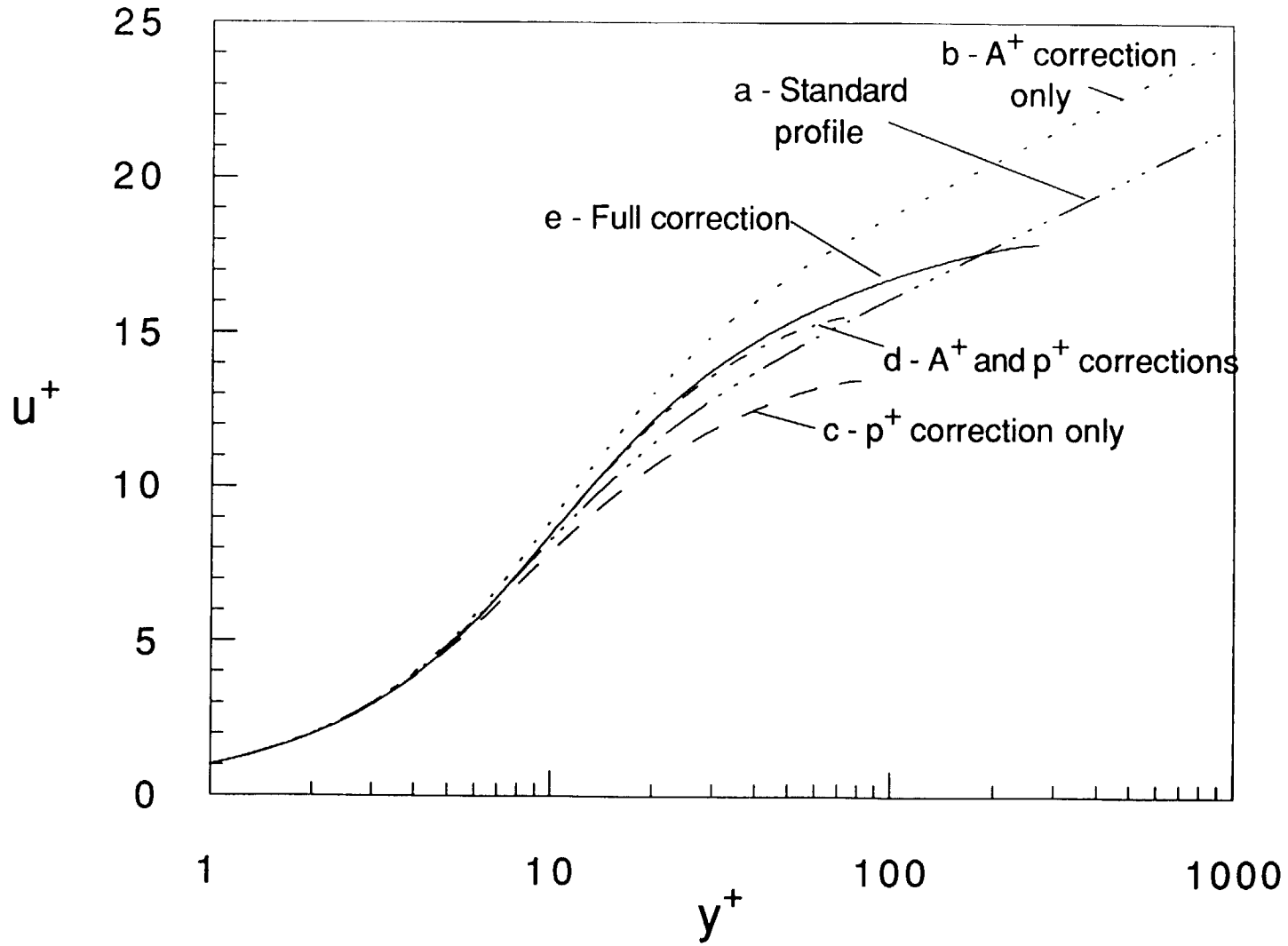

Fig. A.2a: Velocity Profiles Including Various Correction Terms

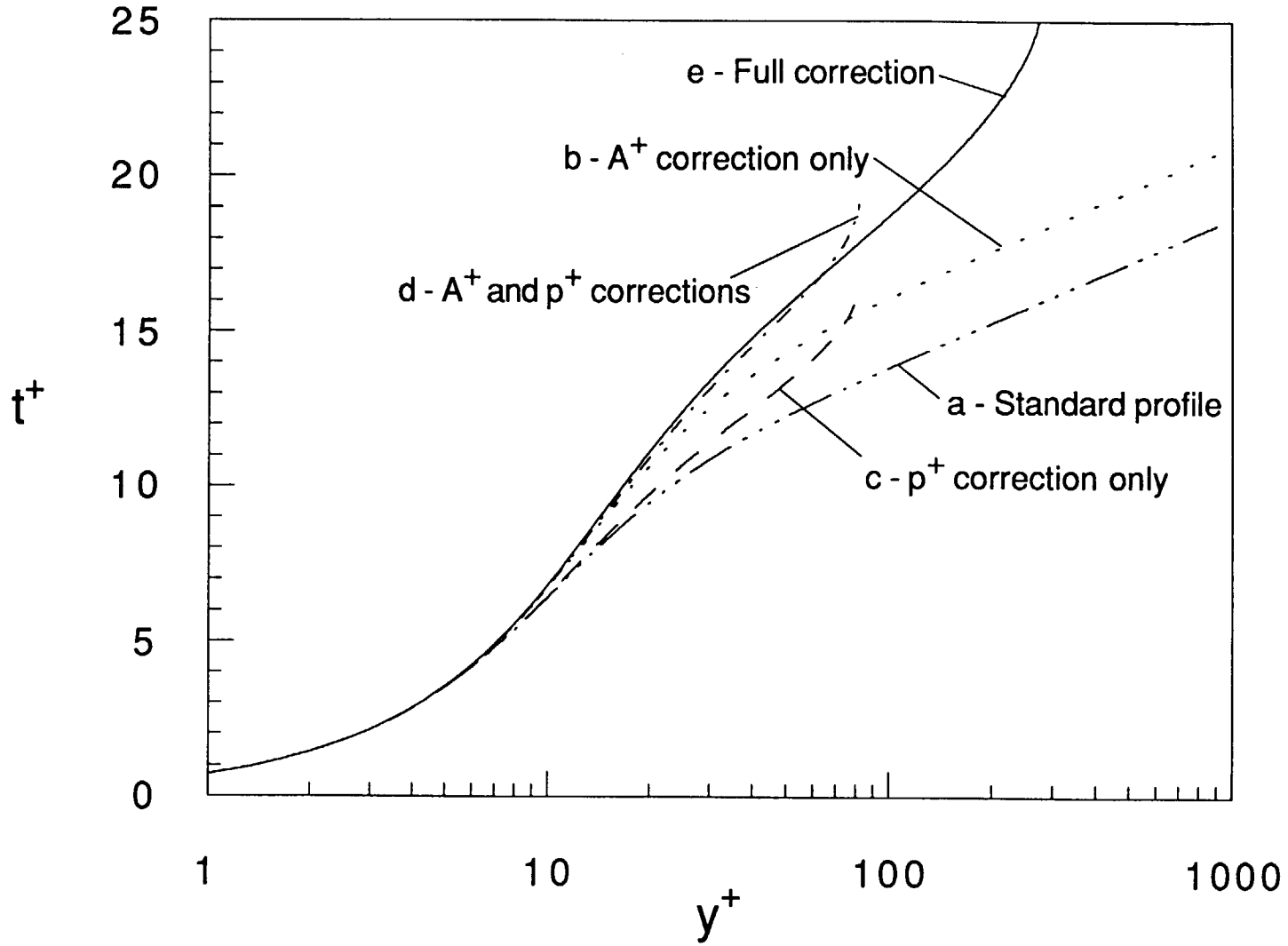

Fig. A.2b: Temperature Profiles Including Various Correction Terms

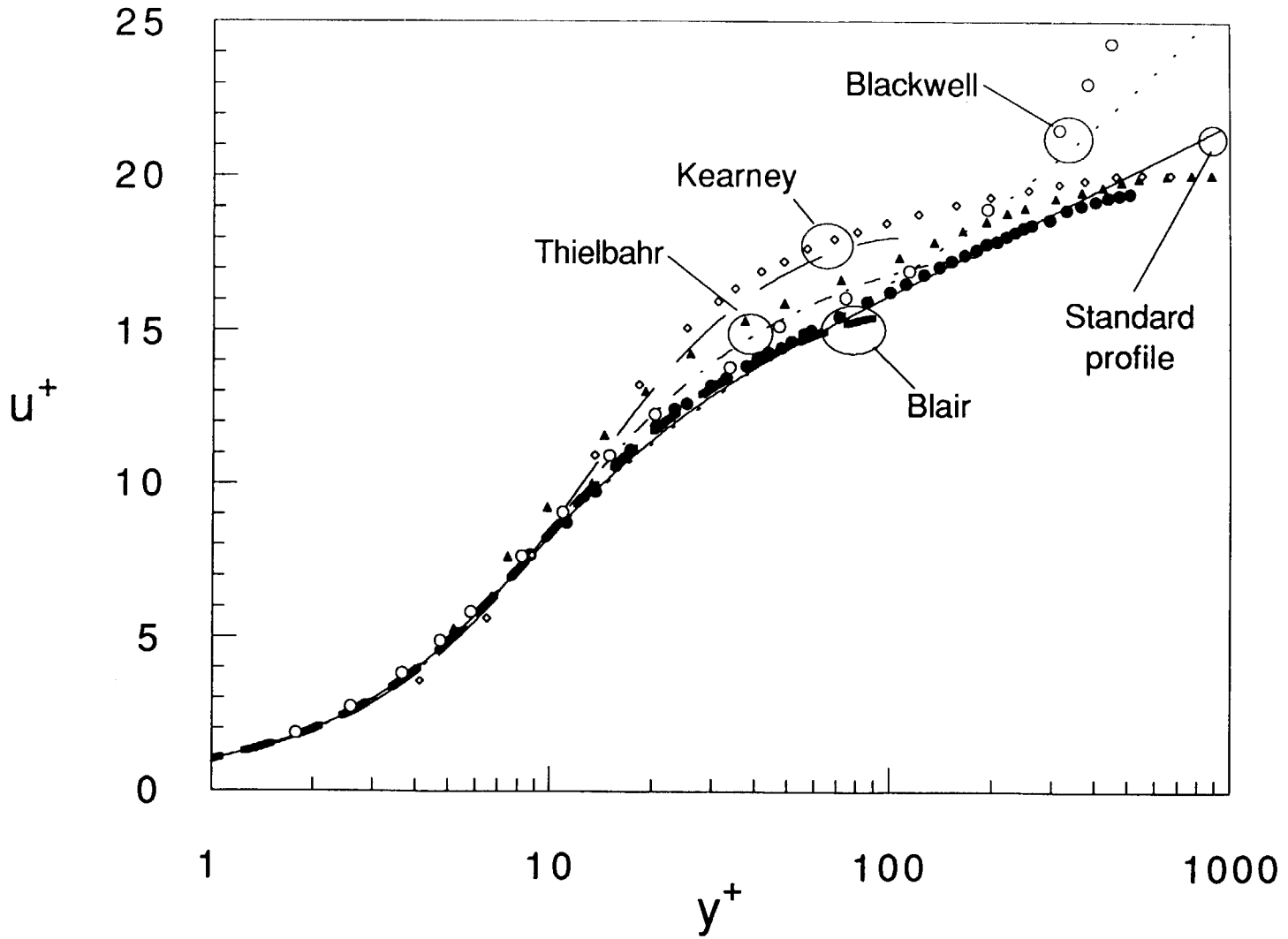

Fig. A.3a: Comparison of Experimental and Calculated Velocity Profiles

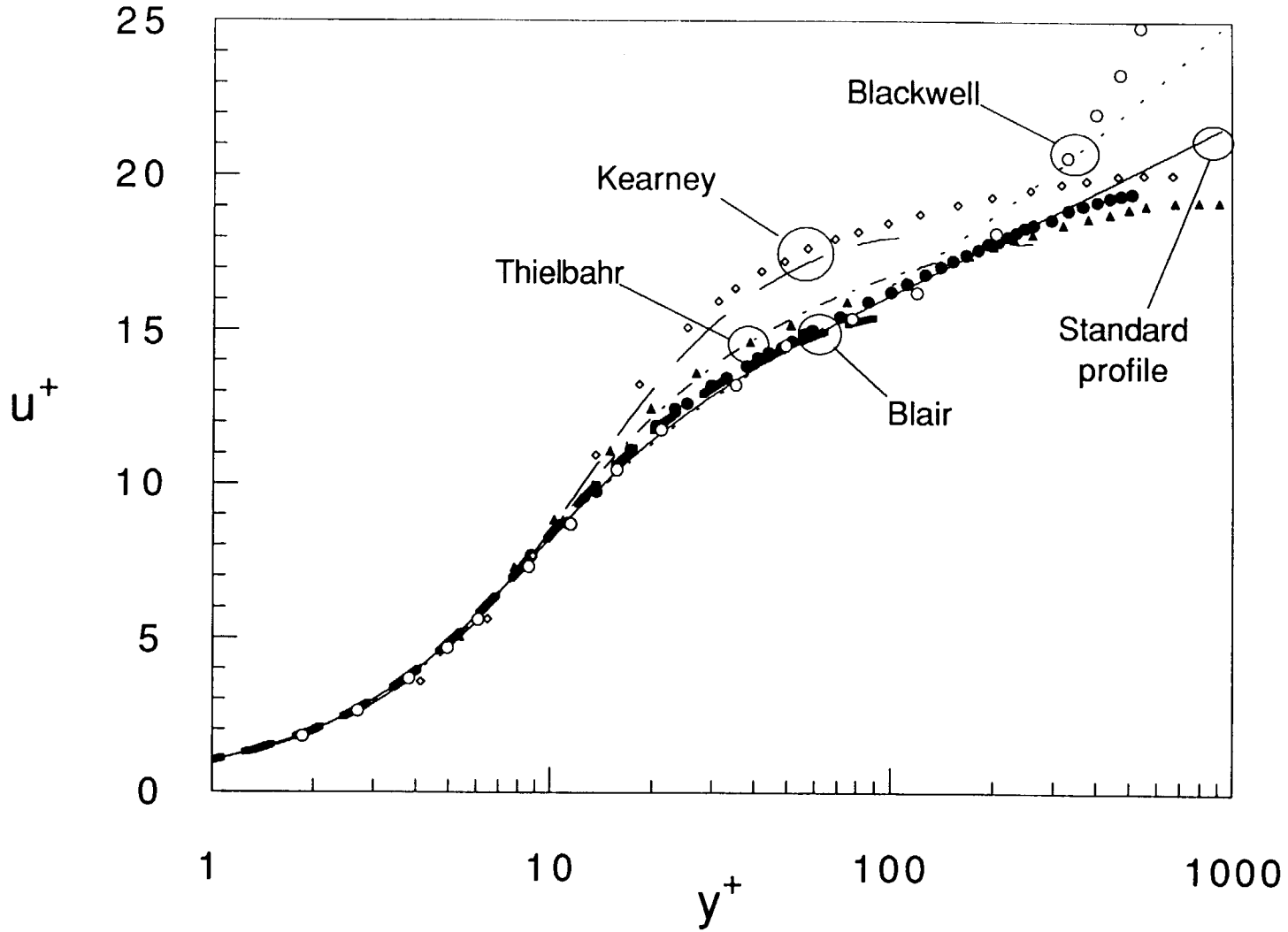

Fig. A.3b: Comparison of Experimental and Calculated Velocity profiles, Adjusted C_f

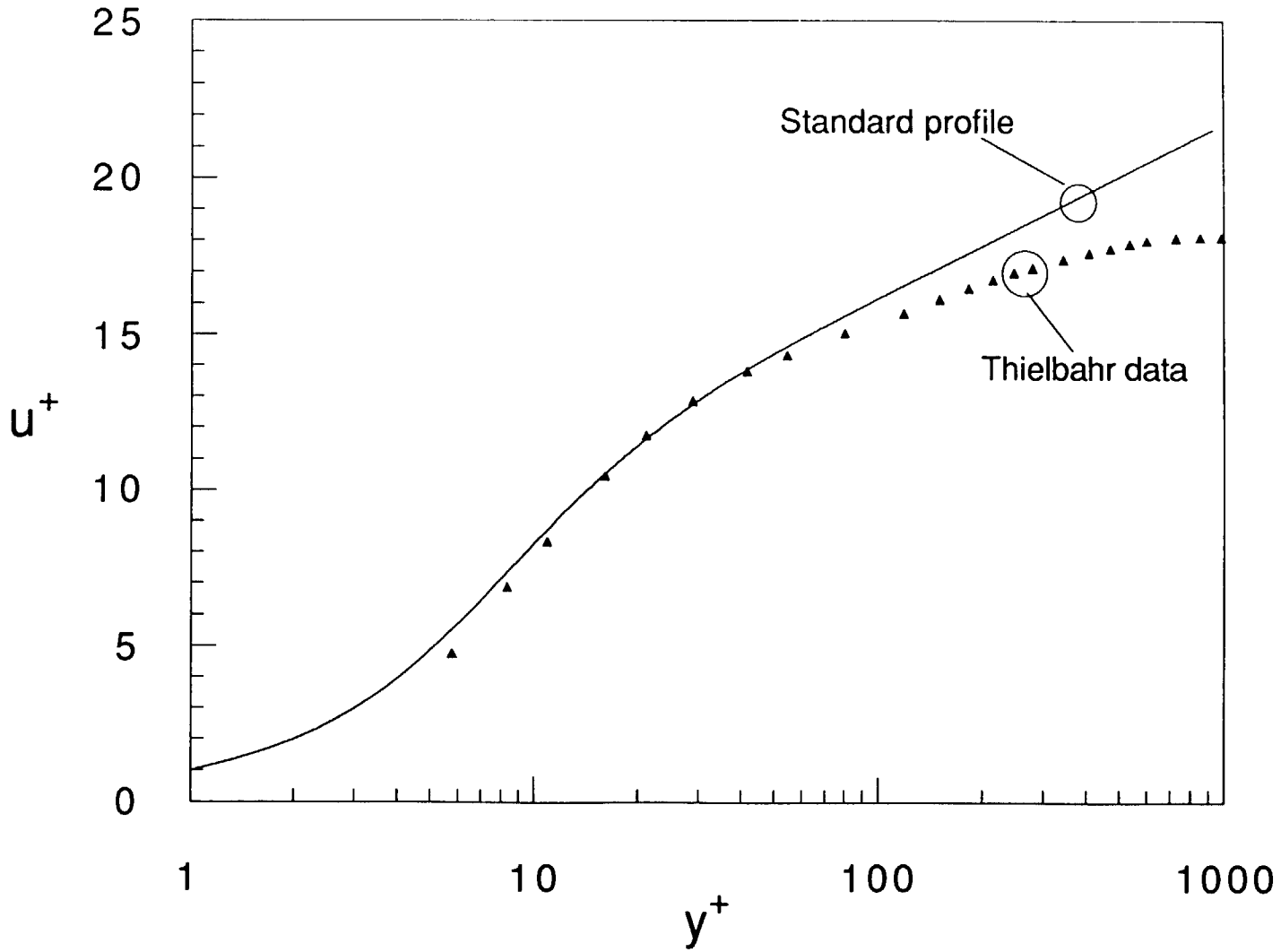

Fig. A.4: Force Fit of Experimental Velocity Data to Standard Law of the Wall

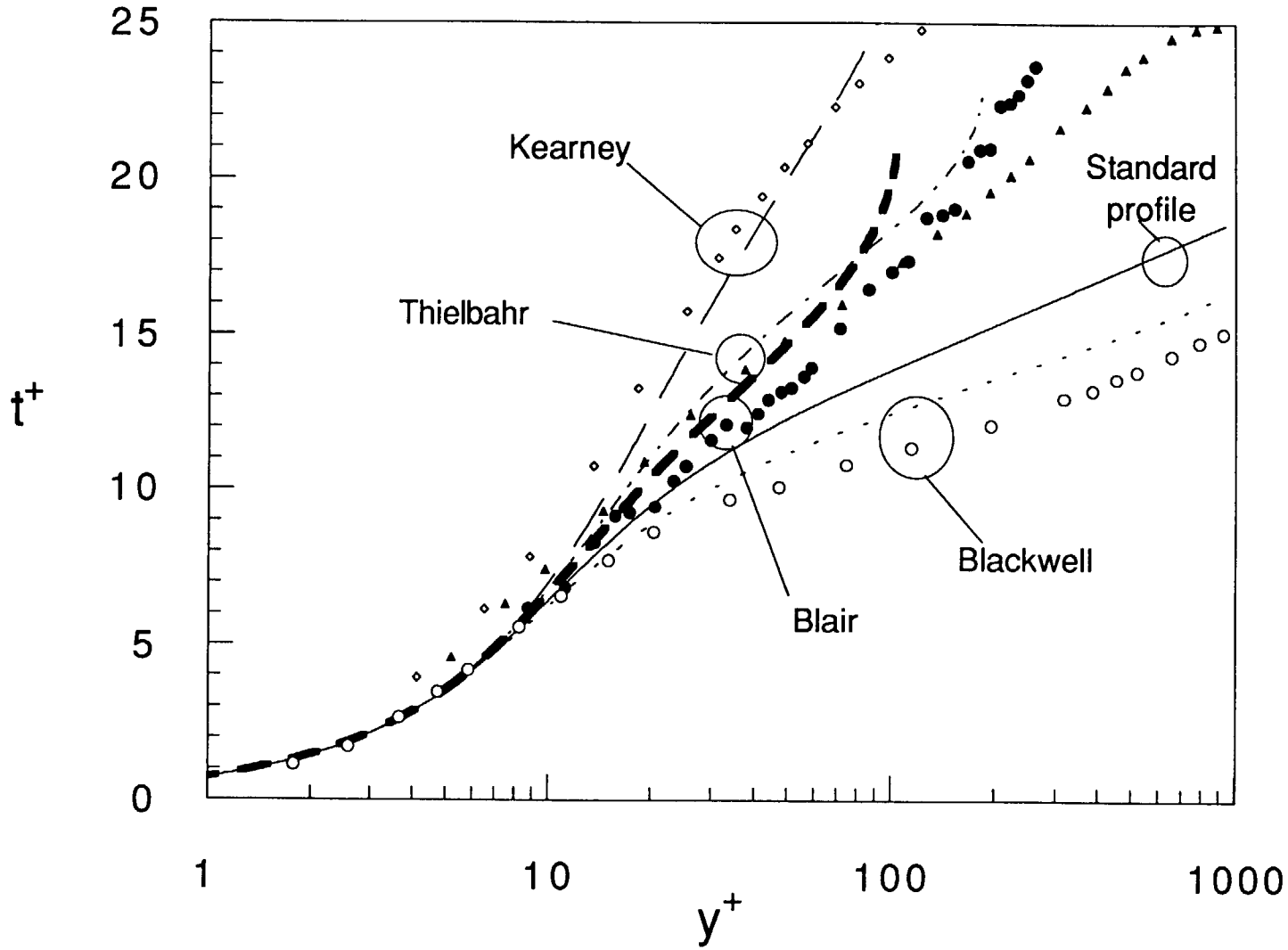

Fig. A.5a: Comparison of Experimental and Calculated Temperature Profiles

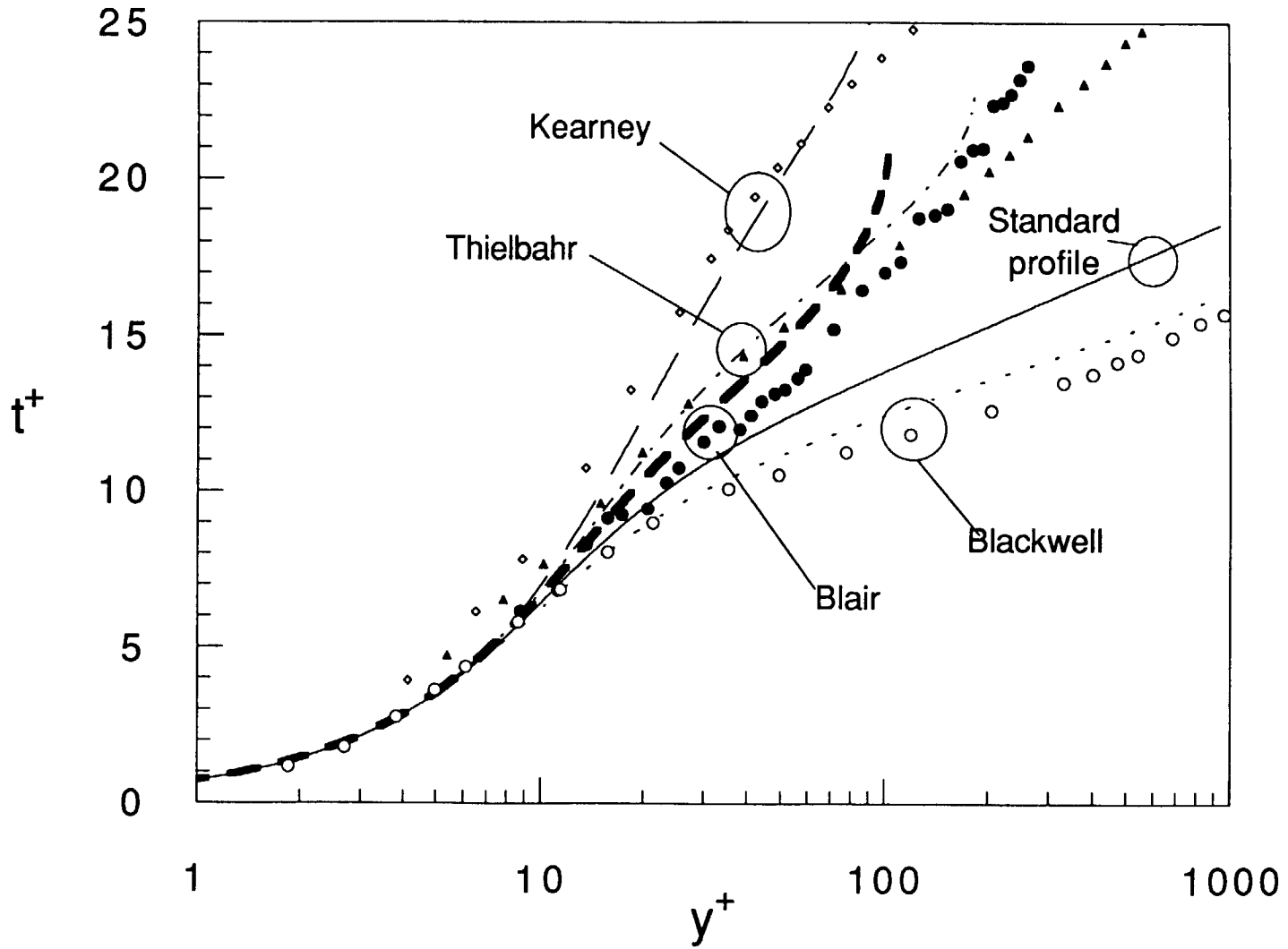

Fig. A.5b: Comparison of Experimental and Calculated Temperature Profiles, Adjusted C_f

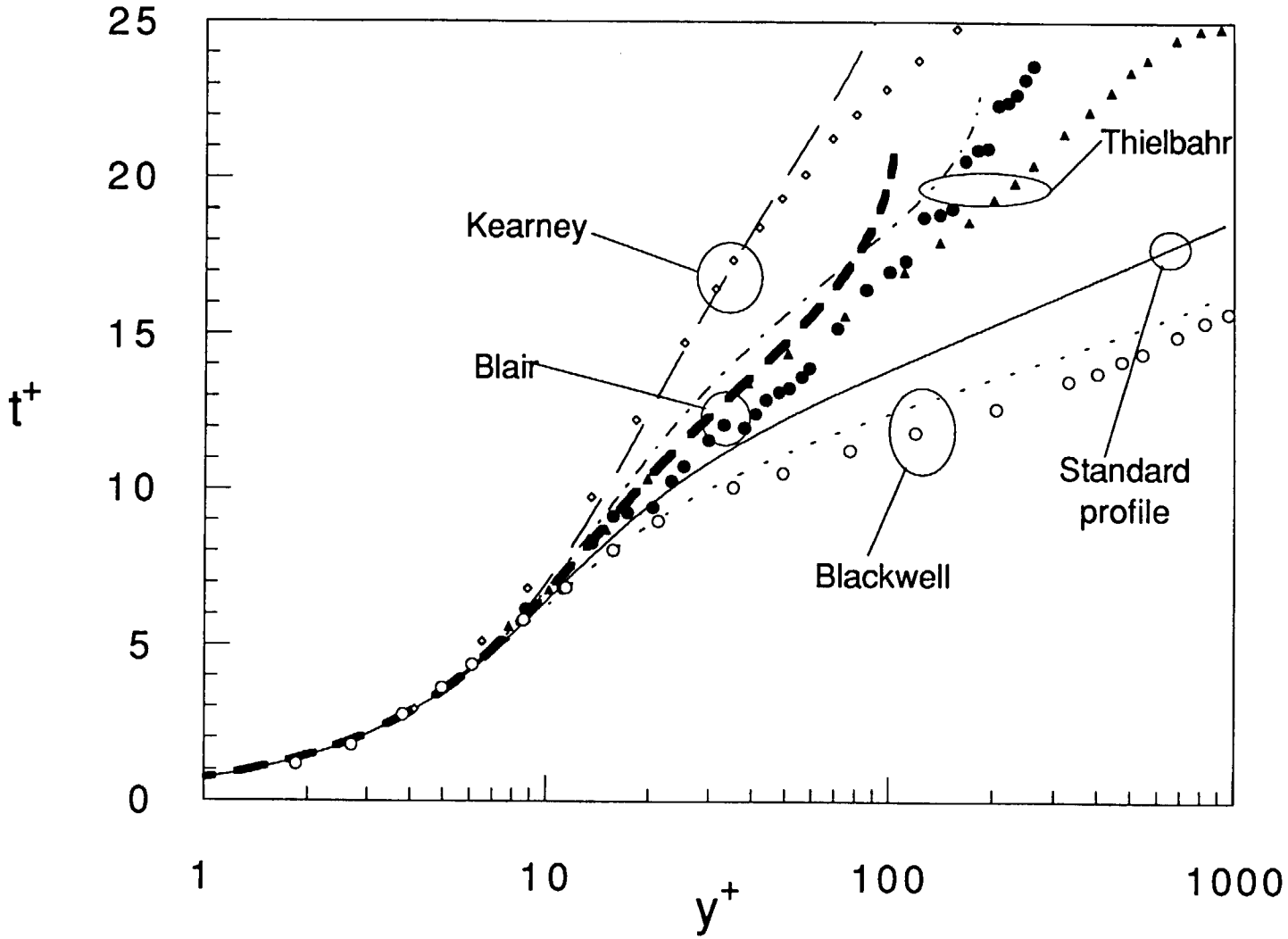

Fig. A.5c: Comparison of Experimental and Calculated Temperature Profiles, Adjusted C_f and t_o

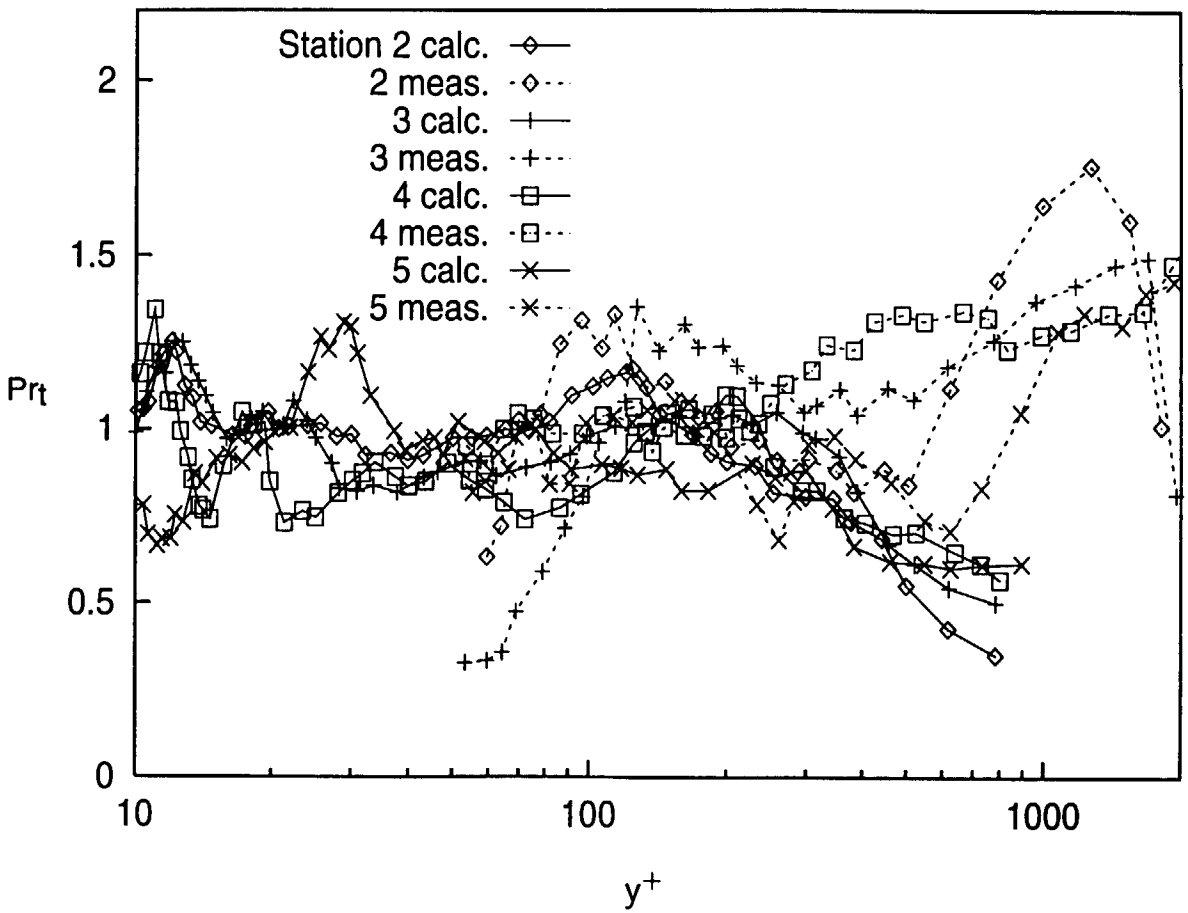

Fig. A.6: Comparison of Calculated and Measured Pr_t Unaccelerated, High FSTI, Concave-Wall Case

APPENDIX B: PROGRAM LISTINGS

C PROGRAMS

Name	Page	Description
s_cal.c	404	Acquires data for calibration of single hot-wire probe. Subsequent processing with swcr.f.
x_cal.c	408	Acquires data for calibration of cross-wire probe and hot-wires of triple-wire probe. Subsequent processing with xwcr.f
cold.c	413	Acquires data from triple-wire probe for determination of cold-wire compensation constant, kcc. Used with kcol.c and kcol.f.
kcol.c	417	Calls program kcol.f to calculate cold wire compensation constant, kcc.
sacq.c	418	Acquires velocity profile data using single hot-wire probe. Raw instantaneous voltage data stored in binary format. Subsequent processing with sred.c, skfric.f.
sred.c	425	Reduces profile data acquired with sacq.c, converting voltages to mean and fluctuating velocities. Further processing with skfric.f.
tacq.c	430	Acquires mean temperature profile data with traversing thermocouple probe. Subsequent processing with tplus.f.
xacq.c	437	Acquires profile data from U and V velocity components with cross-wire probe. Raw instantaneous voltage data stored in binary form. Subsequent processing with xred.c.

xred.c	442	Reduces profile data acquired using xacq.c. Turbulent shear stress among quantities calculated.
vtacq.c	448	Acquires profile data for U and V velocity components and temperature, T, using triple-wire probe. Raw instantaneous voltage data stored in binary form. Subsequent processing with vtred.c, prt.f, and quadrant.f.
vtred.c	455	Reduces profile data acquired with vtacq.c. Turbulent heat flux among quantities calculated. Octant analysis done. Further processing with prt.f and quadrant.f.
facq.c	463	Acquires voltage data from single hot-wire probe for spectral analysis with fred.c
fred.c	467	Processes data acquired with facq.c using Fast Fourier Transform to calculate power spectrum of u' fluctuations.
cacq.c	471	Acquires voltage data from cross-wire probe for spectral analysis with cred.c and hred.c
cred.c	474	Processes data acquired with cacq.c to calculate u' and v' power spectra.
hred.c	479	Processes data acquired with cacq.c to calculate $u'v'$ spectra.

FORTRAN PROGRAMS

Name	Page	Description
swcr.f	484	Calculates calibration constants for single hot-wire using data acquired with s_cal.c
xwcr.f	486	Calculates calibration constants for both wires of cross-wire probe using data acquired with x_cal.c

kcol.f	488	Calculates cold wire compensation constant.
skfric.f	491	Uses output of sred.c to find skin friction coefficients and velocity profiles in wall coordinates.
tplus.f	497	Reduces output of tacq.c to wall coordinates. Local wall temperature, heat flux and Stanton number determined from profile data.
prt.f	505	Reduces output of vtred.c to dimensionless form. Turbulent Prandtl number calculated.
quadrant.f	508	Octant data output by vtred.c nondimensionalized and put in form for plotting.
fplot.f	509	Reduced spectral data sections from fred.c, cred.c and hred.c pieced together.
smoln.f	510	Spectra output by fplot.f smoothed for plotting.
lwall.f	511	Mean velocity and temperature profiles calculated in wall coordinates using method of Appendix A.

```
/*
  Calibrates a single wire probe

  Written:  Ralph Volino       9/22/93


        Command Line:   s_cal

  This program is used to calibrate a single wire probe.
  The calibration is corrected to 25C.  Subsequent measurements
  must also be corrected to 25C.  The operating temperature of
  the probe  is 250C.  The calibration is done using the
  calibration jet.  The static pressure tap is read with the
  fluke multimeter and the hot wire is read with the HP3437A
  voltmeter.


*/

#include <stdio.h>
#include <sys/ugpib.h>
#include <fcntl.h>
#include <string.h>
#include <math.h>
#define  BUFSIZE        32
#define  NOTEXIST       -1
#define  PWR          0.435  /* power used in King's law */
#define  SLOPE        0.244  /* pressure transducer slope */
#define  RAIR          287.  /* gas constant for air */
#define  N1          600   /* # readings to zero pressure transducer */
#define  N0        7000   /* # readings for each data point */
#define  NP        50     /* # hot-wire readings/ pressure reading */
#define  ARAT       -0.89961768  /* area ratio (.8128/2.5654)^2-1 */
#define  CMH2OPA      97.955  /* conversion from cm H2O to Pa */
#define  MMHGPA       132.9   /* conversion from mm H2O to Pa */


main(argc,argv)
int     argc;
char    *argv[];
{

        int     offifa,gainifa,d14,d24,ty,n,i,n2,j,k;
int  flg,ansr,git();
        double  atof(),volt,gft();
        double  press, vel, hwv;
        float   sum1,offset,patm,tatm,tatmo,denair,sum,average;
        char    mybuf[BUFSIZE],o_str[BUFSIZE],readstr[400];
char name[10];
FILE *fd, *fp;


printf("Input a name for the output file: ");
scanf("%s",name);
getchar();
fd = fopen(name,"w");  /* open file for output */

        printf("Input the offset of the signal conditioner on the IFA-100.");
printf("\n(Default=1): ");
flg=0;
while ( flg == 0) {
++flg;
offifa = git();
if ( offifa == -987654 )   /*  check for default flag */
offifa = 1;   /*  default = 1 */
if ( offifa > 9 || offifa <0 ) {
printf("This is an invalid input, try another ");
flg = 0;
}
}

        printf("Input the gain of the signal conditioner on the IFA-100 ");
printf("\n(Default=10): ");
flg=0;
while ( flg == 0) {
++flg;
gainifa = 0;
for (i=0; (ansr = getchar()) != '\n'; i++) {
ansr = ansr - '0';
if (((ansr < 1 || ansr > 9) && i == 0)
        || (ansr != 0 && i > 0 )) {
flg = 0;
printf("Invalid input, try again ");
}
gainifa = 10*gainifa+ansr;
}
if ( i == 0)
gainifa = 10;
}
```

```
/*  Open the Fluke multimeter for reading the pressure transducer */

d14=ibfind("dev14");
               if(d14 < 0){
                fprintf(stderr,"Can't open /dev/dev14 for read\n");
                exit(1);
               }


/*  Open the HP3437A voltmeter for reading the IFA-100 output  */
d24=ibfind("dev13");
ibpad(d24,24);
               if(d24 < 0){
                fprintf(stderr,"Can't open /dev/dev13 for read\n");
                exit(1);
               }


/*  Zero the pressure transducer  */

sprintf(o_str,"F1R0S1T0"); /* fluke on medium rate auto range */
ibwrt(d14,o_str,strlen(o_str));

ty=0;
printf("Zero the pressure transducer ");
while( ansr = getchar() != '\n');
while(ty == 0) {
sum1=0.0;
for (i = 1; i <= N1; i++) {
                 ibrd(d14, mybuf, 13);
                 volt= atof(mybuf);
                 sum1   += volt;
}
sum1 = sum1/N1;
printf("The pressure transducer voltage is %e\n",sum1);
printf("Do you want to adjust the pressure transducer (y,n)? ");
for (i=0; (ansr = getchar()) != '\n' ; i++)
if (i == 0 && ansr == 'n')
ty=1;
}

offset = -sum1/SLOPE;  /* pressure transducer offset */

for (flg=0; flg == 0 ; ) {
flg++;
printf("Input the atmospheric pressure [in. Hg] ");
patm = gft();
if( patm < 28. || patm > 31.) {
printf("%f is not reasonable, try again.\n", patm);
flg = 0;
}
}
patm *= 25.4;


/* Acquire the data from the IFA and the pressure transducer */

tatm = 0;   /* Initializes jet temperature */
ansr = 'y';
for ( i=0; ansr != 'n' ; i++) {
for (flg=0; flg == 0 ; ) {
flg++;
printf("Input the flow temperature [C] ");
tatmo = tatm;
tatm = gft();
if(tatm == -987654.)
tatm = tatmo;
if( tatm < 19. || tatm > 36.) {
printf("%f is out of range, try again.\n",tatm);
flg = 0;
}
}
sum = 0;
sum1 = 0;

printf("Set the flow rate of the jet.");
while( getchar() != '\n');

rng(&d24);    /* sets the range on the HP voltmeter */

denair = patm/RAIR/(tatm+273.15)*MMHGPA;   /* density of air*/

n2 = NO/NP;   /* number of pressure readings */

sprintf(o_str,"D.008SN%dS",NP);
ibwrt(d24,o_str,strlen(o_str));
ibloc(d24);
       for(j=0; j < n2; j++){
ibrd(d24,readstr,NP*7);
```

```
for(k=0; k < NP ; k++) {
sscanf(readstr+(7*k),"%7s",mybuf);
                volt = atof(mybuf);
sum += volt;
        }
ibrd(d14, mybuf, 13);
volt = atof(mybuf);
sum1 += volt;
}

press = sum1/n2;
hwv = sum/(n2*NP);

press = (press+offset)*SLOPE*2.54; /* pressure in cm H20 */
press = 2.*CMH2OPA/denair*press/ARAT;
vel = pow(press, 0.5);  /* velocity from Bernoulli equation */

hwv = hwv/gainifa + offifa; /* decondition hot-wire signal */
hwv = pow( 225./(250.-tatm) , 0.5) * hwv; /* T corr. to H-W */

printf("%f\t%f\n",vel,hwv);
fprintf(fd,"%f\t%f\n",vel,hwv);
fflush(fd);

printf("Do you want to take more data (y,n)? ");
for (j=0; (ansr = getchar()) != '\n' ; j++)
if (j == 0 && ansr == 'n')
break;

}

fclose(fd);          /* This section puts the number of data */
fp = fopen("j1t","w");  /* points at the top of the file  */
fprintf(fp,"%d\n",i);
fclose(fp);
strcpy(mybuf,"cat j1t ");
strcat(mybuf,name);
strcat(mybuf," >j2t");
system(mybuf);
strcpy(mybuf,"cp j2t ");
strcat(mybuf,name);
system(mybuf);
system("rm j2t j1t");

}
```

```
rng(d24)

int *d24;
#define N2   100

{
int flg, i, n;
double atof(),volt;
char mybuf[10],o_str[5],readstr[800];

flg = 0;
sprintf(o_str,"D.008SN%dST1R3",N2);
ibwrt(*d24,o_str,strlen(o_str));
ibloc(*d24);
ibrd(*d24,readstr,N2*7);
        for(i=0; i < N2; i++){
sscanf(readstr+(7*i),"%7s",mybuf);
                volt = atof(mybuf);
if ( volt > 2. || volt < -2. ) {
flg = 1;
break;
}
else if ( volt > .2 || volt < -.2)
flg = 2;
        }
if (flg == 0) {
sprintf(o_str,"R1");
ibwrt(*d24,o_str,strlen(o_str));
ibloc(*d24);
}
if (flg == 2) {
sprintf(o_str,"R2");
ibwrt(*d24,o_str,strlen(o_str));
ibloc(*d24);
}
}


double gft()     /* gets a floating point number */

{
#define MAXLINE 1000

int len,i,flg1,flg2,flg3;
```

```
char line[MAXLINE];
double atof();

flg1 = 0;
while( flg1 == 0) {
flg2 = 0;
flg3 = 0;
len = getline(line,MAXLINE);
if( len == 0 )    /* bail out for blank line */
return(-987654.);
++flg1;
for (i=0; line[i] == ' ' || line[i] == '\t' ; i++)
;    /* get rid of leading blanks  */
if (line[i] == '+' || line[i] == '-' )
i++;
for ( ; i < len ; i++) {
if ( line[i]-'0' < 0 || line[i]-'0' >9) {
if( line[i] == '.' && flg2 == 0 )
flg2 = 1;
else if((line[i] == 'e' || line[i] == 'E') && flg3 == 0) {
flg2 = flg3 = 1;
if (line[i+1] =='+' || line[i+1] == '-')
i++;
}
else  {
flg1 = 0;
printf("Unacceptable input, try again: ");
}
}
}
}
return ( atof(line) );
}


getline(s,lim)  /* get line into s, return length */
char s[];
int lim;
{
int c,i;

i=0;
while(--lim > 0 && (c=getchar()) != EOF && c != '\n')
s[i++] = c;
s[i] = '\0';
return(i);
}


git()     /* gets an integer */

{
#define MAXLINE 1000

int len,i,flg1,flg2;
char line[MAXLINE];
int atoi();

flg1 = 0;
while( flg1 == 0) {
flg2 = 0;
len = getline(line,MAXLINE);
if( len == 0 )    /* bail out for blank line */
return(-987654);
++flg1;
for (i=0; line[i] == ' ' || line[i] == '\t' ; i++)
;    /* get rid of leading blanks  */
if (line[i] == '+' || line[i] == '-' )
i++;
for ( ; i < len ; i++) {
if ( line[i]-'0' < 0 || line[i]-'0' >9 || flg2 == 1 ) {
if( line[i] == '.' && flg2 == 0 )
flg2 = 1;
else  {
flg1 = 0;
printf("Unacceptable input, try again: ");
}
}
}
}
return ( atoi(line) );
}
```

```
/*
  Calibrates a cross wire probe

  Written:  Ralph Volino       10/16/93


        Command Line:   x_cal

  This program is used to calibrate a cross wire
  probe.  The calibration is corrected to 25C.
  Subsequent measurements must also be corrected to
  25C.  The operating temperature of the probe  is
  250C.  The calibration is done using the calibration
  jet.  The static pressure tap is read with the fluke
  multimeter and the hot wires are read with the Norland.


*/

#include <stdio.h>
#include <sys/ugpib.h>
#include <fcntl.h>
#include <string.h>
#include <math.h>
#define  BUFSIZE        40
#define  NOTEXIST       -1
#define  PWR          0.435  /* power used in King's law */
#define  SLOPE        0.244  /* pressure transducer slope */
#define  RAIR          287.  /* gas constant for air */
#define  N1          600   /* number of readings to zero
                              pressure transducer */
#define  NO       4096   /* number of readings for each data point */
#define  NP       850     /* number of pressure readings */
#define  ARAT       -0.89961768  /* area ratio (.8128/2.5654)^2-1 */
#define  CMH2OPA      97.955  /* conversion from cm H20 to Pa */
#define  MMHGPA       132.9   /* conversion from mm H20 to Pa */


main(argc,argv)
int     argc;
char    *argv[];
{

        int     offifa,gainifa,d14,d15,ty,n,i,n2,j,k;
int  flg,ansr,git();
        double  atof(),volt,gft();
double  press, vel, hwv1, hwv2;
double  volt1[4096],volt2[4096];
        float   sum1,offset,patm,tatm,tatmo,denair,sum,average;
        char    mybuf[BUFSIZE],o_str[BUFSIZE],readstr[400];
char name[10];
char    norbuf[8452];
FILE *fd, *fp;


printf("Input a name for the output file: ");
scanf("%s",name);
getchar();
fd = fopen(name,"w");  /* open file for output */

        printf("Input the offset of the signal conditioner on the IFA-100.");
printf("\n(Default=1): ");
flg=0;
while ( flg == 0) {
++flg;
offifa = git();
if ( offifa == -987654 )   /*  check for default flag */
offifa = 1;   /*  default = 1 */
if ( offifa > 9 || offifa <0 ) {
printf("This is an invalid input, try another ");
flg = 0;
}
}

        printf("Input the gain of the signal conditioner on the IFA-100 ");
printf("\n(Default=10): ");
flg=0;
while ( flg == 0) {
++flg;
gainifa = 0;
for (i=0; (ansr = getchar()) != '\n'; i++) {
ansr = ansr - '0';
if (((ansr < 1 || ansr > 9) && i == 0)
         || (ansr != 0 && i > 0 )) {
flg = 0;
printf("Invalid input, try again ");
}
gainifa = 10*gainifa+ansr;
}
if ( i == 0)
```

```
gainifa = 10;
}


/*  Open the Fluke multimeter for reading the pressure transducer */

d14=ibfind("dev14");
                if(d14 < 0){
                fprintf(stderr,"Can't open /dev/dev14 for read\n");
                exit(1);
                }


/*  Open the Norland oscilloscope for reading the IFA-100 output  */
d15=ibfind("dev15");
                if(d15 < 0){
                fprintf(stderr,"Can't open /dev/dev15 for read\n");
                exit(1);
                }


/* Initialize and program the Norland for averaging input voltages */
printf("Do you want to initialize the Norland (y,n)? ");
for (i=0; (ansr = getchar()) != '\n' ; i++)
if (i == 0 && ansr == 'y')
ty=1;
else ty=0;
if(ty == 1) {
printf("Press Reset Key of the Norland");
while( ansr = getchar() != '\n');
sprintf(o_str,"]LAYCL1;<2=");
ibwrt(d15,o_str,strlen(o_str));
sprintf(o_str,"[C5=E0=GC");
ibwrt(d15,o_str,strlen(o_str));

sprintf(o_str,"\\C5=E0=GC");
ibwrt(d15,o_str,strlen(o_str));

}

/*  Zero the pressure transducer  */

sprintf(o_str,"F1R0S1T0");
 /* set up fluke on medium rate auto range */
ibwrt(d14,o_str,strlen(o_str));
```

```
ty=0;
printf("Zero the pressure transducer ");
while( ansr = getchar() != '\n');
while(ty == 0) {
sum1=0.0;
for (i = 1; i <= N1; i++) {
                ibrd(d14, mybuf, 13);
                volt= atof(mybuf);
                sum1   += volt;
}
sum1 = sum1/N1;
printf("The pressure transducer voltage is %e\n",sum1);
printf("Do you want to adjust the pressure transducer (y,n)? ");
for (i=0; (ansr = getchar()) != '\n' ; i++)
if (i == 0 && ansr == 'n')
ty=1;
}

offset = -sum1/SLOPE;  /* pressure transducer offset */

for (flg=0; flg == 0 ; ) {
flg++;
printf("Input the atmospheric pressure [in. Hg] ");
patm = gft();
if( patm < 28. || patm > 31.) {
printf("%f is not reasonable, try again.\n", patm);
flg = 0;
}
}
patm *= 25.4;

printf("Connect the pressure taps, tune the bridge, set to run");
while( ansr = getchar() != '\n');


/* Acquire the data from the IFA and the pressure transducer */

tatm = 0;   /* Initializes jet temperature */
ansr = 'y';
for ( i=0; ansr != 'n' ; i++) {
for (flg=0; flg == 0 ; ) {
flg++;
printf("Input the flow temperature [C] ");
tatmo = tatm;
```

```
tatm = gft();
if(tatm == -987654.)
tatm = tatmo;
if( tatm < 19. || tatm > 36.) {
printf("%f is out of range, try again.\n",tatm);
flg = 0;
}
}
sum = 0;
sum1 = 0;

printf("Set the flow rate of the jet.");
while( getchar() != '\n');

ibwrt(d15,"R",1);  /* send Norland signal to acquire data */

denair = patm/RAIR/(tatm+273.15)*MMHGPA;   /* density of air*/

n2 = NP;   /* number of pressure readings */

       for(j=0; j < n2; j++){   /* read the pressure transducer */
ibrd(d14, mybuf, 13);
volt = atof(mybuf);
sum1 += volt;
}

press = sum1/n2;

press = (press+offset)*SLOPE*2.54; /* pressure in cm H20 */
press = 2.*CMH2OPA/denair*press/ARAT;
vel = pow(press, 0.5);  /* velocity from Bernoulli equation */


ibwrt(d15,"_KCGA",5);
ibrd(d15,norbuf,8452);
norl(volt1,norbuf);

ibwrt(d15,"_KCGC",5);
ibrd(d15,norbuf,8452);
norl(volt2,norbuf);

hwv1=0.;
hwv2=0.;
for(k=0;k<4096;k++)  {
hwv1 += volt1[i];
hwv2 += volt2[i];
}
hwv1 /= 4096.;
hwv2 /= 4096.;

hwv1 = hwv1/gainifa + offifa; /* decondition hot-wire signal */
hwv1 = pow( 225./(250.-tatm) , 0.5) * hwv1; /* T corr. to H-W */

hwv2 = hwv2/gainifa + offifa; /* decondition hot-wire signal */
hwv2 = pow( 225./(250.-tatm) , 0.5) * hwv2; /* T corr. to H-W */

printf("%f\t%f\t%f\n",vel,hwv1,hwv2);
fprintf(fd,"%f\t%f\t%f\n",vel,hwv1,hwv2);
fflush(fd);

printf("Do you want to take more data (y,n)? ");
for (j=0; (ansr = getchar()) != '\n' ; j++)
if (j == 0 && ansr == 'n')
break;

}

fclose(fd);                 /*  This section puts the number of data */
fp = fopen("j1t","w");      /*  points at the top of the file        */
fprintf(fp,"%d\n",i);
fclose(fp);
strcpy(mybuf,"cat j1t ");
strcat(mybuf,name);
strcat(mybuf," >j2t");
system(mybuf);
strcpy(mybuf,"cp j2t ");
strcat(mybuf,name);
system(mybuf);
system("rm j2t j1t");

}

double gft()     /* gets a floating point number */

{
#define MAXLINE 1000

int len,i,flg1,flg2,flg3;
char line[MAXLINE];
double atof();
```

```
flg1 = 0;
while( flg1 == 0) {
flg2 = 0;
flg3 = 0;
len = getline(line,MAXLINE);
if( len == 0 )    /* bail out for blank line */
return(-987654.);
++flg1;
for (i=0; line[i] == ' ' || line[i] == '\t' ; i++)
;    /* get rid of leading blanks  */
if (line[i] == '+' || line[i] == '-' )
i++;
for ( ; i < len ; i++) {
if ( line[i]-'0' < 0 || line[i]-'0' >9) {
if( line[i] == '.' && flg2 == 0 )
flg2 = 1;
else if((line[i] == 'e' || line[i] == 'E') && flg3 == 0) {
flg2 = flg3 = 1;
if (line[i+1] =='+' || line[i+1] == '-')
i++;
}
else  {
flg1 = 0;
printf("Unacceptable input, try again: ");
}
}
}
}
return ( atof(line) );
}


getline(s,lim)  /* get line into s, return length */
char s[];
int lim;
{
int c,i;

i=0;
while(--lim > 0 && (c=getchar()) != EOF && c != '\n')
s[i++] = c;
s[i] = '\0';
return(i);
}
```

```
git()     /* gets an integer */

{
#define MAXLINE 1000

int len,i,flg1,flg2;
char line[MAXLINE];
int atoi();

flg1 = 0;
while( flg1 == 0) {
flg2 = 0;
len = getline(line,MAXLINE);
if( len == 0 )    /* bail out for blank line */
return(-987654);
++flg1;
for (i=0; line[i] == ' ' || line[i] == '\t' ; i++)
;    /* get rid of leading blanks  */
if (line[i] == '+' || line[i] == '-' )
i++;
for ( ; i < len ; i++) {
if ( line[i]-'0' < 0 || line[i]-'0' >9 || flg2 == 1 ) {
if( line[i] == '.' && flg2 == 0 )
flg2 = 1;
else  {
flg1 = 0;
printf("Unacceptable input, try again: ");
}
}
}
}
return ( atoi(line) );
}

norl(v,rdst)

double v[];
char rdst[];

{
int i,j,*pt,ifactor;
int a1,a2;
double factor1,factor2,factor,offset;
```

```
char o_str[40],digit[2];
char *ptrd;
int bit0,bit1,bit2,bit3,hexdigit,sign;


ptrd = rdst;


/* Evaluate factor and offset for Norland */

/* factor */

sscanf(ptrd,"%2x",&ifactor);
factor1 = pow(2.,((double)ifactor -128.));
for (i=0, factor2=0; i<6; i++) {
strncpy(digit,(ptrd+2+i),1);
digit[1]='\0';
sscanf(digit,"%x",&hexdigit);
bit0 = hexdigit & 1;
bit1 = hexdigit & 2;
bit2 = hexdigit & 4;
bit3 = hexdigit & 8;
if(i == 0) {
if(bit3)
sign = -1;
else
sign = 1;
bit3 = 1;
}
if(bit3) factor2 = factor2 + pow(2.,-(double)(i*4+1));
if(bit2) factor2 = factor2 + pow(2.,-(double)(i*4+2));
if(bit1) factor2 = factor2 + pow(2.,-(double)(i*4+3));
if(bit0) factor2 = factor2 + pow(2.,-(double)(i*4+4));
}
factor = (double) sign * factor1 * factor2;

/* offset */

sscanf((ptrd+8),"%2x",&ifactor);
factor1 = pow(2.,((double)ifactor -128.));
for (i=0, factor2=0; i<6; i++) {
strncpy(digit,(ptrd+10+i),1);
digit[1]='\0';
sscanf(digit,"%x",&hexdigit);
bit0 = hexdigit & 1;
bit1 = hexdigit & 2;
bit2 = hexdigit & 4;
bit3 = hexdigit & 8;
if(i == 0) {
if(bit3)
sign = -1;
else
sign = 1;
bit3 = 1;
}
if(bit3) factor2 = factor2 + pow(2.,-(double)(i*4+1));
if(bit2) factor2 = factor2 + pow(2.,-(double)(i*4+2));
if(bit1) factor2 = factor2 + pow(2.,-(double)(i*4+3));
if(bit0) factor2 = factor2 + pow(2.,-(double)(i*4+4));
}
offset = (double) sign * factor1 * factor2;
/* Find voltage for individual data points */

for(j=0,i=256;i<(2*NO+256);j++,i+=2) {
strncpy(digit,(ptrd+i),1);
digit[1]='\0';
a1=*digit;
if(a1 < 0 )
a1 +=256;
strncpy(digit,(ptrd+i+1),1);
digit[1]='\0';
a2=*digit;
if(a2 < 0 )
a2 +=256;
v[j]=(a2*256+a1-32768)*factor+offset;
}
}
```

```
/*
  Calibrates a cold wire compensation

  Written:  Ralph Volino       9/24/93


       Command Line:   cold

  This program is used to calibrate a cold wire on the 3 wire probe.
  The calibration is done using the calibration jet. Derivatives are
  calculated numerically.


*/

#include <stdio.h>
#include <sys/ugpib.h>
#include <fcntl.h>
#include <string.h>
#include <math.h>
#define  BUFSIZE        40
#define  MO      1000   /* number of readings for each data point */
#define  IFAGAINC       1
#define  IFAOFFC        0
#define  CCGAIN       25.494
#define  CCOFF        -6.231e-4
#define  EPSILON      0.108882
#define  V21          (1.0128e-3*9.03)
#define  FREQ         100000.


main(argc,argv)
int     argc;
char    *argv[];
{

        int     offifa,gainifa,d15,ty,n,i,n2,j,k;
int  flg,ansr,git();
        double  atof(),gft();
double  volt1[MO],volt2[MO];
        float   sum1,tatm,cft;
        char    mybuf[BUFSIZE],o_str[BUFSIZE];
char name[10];
FILE *fd;

printf("Input a name for the output file: ");
scanf("%s",name);
getchar();
fd = fopen(name,"w");  /* open file for output */

        printf("Input the offset of the signal conditioner on the IFA-100.");
printf("\n(Default=1): ");
flg=0;
while ( flg == 0) {
++flg;
offifa = git();
if ( offifa == -987654 )   /*  check for default flag */
offifa = 1;   /*  default = 1 */
if ( offifa > 9 || offifa <0 ) {
printf("This is an invalid input, try another ");
flg = 0;
}
}

        printf("Input the gain of the signal conditioner on the IFA-100 ");
printf("\n(Default=10): ");
flg=0;
while ( flg == 0) {
++flg;
gainifa = 0;
for (i=0; (ansr = getchar()) != '\n'; i++) {
ansr = ansr - '0';
if (((ansr < 1 || ansr > 9) && i == 0)
        || (ansr != 0 && i > 0 )) {
flg = 0;
printf("Invalid input, try again ");
}
gainifa = 10*gainifa+ansr;
}
if ( i == 0)
gainifa = 10;
}



/*  Open the Norland oscilloscope for reading the IFA-100 output  */
d15=ibfind("dev15");
```

```
        if(d15 < 0){
                fprintf(stderr,"Can't open /dev/dev15 for read\n");
                exit(1);
        }


/* Initialize and program the Norland */
printf("Do you want to initialize the Norland (y,n)? ");
for (i=0, ty=0; (ansr = getchar()) != '\n' ; i++)
if (i == 0 && ansr == 'y')
ty=1;
if(ty == 1) {
printf("Press Reset Key of the Norland");
while( ansr = getchar() != '\n');
sprintf(o_str,"YEM4096=L10;<6=");
ibwrt(d15,o_str,strlen(o_str));
sprintf(o_str,"[@C5=E<90:625=GC");
ibwrt(d15,o_str,strlen(o_str));
sprintf(o_str,"\\@C5=E<90:625=GC");
ibwrt(d15,o_str,strlen(o_str));
sprintf(o_str,"ZAACCCE80:46=");
ibwrt(d15,o_str,strlen(o_str));


}



for (flg=0; flg == 0 ; ) {
flg++;
printf("Input the flow temperature [C] ");
tatm = gft();
if( tatm < 19. || tatm > 36.) {
printf("%f is out of range, try again.\n",tatm);
flg = 0;
}
}
cft = pow(225./(250.-tatm),0.5);  /* correct for temperature */

printf("Take the data trace, press return when finished");
while( ansr = getchar() != '\n');

nort(&volt1,&d15,1);
nort(&volt2,&d15,2);
```

```
/*  Correct the voltages for gain, offset, etc. */
for(i=0; i< N0; i++) {
volt1[i]=volt1[i]/IFAGAINC+IFAOFFC;
volt1[i]=(volt1[i]-CCOFF)/CCGAIN;
volt2[i]=(volt2[i]/gainifa+offifa)*cft;
}


/*  Output the voltage traces and other data to a file for processing */

fprintf(fd,"%d  %g  %g  %g\n",N0,FREQ,V21,EPSILON);
for(i=0;i<N0;i++)
fprintf(fd,"%f\t%f\n",volt1[i],volt2[i]);
fclose(fd);

}

double gft()     /* gets a floating point number */

{
#define MAXLINE 1000

int len,i,flg1,flg2,flg3;
char line[MAXLINE];
double atof();

flg1 = 0;
while( flg1 == 0) {
flg2 = 0;
flg3 = 0;
len = getline(line,MAXLINE);
if( len == 0 )    /* bail out for blank line */
return(-987654.);
++flg1;
for (i=0; line[i] == ' ' || line[i] == '\t' ; i++)
;    /* get rid of leading blanks  */
if (line[i] == '+' || line[i] == '-' )
i++;
for ( ; i < len ; i++) {
if ( line[i]-'0' < 0 || line[i]-'0' >9) {
if( line[i] == '.' && flg2 == 0 )
flg2 = 1;
else if((line[i] == 'e' || line[i] == 'E') && flg3 == 0) {
flg2 = flg3 = 1;
```

```
if (line[i+1] =='+' || line[i+1] == '-')
i++;
}
else  {
flg1 = 0;
printf("Unacceptable input, try again: ");
}
}
}
}
return ( atof(line) );
}


getline(s,lim)  /* get line into s, return length */
char s[];
int lim;
{
int c,i;

i=0;
while(--lim > 0 && (c=getchar()) != EOF && c != '\n')
s[i++] = c;
s[i] = '\0';
return(i);
}


git()     /* gets an integer */

{
#define MAXLINE 1000

int len,i,flg1,flg2;
char line[MAXLINE];
int atoi();

flg1 = 0;
while( flg1 == 0) {
flg2 = 0;
len = getline(line,MAXLINE);
if( len == 0 )    /* bail out for blank line */
return(-987654);
++flg1;
for (i=0; line[i] == ' ' || line[i] == '\t' ; i++)
;    /* get rid of leading blanks  */
if (line[i] == '+' || line[i] == '-' )
i++;
for ( ; i < len ; i++) {
if ( line[i]-'0' < 0 || line[i]-'0' >9 || flg2 == 1 ) {
if( line[i] == '.' && flg2 == 0 )
flg2 = 1;
else  {
flg1 = 0;
printf("Unacceptable input, try again: ");
}
}
}
}
return ( atoi(line) );
}


nort(v,d15,ch)

double v[];
int *d15;
int ch;

{
int i,j,*pt,ifactor;
int a1,a2;
double factor1,factor2,factor,offset;
char o_str[40],rdst[8452],digit[2];
char *ptrd;
int bit0,bit1,bit2,bit3,hexdigit,sign;


ptrd = rdst;

/* Get data in from the Norland */

if(ch == 1)
sprintf(o_str,"_KCGA");
else
sprintf(o_str,"_KCGC");
ibwrt(*d15,o_str,strlen(o_str));
ibrd(*d15,rdst,8452);

/* Evaluate factor and offset for Norland */
```

```
/* factor */

sscanf(ptrd,"%2x",&ifactor);
factor1 = pow(2.,((double)ifactor -128.));
for (i=0, factor2=0; i<6; i++) {
strncpy(digit,(ptrd+2+i),1);
digit[1]='\0';
sscanf(digit,"%x",&hexdigit);
bit0 = hexdigit & 1;
bit1 = hexdigit & 2;
bit2 = hexdigit & 4;
bit3 = hexdigit & 8;
if(i == 0) {
if(bit3)
sign = -1;
else
sign = 1;
bit3 = 1;
}
if(bit3) factor2 = factor2 + pow(2.,-(double)(i*4+1));
if(bit2) factor2 = factor2 + pow(2.,-(double)(i*4+2));
if(bit1) factor2 = factor2 + pow(2.,-(double)(i*4+3));
if(bit0) factor2 = factor2 + pow(2.,-(double)(i*4+4));
}
factor = (double) sign * factor1 * factor2;

/* offset */

sscanf((ptrd+8),"%2x",&ifactor);
factor1 = pow(2.,((double)ifactor -128.));
for (i=0, factor2=0; i<6; i++) {
strncpy(digit,(ptrd+10+i),1);
digit[1]='\0';
sscanf(digit,"%x",&hexdigit);
bit0 = hexdigit & 1;
bit1 = hexdigit & 2;
bit2 = hexdigit & 4;
bit3 = hexdigit & 8;
if(i == 0) {
if(bit3)
sign = -1;
else
sign = 1;
bit3 = 1;
}
if(bit3) factor2 = factor2 + pow(2.,-(double)(i*4+1));
if(bit2) factor2 = factor2 + pow(2.,-(double)(i*4+2));
if(bit1) factor2 = factor2 + pow(2.,-(double)(i*4+3));
if(bit0) factor2 = factor2 + pow(2.,-(double)(i*4+4));
}
offset = (double) sign * factor1 * factor2;

/* Find voltage for individual data points */

for(j=0,i=256;i<(2*[illegible]0+256);j++,i+=2) {
strncpy(digit,(ptrd+i),1);
digit[1]='\0';
a1=*digit;
if(a1 < 0 )
a1 +=256;
strncpy(digit,(ptrd+i+1),1);
digit[1]='\0';
a2=*digit;
if(a2 < 0 )
a2 +=256;
v[j]=(a2*256+a1-32768)*factor+offset;
}
}
```

```
/*
  Calibrates a cold wire compensation

  Written:  Ralph Volino       9/26/93


        Command Line:   kcol

  This program is used to calibrate a cold wire on the 3 wire probe.
  The calibration is done using the calibration jet. Derivatives are
  calculated numerically.  Uses output of cold.c.  Calls a FORTRAN
  program kolf to do the calculations.


*/

#include <stdio.h>


main(argc,argv)
int     argc;
char    *argv[];

{
int ty=1;
int i,ansr;

while(ty == 1 ) {
system("kolf");
system("gnuplot");
system("rm temp1 temp2");
printf("Do you want to try another kcc (y,n) ? ");
for (i=0; (ansr = getchar()) != '\n' ; i++)
if(i==0 && ansr == 'n')
ty=0;
}
}
```

```
/*
  Acquires data using standard single wire probe

  Written:  Ralph Volino       10/08/93


        Command Line:   sacq

  This program is used to acquire data from a single wire probe
  using the Norland oscilloscopes.  Raw voltage data is acquired
  and saved for future processing. Statistics are also calculated.

*/

#include <stdio.h>
#include <sys/ugpib.h>
#include <fcntl.h>
#include <string.h>
#include <math.h>
#define  BUFSIZE        40
#define  MAXLINE      1000
#define  NOTEXIST       -1
#define  IFA1OFF      1.
#define  IFA1GAIN    10.
#define  THRESH     1.8
#define  PWR       0.435
#define  A1        -1.52481
#define  B1        3.25207
#define  TA        14.
#define  N0        4096


main(argc,argv)
int     argc;
char    *argv[];
{

        int     d15,d08,d03,d11,ty,n,i,j,k;
int     mon[3]={145,146,139};
int  flg,ansr,git(),tc,nt,sta,dv;
int     ndata,addpts,im;
int findwall(),trav(),norl();
        double  atof(),gft(),y[90],ym[90],temp();
double  yp,volt,vlt[3];
        double  patm,tinf,vz,loc,mov,yn;
double  mxt[10]={4.5,4.5,4.0,3.5,3.5,3.0,3.0,2.0,2.0,1.8};
double  visob2,volt1[N0];
double  vinf,y1,sum,u,uold,mstp,vstp;
double  maxtr,dist,pr,movo,movn;
        char    mybuf[BUFSIZE],o_str[BUFSIZE],readstr[400];
char    line[MAXLINE];
char name[20],tal[10],filn[20];
char    norbuf[8500],inam[20];
FILE *fd,*fp;

pr=1./PWR;

printf("Input a base name for the output files: ");
scanf("%s",name);
getchar();

fp = fopen(name,"w");  /*  store processed data */


/*  Open the Fluke multimeter for reading thermocouples */

d08=ibfind("dev8");
              if(d08 < 0){
                      fprintf(stderr,"Can't open /dev/dev08 for read\n");
                      exit(1);
              }

sprintf(o_str,"F1");  /* set up fluke to DC */
ibwrt(d08,o_str,strlen(o_str));


/*  Open the Scanner for reading thermocouples */

d03=ibfind("dev3");
              if(d03 < 0){
                      fprintf(stderr,"Can't open /dev/dev03 for read\n");
                      exit(1);
              }



/*  Open the Norland oscilloscope for reading the IFA-100 output  */
d15=ibfind("dev15");
              if(d15 < 0){
                      fprintf(stderr,"Can't open /dev/dev15 for read\n");
```

```
                exit(1);
        }


/*  Open the motor controller for moving the probe  */
d11=ibfind("dev11");
        if(d11 < 0){
           fprintf(stderr,"Can't open /dev/dev11 for read\n");
           exit(1);
        }



/* Initialize and program the Norland */
printf("Do you want to initialize the Norland (y,n)? ");
for (i=0, ty=0; (ansr = getchar()) != '\n' ; i++)
if (i == 0 && ansr == 'y')
ty=1;
if(ty == 1) {
printf("Press Reset Key of the Norlands");
while( ansr = getchar() != '\n');
sprintf(o_str,"]LAYCL:01=");
ibwrt(d15,o_str,strlen(o_str));

}


for (flg=0; flg == 0 ; ) {
flg++;
printf("Input the atmospheric pressure [in. Hg] ");
patm = gft();
if( patm < 28. || patm > 31.) {
printf("%f is not reasonable, try again.\n", patm);
flg = 0;
}
}
patm *= 25.4;


printf("Enter the TC number closest to the probe ");
tc = git();
printf("Enter the distance (cm) of the probe from this TC\n");
printf("+ for probe downstream of TC, - for upstream :");
dist = gft();
loc = (0.5 + tc)*2.54+dist;
```

```
vstp = 0.4/13.2*(5.+loc*0.15625);


printf("Enter the station number (1 to 10) :");
sta = git();
maxtr = mxt[sta-1];
if(sta>5)
mstp=0.25;
else
mstp=0.5;


/*  ********************************************** */

findwall(&y1,d11,d15);
y[0] = y1;


/*  Dump all the constants out to a file for data reduction */

fprintf(fp,"%g %g %g %g\n",A1,B1,THRESH,PWR);
fprintf(fp,"%g %g\n",IFA1OFF,IFA1GAIN);
fprintf(fp,"%g %g\n",patm,loc);
fprintf(fp,"%d\n",sta);
fflush(fp);



/*  Acquire the raw data from the Norlands and store it  */

ty=0;
for( k=0; ty==0; k++) {

ibwrt(d15,"R",1);

for(i=0;i<3;i++)
vlt[i]    = 0;
for(j=0;j<TA;j++) {
for(i=0;i<3;i++) {
sprintf(o_str,"%d,",mon[i]-1);
ibwrt(d03,o_str,strlen(o_str));
sleep(1);
ibrd(d08, mybuf, 13);
volt = atof(mybuf);
if(i == 0)
```

```
vz=volt;
if(i == 1 && ((vz-volt) > 3e-6 || (volt-vz) > 3e-6))
printf("Check Thermocouples\n");
vlt[i] +=volt;
}
}

visob2 = (vlt[0]+vlt[1])/2.;

vinf   = (vlt[2] - visob2)*1000./TA;
tinf   = temp(vinf);

fprintf(fp,"%f  %f\n",y1,tinf);  /* Store y location and tinf */
fflush(fp);


/*  Open the file for data storage  */

strcpy(filn,name);
ibwrt(d15,"_KCGA",5);
strcat(filn,"_R");
sprintf(o_str,"%d",k+1);
strcat(filn,o_str);
fd = fopen(filn,"w");

ibrd(d15,norbuf,8452);
fprintf(fd,"%s",norbuf);
fflush(fd);
fclose(fd);

norl(volt1,norbuf);
sum = 0;
for(j=0;j<N0;j++)
sum +=volt1[j];
sum /=N0;
sum = sum/IFA1GAIN + IFA1OFF;
u = pow(A1+B1*sum*sum,pr);
printf("%d %f %f\n",k,sum,u);

strcpy(filn,name);
ibwrt(d15,"_KCGC",5);
strcat(filn,"_I");
sprintf(o_str,"%d",k+1);
strcat(filn,o_str);
fd = fopen(filn,"w");

ibrd(d15,norbuf,8452);
fprintf(fd,"%s",norbuf);
fflush(fd);
fclose(fd);

/*   Move to the next y position   */

if(k < 5)
mov = 0.0005;
else  {
movn=vstp/(u-uold)*mov;
if (movn > mstp)
movn=mstp;
if(movn > 2.*mov)
movn=2.*mov;
movo = mov;
mov = movn;
if(mov < 0) {
if(k < 30)
mov = 0.0005;
else
mov = 2*movo;
}
if(mov > mstp)
mov = mstp;
}

uold = u;
if(y1+mov > maxtr)
ty = 1;
else
trav(&y1,mov,maxtr,d11);

}

fclose(fp);
fp = fopen("jnx","w");
fprintf(fp,"%d\n",k);
fclose(fp);
strcpy(o_str,"cat jnx ");
strcat(o_str,name);
strcat(o_str," >jnz");
system(o_str);
strcpy(o_str,"mv jnz ");
```

```
strcat(o_str,name);
system(o_str);
system("rm jnx");
}



double gft()     /* gets a floating point number */

{
#define MAXLINE 1000

int len,i,flg1,flg2,flg3;
char line[MAXLINE];
double atof();

flg1 = 0;
while( flg1 == 0) {
flg2 = 0;
flg3 = 0;
len = getline(line,MAXLINE);
if( len == 0 )    /* bail out for blank line */
return(-987654.);
++flg1;
for (i=0; line[i] == ' ' || line[i] == '\t' ; i++)
;    /* get rid of leading blanks  */
if (line[i] == '+' || line[i] == '-' )
i++;
for ( ; i < len ; i++) {
if ( line[i]-'0' < 0 || line[i]-'0' >9) {
if( line[i] == '.' && flg2 == 0 )
flg2 = 1;
else if((line[i] == 'e' || line[i] == 'E') && flg3 == 0) {
flg2 = flg3 = 1;
if (line[i+1] =='+' || line[i+1] == '-')
i++;
}
else  {
flg1 = 0;
printf("Unacceptable input, try again: ");
}
}
}
}
return ( atof(line) );
}


getline(s,lim)  /* get line into s, return length */
char s[];
int lim;
{
int c,i;

i=0;
while(--lim > 0 && (c=getchar()) != EOF && c != '\n')
s[i++] = c;
s[i] = '\0';
return(i);
}


double temp(v)

double v;

{
double a,b,c,d,t;

a = 0.0878053847;
b = -0.6018211152;
c = 1.113528335;
d = 16.14880077;

t=a*v*v*v*v+b*v*v*v+c*v*v+d*v;

return(t);
}


findwall(y1,d11,d15)

double *y1;
int  d11,d15;

{
char ansr,o_str[BUFSIZE],norbuf[8452];
double sum,sumo,slope,slopo,volt1[N0];
int ii,j,i,ty;
```

```
ibwrt(d11,"Y.D.\n",5);
ibwrt(d11,"Y.B2000.\n",9);
printf("Bring traverse up to wall at fast speed, NOT TOO CLOSE ");
while ( getchar() != '\n');
printf("Switch to AUTO ");
while ( getchar() != '\n');
ibwrt(d11,"Y.B320.\n",8);
printf("Switch to MANUAL and bring probe to wall ");
while ( getchar() != '\n');
printf("Switch to AUTO ");
while ( getchar() != '\n');

sprintf(o_str,"YCL:002=");
ibwrt(d15,o_str,strlen(o_str));

strt: sumo = -999.;
slopo = 999.;

for ( ii = 0; ii < 4; ) {
ibwrt(d15,"R",1);
sleep(11);
ibwrt(d15,"_KCGA",5);
ibrd(d15,norbuf,8452);
norl(volt1,norbuf);
for(sum=0,j=0;j<N0;j++)
sum +=volt1[j];
sum /= N0;
printf("Average Voltage = %g\n",sum);
slope = sum - sumo;
printf("New slope = %f  Old slope = %f\n",slope,slopo);

if(sum < -3.) {
printf("Wire Broken\n");
exit();
}

if(slope > 0.02)
ii +=1;
else
ii = 0;

ibwrt(d11,"Y.M2.G.\n",8);
sleep(1);
slopo = slope;
sumo = sum;
}

printf("Found the wall\n");
ibwrt(d11,"Y.M-11.G.\n",10);

printf("Do you want to find the wall again (y,n)? ");
for (i=0, ty=0; (ansr = getchar()) != '\n' ; i++)
if (i == 0 && ansr == 'y')
ty=1;
if(ty == 1) {
printf("Move in 5 steps manually, switch back to auto ");
while( ansr = getchar() != '\n');
goto strt;
}


*y1 = 0.0;
ibwrt(d11,"Y.B2000.\n",9);
ibwrt(d11,"Y.E.\n",5);

sprintf(o_str,"YCL:01=");
ibwrt(d15,o_str,strlen(o_str));

}

trav(y1,mov,maxtr,d11)

double *y1,mov,maxtr;
int   d11;

{
int stp;
char cst[10],mc[15];

stp = mov*2000;
mov = stp/2000.;
if(mov+*y1 > maxtr) {
mov = 0.;
stp = 0;
printf("Attempt to move beyond allowable travel\n");
}
sprintf(cst,"%d.",stp);
ibwrt(d11,"Y.D.\n",5);
strcpy(mc,"Y.M");
```

```
strcat(mc,cst);
strcat(mc,"G.\n");
ibwrt(d11,mc,strlen(mc));
ibwrt(d11,"Y.E.\n",5);
*y1 +=mov;
sleep(3);
}


norl(v,rdst)

double v[];
char rdst[];

{
int i,j,*pt,ifactor;
int a1,a2;
double factor1,factor2,factor,offset;
char o_str[40],digit[2];
char *ptrd;
int bit0,bit1,bit2,bit3,hexdigit,sign;


ptrd = rdst;


/* Evaluate factor and offset for Norland */

/* factor */

sscanf(ptrd,"%2x",&ifactor);
factor1 = pow(2.,((double)ifactor -128.));
for (i=0, factor2=0; i<6; i++) {
strncpy(digit,(ptrd+2+i),1);
digit[1]='\0';
sscanf(digit,"%x",&hexdigit);
bit0 = hexdigit & 1;
bit1 = hexdigit & 2;
bit2 = hexdigit & 4;
bit3 = hexdigit & 8;
if(i == 0) {
if(bit3)
sign = -1;
else
sign = 1;
bit3 = 1;
}
if(bit3) factor2 = factor2 + pow(2.,-(double)(i*4+1));
if(bit2) factor2 = factor2 + pow(2.,-(double)(i*4+2));
if(bit1) factor2 = factor2 + pow(2.,-(double)(i*4+3));
if(bit0) factor2 = factor2 + pow(2.,-(double)(i*4+4));
}
factor = (double) sign * factor1 * factor2;

/* offset */

sscanf((ptrd+8),"%2x",&ifactor);
factor1 = pow(2.,((double)ifactor -128.));
for (i=0, factor2=0; i<6; i++) {
strncpy(digit,(ptrd+10+i),1);
digit[1]='\0';
sscanf(digit,"%x",&hexdigit);
bit0 = hexdigit & 1;
bit1 = hexdigit & 2;
bit2 = hexdigit & 4;
bit3 = hexdigit & 8;
if(i == 0) {
if(bit3)
sign = -1;
else
sign = 1;
bit3 = 1;
}
if(bit3) factor2 = factor2 + pow(2.,-(double)(i*4+1));
if(bit2) factor2 = factor2 + pow(2.,-(double)(i*4+2));
if(bit1) factor2 = factor2 + pow(2.,-(double)(i*4+3));
if(bit0) factor2 = factor2 + pow(2.,-(double)(i*4+4));
}
offset = (double) sign * factor1 * factor2;
/* Find voltage for individual data points */

for(j=0,i=256;i<(2*N0+256);j++,i+=2) {
strncpy(digit,(ptrd+i),1);
digit[1]='\0';
a1=*digit;
if(a1 < 0 )
a1 +=256;
strncpy(digit,(ptrd+i+1),1);
digit[1]='\0';
a2=*digit;
```

```
if(a2 < 0 )
a2 +=256;
v[j]=(a2*256+a1-32768)*factor+offset;
}
}


git()     /* gets an integer */

{
#define MAXLINE 1000

int len,i,flg1,flg2;
char line[MAXLINE];
int atoi();

flg1 = 0;
while( flg1 == 0) {
flg2 = 0;
len = getline(line,MAXLINE);
if( len == 0 )    /* bail out for blank line */
return(-987654);
++flg1;
for (i=0; line[i] == ' ' || line[i] == '\t' ; i++)
;    /* get rid of leading blanks  */
if (line[i] == '+' || line[i] == '-' )
i++;
for ( ; i < len ; i++) {
if ( line[i]-'0' < 0 || line[i]-'0' >9 || flg2 == 1 ) {
if( line[i] == '.' && flg2 == 0 )
flg2 = 1;
else  {
flg1 = 0;
printf("Unacceptable input, try again: ");
}
}
}
}
return ( atoi(line) );
}
```

```
/*
  Reduces data from single wire probe

  Written:  Ralph Volino       10/08/93


        Command Line:   sred

  This program is used to reduce data from the single wire probe
  acquired using the Norland oscilloscopes.  Raw voltage data
  are converted to velocities.

*/

#include <stdio.h>
#include <fcntl.h>
#include <string.h>
#include <math.h>
#define  BUFSIZE        40
#define  MAXLINE      1000
#define  MAXBUF       9000
#define  NOTEXIST       -1
#define  NO           4096

main(argc,argv)
int     argc;
char    *argv[];
{

        int     n,i,j,k,m,l;
int  git(),sta;
int     ndata,norl();
int     nl,nt,nm;
int     flg[NO];
        double  atof(),gft(),y[90];
        double  patm,tinf[90],loc;
double  ifa1off,ifa1gain;
double  thresh,x;
double  pwr,a1,b1;
double  volt1[NO],volt2[NO];
double  s4m,s7m;
double  s4l,s7l;
double  s4t,s7t;
double  up[NO];
double  ctemp,base1;
double  gamma;
double  ui;
double  um,ul,ut;
double  uprm,uprl,uprt;
        char    mybuf[BUFSIZE],o_str[BUFSIZE],readstr[400];
char    line[MAXLINE];
char name[25],tal[20],filn[25];
char    norbuf[8500],inam[25];
char    s1[10],s2[10],s3[10],s4[10];
FILE *fd,*fp,*fm,*fl,*ft;


printf("Input the base name for the data files: ");
scanf("%s",name);
getchar();

fp = fopen(name,"r");  /*  get constants and y locations of data */

printf("Enter the name of the output file: ");
scanf("%s",inam);
getchar();

strcpy(o_str,inam);
strcat(o_str,"_m");
fm = fopen(o_str,"w");

strcpy(o_str,inam);
strcat(o_str,"_l");
fl = fopen(o_str,"w");

strcpy(o_str,inam);
strcat(o_str,"_t");
ft = fopen(o_str,"w");


/*  Get all the constants for data reduction */

fgets(line,MAXLINE,fp);
sscanf(line,"%d",&ndata);

fgets(line,MAXLINE,fp);
sscanf(line,"%s %s %s %s",s1,s2,s3,s4);
a1 = atof(s1);
b1 = atof(s2);
```

```
thresh = atof(s3);
pwr = atof(s4);

pwr = 1./pwr;

fgets(line,MAXLINE,fp);
sscanf(line,"%s %s",s1,s2);
ifa1off = atof(s1);
ifa1gain = atof(s2);

fgets(line,MAXLINE,fp);
sscanf(line,"%s %s",s1,s2);
patm = atof(s1);
x = atof(s2);

fgets(line,MAXLINE,fp);
sscanf(line,"%d",&sta);

fprintf(fm,"%f %f\n",patm,x);
fprintf(fm,"%d %d\n",sta,ndata);
fflush(ft);
fprintf(fl,"%f %f\n",patm,x);
fprintf(fl,"%d %d\n",sta,ndata);
fflush(fl);
fprintf(ft,"%f %f\n",patm,x);
fprintf(ft,"%d %d\n",sta,ndata);
fflush(ft);

/* Enter the data for the y locations to take measurements  */

for(i=0;i<ndata;i++) {
fgets(line,MAXLINE,fp);
sscanf(line,"%s %s",mybuf,s1);
y[i] = atof(mybuf);
tinf[i] = atof(s1);
}
fclose(fp);


/*  Process the raw data at each y location  */

for (k=0; k<ndata; k++) {

/*  Initialize various summation variables for flow statistics */

s4m=s7m=0.;
s4l=s7l=0.;
s4t=s7t=0.;
nl=nt=0;

ctemp = pow((225./(250.-tinf[k])),.5);

/*  Retrieve the stored raw data and convert to voltages */

for(j=0; j<2; j++) {
strcpy(filn,name);
if(j == 0)
strcpy(tal,"_R");
if(j == 1)
strcpy(tal,"_I");
strcat(filn,tal);
sprintf(o_str,"%d",k+1);
strcat(filn,o_str);
fd = fopen(filn,"r");

fgets(norbuf,MAXBUF,fd);
fclose(fd);
if(j == 0)
norl(volt1,norbuf);
if(j == 1)
norl(volt2,norbuf);
}

/*  Convert voltages to velocities  */

for(j=0; j<NO; j++) {

if(volt2[j]>thresh)
flg[j]=1;
else
flg[j]=2;

volt1[j] = volt1[j]/ifa1gain+ifa1off;

volt1[j] = volt1[j]*ctemp;

base1 = a1+b1*volt1[j]*volt1[j];
up[j] = pow(base1,pwr);

ui = up[j];
```

```
/* Sums for statistics */
if(flg[j] == 2) {
s4l += ui*ui;
s7l += ui;
nl +=1;
}
else {
s4t += ui*ui;
s7t += ui;
nt +=1;
}

}

s4m = s4l+s4t;
s7m = s7l+s7t;
nm = nl+nt;

gamma = (double) nt/(double) nm;

um = s7m/nm;

uprm = pow((s4m/(nm-1.)-s7m*s7m/nm/(nm-1.)),0.5);


if(nl == 0 || nl == 1)
     ul=uprl=0.;

else {
ul = s7l/nl;
uprl = pow((s4l/(nl-1.)-s7l*s7l/nl/(nl-1.)),0.5);
}

if(nt == 0 || nt == 1)
     ut=uprt=0.;

else {
ut = s7t/nt;
uprt = pow((s4t/(nt-1.)-s7t*s7t/nt/(nt-1.)),0.5);
}


fprintf(fm,"%d %f %f %f %f %f %d\n",k,y[k],um,tinf[k],uprm,gamma,nm);
fflush(fm);
fprintf(fl,"%d %f %f %f %f %f %d\n",k,y[k],ul,tinf[k],uprl,gamma,nl);
fflush(fl);
fprintf(ft,"%d %f %f %f %f %f %d\n",k,y[k],ut,tinf[k],uprt,gamma,nt);
fflush(ft);


}

fclose(fm);
fclose(fl);
fclose(ft);
}



double gft()     /* gets a floating point number */

{

int len,i,flg1,flg2,flg3;
char line[MAXLINE];
double atof();

flg1 = 0;
while( flg1 == 0) {
flg2 = 0;
flg3 = 0;
len = getline(line,MAXLINE);
if( len == 0 )    /* bail out for blank line */
return(-987654.);
++flg1;
for (i=0; line[i] == ' ' || line[i] == '\t' ; i++)
;    /* get rid of leading blanks  */
if (line[i] == '+' || line[i] == '-' )
i++;
for ( ; i < len ; i++) {
if ( line[i]-'0' < 0 || line[i]-'0' >9) {
if( line[i] == '.' && flg2 == 0 )
flg2 = 1;
else if((line[i] == 'e' || line[i] == 'E') && flg3 == 0) {
flg2 = flg3 = 1;
if (line[i+1] =='+' || line[i+1] == '-')
i++;
}
else  {
```

```
flg1 = 0;
printf("Unacceptable input, try again: ");
}
}
}
}
return ( atof(line) );
}


getline(s,lim)  /* get line into s, return length */
char s[];
int lim;
{
int c,i;

i=0;
while(--lim > 0 && (c=getchar()) != EOF && c != '\n')
s[i++] = c;
s[i] = '\0';
return(i);
}


git()     /* gets an integer */

{

int len,i,flg1,flg2;
char line[MAXLINE];
int atoi();

flg1 = 0;
while( flg1 == 0) {
flg2 = 0;
len = getline(line,MAXLINE);
if( len == 0 )    /* bail out for blank line */
return(-987654);
++flg1;
for (i=0; line[i] == ' ' || line[i] == '\t' ; i++)
;    /* get rid of leading blanks  */
if (line[i] == '+' || line[i] == '-' )
i++;
for ( ; i < len ; i++) {
if ( line[i]-'0' < 0 || line[i]-'0' >9 || flg2 == 1 ) {
if( line[i] == '.' && flg2 == 0 )
flg2 = 1;
else  {
flg1 = 0;
printf("Unacceptable input, try again: ");
}
}
}
}
return ( atoi(line) );
}



norl(v,rdst)

double v[];
char rdst[];

{
int i,j,*pt,ifactor;
int a1,a2;
double factor1,factor2,factor,offset;
char o_str[40],digit[2];
char *ptrd;
int bit0,bit1,bit2,bit3,hexdigit,sign;


ptrd = rdst;


/* Evaluate factor and offset for Norland */

/* factor */

sscanf(ptrd,"%2x",&ifactor);
factor1 = pow(2.,((double)ifactor -128.));
for (i=0, factor2=0; i<6; i++) {
strncpy(digit,(ptrd+2+i),1);
digit[1]='\0';
sscanf(digit,"%x",&hexdigit);
bit0 = hexdigit & 1;
bit1 = hexdigit & 2;
bit2 = hexdigit & 4;
bit3 = hexdigit & 8;
```

```
if(i == 0) {
if(bit3)
sign = -1;
else
sign = 1;
bit3 = 1;
}
if(bit3) factor2 = factor2 + pow(2.,-(double)(i*4+1));
if(bit2) factor2 = factor2 + pow(2.,-(double)(i*4+2));
if(bit1) factor2 = factor2 + pow(2.,-(double)(i*4+3));
if(bit0) factor2 = factor2 + pow(2.,-(double)(i*4+4));
}
factor = (double) sign * factor1 * factor2;

/* offset */

sscanf((ptrd+8),"%2x",&ifactor);
factor1 = pow(2.,((double)ifactor -128.));
for (i=0, factor2=0; i<6; i++) {
strncpy(digit,(ptrd+10+i),1);
digit[1]='\0';
sscanf(digit,"%x",&hexdigit);
bit0 = hexdigit & 1;
bit1 = hexdigit & 2;
bit2 = hexdigit & 4;
bit3 = hexdigit & 8;
if(i == 0) {
if(bit3)
sign = -1;
else
sign = 1;
bit3 = 1;
}
if(bit3) factor2 = factor2 + pow(2.,-(double)(i*4+1));
if(bit2) factor2 = factor2 + pow(2.,-(double)(i*4+2));
if(bit1) factor2 = factor2 + pow(2.,-(double)(i*4+3));
if(bit0) factor2 = factor2 + pow(2.,-(double)(i*4+4));
}
offset = (double) sign * factor1 * factor2;
/* Find voltage for individual data points */

for(j=0,i=256;i<(2*[illegible]0+256);j++,i+=2) {
strncpy(digit,(ptrd+i),1);
digit[1]='\0';
a1=*digit;
if(a1 < 0 )
a1 +=256;
strncpy(digit,(ptrd+i+1),1);
digit[1]='\0';
a2=*digit;
if(a2 < 0 )
a2 +=256;
v[j]=(a2*256+a1-32768)*factor+offset;
}
}
```

```
/*
  Acquires data using thermocouple probe

  Written:  Ralph Volino       4/03/94


        Command Line:   tacq

  This program is used to acquire data from a thermocouple probe
  using the Fluke multimeter.  Raw voltage data is acquired
  and saved for future processing. Statistics are also calculated.

*/

#include <stdio.h>
#include <sys/ugpib.h>
#include <fcntl.h>
#include <string.h>
#include <math.h>
#define  BUFSIZE        40
#define  MAXLINE      1000
#define  NOTEXIST       -1
#define  RPR        1.985
#define  AREA       0.8361
#define  KLEX       0.197
#define  DXLEX      0.001273556   /* 50.14/1000.*2.54e-2 */
#define  SIGMA      5.67e-8
#define  EMIS       0.85


main(argc,argv)
int     argc;
char    *argv[];
{

        int     d08,d03,d11,ty,n,i,j,k;
int     mon[7]={145,146,148,141,143,142,139};
int  flg,ansr,git(),tc,nt,sta,dv;
int     ndata;
int findwall(),trav();
        double  atof(),gft(),temp();
double  yp,volt,vlt[150];
        double  patm,tinf,vz,loc,mov,yn;
double  mxt[10]={4.1,4.1,3.7,3.1,2.5,2.2,2.0,1.9,1.3,1.2};
double  vinf,y1,tempr,told;
double  maxtr,dist,movo,movn;
        char    mybuf[BUFSIZE],o_str[BUFSIZE],readstr[400];
char    line[MAXLINE];
char name[20];
double  vpr,vhb,coef[5],xt[6],tt[6];
        double  ir,qb;
double  visob2,visob1,vlexb1,vlexb2,vlexb,tlexb,vinsb,tinsb;
double  kins,dxins,qlossb,qfrontb;
double  x1,x2,x3,x4,yt,xy,x2y,dn,nm1,nm2,nm3;
double  twall,tcorr,qrad,qnet,tinfe;
FILE *fp;


x1=x2=x3=x4=yt=xy=x2y=0.;


printf("Input a base name for the output file: ");
scanf("%s",name);
getchar();

fp = fopen(name,"w");  /*  store processed data */


/*  Open the Fluke multimeter for reading thermocouples */

d08=ibfind("dev8");
              if(d08 < 0){
                     fprintf(stderr,"Can't open /dev/dev08 for read\n");
                     exit(1);
              }

sprintf(o_str,"F1");  /* set up fluke to DC */
ibwrt(d08,o_str,strlen(o_str));


/*  Open the Scanner for reading thermocouples */

d03=ibfind("dev3");
              if(d03 < 0){
                     fprintf(stderr,"Can't open /dev/dev03 for read\n");
                     exit(1);
              }
```

```
/*  Open the motor controller for moving the probe  */
d11=ibfind("dev11");
               if(d11 < 0){
                fprintf(stderr,"Can't open /dev/dev11 for read\n");
                exit(1);
               }



for (flg=0; flg == 0 ; ) {
flg++;
printf("Input the atmospheric pressure [in. Hg] ");
patm = gft();
if( patm < 28. || patm > 31.) {
printf("%f is not reasonable, try again.\n", patm);
flg = 0;
}
}
patm *= 25.4;


printf("Enter the TC number closest to the probe ");
tc = git();
printf("Enter the distance (cm) of the probe from this TC\n");
printf("+ for probe downstream of TC, - for upstream :");
dist = gft();
loc = (0.5 + tc)*2.54+dist;

/*  Get the wall heat flux  */

printf("Set the fluke to front panel input");
while ( getchar() != '\n');

sprintf(o_str,"F2SO");  /* set up fluke to AC */
ibwrt(d08,o_str,strlen(o_str));

printf("Turn rotary switch to VPR");
while (getchar() != '\n');
for(j=0,vpr=0;j<4;j++) {
ibrd(d08, mybuf, 13);
volt = atof(mybuf);
vpr +=volt;
sleep(1);
}
vpr /= 4.;

printf("Turn rotary switch to VHB");
while (getchar() != '\n');
for(j=0,vhb=0;j<4;j++) {
ibrd(d08, mybuf, 13);
volt = atof(mybuf);
vhb +=volt;
sleep(1);
}
vhb /= 4.;
printf("%f %f\n",vpr,vhb);

printf("Set the fluke to rear panel input");
while (getchar() != '\n');

sprintf(o_str,"F1");  /* set up fluke to DC */
ibwrt(d08,o_str,strlen(o_str));
sleep(2);

ir = vpr/RPR;
qb = ir*vhb/AREA;
printf("Wall heat flux = %f\n",qb);

for(i=130;i<150;i++)
vlt[i]    = 0;
for(j=0;j<5;j++) {
for(i=0;i<7;i++) {
sprintf(o_str,"%d,",mon[i]-1);
ibwrt(d03,o_str,strlen(o_str));
sleep(1);
ibrd(d08, mybuf, 13);
volt = atof(mybuf);
if(i == 0)
vz=volt;
if(i == 1 && ((vz-volt) > 3e-6 || (volt-vz) > 3e-6))
printf("Check Thermocouples\n");
printf("Run %d , Thermocouple %d , %f volts\n",j+1,i+1,volt);
vlt[mon[i]] +=volt;
}
}
for(i=0;i<7;i++)
vlt[mon[i]] = vlt[mon[i]]*1000./5.;

visob2 = (vlt[145]+vlt[146])/2.;
visob1 = visob2 - vlt[148];
```

```
vlexb1 = vlt[141] - visob2;
vlexb2 = vlt[143] - visob2;
vlexb  = (vlexb1 + vlexb2)/2.;
tlexb  = temp(vlexb);
vinsb  = vlt[142] - visob2;
tinsb  = temp(vinsb);
kins   = 0.04;
dxins  = 4.*2.54/100.;
qlossb = kins*(tlexb-tinsb)/dxins;
qfrontb = qb-qlossb;

vinf   = vlt[139] - visob2;
tinf   = temp(vinf);

/*  Wall temperature */


for(i=0;i<5;i++)
vlt[i]    = 0;
for(k=0;k<5;k++) {
for(i=0,j=tc-2;j<tc+3;i++,j++) {
if(j == 1 || j == 3 || j == 7 || j == 14 || j == 44)
vlt[i] += 99.;
else {
sprintf(o_str,"%d,",j-1);
ibwrt(d03,o_str,strlen(o_str));
sleep(1);
ibrd(d08, mybuf, 13);
volt = atof(mybuf);
vlt[i] +=volt;
}
}
}
for(i=0,j=tc-2,k=0,nt=5;i<5;i++,j++,k++) {
if(vlt[i] == 5*99.) {
nt--;
k--;
}
else {
xt[k] = (.5+j)*2.54;
volt = vlt[i]*1000./5.-visob1;
tt[k] = temp(volt);
}
}
```

```
/*  curve fit the wall temperatures  */
for(i=0;i<nt;i++) {
x1 += xt[i];
x2 += (xt[i]*xt[i]);
x3 += (xt[i]*xt[i]*xt[i]);
x4 += (xt[i]*xt[i]*xt[i]*xt[i]);
yt += tt[i];
xy += (xt[i]*tt[i]);
x2y += (xt[i]*xt[i]*tt[i]);
}
dn = nt*(x2*x4-x3*x3)-x1*(x1*x4-x3*x2)+x2*(x1*x3-x2*x2);
nm1 = yt*(x2*x4-x3*x3)-x1*(xy*x4-x3*x2y)+x2*(xy*x3-x2*x2y);
nm2 = nt*(xy*x4-x3*x2y)-yt*(x1*x4-x3*x2)+x2*(x1*x2y-xy*x2);
nm3 = nt*(x2*x2y-xy*x3)-x1*(x2y*x1-x2*xy)+yt*(x1*x3-x2*x2);
coef[1] = nm1/dn;
coef[2] = nm2/dn;
coef[3] = nm3/dn;

twall = coef[1]+coef[2]*loc+coef[3]*loc*loc;
for(i=0;i<nt;i++)
printf(" %f\n",tt[i]);
printf("Twall = %f\n",twall);
tcorr = qfrontb*DXLEX/KLEX;
twall = twall - tcorr;
printf("Twall corrected = %f\n",twall);
qrad = SIGMA*EMIS*(pow(twall+273.15,4.)-pow(tinf+273.15,4.));
qnet = qfrontb - qrad;

printf("Enter the station number (1 to 10) :");
sta = git();
maxtr = mxt[sta-1];


/*  ******************************************** */

sprintf(o_str,"%d,",143);   /* set scanner for thermocouple probe  */
ibwrt(d03,o_str,strlen(o_str));

findwall(&y1,d11,d08);


/*  Dump all the constants out to a file for data reduction */

fprintf(fp,"%g %g %g %g %g\n",patm,twall,tinf,qnet,loc);
fprintf(fp,"%d\n",sta);
```

```
fflush(fp);



/*  Acquire the data and store it  */

ty=0;
for( k=0; ty==0; k++) {

for(j=0,volt=0.;j<5;j++) {
sleep(1);
ibrd(d08, mybuf, 13);
volt += atof(mybuf);
}
volt = volt/5.*1000.-visob2;

tempr   = temp(volt);

fprintf(fp,"%f  %f %f\n",y1,volt,tempr);  /* Store data */
fflush(fp);


/*   Move to the next y position   */

if(k < 20)
mov = 0.001;
else  {
movn=0.10/(told-tempr)*mov;
if (movn > 0.25)
movn=0.25;
if(movn > 2.*mov)
movn=2.*mov;
movo = mov;
mov = movn;
if(mov < 0) {
if(k < 30)
mov = movo/2.;
else
mov = 2*movo;
}
if(mov<.0005)
mov = .0005;
if(mov > 0.25)
mov = 0.25;
}

told = tempr;
if(y1+mov > maxtr)
ty = 1;
else
trav(&y1,mov,maxtr,d11);

}

for(i=130;i<150;i++)
vlt[i]    = 0;
for(j=0;j<5;j++) {
for(i=0;i<7;i++) {
sprintf(o_str,"%d,",mon[i]-1);
ibwrt(d03,o_str,strlen(o_str));
sleep(1);
ibrd(d08, mybuf, 13);
volt = atof(mybuf);
if(i == 0)
vz=volt;
if(i == 1 && ((vz-volt) > 3e-6 || (volt-vz) > 3e-6))
printf("Check Thermocouples\n");
printf("Run %d , Thermocouple %d , %f volts\n",j+1,i+1,volt);
vlt[mon[i]] +=volt;
}
}
for(i=0;i<7;i++)
vlt[mon[i]] = vlt[mon[i]]*1000./5.;

visob2 = (vlt[145]+vlt[146])/2.;
vinf   = vlt[139] - visob2;
tinfe   = temp(vinf);
fprintf(fp,"%f\n",tinfe);
fflush(fp);

fclose(fp);
fp = fopen("jnx","w");
fprintf(fp,"%d\n",k);
close(fp);
strcpy(o_str,"cat jnx ");
strcat(o_str,name);
strcat(o_str," >jnz");
system(o_str);
strcpy(o_str,"mv jnz ");
strcat(o_str,name);
```

```
system(o_str);
system("rm jnx");
}



double gft()     /* gets a floating point number */

{
#define MAXLINE 1000

int len,i,flg1,flg2,flg3;
char line[MAXLINE];
double atof();

flg1 = 0;
while( flg1 == 0) {
flg2 = 0;
flg3 = 0;
len = getline(line,MAXLINE);
if( len == 0 )    /* bail out for blank line */
return(-987654.);
++flg1;
for (i=0; line[i] == ' ' || line[i] == '\t' ; i++)
;    /* get rid of leading blanks  */
if (line[i] == '+' || line[i] == '-' )
i++;
for ( ; i < len ; i++) {
if ( line[i]-'0' < 0 || line[i]-'0' >9) {
if( line[i] == '.' && flg2 == 0 )
flg2 = 1;
else if((line[i] == 'e' || line[i] == 'E') && flg3 == 0) {
flg2 = flg3 = 1;
if (line[i+1] =='+' || line[i+1] == '-')
i++;
}
else  {
flg1 = 0;
printf("Unacceptable input, try again: ");
}
}
}
}
return ( atof(line) );
}
```

```
getline(s,lim)  /* get line into s, return length */
char s[];
int lim;
{
int c,i;

i=0;
while(--lim > 0 && (c=getchar()) != EOF && c != '\n')
s[i++] = c;
s[i] = '\0';
return(i);
}


double temp(v)

double v;

{
double a,b,c,d,t;

a = 0.0878053847;
b = -0.6018211152;
c = 1.113528335;
d = 16.14880077;

t=a*v*v*v*v+b*v*v*v+c*v*v+d*v;

return(t);
}


findwall(y1,d11,d08)

double *y1;
int  d11,d08;

{
char ansr,o_str[BUFSIZE],mybuf[BUFSIZE];
double sum,sumo,slope,slopo,volt;
int ii,j,i,ty;

ibwrt(d11,"Y.D.\n",5);
```

```
ibwrt(d11,"Y.B2000.\n",9);
printf("Bring traverse up to wall at fast speed, NOT TOO CLOSE ");
while ( getchar() != '\n');
printf("Switch to AUTO ");
while ( getchar() != '\n');
ibwrt(d11,"Y.B320.\n",8);
printf("Switch to MANUAL and bring probe to wall ");
while ( getchar() != '\n');
printf("Switch to AUTO ");
while ( getchar() != '\n');

strt: sumo = -999.;
slopo = 999.;

for ( ii = 0; ii < 4; ) {
for(sum=0,j=0;j<5;j++) {
ibrd(d08, mybuf, 13);
volt = atof(mybuf);
sum +=volt;
}
sum =sum*1000./5.;
printf("Average Voltage = %g\n",sum);
slope = sum - sumo;
printf("New slope = %f  Old slope = %f\n",slope,slopo);

if(sum < -3.) {
printf("Wire Broken\n");
exit();
}

if(slope < -0.002)
ii +=1;
else
ii = 0;

ibwrt(d11,"Y.M2.G.\n",8);
sleep(1);
slopo = slope;
sumo = sum;

}

printf("Found the wall\n");
ibwrt(d11,"Y.M-31.G.\n",10);
printf("Do you want to find the wall again (y,n)? ");
for (i=0, ty=0; (ansr = getchar()) != '\n' ; i++)
if (i == 0 && ansr == 'y')
ty=1;
if(ty == 1) {
printf("Move in 5 steps manually, switch back to auto ");
while( ansr = getchar() != '\n');
goto strt;
}


*y1 = -0.008;
ibwrt(d11,"Y.B2000.\n",9);
ibwrt(d11,"Y.E.\n",5);

}

trav(y1,mov,maxtr,d11)

double *y1,mov,maxtr;
int   d11;

{
int stp;
char cst[10],mc[15];

stp = mov*2000;
mov = stp/2000.;
if(mov+*y1 > maxtr) {
mov = 0.;
stp = 0;
printf("Attempt to move beyond allowable travel\n");
}
sprintf(cst,"%d.",stp);
ibwrt(d11,"Y.D.\n",5);
strcpy(mc,"Y.M");
strcat(mc,cst);
strcat(mc,"G.\n");
ibwrt(d11,mc,strlen(mc));
ibwrt(d11,"Y.E.\n",5);
*y1 +=mov;
sleep(3);
}
```

```
git()     /* gets an integer */

{
#define MAXLINE 1000

int len,i,flg1,flg2;
char line[MAXLINE];
int atoi();

flg1 = 0;
while( flg1 == 0) {
flg2 = 0;
len = getline(line,MAXLINE);
if( len == 0 )    /* bail out for blank line */
return(-987654);
++flg1;
for (i=0; line[i] == ' ' || line[i] == '\t' ; i++)
;    /* get rid of leading blanks  */
if (line[i] == '+' || line[i] == '-' )
i++;
for ( ; i < len ; i++) {
if ( line[i]-'0' < 0 || line[i]-'0' >9 || flg2 == 1 ) {
if( line[i] == '.' && flg2 == 0 )
flg2 = 1;
else  {
flg1 = 0;
printf("Unacceptable input, try again: ");
}
}
}
}
return ( atoi(line) );
}
```

```
/*
  Acquires data using standard cross wire probe

  Written:  Ralph Volino       10/04/93


        Command Line:   xacq

  This program is used to acquire data from a cross wire probe
  using the Norland oscilloscopes.  Raw voltage data is acquired
  and saved for future processing.

*/

#include <stdio.h>
#include <sys/ugpib.h>
#include <fcntl.h>
#include <string.h>
#include <math.h>
#define  BUFSIZE        40
#define  MAXLINE      1000
#define  NOTEXIST       -1
#define  IFA1OFF       1.
#define  IFA2OFF       1.
#define  IFA1GAIN     10.
#define  IFA2GAIN     10.
#define  THRESH      1.8
#define  THETA      0.785398163
#define  PWR        0.435
#define  A1         -1.56300
#define  B1         3.26381
#define  A2         -1.56938
#define  B2         3.15397
#define  TA         14.


main(argc,argv)
int     argc;
char    *argv[];
{

        int     d16,d15,d06,d08,d03,d11,ty,n,i,j,k;
int     mon[3]={145,146,139};
int  flg,ansr,git(),tc,nt,sta,dv;
int     ndata,addpts,im;

int findwall(),trav();
        double  atof(),gft(),y[90],ym[90],temp();
double  yp,volt,vlt[3];
        double  patm,tinf,vz,loc,mov,yn;
double  mxt[10]={4.5,4.5,4.0,3.5,3.5,3.0,3.0,2.0,2.0,1.8};
double  visob2;
double  vinf,y1;
double  maxtr,dist;
        char    mybuf[BUFSIZE],o_str[BUFSIZE],readstr[400];
char    line[MAXLINE];
char name[20],tal[20],filn[20];
char    norbuf[8500],inam[20];
FILE *fd,*fp;



printf("Input a base name for the output files: ");
scanf("%s",name);
getchar();

fp = fopen(name,"w");  /*  store constants and y locations of data */

printf("Enter the name of the y location file: ");
scanf("%s",inam);
getchar();


/*  Open the Fluke multimeter for reading thermocouples */

d08=ibfind("dev8");
              if(d08 < 0){
                      fprintf(stderr,"Can't open /dev/dev08 for read\n");
                      exit(1);
              }

sprintf(o_str,"F1");  /* set up fluke to DC */
ibwrt(d08,o_str,strlen(o_str));


/*  Open the Scanner for reading thermocouples */

d03=ibfind("dev3");
              if(d03 < 0){
              fprintf(stderr,"Can't open /dev/dev03 for read\n");
              exit(1);
```

```
            }

/*  Open the programmable power supply for triggering the Norland */

d06=ibfind("dev6");
            if(d06 < 0){
            fprintf(stderr,"Can't open /dev/dev06 for read\n");
            exit(1);
            }

/*  Open the Norland oscilloscope for reading the IFA-100 output  */
d15=ibfind("dev15");
            if(d15 < 0){
            fprintf(stderr,"Can't open /dev/dev15 for read\n");
            exit(1);
            }

/*  Open the second Norland for reading the IFA-100 output  */
d16=ibfind("dev16");
            if(d16 < 0){
            fprintf(stderr,"Can't open /dev/dev16 for read\n");
            exit(1);
}

/*  Open the motor controller for moving the probe  */
d11=ibfind("dev11");
            if(d11 < 0){
            fprintf(stderr,"Can't open /dev/dev11 for read\n");
            exit(1);
            }

/* Initialize and program the Norland for avrgng input voltages */
printf("Do you want to initialize the Norland (y,n)? ");
for (i=0, ty=0; (ansr = getchar()) != '\n' ; i++)
if (i == 0 && ansr == 'y')
ty=1;
if(ty == 1) {
printf("Press Reset Key of the Norlands");
while( ansr = getchar() != '\n');
sprintf(o_str,"]LAYEL:01=ZME");
ibwrt(d15,o_str,strlen(o_str));
sprintf(o_str,"]LAYAL0=");
ibwrt(d16,o_str,strlen(o_str));
}

for (flg=0; flg == 0 ; ) {
flg++;
printf("Input the atmospheric pressure [in. Hg] ");
patm = gft();
if( patm < 28. || patm > 31.) {
printf("%f is not reasonable, try again.\n", patm);
flg = 0;
}
}
patm *= 25.4;

printf("Enter the TC number closest to the probe ");
tc = git();
printf("Enter the distance (cm) of the probe from this TC\n");
printf("+ for probe downstream of TC, - for upstream :");
dist = gft();
loc = (0.5 + tc)*2.54+dist;

printf("Enter the station number (1 to 10) :");
sta = git();
maxtr = mxt[sta-1];

/* Enter the data for the y locations to take measurements  */

fd = fopen(inam,"r");
fgets(line,MAXLINE,fd);
sscanf(line,"%d",&ndata);
for(i=0;i<ndata;i++) {
fgets(line,MAXLINE,fd);
sscanf(line,"%s",mybuf);
ym[i] = atof(mybuf);
}
close(fd);

/*  ********************************************** */
```

```
findwall(&y1,d11);
y[0] = y1;
for(i=0;i<ndata;i++) {
if(ym[i] > y[0]) {
im = i;
break;
}
}
addpts =  (maxtr - ym[ndata-1])*2+2;
ndata = ndata-im+addpts-1;



/*  Dump all the constants out to a file for data reduction */

fprintf(fp,"%g %g %g %g %g %g %g\n",A1,A2,B1,B2,THRESH,PWR,THETA);
fprintf(fp,"%g %g %g %g\n",IFA1OFF,IFA2OFF,IFA1GAIN,IFA2GAIN);
fprintf(fp,"%g %g\n",patm,loc);
fprintf(fp,"%d %d\n",sta,ndata);
fflush(fp);



/*  Acquire the raw data from the Norlands and store it  */

for( k=0; k<ndata ; k++) {

ibwrt(d06,"2900",4);
ibwrt(d16,"R",1);
ibwrt(d15,"R",1);
sleep(1);
ibwrt(d06,"2000",4);

for(i=0;i<3;i++)
vlt[i]    = 0;
for(j=0;j<TA;j++) {
for(i=0;i<3;i++) {
sprintf(o_str,"%d,",mon[i]-1);
ibwrt(d03,o_str,strlen(o_str));
sleep(1);
ibrd(d08, mybuf, 13);
volt = atof(mybuf);
if(i == 0)
vz=volt;
if(i == 1 && ((vz-volt) > 3e-6 || (volt-vz) > 3e-6))
printf("Check Thermocouples\n");
vlt[i] +=volt;
}
}

visob2 = (vlt[0]+vlt[1])/2.;

vinf   = (vlt[2] - visob2)*1000./TA;
tinf   = temp(vinf);

fprintf(fp,"%f  %f\n",y1,tinf);  /* Store y location and tinf */
printf("%f  %f\n",y1,tinf);  /* Print y location and tinf */
fflush(fp);

ibwrt(d16,"S",1);

/*  Open the files for data storage  */

for(j=0; j<3; j++) {
strcpy(filn,name);
if(j == 0) {
strcpy(tal,"_A");
ibwrt(d15,"_KCGA",5);
dv=d15;
}
if(j == 1) {
strcpy(tal,"_B");
ibwrt(d15,"_KCGC",5);
dv=d15;
}
if(j == 2) {
strcpy(tal,"_C");
ibwrt(d16,"_KCGA",5);
dv=d16;
}
strcat(filn,tal);
sprintf(o_str,"%d",k+1);
strcat(filn,o_str);
fd = fopen(filn,"w");

ibrd(dv,norbuf,8452);
fprintf(fd,"%s",norbuf);
fflush(fd);
fclose(fd);
}
```

```
/*   Move to the next y position   */


if(k != ndata-1) {
if( k > ndata-addpts)
mov = 0.5;
else {
yn = ym[im+k];
mov = yn-y1;
}
trav(&y1,mov,maxtr,d11);
}

}
}



double gft()     /* gets a floating point number */

{
#define MAXLINE 1000

int len,i,flg1,flg2,flg3;
char line[MAXLINE];
double atof();

flg1 = 0;
while( flg1 == 0) {
flg2 = 0;
flg3 = 0;
len = getline(line,MAXLINE);
if( len == 0 )    /* bail out for blank line */
return(-987654.);
++flg1;
for (i=0; line[i] == ' ' || line[i] == '\t' ; i++)
;    /* get rid of leading blanks  */
if (line[i] == '+' || line[i] == '-' )
i++;
for ( ; i < len ; i++) {
if ( line[i]-'0' < 0 || line[i]-'0' >9) {
if( line[i] == '.' && flg2 == 0 )
flg2 = 1;
else if((line[i] == 'e' || line[i] == 'E') && flg3 == 0) {
flg2 = flg3 = 1;
if (line[i+1] =='+' || line[i+1] == '-')
i++;
}
else  {
flg1 = 0;
printf("Unacceptable input, try again: ");
}
}
}
}
return ( atof(line) );
}


getline(s,lim)  /* get line into s, return length */
char s[];
int lim;
{
int c,i;

i=0;
while(--lim > 0 && (c=getchar()) != EOF && c != '\n')
s[i++] = c;
s[i] = '\0';
return(i);
}


git()     /* gets an integer */

{
#define MAXLINE 1000

int len,i,flg1,flg2;
char line[MAXLINE];
int atoi();

flg1 = 0;
while( flg1 == 0) {
flg2 = 0;
len = getline(line,MAXLINE);
if( len == 0 )    /* bail out for blank line */
return(-987654);
++flg1;
```

```
for (i=0; line[i] == ' ' || line[i] == '\t' ; i++)
;    /* get rid of leading blanks  */
if (line[i] == '+' || line[i] == '-' )
i++;
for ( ; i < len ; i++) {
if ( line[i]-'0' < 0 || line[i]-'0' >9 || flg2 == 1 ) {
if( line[i] == '.' && flg2 == 0 )
flg2 = 1;
else  {
flg1 = 0;
printf("Unacceptable input, try again: ");
}
}
}
}
return ( atoi(line) );
}


double temp(v)

double v;

{
double a,b,c,d,t;

a = 0.0878053847;
b = -0.6018211152;
c = 1.113528335;
d = 16.14880077;

t=a*v*v*v*v+b*v*v*v+c*v*v+d*v;

return(t);
}


findwall(y1,d11)

double *y1;
int  d11;

{
ibwrt(d11,"Y.D.\n",5);
ibwrt(d11,"Y.B2000.\n",9);
printf("Bring traverse up to wall at fast speed, NOT TOO CLOSE ");
while ( getchar() != '\n');
printf("Switch to AUTO ");
while ( getchar() != '\n');
ibwrt(d11,"Y.B320.\n",8);
printf("Switch to MANUAL and bring probe to wall ");
while ( getchar() != '\n');
printf("Switch to AUTO ");
while ( getchar() != '\n');
*y1 = 0.06;
ibwrt(d11,"Y.B2000.\n",9);
ibwrt(d11,"Y.E.\n",5);
}

trav(y1,mov,maxtr,d11)

double *y1,mov,maxtr;
int   d11;

{
int stp;
char cst[10],mc[15];

stp = mov*2000;
mov = stp/2000.;
if(mov+*y1 > maxtr) {
mov = 0.;
stp = 0;
printf("Attempt to move beyond allowable travel\n");
}
sprintf(cst,"%d.",stp);
ibwrt(d11,"Y.D.\n",5);
strcpy(mc,"Y.M");
strcat(mc,cst);
strcat(mc,"G.\n");
ibwrt(d11,mc,strlen(mc));
ibwrt(d11,"Y.E.\n",5);
*y1 +=mov;
sleep(3);
}
```

```
/*
  Reduces data from cross wire probe

  Written:  Ralph Volino       10/04/93


        Command Line:   xred

  This program is used to reduce data from the cross wire probe
  acquired using the Norland oscilloscopes.  Raw voltage data
  are converted to velocities.

*/

#include <stdio.h>
#include <fcntl.h>
#include <string.h>
#include <math.h>
#define  BUFSIZE        40
#define  MAXLINE      1000
#define  NOTEXIST       -1
#define  NO           4096

main(argc,argv)
int     argc;
char    *argv[];
{

        int     n,i,j,k,m,l;
int  git(),sta;
int     ndata,norl();
int     nl,nt,nm;
int     flg[NO];
        double  atof(),gft(),y[90];
        double  patm,tinf[90],loc;
double  ifa1off,ifa2off,ifa1gain,ifa2gain;
double  thresh,x;
double  theta,pwr,a1,a2,b1,b2;
double  volt1[NO],volt2[NO],volt3[NO];
double  ld,kt,cfuv,cfv;
double  s1m,s4m,s5m,s7m,s8m,s10m;
double  s1l,s4l,s5l,s7l,s8l,s10l;
double  s1t,s4t,s5t,s7t,s8t,s10t;
double  up[NO],vp[NO];
double  ctemp,base1,base2,uef1,uef2;
double  gamma,c2the;
double  ui,vi;
double  um,vm,upvpm,upvp2m;
double  ul,vl,upvpl,upvp2l;
double  ut,vt,upvpt,upvp2t;
double  uprm,vprm,uprl,vprl,uprt,vprt;
        char    mybuf[BUFSIZE],o_str[BUFSIZE],readstr[400];
char    line[MAXLINE];
char name[20],tal[10],filn[20];
char    norbuf[8500],inam[20];
char    s1[10],s2[10],s3[10],s4[10],s5[10],s6[10],s7[10];
FILE *fd,*fp,*fm,*fl,*ft;



printf("Input the base name for the data files: ");
scanf("%s",name);
getchar();

fp = fopen(name,"r");  /*  get constants and y locations of data */

printf("Enter the name of the output file: ");
scanf("%s",inam);
getchar();

strcpy(o_str,inam);
strcat(o_str,"_m");
fm = fopen(o_str,"w");

strcpy(o_str,inam);
strcat(o_str,"_l");
fl = fopen(o_str,"w");

strcpy(o_str,inam);
strcat(o_str,"_t");
ft = fopen(o_str,"w");


/*  Get all the constants for data reduction */

fgets(line,MAXLINE,fp);
sscanf(line,"%s %s %s %s %s %s %s",s1,s2,s3,s4,s5,s6,s7);
a1 = atof(s1);
a2 = atof(s2);
b1 = atof(s3);
```

```
b2 = atof(s4);
thresh = atof(s5);
pwr = atof(s6);
theta = atof(s7);

pwr = 1./pwr;
c2the = 2.*cos(theta);

fgets(line,MAXLINE,fp);
sscanf(line,"%s %s %s %s",s1,s2,s3,s4);
ifa1off = atof(s1);
ifa2off = atof(s2);
ifa1gain = atof(s3);
ifa2gain = atof(s4);

fgets(line,MAXLINE,fp);
sscanf(line,"%s",s1,s2);
patm = atof(s1);
x = atof(s2);

fgets(line,MAXLINE,fp);
sscanf(line,"%d %d",&sta,&ndata);

fprintf(fm,"%f %f\n",patm,x);
fprintf(fm,"%d %d\n",sta,ndata);
fflush(ft);
fprintf(fl,"%f %f\n",patm,x);
fprintf(fl,"%d %d\n",sta,ndata);
fflush(fl);
fprintf(ft,"%f %f\n",patm,x);
fprintf(ft,"%d %d\n",sta,ndata);
fflush(ft);

/* Enter the data for the y locations to take measurements  */

for(i=0;i<ndata;i++) {
fgets(line,MAXLINE,fp);
sscanf(line,"%s %s",mybuf,s1);
y[i] = atof(mybuf);
tinf[i] = atof(s1);
}
close(fp);


/*  Champagne correction  */

ld = 320.;
kt = -5.e-4*ld+.3;
cfuv = (1.+kt*kt)/(1.-kt*kt);
cfv  = (1.+kt*kt)/(1.-3.*kt*kt+4.*pow(kt,4.));

/*  Process the raw data at each y location  */

for (k=0; k<ndata; k++) {

/*  Initialize various summation variables for flow statistics */

s1m=s4m=s5m=s7m=s8m=s10m=0.;
s1l=s4l=s5l=s7l=s8l=s10l=0.;
s1t=s4t=s5t=s7t=s8t=s10t=0.;
nl=nt=0;

ctemp = pow((225./(250.-tinf[k])),.5);

/*  Retrieve the stored raw data and convert to voltages */

for(j=0; j<3; j++) {
strcpy(filn,name);
if(j == 0)
strcpy(tal,"_A");
if(j == 1)
strcpy(tal,"_B");
if(j == 2)
strcpy(tal,"_C");
strcat(filn,tal);
sprintf(o_str,"%d",k+1);
strcat(filn,o_str);
fd = fopen(filn,"r");

/* fscanf(fd,"%s",norbuf);  */
fgets(norbuf,8452,fd);
fclose(fd);
if(j == 0)
norl(volt1,norbuf);
if(j == 1)
norl(volt2,norbuf);
if(j == 2)
norl(volt3,norbuf);
}
```

```
/*  Convert voltages to velocities  */

for(j=0; j<NO; j++) {

if(volt3[j]>thresh)
flg[j]=1;
else
flg[j]=2;

volt1[j] = volt1[j]/ifa1gain+ifa1off;
volt2[j] = volt2[j]/ifa2gain+ifa2off;

volt1[j] *=ctemp;
volt2[j] *=ctemp;

base1 = a1+b1*volt1[j]*volt1[j];
base2 = a2+b2*volt2[j]*volt2[j];
uef1 = pow(base1,pwr);
uef2 = pow(base2,pwr);
up[j] = (uef1+uef2)/c2the;
vp[j] = (uef1-uef2)/c2the;

ui = up[j];
vi = vp[j];

/* Sums for statistics */
if(flg[j] == 2) {
s1l += ui*vi;
s4l += ui*ui;
s5l += vi*vi;
s7l += ui;
s8l += vi;
s10l += ui*vi*vi;
nl +=1;
}
else {
s1t += ui*vi;
s4t += ui*ui;
s5t += vi*vi;
s7t += ui;
s8t += vi;
s10t += ui*vi*vi;
nt +=1;
}
```



```
}

s1m = s1l+s1t;
s4m = s4l+s4t;
s5m = s5l+s5t;
s7m = s7l+s7t;
s8m = s8l+s8t;
s10m = s10l+s10t;
nm = nl+nt;

gamma = (double) nt/ (double) nm;

um = s7m/nm;
vm = s8m/nm;

uprm = pow((s4m/(nm-1.)-s7m*s7m/nm/(nm-1.)),0.5);
vprm = pow((s5m/(nm-1.)-s8m*s8m/nm/(nm-1.))*cfv,0.5);

upvpm = (s1m/(nm-1.)-s7m*s8m/nm/(nm-1.))*cfuv;

upvp2m = (s10m/(nm-1.)-2.*s8m*s1m/nm/(nm-1.)
-s7m*s5m/nm/(nm-1.)+2.*s7m*s8m*s8m/nm/nm/(nm-1.))*cfv;


if(nl == 0 || nl == 1)
     ul=vl=uprl=vprl=upvpl=upvp2l=0.;

else {
ul = s7l/nl;
vl = s8l/nl;

uprl = pow((s4l/(nl-1.)-s7l*s7l/nl/(nl-1.)),0.5);
vprl = pow((s5l/(nl-1.)-s8l*s8l/nl/(nl-1.))*cfv,0.5);

upvpl = (s1l/(nl-1.)-s7l*s8l/nl/(nl-1.))*cfuv;

upvp2l = (s10l/(nl-1.)-2.*s8l*s1l/nl/(nl-1.)
-s7l*s5l/nl/(nl-1.)+2.*s7l*s8l*s8l/nl/nl/(nl-1.))*cfv;
}

if(nt == 0 || nt == 1)
     ut=vt=uprt=vprt=upvpt=upvp2t=0.;

else {
ut = s7t/nt;
```

```
vt = s8t/nt;

uprt = pow((s4t/(nt-1.)-s7t*s7t/nt/(nt-1.)),0.5);
vprt = pow((s5t/(nt-1.)-s8t*s8t/nt/(nt-1.))*cfv,0.5);

upvpt = (s1t/(nt-1.)-s7t*s8t/nt/(nt-1.))*cfuv;

upvp2t = (s10t/(nt-1.)-2.*s8t*s1t/nt/(nt-1.)
-s7t*s5t/nt/(nt-1.)+2.*s7t*s8t*s8t/nt/nt/(nt-1.))*cfv;
}


fprintf(fm,"%d %f %f %f %f %f %f %f %f %f %d\n",
k,y[k],um,vm,tinf[k],uprm,vprm,upvpm,upvp2m,gamma,nm);
fflush(fm);
fprintf(fl,"%d %f %f %f %f %f %f %f %f %f %d\n",
k,y[k],ul,vl,tinf[k],uprl,vprl,upvpl,upvp2l,gamma,nl);
fflush(fl);
fprintf(ft,"%d %f %f %f %f %f %f %f %f %f %d\n",
k,y[k],ut,vt,tinf[k],uprt,vprt,upvpt,upvp2t,gamma,nt);
fflush(ft);


}

fclose(fm);
fclose(fl);
fclose(ft);
}



double gft()     /* gets a floating point number */

{

int len,i,flg1,flg2,flg3;
char line[MAXLINE];
double atof();

flg1 = 0;
while( flg1 == 0) {
flg2 = 0;
flg3 = 0;
len = getline(line,MAXLINE);

if( len == 0 )    /* bail out for blank line */
return(-987654.);
++flg1;
for (i=0; line[i] == ' ' || line[i] == '\t' ; i++)
;    /* get rid of leading blanks  */
if (line[i] == '+' || line[i] == '-' )
i++;
for ( ; i < len ; i++) {
if ( line[i]-'0' < 0 || line[i]-'0' >9) {
if( line[i] == '.' && flg2 == 0 )
flg2 = 1;
else if((line[i] == 'e' || line[i] == 'E') && flg3 == 0) {
flg2 = flg3 = 1;
if (line[i+1] =='+' || line[i+1] == '-')
i++;
}
else  {
flg1 = 0;
printf("Unacceptable input, try again: ");
}
}
}
}
return ( atof(line) );
}


getline(s,lim)  /* get line into s, return length */
char s[];
int lim;
{
int c,i;

i=0;
while(--lim > 0 && (c=getchar()) != EOF && c != '\n')
s[i++] = c;
s[i] = '\0';
return(i);
}


git()     /* gets an integer */

{
```

```
int len,i,flg1,flg2;
char line[MAXLINE];
int atoi();

flg1 = 0;
while( flg1 == 0) {
flg2 = 0;
len = getline(line,MAXLINE);
if( len == 0 )    /* bail out for blank line */
return(-987654);
++flg1;
for (i=0; line[i] == ' ' || line[i] == '\t' ; i++)
;    /* get rid of leading blanks  */
if (line[i] == '+' || line[i] == '-' )
i++;
for ( ; i < len ; i++) {
if ( line[i]-'0' < 0 || line[i]-'0' >9 || flg2 == 1 ) {
if( line[i] == '.' && flg2 == 0 )
flg2 = 1;
else  {
flg1 = 0;
printf("Unacceptable input, try again: ");
}
}
}
}
return ( atoi(line) );
}



norl(v,rdst)

double v[];
char rdst[];

{
int i,j,*pt,ifactor;
int a1,a2;
double factor1,factor2,factor,offset;
char o_str[40],digit[2];
char *ptrd;
int bit0,bit1,bit2,bit3,hexdigit,sign;

ptrd = rdst;


/* Evaluate factor and offset for Norland */

/* factor */

sscanf(ptrd,"%2x",&ifactor);
factor1 = pow(2.,((double)ifactor -128.));
for (i=0, factor2=0; i<6; i++) {
strncpy(digit,(ptrd+2+i),1);
digit[1]='\0';
sscanf(digit,"%x",&hexdigit);
bit0 = hexdigit & 1;
bit1 = hexdigit & 2;
bit2 = hexdigit & 4;
bit3 = hexdigit & 8;
if(i == 0) {
if(bit3)
sign = -1;
else
sign = 1;
bit3 = 1;
}
if(bit3) factor2 = factor2 + pow(2.,-(double)(i*4+1));
if(bit2) factor2 = factor2 + pow(2.,-(double)(i*4+2));
if(bit1) factor2 = factor2 + pow(2.,-(double)(i*4+3));
if(bit0) factor2 = factor2 + pow(2.,-(double)(i*4+4));
}
factor = (double) sign * factor1 * factor2;

/* offset */

sscanf((ptrd+8),"%2x",&ifactor);
factor1 = pow(2.,((double)ifactor -128.));
for (i=0, factor2=0; i<6; i++) {
strncpy(digit,(ptrd+10+i),1);
digit[1]='\0';
sscanf(digit,"%x",&hexdigit);
bit0 = hexdigit & 1;
bit1 = hexdigit & 2;
bit2 = hexdigit & 4;
bit3 = hexdigit & 8;
if(i == 0) {
if(bit3)
```

```
sign = -1;
else
sign = 1;
bit3 = 1;
}
if(bit3) factor2 = factor2 + pow(2.,-(double)(i*4+1));
if(bit2) factor2 = factor2 + pow(2.,-(double)(i*4+2));
if(bit1) factor2 = factor2 + pow(2.,-(double)(i*4+3));
if(bit0) factor2 = factor2 + pow(2.,-(double)(i*4+4));
}
offset = (double) sign * factor1 * factor2;
/* Find voltage for individual data points */

for(j=0,i=256;i<(2*[illegible]0+256);j++,i+=2) {
strncpy(digit,(ptrd+i),1);
digit[1]='\0';
a1=*digit;
if(a1 < 0 )
a1 +=256;
strncpy(digit,(ptrd+i+1),1);
digit[1]='\0';
a2=*digit;
if(a2 < 0 )
a2 +=256;
v[j]=(a2*256+a1-32768)*factor+offset;
}
}
```

```
/*
  Acquires data using triple wire probe

  Written:  Ralph Volino       10/01/93


        Command Line:   vtacq

  This program is used to acquire data from the triple wire probe
  using the Norland oscilloscopes.  Raw voltage data is acquired
  and saved for future processing.

*/

#include <stdio.h>
#include <sys/ugpib.h>
#include <fcntl.h>
#include <string.h>
#include <math.h>
#define  BUFSIZE        40
#define  MAXLINE      1000
#define  NOTEXIST       -1
#define  IFA1OFF       1.
#define  IFA2OFF       1.
#define  IFA3OFF       1.
#define  IFA4OFF       1.
#define  IFA1GAIN     10.
#define  IFA2GAIN     10.
#define  IFA3GAIN     10.
#define  IFA4GAIN     10.
#define  CCGAIN      202.005
#define  CCOFF      - 0.0071025
#define  CCTC        -0.001767
#define  CURRENT     1.0208e-3
#define  V21         1.0208e-3*9.82
#define  OFFTURB     3.8306
#define  OFFLAM      0.097656
#define  THRESH      1.8
#define  EPSILON     0.1026524
#define  KCC         0.017
#define  DTDR        5.41516
#define  RO          -267.4549
#define  THETA      0.785398163
#define  PWR        0.435
#define  A1         -2.95288
#define  B1         8.33949
#define  A2         -2.84056
#define  B2         8.70155
#define  RPR        1.985
#define  AREA       0.8361
#define  KLEX       0.197
#define  DXLEX      0.001273556   /* 50.14/1000.*2.54e-2 */
#define  SIGMA      5.67e-8
#define  EMIS       0.85


main(argc,argv)
int     argc;
char    *argv[];
{

        int     d16,d15,d06,d08,d03,d11,ty,n,i,j,k;
int     mon[7]={145,146,148,141,143,142,139};
int  flg,ansr,git(),tc,nt,sta,dv;
int     ndata,addpts,im;
int findwall(),trav();
        double  atof(),gft(),y[90],ym[90],temp();
double  yp,vpr,vhb,volt,vlt[150],coef[5],xt[6],tt[6];
        double  patm,tinf,ir,qb,vz,dist,loc,mov,yn;
double  mxt[10]={4.5,4.5,4.0,3.5,3.5,3.0,3.0,2.0,2.0,1.8};
double  visob2,visob1,vlexb1,vlexb2,vlexb,tlexb,vinsb,tinsb;
double  kins,dxins,qlossb,qfrontb,vinf,y1;
double  x1,x2,x3,x4,yt,xy,x2y,dn,nm1,nm2,nm3;
double  twall,tcorr,qrad,qnet,maxtr;
        char    mybuf[BUFSIZE],o_str[BUFSIZE],readstr[400];
char    line[MAXLINE];
char name[20],tal[10],filn[20];
char    norbuf[8500],inam[20];
FILE *fd,*fp;


x1=x2=x3=x4=yt=xy=x2y=0.;

printf("Input a base name for the output files: ");
scanf("%s",name);
getchar();

fp = fopen(name,"w");  /*  store constants and y locations of data */

printf("Enter the name of the y location file: ");
```

```
scanf("%s",inam);
getchar();


/*  Open the Fluke multimeter for reading thermocouples */

d08=ibfind("dev8");
             if(d08 < 0){
             fprintf(stderr,"Can't open /dev/dev08 for read\n");
             exit(1);
             }

/*  Open the Scanner for reading thermocouples */

d03=ibfind("dev3");
             if(d03 < 0){
             fprintf(stderr,"Can't open /dev/dev03 for read\n");
             exit(1);
             }


/*  Open the programmable power supply for triggering the Norland */

d06=ibfind("dev6");
             if(d06 < 0){
             fprintf(stderr,"Can't open /dev/dev06 for read\n");
             exit(1);
             }


/*  Open the Norland oscilloscope for reading the IFA-100 output  */
d15=ibfind("dev15");
             if(d15 < 0){
             fprintf(stderr,"Can't open /dev/dev15 for read\n");
             exit(1);
             }


/*  Open the second Norland for reading the IFA-100 output  */
d16=ibfind("dev16");
              if(d16 < 0){
              fprintf(stderr,"Can't open /dev/dev16 for read\n");
              exit(1);
}
```

```
/*  Open the motor controller for moving the probe  */
d11=ibfind("dev11");
             if(d11 < 0){
             fprintf(stderr,"Can't open /dev/dev11 for read\n");
             exit(1);
             }


/* Initialize and program the Norland for averaging input voltages */
printf("Do you want to initialize the Norland (y,n)? ");
for (i=0, ty=0; (ansr = getchar()) != '\n' ; i++)
if (i == 0 && ansr == 'y')
ty=1;
if(ty == 1) {
printf("Press Reset Key of the Norlands");
while( ansr = getchar() != '\n');
sprintf(o_str,"]LAYEL:01=ZME");
ibwrt(d15,o_str,strlen(o_str));
sprintf(o_str,"]LAYALO=");
ibwrt(d16,o_str,strlen(o_str));

}


for (flg=0; flg == 0 ; ) {
flg++;
printf("Input the atmospheric pressure [in. Hg] ");
patm = gft();
if( patm < 28. || patm > 31.) {
printf("%f is not reasonable, try again.\n", patm);
flg = 0;
}
}
patm *= 25.4;


/*  Get the wall heat flux  */

printf("Set the fluke to front panel input");
while ( getchar() != '\n');

sprintf(o_str,"F2SO");  /* set up fluke to AC */
ibwrt(d08,o_str,strlen(o_str));
```

```
printf("Turn rotary switch to VPR");
while (getchar() != '\n');
for(j=0,vpr=0;j<4;j++) {
ibrd(d08, mybuf, 13);
volt = atof(mybuf);
vpr +=volt;
sleep(1);
}
vpr /= 4.;

printf("Turn rotary switch to VHB");
while (getchar() != '\n');
for(j=0,vhb=0;j<4;j++) {
ibrd(d08, mybuf, 13);
volt = atof(mybuf);
vhb +=volt;
sleep(1);
}
vhb /= 4.;

printf("Set the fluke to rear panel input");
while (getchar() != '\n');

sprintf(o_str,"F1");  /* set up fluke to DC */
ibwrt(d08,o_str,strlen(o_str));

ir = vpr/RPR;
qb = ir*vhb/AREA;
printf("Wall heat flux = %f\n",qb);

for(i=130;i<150;i++)
vlt[i]    = 0;
for(j=0;j<5;j++) {
for(i=0;i<7;i++) {
sprintf(o_str,"%d,",mon[i]-1);
ibwrt(d03,o_str,strlen(o_str));
sleep(1);
ibrd(d08, mybuf, 13);
volt = atof(mybuf);
if(i == 0)
vz=volt;
if(i == 1 && ((vz-volt) > 3e-6 || (volt-vz) > 3e-6))
printf("Check Thermocouples\n");
printf("Run %d , Thermocouple %d , %f volts\n",j+1,i+1,volt);
vlt[mon[i]] +=volt;
}
}
for(i=0;i<7;i++)
vlt[mon[i]] = vlt[mon[i]]*1000./5.;

visob2 = (vlt[145]+vlt[146])/2.;
visob1 = visob2 - vlt[148];
vlexb1 = vlt[141] - visob2;
vlexb2 = vlt[143] - visob2;
vlexb  = (vlexb1 + vlexb2)/2.;
tlexb  = temp(vlexb);
vinsb  = vlt[142] - visob2;
tinsb  = temp(vinsb);
kins   = 0.04;
dxins  = 4.*2.54/100.;
qlossb = kins*(tlexb-tinsb)/dxins;
qfrontb = qb-qlossb;

vinf   = vlt[139] - visob2;
tinf   = temp(vinf);

/*  Wall temperature */

printf("Enter the TC number closest to the probe ");
tc = git();
printf("Enter the distance (cm) of the probe from this TC\n");
printf("+ for probe downstream of TC, - for upstream :");
dist = gft();
loc = (0.5 + tc)*2.54+dist;

for(i=0;i<5;i++)
vlt[i]    = 0;
for(k=0;k<5;k++) {
for(i=0,j=tc-2;j<tc+3;i++,j++) {
if(j == 1 || j == 3 || j == 7 || j == 14 || j == 44)
vlt[i] += 99.;
else {
sprintf(o_str,"%d,",j-1);
ibwrt(d03,o_str,strlen(o_str));
sleep(1);
ibrd(d08, mybuf, 13);
volt = atof(mybuf);
vlt[i] +=volt;
}
```

```
}
}
for(i=0,j=tc-2,k=0,nt=5;i<5;i++,j++,k++) {
if(vlt[i] == 5*99.) {
nt--;
k--;
}
else {
xt[k] = (.5+j)*2.54;
volt = vlt[i]*1000./5.-visob1;
tt[k] = temp(volt);
}
}

/*  curve fit the wall temperatures  */
for(i=0;i<nt;i++) {
x1 += xt[i];
x2 += (xt[i]*xt[i]);
x3 += (xt[i]*xt[i]*xt[i]);
x4 += (xt[i]*xt[i]*xt[i]*xt[i]);
yt += tt[i];
xy += (xt[i]*tt[i]);
x2y += (xt[i]*xt[i]*tt[i]);
}
dn = nt*(x2*x4-x3*x3)-x1*(x1*x4-x3*x2)+x2*(x1*x3-x2*x2);
nm1 = yt*(x2*x4-x3*x3)-x1*(xy*x4-x3*x2y)+x2*(xy*x3-x2*x2y);
nm2 = nt*(xy*x4-x3*x2y)-yt*(x1*x4-x3*x2)+x2*(x1*x2y-xy*x2);
nm3 = nt*(x2*x2y-xy*x3)-x1*(x2y*x1-x2*xy)+yt*(x1*x3-x2*x2);
coef[1] = nm1/dn;
coef[2] = nm2/dn;
coef[3] = nm3/dn;

twall = coef[1]+coef[2]*loc+coef[3]*loc*loc;
for(i=0;i<nt;i++)
printf(" %f\n",tt[i]);
printf("Twall = %f\n",twall);
tcorr = qfrontb*DILEX/KLEX;
twall = twall - tcorr;
printf("Twall corrected = %f\n",twall);
qrad = SIGMA*EMIS*(pow(twall+273.15,4.)-pow(tinf+273.15,4.));
qnet = qfrontb - qrad;
printf("Net convective heat flux = %f\n",qnet);

printf("Enter the station number (1 to 10) :");
sta = git();
maxtr = mxt[sta-1];

/* Enter the data for the y locations to take measurements  */

fd = fopen(inam,"r");
fgets(line,MAXLINE,fd);
sscanf(line,"%d",&ndata);
for(i=0;i<ndata;i++) {
fgets(line,MAXLINE,fd);
sscanf(line,"%s",mybuf);
ym[i] = atof(mybuf);
}
close(fd);

/*  ******************************************** */

findwall(&y1,d11);
y[0] = y1;
for(i=0;i<ndata;i++) {
if(ym[i] > y[0]) {
im = i;
break;
}
}
addpts =  (maxtr - ym[ndata-1])*2+2;
ndata = ndata-im+addpts-1;



/*  Dump all the constants out to a file for data reduction */

fprintf(fp,"%g %g %g %g %g %g %g %g %g %g\n";
CCGAIN,CCOFF,CCTC,CURRENT,EPSILON,V21,KCC,DTDR,RO,THETA);
fprintf(fp,"%g %g %g %g %g %g %g %g %g\n",A1,A2;
B1,B2,THRESH,OFFTURB,OFFLAM,PWR);
fprintf(fp,"%g %g %g %g %g %g %g %g\n",IFA1OFF;
IFA2OFF,IFA3OFF,IFA4OFF,IFA1GAIN,IFA2GAIN,IFA3GAIN,IFA4GAIN);
fprintf(fp,"%g %g %g %g %g\n",patm,qnet,twall,tinf,loc);
fprintf(fp,"%d %d\n",sta,ndata);
fflush(fp);



/*  Acquire the raw data from the Norlands and store it  */
```

```
for( i=0; i<ndata ; i++) {

fprintf(fp,"%f\n",y1);  /* Store the y location */
fflush(fp);

ibwrt(d06,"2900",4);
ibwrt(d16,"R",1);
ibwrt(d15,"R",1);
sleep(1);
ibwrt(d06,"2000",4);
sleep(43);
ibwrt(d16,"S",1);

/*  Open the files for data storage  */

for(j=0; j<4; j++) {
strcpy(filn,name);
if(j == 0) {
strcpy(tal,"_A");
ibwrt(d15,"_KCGA",5);
dv=d15;
}
if(j == 1) {
strcpy(tal,"_B");
ibwrt(d15,"_KCGC",5);
dv=d15;
}
if(j == 2) {
strcpy(tal,"_C");
ibwrt(d16,"_KCGA",5);
dv=d16;
}
if(j == 3) {
strcpy(tal,"_D");
ibwrt(d16,"_KCGC",5);
dv=d16;
}
strcat(filn,tal);
sprintf(o_str,"%d",i+1);
strcat(filn,o_str);
fd = fopen(filn,"w");

ibrd(dv,norbuf,8452);
fprintf(fd,"%s",norbuf);
fflush(fd);
fclose(fd);
}

/*   Move to the next y position   */


if(i != ndata-1) {
if( i > ndata-addpts)
mov = 0.5;
else {
yn = ym[im+i];
mov = yn-y1;
}
trav(&y1,mov,maxtr,d11);
}

}
}



double gft()     /* gets a floating point number */

{
#define MAXLINE 1000

int len,i,flg1,flg2,flg3;
char line[MAXLINE];
double atof();

flg1 = 0;
while( flg1 == 0) {
flg2 = 0;
flg3 = 0;
len = getline(line,MAXLINE);
if( len == 0 )    /* bail out for blank line */
return(-987654.);
++flg1;
for (i=0; line[i] == ' ' || line[i] == '\t' ; i++)
;    /* get rid of leading blanks  */
if (line[i] == '+' || line[i] == '-' )
i++;
for ( ; i < len ; i++) {
if ( line[i]-'0' < 0 || line[i]-'0' >9) {
if( line[i] == '.' && flg2 == 0 )
```

```
flg2 = 1;
else if((line[i] == 'e' || line[i] == 'E') && flg3 == 0) {
flg2 = flg3 = 1;
if (line[i+1] =='+' || line[i+1] == '-')
i++;
}
else  {
flg1 = 0;
printf("Unacceptable input, try again: ");
}
}
}
}
return ( atof(line) );
}


getline(s,lim)  /* get line into s, return length */
char s[];
int lim;
{
int c,i;

i=0;
while(--lim > 0 && (c=getchar()) != EOF && c != '\n')
s[i++] = c;
s[i] = '\0';
return(i);
}


git()     /* gets an integer */

{
#define MAXLINE 1000

int len,i,flg1,flg2;
char line[MAXLINE];
int atoi();

flg1 = 0;
while( flg1 == 0) {
flg2 = 0;
len = getline(line,MAXLINE);
if( len == 0 )    /* bail out for blank line */
return(-987654);
++flg1;
for (i=0; line[i] == ' ' || line[i] == '\t' ; i++)
;    /* get rid of leading blanks  */
if (line[i] == '+' || line[i] == '-' )
i++;
for ( ; i < len ; i++) {
if ( line[i]-'0' < 0 || line[i]-'0' >9 || flg2 == 1 ) {
if( line[i] == '.' && flg2 == 0 )
flg2 = 1;
else  {
flg1 = 0;
printf("Unacceptable input, try again: ");
}
}
}
}
return ( atoi(line) );
}


double temp(v)

double v;

{
double a,b,c,d,t;

a = 0.0878053847;
b = -0.6018211152;
c = 1.113528335;
d = 16.14880077;

t=a*v*v*v*v+b*v*v*v+c*v*v+d*v;

return(t);
}


findwall(y1,d11)

double *y1;
int  d11;

{
```

```
ibwrt(d11,"Y.D.\n",5);
ibwrt(d11,"Y.B2000.\n",9);
printf("Bring traverse up to wall at fast speed, NOT TOO CLOSE ");
while ( getchar() != '\n');
printf("Switch to AUTO ");
while ( getchar() != '\n');
ibwrt(d11,"Y.B320.\n",8);
printf("Switch to MANUAL and bring probe to wall ");
while ( getchar() != '\n');
printf("Switch to AUTO ");
while ( getchar() != '\n');
*y1 = 0.05;
ibwrt(d11,"Y.B2000.\n",9);
ibwrt(d11,"Y.E.\n",5);
}

trav(y1,mov,maxtr,d11)

double *y1,mov,maxtr;
int   d11;

{
int stp;
char cst[10],mc[15];

stp = mov*2000;
mov = stp/2000.;
if(mov+*y1 > maxtr) {
mov = 0.;
stp = 0;
printf("Attempt to move beyond allowable travel\n");
}
sprintf(cst,"%d.",stp);
ibwrt(d11,"Y.D.\n",5);
strcpy(mc,"Y.M");
strcat(mc,cst);
strcat(mc,"G.\n");
ibwrt(d11,mc,strlen(mc));
ibwrt(d11,"Y.E.\n",5);
*y1 +=mov;
sleep(3);
}
```

```
/*
  Reduces data from triple wire probe

  Written:  Ralph Volino       10/03/93


        Command Line:   vtred

  This program is used to reduce data from the triple wire probe
  acquired using the Norland oscilloscopes.  Raw voltage data
  are converted to velocities and temperatures.

*/

#include <stdio.h>
#include <fcntl.h>
#include <string.h>
#include <math.h>
#define  BUFSIZE        40
#define  MAXLINE      1000
#define  NOTEXIST       -1
#define  N0           4096

main(argc,argv)
int     argc;
char    *argv[];
{

        int     n,i,j,k,m,l;
int  git(),sta;
int     ndata,norl();
int     nl,nt,nm;
int     flg[N0];
        double  atof(),gft(),y[90];
        double  patm,tinf,loc;
double  twall,qnet;
double  ifa1off,ifa2off,ifa3off,ifa4off,ifa1gain,ifa2gain,ifa3gain;
double  ifa4gain,ccgain,ccoff,cctc,current,v21,offturb,offlam,thresh;
double  epsilon,kcc,dtdr,r0,theta,pwr,a1,a2,b1,b2;
double  volt1[N0],volt2[N0],volt3[N0],volt4[N0];
double  ld,kt,cfuv,cfv,x;
double  s1m,s2m,s3m,s4m,s5m,s6m,s7m,s8m,s9m,s10m,s11m,s12m,s13m,s14m;
double  s1l,s2l,s3l,s4l,s5l,s6l,s7l,s8l,s9l,s10l,s11l,s12l,s13l,s14l;
double  s1t,s2t,s3t,s4t,s5t,s6t,s7t,s8t,s9t,s10t,s11t,s12t,s13t,s14t;
double  rwire,va,temp[N0],up[N0],vp[N0];
double  numer,denom,ctemp,base1,base2,uef1,uef2;
double  gamma,c2the;
double  ui,vi,ti,hp,hs,q[6],sq[8][6][6];
double  um,vm,tm,upvpm,vptpm,uptpm,upvp2m,vp2tpm;
double  ul,vl,tl,upvpl,vptpl,uptpl,upvp2l,vp2tpl;
double  ut,vt,tt,upvpt,vptpt,uptpt,upvp2t,vp2tpt;
double  uprm,vprm,tprm,uprl,vprl,tprl,uprt,vprt,tprt;
        char    mybuf[BUFSIZE],o_str[BUFSIZE],readstr[400];
char    line[MAXLINE];
char name[40],tal[10],filn[40];
char    norbuf[8500],inam[40];
char    s1[10],s2[10],s3[10],s4[10],s5[10],s6[10],s7[10],s8[10];
char    s9[10],s10[10];
FILE *fd,*fp,*fm,*fl,*ft,*fq;



printf("Input the base name for the data files: ");
scanf("%s",name);
getchar();

fp = fopen(name,"r");  /*  get constants and y locations of data */

printf("Enter the name of the output file: ");
scanf("%s",inam);
getchar();

strcpy(o_str,inam);
strcat(o_str,"_m");
fm = fopen(o_str,"w");

strcpy(o_str,inam);
strcat(o_str,"_l");
fl = fopen(o_str,"w");

strcpy(o_str,inam);
strcat(o_str,"_t");
ft = fopen(o_str,"w");

strcpy(o_str,inam);
strcat(o_str,"_q");
fq = fopen(o_str,"w");

/*  Get all the constants for data reduction */
```

```
fgets(line,MAXLINE,fp);
sscanf(line,"%s %s %s %s %s %s %s %s %s %s",s1,s2,s3,s4,
s5,s6,s7,s8,s9,s10);
ccgain  = atof(s1);
ccoff   = atof(s2);
cctc    = atof(s3);
current = atof(s4);
epsilon = atof(s5);
v21     = atof(s6);
kcc     = atof(s7);
dtdr    = atof(s8);
r0      = atof(s9);
theta   = atof(s10);

c2the = 2.*cos(theta);

fgets(line,MAXLINE,fp);
sscanf(line,"%s %s %s %s %s %s %s %s",s1,s2,s3,s4,s5,s6,s7,s8);
a1 = atof(s1);
a2 = atof(s2);
b1 = atof(s3);
b2 = atof(s4);
thresh = atof(s5);
offturb = atof(s6);
offlam = atof(s7);
pwr = atof(s8);

pwr = 1./pwr;

fgets(line,MAXLINE,fp);
sscanf(line,"%s %s %s %s %s %s %s %s",s1,s2,s3,s4,s5,s6,s7,s8);
ifa1off = atof(s1);
ifa2off = atof(s2);
ifa3off = atof(s3);
ifa4off = atof(s4);
ifa1gain = atof(s5);
ifa2gain = atof(s6);
ifa3gain = atof(s7);
ifa4gain = atof(s8);

fgets(line,MAXLINE,fp);
sscanf(line,"%s %s %s %s %s",s1,s2,s3,s4,s5);
patm = atof(s1);
qnet = atof(s2);
twall = atof(s3);
tinf = atof(s4);
x    =  atof(s5);

fgets(line,MAXLINE,fp);
sscanf(line,"%d %d",&sta,&ndata);

fprintf(fm,"%f %f %f %f %f\n",patm,qnet,twall,tinf,x);
fprintf(fm,"%d %d\n",sta,ndata);
fflush(fm);
fprintf(fl,"%f %f %f %f %f\n",patm,qnet,twall,tinf,x);
fprintf(fl,"%d %d\n",sta,ndata);
fflush(fl);
fprintf(ft,"%f %f %f %f %f\n",patm,qnet,twall,tinf,x);
fprintf(ft,"%d %d\n",sta,ndata);
fflush(ft);

/* Enter the data for the y locations of the measurements  */

for(i=0;i<ndata;i++) {
fgets(line,MAXLINE,fp);
sscanf(line,"%s",mybuf);
y[i] = atof(mybuf);
}
fclose(fp);


/*  Champagne correction  */

ld = 200.;
kt = -5.e-4*ld+.3;
cfuv = (1.+kt*kt)/(1.-kt*kt);
cfv  = (1.+kt*kt)/(1.-3.*kt*kt+4.*pow(kt,4.));

/*  Process the raw data at each y location  */

for (k=0; k<ndata; k++) {

/*  Initialize various summation variables for flow statistics */

s1m=s2m=s3m=s4m=s5m=s6m=s7m=s8m=s9m=s10m=s11m=s12m=s13m=s14m=0.;
s1l=s2l=s3l=s4l=s5l=s6l=s7l=s8l=s9l=s10l=s11l=s12l=s13l=s14l=0.;
s1t=s2t=s3t=s4t=s5t=s6t=s7t=s8t=s9t=s10t=s11t=s12t=s13t=s14t=0.;
nl=nt=0;
```

```
/*  Retrieve the stored raw data and convert to voltages */

for(j=0; j<4; j++) {
strcpy(filn,name);
if(j == 0)
strcpy(tal,"_A");
if(j == 1)
strcpy(tal,"_B");
if(j == 2)
strcpy(tal,"_C");
if(j == 3)
strcpy(tal,"_D");
strcat(filn,tal);
sprintf(o_str,"%d",k+1);
strcat(filn,o_str);
fd = fopen(filn,"r");

fgets(norbuf,8500,fd);
fclose(fd);
if(j == 0)
norl(volt3,norbuf);
if(j == 1)
norl(volt4,norbuf);
if(j == 2)
norl(volt1,norbuf);
if(j == 3)
norl(volt2,norbuf);
}

/*  Convert voltages to velocities and temperatures  */

for(j=0; j<M0; j++) {
volt2[j] = -volt2[j];
if(volt2[j] > offlam+.1 && volt2[j] < offturb-.4) {
flg[j]=3;
goto badpt;
}
else if(volt2[j]>thresh) {
volt2[j] -= offturb;
flg[j]=1;
}
else {
volt2[j] -=offlam;
flg[j]=2;
}

volt1[j] = volt1[j]/ifa3gain+ifa3off;
volt1[j] = (volt1[j]-ccoff)/ccgain;
volt2[j] = volt2[j]/ifa4gain+ifa4off;
volt2[j] = volt2[j]/cctc/ccgain;

volt3[j] = volt3[j]/ifa1gain+ifa1off;
volt4[j] = volt4[j]/ifa2gain+ifa2off;

numer = kcc/volt4[j]/volt4[j]*v21*volt2[j]+volt1[j];
denom = 1.+epsilon*kcc/volt4[j]/volt4[j]*volt2[j];
va = numer/denom;
rwire = va/current;
temp[j] = rwire*dtdr+r0;

ctemp = pow((225./(250.-temp[j])),.5);
volt3[j] *=ctemp;
volt4[j] *=ctemp;
base1 = a1+b1*volt3[j]*volt3[j];
base2 = a2+b2*volt4[j]*volt4[j];
uef1 = pow(base1,pwr);
uef2 = pow(base2,pwr);
up[j] = (uef1+uef2)/c2the;
vp[j] = (uef1-uef2)/c2the;

ti = temp[j];
ui = up[j];
vi = vp[j];

/* Sums for statistics */
if(flg[j] == 2) {
s1l += ui*vi;
s2l += vi*ti;
s3l += ui*ti;
s4l += ui*ui;
s5l += vi*vi;
s6l += ti*ti;
s7l += ui;
s8l += vi;
s9l += ti;
s10l += ui*vi*vi;
s11l += ui*ui*vi;
s12l += vi*vi*vi;
s13l += ti*vi*vi;
s14l += ti*ti*vi;
nl +=1;
```

```
}
else {
s1t += ui*vi;
s2t += vi*ti;
s3t += ui*ti;
s4t += ui*ui;
s5t += vi*vi;
s6t += ti*ti;
s7t += ui;
s8t += vi;
s9t += ti;
s10t += ui*vi*vi;
s11t += ui*ui*vi;
s12t += vi*vi*vi;
s13t += ti*vi*vi;
s14t += ti*ti*vi;
nt +=1;
}
badpt:;

}

s1m = s1l+s1t;
s2m = s2l+s2t;
s3m = s3l+s3t;
s4m = s4l+s4t;
s5m = s5l+s5t;
s6m = s6l+s6t;
s7m = s7l+s7t;
s8m = s8l+s8t;
s9m = s9l+s9t;
s10m = s10l+s10t;
s11m = s11l+s11t;
s12m = s12l+s12t;
s13m = s13l+s13t;
s14m = s14l+s14t;
nm = nl+nt;

gamma = (float) nt/ (float) nm;

um = s7m/nm;
vm = s8m/nm;
tm = s9m/nm;

uprm = pow((s4m/(nm-1.)-s7m*s7m/nm/(nm-1.)),0.5);
vprm = pow((s5m/(nm-1.)-s8m*s8m/nm/(nm-1.))*cfv,0.5);
tprm = pow((s6m/(nm-1.)-s9m*s9m/nm/(nm-1.)),0.5);

upvpm = (s1m/(nm-1.)-s7m*s8m/nm/(nm-1.))*cfuv;
vptpm = (s2m/(nm-1.)-s8m*s9m/nm/(nm-1.))*cfuv;
uptpm = (s3m/(nm-1.)-s7m*s9m/nm/(nm-1.));

upvp2m = (s10m/(nm-1.)-2.*s8m*s1m/nm/(nm-1.)
-s7m*s5m/nm/(nm-1.)+2.*s7m*s8m*s8m/nm/nm/(nm-1.))*cfv;
vp2tpm = (s13m/(nm-1.)-2.*s8m*s2m/nm/(nm-1.)
-s9m*s5m/nm/(nm-1.)+2.*s9m*s8m*s8m/nm/nm/(nm-1.))*cfv;


if(nl == 0 || nl == 1)
     ul=vl=tl=uprl=vprl=tprl=upvpl=vptpl=uptpl=upvp2l=vp2tpl=0.;

else {
ul = s7l/nl;
vl = s8l/nl;
tl = s9l/nl;

uprl = pow((s4l/(nl-1.)-s7l*s7l/nl/(nl-1.)),0.5);
vprl = pow((s5l/(nl-1.)-s8l*s8l/nl/(nl-1.))*cfv,0.5);
tprl = pow((s6l/(nl-1.)-s9l*s9l/nl/(nl-1.)),0.5);

upvpl = (s1l/(nl-1.)-s7l*s8l/nl/(nl-1.))*cfuv;
vptpl = (s2l/(nl-1.)-s8l*s9l/nl/(nl-1.))*cfuv;
uptpl = (s3m/(nl-1.)-s7l*s9l/nl/(nl-1.));

upvp2l = (s10l/(nl-1.)-2.*s8l*s1l/nl/(nl-1.)
-s7l*s5l/nl/(nl-1.)+2.*s7l*s8l*s8l/nl/nl/(nl-1.))*cfv;
vp2tpl = (s13l/(nl-1.)-2.*s8l*s2l/nl/(nl-1.)
-s9l*s5l/nl/(nl-1.)+2.*s9l*s8l*s8l/nl/nl/(nl-1.))*cfv;
}

if(nt == 0 || nt == 1)
     ut=vt=tt=uprt=vprt=tprt=upvpt=vptpt=uptpt=upvp2t=vp2tpt=0.;

else {
ut = s7t/nt;
vt = s8t/nt;
tt = s9t/nt;

uprt = pow((s4t/(nt-1.)-s7t*s7t/nt/(nt-1.)),0.5);
vprt = pow((s5t/(nt-1.)-s8t*s8t/nt/(nt-1.))*cfv,0.5);
```

```
tprt = pow((s6t/(nt-1.)-s9t*s9t/nt/(nt-1.)),0.5);

upvpt = (s1t/(nt-1.)-s7t*s8t/nt/(nt-1.))*cfuv;
vptpt = (s2t/(nt-1.)-s8t*s9t/nt/(nt-1.))*cfuv;
uptpt = (s3m/(nt-1.)-s7t*s9t/nt/(nt-1.));

upvp2t = (s10t/(nt-1.)-2.*s8t*s1t/nt/(nt-1.)
-s7t*s5t/nt/(nt-1.)+2.*s7t*s8t*s8t/nt/nt/(nt-1.))*cfv;
vp2tpt = (s13t/(nt-1.)-2.*s8t*s2t/nt/(nt-1.)
-s9t*s5t/nt/(nt-1.)+2.*s9t*s8t*s8t/nt/nt/(nt-1.))*cfv;
}


/*  Quadrant Analysis  */

for(i=0;i<6;i++)
for(j=0;j<8;j++)
for(l=0;l<6;l++)
sq[j][i][l] = 0.;

for(m=0;m<M0;m++) {
if(flg[m] == 3)
goto skip;
ui = up[m]-um;
vi = vp[m]-vm;
ti = temp[m]-tm;

q[0] = ui*vi*cfuv;
q[1] = vi*ti*cfuv;
q[2] = ui*ti;
q[3] = ui*vi*vi*cfv;
q[4] = vi*vi*ti*cfv;
q[5] = 1.;

if(ui > 0.) {
if(vi > 0.) {
if(ti < 0.)
j=0;
else
j=4;
}
else {
if(ti <0.)
j=3;
else
j=7;
}
}
else {
if(vi > 0.) {
if(ti < 0.)
j=1;
else
j=5;
}
else {
if(ti <0.)
j=2;
else
j=6;
}
}

if(q[0] >= 0)
hp = q[0];
else
hp = -q[0];
if(upvpm >= 0)
hs = upvpm;
else
hs = -upvpm;

for(i=0;i<6;i++)
if(hp >= hs*2.*i )
for(l=0;l<6;l++)
sq[j][l][i] +=q[l];
skip:;
}

fprintf(fm,"%d %f %f %f %f %f %f %f %f %f %f %f %f %f %d\n",
k,y[k],um,vm,tm,uprm,vprm,tprm,upvpm,vptpm,uptpm,upvp2m,vp2tpm,gamma,nm);
fflush(fm);
fprintf(fl,"%d %f %f %f %f %f %f %f %f %f %f %f %f %f %d\n",
k,y[k],ul,vl,tl,uprl,vprl,tprl,upvpl,vptpl,uptpl,upvp2l,vp2tpl,gamma,nl);
fflush(fl);
fprintf(ft,"%d %f %f %f %f %f %f %f %f %f %f %f %f %f %d\n",
k,y[k],ut,vt,tt,uprt,vprt,tprt,upvpt,vptpt,uptpt,upvp2t,vp2tpt,gamma,nt);
fflush(ft);

for(j=0;j<8;j++)
```

```
for(l=0;l<6;l++) {
for(i=0;i<6;i++)
fprintf(fq,"%f  ",sq[j][l][i]);
fprintf(fq,"\n");
}
fflush(fq);

}

fclose(fm);
fclose(fl);
fclose(ft);
fclose(fq);
}



double gft()     /* gets a floating point number */

{

int len,i,flg1,flg2,flg3;
char line[MAXLINE];
double atof();

flg1 = 0;
while( flg1 == 0) {
flg2 = 0;
flg3 = 0;
len = getline(line,MAXLINE);
if( len == 0 )    /* bail out for blank line */
return(-987654.);
++flg1;
for (i=0; line[i] == ' ' || line[i] == '\t' ; i++)
;    /* get rid of leading blanks  */
if (line[i] == '+' || line[i] == '-' )
i++;
for ( ; i < len ; i++) {
if ( line[i]-'0' < 0 || line[i]-'0' >9) {
if( line[i] == '.' && flg2 == 0 )
flg2 = 1;
else if((line[i] == 'e' || line[i] == 'E') && flg3 == 0) {
flg2 = flg3 = 1;
if (line[i+1] =='+' || line[i+1] == '-')
i++;
}
else  {
flg1 = 0;
printf("Unacceptable input, try again: ");
}
}
}
}
return ( atof(line) );
}


getline(s,lim)  /* get line into s, return length */
char s[];
int lim;
{
int c,i;

i=0;
while(--lim > 0 && (c=getchar()) != EOF && c != '\n')
s[i++] = c;
s[i] = '\0';
return(i);
}


git()     /* gets an integer */

{

int len,i,flg1,flg2;
char line[MAXLINE];
int atoi();

flg1 = 0;
while( flg1 == 0) {
flg2 = 0;
len = getline(line,MAXLINE);
if( len == 0 )    /* bail out for blank line */
return(-987654);
++flg1;
for (i=0; line[i] == ' ' || line[i] == '\t' ; i++)
;    /* get rid of leading blanks  */
if (line[i] == '+' || line[i] == '-' )
i++;
```

```
for ( ; i < len ; i++) {
if ( line[i]-'0' < 0 || line[i]-'0' >9 || flg2 == 1 ) {
if( line[i] == '.' && flg2 == 0 )
flg2 = 1;
else  {
flg1 = 0;
printf("Unacceptable input, try again: ");
}
}
}
}
return ( atoi(line) );
}



norl(v,rdst)

double v[];
char rdst[];

{
int i,j,*pt,ifactor;
int a1,a2;
double factor1,factor2,factor,offset;
char o_str[40],digit[2];
char *ptrd;
int bit0,bit1,bit2,bit3,hexdigit,sign;


ptrd = rdst;


/* Evaluate factor and offset for Norland */

/* factor */

sscanf(ptrd,"%2x",&ifactor);
factor1 = pow(2.,((double)ifactor -128.));
for (i=0, factor2=0; i<6; i++) {
strncpy(digit,(ptrd+2+i),1);
digit[1]='\0';
sscanf(digit,"%x",&hexdigit);
bit0 = hexdigit & 1;
bit1 = hexdigit & 2;
bit2 = hexdigit & 4;
bit3 = hexdigit & 8;
if(i == 0) {
if(bit3)
sign = -1;
else
sign = 1;
bit3 = 1;
}
if(bit3) factor2 = factor2 + pow(2.,-(double)(i*4+1));
if(bit2) factor2 = factor2 + pow(2.,-(double)(i*4+2));
if(bit1) factor2 = factor2 + pow(2.,-(double)(i*4+3));
if(bit0) factor2 = factor2 + pow(2.,-(double)(i*4+4));
}
factor = (double) sign * factor1 * factor2;

/* offset */

sscanf((ptrd+8),"%2x",&ifactor);
factor1 = pow(2.,((double)ifactor -128.));
for (i=0, factor2=0; i<6; i++) {
strncpy(digit,(ptrd+10+i),1);
digit[1]='\0';
sscanf(digit,"%x",&hexdigit);
bit0 = hexdigit & 1;
bit1 = hexdigit & 2;
bit2 = hexdigit & 4;
bit3 = hexdigit & 8;
if(i == 0) {
if(bit3)
sign = -1;
else
sign = 1;
bit3 = 1;
}
if(bit3) factor2 = factor2 + pow(2.,-(double)(i*4+1));
if(bit2) factor2 = factor2 + pow(2.,-(double)(i*4+2));
if(bit1) factor2 = factor2 + pow(2.,-(double)(i*4+3));
if(bit0) factor2 = factor2 + pow(2.,-(double)(i*4+4));
}
offset = (double) sign * factor1 * factor2;
/* Find voltage for individual data points */

for(j=0,i=256;i<(2*N0+256);j++,i+=2) {
strncpy(digit,(ptrd+i),1);
```

```
digit[1]='\0';
a1=*digit;
if(a1 < 0 )
a1 +=256;
strncpy(digit,(ptrd+i+1),1);
digit[1]='\0';
a2=*digit;
if(a2 < 0 )
a2 +=256;
v[j]=(a2*256+a1-32768)*factor+offset;
}
}
```

```
/*
  Acquires data using standard single wire probe

  Written:  Ralph Volino       10/09/93


       Command Line:   facq

  This program is used to acquire spectra data from a single wire probe
  using the Norland oscilloscopes.  Raw voltage data is acquired
  and saved for future processing.

*/

#include <stdio.h>
#include <sys/ugpib.h>
#include <fcntl.h>
#include <string.h>
#include <math.h>
#define  BUFSIZE        40
#define  MAXLINE      1000
#define  NOTEXIST       -1
#define  IFA10FF      1.
#define  IFA1GAIN     10.
#define  A1         -1.52481
#define  B1         3.25207
#define  N0         4096


main(argc,argv)
int     argc;
char    *argv[];
{

        int     d11,d15,n,i,j,k;
int  flg,ansr;
        double  tatm,patm,atof(),gft();
        char    mybuf[BUFSIZE],o_str[BUFSIZE];
char    line[MAXLINE];
char name[20],tal[10],filn[20];
char    norbuf[8500];
FILE *fd;


printf("Input a base name for the output files: ");
scanf("%s",name);
getchar();


/*  Open the Norland oscilloscope for reading the IFA-100 output  */
d15=ibfind("dev15");
                if(d15 < 0){
                        fprintf(stderr,"Can't open /dev/dev15 for read\n");
                        exit(1);
                }

/*  Open the motor controller */
d11=ibfind("dev11");
                if(d11 < 0){
                        fprintf(stderr,"Can't open /dev/dev11 for read\n");
                        exit(1);
                }

printf("Do you want to find the wall (y,n)? ");
for (i=0; (ansr = getchar()) != '\n' ; i++)
if (i == 0 && ansr == 'y')
findwall(d11,d15);

for (flg=0; flg == 0 ; ) {
flg++;
printf("Input the atmospheric pressure [in. Hg] ");
patm = gft();
if( patm < 28. || patm > 31.) {
printf("%f is not reasonable, try again.\n", patm);
flg = 0;
}
}
patm *= 25.4;

for (flg=0; flg == 0 ; ) {
flg++;
printf("Input the flow temperature [deg. C] ");
tatm = gft();
if( tatm < 18. || tatm > 35.) {
printf("%f is not reasonable, try again.\n", patm);
flg = 0;
}
}
```

```
/*  Acquire the raw data from the Norlands and store it  */

for( k=0; k<3; k++) {

printf("Set the filter on the IFA-100");
while( (ansr = getchar()) != '\n');

if(k == 0)
sprintf(o_str,"]LAYCL:00001=");
else if(k == 1)
sprintf(o_str,"YCL:0001=");
else
sprintf(o_str,"YCL:001=");

ibwrt(d15,o_str,strlen(o_str));

for( j=0; j<20; j++) {
ibwrt(d15,"R",1);
sleep(k+3);

/*  Open the file for data storage  */

strcpy(filn,name);
ibwrt(d15,"_KCGA",5);
sprintf(o_str,"_%d",k+1);
strcat(filn,o_str);
sprintf(o_str,"_%d",j+1);
strcat(filn,o_str);
fd = fopen(filn,"w");

ibrd(d15,norbuf,8452);
fprintf(fd,"%s",norbuf);
if(j == 0) {
fprintf(fd,"\n%f %f\n",tatm,patm);
fprintf(fd,"%f %f %f %f\n",A1,B1,IFA1OFF,IFA1GAIN);
}
fflush(fd);
fclose(fd);
}
}
}
```

```
double gft()     /* gets a floating point number */

{
#define MAXLINE 1000

int len,i,flg1,flg2,flg3;
char line[MAXLINE];
double atof();

flg1 = 0;
while( flg1 == 0) {
flg2 = 0;
flg3 = 0;
len = getline(line,MAXLINE);
if( len == 0 )    /* bail out for blank line */
return(-987654.);
++flg1;
for (i=0; line[i] == ' ' || line[i] == '\t' ; i++)
;    /* get rid of leading blanks  */
if (line[i] == '+' || line[i] == '-' )
i++;
for ( ; i < len ; i++) {
if ( line[i]-'0' < 0 || line[i]-'0' >9) {
if( line[i] == '.' && flg2 == 0 )
flg2 = 1;
else if((line[i] == 'e' || line[i] == 'E') && flg3 == 0) {
flg2 = flg3 = 1;
if (line[i+1] =='+' || line[i+1] == '-')
i++;
}
else  {
flg1 = 0;
printf("Unacceptable input, try again: ");
}
}
}
}
return ( atof(line) );
}


getline(s,lim)  /* get line into s, return length */
char s[];
int lim;
```

```
{
int c,i;

i=0;
while(--lim > 0 && (c=getchar()) != EOF && c != '\n')
s[i++] = c;
s[i] = '\0';
return(i);
}

findwall(d11,d15)

int  d11,d15;

{
char ansr,o_str[BUFSIZE],norbuf[8452];
double sum,sumo,slope,slopo,volt1[MO];
int ii,j,i,ty,norl();

ibwrt(d11,"Y.D.\n",5);
ibwrt(d11,"Y.B2000.\n",9);
printf("Bring traverse up to wall at fast speed, NOT TOO CLOSE ");
while ( getchar() != '\n');
printf("Switch to AUTO ");
while ( getchar() != '\n');
ibwrt(d11,"Y.B320.\n",8);
printf("Switch to MANUAL and bring probe to wall ");
while ( getchar() != '\n');
printf("Switch to AUTO ");
while ( getchar() != '\n');

sprintf(o_str,"YCL:002=");
ibwrt(d15,o_str,strlen(o_str));

strt: sumo = -999.;
slopo = 999.;

for ( ii = 0; ii < 4; ) {
ibwrt(d15,"R",1);
sleep(11);
ibwrt(d15,"_KCGA",5);
ibrd(d15,norbuf,8452);
norl(volt1,norbuf);
for(sum=0,j=0;j<MO;j++)
sum +=volt1[j];

sum /= MO;
printf("Average Voltage = %g\n",sum);
slope = sum - sumo;
printf("New slope = %f  Old slope = %f\n",slope,slopo);

if(sum < -3.) {
printf("Wire Broken\n");
exit();
}

if(slope > 0.04)
ii +=1;
else
ii = 0;

ibwrt(d11,"Y.M2.G.\n",8);
sleep(1);
slopo = slope;
sumo = sum;

}

printf("Found the wall\n");
ibwrt(d11,"Y.M-11.G.\n",10);

printf("Do you want to find the wall again (y,n)? ");
for (i=0, ty=0; (ansr = getchar()) != '\n' ; i++)
if (i == 0 && ansr == 'y')
ty=1;
if(ty == 1) {
printf("Move in 5 steps manually, switch back to auto ");
while( ansr = getchar() != '\n');
goto strt;
}
}

norl(v,rdst)

double v[];
char rdst[];

{
int i,j,*pt,ifactor;
int a1,a2;
double factor1,factor2,factor,offset;
```

```
char o_str[40],digit[2];
char *ptrd;
int bit0,bit1,bit2,bit3,hexdigit,sign;


ptrd = rdst;


/* Evaluate factor and offset for Borland */

/* factor */

sscanf(ptrd,"%2x",&ifactor);
factor1 = pow(2.,((double)ifactor -128.));
for (i=0, factor2=0; i<6; i++) {
strncpy(digit,(ptrd+2+i),1);
digit[1]='\0';
sscanf(digit,"%x",&hexdigit);
bit0 = hexdigit & 1;
bit1 = hexdigit & 2;
bit2 = hexdigit & 4;
bit3 = hexdigit & 8;
if(i == 0) {
if(bit3)
sign = -1;
else
sign = 1;
bit3 = 1;
}
if(bit3) factor2 = factor2 + pow(2.,-(double)(i*4+1));
if(bit2) factor2 = factor2 + pow(2.,-(double)(i*4+2));
if(bit1) factor2 = factor2 + pow(2.,-(double)(i*4+3));
if(bit0) factor2 = factor2 + pow(2.,-(double)(i*4+4));
}
factor = (double) sign * factor1 * factor2;

/* offset */

sscanf((ptrd+8),"%2x",&ifactor);
factor1 = pow(2.,((double)ifactor -128.));
for (i=0, factor2=0; i<6; i++) {
strncpy(digit,(ptrd+10+i),1);
digit[1]='\0';
sscanf(digit,"%x",&hexdigit);
bit0 = hexdigit & 1;
bit1 = hexdigit & 2;
bit2 = hexdigit & 4;
bit3 = hexdigit & 8;
if(i == 0) {
if(bit3)
sign = -1;
else
sign = 1;
bit3 = 1;
}
if(bit3) factor2 = factor2 + pow(2.,-(double)(i*4+1));
if(bit2) factor2 = factor2 + pow(2.,-(double)(i*4+2));
if(bit1) factor2 = factor2 + pow(2.,-(double)(i*4+3));
if(bit0) factor2 = factor2 + pow(2.,-(double)(i*4+4));
}
offset = (double) sign * factor1 * factor2;
/* Find voltage for individual data points */

for(j=0,i=256;i<(2*N0+256);j++,i+=2) {
strncpy(digit,(ptrd+i),1);
digit[1]='\0';
a1=*digit;
if(a1 < 0 )
a1 +=256;
strncpy(digit,(ptrd+i+1),1);
digit[1]='\0';
a2=*digit;
if(a2 < 0 )
a2 +=256;
v[j]=(a2*256+a1-32768)*factor+offset;
}
}
```

```
/*

Reduces single wire spectra

Written: Ralph Volino        10/10/93

Command Line:   fred

u'2 spectra calculated from saved data
Most of code taken from Numerical Recipes in C

*/

#include <math.h>
#include <malloc.h>
#include <stdio.h>

double *dvector();
void free_dvector();

static double sqrarg;
#define SQR(a) (sqrarg=(a),sqrarg*sqrarg)

#define WINDOW(j,a,b) (1.0-fabs((((j)-1)-(a))*(b)))
/* #define WINDOW(j,a,b) 1.0 */
/* #define WINDOW(j,a,b) (1.0-SQR((((j)-1)-(a))*(b))) */
#define LL      3
#define PWR     0.435
#define M       4096
#define K       10
#define MAXLINE   1000
#define NO      4096

/* spctrm(fp,p,m,k,ovrlap) */
main()
{
FILE *fd;
double p[2050];
int m,k;
int mm,m44,m43,m4,kk,joffn,joff,j2,j;
double w,facp,facm,*w1,sumw=0.0,den=0.0;
int four1();
double ua,upr,total,totalp,hz,tmp;
double off,gain,a1,b1;
int jiff,kp,acq(),nn;
char name[20],filn[20],nam1[20],o_str[30];

printf("Enter the base name of the input files ");
scanf("%s",name);
getchar();

printf("Enter the base name of the output files ");
scanf("%s",filn);
getchar();

k = K;
m = M/2;
mm=m+m;
m43=(m4=mm+mm)+3;
m44=m43+1;
w1=dvector(1,m4);
facm=m-0.5;
facp=1.0/(m+0.5);
for (j=1;j<=mm;j++) sumw += SQR(WINDOW(j,facm,facp));

for (nn=0;nn<LL;nn++) {

den = 0.;
/* Parzen *ua = 0.;
/* Square *upr = 0.;
/* Welch  */
for (j=1;j<=m+2;j++) p[j]=0.0;
for (kk=1;kk<=k;kk++) {
for (joff = -1;joff<=0;joff++) {
jiff=joff+2;
kp = kk*2+joff;
strcpy(nam1,name);
sprintf(o_str,"_%d_%d",nn+1,kp);
strcat(nam1,o_str);
acq(w1,jiff,m4,kp,&total,&totalp,&tmp,&off,&gain,nam1,&a1,&b1);
ua += total;
upr +=totalp;
}
for (j=1;j<=mm;j++) {
j2=j+j;
w=WINDOW(j,facm,facp);
w1[j2] *= w;
w1[j2-1] *= w;
}
four1(w1,mm,1);
```

```
p[1] += (SQR(w1[1])+SQR(w1[2]));
p[m+1] += (SQR(w1[mm+1])+SQR(w1[mm+2]));
for (j=2;j<=m;j++) {
j2=j+j;
p[j] += (SQR(w1[j2])+SQR(w1[j2-1])
+SQR(w1[m44-j2])+SQR(w1[m43-j2]));
}
den += sumw;
}
den *= m4;
ua = ua/2./k;
upr = upr/2./k;

if(nn == 0) hz = 100000.;
else if(nn == 1) hz = 10000.;
else  hz = 1000;

for (j=1;j<=m+1;j++) p[j] = p[j]/(den*hz/mm);

sprintf(o_str,"_%d",LL-nn);
strcpy(nam1,filn);
strcat(nam1,o_str);
fd = fopen(nam1,"w");
fprintf(fd,"%d %f %f %g\n",mm,hz,ua,upr);
for (j=1;j<=m+1;j++) {
fprintf(fd,"%g\n",p[j]);
fflush(fd);
}
fclose(fd);

}
free_dvector(w1,1,m4);
}

#undef SQR
#undef WINDOW

#define SWAP(a,b) tempr=(a);(a)=(b);(b)=tempr

four1(data,nn,isign)
double data[];
int nn,isign;
{
int n,mmax,m,j,istep,i;
double wtemp,wr,wpr,wpi,wi,theta;
double tempr,tempi;

n=nn << 1;
j=1;
for (i=1;i<n;i+=2) {
if (j > i) {
SWAP(data[j],data[i]);
SWAP(data[j+1],data[i+1]);
}
m=n >> 1;
while (m >= 2 && j > m) {
j -= m;
m >>= 1;
}
j += m;
}
mmax=2;
while (n > mmax) {
istep=2*mmax;
theta=6.28318530717959/(isign*mmax);
wtemp=sin(0.5*theta);
wpr = -2.0*wtemp*wtemp;
wpi=sin(theta);
wr=1.0;
wi=0.0;
for (m=1;m<mmax;m+=2) {
for (i=m;i<=n;i+=istep) {
j=i+mmax;
tempr=wr*data[j]-wi*data[j+1];
tempi=wr*data[j+1]+wi*data[j];
data[j]=data[i]-tempr;
data[j+1]=data[i+1]-tempi;
data[i] += tempr;
data[i+1] += tempi;
}
wr=(wtemp=wr)*wpr-wi*wpi+wr;
wi=wi*wpr+wtemp*wpi+wi;
}
mmax=istep;
}
}

#undef SWAP

acq(w1,jiff,m4,kp,total,totalp,tmp,off,gain,nam1,a1,b1)
```

```
double w1[],*total,*totalp,*tmp,*off,*gain,*a1,*b1;
char   nam1[];
int    m4,jiff,kp;

{
char norb[9000],line[MAXLINE];
char s1[10],s2[10],s3[10],s4[10];
int  norl(),i,j;
FILE *fp;
double volt[NO],vlt,a,b,tm,of,gn,ctmp,pw;
double t1,t2;

fp = fopen(nam1,"r");
/* fscanf(fp,"%s",norb);  */
fgets(norb,9000,fp);

if(kp == 1) {
fgets(line,MAXLINE,fp);
fgets(line,MAXLINE,fp);
fgets(line,MAXLINE,fp);
sscanf(line,"%s %s",s1,s2);
*tmp = atof(s1);
fgets(line,MAXLINE,fp);
sscanf(line,"%s %s %s %s",s1,s2,s3,s4);
*a1 = atof(s1);
*b1 = atof(s2);
*off = atof(s3);
*gain = atof(s4);
}
fclose(fp);
norl(volt,norb);
pw = 1./PWR;
a = *a1;
b = *b1;
of = *off;
gn = *gain;
tm = *tmp;
ctmp = pow(225./(250.- tm),0.5);

for(j=jiff,t1=0,t2=0,i=0;j<=m4;j+=2,i++) {
vlt = volt[i]/gn+of;
vlt *= ctmp;
w1[j] = pow((a+b*vlt*vlt),pw);
t1 += w1[j];
t2 += w1[j]*w1[j];
}
*total = t1/m4*2.;
*totalp = (t2-t1*t1/m4*2.)/(m4/2.-1.);
printf("%d   U = %f    u'2 = %f\n",kp,*total,*totalp);

for(j=jiff;j<=m4;j +=2)
w1[j] -= *total;
}

norl(v,rdst)

double v[];
char rdst[];

{
int i,j,*pt,ifactor;
int a1,a2;
double factor1,factor2,factor,offset;
char o_str[40],digit[2];
char *ptrd;
int bit0,bit1,bit2,bit3,hexdigit,sign;


ptrd = rdst;


/* Evaluate factor and offset for Norland */

/* factor */

sscanf(ptrd,"%2x",&ifactor);
factor1 = pow(2.,((double)ifactor -128.));
for (i=0, factor2=0; i<6; i++) {
strncpy(digit,(ptrd+2+i),1);
digit[1]='\0';
sscanf(digit,"%x",&hexdigit);
bit0 = hexdigit & 1;
bit1 = hexdigit & 2;
bit2 = hexdigit & 4;
bit3 = hexdigit & 8;
if(i == 0) {
if(bit3)
sign = -1;
else
```

```
sign = 1;
bit3 = 1;
}
if(bit3) factor2 = factor2 + pow(2.,-(double)(i*4+1));
if(bit2) factor2 = factor2 + pow(2.,-(double)(i*4+2));
if(bit1) factor2 = factor2 + pow(2.,-(double)(i*4+3));
if(bit0) factor2 = factor2 + pow(2.,-(double)(i*4+4));
}
factor = (double) sign * factor1 * factor2;

/* offset */

sscanf((ptrd+8),"%2x",&ifactor);
factor1 = pow(2.,((double)ifactor -128.));
for (i=0, factor2=0; i<6; i++) {
strncpy(digit,(ptrd+10+i),1);
digit[1]='\0';
sscanf(digit,"%x",&hexdigit);
bit0 = hexdigit & 1;
bit1 = hexdigit & 2;
bit2 = hexdigit & 4;
bit3 = hexdigit & 8;
if(i == 0) {
if(bit3)
sign = -1;
else
sign = 1;
bit3 = 1;
}
if(bit3) factor2 = factor2 + pow(2.,-(double)(i*4+1));
if(bit2) factor2 = factor2 + pow(2.,-(double)(i*4+2));
if(bit1) factor2 = factor2 + pow(2.,-(double)(i*4+3));
if(bit0) factor2 = factor2 + pow(2.,-(double)(i*4+4));
}
offset = (double) sign * factor1 * factor2;
/* Find voltage for individual data points */

for(j=0,i=256;i<(2*[illegible]0+256);j++,i+=2) {
strncpy(digit,(ptrd+i),1);
digit[1]='\0';
a1=*digit;
if(a1 < 0 )
a1 +=256;
strncpy(digit,(ptrd+i+1),1);
digit[1]='\0';
a2=*digit;
if(a2 < 0 )
a2 +=256;
v[j]=(a2*256+a1-32768)*factor+offset;
}
}

double *dvector(nl,nh)
int nl,nh;
{
double *v;

v=(double *)malloc((unsigned) (nh-nl+1)*sizeof(double));
return v-nl;
}


void free_dvector(v,nl,nh)
double *v;
int nl,nh;
{
free((char*) (v+nl));
}
```

```
/*
  Acquires data using standard cross wire probe

  Written:  Ralph Volino       10/09/93

        Command Line:   cacq

  This program is used to acquire spectra data from a cross wire probe
  using the Norland oscilloscopes.  Raw voltage data is acquired
  and saved for future processing.

*/

#include <stdio.h>
#include <sys/ugpib.h>
#include <fcntl.h>
#include <string.h>
#include <math.h>
#define  BUFSIZE        40
#define  MAXLINE      1000
#define  NOTEXIST       -1
#define  IFA1OFF         1.
#define  IFA1GAIN       10.
#define  IFA2OFF         1.
#define  IFA2GAIN       10.
#define  A1            -1.56300
#define  B1             3.26381
#define  A2            -1.56938
#define  B2             3.15397


main(argc,argv)
int     argc;
char    *argv[];
{

        int     d15,n,i,j,k;
int  flg,ansr;
        double  tatm,patm,atof(),gft();
        char    mybuf[BUFSIZE],o_str[BUFSIZE];
char    line[MAXLINE];
char name[20],tal[10],filn[20];
char    norbuf[8500];
FILE *fd;

printf("Input a base name for the output files: ");
scanf("%s",name);
getchar();

/*  Open the Norland oscilloscope for reading the IFA-100 output  */
d15=ibfind("dev15");
                if(d15 < 0){
                        fprintf(stderr,"Can't open /dev/dev15 for read\n");
                        exit(1);
                }


for (flg=0; flg == 0 ; ) {
flg++;
printf("Input the atmospheric pressure [in. Hg] ");
patm = gft();
if( patm < 28. || patm > 31.) {
printf("%f is not reasonable, try again.\n", patm);
flg = 0;
}
}
patm *= 25.4;

for (flg=0; flg == 0 ; ) {
flg++;
printf("Input the flow temperature [deg. C] ");
tatm = gft();
if( tatm < 18. || tatm > 35.) {
printf("%f is not reasonable, try again.\n", patm);
flg = 0;
}
}


/*  Acquire the raw data from the Norlands and store it  */

for( k=0; k<3; k++) {

printf("Set the filter on the IFA-100");
while( (ansr = getchar()) != '\n');
```

```
if(k == 0)
sprintf(o_str,"]LAYCL:00001=");
else if(k == 1)
sprintf(o_str,"YCL:0001=");
else
sprintf(o_str,"YCL:001=");

ibwrt(d15,o_str,strlen(o_str));

for( j=0; j<20; j++) {
ibwrt(d15,"R",1);
sleep(k+3);

/*  Open the files for data storage  */

strcpy(filn,name);
ibwrt(d15,"_KCGA",5);
sprintf(o_str,"_%d",k+1);
strcat(filn,o_str);
sprintf(o_str,"_%da",j+1);
strcat(filn,o_str);
fd = fopen(filn,"w");

ibrd(d15,norbuf,8452);
fprintf(fd,"%s",norbuf);
if(j == 0)
fprintf(fd,"\n%f %f\n",tatm,patm);
fprintf(fd,"%f %f %f %f\n",A1,A2,B1,B2);
fprintf(fd,"%f %f %f %f\n",IFA1OFF,IFA1GAIN,IFA2OFF,IFA2GAIN);

fflush(fd);
fclose(fd);

strcpy(filn,name);
ibwrt(d15,"_KCGC",5);
sprintf(o_str,"_%d",k+1);
strcat(filn,o_str);
sprintf(o_str,"_%db",j+1);
strcat(filn,o_str);
fd = fopen(filn,"w");

ibrd(d15,norbuf,8452);
fprintf(fd,"%s",norbuf);
if(j == 0)
fprintf(fd,"\n%f %f\n",tatm,patm);
fprintf(fd,"%f %f %f %f\n",A1,A2,B1,B2);
fprintf(fd,"%f %f %f %f\n",IFA1OFF,IFA1GAIN,IFA2OFF,IFA2GAIN);
fflush(fd);
fclose(fd);
}
}
}



double gft()     /* gets a floating point number */

{
#define MAXLINE 1000

int len,i,flg1,flg2,flg3;
char line[MAXLINE];
double atof();

flg1 = 0;
while( flg1 == 0) {
flg2 = 0;
flg3 = 0;
len = getline(line,MAXLINE);
if( len == 0 )    /* bail out for blank line */
return(-987654.);
++flg1;
for (i=0; line[i] == ' ' || line[i] == '\t' ; i++)
;    /* get rid of leading blanks  */
if (line[i] == '+' || line[i] == '-' )
i++;
for ( ; i < len ; i++) {
if ( line[i]-'0' < 0 || line[i]-'0' >9) {
if( line[i] == '.' && flg2 == 0 )
flg2 = 1;
else if((line[i] == 'e' || line[i] == 'E') && flg3 == 0) {
flg2 = flg3 = 1;
if (line[i+1] =='+' || line[i+1] == '-')
i++;
}
else  {
flg1 = 0;
printf("Unacceptable input, try again: ");
}
```

```
}
}
}
return ( atof(line) );
}


getline(s,lim)  /* get line into s, return length */
char s[];
int lim;
{
int c,i;

i=0;
while(--lim > 0 && (c=getchar()) != EOF && c != '\n')
s[i++] = c;
s[i] = '\0';
return(i);
}
```

```
/*

Reduces cross wire spectra

Written: Ralph Volino    10/10/93

Command Line:  cred

Reduces stored data from the cross wire for
u'2 and v'2 spectra

*/

#include <math.h>
#include <malloc.h>
#include <stdio.h>

double *dvector();
void free_dvector();

static double sqrarg;
#define SQR(a) (sqrarg=(a),sqrarg*sqrarg)

#define WINDOW(j,a,b) (1.0-fabs((((j)-1)-(a))*(b)))    /* Parzen */
/* #define WINDOW(j,a,b) 1.0 */                        /* Square */
/* #define WINDOW(j,a,b) (1.0-SQR((((j)-1)-(a))*(b))) */ /* Welch */
#define LL      3
#define PWR    0.435
#define M      4096
#define K      10
#define MAXLINE   1000
#define N0     4096

/* spctrm(fp,p,m,k,ovrlap) */
main()
{
FILE *fd;
double p[2050],pv[2050];
int m,k;
int mm,m44,m43,m4,kk,joffn,joff,j2,j;
double w,facp,facm,*w1,*w2,sumw=0.0,den=0.0;
int four1();
double ua,upr,totu,totup,totv,totvp,totuv,va,vpr,hz,tmp;
double off1,gain1,off2,gain2,a1,b1,a2,b2;
int jiff,kp,acq(),nn;

char name[40],filn[40],nam1[40],o_str[30];

printf("Enter the base name of the input files ");
scanf("%s",name);
getchar();

printf("Enter the base name of the output files ");
scanf("%s",filn);
getchar();

k = K;
m = M/2;
mm=m+m;
m43=(m4=mm+mm)+3;
m44=m43+1;
w1=dvector(1,m4);
w2=dvector(1,m4);
facm=m-0.5;
facp=1.0/(m+0.5);
for (j=1;j<=mm;j++) sumw += SQR(WINDOW(j,facm,facp));

for (nn=0;nn<LL;nn++) {

den = 0.;
ua = 0.;
upr = 0.;
va = 0.;
vpr = 0.;

for (j=1;j<=m+2;j++) {
p[j]=0.0;
pv[j]=0.0;
}
for (kk=1;kk<=k;kk++) {
for (joff = -1;joff<=0;joff++) {
jiff=joff+2;
kp = kk*2+joff;
strcpy(nam1,name);
sprintf(o_str,"_%d_%d",nn+1,kp);
strcat(nam1,o_str);
acq(w1,w2,jiff,m4,kp,&totu,&totup,&totv,&totvp,&tmp;
&off1,&gain1,&off2,&gain2,nam1,&a1,&b1,&a2,&b2,&totuv);
ua += totu;
upr +=totup;
va += totv;
```

```
vpr +=totvp;
}
for (j=1;j<=mm;j++) {
j2=j+j;
w=WINDOW(j,facm,facp);
w1[j2] *= w;
w1[j2-1] *= w;
w2[j2] *= w;
w2[j2-1] *= w;
}
four1(w1,mm,1);
four1(w2,mm,1);

p[1] += (SQR(w1[1])+SQR(w1[2]));
p[m+1] += (SQR(w1[mm+1])+SQR(w1[mm+2]));

pv[1] += (SQR(w2[1])+SQR(w2[2]));
pv[m+1] += (SQR(w2[mm+1])+SQR(w2[mm+2]));

for (j=2;j<=m;j++) {
j2=j+j;
p[j] += (SQR(w1[j2])+SQR(w1[j2-1])
+SQR(w1[m44-j2])+SQR(w1[m43-j2]));
pv[j] += (SQR(w2[j2])+SQR(w2[j2-1])
+SQR(w2[m44-j2])+SQR(w2[m43-j2]));
}
den += sumw;
}
den *= m4;
ua = ua/2./k;
upr = upr/2./k;
va = va/2./k;
vpr = vpr/2./k;

if(nn == 0) hz = 100000.;
else if(nn == 1) hz = 10000.;
else  hz = 1000;

for (j=1;j<=m+1;j++) {
p[j] /= (den*hz/mm);
pv[j] /= (den*hz/mm);
}

sprintf(o_str,"_%du",LL-nn);
strcpy(nam1,filn);
strcat(nam1,o_str);
fd = fopen(nam1,"w");
fprintf(fd,"%d %f %f %g\n",mm,hz,ua,upr);
for (j=1;j<=m+1;j++)
fprintf(fd,"%g\n",p[j]);
fclose(fd);

sprintf(o_str,"_%dv",LL-nn);
strcpy(nam1,filn);
strcat(nam1,o_str);
fd = fopen(nam1,"w");
fprintf(fd,"%d %f %f %g %g\n",mm,hz,ua,va,vpr);
for (j=1;j<=m+1;j++)
fprintf(fd,"%g\n",pv[j]);
fclose(fd);

}
free_dvector(w1,1,m4);
free_dvector(w2,1,m4);
}

#undef SQR
#undef WINDOW

#define SWAP(a,b) tempr=(a);(a)=(b);(b)=tempr

four1(data,nn,isign)
double data[];
int nn,isign;
{
int n,mmax,m,j,istep,i;
double wtemp,wr,wpr,wpi,wi,theta;
double tempr,tempi;

n=nn << 1;
j=1;
for (i=1;i<n;i+=2) {
if (j > i) {
SWAP(data[j],data[i]);
SWAP(data[j+1],data[i+1]);
}
m=n >> 1;
while (m >= 2 && j > m) {
j -= m;
m >>= 1;
```

```
}
j += m;
}
mmax=2;
while (n > mmax) {
istep=2*mmax;
theta=6.28318530717959/(isign*mmax);
wtemp=sin(0.5*theta);
wpr = -2.0*wtemp*wtemp;
wpi=sin(theta);
wr=1.0;
wi=0.0;
for (m=1;m<mmax;m+=2) {
for (i=m;i<=n;i+=istep) {
j=i+mmax;
tempr=wr*data[j]-wi*data[j+1];
tempi=wr*data[j+1]+wi*data[j];
data[j]=data[i]-tempr;
data[j+1]=data[i+1]-tempi;
data[i] += tempr;
data[i+1] += tempi;
}
wr=(wtemp=wr)*wpr-wi*wpi+wr;
wi=wi*wpr+wtemp*wpi+wi;
}
mmax=istep;
}
}

#undef SWAP

acq(w1,w2,jiff,m4,kp,totu,totup,totv,totvp,tmp,off1;
gain1,off2,gain2,nam1,a1,b1,a2,b2,totuv)

double w1[],*totu,*totup,*tmp,*off1,*gain1,*a1,*b1;
double w2[],*totv,*totvp,*off2,*gain2,*a2,*b2,*totuv;
char   nam1[];
int    m4,jiff,kp;

{
char norb[8452],line[MAXLINE],nme[40];
char s1[10],s2[10],s3[10],s4[10];
int  norl(),i,j;
FILE *fp;
double volt1[NO],vlt,ax,bx,ay,by,tm,of1,gn1,of2,gn2,ctmp,pw;
double t1,t2,t3,t4,t5,volt2[NO],c2th;
double cfv,cfuv,ld,kt,scfv,vlx,vly;

strcpy(nme,nam1);
strcat(nme,"a");
fp = fopen(nme,"r");
fgets(norb,8500,fp);
if(kp == 1) {
fgets(line,MAXLINE,fp);
fgets(line,MAXLINE,fp);
fgets(line,MAXLINE,fp);
sscanf(line,"%s %s",s1,s2);
*tmp = atof(s1);
fgets(line,MAXLINE,fp);
sscanf(line,"%s %s %s %s",s1,s2,s3,s4);
*a1 = atof(s1);
*b1 = atof(s3);
*a2 = atof(s2);
*b2 = atof(s4);
fgets(line,MAXLINE,fp);
sscanf(line,"%s %s %s %s",s1,s2,s3,s4);
*off1 = atof(s1);
*gain1 = atof(s2);
*off2 = atof(s3);
*gain2 = atof(s4);
}
fclose(fp);

norl(volt1,norb);

strcpy(nme,nam1);
strcat(nme,"b");
fp = fopen(nme,"r");
fgets(norb,8500,fp);
fclose(fp);

norl(volt2,norb);

pw = 1./PWR;
ld=320.;
kt = -5.e-4*ld+0.3;
cfuv = (1.+kt*kt)/(1.-kt*kt);
cfv = (1.+kt*kt)/(1.-3.*kt*kt+4.*kt*kt*kt*kt);
scfv = pow(cfv,0.5);
```

```
ax = *a1;
bx = *b1;
ay = *a2;
by = *b2;
of1 = *off1;
gn1 = *gain1;
of2 = *off2;
gn2 = *gain2;
tm = *tmp;
ctmp = pow(225./(250.- tm),0.5);
c2th = 2.*cos(0.785398);

for(j=jiff,t1=t2=t3=t4=t5=0,i=0;j<=m4;j+=2,i++) {
vlx = volt1[i]/gn1+of1;
vlx *= ctmp;
vly = volt2[i]/gn2+of2;
vly *= ctmp;
vlx = pow((ax+bx*vlx*vlx),pw);
vly = pow((ay+by*vly*vly),pw);
w1[j] = (vlx+vly)/c2th;
w2[j] = (vly-vlx)/c2th;
t1 += w1[j];
t2 += w1[j]*w1[j];
t3 += w2[j];
t4 += w2[j]*w2[j];
t5 += w1[j]*w2[j];
}
*totu = t1/m4*2.;
*totv = t3/m4*2.;
*totup = (t2-t1*t1/m4*2.)/(m4/2.-1.);
*totvp = (t4-t3*t3/m4*2.)/(m4/2.-1.)*cfv;
*totuv = (t5-t1*t3/m4*2.)/(m4/2.)*cfuv;

printf("%d  U = %f    u'2 = %f\n",kp,*totu,*totup);
printf("v'2 = %f    u'v' = %f\n",*totvp,*totuv);

for(j=jiff;j<=m4;j+=2) {
w1[j] -= *totu;
w2[j] -= *totv;
w2[j] *= scfv;
}
}

norl(v,rdst)
```

```
double v[];
char rdst[];

{
int i,j,*pt,ifactor;
int a1,a2;
double factor1,factor2,factor,offset;
char o_str[40],digit[2];
char *ptrd;
int bit0,bit1,bit2,bit3,hexdigit,sign;


ptrd = rdst;


/* Evaluate factor and offset for Norland */

/* factor */

sscanf(ptrd,"%2x",&ifactor);
factor1 = pow(2.,((double)ifactor -128.));
for (i=0, factor2=0; i<6; i++) {
strncpy(digit,(ptrd+2+i),1);
digit[1]='\0';
sscanf(digit,"%x",&hexdigit);
bit0 = hexdigit & 1;
bit1 = hexdigit & 2;
bit2 = hexdigit & 4;
bit3 = hexdigit & 8;
if(i == 0) {
if(bit3)
sign = -1;
else
sign = 1;
bit3 = 1;
}
if(bit3) factor2 = factor2 + pow(2.,-(double)(i*4+1));
if(bit2) factor2 = factor2 + pow(2.,-(double)(i*4+2));
if(bit1) factor2 = factor2 + pow(2.,-(double)(i*4+3));
if(bit0) factor2 = factor2 + pow(2.,-(double)(i*4+4));
}
factor = (double) sign * factor1 * factor2;

/* offset */
```

```
sscanf((ptrd+8),"%2x",&ifactor);
factor1 = pow(2.,((double)ifactor -128.));
for (i=0, factor2=0; i<6; i++) {
strncpy(digit,(ptrd+10+i),1);
digit[1]='\0';
sscanf(digit,"%x",&hexdigit);
bit0 = hexdigit & 1;
bit1 = hexdigit & 2;
bit2 = hexdigit & 4;
bit3 = hexdigit & 8;
if(i == 0) {
if(bit3)
sign = -1;
else
sign = 1;
bit3 = 1;
}
if(bit3) factor2 = factor2 + pow(2.,-(double)(i*4+1));
if(bit2) factor2 = factor2 + pow(2.,-(double)(i*4+2));
if(bit1) factor2 = factor2 + pow(2.,-(double)(i*4+3));
if(bit0) factor2 = factor2 + pow(2.,-(double)(i*4+4));
}
offset = (double) sign * factor1 * factor2;
/* Find voltage for individual data points */

for(j=0,i=256;i<(2*NO+256);j++,i+=2) {
strncpy(digit,(ptrd+i),1);
digit[1]='\0';
a1=*digit;
if(a1 < 0 )
a1 +=256;
strncpy(digit,(ptrd+i+1),1);
digit[1]='\0';
a2=*digit;
if(a2 < 0 )
a2 +=256;
v[j]=(a2*256+a1-32768)*factor+offset;
}
}

double *dvector(nl,nh)
int nl,nh;
{
double *v;
v=(double *)malloc((unsigned) (nh-nl+1)*sizeof(double));
return v-nl;
}


void free_dvector(v,nl,nh)
double *v;
int nl,nh;
{
free((char*) (v+nl));
}
```

```
/*

Reduces u'v' spectra

Written:  Ralph Volino    10/12/93

Command Line:  hred

Reduces voltages to get u'v' spectra
Much of code taken from Numerical Recipes in C

*/

#include <math.h>
#include <stdio.h>
#include <malloc.h>

double *dvector();
void free_dvector();

static double sqrarg;
#define SQR(a) (sqrarg=(a),sqrarg*sqrarg)

#define WINDOW(j,a,b) (1.0-fabs((((j)-1)-(a))*(b)))
/* #define WINDOW(j,a,b) 1.0 */
/* #define WINDOW(j,a,b) (1.0-SQR((((j)-1)-(a))*(b))) */
#define LL      3
#define PWR     0.435
#define M       4096
#define K       10
#define MAXLINE   1000
#define NO      4096

/* spctrm(fp,p,m,k,ovrlap) */
main()
{
FILE *fd;
double p[2050];
int m,k;
int mm,m44,m43,m4,kk,joff,j2,j;
double w,facp,facm,*w1,*w2,sumw=0.0,den=0.0;
int four1();
double ua,upr,totu,totup,totv,totvp,totuv,va,vpr,hz,tmp;
double off1,gain1,off2,gain2,a1,b1,a2,b2,upvp;
int jiff,kp,acq(),nn;

char name[40],filn[40],nam1[40],o_str[40];

printf("Enter the base name of the input files ");
scanf("%s",name);
getchar();

printf("Enter the base name of the output files ");
scanf("%s",filn);
getchar();

k = K;
m = M/2;
mm=m+m;
m43=(m4=mm+mm)+3;
m44=m43+1;
w1=dvector(1,m4);
w2=dvector(1,m4);
facm=m-0.5;
facp=1.0/(m+0.5);
for (j=1;j<=mm;j++) sumw += SQR(WINDOW(j,facm,facp));

for (nn=0;nn<LL;nn++) {

/* Parzen */ den = 0.;
/* Square */ va = 0.;
/* Welch  */ vpr = 0.;
             va = 0.;
             vpr = 0.;
             upvp = 0.;

             for (j=1;j<=m+2;j++) {
             p[j]=0.0;
             }
             for (kk=1;kk<=k;kk++) {
             for (joff = -1;joff<=0;joff++) {
             jiff=joff+2;
             kp = kk*2+joff;
             strcpy(nam1,name);
             sprintf(o_str,"_%d_%d",nn+1,kp);
             strcat(nam1,o_str);
             acq(w1,w2,m4,kp,&totu,&totup,&totv,&totvp,&tmp;
             &off1,&gain1,&off2,&gain2,nam1,&a1,&b1,&a2,&b2,&totuv,jiff);
             ua += totu;
             upr +=totup;
             va += totv;
```

```
vpr +=totvp;
upvp +=totuv;
}
for (j=1;j<=mm;j++) {
j2=j+j;
w=WINDOW(j,facm,facp);
w1[j2] *= w;
w1[j2-1] *= w;
w2[j2] *= w;
w2[j2-1] *= w;
}
four1(w1,mm,1);
four1(w2,mm,1);
p[1] = 0;
p[m+1] += w1[mm+1]*w1[mm+4]+w1[mm+2]*w1[mm+3];
p[m+1] += w2[mm+1]*w2[mm+4]+w2[mm+2]*w2[mm+3];


for (j=2;j<=m;j++) {
j2=j+j;
p[j] += w1[j2]*w1[m43-j2]+w1[j2-1]*w1[m44-j2];
p[j] += w2[j2]*w2[m43-j2]+w2[j2-1]*w2[m44-j2];
}
den += sumw;
}
den *= m4;
ua = ua/2./k;
upr = upr/2./k;
va = va/2./k;
vpr = vpr/2./k;
upvp = upvp/2./k,

if(nn == 0) hz = 100000.;
else if(nn == 1) hz = 10000.;
else  hz = 1000;

for (j=1;j<=m+1;j++) {
p[j] /= (den*hz/mm);
}

sprintf(o_str,"_%ds",LL-nn);
strcpy(nam1,filn);
strcat(nam1,o_str);
fd = fopen(nam1,"w");
fprintf(fd,"%d %f %f %f %g %g %g\n",mm,hz,ua,va,upr,vpr,upvp);
for (j=1;j<=m+1;j++)
fprintf(fd,"%g\n",-p[j]);
fclose(fd);

}
free_dvector(w1,1,m4);
free_dvector(w2,1,m4);
}

#undef SQR
#undef WINDOW

#define SWAP(a,b) tempr=(a);(a)=(b);(b)=tempr

four1(data,nn,isign)
double data[];
int nn,isign;
{
int n,mmax,m,j,istep,i;
double wtemp,wr,wpr,wpi,wi,theta;
double tempr,tempi;

n=nn << 1;
j=1;
for (i=1;i<n;i+=2) {
if (j > i) {
SWAP(data[j],data[i]);
SWAP(data[j+1],data[i+1]);
}
m=n >> 1;
while (m >= 2 && j > m) {
j -= m;
m >>= 1;
}
j += m;
}
mmax=2;
while (n > mmax) {
istep=2*mmax;
theta=6.28318530717959/(isign*mmax);
wtemp=sin(0.5*theta);
wpr = -2.0*wtemp*wtemp;
wpi=sin(theta);
wr=1.0;
wi=0.0;
```

```
for (m=1;m<mmax;m+=2) {
for (i=m;i<=n;i+=istep) {
j=i+mmax;
tempr=wr*data[j]-wi*data[j+1];
tempi=wr*data[j+1]+wi*data[j];
data[j]=data[i]-tempr;
data[j+1]=data[i+1]-tempi;
data[i] += tempr;
data[i+1] += tempi;
}
wr=(wtemp=wr)*wpr-wi*wpi+wr;
wi=wi*wpr+wtemp*wpi+wi;
}
mmax=istep;
}
}

#undef SWAP

acq(w1,w2,m4,kp,totu,totup,totv,totvp,tmp;
off1,gain1,off2,gain2,nam1,a1,b1,a2,b2,totuv,jiff)

double w1[],w2[],*totu,*totup,*tmp,*off1,*gain1,*a1,*b1;
double *totv,*totvp,*off2,*gain2,*a2,*b2,*totuv;
char   nam1[];
int    m4,kp,jiff;

{
char norb[8452],line[MAXLINE],nme[40];
char s1[10],s2[10],s3[10],s4[10];
int  norl(),i,j;
FILE *fp;
double volt1[M0],vlt,ax,bx,ay,by,tm,of1,gn1,of2,gn2,ctmp,pw;
double t1,t2,t3,t4,t5,volt2[M0],c2th;
double cfv,cfuv,ld,kt,scfv,vlx,vly;
double up[M0],vp[M0];


strcpy(nme,nam1);
strcat(nme,"a");
fp = fopen(nme,"r");
fgets(norb,8500,fp);

if(kp == 1) {
fgets(line,MAXLINE,fp);
fgets(line,MAXLINE,fp);
fgets(line,MAXLINE,fp);
sscanf(line,"%s %s",s1,s2);
*tmp = atof(s1);
fgets(line,MAXLINE,fp);
sscanf(line,"%s %s %s %s",s1,s2,s3,s4);
*a1 = atof(s1);
*b1 = atof(s3);
*a2 = atof(s2);
*b2 = atof(s4);
fgets(line,MAXLINE,fp);
sscanf(line,"%s %s %s %s",s1,s2,s3,s4);
*off1 = atof(s1);
*gain1 = atof(s2);
*off2 = atof(s3);
*gain2 = atof(s4);
}
fclose(fp);

norl(volt1,norb);

strcpy(nme,nam1);
strcat(nme,"b");
fp = fopen(nme,"r");
fgets(norb,8500,fp);
fclose(fp);

norl(volt2,norb);

pw = 1./PWR;
ld=320.;
kt = -5.e-4*ld+0.3;
cfuv = (1.+kt*kt)/(1.-kt*kt);
cfv = (1.+kt*kt)/(1.-3.*kt*kt+4.*kt*kt*kt*kt);
scfv = pow(cfv,0.5);

ax = *a1;
bx = *b1;
ay = *a2;
by = *b2;
of1 = *off1;
gn1 = *gain1;
of2 = *off2;
gn2 = *gain2;
tm = *tmp;
```

```
ctmp = pow(225./(250.- tm),0.5);
c2th = 2.*cos(0.785398);

for(t1=t2=t3=t4=t5=0,i=0;i<m4/2;i++) {
vlx = volt1[i]/gn1+of1;
vlx *= ctmp;
vly = volt2[i]/gn2+of2;
vly *= ctmp;
vlx = pow((ax+bx*vlx*vlx),pw);
vly = pow((ay+by*vly*vly),pw);
up[i] = (vlx+vly)/c2th;
vp[i] = (vly-vlx)/c2th;

t1 += up[i];
t2 += up[i]*up[i];
t3 += vp[i];
t4 += vp[i]*vp[i];
t5 += up[i]*vp[i];
}
*totu = t1/m4*2.;
*totv = t3/m4*2.;
*totup = (t2-t1*t1/m4*2.)/(m4/2.-1.);
*totvp = (t4-t3*t3/m4*2.)/(m4/2.-1.)*cfv;
*totuv = (t5-t1*t3/m4*2.)/(m4/2.)*cfuv;

printf("%d  U = %f    u'2 = %f\n",kp,*totu,*totup);
printf("v'2 = %f    u'v' = %f\n",*totvp,*totuv);

for(j=1,i=0;j<=m4;j+=2,i++) {
if(jiff ==1) {
w1[j] = up[i] - *totu;
w1[j+1] = vp[i] - *totv;
w1[j+1] *= cfuv;
}
else {
w2[j] = up[i] - *totu;
w2[j+1] = vp[i] - *totv;
w2[j+1] *= cfuv;
}
}
}

norl(v,rdst)

double v[];
```

```
char rdst[];

{
int i,j,*pt,ifactor;
int a1,a2;
double factor1,factor2,factor,offset;
char o_str[40],digit[2];
char *ptrd;
int bit0,bit1,bit2,bit3,hexdigit,sign;


ptrd = rdst;


/* Evaluate factor and offset for Borland */

/* factor */

sscanf(ptrd,"%2x",&ifactor);
factor1 = pow(2.,((double)ifactor -128.));
for (i=0, factor2=0; i<6; i++) {
strncpy(digit,(ptrd+2+i),1);
digit[1]='\0';
sscanf(digit,"%x",&hexdigit);
bit0 = hexdigit & 1;
bit1 = hexdigit & 2;
bit2 = hexdigit & 4;
bit3 = hexdigit & 8;
if(i == 0) {
if(bit3)
sign = -1;
else
sign = 1;
bit3 = 1;
}
if(bit3) factor2 = factor2 + pow(2.,-(double)(i*4+1));
if(bit2) factor2 = factor2 + pow(2.,-(double)(i*4+2));
if(bit1) factor2 = factor2 + pow(2.,-(double)(i*4+3));
if(bit0) factor2 = factor2 + pow(2.,-(double)(i*4+4));
}
factor = (double) sign * factor1 * factor2;

/* offset */

sscanf((ptrd+8),"%2x",&ifactor);
```

```
factor1 = pow(2.,((double)ifactor -128.));
for (i=0, factor2=0; i<6; i++) {
strncpy(digit,(ptrd+10+i),1);
digit[1]='\0';
sscanf(digit,"%x",&hexdigit);
bit0 = hexdigit & 1;
bit1 = hexdigit & 2;
bit2 = hexdigit & 4;
bit3 = hexdigit & 8;
if(i == 0) {
if(bit3)
sign = -1;
else
sign = 1;
bit3 = 1;
}
if(bit3) factor2 = factor2 + pow(2.,-(double)(i*4+1));
if(bit2) factor2 = factor2 + pow(2.,-(double)(i*4+2));
if(bit1) factor2 = factor2 + pow(2.,-(double)(i*4+3));
if(bit0) factor2 = factor2 + pow(2.,-(double)(i*4+4));
}
offset = (double) sign * factor1 * factor2;
/* Find voltage for individual data points */

for(j=0,i=256;i<(2*NO+256);j++,i+=2) {
strncpy(digit,(ptrd+i),1);
digit[1]='\0';
a1=*digit;
if(a1 < 0 )
a1 +=256;
strncpy(digit,(ptrd+i+1),1);
digit[1]='\0';
a2=*digit;
if(a2 < 0 )
a2 +=256;
v[j]=(a2*256+a1-32768)*factor+offset;
}
}

double *dvector(nl,nh)
int nl,nh;
{
double *v;

v=(double *)malloc((unsigned) (nh-nl+1)*sizeof(double));
return v-nl;
}


void free_dvector(v,nl,nh)
double *v;
int nl,nh;
{
free((char*) (v+nl));
}
```

```
      program swcr
c
c      Calculates single hot-wire calibration using data generated by
c      program s_cal.c
c
c      v is velocity array, e is hot-wire voltage array
c
      real v(50),e(50),vc(50),pd(50)
      character*15 f$
      character*15 a$
      write(*,*) "Input the file name of the calibration data"
      read(*,'(a)') f$
      open(10,file=f$,status="old")
      read(10,*) n
      do 30 i=1,n
      read(10,*) v(i),e(i)
30      continue
      close(10)
c
c      power in King's law is 0.435
c
      pwr=0.435
      pw=1./pwr
70      continue
      sum1=0.
      sum2=0.
      sum3=0.
      sum4=0.
      do 40 i=1,n
      x=e(i)**2.
      y=v(i)**pwr
      sum1=sum1+x
      sum2=sum2+y
      sum3=sum3+x**2.
      sum4=sum4+x*y
40      continue
      b=(n*sum4-sum1*sum2)/(n*sum3-sum1**2)
      a=(sum2*sum3-sum1*sum4)/(n*sum3-sum1**2)
      write(*,*) "a= ",a,"  b=",b
c
c      compute difference between data points and calibration
c
      write(*,90)
90      format("Pt",5x,"Volt",5x,"Vel",6x,"Velc",5x,"Pdiff")
      do 50 i=1,n
      vc(i)=(a+b*e(i)**2)**pw
      pd(i)=(v(i)-vc(i))/v(i)*100.
      write(*,91) i,e(i),v(i),vc(i),pd(i)
91      format(i2,5x,4(f7.3,3x))
50      continue
      write(*,*) " "
      write(*,*) "Do you want to save this in a file (y,n)?"
      read(*,'(a)') a$
      if(a$.eq."y") then
      write(*,*) "Enter a file name for the output "
      read(*,'(a)') f$
      open(20,file=f$,status="new")
      write(20,*) "a= ",a,"  b=",b
      write(20,*)
      write(20,90)
      do 60 i=1,n
      write(20,91) i,e(i),v(i),vc(i),pd(i)
60      continue
      close(20)
      endif
c
      write(*,*) "Do you want to remove any points (y,n)?"
      read(*,'(a)') a$
      if(a$.ne."n") then
      call rmpt(n,e,v)
      goto 70
      end if
      end

      subroutine rmpt(n,e,v)
      integer ip(10)
      dimension e(n),v(n)
      write(*,*) "Enter the number of points to remove"
      read(*,*) nr
      if(nr.eq.0) goto 30
      do 10 i=1,nr
      write(*,*) "Enter the ",i," data point to be removed"
      read(*,*) ip(i)
10      continue
      j=0
      k=1
      do 20 i=1,n
      if(i.eq.ip(k)) then
      k=k+1
      else
```

```
      j=j+1
      v(j)=v(i)
      e(j)=e(i)
      end if
20      continue
      n=n-nr
30      return
      end
```

```
      program xwcr
c
c      Calculates cross-wire calibration using data generated by
c      program x_cal.c
c
c      v is velocity array, e1 and e2 are hot-wire voltage arrays
c
      real v(50),e(2,50),e(2,50),vc(2,50),pd(2,50),a(2),b(2)
      character*15 f$
      character*15 a$
      write(*,*) "Input the file name of the calibration data"
      read(*,'(a)') f$
      open(10,file=f$,status="old")
      read(10,*) n
      do 30 i=1,n
      read(10,*) v(i),e(1,i),e(2,i)
30      continue
      close(10)
c
c      power in King's law is 0.435
c
      th=45.*3.141592654/180.
      pwr=0.435
      pw=1./pwr
70      continue
      do 35 m=1,2
      sum1=0.
      sum2=0.
      sum3=0.
      sum4=0.
      do 40 i=1,n
      x=e(m,i)**2.
      y=(v(i)*cos(th))**pwr
      sum1=sum1+x
      sum2=sum2+y
      sum3=sum3+x**2.
      sum4=sum4+x*y
40      continue
      b(m)=(n*sum4-sum1*sum2)/(n*sum3-sum1**2)
      a(m)=(sum2*sum3-sum1*sum4)/(n*sum3-sum1**2)
      write(*,*) "a= ",a(m),"  b=",b(m)
      do 45 i=1,n
      vc(m,i)=((a(m)+b(m)*e(m,i)**2)**pw)/cos(th)
      pd(m,i)=(v(i)-vc(m,i))/v(i)*100.
45      continue
35      continue
c
c      compute difference between data points and calibration
c
      write(*,90)
90      format("Pt",4x,"Volt1",5x,"Volt2",5x,"Vel",7x,"Velc1",5x,
     x "Pdiff1",4x,"Velc2",5x,"Pdiff2")
      do 50 i=1,n
      write(*,91) i,e(1,i),e(2,i),v(i),vc(1,i),pd(1,i),vc(2,i),pd(2,i)
91      format(i2,4x,7(f7.3,3x))
50      continue
      write(*,*) " "
      write(*,*) "Do you want to save this in a file (y,n)?"
      read(*,'(a)') a$
      if(a$.eq."y") then
      write(*,*) "Enter a file name for the output "
      read(*,'(a)') f$
      open(20,file=f$,status="new")
      write(20,*) "a1= ",a(1),"  b1=",b(1)
      write(20,*) "a2= ",a(2),"  b2=",b(2)
      write(20,*)
      write(20,90)
      do 60 i=1,n
      write(20,91) i,e(1,i),e(2,i),v(i),vc(1,i),pd(1,i),vc(2,i),pd(2,i)
60      continue
      close(20)
      endif
c
      write(*,*) "Do you want to remove any points (y,n)?"
      read(*,'(a)') a$
      if(a$.ne."n") then
      call rmpt(n,e,v)
      goto 70
      end if
      end

      subroutine rmpt(n,e,v)
      integer ip(10)
      dimension e(2,n),v(n)
      write(*,*) "Enter the number of points to remove"
      read(*,*) nr
      if(nr.eq.0) goto 30
      do 10 i=1,nr
      write(*,*) "Enter the ",i," data point to be removed"
      read(*,*) ip(i)
```

```
10        continue
          j=0
          k=1
          do 20 i=1,n
          if(i.eq.ip(k)) then
          k=k+1
          else
          j=j+1
          v(j)=v(i)
          e(1,j)=e(1,i)
          e(2,j)=e(2,i)
          end if
20        continue
          n=n-nr
30        return
          end
```

```
c  Calibrates a cold wire compensation
c
c  Written:  Ralph Volino       9/26/93
c
c
c       Command Line:   kcol
c
c  This program is used to calibrate a cold wire on the 3 wire probe.
c  The calibration is done using the calibration jet. Derivatives are
c  calculated numerically.  Uses output of cold.c
c
c
      program kcol
      real t(600),va(600),volt1(600),volt2(600),voltd(600)
      real vf(100),tf(100),coef(10)
      character*20 nam$
c
      write(*,*) "Input the name of the input file: "
      read(*,'(a)') nam$
      open(10,file=nam$,status="old")
c
      np=20
      vmax=-9999.
      vmin=9999.
      read(10,*) n,freq,v21,epsilon
      do 30, i=1,n
      read(10,*) volt1(i),volt2(i)
      t(i)=i/freq
      if(volt1(i).gt.vmax) vmax=volt1(i)
      if(volt1(i).lt.vmin) vmin=volt1(i)
30      continue
      close(10)
c
c        Process the data
c
      do 40, i=30,n-np
      do 50, k=1,np
      vf(k)=volt1(i+k)
      tf(k)=t(i+k)
50      continue
c
      call curvf(np,tf,vf,coef,2)
c
      if(i.eq.30) then
      do 60, ik=i,i+np/2-1
      voltd(ik)=coef(2)+2.*coef(3)*t(ik)
60      continue
      endif
      if(i.eq.n-np-1) then
      do 70, ik=i+np/2+1,n
      voltd(ik)=coef(2)+2.*coef(3)*t(ik)
70      continue
      endif
      voltd(i+np/2)=coef(2)+2.*coef(3)*t(i+np/2)
40      continue
c
      write(*,*) "Input the compensation coefficient, kcc: "
      read(*,*) akcc
c
c       Calculate the compensated voltages
c
      do 80 i=30,n-2
      anum=akcc/volt2(i)/volt2(i)*v21*voltd(i)+volt1(i)
      den=1.+epsilon*akcc/volt2(i)/volt2(i)*voltd(i)
      va(i)=anum/den
80      continue
c
c       Store the results in temporary files for plotting
c
      open(20,file="temp1",status="unknown")
      do 90 i=1,n-2
      write(20,*) t(i),volt1(i)
90      continue
      write(20,*) 0,volt1(n-2)
      close(20)
      open(25,file="temp2",status="unknown")
      open(27,file="temp3",status="unknown")
      write(27,*) v21,epsilon,akcc
      do 95 i=30,n-2
      write(25,*) t(i),va(i)
      write(27,*) volt1(i),va(i),voltd(i)
95      continue
      close(25)
      write(*,*) "Load file kplot int gnuplot"
      write(*,*) "Set yrange to ",vmin," to ",vmax
      end

      subroutine curvf(n,x,y,coef,m1)
      real f(10),g(10),z(10,10),b(10),x(10),y(10)
```

```
      real coef(10),indx(10)
c
      m=m1+1
      do 10 j=1,2*m-1
      f(j)=0.
      g(j)=0.
      do 20 k=1,n
      f(j)=f(j)+x(k)**(j-1)
      g(j)=g(j)+y(k)*x(k)**(j-1)
20      continue
10      continue
      do 30 k=1,m
      do 40 j=1,m
      z(k,j)=f(j+k-1)
40      continue
      b(k)=g(k)
30      continue
      call ludcmp(z,m,10,indx,d)
      call lubksb(z,m,10,indx,b)
      do 50 j=1,m
      coef(j)=b(j)
50      continue
      return
      end

      subroutine ludcmp(a,n,np,indx,d)
      parameter(nmax=100,tiny=1.0e-20)
      dimension a(np,np),indx(n),vv(nmax)
      d=1.
      do 12 i=1,n
      aamax=0.
      do 11 j=1,n
      if (abs(a(i,j)).gt.aamax) aamax=abs(a(i,j))
11      continue
      if(aamax.eq.0.) pause 'singular matrix'
      vv(i)=1./aamax
12      continue
      do 19 j=1,n
      do 14 i=1,j-1
      sum=a(i,j)
      do 13 k=1,i-1
      sum=sum-a(i,k)*a(k,j)
13      continue
      a(i,j)=sum
14      continue
      aamax=0.
      do 16 i=j,n
      sum=a(i,j)
      do 15 k=1,j-1
      sum=sum-a(i,k)*a(k,j)
15      continue
      a(i,j)=sum
      dum=vv(i)*abs(sum)
      if(dum.ge.aamax) then
      imax=i
      aamax=dum
      endif
16      continue
      if(j.ne.imax) then
      do 17 k=1,n
      dum=a(imax,k)
      a(imax,k)=a(j,k)
      a(j,k)=dum
17      continue
      d=-d
      vv(imax)=vv(j)
      endif
      indx(j)=imax
      if(a(j,j).eq.0) a(j,j)=tiny
      if(j.ne.n) then
      dum=1./a(j,j)
      do 18 i=j+1,n
      a(i,j)=a(i,j)*dum
18      continue
      endif
19      continue
      return
      end
c
      subroutine lubksb(a,n,np,indx,b)
      dimension a(np,np),indx(n),b(n)
      ii=0
      do 12 i=1,n
      ll=indx(i)
      sum=b(ll)
      b(ll)=b(i)
      if(ii.ne.0) then
      do 11 j=ii,i-1
      sum=sum-a(i,j)*b(j)
11      continue
```

```
      else if(sum.ne.0) then
      ii=i
      endif
      b(i)=sum
12      continue
      do 14 i=n,1,-1
      sum=b(i)
      if(i.lt.n) then
      do 13 j=i+1,n
      sum=sum-a(i,j)*b(j)
13      continue
      endif
      b(i)=sum/a(i,i)
14      continue
      return
      end
```

```
      program skfric
c
c       Written:  Ralph Volino    3/22/94
c
c       Calculates Cf from mean velocity profile.  Also finds
c       effective y location of points.  Uses Wills correction
c        on the near wall data.
c
      real u(90),y(90),upr(90),gamma(90),ydist(20)
      real vel(20),coef(4),yp(90),up(90)
      real yn(90),un(90),yl(2550),ul(2550),yt(2550),ut(2550)
      character*15 nam$
c
      write(*,*) "Enter the data file name"
      read(*,'(a)') nam$
      open(22,file=nam$,status="old")
c
      read(22,*) patm,x
      read(22,*) ista,ndata
      do 30 i=1,ndata
      read(22,*) k,y(i),u(i),t,upr(i),gamma(i),npt
c
      write(*,*) k,y(i),u(i),upr(i)
30      continue
      close(22)
c
c       Find extrapolated wall velocity, uw
c
      write(*,*) "Enter number of points taken in convex b.l."
      read(*,*) iptr
      write(*,*) "Enter number of points taken in the core"
      read(*,*) icore
      ipoint=icore+iptr
      do 40 i=1+iptr,ipoint
      vel(i-iptr)=u(ndata+1-i)
      ydist(i-iptr)=y(ndata+1-i)
40      continue
      call curvf(icore,ydist,vel,coef,1)
      uw=coef(1)
      sl=coef(2)
      write(*,*) "Uw = ",uw
      call visco(visc,t,patm)
c
      call skf(y,u,ndata,visc,yp,up,cf,uw,x,nto,ibpt,
     x   yn,un,yl,ul,yt,ut,ista,ap,yeff,akac,f1,upr)
c
      write(*,*) ndata,visc,cf,ap,yeff
      call blp(yn,un,ndata-nto-ibpt,visc,x,yeff,d995,del1,
     x   del2,uw,sl)
c
      rex=uw*x/visc/100.
      red1=uw*del1/100./visc
      red2=uw*del2/100./visc
      h=del1/del2
c
c       Print results to output file
c
      write(*,*) "Enter the ouput file name"
      read(*,'(a)') nam$
      open(23,file=nam$,status="new")
      write(23,*) "Station = ",ista
      write(23,*) "patm = ",patm,"    temp = ",t
      write(23,*) "x = ",x,"    visc = ",visc
      write(23,*) "cf = ",cf,"   yeff = ",yeff
      write(23,*) "d99.5 = ",d995,"  del1 = ",del1
      write(23,*) "del2 = ",del2,"   H = ",h
      write(23,*) "Uw = ",uw,"   Rex = ",rex
      write(23,*) "Red1 = ",red1,"    Red2 = ",red2
      write(23,*) "coef1 = ",uw,"   coef2  = ",sl
      write(23,*) "A+ = ",ap
      write(23,*) "K = ",akac,"    f1 = ",f1
      write(23,*) " "
      write(23,*) " "
      write(23,*) "N  y     U     y+     u+     u'     gamma"
      do 98 i=1,ndata-ibpt-nto
      write(23,*) i,yn(i),un(i),yp(i),up(i),upr(i+ibpt+nto)
     x  ,gamma(i+ibpt+nto)
98      continue
      end


      subroutine blp(yn,un,nd,visc,x,yeff,d995,del1,
     x   del2,uw,sl)
c
      real ye(2),ue(2),q1(90),q2(90),coef(2)
      real upot(90)
      dimension un(*),yn(*)
c
      r=0.97
c
```

```
      do 10 i=1,nd
      upot(i)=uw+sl*yn(i)
      u995=.995*upot(i)
      if(un(i).gt.u995) then
      write(*,*) "Edge of boundary layer found between points"
      write(*,*) i-1," and ",i
      c3=uw*0.995
      c4=sl
      m1=i
      ye(1)=yn(m1)
      ye(2)=yn(m1-1)
      ue(1)=un(m1)
      ue(2)=un(m1-1)
      call curvf(2,ye,ue,coef,1)
      ce1=coef(1)
      ce2=coef(2)
      d995=(ce1-c3)/(c4-ce2)
      goto 25
      endif
10      continue
c
      write(*,*) "Edge of boundary layer not found"
25      continue
      write(*,*) "d99.5 = ",d995
      sum1=0
      sum2=0
      mintegr=m1+1
c
      do 20 i=1,mintegr
      upot(i)=uw+sl*yn(i)
      q1(i)=upot(i)-un(i)
      q2(i)=un(i)*(upot(i)-un(i))
20      continue
c
      call integr(yn,q1,mintegr,sum1,uw)
      call integr(yn,q2,mintegr,sum2,0)
c
      c1=uw
      c2=sl
      del1=(-c1+(c1*c1+2.*c2*sum1)**.5)/c2
      del2p=r*(1.-1./(1.+sum2/(r*uw*uw)))
      call newton(c1,c2,sum2,del2p,del2)
c
      return
      end

      subroutine newton(c1,c2,sum2,xp,xn)
c
30      continue
      fofx=c2*c2*xp**3+3*c1*c2*xp**2+3*c1*c1*xp-3*sum2
      deriv=3*c2*c2*xp*xp+6*c1*c2*xp+3*c1*c1
      xn=xp-fofx/deriv
      if(abs(xn-xp).lt.1e-4) goto 20
      xp=xn
      goto 30
20      continue
      return
      end

      subroutine integr(yn,q2,m,sum2,strt)
c
      real q2(90)
      dimension yn(*)
c
      sum2=0.
      do 10 i=0,m-2
      if(i.eq.0) then
      x1=0.
      y21=strt
      else
      x1=yn(i)
      y21=q2(i)
      endif
      x2=yn(i+1)
      x3=yn(i+2)
      y22=q2(i+1)
      y23=q2(i+2)
      b2=((y23-y22)*(x1*x1-x2*x2)-(y21-y22)*(x3*x3-x2*x2))/
     x   ((x3-x2)*(x1*x1-x2*x2)-(x1-x2)*(x3*x3-x2*x2))
      a2=((y21-y22)-b2*(x1-x2))/(x1*x1-x2*x2)
      c2=y21-a2*x1*x1-b2*x1
c
      delar=a2/3.*(x2**3-x1**3)+b2/2.*(x2*x2-x1*x1)+c2*(x2-x1)
      if(i.eq.m-2) then
      delar=a2/3.*(x3**3-x1**3)+b2/2.*(x3*x3-x1*x1)+c2*(x3-x1)
      endif
      sum2=sum2+delar
10      continue
      return
      end
```

```
      subroutine skf(y,u,ndata,visc,yp,up,cf,uw,x,nto,ibpt,
     x   yn,un,yl,ul,yt,ut,ista,ap,yeff,akac,f5,upr)
c
      character an$
      dimension y(*),u(*),yp(*),up(*),yn(*),un(*)
      dimension yl(*),ul(*),yt(*),ut(*),upr(*)
c
70      continue
      write(*,*) "How many data points to take out (near wall)?"
      read(*,*) nto
      write(*,*) "Input Cf"
      read(*,*) cf
      write(*,*) "Input Yeff"
      read(*,*) yeff
      ibpt=0
c
c      Open files for plotting profile in wall coordinates
      open(80,file="dta",status="unknown")
      open(81,file="dtl",status="unknown")
      open(82,file="dtt",status="unknown")
c
      do 17 j=nto+1,ndata
      k=j-nto-ibpt
      yn(k)=y(j)+yeff
      if(yn(k).lt.1.e-6) then
      ibpt=ibpt+1
      goto 17
      endif
c
c      Apply Wills' correction
c
      ba=yn(k)/1.905e-4
      if(ba.le.40) then
      akw=2.423*(4.53*ba**(-1.0278))
      else
      akw=2.423*(76.524*ba**(-1.7893))
      endif
      un(k)=u(j)**0.45-akw
      if(un(k).le.0) un(k)=1.e-10
      un(k)=un(k)**(1./.45)
      un(k)=0.16*u(j)+0.84*un(k)
c
c      Near wall turbulence correction
c
c       uc=un(k)*un(k)-upr(j)*upr(j)
c       if(uc.le.0) then
c       un(k)=1e-10
c       else
c       un(k)=uc**.5
c       endif
c
      up(k)=un(k)/uw/(cf/2.)**0.5
      yp(k)=yn(k)*uw*(cf/2.)**0.5/visc/100.
      write(80,*) yp(k),up(k)
17      continue
c
      write(*,*) "Enter dU/dx at this station"
      read(*,*) dudx
      write(*,*) "Enter d((Cf/2)**.5)/dx at this station"
      read(*,*) dcf
      write(*,*) "Estimate d99.5 at this station [cm]"
      read(*,*) d995
      d995=d995/100.*uw*(cf/2)**.5/visc
      f5=visc/uw*2./cf*dcf
      akac=dudx*visc/uw/uw
      ppl=-akac/(cf/2.)**1.5
      f6=akac/(cf/2.)**0.5
c
c       if(ista.eq.1) then
c       write(*,*) "Enter A+ at this station"
c       read(*,*) ap
c       else
c       write(*,*) "Enter A+ and x [cm] at the upstream station"
c       read(*,*) apu,xu
c       ap=apu
c       xp=x*(cf/2.)**0.5*uw/visc/100.
c       xpu=xu*(cf/2.)**0.5*uw/visc/100.
c       dx=(xp-xpu)/100.
c
c       do 20 i=1,100
c       xl=xu+(x-xu)/100.*i
c       upl=15.625*xl/100.+5.
c       akl=dudx*visc/upl/upl
c       aq=25./(1.-30.175*akl*(2./cf)**1.5)
c       if(ap.le.0.or.ap.gt.200) then
c       ap=150.
c       goto 28
c       endif
```

```
c        ap=(aq-ap)/4000.*dx+ap
20        continue
c       endif
       ap=25./(1.-30.175*akac*(2./cf)**1.5)
       if(ap.le.0.or.aq.gt.150) then
       ap=150.
       endif
       write(*,*) "A+ = ",ap
       write(*,*) "Enter A+ "
       read(*,*) ap
c
28      continue
       sum=0.
       sum1=0.
       sum2=0.
       vanmi=2.
       vanma=800.
       m=2500
       yz=0.
       dy=(vanma-vanmi)/m
c
       do 30 i=1,m
       yz=yz+dy
       sum1=sum1+sum*sum*dy
       sum2=sum2+sum*dy
       fy=(f6+f5)*sum1
       if((yz*ppl+fy).lt.-1) goto 40
       if(yz.gt.40) goto 40
       dfy=(1.+ppl*yz+fy)*dy
       sum=sum+dfy
       yl(i)=yz
       ul(i)=sum
       write(81,*) yl(i),ul(i)
30      continue
c
40      continue
       con=0.41
       sum=0.
       sum1=0.
       sum2=0.
       vanmi=2.
       vanma=800.
       m=2500
       yz=0.
       dy=(vanma-vanmi)/m
       dfy=1.
       rp=-0.97*uw*(cf/2)**.5/visc
       xmlo=.085*d995
c
       do 50 i=1,m
c
c        Curvature correction
c
c        ri=sum/rp/dfy*dy
       ri=2*sum/rp/rp*(sum/(dfy/dy)**2.+rp/dfy*dy)
       crv=1-4.5*ri
c
       yz=yz+dy
       xml=con*yz
c        if(xml.gt.xmlo) xml=xmlo
       a=((xml)*(1.-exp(-yz/ap))*crv)**2.
       sum1=sum1+sum*sum*dy
       sum2=sum2+sum*dy
       fy=(f6+f5)*sum1
       if((yz*ppl+fy).lt.-1) goto 60
       dfy=(-1.+(1.+4*a*(1.+ppl*yz+fy))**0.5)/2./a*dy
       sum=sum+dfy
       yt(i)=yz
       ut(i)=sum
       write(82,*) yt(i),ut(i)
       if(ut(i).gt.50) goto 60
50      continue
c
60      continue
       close(80)
       close(81)
       close(82)
       write(*,*) "Go to another screen, plot the profile"
       write(*,*) " "
       write(*,*) "Do you want to try again [y,n]"
       read(*,'(a)') an$
       if(an$.ne.'n') goto 70
       return
       end


       subroutine visco(visc,t,patm)
c
       visc=9.3277e-8*(t+273.15)-1.2248e-5
       visc=visc*(760./patm)
```

```
      return
      end

      subroutine curvf(n,x,y,coef,m1)
      real f(10),g(10),z(10,10),b(10)
      real indx(10)
      dimension x(*),y(*),coef(*)
c
      m=m1+1
      do 10 j=1,2*m-1
      f(j)=0.
      g(j)=0.
      do 20 k=1,n
      f(j)=f(j)+x(k)**(j-1)
      g(j)=g(j)+y(k)*x(k)**(j-1)
20      continue
10      continue
      do 30 k=1,m
      do 40 j=1,m
      z(k,j)=f(j+k-1)
40      continue
      b(k)=g(k)
30      continue
      call ludcmp(z,m,10,indx,d)
      call lubksb(z,m,10,indx,b)
      do 50 j=1,m
      coef(j)=b(j)
50      continue
      return
      end

      subroutine ludcmp(a,n,np,indx,d)
      parameter(nmax=100,tiny=1.0e-20)
      dimension a(np,np),indx(n),vv(nmax)
      d=1.
      do 12 i=1,n
      aamax=0.
      do 11 j=1,n
      if (abs(a(i,j)).gt.aamax) aamax=abs(a(i,j))
11      continue
      if(aamax.eq.0.) pause 'singular matrix'
      vv(i)=1./aamax
12      continue
      do 19 j=1,n
      do 14 i=1,j-1
      sum=a(i,j)
      do 13 k=1,i-1
      sum=sum-a(i,k)*a(k,j)
13      continue
      a(i,j)=sum
14      continue
      aamax=0.
      do 16 i=j,n
      sum=a(i,j)
      do 15 k=1,j-1
      sum=sum-a(i,k)*a(k,j)
15      continue
      a(i,j)=sum
      dum=vv(i)*abs(sum)
      if(dum.ge.aamax) then
      imax=i
      aamax=dum
      endif
16      continue
      if(j.ne.imax) then
      do 17 k=1,n
      dum=a(imax,k)
      a(imax,k)=a(j,k)
      a(j,k)=dum
17      continue
      d=-d
      vv(imax)=vv(j)
      endif
      indx(j)=imax
      if(a(j,j).eq.0) a(j,j)=tiny
      if(j.ne.n) then
      dum=1./a(j,j)
      do 18 i=j+1,n
      a(i,j)=a(i,j)*dum
18      continue
      endif
19      continue
      return
      end
C
      subroutine lubksb(a,n,np,indx,b)
      dimension a(np,np),indx(n),b(n)
      ii=0
      do 12 i=1,n
      ll=indx(i)
```

```
      sum=b(ll)
      b(ll)=b(i)
      if(ii.ne.0) then
      do 11 j=ii,i-1
      sum=sum-a(i,j)*b(j)
11      continue
      else if(sum.ne.0) then
      ii=i
      endif
      b(i)=sum
12      continue
      do 14 i=n,1,-1
      sum=b(i)
      if(i.lt.n) then
      do 13 j=i+1,n
      sum=sum-a(i,j)*b(j)
13      continue
      endif
      b(i)=sum/a(i,i)
14      continue
      return
      end
```

```
      program tplus
c
c       Written:  Ralph Volino    3/27/94
c
c     Calculates t+ vs y+ from mean temperature profile.  Also finds
c     effective y location of points. Uses previously processed
c     velocity profile to find the enthalpy thickness.  Calculates
c     local turbulent Prandtl number.
c
      real y(90),t(90),uv(90),yv(90)
      real yn(90),un(90),yp(90),tp(90)
      real prt(100),tstg(100)
      character*25 nam$
c
      write(*,*) "Enter the processed velocity data file name"
      read(*,'(a)') nam$
      open(23,file=nam$,status="old")
c
      read(23,*) press,xu
      read(23,*) ista,ndata
      do 98 i=1,ndata
      read(23,*) i1,yv(i),uv(i),zz,zz,zz,zz
98      continue
      close(23)
c
      bpts=0
c
c
      write(*,*) "Enter yeff for the velocity profile"
      read(*,*) yeffu
      do 10 j=1,ndata
      k=j-bpts
      yn(k)=yv(j)+yeffu
      if(yn(k).lt.1.e-6) then
      bpts=bpts+1
      goto 10
      endif
c
c       Apply Wills' correction
c
      ba=yn(k)/2.25e-4
      if(ba.le.40) then
      kw=2.248*(4.53*ba**(-1.0278))
      else
      kw=2.248*(76.524*ba**(-1.7893))
      endif
      un(k)=uv(j)**0.45-kw
      if(un(k).le.0) un(k)=1.e-10
      un(k)=un(k)**(1./.45)
      un(k)=0.16*uv(j)+0.84*un(k)
10      continue
      ndata=ndata-bpts
c
      write(*,*) "Enter coef1 and coef2 from velocity profile"
      read(*,*) uw,slp
      write(*,*) "Enter Cf for this station"
      read(*,*) cf
c
      write(*,*) "Enter dU/dx at this station"
      read(*,*) dudx
      write(*,*) "Enter f1 at this station"
      read(*,*) f5
c
      write(*,*) "Enter A+ at this station"
      read(*,*) ap
c
      write(*,*) "Enter the temperature data file name"
      read(*,'(a)') nam$
      open(22,file=nam$,status="old")
c
      read(22,*) n
      read(22,*) patm,twall,tinf,qnet,xt
      read(22,*) ista
      do 30 i=1,n
      read(22,*) y(i),v,t(i)
      write(*,*) i,y(i),t(i)
30      continue
      read(22,*) tinfe
      close(22)
      write(*,*) "Tinf = ",tinf,"   Tinfe = ",tinfe
c
c       Find the core temperature
c
      write(*,*) "Was the core reached (1), or use Tinfe (2)?"
      read(*,*) icre
      if(icre.eq.2) then
      tinf=tinfe
      else
      write(*,*) "Enter number first and last point to average"
      read(*,*) ipf,ipl
```

```
      sum=0.
      do 40 i=ipf,ipl
      sum=sum+t(i)
40      continue
      tinf=sum/(ipl-ipf+1)
      write(*,*) "Tinf = ",tinf
      endif
c
      tave=(twall+tinf)/2.
      call viscal(visc,tave,patm)
      akac=dudx*visc/uw/uw
      ppl=akac/(cf/2.)**1.5
      f6=akac/(cf/2.)**0.5
c
c       Adjust the velocity for position of probe
c
      ut=uw+dudx*(xt-xu)/100.
      uad=ut/uw
      uw=ut
      do 41 i=1,ndata
      un(i)=un(i)*uad
41      continue
      akac=akac/uad/uad
      ppl=ppl/uad/uad
      f6=f6/uad/uad
      f5=f5/uad
c
      call prtcal(yn,un,ndata,n,yp,tp,cf,uw,xv,xt,prt,
     x  y,t,ap,yeff,tinf,twall,patm,qnet,f5,akac,ppl,f6,f3,
     x  twlo,qwo,qwc,tstg,tstf)
c
      call blp(yn,un,ndata,y,tstg,n,delther,deleth,delcon,
     x  reh,tstf,twall,patm,uw,slp,qwc,rho,cp,tinf,qadd)
c
      rex=uw*xt/visc/100.
      stant=qwc/uw/(twall-tinf)/rho/cp
c
c       Print results to output file
c
      write(*,*) "Enter the ouput file name"
      read(*,'(a)') nam$
      open(23,file=nam$,status="new")
      write(23,*) "Station = ",ista
      write(23,*) "patm = ",patm
      write(23,*) "x = ",xt,"    visc = ",visc
      write(23,*) "cf = ",cf,"   yeff = ",yeff
      write(23,*) "Tw = ",twall,"   Tinf = ",tinf
      write(23,*) "Tw measured = ",twlo," Tw correction = ",twall-twlo
      write(23,*) "Q wall = ",qwc,"  Stanton No. = ",stant
      write(23,*) "Q wall measured (w/Tw measured) = ",qwo
      write(23,*) "Q wall measured (w/Tw corrected) = ",qnet
      write(23,*) "delther = ",delther,"  deleth = ",deleth
      write(23,*) "delcon = ",delcon,"  qadded = ",qadd
      write(23,*) "Uw = ",uw,"   Rex = ",rex
      write(23,*) "Reh = ",reh
      write(23,*) "coef1 = ",uw,"   coef2  = ",slp
      write(23,*) "A+ = ",ap,"    K = ",akac
      write(23,*) "f1 = ",f5,"    f2 = ",f3
      write(23,*) " "
      write(23,*) " "
      write(23,*) "N    y       T        Tnd       y+      t+      Prt"
      do 94 i=1,n
      tnd=(twall-t(i))/(twall-tinf)
      write(23,9) i,y(i),t(i),tnd,yp(i),tp(i),prt(i)
9      format(i2,3x,f6.4,2x,f6.3,3x,f5.3,2x,f7.2,3x,f5.2,3x,f6.3)
94      continue
      end


      subroutine blp(yn,un,ndata,y,t,n,delther,deleth,delcon,
     x  reh,tinf,tw,patm,uw,slp,qw,rho,cp,tinft,qadd)
c
      real q1(90),x(3),f(3)
      real un(90),yn(90),coef(10)
      real y(90),t(100)
c
      r=0.97
c
      tave=(tinf+tw)/2.
      call cpcal(cp,tave)
      call rhocal(rho,tave,patm)
c
      do 10 i=1,n
      if((tw-t(i))/(tw-tinf).gt.0.995) then
      m1=i
      goto 71
      endif
10      continue
      write(*,*) "Edge of boundary layer not found"
      iflag1=5
```

```
      m1=n
71      continue
      write(*,*) "Edge of boundary layer found between points"
      write(*,*) i-1," and ",i
      frac=(.995*(tw-tinf)-tw+t(m1-1))/(t(m1-1)-t(m1))
      delther=frac*(y(m1)-y(m1-1))+y(m1-1)
      if(iflag1.eq.5) then
      y(m1+1)=delther
      t(m1+1)=tinf
      m1=m1+1
      endif
c
      sum1=0
      sum2=0
      mintegr=m1+1
c
      do 20 j=1,mintegr
      do 23 i=1,ndata
      if(y(j).lt.yn(i)) then
      m2=i
      goto 73
      endif
      if(y(j).ge.yn(ndata)) then
      upt=un(ndata)
      goto 74
      endif
23      continue
73      continue
      x(1)=yn(m2-1)
      x(2)=yn(m2)
      x(3)=yn(m2+1)
      f(1)=un(m2-1)
      f(2)=un(m2)
      f(3)=un(m2+1)
c
      call curvf(3,x,f,coef,2)
      upt=coef(1)+coef(2)*y(j)+coef(3)*y(j)*y(j)
74      continue
      q1(j)=upt*(t(j)-tinf)
20      continue
c
      sum1=0
      call integr(y,q1,mintegr,sum1,0)
c
      delp=sum1/uw/(tw-tinf)
      deleth=(-uw+(uw*uw+2.*slp/(tw-tinf)*sum1)**.5)/slp
c
      qadd=uw*deleth*(tw-tinf)*rho*cp/100.
      call condv(cond,tave)
      delcon=cond*(tw-tinft)/qw
      call viscal(visc,tave,patm)
      reh=uw*deleth/visc/100.
c
      return
      end


      subroutine prtcal(yn,un,ndata,n,yp,tp,cf,uw,xv,xt,prt,
     x   yt,t,ap,yeff,tinf,twall,patm,qw,f5,akac,ppl,f6,f3,
     x   twallo,qwo,qwc,tstg,tstf)
c
      character an$
      real yn(90),un(90),yt(90),t(90),yp(90),tp(90)
      real prt(100),tstg(100)
c
c       Correct temperatures for velocity
c
      rc=0.88
      do 11 j=1,n
      call cpcal(cp,t(j))
      do 21 i=1,ndata
      if(yt(j).lt.yn(i)) then
      m2=i
      goto 31
      endif
      if(yt(j).gt.yn(ndata)) then
      velj=un(ndata)
      goto 41
      endif
21      continue
31      continue
      fra=(yt(j)-yn(m2-1))/(yn(m2)-yn(m2-1))
      velj=(un(m2)-un(m2-1))*fra+un(m2-1)
41      continue
      tstg(j)=t(j)
      t(j)=t(j)-velj**2/2./cp*rc
11      continue
      tstf=tinf
      tinf=tinf-velj**2/2./cp/rc
      twallo=twall
```

```
      qwo=qw
61      continue
      write(*,*) "Input Yeff"
      read(*,*) yeff
      write(*,*) "Do you want to adjust twall [y,n]?"
      read(*,'(a)') an$
      if(an$.eq.'y') then
      write(*,*) "Measured Twall = ",twallo
      write(*,*) "Enter Twall"
      read(*,*) twall
c
c      Correct the wall heat flux (radiation loss)
c
      emis=0.85
      qradc=emis*5.67e-8*((twall+273.15)**4-(twallo+273.15)**4)
      qw=qwo-qradc
c
      endif
      qwc=qw
      write(*,*) "Do you want to adjust qwall [y,n]?"
      read(*,'(a)') an$
      if(an$.eq.'y') then
      write(*,*) "Measured qwall = ",qw
      write(*,*) "Enter qwall"
      read(*,*) qwc
      endif
c
      tave=(twall+tinf)/2.
      call condv(cond,tave)
      dtdy=-qwc/cond
      open(27,file="tprx",status="unknown")
      do 51 i=1,n
      write(27,*) yt(i)+yeff,twall-t(i)
51      continue
      tx=-dtdy*0.0005
      open(28,file="tprl",status="unknown")
      write(28,*) 0.0,0.0
      write(28,*) 0.05,tx
      close(27)
      close(28)
      write(*,*) "Go to another screen and look at the profile"
      read(*,'(a)') an$
      write(*,*) "Try another yeff or twall (1) or go on (2)?"
      read(*,*) iasr
      if(iasr.ne.2) goto 61
      bpt=0
      call rhocal(rho,tave,patm)
      call cpcal(cp,tave)
      call viscal(visc,tave,patm)
      do 42 i=1,n
      if(yt(i)+yeff.lt.0.00379) then
      bpt=bpt+1
      goto 42
      endif
      k=i-bpt
      tstg(k)=tstg(i)
      t(k)=t(i)
      yt(k)=yt(i)+yeff
      yp(k)=yt(k)*uw*(cf/2.)**.5/visc/100.
      tp(k)=(twall-t(i))*uw*(cf/2.)**.5/qwc*rho*cp
42      continue
      ti=(twall-tinf)*uw*(cf/2.)**.5/qwc*rho*cp
      n=n-bpt
      call prcalc(pr,tave)
c
c      write(*,*) "Enter dSt/dx"
c      read(*,*) f31
      xm=xt/100.
c      high K
      f31=-.0409676+2*.10573675*xm-3*.115847*xm*xm+4*.0447585*xm**3
c      low K
c      f31=-.03456154+2*.09477014*xm-3*.118264*xm*xm+4*.0550893*xm**3
c
      f3=f31*visc*ti/uw/cf*2.
      call prtfnd(ap,ppl,f6,prt,f5,f3,pr,yp,tp,ti,n,prt,uw,cf,visc)
c
      return
      end


      subroutine prcalc(pr,tave)
      pr=-1.524e-4*(tave+273.15)+.757
      return
      end

      subroutine visco(visc,t,patm)
c
      visc=9.3277e-8*(t+273.15)-1.2248e-5
      visc=visc*(760./patm)
      return
```

```
      end

      subroutine curvf(n,x,y,coef,m1)
      real f(10),g(10),z(10,10),b(10),x(10),y(10)
      real coef(10),indx(10)
c
      m=m1+1
      do 10 j=1,2*m-1
      f(j)=0.
      g(j)=0.
      do 20 k=1,n
      f(j)=f(j)+x(k)**(j-1)
      g(j)=g(j)+y(k)*x(k)**(j-1)
20      continue
10      continue
      do 30 k=1,m
      do 40 j=1,m
      z(k,j)=f(j+k-1)
40      continue
      b(k)=g(k)
30      continue
      call ludcmp(z,m,10,indx,d)
      call lubksb(z,m,10,indx,b)
      do 50 j=1,m
      coef(j)=b(j)
50      continue
      return
      end

      subroutine ludcmp(a,n,np,indx,d)
      parameter(nmax=100,tiny=1.0e-20)
      dimension a(np,np),indx(n),vv(nmax)
      d=1.
      do 12 i=1,n
      aamax=0.
      do 11 j=1,n
      if (abs(a(i,j)).gt.aamax) aamax=abs(a(i,j))
11      continue
      if(aamax.eq.0.) pause 'singular matrix'
      vv(i)=1./aamax
12      continue
      do 19 j=1,n
      do 14 i=1,j-1
      sum=a(i,j)
      do 13 k=1,i-1
      sum=sum-a(i,k)*a(k,j)
13      continue
      a(i,j)=sum
14      continue
      aamax=0.
      do 16 i=j,n
      sum=a(i,j)
      do 15 k=1,j-1
      sum=sum-a(i,k)*a(k,j)
15      continue
      a(i,j)=sum
      dum=vv(i)*abs(sum)
      if(dum.ge.aamax) then
      imax=i
      aamax=dum
      endif
16      continue
      if(j.ne.imax) then
      do 17 k=1,n
      dum=a(imax,k)
      a(imax,k)=a(j,k)
      a(j,k)=dum
17      continue
      d=-d
      vv(imax)=vv(j)
      endif
      indx(j)=imax
      if(a(j,j).eq.0) a(j,j)=tiny
      if(j.ne.n) then
      dum=1./a(j,j)
      do 18 i=j+1,n
      a(i,j)=a(i,j)*dum
18      continue
      endif
19      continue
      return
      end
C
      subroutine lubksb(a,n,np,indx,b)
      dimension a(np,np),indx(n),b(n)
      ii=0
      do 12 i=1,n
      ll=indx(i)
      sum=b(ll)
      b(ll)=b(i)
```

```
      if(ii.ne.0) then
      do 11 j=ii,i-1
      sum=sum-a(i,j)*b(j)
11      continue
      else if(sum.ne.0) then
      ii=i
      endif
      b(i)=sum
12      continue
      do 14 i=n,1,-1
      sum=b(i)
      if(i.lt.n) then
      do 13 j=i+1,n
      sum=sum-a(i,j)*b(j)
13      continue
      endif
      b(i)=sum/a(i,i)
14      continue
      return
      end



      subroutine prtfnd(a,p,ak2,prt,f2,f3,pr,ypd,tpd,
     x   ti,nts,prt,uw,cf,visc)
c
      real p,up(1000),yp(1000),tp(1000),prtc(1000)
      real ypd(100),tpd(100),prt(100),dtd(100)
      real z(6,6),b(6),f(20),g(20),x1(20),y1(20)
      ak=0.41
      e=exp(1.)
C
C   calculate the derivative dt+/dy+ using a curve fit at each pt
C
      do 80 i=1,nts-4
      dtd(i)=0.
      if(i.lt.5) then
      np=3
      nx=i+4
      m1=i
      else
      np=3
      nx=9
      m1=5
      endif
      do 81 j=1,nx
      x1(j)=ypd(i-m1+j)
      y1(j)=tpd(i-m1+j)
81      continue
      do 92 j=1,2*np-1
      f(j)=0.
      g(j)=0.
      do 82 k=1,nx
      f(j)=f(j)+x1(k)**(j-1)
      g(j)=g(j)+y1(k)*x1(k)**(j-1)
82      continue
92      continue
      do 93 k=1,np
      do 84 j=1,np
84      z(k,j)=f(j+k-1)
      b(k)=g(k)
93      continue
      call ludcmp(z,np,6,indx,d)
      call lubksb(z,np,6,indx,b)
      do 85 j=1,np-1
      dtd(i)=dtd(i)+j*b(j+1)*ypd(i)**(j-1)
85      continue
80      continue
      u=0
      dy=1./3.
      y=0
      u2=0
      u1=0
      ut=0
      t=0
      ik=1
      dudy=1.
c
c       curvature correction
c
      rp=-0.97*(cf/2)**.5*uw/visc
c
      do 30 i=1,1000
      if(i.gt.100) then
      dy=1.
      endif
      y=y+dy
C
C       find t+ from the data to match this y+ (linear interpolation)
      do 61 m=ik,nts
      if(y.lt.ypd(m)) then
```

```
      goto 62
      endif
61      continue
      goto 20
62      ik=m-1
      tpl=tpd(m-1)+(tpd(m)-tpd(m-1))*(y-ypd(m-1))/(ypd(m)-ypd(m-1))C
      dtdy=dtd(m-1)+(dtd(m)-dtd(m-1))*(y-ypd(m-1))/(ypd(m)-ypd(m-1))
C      write(*,*) y,tpl,dtdy
C
      vx=1+p*y+(ak2+f2)*u2
      if(vx.le.0) then
      goto 20
      end if
      yp(i)=y
c
      ri=2*u/rp/rp*(u/dudy**2.+rp/dudy)
      crv=1-4.5*ri
c
      v=(ak*y*(1.-e**(-y/a))*crv)**2.
      u=u+(-1+(1.+4.*v*vx)**.5)/(2.*v)*dy
      u2=u2+u*u*dy
      u1=u1+u*dy
      up(i)=u
      dudy=(-1+(1.+4.*v*vx)**.5)/(2.*v)
      ft=(ak2+f2)*ut-(ak2+f3)*ti*u1
      if(ft.gt.1) then
      goto 20
      endif
C      write(*,*) v,dudy,ft,dtdy
      prtc(i)=v*dudy/((1.-ft)/dtdy-1./pr)
      ut=ut+u*tpl*dy
      tp(i)=t
      ii=i
C      write(*,*) yp(i),prt(i),dtdy,ft,v,dudy
30      continue
20       continue
      ik=1
      do 33 i=1,nts-4
      do 34 j=ik,1000
      if(yp(j).gt.ypd(i)) then
      xxx=(ypd(i)-yp(j-1))/(yp(j)-yp(j-1))
      prt(i)=prtc(j-1)+(prtc(j)-prtc(j-1))*xxx
      goto 33
      endif
      ik=j-1
34      continue
33      continue
      return
      end
C
C
      subroutine condv(cond,temp)
      cond=7.305e-5*(temp+273.15)+4.229e-3
      return
      end

      subroutine viscal(visc,temp,press)
      visc=9.3277e-8*(temp+273.15)-1.2248e-5
      visc=visc*760./press
      return
      end

      subroutine cpcal(cp,temp)
      cp=0.053*(temp+273.15)+988.572
      return
      end

      subroutine rhocal(rho,temp,press)
      rho=1.1766*(press/760.)*(300./(temp+273.15))
      return
      end

      subroutine integr(yn,q2,m,sum2,strt)
c
      real q2(90)
      dimension yn(*)
c
      sum2=0.
      do 10 i=0,m-2
      if(i.eq.0) then
      x1=0.
      y21=strt
      else
      x1=yn(i)
      y21=q2(i)
      endif
      x2=yn(i+1)
      x3=yn(i+2)
      y22=q2(i+1)
```

```
      y23=q2(i+2)
      b2=((y23-y22)*(x1*x1-x2*x2)-(y21-y22)*(x3*x3-x2*x2))/
     x   ((x3-x2)*(x1*x1-x2*x2)-(x1-x2)*(x3*x3-x2*x2))
      a2=((y21-y22)-b2*(x1-x2))/(x1*x1-x2*x2)
      c2=y21-a2*x1*x1-b2*x1
c
      delar=a2/3.*(x2**3-x1**3)+b2/2.*(x2*x2-x1*x1)+c2*(x2-x1)
      if(delar.lt.0) then
      delar=y22*(x2-x1)
      write(*,*) "problems integrating for delenth"
      endif
      if(i.eq.m-2) then
      delar=a2/3.*(x3**3-x1**3)+b2/2.*(x3*x3-x1*x1)+c2*(x3-x1)
      if(delar.lt.0) then
      delar=y22*(x3-x1)
      write(*,*) "problems integrating for delenth"
      endif
      endif
      sum2=sum2+delar
10      continue
      return
      end
```

```
c  Calculates Prt from processed triple wire profile
c
c  Written:  Ralph Volino       6/29/94
c
c
c       Command Line:   prt
c
c       This program calculates turbulent Prandtl number using
c       the mean velocity and temperature, and u'v' and v't'
c       profiles obtained with the 3-wire probe
c
      program prt
      real t(60),u(60),uv(60),vt(60),tp(60),up(60),vp(60)
      real ut(60),uv2(60),v2t(60),gamma(60)
      real dudy(60),dtdy(60),pran(60),em(60),eh(60)
      real yf(5),tf(5),coef(10),uf(10),y(60)
      character*20 nam$
c
      write(*,*) "Input the name of the input file: "
      read(*,'(a)') nam$
      open(10,file=nam$,status="old")
c
      write(*,*) "Input the name of the output file: "
      read(*,'(a)') nam$
      open(20,file=nam$,status="new")
c
      write(*,*) "Enter Cf and St"
      read(*,*) cf,st
      write(*,*) "Enter the momemtum thickness"
      read(*,*) del2
      write(*,*) "Enter the enthalpy thickness"
      read(*,*) ent
c
      npt=5
      press=759.
      read(10,*) n,qw,uw
      do 30, i=1,n
      read(10,*) y(i),u(i),v,t(i),up(i),vp(i),tp(i),uv(i),ut(i)
     x  ,vt(i),uv2(i),v2t(i),gamma(i)
30     continue
      close(10)
      visc=16.54e-6
      utau=uw*(cf/2.)**.5
      ttau=qw/1.1436/1004/utau
      delt=ttau/st*utau/uw
c
c        Process the data
c
      do 40, i=1,n
      if(i.lt.(npt+1)/2.) then
      np=(npt+1)/2.+i-1
      str=i
      elseif(i.gt.n-(npt-1)/2.) then
      np=(npt+1)/2.+n-i
      str=(np+1)/2.
      else
      np=npt
      str=(np+1)/2.
      endif
      do 50, k=1,np
      yf(k)=y(i+k-str)
      tf(k)=t(i+k-str)
      uf(k)=u(i+k-str)
50     continue
c
      call curvf(np,yf,uf,coef,2)
      dudy(i)=(coef(2)+2.*coef(3)*y(i))*100.
      call curvf(np,yf,tf,coef,2)
      dtdy(i)=(coef(2)+2.*coef(3)*y(i))*100.
c
      y1=y(i)/del2
      y2=y(i)/ent
      yp=utau*y(i)/visc/100.
      upn=up(i)/utau
      vpn=vp(i)/utau
      uvn=-uv(i)/utau/utau
      tpn=tp(i)/ttau
      tpnd=tp(i)/delt
      vtnd=vt(i)/uw/delt
      vtn=vt(i)/utau/ttau
      utnd=-ut(i)/uw/delt
      utn=-ut(i)/utau/ttau
      uv2nd=-uv2(i)/uw**3
      uv2n=-uv2(i)/utau**3
      v2tnd=-ut(i)/uw/delt/uw
      v2tn=-ut(i)/utau/ttau/utau
c
      em(i)=-uv(i)/dudy(i)
      eh(i)=-vt(i)/dtdy(i)
```

```
      xl=em(i)/dudy(i)
      xlh=-eh(i)/dtdy(i)
      if(xl.le.0) then
      xl=0.
      else
      xl=xl**.5
      endif
      if(xlh.le.0) then
      xlh=0.
      else
      xlh=xlh**.5
      endif
      xl=xl*utau/visc
      xlh=xlh*utau/visc
      pran(i)=(uv(i)/dudy(i))/(vt(i)/dtdy(i))

      write(20,7) y1,y2,yp,upn,vpn,uvn,tpnd,tpn,vtnd,vtn,utnd,utn
     x  ,uv2nd,uv2n,v2tnd,v2tn,dudy(i),dtdy(i),pran(i)
     x  ,em(i),eh(i),xl,xlh,gamma(i),y(i),u(i),t(i)
7     format(2(f6.2,2x),f7.2,2x,13(f9.6,2x),2(f7.0,2x),f6.3,2x,
     x  2(f9.7,2x),2(f7.2,2x),f5.3,2x,f7.4,2x,f5.2,2x,f5.2)
40    continue
      end

      subroutine curvf(n,x,y,coef,m1)
      real f(10),g(10),z(10,10),b(10),x(10),y(10)
      real coef(10),indx(10)
c
      m=m1+1
      do 10 j=1,2*m-1
      f(j)=0.
      g(j)=0.
      do 20 k=1,n
      f(j)=f(j)+x(k)**(j-1)
      g(j)=g(j)+y(k)*x(k)**(j-1)
20    continue
10    continue
      do 30 k=1,m
      do 40 j=1,m
      z(k,j)=f(j+k-1)
40    continue
      b(k)=g(k)
30    continue
      call ludcmp(z,m,10,indx,d)
      call lubksb(z,m,10,indx,b)
      do 50 j=1,m
      coef(j)=b(j)
50    continue
      return
      end

      subroutine ludcmp(a,n,np,indx,d)
      parameter(nmax=100,tiny=1.0e-20)
      dimension a(np,np),indx(n),vv(nmax)
      d=1.
      do 12 i=1,n
      aamax=0.
      do 11 j=1,n
      if (abs(a(i,j)).gt.aamax) aamax=abs(a(i,j))
11    continue
      if(aamax.eq.0.) pause 'singular matrix'
      vv(i)=1./aamax
12    continue
      do 19 j=1,n
      do 14 i=1,j-1
      sum=a(i,j)
      do 13 k=1,i-1
      sum=sum-a(i,k)*a(k,j)
13    continue
      a(i,j)=sum
14    continue
      aamax=0.
      do 16 i=j,n
      sum=a(i,j)
      do 15 k=1,j-1
      sum=sum-a(i,k)*a(k,j)
15    continue
      a(i,j)=sum
      dum=vv(i)*abs(sum)
      if(dum.ge.aamax) then
      imax=i
      aamax=dum
      endif
16    continue
      if(j.ne.imax) then
      do 17 k=1,n
      dum=a(imax,k)
      a(imax,k)=a(j,k)
      a(j,k)=dum
17    continue
```

```
      d=-d
      vv(imax)=vv(j)
      endif
      indx(j)=imax
      if(a(j,j).eq.0) a(j,j)=tiny
      if(j.ne.n) then
      dum=1./a(j,j)
      do 18 i=j+1,n
      a(i,j)=a(i,j)*dum
18      continue
      endif
19      continue
      return
      end
C
      subroutine lubksb(a,n,np,indx,b)
      dimension a(np,np),indx(n),b(n)
      ii=0
      do 12 i=1,n
      ll=indx(i)
      sum=b(ll)
      b(ll)=b(i)
      if(ii.ne.0) then
      do 11 j=ii,i-1
      sum=sum-a(i,j)*b(j)
11      continue
      else if(sum.ne.0) then
      ii=i
      endif
      b(i)=sum
12      continue
      do 14 i=n,1,-1
      sum=b(i)
      if(i.lt.n) then
      do 13 j=i+1,n
      sum=sum-a(i,j)*b(j)
13      continue
      endif
      b(i)=sum/a(i,i)
14      continue
      return
      end
```

```
      program quadrant
      real sq(50,8),q(6),y(50)
      integer np(50)
      character*30 fil$
c
c      Puts quadrant analysis results into form for plotting
c
      write(*,*) "Enter the base data file name"
      read(*,'(a)') fil$
      open(20,file=fil$,status='old')
      read(20,*) p,qw,tw,tinf,x
      read(20,*) ist,n
      do 15 k=1,n
      read(20,*) j,y(k),u,v,t,up,vp,tp,uv,vt,ut,uv2,v2t,g,np(k)
15      continue
      close(20)
      write(*,*) "Enter the quadrant data file name"
      read(*,'(a)') fil$
      open(20,file=fil$,status='old')
      write(*,*) "Enter the quantity to process: 1) uv, 2) vt,"
      write(*,*) "3) ut, 4) uv2, 5) v2t, 6) No. of points"
      read(*,*) l
      write(*,*) "Enter the hole size number (0 - 10 even no.)"
      read(*,*) i
      i=i/2+1
      do 30 k=1,n
      do 40 j=1,8
      do 50 lr=1,6
      read(20,*) q(1),q(2),q(3),q(4),q(5),q(6)
      if(lr.eq.l) sq(k,j)=q(i)
50      continue
40      continue
30      continue
      close(20)
      write(*,*) "Enter the momentum thickness in cm"
      read(*,*) d2
      if(l.eq.1.or.l.eq.4.or.l.eq.5) then
      write(*,*) "Enter Uinf"
      read(*,*) uinf
      endif
      if(l.eq.1) then
      write(*,*) "Enter Cf"
      read(*,*) cf
      endif
      if(l.eq.1) an=uinf*uinf*cf/2.
      if(l.eq.2.or.l.eq.3) then
      tave=(tw+tinf)/2.
      rho=1.1766*p/760.*(300./(273.15+tave))
      cp=0.053*(tave+273.15)+988.572
      an=qw/rho/cp
      endif
      if(l.eq.4) an=uinf*3
      if(l.eq.5) an=uinf*(tw-tinf)
      if(l.eq.6) an=1.
      write(*,*) "Enter the output file name"
      read(*,'(a)') fil$
      open(20,file=fil$,status='new')
      do 60 k=1,n
      write(20,7) y(k)/d2,(sq(k,j)/an/np(k), j=1,8)
7      format(f8.3,8(2x,f9.6))
60      continue
      close(20)
      end
```

```
      program fplot
c
c      Pieces together sections of spectra
c
      character*20 fil$
      write(*,*) "Input the names of the data file"
      read(*,'(a)') fil$
      open(20,file=fil$,status="old")
      write(*,*) "Input the name of the output file"
      read(*,'(a)') fil$
      open(30,file=fil$,status="new")
      do 40 i=1,3
      read(20,*) mm,hz,ua,upr
      m=mm/2.
      do 50 j=1,m+1
      read(20,*) v
      f=hz/mm*(j-1)
      if(i.eq.1.and.f.le.50) then
      write(30,*) f,f*v
      endif
      if(i.eq.2.and.f.le.500.and.f.gt.50) then
      write(30,*) f,f*v
      endif
      if(i.eq.3.and.f.le.10000.and.f.gt.500) then
      write(30,*) f,f*v
      endif
50      continue
40      continue
      close(20)
      close(30)
      end
```

```
      program smoln
c      Smooths spectra for plotting
c
      real f(1000),p(1000)
      character*30 nam$
      write(*,*) "Input the file name"
      read(*,'(a)') nam$
      open(20,file=nam$,status='old')
      write(*,*) "Output file name"
      read(*,'(a)') nam$
      open(30,file=nam$,status='new')
      do 40 i=1,746
      read(20,*) f(i),p(i)
40      continue
      do 70 i=5,30
      sumx=0.
      sumx2=0.
      sumxy=0.
      sumy=0.
      do 64 j=i-3,i+3
      sumy=sumy+log(p(j))
      sumx=sumx+log(f(j))
      sumx2=sumx2+log(f(j))**2.
      sumxy=sumxy+log(f(j))*log(p(j))
64      continue
      am=(7*sumxy-sumx*sumy)/(7*sumx2-sumx*sumx)
      ab=(sumy*sumx2-sumx*sumxy)/(7*sumx2-sumx*sumx)
      write(30,*) f(i),exp(am*log(f(i))+ab)
70      continue
      do 50 i=31,717
      sumx=0.
      sumx2=0.
      sumxy=0.
      sumy=0.
      do 60 j=i-29,i+29
      sumy=sumy+log(p(j))
      sumx=sumx+log(f(j))
      sumx2=sumx2+log(f(j))**2.
      sumxy=sumxy+log(f(j))*log(p(j))
60      continue
      am=(59*sumxy-sumx*sumy)/(59*sumx2-sumx*sumx)
      ab=(sumy*sumx2-sumx*sumxy)/(59*sumx2-sumx*sumx)
      write(30,*) f(i),exp(am*log(f(i))+ab)
50      continue
      end
```

```
c     Calculates velocity and temp. profile taking
c     pressure gradient effects into account.
c
      program lwall
c
      real p,up(1000),yp(1000),tp(1000)
      pr=0.71
      ct=0.2
      prti=0.86
      ak=0.41
      pi=3.141592654
      e=exp(1.)
      write(*,*) "input f2"
      read(*,*) f2
      write(*,*) "input the skin friction coefficient"
      read(*,*) cf
      write(*,*) "input the acceleration, K"
      read(*,*) ak1
      write(*,*) "input f3"
      read(*,*) f3
      write(*,*) "input t+ infinity"
      read(*,*) ti
      write(*,*) "input a file name for result"
      read(*,'(a)'),f$
      open(10,file=f$,status="new")
      p=-ak1/(cf/2.)**1.5
      do 20 k=1,1
      if (p.lt.0) then
      a=25./(7.1*4.25*p+1)
      else
      a=25./(7.1*2.9*p+1)
      endif
      if(a.lt.0) a=99.
      write(*,*) "A+ = ",a
      write(*,*) "input A+"
      read(*,*) a
      u=0
      dy=1./3.
      y=0
      ak2=-p*cf/2.
      u2=0
      u1=0
      ut=0
      t=0
c
      visc=16.e-6
      write(*,*) "Input Uw for curvature correction"
      read(*,*) uw
c
      rp=-0.97*(cf/2)**.5*uw/visc
      dudy=1.
c
      do 30 i=1,1000
      if(i.gt.100) then
      dy=1.
      endif
      y=y+dy
      vx=1+p*y+(ak2+f2)*u2
      if(vx.le.0) then
      goto 20
      end if
      yp(i)=y
c
c     Curvature correction   (not used here)
c      ri=2*u/rp/rp*(u/(dudy)**2.+rp/dudy)
      ri=0
      crv=1-4.5*ri
c
      v=(ak*y*(1.-e**(-y/a))*crv)**2.
      u=u+(-1+(1.+4.*v*vx)**.5)/(2.*v)*dy
      u2=u2+u*u*dy
      u1=u1+u*dy
      up(i)=u
      dudy=(-1+(1.+4.*v*vx)**.5)/(2.*v)
c      pet=pr*ak*ak*y*y*dudy
      pet=pr*v*dudy
      prt=1./(.5/prti+ct*pet/prti**.5-(ct*pet)**2*
     x       (1.-e**(-1./(ct*pet*prti**.5))))
      ft=(ak2+f2)*ut-(ak2+f3/ti)*ti*u1
      t=t+(1-ft)/(1/pr+v/prt*dudy)*dy
      ut=ut+u*t*dy
      tp(i)=t
      ii=i
30      continue
20       continue
      do 40 i=1,ii
      write(10,7) yp(i),tp(i),up(i)
7      format(3f9.3)
40      continue
      end
```

APPENDIX C: TABULATED DATA

KEY TO DATA

Single Hot-Wire Velocity Profiles

x	distance from leading edge of test wall [m]
visc	kinematic viscosity [m^2/s]
cf	skin friction coefficient
yeff	distance profile data has been shifted in the y direction [cm]
d99.5	boundary layer thickness, $\delta_{99.5}$ [cm]
del1	displacement thickness, δ^* [cm]
del2	momentum thickness, θ [cm]
H	shape factor, δ^*/θ
Uw	core velocity extrapolated to the wall, U_{cw} [m/s]
Rex	x-based Reynolds number, Re_x
Red1	displacement thickness Reynolds number, $Re\delta^*$
Red2	displacement thickness Reynolds number, $Re\theta$
coef1 coef2	coef1+coef2*y is equation of line fit to core velocity, coef1=Uw coef1 [m/s], coef2 [m/(s cm)]
A^+	Van Driest damping constant
K	acceleration parameter
f1	parameter used in Appendix A to calculate mean velocity profiles
N	profile point number
y	distance from the wall [cm]
U	mean streamwise velocity [m/s]
y^+, u^+	y and U in wall coordinates

u′	streamwise rms velocity, $\overline{u'}$ [m/s]
gamma	intermittency, γ

Thermocouple Probe Mean Temperature Profiles

patm	atmospheric pressure [mm Hg]
x	distance from the leading edge of the test wall [cm]
cf	skin friction coefficient
yeff	adjustment of raw data so that y-position is one thermocouple-wire radius when the wire is in contact with the test wall [cm]
Tw	wall temperature determined from profile data [°C]
Tinf	free-stream temperature [°C]
Tw measured	embedded thermocouple temperature (not used) [°C]
Tw correction	difference between Tw and Tw measured [°C]
Q wall	convective wall heat flux determined from mean temperature profile (value used to determine St) [W/m^2]
Stanton No.	Stanton number, St
Qwall measured	convective wall heat flux determined based on input power to heater with radiation correction based on Tw (corrected) or Tw measured
delther	thermal boundary layer thickness, $\delta_{t99.5}$ [cm]
deleth	enthalpy thickness, Δ_2 [cm]
delcon	conduction thickness, k(Tw-T∞)/q, (k= conductivity of air) [cm]
qadded	$\int_0^{\delta_{t99.5}} \rho c_p U(T - T_\infty) dy$ [W/m]
Uw	core velocity extrapolated to the wall [m/s]
Rex	x-based Reynolds number, Re_x
Reh	enthalpy thickness Reynolds number, Re_{Δ_2}
coef1 coef2	coef1+coef2*y is equation of line fit to core velocity, coef1=Uw coef1 [m/s], coef2 [m/(s cm)]

A^+	Van Driest damping constant
K	acceleration parameter
f1, f2	parameter used in Appendix A to calculate mean velocity and temperature profiles
N	profile point number
y	distance from the wall [cm]
T	mean temperature [°C]
Tnd	dimensionless temperature, $\frac{T - T_\infty}{T_w - T_\infty}$
y^+, t^+	y and T in wall coordinates
Prt	turbulent Prandtl number, Prt, as calculated in Appendix A

Cross-Wire and Triple-Wire Profiles

x	distance from the leading edge of the test wall [cm]
Patm	atmospheric pressure [mm Hg]
qwall	convective heat flux (determined based on input power to heater with radiation correction) [W/m2]
y	distance from the test wall [cm]
U	mean streamwise velocity [m/s]
V	mean velocity normal to test wall [m/s]
T	mean temperature [°C]
u'	streamwise rms fluctuating velocity, $\overline{u'}$ [m/s]
v'	normal component of rms fluctuating velocity, $\overline{v'}$ [m/s]
t'	rms fluctuating temperature, $\overline{t'}$ [°C]
u'v'	turbulent shear stress, $\overline{u'v'}$ [m^2/s^2]
u't'	streamwise component of turbulent heat flux, $\overline{u't'}$ [°C m/s]
v't'	normal component of turbulent heat flux, $\overline{v't'}$ [°C m/s]

u'v'2	cross-stream transport of turbulent shear stress, $\overline{u'v'^2}$ [m^3/s^3]
v'2t'	cross-stream transport of turbulent heat flux, $\overline{v'^2t'}$ [°C m^2/s^2]
gamma	intermittency, γ
dU/dy	normal gradient of mean streamwise velocity [1/s]
dT/dy	normal gradient of mean temperature [°C/m]
em	eddy viscosity, ε_M [m^2/s]
eh	eddy diffusivity of heat, ε_H [m^2/s]
l	mixing length of momentum, ℓ_M [m]
Prt	turbulent Prandtl number, Pr_t

CONTENTS

	Page
Low FSTI Case	516
Single Hot-Wire Velocity Profiles	517
Triple-Wire Profiles	543
K=0.75×10^{-6} Case	544
Single Hot-Wire Profiles	545
Mean Temperature Profiles	550
Cross-Wire Profiles	555
dU_{cw}/dx=29 s^{-1} Case	558
Single Hot-Wire Profiles	559
Mean Temperature Profiles	570
Cross-Wire Profiles	581
Triple-Wire Profiles	586
dU_{cw}/dx=14 s^{-1} Case	596
Single Hot-Wire Profiles	597
Mean Temperature Profiles	607
Cross-Wire Profiles	618
Triple-Wire Profiles	623

LOW FSTI CASE DATA

	Page
Single Hot-Wire Velocity Profiles	517
Triple-Wire Profiles	543

Station = a1 z=-1.59 downwash

x = 0.361 visc = 1.59800E-05
cf = 3.70000E-03 yeff = 0.
d99.5 = 0.332005 del1 = 6.67784E-02
del2 = 4.19241E-02 H = 1.59284
Ue = 17.6007 Rex = 397613.
Red1 = 735.510 Red2 = 461.760
coef1 = 17.6007 coef2 = 0.147210
A+ = 25.0000
K = 0. f1 = 0.

N	y	U	y+	u+	u'	gamma
1	2.50000E-03	0.590903	1.18435	0.780551	0.268100	4.00000E-02
2	4.50000E-03	1.32826	2.13182	1.75456	0.383800	6.80000E-02
3	7.00000E-03	2.34107	3.31617	3.09243	0.680900	6.90000E-02
4	8.50000E-03	2.96241	4.02677	3.91318	0.625700	6.50000E-02
5	1.00000E-02	3.58699	4.73738	4.73822	0.698000	6.00000E-02
6	1.15000E-02	4.17930	5.44799	5.52063	0.771000	6.80000E-02
7	1.30000E-02	4.74165	6.15859	6.26346	0.975900	8.20000E-02
8	1.45000E-02	5.24011	6.86920	6.92190	0.974500	1.01000E-01
9	1.60000E-02	5.83077	7.57981	7.70213	1.15060	9.80000E-02
10	1.70000E-02	6.22263	8.05355	8.21975	1.13900	1.00000E-01
11	1.80000E-02	6.57644	8.52728	8.68713	1.16960	9.90000E-02
12	1.95000E-02	7.05931	9.23789	9.32496	1.22320	8.20000E-02
13	2.10000E-02	7.50889	9.94850	9.91883	1.28850	9.10000E-02
14	2.25000E-02	7.99304	10.6591	10.55838	1.39150	0.108000
15	2.40000E-02	8.41209	11.3697	11.1119	1.38220	8.00000E-02
16	2.55000E-02	8.87311	12.0803	11.7209	1.50890	1.01000E-01
17	2.70000E-02	9.32427	12.7909	12.3169	1.49810	9.90000E-02
18	2.85000E-02	9.67468	13.5015	12.7797	1.48710	8.80000E-02
19	3.05000E-02	10.11806	14.4490	13.3654	1.59150	9.90000E-02
20	3.25000E-02	10.54536	15.3965	13.9298	1.56530	8.80000E-02
21	3.45000E-02	11.0266	16.3440	14.5655	1.54440	8.10000E-02
22	3.65000E-02	11.3264	17.2914	14.9615	1.66280	8.80000E-02
23	3.95000E-02	11.9817	18.7127	15.8272	1.68690	8.80000E-02
24	4.15000E-02	12.2160	19.6601	16.1367	1.60630	9.30000E-02
25	4.55000E-02	12.7728	21.5551	16.8722	1.54000	6.90000E-02
26	4.90000E-02	13.1853	23.2132	17.4171	1.58940	8.00000E-02
27	5.30000E-02	13.4448	25.1081	17.7599	1.53370	7.70000E-02
28	6.05000E-02	14.0915	28.6612	18.6141	1.50040	7.20000E-02
29	6.60000E-02	14.3482	31.2667	18.9532	1.42850	8.30000E-02
30	7.65000E-02	14.7386	36.2410	19.4689	1.30360	6.40000E-02
31	9.00000E-02	14.8370	42.6364	19.5988	1.45240	8.90000E-02
32	0.117000	14.6615	55.4273	19.3670	1.60970	7.40000E-02
33	0.171000	13.7874	81.0092	18.2124	2.36320	9.90000E-02
34	0.201500	13.9873	95.4582	18.4764	2.48930	9.70000E-02
35	0.262500	16.3671	124.356	21.6201	1.41600	4.60000E-02
36	0.275000	16.7794	130.278	22.1646	1.11910	4.90000E-02
37	0.290000	17.1807	137.384	22.6947	0.900400	4.00000E-02
38	0.308500	17.4240	146.148	23.0161	0.647800	4.40000E-02
39	0.345500	17.6405	163.676	23.3022	0.433200	3.10000E-02
40	0.419500	17.6512	198.733	23.3163	0.267000	2.90000E-02
41	0.567500	17.7200	268.846	23.4071	0.251200	1.80000E-02
42	0.863500	17.7175	409.073	23.4039	0.126800	4.00000E-03
43	1.36350	17.8058	645.942	23.5205	0.110100	0.
44	1.86350	17.8809	882.811	23.6197	9.99000E-02	0.
45	2.36350	17.9349	1119.68	23.6911	1.03100E-01	0.
46	2.86350	18.0129	1356.55	23.7941	0.110300	0.
47	3.36350	18.1080	1593.42	23.9196	0.107800	0.

Station = a2 z=-2.19

x = 0.361 visc = 1.59200E-05
cf = 4.00000E-03 yeff = 0.
d99.5 = 0.330759 del1 = 5.03582E-02
del2 = 2.97678E-02 H = 1.69170
Uw = 17.6195 Rex = 399538.
Red1 = 557.342 Red2 = 329.456
coef1 = 17.6195 coef2 = 0.140897
A+ = 25.0000
K = 0. f1 = 0.

N	y	U	y+	u+	u'	gamma
1	1.00000E-03	0.324160	0.494956	0.411387	0.300100	5.10000E-02
2	1.50000E-03	0.341310	0.742433	0.433152	0.359200	5.90000E-02
3	2.50000E-03	0.758415	1.23739	0.962494	0.452400	7.10000E-02
4	4.00000E-03	1.48349	1.97982	1.88268	0.664100	6.90000E-02
5	5.50000E-03	2.15360	2.72226	2.73311	0.705300	9.40000E-02
6	7.00000E-03	2.72149	3.46469	3.45381	0.793700	9.50000E-02
7	8.50000E-03	3.34085	4.20712	4.23982	0.923300	9.40000E-02
8	1.00000E-02	3.95365	4.94955	5.01752	1.08710	8.60000E-02
9	1.15000E-02	4.50439	5.69199	5.71645	1.23750	1.00000E-01
10	1.30000E-02	5.03242	6.43442	6.38657	1.22940	1.04000E-01
11	1.45000E-02	5.63112	7.17685	7.14637	1.41410	0.122000
12	1.55000E-02	5.95400	7.67181	7.55613	1.35720	0.129000
13	1.70000E-02	6.38914	8.41424	8.10836	1.43820	0.107000
14	1.85000E-02	6.93527	9.15668	8.80145	1.54970	0.120000
15	1.95000E-02	7.30640	9.65163	9.27244	1.62240	0.152000
16	2.05000E-02	7.59693	10.14659	9.64116	1.63970	0.118000
17	2.20000E-02	7.97449	10.8890	10.12031	1.68920	0.128000
18	2.40000E-02	8.45258	11.8789	10.7270	1.82740	0.120000
19	2.60000E-02	8.88321	12.8688	11.2735	1.86100	0.130000
20	2.80000E-02	9.32884	13.8588	11.8391	1.95980	0.125000
21	3.00000E-02	9.79340	14.8487	12.4287	2.01670	0.141000
22	3.20000E-02	10.26368	15.8386	13.0255	2.01760	0.125000
23	3.40000E-02	10.6428	16.8285	13.5066	2.06650	0.134000
24	3.65000E-02	11.0588	18.0659	14.0345	2.07710	0.121000
25	3.95000E-02	11.5407	19.5507	14.6462	2.16290	0.140000
26	4.25000E-02	11.9887	21.0356	15.2147	2.13260	0.117000
27	4.55000E-02	12.3373	22.5205	15.6571	2.19420	0.127000
28	4.95000E-02	12.7219	24.5003	16.1452	2.13520	0.119000
29	5.45000E-02	13.1774	26.9751	16.7233	2.15000	0.122000
30	6.00000E-02	13.5917	29.6973	17.2490	2.03410	0.144000
31	6.65000E-02	14.0123	32.9145	17.7828	1.96260	8.90000E-02
32	7.40000E-02	14.4340	36.6267	18.3180	1.86810	0.114000
33	8.30000E-02	14.7542	41.0813	18.7243	1.67330	7.30000E-02
34	9.70000E-02	15.1898	48.0107	19.2772	1.52840	8.10000E-02
35	0.113000	15.5399	55.9300	19.7215	1.29490	7.10000E-02
36	0.136000	15.8476	67.3139	20.1120	1.26370	5.70000E-02
37	0.173500	16.1059	85.8748	20.4398	1.52960	6.30000E-02
38	0.247000	17.1056	122.254	21.7084	0.911300	5.60000E-02
39	0.283500	17.4275	140.320	22.1170	0.670200	5.00000E-02
40	0.340000	17.6075	168.285	22.3454	0.432700	3.40000E-02
41	0.453000	17.6395	224.215	22.3860	0.212200	2.50000E-02
42	0.679000	17.6993	336.075	22.4619	0.134500	1.80000E-02
43	1.13100	17.7827	559.795	22.5678	0.110800	0.
44	1.63100	17.8428	807.273	22.6441	0.116200	0.
45	2.13100	17.9379	1054.75	22.7647	1.04100E-01	0.
46	2.63100	17.9589	1302.23	22.7914	1.02000E-01	0.
47	3.13100	18.0730	1549.71	22.9361	0.105300	0.
48	3.63100	18.1340	1797.18	23.0135	9.39000E-02	0.

Station = a3 z=-2.69 midspan

x = 0.361 visc = 1.59300E-05
cf = 3.80000E-03 yeff = 0.
d99.5 = 0.316012 del1 = 5.59506E-02
del2 = 3.04422E-02 H = 1.83793
Uw = 17.5729 Rex = 398231.
Red1 = 617.208 Red2 = 335.818
coef1 = 17.5729 coef2 = 0.146621
A+ = 25.0000
K = 0. f1 = 0.

N	y	U	y+	u+	u'	gamma
1	5.00000E-04	0.320480	0.240422	0.418390	0.487200	7.00000E-02
2	1.00000E-03	0.328160	0.480844	0.428416	0.527600	5.90000E-02
3	1.50000E-03	0.352333	0.721266	0.459974	0.588600	7.70000E-02
4	2.50000E-03	0.792856	1.20211	1.03508	0.847900	8.00000E-02
5	4.00000E-03	1.45833	1.92338	1.90387	0.892400	1.02000E-01
6	6.50000E-03	2.42537	3.12549	3.16634	1.05540	9.70000E-02
7	8.00000E-03	2.96219	3.84675	3.86717	1.22810	0.110000
8	9.50000E-03	3.48939	4.56802	4.55544	1.35460	0.137000
9	1.15000E-02	4.10423	5.52970	5.35812	1.59550	0.136000
10	1.35000E-02	4.72433	6.49139	6.16765	1.61520	0.163000
11	1.50000E-02	5.07948	7.21266	6.63131	1.72500	0.143000
12	1.75000E-02	5.78974	8.41477	7.55856	1.96150	0.151000
13	1.90000E-02	6.18577	9.13603	8.07558	2.06890	0.174000
14	2.10000E-02	6.65877	10.09772	8.69310	2.15600	0.166000
15	2.30000E-02	7.04507	11.0594	9.19741	2.29960	0.167000
16	2.55000E-02	7.73126	12.2615	10.09324	2.38620	0.162000
17	2.70000E-02	7.98593	12.9828	10.42571	2.38510	0.169000
18	3.00000E-02	8.55360	14.4253	11.1668	2.62720	0.188000
19	3.25000E-02	8.94844	15.6274	11.6823	2.61990	0.176000
20	3.55000E-02	9.43371	17.0700	12.3158	2.73950	0.172000
21	3.85000E-02	9.78190	18.5125	12.7704	2.73350	0.185000
22	4.25000E-02	10.33436	20.4359	13.4916	2.83300	0.180000
23	4.60000E-02	10.6905	22.1188	13.9565	2.80770	0.169000
24	5.10000E-02	11.1578	24.5230	14.5667	2.78870	0.153000
25	5.60000E-02	11.5111	26.9273	15.0279	2.83760	0.158000
26	6.30000E-02	11.9280	30.2932	15.5721	2.78380	0.150000
27	7.15000E-02	12.5555	34.3803	16.3914	2.73690	0.170000
28	7.80000E-02	12.8192	37.5058	16.7355	2.62110	0.150000
29	9.05000E-02	13.5235	43.5164	17.6550	2.47900	0.122000
30	9.90000E-02	13.9586	47.6035	18.2231	2.35740	0.105000
31	0.108500	14.3174	52.1716	18.6916	2.16390	9.70000E-02
32	0.121500	15.0183	58.4225	19.6065	1.81530	7.90000E-02
33	0.130500	15.3979	62.7501	20.1021	1.63520	8.10000E-02
34	0.142000	15.8325	68.2798	20.6695	1.36590	5.20000E-02
35	0.155000	16.2491	74.5308	21.2133	1.09620	6.10000E-02
36	0.170500	16.5955	81.9839	21.6656	0.952100	5.60000E-02
37	0.192500	16.9471	92.5624	22.1246	0.807300	5.90000E-02
38	0.223500	17.2877	107.469	22.5692	0.590400	3.90000E-02
39	0.269000	17.4711	129.347	22.8087	0.490900	4.50000E-02
40	0.360000	17.5877	173.104	22.9609	0.386400	4.30000E-02
41	0.542000	17.6369	260.617	23.0251	0.350200	2.20000E-02
42	0.906000	17.7026	435.645	23.1109	0.109300	1.00000E-03
43	1.40600	17.7848	676.066	23.2182	0.116000	0.
44	1.90600	17.8429	916.488	23.2941	1.03100E-01	0.
45	2.40600	17.9269	1156.91	23.4038	9.38000E-02	0.
46	2.90600	18.0139	1397.33	23.5174	0.109500	0.
47	3.40600	18.0620	1637.75	23.5801	0.108200	0.

Station = a4 z=-3.24

x = 0.361 visc = 1.59600E-05
cf = 3.25000E-03 yeff = 0.
d99.5 = 0.268630 del1 = 7.25600E-02
del2 = 3.57517E-02 H = 2.02956
Ue = 17.5439 Rex = 396826.
Red1 = 797.611 Red2 = 392.998
coef1 = 17.5439 coef2 = 0.152619
A+ = 25.0000
K = 0. f1 = 0.

N	y	U	y+	u+	u'	gamma
1	5.00000E-04	0.331520	0.221560	0.468766	0.825800	9.80000E-02
2	1.00000E-03	0.348960	0.443119	0.493426	0.909300	0.116000
3	1.50000E-03	0.365125	0.664679	0.516282	0.931700	9.70000E-02
4	2.50000E-03	0.790347	1.10780	1.11754	1.03990	0.111000
5	4.50000E-03	1.57419	1.99404	2.22588	1.12310	0.112000
6	7.50000E-03	2.50423	3.32340	3.54096	1.43710	0.132000
7	9.50000E-03	3.04435	4.20963	4.30469	1.58000	0.160000
8	1.25000E-02	3.82080	5.53899	5.40257	1.76560	0.164000
9	1.50000E-02	4.29764	6.64679	6.07682	2.01380	0.173000
10	1.80000E-02	4.91566	7.97615	6.95069	2.16880	0.193000
11	2.05000E-02	5.35475	9.08395	7.57156	2.36470	0.220000
12	2.35000E-02	5.93096	10.41330	8.38632	2.51210	0.200000
13	2.60000E-02	6.29625	11.5211	8.90284	2.62120	0.210000
14	2.95000E-02	6.74917	13.0720	9.54326	2.64800	0.207000
15	3.35000E-02	7.17140	14.8445	10.14029	2.73270	0.229000
16	3.80000E-02	7.63858	16.8385	10.8009	2.77640	0.212000
17	4.25000E-02	8.11215	18.8326	11.4705	2.87020	0.210000
18	4.70000E-02	8.43328	20.8266	11.9246	2.79310	0.190000
19	5.40000E-02	8.86892	23.9284	12.5406	2.80590	0.210000
20	6.20000E-02	9.45293	27.4734	13.3664	2.86590	0.192000
21	6.85000E-02	9.84743	30.3537	13.9242	2.86240	0.182000
22	7.65000E-02	10.13086	33.8986	14.3249	2.78220	0.171000
23	9.05000E-02	11.0709	40.1023	15.6541	2.67870	0.151000
24	9.75000E-02	11.5491	43.2041	16.3303	2.64210	0.155000
25	1.04500E-01	11.8711	46.3060	16.7856	2.56030	0.124000
26	0.115000	12.6472	50.9587	17.8830	2.43630	0.110000
27	0.121500	13.1173	53.8390	18.5478	2.33560	0.121000
28	0.128000	13.5423	56.7193	19.1487	2.20990	9.60000E-02
29	0.135500	14.1163	60.0427	19.9603	2.01990	9.10000E-02
30	0.142000	14.5531	62.9230	20.5779	1.83710	8.60000E-02
31	0.149000	15.0418	66.0248	21.2689	1.72490	8.40000E-02
32	0.156000	15.3495	69.1266	21.7040	1.54670	5.80000E-02
33	0.167000	15.8774	74.0009	22.4505	1.31900	7.10000E-02
34	0.177000	16.3231	78.4321	23.0808	1.08990	6.40000E-02
35	0.188000	16.6619	83.3064	23.5597	0.938600	5.10000E-02
36	0.204000	17.0098	90.3963	24.0516	0.773900	3.80000E-02
37	0.227000	17.2828	100.5881	24.4377	0.656300	4.60000E-02
38	0.269000	17.4991	119.199	24.7436	0.572000	3.70000E-02
39	0.353000	17.5766	156.421	24.8532	0.325700	3.00000E-02
40	0.521000	17.6388	230.865	24.9411	0.205700	2.50000E-02
41	0.857000	17.6855	379.753	25.0071	1.04700E-01	1.00000E-03
42	1.35700	17.7288	601.313	25.0683	9.16000E-02	0.
43	1.85700	17.8249	822.873	25.2042	0.106100	0.
44	2.35700	17.9249	1044.43	25.3457	0.104900	0.
45	2.85700	17.9759	1265.99	25.4178	0.105400	0.
46	3.35700	18.0520	1487.55	25.5253	1.02100E-01	0.

Station = a5 z=-3.79 upwash

x = 0.361 visc = 1.59700E-05
cf = 2.20000E-03 yeff = 0.
d99.5 = 0.271486 del1 = 9.11756E-02
del2 = 3.95890E-02 H = 2.30305
Uw = 17.5966 Rex = 397769.
Red1 = 1004.621 Red2 = 436.213
coef1 = 17.5966 coef2 = 0.149031
A+ = 25.0000
K = 0. f1 = 0.

N	y	U	y+	u+	u'	gamma
1	5.00000E-04	0.225280	0.182722	0.386009	0.458200	6.20000E-02
2	1.00000E-03	0.232160	0.365443	0.397798	0.489900	7.00000E-02
3	1.50000E-03	0.237440	0.548165	0.406845	0.524700	6.70000E-02
4	2.50000E-03	0.402533	0.913608	0.689727	0.580800	7.60000E-02
5	4.50000E-03	0.311945	1.64449	0.534507	0.767300	9.00000E-02
6	8.50000E-03	1.81798	3.10627	3.11504	0.986600	0.117000
7	1.20000E-02	2.63189	4.38532	4.50966	1.34420	0.165000
8	1.45000E-02	2.97639	5.29893	5.09993	1.41040	0.139000
9	1.90000E-02	3.70529	6.94342	6.34888	1.76250	0.177000
10	2.25000E-02	4.29173	8.22248	7.35373	1.97590	0.202000
11	2.55000E-02	4.57318	9.31880	7.83598	1.91520	0.193000
12	3.10000E-02	5.33068	11.3287	9.13394	2.12260	0.210000
13	3.45000E-02	5.62315	12.6078	9.63507	2.09390	0.185000
14	4.05000E-02	6.27083	14.8005	10.7448	2.25200	0.201000
15	4.50000E-02	6.64232	16.4450	11.3814	2.36940	0.199000
16	5.10000E-02	7.13173	18.6376	12.2200	2.33100	0.205000
17	5.70000E-02	7.31157	20.8303	12.5281	2.18610	0.168000
18	6.90000E-02	7.93645	25.2156	13.5988	2.11220	0.153000
19	7.85000E-02	8.39962	28.6873	14.3924	2.15640	0.127000
20	8.85000E-02	9.00041	32.3417	15.4219	2.21950	0.140000
21	9.65000E-02	9.37384	35.2653	16.0617	2.21230	0.126000
22	0.107000	9.98923	39.1024	17.1162	2.17430	0.122000
23	0.115500	10.56971	42.2087	18.1108	2.14790	0.120000
24	0.122500	11.1447	44.7668	19.0960	2.06590	1.02000E-01
25	0.128500	11.5894	46.9595	19.8581	2.04380	0.106000
26	0.135000	12.0602	49.3349	20.6647	2.02410	9.50000E-02
27	0.141500	12.7218	51.7102	21.7983	1.90800	8.90000E-02
28	0.146000	13.1681	53.3547	22.5631	1.95880	9.70000E-02
29	0.151000	13.5346	55.1819	23.1910	1.82690	7.90000E-02
30	0.156800	14.0070	57.3015	24.0005	1.66610	5.80000E-02
31	0.164000	14.5026	59.9327	24.8496	1.56460	6.40000E-02
32	0.170500	14.9440	62.3081	25.6060	1.49370	7.00000E-02
33	0.177500	15.4684	64.8662	26.5046	1.29340	6.50000E-02
34	0.184000	15.7288	67.2416	26.9508	1.30610	6.20000E-02
35	0.196000	16.3304	71.6269	27.9816	1.09340	5.90000E-02
36	0.205500	16.6309	75.0986	28.4965	0.990100	5.70000E-02
37	0.221000	17.0666	80.7630	29.2430	0.701500	3.30000E-02
38	0.238500	17.3162	87.1582	29.6708	0.749500	4.70000E-02
39	0.273500	17.5632	99.9487	30.0940	0.536500	4.40000E-02
40	0.343500	17.6425	125.530	30.2298	0.346700	2.70000E-02
41	0.483500	17.6876	176.692	30.3071	0.214900	2.40000E-02
42	0.763500	17.7154	279.016	30.3547	0.106100	8.00000E-03
43	1.26350	17.7688	461.738	30.4461	0.107100	0.
44	1.76350	17.8679	644.459	30.6159	0.111300	0.
45	2.26350	17.9369	827.181	30.7343	1.02400E-01	0.
46	2.76350	18.0119	1009.90	30.8628	0.111700	0.
47	3.26350	18.0780	1192.62	30.9759	1.02400E-01	0.

Station = b1 z=-1.59 downwash

x = 0.361 visc = 1.60000E-05
cf = 3.60000E-03 yeff = 0.
d99.5 = 0.332855 del1 = 6.75221E-02
del2 = 4.08870E-02 H = 1.65143
Uw = 16.5115 Rex = 372541.
Red1 = 696.809 Red2 = 421.942
coef1 = 16.5115 coef2 = 0.136973
A+ = 25.0000
K = 0. f1 = 0.

N	y	U	y+	u+	u'	gamma
1	1.00000E-03	0.274240	0.437828	0.391478	0.150600	1.60000E-02
2	1.50000E-03	0.277600	0.656743	0.396274	0.168600	1.50000E-02
3	2.50000E-03	0.510772	1.09457	0.729126	0.207100	1.50000E-02
4	4.50000E-03	1.16521	1.97023	1.66334	0.286100	6.00000E-03
5	7.50000E-03	2.21397	3.28371	3.16044	0.530300	1.50000E-02
6	9.00000E-03	2.75634	3.94046	3.93468	0.520100	1.40000E-02
7	1.05000E-02	3.22202	4.59720	4.59943	0.534600	1.10000E-02
8	1.25000E-02	3.82080	5.47286	5.45418	0.599900	1.40000E-02
9	1.45000E-02	4.37805	6.34851	6.24966	0.732800	2.70000E-02
10	1.65000E-02	4.97202	7.22417	7.09756	0.807300	2.50000E-02
11	1.80000E-02	5.46507	7.88091	7.80138	0.698900	2.20000E-02
12	1.95000E-02	5.91806	8.53765	8.44804	0.950600	2.90000E-02
13	2.10000E-02	6.27969	9.19440	8.96425	0.900600	1.50000E-02
14	2.30000E-02	6.77710	10.07005	9.67432	0.991500	2.30000E-02
15	2.50000E-02	7.26896	10.9457	10.37643	0.608700	2.10000E-02
16	2.70000E-02	7.70393	11.8214	10.9974	1.07580	1.60000E-02
17	2.90000E-02	8.13313	12.6970	11.6100	1.14760	2.40000E-02
18	3.10000E-02	8.54028	13.5727	12.1912	1.20960	3.00000E-02
19	3.35000E-02	9.08673	14.6673	12.9713	1.18630	2.10000E-02
20	3.55000E-02	9.42974	15.5429	13.4609	1.18370	1.70000E-02
21	3.80000E-02	9.84840	16.6375	14.0586	1.20050	1.50000E-02
22	4.10000E-02	10.32616	17.9510	14.7406	1.26060	1.80000E-02
23	4.40000E-02	10.8202	19.2645	15.4458	1.20070	2.70000E-02
24	4.70000E-02	11.1545	20.5779	15.9231	1.22810	2.40000E-02
25	5.15000E-02	11.5567	22.5482	16.4972	1.24130	2.00000E-02
26	5.70000E-02	12.1103	24.9562	17.2874	1.20170	2.50000E-02
27	6.20000E-02	12.5126	27.1454	17.8617	1.12630	1.40000E-02
28	6.80000E-02	12.7769	29.7723	18.2391	1.14280	1.60000E-02
29	7.95000E-02	13.2726	34.8074	18.9466	1.10750	1.70000E-02
30	9.10000E-02	13.4308	39.8424	19.1724	1.17170	1.90000E-02
31	0.114000	13.4964	49.9124	19.2662	1.36130	1.50000E-02
32	0.160000	13.1926	70.0526	18.8325	1.85530	1.60000E-02
33	0.234000	14.8845	102.4518	21.2476	1.38770	2.00000E-02
34	0.255500	15.5910	111.865	22.2562	0.896400	1.30000E-02
35	0.270500	15.9204	118.433	22.7263	0.667600	1.00000E-02
36	0.293000	16.2368	128.284	23.1781	0.562700	1.20000E-02
37	0.328500	16.4684	143.827	23.5086	0.313000	1.00000E-02
38	0.399500	16.5692	174.912	23.6525	0.174400	9.00000E-03
39	0.541500	16.5709	237.084	23.6550	0.140400	7.00000E-03
40	0.825500	16.6305	361.427	23.7400	0.110700	1.00000E-03
41	1.32550	16.6848	580.342	23.8175	0.107400	0.
42	1.82550	16.7659	799.256	23.9333	1.03500E-01	0.
43	2.32550	16.8269	1018.17	24.0204	1.03300E-01	0.
44	2.82550	16.8919	1237.08	24.1132	0.105400	0.
45	3.32550	16.9740	1456.00	24.2303	9.87000E-02	0.

Station = b2 z=-2.19

x = 0.361 visc = 1.60000E-05
cf = 3.70000E-03 yeff = 0.
d99.5 = 0.280972 del1 = 5.14789E-02
del2 = 2.81582E-02 H = 1.82820
Uw = 16.4463 Rex = 371070.
Red1 = 529.149 Red2 = 289.437
coef1 = 16.4463 coef2 = 0.159764
A+ = 25.0000
K = 0. f1 = 0.

N	y	U	y+	u+	u'	gamma
1	1.00000E-03	0.272800	0.442115	0.385646	0.197000	1.40000E-02
2	1.50000E-03	0.276800	0.663173	0.391301	0.205600	8.00000E-03
3	2.50000E-03	0.535287	1.10529	0.756714	0.269000	8.00000E-03
4	4.50000E-03	1.22230	1.98952	1.72791	0.577400	6.00000E-03
5	7.00000E-03	2.11461	3.09481	2.98933	0.543000	1.50000E-02
6	8.50000E-03	2.62249	3.75798	3.70731	0.619600	1.30000E-02
7	1.00000E-02	3.12222	4.42115	4.41376	0.728700	2.90000E-02
8	1.20000E-02	3.71715	5.30538	5.25478	0.794700	1.60000E-02
9	1.40000E-02	4.40247	6.18961	6.22359	0.899500	1.60000E-02
10	1.55000E-02	4.85548	6.85278	6.86400	1.04410	2.30000E-02
11	1.70000E-02	5.29761	7.51596	7.48901	1.09260	2.30000E-02
12	1.85000E-02	5.67157	8.17913	8.01766	1.09800	1.60000E-02
13	2.05000E-02	6.16646	9.06336	8.71727	1.22500	3.10000E-02
14	2.25000E-02	6.58655	9.94759	9.31113	1.37410	2.90000E-02
15	2.50000E-02	7.27883	11.0529	10.28979	1.36950	3.80000E-02
16	2.65000E-02	7.64740	11.7160	10.8108	1.43330	2.70000E-02
17	2.85000E-02	8.01194	12.6003	11.3262	1.42400	2.90000E-02
18	3.10000E-02	8.46191	13.7056	11.9623	1.53280	3.70000E-02
19	3.35000E-02	8.90397	14.8109	12.5872	1.55790	2.80000E-02
20	3.60000E-02	9.28714	15.9161	13.1288	1.59780	2.50000E-02
21	3.90000E-02	9.81681	17.2425	13.8776	1.61460	3.90000E-02
22	4.15000E-02	10.20649	18.3478	14.4285	1.68990	3.30000E-02
23	4.45000E-02	10.46110	19.6741	14.7884	1.58900	2.00000E-02
24	5.05000E-02	11.1169	22.3268	15.7155	1.63100	2.50000E-02
25	5.50000E-02	11.7029	24.3163	16.5440	1.58890	2.50000E-02
26	5.85000E-02	11.8601	25.8637	16.7662	1.60950	3.10000E-02
27	6.55000E-02	12.4618	28.9585	17.6168	1.48110	1.60000E-02
28	7.10000E-02	12.7887	31.3902	18.0789	1.39120	1.60000E-02
29	7.95000E-02	13.2167	35.1481	18.6839	1.27250	1.90000E-02
30	8.95000E-02	13.7068	39.5693	19.3767	1.10150	1.50000E-02
31	9.95000E-02	14.1276	43.9904	19.9717	0.951900	1.40000E-02
32	0.111000	14.4151	49.0748	20.3780	0.882400	8.00000E-03
33	0.131000	14.8362	57.9171	20.9734	0.830900	1.10000E-02
34	0.154500	15.1414	68.3068	21.4048	0.891000	1.70000E-02
35	0.193000	15.5824	85.3282	22.0283	0.939000	1.50000E-02
36	0.236500	16.0464	104.5602	22.6841	0.554200	8.00000E-03
37	0.283500	16.4296	125.340	23.2259	0.282000	5.00000E-03
38	0.345000	16.5396	152.530	23.3814	0.363400	8.00000E-03
39	0.468000	16.5416	206.910	23.3842	0.170700	8.00000E-03
40	0.714000	16.5793	315.670	23.4375	0.106300	2.00000E-03
41	1.20600	16.6177	533.191	23.4918	9.22000E-02	0.
42	1.70600	16.6979	754.248	23.6051	0.105200	0.
43	2.20600	16.7959	975.306	23.7437	1.03200E-01	0.
44	2.70600	16.8479	1196.36	23.8172	1.00100E-01	0.
45	3.20600	16.9290	1417.42	23.9318	0.109000	0.
46	2.70600	16.9639	1196.36	23.9812	9.79000E-02	0.

Station = b3 z=-3.24 midspan

x = 0.361 visc = 1.59900E-05
cf = 3.20000E-03 yeff = 0.
d99.5 = 0.307932 del1 = 6.01724E-02
del2 = 3.06232E-02 H = 1.96493
Uw = 16.4834 Rex = 372139.
Red1 = 620.290 Red2 = 315.681
coef1 = 16.4834 coef2 = 0.130786
A+ = 25.0000
K = 0. f1 = 0.

N	y	U	y+	u+	u'	gamma
1	5.00000E-04	0.246080	0.206171	0.373224	0.247500	1.10000E-02
2	1.00000E-03	0.255520	0.412342	0.387542	0.281000	1.00000E-02
3	1.50000E-03	0.260480	0.618514	0.395064	0.324200	1.60000E-02
4	2.50000E-03	0.480968	1.03086	0.729474	0.393700	1.20000E-02
5	4.50000E-03	1.12178	1.85554	1.70138	0.522700	1.30000E-02
6	7.50000E-03	2.00430	3.09257	3.03988	0.909500	2.10000E-02
7	9.50000E-03	2.51519	3.91725	3.81473	0.869100	2.40000E-02
8	1.25000E-02	3.41142	5.15428	5.17403	1.08210	2.20000E-02
9	1.45000E-02	3.81938	5.97896	5.79277	1.25400	2.30000E-02
10	1.70000E-02	4.45318	7.00982	6.75404	1.36260	3.90000E-02
11	1.90000E-02	4.82573	7.83451	7.31909	1.47380	4.90000E-02
12	2.15000E-02	5.45949	8.86536	8.28030	1.57580	4.00000E-02
13	2.35000E-02	5.81182	9.69005	8.81466	1.65910	3.80000E-02
14	2.65000E-02	6.36133	10.9271	9.64810	1.76710	4.00000E-02
15	2.90000E-02	6.79893	11.9579	10.31180	1.82360	4.20000E-02
16	3.15000E-02	7.20262	12.9888	10.9241	1.91450	4.20000E-02
17	3.45000E-02	7.64215	14.2258	11.5907	1.95720	4.20000E-02
18	3.80000E-02	8.10589	15.6690	12.2940	2.11060	5.00000E-02
19	4.15000E-02	8.50824	17.1122	12.9043	2.11040	4.70000E-02
20	4.55000E-02	9.09612	18.7616	13.7959	2.14460	4.60000E-02
21	4.85000E-02	9.34427	19.9986	14.1723	2.14660	4.30000E-02
22	5.45000E-02	9.94070	22.4727	15.0768	2.15010	4.20000E-02
23	5.95000E-02	10.29405	24.5344	15.6128	2.11340	3.30000E-02
24	6.65000E-02	10.8288	27.4208	16.4238	2.12260	3.80000E-02
25	7.30000E-02	11.3007	30.1010	17.1395	1.98460	3.10000E-02
26	7.95000E-02	11.7086	32.7812	17.7581	1.92290	2.70000E-02
27	8.75000E-02	12.2373	36.0800	18.5601	1.85240	2.30000E-02
28	9.50000E-02	12.5982	39.1725	19.1075	1.73250	1.50000E-02
29	0.105000	13.2711	43.2959	20.1281	1.58310	1.50000E-02
30	0.112000	13.5299	46.1823	20.5205	1.43300	1.50000E-02
31	0.125500	14.2165	51.7490	21.5619	1.13410	6.00000E-03
32	0.135000	14.6460	55.6662	22.2132	0.991300	1.30000E-02
33	0.146000	14.9554	60.2020	22.6826	0.855300	1.30000E-02
34	0.163500	15.3932	67.4180	23.3466	0.643800	1.20000E-02
35	0.183500	15.8268	75.6648	24.0041	0.447600	7.00000E-03
36	0.206500	16.0881	85.1487	24.4004	0.402700	1.20000E-02
37	0.250500	16.3838	103.2918	24.8489	0.299000	5.00000E-03
38	0.325000	16.4583	134.011	24.9620	0.254900	1.00000E-02
39	0.474000	16.5036	195.450	25.0307	0.143000	7.00000E-03
40	0.772000	16.5524	318.328	25.1047	0.107100	1.00000E-03
41	1.27200	16.6768	524.499	25.2933	8.45000E-02	0.
42	1.77200	16.7229	730.671	25.3632	9.62000E-02	0.
43	2.27200	16.7899	936.842	25.4649	9.60000E-02	0.
44	2.77200	16.8509	1143.01	25.5575	0.106000	0.
45	3.27200	16.8930	1349.18	25.6212	1.01700E-01	0.

Station = b4 z=-3.24

x = 0.361 visc = 1.60000E-05
cf = 2.45000E-03 yeff = 0.
d99.5 = 0.280231 del1 = 7.71034E-02
del2 = 3.48763E-02 H = 2.21077
Uw = 16.4617 Rex = 371417.
Red1 = 793.283 Red2 = 358.827
coef1 = 16.4617 coef2 = 0.144269
A+ = 25.0000
K = 0. f1 = 0.

N	y	U	y+	u+	u'	gamma
1	5.00000E-04	0.213120	0.180050	0.369898	0.283600	1.00000E-02
2	1.00000E-03	0.218560	0.360100	0.379339	0.317500	7.00000E-03
3	1.50000E-03	0.224960	0.540149	0.390448	0.358100	1.00000E-02
4	2.50000E-03	0.372297	0.900249	0.646171	0.414200	1.10000E-02
5	4.50000E-03	0.851805	1.62045	1.47842	0.523700	1.00000E-02
6	8.50000E-03	1.71943	3.06085	2.98429	0.749100	1.30000E-02
7	1.20000E-02	2.45994	4.32120	4.26955	0.985100	2.70000E-02
8	1.50000E-02	3.03997	5.40149	5.27627	1.20480	2.70000E-02
9	1.80000E-02	3.48944	6.48179	6.05638	1.33770	4.20000E-02
10	2.15000E-02	4.01170	7.74214	6.96284	1.39320	3.80000E-02
11	2.50000E-02	4.56966	9.00249	7.93125	1.59310	4.70000E-02
12	2.80000E-02	4.85018	10.08279	8.41813	1.57620	4.10000E-02
13	3.30000E-02	5.59064	11.8833	9.70328	1.84830	5.60000E-02
14	3.65000E-02	5.93679	13.1436	10.30407	1.89340	6.80000E-02
15	4.15000E-02	6.42081	14.9441	11.1441	1.91780	4.70000E-02
16	4.65000E-02	6.93026	16.7446	12.0284	2.01970	5.20000E-02
17	5.15000E-02	7.32985	18.5451	12.7219	1.98400	4.80000E-02
18	5.75000E-02	7.80878	20.7057	13.5532	2.01590	4.10000E-02
19	6.35000E-02	8.32898	22.8663	14.4560	2.08790	4.60000E-02
20	6.90000E-02	8.64009	24.8469	14.9960	1.97950	3.50000E-02
21	7.75000E-02	9.28372	27.9077	16.1131	2.04180	3.70000E-02
22	8.40000E-02	9.71457	30.2484	16.8609	1.97030	2.20000E-02
23	9.15000E-02	10.22820	32.9491	17.7524	1.95090	3.20000E-02
24	9.85000E-02	10.6962	35.4698	18.5647	1.87080	2.10000E-02
25	0.106000	11.2729	38.1706	19.5657	1.78090	1.90000E-02
26	0.112500	11.7103	40.5112	20.3247	1.77100	2.00000E-02
27	0.119500	12.1685	43.0319	21.1200	1.64300	1.80000E-02
28	0.127000	12.7586	45.7327	22.1442	1.48380	1.70000E-02
29	0.133000	13.1424	47.8933	22.8103	1.40440	1.30000E-02
30	0.140500	13.6322	50.5940	23.6605	1.23920	7.00000E-03
31	0.148000	13.9861	53.2947	24.2746	1.16570	1.50000E-02
32	0.158500	14.6110	57.0758	25.3593	0.906700	5.00000E-03
33	0.166500	14.8517	59.9566	25.7770	0.940300	2.60000E-02
34	0.182500	15.4268	65.7182	26.7752	0.585300	7.00000E-03
35	0.196000	15.7716	70.5795	27.3736	0.524400	6.00000E-03
36	0.215500	16.0895	77.6015	27.9255	0.476000	1.40000E-02
37	0.246000	16.3596	88.5845	28.3943	0.302400	7.00000E-03
38	0.302500	16.4590	108.930	28.5667	0.236700	7.00000E-03
39	0.415500	16.5053	149.621	28.6471	0.198300	7.00000E-03
40	0.641500	16.5632	231.004	28.7476	0.116900	3.00000E-03
41	1.09350	16.6007	393.769	28.8127	9.50000E-02	0.
42	1.59350	16.6828	573.819	28.9553	9.88000E-02	0.
43	2.09350	16.7869	753.868	29.1359	9.26000E-02	0.
44	2.59350	16.8369	933.918	29.2227	1.00000E-01	0.
45	3.09350	16.9050	1113.97	29.3408	9.57000E-02	0.
46	3.59350	16.9760	1294.02	29.4640	0.115300	0.

Station = b5 z=-3.79 upwash

x = 0.361 visc = 1.59900E-05
cf = 2.10000E-03 yeff = 0.
d99.5 = 0.290065 del1 = 8.80755E-02
del2 = 3.76160E-02 H = 2.34144
Uw = 16.4725 Rex = 371893.
Red1 = 907.334 Red2 = 387.512
coef1 = 16.4725 coef2 = 0.127358
A+ = 25.0000
K = 0. f1 = 0.

N	y	U	y+	u+	u'	gamma
1	5.00000E-04	0.201600	0.166908	0.377690	0.266300	8.00000E-03
2	1.00000E-03	0.207520	0.333816	0.388781	0.345200	5.00000E-03
3	1.50000E-03	0.215520	0.500724	0.403768	0.383700	1.90000E-02
4	2.50000E-03	0.354182	0.834539	0.663545	0.431100	1.70000E-02
5	4.50000E-03	0.802423	1.50217	1.50331	0.470600	1.20000E-02
6	8.50000E-03	1.56933	2.83743	2.94008	0.611300	1.80000E-02
7	1.25000E-02	2.28241	4.17270	4.27601	0.797000	3.00000E-02
8	1.65000E-02	2.84372	5.50796	5.32760	0.927200	3.10000E-02
9	2.05000E-02	3.33212	6.84322	6.24260	1.11520	4.00000E-02
10	2.50000E-02	3.84344	8.34539	7.20053	1.19450	4.00000E-02
11	2.95000E-02	4.31225	9.84756	8.07884	1.18590	3.60000E-02
12	3.45000E-02	4.90903	11.5166	9.19688	1.43300	3.80000E-02
13	3.85000E-02	5.24927	12.8519	9.83431	1.42070	3.50000E-02
14	4.45000E-02	5.79430	14.8548	10.8554	1.42630	4.10000E-02
15	5.00000E-02	6.17471	16.6908	11.5681	1.40160	3.40000E-02
16	5.70000E-02	6.67345	19.0275	12.5025	1.42530	2.80000E-02
17	6.40000E-02	7.19604	21.3642	13.4815	1.49720	2.90000E-02
18	7.05000E-02	7.57223	23.5340	14.1863	1.40210	2.30000E-02
19	7.90000E-02	8.16225	26.3714	15.2917	1.47530	2.10000E-02
20	8.60000E-02	8.59689	28.7082	16.1059	1.42230	1.60000E-02
21	9.40000E-02	9.15824	31.3787	17.1576	1.43320	1.20000E-02
22	1.01000E-01	9.69689	33.7154	18.1667	1.43420	2.00000E-02
23	0.107500	10.14123	35.8852	18.9992	1.34940	1.10000E-02
24	0.114500	10.6754	38.2219	20.0000	1.37210	1.50000E-02
25	0.121000	11.0445	40.3917	20.6914	1.28090	1.10000E-02
26	0.129500	11.8165	43.2291	22.1377	1.26590	1.40000E-02
27	0.135000	12.2171	45.0651	22.8883	1.20340	9.00000E-03
28	0.141500	12.7048	47.2349	23.8019	1.13920	1.20000E-02
29	0.148000	13.1564	49.4047	24.6480	1.10690	9.00000E-03
30	0.155000	13.5960	51.7414	25.4716	1.01360	9.00000E-03
31	0.162500	14.0206	54.2451	26.2670	0.985100	2.00000E-02
32	0.171000	14.4822	57.0825	27.1318	0.815400	4.00000E-03
33	0.180000	14.8817	60.0868	27.8804	0.683700	7.00000E-03
34	0.191000	15.3224	63.7588	28.7059	0.639800	8.00000E-03
35	0.203500	15.6210	67.9315	29.2654	0.482800	5.00000E-03
36	0.224000	16.0549	74.7747	30.0782	0.498900	8.00000E-03
37	0.247500	16.2667	82.6194	30.4750	0.485200	2.00000E-02
38	0.294500	16.4438	98.3087	30.8069	0.243300	5.00000E-03
39	0.388500	16.5191	129.687	30.9478	0.178900	7.00000E-03
40	0.576500	16.5220	192.445	30.9534	0.130200	3.00000E-03
41	0.952500	16.5996	317.959	31.0987	0.115900	0.
42	1.45250	16.6588	484.867	31.2096	1.00700E-01	0.
43	1.95250	16.7199	651.775	31.3241	9.78000E-02	0.
44	2.44250	16.7669	815.345	31.4122	9.86000E-02	0.
45	2.95250	16.8489	985.591	31.5659	1.01700E-01	0.
46	3.45250	16.9220	152.50	31.7026	9.65000E-02	0.

Station = c1 z=-1.59 downwash
x = 0.361 visc = 1.61600E-05
cf = 4.10000E-03 yeff = 0.
d99.5 = 0.341839 del1 = 6.35699E-02
del2 = 4.07665E-02 H = 1.55936
Uw = 18.0578 Rex = 403395.
Red1 = 710.354 Red2 = 455.541
coef1 = 18.0578 coef2 = 0.156081
A+ = 25.0000
K = 0. f1 = 0.

N	y	U	y+	u+	u'	gamma
1	5.00000E-04	0.328000	0.252971	0.401173	0.525500	7.70000E-02
2	1.00000E-03	0.331840	0.505942	0.405870	0.318000	7.60000E-02
3	1.50000E-03	0.339447	0.758913	0.415174	0.276400	7.60000E-02
4	2.50000E-03	0.745050	1.26485	0.911262	0.369500	9.90000E-02
5	4.50000E-03	1.67031	2.27674	2.04294	0.486400	1.03000E-01
6	6.00000E-03	2.39664	3.03565	2.93130	0.889600	0.113000
7	7.00000E-03	2.84888	3.54159	3.48443	0.724300	0.119000
8	8.00000E-03	3.29358	4.04754	4.02834	1.01240	0.120000
9	9.00000E-03	3.73081	4.55348	4.56311	0.847300	0.108000
10	1.05000E-02	4.34802	5.31239	5.31801	1.16590	0.118000
11	1.20000E-02	5.02999	6.07130	6.15212	0.992200	0.112000
12	1.30000E-02	5.46016	6.57725	6.67826	1.03890	0.114000
13	1.40000E-02	5.80159	7.08319	7.09586	1.07280	0.121000
14	1.55000E-02	6.43168	7.84210	7.86652	1.23270	0.118000
15	1.65000E-02	6.74480	8.34804	8.24949	1.28570	0.131000
16	1.80000E-02	7.21356	9.10695	8.82282	1.37390	0.117000
17	2.00000E-02	7.85401	10.11884	9.60615	1.41110	0.126000
18	2.05000E-02	8.17880	10.37181	10.00340	1.38190	0.119000
19	2.20000E-02	8.63755	11.1307	10.56449	1.44460	0.112000
20	2.35000E-02	9.13711	11.8896	11.1755	1.59440	0.152000
21	2.50000E-02	9.52612	12.6485	11.6513	1.62610	0.127000
22	2.70000E-02	10.09382	13.6604	12.3456	1.55940	0.130000
23	2.85000E-02	10.41527	14.4193	12.7388	1.67830	0.140000
24	3.05000E-02	10.8297	15.4312	13.2457	1.73260	0.123000
25	3.30000E-02	11.4371	16.6961	13.9886	1.77500	0.117000
26	3.50000E-02	11.8231	17.7080	14.4607	1.79170	0.133000
27	3.75000E-02	12.3355	18.9728	15.0875	1.68370	0.128000
28	3.95000E-02	12.5871	19.9847	15.3951	1.88370	0.129000
29	4.35000E-02	13.2127	22.0085	16.1603	1.82190	0.131000
30	4.65000E-02	13.5733	23.5263	16.6013	1.71330	0.112000
31	5.05000E-02	13.9878	25.5501	17.1083	1.68850	0.112000
32	5.50000E-02	14.3327	27.8268	17.5302	1.70330	0.107000
33	6.15000E-02	14.7856	31.1154	18.0841	1.59440	0.105000
34	6.85000E-02	15.1288	34.6570	18.5038	1.44900	9.70000E-02
35	7.85000E-02	15.3255	39.7164	18.7444	1.48380	9.00000E-02
36	9.85000E-02	15.4722	49.8353	18.9239	1.37280	9.70000E-02
37	0.138500	14.7974	70.0730	18.0986	1.91890	0.108000
38	0.167500	14.3929	84.7453	17.6038	2.37210	0.141000
39	0.203000	14.4812	102.7062	17.7118	2.60730	0.171000
40	0.274000	17.1813	138.628	21.0143	1.26420	9.80000E-02
41	0.287000	17.5396	145.205	21.4524	0.937200	5.30000E-02
42	0.305000	17.8429	154.312	21.8234	0.611900	5.10000E-02
43	0.334500	18.0063	169.238	22.0234	0.569700	6.30000E-02
44	0.393500	18.1230	199.088	22.1660	0.317100	3.70000E-02
45	0.511500	18.1338	258.789	22.1792	0.234700	3.80000E-02
46	0.747500	18.1744	378.192	22.2289	0.119400	1.30000E-02
47	1.21950	18.2567	616.996	22.3296	9.87000E-02	0.
48	1.71950	18.3269	869.967	22.4154	1.02100E-01	0.
49	2.21950	18.3939	1122.94	22.4974	1.00100E-01	0.
50	2.71950	18.4759	1375.91	22.5977	8.06000E-02	0.
51	3.21950	18.5530	1628.88	22.6919	1.00300E-01	0.
52	3.71950	18.6520	1881.85	22.8130	0.107900	0.

Station = c2 z=-2.19

x = 0.361 visc = 1.61500E-05
cf = 3.80000E-03 yeff = 0.
d99.5 = 0.315950 del1 = 4.98164E-02
del2 = 2.88252E-02 H = 1.72823
Uw = 18.0258 Rex = 402930.
Red1 = 556.025 Red2 = 321.732
coef1 = 18.0258 coef2 = 0.149207
A+ = 25.0000
K = 0. f1 = 0.

N	y	U	y+	u+	u'	gamma
1	1.50000E-03	0.326357	0.729776	0.415357	0.314600	7.10000E-02
2	2.50000E-03	0.659069	1.21629	0.838803	0.838100	9.60000E-02
3	4.50000E-03	1.49549	2.18933	1.90332	0.835200	1.03000E-01
4	6.50000E-03	2.30355	3.16236	2.93175	1.04710	8.50000E-02
5	8.00000E-03	2.96655	3.89214	3.77555	1.06190	0.132000
6	9.00000E-03	3.44588	4.37866	4.38561	1.10050	0.119000
7	1.00000E-02	3.86163	4.86518	4.91473	1.12160	0.121000
8	1.15000E-02	4.38311	5.59495	5.57842	1.27550	0.141000
9	1.30000E-02	5.05437	6.32473	6.43273	1.28790	0.164000
10	1.40000E-02	5.43340	6.81125	6.91513	1.47460	0.156000
11	1.50000E-02	5.76956	7.29776	7.34297	1.54520	0.152000
12	1.65000E-02	6.25844	8.02754	7.96517	1.54770	0.157000
13	1.80000E-02	6.81773	8.75732	8.67699	1.73320	0.156000
14	1.90000E-02	7.11376	9.24383	9.05374	1.81660	0.159000
15	2.05000E-02	7.58121	9.97361	9.64867	1.82430	0.168000
16	2.20000E-02	8.02965	10.7034	10.21941	2.05820	0.163000
17	2.35000E-02	8.48655	11.4332	10.8009	2.00240	0.154000
18	2.50000E-02	8.82808	12.1629	11.2356	2.03460	0.163000
19	2.70000E-02	9.34210	13.1360	11.8898	2.17300	0.153000
20	2.90000E-02	9.79940	14.1090	12.4718	2.26750	0.192000
21	3.10000E-02	10.20944	15.0820	12.9936	2.36960	0.169000
22	3.35000E-02	10.7668	16.2983	13.7030	2.40950	0.185000
23	3.55000E-02	11.1657	17.2714	14.2107	2.41860	0.167000
24	3.80000E-02	11.5737	18.4877	14.7300	2.44510	0.158000
25	4.10000E-02	12.0448	19.9472	15.3295	2.40640	0.150000
26	4.40000E-02	12.3535	21.4068	15.7224	2.44820	0.163000
27	4.90000E-02	12.9530	23.8394	16.4854	2.43230	0.160000
28	5.30000E-02	13.2134	25.7854	16.8168	2.38530	0.143000
29	6.05000E-02	13.7990	29.4343	17.5621	2.34370	0.136000
30	6.70000E-02	14.2285	32.5967	18.1088	2.26960	0.129000
31	7.45000E-02	14.5473	36.2456	18.5144	2.15410	0.135000
32	8.65000E-02	15.0529	42.0838	19.1580	2.00110	0.129000
33	9.85000E-02	15.4932	47.9220	19.7183	1.82630	0.114000
34	0.112000	15.8545	54.4900	20.1781	1.51420	9.30000E-02
35	0.130500	16.2365	63.4905	20.6643	1.36830	8.20000E-02
36	0.154500	16.5609	75.1670	21.0772	1.32750	8.20000E-02
37	0.191500	16.8201	93.1681	21.4070	1.46270	9.60000E-02
38	0.263500	17.7360	128.197	22.5727	0.778100	6.70000E-02
39	0.302500	17.9638	147.172	22.8627	0.616600	5.20000E-02
40	0.380500	18.0739	185.120	23.0028	0.309600	4.30000E-02
41	0.536500	18.1099	261.017	23.0486	0.151500	2.80000E-02
42	0.848500	18.1625	412.810	23.1156	0.193000	8.00000E-03
43	1.34850	18.2258	656.069	23.1961	0.112100	0.
44	1.84850	18.3119	899.328	23.3057	0.111500	0.
45	2.34850	18.3569	1142.59	23.3630	0.108500	0.
46	2.84850	18.4619	1385.85	23.4967	9.98000E-02	0.
47	3.34850	18.5240	1629.10	23.5756	9.66000E-02	0.

Station = c3 z=-2.69 midspan

x = 0.361 visc = 1.61500E-05
cf = 3.25000E-03 yeff = 0.
d99.5 = 0.299662 del1 = 5.95002E-02
del2 = 3.19093E-02 H = 1.86467
Uw = 18.0200 Rex = 402800.
Red1 = 663.897 Red2 = 356.041
coef1 = 18.0200 coef2 = 0.152619
A+ = 25.0000
K = 0. f1 = 0.

N	y	U	y+	u+	u'	gamma
1	1.00000E-03	0.294240	0.449789	0.405061	0.411100	6.60000E-02
2	1.50000E-03	0.303791	0.674683	0.418210	0.726700	6.80000E-02
3	2.50000E-03	0.624952	1.12447	0.860332	0.596200	9.10000E-02
4	4.50000E-03	1.39714	2.02405	1.92335	0.916900	0.140000
5	7.00000E-03	2.29749	3.14852	3.16280	1.09980	0.148000
6	8.50000E-03	2.86355	3.82320	3.94207	1.46500	0.146000
7	1.00000E-02	3.40188	4.49789	4.68315	1.47040	0.148000
8	1.15000E-02	3.84462	5.17257	5.29263	1.59550	0.178000
9	1.35000E-02	4.37387	6.07215	6.02123	1.77430	0.202000
10	1.55000E-02	5.04670	6.97173	6.94747	2.01130	0.194000
11	1.70000E-02	5.56782	7.64641	7.66485	2.11480	0.516000
12	1.85000E-02	5.92156	8.32109	8.15182	2.27630	0.217000
13	2.05000E-02	6.33715	9.22067	8.72395	2.41970	0.219000
14	2.30000E-02	7.06182	10.34514	9.72155	2.49260	0.218000
15	2.45000E-02	7.33784	11.0198	10.10152	2.56840	0.234000
16	2.70000E-02	7.89984	12.1443	10.8752	2.70270	0.239000
17	2.90000E-02	8.18564	13.0439	11.2686	2.78150	0.235000
18	3.25000E-02	8.96234	14.6181	12.3379	2.89780	0.236000
19	3.45000E-02	9.21070	15.5177	12.6798	2.97500	0.237000
20	3.85000E-02	9.77892	17.3169	13.4620	2.98570	0.235000
21	4.20000E-02	10.27991	18.8911	14.1517	3.06340	0.227000
22	4.55000E-02	10.6821	20.4654	14.7054	3.14420	0.243000
23	4.95000E-02	10.9044	22.2645	15.0113	3.05060	0.215000
24	5.75000E-02	11.6761	25.8629	16.0737	3.04630	0.213000
25	6.25000E-02	11.8805	28.1118	16.3551	3.07640	0.215000
26	7.25000E-02	12.3746	32.6097	17.0354	2.98120	0.198000
27	8.25000E-02	12.8330	37.1076	17.6664	2.88770	0.186000
28	9.35000E-02	13.4658	42.0553	18.5375	2.79290	0.183000
29	1.02000E-01	13.9437	45.8785	19.1953	2.56700	0.150000
30	0.110500	14.4569	49.7017	19.9019	2.43270	0.158000
31	0.118500	14.8227	53.3000	20.4055	2.22800	0.135000
32	0.129000	15.3526	58.0228	21.1349	2.01600	0.134000
33	0.138500	15.7760	62.2958	21.7178	1.79690	0.122000
34	0.149500	16.3304	67.2434	22.4809	1.47130	8.00000E-02
35	0.159000	16.5844	71.5164	22.8307	1.33430	7.60000E-02
36	0.177500	17.1490	79.8375	23.6079	1.10160	6.70000E-02
37	0.193500	17.4011	87.0341	23.9549	0.991400	7.70000E-02
38	0.225000	17.6787	101.2025	24.3371	0.861100	7.00000E-02
39	0.282000	17.9634	126.840	24.7290	0.502000	5.00000E-02
40	0.382500	18.0329	172.044	24.8247	0.336600	3.80000E-02
41	0.583500	18.1070	262.452	24.9268	0.142600	1.80000E-02
42	0.985500	18.1796	443.267	25.0267	0.109600	1.00000E-03
43	1.48550	18.2438	668.161	25.1151	9.74000E-02	0.
44	1.98550	18.3229	893.056	25.2239	0.106600	0.
45	2.48550	18.3819	1117.95	25.3052	9.95000E-02	0.
46	2.98550	18.4729	1342.84	25.4305	0.106000	0.
47	3.48550	18.5650	1567.74	25.5572	9.79000E-02	0.

Station = c4 z=-3.24
x = 0.361 visc = 1.61400E-05
cf = 2.40000E-03 yeff = 0.
d99.5 = 0.283840 del1 = 8.14809E-02
del2 = 3.80685E-02 H = 2.14037
Ue = 17.9830 Rex = 402222.
Red1 = 907.851 Red2 = 424.155
coef1 = 17.9830 coef2 = 0.148340
A+ = 25.0000
K = 0. f1 = 0.

N	y	U	y+	u+	u'	gamma
1	1.50000E-03	0.243200	0.578949	0.390401	0.691900	6.40000E-02
2	2.50000E-03	0.402125	0.964915	0.645517	0.501900	8.50000E-02
3	4.50000E-03	0.945087	1.73685	1.51712	0.745300	0.110000
4	8.50000E-03	2.00832	3.28071	3.22390	1.19890	0.164000
5	1.10000E-02	2.64319	4.24563	4.24302	1.49600	0.179000
6	1.35000E-02	3.16802	5.21054	5.08551	1.68030	0.195000
7	1.60000E-02	3.72388	6.17546	5.97783	1.87400	0.212000
8	1.85000E-02	4.15399	7.14037	6.66827	1.91130	0.226000
9	2.15000E-02	4.78461	8.29827	7.68058	2.29140	0.258000
10	2.40000E-02	5.14532	9.26319	8.25960	2.32340	0.238000
11	2.75000E-02	5.79693	10.6141	9.30561	2.57100	0.249000
12	3.00000E-02	6.03564	11.5790	9.68881	2.59380	0.254000
13	3.50000E-02	6.70019	13.5088	10.7556	2.72120	0.246000
14	3.85000E-02	7.23878	14.8597	11.6202	2.97880	0.266000
15	4.15000E-02	7.50018	16.0176	12.0398	2.91820	0.262000
16	4.70000E-02	8.04876	18.1404	12.9204	2.95340	0.268000
17	5.20000E-02	8.53468	20.0702	13.7004	3.06210	0.263000
18	5.70000E-02	8.69473	22.0001	13.9574	2.99100	0.256000
19	6.70000E-02	9.25425	25.8597	14.8555	2.97990	0.236000
20	7.60000E-02	9.80003	29.3334	15.7317	2.98170	0.242000
21	8.40000E-02	10.07411	32.4212	16.1716	2.91350	0.185000
22	9.85000E-02	10.8551	38.0177	17.4253	2.88870	0.192000
23	0.107500	11.4502	41.4914	18.3806	2.91380	0.266000
24	0.115000	12.0546	44.3861	19.3509	2.85540	0.184000
25	0.121000	12.3047	46.7019	19.7523	2.67390	0.171000
26	0.133000	13.2583	51.3335	21.2831	2.49310	0.142000
27	0.139000	13.7860	53.6493	22.1301	2.46680	0.151000
28	0.144500	14.1595	55.7721	22.7299	2.31050	0.146000
29	0.151500	14.6922	58.4739	23.5849	2.16510	0.142000
30	0.158000	15.0828	60.9827	24.2119	1.94490	1.01000E-01
31	0.166000	15.5924	64.0704	25.0300	1.77780	1.03000E-01
32	0.173500	16.0699	66.9651	25.7965	1.61350	9.90000E-02
33	0.181000	16.4174	69.8599	26.3543	1.38880	7.50000E-02
34	0.191500	16.8441	73.9125	27.0392	1.17760	7.90000E-02
35	0.203500	17.1577	78.5441	27.5427	1.10890	8.80000E-02
36	0.222500	17.6006	85.8775	28.2536	0.832200	6.00000E-02
37	0.243500	17.7334	93.9828	28.4668	0.790100	7.50000E-02
38	0.285500	17.9435	110.193	28.8041	0.574600	4.40000E-02
39	0.369500	18.0138	142.614	28.9169	0.493800	5.00000E-02
40	0.537500	18.0589	207.457	28.9893	0.155100	2.20000E-02
41	0.873500	18.1055	337.141	29.0642	9.9800E-02	2.00000E-03
42	1.37350	18.2038	530.125	29.2219	0.107200	0.
43	1.87350	18.2479	723.108	29.2927	1.00000E-01	0.
44	2.37350	18.3379	916.091	29.4373	1.04000E-01	0.
45	2.87350	18.4059	1109.07	29.5464	9.62000E-02	0.
46	3.37350	18.4860	1302.06	29.6749	0.109200	0.

Station = c5 z=-3.79 upwash
x = 0.361 visc = 1.61300E-05
cf = 2.25000E-03 yeff = 0.
d99.5 = 0.284155 del1 = 9.34640E-02
del2 = 4.12376E-02 H = 2.26647
Uw = 17.9971 Rex = 402787.
Red1 = 1042.83 Red2 = 460.109
coef1 = 17.9971 coef2 = 0.149402
A+ = 25.0000
K = 0. f1 = 0.

N	y	U	y+	u+	u'	gamma
1	5.00000E-04	0.239680	0.187117	0.397058	0.836400	1.03000E-01
2	1.00000E-03	0.236000	0.374234	0.390962	0.493100	9.70000E-02
3	1.50000E-03	0.244160	0.561351	0.404480	0.525700	9.20000E-02
4	2.50000E-03	0.427317	0.935586	0.707900	0.845200	0.117000
5	4.50000E-03	0.947131	1.68405	1.56903	0.761700	0.114000
6	8.50000E-03	1.94101	3.18099	3.21551	1.18230	0.184000
7	1.10000E-02	2.47048	4.11658	4.09265	1.49480	0.179000
8	1.45000E-02	3.15550	5.42640	5.22745	1.60790	0.219000
9	1.75000E-02	3.64561	6.54910	6.03938	1.77600	0.232000
10	2.10000E-02	4.23676	7.85892	7.01869	2.14440	0.248000
11	2.40000E-02	4.64349	8.98162	7.69248	2.15560	0.243000
12	2.75000E-02	5.06089	10.29144	8.38396	2.23690	0.243000
13	3.15000E-02	5.54834	11.7884	9.19147	2.33240	0.258000
14	3.55000E-02	6.02425	13.2853	9.97987	2.39500	0.254000
15	3.95000E-02	6.52136	14.7823	10.8034	2.60050	0.272000
16	4.35000E-02	6.82195	16.2792	11.3014	2.51430	0.253000
17	5.00000E-02	7.33830	18.7117	12.1568	2.67580	0.249000
18	5.60000E-02	7.69720	20.9571	12.7513	2.57630	0.253000
19	6.45000E-02	8.05552	24.1381	13.3449	2.45920	0.217000
20	7.65000E-02	8.61916	28.6289	14.2787	2.44210	0.216000
21	8.70000E-02	8.91890	32.5584	14.7752	2.40260	0.185000
22	1.04500E-01	9.65787	39.1075	15.9994	2.25610	0.148000
23	0.116000	10.52484	43.4112	17.4356	2.42650	0.176000
24	0.122500	10.8129	45.8437	17.9128	2.29030	0.142000
25	0.133500	11.7701	49.9603	19.4986	2.33100	0.141000
26	0.139000	12.2996	52.0186	20.3758	2.27270	0.148000
27	0.144000	12.7041	53.8897	21.0458	2.20160	0.140000
28	0.150000	13.2606	56.1351	21.9677	2.06380	0.144000
29	0.155000	13.6060	58.0063	22.5399	2.01740	0.114000
30	0.162000	14.2005	60.6260	23.5247	1.97870	0.129000
31	0.167500	14.6718	62.6842	24.3056	1.84940	9.50000E-02
32	0.173000	15.0942	64.7425	25.0052	1.77780	0.117000
33	0.179500	15.5715	67.1751	25.7961	1.56930	9.90000E-02
34	0.186000	15.9389	69.6076	26.4047	1.58470	9.60000E-02
35	0.194500	16.4233	72.7886	27.2072	1.30410	7.50000E-02
36	0.203000	16.7778	75.9696	27.7943	1.11610	7.20000E-02
37	0.214500	17.1723	80.2733	28.4479	1.13620	7.90000E-02
38	0.229000	17.5138	85.6997	29.0137	0.768400	5.70000E-02
39	0.250000	17.7696	93.5586	29.4374	0.727700	8.00000E-02
40	0.291000	17.9856	108.902	29.7952	0.468300	4.00000E-02
41	0.373000	18.0468	139.589	29.8967	0.248400	3.00000E-02
42	0.537000	18.0739	200.964	29.9415	0.168000	2.90000E-02
43	0.865000	18.1155	323.713	30.0105	0.228100	1.00000E-03
44	1.36500	18.1958	510.830	30.1434	1.00000E-01	0.
45	1.86500	18.2849	697.947	30.2910	9.86000E-02	0.
46	2.36500	18.3419	885.064	30.3855	9.30000E-02	0.
47	2.86500	18.4339	1072.18	30.5380	0.111200	0.
48	3.36500	18.4950	1259.30	30.6391	9.44000E-02	0.

Station = d1 z=-1.59 downwash

x = 0.361 visc = 1.62500E-05
cf = 4.45000E-03 yeff = 0.
d99.5 = 0.355209 del1 = 6.38822E-02
del2 = 4.24693E-02 H = 1.50420
Uw = 19.1109 Rex = 424556.
Red1 = 751.291 Red2 = 499.463
coef1 = 19.1109 coef2 = 0.158691
A+ = 25.0000
K = 0. f1 = 0.

N	y	U	y+	u+	u'	gamma
1	1.00000E-03	0.387360	0.554745	0.429703	0.798700	0.391000
2	1.50000E-03	0.426567	0.832117	0.473196	0.714700	0.386000
3	2.50000E-03	1.00204	1.38686	1.11158	0.753000	0.426000
4	4.00000E-03	1.94647	2.21898	2.15924	0.731300	0.425000
5	5.00000E-03	2.47783	2.77372	2.74869	0.849100	0.434000
6	6.00000E-03	3.03397	3.32847	3.36561	1.15530	0.446000
7	7.00000E-03	3.50249	3.88321	3.88536	1.20980	0.403000
8	8.00000E-03	3.98215	4.43796	4.41745	1.25620	0.413000
9	9.00000E-03	4.44257	4.99270	4.92820	1.24660	0.413000
10	1.05000E-02	5.14872	5.82482	5.71154	1.24850	0.413000
11	1.15000E-02	5.62412	6.37956	6.23890	1.46540	0.416000
12	1.25000E-02	6.11839	6.93431	6.78721	1.60370	0.419000
13	1.35000E-02	6.56621	7.48905	7.28397	1.45560	0.390000
14	1.45000E-02	6.93815	8.04380	7.69657	1.48300	0.370000
15	1.60000E-02	7.55136	8.87591	8.37681	1.50250	0.353000
16	1.70000E-02	7.91524	9.43066	8.78047	1.73470	0.401000
17	1.85000E-02	8.45801	10.26277	9.38257	1.75190	0.390000
18	1.95000E-02	8.85028	10.8175	9.81772	1.85790	0.412000
19	2.05000E-02	9.27850	11.3723	10.29275	1.82920	0.388000
20	2.15000E-02	9.58158	11.9270	10.6290	1.91210	0.377000
21	2.30000E-02	10.12887	12.7591	11.2361	1.83420	0.397000
22	2.40000E-02	10.34460	13.3139	11.4754	2.02060	0.415000
23	2.60000E-02	10.8767	14.4234	12.0656	1.92910	0.399000
24	2.75000E-02	11.2878	15.2555	12.5217	2.05330	0.407000
25	2.90000E-02	11.7049	16.0876	12.9844	2.15360	0.400000
26	3.05000E-02	12.0956	16.9197	13.4178	2.07780	0.398000
27	3.20000E-02	12.5475	17.7518	13.9191	2.04420	0.376000
28	3.35000E-02	12.7627	18.5839	14.1578	2.15150	0.414000
29	3.65000E-02	13.3849	20.2482	14.8481	2.14210	0.401000
30	3.85000E-02	13.7103	21.3577	15.2090	2.18580	0.391000
31	4.15000E-02	14.1166	23.0219	15.6597	2.29030	0.411000
32	4.50000E-02	14.5693	24.9635	16.1619	2.25970	0.396000
33	4.85000E-02	14.9011	26.9051	16.5300	2.34850	0.438000
34	5.35000E-02	15.3313	29.6788	17.0072	2.16450	0.402000
35	5.90000E-02	15.7709	32.7299	17.4948	2.05980	0.381000
36	6.50000E-02	15.9324	36.0584	17.6740	2.08090	0.412000
37	7.70000E-02	16.3691	42.7153	18.1584	1.82120	0.370000
38	9.10000E-02	16.5080	50.4817	18.3125	1.74290	0.361000
39	0.119000	16.1151	66.0146	17.8767	2.05890	0.487000
40	0.153500	15.5211	85.1533	17.2178	2.49830	0.576000
41	0.182000	15.2448	100.9635	16.9112	2.67370	0.634000
42	0.232500	16.1962	128.978	17.9666	2.60650	0.594000
43	0.259000	17.1879	143.679	19.0667	2.21680	0.481000
44	0.272000	17.8012	150.891	19.7471	1.82400	0.384000
45	0.282500	18.1444	156.715	20.1278	1.52600	0.347000
46	0.297500	18.4557	165.036	20.4731	1.46360	0.321000
47	0.321500	18.8741	178.350	20.9372	1.08660	0.267000
48	0.350000	19.0675	194.161	21.1518	0.738400	0.201000
49	0.407000	19.1141	225.781	21.2035	0.693300	0.168000
50	0.521000	19.1998	289.022	21.2985	0.450400	8.90000E-02

51	0.749000	19.2443	415.504	21.3480	0.299500	1.70000E-02
52	1.20500	19.2837	668.467	21.3917	1.03000E-01	0.
53	1.70500	19.3968	945.839	21.5172	1.00500E-01	0.
54	2.20500	19.4729	1223.21	21.6015	1.02600E-01	0.
55	2.70500	19.5389	1500.58	21.6748	0.108100	0.
56	3.20500	19.6140	1777.96	21.7580	9.55000E-02	0.
57	3.70500	19.6960	2055.33	21.8490	9.51000E-02	0.

Station = d2 z=-2.19

x = 0.361 visc = 1.62300E-05
cf = 3.85000E-03 yeff = 0.
d99.5 = 0.361053 del1 = 5.09754E-02
del2 = 3.07203E-02 H = 1.65934
Uw = 19.1405 Rex = 425738.
Red1 = 601.166 Red2 = 362.293
coef1 = 19.1405 coef2 = 0.160033
A+ = 25.0000
K = 0. f1 = 0.

N	y	U	y+	u+	u'	gamma
1	1.50000E-03	0.382966	0.776141	0.456029	0.746600	0.352000
2	2.50000E-03	0.786337	1.29357	0.936356	0.819100	0.364000
3	4.50000E-03	1.74341	2.32842	2.07602	0.847700	0.374000
4	6.00000E-03	2.52443	3.10456	3.00604	1.12190	0.398000
5	7.00000E-03	2.96301	3.62199	3.52830	1.31130	0.421000
6	8.00000E-03	3.38748	4.13942	4.03376	1.28610	0.437000
7	9.00000E-03	3.95872	4.65684	4.71397	1.45260	0.432000
8	1.00000E-02	4.40652	5.17427	5.24721	1.44700	0.425000
9	1.10000E-02	4.78923	5.69170	5.70293	1.49460	0.432000
10	1.25000E-02	5.37755	6.46784	6.40349	1.60290	0.428000
11	1.40000E-02	6.02289	7.24398	7.17196	1.73920	0.434000
12	1.50000E-02	6.38350	7.76140	7.60136	1.75620	0.415000
13	1.65000E-02	6.96283	8.53755	8.29121	1.88770	0.398000
14	1.75000E-02	7.38370	9.05497	8.79238	1.96300	0.403000
15	1.85000E-02	7.79569	9.57240	9.28297	2.07310	0.408000
16	1.95000E-02	8.10110	10.08983	9.64664	2.10710	0.398000
17	2.10000E-02	8.58607	10.8660	10.22414	2.29570	0.415000
18	2.25000E-02	9.03816	11.6421	10.7625	2.35490	0.417000
19	2.40000E-02	9.59940	12.4182	11.4308	2.32190	0.417000
20	2.50000E-02	9.82381	12.9357	11.6980	2.50420	0.405000
21	2.70000E-02	10.36426	13.9705	12.3416	2.47000	0.407000
22	2.85000E-02	10.6185	14.7467	12.6444	2.61690	0.448000
23	3.15000E-02	11.4447	16.2990	13.6281	2.72030	0.413000
24	3.30000E-02	11.7104	17.0751	13.9446	2.81510	0.426000
25	3.55000E-02	12.3075	18.3687	14.6555	2.79010	0.428000
26	3.75000E-02	12.5017	19.4035	14.8868	2.84430	0.425000
27	4.15000E-02	13.1672	21.4732	15.6793	2.87760	0.423000
28	4.45000E-02	13.5589	23.0255	16.1457	2.88270	0.436000
29	4.80000E-02	13.9574	24.8365	16.6202	2.83480	0.439000
30	5.20000E-02	14.1559	26.9062	16.8566	2.89540	0.424000
31	6.00000E-02	14.7864	31.0456	17.6074	2.84740	0.414000
32	6.60000E-02	15.1569	34.1502	18.0485	2.75510	0.399000
33	7.40000E-02	15.5166	38.2896	18.4769	2.64330	0.367000
34	8.50000E-02	15.9072	43.9813	18.9420	2.49860	0.400000
35	9.90000E-02	16.3078	51.2253	19.4190	2.24960	0.360000
36	0.116500	16.8151	60.2802	20.0231	1.95480	0.356000
37	0.133500	17.1716	69.0765	20.4476	1.73710	0.350000
38	0.157500	17.4060	81.4948	20.7267	1.71550	0.368000
39	0.205500	17.9337	106.331	21.3551	1.65260	0.353000
40	0.251000	18.5025	129.874	22.0324	1.40630	0.287000
41	0.291000	18.9265	150.571	22.5373	0.816800	0.187000
42	0.338000	19.0763	174.890	22.7157	0.639200	0.167000
43	0.432000	19.1833	223.529	22.8431	0.445800	0.110000
44	0.620000	19.2471	320.805	22.9191	0.425200	4.70000E-02
45	0.996000	19.3046	515.357	22.9876	9.990E-02	2.00E-03
46	1.49600	19.3718	774.071	23.0676	9.940 0E-02	0.
47	1.99600	19.4519	1032.78	23.1630	9.17000E-02	0.
48	2.49600	19.5239	1291.50	23.2487	9.82000E-02	0.
49	2.99600	19.6329	1550.21	23.3786	1.04100E-01	0.
50	3.49600	19.7050	1808.92	23.4643	0.115800	0.

Station = d3 z=-2.69 midspan

x = 0.361 visc = 1.62000E-05
cf = 3.40000E-03 yeff = 0.
d99.5 = 0.313311 del1 = 5.92559E-02
del2 = 3.29197E-02 H = 1.80001
Uw = 19.1188 Rex = 426042.
Red1 = 699.321 Red2 = 388.509
coef1 = 19.1188 coef2 = 0.167798
A+ = 25.0000
K = 0. f1 = 0.

N	y	U	y+	u+	u'	gamma
1	1.50000E-03	0.353494	0.729895	0.448433	1.13990	0.320000
2	2.50000E-03	0.746038	1.21649	0.946404	1.13670	0.359000
3	4.50000E-03	1.57272	2.18969	1.99512	1.04170	0.408000
4	7.00000E-03	2.69776	3.40618	3.42230	1.59040	0.446000
5	8.00000E-03	3.10796	3.89278	3.94268	1.45370	0.452000
6	9.50000E-03	3.67502	4.62267	4.66203	1.71350	0.461000
7	1.10000E-02	4.18474	5.35257	5.30866	1.77130	0.456000
8	1.25000E-02	4.81835	6.08246	6.11244	1.99210	0.455000
9	1.35000E-02	5.07530	6.56906	6.43839	1.97340	0.487000
10	1.55000E-02	5.70423	7.54225	7.23623	2.24370	0.449000
11	1.70000E-02	6.24307	8.27215	7.91980	2.41500	0.476000
12	1.80000E-02	6.55301	8.75874	8.31297	2.44580	0.471000
13	1.95000E-02	6.95049	9.48864	8.81721	2.52770	0.474000
14	2.15000E-02	7.45646	10.46183	9.45907	2.73130	0.488000
15	2.35000E-02	7.99808	11.4350	10.14615	2.84120	0.480000
16	2.50000E-02	8.38033	12.1649	10.6311	2.94980	0.475000
17	2.70000E-02	8.88168	13.1381	11.2671	3.03970	0.472000
18	2.90000E-02	9.27391	14.1113	11.7646	3.13720	0.470000
19	3.15000E-02	9.77350	15.3278	12.3984	3.25940	0.507000
20	3.40000E-02	10.20150	16.5443	12.9414	3.34890	0.504000
21	3.70000E-02	10.8296	18.0041	13.7381	3.34700	0.467000
22	3.90000E-02	10.9095	18.9773	13.8395	3.45630	0.505000
23	4.30000E-02	11.5501	20.9237	14.6522	3.44560	0.469000
24	4.60000E-02	11.8803	22.3835	15.0711	3.46320	0.471000
25	5.05000E-02	12.1539	24.5731	15.4181	3.57120	0.484000
26	5.90000E-02	12.8428	28.7092	16.2920	3.46130	0.464000
27	6.50000E-02	13.0363	31.6288	16.5375	3.44560	0.456000
28	7.70000E-02	13.6923	37.4680	17.3697	3.39210	0.470000
29	8.60000E-02	14.1625	41.8473	17.9662	3.29380	0.459000
30	9.55000E-02	14.4288	46.4700	18.3040	3.27770	0.451000
31	0.113500	15.1993	55.2287	19.2814	2.97220	0.430000
32	0.125000	15.7566	60.8246	19.9884	2.75630	0.413000
33	0.135000	16.2103	65.6906	20.5639	2.55560	0.360000
34	0.146000	16.7407	71.0431	21.2369	2.30200	0.368000
35	0.156000	17.1379	75.9091	21.7407	2.00030	0.309000
36	0.168500	17.5891	81.9916	22.3130	1.78220	0.285000
37	0.182000	18.0111	88.5606	22.8484	1.50260	0.261000
38	0.198000	18.3351	96.3462	23.2595	1.40110	0.243000
39	0.222500	18.7104	108.268	23.7355	0.974700	0.181000
40	0.255000	18.8816	124.082	23.9527	0.954300	0.182000
41	0.320000	19.0980	155.711	24.2273	0.746600	0.143000
42	0.450000	19.1874	218.969	24.3406	0.465600	9.70000E-02
43	0.710000	19.2733	345.484	24.4496	0.141900	3.40000E-02
44	1.21000	19.3267	588.782	24.5174	9.77000E-02	0.
45	1.71000	19.3968	832.081	24.6063	0.117600	0.
46	2.21000	19.4939	1075.38	24.7295	9.87000E-02	0.
47	2.71000	19.5699	1318.68	24.8259	9.56000E-02	0.
48	3.21000	19.6600	1561.98	24.9401	1.01300E-01	0.

Station = d4 z=-3.24

x = 0.361 visc = 1.61800E-05
cf = 2.90000E-03 yeff = 0.
d99.5 = 0.367107 del1 = 7.79691E-02
del2 = 4.03640E-02 H = 1.93165
Uw = 19.2340 Rex = 429139.
Red1 = 926.858 Red2 = 479.827
coef1 = 19.2340 coef2 = 0.156000
A+ = 25.0000
K = 0. f1 = 0.

N	y	U	y+	u+	u'	gamma
1	5.00000E-04	0.297120	0.226331	0.405676	1.12360	0.302000
2	1.00000E-03	0.298720	0.452663	0.407860	0.943000	0.312000
3	1.50000E-03	0.305936	0.678994	0.417712	1.05750	0.316000
4	2.50000E-03	0.638632	1.13166	0.871961	1.33490	0.387000
5	4.50000E-03	1.40218	2.03698	1.91448	1.43960	0.450000
6	7.00000E-03	2.30754	3.16864	3.15062	1.63590	0.474000
7	9.00000E-03	2.97673	4.07396	4.06430	1.92840	0.511000
8	1.05000E-02	3.43299	4.75296	4.68726	2.02950	0.519000
9	1.25000E-02	3.98619	5.65828	5.44258	2.22320	0.498000
10	1.45000E-02	4.57482	6.56361	6.24627	2.35140	0.535000
11	1.60000E-02	5.11180	7.24260	6.97945	2.53110	0.542000
12	1.75000E-02	5.47618	7.92159	7.47696	2.76430	0.531000
13	1.95000E-02	5.85053	8.82692	7.98808	2.77570	0.526000
14	2.20000E-02	6.39481	9.95858	8.73121	2.97740	0.530000
15	2.40000E-02	6.84797	10.8639	9.34993	3.06100	0.568000
16	2.60000E-02	7.15772	11.7692	9.77285	3.19740	0.560000
17	2.90000E-02	7.78933	13.1272	10.6352	3.34810	0.564000
18	3.10000E-02	8.07902	14.0325	11.0308	3.43140	0.559000
19	3.45000E-02	8.60861	15.6169	11.7538	3.44428	0.556000
20	3.75000E-02	9.05745	16.9748	12.3667	3.51240	0.578000
21	4.05000E-02	9.22146	18.3328	12.5906	3.51180	0.551000
22	4.65000E-02	9.90760	21.0488	13.5274	3.62390	0.567000
23	5.05000E-02	10.18872	22.8595	13.9113	3.51510	0.572000
24	5.75000E-02	10.6076	26.0281	14.4832	3.57890	0.579000
25	6.60000E-02	11.0369	29.8757	15.0694	3.52390	0.579000
26	7.60000E-02	11.3228	34.4023	15.4597	3.50740	0.577000
27	9.35000E-02	11.8434	42.3240	16.1704	3.48580	0.557000
28	0.110500	12.8240	50.0192	17.5094	3.49470	0.573000
29	0.119000	13.1368	53.8668	17.9365	3.36100	0.563000
30	0.132500	14.0498	59.9778	19.1831	3.27370	0.537000
31	0.139500	14.6107	63.1464	19.9488	3.08580	0.521000
32	0.145500	15.0093	65.8624	20.4931	2.95120	0.498000
33	0.153000	15.5421	69.2574	21.2205	2.84080	0.482000
34	0.160000	15.8977	72.4260	21.7061	2.68100	0.446000
35	0.169500	16.6734	76.7263	22.7652	2.38510	0.386000
36	0.175500	17.0118	79.4423	23.2273	2.11130	0.342000
37	0.184000	17.4074	83.2899	23.7674	1.97360	0.316000
38	0.194500	17.8850	88.0429	24.4195	1.62800	0.268000
39	0.205000	18.2676	92.7958	24.9418	1.51010	0.268000
40	0.218500	18.6042	98.9068	25.4014	1.21550	0.197000
41	0.238500	18.9040	107.960	25.8108	0.861100	0.184000
42	0.271500	19.0270	122.898	25.9787	0.944400	0.202000
43	0.337500	19.1723	152.774	26.1771	0.736100	0.151000
44	0.479500	19.2816	217.052	26.3262	0.432100	9.80000E-02
45	0.733500	19.3743	332.028	26.4529	0.173800	1.70000E-02
46	1.23350	19.4267	558.359	26.5245	9.61000E-02	0.
47	1.73350	19.5109	784.690	26.6393	0.109600	0.
48	2.23350	19.5749	1011.02	26.7268	0.109400	0.
49	2.73350	19.6529	1237.35	26.8333	9.21000E-02	0.
50	3.23350	19.7460	1463.68	26.9603	9.90000E-02	0.

Station = d5 z=-3.79 upwash

x = 0.361 visc = 1.61700E-05
cf = 2.45000E-03 yeff = 0.
d99.5 = 0.334747 del1 = 9.20223E-02
del2 = 4.40098E-02 H = 2.09095
Uw = 19.2323 Rex = 429367.
Red1 = 1094.50 Red2 = 523.444
coef1 = 19.2323 coef2 = 0.162106
A+ = 25.0000
K = 0. f1 = 0.

N	y	U	y+	u+	u'	gamma
1	1.00000E-03	0.271840	0.416284	0.403844	0.852900	0.226000
2	1.50000E-03	0.280480	0.624425	0.416680	0.904400	0.246000
3	2.50000E-03	0.536185	1.04071	0.796555	1.13030	0.276000
4	4.50000E-03	1.23362	1.87328	1.83266	1.24920	0.361000
5	7.00000E-03	1.97016	2.91399	2.92686	1.35100	0.369000
6	9.00000E-03	2.51911	3.74655	3.74237	1.88550	0.389000
7	1.15000E-02	3.16856	4.78726	4.70721	1.82860	0.418000
8	1.40000E-02	3.88056	5.82797	5.76495	2.09950	0.450000
9	1.60000E-02	4.23112	6.66054	6.28573	2.34190	0.451000
10	1.90000E-02	4.96918	7.90939	7.38220	2.49400	0.475000
11	2.10000E-02	5.35734	8.74195	7.95885	2.68090	0.482000
12	2.35000E-02	5.89157	9.78266	8.75250	2.77580	0.517000
13	2.55000E-02	6.16187	10.6152	9.15404	2.80490	0.507000
14	2.90000E-02	6.62766	12.0722	9.84602	2.89860	0.476000
15	3.25000E-02	7.17784	13.5292	10.6634	3.14220	0.501000
16	3.55000E-02	7.63802	14.7781	11.3470	3.11910	0.537000
17	3.85000E-02	8.03424	16.0269	11.9356	3.21690	0.519000
18	4.20000E-02	8.11665	17.4839	12.0581	3.14850	0.497000
19	4.90000E-02	8.82114	20.3979	13.1046	3.20040	0.513000
20	5.40000E-02	9.03943	22.4793	13.4289	3.11240	0.505000
21	6.40000E-02	9.45503	26.6421	14.0464	3.07130	0.511000
22	7.60000E-02	9.77008	31.6375	14.5144	3.07630	0.467000
23	9.55000E-02	10.39849	39.7551	15.4480	3.10010	0.458000
24	0.111000	10.9025	46.2075	16.1967	2.97910	0.452000
25	0.126000	11.7669	52.4517	17.4809	3.06400	0.459000
26	0.134500	12.5629	55.9901	18.6634	3.16080	0.544000
27	0.139500	12.8115	58.0716	19.0327	3.09970	0.512000
28	0.149500	13.8223	62.2344	20.5343	3.04060	0.524000
29	0.154000	14.0767	64.1077	20.9123	2.89420	0.501000
30	0.162500	14.8483	67.6461	22.0586	2.59220	0.445000
31	0.168000	15.2687	69.9356	22.6831	2.57090	0.408000
32	0.174500	15.8281	72.6415	23.5141	2.45810	0.382000
33	0.180000	16.2714	74.9310	24.1727	2.29210	0.351000
34	0.186000	16.7157	77.4287	24.8328	2.08510	0.325000
35	0.192500	17.1590	80.1346	25.4914	2.05660	0.301000
36	0.199500	17.5224	83.0486	26.0312	1.75770	0.262000
37	0.209000	17.9119	87.0033	26.6098	1.65920	0.243000
38	0.221000	18.2924	91.9987	27.1751	1.41160	0.216000
39	0.236500	18.6880	98.4511	27.7628	1.20490	0.180000
40	0.256000	18.9426	106.569	28.1410	1.20930	0.171000
41	0.294000	19.1565	122.387	28.4589	0.871400	0.141000
42	0.370000	19.2197	154.025	28.5527	0.726300	0.129000
43	0.522000	19.3478	217.300	28.7430	0.422200	7.80000E-02
44	0.826000	19.3794	343.850	28.7900	0.105700	6.00000E-03
45	1.32600	19.4458	551.992	28.8886	0.105100	0.
46	1.82600	19.5079	760.134	28.9808	9.93000E-02	0.
47	2.32600	19.6119	968.275	29.1354	9.97000E-02	0.
48	2.82600	19.6819	1176.42	29.2394	9.09000E-02	0.
49	3.32600	19.7850	1384.56	29.3925	1.01400E-01	0.

Station = e1 z=-1.59 downwash

x = 0.361 visc = 1.63000E-05
cf = 4.47000E-03 yeff = 0.
d99.5 = 0.512255 del1 = 6.44502E-02
del2 = 4.39273E-02 H = 1.46720
Ue = 20.0320 Rex = 443653.
Red1 = 792.066 Red2 = 539.848
coef1 = 20.0320 coef2 = 0.161377
A+ = 25.0000
K = 0. f1 = 0.

N	y	U	y+	u+	u'	gamma
1	1.00000E-03	0.421120	0.581000	0.444674	0.978300	0.836000
2	1.50000E-03	0.469908	0.871500	0.496192	1.12390	0.815000
3	2.50000E-03	1.11749	1.45250	1.18000	0.989700	0.853000
4	3.50000E-03	1.79979	2.03350	1.90046	1.00430	0.863000
5	4.50000E-03	2.42709	2.61450	2.56284	0.925000	0.868000
6	5.50000E-03	3.00867	3.19550	3.17696	1.15330	0.866000
7	6.50000E-03	3.55911	3.77650	3.75818	1.27830	0.860000
8	7.50000E-03	4.10680	4.35750	4.33650	1.28910	0.847000
9	8.50000E-03	4.67045	4.93850	4.93168	1.46440	0.853000
10	9.50000E-03	5.23098	5.51950	5.52356	1.47340	0.837000
11	1.05000E-02	5.88467	6.10050	6.21381	1.57740	0.828000
12	1.15000E-02	6.34594	6.68150	6.70089	1.67270	0.831000
13	1.25000E-02	6.83430	7.26250	7.21656	1.66230	0.827000
14	1.35000E-02	7.29476	7.84350	7.70277	1.58140	0.816000
15	1.45000E-02	7.72965	8.42450	8.16199	1.83190	0.823000
16	1.55000E-02	8.24183	9.00550	8.70282	1.77370	0.820000
17	1.65000E-02	8.58092	9.58650	9.06088	2.00800	0.824000
18	1.80000E-02	9.25350	10.45800	9.77107	2.00000	0.813000
19	1.90000E-02	9.70047	11.0390	10.24305	2.14260	0.827000
20	2.00000E-02	10.03248	11.6200	10.5936	2.13160	0.814000
21	2.15000E-02	10.51026	12.4915	11.0981	2.20750	0.827000
22	2.30000E-02	11.0119	13.3630	11.6278	2.25480	0.817000
23	2.45000E-02	11.5197	14.2345	12.1641	2.29620	0.841000
24	2.60000E-02	11.9949	15.1060	12.6658	2.34590	0.825000
25	2.75000E-02	12.4508	15.9775	13.1472	2.33710	0.824000
26	2.90000E-02	12.8154	16.8490	13.5322	2.33230	0.834000
27	3.10000E-02	13.1509	18.0110	13.8865	2.44690	0.853000
28	3.40000E-02	13.8423	19.7540	14.6165	2.49730	0.842000
29	3.60000E-02	14.2139	20.9160	15.0089	2.49950	0.841000
30	3.85000E-02	14.6234	22.3685	15.4413	2.51240	0.844000
31	4.15000E-02	15.0910	24.1115	15.9350	2.49830	0.840000
32	4.45000E-02	15.3799	25.8545	16.2401	2.45770	0.839000
33	4.95000E-02	15.9909	28.7595	16.8854	2.36670	0.836000
34	5.35000E-02	16.2462	31.0835	17.1549	2.35550	0.842000
35	6.15000E-02	16.6962	35.7315	17.6301	2.25640	0.819000
36	7.05000E-02	16.9174	40.9605	17.8636	2.22250	0.822000
37	8.85000E-02	17.1331	51.4185	18.0914	2.02820	0.834000
38	0.124500	16.7150	72.3345	17.6500	2.05830	0.881000
39	0.166000	16.1862	96.4460	17.0916	2.54060	0.913000
40	0.204500	16.4079	118.815	17.3257	2.79000	0.908000
41	0.281500	18.6913	163.552	19.7368	1.81330	0.808000
42	0.298000	19.2016	173.138	20.2756	1.53070	0.744000
43	0.314000	19.5019	182.434	20.5927	1.26830	0.714000
44	0.340500	19.7283	197.831	20.8317	0.956800	0.670000
45	0.393500	19.9269	228.624	21.0415	0.824200	0.579000
46	0.499500	20.0066	290.210	21.1256	1.05340	0.268000
47	0.711500	20.1383	413.382	21.2647	0.343700	3.70000E-02
48	1.13550	20.2127	659.726	21.3432	9.89000E-02	0.
49	1.63550	20.3028	950.226	21.4384	1.03400E-01	0.
50	2.13550	20.3679	1240.73	21.5071	1.01600E-01	0.

Station = e2 z=-2.19

x = 0.361 visc = 1.63000E-05
cf = 4.13000E-03 yeff = 0.
d99.5 = 0.462376 del1 = 5.18481E-02
del2 = 3.30372E-02 H = 1.56939
Ue = 20.0191 Rex = 443368.
Red1 = 636.780 Red2 = 405.751
coef1 = 20.0191 coef2 = 0.162195
A+ = 25.0000
K = 0. f1 = 0.

N	y	U	y+	u+	u'	gamma
1	2.50000E-03	0.950717	1.39527	1.04507	0.977100	0.776000
2	4.50000E-03	2.02582	2.51148	2.22688	1.06770	0.796000
3	6.00000E-03	2.97570	3.34864	3.27103	1.33770	0.821000
4	7.00000E-03	3.44648	3.90674	3.78853	1.28380	0.809000
5	8.00000E-03	4.00342	4.46485	4.40075	1.65620	0.810000
6	9.00000E-03	4.58188	5.02296	5.03662	1.59960	0.828000
7	1.00000E-02	5.15056	5.58106	5.66174	1.85810	0.834000
8	1.10000E-02	5.62269	6.13917	6.18073	1.83590	0.811000
9	1.20000E-02	6.10565	6.69728	6.71163	1.89190	0.798000
10	1.30000E-02	6.59942	7.25538	7.25440	2.04540	0.802000
11	1.40000E-02	7.08503	7.81349	7.78820	2.11350	0.825000
12	1.50000E-02	7.51108	8.37159	8.25653	2.08489	0.805000
13	1.60000E-02	8.00691	8.92970	8.80158	2.17590	0.809000
14	1.70000E-02	8.31561	9.48781	9.14092	2.31380	0.800000
15	1.85000E-02	8.86289	10.32496	9.74251	2.52090	0.813000
16	1.95000E-02	9.37393	10.8831	10.30427	2.47660	0.809000
17	2.05000E-02	9.71156	11.4412	10.6754	2.47520	0.806000
18	2.20000E-02	10.28820	12.2783	11.3093	2.67470	0.810000
19	2.30000E-02	10.55848	12.8364	11.6064	2.72900	0.821000
20	2.45000E-02	11.0538	13.6736	12.1508	2.70240	0.820000
21	2.60000E-02	11.3976	14.5108	12.5288	2.81900	0.805000
22	2.80000E-02	11.9410	15.6270	13.1262	2.85480	0.804000
23	2.95000E-02	12.3292	16.4641	13.5529	2.88640	0.798000
24	3.10000E-02	12.5996	17.3013	13.8501	2.98350	0.834000
25	3.35000E-02	13.2817	18.6966	14.5999	2.92450	0.823000
26	3.50000E-02	13.4324	19.5337	14.7655	2.98470	0.817000
27	3.80000E-02	13.8372	21.2080	15.2105	3.09430	0.821000
28	4.15000E-02	14.4045	23.1614	15.8341	3.11500	0.819000
29	4.45000E-02	14.7360	24.8357	16.1985	2.96710	0.834000
30	4.90000E-02	15.0960	27.3472	16.5942	3.01970	0.822000
31	5.50000E-02	15.4712	30.6958	17.0066	3.05470	0.822000
32	6.30000E-02	15.9217	35.1607	17.5019	2.92030	0.814000
33	7.20000E-02	16.3367	40.1837	17.9580	2.74420	0.792000
34	8.30000E-02	16.5812	46.3228	18.2269	2.73200	0.780000
35	0.105000	17.1824	58.6012	18.8877	2.40780	0.767000
36	0.123500	17.5514	68.9261	19.2934	2.12810	0.792000
37	0.148500	17.8307	82.8788	19.6004	2.03780	0.806000
38	0.183500	18.4031	102.4125	20.2296	1.94680	0.781000
39	0.233000	18.8998	130.039	20.7755	1.76630	0.714000
40	0.272500	19.4490	152.084	21.3793	1.34950	0.634000
41	0.308500	19.7118	172.176	21.6681	1.24440	0.574000
42	0.377000	19.8787	210.406	21.8517	1.15660	0.459000
43	0.514000	20.0637	286.867	22.0550	0.589100	0.184000
44	0.788000	20.1574	439.788	22.1580	0.185900	1.70000E-02
45	1.28800	20.2437	718.841	22.2529	9.90000E-02	0.
46	1.78800	20.2939	997.894	22.3080	1.02100E-01	0.
47	2.28800	20.3869	1276.95	22.4103	9.80000E-02	0.
48	2.78800	20.4589	1556.00	22.4894	9.08000E-02	0.
49	3.28800	20.5670	1835.05	22.6082	1.01300E-01	0.

Station = e3 z=-2.69 midspan

x = 0.361 visc = 1.63100E-05
cf = 4.27000E-03 yeff = 0.
d99.5 = 0.413891 del1 = 5.78965E-02
del2 = 3.48244E-02 H = 1.66253
Ue = 19.9756 Rex = 442133.
Red1 = 709.086 Red2 = 426.512
coef1 = 19.9756 coef2 = 0.167257
A+ = 25.0000
K = 0. f1 = 0.

N	y	U	y+	u+	u'	gamma
1	5.00000E-04	0.390560	0.282954	0.423144	1.20840	0.725000
2	1.00000E-03	0.395520	0.565908	0.428518	0.764500	0.735000
3	1.50000E-03	0.452523	0.848862	0.490276	0.952500	0.748000
4	2.50000E-03	1.06750	1.41477	1.15656	1.28160	0.777000
5	3.50000E-03	1.73046	1.98068	1.87483	1.40160	0.782000
6	4.50000E-03	2.32584	2.54659	2.51988	1.62290	0.806000
7	5.50000E-03	2.86068	3.11249	3.09934	1.55470	0.800000
8	6.50000E-03	3.35633	3.67840	3.63635	1.91700	0.794000
9	7.50000E-03	3.81662	4.24431	4.13504	1.77160	0.796000
10	8.50000E-03	4.34404	4.81022	4.70645	2.02590	0.791000
11	9.50000E-03	4.82542	5.37613	5.22799	2.08740	0.803000
12	1.05000E-02	5.22256	5.94203	5.65827	2.25330	0.811000
13	1.20000E-02	5.93065	6.79090	6.42544	2.39760	0.805000
14	1.30000E-02	6.27063	7.35680	6.79378	2.53290	0.801000
15	1.45000E-02	6.85405	8.20566	7.42587	2.55410	0.804000
16	1.55000E-02	7.25640	8.77157	7.86179	2.72570	0.804000
17	1.65000E-02	7.62325	9.33748	8.25924	2.80760	0.793000
18	1.75000E-02	7.86148	9.90339	8.51735	2.93190	0.813000
19	1.95000E-02	8.53110	11.0352	9.24283	3.02730	0.809000
20	2.10000E-02	8.96603	11.8841	9.71406	3.15530	0.814000
21	2.25000E-02	9.40807	12.7329	10.19298	3.26370	0.803000
22	2.40000E-02	9.97591	13.5818	10.8082	3.26490	0.798000
23	2.50000E-02	10.13835	14.1477	10.9842	3.33970	0.813000
24	2.70000E-02	10.46828	15.2795	11.3416	3.43490	0.814000
25	3.00000E-02	11.1191	16.9772	12.0468	3.52410	0.818000
26	3.20000E-02	11.4526	18.1091	12.4081	3.60660	0.808000
27	3.50000E-02	12.0200	19.8068	13.0228	3.58280	0.812000
28	3.75000E-02	12.2828	21.2215	13.3075	3.66370	0.834000
29	4.20000E-02	12.7937	23.7681	13.8610	3.68980	0.808000
30	4.65000E-02	13.1935	26.3147	14.2942	3.64330	0.830000
31	5.20000E-02	13.7240	29.4272	14.8689	3.59800	0.819000
32	5.70000E-02	13.8564	32.2568	15.0124	3.58460	0.828000
33	6.70000E-02	14.2355	37.9158	15.4232	3.52350	0.840000
34	8.05000E-02	14.6746	45.5556	15.8989	3.50020	0.814000
35	9.60000E-02	15.2743	54.3272	16.5487	3.35510	0.797000
36	0.109000	15.7337	61.6840	17.0463	3.27260	0.787000
37	0.123000	16.4259	69.6067	17.7963	2.94730	0.758000
38	0.133000	16.8317	75.2658	18.2359	2.78080	0.740000
39	0.145000	17.3114	82.0566	18.7557	2.58080	0.735000
40	0.157500	17.8848	89.1305	19.3769	2.18460	0.706000
41	0.168000	18.1968	95.0725	19.7150	1.98460	0.708000
42	0.184500	18.6961	104.4100	20.2559	1.77480	0.653000
43	0.201000	19.0322	113.747	20.6200	1.63630	0.611000
44	0.225500	19.4244	127.612	21.0449	1.32350	0.556000
45	0.256500	19.5915	145.155	21.2260	1.38520	0.525000
46	0.318500	19.7939	180.242	21.4453	1.34470	0.437000
47	0.442500	19.9903	250.414	21.6581	0.839900	0.223000
48	0.690500	20.0922	390.759	21.7685	0.395400	4.10000E-02
49	1.18650	20.1797	671.450	21.8633	9.82000E-02	0.
50	1.68650	20.2558	954.404	21.9458	9.78000E-02	0.

Station = e4 z=-3.24

x = 0.361 visc = 1.63300E-05
cf = 3.15000E-03 yeff = 0.
d99.5 = 0.385928 del1 = 7.68143E-02
del2 = 4.18063E-02 H = 1.83739
Ue = 19.9935 Rex = 441987.
Red1 = 940.470 Red2 = 511.852
coef1 = 19.9935 coef2 = 0.169022
A+ = 25.0000
K = 0. f1 = 0.

N	y	U	y+	u+	u'	gamma
1	1.00000E-03	0.335520	0.485895	0.422853	1.01700	0.616000
2	1.50000E-03	0.346965	0.728843	0.437277	0.987000	0.651000
3	2.50000E-03	0.796373	1.21474	1.00366	1.43660	0.714000
4	4.00000E-03	1.49889	1.94358	1.88904	1.53600	0.742000
5	6.00000E-03	2.27267	2.91537	2.86423	1.66460	0.773000
6	8.00000E-03	3.05554	3.88716	3.85087	1.94480	0.771000
7	9.50000E-03	3.61128	4.61601	4.55126	2.02680	0.766000
8	1.10000E-02	4.28470	5.34485	5.39997	2.36800	0.766000
9	1.20000E-02	4.62972	5.83074	5.83480	2.39720	0.765000
10	1.35000E-02	5.12220	6.55959	6.45546	2.62740	0.783000
11	1.50000E-02	5.46344	7.28843	6.88552	2.73740	0.774000
12	1.75000E-02	6.18343	8.50317	7.79293	2.88040	0.792000
13	1.90000E-02	6.55270	9.23201	8.25832	3.01880	0.790000
14	2.10000E-02	7.12943	10.20380	8.98516	3.14580	0.796000
15	2.25000E-02	7.55849	10.9326	9.52590	3.28040	0.790000
16	2.40000E-02	7.86419	11.6615	9.91117	3.36100	0.784000
17	2.65000E-02	8.29927	12.8762	10.45950	3.44280	0.784000
18	2.95000E-02	8.86385	14.3339	11.1710	3.54820	0.796000
19	3.20000E-02	9.34422	15.5487	11.7764	3.62860	0.791000
20	3.45000E-02	9.80197	16.7634	12.3533	3.68560	0.807000
21	3.70000E-02	10.05469	17.9781	12.6718	3.70120	0.803000
22	4.20000E-02	10.46810	20.4076	13.1929	3.65840	0.800000
23	4.80000E-02	11.0913	23.3230	13.9782	3.73320	0.826000
24	5.25000E-02	11.3413	25.5095	14.2934	3.68500	0.796000
25	6.15000E-02	11.8263	29.8826	14.9046	3.75540	0.814000
26	7.10000E-02	12.1827	34.4986	15.3537	3.66660	0.813000
27	8.45000E-02	12.5085	41.0582	15.7643	3.62720	0.829000
28	0.105500	13.1554	51.2620	16.5796	3.67000	0.808000
29	0.121500	13.8889	59.0363	17.5041	3.55980	0.808000
30	0.132000	14.4606	64.1382	18.2245	3.50080	0.800000
31	0.141000	15.0647	68.5113	18.9859	3.36120	0.775000
32	0.148000	15.4355	71.9125	19.4532	3.25940	0.783000
33	0.157000	16.1963	76.2856	20.4121	3.01540	0.739000
34	0.162500	16.6437	78.9580	20.9760	2.76720	0.731000
35	0.168500	16.9362	81.8734	21.3446	2.70900	0.688000
36	0.178500	17.5329	86.7323	22.0966	2.45960	0.666000
37	0.186500	18.0484	90.6195	22.7463	2.20580	0.610000
38	0.194000	18.3509	94.2637	23.1275	2.10200	0.574000
39	0.206000	18.8175	100.0945	23.7156	1.68680	0.525000
40	0.218500	19.0831	106.168	24.0503	1.77700	0.485000
41	0.242000	19.5530	117.587	24.6425	1.25740	0.421000
42	0.267000	19.7138	129.734	24.8452	1.19960	0.358000
43	0.317000	19.8759	154.029	25.0494	0.894600	0.295000
44	0.417000	19.9961	202.618	25.2009	0.774200	0.180000
45	0.617000	20.0931	299.797	25.3231	0.380800	5.50000E-02
46	1.01700	20.1606	494.156	25.4083	1.012E-01	1.00000E-03
47	1.51700	20.2668	737.103	25.5421	1.04800E-01	0.
48	2.01700	20.3269	980.051	25.6178	0.108800	0.
49	2.51700	20.4109	1223.00	25.7237	9.72000E-02	0.
50	3.01700	20.4949	1465.95	25.8296	9.50000E-02	0.
51	3.51700	20.5990	1708.89	25.9607	1.01400E-01	0.

Station = e5 z=-3.79 upwash
x = 0.361 visc = 1.63300E-05
cf = 2.85000E-03 yeff = 0.
d99.5 = 0.382819 del1 = 8.90439E-02
del2 = 4.59719E-02 H = 1.93692
Ue = 20.0269 Rex = 442726.
Red1 = 1092.02 Red2 = 563.794
coef1 = 20.0269 coef2 = 0.170613
A+ = 25.0000
K = 0. f1 = 0.

N	y	U	y+	u+	u'	gamma
1	1.00000E-03	0.311200	0.462951	0.411641	1.24540	0.500000
2	1.50000E-03	0.327248	0.694427	0.432868	1.44420	0.517000
3	2.50000E-03	0.671035	1.15738	0.887614	1.14450	0.579000
4	4.50000E-03	1.49985	2.08328	1.98393	1.42560	0.669000
5	6.50000E-03	2.23087	3.00918	2.95089	1.61620	0.697000
6	8.00000E-03	2.82118	3.70361	3.73173	1.88410	0.704000
7	9.50000E-03	3.29874	4.39803	4.36341	2.03580	0.714000
8	1.15000E-02	3.94297	5.32394	5.21558	2.30310	0.727000
9	1.20000E-02	4.31616	5.55541	5.70921	2.32990	0.740000
10	1.50000E-02	4.94164	6.94427	6.53656	2.53810	0.717000
11	1.70000E-02	5.25485	7.87017	6.95087	2.64960	0.743000
12	2.05000E-02	6.31164	9.49050	8.34875	2.94530	0.754000
13	2.20000E-02	6.59250	10.18492	8.72025	3.02400	0.752000
14	2.50000E-02	7.23044	11.5738	9.56409	3.24280	0.766000
15	2.70000E-02	7.56147	12.4997	10.00196	3.30350	0.768000
16	3.00000E-02	8.15799	13.8885	10.7910	3.32310	0.773000
17	3.25000E-02	8.61884	15.0459	11.4006	3.40600	0.789000
18	3.50000E-02	8.82685	16.2033	11.6757	3.42340	0.781000
19	4.00000E-02	9.46148	18.5180	12.5152	3.37800	0.798000
20	4.40000E-02	9.90978	20.3698	13.1082	3.47710	0.778000
21	4.85000E-02	10.00403	22.4531	13.2329	3.44560	0.775000
22	5.75000E-02	10.6684	26.6197	14.1117	3.43920	0.778000
23	6.40000E-02	11.0089	29.6289	14.5620	3.33890	0.798000
24	7.35000E-02	11.1942	34.0269	14.8072	3.34090	0.791000
25	9.25000E-02	11.4783	42.8230	15.1830	3.30530	0.788000
26	0.127000	12.5897	58.7948	16.6530	3.46290	0.791000
27	0.142500	13.5236	65.9705	17.8883	3.35440	0.804000
28	0.150500	14.0923	69.6741	18.6406	3.26990	0.788000
29	0.157500	14.7178	72.9148	19.4681	3.23920	0.771000
30	0.163000	15.1832	75.4610	20.0837	3.08030	0.769000
31	0.168500	15.5796	78.0073	20.6080	2.94430	0.733000
32	0.175000	16.2900	81.0164	21.5476	2.79260	0.698000
33	0.179500	16.5543	83.0997	21.8972	2.71510	0.693000
34	0.188000	17.1917	87.0348	22.7404	2.49910	0.618000
35	0.194500	17.5921	90.0440	23.2700	2.32610	0.565000
36	0.202500	18.0605	93.7476	23.8895	2.16900	0.506000
37	0.211000	18.5678	97.6827	24.5607	1.83520	0.449000
38	0.219000	18.8642	101.3863	24.9527	1.71290	0.398000
39	0.232500	19.1937	107.636	25.3886	1.57760	0.373000
40	0.253000	19.5114	117.127	25.8088	1.35480	0.319000
41	0.285000	19.7923	131.941	26.1803	1.14350	0.282000
42	0.342000	19.9473	158.329	26.3854	0.917700	0.234000
43	0.456000	20.0724	211.106	26.5508	0.621400	0.156000
44	0.684000	20.1392	316.659	26.6392	0.354400	3.90000E-02
45	1.14000	20.2247	527.764	26.7523	9.69000E-02	0.
46	1.64000	20.3048	759.240	26.8583	9.95000E-02	0.
47	2.14000	20.3829	990.715	26.9615	9.87000E-02	0.
48	2.64000	20.4829	1222.19	27.0939	9.51000E-02	0.
49	3.14000	20.5669	1453.67	27.2050	9.33000E-02	0.
50	3.64000	20.6450	1685.14	27.3082	9.55000E-02	0.

Station 3 downwash dU/dx=29s-1

x = 9.56000 cm, qwall = 170.900 W/m2

y	U	V	T	u'	v'	t'	u'v'	v't'	u't'	u'v'2	v'2t'	gamma	dU/dy	dT/dy	em	eh	Prt
0.0500	7.130	-0.040	22.93	1.1090	0.3330	0.9810	-0.0800	0.1550	-0.8490	-0.140	0.117	0.535	1974.0	-1938.7	0.405E-04	0.800E-04	0.507
0.0520	7.170	-0.050	22.90	1.0580	0.3340	0.9420	-0.0810	0.1580	-0.7640	-0.125	0.100	0.552	1747.3	-23.9	0.464E-04	0.660E-02	0.007
0.0620	7.350	-0.080	22.88	1.1100	0.3430	0.9230	-0.0670	0.1470	-0.7910	-0.139	0.105	0.550	1946.9	-860.9	0.344E-04	0.171E-03	0.202
0.0770	7.660	-0.030	22.66	1.2530	0.3150	0.9650	-0.0340	0.1090	-0.9520	-0.139	0.086	0.558	1957.5	-1637.0	0.174E-04	0.666E-04	0.261
0.1070	8.210	-0.150	22.02	1.0620	0.3230	0.9420	-0.0380	0.1190	-0.7180	-0.134	0.106	0.509	1177.5	-1350.6	0.323E-04	0.881E-04	0.366
0.1670	8.430	-0.220	21.63	1.0440	0.4000	1.0040	-0.0640	0.1720	-0.6940	-0.156	0.160	0.522	483.5	-727.0	0.132E-03	0.237E-03	0.560
0.2370	8.500	-0.280	21.40	1.0050	0.4500	0.9460	-0.0270	0.1720	-0.5130	-0.153	0.162	0.549	238.3	-368.7	0.113E-03	0.466E-03	0.243
0.3870	8.910	-0.250	21.00	0.9230	0.4420	0.8600	-0.0540	0.1520	-0.4140	-0.159	0.160	0.465	238.6	-254.9	0.226E-03	0.596E-03	0.380
0.5870	9.460	-0.160	20.51	0.4370	0.2760	0.4560	-0.0200	0.0420	-0.0860	-0.051	0.057	0.234	176.1	-158.2	0.114E-03	0.266E-03	0.428
0.8370	9.650	-0.080	20.36	0.1150	0.1070	0.1140	0.0000	0.0030	-0.0020	-0.001	0.004	0.023	87.4	-71.6	0.000E+00	0.419E-04	0.000
1.0870	9.690	-0.050	20.34	0.0670	0.0380	0.0240	0.0000	0.0000	0.0000	0.000	0.000	0.000	24.6	-7.6	0.000E+00	0.000E+00	NaN
1.4370	9.720	-0.040	20.35	0.0550	0.0180	0.0230	0.0000	0.0000	0.0000	0.000	0.000	0.000	13.6	0.4	0.000E+00	0.000E+00	NaN
1.3870	9.780	-0.040	20.37	0.0600	0.0150	0.0260	0.0000	0.0000	0.0000	0.000	0.000	0.000	9.3	2.7	0.000E+00	0.000E+00	NaN
2.4370	9.830	-0.030	20.36	0.0520	0.0160	0.0260	0.0000	0.0000	0.0000	0.000	0.000	0.000	9.9	-0.3	0.000E+00	0.000E+00	NaN
3.1360	9.930	-0.020	20.35	0.0630	0.0150	0.0240	0.0000	0.0000	0.0000	0.000	0.000	0.000	9.9	-0.4	0.000E+00	0.000E+00	NaN
4.1370	10.030	-0.020	20.36	0.0670	0.0150	0.0230	0.0000	0.0000	0.0000	0.000	0.000	0.000	9.3	-0.1	0.000E+00	0.000E+00	NaN
4.6370	10.080	-0.020	20.35	0.0610	0.0160	0.0240	0.0000	0.0000	0.0000	0.000	0.000	0.000	-15.1	-55.3	0.000E+00	0.000E+00	NaN

Station 3 upwash dU/dx=29s-1

x = 9.57000 cm, qwall = 169.200 W/m2

y	U	V	T	u'	v'	t'	u'v'	v't'	u't'	u'v'2	v'2t'	gamma	dU/dy	dT/dy	em	eh	Prt
0.0500	5.420	0.260	24.81	1.3820	0.7610	1.1370	-0.0150	0.4790	-0.7700	-0.349	0.450	0.677	-1287.5	-4801.7	-.117E-04	0.998E-04	-.117
0.0520	5.410	0.240	24.73	1.4070	0.7580	1.1330	-0.0080	0.4710	-0.7850	-0.334	0.450	0.613	2417.5	-1643.1	0.331E-05	0.287E-03	0.012
0.0620	5.690	0.200	24.61	1.4070	0.7740	1.1400	-0.0380	0.4880	-0.7830	-0.377	0.460	0.644	2372.0	-1399.3	0.160E-04	0.349E-03	0.046
0.0770	6.020	0.280	24.41	1.5280	0.7430	1.0100	0.0230	0.3660	-0.8400	-0.398	0.350	0.649	1680.9	-1593.2	-.137E-04	0.230E-03	-.060
0.1070	6.300	0.090	23.86	1.4280	0.6610	1.0090	-0.0960	0.3220	-0.8370	-0.326	0.257	0.709	1040.2	-1272.3	0.923E-04	0.253E-03	0.365
0.1670	6.760	0.100	23.39	1.2440	0.5950	0.9910	-0.1030	0.2300	-0.7710	-0.105	0.108	0.771	679.5	-863.7	0.152E-03	0.266E-03	0.569
0.2370	7.100	0.040	22.96	1.2210	0.6030	1.0540	-0.1890	0.2840	-0.9020	-0.045	0.034	0.818	598.7	-636.6	0.316E-03	0.446E-03	0.708
0.3870	7.990	-0.060	22.09	1.0150	0.5850	0.9630	-0.2140	0.3060	-0.5750	-0.124	0.106	0.778	502.5	-510.0	0.426E-03	0.600E-03	0.710
0.5870	8.870	-0.100	21.22	0.8460	0.4590	0.7560	-0.0820	0.1790	-0.3470	-0.110	0.127	0.595	371.4	-350.7	0.221E-03	0.510E-03	0.433
0.8370	9.610	-0.060	20.60	0.3020	0.1970	0.3030	-0.0030	0.0210	-0.0410	-0.016	0.025	0.138	201.1	-180.7	0.149E-04	0.116E-03	0.128
1.0870	9.700	-0.030	20.52	0.0810	0.0670	0.0660	0.0000	0.0010	0.0000	-0.001	0.002	0.005	88.7	-70.4	0.000E+00	0.142E-04	0.000
1.4370	9.740	-0.030	20.52	0.0610	0.0200	0.0250	0.0000	0.0000	0.0000	0.000	0.000	0.000	16.9	-6.1	0.000E+00	0.000E+00	NaN
1.8370	9.790	-0.030	20.52	0.0540	0.0150	0.0280	0.0000	0.0000	0.0000	0.000	0.000	0.000	12.4	0.6	0.000E+00	0.000E+00	NaN
2.4370	9.870	-0.030	20.53	0.0660	0.0160	0.0230	0.0000	0.0000	0.0000	0.000	0.000	0.000	12.4	0.7	0.000E+00	0.000E+00	NaN
3.1360	9.950	-0.020	20.53	0.0580	0.0160	0.0240	0.0000	0.0000	0.0000	0.000	0.000	0.000	12.1	0.5	0.000E+00	0.000E+00	NaN
4.1370	10.070	-0.020	20.54	0.0640	0.0150	0.0240	0.0000	0.0000	0.0000	0.000	0.000	0.000	12.1	-0.3	0.000E+00	0.000E+00	NaN
4.6370	10.130	-0.020	20.53	0.0630	0.0170	0.0250	0.0000	0.0000	0.0000	0.000	0.000	0.000	-13.0	-55.7	0.000E+00	0.000E+00	NaN

$K=0.75\times10^{-6}$ CASE DATA

	Page
Single Hot-Wire Profiles	545
Mean Temperature Profiles	550
Cross-Wire Profiles	555

Station = 1 K=0.75x10-6

x = 10.6000 visc = 1.58364E-05
cf = 6.00000E-03 yeff = -1.50000E-03
d99.5 = 0.450052 del1 = 6.90487E-02
del2 = 3.74294E-02 H = 1.84477
Uw = 8.19867 Rex = 54877.2
Red1 = 357.471 Red2 = 193.776
coef1 = 8.19867 coef2 = 0.205407
A+ = 26.6600
K = 7.50000E-07 f1 = 4.70019E-06

N	y	U	y+	u+	u'
1	5.000E-04	1.0000E-10	0.141781	2.23E-10	0.333676
2	1.500E-03	1.0000E-10	0.425342	2.23E-10	0.402146
3	3.500E-03	1.0000E-10	0.992464	2.23E-10	0.457270
4	7.500E-03	0.934184	2.12671	2.08031	0.600075
5	1.150E-02	1.54519	3.26095	3.44094	0.747644
6	1.550E-02	2.01675	4.39520	4.49105	0.855769
7	1.950E-02	2.42502	5.52944	5.40022	0.927103
8	2.400E-02	2.82290	6.80547	6.28625	1.05100
9	2.850E-02	3.20288	8.08149	7.13242	1.13061
10	3.300E-02	3.54114	9.35752	7.88567	1.16781
11	3.850E-02	3.94570	10.9171	8.78658	1.19059
12	4.400E-02	4.23498	12.4767	9.43077	1.22729
13	5.150E-02	4.61984	14.6034	10.28780	1.25238
14	5.950E-02	5.05583	16.8719	11.2587	1.27440
15	6.700E-02	5.30234	18.9986	11.8076	1.30844
16	7.900E-02	5.75524	22.4013	12.8162	1.27118
17	9.000E-02	6.11540	25.5205	13.6182	1.24807
18	1.025E-01	6.43570	29.0650	14.3315	1.24860
19	0.118500	6.74798	33.6020	15.0269	1.21699
20	0.139500	7.08828	39.5568	15.7847	1.13669
21	0.165500	7.38508	46.9294	16.4456	1.09800
22	0.201500	7.66426	57.1376	17.0674	1.00572
23	0.256000	8.00720	72.5917	17.8310	0.907701
24	0.322500	8.12583	91.4485	18.0952	0.833130
25	0.455500	8.25543	129.162	18.3838	0.760209
26	0.721500	8.31059	204.589	18.5066	0.753960
27	1.22150	8.41443	346.370	18.7379	0.733108
28	1.72150	8.53805	488.151	19.0132	0.733997
29	2.22150	8.61535	629.931	19.1853	0.712864
30	2.72150	8.67583	771.712	19.3200	0.704758
31	3.22150	8.67810	913.492	19.3250	0.709979
32	3.72150	8.75033	1055.27	19.4859	0.687430
33	4.22150	8.75226	1197.05	19.4902	0.700499
34	4.72150	8.79880	1338.83	19.5938	0.696722
35	5.22150	8.80502	1480.61	19.6077	0.690835
36	5.72150	8.82340	1622.40	19.6486	0.687028
37	6.22150	8.82680	1764.18	19.6562	0.694461
38	6.72150	8.83674	1905.96	19.6783	0.712291
39	7.22150	8.83206	2047.74	19.6679	0.712192
40	7.72150	8.80016	2189.52	19.5969	0.727927
41	8.22150	8.80688	2331.30	19.6118	0.735858
42	8.72150	8.78049	2473.08	19.5531	0.756680
43	9.22150	8.71620	2614.86	19.4099	0.797959
44	9.72150	8.59615	2756.64	19.1425	0.826244
45	10.22150	8.31919	2898.42	18.5258	0.871601

Station = 2 K=0.75x10-6

x = 35.3000 visc = 1.58855E-05
cf = 6.40000E-03 yeff = -1.50000E-03
d99.5 = 2.19560 del1 = 0.137088
del2 = 1.02539E-01 H = 1.33694
Ue = 9.15425 Rex = 203421.
Red1 = 789.991 Red2 = 590.893
coef1 = 9.15425 coef2 = 6.27211E-02
A+ = 28.4400
K = 7.50000E-07 f1 = 0.

N	y	U	y+	u+	u'
1	5.000E-04	1.000E-10	0.162992	1.93E-10	0.323758
2	1.500E-03	1.000E-10	0.488977	1.93E-10	0.400811
3	3.500E-03	0.386586	1.14095	0.746532	0.467620
4	7.500E-03	1.29469	2.44488	2.50015	0.641532
5	1.050E-02	1.94517	3.42284	3.75630	0.775622
6	1.300E-02	2.34512	4.23780	4.52864	0.880485
7	1.600E-02	2.80547	5.21575	5.41761	0.967062
8	1.900E-02	3.15046	6.19370	6.08382	1.02574
9	2.300E-02	3.60658	7.49764	6.96462	1.12245
10	2.650E-02	3.97992	8.63859	7.68557	1.14118
11	3.050E-02	4.30110	9.94252	8.30581	1.18700
12	3.550E-02	4.70839	11.5724	9.09232	1.20244
13	4.050E-02	5.10828	13.2024	9.86454	1.22677
14	4.550E-02	5.34532	14.8323	10.32228	1.22531
15	5.450E-02	5.76799	17.7661	11.1385	1.22219
16	6.350E-02	6.11874	20.7000	11.8158	1.16929
17	7.450E-02	6.40555	24.2858	12.3697	1.16343
18	9.050E-02	6.73949	29.5016	13.0146	1.08600
19	0.111000	7.05069	36.1843	13.6155	1.03370
20	0.138500	7.29253	45.1488	14.0825	0.962046
21	0.187000	7.62432	60.9591	14.7232	0.883742
22	0.248000	7.88818	80.8441	15.2328	0.853249
23	0.342500	8.18463	111.650	15.8052	0.797101
24	0.473500	8.47097	154.354	16.3582	0.764258
25	0.659500	8.74683	214.987	16.8909	0.705848
26	0.935500	8.98586	304.958	17.3525	0.666744
27	1.40500	9.11476	458.008	17.6014	0.606066
28	1.90500	9.21348	621.000	17.7920	0.583156
29	2.40500	9.26976	783.992	17.9007	0.574931
30	2.90500	9.29047	946.985	17.9407	0.569935
31	3.40500	9.35583	1109.98	18.0669	0.569220
32	3.90500	9.39633	1272.97	18.1451	0.568276
33	4.40500	9.42481	1435.96	18.2001	0.572466
34	4.90500	9.45106	1598.95	18.2508	0.579937
35	5.40500	9.49370	1761.95	18.3332	0.562530
36	5.90500	9.50336	1924.94	18.3518	0.582687
37	6.40500	9.51536	2087.93	18.3750	0.583375
38	6.90500	9.50046	2250.92	18.3462	0.593084
39	7.40500	9.49603	2413.91	18.3377	0.603781
40	7.90500	9.43888	2576.91	18.2273	0.625714
41	8.40500	9.35486	2739.90	18.0651	0.650171
42	8.90500	9.16409	2902.89	17.6967	0.710525

Station = 3 K=0.75x10-6

x = 61.0000 visc = 1.59069E-05
cf = 6.00000E-03 yeff = -1.00000E-03
d99.5 = 2.76647 del1 = 0.164510
del2 = 0.126062 H = 1.30500
Uw = 10.33877 Rex = 396471.
Red1 = 1069.24 Red2 = 819.341
coef1 = 10.33877 coef2 = 6.65385E-02
A+ = 28.8300
K = 7.50000E-07 f1 = -2.71815E-06

N	y	U	y+	u+	u'
1	5.00000E-04	1.000E-10	0.177997	1.77E-10	0.315282
2	1.00000E-03	1.000E-10	0.355994	1.77E-10	0.350634
3	2.00000E-03	1.000E-10	0.711988	1.77E-10	0.420385
4	4.00000E-03	0.609668	1.42398	1.07662	0.511997
5	8.00000E-03	1.56270	2.84795	2.75960	0.707260
6	1.05000E-02	2.17934	3.73794	3.84853	0.856746
7	1.25000E-02	2.48999	4.44992	4.39712	0.912016
8	1.60000E-02	3.11850	5.69590	5.50701	1.06471
9	1.85000E-02	3.47034	6.58589	6.12833	1.12344
10	2.15000E-02	3.90735	7.65387	6.90007	1.20232
11	2.40000E-02	4.20513	8.54385	7.42592	1.24801
12	2.75000E-02	4.56286	9.78983	8.05763	1.29347
13	3.15000E-02	4.91327	11.2138	8.67643	1.31634
14	3.60000E-02	5.34486	12.8158	9.43859	1.33112
15	4.00000E-02	5.61879	14.2398	9.92232	1.35562
16	4.60000E-02	6.03277	16.3757	10.6534	1.33959
17	5.20000E-02	6.30632	18.5117	11.1364	1.32412
18	6.10000E-02	6.70715	21.7156	11.8443	1.28901
19	7.05000E-02	6.94504	25.0976	12.2644	1.25685
20	8.75000E-02	7.41698	31.1495	13.0978	1.20147
21	1.02500E-01	7.62840	36.4894	13.4711	1.15859
22	0.132500	7.97992	47.1692	14.0919	1.08136
23	0.168500	8.25563	59.9850	14.5788	1.00347
24	0.223500	8.58869	79.5646	15.1669	0.965780
25	0.291000	8.84071	103.5942	15.6120	0.902488
26	0.402000	9.20600	143.110	16.2570	0.858136
27	0.525500	9.48696	187.075	16.7532	0.796630
28	0.705500	9.76680	251.154	17.2474	0.722506
29	0.969000	9.99737	344.958	17.6545	0.648586
30	1.43800	10.24433	511.919	18.0906	0.566832
31	1.93800	10.35928	689.916	18.2936	0.522571
32	2.43800	10.44011	867.913	18.4364	0.511412
33	2.93800	10.48736	1045.91	18.5198	0.488462
34	3.43800	10.55421	1223.91	18.6379	0.485430
35	3.93800	10.5868	1401.90	18.6953	0.483213
36	4.43800	10.6175	1579.90	18.7496	0.488120
37	4.93800	10.6678	1757.90	18.8384	0.483076
38	5.43800	10.7062	1935.90	18.9063	0.493184
39	5.93800	10.7048	2113.89	18.9038	0.498842
40	6.43800	10.6989	2291.89	18.8935	0.507863
41	6.93800	10.6797	2469.89	18.8594	0.521814
42	7.43800	10.5819	2647.88	18.6868	0.553747
43	7.93800	10.16523	2825.88	17.9510	0.637594

Station = 4 K=0.75x10-6

x = 86.1000 visc = 1.59340E-05
cf = 5.80000E-03 yeff = -1.50000E-03
d99.5 = 2.33285 del1 = 0.155562
del2 = 0.120064 H = 1.29565
Uw = 11.5859 Rex = 626047.
Red1 = 1131.11 Red2 = 873.007
coef1 = 11.5859 coef2 = 5.89633E-02
A+ = 29.1600
K = 7.50000E-07 f1 = -8.53632E-07

N	y	U	y+	u+	u'
1	5.00000E-04	1.000E-10	0.195782	1.603E-10	0.383104
2	1.50000E-03	1.000E-10	0.587346	1.603E-10	0.467799
3	3.50000E-03	0.656311	1.37047	1.05192	0.582578
4	6.00000E-03	1.47298	2.34939	2.36085	0.730649
5	8.00000E-03	1.98842	3.13251	3.18698	0.840334
6	1.00000E-02	2.50912	3.91564	4.02154	0.938680
7	1.20000E-02	2.97646	4.69877	4.77059	1.04422
8	1.40000E-02	3.40267	5.48190	5.45370	1.14203
9	1.60000E-02	3.76117	6.26503	6.02829	1.20669
10	1.85000E-02	4.26974	7.24394	6.84341	1.31502
11	2.05000E-02	4.51348	8.02707	7.23407	1.29896
12	2.45000E-02	5.11488	9.59332	8.19799	1.41196
13	2.70000E-02	5.43788	10.57223	8.71568	1.47151
14	3.00000E-02	5.80958	11.7469	9.31143	1.45794
15	3.35000E-02	6.14821	13.1174	9.85418	1.46174
16	3.75000E-02	6.47617	14.6837	10.37982	1.44959
17	4.25000E-02	6.82656	16.6415	10.9414	1.46057
18	4.85000E-02	7.22087	18.9909	11.5734	1.42137
19	5.50000E-02	7.47422	21.5360	11.9795	1.41351
20	6.55000E-02	7.91395	25.6475	12.6843	1.35604
21	7.55000E-02	8.17000	29.5631	13.0946	1.31728
22	9.20000E-02	8.53463	36.0239	13.6791	1.24681
23	0.111000	8.84724	43.4636	14.1801	1.17070
24	0.136500	9.10080	53.4485	14.5865	1.12011
25	0.178500	9.41123	69.8942	15.0840	1.07348
26	0.234500	9.76871	91.8218	15.6570	0.999636
27	0.299000	10.04526	117.078	16.1003	0.968984
28	0.394000	10.34637	154.276	16.5829	0.912199
29	0.523000	10.6207	204.788	17.0226	0.861165
30	0.715000	10.9519	279.968	17.5534	0.765865
31	0.953000	11.2089	373.161	17.9653	0.682942
32	1.33200	11.3851	521.563	18.2477	0.617038
33	1.83200	11.5626	717.346	18.5322	0.526795
34	2.33200	11.6653	913.128	18.6969	0.475460
35	2.83200	11.7386	1108.91	18.8142	0.438717
36	3.33200	11.7806	1304.69	18.8816	0.430326
37	3.83200	11.8092	1500.47	18.9274	0.423129
38	4.33200	11.8299	1696.26	18.9607	0.422790
39	4.83200	11.8628	1892.04	19.0133	0.430791
40	5.33200	11.8920	2087.82	19.0602	0.430114
41	5.83200	11.8592	2283.60	19.0076	0.432425
42	6.33200	11.7865	2479.38	18.8910	0.463883
43	6.83200	11.5540	2675.17	18.5184	0.534938
44	7.33200	10.39761	2870.95	16.6650	0.783310

Station = 5 K=0.75x10-6

x = 110.800 visc = 1.59538E-05
cf = 5.60000E-03 yeff = -1.50000E-03
d99.5 = 2.53413 del1 = 0.147548
del2 = 0.114316 H = 1.29071
Uw = 13.2966 Rex = 923454.
Red1 = 1229.73 Red2 = 952.755
coef1 = 13.2966 coef2 = 3.89102E-02
A+ = 29.4400
K = 7.50000E-07 f1 = -1.62836E-06

N	y	U	y+	u+	u'
1	5.00000E-04	1.000E-10	0.220508	1.42E-10	0.417830
2	1.50000E-03	1.000E-10	0.661525	1.42E-10	0.522570
3	3.00000E-03	0.665717	1.32305	0.946175	0.608590
4	5.00000E-03	1.47546	2.20508	2.09705	0.770807
5	6.50000E-03	2.01761	2.86661	2.86761	0.868504
6	8.00000E-03	2.48061	3.52813	3.52566	0.991470
7	9.50000E-03	2.96425	4.18966	4.21305	1.05991
8	1.10000E-02	3.42337	4.85118	4.86559	1.15978
9	1.25000E-02	3.83777	5.51270	5.45458	1.24938
10	1.40000E-02	4.17041	6.17423	5.92735	1.31807
11	1.60000E-02	4.57607	7.05626	6.50391	1.34048
12	1.80000E-02	5.02235	7.93830	7.13820	1.43588
13	1.95000E-02	5.33291	8.59982	7.57959	1.46981
14	2.15000E-02	5.65620	9.48185	8.03908	1.53022
15	2.40000E-02	6.16363	10.5844	8.76029	1.57753
16	2.60000E-02	6.37335	11.4664	9.05837	1.57165
17	3.00000E-02	6.91818	13.2305	9.83272	1.59771
18	3.30000E-02	7.24496	14.5535	10.29717	1.59886
19	3.65000E-02	7.60981	16.0971	10.8157	1.60080
20	4.05000E-02	7.93267	17.8612	11.2746	1.58565
21	4.55000E-02	8.28249	20.0662	11.7718	1.57280
22	5.15000E-02	8.61140	22.7123	12.2393	1.54741
23	5.90000E-02	8.95629	26.0200	12.7295	1.51037
24	6.80000E-02	9.31260	29.9891	13.2359	1.44640
25	7.85000E-02	9.58204	34.6198	13.6188	1.38710
26	9.50000E-02	9.92965	41.8966	14.1129	1.32420
27	0.115000	10.22921	50.7169	14.5387	1.26545
28	0.143000	10.56666	63.0653	15.0183	1.17425
29	0.177500	10.8799	78.2804	15.4634	1.16165
30	0.222000	11.2048	97.9056	15.9253	1.08063
31	0.278500	11.4963	122.823	16.3396	1.07086
32	0.357000	11.8439	157.443	16.8336	1.03088
33	0.448500	12.1232	197.796	17.2306	0.942710
34	0.583500	12.4439	257.333	17.6863	0.880809
35	0.755000	12.6609	332.967	17.9948	0.803105
36	1.07950	12.9718	476.077	18.4367	0.662076
37	1.50900	13.1313	665.494	18.6634	0.577729
38	2.00900	13.2651	886.002	18.8535	0.499257
39	2.50900	13.3247	1106.51	18.9382	0.454693
40	3.00900	13.4039	1327.02	19.0508	0.413059
41	3.50900	13.4275	1547.53	19.0844	0.396594
42	4.00900	13.4466	1768.03	19.1115	0.382213
43	4.50900	13.4669	1988.54	19.1403	0.380530
44	5.00900	13.4484	2209.05	19.1140	0.383946
45	5.50900	13.3878	2429.56	19.0279	0.421412
46	6.00900	12.9134	2650.07	18.3537	0.609558

Station = 1 K=0.75x10-6

patm = 754.000
x = 7.80000 visc = 1.60642E-05
cf = 6.00000E-03 yeff = 1.30000E-03
Tw = 29.7200 Tinf = 28.0282
Tw measured = 29.9660 Tw correction = -0.246000
Q wall = 71.5000 Stanton No. = 4.47379E-03
Q wall measured (w/Tw measured) = 77.2100
Q wall measured (w/Tw corrected) = 78.5292
delther = 0.279706 deleth = 2.37343E-02
delcon = 6.22140E-04 qadded = 3.69655
Uw = 8.11080 Rex = 39382.1
Reh = 119.920
coef1 = 8.11080 coef2 = 0.205407
A+ = 26.6600 K = 7.50000E-07
f1 = 4.75092E-06 f2 = -4.07539E-05

N	y	T	Tnd	y+	t+	Prt
1	0.0043	29.598	0.072	1.19	0.89	-0.025
2	0.0053	29.571	0.088	1.47	1.08	-0.019
3	0.0063	29.541	0.106	1.74	1.29	0.028
4	0.0073	29.522	0.117	2.02	1.43	0.081
5	0.0083	29.496	0.132	2.30	1.62	0.386
6	0.0093	29.473	0.146	2.57	1.79	-0.107
7	0.0103	29.427	0.173	2.85	2.12	-0.413
8	0.0113	29.419	0.178	3.13	2.17	-0.935
9	0.0123	29.380	0.201	3.40	2.46	-1.073
10	0.0133	29.341	0.224	3.68	2.74	1.012
11	0.0153	29.304	0.246	4.23	3.01	0.381
12	0.0193	29.215	0.298	5.34	3.65	0.547
13	0.0243	29.099	0.367	6.73	4.49	0.751
14	0.0293	29.009	0.420	8.11	5.15	0.944
15	0.0358	28.876	0.499	9.91	6.10	1.198
16	0.0413	28.783	0.554	11.43	6.78	1.334
17	0.0483	28.700	0.603	13.37	7.38	1.422
18	0.0583	28.570	0.680	16.14	8.32	1.537
19	0.0673	28.476	0.735	18.63	9.00	1.533
20	0.0788	28.398	0.781	21.81	9.57	1.543
21	0.0968	28.283	0.849	26.79	10.40	1.459
22	0.1163	28.199	0.899	32.19	11.01	1.109
23	0.1448	28.125	0.943	40.08	11.55	0.744
24	0.1928	28.079	0.970	53.36	11.88	0.584
25	0.2888	28.049	0.988	79.93	12.09	0.902
26	0.4808	28.044	0.990	133.08	12.13	0.000
27	0.8648	28.034	0.997	239.36	12.20	0.000
28	1.3648	28.040	0.993	377.75	12.16	0.000
29	1.6148	28.050	0.987	446.94	12.09	0.000
30	1.7398	28.039	0.993	481.54	12.16	0.000
31	1.9898	28.036	0.995	550.73	12.19	0.000
32	2.4898	28.032	0.998	689.12	12.22	0.000
33	2.9898	28.036	0.996	827.51	12.19	0.000
34	3.4898	28.038	0.994	965.90	12.17	0.000
35	3.9898	28.044	0.991	1104.29	12.13	0.000
36	4.4898	28.044	0.991	1242.68	12.13	0.000
37	4.9898	28.035	0.996	1381.07	12.20	0.000
38	5.4898	28.034	0.996	1519.46	12.20	0.000
39	2.9898	28.042	0.992	827.51	12.15	0.000
40	6.4898	28.034	0.996	1796.24	12.20	0.000
41	6.9898	28.034	0.996	1934.63	12.20	0.000
42	7.4898	28.034	0.996	2073.02	12.20	0.000
43	7.9898	28.041	0.993	2211.41	12.15	0.000
44	8.4898	28.048	0.989	2349.79	12.10	0.000

Station = 2 K=0.75x10-6

patm = 754.000
x = 32.8000 visc = 1.60877E-05
cf = 6.40000E-03 yeff = -8.70000E-03
Tw = 30.2500 Tinf = 28.0310
Tw measured = 30.4570 Tw correction = -0.207001
Q wall = 75.1156 Stanton No. = 3.21190E-03
Q wall measured (w/Tw measured) = 74.0000
Q wall measured (w/Tw corrected) = 75.1156
delther = 1.52136 deleth = 0.111118
delcon = 7.77336E-04 qadded = 25.3998
Uw = 9.05658 Rex = 184647.
Reh = 625.917
coef1 = 9.05658 coef2 = 6.27211E-02
A+ = 28.4400 K = 7.50000E-07
f1 = 0. f2 = -2.94249E-05

N	y	T	Tnd	y+	t+	Prt
1	0.0053	30.066	0.083	1.69	1.46	0.003
2	0.0093	30.009	0.109	2.96	1.91	0.086
3	0.0173	29.757	0.222	5.51	3.91	2.165
4	0.0208	29.665	0.263	6.63	4.64	2.047
5	0.0248	29.536	0.322	7.90	5.67	2.135
6	0.0283	29.443	0.364	9.02	6.40	2.444
7	0.0323	29.376	0.394	10.29	6.94	2.170
8	0.0393	29.243	0.454	12.52	7.99	1.880
9	0.0453	29.121	0.509	14.44	8.96	1.735
10	0.0508	29.077	0.529	16.19	9.31	1.702
11	0.0618	28.967	0.578	19.70	10.18	1.753
12	0.0738	28.841	0.635	23.52	11.19	1.703
13	0.0848	28.771	0.667	27.03	11.74	1.561
14	0.1038	28.687	0.704	33.08	12.41	1.617
15	0.1313	28.597	0.745	41.84	13.12	1.627
16	0.1683	28.523	0.778	53.64	13.71	1.790
17	0.2298	28.426	0.822	73.24	14.48	2.576
18	0.3078	28.349	0.857	98.09	15.09	3.991
19	0.4328	28.257	0.898	137.93	15.82	******
20	0.6038	28.173	0.936	192.43	16.48	0.000
21	0.8568	28.150	0.947	273.05	16.67	0.000
22	1.3263	28.061	0.986	422.68	17.37	0.000
23	1.8263	28.048	0.993	582.03	17.48	0.000
24	2.3263	28.040	0.996	741.37	17.54	0.000
25	2.8263	28.040	0.996	900.72	17.54	0.000
26	3.3263	28.046	0.993	1060.06	17.49	0.000
27	3.8263	28.036	0.998	1219.41	17.57	0.000
28	4.3263	28.046	0.993	1378.76	17.50	0.000
29	4.8263	28.049	0.992	1538.10	17.47	0.000
30	5.3263	28.042	0.995	1697.45	17.52	0.000
31	5.8263	28.048	0.992	1856.79	17.48	0.000
32	6.3263	28.045	0.994	2016.14	17.50	0.000
33	6.8263	28.038	0.997	2175.48	17.56	0.000
34	7.3263	28.038	0.997	2334.83	17.56	0.000

Station = 3 K=0.75x10-6

patm = 754.000
x = 58.2000 visc = 1.60967E-05
cf = 6.00000E-03 yeff = -7.10000E-03
Tw = 30.4190 Tinf = 28.0097
Tw measured = 30.6560 Tw correction = -0.237000
Q wall = 83.8000 Stanton No. = 2.93123E-03
Q wall measured (w/Tw measured) = 72.1000
Q wall measured (w/Tw corrected) = 73.3796
delther = 2.37065 deleth = 0.153388
delcon = 7.56700E-04 qadded = 42.7011
Uw = 10.19932 Rex = 368771.
Reh = 972.583
coef1 = 10.19932 coef2 = 6.65385E-02
A+ = 28.8300 K = 7.50000E-07
f1 = -2.75531E-06 f2 = -5.69263E-06

N	y	T	Tnd	y+	t+	Prt
1	0.0039	30.163	0.106	1.35	1.99	0.001
2	0.0049	30.093	0.135	1.70	2.53	0.001
3	0.0064	30.077	0.142	2.22	2.65	0.003
4	0.0094	30.036	0.159	3.27	2.97	0.025
5	0.0154	29.939	0.199	5.35	3.72	0.235
6	0.0224	29.707	0.295	7.78	5.52	0.709
7	0.0259	29.611	0.335	9.00	6.27	0.974
8	0.0299	29.524	0.371	10.39	6.94	1.258
9	0.0349	29.431	0.410	12.12	7.66	1.515
10	0.0409	29.337	0.449	14.21	8.39	1.386
11	0.0484	29.220	0.498	16.81	9.30	1.400
12	0.0559	29.150	0.527	19.42	9.85	1.443
13	0.0684	29.017	0.582	23.76	10.88	1.511
14	0.0794	28.949	0.610	27.58	11.40	1.451
15	0.0989	28.829	0.660	34.35	12.33	1.463
16	0.1184	28.753	0.692	41.13	12.92	1.382
17	0.1489	28.682	0.721	51.72	13.47	1.337
18	0.2019	28.571	0.767	70.13	14.34	1.478
19	0.2604	28.500	0.797	90.45	14.88	1.552
20	0.3624	28.405	0.836	125.88	15.62	1.746
21	0.4964	28.308	0.876	172.43	16.38	2.075
22	0.6669	28.223	0.912	231.65	17.04	2.348
23	0.9189	28.166	0.935	319.19	17.48	2.923
24	1.4189	28.070	0.975	492.86	18.22	4.504
25	1.9189	28.063	0.978	666.54	18.27	6.198
26	2.4189	28.035	0.989	840.22	18.49	9.416
27	2.9189	28.022	0.995	1013.90	18.59	0.000
28	3.4189	28.034	0.990	1187.58	18.50	0.000
29	3.9189	28.021	0.995	1361.26	18.60	0.000
30	4.4189	28.015	0.998	1534.93	18.65	0.000
31	4.9189	28.024	0.994	1708.61	18.57	0.000
32	5.4189	28.027	0.993	1882.29	18.55	0.000
33	5.9189	28.020	0.996	2055.97	18.61	0.000

Station = 4 K=0.75x10-6

patm = 754.000
x = 84.4000 visc = 1.60900E-05
cf = 5.80000E-03 yeff = -1.22000E-02
Tw = 30.3100 Tinf = 27.9789
Tw measured = 30.5280 Tw correction = -0.218000
Q wall = 90.6000 Stanton No. = 2.90956E-03
Q wall measured (w/Tw measured) = 74.4900
Q wall measured (w/Tw corrected) = 75.6656
delther = 3.64302 deleth = 0.229623
delcon = 6.77065E-04 qadded = 69.0902
Uw = 11.4795 Rex = 602159.
Reh = 1639.31
coef1 = 11.4795 coef2 = 5.89633E-02
A+ = 29.1600 K = 7.50000E-07
f1 = -8.61542E-07 f2 = -5.58111E-06

N	y	T	Tnd	y+	t+	Prt
1	0.0058	30.115	0.084	2.23	1.55	-0.037
2	0.0138	29.845	0.199	5.31	3.69	1.361
3	0.0168	29.722	0.252	6.46	4.67	1.033
4	0.0193	29.658	0.280	7.42	5.18	1.049
5	0.0238	29.555	0.324	9.15	5.99	1.159
6	0.0288	29.451	0.368	11.07	6.82	1.182
7	0.0343	29.341	0.416	13.19	7.69	1.188
8	0.0398	29.251	0.454	15.30	8.41	1.234
9	0.0468	29.151	0.497	18.00	9.20	1.211
10	0.0548	29.093	0.522	21.07	9.67	1.165
11	0.0708	28.978	0.571	27.23	10.58	1.245
12	0.0878	28.888	0.610	33.76	11.29	1.283
13	0.1103	28.791	0.652	42.42	12.06	1.368
14	0.1383	28.706	0.688	53.18	12.74	1.328
15	0.1788	28.635	0.719	68.76	13.30	1.407
16	0.2493	28.527	0.765	95.87	14.16	1.551
17	0.3298	28.482	0.784	126.82	14.52	1.700
18	0.4908	28.347	0.842	188.73	15.59	2.243
19	0.6388	28.288	0.867	245.65	16.05	2.662
20	0.9348	28.196	0.907	359.47	16.79	4.131
21	1.3403	28.128	0.936	515.40	17.33	7.831
22	1.8403	28.077	0.958	707.67	17.73	27.314
23	2.3403	28.033	0.977	899.94	18.08	0.000
24	2.8403	28.030	0.978	1092.22	18.11	0.000
25	3.3403	28.013	0.985	1284.49	18.24	0.000
26	3.8403	28.006	0.988	1476.76	18.30	0.000
27	4.3403	28.003	0.990	1669.03	18.32	0.000
28	4.8403	27.995	0.993	1861.30	18.38	0.000
29	5.3403	27.998	0.992	2053.57	18.36	0.000

Station = 5 K=0.75x10-6

patm = 754.000
x = 107.700 visc = 1.60822E-05
cf = 5.60000E-03 yeff = 1.60000E-03
Tw = 30.1000 Tinf = 27.9445
Tw measured = 30.3760 Tw correction = -0.275999
Q wall = 86.7000 Stanton No. = 2.64960E-03
Q wall measured (w/Tw measured) = 75.0500
Q wall measured (w/Tw corrected) = 76.5358
delther = 3.15322 deleth = 0.233577
delcon = 6.54030E-04 qadded = 72.9367
Uw = 13.0410 Rex = 873338.
Reh = 1895.60
coef1 = 13.0410 coef2 = 3.89102E-02
A+ = 29.4400 K = 7.50000E-07
f1 = -1.66028E-06 f2 = -1.00472E-05

N	y	T	Tnd	y+	t+	Prt
1	0.0046	29.974	0.059	1.98	1.17	0.066
2	0.0056	29.937	0.075	2.41	1.51	-0.367
3	0.0066	29.898	0.094	2.84	1.87	-0.104
4	0.0076	29.877	0.103	3.26	2.06	-0.124
5	0.0086	29.825	0.128	3.69	2.55	-0.180
6	0.0096	29.785	0.146	4.12	2.92	-0.288
7	0.0106	29.754	0.160	4.55	3.20	-0.571
8	0.0116	29.705	0.183	4.98	3.66	-1.083
9	0.0126	29.678	0.196	5.41	3.91	3.316
10	0.0136	29.638	0.214	5.84	4.28	0.997
11	0.0156	29.604	0.230	6.70	4.60	0.824
12	0.0196	29.502	0.277	8.42	5.54	0.884
13	0.0241	29.394	0.328	10.35	6.55	1.066
14	0.0291	29.298	0.372	12.50	7.43	1.206
15	0.0351	29.212	0.412	15.08	8.23	1.348
16	0.0436	29.099	0.464	18.73	9.27	1.380
17	0.0526	29.014	0.504	22.59	10.07	1.351
18	0.0656	28.917	0.549	28.18	10.96	1.442
19	0.0821	28.845	0.582	35.27	11.63	1.587
20	0.1106	28.745	0.629	47.51	12.56	1.737
21	0.1461	28.633	0.680	62.76	13.59	1.892
22	0.1851	28.582	0.704	79.51	14.07	2.090
23	0.2046	28.563	0.713	87.89	14.24	2.017
24	0.2386	28.528	0.729	102.49	14.57	2.025
25	0.3066	28.463	0.760	131.70	15.17	2.312
26	0.4381	28.353	0.810	188.19	16.19	4.028
27	0.5891	28.257	0.855	253.05	17.07	8.637
28	0.7881	28.212	0.876	338.53	17.50	0.000
29	1.1861	28.106	0.925	509.50	18.47	0.000
30	1.6621	28.052	0.950	713.97	18.98	0.000
31	2.1621	28.005	0.972	928.75	19.42	0.000
32	2.6621	27.994	0.977	1143.53	19.52	0.000
33	3.1621	27.977	0.985	1358.30	19.67	0.000
34	3.6621	27.970	0.988	1573.08	19.74	0.000
35	4.1621	27.964	0.991	1787.86	19.80	0.000

Station 1 K=0.75x10-6

y	U	V	u'	v'	u'v'	dU/dy	em	l
0.080	6.155	-0.629	1.070	0.759	-0.296	3127.3	0.947E-04	0.0002
0.092	6.491	-0.665	1.088	0.723	-0.280	2488.5	0.113E-03	0.0002
0.105	6.768	-0.712	1.065	0.724	-0.290	2125.4	0.136E-03	0.0003
0.124	7.135	-0.774	1.040	0.660	-0.250	1654.0	0.151E-03	0.0003
0.145	7.403	-0.805	1.015	0.620	-0.227	1291.5	0.176E-03	0.0004
0.175	7.735	-0.818	0.975	0.541	-0.213	882.1	0.241E-03	0.0005
0.212	7.941	-0.842	0.917	0.464	-0.164	576.3	0.285E-03	0.0007
0.282	8.190	-0.855	0.835	0.408	-0.125	286.6	0.436E-03	0.0012
0.395	8.354	-0.867	0.762	0.389	-0.078	124.3	0.627E-03	0.0022
0.621	8.437	-0.882	0.749	0.442	-0.091	40.7	0.224E-02	0.0074
1.073	8.502	-0.899	0.741	0.519	-0.111	19.1	0.582E-02	0.0175
1.573	8.597	-0.928	0.722	0.565	-0.100	15.5	0.645E-02	0.0204
2.073	8.668	-0.957	0.702	0.601	-0.097	13.6	0.715E-02	0.0230
2.573	8.733	-0.964	0.693	0.633	-0.104	10.8	0.965E-02	0.0299
3.073	8.773	-0.960	0.704	0.642	-0.094	7.7	0.121E-01	0.0396
3.573	8.814	-0.973	0.676	0.641	-0.071	5.7	0.125E-01	0.0469
4.073	8.821	-0.964	0.686	0.638	-0.071	3.3	0.215E-01	0.0807
4.573	8.851	-0.986	0.684	0.644	-0.064	2.7	0.235E-01	0.0930
5.073	8.837	-0.969	0.683	0.649	-0.069	3.3	0.212E-01	0.0806
5.573	8.874	-0.979	0.681	0.636	-0.049	3.2	0.151E-01	0.0683
6.073	8.891	-1.006	0.688	0.627	-0.053	3.0	0.176E-01	0.0762
6.573	8.905	-1.004	0.686	0.624	-0.042	1.0	0.437E-01	0.2131
7.073	8.897	-0.979	0.687	0.617	-0.028	-2.9	-0.972E-02	0.0581
7.573	8.895	-0.990	0.713	0.587	-0.034	-7.5	-0.456E-02	0.0247
8.073	8.824	-0.943	0.733	0.570	-0.017	-12.0	-0.142E-02	0.0109
8.573	8.755	-0.889	0.748	0.538	-0.006	-21.0	-0.286E-03	0.0037
9.073	8.668	-0.832	0.770	0.508	0.027	-31.6	0.855E-03	0.0000
9.573	8.449	-0.706	0.821	0.480	0.028	-51.1	0.548E-03	0.0000

Station 2 K=0.75x10-6

y	U	V	u'	v'	u'v'	dU/dy	em	l
0.101	6.305	-0.393	0.993	0.812	-0.264	3126.9	0.844E-04	0.0002
0.109	6.536	-0.438	0.998	0.773	-0.260	2528.1	0.103E-03	0.0002
0.122	6.817	-0.423	0.977	0.730	-0.230	2105.8	0.109E-03	0.0002
0.140	7.152	-0.475	0.938	0.660	-0.225	1565.9	0.144E-03	0.0003
0.162	7.413	-0.497	0.931	0.629	-0.229	1107.6	0.207E-03	0.0004
0.196	7.646	-0.518	0.874	0.581	-0.209	733.0	0.285E-03	0.0006
0.253	7.993	-0.558	0.829	0.523	-0.189	478.5	0.395E-03	0.0009
0.319	8.182	-0.585	0.819	0.504	-0.189	332.3	0.569E-03	0.0013
0.451	8.489	-0.634	0.765	0.475	-0.168	204.6	0.821E-03	0.0020
0.623	8.763	-0.669	0.726	0.476	-0.150	145.1	0.103E-02	0.0027
0.873	9.020	-0.719	0.661	0.470	-0.119	85.7	0.139E-02	0.0040
1.262	9.188	-0.754	0.626	0.491	-0.098	41.1	0.238E-02	0.0076
1.762	9.269	-0.798	0.587	0.526	-0.089	18.4	0.483E-02	0.0162
2.262	9.319	-0.852	0.571	0.553	-0.103	11.4	0.905E-02	0.0282
2.762	9.378	-0.901	0.567	0.564	-0.096	8.8	0.109E-01	0.0353
3.262	9.418	-0.925	0.564	0.576	-0.101	7.4	0.136E-01	0.0428
3.762	9.439	-0.962	0.554	0.590	-0.092	6.8	0.135E-01	0.0446
4.262	9.474	-0.998	0.563	0.587	-0.093	6.6	0.141E-01	0.0464
4.762	9.520	-1.035	0.553	0.580	-0.090	6.6	0.136E-01	0.0452
5.262	9.542	-1.070	0.565	0.582	-0.089	4.7	0.189E-01	0.0635
5.762	9.571	-1.109	0.566	0.559	-0.078	3.5	0.222E-01	0.0794
6.262	9.566	-1.122	0.564	0.561	-0.064	2.1	0.299E-01	0.1182
6.762	9.596	-1.124	0.591	0.526	-0.062	-2.0	-0.307E-01	0.1232
7.262	9.583	-1.142	0.583	0.507	-0.045	-7.0	-0.639E-02	0.0301
7.762	9.512	-1.117	0.605	0.466	-0.031	-15.7	-0.197E-02	0.0112
8.262	9.432	-1.078	0.624	0.431	-0.016	-44.6	-0.359E-03	0.0028
8.762	9.278	-1.022	0.689	0.399	0.006	-89.6	0.670E-04	0.0000
9.262	8.586	-0.878	0.786	0.468	0.062	-151.6	0.409E-03	0.0000

Station 3 K=0.75x10-6

y	U	V	u'	v'	u'v'	dU/dy	em	l
0.081	7.105	-0.496	1.062	0.905	-0.351	3606.8	0.973E-04	0.0002
0.088	7.330	-0.518	1.054	0.855	-0.312	2743.7	0.114E-03	0.0002
0.100	7.595	-0.532	1.030	0.802	-0.302	2041.0	0.148E-03	0.0003
0.118	7.863	-0.572	1.006	0.747	-0.274	1450.2	0.189E-03	0.0004
0.144	8.163	-0.593	0.984	0.700	-0.290	1037.3	0.280E-03	0.0005
0.179	8.437	-0.613	0.957	0.643	-0.293	752.7	0.389E-03	0.0007
0.230	8.731	-0.663	0.918	0.601	-0.270	528.5	0.511E-03	0.0010
0.299	9.000	-0.680	0.868	0.558	-0.239	391.1	0.611E-03	0.0013
0.402	9.332	-0.738	0.826	0.535	-0.227	285.0	0.797E-03	0.0017
0.525	9.618	-0.770	0.780	0.502	-0.202	208.4	0.969E-03	0.0022
0.698	9.870	-0.806	0.700	0.489	-0.166	132.9	0.125E-02	0.0031
0.971	10.097	-0.841	0.639	0.479	-0.141	76.3	0.185E-02	0.0049
1.453	10.307	-0.882	0.550	0.497	-0.120	39.7	0.303E-02	0.0087
1.953	10.433	-0.936	0.519	0.506	-0.093	22.5	0.414E-02	0.0136
2.453	10.507	-0.970	0.506	0.543	-0.103	14.0	0.736E-02	0.0229
2.953	10.551	-1.012	0.481	0.562	-0.092	9.9	0.926E-02	0.0305
3.453	10.598	-1.039	0.471	0.557	-0.091	8.7	0.105E-01	0.0348
3.953	10.636	-1.050	0.474	0.563	-0.088	8.0	0.110E-01	0.0372
4.453	10.681	-1.100	0.471	0.549	-0.085	6.7	0.127E-01	0.0435
4.953	10.709	-1.133	0.471	0.528	-0.072	6.1	0.118E-01	0.0441
5.453	10.729	-1.139	0.481	0.513	-0.075	3.3	0.227E-01	0.0830
5.953	10.764	-1.163	0.476	0.481	-0.052	1.0	0.510E-01	0.2234
6.453	10.736	-1.136	0.488	0.444	-0.040	-6.0	-0.664E-02	0.0332
6.953	10.731	-1.117	0.511	0.409	-0.027	-22.7	-0.119E-02	0.0072
7.453	10.595	-1.066	0.554	0.366	-0.001	-47.3	-0.212E-04	0.0007
7.953	10.266	-0.980	0.655	0.366	0.032	-78.9	0.406E-03	0.0000

Station 4 K=0.75x10-6

y	U	V	u'	v'	u'v'	dU/dy	em	l
0.092	8.112	-0.505	1.151	0.976	-0.414	2866.5	0.144E-03	0.0002
0.099	8.302	-0.505	1.143	0.963	-0.396	2516.5	0.157E-03	0.0003
0.113	8.620	-0.508	1.116	0.898	-0.392	2119.3	0.185E-03	0.0003
0.130	8.948	-0.524	1.074	0.808	-0.357	1636.6	0.218E-03	0.0004
0.151	9.199	-0.567	1.081	0.753	-0.352	1184.3	0.297E-03	0.0005
0.185	9.484	-0.599	1.027	0.695	-0.311	807.9	0.385E-03	0.0007
0.232	9.788	-0.630	1.005	0.646	-0.311	606.8	0.513E-03	0.0009
0.293	10.109	-0.690	0.960	0.610	-0.292	451.7	0.646E-03	0.0012
0.370	10.342	-0.706	0.935	0.596	-0.295	334.4	0.882E-03	0.0016
0.501	10.706	-0.766	0.851	0.542	-0.232	228.7	0.101E-02	0.0021
0.645	10.961	-0.809	0.786	0.530	-0.224	164.8	0.136E-02	0.0029
0.871	11.192	-0.852	0.715	0.543	-0.210	95.6	0.220E-02	0.0048
1.261	11.423	-0.903	0.621	0.537	-0.173	55.2	0.313E-02	0.0075
1.761	11.614	-0.982	0.531	0.530	-0.132	32.1	0.412E-02	0.0113
2.261	11.712	-1.024	0.470	0.556	-0.112	19.7	0.570E-02	0.0170
2.761	11.783	-1.076	0.442	0.541	-0.094	11.5	0.816E-02	0.0266
3.261	11.830	-1.144	0.424	0.538	-0.090	8.6	0.105E-01	0.0350
3.761	11.843	-1.169	0.420	0.536	-0.074	6.0	0.124E-01	0.0456
4.261	11.896	-1.213	0.418	0.504	-0.062	4.2	0.146E-01	0.0587
4.761	11.899	-1.211	0.416	0.498	-0.062	2.5	0.250E-01	0.1004
5.261	11.908	-1.223	0.420	0.458	-0.042	-1.6	-0.256E-01	0.1249
5.761	11.899	-1.204	0.416	0.423	-0.037	-10.4	-0.355E-02	0.0185
6.261	11.855	-1.161	0.448	0.379	-0.021	-24.5	-0.855E-03	0.0059
6.761	11.665	-1.100	0.507	0.340	0.008	-54.8	0.146E-03	0.0000

Station 5 K=0.75x10-6

y	U	V	u'	v'	u'v'	dU/dy	em	l
0.099	9.546	-0.790	1.254	1.056	-0.534	2742.9	0.195E-03	0.0003
0.106	9.734	-0.786	1.213	1.007	-0.477	2646.6	0.180E-03	0.0003
0.120	10.069	-0.796	1.208	0.962	-0.504	2079.9	0.242E-03	0.0003
0.137	10.343	-0.848	1.187	0.897	-0.483	1636.4	0.295E-03	0.0004
0.161	10.689	-0.902	1.111	0.814	-0.425	1189.7	0.357E-03	0.0005
0.188	10.901	-0.916	1.107	0.774	-0.421	917.5	0.459E-03	0.0007
0.239	11.288	-0.979	1.078	0.698	-0.387	657.2	0.589E-03	0.0009
0.292	11.572	-1.031	1.049	0.667	-0.364	543.1	0.670E-03	0.0011
0.367	11.932	-1.081	0.986	0.651	-0.353	406.5	0.868E-03	0.0015
0.450	12.193	-1.113	0.934	0.609	-0.316	309.4	0.102E-02	0.0018
0.576	12.491	-1.182	0.880	0.588	-0.290	203.5	0.143E-02	0.0026
0.746	12.720	-1.227	0.765	0.579	-0.248	135.3	0.183E-02	0.0037
1.041	12.998	-1.296	0.678	0.550	-0.205	77.4	0.265E-02	0.0059
1.465	13.185	-1.367	0.578	0.566	-0.170	42.3	0.402E-02	0.0097
1.965	13.287	-1.445	0.496	0.563	-0.129	22.1	0.584E-02	0.0162
2.465	13.382	-1.518	0.435	0.547	-0.099	13.6	0.730E-02	0.0232
2.965	13.421	-1.567	0.408	0.536	-0.077	9.5	0.814E-02	0.0293
3.465	13.457	-1.628	0.393	0.512	-0.064	6.1	0.105E-01	0.0415
3.965	13.486	-1.673	0.376	0.482	-0.052	4.1	0.127E-01	0.0556
4.465	13.502	-1.674	0.372	0.446	-0.043	-0.2	-0.196	0.9445
4.965	13.501	-1.677	0.381	0.398	-0.025	-14.2	-0.176E-02	0.0111
5.465	13.444	-1.673	0.416	0.344	-0.011	-79.2	-0.139E-03	0.0013
5.965	13.159	-1.606	0.547	0.360	0.028	-185.0	0.151E-03	0.0000
6.465	11.694	-1.367	0.819	0.640	0.094	-332.7	0.283E-03	0.0000

$dU_{CW}/dx=29s^{-1}$ CASE DATA

	Page
Single Hot-Wire Profiles	559
Mean Temperature Profiles	570
Cross-Wire Profiles	581
Triple-Wire Profiles	586

Station = 1 dU/dx=29s-1

patm = 758.190 temp = 29.1709
x = 10.03000 visc = 1.59897E-05
cf = 5.70000E-03 yeff = 0.
d99.5 = 1.00640 del1 = 7.83838E-02
del2 = 5.39428E-02 H = 1.45309
Uw = 13.1298 Rex = 82360.4
Red1 = 643.642 Red2 = 442.946
coef1 = 13.1298 coef2 = 0.111764
A+ = 42.7187
K = 2.73137E-06 f1 = 3.95556E-06

N	y	U	y+	u+	u'	gamma
1	5.00000E-04	1.000E-10	0.219185	1.427E-10	0.591343	0.358154
2	1.00000E-03	1.000E-10	0.438369	1.427E-10	0.568327	0.352539
3	1.50000E-03	1.000E-10	0.657554	1.427E-10	0.616551	0.385254
4	2.00000E-03	1.000E-10	0.876739	1.427E-10	0.641375	0.408691
5	2.50000E-03	0.240500	1.09592	0.343112	0.683385	0.400391
6	3.50000E-03	0.925241	1.53429	1.32000	0.760433	0.402588
7	4.50000E-03	1.36093	1.97266	1.94158	0.834950	0.451172
8	5.50000E-03	1.74119	2.41103	2.48409	0.904885	0.445312
9	7.00000E-03	2.20064	3.06859	3.13957	0.960161	0.470947
10	8.50000E-03	2.64154	3.72614	3.76857	1.07122	0.484619
11	9.50000E-03	3.02162	4.16451	4.31083	1.14630	0.514893
12	1.05000E-02	3.27171	4.60288	4.66761	1.20623	0.538574
13	1.25000E-02	3.71362	5.47962	5.29807	1.26816	0.560303
14	1.40000E-02	4.09662	6.13717	5.84448	1.37911	0.573975
15	1.55000E-02	4.40006	6.79472	6.27739	1.39535	0.587158
16	1.70000E-02	4.78806	7.45228	6.83093	1.46164	0.612305
17	1.80000E-02	5.02052	7.89065	7.16258	1.53677	0.605469
18	1.95000E-02	5.32838	8.54820	7.60179	1.53460	0.635742
19	2.05000E-02	5.48733	8.98657	7.82855	1.58941	0.625488
20	2.30000E-02	5.87781	10.08249	8.38563	1.59764	0.644531
21	2.45000E-02	6.08892	10.7400	8.68681	1.61927	0.660645
22	2.70000E-02	6.45217	11.8360	9.20506	1.62153	0.670898
23	2.90000E-02	6.72416	12.7127	9.59309	1.64519	0.679688
24	3.10000E-02	6.98451	13.5894	9.96452	1.66970	0.690430
25	3.30000E-02	7.22141	14.4662	10.30249	1.67862	0.685303
26	3.55000E-02	7.56915	15.5621	10.7986	1.66488	0.676758
27	3.75000E-02	7.78770	16.4388	11.1104	1.68045	0.703613
28	4.00000E-02	7.96896	17.5348	11.3690	1.66828	0.699951
29	4.35000E-02	8.28351	19.0691	11.8177	1.64501	0.712158
30	4.65000E-02	8.60753	20.3842	12.2800	1.64204	0.710693
31	4.90000E-02	8.74444	21.4801	12.4753	1.59733	0.707764
32	5.45000E-02	9.08052	23.8911	12.9548	1.56155	0.723877
33	5.90000E-02	9.36227	25.8638	13.3568	1.56681	0.712646
34	6.30000E-02	9.55703	27.6173	13.6346	1.48741	0.719727
35	6.90000E-02	9.79136	30.2475	13.9689	1.46103	0.721191
36	7.60000E-02	10.11908	33.3161	14.4365	1.41597	0.705566
37	8.15000E-02	10.30290	35.7271	14.6987	1.37484	0.711914
38	9.00000E-02	10.56960	39.4532	15.0792	1.32679	0.698975
39	9.85000E-02	10.7418	43.1794	15.3248	1.24186	0.693115
40	0.111500	10.9442	48.8782	15.6137	1.23869	0.689941
41	0.129000	11.2002	56.5496	15.9789	1.17439	0.659912
42	0.147500	11.3916	64.6595	16.2520	1.15474	0.638916
43	0.173000	11.6351	75.8379	16.5994	1.09291	0.624023
44	0.201000	11.8618	88.1122	16.9227	1.04578	0.596924
45	0.234000	12.0435	102.5784	17.1820	1.03791	0.570312
46	0.281500	12.2410	123.401	17.4638	1.03930	0.535156
47	0.345500	12.4734	151.457	17.7953	0.985209	0.467773
48	0.418000	12.6837	183.238	18.0953	0.971778	0.425049
49	0.507500	12.8164	222.472	18.2847	0.938155	0.371094

50	0.683000	12.9957	299.406	18.5404	0.876510	0.306641
51	0.941000	13.1577	412.505	18.7716	0.813383	0.249023
52	1.36600	13.2803	598.812	18.9464	0.779513	0.227051
53	1.86600	13.3464	817.997	19.0408	0.762157	0.235596
54	2.36600	13.3884	1037.18	19.1007	0.762120	0.226807
55	2.86600	13.4476	1256.37	19.1851	0.748881	0.234619
56	3.36600	13.4787	1475.55	19.2295	0.753781	0.239990
57	3.86600	13.5140	1694.74	19.2799	0.745619	0.242676
58	4.36600	13.4865	1913.92	19.2407	0.744068	0.235840

Station = 2 dU/dx=29s-1

patm = 757.682 temp = 29.2224
x = 18.8500 visc = 1.60052E-05
cf = 5.90000E-03 yeff = 1.00000E-03
d99.5 = 0.783126 del1 = 5.95217E-02
del2 = 4.08396E-02 H = 1.45745
Uw = 15.5873 Rex = 183578.
Red1 = 579.675 Red2 = 397.732
coef1 = 15.5873 coef2 = 0.211542
A+ = 42.5532
K = 1.93988E-06 f1 = 1.01811E-06

N	y	U	y+	u+	u'	gamma
1	1.00000E-03	1.00E-10	0.528957	1.18E-10	0.768148	0.464355
2	1.50000E-03	1.00E-10	0.793435	1.18E-10	0.781056	0.459473
3	2.00000E-03	0.310442	1.05791	0.366690	0.813298	0.484375
4	2.50000E-03	0.844132	1.32239	0.997076	0.813472	0.479980
5	3.00000E-03	1.21279	1.58687	1.43253	0.835957	0.482910
6	3.50000E-03	1.55337	1.85135	1.83482	0.887803	0.493896
7	4.50000E-03	2.18450	2.38031	2.58030	0.999049	0.514648
8	5.50000E-03	2.70088	2.90926	3.19025	1.07684	0.523926
9	7.50000E-03	3.34651	3.96718	3.95285	1.21219	0.560791
10	1.00000E-02	4.44861	5.28957	5.25464	1.36847	0.592041
11	1.15000E-02	4.99859	6.08300	5.90427	1.47748	0.624023
12	1.35000E-02	5.56678	7.14092	6.57540	1.57639	0.634033
13	1.60000E-02	6.44640	8.46331	7.61440	1.69329	0.662598
14	1.75000E-02	6.87107	9.25675	8.11601	1.72655	0.683105
15	1.95000E-02	7.34761	10.31466	8.67890	1.74457	0.694336
16	2.20000E-02	7.97356	11.6371	9.41826	1.81759	0.695801
17	2.40000E-02	8.45696	12.6950	9.98924	1.83089	0.699707
18	2.65000E-02	8.94847	14.0174	10.56980	1.81775	0.725586
19	2.95000E-02	9.44687	15.6042	11.1585	1.82129	0.732910
20	3.25000E-02	9.87874	17.1911	11.6686	1.82293	0.726807
21	3.65000E-02	10.30656	19.3069	12.1740	1.82887	0.745850
22	4.15000E-02	10.8566	21.9517	12.8236	1.78172	0.744629
23	4.65000E-02	11.3654	24.5965	13.4246	1.72058	0.749023
24	5.15000E-02	11.6322	27.2413	13.7398	1.69228	0.742920
25	6.20000E-02	12.2675	32.7953	14.4902	1.57767	0.731445
26	7.05000E-02	12.6017	37.2915	14.8849	1.51612	0.739258
27	8.40000E-02	13.0190	44.4324	15.3778	1.40263	0.728516
28	1.01500E-01	13.4118	53.6891	15.8418	1.28757	0.703857
29	0.124500	13.7891	65.8551	16.2875	1.20500	0.680908
30	0.156500	14.1090	82.7818	16.6653	1.11678	0.652344
31	0.208000	14.5009	110.023	17.1282	1.01633	0.596680
32	0.276000	14.8954	145.992	17.5943	0.943081	0.521240
33	0.364500	15.1805	192.805	17.9310	0.881737	0.432861
34	0.524000	15.4846	277.173	18.2902	0.817747	0.318115
35	0.791000	15.6808	418.405	18.5220	0.743114	0.264404
36	1.29100	15.8760	682.883	18.7526	0.697142	0.224854
37	1.79100	15.9660	947.362	18.8588	0.673947	0.222656
38	2.29100	16.0755	1211.84	18.9881	0.666742	0.219727
39	2.79100	16.1962	1476.32	19.1307	0.656130	0.233154
40	3.29100	16.2500	1740.80	19.1942	0.653261	0.209961
41	3.79100	16.3779	2005.28	19.3454	0.643231	0.220215
42	4.29100	16.4598	2269.75	19.4420	0.669780	0.232422

Station = 3 dU/dx=29s-1

patm = 757.428 temp = 29.2131
x = 25.9700 visc = 1.60097E-05
cf = 5.80000E-03 yeff = 5.00000E-04
d99.5 = 0.793014 del1 = 5.85270E-02
del2 = 4.08564E-02 H = 1.43250
Ue = 17.8056 Rex = 288832.
Red1 = 650.924 Red2 = 454.396
coef1 = 17.8056 coef2 = 0.244158
A+ = 37.6603
K = 1.43655E-06 f1 = 0.

N	y	U	y+	u+	u'	gamma
1	5.00000E-04	1.000E-10	0.299463	1.04E-10	0.840161	0.621826
2	1.00000E-03	1.000E-10	0.598926	1.04E-10	0.851044	0.616943
3	1.50000E-03	1.000E-10	0.898389	1.04E-10	0.903488	0.624512
4	2.00000E-03	0.684517	1.19785	0.713885	0.933485	0.633789
5	2.50000E-03	1.28220	1.49731	1.33721	0.979398	0.636230
6	3.00000E-03	1.75397	1.79678	1.82922	1.05627	0.675049
7	4.00000E-03	2.56705	2.39570	2.67719	1.15504	0.664795
8	5.00000E-03	3.21606	2.99463	3.35404	1.24391	0.691406
9	7.00000E-03	4.02436	4.19248	4.19702	1.35038	0.709473
10	9.50000E-03	5.34641	5.68979	5.57578	1.56082	0.728271
11	1.10000E-02	6.01803	6.58818	6.27622	1.68306	0.736328
12	1.25000E-02	6.63279	7.48657	6.91735	1.77051	0.762695
13	1.45000E-02	7.25516	8.68442	7.56642	1.86246	0.767822
14	1.70000E-02	8.17776	10.18174	8.52861	1.94841	0.784424
15	1.85000E-02	8.70019	11.0801	9.07345	1.98158	0.805420
16	2.05000E-02	9.21520	12.2780	9.61056	1.99133	0.812744
17	2.30000E-02	9.83563	13.7753	10.25761	2.03826	0.809814
18	2.55000E-02	10.46603	15.2726	10.9151	2.03126	0.822510
19	2.80000E-02	10.8712	16.7699	11.3376	2.03771	0.827881
20	3.20000E-02	11.4780	19.1656	11.9704	1.96343	0.825439
21	3.60000E-02	12.0216	21.5613	12.5374	1.96669	0.826416
22	4.05000E-02	12.5200	24.2565	13.0572	1.90506	0.827881
23	4.65000E-02	13.0821	27.8500	13.6434	1.83895	0.835449
24	5.30000E-02	13.5250	31.7431	14.1052	1.76516	0.841309
25	6.20000E-02	14.0448	37.1334	14.6473	1.70466	0.824951
26	7.20000E-02	14.4406	43.1227	15.0602	1.62506	0.813965
27	8.75000E-02	14.9802	52.4060	15.6229	1.49281	0.797119
28	0.105000	15.3475	62.8872	16.0060	1.40092	0.777588
29	0.133000	15.8124	79.6571	16.4908	1.28791	0.750244
30	0.168500	16.2283	100.9190	16.9245	1.16926	0.703369
31	0.219000	16.6403	131.165	17.3542	1.07267	0.641357
32	0.291000	17.0742	174.287	17.8068	0.957764	0.561035
33	0.388500	17.4185	232.683	18.1658	0.843623	0.435547
34	0.555500	17.7538	332.703	18.5155	0.736575	0.334473
35	0.847000	17.9458	507.290	18.7157	0.679301	0.249756
36	1.34700	18.1613	806.753	18.9405	0.632044	0.228027
37	1.84700	18.2657	1106.22	19.0494	0.616059	0.225342
38	2.34700	18.3810	1405.68	19.1696	0.593329	0.218750
39	2.84700	18.4956	1705.14	19.2891	0.599684	0.212402
40	3.34700	18.6159	2004.60	19.4146	0.604576	0.230957
41	3.84700	18.7107	2304.07	19.5135	0.588649	0.216797

Station = 4 dU/dx=29s-1

patm = 757.428 temp = 29.2219
x = 35.1900 visc = 1.60105E-05
cf = 5.90000E-03 yeff = 1.00000E-03
d99.5 = 0.720051 del1 = 5.40352E-02
del2 = 3.84883E-02 H = 1.40394
Uw = 21.0063 Rex = 461705.
Red1 = 708.961 Red2 = 504.980
coef1 = 21.0063 coef2 = 0.248853
A+ = 32.9352
K = 1.06846E-06 f1 = -1.83956E-06

N	y	U	y+	u+	u'	gamma
1	1.00000E-03	1.000E-10	0.712617	8.76E-11	1.23032	0.815674
2	1.50000E-03	0.440333	1.06893	0.385940	1.23770	0.807861
3	2.00000E-03	1.51362	1.42523	1.32664	1.26994	0.819336
4	2.50000E-03	2.18644	1.78154	1.91636	1.33322	0.811523
5	3.00000E-03	2.78809	2.13785	2.44369	1.32896	0.818115
6	3.50000E-03	3.29099	2.49416	2.88446	1.39218	0.825195
7	4.50000E-03	4.21114	3.20678	3.69095	1.52368	0.850098
8	5.50000E-03	4.92693	3.91939	4.31832	1.63928	0.841309
9	7.00000E-03	5.78182	4.98832	5.06761	1.73495	0.855469
10	9.00000E-03	6.89288	6.41355	6.04143	1.86845	0.880615
11	1.10000E-02	7.95848	7.83878	6.97539	1.96687	0.881348
12	1.25000E-02	8.84146	8.90771	7.74930	2.07507	0.890625
13	1.40000E-02	9.62121	9.97663	8.43273	2.14474	0.899414
14	1.55000E-02	10.27454	11.0456	9.00536	2.14661	0.899170
15	1.70000E-02	10.7508	12.1145	9.42280	2.18475	0.895020
16	2.00000E-02	11.8446	14.2523	10.38149	2.20539	0.906250
17	2.20000E-02	12.2380	15.6776	10.7263	2.19590	0.909668
18	2.60000E-02	13.2807	18.5280	11.6402	2.19085	0.907959
19	2.85000E-02	13.7141	20.3096	12.0201	2.15108	0.910889
20	3.35000E-02	14.5556	23.8727	12.7576	2.08710	0.900146
21	3.75000E-02	14.9888	26.7231	13.1373	2.06311	0.895508
22	4.45000E-02	15.7314	31.7114	13.7881	1.97800	0.898438
23	5.10000E-02	16.2228	36.3435	14.2189	1.85410	0.890381
24	6.05000E-02	16.8382	43.1133	14.7583	1.74650	0.883301
25	7.15000E-02	17.2436	50.9521	15.1135	1.66308	0.871582
26	9.05000E-02	17.8174	64.4918	15.6164	1.56877	0.864990
27	0.113000	18.3679	80.5257	16.0990	1.44331	0.832031
28	0.141000	18.8324	100.4790	16.5061	1.35321	0.807617
29	0.182000	19.3501	129.696	16.9598	1.23730	0.747314
30	0.236500	19.8927	168.534	17.4354	1.08196	0.665283
31	0.304500	20.2934	216.992	17.7866	0.976614	0.561523
32	0.420500	20.6933	299.655	18.1371	0.823413	0.425293
33	0.619500	21.0231	441.466	18.4261	0.684503	0.285400
34	1.01800	21.2507	725.444	18.6257	0.591159	0.223389
35	1.51800	21.3742	1081.75	18.7339	0.549242	0.210693
36	2.01800	21.5155	1438.06	18.8578	0.538655	0.208252
37	2.51800	21.6052	1794.37	18.9364	0.546491	0.208740
38	3.01800	21.7591	2150.68	19.0712	0.549956	0.199707

Station = 5 dU/dx=29s-1

patm = 757.428 temp = 29.2312
x = 42.3100 visc = 1.60114E-05
cf = 5.65000E-03 yeff = -5.00000E-04
d99.5 = 0.662155 del1 = 5.43106E-02
del2 = 3.86159E-02 H = 1.40643
Uw = 23.5767 Rex = 623013.
Red1 = 799.722 Red2 = 568.618
coef1 = 23.5767 coef2 = 0.227748
A+ = 31.2097
K = 8.48239E-07 f1 = -4.47137E-06

N	y	U	y+	u+	u'	gamma
1	5.00000E-04	1.000E-10	0.391321	7.98E-11	1.25511	0.892334
2	1.00000E-03	1.000E-10	0.782642	7.98E-11	1.25984	0.896729
3	1.50000E-03	0.688348	1.17396	0.549307	1.24571	0.892578
4	2.00000E-03	1.70416	1.56528	1.35994	1.29830	0.902588
5	3.00000E-03	3.25815	2.34793	2.60003	1.47609	0.907715
6	4.00000E-03	4.36569	3.13057	3.48386	1.56148	0.913330
7	5.00000E-03	5.34219	3.91321	4.26311	1.69389	0.923096
8	6.50000E-03	6.29459	5.08718	5.02313	1.83427	0.910400
9	8.50000E-03	7.64502	6.65246	6.10079	2.01062	0.929932
10	1.00000E-02	8.78976	7.82642	7.01430	2.12488	0.939941
11	1.10000E-02	9.55136	8.60907	7.62206	2.14212	0.937744
12	1.25000E-02	10.24490	9.78303	8.17552	2.22153	0.939697
13	1.45000E-02	11.2537	11.3483	8.98051	2.28528	0.939697
14	1.60000E-02	11.9913	12.5223	9.56913	2.34228	0.946289
15	1.80000E-02	12.6577	14.0876	10.10095	2.33810	0.944336
16	2.05000E-02	13.5955	16.0442	10.8493	2.33387	0.944580
17	2.25000E-02	14.0981	17.6095	11.2504	2.32179	0.944580
18	2.60000E-02	14.9876	20.3487	11.9602	2.28218	0.944092
19	2.95000E-02	15.6118	23.0879	12.4584	2.23686	0.948242
20	3.40000E-02	16.3107	26.6098	13.0161	2.16053	0.941406
21	3.90000E-02	16.9419	30.5231	13.5197	2.05990	0.938965
22	4.55000E-02	17.5802	35.6102	14.0292	2.00505	0.936035
23	5.30000E-02	18.1653	41.4800	14.4961	1.91268	0.925049
24	6.35000E-02	18.7158	49.6978	14.9353	1.80599	0.924805
25	7.80000E-02	19.4041	61.0461	15.4846	1.73560	0.910889
26	9.40000E-02	19.8778	73.5684	15.8626	1.64577	0.892090
27	0.120000	20.5209	93.9171	16.3758	1.54114	0.873291
28	0.151000	21.1573	118.179	16.8837	1.45433	0.840088
29	0.187500	21.6896	146.745	17.3085	1.34202	0.795654
30	0.239000	22.2526	187.052	17.7578	1.21914	0.714111
31	0.308000	22.7421	241.054	18.1484	1.09313	0.620850
32	0.413500	23.2205	323.623	18.5302	0.874850	0.464600
33	0.580000	23.5570	453.933	18.7987	0.695785	0.332031
34	0.913000	23.7702	714.552	18.9689	0.591308	0.244141
35	1.41300	23.9137	1105.87	19.0833	0.526057	0.214355
36	1.91300	23.9928	1497.19	19.1465	0.518944	0.195312
37	2.41300	24.1245	1888.52	19.2515	0.506005	0.196289
38	2.91300	24.2186	2279.84	19.3267	0.515805	0.208984
39	3.41300	24.3605	2671.16	19.4399	0.526500	0.211426

Station = 6 dU/dx=29s-1

patm = 757.682 temp = 29.2072
x = 50.4300 visc = 1.60038E-05
cf = 5.30000E-03 yeff = 1.50000E-03
d99.5 = 0.742298 del1 = 6.42254E-02
del2 = 4.64525E-02 H = 1.38260
Ue = 25.4109 Rex = 800730.
Red1 = 1019.77 Red2 = 737.575
coef1 = 25.4109 coef2 = 0.308559
A+ = 30.2311
K = 7.29858E-07 f1 = -3.94516E-06

N	y	U	y+	u+	u'	gamma
1	1.50000E-03	1.55682	1.22606	1.19013	1.56301	0.938721
2	2.00000E-03	2.60616	1.63475	1.99231	1.55319	0.948975
3	2.50000E-03	3.26498	2.04343	2.49596	1.55001	0.949707
4	3.00000E-03	3.79919	2.45212	2.90434	1.59540	0.949219
5	3.50000E-03	4.18768	2.86081	3.20133	1.53211	0.943604
6	4.00000E-03	4.66216	3.26949	3.56406	1.58280	0.950684
7	5.00000E-03	5.79284	4.08686	4.42842	1.71957	0.952393
8	6.00000E-03	6.70030	4.90424	5.12214	1.88492	0.951904
9	7.00000E-03	7.39398	5.72161	5.65243	1.94634	0.951416
10	9.00000E-03	8.70731	7.35636	6.65643	2.02292	0.957764
11	1.10000E-02	10.00257	8.99110	7.64661	2.17270	0.952148
12	1.25000E-02	10.9809	10.21716	8.39450	2.23978	0.959961
13	1.40000E-02	11.8678	11.4432	9.07254	2.30722	0.963379
14	1.55000E-02	12.6374	12.6693	9.66085	2.30820	0.965576
15	1.75000E-02	13.3428	14.3040	10.20008	2.26976	0.962158
16	2.05000E-02	14.4182	16.7561	11.0222	2.33238	0.960938
17	2.30000E-02	15.0016	18.7996	11.4682	2.35812	0.967529
18	2.70000E-02	15.8354	22.0691	12.1056	2.28007	0.960449
19	3.10000E-02	16.5157	25.3386	12.6256	2.21790	0.961182
20	3.65000E-02	17.3448	29.8341	13.2595	2.16780	0.953857
21	4.25000E-02	17.8433	34.7383	13.6406	2.05847	0.952881
22	5.35000E-02	18.7215	43.7295	14.3119	1.99846	0.947998
23	6.40000E-02	19.3417	52.3119	14.7860	1.92238	0.937012
24	7.85000E-02	20.0040	64.1638	15.2924	1.83692	0.936279
25	9.70000E-02	20.6084	79.2852	15.7544	1.79121	0.923828
26	0.123000	21.3574	100.5369	16.3270	1.72163	0.902344
27	0.152000	22.0489	124.241	16.8556	1.67457	0.895996
28	0.187000	22.7817	152.849	17.4158	1.64954	0.859131
29	0.227000	23.3815	185.544	17.8744	1.52519	0.799316
30	0.282500	24.0388	230.908	18.3768	1.36257	0.730469
31	0.352500	24.5736	288.124	18.7857	1.15454	0.618652
32	0.462000	25.0659	377.626	19.1620	0.931444	0.467773
33	0.645000	25.4358	527.206	19.4447	0.726067	0.331299
34	0.895000	25.6339	731.549	19.5962	0.593283	0.258545
35	1.14500	25.7721	935.892	19.7018	0.524859	0.216553
36	1.39500	25.8338	1140.24	19.7490	0.505214	0.219727
37	1.64500	25.9163	1344.58	19.8120	0.492344	0.201660
38	1.89500	25.9836	1548.92	19.8635	0.494809	0.198975
39	2.14500	26.0508	1753.26	19.9149	0.492629	0.199951
40	2.39500	26.1355	1957.61	19.9796	0.479454	0.205566
41	2.64500	26.2151	2161.95	20.0405	0.475450	0.185791
42	2.89500	26.3237	2366.29	20.1235	0.492095	0.197754

Station = 7 dU/dx=29s-1

patm = 757.555 temp = 29.2482
x = 58.2500 visc = 1.60103E-05
cf = 5.10000E-03 yeff = 2.50000E-03
d99.5 = 0.769978 del1 = 7.02820E-02
del2 = 5.19049E-02 H = 1.35405
Uw = 27.1914 Rex = 989298.
Red1 = 1193.65 Red2 = 881.536
coef1 = 27.1914 coef2 = 0.345907
A+ = 29.5304
K = 6.37667E-07 f1 = 0.

N	y	U	y+	u+	u'	gamma
1	2.50000E-03	3.95653	2.14408	2.88146	1.72174	0.958008
2	3.00000E-03	4.61431	2.57290	3.36052	1.75083	0.955811
3	3.50000E-03	5.20425	3.00171	3.79016	1.75332	0.954346
4	4.00000E-03	5.76936	3.43053	4.20172	1.82001	0.963867
5	4.50000E-03	6.22237	3.85935	4.53163	1.87172	0.954834
6	5.00000E-03	6.64860	4.28816	4.84205	1.88987	0.960938
7	6.00000E-03	7.65286	5.14580	5.57343	2.01577	0.964355
8	7.00000E-03	8.44301	6.00343	6.14888	2.10944	0.964111
9	8.50000E-03	9.51742	7.28988	6.93136	2.21236	0.969727
10	1.05000E-02	10.7478	9.00514	7.82744	2.30975	0.962891
11	1.30000E-02	12.4089	11.1492	9.03718	2.37876	0.968018
12	1.45000E-02	13.2270	12.4357	9.63294	2.43924	0.966797
13	1.65000E-02	14.0094	14.1509	10.20280	2.47839	0.970703
14	1.95000E-02	15.2382	16.7238	11.0977	2.44652	0.960449
15	2.15000E-02	15.7031	18.4391	11.4363	2.46420	0.963379
16	2.60000E-02	16.7968	22.2984	12.2328	2.36142	0.960938
17	3.00000E-02	17.4518	25.7290	12.7098	2.34908	0.962646
18	3.65000E-02	18.3230	31.3036	13.3443	2.29088	0.956055
19	4.40000E-02	19.1813	37.7358	13.9694	2.21453	0.952881
20	5.20000E-02	19.7581	44.5969	14.3895	2.12143	0.946289
21	6.55000E-02	20.5292	56.1749	14.9510	1.98541	0.950439
22	8.20000E-02	21.2983	70.3259	15.5112	1.92140	0.936523
23	1.02000E-01	22.0157	87.4785	16.0337	1.86984	0.927246
24	0.127500	22.6952	109.348	16.5285	1.87550	0.922607
25	0.161500	23.4387	138.508	17.0700	1.80622	0.895996
26	0.203500	24.2184	174.528	17.6378	1.73271	0.882324
27	0.252000	24.8922	216.123	18.1285	1.68311	0.815186
28	0.317500	25.6322	272.298	18.6674	1.51598	0.750732
29	0.398000	26.2915	341.338	19.1476	1.27254	0.632324
30	0.509500	26.7975	436.964	19.5161	1.04648	0.488281
31	0.710500	27.2675	609.348	19.8584	0.736733	0.337158
32	0.960500	27.4954	823.756	20.0244	0.587315	0.265625
33	1.21050	27.6175	1038.16	20.1133	0.522231	0.228027
34	1.46050	27.6970	1252.57	20.1712	0.489158	0.209961
35	1.71050	27.7896	1466.98	20.2387	0.490363	0.201172
36	1.96050	27.8430	1681.39	20.2775	0.458551	0.200195
37	2.21050	27.9697	1895.80	20.3698	0.465335	0.191895
38	2.46050	28.0350	2110.21	20.4173	0.468631	0.192383
39	2.71050	28.1348	2324.61	20.4901	0.486379	0.202881
40	2.96050	28.1940	2539.02	20.5331	0.501194	0.203125

Station = 8 dU/dx=29s-1

patm = 757.428 temp = 29.3226
x = 66.1100 visc = 1.60200E-05
cf = 5.30000E-03 yeff = 1.00000E-03
d99.5 = 0.656221 del1 = 6.25045E-02
del2 = 4.60231E-02 H = 1.35811
Uw = 29.1726 Rex = 1.20388E+06
Red1 = 1138.22 Red2 = 838.089
coef1 = 29.1726 coef2 = 0.524010
A+ = 28.5844
K = 5.54327E-07 f1 = -6.56900E-07

N	y	U	y+	u+	u'	gamma
1	1.00000E-03	1.00E-10	0.937427	6.66E-11	1.61198	0.960205
2	1.50000E-03	2.11089	1.40614	1.40562	1.64377	0.962158
3	2.00000E-03	3.34968	1.87485	2.23051	1.67341	0.958008
4	2.50000E-03	4.29595	2.34357	2.86062	1.79981	0.956299
5	3.00000E-03	5.09571	2.81228	3.39318	1.77880	0.958252
6	3.50000E-03	5.82402	3.28099	3.87814	1.87804	0.962891
7	4.50000E-03	7.26749	4.21842	4.83934	1.97082	0.969238
8	5.50000E-03	8.41446	5.15585	5.60309	2.11513	0.964111
9	6.50000E-03	9.42000	6.09327	6.27267	2.27615	0.968262
10	8.00000E-03	10.6755	7.49941	7.10867	2.34991	0.971191
11	9.50000E-03	11.9190	8.90556	7.93673	2.45426	0.968018
12	1.15000E-02	13.2236	10.7804	8.80542	2.50289	0.969971
13	1.35000E-02	14.3706	12.6553	9.56921	2.56608	0.972656
14	1.55000E-02	15.4764	14.5301	10.30554	2.58301	0.961426
15	1.75000E-02	16.5403	16.4050	11.0140	2.62447	0.968018
16	1.95000E-02	16.9482	18.2798	11.2856	2.58289	0.966309
17	2.40000E-02	18.2868	22.4982	12.1769	2.53716	0.965088
18	2.75000E-02	19.0310	25.7792	12.6725	2.52214	0.963867
19	3.30000E-02	19.9056	30.9351	13.2549	2.43168	0.958496
20	3.95000E-02	20.6771	37.0284	13.7686	2.33995	0.949951
21	4.85000E-02	21.5770	45.4652	14.3679	2.24051	0.951416
22	5.90000E-02	22.2257	55.3082	14.7998	2.15225	0.944580
23	7.60000E-02	23.0721	71.2444	15.3635	2.02693	0.938721
24	9.65000E-02	23.7979	90.4617	15.8467	2.02023	0.935791
25	0.124500	24.6231	116.710	16.3963	1.94940	0.919678
26	0.158500	25.4774	148.582	16.9651	1.92999	0.908691
27	0.197500	26.1980	185.142	17.4449	1.88497	0.879150
28	0.251000	27.0143	235.294	17.9885	1.79101	0.841064
29	0.316000	27.7913	296.227	18.5059	1.59721	0.770752
30	0.399000	28.5093	374.033	18.9840	1.42387	0.659668
31	0.513500	29.0723	481.369	19.3589	1.18805	0.524658
32	0.716500	29.4966	671.666	19.6415	0.876570	0.371826
33	0.966500	29.6531	906.023	19.7456	0.738414	0.320801
34	1.21650	29.8621	1140.38	19.8848	0.565542	0.235107
35	1.46650	29.9778	1374.74	19.9618	0.495881	0.201416
36	1.71650	30.0579	1609.09	20.0152	0.472234	0.193359
37	1.96650	30.1619	1843.45	20.0844	0.449261	0.187988

Station = 9 dU/dx=29s-1

patm = 757.428 temp = 29.3097
x = 73.9300 visc = 1.60187E-05
cf = 5.00000E-03 yeff = 2.50000E-03
d99.5 = 0.865280 del1 = 7.27015E-02
del2 = 5.48091E-02 H = 1.32645
Ue = 31.8585 Rex = 1.47034E+06
Red1 = 1445.90 Red2 = 1090.06
coef1 = 31.8585 coef2 = 0.571484
A+ = 28.1911
K = 4.64766E-07 f1 = -1.26105E-06

N	y	U	y+	u+	u'	gamma
1	2.50000E-03	4.86859	2.48603	3.05639	1.83636	0.967773
2	3.00000E-03	5.42795	2.98324	3.40754	1.83377	0.968750
3	3.50000E-03	6.05318	3.48044	3.80004	1.87547	0.964844
4	4.00000E-03	6.70033	3.97765	4.20631	1.87947	0.963867
5	4.50000E-03	7.31701	4.47485	4.59345	2.00468	0.964844
6	5.00000E-03	7.97917	4.97206	5.00914	2.06051	0.967285
7	6.00000E-03	9.24151	5.96647	5.80161	2.14565	0.973389
8	7.00000E-03	10.37798	6.96088	6.51505	2.31209	0.969971
9	8.00000E-03	11.3734	7.95529	7.13996	2.38829	0.970215
10	9.50000E-03	12.7461	9.44691	8.00167	2.51859	0.970215
11	1.10000E-02	13.9307	10.9385	8.74536	2.57518	0.966553
12	1.30000E-02	15.1916	12.9274	9.53694	2.66197	0.968994
13	1.50000E-02	16.2467	14.9162	10.19930	2.66501	0.975098
14	1.75000E-02	17.5099	17.4022	10.9923	2.64514	0.967285
15	2.00000E-02	18.5746	19.8882	11.6607	2.69050	0.967285
16	2.25000E-02	19.2911	22.3743	12.1105	2.63023	0.966797
17	2.70000E-02	20.3145	26.8491	12.7529	2.55273	0.968750
18	3.20000E-02	21.1554	31.8212	13.2809	2.51634	0.961914
19	3.90000E-02	22.0858	38.7821	13.8650	2.45429	0.955322
20	4.75000E-02	22.9480	47.2346	14.4062	2.30946	0.955078
21	5.90000E-02	23.7698	58.6703	14.9222	2.29801	0.948486
22	7.45000E-02	24.6706	74.0837	15.4877	2.20773	0.941650
23	9.35000E-02	25.3840	92.9775	15.9355	2.19159	0.934570
24	0.122000	26.4179	121.318	16.5846	2.14634	0.927002
25	0.152000	27.3100	151.151	17.1446	2.11777	0.914551
26	0.187500	27.9652	186.452	17.5559	2.08241	0.896484
27	0.245000	29.0476	243.631	18.2354	1.91886	0.866455
28	0.301500	29.7661	299.815	18.6865	1.77194	0.804199
29	0.385000	30.5691	382.849	19.1905	1.56835	0.709473
30	0.496000	31.2676	493.228	19.6291	1.32867	0.582275
31	0.665500	31.8396	661.781	19.9881	1.01117	0.441406
32	0.915500	32.2827	910.384	20.2663	0.715206	0.273193
33	1.16550	32.5188	1158.99	20.4145	0.555922	0.227783
34	1.41550	32.6687	1407.59	20.5086	0.481188	0.200684
35	1.66550	32.7900	1656.19	20.5848	0.455087	0.187744
36	1.91550	32.9567	1904.80	20.6895	0.442233	0.171631

Station = 10 dU/dx=29s-1

patm = 757.174 temp = 29.4028
x = 81.7500 visc = 1.60328E-05
cf = 5.10000E-03 yeff = 2.00000E-03
d99.5 = 0.846639 del1 = 6.75840E-02
del2 = 5.16733E-02 H = 1.30791
Uw = 34.7172 Rex = 1.77020E+06
Red1 = 1463.45 Red2 = 1118.92
coef1 = 34.7172 coef2 = 0.736084
A+ = 27.7005
K = 3.91721E-07 f1 = 1.15218E-06

N	y	U	y+	u+	u'	gamma
1	2.00000E-03	5.13445	2.18693	2.92873	2.05655	0.973145
2	2.50000E-03	6.20263	2.73366	3.53803	2.04328	0.972168
3	3.00000E-03	7.14868	3.28039	4.07766	2.07986	0.970703
4	3.50000E-03	7.89578	3.82712	4.50381	2.14176	0.976562
5	4.00000E-03	8.71919	4.37385	4.97349	2.20902	0.971436
6	4.50000E-03	9.34166	4.92058	5.32856	2.24366	0.974365
7	5.50000E-03	10.9234	6.01405	6.23082	2.43044	0.974121
8	6.00000E-03	11.5029	6.56078	6.56135	2.45181	0.974365
9	7.50000E-03	12.8385	8.20097	7.32317	2.49763	0.976562
10	9.50000E-03	14.6640	10.38790	8.36444	2.62949	0.976807
11	1.15000E-02	16.2821	12.5748	9.28743	2.76411	0.973145
12	1.30000E-02	17.4485	14.2150	9.95275	2.83734	0.966797
13	1.50000E-02	18.5912	16.4019	10.6046	2.81885	0.971924
14	1.75000E-02	19.8777	19.1356	11.3384	2.77904	0.970459
15	2.00000E-02	20.9941	21.8693	11.9752	2.79787	0.969238
16	2.30000E-02	21.9815	25.1497	12.5384	2.75295	0.961914
17	2.65000E-02	22.7256	28.9768	12.9629	2.67202	0.963379
18	3.30000E-02	23.8718	36.0843	13.6167	2.58917	0.961670
19	4.00000E-02	24.7784	43.7385	14.1338	2.50211	0.959717
20	4.95000E-02	25.8026	54.1264	14.7180	2.43098	0.954346
21	6.05000E-02	26.6172	66.1545	15.1827	2.34238	0.953613
22	7.70000E-02	27.5059	84.1967	15.6896	2.33848	0.942383
23	9.85000E-02	28.4784	107.706	16.2443	2.32866	0.936279
24	0.124500	29.3499	136.136	16.7414	2.28735	0.926025
25	0.159000	30.3632	173.861	17.3194	2.20352	0.908203
26	0.198000	31.2101	216.506	17.8025	2.11823	0.887939
27	0.251000	32.0726	274.459	18.2945	1.99925	0.850830
28	0.321500	32.8962	351.548	18.7642	1.88688	0.780273
29	0.419000	33.6978	458.161	19.2215	1.63295	0.685791
30	0.558000	34.4445	610.152	19.6474	1.31574	0.539307
31	0.772000	35.0494	844.154	19.9925	0.961279	0.371826
32	1.02200	35.4426	1117.52	20.2167	0.670030	0.239258
33	1.27200	35.6633	1390.89	20.3426	0.546019	0.211670
34	1.52200	35.8569	1664.25	20.4530	0.458934	0.180908
35	1.77200	35.9960	1937.62	20.5324	0.428582	0.164551

Station = 1 dU/dx=29s-1

patm = 749.300
x = 7.35000 visc = 1.65186E-05
cf = 5.70000E-03 yeff = 1.30000E-03
Tw = 35.3400 Tinf = 30.3748
Tw measured = 35.0475 Tw correction = 0.292500
Q wall = 367.000 Stanton No. = 5.24231E-03
Q wall measured (w/Tw measured) = 380.602
Q wall measured (w/Tw corrected) = 378.949
delther = 0.328260 deleth = 2.37045E-02
delcon = 3.59687E-04 qadded = 16.2894
Uw = 12.3406 Rex = 54909.7
Reh = 176.941
coef1 = 12.3406 coef2 = 0.111764
A+ = 42.7187 K = 3.19417E-06
f1 = 4.20853E-06 f2 = -1.07500E-04

N	y	T	Tnd	y+	t+	Prt
1	0.0043	34.742	0.120	1.71	1.23	0.041
2	0.0053	34.600	0.149	2.11	1.52	0.233
3	0.0063	34.464	0.176	2.51	1.80	0.030
4	0.0073	34.354	0.199	2.91	2.02	0.040
5	0.0083	34.247	0.220	3.31	2.24	0.056
6	0.0093	34.114	0.247	3.71	2.52	0.070
7	0.0103	34.003	0.269	4.11	2.74	0.086
8	0.0113	33.867	0.297	4.50	3.02	0.109
9	0.0123	33.766	0.317	4.90	3.23	0.132
10	0.0133	33.668	0.337	5.30	3.43	0.148
11	0.0143	33.580	0.354	5.70	3.61	0.163
12	0.0153	33.473	0.376	6.10	3.83	0.171
13	0.0163	33.365	0.398	6.50	4.05	0.183
14	0.0173	33.287	0.414	6.90	4.21	0.194
15	0.0183	33.205	0.430	7.29	4.38	0.202
16	0.0198	33.106	0.450	7.89	4.58	0.212
17	0.0213	33.021	0.467	8.49	4.76	0.230
18	0.0233	32.913	0.489	9.29	4.98	0.273
19	0.0248	32.789	0.514	9.89	5.23	0.306
20	0.0263	32.700	0.532	10.48	5.42	0.346
21	0.0278	32.647	0.542	11.08	5.52	0.387
22	0.0308	32.473	0.577	12.28	5.88	0.456
23	0.0323	32.417	0.589	12.87	6.00	0.480
24	0.0358	32.242	0.624	14.27	6.35	0.565
25	0.0378	32.179	0.637	15.07	6.48	0.607
26	0.0408	32.025	0.668	16.26	6.80	0.646
27	0.0428	31.949	0.683	17.06	6.96	0.680
28	0.0453	31.896	0.694	18.06	7.07	0.696
29	0.0508	31.740	0.725	20.25	7.38	0.779
30	0.0543	31.647	0.744	21.64	7.57	0.820
31	0.0583	31.545	0.764	23.24	7.79	0.910
32	0.0618	31.475	0.778	24.63	7.93	0.996
33	0.0673	31.346	0.804	26.83	8.19	1.089
34	0.0718	31.263	0.821	28.62	8.36	1.149
35	0.0773	31.183	0.837	30.81	8.53	1.213
36	0.0843	31.103	0.853	33.60	8.69	1.303
37	0.0933	31.010	0.872	37.19	8.88	1.418
38	0.1033	30.920	0.890	41.18	9.07	1.641
39	0.1143	30.847	0.905	45.56	9.22	2.075
40	0.1298	30.761	0.922	51.74	9.39	3.383
41	0.1483	30.710	0.932	59.11	9.50	16.702
42	0.1853	30.590	0.957	73.86	9.74	0.000
43	0.2168	30.526	0.970	86.42	9.88	0.000
44	0.2678	30.465	0.982	106.74	10.00	0.000
45	0.3548	30.416	0.992	141.42	10.10	0.000
46	0.5293	30.386	0.998	210.98	10.16	0.000
47	0.7793	30.378	0.999	310.63	10.18	0.000
48	1.0293	30.380	0.999	410.28	10.17	0.000
49	1.2793	30.382	0.998	509.93	10.17	0.000
50	1.5293	30.382	0.999	609.57	10.17	0.000
51	1.7793	30.391	0.997	709.22	10.15	0.000
52	2.0293	30.398	0.995	808.87	10.14	0.000
53	2.2793	30.391	0.997	908.52	10.15	0.000
54	2.5293	30.394	0.996	1008.17	10.15	0.000
55	2.7793	30.400	0.995	1107.82	10.13	0.000
56	3.0293	30.406	0.994	1207.47	10.12	0.000
57	3.2793	30.403	0.994	1307.12	10.13	0.000
58	3.5293	30.416	0.992	1406.77	10.10	0.000
59	3.7793	30.416	0.992	1506.42	10.10	0.000
60	4.0293	30.425	0.990	1606.07	10.08	0.000

Station = 2 dU/dx=29s-1

patm = 751.078
x = 15.7100 visc = 1.65787E-05
cf = 5.90000E-03 yeff = 2.30000E-03
Tw = 36.4000 Tinf = 29.8364
Tw measured = 37.6429 Tw correction = -1.24290
Q wall = 390.000 Stanton No. = 3.54164E-03
Q wall measured (w/Tw measured) = 361.881
Q wall measured (w/Tw corrected) = 369.031
delther = 0.581971 deleth = 4.50009E-02
delcon = 4.47786E-04 qadded = 48.5330
Uw = 14.6626 Rex = 138944.
Reh = 399.413
coef1 = 14.6626 coef2 = 0.211542
A+ = 42.5532 K = 2.27082E-06
f1 = 1.08231E-06 f2 = -7.42953E-05

N	y	T	Tnd	y+	t+	Prt
1	0.0043	35.781	0.094	2.07	1.45	-0.002
2	0.0053	35.604	0.121	2.56	1.86	1.407
3	0.0063	35.490	0.139	3.04	2.13	0.600
4	0.0073	35.341	0.161	3.52	2.48	0.192
5	0.0083	35.189	0.185	4.00	2.83	0.164
6	0.0093	35.050	0.206	4.49	3.16	0.161
7	0.0098	35.023	0.210	4.73	3.22	0.177
8	0.0108	34.884	0.231	5.21	3.54	0.201
9	0.0118	34.766	0.249	5.69	3.82	0.219
10	0.0123	34.733	0.254	5.93	3.89	0.259
11	0.0138	34.551	0.282	6.66	4.32	0.445
12	0.0143	34.479	0.293	6.90	4.49	0.452
13	0.0153	34.407	0.304	7.38	4.66	0.502
14	0.0168	34.179	0.338	8.10	5.19	0.595
15	0.0173	34.136	0.345	8.34	5.29	0.579
16	0.0178	34.116	0.348	8.58	5.34	0.595
17	0.0183	34.080	0.353	8.83	5.42	0.586
18	0.0193	33.943	0.374	9.31	5.74	0.492
19	0.0203	33.880	0.384	9.79	5.89	0.574
20	0.0218	33.749	0.404	10.51	6.20	0.729
21	0.0228	33.696	0.412	11.00	6.32	0.792
22	0.0253	33.459	0.448	12.20	6.87	0.958
23	0.0263	33.312	0.471	12.68	7.22	1.030
24	0.0268	33.366	0.462	12.92	7.09	1.014
25	0.0283	33.231	0.483	13.65	7.40	1.047
26	0.0293	33.143	0.496	14.13	7.61	0.976
27	0.0303	33.067	0.508	14.61	7.79	0.933
28	0.0318	33.004	0.517	15.34	7.94	1.077
29	0.0343	32.846	0.542	16.54	8.31	1.068
30	0.0358	32.786	0.551	17.26	8.45	1.131
31	0.0388	32.615	0.577	18.71	8.85	1.358
32	0.0403	32.568	0.584	19.44	8.96	1.423
33	0.0438	32.331	0.620	21.12	9.51	1.519
34	0.0453	32.242	0.633	21.85	9.72	1.512
35	0.0468	32.225	0.636	22.57	9.76	1.548
36	0.0503	32.096	0.656	24.26	10.06	1.520
37	0.0528	31.997	0.671	25.46	10.29	1.386
38	0.0553	31.980	0.673	26.67	10.33	1.435
39	0.0608	31.772	0.705	29.32	10.82	1.719
40	0.0633	31.744	0.709	30.53	10.88	1.802
41	0.0688	31.593	0.732	33.18	11.24	2.074
42	0.0723	31.523	0.743	34.87	11.40	2.225
43	0.0778	31.404	0.761	37.52	11.68	2.362
44	0.0823	31.325	0.773	39.69	11.86	2.602
45	0.0883	31.215	0.790	42.58	12.12	2.833
46	0.0938	31.175	0.796	45.24	12.21	3.164
47	0.1048	31.059	0.814	50.54	12.48	4.358
48	0.1143	30.943	0.831	55.12	12.75	6.796
49	0.1228	30.867	0.843	59.22	12.93	12.969
50	0.1343	30.787	0.855	64.77	13.12	******
51	0.1488	30.681	0.871	71.76	13.37	0.000
52	0.1628	30.562	0.889	78.51	13.64	0.000
53	0.1743	30.522	0.896	84.06	13.74	0.000
54	0.1978	30.415	0.912	95.39	13.99	0.000
55	0.2203	30.329	0.925	106.24	14.19	0.000
56	0.2468	30.258	0.936	119.02	14.35	0.000
57	0.2858	30.155	0.952	137.83	14.60	0.000
58	0.3243	30.085	0.962	156.40	14.76	0.000
59	0.3803	30.004	0.974	183.40	14.95	0.000
60	0.4518	29.957	0.982	217.88	15.06	0.000
61	0.5953	29.905	0.989	287.09	15.18	0.000
62	0.8453	29.874	0.994	407.65	15.25	0.000
63	1.0953	29.866	0.995	528.22	15.27	0.000
64	1.3453	29.878	0.994	648.78	15.24	0.000
65	1.5953	29.868	0.995	769.35	15.27	0.000
66	1.8453	29.867	0.995	889.91	15.27	0.000
67	2.0953	29.867	0.995	1010.48	15.27	0.000
68	2.3453	29.873	0.994	1131.04	15.25	0.000
69	2.5953	29.875	0.994	1251.61	15.25	0.000
70	2.8453	29.868	0.995	1372.17	15.27	0.000

71	3.0953	29.874	0.994	1492.74	15.25	0.000
72	3.3453	29.877	0.994	1613.30	15.24	0.000
73	3.5953	29.873	0.994	1733.86	15.25	0.000
74	3.8453	29.869	0.995	1854.43	15.26	0.000
75	4.0953	29.865	0.996	1974.99	15.27	0.000

Station = 3 dU/dx=29s-1

patm = 751.332
x = 23.6300 visc = 1.65854E-05
cf = 5.80000E-03 yeff = 2.80000E-03
Tw = 36.4000 Tinf = 29.7769
Tw measured = 37.9161 Tw correction = -1.51610
Q wall = 415.000 Stanton No. = 3.19823E-03
Q wall measured (w/Tw measured) = 360.935
Q wall measured (w/Tw corrected) = 369.668
delther = 0.851673 deleth = 6.31283E-02
delcon = 4.24618E-04 qadded = 79.6578
Uw = 17.1165 Rex = 243867.
Reh = 654.321
coef1 = 17.1165 coef2 = 0.244158
A+ = 37.6603 K = 1.66706E-06
f1 = 0. f2 = -3.73913E-05

N	y	T	Tnd	y+	t+	Prt
1	0.0038	35.798	0.091	2.12	1.53	0.016
2	0.0048	35.678	0.109	2.68	1.84	0.205
3	0.0058	35.485	0.138	3.24	2.33	-1.215
4	0.0068	35.348	0.159	3.80	2.67	0.832
5	0.0078	35.166	0.186	4.36	3.14	0.416
6	0.0088	35.021	0.208	4.91	3.51	0.385
7	0.0098	34.939	0.221	5.47	3.72	0.352
8	0.0108	34.747	0.250	6.03	4.20	0.345
9	0.0113	34.723	0.253	6.31	4.26	0.367
10	0.0123	34.599	0.272	6.87	4.58	0.423
11	0.0133	34.487	0.289	7.43	4.86	0.500
12	0.0138	34.448	0.295	7.71	4.97	0.492
13	0.0153	34.257	0.323	8.54	5.45	0.614
14	0.0163	34.178	0.335	9.10	5.65	0.627
15	0.0173	34.038	0.357	9.66	6.01	0.654
16	0.0178	34.008	0.361	9.94	6.08	0.685
17	0.0193	33.882	0.380	10.78	6.40	0.696
18	0.0208	33.791	0.394	11.62	6.64	0.736
19	0.0223	33.658	0.414	12.45	6.97	0.748
20	0.0233	33.550	0.430	13.01	7.25	0.786
21	0.0243	33.490	0.439	13.57	7.40	0.844
22	0.0263	33.376	0.457	14.69	7.69	0.966
23	0.0283	33.262	0.474	15.80	7.98	1.042
24	0.0298	33.179	0.486	16.64	8.19	1.062
25	0.0318	33.018	0.511	17.76	8.60	1.154
26	0.0328	32.932	0.524	18.32	8.82	1.213
27	0.0343	32.881	0.531	19.16	8.95	1.245
28	0.0373	32.748	0.551	20.83	9.29	1.230
29	0.0398	32.628	0.569	22.23	9.59	1.184
30	0.0418	32.578	0.577	23.34	9.72	1.190
31	0.0458	32.411	0.602	25.58	10.14	1.279
32	0.0483	32.299	0.619	26.97	10.43	1.362
33	0.0508	32.264	0.624	28.37	10.52	1.430
34	0.0558	32.137	0.644	31.16	10.84	1.577
35	0.0598	32.028	0.660	33.40	11.12	1.588
36	0.0633	31.860	0.686	35.35	11.55	1.614
37	0.0653	31.829	0.690	36.47	11.62	1.708
38	0.0698	31.782	0.697	38.98	11.74	1.724
39	0.0788	31.641	0.719	44.01	12.10	1.745
40	0.0853	31.544	0.733	47.64	12.35	1.790
41	0.0923	31.425	0.751	51.55	12.65	2.054
42	0.0983	31.355	0.762	54.90	12.83	2.290
43	0.1068	31.281	0.773	59.64	13.02	2.542
44	0.1188	31.158	0.791	66.35	13.33	2.896
45	0.1288	31.035	0.810	71.93	13.64	3.284
46	0.1368	31.008	0.814	76.40	13.71	3.735
47	0.1533	30.914	0.828	85.61	13.95	5.064
48	0.1718	30.784	0.848	95.94	14.28	7.872
49	0.1863	30.685	0.863	104.04	14.53	13.892
50	0.2008	30.660	0.867	112.14	14.60	59.842
51	0.2303	30.510	0.889	128.61	14.98	0.000
52	0.2503	30.450	0.898	139.78	15.13	0.000
53	0.2848	30.313	0.919	159.05	15.48	0.000
54	0.3103	30.266	0.926	173.29	15.60	0.000
55	0.3618	30.175	0.940	202.05	15.83	0.000
56	0.4198	30.081	0.954	234.44	16.07	0.000
57	0.4833	29.998	0.967	269.90	16.28	0.000
58	0.5613	29.930	0.977	313.46	16.45	0.000
59	0.6803	29.893	0.982	379.92	16.55	0.000
60	0.9188	29.849	0.989	513.11	16.66	0.000
61	1.1688	29.821	0.993	652.73	16.73	0.000
62	1.4188	29.820	0.994	792.34	16.73	0.000
63	1.6688	29.819	0.994	931.96	16.74	0.000
64	1.9188	29.828	0.992	1071.57	16.71	0.000
65	2.1688	29.820	0.993	1211.19	16.73	0.000
66	2.4188	29.823	0.993	1350.80	16.73	0.000
67	2.6688	29.825	0.993	1490.42	16.72	0.000
68	2.9188	29.828	0.992	1630.03	16.71	0.000
69	3.1688	29.824	0.993	1769.65	16.72	0.000
70	3.4188	29.816	0.994	1909.26	16.74	0.000
71	3.6688	29.822	0.993	2048.88	16.73	0.000

Station = 4 dU/dx=29s-1

patm = 750.570
x = 31.7500 visc = 1.65883E-05
cf = 5.90000E-03 yeff = 2.80000E-03
Tw = 35.7150 Tinf = 29.7604
Tw measured = 37.5788 Tw correction = -1.86380
Q wall = 367.000 Stanton No. = 2.69314E-03
Q wall measured (w/Tw measured) = 364.553
Q wall measured (w/Tw corrected) = 375.236
delther = 0.964827 deleth = 8.80275E-02
delcon = 4.31310E-04 qadded = 115.087
Uw = 19.9933 Rex = 382671.
Reh = 1066.62
coef1 = 19.9933 coef2 = 0.248853
A+ = 32.9352 K = 1.22205E-06
f1 = -1.93277E-06 f2 = -1.74569E-05

N	y	T	Tnd	y+	t+	Prt
1	0.0038	35.194	0.088	2.50	1.77	0.036
2	0.0048	35.061	0.110	3.16	2.22	-0.400
3	0.0058	34.920	0.133	3.82	2.69	-0.416
4	0.0068	34.767	0.159	4.48	3.21	1.770
5	0.0078	34.587	0.190	5.14	3.82	1.187
6	0.0088	34.487	0.206	5.80	4.16	0.851
7	0.0098	34.372	0.225	6.45	4.55	0.700
8	0.0108	34.267	0.243	7.11	4.91	0.595
9	0.0118	34.174	0.259	7.77	5.22	0.529
10	0.0128	34.058	0.278	8.43	5.61	0.536
11	0.0138	33.981	0.291	9.09	5.87	0.544
12	0.0148	33.913	0.303	9.75	6.11	0.557
13	0.0163	33.836	0.316	10.73	6.37	0.613
14	0.0183	33.729	0.333	12.05	6.73	0.673
15	0.0203	33.569	0.360	13.37	7.27	0.766
16	0.0213	33.459	0.379	14.03	7.64	0.825
17	0.0223	33.440	0.382	14.69	7.71	0.890
18	0.0248	33.370	0.394	16.33	7.94	0.977
19	0.0288	33.156	0.430	18.97	8.67	1.121
20	0.0303	33.092	0.441	19.95	8.89	1.117
21	0.0333	32.912	0.471	21.93	9.50	1.237
22	0.0348	32.906	0.472	22.92	9.52	1.345
23	0.0383	32.742	0.499	25.22	10.07	1.345
24	0.0403	32.746	0.499	26.54	10.06	1.367
25	0.0448	32.601	0.523	29.50	10.55	1.487
26	0.0478	32.493	0.541	31.48	10.92	1.600
27	0.0508	32.429	0.552	33.46	11.13	1.662
28	0.0558	32.259	0.580	36.75	11.71	1.826
29	0.0588	32.205	0.589	38.72	11.89	1.824
30	0.0648	32.135	0.601	42.68	12.13	1.867
31	0.0738	31.943	0.634	48.60	12.78	2.011
32	0.0783	31.899	0.641	51.57	12.93	2.009
33	0.0878	31.732	0.669	57.82	13.49	2.198
34	0.0938	31.658	0.681	61.77	13.75	2.340
35	0.1018	31.574	0.695	67.04	14.03	2.345
36	0.1118	31.502	0.707	73.63	14.27	2.462
37	0.1268	31.352	0.733	83.51	14.78	2.634
38	0.1368	31.249	0.750	90.09	15.13	2.851
39	0.1468	31.246	0.750	96.68	15.14	3.119
40	0.1673	31.050	0.783	110.18	15.81	3.706
41	0.1778	31.006	0.791	117.09	15.96	3.937
42	0.1988	30.882	0.812	130.92	16.38	4.654
43	0.2163	30.765	0.831	142.45	16.77	5.441
44	0.2318	30.723	0.838	152.66	16.91	5.776
45	0.2628	30.586	0.861	173.07	17.38	7.736
46	0.2858	30.496	0.876	188.22	17.68	9.805
47	0.3118	30.458	0.883	205.34	17.81	14.369
48	0.3643	30.295	0.910	239.92	18.36	******
49	0.3968	30.205	0.925	261.32	18.67	0.000
50	0.4338	30.157	0.933	285.69	18.83	0.000
51	0.5083	30.041	0.953	334.75	19.22	0.000
52	0.5733	29.990	0.961	377.56	19.40	0.000
53	0.7033	29.913	0.974	463.17	19.66	0.000
54	0.8763	29.865	0.982	577.11	19.82	0.000
55	1.1263	29.828	0.989	741.75	19.95	0.000
56	1.3763	29.820	0.990	906.39	19.97	0.000
57	1.6263	29.819	0.990	1071.04	19.98	0.000
58	1.8763	29.818	0.990	1235.68	19.98	0.000
59	2.1263	29.820	0.990	1400.32	19.97	0.000
60	2.3763	29.819	0.990	1564.97	19.98	0.000
61	2.6263	29.818	0.990	1729.61	19.98	0.000
62	2.8763	29.807	0.992	1894.25	20.02	0.000

Station = 5 dU/dx=29s-1

patm = 750.316
x = 39.4700 visc = 1.65947E-05
cf = 5.65000E-03 yeff = 1.80000E-03
Tw = 35.7900 Tinf = 29.7542
Tw measured = 37.5362 Tw correction = -1.74620
Q wall = 380.000 Stanton No. = 2.42004E-03
Q wall measured (w/Tw measured) = 365.915
Q wall measured (w/Tw corrected) = 375.926
delther = 1.14583 deleth = 9.69804E-02
delcon = 4.22312E-04 qadded = 144.551
Uw = 22.7404 Rex = 540874.
Reh = 1335.60
coef1 = 22.7404 coef2 = 0.227748
A+ = 31.2097 K = 9.44995E-07
f1 = -4.63581E-06 f2 = -8.31035E-06

N	y	T	Tnd	y+	t+	Prt
1	0.0038	35.215	0.095	2.78	2.09	0.033
2	0.0048	35.110	0.113	3.52	2.48	0.144
3	0.0058	34.965	0.137	4.25	3.00	0.377
4	0.0068	34.826	0.160	4.98	3.51	0.732
5	0.0078	34.694	0.182	5.71	3.99	0.841
6	0.0088	34.562	0.203	6.45	4.47	0.945
7	0.0098	34.417	0.227	7.18	5.00	1.004
8	0.0108	34.319	0.244	7.91	5.35	0.924
9	0.0118	34.224	0.259	8.65	5.70	0.834
10	0.0128	34.129	0.275	9.38	6.05	0.855
11	0.0138	33.996	0.297	10.11	6.53	0.894
12	0.0143	34.004	0.296	10.48	6.50	0.939
13	0.0148	33.967	0.302	10.84	6.64	0.991
14	0.0158	33.859	0.320	11.58	7.03	1.062
15	0.0163	33.825	0.326	11.94	7.15	1.095
16	0.0178	33.708	0.345	13.04	7.58	1.306
17	0.0193	33.571	0.368	14.14	8.08	1.324
18	0.0203	33.500	0.379	14.87	8.34	1.314
19	0.0218	33.429	0.391	15.97	8.59	1.349
20	0.0248	33.249	0.421	18.17	9.25	1.335
21	0.0263	33.148	0.438	19.27	9.62	1.329
22	0.0278	33.072	0.450	20.37	9.89	1.347
23	0.0303	32.967	0.468	22.20	10.28	1.382
24	0.0328	32.900	0.479	24.03	10.52	1.353
25	0.0368	32.734	0.506	26.96	11.13	1.430
26	0.0393	32.675	0.516	28.79	11.34	1.500
27	0.0438	32.522	0.541	32.09	11.90	1.597
28	0.0468	32.418	0.559	34.29	12.28	1.656
29	0.0498	32.366	0.567	36.48	12.47	1.644
30	0.0558	32.207	0.594	40.88	13.04	1.639
31	0.0598	32.162	0.601	43.81	13.21	1.574
32	0.0678	32.029	0.623	49.67	13.69	1.620
33	0.0743	31.956	0.635	54.43	13.96	1.693
34	0.0838	31.830	0.656	61.39	14.42	1.739
35	0.0918	31.700	0.678	67.26	14.89	1.850
36	0.0978	31.658	0.685	71.65	15.04	1.881
37	0.1103	31.536	0.705	80.81	15.49	1.936
38	0.1208	31.473	0.715	88.50	15.72	1.901
39	0.1388	31.324	0.740	101.69	16.26	2.030
40	0.1513	31.271	0.749	110.85	16.45	2.180
41	0.1768	31.137	0.771	129.53	16.94	2.463
42	0.1968	30.947	0.802	144.18	17.63	2.650
43	0.2073	30.958	0.801	151.87	17.59	2.746
44	0.2288	30.836	0.821	167.63	18.03	2.965
45	0.2473	30.742	0.836	181.18	18.38	3.060
46	0.2673	30.684	0.846	195.83	18.59	3.001
47	0.3038	30.536	0.871	222.57	19.13	3.335
48	0.3293	30.478	0.880	241.25	19.34	3.358
49	0.3753	30.347	0.902	274.96	19.82	3.513
50	0.4113	30.285	0.912	301.33	20.04	3.615
51	0.4728	30.158	0.933	346.39	20.50	3.614
52	0.5223	30.107	0.942	382.65	20.69	3.590
53	0.6213	30.023	0.956	455.18	21.00	3.820
54	0.7423	29.956	0.967	543.83	21.24	4.570
55	0.9273	29.882	0.979	679.37	21.51	7.918
56	1.1773	29.854	0.983	862.52	21.61	0.000
57	1.4273	29.840	0.986	1045.68	21.66	0.000
58	1.6773	29.829	0.988	1228.84	21.70	0.000
59	1.9273	29.822	0.989	1411.99	21.73	0.000
60	2.1773	29.827	0.988	1595.15	21.71	0.000
61	2.4273	29.823	0.989	1778.31	21.72	0.000

Station = 6 dU/dx=29s-1

patm = 750.316
x = 47.9900 visc = 1.65282E-05
cf = 5.30000E-03 yeff = 1.80000E-03
Tw = 35.2000 Tinf = 29.6815
Tw measured = 36.1461 Tw correction = -0.946098
Q wall = 369.000 Stanton No. = 2.36478E-03
Q wall measured (w/Tw measured) = 372.842
Q wall measured (w/Tw corrected) = 378.214
delther = 1.30698 deleth = 0.110630
delcon = 3.97295E-04 qadded = 161.271
Uw = 24.6924 Rex = 716946.
Reh = 1657.23
coef1 = 24.6924 coef2 = 0.308559
A+ = 30.2311 K = 7.98284E-07
f1 = -4.05996E-06 f2 = -5.24364E-06

N	y	T	Tnd	y+	t+	Prt
1	0.0038	34.655	0.099	2.93	2.15	-1.034
2	0.0048	34.522	0.123	3.71	2.68	0.364
3	0.0058	34.392	0.146	4.48	3.19	0.870
4	0.0068	34.248	0.173	5.25	3.76	1.106
5	0.0078	34.140	0.192	6.02	4.18	1.162
6	0.0088	33.978	0.221	6.79	4.82	1.057
7	0.0098	33.877	0.240	7.57	5.22	1.059
8	0.0108	33.767	0.260	8.34	5.66	0.949
9	0.0118	33.656	0.280	9.11	6.09	0.921
10	0.0128	33.600	0.290	9.88	6.32	0.818
11	0.0138	33.482	0.311	10.65	6.78	0.839
12	0.0143	33.479	0.312	11.04	6.79	0.803
13	0.0158	33.354	0.334	12.20	7.28	0.818
14	0.0173	33.302	0.344	13.35	7.49	0.886
15	0.0203	33.091	0.382	15.67	8.33	0.962
16	0.0218	33.033	0.393	16.83	8.55	1.032
17	0.0243	32.912	0.415	18.76	9.03	1.089
18	0.0268	32.815	0.432	20.69	9.41	1.127
19	0.0293	32.728	0.448	22.62	9.76	1.099
20	0.0323	32.625	0.467	24.93	10.17	1.156
21	0.0358	32.510	0.487	27.64	10.62	1.183
22	0.0388	32.495	0.490	29.95	10.68	1.211
23	0.0453	32.313	0.523	34.97	11.40	1.267
24	0.0488	32.234	0.537	37.67	11.71	1.277
25	0.0538	32.163	0.550	41.53	11.99	1.322
26	0.0613	32.052	0.570	47.32	12.42	1.443
27	0.0688	31.987	0.582	53.11	12.68	1.439
28	0.0813	31.816	0.613	62.76	13.36	1.638
29	0.0888	31.728	0.629	68.55	13.71	1.742
30	0.0978	31.654	0.643	75.50	13.99	1.857
31	0.1113	31.501	0.670	85.92	14.60	2.008
32	0.1203	31.442	0.681	92.87	14.83	2.028
33	0.1373	31.330	0.701	105.99	15.28	2.166
34	0.1533	31.209	0.723	118.34	15.75	2.297
35	0.1673	31.129	0.738	129.15	16.07	2.305
36	0.1863	30.998	0.762	143.81	16.59	2.435
37	0.2013	30.931	0.774	155.39	16.85	2.497
38	0.2258	30.807	0.796	174.31	17.34	2.523
39	0.2468	30.776	0.802	190.52	17.46	2.590
40	0.2888	30.581	0.837	222.94	18.23	2.777
41	0.3113	30.535	0.845	240.31	18.41	2.839
42	0.3568	30.375	0.874	275.43	19.05	2.950
43	0.3863	30.294	0.889	298.20	19.37	3.064
44	0.4238	30.215	0.903	327.15	19.68	2.876
45	0.4743	30.195	0.907	366.13	19.76	2.732
46	0.5753	30.004	0.942	444.10	20.51	2.482
47	0.6293	29.986	0.945	485.79	20.58	2.296
48	0.7378	29.931	0.955	569.54	20.80	2.215
49	0.9453	29.866	0.967	729.72	21.05	2.303
50	1.1953	29.801	0.978	922.71	21.31	2.010
51	1.4453	29.787	0.981	1115.69	21.37	0.000
52	1.6953	29.769	0.984	1308.68	21.44	0.000
53	1.9453	29.767	0.984	1501.67	21.44	0.000
54	2.1953	29.759	0.986	1694.65	21.48	0.000

Station = 7 dU/dx=29s-1

patm = 750.062
x = 55.6100 visc = 1.65501E-05
cf = 5.10000E-03 yeff = 2.80000E-03
Tw = 35.0650 Tinf = 29.6547
Tw measured = 36.4660 Tw correction = -1.40100
Q wall = 343.000 Stanton No. = 2.09633E-03
Q wall measured (w/Tw measured) = 371.564
Q wall measured (w/Tw corrected) = 379.526
delther = 1.30435 deleth = 0.126928
delcon = 4.18965E-04 qadded = 191.817
Uw = 26.4140 Rex = 887538.
Reh = 2033.91
coef1 = 26.4140 coef2 = 0.345907
A+ = 29.5304 K = 6.98535E-07
f1 = 0. f2 = -5.78175E-06

N	y	T	Tnd	y+	t+	Prt
1	0.0038	34.582	0.089	3.08	2.15	-0.313
2	0.0048	34.482	0.108	3.89	2.60	-0.353
3	0.0058	34.304	0.141	4.70	3.39	-0.845
4	0.0068	34.168	0.166	5.51	4.00	5.721
5	0.0078	34.042	0.189	6.32	4.56	1.970
6	0.0088	33.913	0.213	7.13	5.13	1.662
7	0.0098	33.821	0.230	7.94	5.54	1.367
8	0.0108	33.726	0.247	8.75	5.96	1.305
9	0.0118	33.651	0.261	9.56	6.30	1.251
10	0.0128	33.527	0.284	10.37	6.85	1.168
11	0.0138	33.438	0.301	11.18	7.25	1.204
12	0.0148	33.368	0.314	11.99	7.56	1.195
13	0.0163	33.272	0.331	13.21	7.99	1.113
14	0.0178	33.219	0.341	14.42	8.22	1.024
15	0.0213	33.013	0.379	17.26	9.14	1.121
16	0.0228	32.968	0.388	18.47	9.34	1.178
17	0.0263	32.832	0.413	21.31	9.95	1.312
18	0.0288	32.743	0.429	23.33	10.34	1.394
19	0.0323	32.603	0.455	26.17	10.97	1.402
20	0.0348	32.523	0.470	28.19	11.32	1.442
21	0.0383	32.455	0.482	31.03	11.63	1.425
22	0.0438	32.339	0.504	35.48	12.15	1.371
23	0.0493	32.269	0.517	39.94	12.46	1.343
24	0.0578	32.134	0.542	46.83	13.06	1.429
25	0.0648	32.069	0.554	52.50	13.35	1.516
26	0.0768	31.932	0.579	62.22	13.96	1.652
27	0.0863	31.854	0.594	69.91	14.31	1.785
28	0.0993	31.722	0.618	80.45	14.89	1.938
29	0.1098	31.690	0.624	88.95	15.04	2.111
30	0.1313	31.494	0.660	106.37	15.91	2.429
31	0.1428	31.457	0.667	115.69	16.08	2.596
32	0.1658	31.278	0.700	134.32	16.87	2.930
33	0.1793	31.218	0.711	145.26	17.14	3.226
34	0.2038	31.089	0.735	165.11	17.72	3.579
35	0.2243	31.014	0.749	181.71	18.05	4.004
36	0.2543	30.859	0.777	206.02	18.74	4.305
37	0.2743	30.757	0.796	222.22	19.20	4.686
38	0.2948	30.654	0.815	238.83	19.65	5.027
39	0.3158	30.600	0.825	255.84	19.89	5.349
40	0.3583	30.514	0.841	290.27	20.27	5.658
41	0.4128	30.346	0.872	334.43	21.03	6.305
42	0.4468	30.261	0.888	361.97	21.40	6.825
43	0.4883	30.201	0.899	395.59	21.67	7.863
44	0.5633	30.121	0.914	456.35	22.03	10.512
45	0.6633	30.018	0.933	537.37	22.49	21.970
46	0.7653	29.933	0.949	620.00	22.87	0.000
47	0.8898	29.875	0.959	720.86	23.12	0.000
48	1.1143	29.806	0.972	902.74	23.43	0.000
49	1.3643	29.768	0.979	1105.27	23.60	0.000
50	1.6143	29.763	0.980	1307.81	23.62	0.000
51	1.8643	29.748	0.983	1510.34	23.69	0.000

Station = 8 dU/dx=29s-1

patm = 750.062
x = 63.9300 visc = 1.65543E-05
cf = 5.30000E-03 yeff = 1.80000E-03
Tw = 35.0300 Tinf = 29.6283
Tw measured = 36.5072 Tw correction = -1.47720
Q wall = 395.000 Stanton No. = 2.23862E-03
Q wall measured (w/Tw measured) = 371.701
Q wall measured (w/Tw corrected) = 380.096
delther = 1.41584 deleth = 0.138320
delcon = 3.63242E-04 qadded = 221.980
Uw = 28.5306 Rex = 1.10180E+06
Reh = 2393.98
coef1 = 28.5306 coef2 = 0.524010
A+ = 28.5844 K = 5.98887E-07
f1 = -6.71681E-07 f2 = -4.09643E-06

N	y	T	Tnd	y+	t+	Prt
1	0.0038	34.468	0.104	3.39	2.39	-0.131
2	0.0048	34.315	0.132	4.28	3.05	-0.583
3	0.0058	34.134	0.166	5.17	3.82	******
4	0.0068	34.020	0.187	6.07	4.30	1.141
5	0.0078	33.884	0.212	6.96	4.88	0.996
6	0.0088	33.777	0.232	7.85	5.34	0.991
7	0.0098	33.683	0.249	8.74	5.74	0.986
8	0.0108	33.570	0.270	9.64	6.22	0.969
9	0.0118	33.471	0.289	10.53	6.64	0.951
10	0.0128	33.378	0.306	11.42	7.04	0.963
11	0.0138	33.298	0.321	12.31	7.38	0.940
12	0.0148	33.272	0.325	13.20	7.49	0.848
13	0.0173	33.127	0.352	15.44	8.11	0.889
14	0.0193	33.017	0.373	17.22	8.58	0.935
15	0.0213	32.950	0.385	19.00	8.86	1.007
16	0.0243	32.793	0.414	21.68	9.53	1.133
17	0.0263	32.756	0.421	23.47	9.69	1.154
18	0.0308	32.613	0.447	27.48	10.30	1.219
19	0.0343	32.491	0.470	30.60	10.82	1.253
20	0.0373	32.440	0.480	33.28	11.04	1.227
21	0.0433	32.309	0.504	38.63	11.59	1.274
22	0.0483	32.271	0.511	43.09	11.75	1.249
23	0.0588	32.106	0.541	52.46	12.46	1.334
24	0.0658	32.044	0.553	58.71	12.72	1.423
25	0.0783	31.903	0.579	69.86	13.32	1.560
26	0.0878	31.825	0.593	78.34	13.65	1.695
27	0.1013	31.705	0.615	90.38	14.16	1.794
28	0.1133	31.630	0.629	101.09	14.48	1.915
29	0.1313	31.499	0.654	117.15	15.04	2.024
30	0.1463	31.410	0.670	130.53	15.42	2.149
31	0.1648	31.304	0.690	147.04	15.88	2.297
32	0.1833	31.244	0.701	163.54	16.13	2.482
33	0.2193	31.088	0.730	195.66	16.80	2.816
34	0.2443	30.946	0.756	217.97	17.40	3.132
35	0.2633	30.865	0.771	234.92	17.74	3.353
36	0.2883	30.796	0.784	257.22	18.04	3.703
37	0.3288	30.669	0.807	293.36	18.58	4.034
38	0.3633	30.522	0.835	324.14	19.21	4.233
39	0.3878	30.474	0.843	346.00	19.41	4.450
40	0.4373	30.347	0.867	390.16	19.95	4.864
41	0.4783	30.283	0.879	426.74	20.22	4.994
42	0.5483	30.137	0.906	489.20	20.85	5.199
43	0.5978	30.092	0.914	533.36	21.04	5.319
44	0.6973	29.995	0.932	622.14	21.45	5.969
45	0.8063	29.921	0.946	719.39	21.77	7.371
46	0.9578	29.870	0.955	854.56	21.99	0.000
47	1.2078	29.793	0.970	1077.61	22.31	0.000
48	1.4578	29.760	0.976	1300.66	22.45	0.000
49	1.7078	29.739	0.980	1523.71	22.54	0.000

Station = 9 dU/dx=29s-1

patm = 749.427
x = 71.5500 visc = 1.65493E-05
cf = 5.00000E-03 yeff = 2.80000E-03
Tw = 35.3500 Tinf = 29.7186
Tw measured = 35.9318 Tw correction = -0.581802
Q wall = 403.000 Stanton No. = 2.00937E-03
Q wall measured (w/Tw measured) = 375.122
Q wall measured (w/Tw corrected) = 378.424
delther = 1.45431 deleth = 0.154304
delcon = 3.71425E-04 qadded = 278.051
Uw = 31.1576 Rex = 1.34708E+06
Reh = 2909.94
coef1 = 31.1576 coef2 = 0.571484
A+ = 28.1911 K = 5.02005E-07
f1 = -1.28942E-06 f2 = 7.25550E-07

N	y	T	Tnd	y+	t+	Prt
1	0.0038	34.740	0.108	3.59	2.70	0.141
2	0.0048	34.616	0.130	4.53	3.24	0.712
3	0.0058	34.459	0.158	5.48	3.94	1.950
4	0.0068	34.316	0.184	6.42	4.57	1.616
5	0.0078	34.160	0.211	7.37	5.26	1.386
6	0.0088	34.018	0.237	8.31	5.89	1.324
7	0.0098	33.934	0.251	9.26	6.26	1.327
8	0.0108	33.839	0.268	10.20	6.68	1.265
9	0.0118	33.731	0.288	11.14	7.16	1.145
10	0.0128	33.662	0.300	12.09	7.47	1.113
11	0.0138	33.531	0.323	13.03	8.04	1.144
12	0.0148	33.479	0.332	13.98	8.27	1.095
13	0.0168	33.392	0.348	15.87	8.66	1.062
14	0.0193	33.260	0.371	18.23	9.24	1.118
15	0.0213	33.153	0.390	20.12	9.72	1.136
16	0.0233	33.068	0.405	22.01	10.09	1.222
17	0.0263	32.936	0.429	24.84	10.68	1.305
18	0.0288	32.876	0.439	27.20	10.94	1.303
19	0.0338	32.719	0.467	31.92	11.64	1.279
20	0.0373	32.649	0.480	35.23	11.95	1.231
21	0.0433	32.529	0.501	40.90	12.48	1.201
22	0.0488	32.467	0.512	46.09	12.75	1.203
23	0.0593	32.358	0.531	56.01	13.23	1.252
24	0.0708	32.231	0.554	66.87	13.80	1.367
25	0.0808	32.117	0.574	76.31	14.30	1.457
26	0.0903	32.018	0.592	85.29	14.73	1.560
27	0.1008	31.968	0.601	95.20	14.96	1.636
28	0.1218	31.796	0.631	115.04	15.72	1.704
29	0.1353	31.695	0.649	127.79	16.16	1.721
30	0.1503	31.637	0.659	141.95	16.42	1.771
31	0.1803	31.486	0.686	170.29	17.09	1.941
32	0.2023	31.389	0.703	191.07	17.52	2.014
33	0.2273	31.261	0.726	214.68	18.09	2.061
34	0.2488	31.183	0.740	234.98	18.43	2.200
35	0.2798	31.040	0.765	264.26	19.06	2.260
36	0.3033	30.948	0.782	286.46	19.47	2.289
37	0.3308	30.944	0.782	312.43	19.48	2.264
38	0.3863	30.713	0.823	364.85	20.51	2.277
39	0.4113	30.702	0.825	388.46	20.56	2.237
40	0.4618	30.557	0.851	436.16	21.20	2.279
41	0.4988	30.522	0.857	471.10	21.35	2.351
42	0.5728	30.388	0.881	540.99	21.95	2.125
43	0.6313	30.292	0.898	596.24	22.37	2.090
44	0.6953	30.235	0.908	656.69	22.62	0.000
45	0.8178	30.131	0.927	772.39	23.08	0.000
46	0.9428	30.067	0.938	890.45	23.37	0.000
47	1.1553	29.983	0.953	1091.15	23.74	0.000

Station = 10 dU/dx=29s-1

patm = 749.808
x = 78.9100 visc = 1.65238E-05
cf = 5.10000E-03 yeff = 1.80000E-03
Tw = 34.8700 Tinf = 29.3829
Tw measured = 35.7972 Tw correction = -0.927200
Q wall = 427.000 Stanton No. = 2.00610E-03
Q wall measured (w/Tw measured) = 375.588
Q wall measured (w/Tw corrected) = 380.835
delther = 1.91704 deleth = 0.157893
delcon = 3.41233E-04 qadded = 294.416
Uw = 33.8809 Rex = 1.61799E+06
Reh = 3246.08
coef1 = 33.8809 coef2 = 0.736084
A+ = 27.7005 K = 4.23894E-07
f1 = 1.18062E-06 f2 = 1.13077E-05

N	y	T	Tnd	y+	t+	Prt
1	0.0038	34.267	0.110	3.95	2.77	-0.683
2	0.0048	34.106	0.139	4.99	3.51	-1.826
3	0.0058	33.930	0.171	6.03	4.32	7.320
4	0.0068	33.788	0.197	7.07	4.97	2.305
5	0.0078	33.621	0.228	8.11	5.74	1.651
6	0.0088	33.507	0.248	9.15	6.26	1.426
7	0.0098	33.376	0.272	10.19	6.86	1.237
8	0.0108	33.297	0.287	11.23	7.23	1.153
9	0.0118	33.201	0.304	12.27	7.67	1.085
10	0.0128	33.124	0.318	13.31	8.02	1.061
11	0.0138	33.069	0.328	14.35	8.27	1.025
12	0.0158	32.945	0.351	16.44	8.84	1.089
13	0.0173	32.823	0.373	18.00	9.40	1.114
14	0.0188	32.770	0.383	19.56	9.64	1.145
15	0.0218	32.645	0.406	22.68	10.22	1.191
16	0.0248	32.492	0.433	25.80	10.92	1.168
17	0.0268	32.462	0.439	27.88	11.06	1.102
18	0.0313	32.334	0.462	32.56	11.65	1.134
19	0.0353	32.237	0.480	36.72	12.09	1.108
20	0.0403	32.192	0.488	41.92	12.30	1.107
21	0.0503	32.011	0.521	52.32	13.13	1.194
22	0.0563	31.901	0.541	58.56	13.64	1.190
23	0.0623	31.833	0.554	64.80	13.95	1.198
24	0.0728	31.755	0.568	75.73	14.30	1.216
25	0.0888	31.624	0.592	92.37	14.91	1.165
26	0.1028	31.503	0.614	106.93	15.46	1.147
27	0.1158	31.431	0.627	120.45	15.80	1.167
28	0.1373	31.291	0.652	142.82	16.44	1.201
29	0.1548	31.245	0.661	161.02	16.65	1.202
30	0.1898	31.059	0.695	197.43	17.50	1.241
31	0.2108	30.980	0.709	219.27	17.86	1.260
32	0.2418	30.821	0.738	251.52	18.60	1.248
33	0.2628	30.744	0.752	273.36	18.95	1.266
34	0.2933	30.679	0.764	305.09	19.25	1.200
35	0.3488	30.517	0.793	362.82	19.99	1.155
36	0.3863	30.463	0.803	401.83	20.24	1.100
37	0.4618	30.273	0.838	480.36	21.11	1.103
38	0.5048	30.205	0.850	525.09	21.42	1.098
39	0.5738	30.091	0.871	596.87	21.95	1.045
40	0.6403	29.978	0.892	666.04	22.47	0.991
41	0.7018	29.924	0.901	730.01	22.72	0.000
42	0.8248	29.808	0.923	857.95	23.25	0.000
43	0.9388	29.741	0.935	976.54	23.56	0.000
44	1.1228	29.701	0.942	1167.93	23.74	0.000

Station 1 dU/dx=29s-1
x = 10.03000 cm, Patm = 742.315 mm Hg, T = 29.5304 deg C

y	U	V	u'	v'	u'v'	u'v'2	dU/dy	em	l	gamma
0.060	9.531	-0.354	1.149	1.027	-0.269	-0.527	-5287.7	-0.508E-04	0.00010	0.379
0.063	9.475	-0.716	1.140	1.023	-0.343	-0.550	3156.3	0.109E-03	0.00019	0.388
0.069	9.806	-0.767	1.152	0.981	-0.376	-0.507	2473.3	0.152E-03	0.00025	0.389
0.075	9.840	-0.578	1.131	0.910	-0.303	-0.445	2579.4	0.117E-03	0.00021	0.397
0.081	9.994	-0.527	1.129	0.917	-0.331	-0.495	2038.7	0.162E-03	0.00028	0.410
0.090	10.208	-0.540	1.106	0.835	-0.269	-0.372	2489.9	0.108E-03	0.00021	0.421
0.098	10.409	-0.540	1.082	0.769	-0.264	-0.329	2246.0	0.117E-03	0.00023	0.418
0.111	10.707	-0.578	1.045	0.703	-0.230	-0.243	1788.3	0.128E-03	0.00027	0.429
0.128	10.898	-0.549	1.028	0.641	-0.222	-0.166	1332.8	0.167E-03	0.00035	0.432
0.147	11.134	-0.573	0.998	0.595	-0.208	-0.133	980.7	0.212E-03	0.00047	0.420
0.172	11.338	-0.597	0.982	0.548	-0.197	-0.100	773.2	0.255E-03	0.00057	0.449
0.200	11.487	-0.598	0.976	0.526	-0.190	-0.089	589.5	0.323E-03	0.00074	0.433
0.234	11.676	-0.623	0.964	0.513	-0.179	-0.089	483.5	0.371E-03	0.00088	0.411
0.281	11.886	-0.654	0.925	0.487	-0.161	-0.071	379.5	0.424E-03	0.00106	0.400
0.345	12.042	-0.664	0.930	0.483	-0.151	-0.069	264.0	0.572E-03	0.00147	0.381
0.417	12.218	-0.710	0.891	0.482	-0.137	-0.068	183.9	0.744E-03	0.00201	0.346
0.507	12.320	-0.740	0.865	0.499	-0.112	-0.069	127.4	0.882E-03	0.00263	0.334
0.683	12.471	-0.776	0.810	0.531	-0.080	-0.040	76.6	0.105E-02	0.00370	0.288
0.941	12.624	-0.843	0.745	0.564	-0.050	-0.029	42.7	0.118E-02	0.00525	0.259
1.365	12.668	-0.939	0.747	0.637	-0.033	-0.030	19.3	0.171E-02	0.00941	0.253
1.865	12.737	-1.063	0.704	0.666	-0.018	-0.011	8.6	0.204E-02	0.01539	0.258
2.365	12.771	-1.187	0.703	0.710	-0.028	-0.026	5.3	0.532E-02	0.03177	0.268
2.866	12.776	-1.300	0.699	0.730	0.004	0.000	3.1	-0.132E-02	0.00000	0.274
3.366	12.781	-1.422	0.693	0.739	0.007	-0.019	0.4	-0.153E-01	0.00000	0.280
3.866	12.811	-1.562	0.691	0.742	0.022	-0.017	-2.6	0.842E-02	0.00000	0.283
4.366	12.765	-1.680	0.687	0.709	0.007	-0.024	-48.2	0.136E-03	0.00000	0.295

Station 2 dU/dx=29s-1
x = 18.7500 cm, Patm = 741.680 mm Hg, T = 29.2576 deg C

y	U	V	u'	v'	u'v'	u'v'2	dU/dy	em	l	gamma
0.060	11.458	1.458	1.158	1.089	0.028	-0.589	2451.7	-0.115E-04	0.00000	0.491
0.061	11.484	1.425	1.138	1.068	0.029	-0.576	-1.4	0.206E-01	0.00000	0.466
0.069	11.622	0.410	1.150	1.069	-0.121	-0.648	4217.9	0.288E-04	0.00008	0.463
0.083	12.471	-0.397	1.198	1.018	-0.298	-0.634	3514.1	0.847E-04	0.00016	0.458
0.101	12.791	-0.180	1.149	0.884	-0.240	-0.529	2626.8	0.912E-04	0.00019	0.479
0.123	13.165	-0.142	1.070	0.757	-0.248	-0.349	1456.7	0.170E-03	0.00034	0.458
0.155	13.567	-0.154	0.996	0.653	-0.214	-0.232	1082.2	0.198E-03	0.00043	0.482
0.206	13.937	-0.193	0.957	0.566	-0.187	-0.139	716.6	0.261E-03	0.00060	0.438
0.275	14.305	-0.232	0.889	0.520	-0.173	-0.108	467.1	0.371E-03	0.00089	0.389
0.363	14.585	-0.281	0.835	0.476	-0.125	-0.070	297.1	0.421E-03	0.00119	0.346
0.523	14.872	-0.334	0.770	0.492	-0.086	-0.048	148.0	0.583E-03	0.00199	0.283
0.790	15.053	-0.429	0.699	0.552	-0.051	-0.028	67.2	0.755E-03	0.00335	0.245
1.290	15.179	-0.601	0.664	0.629	-0.043	-0.031	27.4	0.156E-02	0.00753	0.226
1.790	15.282	-0.775	0.638	0.678	-0.022	-0.029	15.8	0.141E-02	0.00944	0.224
2.290	15.324	-0.905	0.644	0.723	-0.005	-0.031	13.0	0.406E-03	0.00560	0.228
2.790	15.375	-1.086	0.621	0.718	-0.010	-0.012	11.2	0.866E-03	0.00878	0.237
3.290	15.457	-1.213	0.630	0.725	-0.001	-0.021	11.6	0.106E-03	0.00303	0.233
3.790	15.497	-1.385	0.625	0.727	0.017	-0.027	10.1	-0.170E-02	0.00000	0.247
4.290	15.552	-1.513	0.628	0.718	0.028	-0.015	-35.3	0.799E-03	0.00000	0.250

Station 3 dU/dx=29s-1
x = 26.1700 cm, Patm = 741.680 mm Hg, T = 29.1269 deg C

y	U	V	u'	v'	u'v'	u'v'2	dU/dy	em	l	gamma
0.060	12.140	2.127	1.201	1.192	0.036	-0.665	-962.2	0.376E-04	0.00000	0.633
0.062	12.129	2.089	1.182	1.220	0.098	-0.679	4455.9	-0.221E-04	0.00000	0.640
0.071	12.712	1.573	1.218	1.187	0.009	-0.733	7474.2	-0.121E-05	0.00000	0.613
0.087	14.096	0.257	1.295	1.237	-0.272	-1.004	5262.6	0.518E-04	0.00010	0.585
0.105	14.391	-0.631	1.270	1.085	-0.392	-0.913	3540.4	0.111E-03	0.00018	0.592
0.132	15.035	-0.603	1.169	0.897	-0.371	-0.553	1768.9	0.210E-03	0.00034	0.577
0.168	15.549	-0.597	1.094	0.754	-0.348	-0.352	1385.0	0.252E-03	0.00043	0.556
0.218	16.029	-0.650	0.991	0.643	-0.274	-0.224	889.8	0.308E-03	0.00059	0.499
0.290	16.486	-0.704	0.895	0.555	-0.229	-0.136	556.4	0.411E-03	0.00086	0.439
0.387	16.817	-0.757	0.791	0.512	-0.171	-0.102	323.8	0.530E-03	0.00128	0.360
0.554	17.124	-0.835	0.702	0.500	-0.101	-0.057	155.4	0.647E-03	0.00204	0.276
0.846	17.329	-0.958	0.637	0.557	-0.061	-0.041	68.9	0.880E-03	0.00357	0.219
1.346	17.459	-1.163	0.596	0.646	-0.039	-0.034	27.2	0.145E-02	0.00729	0.230
1.846	17.534	-1.351	0.575	0.680	-0.033	-0.025	17.3	0.191E-02	0.01051	0.222
2.346	17.592	-1.523	0.577	0.708	-0.012	-0.028	14.0	0.850E-03	0.00778	0.232
2.846	17.694	-1.690	0.569	0.733	-0.001	-0.015	13.9	0.615E-04	0.00210	0.243
3.346	17.729	-1.854	0.572	0.716	0.004	-0.020	13.2	-0.320E-03	0.00000	0.250
3.846	17.814	-1.941	0.577	0.688	0.020	-0.006	-49.8	0.396E-03	0.00000	0.241

Station 4 dU/dx=29s-1
x = 34.7900 cm, Patm = 742.442 mm Hg, T = 29.1076 deg C

y	U	V	u'	v'	u'v'	u'v'2	dU/dy	em	l	gamma
0.060	13.989	3.009	1.270	1.279	0.156	-0.698	3621.7	-0.430E-04	0.00000	0.773
0.070	14.458	2.617	1.276	1.292	0.080	-0.780	7122.2	-0.113E-04	0.00000	0.757
0.090	15.993	1.277	1.346	1.277	-0.224	-1.048	5510.0	0.407E-04	0.00009	0.733
0.112	16.883	-0.369	1.341	1.138	-0.487	-0.895	4057.4	0.120E-03	0.00017	0.695
0.140	17.577	-0.389	1.285	0.958	-0.436	-0.648	2339.1	0.186E-03	0.00028	0.671
0.181	18.209	-0.387	1.163	0.796	-0.368	-0.442	1458.7	0.253E-03	0.00042	0.607
0.235	18.772	-0.433	1.046	0.674	-0.319	-0.265	936.2	0.341E-03	0.00060	0.538
0.303	19.204	-0.474	0.954	0.594	-0.255	-0.188	583.8	0.436E-03	0.00086	0.461
0.419	19.607	-0.547	0.792	0.536	-0.189	-0.116	314.7	0.601E-03	0.00138	0.349
0.618	19.967	-0.645	0.647	0.523	-0.095	-0.053	144.9	0.657E-03	0.00213	0.243
1.016	20.160	-0.842	0.577	0.603	-0.051	-0.051	54.6	0.932E-03	0.00413	0.216
1.516	20.258	-1.023	0.535	0.686	-0.022	-0.042	23.2	0.931E-03	0.00633	0.217
2.016	20.331	-1.199	0.523	0.709	-0.028	-0.028	18.2	0.153E-02	0.00917	0.208
2.516	20.425	-1.356	0.528	0.719	-0.012	-0.021	20.1	0.605E-03	0.00548	0.201
3.016	20.533	-1.485	0.535	0.702	0.010	-0.029	-109.3	0.889E-04	0.00000	0.227

Station 5 dU/dx=29s-1
x = 42.5100 cm, Patm = 742.569 mm Hg, T = 29.0877 deg C

y	U	V	u'	v'	u'v'	u'v'2	dU/dy	em	l	gamma
0.060	14.669	3.558	1.280	1.244	0.442	-0.563	3935.6	-0.112E-03	0.00000	0.859
0.064	14.828	3.554	1.290	1.263	0.419	-0.634	3660.0	-0.115E-03	0.00000	0.853
0.078	15.421	3.326	1.342	1.340	0.157	-0.657	4957.3	-0.317E-04	0.00000	0.840
0.094	16.394	2.498	1.379	1.350	-0.124	-0.820	5519.8	0.224E-04	0.00006	0.811
0.120	17.981	-0.466	1.475	1.377	-0.660	-1.364	5101.9	0.129E-03	0.00016	0.786
0.152	19.379	-0.589	1.391	1.140	-0.582	-0.874	3688.8	0.158E-03	0.00021	0.746
0.188	20.140	-0.616	1.297	0.952	-0.478	-0.587	2322.3	0.206E-03	0.00030	0.697
0.239	20.949	-0.653	1.187	0.773	-0.396	-0.382	1344.3	0.295E-03	0.00047	0.622
0.308	21.560	-0.671	1.059	0.671	-0.329	-0.321	850.4	0.387E-03	0.00067	0.528
0.414	22.119	-0.697	0.903	0.565	-0.238	-0.184	457.4	0.519E-03	0.00107	0.405
0.581	22.519	-0.764	0.715	0.545	-0.147	-0.113	205.1	0.719E-03	0.00187	0.305
0.913	22.737	-0.893	0.574	0.587	-0.059	-0.049	69.9	0.848E-03	0.00348	0.215
1.413	22.826	-1.039	0.529	0.660	-0.043	-0.045	23.8	0.179E-02	0.00868	0.193
1.913	22.891	-1.171	0.503	0.701	-0.032	-0.036	16.3	0.198E-02	0.01101	0.196
2.413	22.964	-1.235	0.498	0.708	-0.011	-0.020	18.3	0.595E-03	0.00570	0.196
2.913	23.076	-1.311	0.507	0.676	-0.009	-0.020	22.4	0.421E-03	0.00433	0.199
3.413	23.192	-1.396	0.518	0.599	0.008	-0.010	-89.4	0.847E-04	0.00000	0.201

Station 6 dU/dx=29s-1
x = 50.6300 cm, Patm = 742.950 mm Hg, T = 29.0097 deg C

y	U	V	u'	v'	u'v'	u'v'2	dU/dy	em	l	gamma
0.060	14.897	3.370	1.262	1.186	0.390	-0.382	-18.8	0.207E-01	0.00000	0.892
0.062	14.907	3.396	1.281	1.218	0.448	-0.456	1959.5	-0.228E-03	0.00000	0.903
0.076	15.342	3.668	1.295	1.314	0.292	-0.309	3900.7	-0.748E-04	0.00000	0.893
0.095	16.327	3.133	1.401	1.414	-0.065	-0.500	5744.4	0.112E-04	0.00004	0.872
0.121	18.437	1.385	1.494	1.471	-0.512	-0.893	5719.9	0.895E-04	0.00013	0.840
0.150	19.737	-0.640	1.534	1.340	-0.830	-0.772	4505.6	0.184E-03	0.00020	0.827
0.185	20.789	-0.687	1.496	1.159	-0.772	-0.724	2862.9	0.270E-03	0.00031	0.780
0.226	21.679	-0.781	1.440	0.996	-0.643	-0.587	2065.3	0.311E-03	0.00039	0.742
0.281	22.597	-0.802	1.324	0.845	-0.481	-0.471	1443.0	0.333E-03	0.00048	0.668
0.350	23.305	-0.792	1.237	0.722	-0.431	-0.373	945.1	0.456E-03	0.00069	0.571
0.460	23.950	-0.854	1.013	0.606	-0.297	-0.280	513.3	0.579E-03	0.00106	0.445
0.643	24.429	-0.903	0.743	0.553	-0.173	-0.136	240.8	0.720E-03	0.00173	0.301
0.893	24.678	-0.957	0.580	0.596	-0.092	-0.100	95.4	0.968E-03	0.00318	0.208
1.143	24.772	-1.022	0.519	0.614	-0.059	-0.052	41.4	0.142E-02	0.00586	0.200
1.393	24.822	-1.086	0.501	0.669	-0.055	-0.051	24.4	0.225E-02	0.00961	0.186
1.643	24.875	-1.132	0.487	0.674	-0.039	-0.039	22.1	0.177E-02	0.00894	0.190
1.893	24.932	-1.151	0.479	0.684	-0.020	-0.025	22.9	0.857E-03	0.00612	0.185
2.143	24.994	-1.189	0.477	0.695	-0.019	-0.031	25.3	0.741E-03	0.00541	0.185
2.394	25.049	-1.192	0.469	0.690	-0.006	-0.021	28.7	0.200E-03	0.00264	0.187
2.644	25.133	-1.224	0.475	0.666	-0.007	-0.020	34.2	0.217E-03	0.00252	0.188
2.894	25.221	-1.217	0.486	0.625	0.000	-0.023	-43.6	0.307E-05	0.00000	0.178

Station 7 dU/dx=29s-1
x = 58.2500 cm, Patm = 742.950 mm Hg, T = 29.0021 deg C

y	U	V	u'	v'	u'v'	u'v'2	dU/dy	em	l	gamma
0.060	16.012	3.836	1.364	1.365	0.270	-0.440	1339.9	-0.201E-03	0.00000	0.888
0.063	16.069	3.797	1.416	1.360	0.269	-0.314	3781.3	-0.712E-04	0.00000	0.895
0.079	17.020	3.219	1.468	1.459	-0.014	-0.541	7064.1	0.191E-05	0.00002	0.886
0.100	18.907	1.677	1.579	1.519	-0.587	-1.008	6789.3	0.864E-04	0.00011	0.862
0.124	20.461	-0.863	1.676	1.449	-1.010	-0.947	5468.6	0.185E-03	0.00018	0.840
0.159	21.543	-0.916	1.628	1.267	-0.888	-0.750	3356.1	0.265E-03	0.00028	0.812
0.201	22.595	-1.021	1.618	1.118	-0.839	-0.599	2259.2	0.371E-03	0.00041	0.792
0.249	23.437	-1.046	1.584	1.013	-0.765	-0.612	1732.2	0.442E-03	0.00051	0.740
0.315	24.416	-1.139	1.429	0.884	-0.648	-0.624	1233.1	0.526E-03	0.00065	0.671
0.396	25.128	-1.180	1.305	0.762	-0.515	-0.547	850.2	0.605E-03	0.00084	0.574
0.507	25.761	-1.199	1.059	0.648	-0.364	-0.362	484.8	0.751E-03	0.00124	0.440
0.707	26.266	-1.266	0.767	0.600	-0.212	-0.198	226.9	0.933E-03	0.00203	0.291
0.957	26.508	-1.336	0.593	0.607	-0.108	-0.097	95.1	0.114E-02	0.00345	0.224
1.207	26.596	-1.392	0.513	0.650	-0.072	-0.074	45.2	0.159E-02	0.00593	0.205
1.457	26.680	-1.447	0.472	0.665	-0.054	-0.045	30.1	0.180E-02	0.00773	0.183
1.707	26.745	-1.495	0.472	0.663	-0.043	-0.036	28.5	0.149E-02	0.00725	0.189
1.957	26.810	-1.512	0.460	0.664	-0.018	-0.031	30.0	0.610E-03	0.00451	0.188
2.208	26.887	-1.534	0.459	0.671	-0.018	-0.015	33.8	0.523E-03	0.00394	0.178
2.458	26.985	-1.556	0.464	0.632	-0.011	-0.015	35.1	0.322E-03	0.00303	0.172
2.708	27.080	-1.555	0.454	0.599	-0.006	-0.017	33.1	0.182E-03	0.00234	0.174
2.958	27.153	-1.594	0.484	0.537	-0.008	-0.017	-53.3	-0.154E-03	0.00170	0.182

Station 8 dU/dx=29s-1
x = 66.3100 cm, Patm = 743.712 mm Hg, T = 28.9904 deg C

y	U	V	u'	v'	u'v'	u'v'2	dU/dy	em	l	gamma
0.060	17.276	4.224	1.390	1.268	0.575	-0.490	624.3	-0.921E-03	0.00000	0.899
0.075	17.691	4.292	1.443	1.378	0.275	-0.359	5400.4	-0.509E-04	0.00000	0.894
0.095	19.446	3.023	1.541	1.484	-0.258	-0.692	7876.5	0.327E-04	0.00006	0.873
0.123	22.672	-1.197	1.786	1.545	-1.190	-1.265	6965.0	0.171E-03	0.00016	0.849
0.157	23.629	-0.963	1.749	1.299	-1.053	-0.761	4408.8	0.239E-03	0.00023	0.819
0.197	24.601	-1.041	1.714	1.192	-0.984	-0.668	2188.2	0.450E-03	0.00045	0.785
0.250	25.548	-1.130	1.681	1.073	-0.896	-0.758	1675.5	0.535E-03	0.00056	0.752
0.315	26.438	-1.213	1.602	0.960	-0.779	-0.722	1208.3	0.645E-03	0.00073	0.686
0.398	27.156	-1.242	1.475	0.840	-0.670	-0.607	854.6	0.784E-03	0.00096	0.604
0.512	27.930	-1.345	1.197	0.697	-0.452	-0.457	537.6	0.841E-03	0.00125	0.482
0.715	28.527	-1.411	0.842	0.626	-0.261	-0.271	266.8	0.980E-03	0.00192	0.329
0.965	28.803	-1.508	0.622	0.617	-0.138	-0.153	112.9	0.122E-02	0.00329	0.226
1.215	28.924	-1.576	0.529	0.646	-0.082	-0.097	52.3	0.156E-02	0.00546	0.189
1.465	29.026	-1.584	0.483	0.670	-0.065	-0.072	33.2	0.196E-02	0.00768	0.183
1.715	29.070	-1.653	0.444	0.664	-0.036	-0.043	25.7	0.142E-02	0.00743	0.174
1.965	29.145	-1.639	0.438	0.646	-0.022	-0.023	-181.4	-0.122E-03	0.00082	0.173

Station 9 dU/dx=29s-1
x = 74.0300 cm, Patm = 743.712 mm Hg, T = 29.0326 deg C

y	U	V	u'	v'	u'v'	u'v'2	dU/dy	em	l	gamma
0.060	18.769	4.287	1.547	1.491	0.140	-0.382	4535.6	-0.309E-04	0.00000	0.908
0.072	19.530	3.702	1.619	1.589	-0.110	-0.633	10241.3	0.107E-04	0.00003	0.899
0.091	21.924	1.881	1.784	1.654	-0.755	-1.188	9107.4	0.829E-04	0.00010	0.873
0.119	24.145	-1.250	1.885	1.574	-1.302	-1.160	6644.3	0.196E-03	0.00017	0.844
0.149	25.202	-1.281	1.886	1.420	-1.274	-1.079	4190.4	0.304E-03	0.00027	0.837
0.185	26.293	-1.398	1.856	1.273	-1.174	-0.885	2631.0	0.446E-03	0.00041	0.798
0.242	27.418	-1.519	1.852	1.157	-1.122	-0.972	1875.3	0.598E-03	0.00056	0.761
0.299	28.276	-1.588	1.736	1.037	-0.963	-0.875	1373.5	0.701E-03	0.00071	0.719
0.382	29.132	-1.673	1.551	0.912	-0.797	-0.851	944.0	0.844E-03	0.00095	0.639
0.493	29.903	-1.770	1.340	0.783	-0.604	-0.637	609.7	0.990E-03	0.00127	0.522
0.663	30.546	-1.817	1.013	0.697	-0.401	-0.450	340.0	0.118E-02	0.00186	0.378
0.913	30.977	-1.891	0.733	0.664	-0.242	-0.278	175.5	0.138E-02	0.00281	0.255
1.163	31.211	-1.950	0.569	0.654	-0.142	-0.159	110.6	0.129E-02	0.00341	0.203
1.413	31.530	-2.022	0.493	0.649	-0.079	-0.094	80.9	0.971E-03	0.00346	0.177
1.663	31.652	-2.060	0.443	0.639	-0.042	-0.052	51.5	0.825E-03	0.00400	0.160
1.913	31.768	-2.089	0.432	0.623	-0.027	-0.029	-196.4	-0.135E-03	0.00083	0.156

Station 10 dU/dx=29s-1
x = 82.0500 cm, Patm = 744.728 mm Hg, T = 28.9933 deg C

y	U	V	u'	v'	u'v'	u'v'2	dU/dy	em	l	gamma
0.060	20.746	4.570	1.656	1.542	0.227	-0.412	5139.7	-0.442E-04	0.00000	0.906
0.075	21.883	3.914	1.742	1.646	-0.149	-0.656	11932.1	0.125E-04	0.00003	0.894
0.097	25.111	1.353	1.927	1.743	-0.866	-1.544	9679.3	0.895E-04	0.00010	0.870
0.122	26.933	-1.538	2.020	1.636	-1.438	-1.328	7261.4	0.198E-03	0.00017	0.851
0.157	28.331	-1.603	1.986	1.429	-1.295	-1.255	3967.5	0.326E-03	0.00029	0.819
0.196	29.415	-1.697	2.000	1.303	-1.295	-1.099	2671.7	0.485E-03	0.00043	0.788
0.249	30.523	-1.765	1.940	1.167	-1.174	-0.989	1878.3	0.625E-03	0.00058	0.752
0.319	31.495	-1.892	1.762	1.034	-0.986	-0.915	1304.2	0.756E-03	0.00076	0.704
0.417	32.415	-2.011	1.601	0.912	-0.880	-0.845	864.2	0.102E-02	0.00109	0.604
0.556	33.281	-2.143	1.288	0.793	-0.616	-0.710	530.8	0.116E-02	0.00148	0.476
0.770	33.909	-2.271	0.960	0.716	-0.411	-0.512	279.9	0.147E-02	0.00229	0.323
1.020	34.299	-2.357	0.675	0.669	-0.209	-0.272	144.0	0.145E-02	0.00318	0.229
1.270	34.514	-2.422	0.517	0.660	-0.117	-0.168	88.1	0.133E-02	0.00389	0.185
1.520	34.675	-2.478	0.453	0.654	-0.076	-0.094	62.4	0.122E-02	0.00443	0.160
1.770	34.822	-2.531	0.423	0.613	-0.041	-0.070	-255.5	-0.160E-03	0.00079	0.140

Station 1 dU/dx=29s-1
x = 13.3100 cm, qwall = 361.200 W/m2

y	U	V	T	u'	v'	t'	u'v'	v't'	u't'	u'v'2	v'2t'	gamma	dU/dy	dT/dy	em	eh	Prt
0.0710	10.980	-0.290	33.52	1.3330	0.6860	0.5970	-0.2410	0.1870	-0.3570	-.318	0.161	0.802	5071.6	-1914.2	0.475E-04	0.977E-04	0.486
0.0760	11.160	-0.300	33.45	1.3470	0.6710	0.5650	-0.2370	0.1680	-0.3120	-.297	0.132	0.782	2272.2	-1032.9	0.104E-03	0.163E-03	0.641
0.0790	11.150	-0.270	33.44	1.3100	0.6550	0.5680	-0.2650	0.1750	-0.3330	-.266	0.125	0.784	1996.0	-933.6	0.133E-03	0.187E-03	0.708
0.0840	11.260	-0.300	33.39	1.3190	0.6220	0.5420	-0.2420	0.1440	-0.3240	-.234	0.102	0.764	1418.7	-723.8	0.171E-03	0.199E-03	0.857
0.0950	11.420	-0.280	33.32	1.2710	0.6070	0.5110	-0.2450	0.1340	-0.2820	-.222	0.106	0.743	1372.1	-713.2	0.179E-03	0.188E-03	0.950
0.1010	11.500	-0.290	33.27	1.2390	0.5840	0.4840	-0.2400	0.1170	-0.2720	-.191	0.086	0.718	1248.1	-607.7	0.192E-03	0.193E-03	0.999
0.1090	11.580	-0.290	33.22	1.2310	0.5880	0.4630	-0.2430	0.1170	-0.2490	-.164	0.082	0.702	1106.2	-568.6	0.220E-03	0.206E-03	1.068
0.1180	11.690	-0.290	33.19	1.2100	0.5620	0.4400	-0.2410	0.1090	-0.2190	-.156	0.073	0.705	1013.8	-479.8	0.238E-03	0.227E-03	1.046
0.1290	11.780	-0.300	33.13	1.2120	0.5550	0.4130	-0.2460	0.1000	-0.2280	-.160	0.065	0.676	951.2	-440.1	0.259E-03	0.227E-03	1.138
0.1410	11.900	-0.300	33.08	1.1690	0.5350	0.3920	-0.2250	0.0810	-0.1920	-.107	0.055	0.636	817.3	-415.8	0.275E-03	0.195E-03	1.413
0.1560	12.020	-0.290	33.02	1.1470	0.5150	0.3440	-0.2000	0.0680	-0.1610	-.099	0.038	0.607	718.8	-326.3	0.278E-03	0.208E-03	1.335
0.1730	12.100	-0.300	32.98	1.1130	0.5230	0.3160	-0.2060	0.0640	-0.1380	-.092	0.036	0.547	596.0	-260.1	0.346E-03	0.246E-03	1.405
0.2010	12.270	-0.300	32.92	1.1090	0.5150	0.2810	-0.1880	0.0580	-0.1280	-.092	0.032	0.480	503.8	-192.5	0.373E-03	0.301E-03	1.239
0.2300	12.400	-0.310	32.87	1.0760	0.5010	0.2350	-0.1860	0.0460	-0.1020	-.085	0.024	0.376	444.5	-156.8	0.418E-03	0.293E-03	1.426
0.2780	12.580	-0.310	32.81	1.0440	0.5120	0.1890	-0.1890	0.0410	-0.0810	-.078	0.018	0.289	327.7	-104.0	0.577E-03	0.394E-03	1.463
0.3440	12.740	-0.320	32.77	1.0320	0.5020	0.1410	-0.1790	0.0310	-0.0570	-.083	0.016	0.172	254.4	-66.5	0.704E-03	0.466E-03	1.509
0.4710	13.010	-0.330	32.71	0.9560	0.5240	0.0780	-0.1360	0.0180	-0.0290	-.066	0.010	0.049	152.7	-31.4	0.891E-03	0.574E-03	1.553
0.7210	13.190	-0.350	32.69	0.8790	0.5500	0.0350	-0.0920	0.0090	-0.0130	-.034	0.003	0.004	75.2	-8.5	0.122E-02	0.106E-02	1.156
0.9710	13.300	-0.390	32.70	0.8460	0.5900	0.0260	-0.0740	0.0070	-0.0100	-.032	0.001	0.000	35.2	-0.4	0.210E-02	0.176E-01	0.119
1.2200	13.350	-0.430	32.70	0.8340	0.6490	0.0230	-0.1000	0.0070	-0.0100	-.031	0.000	0.000	21.2	0.8	0.471E-02	-.869E-02	-.542
1.4700	13.370	-0.460	32.70	0.8010	0.6650	0.0220	-0.0730	0.0070	-0.0080	-.037	0.000	0.000	13.2	0.0	0.552E-02	-.140E+01	-.004
1.7200	13.420	-0.520	32.70	0.7910	0.6770	0.0220	-0.0650	0.0080	-0.0080	-.027	0.000	0.000	10.4	0.8	0.625E-02	-.101E-01	-.618
1.9700	13.430	-0.590	32.70	0.7940	0.7010	0.0220	-0.0500	0.0080	-0.0080	-.039	0.000	0.000	8.4	1.2	0.595E-02	-.668E-02	-.891
2.2200	13.450	-0.630	32.71	0.7740	0.7250	0.0220	-0.0520	0.0090	-0.0080	-.036	-.001	0.000	6.0	1.2	0.867E-02	-.747E-02	*****
2.4710	13.460	-0.680	32.71	0.7710	0.7280	0.0210	-0.0410	0.0090	-0.0010	-.020	0.000	0.000	5.2	0.0	0.790E-02	0.664E+00	0.012
2.7210	13.480	-0.740	32.71	0.7790	0.7380	0.0220	-0.0430	0.0100	-0.0080	-.029	0.001	0.000	4.0	-0.4	0.108E-01	0.245E-01	0.439
2.9700	13.480	-0.800	32.70	0.7530	0.7430	0.0220	-0.0310	0.0100	-0.0070	-.021	0.000	0.000	4.4	0.0	0.704E-02	-.910E+00	-.008
3.2210	13.490	-0.860	32.71	0.7460	0.7480	0.0210	-0.0220	0.0100	-0.0070	-.024	0.000	0.000	4.4	0.4	0.500E-02	-.256E-01	-.195
3.4710	13.510	-0.900	32.71	0.7490	0.7440	0.0210	-0.0200	0.0100	-0.0070	-.007	0.000	0.000	4.4	0.0	0.455E-02	0.742E+00	0.006
3.7210	13.520	-0.990	32.71	0.7600	0.7320	0.0210	-0.0070	0.0100	-0.0070	-.022	0.000	0.000	3.2	-0.6	0.219E-02	0.162E-01	0.135
3.9710	13.520	-1.040	32.70	0.7580	0.7590	0.0220	-0.0050	0.0100	-0.0070	-.021	0.001	0.000	0.9	-0.2	0.559E-02	0.467E-01	0.120
4.4700	13.520	-1.150	32.71	0.7590	0.7520	0.0220	-0.0050	0.0110	-0.0060	-.013	0.001	0.000	-38.0	-89.6	-.132E-03	0.123E-03	*****

Station 2 dU/dx=29s-1
x = 15.5600 cm, qwall = 365.000 W/m2

y	U	V	T	u'	v'	t'	u'v'	v't'	u't'	u'v'2	v'2t'	gamma	dU/dy	dT/dy	em	eh	Prt
0.0740	11.630	-0.150	35.01	1.6000	1.0610	0.9430	-0.3040	0.4790	-0.7140	-1.088	0.478	0.898	3880.5	120.6	0.783E-04	-.397E-02	-.020
0.0770	11.750	-0.180	35.00	1.5930	1.0550	0.9680	-0.3460	0.5300	-0.7530	-1.050	0.482	0.896	4518.0	-655.7	0.766E-04	0.808E-03	0.095
0.0810	11.950	-0.050	34.95	1.6530	1.0520	0.9630	-0.3040	0.4980	-0.7710	-1.088	0.425	0.895	4069.2	-1372.1	0.747E-04	0.363E-03	0.206
0.0860	12.160	-0.010	34.87	1.6880	0.9900	0.9510	-0.2330	0.4160	-0.7430	-0.959	0.385	0.908	3325.5	-2375.9	0.701E-04	0.175E-03	0.400
0.0890	12.190	-0.010	34.79	1.6790	0.9600	0.9330	-0.1810	0.4120	-0.7150	-0.923	0.395	0.903	3667.6	-2313.4	0.494E-04	0.178E-03	0.277
0.0910	12.300	-0.020	34.72	1.6460	0.9540	0.9280	-0.1950	0.3960	-0.7090	-0.897	0.377	0.913	3396.5	-2626.9	0.574E-04	0.151E-03	0.381
0.0960	12.510	0.030	34.62	1.6000	0.9410	0.9150	-0.2880	0.3920	-0.6980	-0.927	0.370	0.907	3487.2	-1964.6	0.826E-04	0.200E-03	0.414
0.1010	12.610	0.000	34.55	1.5740	0.8940	0.9100	-0.2390	0.3410	-0.6850	-0.780	0.350	0.902	3053.7	-1757.0	0.783E-04	0.194E-03	0.403
0.1050	12.740	0.020	34.47	1.5690	0.8670	0.8830	-0.2630	0.3170	-0.6420	-0.717	0.307	0.908	2775.4	-1668.6	0.948E-04	0.190E-03	0.499
0.1130	12.990	-0.010	34.33	1.5250	0.8340	0.8800	-0.2780	0.3220	-0.6480	-0.634	0.329	0.903	2775.0	-1599.2	0.100E-03	0.201E-03	0.498
0.1190	13.130	0.000	34.25	1.4560	0.8040	0.8550	-0.2790	0.2810	-0.6020	-0.612	0.285	0.897	2444.4	-1404.0	0.114E-03	0.200E-03	0.570
0.1280	13.340	0.010	34.13	1.3860	0.7500	0.8290	-0.2710	0.2630	-0.5410	-0.467	0.242	0.895	1948.6	-1194.3	0.139E-03	0.220E-03	0.632
0.1400	13.530	0.010	34.01	1.3620	0.7230	0.7780	-0.2500	0.2270	-0.4800	-0.375	0.197	0.888	1624.2	-1061.7	0.154E-03	0.214E-03	0.720
0.1520	13.660	-0.010	33.88	1.3070	0.6950	0.7590	-0.2620	0.2130	-0.4670	-0.361	0.210	0.872	1373.9	-872.2	0.191E-03	0.244E-03	0.781
0.1600	13.840	-0.020	33.81	1.2570	0.6390	0.7140	-0.2360	0.1810	-0.4160	-0.289	0.150	0.860	1274.2	-808.0	0.185E-03	0.224E-03	0.827
0.1760	13.990	-0.010	33.72	1.2080	0.6250	0.6720	-0.2400	0.1690	-0.3720	-0.239	0.149	0.844	1079.3	-636.9	0.222E-03	0.265E-03	0.838
0.1940	14.130	-0.020	33.61	1.1930	0.5940	0.6560	-0.2520	0.1540	-0.3540	-0.214	0.138	0.821	851.6	-588.2	0.296E-03	0.262E-03	1.130
0.2170	14.350	-0.020	33.46	1.1340	0.5590	0.5870	-0.2390	0.1330	-0.3050	-0.171	0.100	0.788	741.9	-500.7	0.322E-03	0.266E-03	1.213
0.2360	14.470	-0.020	33.38	1.0890	0.5490	0.5350	-0.2210	0.1240	-0.2600	-0.119	0.080	0.772	654.7	-421.3	0.338E-03	0.294E-03	1.147
0.2610	14.600	-0.050	33.31	1.0650	0.5240	0.5130	-0.2250	0.1110	-0.2510	-0.128	0.066	0.714	511.1	-312.4	0.440E-03	0.355E-03	1.239
0.2950	14.750	-0.040	33.21	1.0340	0.5070	0.4590	-0.2130	0.0960	-0.2000	-0.093	0.054	0.660	450.8	-271.7	0.472E-03	0.353E-03	1.337
0.3380	14.950	-0.060	33.09	0.9840	0.5080	0.3780	-0.1970	0.0870	-0.1490	-0.101	0.048	0.585	385.7	-223.5	0.511E-03	0.389E-03	1.312
0.4170	15.190	-0.090	32.97	0.9180	0.4900	0.2870	-0.1670	0.0640	-0.0920	-0.073	0.031	0.415	279.1	-141.3	0.598E-03	0.453E-03	1.321
0.4840	15.350	-0.120	32.91	0.8740	0.4960	0.2320	-0.1400	0.0630	-0.0660	-0.071	0.029	0.288	197.7	-94.5	0.708E-03	0.667E-03	1.062
0.6180	15.500	-0.150	32.82	0.8210	0.5090	0.1380	-0.1190	0.0310	-0.0340	-0.057	0.016	0.141	112.9	-49.1	0.105E-02	0.631E-03	1.671
0.8680	15.680	-0.220	32.77	0.7800	0.5530	0.0670	-0.0880	0.0160	-0.0150	-0.049	0.008	0.034	59.2	-19.4	0.149E-02	0.823E-03	1.806
1.1180	15.750	-0.310	32.76	0.7350	0.6000	0.0370	-0.0830	0.0100	-0.0080	-0.040	0.005	0.007	37.2	-6.4	0.223E-02	0.156E-02	1.428
1.3680	15.850	-0.400	32.75	0.7260	0.6320	0.0220	-0.0670	0.0060	-0.0050	-0.037	0.002	0.001	25.2	-2.8	0.266E-02	0.214E-02	1.241
1.6180	15.880	-0.440	32.75	0.7020	0.6540	0.0200	-0.0580	0.0060	-0.0040	-0.029	0.002	0.000	20.8	-2.0	0.279E-02	0.300E-02	0.930
1.8680	15.930	-0.510	32.74	0.7220	0.7050	0.0190	-0.0670	0.0070	-0.0050	-0.047	0.001	0.000	17.2	-1.2	0.390E-02	0.580E-02	0.671
2.1180	15.970	-0.580	32.74	0.6910	0.6930	0.0170	-0.0450	0.0060	-0.0040	-0.035	0.001	0.000	18.8	-0.8	0.239E-02	0.745E-02	0.321
2.3680	16.020	-0.630	32.74	0.6990	0.7080	0.0170	-0.0430	0.0060	-0.0040	-0.031	0.000	0.000	18.4	0.0	0.234E-02	0.123E+01	0.002
2.6180	16.070	-0.720	32.74	0.6800	0.7020	0.0170	-0.0340	0.0060	-0.0030	-0.032	0.001	0.000	18.0	-0.8	0.189E-02	0.745E-02	0.254
2.8680	16.110	-0.810	32.74	0.6800	0.7190	0.0160	-0.0310	0.0070	-0.0030	-0.026	0.001	0.000	16.8	-0.4	0.185E-02	0.177E-01	0.104
3.1180	16.150	-0.860	32.73	0.6820	0.7270	0.0170	-0.0340	0.0070	-0.0030	-0.019	0.000	0.000	15.2	0.0	0.224E-02	0.144E+01	0.002
3.3680	16.190	-0.930	32.74	0.6790	0.7200	0.0170	-0.0060	0.0070	-0.0030	-0.027	0.001	0.000	14.0	1.6	0.430E-03	-.443E-02	-.097
3.6180	16.220	-1.010	32.74	0.6840	0.7220	0.0170	-0.0140	0.0080	-0.0030	-0.028	0.000	0.000	-20.4	-67.1	-.686E-03	0.119E-03	*****

Station 3 dU/dx=29s-1
x = 17.7700 cm, qwall = 359.100 W/m2

y	U	V	T	u'	v'	t'	u'v'	v't'	u't'	u'v'2	v'2t'	gamma	dU/dy	dT/dy	em	eh	Prt
0.0830	13.360	-0.630	35.03	1.7500	1.2240	0.9590	-0.5700	0.5740	-0.7920	-1.450	0.539	0.933	19823.9	-1533.2	0.288E-04	0.374E-03	0.077
0.0870	13.980	-0.090	34.97	1.8420	1.1860	0.9330	-0.4360	0.4910	-0.7700	-1.563	0.486	0.930	8596.0	-2014.9	0.507E-04	0.244E-03	0.208
0.0950	14.200	-0.110	34.79	1.7990	1.1090	0.9240	-0.4030	0.4340	-0.7920	-1.313	0.428	0.939	4704.8	-1993.6	0.857E-04	0.218E-03	0.393
0.1010	14.450	-0.130	34.68	1.7360	1.0930	0.9230	-0.3790	0.4200	-0.7520	-1.356	0.508	0.942	3388.8	-1848.7	0.112E-03	0.227E-03	0.492
0.1050	14.630	-0.120	34.60	1.6950	1.0110	0.9050	-0.4190	0.3860	-0.7570	-1.103	0.412	0.935	3476.0	-1716.1	0.121E-03	0.225E-03	0.536
0.1130	14.830	-0.130	34.48	1.6810	0.9840	0.8870	-0.4340	0.3580	-0.7430	-1.074	0.399	0.932	2756.3	-1571.9	0.157E-03	0.228E-03	0.691
0.1220	15.040	-0.160	34.35	1.6010	0.9270	0.8570	-0.4070	0.3300	-0.6900	-0.858	0.350	0.929	2352.6	-1394.7	0.173E-03	0.237E-03	0.731
0.1320	15.310	-0.180	34.19	1.5540	0.8550	0.8370	-0.3900	0.2910	-0.6470	-0.651	0.271	0.928	2143.5	-1235.7	0.182E-03	0.235E-03	0.773
0.1400	15.430	-0.180	34.13	1.5060	0.8300	0.7960	-0.3870	0.2560	-0.6060	-0.612	0.226	0.916	1950.3	-1088.2	0.198E-03	0.235E-03	0.843
0.1560	15.720	-0.200	33.97	1.4120	0.7830	0.7770	-0.3430	0.2420	-0.5450	-0.492	0.211	0.924	1489.6	-826.9	0.230E-03	0.293E-03	0.787
0.1740	15.950	-0.220	33.83	1.3460	0.7350	0.7530	-0.3770	0.2150	-0.5270	-0.408	0.202	0.892	1184.7	-679.7	0.318E-03	0.316E-03	1.006
0.1870	16.080	-0.220	33.77	1.2830	0.7150	0.7180	-0.3510	0.1860	-0.4730	-0.394	0.183	0.887	1044.4	-597.3	0.336E-03	0.311E-03	1.079
0.2050	16.230	-0.220	33.67	1.2330	0.6770	0.6800	-0.3430	0.1980	-0.4180	-0.283	0.154	0.871	937.5	-528.4	0.366E-03	0.375E-03	0.976
0.2360	16.550	-0.240	33.50	1.1360	0.6220	0.6310	-0.3100	0.1590	-0.3470	-0.215	0.109	0.845	803.5	-466.0	0.386E-03	0.341E-03	1.131
0.2570	16.690	-0.250	33.41	1.0910	0.6160	0.5860	-0.3050	0.1620	-0.3120	-0.214	0.115	0.831	693.2	-390.3	0.440E-03	0.415E-03	1.060
0.2810	16.830	-0.260	33.33	1.0490	0.5860	0.5580	-0.2710	0.1410	-0.2870	-0.171	0.088	0.796	544.1	-339.9	0.498E-03	0.415E-03	1.201
0.3050	16.950	-0.270	33.27	1.0250	0.5720	0.5420	-0.2660	0.1380	-0.2540	-0.155	0.089	0.784	467.6	-314.2	0.569E-03	0.439E-03	1.295
0.3520	17.130	-0.310	33.10	0.9590	0.5470	0.4680	-0.2340	0.1160	-0.1960	-0.123	0.065	0.700	378.3	-265.7	0.619E-03	0.437E-03	1.417
0.4030	17.310	-0.320	33.00	0.8930	0.5290	0.4130	-0.2120	0.1040	-0.1540	-0.123	0.060	0.607	304.5	-205.2	0.696E-03	0.507E-03	1.373
0.4630	17.480	-0.360	32.91	0.8630	0.5230	0.3520	-0.1860	0.0930	-0.1150	-0.093	0.044	0.498	234.6	-134.3	0.793E-03	0.692E-03	1.145
0.5420	17.590	-0.400	32.83	0.7940	0.5240	0.2820	-0.1490	0.0740	-0.0790	-0.081	0.038	0.380	158.7	-90.3	0.939E-03	0.819E-03	1.146
0.6830	17.760	-0.450	32.75	0.7450	0.5510	0.1930	-0.1230	0.0520	-0.0430	-0.071	0.031	0.219	101.2	-50.3	0.122E-02	0.103E-02	1.174
0.9000	17.920	-0.530	32.69	0.7020	0.5700	0.1130	-0.0930	0.0280	-0.0190	-0.055	0.019	0.083	61.8	-23.2	0.151E-02	0.120E-02	1.250
1.1510	18.000	-0.610	32.67	0.6610	0.6360	0.0620	-0.0890	0.0150	-0.0090	-0.057	0.009	0.031	37.5	-9.0	0.238E-02	0.167E-02	1.427
1.4010	18.060	-0.700	32.66	0.6480	0.6580	0.0350	-0.0710	0.0100	-0.0050	-0.033	0.004	0.011	27.2	-3.6	0.261E-02	0.278E-02	0.940
1.6510	18.140	-0.790	32.66	0.6250	0.6750	0.0240	-0.0540	0.0070	-0.0020	-0.035	0.002	0.001	24.4	-2.8	0.221E-02	0.249E-02	0.888
1.9000	18.190	-0.850	32.65	0.6280	0.6960	0.0210	-0.0430	0.0070	-0.0020	-0.038	0.002	0.001	22.4	-2.4	0.192E-02	0.291E-02	0.660
2.1500	18.240	-0.950	32.64	0.6190	0.7250	0.0170	-0.0510	0.0060	-0.0020	-0.028	0.000	0.000	20.8	-2.8	0.245E-02	0.214E-02	1.143
2.4000	18.290	-1.000	32.64	0.6120	0.7320	0.0160	-0.0450	0.0050	-0.0010	-0.038	0.001	0.000	21.2	-2.0	0.212E-02	0.250E-02	0.850
2.6500	18.350	-1.090	32.63	0.6210	0.7200	0.0160	-0.0180	0.0060	-0.0010	-0.022	0.000	0.000	18.8	-1.2	0.957E-03	0.500E-02	0.192
2.9010	18.400	-1.150	32.63	0.6060	0.7240	0.0160	-0.0370	0.0060	-0.0010	-0.026	0.000	0.000	17.2	-1.6	0.215E-02	0.375E-02	0.573
3.1500	18.420	-1.240	32.63	0.6160	0.7230	0.0150	-0.0090	0.0060	-0.0010	-0.018	0.001	0.000	17.2	-0.8	0.524E-03	0.713E-02	0.073
3.4000	18.470	-1.330	32.62	0.6150	0.7390	0.0150	-0.0140	0.0060	-0.0010	-0.014	0.000	0.000	19.3	-1.2	0.726E-03	0.519E-02	0.140
3.9000	18.590	-1.480	32.62	0.6310	0.7110	0.0160	-0.0060	0.0060	0.0000	-0.022	0.000	0.000	-42.6	-123.0	-.141E-03	0.488E-04	*****

Station 4 dU/dx=29s-1
x = 20.7400 cm, qwall = 359.800 W/m2

y	U	V	T	u'	v'	t'	u'v'	v't'	u't'	u'v'2	v'2t'	gamma	dU/dy	dT/dy	em	eh	Prt
0.1080	15.680	-0.610	35.14	1.7830	1.2900	0.8630	-0.7000	0.4770	-0.7070	-1.841	0.225	0.953	14947.3	-1062.6	0.468E-04	0.449E-03	0.104
0.1150	16.520	-0.130	35.06	1.9170	1.3090	0.8620	-0.5010	0.4370	-0.7290	-2.106	0.584	0.946	7971.8	-1502.0	0.628E-04	0.291E-03	0.216
0.1310	17.130	0.010	34.79	1.8270	1.0950	0.8310	-0.5010	0.3220	-0.7100	-1.311	0.345	0.947	4288.4	-1463.5	0.117E-03	0.220E-03	0.531
0.1400	17.400	0.000	34.67	1.7650	1.0550	0.8000	-0.4560	0.2930	-0.6410	-1.173	0.329	0.944	3035.9	-1358.6	0.150E-03	0.216E-03	0.696
0.1540	17.840	-0.060	34.48	1.6230	0.9610	0.7710	-0.4360	0.2600	-0.6000	-0.813	0.252	0.941	2466.9	-1149.2	0.177E-03	0.226E-03	0.781
0.1680	18.070	-0.050	34.36	1.5730	0.8900	0.7640	-0.4150	0.2270	-0.5920	-0.693	0.212	0.939	2016.5	-975.4	0.206E-03	0.233E-03	0.884
0.1900	18.450	-0.050	34.15	1.4690	0.8320	0.7320	-0.4620	0.2130	-0.5460	-0.556	0.191	0.929	1638.9	-779.2	0.282E-03	0.273E-03	1.031
0.2080	18.710	-0.040	34.06	1.4030	0.7720	0.7070	-0.4480	0.2090	-0.5270	-0.465	0.180	0.923	1424.0	-711.0	0.315E-03	0.294E-03	1.070
0.2230	18.980	-0.100	33.93	1.3320	0.7260	0.6750	-0.3900	0.1820	-0.4600	-0.376	0.139	0.912	1294.9	-621.4	0.301E-03	0.293E-03	1.028
0.2450	19.160	-0.090	33.80	1.2730	0.6730	0.6520	-0.3740	0.1780	-0.4080	-0.290	0.121	0.894	1072.3	-572.6	0.349E-03	0.311E-03	1.122
0.2800	19.520	-0.130	33.64	1.1860	0.6360	0.6310	-0.3490	0.1680	-0.3870	-0.248	0.116	0.880	786.9	-402.0	0.443E-03	0.418E-03	1.061
0.3080	19.670	-0.130	33.56	1.1340	0.6130	0.5920	-0.3320	0.1550	-0.3370	-0.193	0.089	0.853	694.0	-344.5	0.478E-03	0.450E-03	1.063
0.3330	19.850	-0.140	33.47	1.0990	0.5920	0.5310	-0.3070	0.1500	-0.3120	-0.181	0.079	0.837	565.7	-301.4	0.543E-03	0.498E-03	1.091
0.3830	20.100	-0.190	33.33	1.0060	0.5700	0.5170	-0.2790	0.1430	-0.2480	-0.183	0.090	0.765	462.0	-259.4	0.604E-03	0.551E-03	1.095
0.4360	20.310	-0.230	33.21	0.9230	0.4360	0.4630	-0.2270	0.1200	-0.1910	-0.125	0.068	0.673	335.7	-205.6	0.676E-03	0.584E-03	1.158
0.5040	20.450	-0.250	33.10	0.8450	0.5410	0.4060	-0.1900	0.1110	-0.1430	-0.110	0.059	0.592	238.9	-155.4	0.795E-03	0.714E-03	1.113
0.5860	20.630	-0.310	32.99	0.7660	0.5240	0.3400	-0.1450	0.0880	-0.0920	-0.086	0.046	0.445	167.2	-110.4	0.867E-03	0.797E-03	1.088
0.7270	20.790	-0.360	32.89	0.6990	0.5560	0.2530	-0.1190	0.0710	-0.0590	-0.072	0.040	0.291	110.1	-65.9	0.108E-02	0.108E-02	1.004
0.8990	20.920	-0.430	32.82	0.6650	0.5710	0.1640	-0.0900	0.0410	-0.0310	-0.051	0.023	0.156	62.4	-35.4	0.144E-02	0.116E-02	1.245
1.1490	20.990	-0.530	32.78	0.6210	0.6300	0.1000	-0.0720	0.0270	-0.0110	-0.058	0.020	0.066	36.1	-15.1	0.199E-02	0.179E-02	1.113
1.3990	21.060	-0.630	32.76	0.6000	0.6660	0.0700	-0.0780	0.0180	-0.0070	-0.067	0.017	0.033	24.0	-5.6	0.325E-02	0.322E-02	1.011
1.6490	21.130	-0.710	32.76	0.5850	0.6760	0.0380	-0.0660	0.0110	-0.0030	-0.027	0.008	0.010	18.8	-1.6	0.351E-02	0.688E-02	0.510
1.8990	21.150	-0.800	32.76	0.5700	0.6920	0.0260	-0.0470	0.0070	-0.0010	-0.030	0.003	0.004	17.2	0.4	0.274E-02	-.166E-01	-.166
2.1500	21.180	-0.900	32.76	0.5600	0.7140	0.0210	-0.0480	0.0070	0.0000	-0.027	0.002	0.001	16.2	0.8	0.297E-02	-.871E-02	-.340
2.6500	21.300	-1.050	32.77	0.5700	0.7100	0.0160	-0.0360	0.0050	0.0000	-0.022	0.000	0.000	20.6	0.8	0.175E-02	-.636E-02	-.274
2.9000	21.350	-1.150	32.77	0.5640	0.7050	0.0160	-0.0280	0.0050	-0.0010	-0.022	0.000	0.000	20.9	0.4	0.134E-02	-.115E-01	-.117
3.4000	21.450	-1.300	32.77	0.5780	0.6760	0.0160	-0.0100	0.0050	-0.0010	-0.019	0.000	0.000	-85.3	-166.2	-.117E-03	0.301E-04	*****

Station 5 dU/dx=29s-1
x = 23.5800 cm, qwall = 364.800 W/m2

y	U	V	T	u'	v'	t'	u'v'	v't'	u't'	u'v'2	v'2t'	gamma	dU/dy	dT/dy	em	eh	Prt
0.1040	17.380	-1.050	35.07	1.9370	1.4650	0.7330	-0.9960	0.4210	-0.6500	-2.110	0.389	0.944	18560.8	-986.2	0.537E-04	0.427E-03	0.126
0.1140	18.690	-0.090	34.95	2.0810	1.3780	0.7200	-0.7450	0.3440	-0.6650	-2.057	0.252	0.941	9180.1	-1276.7	0.812E-04	0.269E-03	0.301
0.1210	18.960	-0.090	34.85	1.9740	1.3240	0.7110	-0.6470	0.3090	-0.6290	-1.746	0.275	0.939	6839.5	-1327.1	0.946E-04	0.233E-03	0.406
0.1340	19.580	-0.130	34.68	1.8870	1.1390	0.6950	-0.5900	0.2550	-0.6370	-1.246	0.236	0.950	3885.0	-1257.6	0.152E-03	0.203E-03	0.749
0.1420	19.900	-0.150	34.56	1.7660	1.0480	0.6740	-0.5300	0.2220	-0.5650	-1.007	0.213	0.938	3508.4	-1149.8	0.151E-03	0.193E-03	0.782
0.1590	20.310	-0.140	34.41	1.7090	0.9700	0.6760	-0.5880	0.2160	-0.5880	-0.808	0.177	0.933	2516.5	-929.7	0.234E-03	0.232E-03	1.006
0.1750	20.670	-0.130	34.28	1.6400	0.9200	0.6670	-0.5430	0.2030	-0.5700	-0.667	0.185	0.931	2093.7	-778.9	0.259E-03	0.261E-03	0.995
0.2020	21.190	-0.150	34.08	1.5290	0.7920	0.6670	-0.4770	0.1880	-0.5650	-0.441	0.150	0.921	1693.3	-657.0	0.282E-03	0.286E-03	0.985
0.2200	21.450	-0.150	33.98	1.4710	0.7640	0.6560	-0.4810	0.1890	-0.5360	-0.405	0.111	0.922	1454.8	-592.9	0.331E-03	0.319E-03	1.037
0.2330	21.640	-0.170	33.90	1.4040	0.7110	0.6350	-0.4150	0.1620	-0.4840	-0.346	0.104	0.915	1280.9	-541.4	0.324E-03	0.299E-03	1.083
0.2590	21.930	-0.190	33.77	1.3220	0.6740	0.6170	-0.4130	0.1660	-0.4460	-0.325	0.123	0.919	1068.0	-486.2	0.387E-03	0.341E-03	1.133
0.2830	22.150	-0.180	33.66	1.2790	0.6570	0.6000	-0.4030	0.1740	-0.4190	-0.264	0.099	0.883	914.5	-427.9	0.441E-03	0.407E-03	1.084
0.3320	22.550	-0.210	33.48	1.1580	0.6170	0.5770	-0.3550	0.1530	-0.3560	-0.242	0.084	0.850	689.6	-346.7	0.515E-03	0.441E-03	1.166
0.3570	22.710	-0.230	33.39	1.1050	0.5920	0.5510	-0.3150	0.1550	-0.3240	-0.226	0.089	0.827	602.7	-308.1	0.523E-03	0.503E-03	1.039
0.4020	22.920	-0.250	33.27	1.0140	0.5660	0.5120	-0.2800	0.1430	-0.2630	-0.188	0.077	0.766	434.2	-249.3	0.645E-03	0.574E-03	1.124
0.4680	23.150	-0.280	33.14	0.9030	0.5430	0.4590	-0.2360	0.1250	-0.1930	-0.150	0.067	0.678	304.1	-185.0	0.776E-03	0.676E-03	1.149
0.5320	23.280	-0.300	33.04	0.8310	0.5380	0.4180	-0.2040	0.1130	-0.1500	-0.119	0.059	0.587	225.8	-143.0	0.904E-03	0.790E-03	1.144
0.6360	23.480	-0.340	32.92	0.7270	0.5520	0.3380	-0.1520	0.0920	-0.0870	-0.099	0.053	0.459	143.2	-95.2	0.106E-02	0.966E-03	1.099
0.7740	23.600	-0.390	32.84	0.6620	0.5770	0.2610	-0.1200	0.0760	-0.0550	-0.080	0.049	0.311	87.0	-57.4	0.138E-02	0.132E-02	1.042
0.9440	23.660	-0.440	32.78	0.6010	0.6180	0.1930	-0.0920	0.0560	-0.0280	-0.068	0.044	0.190	47.6	-30.8	0.193E-02	0.182E-02	1.061
1.1950	23.770	-0.500	32.74	0.5800	0.6470	0.1220	-0.0940	0.0350	-0.0460	-0.061	0.030	0.096	29.2	-15.4	0.322E-02	0.227E-02	1.422
1.4450	23.810	-0.580	32.72	0.5520	0.6680	0.0780	-0.0570	0.0210	-0.0050	-0.055	0.019	0.043	21.6	-8.0	0.264E-02	0.263E-02	1.005
1.6950	23.850	-0.650	32.70	0.5500	0.6900	0.0590	-0.0610	0.0150	-0.0020	-0.031	0.012	0.021	16.0	-4.0	0.381E-02	0.375E-02	1.017
1.9450	23.890	-0.710	32.70	0.5360	0.6880	0.0380	-0.0430	0.0100	0.0000	-0.027	0.007	0.010	16.4	-2.4	0.262E-02	0.424E-02	0.618
2.1950	23.930	-0.780	32.70	0.5160	0.7160	0.0260	-0.0430	0.0070	0.0000	-0.031	0.004	0.003	16.7	-0.8	0.257E-02	0.848E-02	0.303
2.6950	24.020	-0.900	32.69	0.5260	0.6950	0.0170	-0.0240	0.0050	-0.0010	-0.026	0.000	0.000	15.7	-0.8	0.153E-02	0.637E-02	0.240
3.1950	24.090	-1.010	32.69	0.5440	0.6610	0.0170	-0.0230	0.0050	-0.0020	-0.024	0.005	0.000	-123.3	-189.8	-.187E-03	0.263E-04	*****

Station 6 dU/dx=29s-1
x = 25.8800 cm, qwall = 368.500 W/m2

y	U	V	T	u'	v'	t'	u'v'	v't'	u't'	u'v'2	v'2t'	gamma	dU/dy	dT/dy	em	eh	Prt
0.0970	18.820	0.090	34.57	1.9560	1.4710	0.6160	-0.9140	0.3070	-0.5370	-1.759	0.187	0.933	582.7	-47.0	0.157E-02	0.653E-02	0.240
0.1090	19.170	-0.180	34.55	2.0640	1.4950	0.6210	-1.0010	0.3370	-0.5830	-2.158	0.308	0.930	4576.7	-343.2	0.219E-03	0.982E-03	0.223
0.1190	19.900	0.190	34.51	2.1730	1.4620	0.6080	-0.8410	0.2660	-0.5390	-1.820	0.193	0.929	4732.2	-690.3	0.178E-03	0.385E-03	0.461
0.1310	20.400	0.200	34.37	2.1010	1.3130	0.6020	-0.8960	0.2310	-0.5920	-1.520	0.203	0.934	4786.2	-936.3	0.187E-03	0.247E-03	0.759
0.1470	21.100	0.160	34.19	2.0040	1.1850	0.5850	-0.8160	0.2050	-0.5670	-1.026	0.149	0.937	3587.8	-915.2	0.227E-03	0.224E-03	1.015
0.1620	21.580	0.150	34.08	1.9250	1.0800	0.5880	-0.7670	0.1900	-0.5930	-0.798	0.123	0.928	3173.5	-795.8	0.242E-03	0.239E-03	1.012
0.1730	21.830	0.150	34.01	1.8620	1.0510	0.5870	-0.7350	0.1630	-0.5560	-0.810	0.122	0.923	2776.9	-697.8	0.265E-03	0.234E-03	1.133
0.1900	22.350	0.120	33.88	1.8010	1.0000	0.5950	-0.7330	0.1820	-0.5550	-0.617	0.100	0.913	2504.4	-663.4	0.293E-03	0.274E-03	1.067
0.2120	22.840	0.120	33.75	1.7930	0.9140	0.5910	-0.7230	0.1780	-0.5760	-0.585	0.109	0.919	2151.3	-622.2	0.336E-03	0.286E-03	1.175
0.2300	23.180	0.100	33.64	1.6880	0.8650	0.5880	-0.6030	0.1690	-0.5460	-0.484	0.081	0.919	1871.2	-559.8	0.322E-03	0.302E-03	1.068
0.2470	23.480	0.110	33.54	1.6810	0.8380	0.5980	-0.6410	0.1800	-0.5670	-0.491	0.120	0.918	1675.5	-533.6	0.383E-03	0.337E-03	1.134
0.2810	24.010	0.080	33.39	1.5490	0.7660	0.5970	-0.5430	0.1750	-0.5510	-0.421	0.115	0.917	1359.0	-447.4	0.400E-03	0.391E-03	1.021
0.3060	24.270	0.080	33.27	1.4850	0.7140	0.5840	-0.4900	0.1570	-0.5090	-0.377	0.102	0.898	1161.4	-396.1	0.422E-03	0.396E-03	1.064
0.3550	24.780	0.070	33.11	1.3680	0.6490	0.5650	-0.4390	0.1670	-0.4510	-0.350	0.106	0.874	844.4	-324.4	0.520E-03	0.515E-03	1.010
0.3950	25.060	0.050	32.99	1.2220	0.6040	0.5540	-0.3370	0.1510	-0.3810	-0.250	0.093	0.839	687.5	-272.6	0.490E-03	0.554E-03	0.885
0.4340	25.270	0.070	32.89	1.1450	0.6100	0.5270	-0.3570	0.1590	-0.3440	-0.289	0.103	0.795	526.6	-235.5	0.678E-03	0.675E-03	1.004
0.4720	25.480	0.040	32.81	1.0250	0.5530	0.4980	-0.2660	0.1370	-0.2750	-0.179	0.074	0.743	430.7	-200.2	0.618E-03	0.684E-03	0.902
0.5250	25.640	0.020	32.72	0.9620	0.5630	0.4570	-0.2600	0.1350	-0.2240	-0.176	0.074	0.674	317.8	-159.7	0.818E-03	0.846E-03	0.967
0.6150	25.850	0.010	32.60	0.8340	0.5470	0.3910	-0.2040	0.1100	-0.1550	-0.129	0.059	0.561	206.3	-113.9	0.989E-03	0.966E-03	1.024
0.7410	26.050	-0.030	32.50	0.7260	0.5650	0.3230	-0.1530	0.0930	-0.0900	-0.111	0.056	0.429	131.9	-75.4	0.116E-02	0.123E-02	0.940
0.9170	26.170	-0.080	32.41	0.6510	0.6060	0.2480	-0.1290	0.0740	-0.0540	-0.101	0.053	0.280	75.2	-43.5	0.172E-02	0.170E-02	1.008
1.1670	26.290	-0.130	32.35	0.5810	0.6260	0.1600	-0.0780	0.0450	-0.0190	-0.061	0.032	0.149	41.3	-21.6	0.189E-02	0.208E-02	0.908
1.4170	26.360	-0.180	32.32	0.5550	0.6740	0.1100	-0.0720	0.0320	-0.0090	-0.050	0.026	0.082	32.4	-10.4	0.222E-02	0.308E-02	0.722
1.6670	26.420	-0.230	32.31	0.5380	0.6820	0.0760	-0.0710	0.0210	-0.0050	-0.057	0.018	0.044	28.7	-5.6	0.248E-02	0.376E-02	0.658
1.9170	26.510	-0.260	32.30	0.5340	0.6900	0.0550	-0.0600	0.0140	-0.0020	-0.031	0.013	0.022	29.3	-3.0	0.205E-02	0.461E-02	0.444
2.4170	26.650	-0.360	32.29	0.5170	0.6830	0.0250	-0.0450	0.0070	0.0010	-0.015	0.004	0.004	27.4	-1.0	0.164E-02	0.668E-02	0.246
2.9170	26.780	-0.410	32.29	0.5360	0.6170	0.0160	-0.0320	0.0040	0.0020	-0.019	0.001	0.001	-158.5	-229.0	-.202E-03	0.175E-04	*****

Station 7 dU/dx=29s-1
x = 27.1100 cm, qwall = 366.500 W/m2

y	U	V	T	u'	v'	t'	u'v'	v't'	u't'	u'v'2	v'2t'	gamma	dU/dy	dT/dy	em	eh	Prt
0.1050	20.300	-0.160	34.96	2.1930	1.4290	0.5630	-1.0150	0.2210	-0.5460	-1.577	0.152	0.918	6511.0	-1805.6	0.156E-03	0.122E-03	1.274
0.1240	21.250	-0.240	34.71	2.1220	1.3090	0.5530	-0.9840	0.2060	-0.5790	-1.462	0.149	0.914	4081.9	-1028.5	0.241E-03	0.200E-03	1.204
0.1360	21.560	-0.260	34.64	2.1000	1.2170	0.5500	-1.0180	0.2040	-0.5740	-0.971	0.110	0.911	3652.6	-898.7	0.279E-03	0.227E-03	1.228
0.1590	22.350	-0.260	34.46	2.0040	1.0910	0.5440	-0.9370	0.1780	-0.5900	-0.672	0.104	0.896	2838.6	-696.1	0.330E-03	0.256E-03	1.291
0.1740	22.790	-0.290	34.34	1.9420	1.0580	0.5410	-0.9240	0.1770	-0.5460	-0.618	0.101	0.907	2651.9	-660.8	0.348E-03	0.268E-03	1.301
0.1990	23.270	-0.310	34.21	1.9100	0.9870	0.5540	-0.8850	0.1830	-0.5970	-0.463	0.065	0.902	2196.0	-539.2	0.403E-03	0.339E-03	1.187
0.2250	23.840	-0.360	34.08	1.8500	0.9470	0.5600	-0.8640	0.1800	-0.5920	-0.573	0.115	0.904	1844.5	-460.5	0.468E-03	0.391E-03	1.198
0.2390	24.150	-0.350	34.02	1.7880	0.9100	0.5570	-0.7960	0.1820	-0.5840	-0.551	0.105	0.906	1812.6	-462.0	0.439E-03	0.394E-03	1.115
0.2630	24.440	-0.360	33.92	1.7720	0.8680	0.5620	-0.7750	0.1840	-0.5820	-0.576	0.111	0.900	1516.4	-445.3	0.511E-03	0.413E-03	1.237
0.2970	24.980	-0.400	33.75	1.6920	0.8010	0.5650	-0.6740	0.1880	-0.5850	-0.535	0.125	0.897	1268.4	-396.3	0.531E-03	0.474E-03	1.120
0.3440	25.500	-0.410	33.60	1.5650	0.7470	0.5540	-0.6170	0.1790	-0.5430	-0.433	0.106	0.876	988.1	-323.5	0.624E-03	0.553E-03	1.129
0.3690	25.710	-0.430	33.53	1.4780	0.7070	0.5460	-0.5350	0.1670	-0.5050	-0.444	0.111	0.867	866.4	-285.5	0.617E-03	0.585E-03	1.056
0.4020	25.960	-0.440	33.43	1.4290	0.6910	0.5490	-0.5300	0.1840	-0.4860	-0.423	0.124	0.835	721.0	-263.4	0.735E-03	0.699E-03	1.052
0.4690	26.390	-0.460	33.28	1.2390	0.6420	0.5160	-0.4310	0.1690	-0.3880	-0.365	0.128	0.776	548.7	-215.7	0.786E-03	0.784E-03	1.003
0.5070	26.560	-0.480	33.20	1.1580	0.6160	0.4950	-0.3890	0.1580	-0.3460	-0.339	0.111	0.733	463.4	-187.0	0.839E-03	0.845E-03	0.994
0.5650	26.800	-0.490	33.10	1.0270	0.5940	0.4510	-0.3150	0.1410	-0.2640	-0.288	0.101	0.654	335.6	-153.2	0.938E-03	0.921E-03	1.019
0.6700	27.040	-0.530	32.98	0.8620	0.5670	0.3880	-0.2230	0.1180	-0.1720	-0.194	0.079	0.539	210.4	-103.3	0.106E-02	0.114E-02	0.928
0.7630	27.160	-0.540	32.91	0.7700	0.5910	0.3570	-0.1950	0.1110	-0.1290	-0.169	0.071	0.447	138.9	-74.5	0.140E-02	0.149E-02	0.943
0.9520	27.340	-0.600	32.81	0.6300	0.5990	0.2540	-0.1350	0.0770	-0.0570	-0.110	0.053	0.280	80.0	-44.1	0.169E-02	0.175E-02	0.966
1.1570	27.450	-0.690	32.75	0.5670	0.6140	0.1960	-0.0810	0.0570	-0.0250	-0.067	0.043	0.187	52.7	-27.0	0.154E-02	0.211E-02	0.728
1.4070	27.550	-0.720	32.71	0.5270	0.6440	0.1410	-0.0710	0.0400	-0.0150	-0.064	0.036	0.111	35.1	-15.4	0.203E-02	0.259E-02	0.781
1.6570	27.590	-0.770	32.69	0.5100	0.6640	0.1030	-0.0640	0.0270	-0.0060	-0.041	0.023	0.071	28.1	-9.7	0.228E-02	0.279E-02	0.818
2.1570	27.740	-0.840	32.65	0.4890	0.6490	0.0510	-0.0360	0.0120	0.0000	-0.037	0.013	0.021	25.9	-3.6	0.139E-02	0.330E-02	0.421
2.6570	27.860	-0.980	32.65	0.5060	0.6060	0.0270	-0.0290	0.0050	0.0020	-0.016	0.005	0.005	-213.5	-284.8	-.136E-03	0.176E-04	*****

Station 8 dU/dx=29s-1
x = 29.2400 cm, qwall = 366.100 W/m2

y	U	V	T	u'	v'	t'	u'v'	v't'	u't'	u'v'2	v'2t'	gamma	dU/dy	dT/dy	em	eh	Prt
0.1580	23.890	-0.460	34.46	2.1190	1.1870	0.5170	-1.1260	0.1980	-0.5840	-0.986	0.110	0.898	3055.5	-593.1	0.369E-03	0.334E-03	1.104
0.1910	24.780	-0.510	34.27	2.0350	1.0850	0.5240	-1.0930	0.2030	-0.5980	-0.723	0.101	0.893	2367.2	-523.5	0.462E-03	0.388E-03	1.191
0.2060	25.110	-0.540	34.19	2.0140	1.0410	0.5210	-1.0460	0.1940	-0.5880	-0.686	0.075	0.896	2141.1	-492.2	0.489E-03	0.394E-03	1.240
0.2280	25.520	-0.570	34.10	1.9700	1.0160	0.5280	-1.0180	0.2010	-0.6170	-0.577	0.102	0.897	1889.0	-450.6	0.539E-03	0.446E-03	1.208
0.2470	25.860	-0.560	34.01	1.9490	0.9720	0.5320	-1.0010	0.1960	-0.6260	-0.695	0.106	0.891	1765.9	-436.7	0.567E-03	0.449E-03	1.263
0.2870	26.560	-0.620	33.84	1.8720	0.9320	0.5420	-0.9360	0.2070	-0.6330	-0.631	0.135	0.899	1504.3	-401.9	0.622E-03	0.515E-03	1.208
0.3100	26.860	-0.650	33.73	1.8020	0.8870	0.5410	-0.8580	0.2030	-0.6100	-0.609	0.136	0.898	1381.8	-379.8	0.621E-03	0.534E-03	1.162
0.3340	27.160	-0.690	33.67	1.7420	0.8640	0.5410	-0.8140	0.1970	-0.5910	-0.650	0.132	0.893	1209.8	-348.2	0.673E-03	0.566E-03	1.189
0.3690	27.580	-0.690	33.54	1.6470	0.8210	0.5370	-0.7580	0.2010	-0.5580	-0.559	0.133	0.879	1061.6	-295.9	0.714E-03	0.679E-03	1.051
0.4390	28.190	-0.760	33.36	1.5170	0.7540	0.5360	-0.6590	0.2030	-0.5300	-0.598	0.154	0.838	691.1	-244.0	0.954E-03	0.832E-03	1.146
0.4750	28.350	-0.770	33.29	1.4260	0.7370	0.5180	-0.6080	0.1930	-0.4710	-0.570	0.154	0.804	593.0	-210.1	0.103E-02	0.919E-03	1.116
0.5230	28.590	-0.800	33.18	1.2860	0.6900	0.4970	-0.5080	0.1750	-0.3960	-0.455	0.138	0.745	443.8	-182.1	0.114E-02	0.961E-03	1.191
0.6170	28.970	-0.840	33.05	1.1160	0.6660	0.4570	-0.4230	0.1650	-0.3200	-0.406	0.132	0.663	340.9	-140.7	0.124E-02	0.117E-02	1.058
0.6910	29.180	-0.890	32.95	0.9640	0.6340	0.4170	-0.3400	0.1470	-0.2380	-0.330	0.121	0.556	257.7	-109.2	0.132E-02	0.135E-02	0.980
0.8330	29.400	-0.960	32.83	0.7910	0.6260	0.3390	-0.2400	0.1150	-0.1420	-0.246	0.098	0.444	150.2	-72.3	0.160E-02	0.159E-02	1.004
0.9540	29.560	-0.970	32.78	0.6680	0.6110	0.2910	-0.1600	0.0960	-0.0790	-0.146	0.075	0.345	100.0	-48.9	0.160E-02	0.196E-02	0.815
1.1960	29.670	-1.050	32.70	0.5640	0.6510	0.2200	-0.1100	0.0730	-0.0410	-0.113	0.066	0.212	58.5	-27.3	0.188E-02	0.267E-02	0.704
1.4460	29.800	-1.130	32.65	0.5160	0.6390	0.1470	-0.0710	0.0400	-0.0160	-0.064	0.035	0.132	39.1	-17.1	0.182E-02	0.233E-02	0.779
1.9460	29.940	-1.280	32.61	0.4590	0.6390	0.0770	-0.0360	0.0190	-0.0020	-0.024	0.017	0.048	-494.3	-590.2	-.728E-04	0.322E-04	*****

Station 9 dU/dx=29s-1
x = 32.1200 cm, qwall = 371.500 W/m2

y	U	V	T	u'	v'	t'	u'v'	v't'	u't'	u'v'2	v'2t'	gamma	dU/dy	dT/dy	em	eh	Prt
0.0830	22.360	-1.450	34.35	2.1990	1.6430	0.5120	-1.6490	0.2940	-0.5640	-1.494	0.193	0.910	23147.9	-316.9	0.712E-04	0.928E-03	0.077
0.0910	23.890	-0.520	34.31	2.3990	1.6380	0.5030	-1.6260	0.2740	-0.6110	-2.267	0.227	0.906	13868.2	-806.8	0.117E-03	0.340E-03	0.345
0.1060	25.040	0.000	34.16	2.4550	1.4670	0.4980	-1.3090	0.2030	-0.6470	-1.552	0.131	0.900	9283.3	-750.9	0.141E-03	0.270E-03	0.522
0.1160	25.510	-0.060	34.10	2.3850	1.4010	0.5020	-1.2870	0.2030	-0.6520	-1.418	0.130	0.901	5027.1	-671.2	0.256E-03	0.302E-03	0.846
0.1210	26.640	-0.070	34.07	2.4240	1.3590	0.5050	-1.3360	0.1980	-0.6680	-1.154	0.119	0.901	4704.6	-628.9	0.284E-03	0.315E-03	0.902
0.1300	26.080	-0.110	34.01	2.3540	1.2870	0.5010	-1.2570	0.2110	-0.6460	-1.167	0.115	0.898	2488.6	-651.9	0.505E-03	0.324E-03	1.561
0.1420	26.440	-0.080	33.93	2.3230	1.2720	0.5000	-1.3180	0.2090	-0.6610	-1.128	0.158	0.896	1171.9	-628.2	0.112E-02	0.333E-03	3.380
0.1600	27.030	-0.110	33.82	2.2740	1.1750	0.5070	-1.2590	0.2020	-0.6650	-0.970	0.114	0.896	2907.9	-554.0	0.433E-03	0.365E-03	1.187
0.1830	27.610	-0.130	33.72	2.2390	1.1460	0.5050	-1.2820	0.1990	-0.6730	-0.823	0.110	0.898	2580.7	-484.1	0.497E-03	0.411E-03	1.208
0.2050	28.210	-0.180	33.60	2.2220	1.0960	0.5150	-1.2230	0.2130	-0.7090	-0.803	0.103	0.887	2227.6	-424.7	0.549E-03	0.502E-03	1.095
0.2330	28.710	-0.200	33.50	2.1360	1.0450	0.5200	-1.1510	0.2040	-0.7100	-0.793	0.106	0.892	1933.5	-385.2	0.595E-03	0.530E-03	1.124
0.2510	29.050	-0.200	33.44	2.0670	1.0230	0.5180	-1.0980	0.2080	-0.6750	-0.841	0.131	0.895	1710.0	-348.1	0.642E-03	0.598E-03	1.074
0.2880	29.650	-0.270	33.31	2.0090	0.9700	0.5370	-1.0040	0.2250	-0.6940	-0.751	0.136	0.900	1496.2	-337.4	0.671E-03	0.667E-03	1.006
0.3350	30.290	-0.290	33.15	1.8450	0.9440	0.5310	-0.9400	0.2220	-0.6370	-0.864	0.180	0.901	1150.5	-297.7	0.817E-03	0.746E-03	1.096
0.3650	30.540	-0.320	33.07	1.7900	0.8690	0.5320	-0.8390	0.2020	-0.6230	-0.693	0.145	0.890	966.2	-260.3	0.868E-03	0.776E-03	1.119
0.3970	30.860	-0.330	32.99	1.7270	0.8550	0.5290	-0.8580	0.2220	-0.6050	-0.783	0.173	0.873	798.0	-221.3	0.108E-02	0.100E-02	1.072
0.4350	31.110	-0.360	32.92	1.6560	0.8260	0.5310	-0.7350	0.2080	-0.5840	-0.670	0.164	0.856	714.6	-197.9	0.103E-02	0.105E-02	0.979
0.4690	31.330	-0.360	32.86	1.5660	0.8190	0.5220	-0.7380	0.2200	-0.5440	-0.689	0.175	0.835	614.0	-185.6	0.120E-02	0.119E-02	1.014
0.5360	31.720	-0.430	32.73	1.3870	0.7770	0.5060	-0.6250	0.2090	-0.4690	-0.629	0.190	0.776	513.3	-173.2	0.122E-02	0.121E-02	1.009
0.5850	31.950	-0.440	32.64	1.2970	0.7330	0.4690	-0.5560	0.1890	-0.3970	-0.553	0.165	0.717	425.4	-149.7	0.131E-02	0.126E-02	1.035
0.6690	32.240	-0.500	32.54	1.1190	0.6980	0.4330	-0.4290	0.1650	-0.3080	-0.414	0.132	0.646	300.2	-109.5	0.143E-02	0.151E-02	0.949
0.7440	32.390	-0.490	32.49	1.0370	0.6990	0.4150	-0.4210	0.1660	-0.2720	-0.458	0.157	0.579	225.5	-84.0	0.187E-02	0.198E-02	0.945
0.8950	32.660	-0.550	32.37	0.8180	0.6690	0.3420	-0.2840	0.1300	-0.1560	-0.309	0.122	0.429	146.8	-59.2	0.194E-02	0.220E-02	0.881
1.0310	32.800	-0.620	32.32	0.7020	0.6770	0.2950	-0.2220	0.1130	-0.1090	-0.230	0.106	0.335	112.1	-46.6	0.198E-02	0.242E-02	0.817
1.5310	33.090	-0.740	32.20	0.4930	0.6650	0.1630	-0.0760	0.0470	-0.0180	-0.066	0.041	0.158	-962.1	-1055.7	-.790E-04	0.445E-04	*****

Station 10 dU/dx=29s-1
x = 33.9400 cm, qwall = 372.000 W/m2

y	U	V	T	u'	v'	t'	u'v'	v't'	u't'	u'v'2	v'2t'	gamma	dU/dy	dT/dy	em	eh	Prt
0.0560	22.340	-3.370	34.68	2.1450	1.7360	0.4750	-1.9670	0.2880	-0.4960	-1.943	0.156	0.888	9264.9	3.8	0.212E-03	-.749E-01	-.003
0.0650	23.710	-2.850	34.65	2.3000	1.7550	0.4870	-2.2150	0.3220	-0.6090	-1.975	0.225	0.887	18319.9	-559.3	0.121E-03	0.576E-03	0.210
0.0720	25.520	-1.200	34.59	2.4380	1.6440	0.4760	-1.7200	0.2530	-0.6260	-2.060	0.162	0.883	15136.8	-706.7	0.114E-03	0.358E-03	0.317
0.0830	26.740	-0.560	34.50	2.5000	1.4900	0.4830	-1.4130	0.2250	-0.6360	-1.949	0.201	0.887	11154.9	-836.8	0.127E-03	0.269E-03	0.471
0.0930	27.220	-0.560	34.41	2.4360	1.4110	0.4710	-1.4410	0.2030	-0.6080	-1.398	0.133	0.878	6534.4	-804.1	0.221E-03	0.252E-03	0.874
0.1140	28.300	-0.670	34.25	2.3480	1.2660	0.4780	-1.3400	0.2020	-0.6230	-1.065	0.104	0.873	4037.3	-675.7	0.332E-03	0.299E-03	1.110
0.1280	28.680	-0.690	34.18	2.3270	1.2600	0.4750	-1.3900	0.2070	-0.6580	-1.258	0.148	0.861	3501.8	-589.3	0.397E-03	0.351E-03	1.130
0.1480	29.310	-0.690	34.06	2.3030	1.1770	0.4880	-1.4050	0.2120	-0.6660	-1.062	0.141	0.871	2750.6	-505.4	0.511E-03	0.419E-03	1.218
0.1670	29.810	-0.760	33.98	2.2450	1.1380	0.4800	-1.3850	0.2050	-0.6450	-1.054	0.117	0.875	2556.1	-473.1	0.542E-03	0.433E-03	1.250
0.1990	30.500	-0.840	33.84	2.1680	1.0640	0.4950	-1.2410	0.2070	-0.6550	-0.800	0.107	0.881	2079.7	-402.3	0.597E-03	0.515E-03	1.160
0.2170	30.930	-0.870	33.76	2.1200	1.0330	0.5060	-1.2200	0.2180	-0.6690	-0.843	0.123	0.885	1885.2	-380.9	0.647E-03	0.572E-03	1.131
0.2550	31.490	-0.910	33.64	2.0550	0.9800	0.5200	-1.1270	0.2140	-0.7010	-0.821	0.136	0.879	1497.5	-324.0	0.753E-03	0.660E-03	1.140
0.2920	32.020	-0.960	33.53	1.9160	0.9600	0.5110	-1.0580	0.2250	-0.6390	-0.898	0.162	0.874	1232.5	-296.9	0.858E-03	0.758E-03	1.133
0.3140	32.230	-0.970	33.46	1.8960	0.9450	0.5260	-1.0570	0.2250	-0.6540	-0.843	0.163	0.875	1109.6	-281.0	0.953E-03	0.801E-03	1.190
0.3580	32.700	-1.030	33.34	1.7850	0.9120	0.5230	-0.9960	0.2360	-0.6160	-0.913	0.180	0.880	880.8	-250.9	0.113E-02	0.940E-03	1.202
0.3930	32.930	-1.050	33.27	1.7390	0.8760	0.5230	-0.9240	0.2310	-0.6170	-0.828	0.181	0.857	792.5	-226.5	0.117E-02	0.102E-02	1.143
0.4410	33.290	-1.100	33.16	1.6440	0.8330	0.5130	-0.8730	0.2210	-0.5620	-0.861	0.199	0.825	652.5	-199.4	0.134E-02	0.111E-02	1.207
0.5110	33.720	-1.160	33.03	1.4390	0.7980	0.4940	-0.7210	0.2240	-0.4810	-0.729	0.193	0.777	520.8	-170.8	0.138E-02	0.131E-02	1.056
0.5540	33.900	-1.200	32.97	1.3420	0.7740	0.4820	-0.6380	0.2050	-0.4270	-0.690	0.193	0.737	438.9	-149.9	0.145E-02	0.137E-02	1.063
0.6400	34.190	-1.230	32.85	1.1620	0.7450	0.4490	-0.5270	0.1870	-0.3320	-0.563	0.168	0.674	312.9	-118.8	0.168E-02	0.157E-02	1.070
0.7070	34.400	-1.310	32.78	1.0250	0.6910	0.4170	-0.4100	0.1600	-0.2700	-0.431	0.146	0.602	253.2	-99.5	0.162E-02	0.161E-02	1.008
0.8420	34.640	-1.370	32.68	0.8560	0.6850	0.3630	-0.3200	0.1440	-0.1860	-0.378	0.139	0.489	174.3	-69.7	0.184E-02	0.206E-02	0.889
0.9230	34.740	-1.420	32.63	0.7840	0.7070	0.3430	-0.2880	0.1380	-0.1550	-0.380	0.154	0.406	134.9	-57.6	0.213E-02	0.240E-02	0.891
1.4230	35.140	-1.600	32.48	0.4990	0.6670	0.1940	-0.0890	0.0620	-0.0310	-0.103	0.068	0.180	-1214.4	-1282.7	-.733E-04	0.483E-04	*****

$dU_{cw}/dx=14s^{-1}$ CASE DATA

	Page
Single Hot-Wire Profiles	597
Mean Temperature Profiles	607
Cross-Wire Profiles	618
Triple-Wire Profiles	623

Station = 1 dU/dx=14s-1

patm = 754.380 temp = 27.2056
x = 9.93000 visc = 1.58857E-05
cf = 7.20000E-03 yeff = 1.00000E-03
d99.5 = 1.60950 del1 = 1.00301E-01
del2 = 6.64509E-02 H = 1.50940
Ue = 6.56151 Rex = 41015.3
Red1 = 414.288 Red2 = 274.472
coef1 = 6.56151 coef2 = 4.82823E-02
A+ = 52.8360
K = 5.29482E-06 f1 = -2.55824E-05

N	y	U	y+	u+	u'	gamma
1	1.00000E-03	1.0000E-10	0.247827	2.54E-10	0.236234	2.66110E-02
2	1.50000E-03	1.0000E-10	0.371740	2.54E-10	0.250820	2.61230E-02
3	2.00000E-03	1.0000E-10	0.495653	2.54E-10	0.252425	3.07620E-02
4	2.50000E-03	1.0000E-10	0.619566	2.54E-10	0.252690	3.02730E-02
5	3.00000E-03	2.5233E-02	0.743480	6.41E-02	0.259447	2.73440E-02
6	3.50000E-03	0.185117	0.867393	0.470210	0.275501	3.34470E-02
7	4.50000E-03	0.384755	1.11522	0.977301	0.297015	3.97950E-02
8	6.50000E-03	0.623719	1.61087	1.58429	0.319088	3.66210E-02
9	1.05000E-02	1.09450	2.60218	2.78009	0.401138	4.56540E-02
10	1.35000E-02	1.41078	3.34566	3.58348	0.479886	4.88280E-02
11	1.60000E-02	1.61433	3.96523	4.10050	0.502847	5.68850E-02
12	1.95000E-02	1.90996	4.83262	4.85143	0.583162	6.86040E-02
13	2.25000E-02	2.08689	5.57610	5.30083	0.612155	7.03120E-02
14	2.65000E-02	2.32947	6.56740	5.91701	0.659797	9.27730E-02
15	3.05000E-02	2.59583	7.55871	6.59358	0.699414	1.01074E-01
16	3.35000E-02	2.81527	8.30219	7.15098	0.727426	0.109619
17	3.65000E-02	2.98133	9.04567	7.57276	0.758423	0.130615
18	4.05000E-02	3.17324	10.03698	8.06023	0.772245	0.131836
19	4.50000E-02	3.41164	11.1522	8.66579	0.796774	0.150879
20	4.90000E-02	3.59322	12.1435	9.12701	0.811078	0.164062
21	5.35000E-02	3.78804	13.2587	9.62186	0.805834	0.177490
22	5.85000E-02	4.01654	14.4979	10.20226	0.809811	0.201172
23	6.30000E-02	4.14269	15.6131	10.52271	0.823214	0.203613
24	7.10000E-02	4.40004	17.5957	11.1764	0.798991	0.226807
25	7.75000E-02	4.56141	19.2066	11.5863	0.809597	0.224609
26	8.60000E-02	4.80704	21.3131	12.2102	0.774132	0.262695
27	9.30000E-02	4.90361	23.0479	12.4555	0.770001	0.272461
28	0.107500	5.12721	26.6414	13.0234	0.738491	0.290527
29	0.121000	5.31888	29.9870	13.5103	0.691511	0.309082
30	0.136000	5.46497	33.7044	13.8814	0.674703	0.315918
31	0.157500	5.65053	39.0327	14.3527	0.639281	0.335449
32	0.182000	5.75784	45.1044	14.6253	0.592588	0.348633
33	0.230000	5.95904	57.0001	15.1364	0.560828	0.330566
34	0.279000	6.09443	69.1436	15.4803	0.525844	0.332031
35	0.355000	6.21128	87.9784	15.7771	0.494234	0.299072
36	0.489500	6.35609	121.311	16.1449	0.453713	0.237793
37	0.682500	6.43924	169.142	16.3561	0.425112	0.190186
38	1.06900	6.54893	264.927	16.6347	0.397521	0.128418
39	1.56900	6.60186	388.840	16.7692	0.375901	0.129150
40	2.06900	6.65807	512.753	16.9119	0.364204	0.118408
41	2.56900	6.70004	636.667	17.0185	0.361092	0.131104
42	3.06900	6.71015	760.580	17.0442	0.359795	0.120850
43	3.56900	6.72694	884.493	17.0869	0.357934	0.131104
44	4.06900	6.72881	1008.41	17.0916	0.362790	0.129150

Station = 2 dU/dx=14s-1

patm = 754.634 temp = 27.1873
x = 18.9500 visc = 1.58787E-05
cf = 6.40000E-03 yeff = 3.00000E-03
d99.5 = 0.808502 del1 = 7.22274E-02
del2 = 4.26881E-02 H = 1.69198
Uw = 7.70834 Rex = 91993.2
Red1 = 350.630 Red2 = 207.230
coef1 = 7.70834 coef2 = 0.110832
A+ = 63.6017
K = 3.83482E-06 f1 = -1.90351E-05

N	y	U	y+	u+	u'	gamma
1	3.00000E-03	0.188008	0.823840	0.431162	0.186917	1.78220E-02
2	3.50000E-03	0.271067	0.961146	0.621644	0.193916	1.95310E-02
3	4.00000E-03	0.348674	1.09845	0.799620	0.199343	2.17290E-02
4	4.50000E-03	0.424386	1.23576	0.973252	0.212489	2.05080E-02
5	5.00000E-03	0.491694	1.37307	1.12761	0.239094	2.46580E-02
6	5.50000E-03	0.563267	1.51037	1.29175	0.250025	2.51460E-02
7	6.50000E-03	0.705121	1.78499	1.61707	0.274644	2.88090E-02
8	8.50000E-03	0.945709	2.33421	2.16881	0.316925	2.80760E-02
9	1.20000E-02	1.44250	3.29536	3.30810	0.420134	3.46680E-02
10	1.45000E-02	1.72444	3.98189	3.95469	0.473719	4.24800E-02
11	1.75000E-02	2.04202	4.80573	4.68300	0.550233	4.63870E-02
12	2.00000E-02	2.26117	5.49226	5.18559	0.608287	5.90820E-02
13	2.35000E-02	2.61529	6.45341	5.99770	0.669881	6.15230E-02
14	2.60000E-02	2.82458	7.13994	6.47766	0.724715	7.08010E-02
15	2.95000E-02	3.16498	8.10109	7.25830	0.763446	7.66600E-02
16	3.20000E-02	3.34849	8.78762	7.67915	0.802954	9.20410E-02
17	3.60000E-02	3.67165	9.88608	8.42027	0.836151	1.00342E-01
18	3.90000E-02	3.94012	10.7099	9.03595	0.888218	0.110840
19	4.20000E-02	4.14096	11.5338	9.49654	0.884294	0.114258
20	4.55000E-02	4.34323	12.4949	9.96040	0.913231	0.122559
21	5.05000E-02	4.63408	13.8680	10.6274	0.923656	0.146240
22	5.45000E-02	4.83125	14.9664	11.0796	0.944216	0.145996
23	6.00000E-02	5.09874	16.4768	11.6930	0.936126	0.161865
24	6.50000E-02	5.30450	17.8499	12.1649	0.947325	0.178223
25	7.15000E-02	5.54408	19.6348	12.7143	0.935560	0.186768
26	7.85000E-02	5.77944	21.5571	13.2541	0.891418	0.213379
27	8.60000E-02	5.99580	23.6167	13.7503	0.898894	0.231934
28	9.50000E-02	6.18877	26.0883	14.1928	0.855767	0.240234
29	0.107000	6.43858	29.3836	14.7657	0.812593	0.249756
30	0.119000	6.57128	32.6790	15.0700	0.792480	0.272949
31	0.142500	6.82750	39.1324	15.6576	0.717533	0.290527
32	0.165500	6.97104	45.4485	15.9868	0.661497	0.310303
33	0.206500	7.19484	56.7076	16.5001	0.574449	0.306152
34	0.253000	7.33089	69.4771	16.8121	0.522118	0.300781
35	0.339500	7.48893	93.2312	17.1745	0.459718	0.291016
36	0.478000	7.61513	131.265	17.4639	0.409049	0.251709
37	0.754000	7.74713	207.058	17.7666	0.356755	0.189209
38	1.25400	7.85971	344.365	18.0248	0.333179	0.155273
39	1.75400	7.90379	481.672	18.1259	0.317799	0.141846
40	2.25400	7.96322	618.978	18.2622	0.317670	0.138916
41	2.75400	8.02032	756.285	18.3931	0.313171	0.133301
42	3.25400	8.06899	893.591	18.5048	0.308899	0.152832
43	3.75400	8.11064	1030.90	18.6003	0.312914	0.142334
44	4.25400	8.15784	1168.20	18.7085	0.306270	0.154297

Station = 3 dU/dx=14s-1

patm = 754.888 temp = 27.1590
x = 26.0700 visc = 1.58707E-05
cf = 6.10000E-03 yeff = 1.00000E-03
d99.5 = 0.902575 del1 = 7.02895E-02
del2 = 4.33282E-02 H = 1.62226
Ue = 8.73825 Rex = 143539.
Red1 = 387.008 Red2 = 238.561
coef1 = 8.73825 coef2 = 0.125624
A+ = 60.0372
K = 2.98263E-06 f1 = -3.41213E-06

N	y	U	y+	u+	u'	gamma
1	1.00000E-03	1.000E-10	0.304074	2.072E-10	0.219575	4.22360E-02
2	1.50000E-03	1.000E-10	0.456111	2.072E-10	0.210693	3.51560E-02
3	2.00000E-03	1.000E-10	0.608147	2.072E-10	0.219253	4.51660E-02
4	2.50000E-03	9.906E-02	0.760184	0.205263	0.228440	4.24800E-02
5	3.00000E-03	0.236996	0.912221	0.491097	0.237691	4.68750E-02
6	3.50000E-03	0.344450	1.06426	0.713760	0.255161	4.78520E-02
7	4.50000E-03	0.549137	1.36833	1.13791	0.316811	4.90720E-02
8	6.50000E-03	0.867413	1.97648	1.79743	0.363082	5.41990E-02
9	1.00000E-02	1.48829	3.04074	3.08399	0.474776	6.98240E-02
10	1.25000E-02	1.87272	3.80092	3.88059	0.553327	7.10450E-02
11	1.50000E-02	2.22367	4.56111	4.60783	0.623548	8.56930E-02
12	1.75000E-02	2.56018	5.32129	5.30513	0.710031	9.69240E-02
13	1.95000E-02	2.80826	5.92944	5.81919	0.749898	9.64360E-02
14	2.25000E-02	3.19808	6.84166	6.62697	0.832245	0.107422
15	2.45000E-02	3.39878	7.44980	7.04286	0.876996	0.117188
16	2.80000E-02	3.76925	8.51406	7.81053	0.941504	0.134766
17	3.10000E-02	4.10295	9.42628	8.50201	0.977672	0.149170
18	3.35000E-02	4.32939	10.18647	8.97124	1.01965	0.147705
19	3.70000E-02	4.61701	11.2507	9.56723	1.05982	0.165771
20	4.05000E-02	4.88021	12.3150	10.11263	1.07122	0.177490
21	4.45000E-02	5.16398	13.5313	10.7007	1.08110	0.181885
22	4.85000E-02	5.42421	14.7476	11.2399	1.08538	0.199951
23	5.30000E-02	5.67236	16.1159	11.7541	1.10314	0.212646
24	5.85000E-02	5.97635	17.7883	12.3840	1.09118	0.219238
25	6.35000E-02	6.20606	19.3087	12.8600	1.07401	0.229492
26	7.00000E-02	6.41344	21.2852	13.2897	1.07224	0.241943
27	7.95000E-02	6.77638	24.1739	14.0418	1.04506	0.278564
28	8.70000E-02	6.98088	26.4544	14.4656	1.02225	0.287842
29	9.75000E-02	7.23760	29.6472	14.9976	0.967444	0.288818
30	0.109500	7.41130	33.2961	15.3575	0.916158	0.319580
31	0.130000	7.71750	39.5296	15.9920	0.856507	0.324463
32	0.149500	7.88459	45.4590	16.3382	0.779596	0.344238
33	0.183000	8.05685	55.6455	16.6952	0.702985	0.362793
34	0.239500	8.24730	72.8256	17.0898	0.578748	0.346680
35	0.325500	8.46364	98.9760	17.5381	0.466230	0.326660
36	0.440500	8.62020	133.944	17.8625	0.404545	0.280273
37	0.650000	8.72836	197.648	18.0867	0.347394	0.225342
38	1.06900	8.86038	325.055	18.3602	0.311863	0.181641
39	1.56900	8.92873	477.092	18.5019	0.291439	0.164551
40	2.06900	9.00335	629.128	18.6565	0.289598	0.159180
41	2.56900	9.05822	781.165	18.7702	0.283472	0.164551
42	3.06900	9.12363	933.202	18.9057	0.280972	0.165527
43	3.56900	9.17354	1085.24	19.0091	0.291831	0.172607

Station = 4 dU/dx=14s-1

patm = 752.983 temp = 28.1081
x = 34.4900 visc = 1.60002E-05
cf = 6.20000E-03 yeff = -1.50000E-03
d99.5 = 0.627761 del1 = 5.72847E-02
del2 = 3.43923E-02 H = 1.66563
Uw = 10.25741 Rex = 221109.
Red1 = 367.242 Red2 = 220.483
coef1 = 10.25741 coef2 = 0.112224
A+ = 50.0395
K = 2.18223E-06 f1 = -8.63461E-06

N	y	U	y+	u+	u'	gamma
1	5.00000E-04	1.000E-10	0.178470	1.751E-10	0.295802	0.168213
2	1.00000E-03	1.000E-10	0.356939	1.751E-10	0.315930	0.180176
3	2.00000E-03	1.000E-10	0.713878	1.751E-10	0.375619	0.210449
4	4.00000E-03	0.750386	1.42776	1.31391	0.439589	0.237549
5	7.00000E-03	1.52943	2.49857	2.67801	0.580989	0.265625
6	9.00000E-03	1.93382	3.21245	3.38608	0.634183	0.292236
7	1.20000E-02	2.59101	4.28327	4.53681	0.770654	0.311035
8	1.40000E-02	2.91077	4.99715	5.09670	0.845669	0.328125
9	1.65000E-02	3.38107	5.88949	5.92020	0.938526	0.367920
10	1.85000E-02	3.64335	6.60337	6.37943	0.974486	0.357422
11	2.20000E-02	4.19219	7.85266	7.34045	1.08080	0.398438
12	2.40000E-02	4.44946	8.56654	7.79091	1.11407	0.411377
13	2.70000E-02	4.86265	9.63735	8.51440	1.18599	0.422363
14	2.95000E-02	5.16180	10.52970	9.03821	1.20211	0.445312
15	3.25000E-02	5.52498	11.6005	9.67413	1.24425	0.458008
16	3.55000E-02	5.87164	12.6713	10.28112	1.23961	0.459229
17	3.80000E-02	6.05952	13.5637	10.6101	1.28122	0.460449
18	4.30000E-02	6.48349	15.3484	11.3525	1.28102	0.457764
19	4.70000E-02	6.73247	16.7761	11.7884	1.27518	0.480469
20	5.30000E-02	7.16380	18.9178	12.5437	1.28008	0.495605
21	5.75000E-02	7.37189	20.5240	12.9080	1.28166	0.494141
22	6.50000E-02	7.78055	23.2010	13.6236	1.25205	0.502930
23	7.10000E-02	8.04438	25.3427	14.0856	1.23315	0.517334
24	7.90000E-02	8.30049	28.1982	14.5340	1.18610	0.520508
25	8.95000E-02	8.56955	31.9460	15.0051	1.14246	0.533691
26	1.02500E-01	8.86188	36.5862	15.5170	1.05475	0.540771
27	0.117500	9.06282	41.9403	15.8688	1.00238	0.525146
28	0.143000	9.38756	51.0423	16.4374	0.882537	0.536133
29	0.169500	9.56861	60.5012	16.7545	0.812790	0.520996
30	0.218500	9.78072	77.9912	17.1259	0.679093	0.496094
31	0.297000	9.95370	106.011	17.4287	0.547665	0.452881
32	0.449000	10.16566	160.266	17.7999	0.411854	0.372314
33	0.688500	10.31427	245.752	18.0601	0.323805	0.260498
34	1.16800	10.40685	416.905	18.2222	0.277208	0.182373
35	1.66800	10.43962	595.374	18.2796	0.270328	0.170654
36	2.16800	10.49112	773.844	18.3697	0.261050	0.170410
37	2.66800	10.55716	952.313	18.4854	0.258419	0.167969
38	3.16800	10.6074	1130.78	18.5733	0.259530	0.177979

Station = 5 dU/dx=14s-1

patm = 752.983 temp = 28.0128
x = 42.3100 visc = 1.59912E-05
cf = 5.50000E-03 yeff = -1.25000E-03
d99.5 = 0.653143 del1 = 5.94947E-02
del2 = 3.57768E-02 H = 1.66294
Uw = 11.5785 Rex = 306346.
Red1 = 430.772 Red2 = 259.043
coef1 = 11.5785 coef2 = 0.139585
A+ = 43.9040
K = 1.71171E-06 f1 = -1.33140E-05

N	y	U	y+	u+	u'	gamma
1	2.50000E-04	1.000E-10	9.492E-02	1.647E-10	0.335371	0.273926
2	7.50000E-04	1.000E-10	0.284772	1.647E-10	0.358443	0.297852
3	1.25000E-03	1.000E-10	0.474620	1.647E-10	0.373330	0.287354
4	2.25000E-03	1.000E-10	0.854316	1.647E-10	0.444673	0.322266
5	4.25000E-03	0.808755	1.61371	1.33199	0.509391	0.344727
6	8.25000E-03	1.85234	3.13249	3.05073	0.702171	0.402344
7	1.02500E-02	2.32856	3.89188	3.83504	0.810810	0.417725
8	1.27500E-02	2.85787	4.84112	4.70679	0.920747	0.433105
9	1.47500E-02	3.23292	5.60052	5.32449	1.01260	0.449219
10	1.72500E-02	3.78634	6.54975	6.23595	1.11130	0.488037
11	1.92500E-02	4.04557	7.30915	6.66288	1.18975	0.498047
12	2.22500E-02	4.67295	8.44823	7.69615	1.26562	0.511230
13	2.42500E-02	4.87813	9.20763	8.03407	1.28319	0.518555
14	2.82500E-02	5.42545	10.7264	8.93549	1.36135	0.544922
15	3.07500E-02	5.84546	11.6757	9.62723	1.40629	0.563965
16	3.32500E-02	6.16526	12.6249	10.15393	1.41621	0.561768
17	3.62500E-02	6.54190	13.7640	10.7742	1.42330	0.573975
18	3.92500E-02	6.89038	14.9031	11.3482	1.45135	0.581543
19	4.27500E-02	7.25080	16.2320	11.9418	1.46237	0.604736
20	4.62500E-02	7.51999	17.5609	12.3851	1.47189	0.599854
21	5.12500E-02	7.93598	19.4594	13.0702	1.45195	0.622314
22	5.57500E-02	8.26877	21.1680	13.6183	1.44436	0.621582
23	6.07500E-02	8.56625	23.0665	14.1083	1.41052	0.621094
24	6.72500E-02	8.93287	25.5346	14.7121	1.36822	0.641113
25	7.42500E-02	9.15018	28.1924	15.0700	1.36429	0.636719
26	8.62500E-02	9.60794	32.7488	15.8239	1.27960	0.659668
27	9.62500E-02	9.90570	36.5457	16.3143	1.19790	0.643555
28	0.108750	10.08637	41.2919	16.6118	1.13498	0.654053
29	0.134250	10.42580	50.9742	17.1709	1.02279	0.644531
30	0.162250	10.6908	61.6057	17.6073	0.902766	0.631592
31	0.202250	10.9268	76.7935	17.9960	0.757287	0.617676
32	0.265750	11.1228	100.9042	18.3188	0.636094	0.580322
33	0.386750	11.4002	146.847	18.7757	0.492942	0.482910
34	0.548750	11.5694	208.358	19.0543	0.368549	0.382812
35	0.872750	11.7008	331.380	19.2707	0.290979	0.250977
36	1.37275	11.7712	521.228	19.3866	0.248731	0.198486
37	1.87275	11.8352	711.075	19.4922	0.250835	0.200684
38	2.37275	11.8912	900.924	19.5843	0.244276	0.206787
39	2.87275	11.9790	1090.77	19.7288	0.248489	0.200439
40	3.37275	12.0548	1280.62	19.8538	0.255050	0.219238

Station = 6 dU/dx=14s-1

patm = 752.856 temp = 27.8316
x = 50.3300 visc = 1.59768E-05
cf = 5.30000E-03 yeff = -1.75000E-03
d99.5 = 0.629282 del1 = 6.55674E-02
del2 = 4.09510E-02 H = 1.60112
Uw = 12.5293 Rex = 394696.
Red1 = 514.190 Red2 = 321.145
coef1 = 12.5293 coef2 = 0.203367
A+ = 40.1746
K = 1.46046E-06 f1 = 5.02364E-06

N	y	U	y+	u+	u'	gamma
1	2.50000E-04	1.000E-10	1.01E-01	1.55E-10	0.471187	0.559814
2	7.50000E-04	1.000E-10	0.302775	1.55E-10	0.514292	0.577637
3	1.75000E-03	1.000E-10	0.706475	1.55E-10	0.579371	0.586426
4	3.75000E-03	0.725983	1.51388	1.12558	0.666879	0.615967
5	7.25000E-03	1.87176	2.92683	2.90201	0.931694	0.657715
6	8.75000E-03	2.27514	3.53238	3.52743	1.02361	0.661377
7	1.17500E-02	3.08989	4.74348	4.79063	1.17694	0.688477
8	1.37500E-02	3.42969	5.55088	5.31747	1.24164	0.689941
9	1.72500E-02	4.23326	6.96383	6.56334	1.42995	0.715088
10	1.92500E-02	4.57152	7.77123	7.08779	1.44677	0.732178
11	2.22500E-02	5.13875	8.98233	7.96723	1.56280	0.730469
12	2.42500E-02	5.45451	9.78973	8.45679	1.56913	0.746582
13	2.72500E-02	5.93960	11.0008	9.20889	1.62483	0.753174
14	2.97500E-02	6.31140	12.0101	9.78533	1.62942	0.758301
15	3.27500E-02	6.70549	13.2212	10.39634	1.67747	0.771973
16	3.62500E-02	7.08773	14.6341	10.9890	1.67415	0.779297
17	4.02500E-02	7.48129	16.2489	11.5992	1.65671	0.781494
18	4.42500E-02	7.86480	17.8637	12.1938	1.63306	0.785156
19	4.87500E-02	8.18110	19.6804	12.6842	1.59035	0.788330
20	5.47500E-02	8.58669	22.1026	13.3130	1.59751	0.796143
21	6.12500E-02	9.00027	24.7266	13.9542	1.56927	0.795898
22	6.77500E-02	9.31941	27.3507	14.4490	1.55274	0.806396
23	7.62500E-02	9.65932	30.7821	14.9760	1.50251	0.800781
24	8.67500E-02	9.99628	35.0210	15.4984	1.41831	0.811768
25	9.97500E-02	10.39200	40.2691	16.1120	1.36052	0.799316
26	0.113250	10.6449	45.7191	16.5040	1.30972	0.806396
27	0.135750	10.9868	54.8023	17.0342	1.19973	0.802002
28	0.162750	11.2898	65.7022	17.5040	1.07932	0.790283
29	0.199250	11.5572	80.4373	17.9185	0.972469	0.762695
30	0.256250	11.8912	103.4482	18.4364	0.806924	0.710938
31	0.326250	12.1105	131.707	18.7763	0.685603	0.682617
32	0.457250	12.4317	184.592	19.2743	0.482556	0.546143
33	0.624750	12.5924	252.212	19.5235	0.368416	0.416992
34	0.874750	12.7176	353.137	19.7176	0.297511	0.316162
35	1.12475	12.7848	454.062	19.8219	0.261173	0.247559
36	1.37475	12.8342	554.987	19.8984	0.249844	0.224609
37	1.62475	12.8704	655.912	19.9546	0.240873	0.217529
38	1.87475	12.9091	756.837	20.0146	0.234912	0.213867
39	2.12475	12.9596	857.762	20.0928	0.236598	0.206543
40	2.37475	13.0033	958.687	20.1606	0.238380	0.218262
41	2.62475	13.0527	1059.61	20.2372	0.237177	0.214844
42	2.87475	13.1019	1160.54	20.3135	0.241095	0.220215

Station = 7 dU/dx=14s-1

patm = 752.856 temp = 27.7081
x = 58.0500 visc = 1.59652E-05
cf = 5.85000E-03 yeff = -1.00000E-03
d99.5 = 0.752726 del1 = 7.11703E-02
del2 = 4.80800E-02 H = 1.48025
Uw = 13.6027 Rex = 494598.
Red1 = 606.385 Red2 = 409.651
coef1 = 13.6027 coef2 = 0.212817
A+ = 35.4068
K = 1.23816E-06 f1 = 8.50668E-06

N	y	U	y+	u+	u'	gamma
1	5.00000E-04	1.000E-10	0.230400	1.36E-10	0.650892	0.813965
2	1.00000E-03	1.000E-10	0.460800	1.36E-10	0.667700	0.802734
3	1.50000E-03	1.000E-10	0.691201	1.36E-10	0.694491	0.797852
4	2.50000E-03	0.411279	1.15200	0.560047	0.765315	0.818115
5	4.00000E-03	1.31470	1.84320	1.78706	0.865427	0.821045
6	6.50000E-03	2.28741	2.99520	3.10926	1.03396	0.834473
7	8.50000E-03	2.85651	3.91680	3.88282	1.14671	0.845703
8	1.15000E-02	3.92627	5.29921	5.33695	1.33929	0.874512
9	1.30000E-02	4.26293	5.99041	5.79456	1.39736	0.863525
10	1.60000E-02	5.06228	7.37281	6.88112	1.51475	0.877930
11	1.75000E-02	5.34072	8.06401	7.25960	1.56972	0.878418
12	2.10000E-02	6.11465	9.67681	8.31159	1.66400	0.889404
13	2.30000E-02	6.40240	10.5984	8.70273	1.67839	0.886475
14	2.70000E-02	7.01843	12.4416	9.54010	1.69849	0.897217
15	3.00000E-02	7.50316	13.8240	10.19898	1.73216	0.898438
16	3.25000E-02	7.84724	14.9760	10.6667	1.72565	0.911377
17	3.65000E-02	8.23040	16.8192	11.1875	1.69495	0.907471
18	4.15000E-02	8.67015	19.1232	11.7853	1.67472	0.911377
19	4.65000E-02	9.14269	21.4272	12.4276	1.65370	0.918945
20	5.15000E-02	9.43401	23.7312	12.8236	1.64232	0.908691
21	5.95000E-02	9.89118	27.4176	13.4450	1.56225	0.913574
22	6.75000E-02	10.27106	31.1040	13.9614	1.49343	0.913330
23	7.70000E-02	10.53471	35.4816	14.3197	1.44696	0.915771
24	9.35000E-02	10.9857	43.0848	14.9328	1.35553	0.909912
25	0.110500	11.2723	50.9185	15.3223	1.32066	0.906738
26	0.137000	11.6862	63.1297	15.8849	1.23184	0.900635
27	0.166000	12.0025	76.4929	16.3148	1.13030	0.889893
28	0.207500	12.3327	95.6161	16.7637	1.03781	0.876221
29	0.264500	12.6793	121.882	17.2348	0.918064	0.839355
30	0.337500	13.0226	155.520	17.7014	0.780698	0.786621
31	0.432500	13.2996	199.296	18.0781	0.640219	0.695801
32	0.585500	13.5617	269.799	18.4343	0.473619	0.546875
33	0.835500	13.7608	384.999	18.7049	0.330465	0.363037
34	1.08550	13.8423	500.199	18.8157	0.280562	0.295898
35	1.33550	13.8870	615.399	18.8764	0.255780	0.269043
36	1.58550	13.9432	730.599	18.9529	0.240648	0.240723
37	1.83550	13.9934	845.799	19.0212	0.237267	0.232422
38	2.08550	14.0451	960.999	19.0913	0.233443	0.244141
39	2.33550	14.1009	1076.20	19.1672	0.236462	0.229736
40	2.58550	14.1395	1191.40	19.2197	0.237623	0.237549
41	2.83550	14.2068	1306.60	19.3112	0.244219	0.240234

Station = 8 dU/dx=14s-1

patm = 752.983 temp = 27.6568
x = 65.8700 visc = 1.59577E-05
cf = 6.00000E-03 yeff = -4.00000E-03
d99.5 = 0.741104 del1 = 6.98292E-02
del2 = 4.84165E-02 H = 1.44226
Uw = 14.5629 Rex = 601127.
Red1 = 637.259 Red2 = 441.847
coef1 = 14.5629 coef2 = 0.283715
A+ = 32.4248
K = 1.07975E-06 f1 = 5.44235E-07

N	y	U	y+	u+	u'	gamma
1	1.50000E-03	1.000E-10	0.749774	1.25E-10	0.659731	0.895020
2	5.00000E-03	2.12896	2.49925	2.66906	0.968442	0.919922
3	6.50000E-03	2.74585	3.24902	3.44245	1.10070	0.924072
4	8.00000E-03	3.32362	3.99879	4.16679	1.20508	0.922607
5	1.00000E-02	4.02230	4.99849	5.04272	1.31308	0.924805
6	1.20000E-02	4.72423	5.99819	5.92273	1.44184	0.935547
7	1.40000E-02	5.27337	6.99789	6.61118	1.54546	0.937012
8	1.60000E-02	5.80326	7.99759	7.27550	1.60942	0.940186
9	1.85000E-02	6.48915	9.24721	8.13540	1.68226	0.947266
10	2.00000E-02	6.80835	9.99699	8.53557	1.70815	0.953857
11	2.30000E-02	7.41781	11.4965	9.29965	1.71086	0.952881
12	2.55000E-02	7.86395	12.7462	9.85897	1.75949	0.953125
13	2.85000E-02	8.30378	14.2457	10.41038	1.74481	0.957031
14	3.20000E-02	8.72625	15.9952	10.9400	1.75117	0.958252
15	3.65000E-02	9.21342	18.2445	11.5508	1.70769	0.963379
16	4.10000E-02	9.62910	20.4938	12.0719	1.71100	0.962646
17	4.70000E-02	10.06987	23.4929	12.6245	1.65633	0.958740
18	5.35000E-02	10.55569	26.7419	13.2336	1.57272	0.960449
19	6.05000E-02	10.8452	30.2409	13.5966	1.54518	0.960693
20	7.25000E-02	11.3395	36.2391	14.2163	1.43839	0.959961
21	8.45000E-02	11.6694	42.2373	14.6299	1.40195	0.957764
22	1.03000E-01	12.0505	51.4845	15.1076	1.29983	0.959229
23	0.126500	12.4224	63.2309	15.5739	1.25712	0.950684
24	0.158000	12.7842	78.9762	16.0274	1.15365	0.943604
25	0.200500	13.1664	100.2198	16.5066	1.06218	0.934814
26	0.254500	13.5117	127.212	16.9395	0.981744	0.912842
27	0.331000	13.8540	165.450	17.3686	0.864863	0.871338
28	0.439500	14.2384	219.684	17.8506	0.704741	0.775391
29	0.576000	14.5277	287.913	18.2133	0.570499	0.644043
30	0.804000	14.7661	401.879	18.5122	0.372477	0.451904
31	1.05400	14.8795	526.841	18.6543	0.288489	0.328369
32	1.30400	14.9428	651.804	18.7336	0.254076	0.286133
33	1.55400	15.0057	776.766	18.8125	0.237156	0.254395
34	1.80400	15.0616	901.728	18.8826	0.227904	0.256592

Station = 9 dU/dx=14s-1

patm = 753.364 temp = 27.5726
x = 73.5300 visc = 1.59417E-05
cf = 5.90000E-03 yeff = -6.00000E-03
d99.5 = 0.763479 del1 = 7.65738E-02
del2 = 5.39834E-02 H = 1.41847
Uw = 15.4032 Rex = 710463.
Red1 = 739.873 Red2 = 521.599
coef1 = 15.4032 coef2 = 0.400854
A+ = 30.9576
K = 9.64193E-07 f1 = -2.04676E-06

N	y	U	y+	u+	u'	gamma
1	3.50000E-03	1.47342	1.83677	1.76118	0.905077	0.956787
2	6.00000E-03	2.76265	3.14876	3.30219	1.10765	0.959473
3	7.50000E-03	3.38065	3.93595	4.04090	1.25927	0.964844
4	9.00000E-03	4.10204	4.72313	4.90317	1.37182	0.969727
5	1.05000E-02	4.63907	5.51032	5.54508	1.46792	0.968262
6	1.30000E-02	5.43920	6.82230	6.50148	1.57741	0.966797
7	1.50000E-02	5.96444	7.87189	7.12931	1.64400	0.977295
8	1.75000E-02	6.75061	9.18387	8.06902	1.73733	0.974365
9	1.95000E-02	7.12189	10.23346	8.51281	1.73641	0.977539
10	2.25000E-02	7.84458	11.8078	9.37664	1.75963	0.981689
11	2.50000E-02	8.24200	13.1198	9.85168	1.80022	0.977783
12	2.85000E-02	8.75797	14.9566	10.46842	1.81082	0.983398
13	3.20000E-02	9.24825	16.7934	11.0545	1.77224	0.979004
14	3.60000E-02	9.64494	18.8925	11.5286	1.71572	0.984131
15	4.20000E-02	10.13734	22.0413	12.1172	1.72054	0.976807
16	4.85000E-02	10.6323	25.4524	12.7088	1.66077	0.978027
17	5.55000E-02	10.9905	29.1260	13.1370	1.58277	0.982666
18	6.65000E-02	11.4732	34.8987	13.7139	1.52384	0.975342
19	7.90000E-02	11.8763	41.4586	14.1958	1.43589	0.974365
20	9.55000E-02	12.2387	50.1177	14.6290	1.36771	0.976318
21	0.120000	12.6657	62.9751	15.1393	1.30517	0.970703
22	0.150000	13.0990	78.7189	15.6573	1.23306	0.971191
23	0.186500	13.5125	97.8738	16.1515	1.15978	0.966309
24	0.233000	13.9310	122.277	16.6518	1.09967	0.955078
25	0.290500	14.3302	152.452	17.1289	1.01682	0.929199
26	0.366000	14.7407	192.074	17.6195	0.892137	0.887939
27	0.462000	15.0711	242.454	18.0146	0.766540	0.819336
28	0.613500	15.4459	321.960	18.4625	0.569050	0.655029
29	0.825500	15.7093	433.216	18.7773	0.416330	0.475342
30	1.07550	15.8468	564.415	18.9418	0.319178	0.380859
31	1.32550	15.9559	695.613	19.0722	0.265006	0.312012
32	1.57550	16.0364	826.811	19.1684	0.242021	0.287598
33	1.82550	16.1206	958.009	19.2690	0.228434	0.265869

Station = 10 dU/dx=14s-1

patm = 753.491 temp = 27.6168
x = 81.6500 visc = 1.59432E-05
cf = 5.80000E-03 yeff = -4.00000E-03
d99.5 = 0.866667 del1 = 7.71431E-02
del2 = 5.54618E-02 H = 1.39092
Ue = 16.9264 Rex = 866855.
Red1 = 819.006 Red2 = 588.822
coef1 = 16.9264 coef2 = 0.409863
A+ = 30.0108
K = 7.98540E-07 f1 = -1.84809E-06

N	y	U	y+	u+	u'	gamma
1	1.50000E-03	1.00E-10	0.857592	1.10E-10	0.810392	0.965332
2	5.50000E-03	2.96591	3.14450	3.25382	1.21855	0.969971
3	7.00000E-03	3.78321	4.00210	4.15046	1.32662	0.977539
4	8.50000E-03	4.49799	4.85969	4.93463	1.47248	0.976074
5	1.00000E-02	5.20426	5.71728	5.70946	1.56883	0.977295
6	1.15000E-02	5.81866	6.57487	6.38350	1.64157	0.979736
7	1.35000E-02	6.41095	7.71833	7.03329	1.71154	0.983398
8	1.60000E-02	7.32667	9.14764	8.03790	1.83018	0.985352
9	1.75000E-02	7.72991	10.00524	8.48028	1.87147	0.986084
10	2.00000E-02	8.39284	11.4346	9.20757	1.92283	0.987305
11	2.25000E-02	8.90734	12.8639	9.77201	1.91722	0.987061
12	2.55000E-02	9.51843	14.5791	10.44243	1.93194	0.986816
13	2.85000E-02	10.08976	16.2942	11.0692	1.87229	0.987793
14	3.15000E-02	10.40679	18.0094	11.4170	1.90743	0.987549
15	3.75000E-02	11.0420	21.4398	12.1139	1.81545	0.983887
16	4.35000E-02	11.5767	24.8702	12.7005	1.76659	0.987061
17	5.00000E-02	11.9605	28.5864	13.1216	1.73235	0.985107
18	6.00000E-02	12.5165	34.3037	13.7315	1.65464	0.984863
19	7.05000E-02	12.8525	40.3068	14.1002	1.53260	0.984131
20	8.85000E-02	13.3892	50.5979	14.6889	1.45810	0.981689
21	0.108000	13.8255	61.7466	15.1676	1.34915	0.981934
22	0.133500	14.2091	76.3257	15.5885	1.28229	0.976562
23	0.171500	14.6953	98.0513	16.1218	1.21417	0.973389
24	0.216000	15.1064	123.493	16.5728	1.15503	0.962891
25	0.276500	15.6410	158.083	17.1593	1.04312	0.947021
26	0.340500	16.0315	194.673	17.5877	0.968032	0.920166
27	0.432000	16.4212	246.986	18.0153	0.876379	0.866455
28	0.564000	16.8080	322.455	18.4396	0.684039	0.732178
29	0.755500	17.0941	431.940	18.7535	0.515130	0.572266
30	1.00550	17.3255	574.872	19.0073	0.356380	0.413086
31	1.25550	17.4515	717.804	19.1456	0.301402	0.346191
32	1.50550	17.5516	860.736	19.2555	0.247329	0.300049
33	1.75550	17.6364	1003.668	19.3484	0.228190	0.268555

Station = 1 dU/dx=14s-1

patm = 751.332
x = 7.35000 visc = 1.61512E-05
cf = 7.20000E-03 yeff = 1.30000E-03
Tw = 31.3000 Tinf = 27.3603
Tw measured = 31.2889 Tw correction = 1.10989E-02
Q wall = 163.000 Stanton No. = 5.76632E-03
Q wall measured (w/Tw measured) = 180.616
Q wall measured (w/Tw corrected) = 180.556
delther = 0.409699 deleth = 3.06256E-02
delcon = 6.36291E-04 qadded = 8.60687
Uw = 6.19128 Rex = 28174.9
Reh = 117.394
coef1 = 6.19128 coef2 = 4.82823E-02
A+ = 52.8360 K = 6.04639E-06
f1 = -2.71122E-05 f2 = -2.05321E-04

N	y	T	Tnd	y+	t+	Prt
1	0.0043	31.038	0.067	0.99	0.69	0.002
2	0.0053	30.972	0.083	1.22	0.87	-0.020
3	0.0063	30.917	0.097	1.45	1.01	-0.024
4	0.0073	30.848	0.115	1.68	1.19	-0.011
5	0.0083	30.786	0.130	1.91	1.36	-0.018
6	0.0093	30.718	0.148	2.14	1.54	-0.039
7	0.0103	30.652	0.164	2.37	1.71	-0.046
8	0.0113	30.590	0.180	2.60	1.87	0.072
9	0.0123	30.531	0.195	2.83	2.03	0.081
10	0.0133	30.466	0.212	3.06	2.20	0.052
11	0.0148	30.394	0.230	3.40	2.39	0.050
12	0.0168	30.292	0.256	3.86	2.66	0.068
13	0.0188	30.178	0.285	4.32	2.96	0.091
14	0.0203	30.109	0.302	4.67	3.15	0.121
15	0.0228	29.974	0.336	5.24	3.50	0.170
16	0.0243	29.879	0.361	5.59	3.75	0.197
17	0.0263	29.810	0.378	6.05	3.93	0.224
18	0.0293	29.630	0.424	6.74	4.41	0.253
19	0.0308	29.597	0.432	7.08	4.50	0.271
20	0.0338	29.459	0.467	7.77	4.86	0.300
21	0.0358	29.383	0.487	8.23	5.06	0.334
22	0.0388	29.288	0.511	8.92	5.31	0.364
23	0.0418	29.153	0.545	9.61	5.67	0.410
24	0.0443	29.100	0.558	10.19	5.81	0.438
25	0.0488	28.935	0.600	11.22	6.25	0.503
26	0.0513	28.866	0.618	11.80	6.43	0.532
27	0.0553	28.806	0.633	12.72	6.59	0.566
28	0.0623	28.615	0.682	14.33	7.09	0.676
29	0.0658	28.523	0.705	15.13	7.34	0.712
30	0.0698	28.486	0.714	16.05	7.43	0.777
31	0.0778	28.295	0.763	17.89	7.94	0.916
32	0.0818	28.278	0.767	18.81	7.98	0.931
33	0.0903	28.136	0.803	20.77	8.36	1.057
34	0.0963	28.086	0.816	22.15	8.49	1.184
35	0.1083	27.940	0.853	24.91	8.87	1.366
36	0.1163	27.890	0.865	26.75	9.01	1.627
37	0.1328	27.771	0.896	30.54	9.32	2.299
38	0.1468	27.708	0.912	33.77	9.49	3.631
39	0.1693	27.615	0.935	38.94	9.73	-6.791
40	0.1938	27.555	0.951	44.58	9.89	0.000
41	0.2353	27.485	0.968	54.12	10.08	0.000
42	0.2953	27.428	0.983	67.92	10.23	0.000
43	0.4023	27.388	0.993	92.53	10.33	0.000
44	0.6168	27.368	0.998	141.87	10.39	0.000
45	0.8668	27.367	0.998	199.37	10.39	0.000
46	1.1168	27.364	0.999	256.87	10.40	0.000
47	1.3668	27.363	0.999	314.37	10.40	0.000
48	1.6168	27.367	0.998	371.88	10.39	0.000
49	1.8668	27.366	0.998	429.38	10.39	0.000
50	2.1168	27.363	0.999	486.88	10.40	0.000
51	2.3668	27.370	0.998	544.38	10.38	0.000
52	2.6168	27.356	1.001	601.88	10.42	0.000
53	2.8668	27.366	0.999	659.39	10.39	0.000
54	3.1168	27.369	0.998	716.89	10.38	0.000
55	3.3668	27.373	0.997	774.39	10.37	0.000
56	3.6168	27.363	0.999	831.89	10.40	0.000
57	3.8668	27.369	0.998	889.39	10.38	0.000

Station = 2 dU/dx=14s-1

patm = 751.332
x = 15.9100 visc = 1.62434E-05
cf = 6.40000E-03 yeff = -2.00000E-04
Tw = 32.6300 Tinf = 27.3211
Tw measured = 33.2729 Tw correction = -0.642899
Q wall = 176.000 Stanton No. = 3.94197E-03
Q wall measured (w/Tw measured) = 169.464
Q wall measured (w/Tw corrected) = 173.019
delther = 0.633747 deleth = 5.17615E-02
delcon = 7.95542E-04 qadded = 22.9654
Uw = 7.27210 Rex = 71228.2
Reh = 232.167
coef1 = 7.27210 coef2 = 0.110832
A+ = 63.6017 K = 4.40768E-06
f1 = -2.01770E-05 f2 = -1.53948E-04

N	y	T	Tnd	y+	t+	Prt
1	0.0038	32.338	0.055	0.96	0.79	0.000
2	0.0048	32.296	0.063	1.22	0.90	0.000
3	0.0058	32.250	0.072	1.47	1.03	0.001
4	0.0068	32.188	0.083	1.73	1.19	0.003
5	0.0078	32.100	0.100	1.98	1.43	0.006
6	0.0088	32.039	0.111	2.23	1.60	0.013
7	0.0098	31.977	0.123	2.49	1.77	0.022
8	0.0108	31.911	0.135	2.74	1.94	0.029
9	0.0118	31.879	0.142	2.99	2.03	0.031
10	0.0138	31.748	0.166	3.50	2.38	0.082
11	0.0153	31.644	0.186	3.88	2.67	0.095
12	0.0163	31.543	0.205	4.14	2.94	0.114
13	0.0173	31.504	0.212	4.39	3.04	0.142
14	0.0198	31.347	0.242	5.02	3.47	0.141
15	0.0213	31.314	0.248	5.40	3.56	0.139
16	0.0248	31.121	0.284	6.29	4.08	0.203
17	0.0263	30.997	0.308	6.67	4.41	0.259
18	0.0278	30.905	0.325	7.05	4.66	0.308
19	0.0293	30.879	0.330	7.43	4.73	0.356
20	0.0323	30.712	0.361	8.20	5.19	0.370
21	0.0343	30.600	0.382	8.70	5.49	0.388
22	0.0358	30.535	0.395	9.08	5.66	0.416
23	0.0383	30.452	0.410	9.72	5.89	0.507
24	0.0413	30.334	0.432	10.48	6.21	0.591
25	0.0438	30.190	0.460	11.11	6.60	0.680
26	0.0458	30.160	0.465	11.62	6.68	0.805
27	0.0498	29.982	0.499	12.64	7.16	0.955
28	0.0518	29.864	0.521	13.14	7.48	1.066
29	0.0533	29.854	0.523	13.53	7.50	1.093
30	0.0568	29.683	0.555	14.41	7.97	1.271
31	0.0588	29.673	0.557	14.92	7.99	1.274
32	0.0633	29.469	0.595	16.06	8.54	1.185
33	0.0653	29.456	0.598	16.57	8.58	1.298
34	0.0698	29.284	0.630	17.71	9.04	1.226
35	0.0723	29.195	0.647	18.35	9.28	1.329
36	0.0753	29.270	0.633	19.11	9.08	1.279
37	0.0813	29.024	0.679	20.63	9.75	1.455
38	0.0833	29.066	0.671	21.14	9.63	1.493
39	0.0878	28.928	0.697	22.28	10.01	1.897
40	0.0913	28.852	0.712	23.17	10.21	2.530
41	0.0958	28.815	0.719	24.31	10.31	2.573
42	0.1048	28.611	0.757	26.59	10.87	3.504
43	0.1093	28.518	0.775	27.74	11.12	3.719
44	0.1143	28.462	0.785	29.00	11.27	4.258
45	0.1233	28.379	0.801	31.29	11.49	5.807
46	0.1338	28.247	0.826	33.95	11.85	9.192
47	0.1418	28.204	0.834	35.98	11.96	32.968
48	0.1583	28.111	0.851	40.17	12.22	-1.761
49	0.1763	27.943	0.883	44.74	12.67	0.000
50	0.1868	27.870	0.897	47.40	12.87	0.000
51	0.2013	27.784	0.913	51.08	13.10	0.000
52	0.2183	27.757	0.918	55.39	13.17	0.000
53	0.2528	27.661	0.936	64.15	13.43	0.000
54	0.2888	27.608	0.946	73.28	13.58	0.000
55	0.3573	27.505	0.965	90.67	13.85	0.000
56	0.4243	27.422	0.981	107.67	14.08	0.000
57	0.5058	27.389	0.987	128.35	14.17	0.000
58	0.6693	27.349	0.995	169.84	14.28	0.000
59	0.9193	27.335	0.997	233.27	14.31	0.000
60	1.1693	27.332	0.998	296.71	14.32	0.000
61	1.4193	27.331	0.998	360.15	14.32	0.000
62	1.6693	27.328	0.999	423.59	14.33	0.000
63	1.9193	27.328	0.999	487.03	14.33	0.000
64	2.1693	27.334	0.998	550.47	14.32	0.000
65	2.4193	27.327	0.999	613.90	14.33	0.000
66	2.6693	27.331	0.998	677.34	14.33	0.000
67	2.9193	27.324	0.999	740.78	14.34	0.000
68	3.1693	27.334	0.998	804.22	14.32	0.000
69	3.4193	27.327	0.999	867.66	14.34	0.000
70	3.6693	27.323	1.000	931.09	14.34	0.000
71	3.9193	27.330	0.998	994.53	14.33	0.000

Station = 3 dU/dx=14s-1

patm = 751.078
x = 23.2300 visc = 1.62826E-05
cf = 6.10000E-03 yeff = -2.00000E-04
Tw = 33.0600 Tinf = 27.3750
Tw measured = 33.9232 Tw correction = -0.863197
Q wall = 176.000 Stanton No. = 3.21710E-03
Q wall measured (w/Tw measured) = 166.979
Q wall measured (w/Tw corrected) = 171.777
delther = 0.867674 deleth = 6.56361E-02
delcon = 8.52474E-04 qadded = 35.6344
Uw = 8.33071 Rex = 118852.
Reh = 336.657
coef1 = 8.33071 coef2 = 0.125624
A+ = 60.0372 K = 3.36676E-06
f1 = -3.57905E-06 f2 = -9.16494E-05

N	y	T	Tnd	y+	t+	Prt
1	0.0038	32.857	0.036	1.08	0.61	-0.001
2	0.0048	32.782	0.049	1.36	0.84	-0.002
3	0.0058	32.688	0.065	1.64	1.12	-0.003
4	0.0068	32.652	0.072	1.93	1.23	-0.005
5	0.0078	32.571	0.086	2.21	1.48	-0.009
6	0.0088	32.473	0.103	2.49	1.77	-0.017
7	0.0098	32.411	0.114	2.78	1.96	-0.028
8	0.0108	32.333	0.128	3.06	2.19	-0.046
9	0.0118	32.265	0.140	3.34	2.40	-0.064
10	0.0128	32.206	0.150	3.63	2.58	0.932
11	0.0153	32.059	0.176	4.33	3.02	0.746
12	0.0168	31.916	0.201	4.76	3.45	1.983
13	0.0178	31.899	0.204	5.04	3.50	3.216
14	0.0198	31.749	0.231	5.61	3.96	0.953
15	0.0213	31.654	0.247	6.03	4.24	0.586
16	0.0228	31.540	0.267	6.46	4.59	0.561
17	0.0238	31.481	0.278	6.74	4.77	0.625
18	0.0263	31.366	0.298	7.45	5.11	0.548
19	0.0283	31.288	0.312	8.02	5.35	0.598
20	0.0308	31.104	0.344	8.73	5.91	0.820
21	0.0323	31.035	0.356	9.15	6.11	0.951
22	0.0343	30.943	0.372	9.72	6.39	1.157
23	0.0363	30.822	0.394	10.28	6.76	1.275
24	0.0383	30.704	0.414	10.85	7.12	1.062
25	0.0398	30.651	0.424	11.28	7.27	1.079
26	0.0428	30.503	0.450	12.13	7.72	1.091
27	0.0448	30.408	0.466	12.69	8.01	1.058
28	0.0468	30.401	0.468	13.26	8.03	1.063
29	0.0513	30.181	0.506	14.53	8.69	1.096
30	0.0533	30.095	0.522	15.10	8.95	1.147
31	0.0558	30.010	0.537	15.81	9.21	1.215
32	0.0588	29.920	0.552	16.66	9.48	1.355
33	0.0618	29.884	0.559	17.51	9.59	1.246
34	0.0683	29.660	0.598	19.35	10.27	1.394
35	0.0713	29.607	0.607	20.20	10.43	1.578
36	0.0768	29.445	0.636	21.76	10.92	1.865
37	0.0803	29.366	0.650	22.75	11.15	2.047
38	0.0848	29.323	0.657	24.02	11.29	2.146
39	0.0938	29.036	0.708	26.57	12.15	2.528
40	0.0968	29.046	0.706	27.42	12.12	2.565
41	0.1033	28.943	0.724	29.27	12.43	2.875
42	0.1093	28.812	0.747	30.96	12.83	3.322
43	0.1138	28.772	0.754	32.24	12.95	3.134
44	0.1233	28.686	0.769	34.93	13.21	4.023
45	0.1348	28.530	0.797	38.19	13.68	5.297
46	0.1418	28.405	0.819	40.17	14.06	6.566
47	0.1473	28.388	0.822	41.73	14.11	8.599
48	0.1588	28.371	0.825	44.99	14.16	19.102
49	0.1823	28.177	0.859	51.65	14.75	0.000
50	0.1943	28.078	0.876	55.05	15.05	0.000
51	0.2063	28.071	0.878	58.45	15.07	0.000
52	0.2308	27.988	0.892	65.39	15.32	0.000
53	0.2608	27.846	0.917	73.89	15.75	0.000
54	0.2818	27.816	0.922	79.83	15.84	0.000
55	0.3243	27.703	0.942	91.87	16.18	0.000
56	0.3623	27.673	0.948	102.64	16.27	0.000
57	0.4383	27.577	0.965	124.17	16.56	0.000
58	0.5178	27.494	0.979	146.69	16.81	0.000
59	0.6143	27.454	0.986	174.03	16.93	0.000
60	0.8073	27.421	0.992	228.71	17.03	0.000
61	1.0573	27.400	0.996	299.54	17.09	0.000
62	1.3073	27.390	0.997	370.36	17.12	0.000
63	1.5573	27.390	0.997	441.19	17.12	0.000
64	1.8073	27.393	0.997	512.01	17.11	0.000
65	2.0573	27.386	0.998	582.84	17.13	0.000
66	2.3073	27.379	0.999	653.66	17.16	0.000
67	2.5573	27.389	0.998	724.49	17.13	0.000
68	2.8073	27.382	0.999	795.31	17.15	0.000
69	3.0573	27.382	0.999	866.14	17.15	0.000
70	3.3073	27.382	0.999	936.96	17.15	0.000
71	3.5573	27.385	0.998	1007.79	17.14	0.000

Station = 4 dU/dx=14s-1

patm = 750.951
x = 31.4500 visc = 1.62958E-05
cf = 6.20000E-03 yeff = 8.00000E-04
Tw = 33.3200 Tinf = 27.3403
Tw measured = 34.1636 Tw correction = -0.843601
Q wall = 194.000 Stanton No. = 2.86133E-03
Q wall measured (w/Tw measured) = 165.696
Q wall measured (w/Tw corrected) = 170.397
delther = 0.909266 deleth = 7.39832E-02
delcon = 8.13737E-04 qadded = 49.6730
Uw = 9.82117 Rex = 189543.
Reh = 446.975
coef1 = 9.82117 coef2 = 0.112224
A+ = 50.0395 K = 2.42438E-06
f1 = -9.01814E-06 f2 = -3.39228E-05

N	y	T	Tnd	y+	t+	Prt
1	0.0038	33.008	0.052	1.28	1.02	0.000
2	0.0048	32.962	0.060	1.61	1.17	0.001
3	0.0058	32.913	0.068	1.95	1.33	0.005
4	0.0068	32.815	0.084	2.29	1.64	0.020
5	0.0078	32.750	0.095	2.62	1.86	0.092
6	0.0088	32.688	0.106	2.96	2.06	-0.206
7	0.0098	32.590	0.122	3.30	2.37	-0.107
8	0.0108	32.532	0.132	3.63	2.57	-0.382
9	0.0118	32.450	0.145	3.97	2.83	1.067
10	0.0128	32.378	0.157	4.31	3.06	1.162
11	0.0138	32.245	0.180	4.64	3.50	0.536
12	0.0148	32.254	0.178	4.98	3.47	0.413
13	0.0153	32.225	0.183	5.15	3.56	0.370
14	0.0158	32.143	0.197	5.32	3.83	0.326
15	0.0163	32.124	0.200	5.48	3.89	0.455
16	0.0173	32.058	0.211	5.82	4.11	2.137
17	0.0188	31.963	0.227	6.33	4.42	1.047
18	0.0208	31.816	0.252	7.00	4.89	0.865
19	0.0218	31.731	0.266	7.33	5.17	1.060
20	0.0233	31.681	0.274	7.84	5.33	0.979
21	0.0263	31.462	0.311	8.85	6.05	1.030
22	0.0278	31.344	0.331	9.35	6.43	1.052
23	0.0288	31.307	0.337	9.69	6.55	1.091
24	0.0313	31.241	0.348	10.53	6.77	1.198
25	0.0353	30.936	0.399	11.88	7.76	1.480
26	0.0363	30.896	0.405	12.21	7.89	1.585
27	0.0388	30.755	0.429	13.05	8.35	1.940
28	0.0403	30.770	0.426	13.56	8.30	1.344
29	0.0408	30.617	0.452	13.73	8.80	1.236
30	0.0413	30.646	0.447	13.89	8.70	1.252
31	0.0423	30.564	0.461	14.23	8.97	1.223
32	0.0438	30.547	0.464	14.74	9.02	1.229
33	0.0468	30.448	0.480	15.75	9.35	1.065
34	0.0498	30.306	0.504	16.75	9.81	1.415
35	0.0518	30.237	0.516	17.43	10.03	1.470
36	0.0548	30.144	0.531	18.44	10.34	1.712
37	0.0583	29.944	0.565	19.61	10.99	1.842
38	0.0598	29.904	0.571	20.12	11.12	1.842
39	0.0633	29.860	0.579	21.30	11.26	1.856
40	0.0703	29.570	0.627	23.65	12.20	1.728
41	0.0723	29.553	0.630	24.32	12.26	1.663
42	0.0768	29.448	0.648	25.84	12.60	1.819
43	0.0813	29.352	0.664	27.35	12.92	1.934
44	0.0858	29.269	0.677	28.87	13.18	1.807
45	0.0918	29.147	0.698	30.88	13.58	1.867
46	0.0963	28.998	0.723	32.40	14.07	1.909
47	0.0993	28.978	0.726	33.41	14.13	1.921
48	0.1058	28.908	0.738	35.60	14.36	1.850
49	0.1153	28.806	0.755	38.79	14.69	1.789
50	0.1248	28.680	0.776	41.99	15.10	1.838
51	0.1323	28.610	0.788	44.51	15.33	2.047
52	0.1433	28.511	0.804	48.21	15.65	2.255
53	0.1543	28.411	0.821	51.91	15.97	2.330
54	0.1653	28.322	0.836	55.61	16.27	2.353
55	0.1778	28.197	0.857	59.82	16.67	2.386
56	0.1878	28.203	0.856	63.18	16.65	2.259
57	0.2083	28.156	0.864	70.08	16.81	2.466
58	0.2493	28.004	0.889	83.87	17.30	3.301
59	0.2763	27.911	0.905	92.96	17.60	4.176
60	0.3058	27.795	0.924	102.88	17.98	6.215
61	0.3313	27.812	0.921	111.46	17.93	9.094
62	0.3823	27.692	0.941	128.62	18.31	43.552
63	0.4253	27.642	0.949	143.09	18.48	0.000
64	0.5113	27.527	0.969	172.02	18.85	0.000
65	0.5858	27.487	0.976	197.08	18.98	0.000
66	0.7353	27.427	0.986	247.38	19.18	0.000
67	0.9853	27.367	0.996	331.49	19.37	0.000
68	1.2353	27.363	0.996	415.60	19.39	0.000
69	1.4853	27.353	0.998	499.71	19.42	0.000
70	1.7353	27.360	0.997	583.82	19.40	0.000

71	1.9853	27.350	0.998	667.93	19.43	0.000
72	2.2353	27.356	0.997	752.04	19.41	0.000
73	2.4853	27.342	1.000	836.15	19.45	0.000
74	2.7353	27.355	0.997	920.26	19.41	0.000
75	2.9853	27.355	0.998	1004.37	19.41	0.000

Station = 5 dU/dx=14s-1

patm = 750.824
x = 39.5700 visc = 1.63007E-05
cf = 5.50000E-03 yeff = 8.00000E-04
Tw = 33.1500 Tinf = 27.3280
Tw measured = 34.2051 Tw correction = -1.05510
Q wall = 189.000 Stanton No. = 2.51364E-03
Q wall measured (w/Tw measured) = 165.964
Q wall measured (w/Tw corrected) = 171.840
delther = 1.15526 deleth = 8.55393E-02
delcon = 8.13057E-04 qadded = 63.4890
Uw = 11.1853 Rex = 271523.
Reh = 588.757
coef1 = 11.1853 coef2 = 0.139585
A+ = 43.9040 K = 1.86966E-06
f1 = -1.37820E-05 f2 = -6.74897E-06

N	y	T	Tnd	y+	t+	Prt
1	0.0038	32.837	0.054	1.37	1.12	0.000
2	0.0048	32.785	0.063	1.73	1.31	0.002
3	0.0058	32.733	0.072	2.09	1.50	0.011
4	0.0068	32.654	0.085	2.45	1.78	0.032
5	0.0078	32.576	0.099	2.82	2.06	0.083
6	0.0088	32.501	0.111	3.18	2.33	0.181
7	0.0098	32.475	0.116	3.54	2.42	0.304
8	0.0108	32.351	0.137	3.90	2.86	0.362
9	0.0118	32.299	0.146	4.26	3.05	0.430
10	0.0128	32.246	0.155	4.62	3.24	0.749
11	0.0143	32.132	0.175	5.16	3.65	2.200
12	0.0158	32.024	0.193	5.70	4.04	1.153
13	0.0173	31.929	0.210	6.25	4.38	1.518
14	0.0188	31.801	0.232	6.79	4.83	1.409
15	0.0198	31.726	0.245	7.15	5.10	1.246
16	0.0213	31.666	0.255	7.69	5.32	1.098
17	0.0243	31.456	0.291	8.77	6.07	0.884
18	0.0253	31.416	0.298	9.13	6.21	0.899
19	0.0278	31.285	0.320	10.04	6.68	1.058
20	0.0298	31.163	0.341	10.76	7.12	1.144
21	0.0313	31.139	0.345	11.30	7.21	1.208
22	0.0348	30.911	0.384	12.56	8.02	1.507
23	0.0363	30.826	0.399	13.11	8.33	1.558
24	0.0378	30.799	0.404	13.65	8.43	1.692
25	0.0413	30.565	0.444	14.91	9.27	1.822
26	0.0428	30.544	0.448	15.45	9.34	1.693
27	0.0458	30.422	0.469	16.53	9.78	1.745
28	0.0483	30.260	0.496	17.44	10.36	1.633
29	0.0498	30.237	0.500	17.98	10.44	1.507
30	0.0528	30.173	0.511	19.06	10.67	1.528
31	0.0583	29.902	0.558	21.05	11.64	1.442
32	0.0603	29.983	0.544	21.77	11.35	1.424
33	0.0643	29.818	0.572	23.21	11.94	1.551
34	0.0668	29.765	0.581	24.12	12.13	1.712
35	0.0713	29.633	0.604	25.74	12.61	1.885
36	0.0748	29.543	0.619	27.00	12.93	2.204
37	0.0788	29.464	0.633	28.45	13.21	2.014
38	0.0838	29.252	0.669	30.25	13.97	1.970
39	0.0863	29.196	0.679	31.16	14.17	1.918
40	0.0908	29.152	0.687	32.78	14.33	1.758
41	0.0998	29.108	0.694	36.03	14.49	1.442
42	0.1178	28.778	0.751	42.53	15.67	1.576
43	0.1228	28.823	0.743	44.33	15.51	1.594
44	0.1333	28.740	0.758	48.12	15.81	1.613
45	0.1463	28.499	0.799	52.82	16.67	1.692
46	0.1518	28.459	0.806	54.80	16.81	1.576
47	0.1628	28.422	0.812	58.77	16.94	1.619
48	0.1848	28.368	0.821	66.72	17.14	1.486
49	0.2268	28.133	0.862	81.88	17.98	1.453
50	0.2448	28.064	0.874	88.38	18.23	1.506
51	0.2708	27.981	0.888	97.76	18.53	1.581
52	0.3023	27.871	0.907	109.14	18.92	1.597
53	0.3313	27.848	0.911	119.61	19.00	1.406
54	0.3898	27.738	0.930	140.73	19.40	1.353
55	0.4433	27.671	0.941	160.04	19.63	1.249
56	0.5248	27.562	0.960	189.46	20.03	1.139
57	0.5998	27.518	0.967	216.54	20.18	1.048
58	0.7498	27.455	0.978	270.69	20.41	0.875
59	0.9898	27.395	0.988	357.34	20.62	0.693
60	1.2398	27.365	0.994	447.59	20.73	0.492
61	1.4898	27.358	0.995	537.85	20.76	0.356
62	1.7398	27.355	0.995	628.10	20.77	0.000
63	1.9898	27.344	0.997	718.36	20.81	0.000
64	2.2398	27.344	0.997	808.61	20.81	0.000
65	2.4898	27.347	0.997	898.87	20.80	0.000

Station = 6 dU/dx=14s-1

patm = 750.824
x = 44.7500 visc = 1.62897E-05
cf = 5.30000E-03 yeff = 8.00000E-04
Tw = 32.9900 Tinf = 27.3954
Tw measured = 33.8969 Tw correction = -0.906898
Q wall = 195.000 Stanton No. = 2.57348E-03
Q wall measured (w/Tw measured) = 168.128
Q wall measured (w/Tw corrected) = 173.167
delther = 1.18767 deleth = 9.40558E-02
delcon = 7.57176E-04 qadded = 70.2129
Uw = 11.7286 Rex = 322199.
Reh = 678.984
coef1 = 11.7286 coef2 = 0.203367
A+ = 40.1746 K = 1.69932E-06
f1 = 5.36661E-06 f2 = 1.18769E-06

N	y	T	Tnd	y+	t+	Prt
1	0.0038	32.745	0.044	1.41	0.88	-0.001
2	0.0048	32.685	0.054	1.78	1.09	-0.014
3	0.0058	32.597	0.070	2.16	1.40	-0.019
4	0.0068	32.500	0.088	2.53	1.75	-0.033
5	0.0078	32.428	0.100	2.90	2.01	-0.062
6	0.0088	32.349	0.114	3.27	2.29	-0.095
7	0.0098	32.232	0.135	3.64	2.71	-0.172
8	0.0108	32.206	0.140	4.01	2.81	1.946
9	0.0118	32.121	0.155	4.39	3.11	2.513
10	0.0128	32.019	0.174	4.76	3.47	0.919
11	0.0133	31.980	0.181	4.94	3.61	0.682
12	0.0148	31.947	0.186	5.50	3.73	0.812
13	0.0183	31.648	0.240	6.80	4.80	0.752
14	0.0193	31.576	0.253	7.17	5.06	0.790
15	0.0208	31.549	0.258	7.73	5.15	0.866
16	0.0243	31.312	0.300	9.03	6.00	0.898
17	0.0258	31.204	0.319	9.59	6.39	0.803
18	0.0268	31.141	0.330	9.96	6.61	0.856
19	0.0288	31.071	0.343	10.71	6.86	0.976
20	0.0323	30.919	0.370	12.01	7.41	0.946
21	0.0343	30.875	0.378	12.75	7.56	0.966
22	0.0388	30.635	0.421	14.42	8.42	1.283
23	0.0403	30.572	0.432	14.98	8.65	1.414
24	0.0433	30.433	0.457	16.09	9.14	1.465
25	0.0453	30.445	0.455	16.84	9.10	1.351
26	0.0463	30.310	0.479	17.21	9.58	1.204
27	0.0468	30.307	0.480	17.40	9.59	1.146
28	0.0483	30.274	0.486	17.95	9.71	1.050
29	0.0513	30.178	0.503	19.07	10.06	1.109
30	0.0548	30.166	0.505	20.37	10.10	1.161
31	0.0618	29.895	0.553	22.97	11.07	1.474
32	0.0643	29.858	0.560	23.90	11.20	1.611
33	0.0693	29.676	0.592	25.76	11.85	1.822
34	0.0718	29.676	0.592	26.69	11.85	1.982
35	0.0773	29.563	0.613	28.73	12.26	1.899
36	0.0823	29.401	0.641	30.59	12.83	1.895
37	0.0853	29.338	0.653	31.71	13.06	1.849
38	0.0903	29.235	0.671	33.57	13.43	1.870
39	0.0953	29.192	0.679	35.42	13.58	1.730
40	0.1058	29.068	0.701	39.33	14.02	1.546
41	0.1143	28.982	0.716	42.49	14.33	1.647
42	0.1243	28.869	0.737	46.20	14.74	1.676
43	0.1333	28.805	0.748	49.55	14.96	1.743
44	0.1478	28.613	0.782	54.94	15.65	1.793
45	0.1553	28.544	0.795	57.73	15.90	1.766
46	0.1663	28.608	0.783	61.81	15.67	1.699
47	0.1883	28.446	0.812	69.99	16.25	1.632
48	0.2018	28.337	0.832	75.01	16.64	1.539
49	0.2143	28.369	0.826	79.66	16.52	1.669
50	0.2398	28.164	0.863	89.14	17.26	1.836
51	0.2523	28.272	0.843	93.78	16.87	1.773
52	0.2773	28.123	0.870	103.07	17.40	1.825
53	0.2938	28.043	0.884	109.21	17.69	2.025
54	0.3148	28.082	0.877	117.01	17.55	1.946
55	0.3573	27.913	0.907	132.81	18.15	2.393
56	0.3828	27.896	0.910	142.29	18.21	2.250
57	0.4338	27.780	0.931	161.25	18.63	2.217
58	0.4778	27.736	0.939	177.60	18.79	2.323
59	0.5658	27.633	0.957	210.31	19.16	2.091
60	0.6523	27.623	0.959	242.46	19.19	2.140
61	0.8253	27.510	0.980	306.77	19.60	2.264
62	0.9798	27.476	0.986	364.20	19.72	2.430
63	1.2298	27.436	0.993	457.13	19.86	0.000
64	1.4798	27.416	0.996	550.05	19.93	0.000
65	1.7298	27.419	0.996	642.98	19.92	0.000
66	1.9798	27.409	0.998	735.91	19.96	0.000

Station = 7 dU/dx=14s-1

patm = 750.824
x = 55.3100 visc = 1.62610E-05
cf = 5.85000E-03 yeff = 1.80000E-03
Tw = 32.6000 Tinf = 27.3486
Tw measured = 33.3128 Tw correction = -0.712803
Q wall = 206.000 Stanton No. = 2.56992E-03
Q wall measured (w/Tw measured) = 171.304
Q wall measured (w/Tw corrected) = 175.245
delther = 1.79056 deleth = 0.132146
delcon = 6.72378E-04 qadded = 103.8215
Uw = 13.2095 Rex = 449308.
Reh = 1075.71
coef1 = 13.2095 coef2 = 0.212817
A+ = 35.4068 K = 1.33729E-06
f1 = 8.75989E-06 f2 = -2.46730E-07

N	y	T	Tnd	y+	t+	Prt
1	0.0038	32.228	0.071	1.67	1.49	0.001
2	0.0048	32.178	0.080	2.11	1.69	0.003
3	0.0058	32.135	0.089	2.55	1.86	0.011
4	0.0068	32.066	0.102	2.99	2.14	0.035
5	0.0078	32.004	0.114	3.44	2.39	0.127
6	0.0088	31.932	0.127	3.88	2.68	0.502
7	0.0098	31.840	0.145	4.32	3.05	4.294
8	0.0108	31.729	0.166	4.76	3.49	16.728
9	0.0118	31.682	0.175	5.20	3.68	5.174
10	0.0128	31.600	0.190	5.64	4.01	1.526
11	0.0138	31.527	0.204	6.08	4.30	0.798
12	0.0148	31.452	0.219	6.52	4.60	0.629
13	0.0163	31.353	0.238	7.18	5.00	0.621
14	0.0178	31.273	0.253	7.84	5.32	0.595
15	0.0198	31.187	0.269	8.72	5.67	0.643
16	0.0223	31.057	0.294	9.82	6.19	0.811
17	0.0243	30.961	0.312	10.70	6.57	0.891
18	0.0263	30.868	0.330	11.58	6.94	1.026
19	0.0288	30.715	0.359	12.68	7.55	1.147
20	0.0303	30.639	0.373	13.34	7.86	1.212
21	0.0323	30.614	0.378	14.22	7.96	1.238
22	0.0368	30.395	0.420	16.21	8.84	1.250
23	0.0388	30.355	0.428	17.09	9.00	1.215
24	0.0428	30.206	0.456	18.85	9.60	1.311
25	0.0453	30.194	0.458	19.95	9.64	1.410
26	0.0508	29.969	0.501	22.37	10.55	1.452
27	0.0533	29.964	0.502	23.47	10.56	1.499
28	0.0583	29.818	0.530	25.67	11.15	1.526
29	0.0618	29.735	0.546	27.22	11.48	1.619
30	0.0658	29.661	0.560	28.98	11.78	1.535
31	0.0718	29.577	0.576	31.62	12.12	1.708
32	0.0793	29.471	0.596	34.92	12.54	1.745
33	0.0863	29.332	0.622	38.01	13.10	1.751
34	0.0913	29.242	0.639	40.21	13.46	1.765
35	0.0968	29.191	0.649	42.63	13.66	1.742
36	0.1083	29.055	0.675	47.69	14.21	1.620
37	0.1168	29.051	0.676	51.44	14.23	1.505
38	0.1343	28.960	0.693	59.14	14.59	1.734
39	0.1538	28.816	0.721	67.73	15.17	2.033
40	0.1678	28.664	0.750	73.90	15.78	2.181
41	0.1768	28.637	0.755	77.86	15.89	2.344
42	0.1953	28.517	0.778	86.01	16.37	2.454
43	0.2108	28.480	0.785	92.83	16.52	2.292
44	0.2423	28.346	0.810	106.71	17.05	2.329
45	0.2658	28.345	0.810	117.05	17.06	2.534
46	0.3133	28.175	0.843	137.97	17.74	2.888
47	0.3418	28.052	0.866	150.52	18.23	3.151
48	0.3648	28.041	0.868	160.65	18.27	3.328
49	0.4113	27.928	0.890	181.13	18.73	3.806
50	0.4528	27.874	0.900	199.41	18.94	3.745
51	0.5323	27.774	0.919	234.42	19.35	4.176
52	0.6128	27.670	0.939	269.87	19.76	5.120
53	0.6913	27.600	0.952	304.44	20.04	5.919
54	0.8048	27.556	0.960	354.42	20.22	8.856
55	1.0323	27.466	0.978	454.61	20.58	0.000
56	1.2823	27.436	0.983	564.71	20.70	0.000
57	1.5323	27.419	0.987	674.81	20.77	0.000
58	1.7823	27.399	0.990	784.90	20.85	0.000

Station = 8 dU/dx=14s-1

patm = 751.078
x = 63.5300 visc = 1.62371E-05
cf = 6.00000E-03 yeff = 1.80000E-03
Tw = 31.9600 Tinf = 27.3865
Tw measured = 32.8680 Tw correction = -0.908001
Q wall = 194.000 Stanton No. = 2.57687E-03
Q wall measured (w/Tw measured) = 173.873
Q wall measured (w/Tw corrected) = 178.867
delther = 1.46694 deleth = 0.140818
delcon = 6.21300E-04 qadded = 103.1758
Uw = 14.2271 Rex = 556655.
Reh = 1237.13
coef1 = 14.2271 coef2 = 0.283715
A+ = 32.4248 K = 1.15114E-06
f1 = 5.57080E-07 f2 = -7.91743E-06

N	y	T	Tnd	y+	t+	Prt
1	0.0038	31.640	0.070	1.83	1.49	0.001
2	0.0048	31.607	0.077	2.31	1.64	0.004
3	0.0058	31.556	0.088	2.79	1.88	0.027
4	0.0068	31.492	0.102	3.27	2.17	0.128
5	0.0078	31.413	0.120	3.75	2.54	-0.248
6	0.0088	31.301	0.144	4.24	3.06	-1.411
7	0.0098	31.255	0.154	4.72	3.28	-0.133
8	0.0108	31.163	0.174	5.20	3.71	3.687
9	0.0118	31.087	0.191	5.68	4.06	0.914
10	0.0128	31.014	0.207	6.16	4.40	0.637
11	0.0138	30.970	0.216	6.64	4.60	0.619
12	0.0158	30.903	0.231	7.61	4.91	0.638
13	0.0188	30.710	0.273	9.05	5.81	0.830
14	0.0203	30.629	0.291	9.77	6.19	0.896
15	0.0223	30.532	0.312	10.73	6.64	1.041
16	0.0243	30.458	0.328	11.70	6.98	1.180
17	0.0273	30.318	0.359	13.14	7.63	1.159
18	0.0293	30.273	0.369	14.10	7.84	1.185
19	0.0333	30.110	0.405	16.03	8.60	1.249
20	0.0358	30.023	0.424	17.23	9.01	1.280
21	0.0388	29.968	0.436	18.68	9.26	1.269
22	0.0448	29.813	0.469	21.56	9.98	1.338
23	0.0488	29.733	0.487	23.49	10.35	1.317
24	0.0538	29.654	0.504	25.90	10.72	1.354
25	0.0603	29.517	0.534	29.03	11.36	1.442
26	0.0653	29.486	0.541	31.43	11.50	1.449
27	0.0753	29.325	0.576	36.25	12.25	1.565
28	0.0818	29.314	0.579	39.38	12.30	1.597
29	0.0948	29.104	0.624	45.63	13.28	1.624
30	0.1008	29.103	0.625	48.52	13.28	1.681
31	0.1133	28.989	0.650	54.54	13.81	1.676
32	0.1243	28.988	0.650	59.83	13.82	1.804
33	0.1468	28.844	0.681	70.66	14.49	1.912
34	0.1628	28.760	0.700	78.37	14.88	2.188
35	0.1823	28.613	0.732	87.75	15.56	2.390
36	0.1958	28.592	0.736	94.25	15.65	2.624
37	0.2228	28.511	0.754	107.25	16.03	2.605
38	0.2573	28.361	0.787	123.85	16.73	2.847
39	0.2803	28.330	0.794	134.93	16.87	2.954
40	0.3268	28.262	0.809	157.31	17.19	3.573
41	0.3978	28.026	0.860	191.49	18.29	4.348
42	0.4278	27.982	0.870	205.93	18.49	4.605
43	0.4883	27.907	0.886	235.05	18.84	5.571
44	0.5723	27.787	0.913	275.48	19.40	6.853
45	0.6428	27.736	0.924	309.42	19.63	7.608
46	0.7843	27.613	0.951	377.53	20.21	16.390
47	0.9003	27.559	0.962	433.37	20.46	******
48	1.1203	27.479	0.980	539.27	20.83	0.000
49	1.3703	27.452	0.986	659.61	20.96	0.000
50	1.6203	27.415	0.994	779.95	21.13	0.000
51	1.8703	27.414	0.994	900.29	21.13	0.000

Station = 9 dU/dx=14s-1

patm = 751.332
x = 71.5500 visc = 1.61982E-05
cf = 5.90000E-03 yeff = 1.80000E-03
Tw = 31.5600 Tinf = 27.3043
Tw measured = 32.2272 Tw correction = -0.667200
Q wall = 182.000 Stanton No. = 2.44203E-03
Q wall measured (w/Tw measured) = 177.549
Q wall measured (w/Tw corrected) = 181.200
delther = 1.43376 deleth = 0.168277
delcon = 6.15851E-04 qadded = 121.373
Uw = 15.1191 Rex = 667833.
Reh = 1573.72
coef1 = 15.1191 coef2 = 0.400854
A+ = 30.9576 K = 1.01688E-06
f1 = -2.08522E-06 f2 = -1.61176E-05

N	y	T	Tnd	y+	t+	Prt
1	0.0038	31.292	0.063	1.93	1.40	0.008
2	0.0048	31.225	0.079	2.44	1.75	0.042
3	0.0058	31.165	0.093	2.95	2.07	0.336
4	0.0068	31.102	0.108	3.46	2.39	6.054
5	0.0078	31.019	0.127	3.96	2.83	14.406
6	0.0088	30.940	0.146	4.47	3.24	13.840
7	0.0098	30.867	0.163	4.98	3.62	4.778
8	0.0108	30.817	0.175	5.49	3.89	1.452
9	0.0118	30.753	0.190	6.00	4.22	0.971
10	0.0128	30.680	0.207	6.50	4.60	0.814
11	0.0138	30.620	0.221	7.01	4.91	0.743
12	0.0153	30.560	0.235	7.77	5.23	0.751
13	0.0178	30.422	0.267	9.04	5.95	0.829
14	0.0198	30.367	0.280	10.06	6.24	0.879
15	0.0238	30.202	0.319	12.09	7.10	1.043
16	0.0263	30.081	0.347	13.36	7.73	1.118
17	0.0283	30.050	0.355	14.38	7.89	1.163
18	0.0323	29.912	0.387	16.41	8.62	1.279
19	0.0353	29.847	0.403	17.94	8.96	1.270
20	0.0403	29.742	0.427	20.48	9.50	1.308
21	0.0453	29.614	0.457	23.02	10.17	1.403
22	0.0493	29.562	0.469	25.05	10.44	1.389
23	0.0573	29.451	0.496	29.12	11.03	1.421
24	0.0648	29.353	0.519	32.93	11.54	1.462
25	0.0728	29.274	0.537	36.99	11.95	1.508
26	0.0833	29.232	0.547	42.33	12.17	1.621
27	0.1043	29.031	0.594	53.00	13.22	1.935
28	0.1148	28.950	0.613	58.34	13.64	2.083
29	0.1283	28.932	0.618	65.19	13.74	2.321
30	0.1558	28.777	0.654	79.17	14.55	2.763
31	0.1738	28.656	0.682	88.32	15.18	2.870
32	0.1893	28.608	0.694	96.19	15.43	3.141
33	0.2203	28.543	0.709	111.94	15.77	3.799
34	0.2698	28.394	0.744	137.10	16.55	4.798
35	0.3038	28.273	0.772	154.37	17.18	5.890
36	0.3323	28.241	0.780	168.86	17.35	7.263
37	0.3898	28.110	0.811	198.07	18.04	11.817
38	0.4348	28.019	0.832	220.94	18.51	19.470
39	0.4853	27.912	0.857	246.60	19.07	63.629
40	0.5333	27.900	0.860	270.99	19.13	0.000
41	0.6298	27.752	0.895	320.03	19.90	0.000
42	0.6963	27.666	0.915	353.82	20.36	0.000
43	0.7738	27.648	0.919	393.20	20.45	0.000
44	0.9288	27.557	0.941	471.96	20.92	0.000
45	1.1033	27.487	0.957	560.64	21.29	0.000

Station = 10 dU/dx=14s-1

patm = 751.332
x = 79.1100 visc = 1.61929E-05
cf = 5.80000E-03 yeff = -2.00000E-04
Tw = 31.2400 Tinf = 27.2575
Tw measured = 32.1347 Tw correction = -0.894701
Q wall = 172.000 Stanton No. = 2.25010E-03
Q wall measured (w/Tw measured) = 178.272
Q wall measured (w/Tw corrected) = 183.158
delther = 2.41964 deleth = 0.186703
delcon = 6.09530E-04 qadded = 136.838
Uw = 16.5619 Rex = 809127.
Reh = 1914.57
coef1 = 16.5619 coef2 = 0.409863
A+ = 30.0108 K = 8.47142E-07
f1 = -1.88876E-06 f2 = -2.04028E-05

N	y	T	Tnd	y+	t+	Prt
1	0.0038	31.071	0.042	2.10	1.01	-0.006
2	0.0048	30.941	0.075	2.65	1.79	-0.022
3	0.0058	30.867	0.094	3.20	2.24	-0.067
4	0.0068	30.807	0.109	3.76	2.60	-0.173
5	0.0078	30.756	0.121	4.31	2.91	-0.444
6	0.0088	30.660	0.146	4.86	3.49	27.260
7	0.0098	30.590	0.163	5.41	3.91	1.823
8	0.0108	30.542	0.175	5.97	4.19	1.381
9	0.0118	30.472	0.193	6.52	4.62	1.064
10	0.0128	30.418	0.206	7.07	4.94	0.689
11	0.0153	30.342	0.226	8.45	5.40	0.774
12	0.0188	30.146	0.275	10.39	6.58	1.033
13	0.0208	30.123	0.280	11.49	6.71	1.119
14	0.0248	29.947	0.325	13.70	7.77	1.289
15	0.0268	29.873	0.343	14.81	8.22	1.375
16	0.0298	29.797	0.362	16.46	8.67	1.353
17	0.0343	29.698	0.387	18.95	9.27	1.502
18	0.0388	29.602	0.411	21.44	9.84	1.453
19	0.0438	29.533	0.429	24.20	10.26	1.515
20	0.0518	29.371	0.469	28.62	11.23	1.655
21	0.0568	29.329	0.480	31.38	11.49	1.662
22	0.0668	29.234	0.504	36.91	12.06	1.785
23	0.0778	29.119	0.533	42.98	12.75	1.886
24	0.0878	29.096	0.538	48.51	12.89	1.933
25	0.1078	28.937	0.578	59.56	13.85	2.384
26	0.1208	28.895	0.589	66.74	14.10	2.651
27	0.1468	28.753	0.625	81.11	14.95	3.436
28	0.1653	28.701	0.638	91.33	15.26	4.194
29	0.2028	28.548	0.676	112.05	16.18	5.772
30	0.2283	28.444	0.702	126.13	16.81	7.772
31	0.2533	28.378	0.719	139.95	17.20	10.566
32	0.2933	28.328	0.731	162.05	17.50	24.523
33	0.3738	28.142	0.778	206.52	18.62	0.000
34	0.4183	28.008	0.812	231.11	19.43	0.000
35	0.4518	27.957	0.824	249.62	19.74	0.000
36	0.5193	27.898	0.839	286.91	20.09	0.000
37	0.6403	27.713	0.886	353.76	21.20	0.000
38	0.7068	27.676	0.895	390.50	21.42	0.000
39	0.8403	27.548	0.927	464.26	22.19	0.000
40	0.9468	27.521	0.934	523.10	22.36	0.000
41	1.1598	27.489	0.942	640.78	22.55	0.000

Station 1 dU/dx=14s-1
x = 10.53000 cm, Patm = 755.142 mm Hg, T = 26.8510 deg C

y	U	V	u'	v'	u'v'	u'v'2	dU/dy	em	l	gamma
0.060	3.337	1.283	0.634	0.632	-0.081	0.240	*******	0.731E-06	0.00000	0.313
0.062	5.115	-0.500	1.002	1.014	-0.679	0.805	19480.6	0.348E-04	0.00004	0.306
0.068	4.565	0.100	0.703	0.417	-0.030	-0.043	3680.1	0.815E-05	0.00005	0.277
0.074	4.399	-0.271	0.686	0.436	-0.076	-0.043	-2082.5	-0.367E-04	0.00013	0.280
0.081	4.442	-0.126	0.685	0.428	-0.067	-0.042	912.0	0.738E-04	0.00028	0.312
0.090	4.717	-0.151	0.691	0.422	-0.072	-0.054	2233.2	0.323E-04	0.00012	0.319
0.101	4.996	-0.171	0.679	0.407	-0.071	-0.056	2295.2	0.311E-04	0.00012	0.352
0.116	5.284	-0.216	0.655	0.381	-0.071	-0.056	1728.6	0.413E-04	0.00015	0.373
0.132	5.487	-0.229	0.639	0.362	-0.069	-0.050	1314.6	0.522E-04	0.00020	0.410
0.149	5.706	-0.252	0.621	0.324	-0.067	-0.042	988.0	0.682E-04	0.00026	0.415
0.179	5.912	-0.266	0.581	0.289	-0.059	-0.030	662.4	0.884E-04	0.00037	0.454
0.221	6.091	-0.288	0.553	0.252	-0.052	-0.019	416.2	0.125E-03	0.00055	0.471
0.268	6.243	-0.302	0.516	0.240	-0.047	-0.017	273.7	0.170E-03	0.00079	0.488
0.347	6.372	-0.314	0.485	0.229	-0.039	-0.009	158.3	0.245E-03	0.00124	0.482
0.491	6.513	-0.342	0.452	0.243	-0.032	-0.007	85.9	0.377E-03	0.00210	0.469
0.702	6.621	-0.382	0.406	0.254	-0.026	-0.004	44.5	0.574E-03	0.00359	0.407
1.125	6.697	-0.433	0.377	0.288	-0.022	-0.003	18.0	0.123E-02	0.00824	0.389
1.625	6.734	-0.504	0.375	0.317	-0.020	-0.003	9.2	0.221E-02	0.01546	0.370
2.124	6.769	-0.565	0.371	0.337	-0.018	-0.004	6.0	0.304E-02	0.02247	0.385
2.624	6.805	-0.625	0.357	0.336	-0.014	-0.004	3.8	0.383E-02	0.03197	0.377
3.124	6.812	-0.690	0.353	0.352	-0.011	-0.004	1.9	0.573E-02	0.05514	0.374
3.624	6.806	-0.743	0.350	0.345	-0.008	-0.001	0.7	0.122E-01	0.13644	0.400
4.124	6.816	-0.805	0.353	0.345	-0.002	-0.003	-20.6	-0.881E-04	0.00207	0.390

Station 2 dU/dx=14s-1
x = 19.0500 cm, Patm = 755.142 mm Hg, T = 26.8103 deg C

y	U	V	u'	v'	u'v'	u'v'2	dU/dy	em	l	gamma
0.060	4.977	0.837	0.768	0.405	0.098	-0.038	2701.2	-0.362E-04	0.00000	0.313
0.062	5.019	0.831	0.779	0.409	0.106	-0.044	2096.1	-0.507E-04	0.00000	0.302
0.069	5.192	0.745	0.790	0.410	0.083	-0.045	2708.9	-0.306E-04	0.00000	0.312
0.078	5.475	0.571	0.808	0.434	0.056	-0.065	2240.3	-0.250E-04	0.00000	0.279
0.087	5.787	0.380	0.836	0.448	0.002	-0.077	1749.0	-0.135E-05	0.00000	0.270
0.101	5.622	0.020	0.794	0.483	-0.060	-0.086	1554.8	0.388E-04	0.00016	0.268
0.116	6.098	-0.016	0.792	0.469	-0.065	-0.099	1705.7	0.382E-04	0.00015	0.299
0.135	6.584	-0.037	0.754	0.439	-0.063	-0.101	2157.6	0.291E-04	0.00012	0.354
0.166	7.019	-0.073	0.682	0.371	-0.056	-0.069	1309.3	0.425E-04	0.00018	0.379
0.202	7.325	-0.092	0.606	0.316	-0.055	-0.050	770.3	0.718E-04	0.00031	0.415
0.262	7.572	-0.100	0.532	0.273	-0.053	-0.032	396.5	0.133E-03	0.00058	0.439
0.352	7.771	-0.125	0.455	0.237	-0.039	-0.014	194.5	0.202E-03	0.00102	0.441
0.506	7.914	-0.153	0.412	0.243	-0.031	-0.008	85.3	0.367E-03	0.00207	0.442
0.813	8.027	-0.202	0.361	0.272	-0.022	-0.005	36.0	0.619E-03	0.00415	0.394
1.314	8.111	-0.285	0.336	0.308	-0.019	-0.003	17.2	0.113E-02	0.00812	0.382
1.814	8.167	-0.367	0.320	0.325	-0.014	-0.004	10.8	0.129E-02	0.01090	0.366
2.314	8.218	-0.453	0.314	0.344	-0.010	-0.005	8.8	0.119E-02	0.01163	0.381
2.814	8.244	-0.510	0.317	0.345	-0.010	-0.005	7.3	0.134E-02	0.01351	0.376
3.314	8.293	-0.603	0.309	0.349	-0.004	-0.002	6.4	0.674E-03	0.01025	0.393
3.814	8.313	-0.675	0.302	0.344	0.002	-0.003	5.5	-0.306E-03	0.00000	0.386
4.314	8.344	-0.732	0.311	0.334	0.002	-0.003	-18.4	0.122E-03	0.00000	0.395

Station 3 dU/dx=14s-1
x = 26.4700 cm, Patm = 755.396 mm Hg, T = 26.7601 deg C

y	U	V	u'	v'	u'v'	u'v'2	dU/dy	em	l	gamma
0.060	6.287	0.667	0.941	0.498	0.079	-0.109	1469.3	-0.535E-04	0.00000	0.360
0.061	6.284	0.664	0.940	0.499	0.067	-0.106	1516.4	-0.439E-04	0.00000	0.359
0.067	6.430	0.544	0.935	0.521	0.034	-0.121	2839.4	-0.121E-04	0.00000	0.368
0.075	6.727	0.320	0.956	0.531	-0.003	-0.140	1882.3	0.160E-05	0.00003	0.338
0.083	6.660	-0.209	0.941	0.572	-0.090	-0.152	1557.8	0.578E-04	0.00019	0.333
0.095	6.844	-0.131	0.931	0.571	-0.098	-0.173	1804.5	0.545E-04	0.00017	0.359
0.108	7.295	-0.168	0.884	0.557	-0.093	-0.185	2369.5	0.394E-04	0.00013	0.387
0.125	7.703	-0.223	0.853	0.506	-0.087	-0.177	2093.4	0.415E-04	0.00014	0.421
0.151	8.056	-0.244	0.779	0.445	-0.095	-0.131	1285.7	0.741E-04	0.00024	0.431
0.183	8.328	-0.265	0.691	0.387	-0.085	-0.096	814.5	0.104E-03	0.00036	0.457
0.225	8.559	-0.287	0.613	0.333	-0.068	-0.064	507.3	0.134E-03	0.00051	0.479
0.301	8.809	-0.302	0.500	0.292	-0.059	-0.037	283.8	0.208E-03	0.00086	0.510
0.413	8.989	-0.326	0.422	0.262	-0.046	-0.018	143.7	0.322E-03	0.00150	0.488
0.629	9.127	-0.380	0.352	0.265	-0.031	-0.009	62.3	0.490E-03	0.00280	0.443
1.046	9.252	-0.485	0.314	0.298	-0.019	-0.005	27.2	0.685E-03	0.00502	0.395
1.546	9.321	-0.574	0.299	0.331	-0.017	-0.005	13.6	0.122E-02	0.00947	0.413
2.046	9.357	-0.670	0.285	0.331	-0.011	-0.004	8.6	0.125E-02	0.01203	0.394
2.546	9.394	-0.745	0.286	0.347	-0.009	-0.003	7.8	0.119E-02	0.01234	0.398
3.046	9.431	-0.819	0.286	0.337	-0.005	-0.003	8.6	0.634E-03	0.00856	0.405
3.546	9.479	-0.871	0.289	0.336	-0.002	-0.002	-32.7	-0.467E-04	0.00120	0.412

Station 4 dU/dx=14s-1
x = 34.8900 cm, Patm = 755.650 mm Hg, T = 26.7141 deg C

y	U	V	u'	v'	u'v'	u'v'2	dU/dy	em	l	gamma
0.060	7.092	1.147	1.046	0.612	0.180	-0.169	3962.7	-0.453E-04	0.00000	0.517
0.067	7.319	1.080	1.039	0.605	0.135	-0.185	3164.6	-0.425E-04	0.00000	0.498
0.072	7.459	0.954	1.069	0.615	0.117	-0.213	3377.4	-0.348E-04	0.00000	0.499
0.080	7.751	0.742	1.087	0.637	0.073	-0.246	3261.8	-0.224E-04	0.00000	0.498
0.090	8.189	0.458	1.081	0.666	-0.029	-0.273	2605.0	0.112E-04	0.00007	0.479
0.104	8.209	-0.252	1.071	0.715	-0.162	-0.319	2155.4	0.752E-04	0.00019	0.491
0.119	8.637	-0.126	1.018	0.659	-0.136	-0.331	1995.7	0.680E-04	0.00018	0.509
0.144	9.266	-0.188	0.941	0.597	-0.141	-0.295	1997.8	0.705E-04	0.00019	0.545
0.170	9.646	-0.229	0.842	0.515	-0.119	-0.216	1362.1	0.877E-04	0.00025	0.568
0.220	10.018	-0.256	0.725	0.412	-0.098	-0.117	667.7	0.147E-03	0.00047	0.583
0.298	10.290	-0.267	0.588	0.337	-0.089	-0.061	343.9	0.260E-03	0.00087	0.587
0.450	10.585	-0.324	0.428	0.285	-0.052	-0.026	157.7	0.332E-03	0.00145	0.551
0.689	10.751	-0.382	0.328	0.278	-0.033	-0.011	70.9	0.459E-03	0.00255	0.476
1.169	10.871	-0.492	0.285	0.309	-0.019	-0.005	24.4	0.794E-03	0.00571	0.423
1.669	10.922	-0.588	0.273	0.339	-0.014	-0.004	12.5	0.111E-02	0.00943	0.411
2.170	10.969	-0.674	0.261	0.344	-0.009	-0.005	9.2	0.969E-03	0.01028	0.424
2.670	11.009	-0.749	0.262	0.338	-0.004	-0.004	8.9	0.426E-03	0.00691	0.430
3.170	11.057	-0.807	0.267	0.329	0.000	-0.003	-53.9	0.676E-05	0.00000	0.444

Station 5 dU/dx=14s-1
x = 42.5100 cm, Patm = 755.904 mm Hg, T = 26.6810 deg C

y	U	V	u'	v'	u'v'	u'v'2	dU/dy	em	l	gamma
0.060	7.474	1.346	1.130	0.698	0.232	-0.239	4156.8	-0.559E-04	0.00000	0.630
0.062	7.551	1.336	1.148	0.690	0.249	-0.223	2711.6	-0.918E-04	0.00000	0.646
0.068	7.734	1.246	1.146	0.708	0.211	-0.239	3485.9	-0.607E-04	0.00000	0.628
0.075	8.003	1.120	1.131	0.706	0.180	-0.274	3866.1	-0.465E-04	0.00000	0.634
0.087	8.513	0.814	1.178	0.754	0.109	-0.362	3675.1	-0.296E-04	0.00000	0.635
0.097	8.956	0.477	1.196	0.776	-0.004	-0.388	3363.6	0.110E-05	0.00002	0.625
0.109	9.090	-0.388	1.168	0.815	-0.176	-0.431	2972.2	0.593E-04	0.00014	0.603
0.135	10.040	-0.273	1.120	0.760	-0.205	-0.509	2608.8	0.785E-04	0.00017	0.650
0.163	10.714	-0.330	0.999	0.627	-0.187	-0.368	2116.8	0.885E-04	0.00020	0.672
0.203	11.184	-0.368	0.837	0.510	-0.125	-0.208	1112.3	0.113E-03	0.00032	0.707
0.267	11.522	-0.372	0.705	0.402	-0.111	-0.111	522.1	0.212E-03	0.00064	0.690
0.387	11.857	-0.396	0.519	0.319	-0.076	-0.045	245.7	0.311E-03	0.00113	0.664
0.550	12.064	-0.450	0.384	0.282	-0.043	-0.019	117.1	0.371E-03	0.00178	0.586
0.873	12.207	-0.504	0.299	0.303	-0.025	-0.010	42.7	0.595E-03	0.00374	0.488
1.374	12.273	-0.588	0.267	0.332	-0.017	-0.007	16.7	0.103E-02	0.00786	0.447
1.874	12.323	-0.636	0.248	0.343	-0.012	-0.004	10.4	0.113E-02	0.01040	0.427
2.374	12.370	-0.685	0.247	0.346	-0.009	-0.003	11.2	0.779E-03	0.00832	0.453
2.874	12.420	-0.703	0.254	0.324	-0.003	-0.002	14.0	0.190E-03	0.00369	0.460
3.374	12.506	-0.739	0.263	0.292	-0.001	-0.002	-44.3	-0.251E-04	0.00075	0.484

Station 6 dU/dx=14s-1
x = 50.3300 cm, Patm = 756.158 mm Hg, T = 26.6096 deg C

y	U	V	u'	v'	u'v'	u'v'2	dU/dy	em	l	gamma
0.060	8.506	1.344	1.266	0.873	0.213	-0.440	-311.6	0.685E-03	0.00000	0.805
0.063	8.521	1.268	1.254	0.873	0.216	-0.413	2919.6	-0.741E-04	0.00000	0.798
0.069	8.820	1.127	1.270	0.883	0.165	-0.478	4132.7	-0.398E-04	0.00000	0.797
0.078	9.211	0.864	1.289	0.901	0.067	-0.515	4124.1	-0.164E-04	0.00000	0.800
0.088	9.686	0.501	1.302	0.956	-0.034	-0.615	3029.5	0.114E-04	0.00006	0.784
0.101	9.699	-0.193	1.283	1.001	-0.302	-0.651	2481.6	0.122E-03	0.00022	0.798
0.115	10.176	-0.136	1.243	0.914	-0.280	-0.635	2381.3	0.118E-03	0.00022	0.800
0.138	10.871	-0.226	1.211	0.820	-0.277	-0.580	2543.5	0.109E-03	0.00021	0.808
0.164	11.391	-0.255	1.099	0.711	-0.240	-0.454	1787.8	0.134E-03	0.00027	0.810
0.201	11.806	-0.281	0.988	0.586	-0.186	-0.275	1074.9	0.173E-03	0.00040	0.812
0.257	12.182	-0.291	0.856	0.485	-0.142	-0.158	647.7	0.219E-03	0.00058	0.808
0.328	12.525	-0.315	0.698	0.401	-0.120	-0.105	398.6	0.301E-03	0.00087	0.782
0.459	12.805	-0.335	0.513	0.321	-0.074	-0.039	206.6	0.358E-03	0.00132	0.712
0.626	12.987	-0.359	0.393	0.295	-0.050	-0.022	104.0	0.484E-03	0.00216	0.620
0.876	13.122	-0.409	0.302	0.300	-0.028	-0.013	47.1	0.588E-03	0.00353	0.531
1.127	13.181	-0.415	0.270	0.319	-0.023	-0.010	24.0	0.942E-03	0.00627	0.482
1.377	13.214	-0.448	0.250	0.329	-0.017	-0.007	15.5	0.108E-02	0.00834	0.488
1.627	13.242	-0.463	0.250	0.332	-0.012	-0.005	14.0	0.876E-03	0.00790	0.453
1.877	13.286	-0.479	0.248	0.332	-0.012	-0.004	14.1	0.866E-03	0.00784	0.463
2.126	13.320	-0.485	0.238	0.337	-0.010	-0.004	14.8	0.680E-03	0.00678	0.479
2.376	13.351	-0.493	0.242	0.335	-0.007	-0.005	16.1	0.457E-03	0.00532	0.478
2.626	13.394	-0.495	0.242	0.318	-0.003	-0.003	20.1	0.131E-03	0.00255	0.470
2.876	13.451	-0.508	0.246	0.298	-0.004	-0.002	-19.4	-0.180E-03	0.00305	0.468

Station 7 dU/dx=14s-1
x = 58.3500 cm, Patm = 756.412 mm Hg, T = 26.5150 deg C

y	U	V	u'	v'	u'v'	u'v'2	dU/dy	em	l	gamma
0.060	9.347	1.347	1.242	0.958	0.057	-0.509	7983.8	-0.711E-05	0.00000	0.921
0.060	9.315	1.304	1.244	0.943	0.110	-0.449	3859.2	-0.285E-04	0.00000	0.928
0.068	9.672	1.105	1.238	0.969	-0.013	-0.552	4271.0	0.310E-05	0.00003	0.919
0.078	10.084	0.750	1.293	1.004	-0.100	-0.620	3462.7	0.288E-04	0.00009	0.912
0.094	10.439	-0.457	1.279	1.061	-0.401	-0.708	2735.9	0.147E-03	0.00023	0.914
0.112	10.914	-0.309	1.218	0.963	-0.404	-0.600	2370.7	0.170E-03	0.00027	0.914
0.138	11.571	-0.403	1.180	0.825	-0.349	-0.495	2035.0	0.172E-03	0.00029	0.918
0.167	11.996	-0.448	1.096	0.728	-0.308	-0.337	1494.4	0.206E-03	0.00037	0.928
0.208	12.429	-0.485	1.018	0.625	-0.256	-0.241	965.4	0.265E-03	0.00052	0.914
0.265	12.835	-0.531	0.918	0.541	-0.228	-0.180	672.1	0.339E-03	0.00071	0.906
0.338	13.211	-0.561	0.793	0.467	-0.176	-0.130	467.7	0.377E-03	0.00090	0.867
0.433	13.547	-0.596	0.654	0.398	-0.129	-0.078	310.3	0.417E-03	0.00116	0.835
0.586	13.841	-0.631	0.484	0.328	-0.079	-0.043	172.6	0.456E-03	0.00163	0.729
0.836	14.061	-0.687	0.335	0.304	-0.039	-0.015	75.5	0.510E-03	0.00260	0.598
1.086	14.138	-0.709	0.276	0.320	-0.025	-0.011	34.3	0.725E-03	0.00460	0.550
1.336	14.181	-0.737	0.257	0.333	-0.018	-0.009	17.9	0.102E-02	0.00755	0.500
1.586	14.210	-0.748	0.243	0.324	-0.014	-0.005	14.7	0.947E-03	0.00802	0.504
1.836	14.249	-0.765	0.243	0.330	-0.011	-0.005	16.8	0.653E-03	0.00624	0.503
2.086	14.288	-0.765	0.239	0.328	-0.010	-0.004	18.6	0.560E-03	0.00549	0.492
2.336	14.352	-0.780	0.231	0.316	-0.005	-0.003	19.6	0.277E-03	0.00376	0.495
2.586	14.392	-0.788	0.239	0.309	-0.004	-0.003	18.8	0.190E-03	0.00318	0.494
2.836	14.442	-0.808	0.241	0.278	0.000	-0.001	-26.9	-0.112E-05	0.00020	0.477

Station 8 dU/dx=14s-1
x = 66.1700 cm, Patm = 756.666 mm Hg, T = 26.4477 deg C

y	U	V	u'	v'	u'v'	u'v'2	dU/dy	em	l	gamma
0.060	10.126	1.604	1.226	1.025	0.048	-0.520	5298.1	-0.901E-05	0.00000	0.967
0.064	10.359	1.471	1.266	1.002	0.029	-0.571	4746.8	-0.602E-05	0.00000	0.962
0.076	10.909	1.089	1.269	1.051	-0.109	-0.565	4650.7	0.234E-04	0.00007	0.964
0.088	11.578	0.592	1.315	1.073	-0.227	-0.734	3362.2	0.676E-04	0.00014	0.957
0.107	11.688	-0.221	1.237	1.059	-0.464	-0.641	2335.7	0.199E-03	0.00029	0.959
0.131	12.343	-0.288	1.183	0.902	-0.379	-0.503	1764.9	0.215E-03	0.00035	0.959
0.162	12.886	-0.359	1.135	0.768	-0.361	-0.359	1624.3	0.222E-03	0.00037	0.961
0.204	13.340	-0.408	1.058	0.667	-0.308	-0.219	1065.2	0.289E-03	0.00052	0.954
0.258	13.762	-0.451	0.981	0.597	-0.272	-0.173	761.8	0.357E-03	0.00068	0.949
0.335	14.257	-0.507	0.871	0.513	-0.213	-0.135	548.3	0.388E-03	0.00084	0.927
0.443	14.688	-0.550	0.717	0.436	-0.155	-0.098	363.5	0.427E-03	0.00108	0.879
0.580	15.009	-0.565	0.568	0.367	-0.103	-0.059	211.7	0.488E-03	0.00152	0.786
0.808	15.267	-0.628	0.386	0.315	-0.056	-0.029	96.9	0.582E-03	0.00245	0.645
1.058	15.369	-0.659	0.306	0.323	-0.039	-0.022	43.7	0.900E-03	0.00454	0.547
1.308	15.420	-0.685	0.259	0.322	-0.023	-0.010	23.2	0.979E-03	0.00650	0.522
1.558	15.456	-0.704	0.245	0.332	-0.020	-0.008	19.2	0.102E-02	0.00728	0.510
1.808	15.513	-0.718	0.235	0.331	-0.013	-0.006	-111.5	-0.113E-03	0.00101	0.508

Station 9 dU/dx=14s-1
x = 74.5300 cm, Patm = 756.666 mm Hg, T = 26.4175 deg C

y	U	V	u'	v'	u'v'	u'v'2	dU/dy	em	l	gamma
0.060	11.408	1.337	1.315	1.070	-0.122	-0.558	-322.9	-0.377E-03	0.00108	0.983
0.062	11.410	1.314	1.331	1.096	-0.162	-0.639	6173.9	0.262E-04	0.00007	0.982
0.072	11.989	0.888	1.325	1.111	-0.255	-0.709	3731.8	0.683E-04	0.00014	0.984
0.085	12.250	-0.092	1.335	1.156	-0.467	-0.720	2826.1	0.165E-03	0.00024	0.978
0.101	12.577	-0.336	1.273	1.055	-0.487	-0.597	2156.5	0.226E-03	0.00032	0.975
0.126	13.194	-0.431	1.233	0.934	-0.480	-0.520	2005.5	0.240E-03	0.00035	0.975
0.155	13.696	-0.464	1.180	0.806	-0.423	-0.306	1636.2	0.259E-03	0.00040	0.976
0.192	14.178	-0.515	1.112	0.732	-0.386	-0.241	1175.3	0.328E-03	0.00053	0.969
0.238	14.566	-0.550	1.064	0.667	-0.340	-0.206	895.7	0.379E-03	0.00065	0.970
0.296	15.028	-0.595	0.992	0.588	-0.301	-0.170	688.2	0.438E-03	0.00080	0.957
0.372	15.474	-0.636	0.901	0.521	-0.250	-0.148	517.6	0.482E-03	0.00097	0.936
0.468	15.811	-0.682	0.783	0.454	-0.196	-0.117	350.8	0.560E-03	0.00126	0.902
0.619	16.196	-0.759	0.609	0.399	-0.136	-0.091	213.0	0.639E-03	0.00173	0.805
0.831	16.482	-0.808	0.450	0.349	-0.080	-0.047	118.5	0.678E-03	0.00239	0.693
1.082	16.630	-0.854	0.316	0.332	-0.043	-0.025	58.5	0.735E-03	0.00355	0.597
1.332	16.704	-0.893	0.269	0.337	-0.029	-0.015	32.7	0.872E-03	0.00516	0.546
1.582	16.771	-0.914	0.240	0.326	-0.016	-0.007	23.1	0.714E-03	0.00556	0.534
1.832	16.820	-0.932	0.234	0.319	-0.013	-0.006	-122.7	-0.107E-03	0.00093	0.516

Station 10 dU/dx=14s-1
x = 82.1500 cm, Patm = 756.920 mm Hg, T = 26.4063 deg C

y	U	V	u'	v'	u'v'	u'v'2	dU/dy	em	l	gamma
0.060	13.674	-0.467	1.357	1.187	-0.596	-0.837	-861.8	-0.692E-03	0.00090	0.982
0.064	13.673	-0.397	1.365	1.154	-0.602	-0.749	2281.0	0.264E-03	0.00034	0.982
0.074	13.991	-0.421	1.350	1.083	-0.577	-0.645	2542.9	0.227E-03	0.00030	0.981
0.093	14.456	-0.528	1.293	0.961	-0.495	-0.553	2246.8	0.220E-03	0.00031	0.979
0.112	14.783	-0.554	1.253	0.891	-0.519	-0.452	1797.5	0.289E-03	0.00040	0.979
0.138	15.214	-0.608	1.166	0.807	-0.435	-0.305	1399.2	0.311E-03	0.00047	0.979
0.175	15.610	-0.659	1.144	0.744	-0.408	-0.250	1100.3	0.370E-03	0.00058	0.977
0.220	16.043	-0.704	1.093	0.673	-0.381	-0.206	845.6	0.450E-03	0.00073	0.974
0.280	16.442	-0.754	1.031	0.602	-0.326	-0.175	666.6	0.489E-03	0.00086	0.965
0.344	16.846	-0.808	0.947	0.554	-0.279	-0.176	512.6	0.545E-03	0.00103	0.950
0.435	17.187	-0.835	0.843	0.487	-0.235	-0.136	371.7	0.634E-03	0.00131	0.917
0.567	17.549	-0.870	0.689	0.431	-0.177	-0.107	237.3	0.745E-03	0.00177	0.846
0.759	17.859	-0.914	0.500	0.372	-0.100	-0.059	141.3	0.706E-03	0.00224	0.737
1.010	18.046	-0.953	0.381	0.341	-0.062	-0.039	73.4	0.847E-03	0.00340	0.633
1.260	18.173	-0.986	0.268	0.330	-0.029	-0.016	42.4	0.696E-03	0.00405	0.564
1.510	18.224	-0.993	0.240	0.328	-0.020	-0.011	27.5	0.713E-03	0.00509	0.550
1.760	18.300	-1.024	0.226	0.316	-0.013	-0.006	-136.9	-0.978E-04	0.00085	0.510

Station 1 dU/dx=14s-1
x = 10.33000 cm, Patm = 758.952 mm Hg,
Tatm = 26.1555 deg C, qwall = 175.057W/m2

y	U	V	T	u'	v'	t'	u'v'	v't'	u't'	u'v'2	v'2t'	gamma	dU/dy	dT/dy	em	eh	Prt
0.0500	4.721	-0.304	28.35	0.8173	0.2883	0.6003	-0.0561	0.1070	-0.3080	-.032	0.029	0.450	2147.7	-1806.7	0.261E-04	0.592E-04	0.441
0.0535	4.793	-0.299	28.29	0.8258	0.2792	0.6114	-0.0626	0.1074	-0.3147	-.037	0.031	0.465	1784.9	-1772.1	0.351E-04	0.606E-04	0.579
0.0605	4.916	-0.293	28.15	0.8275	0.2843	0.5920	-0.0680	0.1064	-0.3104	-.038	0.034	0.482	1954.9	-1928.6	0.348E-04	0.552E-04	0.630
0.0640	5.010	-0.298	28.07	0.7968	0.2845	0.5864	-0.0588	0.1029	-0.2817	-.035	0.033	0.476	2113.9	-1959.7	0.278E-04	0.525E-04	0.530
0.0685	5.079	-0.306	28.00	0.8066	0.2853	0.5857	-0.0619	0.1056	-0.2975	-.038	0.031	0.476	2200.2	-1926.6	0.281E-04	0.548E-04	0.513
0.0760	5.279	-0.296	27.85	0.7928	0.2619	0.5533	-0.0551	0.0886	-0.2607	-.032	0.027	0.468	1866.1	-1696.3	0.295E-04	0.522E-04	0.566
0.0800	5.331	-0.293	27.78	0.7914	0.2698	0.5552	-0.0593	0.0898	-0.2728	-.032	0.030	0.472	1776.0	-1660.1	0.334E-04	0.541E-04	0.617
0.0885	5.447	-0.285	27.66	0.7642	0.2682	0.5450	-0.0681	0.0876	-0.2598	-.036	0.033	0.494	1360.9	-1415.1	0.500E-04	0.619E-04	0.808
0.0945	5.531	-0.292	27.57	0.7486	0.2539	0.5111	-0.0572	0.0759	-0.2295	-.029	0.025	0.468	1346.4	-1315.1	0.425E-04	0.577E-04	0.736
0.1065	5.693	-0.283	27.44	0.7175	0.2454	0.4858	-0.0585	0.0687	-0.2070	-.030	0.024	0.459	1227.6	-1098.8	0.477E-04	0.626E-04	0.762
0.1145	5.787	-0.282	27.34	0.6959	0.2411	0.4547	-0.0591	0.0612	-0.1860	-.027	0.022	0.449	1099.6	-925.6	0.537E-04	0.661E-04	0.813
0.1310	5.944	-0.279	27.22	0.6669	0.2339	0.4201	-0.0585	0.0510	-0.1652	-.024	0.018	0.419	822.8	-707.5	0.711E-04	0.720E-04	0.987
0.1450	6.036	-0.279	27.14	0.6506	0.2293	0.3975	-0.0584	0.0493	-0.1504	-.023	0.018	0.399	644.1	-556.6	0.906E-04	0.886E-04	1.022
0.1675	6.145	-0.274	27.03	0.6041	0.2205	0.3371	-0.0510	0.0383	-0.1153	-.020	0.014	0.355	449.4	-406.5	0.114E-03	0.943E-04	1.205
0.1920	6.232	-0.267	26.96	0.5774	0.2127	0.2983	-0.0480	0.0306	-0.0862	-.014	0.009	0.337	345.1	-296.9	0.139E-03	0.103E-03	1.352
0.2340	6.348	-0.278	26.87	0.5477	0.2172	0.2373	-0.0477	0.0249	-0.0655	-.015	0.009	0.256	247.0	-177.1	0.193E-03	0.141E-03	1.373
0.2935	6.460	-0.278	26.81	0.5044	0.2194	0.1792	-0.0419	0.0177	-0.0408	-.009	0.005	0.179	174.1	-100.8	0.241E-03	0.175E-03	1.374
0.4010	6.593	-0.292	26.75	0.4602	0.2269	0.1050	-0.0323	0.0104	-0.0204	-.007	0.003	0.081	99.5	-45.4	0.324E-03	0.230E-03	1.410
0.6155	6.700	-0.322	26.71	0.4260	0.2596	0.0448	-0.0311	0.0053	-0.0099	-.006	0.001	0.012	48.2	-16.6	0.644E-03	0.318E-03	2.026
0.8655	6.764	-0.346	26.70	0.3983	0.2743	0.0308	-0.0256	0.0033	-0.0063	-.003	0.000	0.001	23.9	-5.1	0.107E-02	0.662E-03	1.620
1.1155	6.796	-0.368	26.70	0.3946	0.2984	0.0229	-0.0284	0.0033	-0.0062	-.004	0.000	0.000	14.3	-0.4	0.198E-02	0.819E-02	0.242
1.3655	6.828	-0.402	26.70	0.3841	0.3135	0.0219	-0.0282	0.0033	-0.0059	-.005	0.000	0.000	10.5	0.2	0.269E-02	-.158E-01	-.171
1.6155	6.847	-0.429	26.71	0.3797	0.3293	0.0216	-0.0285	0.0037	-0.0057	-.001	0.000	0.000	9.8	0.7	0.290E-02	-.541E-02	-.537
1.8655	6.869	-0.454	26.70	0.3733	0.3410	0.0212	-0.0226	0.0038	-0.0054	-.005	0.000	0.000	7.6	-0.4	0.295E-02	0.985E-02	0.300
2.1155	6.898	-0.484	26.71	0.3760	0.3462	0.0214	-0.0196	0.0039	-0.0056	-.003	0.000	0.000	6.7	-0.5	0.293E-02	0.845E-02	0.347
2.3655	6.898	-0.508	26.70	0.3683	0.3493	0.0208	-0.0172	0.0040	-0.0052	-.005	0.000	0.000	5.5	-0.1	0.316E-02	0.589E-01	0.054
2.6155	6.916	-0.527	26.70	0.3668	0.3548	0.0208	-0.0186	0.0042	-0.0053	-.001	0.000	0.000	3.0	-0.1	0.615E-02	0.389E-01	0.158
2.8655	6.928	-0.571	26.70	0.3659	0.3532	0.0205	-0.0209	0.0043	-0.0051	-.003	0.000	0.000	4.5	0.5	0.468E-02	-.884E-02	-.530
3.1155	6.920	-0.603	26.70	0.3647	0.3485	0.0201	-0.0125	0.0039	-0.0051	-.003	0.000	0.000	3.4	-0.2	0.371E-02	0.179E-01	0.207
3.3655	6.951	-0.635	26.70	0.3658	0.3627	0.0202	-0.0098	0.0043	-0.0050	-.005	0.000	0.000	3.3	-0.2	0.294E-02	0.202E-01	0.145
3.6155	6.947	-0.653	26.70	0.3637	0.3599	0.0202	-0.0098	0.0043	-0.0049	-.004	0.000	0.000	4.0	0.0	0.243E-02	-.123E+00	-.020
3.8655	6.957	-0.683	26.70	0.3634	0.3550	0.0199	-0.0086	0.0041	-0.0048	-.003	0.000	0.000	2.1	0.3	0.410E-02	-.125E-01	-.327
4.3655	6.971	-0.760	26.71	0.3681	0.3573	0.0198	-0.0080	0.0042	-0.0050	-.004	0.000	0.000	-17.6	-77.7	-.456E-03	0.538E-04	*****

Station 2 dU/dx=14s-1
x = 18.7500 cm, Patm = 759.206 mm Hg,
Tatm = 26.3293 deg C, qwall = 170.515W/m2

y	U	V	T	u'	v'	t'	u'v'	v't'	u't'	u'v'2	v'2t'	gamma	dU/dy	dT/dy	em	eh	Prt
0.0500	5.490	-0.621	29.66	0.9774	0.3142	0.7911	-0.0971	0.1433	-0.4985	-.046	0.037	0.484	3276.8	-1099.9	0.296E-04	0.130E-03	0.227
0.0515	5.483	-0.635	29.67	0.9821	0.3174	0.7919	-0.1068	0.1446	-0.4906	-.048	0.041	0.495	672.3	-984.3	0.159E-03	0.147E-03	1.082
0.0530	5.513	-0.658	29.64	0.9727	0.3106	0.7880	-0.0997	0.1391	-0.4879	-.043	0.041	0.484	106.0	207.1	0.941E-03	-.672E-03	*****
0.0565	5.483	-0.697	29.70	0.9807	0.3244	0.7868	-0.1163	0.1533	-0.4860	-.048	0.043	0.490	608.8	188.4	0.191E-03	-.814E-03	-.235
0.0585	5.504	-0.704	29.67	0.9986	0.3253	0.7997	-0.1234	0.1611	-0.5353	-.052	0.045	0.483	994.6	-52.8	0.124E-03	0.305E-02	0.041
0.0630	5.598	-0.728	29.67	1.0150	0.3193	0.7753	-0.1213	0.1542	-0.5103	-.050	0.038	0.489	1610.1	-1161.1	0.754E-04	0.133E-03	0.568
0.0650	5.645	-0.702	29.62	0.9959	0.3323	0.8012	-0.1230	0.1732	-0.5206	-.056	0.044	0.488	438.5	-1365.8	0.280E-03	0.127E-03	2.211
0.0695	5.679	-0.548	29.54	1.0146	0.3526	0.7997	-0.0996	0.1762	-0.5471	-.059	0.052	0.501	-176.7	-2504.0	-.564E-03	0.704E-04	*****
0.0720	5.486	-0.292	29.49	0.9919	0.3333	0.7946	-0.0531	0.1535	-0.5345	-.052	0.047	0.516	472.7	-2516.4	0.112E-03	0.610E-04	1.840
0.0750	5.645	-0.280	29.36	0.9810	0.3241	0.7921	-0.0524	0.1418	-0.5325	-.051	0.044	0.524	1172.5	-3067.5	0.447E-04	0.462E-04	0.967
0.0810	5.813	-0.253	29.21	0.9747	0.3243	0.8174	-0.0482	0.1531	-0.5458	-.052	0.049	0.536	2718.2	-3019.4	0.177E-04	0.507E-04	0.350
0.0830	5.877	-0.251	29.11	0.9550	0.3219	0.8038	-0.0535	0.1486	-0.5133	-.053	0.051	0.535	2711.1	-2972.7	0.197E-04	0.500E-04	0.395
0.0875	5.960	-0.234	29.01	0.9629	0.3310	0.8162	-0.0538	0.1524	-0.5355	-.062	0.054	0.568	2622.3	-3027.6	0.205E-04	0.503E-04	0.408
0.0910	6.094	-0.232	28.89	0.9447	0.3075	0.8064	-0.0407	0.1350	-0.5020	-.050	0.049	0.568	2531.6	-2695.6	0.161E-04	0.501E-04	0.321
0.0955	6.194	-0.221	28.76	0.9375	0.3143	0.8178	-0.0455	0.1385	-0.5044	-.060	0.051	0.577	2542.6	-2583.8	0.179E-04	0.536E-04	0.334
0.1045	6.391	-0.208	28.57	0.9000	0.3182	0.7923	-0.0436	0.1364	-0.4570	-.057	0.053	0.604	1955.0	-2144.2	0.223E-04	0.636E-04	0.350
0.1090	6.473	-0.200	28.49	0.9067	0.3163	0.8099	-0.0501	0.1388	-0.4792	-.063	0.060	0.599	1934.0	-2105.2	0.259E-04	0.659E-04	0.393
0.1140	6.557	-0.199	28.37	0.8691	0.3108	0.7851	-0.0420	0.1322	-0.4397	-.057	0.058	0.606	1790.5	-2052.8	0.234E-04	0.644E-04	0.364
0.1230	6.731	-0.201	28.19	0.8552	0.2897	0.7645	-0.0426	0.1143	-0.4250	-.054	0.051	0.602	1517.3	-1718.6	0.281E-04	0.665E-04	0.422
0.1335	6.846	-0.184	28.07	0.8318	0.2944	0.7543	-0.0539	0.1145	-0.3974	-.056	0.051	0.628	1248.0	-1389.1	0.432E-04	0.824E-04	0.524
0.1415	6.941	-0.187	27.94	0.8022	0.2785	0.7356	-0.0455	0.1080	-0.3642	-.045	0.048	0.590	1024.7	-1176.6	0.444E-04	0.918E-04	0.483
0.1580	7.094	-0.173	27.77	0.7633	0.2683	0.7016	-0.0549	0.0979	-0.3379	-.042	0.045	0.600	850.7	-1008.0	0.645E-04	0.971E-04	0.664
0.1760	7.215	-0.163	27.62	0.7019	0.2645	0.6427	-0.0476	0.0835	-0.2791	-.038	0.037	0.576	676.7	-821.5	0.704E-04	0.102E-03	0.693
0.1865	7.297	-0.169	27.53	0.6918	0.2580	0.6324	-0.0510	0.0794	-0.2606	-.035	0.037	0.573	587.8	-714.2	0.868E-04	0.111E-03	0.780
0.2010	7.367	-0.163	27.43	0.6612	0.2462	0.5996	-0.0537	0.0726	-0.2427	-.030	0.031	0.537	504.8	-603.0	0.106E-03	0.120E-03	0.883
0.2180	7.437	-0.162	27.36	0.6295	0.2498	0.5665	-0.0530	0.0707	-0.2047	-.029	0.031	0.517	397.1	-462.6	0.134E-03	0.153E-03	0.874
0.2525	7.556	-0.159	27.23	0.5689	0.2415	0.4975	-0.0494	0.0583	-0.1628	-.022	0.025	0.461	295.6	-333.8	0.167E-03	0.175E-03	0.959
0.2885	7.629	-0.157	27.13	0.5324	0.2338	0.4256	-0.0491	0.0462	-0.1166	-.019	0.018	0.410	235.5	-258.6	0.208E-03	0.179E-03	1.167
0.3570	7.774	-0.166	27.00	0.4847	0.2394	0.3183	-0.0451	0.0364	-0.0765	-.013	0.013	0.318	152.3	-157.6	0.296E-03	0.231E-03	1.283
0.4240	7.832	-0.170	26.93	0.4416	0.2338	0.2466	-0.0341	0.0259	-0.0444	-.009	0.008	0.235	111.3	-104.0	0.307E-03	0.249E-03	1.230
0.5055	7.896	-0.184	26.87	0.4126	0.2451	0.1823	-0.0329	0.0189	-0.0282	-.008	0.005	0.170	67.8	-57.5	0.485E-03	0.329E-03	1.475
0.6690	7.980	-0.205	26.83	0.3905	0.2594	0.1050	-0.0273	0.0114	-0.0135	-.008	0.004	0.069	42.4	-25.0	0.643E-03	0.456E-03	1.411
0.9190	8.037	-0.240	26.81	0.3689	0.2917	0.0466	-0.0276	0.0059	-0.0069	-.004	0.001	0.019	25.1	-8.6	0.110E-02	0.686E-03	1.604
1.1690	8.075	-0.290	26.80	0.3552	0.3121	0.0288	-0.0241	0.0040	-0.0050	-.006	0.001	0.006	16.5	-3.3	0.147E-02	0.123E-02	1.193
1.4190	8.130	-0.327	26.79	0.3487	0.3241	0.0203	-0.0225	0.0031	-0.0039	-.005	0.000	0.001	12.9	-1.0	0.174E-02	0.299E-02	0.583
1.6690	8.139	-0.356	26.80	0.3339	0.3371	0.0191	-0.0232	0.0034	-0.0038	-.004	0.000	0.000	9.8	-0.3	0.237E-02	0.130E-01	0.182
1.9190	8.167	-0.382	26.80	0.3300	0.3478	0.0176	-0.0210	0.0032	-0.0035	-.003	0.000	0.000	8.0	0.8	0.263E-02	-.396E-02	-.664
2.1695	8.179	-0.420	26.80	0.3312	0.3530	0.0168	-0.0188	0.0031	-0.0034	-.003	0.000	0.000	9.4	0.8	0.200E-02	-.407E-02	-.490
2.4195	8.210	-0.454	26.80	0.3458	0.3572	0.0170	-0.0186	0.0033	-0.0037	-.003	0.000	0.000	-30.2	-205.4	-.616E-03	0.160E-04	*****

2.6695	8.235	-0.491	26.81	0.3297	0.3580	0.0167	-0.0184	0.0035	-0.0033	-.005	0.000	0.000	-49.8	-308.1	-.370E-03	0.113E-04	*****
2.9195	7.762	-0.506	24.23	0.3139	0.3441	0.0034	-0.0119	0.0001	-0.0001	-.003	0.000	0.000	-50.1	-308.7	-.238E-03	0.483E-06	*****
3.1695	7.781	-0.531	24.23	0.3217	0.3457	0.0038	-0.0115	0.0002	-0.0002	-.003	0.000	0.000	-31.0	-206.2	-.370E-03	0.941E-06	*****
3.4195	7.811	-0.574	24.23	0.3175	0.3408	0.0039	-0.0084	0.0002	-0.0002	-.003	0.000	0.000	7.6	-0.1	0.111E-02	0.194E-02	0.574
3.6695	7.823	-0.607	24.23	0.3162	0.3412	0.0101	-0.0083	0.0003	-0.0002	-.003	0.000	0.001	7.4	-0.2	0.112E-02	0.128E-02	0.870
3.9195	7.836	-0.644	24.23	0.3193	0.3423	0.0037	-0.0042	0.0003	-0.0002	-.004	0.000	0.000	6.8	0.0	0.622E-03	-.160E-01	-.039
4.4195	7.880	-0.698	24.23	0.3214	0.3319	0.0037	-0.0042	0.0003	-0.0002	-.002	0.000	0.000	-12.8	-70.0	-.326E-03	0.412E-05	*****

Station 3 dU/dx=14s-1
x = 26.3700 cm, Patm = 759.206 mm Hg,
Tatm = 26.4981 deg C, qwall = 167.217W/m2

y	U	V	T	u'	v'	t'	u'v'	v't'	u't'	u'v'2	v'2t'	gamma	dU/dy	dT/dy	em	eh	Prt
0.0500	6.153	-0.961	30.04	1.1644	0.4192	0.9007	-0.2261	0.2617	-0.6945	-.110	0.080	0.582	-913.2	-2514.1	-.248E-03	0.104E-03	*****
0.0510	6.144	-0.945	30.04	1.1753	0.4238	0.8851	-0.2113	0.2493	-0.6809	-.120	0.075	0.579	810.9	-910.8	0.261E-03	0.274E-03	0.952
0.0530	6.200	-0.933	30.02	1.1883	0.4302	0.8994	-0.2017	0.2626	-0.7190	-.114	0.090	0.567	2455.9	-1531.0	0.821E-04	0.171E-03	0.479
0.0555	6.326	-0.830	29.96	1.2153	0.4492	0.9059	-0.2087	0.2700	-0.7373	-.139	0.102	0.591	1129.9	-2589.0	0.185E-03	0.104E-03	1.771
0.0585	6.189	-0.416	29.85	1.1539	0.4088	0.9058	-0.0956	0.2174	-0.7055	-.103	0.078	0.586	835.0	-3116.4	0.114E-03	0.698E-04	1.641
0.0615	6.262	-0.401	29.76	1.1630	0.4098	0.9247	-0.1020	0.2270	-0.7321	-.108	0.080	0.606	1144.1	-3339.7	0.891E-04	0.680E-04	1.311
0.0680	6.501	-0.375	29.55	1.1466	0.4174	0.9282	-0.0936	0.2216	-0.7167	-.116	0.101	0.631	3396.3	-3125.3	0.276E-04	0.709E-04	0.389
0.0710	6.626	-0.364	29.46	1.1374	0.4139	0.9438	-0.0932	0.2240	-0.7155	-.121	0.095	0.630	3457.4	-3222.4	0.269E-04	0.695E-04	0.388
0.0765	6.782	-0.349	29.29	1.1418	0.4100	0.9529	-0.1004	0.2214	-0.7238	-.129	0.108	0.667	2999.7	-2931.6	0.335E-04	0.755E-04	0.443
0.0800	6.910	-0.350	29.16	1.1089	0.4050	0.9427	-0.0904	0.2134	-0.7076	-.122	0.108	0.660	2678.2	-2730.0	0.337E-04	0.782E-04	0.432
0.0845	7.000	-0.339	29.08	1.0867	0.3930	0.9369	-0.0820	0.2049	-0.6744	-.114	0.098	0.669	2431.0	-2353.3	0.337E-04	0.871E-04	0.387
0.0935	7.190	-0.320	28.89	1.0559	0.4085	0.9376	-0.1001	0.2141	-0.6514	-.133	0.106	0.689	2227.0	-2111.8	0.449E-04	0.101E-03	0.443
0.0965	7.266	-0.335	28.82	1.0617	0.3868	0.9332	-0.0940	0.2016	-0.6495	-.120	0.106	0.701	2129.4	-2034.9	0.442E-04	0.991E-04	0.446
0.1030	7.412	-0.327	28.68	1.0319	0.3811	0.9128	-0.0890	0.1876	-0.6280	-.121	0.105	0.686	2051.8	-1982.0	0.434E-04	0.947E-04	0.458
0.1090	7.512	-0.326	28.59	1.0278	0.3744	0.9121	-0.0829	0.1724	-0.6180	-.116	0.097	0.707	1779.0	-1777.8	0.466E-04	0.970E-04	0.481
0.1135	7.603	-0.329	28.49	0.9871	0.3652	0.8993	-0.0816	0.1776	-0.5699	-.104	0.098	0.700	1602.0	-1647.1	0.509E-04	0.108E-03	0.472
0.1230	7.729	-0.316	28.36	0.9536	0.3601	0.8880	-0.0932	0.1699	-0.5606	-.108	0.095	0.691	1324.6	-1427.8	0.704E-04	0.119E-03	0.591
0.1345	7.873	-0.325	28.19	0.9101	0.3477	0.8515	-0.0774	0.1508	-0.4892	-.093	0.081	0.701	1080.4	-1085.9	0.717E-04	0.139E-03	0.516
0.1415	7.914	-0.314	28.16	0.8852	0.3487	0.8559	-0.0870	0.1613	-0.4831	-.092	0.089	0.690	874.4	-959.7	0.995E-04	0.168E-03	0.592
0.1470	7.995	-0.296	28.09	0.8727	0.3455	0.8520	-0.0956	0.1603	-0.4869	-.092	0.097	0.681	759.7	-815.6	0.126E-03	0.196E-03	0.640
0.1585	8.043	-0.293	28.01	0.8480	0.3316	0.8211	-0.0993	0.1449	-0.4518	-.078	0.079	0.678	734.9	-855.7	0.135E-03	0.169E-03	0.798
0.1820	8.224	-0.293	27.81	0.7590	0.3175	0.7537	-0.0803	0.1240	-0.3497	-.064	0.068	0.657	578.4	-627.2	0.139E-03	0.198E-03	0.702
0.1940	8.280	-0.293	27.71	0.7421	0.3046	0.7153	-0.0755	0.1056	-0.3189	-.059	0.060	0.638	571.3	-619.7	0.132E-03	0.170E-03	0.775
0.2060	8.334	-0.298	27.71	0.7158	0.2986	0.7226	-0.0754	0.1059	-0.3204	-.052	0.057	0.641	481.4	-504.3	0.157E-03	0.210E-03	0.746
0.2305	8.462	-0.299	27.55	0.6503	0.3051	0.6499	-0.0778	0.0991	-0.2422	-.055	0.053	0.593	397.4	-425.8	0.196E-03	0.233E-03	0.841
0.2605	8.541	-0.304	27.43	0.5917	0.2713	0.5782	-0.0629	0.0728	-0.1997	-.034	0.035	0.554	299.2	-355.6	0.210E-03	0.205E-03	1.027
0.2815	8.601	-0.298	27.39	0.5792	0.2767	0.5580	-0.0624	0.0725	-0.1831	-.036	0.037	0.531	240.1	-270.3	0.260E-03	0.268E-03	0.970
0.3240	8.681	-0.311	27.30	0.5366	0.2751	0.4908	-0.0622	0.0666	-0.1365	-.031	0.032	0.503	207.9	-209.5	0.299E-03	0.318E-03	0.941
0.3620	8.775	-0.327	27.21	0.4861	0.2704	0.4267	-0.0542	0.0552	-0.1061	-.024	0.025	0.433	172.0	-183.6	0.315E-03	0.300E-03	1.050
0.4380	8.865	-0.344	27.10	0.4281	0.2668	0.3344	-0.0450	0.0408	-0.0616	-.015	0.017	0.353	123.1	-117.4	0.365E-03	0.347E-03	1.051
0.5175	8.937	-0.355	27.05	0.4068	0.2653	0.2764	-0.0397	0.0334	-0.0446	-.011	0.011	0.282	85.7	-75.2	0.463E-03	0.444E-03	1.045
0.6140	9.014	-0.385	26.99	0.3726	0.2702	0.1944	-0.0342	0.0235	-0.0243	-.011	0.008	0.186	59.5	-45.5	0.575E-03	0.516E-03	1.115
0.8070	9.073	-0.435	26.94	0.3423	0.2799	0.1169	-0.0237	0.0132	-0.0096	-.006	0.005	0.091	34.9	-23.2	0.680E-03	0.571E-03	1.192
1.0570	9.140	-0.476	26.92	0.3323	0.3114	0.0570	-0.0250	0.0072	-0.0054	-.006	0.003	0.030	19.6	-9.3	0.127E-02	0.772E-03	1.648
1.3070	9.167	-0.508	26.91	0.3159	0.3231	0.0378	-0.0231	0.0051	-0.0042	-.006	0.002	0.013	15.5	-2.9	0.149E-02	0.177E-02	0.846
1.5570	9.192	-0.553	26.91	0.3158	0.3374	0.0231	-0.0197	0.0033	-0.0032	-.007	0.001	0.003	15.1	-0.7	0.130E-02	0.468E-02	0.278
1.8070	9.241	-0.613	26.91	0.3049	0.3461	0.0176	-0.0227	0.0029	-0.0027	-.005	0.000	0.001	15.6	-0.7	0.146E-02	0.394E-02	0.370
2.0570	9.292	-0.656	26.91	0.3041	0.3532	0.0150	-0.0157	0.0027	-0.0024	-.005	0.000	0.000	15.2	-0.5	0.103E-02	0.589E-02	0.176
2.3070	9.312	-0.684	26.90	0.3016	0.3628	0.0145	-0.0177	0.0027	-0.0023	-.006	0.000	0.000	13.6	-0.4	0.130E-02	0.593E-02	0.219

2.5570	9.346	-0.729	26.91	0.3046	0.3628	0.0142	-0.0183	0.0028	-0.0023	-.005	0.000	0.000	12.3	0.2	0.148E-02	-.148E-01	-.100
2.8070	9.383	-0.783	26.91	0.3064	0.3595	0.0137	-0.0138	0.0027	-0.0023	-.004	0.000	0.000	10.9	0.3	0.127E-02	-.867E-02	-.146
3.0570	9.410	-0.812	26.91	0.3104	0.3630	0.0138	-0.0118	0.0028	-0.0024	-.002	0.000	0.000	8.8	-0.1	0.135E-02	0.321E-01	0.042
3.3070	9.416	-0.860	26.91	0.2990	0.3501	0.0135	-0.0066	0.0027	-0.0020	-.003	0.000	0.000	6.6	0.3	0.100E-02	-.802E-02	-.125
3.5570	9.440	-0.898	26.91	0.3019	0.3423	0.0133	-0.0042	0.0028	-0.0019	-.003	0.000	0.000	-9.9	-56.4	-.423E-03	0.491E-04	*****

Station 4 dU/dx=14s-1
x = 34.9900 cm, Patm = 759.460 mm Hg,
Tatm = 26.7098 deg C, qwall = 169.277W/m2

y	U	V	T	u'	v'	t'	u'v'	v't'	u't'	u'v'2	v'2t'	gamma	dU/dy	dT/dy	em	eh	Prt
0.0500	7.453	-0.761	29.89	1.3360	0.5078	0.9174	-0.1578	0.2061	-0.6628	-.195	0.078	0.762	-894.1	1253.1	-.176E-03	-.164E-03	1.073
0.0505	7.434	-0.753	29.93	1.3408	0.5153	0.9211	-0.1932	0.2315	-0.6622	-.196	0.082	0.771	-703.2	1763.0	-.275E-03	-.131E-03	2.093
0.0535	7.451	-0.837	29.93	1.3282	0.5128	0.9193	-0.1991	0.2207	-0.6228	-.197	0.091	0.774	633.6	196.7	0.314E-03	-.112E-02	-.280
0.0570	7.500	-0.916	29.90	1.3301	0.5189	0.9107	-0.2048	0.2317	-0.6313	-.217	0.091	0.781	1061.5	-248.9	0.193E-03	0.931E-03	0.207
0.0585	7.496	-0.923	29.94	1.3266	0.5177	0.9100	-0.2247	0.2339	-0.6476	-.203	0.091	0.774	1107.3	-221.8	0.203E-03	0.105E-02	0.192
0.0620	7.550	-1.015	29.90	1.3143	0.5167	0.9018	-0.2249	0.2312	-0.6134	-.208	0.082	0.766	1061.1	-205.0	0.212E-03	0.113E-02	0.188
0.0690	7.621	-1.089	29.89	1.3488	0.5440	0.9197	-0.2772	0.2862	-0.6682	-.236	0.109	0.773	1250.3	-603.4	0.222E-03	0.474E-03	0.467
0.0710	7.662	-1.085	29.86	1.3187	0.5455	0.9014	-0.2691	0.2729	-0.6409	-.256	0.107	0.761	887.8	-789.7	0.303E-03	0.346E-03	0.877
0.0755	7.712	-1.015	29.83	1.3390	0.5517	0.9146	-0.2324	0.2795	-0.6811	-.236	0.118	0.765	886.3	-1311.4	0.262E-03	0.213E-03	1.230
0.0800	7.695	-0.697	29.76	1.3553	0.5927	0.9231	-0.1972	0.3037	-0.7250	-.255	0.142	0.790	1586.6	-2032.1	0.124E-03	0.149E-03	0.832
0.0845	7.789	-0.445	29.65	1.3394	0.5587	0.9215	-0.1265	0.2684	-0.7081	-.247	0.133	0.794	2368.8	-2644.9	0.534E-04	0.101E-03	0.526
0.0905	8.044	-0.413	29.43	1.3160	0.5438	0.9340	-0.1320	0.2535	-0.7318	-.242	0.133	0.809	3245.3	-2852.1	0.407E-04	0.889E-04	0.458
0.0950	8.167	-0.392	29.33	1.3024	0.5461	0.9426	-0.1346	0.2545	-0.7237	-.257	0.141	0.812	3057.0	-2657.7	0.440E-04	0.957E-04	0.460
0.0980	8.254	-0.378	29.25	1.2909	0.5332	0.9447	-0.1393	0.2450	-0.7295	-.250	0.142	0.826	2724.1	-2329.9	0.511E-04	0.105E-03	0.486
0.1045	8.421	-0.372	29.10	1.2495	0.5242	0.9548	-0.1219	0.2480	-0.6973	-.226	0.145	0.836	2695.5	-2226.3	0.452E-04	0.111E-03	0.406
0.1140	8.690	-0.364	28.90	1.1958	0.5110	0.9470	-0.1144	0.2323	-0.6626	-.224	0.144	0.842	2211.3	-1913.9	0.517E-04	0.121E-03	0.426
0.1235	8.863	-0.346	28.73	1.1505	0.4966	0.9389	-0.1232	0.2136	-0.6408	-.212	0.136	0.839	1687.6	-1499.7	0.730E-04	0.142E-03	0.512
0.1310	8.961	-0.349	28.63	1.1359	0.4970	0.9170	-0.1500	0.2261	-0.6191	-.211	0.139	0.845	1379.7	-1303.2	0.109E-03	0.174E-03	0.626
0.1420	9.072	-0.327	28.54	1.0925	0.4717	0.9215	-0.1546	0.1982	-0.5903	-.182	0.120	0.849	1246.1	-1141.4	0.124E-03	0.174E-03	0.715
0.1530	9.235	-0.332	28.39	1.0440	0.4701	0.8766	-0.1281	0.1866	-0.5138	-.186	0.125	0.837	1214.4	-1099.4	0.105E-03	0.170E-03	0.621
0.1640	9.373	-0.332	28.26	1.0061	0.4440	0.8709	-0.1322	0.1755	-0.5102	-.154	0.107	0.837	1067.4	-1014.0	0.124E-03	0.173E-03	0.715
0.1765	9.495	-0.335	28.15	0.9531	0.4259	0.8521	-0.1285	0.1585	-0.4660	-.134	0.106	0.826	889.1	-856.3	0.145E-03	0.185E-03	0.781
0.1865	9.536	-0.313	28.09	0.9181	0.4331	0.8530	-0.1258	0.1695	-0.4526	-.131	0.104	0.818	761.6	-731.0	0.165E-03	0.232E-03	0.713
0.2070	9.715	-0.328	27.93	0.8439	0.3921	0.7965	-0.1039	0.1347	-0.3841	-.102	0.086	0.799	624.8	-609.3	0.166E-03	0.221E-03	0.752
0.2480	9.903	-0.322	27.74	0.7590	0.3680	0.7288	-0.1063	0.1157	-0.3120	-.083	0.078	0.752	446.5	-477.5	0.238E-03	0.242E-03	0.982
0.2750	9.994	-0.322	27.59	0.7086	0.3611	0.6765	-0.1036	0.1078	-0.2720	-.078	0.064	0.717	334.9	-369.3	0.309E-03	0.292E-03	1.059
0.3045	10.101	-0.334	27.51	0.6390	0.3489	0.6344	-0.0997	0.1008	-0.2194	-.070	0.060	0.668	286.6	-317.0	0.348E-03	0.318E-03	1.093
0.3300	10.142	-0.330	27.46	0.6106	0.3212	0.6021	-0.0842	0.0867	-0.1958	-.046	0.041	0.661	252.5	-244.5	0.333E-03	0.354E-03	0.941
0.3810	10.271	-0.342	27.33	0.5476	0.3091	0.5194	-0.0725	0.0703	-0.1478	-.038	0.035	0.570	192.7	-208.4	0.376E-03	0.338E-03	1.114
0.4240	10.346	-0.357	27.25	0.4937	0.3008	0.4763	-0.0629	0.0660	-0.1137	-.027	0.030	0.519	163.3	-177.2	0.385E-03	0.372E-03	1.033
0.5100	10.432	-0.372	27.14	0.4306	0.2988	0.3945	-0.0537	0.0537	-0.0709	-.022	0.024	0.424	104.1	-118.9	0.516E-03	0.452E-03	1.142
0.5845	10.510	-0.401	27.06	0.3938	0.2923	0.3139	-0.0440	0.0418	-0.0481	-.017	0.017	0.345	77.7	-88.4	0.566E-03	0.473E-03	1.197
0.7340	10.585	-0.425	26.98	0.3512	0.2944	0.2213	-0.0324	0.0298	-0.0263	-.012	0.011	0.218	47.8	-48.3	0.677E-03	0.617E-03	1.098
0.9840	10.654	-0.482	26.92	0.3124	0.3109	0.1137	-0.0283	0.0146	-0.0100	-.009	0.006	0.095	25.7	-20.5	0.110E-02	0.710E-03	1.554
1.2340	10.700	-0.532	26.90	0.2921	0.3444	0.0709	-0.0213	0.0094	-0.0045	-.008	0.004	0.040	15.7	-8.8	0.136E-02	0.107E-02	1.271
1.4840	10.727	-0.579	26.89	0.2850	0.3426	0.0419	-0.0186	0.0052	-0.0028	-.005	0.002	0.013	11.4	-3.5	0.163E-02	0.147E-02	1.110
1.7340	10.744	-0.620	26.88	0.2809	0.3503	0.0260	-0.0155	0.0037	-0.0020	-.004	0.001	0.007	10.1	-1.9	0.153E-02	0.199E-02	0.769
1.9840	10.775	-0.666	26.89	0.2807	0.3553	0.0215	-0.0205	0.0032	-0.0020	-.003	0.001	0.002	9.6	-1.4	0.213E-02	0.221E-02	0.966
2.2345	10.803	-0.727	26.88	0.2737	0.3560	0.0141	-0.0159	0.0024	-0.0016	-.005	0.000	0.000	10.5	-1.2	0.151E-02	0.199E-02	0.759

2.4845	10.818	-0.742	26.87	0.2698	0.3549	0.0186	-0.0131	0.0022	-0.0013	-.003	0.000	0.000	10.3	-1.5	0.127E-02	0.148E-02	0.856
2.7345	10.853	-0.810	26.87	0.2747	0.3611	0.0122	-0.0107	0.0024	-0.0014	-.004	0.000	0.000	9.6	-0.7	0.112E-02	0.337E-02	0.331
2.9845	10.879	-0.852	26.87	0.2760	0.3454	0.0117	-0.0045	0.0022	-0.0012	-.003	0.000	0.000	9.1	-0.1	0.497E-03	0.220E-01	0.023
3.4845	10.910	-0.931	26.87	0.2871	0.3371	0.0117	-0.0035	0.0022	-0.0013	-.004	0.000	0.000	-45.2	-128.2	-.775E-04	0.173E-04	*****

Station 5 dU/dx=14s-1
x = 42.4100 cm, Patm = 759.714 mm Hg,
Tatm = 26.7280 deg C, qwall = 170.669W/m2

y	U	V	T	u'	v'	t'	u'v'	v't'	u't'	u'v'2	v'2t'	gamma	dU/dy	dT/dy	em	eh	Prt
0.0500	8.671	-0.910	29.76	1.4290	0.5928	0.8537	-0.1880	0.2252	-0.5684	-.330	0.090	0.788	-3011.2	-621.4	-.624E-04	0.362E-03	-.172
0.0515	8.628	-0.921	29.77	1.4549	0.5822	0.8585	-0.1869	0.2176	-0.5902	-.304	0.092	0.808	-1940.1	643.6	-.963E-04	-.338E-03	0.285
0.0570	8.611	-0.987	29.78	1.4576	0.5798	0.8570	-0.2054	0.2238	-0.6172	-.286	0.092	0.801	566.2	-95.7	0.363E-03	0.234E-02	0.155
0.0590	8.638	-1.026	29.76	1.4614	0.5888	0.8509	-0.2459	0.2286	-0.6264	-.340	0.101	0.796	1155.0	-249.3	0.213E-03	0.917E-03	0.232
0.0630	8.711	-1.089	29.76	1.4654	0.5820	0.8431	-0.2442	0.2285	-0.6012	-.321	0.092	0.804	1656.9	-414.5	0.147E-03	0.551E-03	0.267
0.0660	8.779	-1.106	29.73	1.4867	0.5985	0.8477	-0.2622	0.2426	-0.6367	-.355	0.110	0.805	1640.8	-284.2	0.160E-03	0.854E-03	0.187
0.0700	8.809	-1.109	29.72	1.4968	0.6147	0.8590	-0.2777	0.2556	-0.6542	-.406	0.124	0.800	1946.6	-585.3	0.143E-03	0.437E-03	0.327
0.0735	8.884	-1.064	29.73	1.4762	0.6231	0.8634	-0.2696	0.2764	-0.6347	-.391	0.134	0.807	1804.2	-1170.5	0.149E-03	0.236E-03	0.633
0.0775	9.021	-0.864	29.65	1.4722	0.6612	0.8690	-0.2373	0.2982	-0.6927	-.426	0.160	0.804	1916.1	-1964.1	0.124E-03	0.152E-03	0.816
0.0825	9.040	-0.418	29.50	1.4604	0.6307	0.8748	-0.1155	0.2518	-0.7238	-.384	0.151	0.816	2344.0	-2634.2	0.493E-04	0.956E-04	0.515
0.0850	9.105	-0.369	29.46	1.4445	0.6468	0.8618	-0.1250	0.2613	-0.6571	-.402	0.159	0.837	2230.5	-2687.8	0.560E-04	0.972E-04	0.577
0.0895	9.277	-0.362	29.32	1.4134	0.6103	0.8685	-0.0881	0.2362	-0.6927	-.378	0.148	0.832	3403.5	-2480.8	0.259E-04	0.952E-04	0.272
0.0985	9.572	-0.328	29.11	1.3456	0.5943	0.8911	-0.0713	0.2271	-0.6650	-.339	0.139	0.864	3179.2	-2280.3	0.224E-04	0.996E-04	0.225
0.1165	10.082	-0.291	28.76	1.2559	0.5429	0.8660	-0.1223	0.1994	-0.6076	-.300	0.148	0.878	2266.1	-1617.0	0.540E-04	0.123E-03	0.437
0.1215	10.200	-0.278	28.68	1.2135	0.5320	0.8642	-0.1263	0.2019	-0.5650	-.301	0.151	0.872	2070.7	-1527.8	0.610E-04	0.132E-03	0.462
0.1320	10.362	-0.269	28.55	1.1180	0.5038	0.8638	-0.0876	0.1724	-0.5141	-.216	0.121	0.880	1514.2	-1215.7	0.579E-04	0.142E-03	0.408
0.1450	10.536	-0.244	28.40	1.0853	0.4780	0.8529	-0.1202	0.1639	-0.5276	-.217	0.130	0.870	1201.2	-1051.9	0.100E-03	0.156E-03	0.642
0.1505	10.583	-0.239	28.35	1.0803	0.4678	0.8478	-0.1103	0.1600	-0.5097	-.189	0.107	0.878	1128.7	-1001.0	0.977E-04	0.160E-03	0.611
0.1615	10.708	-0.234	28.24	1.0050	0.4541	0.8272	-0.1270	0.1500	-0.4717	-.173	0.112	0.878	999.5	-854.6	0.127E-03	0.175E-03	0.724
0.1835	10.906	-0.219	28.08	0.9353	0.4369	0.7819	-0.1152	0.1313	-0.4061	-.145	0.094	0.866	802.7	-706.1	0.143E-03	0.186E-03	0.772
0.2255	11.151	-0.225	27.84	0.8228	0.3908	0.7267	-0.1066	0.0999	-0.3130	-.102	0.080	0.830	530.2	-482.6	0.201E-03	0.207E-03	0.972
0.2435	11.255	-0.229	27.77	0.7557	0.3808	0.6931	-0.1071	0.0960	-0.2743	-.083	0.065	0.800	444.7	-420.7	0.241E-03	0.228E-03	1.055
0.2695	11.346	-0.229	27.67	0.7054	0.3563	0.6664	-0.0897	0.0918	-0.2463	-.065	0.052	0.786	347.5	-332.8	0.258E-03	0.276E-03	0.936
0.3010	11.433	-0.229	27.58	0.6551	0.3456	0.6379	-0.0958	0.0917	-0.2110	-.058	0.051	0.767	262.4	-285.0	0.365E-03	0.322E-03	1.134
0.3300	11.489	-0.227	27.51	0.6139	0.3383	0.6098	-0.0856	0.0795	-0.1818	-.047	0.040	0.733	228.0	-245.4	0.375E-03	0.324E-03	1.160
0.3885	11.622	-0.246	27.37	0.5448	0.3294	0.5356	-0.0777	0.0773	-0.1454	-.044	0.041	0.657	185.6	-201.3	0.419E-03	0.384E-03	1.091
0.4420	11.717	-0.254	27.28	0.4862	0.3084	0.4767	-0.0660	0.0635	-0.1064	-.032	0.030	0.592	147.8	-167.8	0.446E-03	0.378E-03	1.180
0.5235	11.787	-0.274	27.17	0.4396	0.2995	0.4044	-0.0558	0.0541	-0.0772	-.025	0.024	0.491	97.7	-117.1	0.571E-03	0.463E-03	1.234
0.5985	11.851	-0.280	27.10	0.3870	0.3018	0.3510	-0.0430	0.0484	-0.0514	-.019	0.020	0.410	70.8	-87.1	0.606E-03	0.555E-03	1.092
0.7485	11.934	-0.310	27.02	0.3501	0.2986	0.2516	-0.0384	0.0327	-0.0307	-.015	0.013	0.272	45.0	-46.4	0.855E-03	0.704E-03	1.214
0.9885	11.988	-0.340	26.96	0.3052	0.3259	0.1593	-0.0269	0.0222	-0.0122	-.010	0.010	0.140	25.2	-24.0	0.107E-02	0.925E-03	1.156
1.2390	12.033	-0.378	26.92	0.2854	0.3389	0.0940	-0.0233	0.0126	-0.0058	-.007	0.006	0.066	15.7	-11.1	0.148E-02	0.114E-02	1.304
1.4890	12.069	-0.422	26.91	0.2738	0.3415	0.0581	-0.0190	0.0071	-0.0033	-.006	0.004	0.034	13.2	-5.1	0.144E-02	0.138E-02	1.042
1.7390	12.088	-0.460	26.90	0.2689	0.3561	0.0355	-0.0192	0.0044	-0.0019	-.006	0.001	0.014	11.1	-1.5	0.173E-02	0.300E-02	0.575
1.9890	12.125	-0.494	26.90	0.2646	0.3573	0.0275	-0.0164	0.0036	-0.0014	-.005	0.001	0.007	9.5	-1.1	0.174E-02	0.333E-02	0.522
2.2385	12.144	-0.536	26.90	0.2613	0.3482	0.0194	-0.0161	0.0026	-0.0012	-.005	0.000	0.002	9.2	-0.7	0.175E-02	0.387E-02	0.452
2.4885	12.159	-0.559	26.90	0.2601	0.3517	0.0129	-0.0120	0.0024	-0.0010	-.003	0.000	0.001	8.0	-0.5	0.151E-02	0.451E-02	0.335
2.9885	12.201	-0.619	26.90	0.2671	0.3360	0.0113	-0.0056	0.0021	-0.0010	-.003	0.000	0.000	16.1	-0.3	0.350E-03	0.806E-02	0.043
3.4885	12.315	-0.653	26.90	0.2836	0.3023	0.0107	-0.0036	0.0017	-0.0010	-.003	0.000	0.000	-32.5	-129.4	-.112E-03	0.134E-04	*****

Station 6 dU/dx=14s-1
x = 50.4300 cm, Patm = 760.222 mm Hg,
Tatm = 26.8586 deg C, qwall = 172.774W/m2

y	U	V	T	u'	v'	t'	u'v'	v't'	u't'	u'v'2	v'2t'	gamma	dU/dy	dT/dy	em	eh	Prt
0.0500	9.237	-0.785	29.74	1.6311	0.7228	0.8345	-0.2205	0.2300	-0.6046	-.460	0.109	0.859	-2558.6	-4101.0	-.862E-04	0.561E-04	*****
0.0505	9.207	-0.823	29.75	1.6331	0.7201	0.8256	-0.2536	0.2188	-0.5862	-.510	0.114	0.844	-887.6	-187.3	-.286E-03	0.117E-02	-.245
0.0535	9.206	-0.861	29.74	1.6568	0.7167	0.8189	-0.2544	0.1981	-0.5989	-.506	0.101	0.850	-352.4	75.4	-.722E-03	-.263E-02	0.275
0.0605	9.230	-0.929	29.76	1.6360	0.7229	0.8263	-0.2799	0.2295	-0.5755	-.495	0.109	0.858	777.5	-43.4	0.360E-03	0.529E-02	0.068
0.0630	9.280	-0.963	29.76	1.6110	0.7309	0.8257	-0.2666	0.2469	-0.5657	-.529	0.114	0.858	878.0	-92.7	0.304E-03	0.266E-02	0.114
0.0685	9.327	-1.017	29.74	1.6400	0.7309	0.8185	-0.3231	0.2483	-0.6104	-.577	0.113	0.859	756.1	-231.5	0.427E-03	0.107E-02	0.398
0.0705	9.339	-1.010	29.74	1.6408	0.7443	0.8210	-0.3400	0.2492	-0.5628	-.578	0.127	0.857	718.0	-183.2	0.474E-03	0.136E-02	0.348
0.0760	9.358	-1.024	29.72	1.6990	0.7378	0.8270	-0.3134	0.2629	-0.6519	-.562	0.133	0.848	1248.4	-306.1	0.251E-03	0.859E-03	0.292
0.0810	9.429	-0.965	29.73	1.6787	0.7764	0.8381	-0.3876	0.2881	-0.6758	-.636	0.166	0.856	1126.8	-550.1	0.344E-03	0.524E-03	0.657
0.0840	9.554	-0.910	29.68	1.6647	0.7699	0.8455	-0.3187	0.2889	-0.6760	-.604	0.153	0.865	1314.0	-881.5	0.243E-03	0.328E-03	0.740
0.0890	9.510	-0.606	29.65	1.6568	0.8117	0.8347	-0.2948	0.3044	-0.6829	-.664	0.175	0.869	1297.6	-1466.9	0.227E-03	0.208E-03	1.095
0.0940	9.586	-0.358	29.53	1.6289	0.7588	0.8275	-0.2060	0.2561	-0.7258	-.579	0.179	0.872	1767.4	-1714.5	0.117E-03	0.149E-03	0.780
0.1045	9.946	-0.272	29.33	1.5732	0.7485	0.8360	-0.2035	0.2540	-0.6643	-.608	0.174	0.887	3119.6	-2030.8	0.652E-04	0.125E-03	0.522
0.1130	10.251	-0.276	29.15	1.4950	0.7158	0.8365	-0.1829	0.2392	-0.6565	-.567	0.172	0.896	2926.6	-1786.6	0.625E-04	0.134E-03	0.467
0.1230	10.533	-0.263	28.97	1.4394	0.6674	0.8265	-0.1908	0.2068	-0.6223	-.477	0.164	0.901	2582.6	-1561.9	0.739E-04	0.132E-03	0.558
0.1320	10.672	-0.214	28.87	1.4032	0.6677	0.8215	-0.2216	0.2194	-0.6000	-.460	0.177	0.913	2121.6	-1244.1	0.104E-03	0.176E-03	0.592
0.1465	11.027	-0.231	28.69	1.3040	0.5960	0.8184	-0.1679	0.1781	-0.5476	-.334	0.135	0.915	1684.0	-950.0	0.997E-04	0.188E-03	0.532
0.1540	11.086	-0.216	28.65	1.2693	0.5914	0.8065	-0.1667	0.1720	-0.5333	-.329	0.125	0.921	1609.8	-923.1	0.104E-03	0.186E-03	0.556
0.1650	11.249	-0.188	28.56	1.2433	0.5864	0.8089	-0.2093	0.1776	-0.5494	-.320	0.148	0.914	1188.1	-776.5	0.176E-03	0.229E-03	0.770
0.1870	11.498	-0.183	28.38	1.1363	0.5265	0.7870	-0.1705	0.1516	-0.4558	-.239	0.113	0.908	1026.7	-725.9	0.166E-03	0.209E-03	0.795
0.2005	11.626	-0.177	28.29	1.0815	0.5068	0.7607	-0.1762	0.1374	-0.4444	-.224	0.106	0.905	865.2	-644.5	0.204E-03	0.213E-03	0.955
0.2130	11.724	-0.191	28.21	1.0189	0.4948	0.7443	-0.1612	0.1228	-0.3977	-.203	0.105	0.900	766.7	-579.2	0.210E-03	0.212E-03	0.991
0.2385	11.875	-0.163	28.09	0.9445	0.4654	0.7129	-0.1486	0.1131	-0.3575	-.151	0.084	0.881	641.4	-488.6	0.232E-03	0.231E-03	1.001
0.2510	12.001	-0.169	28.00	0.8955	0.4349	0.6885	-0.1310	0.1013	-0.3251	-.138	0.075	0.860	588.2	-447.0	0.223E-03	0.227E-03	0.982
0.2760	12.105	-0.170	27.92	0.8518	0.4288	0.6831	-0.1392	0.1004	-0.3135	-.129	0.075	0.863	504.4	-370.8	0.276E-03	0.271E-03	1.019
0.2925	12.180	-0.165	27.86	0.7844	0.3982	0.6410	-0.1217	0.0906	-0.2662	-.094	0.053	0.837	398.1	-302.1	0.306E-03	0.300E-03	1.019
0.3135	12.276	-0.171	27.79	0.7396	0.3906	0.6199	-0.1100	0.0910	-0.2338	-.091	0.059	0.822	361.8	-292.1	0.304E-03	0.312E-03	0.975
0.3560	12.375	-0.168	27.70	0.6851	0.3547	0.5930	-0.0996	0.0854	-0.2121	-.060	0.037	0.775	279.3	-239.6	0.357E-03	0.357E-03	1.000
0.3815	12.469	-0.178	27.62	0.6196	0.3484	0.5540	-0.0858	0.0756	-0.1706	-.055	0.037	0.758	241.4	-216.1	0.355E-03	0.350E-03	1.015
0.4325	12.565	-0.182	27.54	0.5723	0.3434	0.5198	-0.0865	0.0755	-0.1491	-.051	0.035	0.706	206.0	-179.0	0.420E-03	0.422E-03	0.995
0.4765	12.649	-0.183	27.46	0.5211	0.3216	0.4700	-0.0754	0.0660	-0.1155	-.038	0.029	0.643	159.6	-135.7	0.472E-03	0.486E-03	0.971
0.5645	12.762	-0.205	27.38	0.4632	0.3101	0.4201	-0.0630	0.0611	-0.0913	-.029	0.024	0.565	116.7	-104.6	0.540E-03	0.584E-03	0.924
0.6510	12.840	-0.207	27.28	0.3904	0.3069	0.3551	-0.0473	0.0515	-0.0564	-.020	0.019	0.459	82.4	-80.2	0.574E-03	0.642E-03	0.895
0.8240	12.932	-0.230	27.18	0.3442	0.3144	0.2576	-0.0416	0.0386	-0.0283	-.018	0.016	0.319	47.1	-53.4	0.883E-03	0.722E-03	1.223
0.9785	12.976	-0.267	27.13	0.3029	0.3232	0.1968	-0.0285	0.0278	-0.0166	-.012	0.012	0.204	31.9	-32.8	0.891E-03	0.847E-03	1.052
1.2290	13.037	-0.294	27.08	0.2807	0.3266	0.1203	-0.0229	0.0154	-0.0081	-.009	0.007	0.109	20.7	-15.4	0.111E-02	0.998E-03	1.110
1.4790	13.072	-0.312	27.06	0.2633	0.3434	0.0805	-0.0216	0.0105	-0.0042	-.008	0.005	0.059	16.5	-7.5	0.131E-02	0.140E-02	0.936
1.7290	13.117	-0.346	27.06	0.2546	0.3514	0.0501	-0.0166	0.0063	-0.0020	-.005	0.003	0.025	14.1	-3.7	0.118E-02	0.170E-02	0.694
1.9790	13.142	-0.368	27.05	0.2493	0.3498	0.0370	-0.0130	0.0041	-0.0014	-.005	0.001	0.013	NaN	NaN	-NaN	-NaN	NaN
2.4790	13.207	-0.414	27.04	0.2488	0.3424	0.0154	-0.0107	0.0021	-0.0009	-.005	0.000	0.002	NaN	NaN	-NaN	-NaN	NaN

Station 7 dU/dx=14s-1
x = 58.2500 cm, Patm = 760.476 mm Hg,
Tatm = 26.8983 deg C, qwall = 175.417W/m2

y	U	V	T	u'	v'	t'	u'v'	v't'	u't'	u'v'2	v'2t'	gamma	dU/dy	dT/dy	em	eh	Prt
0.0500	9.445	-1.192	29.58	1.6208	0.7908	0.7287	-0.3939	0.1912	-0.3844	-.555	0.050	0.917	*******	-5306.9	-.352E-04	0.360E-04	-.977
0.0510	9.404	-1.195	29.57	1.6580	0.8274	0.7340	-0.4587	0.2127	-0.4399	-.635	0.078	0.917	431.4	-814.2	0.106E-02	0.261E-03	4.071
0.0560	9.517	-1.257	29.55	1.6484	0.8158	0.7252	-0.4995	0.2174	-0.4270	-.673	0.067	0.916	1977.5	-417.1	0.253E-03	0.521E-03	0.485
0.0595	9.627	-1.306	29.54	1.6331	0.8144	0.7296	-0.4913	0.2156	-0.4353	-.618	0.091	0.921	2127.0	-360.1	0.231E-03	0.599E-03	0.386
0.0635	9.678	-1.318	29.53	1.6626	0.8481	0.7258	-0.5296	0.2284	-0.4426	-.740	0.100	0.917	2076.9	-372.6	0.255E-03	0.613E-03	0.416
0.0700	9.795	-1.273	29.50	1.6578	0.8519	0.7290	-0.4812	0.2616	-0.4486	-.703	0.114	0.920	2082.3	-639.8	0.231E-03	0.409E-03	0.565
0.0770	10.051	-1.144	29.44	1.6663	0.8625	0.7176	-0.4763	0.2495	-0.4574	-.787	0.121	0.924	2221.9	-1015.1	0.214E-03	0.246E-03	0.872
0.0840	10.068	-0.489	29.36	1.6401	0.8902	0.7309	-0.3372	0.2637	-0.5286	-.723	0.145	0.928	2539.2	-1448.8	0.133E-03	0.182E-03	0.729
0.0890	10.269	-0.401	29.28	1.5941	0.8577	0.7209	-0.3587	0.2310	-0.4996	-.728	0.128	0.934	2418.2	-1506.2	0.148E-03	0.153E-03	0.967
0.0945	10.442	-0.376	29.17	1.5622	0.8443	0.7266	-0.3302	0.2277	-0.4899	-.692	0.134	0.936	3202.8	-1621.4	0.103E-03	0.140E-03	0.734
0.1060	10.762	-0.376	29.02	1.5410	0.7818	0.7336	-0.3073	0.1932	-0.5080	-.567	0.123	0.942	2728.3	-1369.8	0.113E-03	0.141E-03	0.799
0.1145	11.019	-0.343	28.90	1.4759	0.7464	0.7226	-0.3107	0.1884	-0.5016	-.524	0.143	0.939	2432.2	-1192.4	0.128E-03	0.158E-03	0.809
0.1320	11.364	-0.335	28.72	1.3891	0.7141	0.7140	-0.3446	0.1792	-0.4911	-.492	0.134	0.934	1841.8	-950.1	0.187E-03	0.189E-03	0.992
0.1515	11.637	-0.337	28.57	1.3072	0.6716	0.6987	-0.3092	0.1651	-0.4406	-.332	0.113	0.951	1445.6	-764.0	0.214E-03	0.216E-03	0.990
0.1660	11.832	-0.334	28.47	1.2527	0.6308	0.7067	-0.2975	0.1441	-0.4440	-.301	0.104	0.942	1222.2	-700.9	0.243E-03	0.206E-03	1.184
0.1745	11.960	-0.337	28.40	1.2380	0.6213	0.6989	-0.2882	0.1466	-0.4528	-.308	0.114	0.947	1167.4	-639.6	0.247E-03	0.229E-03	1.077
0.1930	12.121	-0.331	28.29	1.1640	0.5989	0.6883	-0.2666	0.1304	-0.4022	-.258	0.089	0.944	964.2	-550.0	0.276E-03	0.237E-03	1.166
0.2085	12.265	-0.346	28.24	1.1158	0.5705	0.6713	-0.2487	0.1193	-0.3891	-.239	0.081	0.940	837.9	-495.6	0.297E-03	0.241E-03	1.233
0.2400	12.522	-0.338	28.07	1.0117	0.5232	0.6500	-0.2150	0.1126	-0.3439	-.166	0.071	0.926	711.5	-436.6	0.302E-03	0.258E-03	1.171
0.2635	12.635	-0.342	27.98	0.9859	0.5122	0.6416	-0.2249	0.1131	-0.3338	-.157	0.064	0.920	620.0	-411.1	0.363E-03	0.275E-03	1.318
0.3110	12.925	-0.368	27.81	0.8847	0.4606	0.6176	-0.1791	0.0963	-0.2852	-.131	0.059	0.879	506.5	-325.6	0.354E-03	0.296E-03	1.196
0.3400	13.042	-0.348	27.74	0.8430	0.4433	0.6047	-0.1783	0.1049	-0.2763	-.112	0.054	0.867	423.5	-280.4	0.421E-03	0.374E-03	1.125
0.3625	13.152	-0.356	27.65	0.7776	0.4218	0.5810	-0.1516	0.0939	-0.2365	-.105	0.054	0.838	357.9	-255.1	0.424E-03	0.368E-03	1.151
0.4090	13.269	-0.365	27.56	0.7145	0.4133	0.5523	-0.1419	0.0956	-0.2082	-.097	0.053	0.799	288.1	-218.4	0.493E-03	0.438E-03	1.126
0.4505	13.382	-0.381	27.48	0.6562	0.3789	0.5246	-0.1198	0.0864	-0.1749	-.070	0.041	0.762	241.0	-187.6	0.497E-03	0.461E-03	1.079
0.5300	13.563	-0.395	27.33	0.5561	0.3522	0.4637	-0.0960	0.0785	-0.1204	-.060	0.036	0.659	182.5	-148.8	0.526E-03	0.528E-03	0.997
0.6105	13.677	-0.399	27.24	0.4615	0.3240	0.4088	-0.0699	0.0641	-0.0852	-.038	0.028	0.565	126.8	-108.8	0.551E-03	0.590E-03	0.935
0.6890	13.723	-0.407	27.19	0.4249	0.3247	0.3768	-0.0643	0.0628	-0.0748	-.031	0.026	0.494	85.6	-75.5	0.751E-03	0.831E-03	0.904
0.8025	13.817	-0.438	27.11	0.3557	0.3151	0.3113	-0.0440	0.0478	-0.0444	-.022	0.021	0.380	57.2	-54.1	0.770E-03	0.883E-03	0.872
1.0300	13.900	-0.449	27.03	0.3088	0.3245	0.2093	-0.0336	0.0318	-0.0201	-.016	0.013	0.233	38.6	-33.1	0.870E-03	0.960E-03	0.906
1.2800	13.974	-0.490	26.97	0.2693	0.3294	0.1466	-0.0234	0.0210	-0.0092	-.009	0.009	0.142	24.0	-17.6	0.975E-03	0.120E-02	0.815
1.5300	14.020	-0.521	26.95	0.2550	0.3390	0.0990	-0.0181	0.0132	-0.0046	-.008	0.006	0.086	18.3	-10.3	0.991E-03	0.128E-02	0.777
1.7800	14.048	-0.533	26.93	0.2437	0.3341	0.0675	-0.0148	0.0080	-0.0023	-.005	0.004	0.043	14.0	-5.7	0.105E-02	0.140E-02	0.750
2.2800	14.112	-0.565	26.92	0.2466	0.3318	0.0314	-0.0101	0.0035	-0.0011	-.004	0.001	0.013	17.4	-2.2	0.584E-03	0.161E-02	0.363
2.7800	14.219	-0.593	26.91	0.2494	0.2908	0.0211	-0.0080	0.0019	-0.0010	-.003	0.001	0.003	-86.0	-213.8	-.924E-04	0.887E-05	*****

Station 8 dU/dx=14s-1
x = 66.2100 cm, Patm = 760.476 mm Hg,
Tatm = 26.7908 deg C, qwall = 178.738W/m2

y	U	V	T	u'	v'	t'	u'v'	v't'	u't'	u'v'2	v'2t'	gamma	dU/dy	dT/dy	em	eh	Prt
0.0500	10.854	-0.504	29.12	1.6123	0.8162	0.6330	-0.2328	0.1402	-0.3641	-.626	0.059	0.948	-2362.1	884.5	-.985E-04	-.158E-03	0.622
0.0515	10.822	-0.522	29.13	1.6219	0.7933	0.6256	-0.2417	0.1342	-0.3218	-.576	0.029	0.955	-1538.2	326.4	-.157E-03	-.411E-03	0.382
0.0580	10.786	-0.588	29.14	1.6262	0.8324	0.6333	-0.3081	0.1469	-0.3274	-.651	0.081	0.947	-20.9	106.6	-.148E-01	-.138E-02	*****
0.0630	10.836	-0.705	29.14	1.6331	0.8207	0.6224	-0.3255	0.1451	-0.3187	-.677	0.059	0.949	635.0	-44.6	0.513E-03	0.326E-02	0.157
0.0730	10.927	-0.895	29.14	1.6661	0.8656	0.6301	-0.3942	0.1661	-0.3493	-.741	0.088	0.946	1295.9	-397.6	0.304E-03	0.418E-03	0.728
0.0800	11.094	-0.692	29.09	1.6806	0.9030	0.6278	-0.3946	0.1928	-0.3734	-.862	0.117	0.951	1525.9	-706.6	0.259E-03	0.273E-03	0.948
0.0925	11.224	-0.121	28.96	1.5980	0.8878	0.6214	-0.3183	0.1642	-0.3944	-.733	0.116	0.956	2004.3	-1057.1	0.159E-03	0.155E-03	1.022
0.0990	11.413	-0.068	28.87	1.5282	0.8397	0.6188	-0.2958	0.1571	-0.3747	-.608	0.072	0.952	2041.1	-1037.0	0.145E-03	0.152E-03	0.957
0.1110	11.709	-0.047	28.75	1.4565	0.8048	0.6238	-0.3229	0.1471	-0.3768	-.571	0.101	0.961	2319.0	-950.9	0.139E-03	0.155E-03	0.900
0.1220	11.943	-0.029	28.67	1.4390	0.7541	0.6187	-0.3350	0.1401	-0.3938	-.449	0.083	0.961	1989.4	-792.8	0.168E-03	0.177E-03	0.953
0.1445	12.316	-0.014	28.51	1.3357	0.7045	0.6093	-0.3165	0.1252	-0.3709	-.326	0.078	0.959	1533.0	-627.2	0.206E-03	0.200E-03	1.034
0.1610	12.538	-0.007	28.41	1.2572	0.6697	0.5971	-0.2973	0.1058	-0.3561	-.272	0.063	0.960	1309.1	-576.6	0.227E-03	0.183E-03	1.238
0.1805	12.773	-0.014	28.32	1.1982	0.6222	0.5993	-0.2796	0.1009	-0.3374	-.217	0.059	0.958	1094.2	-489.1	0.256E-03	0.206E-03	1.239
0.1940	12.914	-0.005	28.24	1.1735	0.6007	0.5925	-0.2696	0.0994	-0.3444	-.210	0.058	0.950	984.1	-454.1	0.274E-03	0.219E-03	1.252
0.2210	13.133	-0.001	28.14	1.1208	0.5700	0.5804	-0.2771	0.1001	-0.3213	-.186	0.051	0.950	803.6	-402.8	0.345E-03	0.249E-03	1.387
0.2555	13.388	0.014	28.01	1.0512	0.5535	0.5789	-0.2650	0.1048	-0.3224	-.168	0.054	0.945	671.6	-342.0	0.395E-03	0.306E-03	1.287
0.2785	13.535	0.003	27.93	0.9861	0.5248	0.5834	-0.2363	0.0993	-0.3018	-.137	0.048	0.937	610.8	-324.1	0.387E-03	0.306E-03	1.263
0.3250	13.774	-0.005	27.80	0.9240	0.4968	0.5670	-0.2165	0.0981	-0.2745	-.141	0.047	0.924	505.2	-275.7	0.429E-03	0.356E-03	1.204
0.3960	14.101	-0.014	27.62	0.7994	0.4385	0.5406	-0.1600	0.0839	-0.2297	-.106	0.049	0.873	391.7	-224.3	0.408E-03	0.374E-03	1.092
0.4260	14.214	-0.021	27.56	0.7741	0.4067	0.5231	-0.1467	0.0876	-0.2195	-.087	0.037	0.844	345.7	-204.1	0.424E-03	0.429E-03	0.989
0.4865	14.387	-0.029	27.45	0.6884	0.3960	0.4926	-0.1332	0.0818	-0.1778	-.087	0.040	0.795	250.3	-169.1	0.532E-03	0.484E-03	1.099
0.5705	14.533	-0.032	27.33	0.5974	0.3590	0.4518	-0.1056	0.0765	-0.1453	-.062	0.035	0.683	179.3	-129.3	0.589E-03	0.592E-03	0.996
0.6410	14.662	-0.059	27.24	0.5146	0.3372	0.4115	-0.0798	0.0656	-0.1050	-.048	0.030	0.611	134.4	-100.7	0.593E-03	0.651E-03	0.912
0.7825	14.781	-0.053	27.15	0.4249	0.3352	0.3541	-0.0683	0.0635	-0.0698	-.036	0.028	0.481	85.3	-68.3	0.801E-03	0.930E-03	0.861
0.8985	14.855	-0.072	27.07	0.3627	0.3324	0.2871	-0.0525	0.0471	-0.0423	-.031	0.024	0.368	57.1	-50.4	0.921E-03	0.935E-03	0.984
1.1185	14.940	-0.097	27.00	0.2915	0.3266	0.2113	-0.0316	0.0313	-0.0188	-.013	0.013	0.258	34.7	-31.3	0.910E-03	0.999E-03	0.912
1.3685	15.000	-0.128	26.95	0.2569	0.3324	0.1513	-0.0236	0.0224	-0.0089	-.008	0.011	0.155	22.7	-16.1	0.104E-02	0.139E-02	0.746
1.6185	15.035	-0.159	26.92	0.2476	0.3329	0.0978	-0.0186	0.0134	-0.0043	-.008	0.007	0.080	16.7	-6.5	0.111E-02	0.206E-02	0.541
1.8685	15.080	-0.180	26.92	0.2364	0.3378	0.0751	-0.0152	0.0095	-0.0027	-.005	0.005	0.049	-103.7	-225.2	-.146E-03	0.423E-04	*****

REPORT DOCUMENTATION PAGE

Form Approved
OMB No. 0704-0188

1. AGENCY USE ONLY (*Leave blank*)	2. REPORT DATE	3. REPORT TYPE AND DATES COVERED
	October 1995	Final Contractor Report

4. TITLE AND SUBTITLE

Measurements in Transitional Boundary Layers Under High Free-Stream Turbulence and Strong Acceleration Conditions

5. FUNDING NUMBERS

WU-505-62-52
G-NAG3-1249

6. AUTHOR(S)

Ralph J. Volino and Terrence W. Simon

7. PERFORMING ORGANIZATION NAME(S) AND ADDRESS(ES)

University of Minnesota
111 Church Street N.E.
Minneapolis, Minnesota 55455-0111

8. PERFORMING ORGANIZATION REPORT NUMBER

E-9976

9. SPONSORING/MONITORING AGENCY NAME(S) AND ADDRESS(ES)

National Aeronautics and Space Administration
Lewis Research Center
Cleveland, Ohio 44135-3191

10. SPONSORING/MONITORING AGENCY REPORT NUMBER

NASA CR-198413

11. SUPPLEMENTARY NOTES

Project Manager, Frederick F. Simon, Internal Fluid Division, NASA Lewis Research Center, organization code 2630, (216) 433-5894.

12a. DISTRIBUTION/AVAILABILITY STATEMENT

Unclassified - Unlimited
Subject Category 34

This publication is available from the NASA Center for Aerospace Information, (301) 621-0390.

12b. DISTRIBUTION CODE

13. ABSTRACT ***(Maximum 200 words)***

Measurements from transitional, heated boundary layers along a concave-curved test wall are presented and discussed. A boundary layer subject to low free-stream turbulence intensity (FSTI), which contains stationary streamwise (Görtler) vortices, is documented. The low FSTI measurements are followed by measurements in boundary layers subject to high (initially 8%) free-stream turbulence intensity and moderate to strong streamwise acceleration. Conditions were chosen to simulate those present on the downstream half of the pressure side of a gas turbine airfoil. Mean flow characteristics as well as turbulence statistics, including the turbulent shear stress, turbulent heat flux, and turbulent Prandtl number, are documented. A technique called "octant analysis" is introduced and applied to several cases from the literature as well as to data from the present study. Spectral analysis was applied to describe the effects of turbulence scales of different sizes during transition. To the authors' knowledge, this is the first detailed documentation of boundary layer transition under such high free-stream turbulence conditions.

14. SUBJECT TERMS

Transition; Heat transfer; Curvature; Turbulence; Pressure gradient

15. NUMBER OF PAGES

660

16. PRICE CODE

A25

17. SECURITY CLASSIFICATION OF REPORT	18. SECURITY CLASSIFICATION OF THIS PAGE	19. SECURITY CLASSIFICATION OF ABSTRACT	20. LIMITATION OF ABSTRACT
Unclassified	Unclassified	Unclassified	